1312

PHILIPS TECHNICAL REVIEW

20. JULI 1949
N.V. PHILIPS' GLOEILAMPENFABRIEKEN
BIBLIOTHEEK
LABORATORIUM
WETENSCHAPP. ONDERZOEK



VOLUME 10

1948/1949

PHILIPS RESEARCH LABORATORIES - EINDHOVEN

CONTENTS

VOLUME 10, 1948/1949

LIGHT SOURCES AND ILLUMINATION

Page

A rapid-action starter switch for fluorescent lamps, by Th. Hehenkamp 141

The new candle, by W. de Groot 150

Basic principles for the formulation of illumination standards, by A. A. Kruithof and A. M. Kruithof 214

A flash lamp for illuminating vapour tracks in the Wilson cloud chamber, by N. Warmoltz and A. M. C. Helmer . . . 178

Page

Forcing tulips with artificial light, by R. van der Veen 282

On the illumination of traffic tunnels, by A. M. Kruithof 299

Storing seed potatoes in artificially-lighted cellars, by R. van der Veen. 318

The illumination of coal-mines and the attendant risk of explosions, by G. D. Rieck 334

TELECOMMUNICATION

Electromagnetic waves in wave guides, by W. Opechowski, ...

I. General theoretical principles; rectangular wave guides 13

II. Coaxial cables and circular wave guides 46

Projection-television receiver,

I. The optical system for the projection, by P. M. van Alphen and H. Rinia 69

II. The cathode-ray tube, by J. de Gier 97

III. The 25 kV anode voltage supply unit, by G. J. Siezen and F. Kerkhof 125

IV. The circuits for deflecting the electron beam, by J. Haantjes and F. Kerkhof 307

V. The synchronisation, by J. Haantjes and F. Kerkhof 364

Experimental transmitting and receiving equipment for high-speed facsimile transmission,

I. General, by H. Rinia, D. Kleis and M. van Tol 189

II. Details of the transmitter, by D. Kleis, F. C. W. Slooff and J. M. Unk 257

III. Details of the receiver, by F. C. W. Slooff, M. van Tol and J. M. Unk 265

IV. Transmission of the signals, by D. Kleis and M. van Tol 289

V. Synchronization of transmitter and receiver, by D. Kleis and M. van Tol 325

A transmitting valve cooler with increased turbulence of the cooling water, by M. J. Snijders 239

Glass transmitting valves of high efficiency in the 100 Mc/s range, by E. G. Dorgelo 273

Secondary emission in output valves, by J. L. H. Jonker 346

A 48-channel carrier telephone system, II. Construction of the apparatus, by G. H. Bast, D. Goedhart and J. F. Schouten 353

SOUND

Duplication of concerts, by R. Vermeulen 169

A demonstration studio for sound recording and reproduction and for sound film projection, by the Electro-Acoustics Department 196

X-RAYS

X-Ray spectrometer with Geiger counter for measuring powder diffraction patterns, by J. Bleeksma, G. Kloos and H. J. Di Giovanni 1

A diagnostic X-ray apparatus with exposure technique indication and overload protection, by A. Nemet, W. A. Bayfield and M. Berindei 37

A miniature X-ray apparatus for dentists, by J. Fransen. 221

A transportable X-ray apparatus for mass chest survey, by H. J. Di Giovanni, W. Kes and K. Lowitzsch 105

An improved X-ray diffraction camera, by W. Parrish and E. Cisney 157

A direct-reading dynamic electrometer, by J. van Hengel and W. J. Oosterkamp . 338

ELECTROTECHNICS

	Page
The origin of the Giorgi system of electrical units, by W. de Groot	55
The rationalized Giorgi system with absolute volt and ampere as applied in electrical engineering, by P. Cornelius	79
Stabilization of the accelerating voltage in an electron microscope, by A. C. van Dorsten	135
A rapid-action starter switch for fluorescent lamps, by Th. Hehenkamp	141
Soft iron for the electromagnet of a cyclotron, by J. J. Went	246
A direct-reading dynamic electrometer, by J. van Hengel and W. J. Oosterkamp	338

MATERIALS AND THEIR RESEARCH

	Page
The part played by oxygen and nitrogen in arc-welding, by J. D. Fast	26
The effect of the melting point and the volume magneto-striction on the thermal expansion of alloys, by J. J. Went	87
The function of the coating of welding rods, by J. D. Fast	114
Ceramics and their manufacture, by R. A. IJdens	205
Ceramic materials with a high dielectric constant, by E. J. W. Verwey and R. D. Bügel	231
Soft iron for the electromagnet of a cyclotron, by J. J. Went	246

MISCELLANEOUS

	Page
The origin of the Giorgi system of electrical units, by W. de Groot	55
Conical disc springs, by J. A. Haringx	61
The rationalized Giorgi system with absolute volt and ampere as applied in electrical engineering, by P. Cornelius	79
Examining mirrors for projection television	286

VOL. 10 No. 1, pp. 1-36 JULY 1948

Philips Technical Review

DEALING WITH TECHNICAL PROBLEMS
RELATING TO THE PRODUCTS, PROCESSES AND INVESTIGATIONS OF
THE PHILIPS INDUSTRIES

EDITED BY THE RESEARCH LABORATORY OF N.V. PHILIPS' GLOEILAMPENFABRIEKEN, EINDHOVEN, NETHERLANDS.

X-RAY SPECTROMETER WITH GEIGER COUNTER FOR MEASURING POWDER DIFFRACTION PATTERNS

by J. BLEEKSMA *), G. KLOOS *) and H. J. DI GIOVANNI *).

539.26:535.322.1:
539.16.08

With the spectrometer described in this paper, which was engineered by North American Philips Co., Inc., along the lines indicated by H. Friedman, X-ray diffraction patterns are traversed by a Geiger counter tube detector instead of being recorded in the conventional fashion on photographic film. The Geiger counter tube, also developed by H. Friedman in a form especially adapted to the measurement of X-ray intensities, is applied in a well known focusing arrangement, making use of a large flat specimen (dimensions of active area, e.g., 1 × 2 cm). Due to the extremely high sensitivity of the counter tube, to the high apparent X-ray "brightness" of the focal spot which is used at a glancing angle of only 1.5°, and to the large specimen surface contributing to the diffraction intensity, an X-ray tube rating as low as 125 W is sufficient. The measurement of the intensity of the diffraction lines is effected, *a*) by counting the current pulses produced in the Geiger tube by the entering X-ray quanta, a scaling circuit making this possible at radiation intensities of several thousand quanta per second at the tube window, or *b*) by measuring, after amplification, the mean value of the current through the Geiger tube by means of a milliammeter; the milliammeter reading can be automatically recorded while the spectrum is being scanned, thus producing a chart which immediately indicates the relative line intensity as a function of the diffraction angle. The scanning speed, as well as the averaging time for the mean current measurement, can be chosen between wide limits. The accuracy of the determination of diffraction angles and relative intensities, and the resolving power for adjacent diffraction lines are better than with the commonly used photographic methods, under comparable electric and geometric conditions. Moreover the Geiger counter spectrometer offers additional distinct advantages for applications in which the accurate measurement of only a few lines is desired. A more detailed account of the special techniques and possibilities of the instrument will be given later.

The use of X-ray diffraction technique for chemical analysis, for metallurgical investigations, etc. has become rather commonplace in the past two decades. From an interesting laboratory phenomenon, X-ray diffraction has thus become an invaluable tool for industry. Many examples of its industrial application have been given in papers in this Review [1]).

Actually, it has been apparent for a number of years that the possible fields of application of the method are much wider than those covered at the moment. The limitations on the use of X-ray diffraction are generally not set by the results of which the method is capable, but more commonly by the time and cost involved in its practical adaptation to a particular type of problem.

In the past few years a very promising line has been opened in the field of X-ray diffraction techniques by the development of a new instrument, the Geiger counter spectrometer. By means of this instrument the desired information can in certain cases be obtained in much less time than with the conventional photographic procedure. Moreover, routine measurements can be made by relatively unskilled operators, while at the same time the accuracy of the results is in general better than with commonly used photographic methods. Although it is not to be supposed — because of certain limitations of the new method — that the photographic techniques will be superseded, we may

*) North American Philips Co., Inc., New York, N.Y.

[1]) Cf. the series of articles by W. G. Burgers in Philips Techn. Rev. 1 (1936) and 2 (1937), the summarizing article in 5, 161, 1940, and another series by J. F. H. Custers in Philips Techn. Rev. 7 (1942).

safely expect that a considerable increase in the industrial use of X-ray diffraction will be brought about by this instrument.

In this paper a succinct description of the principle and design of the Geiger counter spectrometer is given. Limits of accuracy, techniques of practical use and a number of special applications will be described in a second paper.

Brief outline of X-ray diffraction; photographic method

The diffraction of an X-ray beam striking a crystal can be described as a reflection, one set of the lattice planes in which the atoms are arranged acting as a mirror (*fig. 1*), under the condition that the angle Θ of "reflection", the X-ray wavelength λ and the spacing d between successive parallel lattice planes of the set conform to the well-known Bragg equation:

$$n\lambda = 2\,d \sin \Theta,$$

where n is an integer indicating the order of the diffraction.

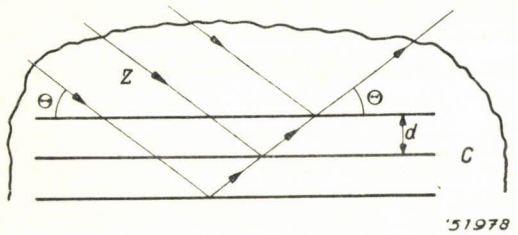


Fig. 1. Diffraction of a beam of X-rays Z impingent on a crystal C can be described as a reflection at a set of lattice planes, conforming to the Bragg relation between the angle Θ, the wavelength λ of the rays and the spacing d of the parallel atomic planes.

In a single crystal of a material a series of different sets of lattice planes can be distinguished, every set possessing a specific "planar spacing value" d and a specific orientation within the crystal. Using X-rays of one single wavelength, reflection at a given lattice plane will occur only if the crystal has an appropriate position with respect to the beam, the required angle between the beam and the plane being fixed (Θ). The intensity of the reflected beam depends on the arrangement, kind and density of the atoms in the plane, and on the perfection of the crystal, as well as on the absorption of the X-rays in the material.

In most practical applications the substance under examination is not a single crystal, but a polycrystalline material, e.g. a powder. Assuming the tiny crystals of the powder to be oriented entirely at random, there will always be a number of crystals showing the orientation required for a specific lattice plane to act as a mirror and hence giving rise to a diffraction of X-rays in the corresponding direction Θ. The angle Θ being fixed only with respect to the incident beam, and rotational symmetry prevailing because of the random orientation of the crystals, the diffracted X-rays form a cone with included angle 4Θ around the primary beam. The entire diffracted radiation from the powder specimen consists of a series of such coaxial cones, belonging to different sets of lattice planes in the elementary crystal (*fig. 2*).

A hypothetical sphere arranged around the powder specimen is intersected by the cones in a series of concentric rings, the central spot being formed by the primary beam. By laying a narrow strip of photographic film in a circle around the specimen, a small part of every ring is recorded on each side of

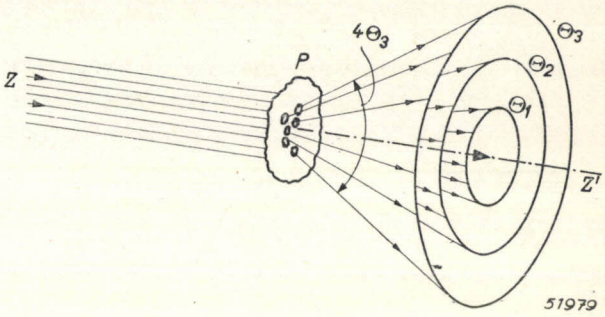


Fig. 2. When a polycrystalline specimen P containing crystallites oriented at random is placed in a monochromatic X-ray beam Z, the rays diffracted at a Bragg angle Θ by the suitably oriented crystallites form a cone with included angle 4Θ around the direction Z' of the primary beam. Different lattice planes (spacing values d) give rise to different cones.

the central spot. In this way the well-known diffraction pattern (Debye-Scherrer photograph) of the specimen substance is obtained (*fig. 3*).

After this brief recapitulation of the principles of X-ray diffraction, the photographic method for the measurement of diffraction patterns requires little further explanation. The arrangement generally used is shown in *fig. 4*. The specimen is formed, for example, by a small cylindrical tube filled with the powder under examination and placed along the axis of a cylindrical camera. The X-rays emanating from the anode of an X-ray tube are collimated by means of a pair of pin-hole apertures of say 0.5 mm width; the fine pencil of X-rays thus obtained enters the camera and impinges on the specimen. A film is laid against the whole inner circumference of the cylindrical wall of the camera. With ordinary equipment the exposure times necessary for obtaining a diffraction pattern of sufficient density vary between 15 minutes and more than 10 hours. In cases where the exact knowledge of relative

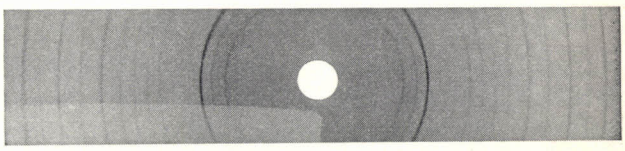


Fig. 3. Diffraction pattern of a specimen obtained on a photographic film. The "lines" (rings) are the intersections of the film with the series of cones shown in fig. 2. (The shadow along the lower left hand edge of the pattern is produced by a thin nickel filter, offering a means of identifying undesired Kβ-lines of the copper radiation; cf. footnote [8]).)

intensities of the diffraction lines is required (e.g., for quantitative analysis of mixtures), the density of the film pattern must be measured by means of a microphotometer.

This is not the place to dwell on the various types of information which can be read from the position, the intensity and the shape of the lines in the diffraction pattern [2]). We confine

[2]) Cf. e.g. W. G. Burgers, Philips Techn. Rev. **5**, 157, 1940.

ourselves to mentioning the identification of substances by means of the so-called "fingerprint" method. The crystal lattice being different for all substances, each having its specific planar spacing values and corresponding diffraction intensities, no two patterns are exactly alike. Hence, a sub-

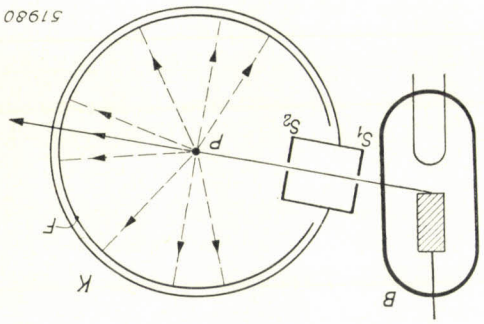


Fig. 4. For the photographic recording of powder diffraction patterns, a cylindrical camera is commonly used. The X-rays emitted by the tube B are collimated in a narrow beam by pin-hole apertures S_1, S_2, impinge on the thin cylindrical specimen P at the centre of the camera K, and are diffracted onto the film strip F.

stance can be unambiguously identified by the spacing values derived from a number of lines in its diffraction pattern. The spacing values of most of the commonly occurring substances have been listed in a catalog, compiled by the American Society for Testing Materials and indexed according to the three strongest diffraction lines (the "fingerprints" of each substance). Such a catalog offers a simple means of chemical identification and analysis of mixtures.

Principles of the Geiger counter spectrometer

In the photographic method for investigating diffraction patterns, local radiation intensities are measured by the blackening of a photographic film. There are other, and in some cases, more efficient means for radiation measurements; one of these is the Geiger counter tube, *fig. 5*. When a single X-ray quantum is absorbed in such a tube, it sets free a photo-electron which gives rise to a short discharge through the gas filling between the wire anode and the surrounding cylindrical cathode. By counting the short current pulses through the Geiger tube produced by the absorbed quanta, the rate of the arrival of quanta, i.e. the radiation intensity, is measured. We shall give below a more detailed account of the properties of the Geiger tube and of its adaptation to our special purpose.

While the photographic film registers all diffracted beams simultaneously, the Geiger tube can measure the mean intensity at only one spot at a time, viz. at the instantaneous position of the window through which the X-rays enter the tube. Therefore, the Geiger tube must be moved along the circle on which the film would have been mounted in the photographic method, and the intensities at different diffraction angles must be measured one after the other. The simultaneous recording of the whole spectrum of diffraction lines would seem to be an inherent advantage of the film — and in fact for some purposes it is — but in general this advantage is outweighed by the greater sensitivity of the Geiger tube: to obtain a sufficient blackening of the film, with a wavelength of 1.5 Å, an incident radiation energy of about 2 erg per cm^2 is necessary, while one single line can be recorded by the Geiger counter using only say 4×10^{-4} erg/cm^2 (for a precision of about 5% in the intensity measurement).

A local radiation detector, such as the Geiger tube, is used to best advantage in conjunction with a focusing arrangement; cf. *fig. 6*. Instead of the small cylindrical specimen previously mentioned, a large flat specimen with dimensions of perhaps 1×2 cm is used. A divergent X-ray beam, emerging from the slit A, irradiates this specimen at an angle Θ. Considering only the crystallites (of appropriate orientation) lying at the surface of the specimen, it is seen that the rays reflected at the angle Θ from all points of the specimen very nearly converge to a single line at point B in fig. 6; at this point the entrance window of the Geiger tube is placed. The "focusing" at B would be exact if the specimen were curved to conform to the circle

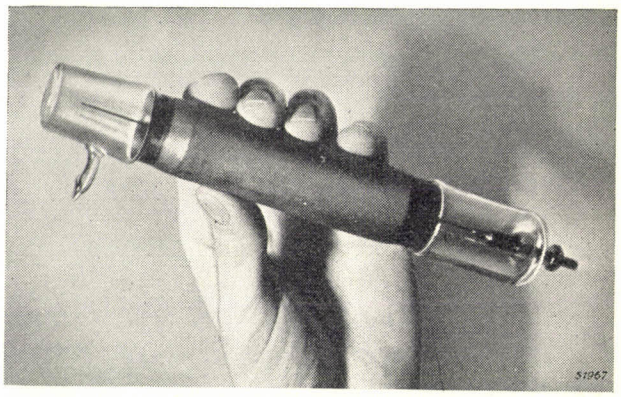


Fig. 5. A Geiger counter tube for X-ray measurements. Along the axis of a cylindrical electrode which forms part of the tube wall, a straight wire electrode is placed. Between these electrodes a high d.c. voltage is applied, the wire acting as the anode.

drawn through points A, B and P; all angles inscribed in this "focusing" circle on the chord joining A and B are equal, and so are the values of angle Θ for all the paths of incident and reflected beams going through A and B. The deviation of the flat specimen from the focusing circle is, within certain limits, not serious, but obviously the specimen must be made to conform as nearly as possible

to the circle, i.e. it must be tangent to the circle in P. Therefore, on moving the Geiger tube (i.e. point B) on the scanning circle C around the axis P, the specimen must rotate around the same axis at half the angular speed of the Geiger tube, thus always maintaining the mirror position between points A and B which is necessary for the osculating condition mentioned above.

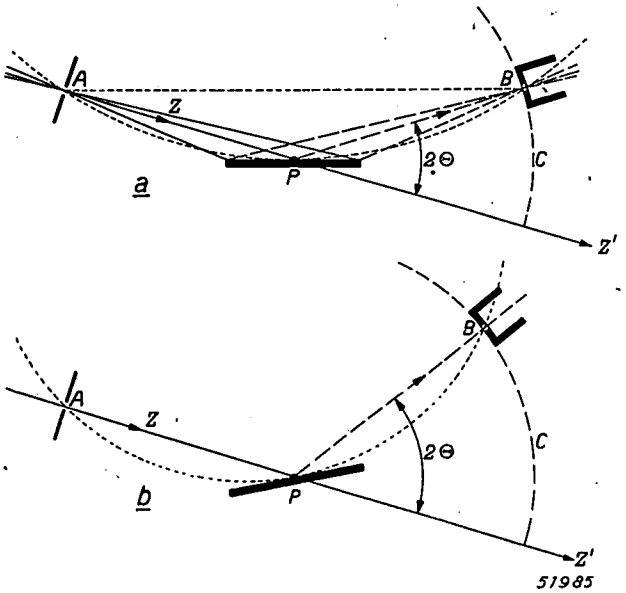


Fig. 6. Focusing arrangment. A divergent X-ray beam Z coming from slit A irradiates the surface of the flat specimen indicated by the heavy line through P. All the rays (dotted lines) diffracted at Bragg angle Θ by suitably oriented crystallites at the surface very nearly converge to a single line, projected at point B. Here the receiving slit of the Geiger counter tube is placed. When the counter tube is moved along the circle C around axis P, in order to scan subsequent angles 2Θ, the flat specimen must rotate around P in such a way that it is always tangent to the focussing circle through A, P, B (compare a and b).

With the conventional non-focusing arrangement with cylindrical specimen, the diffraction lines obtained have a width comparable to the diameter of the specimen. Therefore the specimen (and hence the irradiating pencil of X-rays) must be very narrow in order to obtain sufficient resolution of the lines on the film, although larger specimens and correspondingly wider beams would be desirable for rapid recording of lines. The large flat specimen used in the focusing arrangement receives and reflects about 10 to 20 times as much radiation as the cylindrical specimens used in ordinary photographic technique.

Incidentally, it will be noted that in the focusing arrangement it is presupposed that the diffracted X-rays contributing to the measured intensity originate from suitably oriented crystallites in a very thin specimen layer. A thin specimen can be prepared from most materials by one of several methods. In cases where a fairly thick specimen must be examined, the diffracted energy contributed from crystallites lying at some depth beneath the surface will give rise to a greater line width. This point will be dealt with more extensively in the second article.

The principle outlined in this section, viz. the use of a local radiation detector in a focusing arrangement, is not new. It was developed and applied as early as in 1913 by Bragg [3]), who, however, made use of an ionization chamber as radiation detector. Because of the low sensitivity of this detector and the constant care it requires, the method could not then compete on equal terms with the photographic method and never was used on a large scale. In fact the new impetus given to the method to-day is largely due to the replacement of the ionization chamber by the Geiger counter tube which in the meantime has been developed from a somewhat unfamiliar laboratory instrument, used mainly for cosmic ray experiments, into a rugged and reliable device of utmost sensitivity. The change-over to the Geiger counter was initiated by H. Friedman [4]), who also changed the design of the Geiger tube so as to render it particularly sensitive to the X-rays used for the diffraction measurements. Friedman's ideas were executed in a practical form by the North American Philips Company, Inc., which engineered and produced the spectrometer described in the following section.

General description of the apparatus

The set-up

The set-up of the apparatus is shown in *figs 7* and *8*. The source of the X-ray beam (focal spot of the X-ray tube) and the entrance slit of the Geiger tube are each spaced 13 cm from the specimen axis. The width of slit S_1 controls the divergence of the primary X-ray beam, and may be chosen so that at a Bragg angle of, e.g., $\Theta = 15°$ a 1×2 cm surface of the specimen is irradiated. The Geiger counter

[3]) W. H. Bragg, Proc. Roy. Soc. A **88**, 428-438, 1913. In this paper the arrangement was applied to single crystals; the application to powder specimens was described by Bragg in Proc. Phys. Soc. **33**, 222-224, 1921.

[4]) H. Friedman, Geiger counter spectrometer for industrial research, Electronics, April 1945, p.p. 132-137. This apparatus, showing most of the features incorporated in the present design, was constructed in the Naval Research Laboratory at Washington, D.C. The present design is in part an outgrowth of machines which Friedman also aided in designing, and which were built at an earlier date by North American Philips Co. and widely used during the war for accurately controlling the orientation of quartz oscillator plates; see W. Parrish and S. G. Gordon, Precise angular control of quartz-cutting by X-rays, Amer. Mineralogist **30**, 326-346, 1945. — An independent development of similar ideas appears to have taken place in Germany in the beginning of the war: R. Lindemann and A. Trost, Das Interferenz-Zählrohr als Hilfsmittel der Feinstrukturforschung mit Röntgenstrahlen, Z. Physik **115**, 456-468, 1940.

tube entrance slit S_2 must be narrow in order to obtain a high resolving power for adjacent diffraction lines. On the other hand, more diffracted radiation enters the counter tube, and hence measurements may be speeded up, with a wider slit. As an adequate compromise to cover the ordinary range of requirements, the width of the entrance slit can be adjusted to 0.25, 0.5 or 1.0 mm.

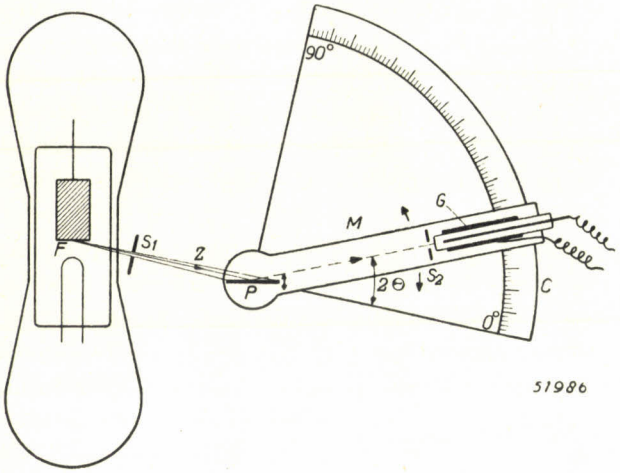


Fig. 7. Set-up of the Geiger counter spectrometer. The divergence of the X-ray beam Z emitted from the small focal spot F is controlled by the slit S_1. Slit S_2 confines the diffracted beam entering the Geiger counter tube G. This tube is mounted on the goniometer arm M and slides along the goniometer circle C which carries a Bragg angle scale from $2\Theta = 0°$ to 90°. The specimen holder P is geared with the goniometer arm M so as to rotate at half the angular speed of the counter tube.

The Geiger counter tube is mounted on a scanning arm pivoted at the specimen axis. The position of the arm corresponds to the angle $2\,\Theta$, i.e. twice the Bragg angle, and is read on a goniometer scale and vernier graduated to 0.01°. The specimen holder is geared with the scanning arm so as to rotate at half the angular speed of the counter in accordance with the focusing condition described above. The mechanism is free of backlash to such a degree that resetting is possible with an accuracy of $\pm$ 0.01°. The exact positioning of the specimen holder and the goniometer scale is accomplished with the aid of a flat single quartz crystal whose surface is cut parallel to a known lattice plane (with precisely known spacing value d).

The focal spot

It has been pointed out above that the focal spot of the X-ray tube acts as the geometric origin of the divergent beam falling on the specimen. A previ-

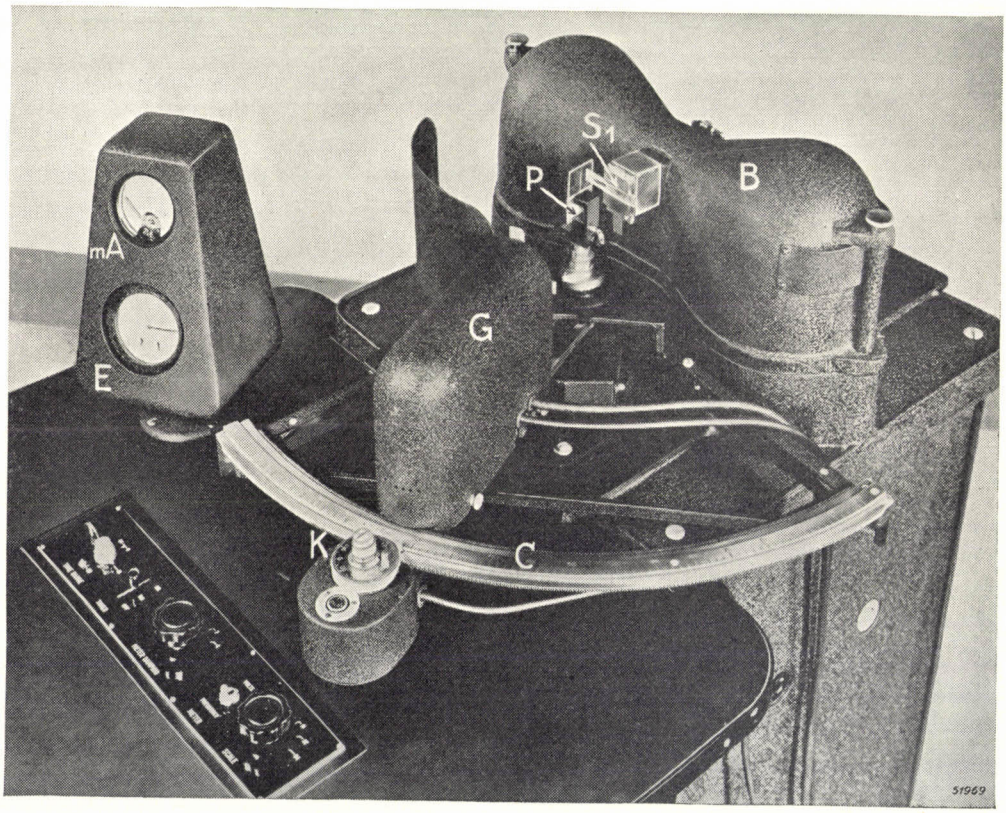


Fig. 8. Photograph of the desk of the Geiger counter spectrometer, showing the arrangement of X-ray tube housing B, slit S_1, specimen holder P, Geiger counter tube housing G and goniometer circle C. K is the vernier knob for moving the counter tube over the goniometer scale; mA and E are the instruments for reading the diffraction intensities, described below.

ously used solution consisted in using as the beam origin a narrow "source slit" irradiated by a large focal spot. Obviously the present solution is more economical with regard to the use of the X-ray energy. In this case very small dimensions of the focal spot are required. The condition of sufficient resolving power for most practical purposes allows a source width of 0.25 mm, while the height of the source, being parallel to the "lines" in the diffraction pattern, can be made comparatively large, e.g. 2.5 mm. These required dimensions apply, however, to the apparent focal spot, i.e. the projection of the focal spot in the direction of the useful beam. The real width of the focal spot can be made much larger by having the useful beam oriented obliquely to the anode surface, resulting in an increase in beam intensity [5]). In our case the intensity is 35 times the value in the direction normal to the anode, as the beam includes the exceptionally small angle of 1.5° with the anode; the real width of the focal spot in this case is 7 mm, the apparent width 0.2 mm (*fig. 9*).

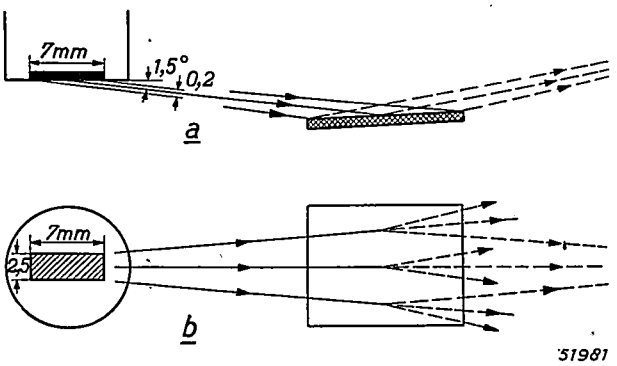


Fig. 9. *a*) The real width of the focal spot is 7 mm, while the "apparent width", due to the very small projection angle of 1.5°, is only 0.2 mm. *b*) The apparent height of the focal spot, being parallel to the diffraction lines (and to the entrance slit of the Geiger counter tube), is equal to the real height, i.e., about 2.5 mm.

As the large height of 2.5 mm for the beam source (focal spot dimensions perpendicular to plane of fig. 7) is only permissible when it is parallel to the diffraction lines, it will be evident that the axis of an X-ray tube of conventional design must lie in the plane traversed by the scanning Geiger tube. Since, for the sake of convenience, the goniometer scale is arranged in a horizontal plane, the X-ray tube must also be mounted horizontally (figs 7 and 8). This entails the limitation of the goniometer scale to an angle $2\Theta = 90°$, as the further movement of the counter tube needed for traversing larger angles is prevented by the X-ray tube housing.

The very small angle between the anode surface and the useful X-ray beam requires extremely careful polishing of the surface, as minute irregularities would otherwise be likely to intercept part of the beam. During the life of X-ray tubes, some roughness of the anode surface is ordinarily produced by the evaporation of material from the hot focal spot. In our case, however, this roughness remains imperceptibly small, owing to the very low specific focal spot loading. In fact, due to the high sensitivity of the detecting device and the large gain in intensity achieved by use of the focusing arrangement, an X-ray tube power as low as 125 W is sufficient. The specific loading of the 2.5 × 7 mm focal spot therefore is only about 7 W/mm², while in high-power water-cooled X-ray tubes specific loads of 60 to 80 W/mm² are quite common.

The X-ray tube

The X-ray tube is fed with a.c. and driven at 35 kV (peak value) and 5 to 6 mA (mean value). The small power of 125 W can easily be dissipated by air cooling instead of requiring the usual water cooling — a very welcome simplification of working conditions. The filament current and tube voltage transformers are supplied by a stabiliser. Moreover, means are provided which correct for drift of the filament current during the warm-up period. These precautions are necessary because the diffraction lines of a pattern are not measured simultaneously but successively; as a consequence, the intensity of the primary X-ray beam must be kept constant during the whole scanning time in order to avoid errors in the relative line intensities.

As is usual in X-ray diffraction practice, the X-ray tube is made readily interchangeable to facilitate the selection of a suitable target material for the focal spot. Tubes with molybdenum, copper or iron target are available at present, yielding the characteristic radiation of these elements at 0.7107, 1.5418 and 1.9273 Å respectively (weighted mean value of $K\alpha_1$ and $K\alpha_2$ lines). Thus for practically all specimens a radiation with sufficiently long wavelength can be used to avoid the excitation in the specimen atoms of their own characteristic radiation (fluorescence), which would increase the undesired background intensity of the diffraction pattern.

Circuit for the intensity measurements

The current pulses produced in the Geiger counter tube by the arriving X-ray quanta are preamplified in two amplifier stages, then in a third stage the pulses are equalized, i.e., they are given a definite shape independent of the duration and intensity of the discharge in the counter tube, which may vary

[5]) See e.g. Philips Techn. Rev. 3, 261, 1938.

to a certain degree. The rate of the production of pulses, which is used as a measure of the X-ray intensity, can be determined in two ways:

a) A mechanical register is provided, similar to those used for registering telephone calls, that is actuated by a relay into which the pulses are fed (*fig. 10*). Because of the inertia of the mechanical register, its resolving power for successive pulses

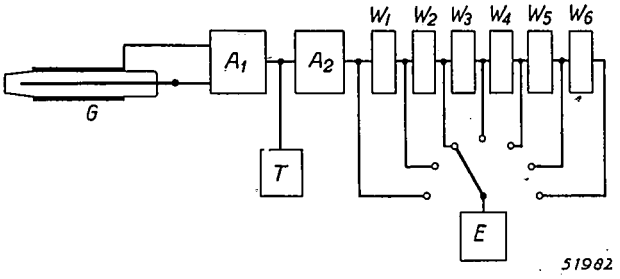


Fig. 10. Schematic circuit for counting the pulses produced in the Geiger counter tube G. The pulses are preamplified in A_1, then once more amplified and equalized in A_2, and counted by the electromechanical register E (cf. also fig. 8). At pulse rates greater than about 60 per second, the pulses are scaled down by a number of scale-of-two circuits $W_1 \ldots W_6$, allowing a maximum scaling down factor of 64. The counting interval is controlled by the timer T.

is limited to about 60 counts per second. In order to profit by the much higher resolving power of the Geiger tube itself (several thousand pulses per second), a scaling circuit is inserted between the tube and the counting system. This well-known device consists of a number of scale-of-two (flip-flop) circuits connected in series. Every one of these scale-of-two circuits[6]) essentially contains two twin-triodes connected in such a way that only one of the two can be in a conducting state at a time, while an arriving pulse of a given polarity causes both tubes to change their state; therefore, in the output of the circuit only one pulse (of a given polarity) occurs for every two pulses arriving at the input. In our case, six such units are provided. The output of the last scaler unit actuates a relay-tube which passes the impulses on to the register.

For the measurement of high intensities the full scaling down factor of $2^6 = 64$ is used; for smaller intensities intermediate factors can be chosen by omitting a number of the scale-of-two units. Often it will be sufficient to count the pulses received during a period of half a minute or so. The time period over which the counter will operate is controlled by a timer, cutting off the pulse output between timing intervals and allowing for a continuously variable setting up to 64 sec. The settings of 64, 32 and 16 seconds are marked, as with these settings the number of counts registered is directly equal to the number of counts per second when using 6, 5, or 4 scaling-down units respectively.

b) The rate of arrival of quanta can also be determined by measuring the mean value of the current flowing at the amplifier output. This current is used to charge a condenser C shunted by a resistor R (*fig. 11*). The voltage rise on C within certain limits is proportional to the number of pulses per second, all pulses yielding identical contributions owing to the equalization stage mentioned above and to proper design of the circuit (such that the voltage rise for each pulse is approximately independent of the voltage already attained on C). The leakage current through R being proportional to the voltage on C, a milliammeter connected in series with R indicates directly the X-ray intensity entering the Geiger tube.

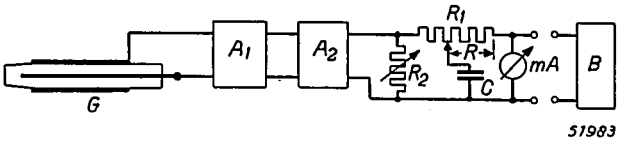


Fig. 11. Circuit for measuring the mean value of the current flowing through the Geiger tube. The amplified and equalized pulses are fed to a condenser C (the resistor R_2 serves for amplitude adjustment), whose voltage rises approximately in proportion to the number of pulses per second. This voltage is measured by the leakage current flowing through the adjustable part R of the resistor R_1 and is read off the milliammeter mA (cf. fig. 8), whose deflection can also be recorded by a separate strip chart recorder B.

The deflection of the milliammeter can be recorded continuously by a separate strip chart recorder (*fig. 12*), while the Geiger tube is moving along the goniometer scale. To effect the movement of the Geiger counter, a small synchronous motor is used. The chart in the recorder also being driven by a synchronous motor, a definite relationship is established between the abscissae of the chart and the Bragg angles, and the recorded curve immediately represents the intensity distribution in the diffraction pattern (*fig. 13*). The time for scanning 90 degrees can be varied between 6 hours and 45 minutes. For this purpose an interchangeable series of motors is provided, the one desired being connected to the vernier knob effecting the movement of the goniometer arm. (This is a simpler solution than a single stationary motor with controllable gear wheel drive.)

The intensity indicated by the milliammeter is a mean value, averaged over a time which depends on the product RC of the circuit described above

[6]) The first device of this kind, using thyratrons, was developed by C. E. Wynn-Williams: A thyratron "scale-of-two" automatic counter, Proc. Roy. Soc. A **136**, 312-324, 1932. A modern and widely adopted counting system is described by H. Lifschutz, A complete Geiger-Müller counter system, Rev. Sci. Instr. **10**, 21-26, 1939.

(fig. 11). A point of major importance in all work with Geiger counter tubes, and which will be considered in greater detail in the second article that is to appear subsequently, is the random time distribution of the X-ray quanta absorbed in the counter tube. The ensuing current intensity fluctuations would tend to render the position of a rate of e.g. 2 degrees/minute, will be desirable; a time constant of 2 seconds is suitable for this purpose. If subsequently the spectrum is more accurately scanned, e.g. at 0.25 degree/minute, the time constant may be set to say 5 seconds.

Finally, it may be mentioned that a test multivibrator is incorporated, delivering pulses at a

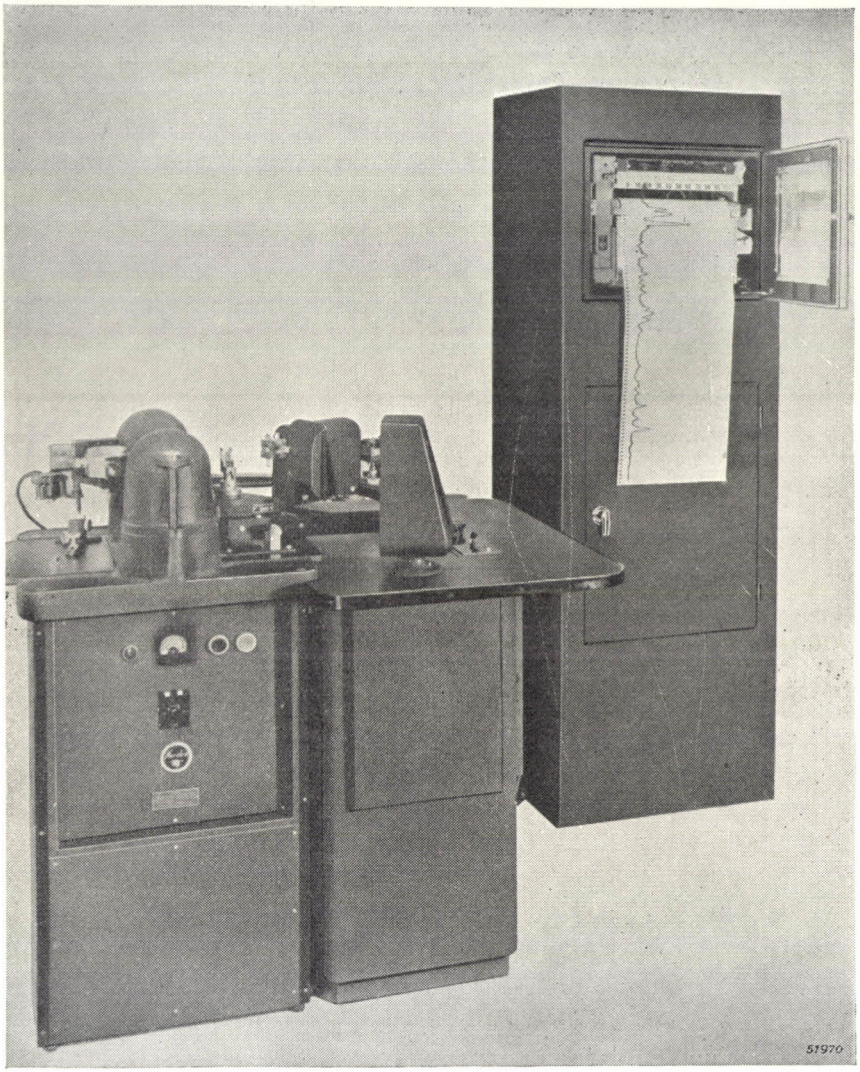


Fig. 12. The Geiger counter spectrometer with strip chart recorder.

line peak indefinite if at a given scanning speed the averaging time (time constant) is made too short. On the other hand, if one adopts a very large time constant, it is evident that two closely adjacent diffraction lines will not be resolved because the averaging time will cover the time of traversing both lines. With a view to adapting the time constant to the scanning speed (and slit width) actually chosen, an adjustment by a suitable choice of the resistance R is provided. For many purposes a preliminary rapid scanning of the spectrum, at a fixed, known frequency and which, substituted for the Geiger counter tube, is used to check the functioning of both intensity measuring devices.

Adaptation of the Geiger counter tube to the diffraction measurements

To obtain the greatest possible sensitivity the Geiger counter ought to deliver a discharge pulse for every single X-ray quantum entering the receiving slit. With the design of the counter devel-

oped by H. Friedman [7]) this ideal is approached very closely. *Fig. 14,* representing a modified construction incorporated in most of the spectrometer units at present in use, shows the essential features of the design (cf. also fig. 5). The X-ray beam enters the tube at one end through a window of Lindemann glass, which is highly transparent for X-rays. This window, being 250 microns thick, transmits about 75% of the radiation with wavelength 1.5 Å (Kα-radiation of a copper target [8])). The beam then travels through the whole length of the tube more or less parallel to the central wire anode, at a distance of a few mm from this wire. It is essential for the beam to be absorbed as completely as possible in the gas filling of the counter tube, and not to strike the central wire nor the surrounding cylindrical cathode. A photo-electron is easily produced in the gas and almost certainly will trigger a discharge, while only a small number of photo-electrons would be liberated from the electrode metal and these would have a high probability of vanishing in the metal or elsewerhe (see below) without being counted.

The tube is in most cases filled with argon, which strongly absorbs the characteristic radiation of copper or iron targets (*fig. 15*). If a molybdenum target is used, a Geiger counter tube filled with krypton is better suited.

With an argon pressure of 30 cm Hg, 42% of the quanta of 1.5 Å wavelength entering the tube give rise to a discharge. Taking into account the absorption of the window, it is seen that an over-all efficiency of the counter of about 30% is achieved (percentage of quanta arriving at the tube window which is counted), a very high value indeed compared to the values of only a few percent obtained with former types of counter tubes.

During the past year still higher efficiencies have been attained by means of a counter tube provided with a mica window instead of the

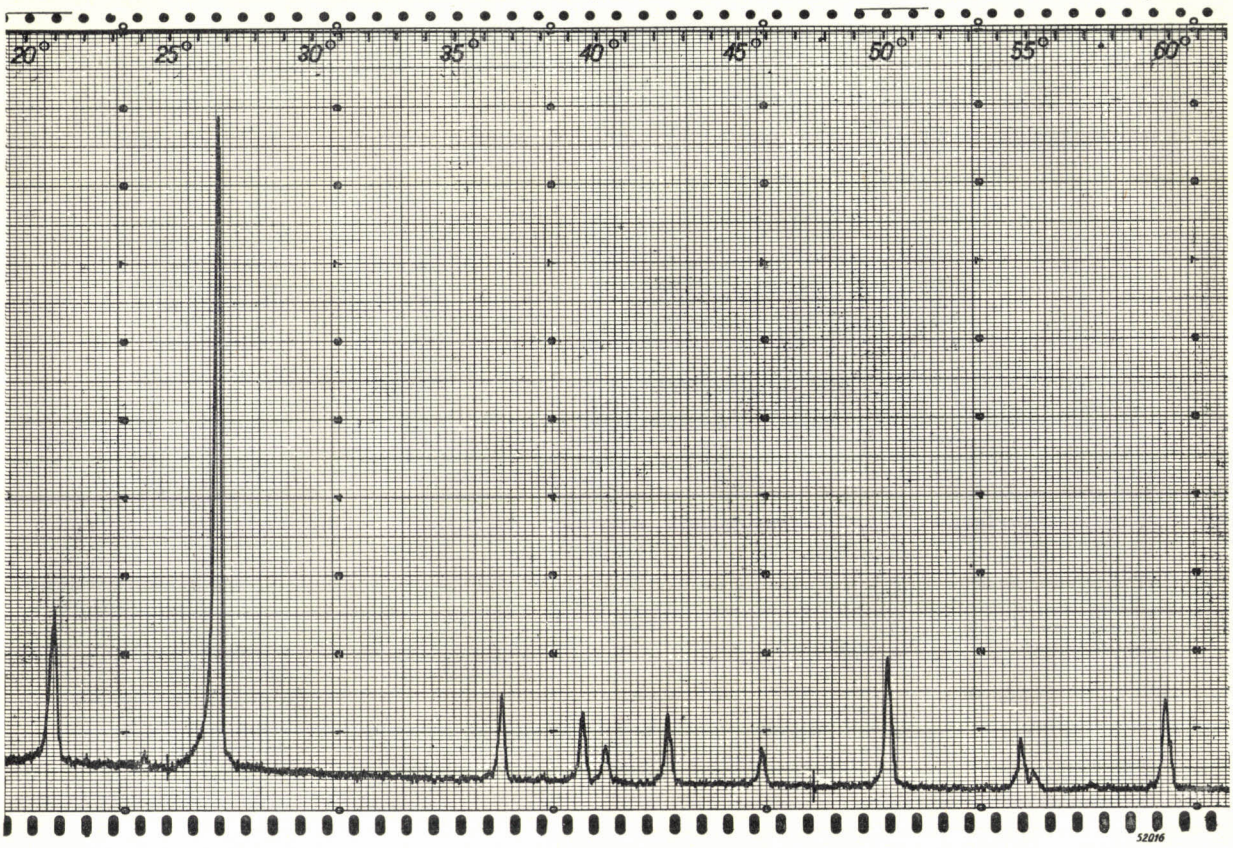


Fig. 13. Example of a diffraction pattern recorded with the Geiger counter spectrometer. The curve shows immediately the relative line intensities as a function of the Bragg angle (2Θ). (The section of the spectrum shown here was recorded in appr. 3 hours.)

[7]) H. Friedman, l.c. and U.S. Pat. 2386785.

[8]) The other components (Kβ-lines) of the copper radiation and part of the "white radiation", which produce a background and diffraction spectra of their own and whose superposition on the desired spectrum would cause serious errors, are eliminated by means of a thin nickel filter placed before the window.

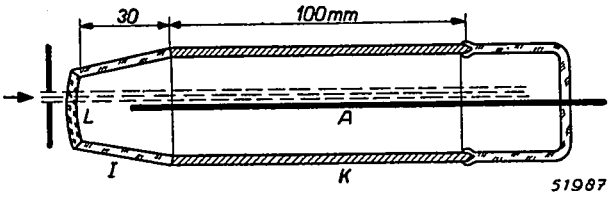


Fig. 14. Geiger counter tube for X-ray intensity measurements (longitudinal cross section of the tube shown in fig. 5). The X-ray beam enters the tube in a longitudinal direction and travels through it a short distance from and more or less parallel to the wire anode *A*. The entrance window *L* is made of Lindemann glass, sealed to the chrome iron cathode cylinder *K* via a short cylinder of soft glass *I*. The tube, if used for the measurement of copper or iron radiation, is filled with argon at a pressure of about 30 cm Hg and contains a small amount of an organic quenching vapor.

window of Lindemann glass. A tube of this type is shown in *fig. 16*. The mica window, having a thickness of only 12 microns, is sealed vacuum-tight to the chrome-iron cathode cylinder by a newly developed technique [9]). It transmits 86% of the incident copper *Kα*-radiation. Moreover, with this type of tube there is hardly any "dead space" between the window and the active counting volume. In the Lindemann window type of tube, the window could not be sealed directly to this metal cylinder; therefore, a short cylinder of soft glass was used as an intermediary (cf. figs 5 and 14). As the absorption of the X-rays in the gas is useful only when it takes place in the section within the cathode cylinder, the intermediate glass section entailed the existence of an inactive column of gas about 3 cm long, preceding the active column. Owing to the avoidance of this dead space in the mica window tubes, 55% of the entering quanta give rise to a discharge. Thus the over-all efficiency is increased to 0.86 × 0.55 = about 50%, for the copper radiation.

The increase in efficiency is even more pronounced in the case of iron radiation, which is rather strongly absorbed in the Lindemann glass windows formerly used. Thus, measurements with iron radiation are considerably speeded up when using the mica window Geiger counter; still higher speed will be achieved when this counter tube is used in conjunction with an X-ray tube similarly provided with a mica window for the emerging X-rays.

As a consequence of the dead space in the Lindemann window tubes, the efficiency of these tubes exhibits an optimum at a definite gas pressure. Since the absorption by the gas increases with increasing gas pressure, a high pressure favors the complete absorption of the entering X-ray quanta in the tube — but then most of them are absorbed in the first, inactive part of the tube. With very low pressure, absorption in this part of the tube is negligible, but then the absorption in the useful part of the gas column also is far from complete and a considerable part of the quanta will pass through to the other end of the tube uncounted. Evidently, an optimum must exist at an intermediate pressure. The argon pressure actually chosen, about 30 cm Hg as mentioned above, is near the optimum.

With the mica window type of tube, in which practically no dead space with undesired absorption occurs, a higher argon pressure would be permissible, yielding a higher efficiency. However, a limit to the permissible increase of the pressure is set by the increase of the voltage which must be applied between the electrodes. We shall later return briefly to this point.

When the intensity of the X-ray beam is very high, the quanta enter the tube at such a rate that the time interval between some of them will be shorter than the "dead time" of the counter tube, i.e., the time necessary for the restoration of tube conditions necessary to ensure a response to a succeeding absorbed quantum. In this case not all

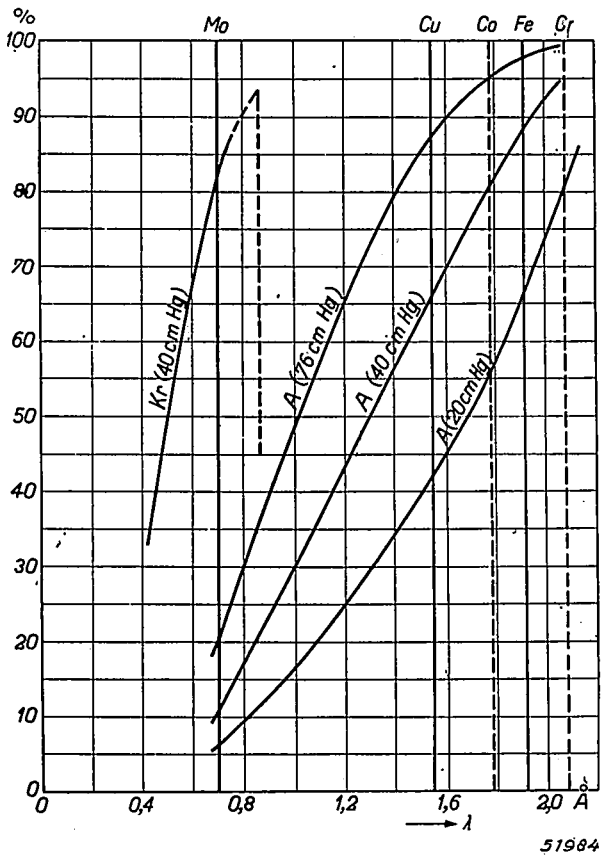


Fig. 15. Absorption of a column of 10 cm of argon (A) or krypton (Kr) for X-rays of different wavelengths, at different pressures. The characteristic radiation of copper (Cu $K\alpha$ = 1.5418 Å), is strongly absorbed by argon, as well as that of iron (1.9373 Å), chromium, cobalt. For the radiation of molybdenum (0.7107 Å), the argon filled Geiger tube is not effective and must be replaced by one filled with krypton. (The absorption edge, where the absorption suddenly becomes small with increasing wavelength, lies at 0.86 Å for krypton, at 3.87 Å for argon).

[9]) The technique is similar to the one described by J. S. Donal Jr. in Rev. Sci. Instr. **13**, 266, 1942; cf. also L. Malter, R. L. Jepsen and L. R. Blom, R. C. A. Review **7**, 623, 1946 (December).

absorbed quanta give rise to separate counts. Such counting losses, causing a non-linear response of the counting system to variations in X-ray intensity, affect the efficiency of the counter tube unfavorably and ultimately set a limit to the permissible intensity of the diffracted X-ray beam. In view of this undesirable limitation, measures are taken to make the dead time very short. A well-known and effective means is the addition of a small amount of an organic vapor to the gas. By a mechanism of a rather complex nature which is not yet completely understood, the vapor tends to reduce the number of charged particles available for maintaining the discharge so that it is rapidly quenched. Formerly, alcohol was generally used as a quenching component. This, however, had the drawback of being soon decomposed by the process in which it was involved. To-day other compounds are used, e.g., methylene bromide, which is more stable and equally efficient; thus, the life of a Geiger counter tube in constant use may amount to many months or even several years (the total number of counts performed amounting to the order of 10^9), while the tubes lasted for at most a few months with the argon-alcohol filling. The quenching speed is such that up to 600 absorbed quanta per second may be counted without appreciable loss. However, counting is still possible at rates up to 3000 counts/second (taking into account the non-linearity correction). This corresponds to a beam intensity of approximately 10^4 quanta per second arriving at the tube window (on the basis of a 30% overall counting efficiency). Since each quantum of the copper radiation at 1.5 Å represents an energy of approximately 10^{-8} erg, the permissible beam intensity is about 10^{-4} erg/sec. If necessary, the intensity can be kept within this limit by reducing the height of the primary beam divergence slit and the Geiger tube entrance slit, which is controllable between 1 and 6 mm by means of two horizontal wedge-shaped diaphragms.

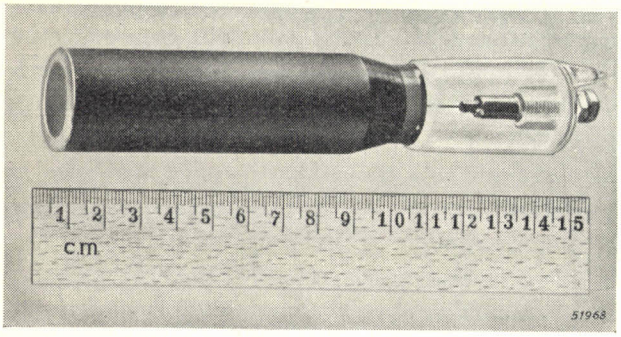


Fig. 16. Geiger counter tube, similar to that in figs 5 and 14, but provided with a mica window. The window is 12 microns thick and is sealed vacuum-tight to the chrome iron cathode cylinder. The axial anode wire, which nearly touches the window, carries a glass bead at its end, in view of the high field strength occurring at this point.

In connection with the last remark it is interesting to note that the intensity recorded by the counter tube does not vary linearly with the entrance slit height. This is due to the fact that in the outer part of the cylindrical gas column, near the wall, the field strength is much less than near the wire anode in the centre. The quenching vapor, trapping electrons as it is intended to do, eliminates many of the primary photo-electrons in the outer part of the tube which ought otherwise to produce a discharge pulse, while photo-electrons produced near the wire are accelerated rapidly enough to escape being passively absorbed. Thus there exists in the gas column a cylindrical "active volume", located around the anode wire. With the present type of counter tube at 3 mm from the wire the probability of an electron triggering a discharge is reduced to one half of the value at 1 mm.

We conclude this section with a few remarks on the voltage applied to the Geiger counter tube. This voltage should be chosen well up on the "plateau" of the counter tube, i.e. the voltage region where the desired intense short pulses with amplitude nearly independent of voltage can be obtained. Thus the functioning of the tube is made as nearly as possible independent of the voltage supply. On the other hand it is desirable to choose the voltage at the low voltage end of the "plateau", because during the life of the tube the plateau gradually shrinks at the high voltage end (and extends to lower voltages). This is due to the gradual disappearance of the quenching vapor. In our case a voltage of about 1400 V is applied, which at the argon pressure of 30 cm Hg (upper and lower limits of the plateau depend also on the gas pressure) is a suitable compromise.

The use of the Geiger counter spectrometer

As the results obtainable with the spectrometer will be treated in a separate article, only a very brief survey is given here.

The peaks of diffraction lines can usually be located on spectrometer charts with an error no greater than $\pm$ 0.02°. This compares very favorably with the error of $\pm$ 0.1° generally inherent in photographic diffraction measurements. The resolving power likewise is beyond that attainable in the common photographic procedure. Usually the resolution of two diffraction lines obtained from one

lattice plane (spacing value d) with two slightly different wavelengths, e.g. Cu $K\alpha_1$ and $K\alpha_2$ (1.54050 and 1.54434 Å), is given as a criterion. From the Bragg equation it is easily seen that the angle difference for two such lines increases with angle Θ (diminishing d). On spectrometer recordings Cu $K\alpha_1$ and $K\alpha_2$ are clearly distinguishable even at $\Theta = 30°$ and completely resolved at $\Theta = 40°$, while on a film taken with a conventional powder camera (114 mm diameter) resolution of these lines starts only at $\Theta =$ about 50° and complete resolution is not obtained before $\Theta =$ about 60°.

One of the outstanding features of the new instrument is the ease with which quantitative measurements of relative line intensities are obtained. In the photographic procedure these measurements are rather difficult and time consuming because of their sensitivity to the exposure and developing conditions of the film and because of the necessary recording with a microphotometer. The advantage of the Geiger counter spectrometer becomes especially apparent if the position of the lines we are interested in is already known from a photographic diffraction pattern, whereupon the intensities of these lines can be accurately determined by scanning with the counter tube only those limited portions of the spectrum containing the lines under consideration. The time saving achieved in such cases can be quite spectacular.

A further advantage of the Geiger counter spectrometer as compared with the photographic method is the weaker and more evenly distributed background of the spectrum, which improves the possibility of measuring very weak lines and makes feasible the measurement of lines at very low Bragg angles (spacing values up to 150 Å). These points will be discussed more fully in the second article.

As to other specific applications of the spectrometer, it is evident that the use of a local radiation detector is ideally suited for experiments in which one or two diffraction lines must be continuously observed, e.g., the investigation of phase changes in a specimen. In such investigations it is also an important feature that, with the spectrometer, heating or cooling of the specimen is possible in a simple way without danger to the measuring device, and that, furthermore, the specimen is freely accessible for adjustments during the measurements. (Since of course the operator must not be exposed to the X-rays when making such adjustments, a shutter is incorporated which automatically cuts off the primary beam when the operator lifts the barrier flag located before the specimen.)

Finally, attention may be drawn to the fact that the charts obtained with the spectrometer offer no indication as to whether the intensity along a diffraction line is uniform or not. Therefore, special precautions are required in the preparation of the flat specimen in order to avoid a preferred orientation of the crystallites (texture) which would give rise to a non-uniform intensity distribution and thereby introduce errors into the intensity measurements.

ELECTROMAGNETIC WAVES IN WAVE GUIDES

by W. OPECHOWSKI.

538.566.5:621.392.26

PART I. GENERAL THEORETICAL PRINCIPLES; RECTANGULAR WAVE GUIDES.

In the domain of microwaves the ideas commonly held in regard to the theory of resonant circuits and transmission lines are limited in validity. A rigorous theory of the electromagnetic phenomena must therefore, in this field, be based directly upon the fundamental equations of the Maxwell theory. It is in this manner that the present article deals with the propagation of electromagnetic waves in what are called wave guides, *i.e.* long metal tubes as used in high-frequency technique for transmitting electromagnetic energy over short distances (*e.g.* inside an apparatus). In Part I the theory of rectangular wave guides is explained (in Part II, which will be published later, circular wave guides will be discussed). As an introduction the properties of plane electromagnetic waves in an unbounded conducting medium are dealt with and the methods for solving the basic equations of the Maxwell theory are summarized.

Resonant circuits employed in the range of decimeter and centimeter waves (microwaves) have been extensively discussed in a series of articles already published in this journal [1] [2] [3] [4]. The last two articles particularly discussed the theoretical principles and practical applications of electromagnetic cavity resonators, dealing with the theory of cavity resonators mainly by means of a suitable generalization of concepts such as "capacitance", "self-inductance" and "impedance" with which we are familiar in the range of lower frequencies. We have said "mainly", for other problems also arose which could not be dealt with in this manner and in those cases it could only be stated what results are obtained by a direct solution of the Maxwell equations. As is known, these equations form the theoretical basis of all electromagnetic phenomena (excepting of course atomic structure of the charge and radiation as manifested in the existence of electrons and photons).

It is not surprising that when dealing with very high frequencies one is often at a loss to know what is to be understood by the concepts mentioned, for even the possibility of introducing these concepts, starting from the fundamentals of the Maxwell theory, arose from the very fact that one's interest was consciously limited to not too rapidly alternating electric currents and electromagnetic fields. Thanks to this limitation it became possible with the aid of these concepts to work out a theory of resonant circuits and transmission lines for this range. The great advantage of this theory is that it can be further applied with hardly any reference to the Maxwell equations, which are unnecessarily general for a description of the low frequency phenomena. That the equations of this theory are also for very high frequencies (let us say $\nu > 10^9$ c/s) in certain cases equivalent to the Maxwell equations is essentially due to the fact that the concept of electric (conduction) current holds for any frequency, since current is a quantity that occurs also in the Maxwell equations. In an imaginary strange world where exclusively high-frequency electromagnetic phenomena existed one would presumably not immediately have felt any call for introducing such concepts as capacitance and self-inductance.

The only generally valid manner of approaching the problems arising in the domain of very high frequencies is, therefore, to start directly from the basic equations of the Maxwell theory. By this we do not mean to say that it can never be desirable to follow some roundabout way that may be available via the range of lower frequencies with their specific concepts. On the contrary, firstly, because for anyone better acquainted with these concepts than with the Maxwell equations such can hardly constitute a roundabout method, and secondly because extension of the terminology of resonant circuits and transmission lines to the range of microwaves leads to a more uniform language, which in itself may be useful. As a matter of fact in this journal wide use will be made of the "language" of resonant circuits and transmission

[1] C. G. A. von Lindern and G. de Vries, Resonant circuits for very high frequencies, Philips Techn. Rev. **6**, 217-224, 1941.
[2] C. G. A. von Lindern and G. de Vries, Lecher systems, Philips Technical Rev. **6**, 240-249, 1941.
[3] C. G. A. von Lindern and G. de Vries, Flat cavities as electrical resonators, Philips Techn. Rev. **8**, 149-160, 1946 (No. 5).
[4] G. de Vries, Electromagnetic cavity resonators, Philips Techn. Rev. **9**, 73-84, 1947 (No. 3).

lines when discussing a device which for high frequencies performs a function of no less importance than the cavity resonator. We refer to the "wave guides", serving to convey electromagnetic energy within a transmitting or receiving apparatus from one point to another. Wave guides are long metal tubes which may be, for instance, rectangular, circular or elliptical in cross section and through which electromagnetic waves can be propagated. Governing the whole of the high-frequency technique is the phenomenon that owing to skin effect the current flows only in a thin surface layer of a conductor and scarcely does anything more than dissipate energy. Consequently the energy transmission takes place substantially not in the conductor but by means of an electromagnetic wave around the conductor or, as in the case of wave guides, inside a space bounded by conductors. The function of the conductors is merely to mark out, as it were, the path for the wave.

In this article we shall study the propagation of electromagnetic waves in cases where conductors are present (particularly in wave guides), starting from the basic equations of the Maxwell theory. We shall only incidentally consider in how far the same results could be deduced by an extension of the concepts commonly used for low frequencies; the question where the limits of such an extension lie has been sufficiently dealt with in the articles already quoted [5]). Neither shall we enter into the engineering aspect of wave guides, this being reserved for other articles to be subsequently published in this journal. Of course we shall not omit to bring forward whatever may be of particular technical importance. In the following section a summary is given of the general mathematical formulation of the fundamentals of the Maxwell theory. The actual subject of the present article begins with the next section on plane waves.

Basic equations of the Maxwell theory

In the Maxwell theory the electromagnetic phenomena are described with the aid of two kinds of quantities, one relating to the electric charges at rest and in motion, the other relating to the electromagnetic field.

As a rule two quantities suffice to describe the behaviour of the electric charges: the charge density ϱ, *i.e.* the amount of charge per unit volume, and the current density **J**, *i.e.* the amount of charge which per unit time passes a unit surface perpendicular to the direction of motion; by printing **J** in heavy type we indicate that it is a vector. The quantities ϱ and **J** are not independent of each other, for when we consider a volume τ containing electric charges and enveloped by a closed surface S then, in virtue of the law of conservation of the charge, the following equation must hold:

$$\oint\oint J_n \, dS = -\frac{d}{dt}\iiint \varrho \, d\tau, \quad \ldots\ldots \quad (I)$$

where t is the time and J_n the component of **J** along the normal to the surface at the point considered on the surface; as positive direction of the normal the direction outwards is chosen (we shall consistently keep to this latter convention in this article). The integral on the left means that the surface S has to be divided into infinitesimal elements dS, the product $J_n \cdot dS$ then having to be found for each element and all these products added up. The small circles remind us that S is a closed surface.

The electromagnetic field is usually characterized by four vectors whose physical significance is here assumed to be known: the electric field strength **E**, the magnetic field strength **H**, the magnetic induction **B** and the electric displacement **D**. The essence of the Maxwell theory is now comprised in two equations correlating **E** and **B** respectively **H** and **D**.

One equation reads as follows:

$$\oint E_l \, dl = -\frac{d}{dt}\iint B_n \, dS \ldots\ldots\ldots \quad (II)$$

Here the integral on the right extends over an arbitrary surface S bounded by the closed curve (contour) l along which the integral on the left has been taken; the curve l is as a matter of fact an arbitrary curve. B_n is the component of **B** at the point considered on the surface S in a direction perpendicular to the surface. The meaning of the integral on the right is analogous to that of the integral of the left-hand side of eq. (I) except that there the surface was closed. E_l is the component of **E** at the point considered on the curve l along the tangent at that point. The meaning of the "line integral" of the left-hand side of eq. (II) — where the circle indicates that l is a closed curve — is roughly speaking as follows: the curve l is divided into infinitesimal elements dl; the product $E_l \cdot dl$ is found for each element and all these products are added up. The minus sign in eq. (II) is necessary to conform to what has been agreed upon concerning the positive directions of the normal to the surface and of the tangent to the curve; in this article we shall follow consistently the "corkscrew rule", well known from the text books (*fig. 1*).

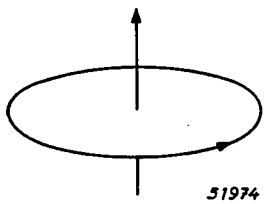


Fig. 1. The relation between the positive direction along a contour and the positive direction of the normal of the surface bounded by this contour, according to the usual convention ("corkscrew rule").

Eq. (II) gives expression to Faraday's law of induction. If we imagine the curve l to be formed by a wire then the integral on the left-hand side of the equation represents the e.m.f. induced in the wire by the variation of the magnetic flux $\iint B_n dS$; the validity of eq. (II) however is postulated in the Maxwell theory also for vacuum, that is to say also in the

[5]) See particularly pp. 222-223 of the article quoted in footnote 1 and pp. 78-79 of the article quoted in footnote 4.

absence of any conductor that makes the contour l as it were tangible. If, as is usual in electrotechnics, the e.m.f. is to be expressed in volts and we agree to measure length in metres and time in seconds, then from eq. (II) it immediately follows that the unit of **E** is volt/m and that of **B** volt · sec/m².

The other fundamental equation of the Maxwell theory is:

$$\oint H_l \, dl = \iint J_n \, dS + \frac{d}{dt} \iint D_n \, dS \quad . \quad . \quad . \quad \text{(III)}$$

Here again on the right-hand side we have an integration over an arbitrary surface bounded by an also arbitrary contour along which the integral on the left has been taken. The meaning of the symbols is analogous to that of the symbols in eq. (II). Supposing for a moment that **D** is independent of time, then the second term on the right in eq. (III) is zero. The equation then gives expression to the well-known fact that the "magnetomotive force", *i.e.* the line integral of the left-hand side measured along a curve enclosing a conductor (*e.g.* a wire), is equal to the total current intensity flowing in the conductor. The second term on the right in eq. (III) represents the so-called displacement current introduced by Maxwell in his theory. The necessity of introducing such a term can be illustrated with all kinds of examples, which we shall not enter upon here. We would observe however that if the displacement current were to be omitted from equation (III) we should be acting contrary to the law of the conservation of charge (eq. (I)).

Expressing the total current intensity in amperes — again in accordance with technical usage — and measuring length in metres and time in seconds in the same way as before, it follows from eq. (III) that the unit of **H** is amp/m and that of **D** amp · sec/m².

From equations (I), (II) and (III) it can further be immediately deduced that:

$$\oint\oint B_n \, dS = \text{constant},$$

$$\oint\oint D_n \, dS - \iiint \varrho \, d\tau = \text{constant}.$$

The physical significance of these equations leads to the conclusion that the constants on the right-hand side of the two equations have to be put equal to zero (think, in particular, of magnetostatics and electrostatics!). Hence:

$$\oint\oint B_n \, dS = 0, \quad . \quad . \quad . \quad . \quad . \quad . \quad . \quad . \quad \text{(IV)}$$

$$\oint\oint D_n \, dS = \iiint \varrho \, d\tau \quad . \quad . \quad . \quad . \quad . \quad \text{(V)}$$

Equations (IV) and (V) thus fulfil the function of supplementary conditions which **B** and **D** have to satisfy.

The two basic equations (II) and (III) of the Maxwell theory are absolutely general, in the sense that nothing is assumed in regard to the electromagnetic properties of the medium. They are not, however, sufficient to determine the five quantities **E**, **B**, **H**, **D** and **J**. They only give a relation between **E** and **B** (eq. (II)) and between **H**, **D** and **J** (eq. (III)) but say nothing about the relation of **E** and **B** on the one hand to **H**, **D** and **J** on the other hand. It is in the nature of the latter relation that the electromagnetic properties of the medium find expression, that is to say, as a rule this relation differs according to the medium in which the electromagnetic field may be present. For homogeneous, isotropic media the following relations mostly [6]) hold with sufficient approximation:

$$\mathbf{D} = \varepsilon \mathbf{E}, \quad . \quad . \quad . \quad . \quad . \quad . \quad . \quad . \quad \text{(VI)}$$

$$\mathbf{B} = \mu \mathbf{H}, \quad . \quad . \quad . \quad . \quad . \quad . \quad . \quad . \quad \text{(VII)}$$

$$\mathbf{J} = \sigma \mathbf{E}, \quad . \quad . \quad . \quad . \quad . \quad . \quad . \quad . \quad \text{(VIII)}$$

in which the dielectric constant ε, the magnetic permeability μ and the specific conductivity σ are constants depending upon the nature of the medium. The units in which these three constants are expressed follow immediately from the units chosen above for **D**, **E**, **B**, **H** and **J**. The unit of ε is amp·sec·volt^{-1}·m^{-1} or (definition of coulomb) coulomb·volt^{-1}·m^{-1} or (definition of farad) farad·m^{-1}, that of μ is volt·amp^{-1}·sec·m^{-1} or (definition of henry) henry·m^{-1} and that of σ is amp·volt^{-1}·m^{-1} or (definition of ohm) ohm^{-1}·m^{-1}.

Substituting in the equations (II) and (III) the expressions (VI, VII, VIII) for the quantities **D**, **B** and **J**, we obtain two equations between the quantities **E** and **H** (eqs. (1) and (2) below) which will form the basis of what follows in this article. By performing the same substitution in (IV) and (V) we obtain two supplementary equations (eqs. (3) and (4) below).

In the foregoing we have used the terms volt and ampere without any further definition; the other electromagnetic units have been defined with the aid of volt, ampere, metre (as length unit) and second (as time unit). By expressing all quantities in volts, amperes and the units derived therefrom in the manner indicated above we have introduced the so-called rationalized Giorgi system of electromagnetic units. The Giorgi system will be discussed separately in two articles that will appear shortly in this journal, when the definition of volt and ampere will be given. Here we shall only mention that the magnetic permeability of vacuum in this system has the value:

$$\mu_0 = \frac{4\pi}{10^7} \frac{\text{henry}}{\text{metre}} \quad . \quad . \quad . \quad . \quad . \quad . \quad . \quad . \quad \text{(IX)}$$

From (IX) and a relation which we shall deduce later, *viz.* eq. (16), it follows that the value of the dielectric constant ε_0 of vacuum is:

$$\varepsilon_0 = \frac{10^7}{4\pi c^2} \frac{\text{farad}}{\text{meter}}, \quad . \quad . \quad . \quad . \quad . \quad . \quad . \quad . \quad \text{(X)}$$

in which c indicates the numerical value of the velocity of light in m/sec.

Plane waves in an unbounded conducting medium

We shall first apply the fundamental equations of the Maxwell theory to the case of an unbounded, homogeneous and isotropic medium, which is thus characterized by given, constant values of ε, μ and σ. (These constants may still be functions of the frequency of the electromagnetic waves considered.)

In fact such a case does not occur in practice, but it will serve as starting point for the investigation of wave guides. Moreover, already in this case we shall obtain certain results not without interest for the interpretation of technically important facts. The equations for the electric and magnetic field strengths **E** and **H** then assume the following form:

$$\oint E_l \, dl = -\mu \frac{d}{dt} \iint H_n \, dS, \quad . \quad . \quad . \quad . \quad \text{(1)}$$

[6]) We say "mostly" because for ferromagnetic media (particularly iron) equation (VII) no longer applies, and for substances showing the Hall effect (VIII) is no longer correct.

$$\oint H_l \, \mathrm{d}l = \sigma \iint E_n \, \mathrm{d}S + \varepsilon \frac{\mathrm{d}}{\mathrm{d}t} \iint E_n \, dS; \quad . \quad (2)$$

to which are to be added the two conditions which the solutions of (1) and (2) have to satisfy:

$$\oint \oint H_n \, \mathrm{d}S = 0, \quad . \quad . \quad . \quad . \quad . \quad (3)$$

$$\varepsilon \oint \oint E_n \, \mathrm{d}S = \iiint \varrho \, \mathrm{d}\tau . \quad . \quad . \quad (4)$$

Here it is assumed that all quantities are expressed in units of the rationalized Giorgi sytems. The notation employed has been explained in the preceding section.

By choosing suitable integration contours and surfaces we shall be able to deduce differential equations valid for such a medium. We shall confine ourselves to the particular case where **E** and **H** depend only upon one coordinate, for instance z, of a rectangular system of coordinates, and the time. This suffices for our purpose, for what we want to show is that a plane wave propagated in any direction is a solution of the fundamental equations (1) and (2), after which we shall investigate the properties of such a wave; here the word "plane" means that in any plane perpendicular to the direction of propagation the **E** and **H** vectors respectively are everywhere equal at any given moment; if we now take the z-axis parallel to the direction of propagation then **E** and **H** are indeed dependent only upon z and t.

In order to deduce the said differential equations we first apply eq. (1) to the contour shown in *fig. 2a*; as surface S we take the rectangle bounded

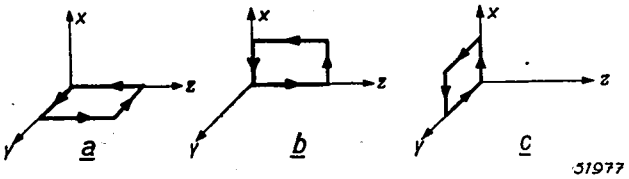


Fig. 2. Integration contours for deduction of equations (5)-(6) from equations (1)-(2).

by this contour in the y-z plane. Since the contributions to the line integral of the two lengths of line parallel to the z-axis cancel each other (**E** and **H** depending only upon z and t) we find

$$y \cdot E_y(0,t) - y \cdot E_y(z,t) = \mu y \int_0^z \frac{\partial}{\partial t} H_x(\zeta, t) \, \mathrm{d}\zeta .$$

By differentiation with respect to z we obtain

$$\frac{\partial E_y}{\partial z} = \mu \frac{\partial H_x}{\partial t} . \quad . \quad . \quad . \quad . \quad . \quad (5a)$$

By applying eq. (1) to the contours of figs 2*b* and 2*c* we find in the same way:

$$-\frac{\partial E_x}{\partial z} = \mu \frac{\partial H_y}{\partial t} . \quad . \quad . \quad . \quad . \quad . \quad (5b)$$

and

$$0 = \mu \frac{\partial H_z}{\partial t} . \quad . \quad . \quad . \quad . \quad . \quad (5c)$$

By carrying out the same operations with eq. (2) we obtain:

$$-\frac{\partial H_y}{\partial z} = \sigma E_x + \varepsilon \frac{\partial E_x}{\partial t}, \quad . \quad . \quad . \quad . \quad (6a)$$

$$\frac{\partial H_x}{\partial z} = \sigma E_y + \varepsilon \frac{\partial E_y}{\partial t}, \quad . \quad . \quad . \quad (6b)$$

$$0 = \sigma E_z + \varepsilon \frac{\partial E_z}{\partial t} . \quad . \quad . \quad . \quad . \quad (6c)$$

Thus six simultaneous differential equations (5)-(6) have been derived for the six quantities $E_x \ldots H_z$, each of which is a function of only z and t.

We shall now prove that a plane wave running in the z direction represents a solution of (5)-(6).

For the sake of simplicity, in what follows we shall consider only linearly polarized, harmonic plane waves.

"Linearly polarized" means that **E**, respectively **H**, has always the same direction for any value of z. By "harmonic" is to be understood that **E** and **H** depend sinusoidally upon z and t. The mathematical expression for such a plane wave is, therefore, in the well-known complex representation:

$$\left.\begin{aligned} \mathbf{E} &= \mathbf{E}^\circ \, \mathrm{e}^{j(\omega t - kz + \eta)}, \\ \mathbf{H} &= \mathbf{H}^\circ \, \mathrm{e}^{j(\omega t - kz)}, \end{aligned}\right\} \quad . \quad . \quad . \quad . \quad (7)$$

where the symbols have the following meanings: $\mathbf{E}^\circ$, $\mathbf{H}^\circ$ are two real constant vectors (of which we know nothing more at the moment); the length of the vectors $\mathbf{E}^\circ$ and $\mathbf{H}^\circ$ will be denoted by E° and H° respectively;

$\omega = 2\pi\nu$ radial frequency, (ν frequency),
η phase difference between the **E** and **H** vectors,
j the imaginary unit, $+\sqrt{-1}$,
k a constant.

It will appear that (7) is indeed a solution of (5)-(6), provided k, η and E°/H° depend in a certain manner upon μ, ε, σ and ω. This dependence is found by substituting (7) in eq. (5)-(6) and

seeking the consequences of the requirement that (7) is a solution of these equations.

With a suitable choice of the system of coordinates this substitution yields:

$$\left.\begin{aligned} kE^\circ &= \mu\,\omega\,H^\circ\,e^{-j\eta}, \\ (\sigma + j\omega\varepsilon)\,E^\circ &= j\,k\,H^\circ\,e^{-j\eta}, \end{aligned}\right\} \quad . \quad . \quad . \quad (8)$$

where

$$E^\circ = E_x^\circ,\ H^\circ = H_y^\circ,\ E_y^\circ = H_x^\circ = 0, \quad (9a)$$

$$E_z^\circ = H_z^\circ = 0 \quad . \quad . \quad . \quad . \quad . \quad . \quad (9b)$$

Eq. (9b) expresses the fact that the wave is transverse, whereas equations (9a) and (9b) together express the fact that the electric vector and the magnetic vector are at right-angles to each other.

Further from (8) it immediately follows that:

$$k^2 = \mu\omega\,(\varepsilon\omega - j\sigma), \quad . \quad . \quad . \quad . \quad (10)$$

$$\frac{E^\circ}{H^\circ} = \frac{\mu\omega}{k\,e^{j\eta}}.$$

Since we have assumed that E°, H°, μ and ω are real, according to the last equations also $k\,e^{j\eta}$ must be real; k is therefore a complex number for which the following holds:

$$k = |k|\,e^{-j\eta}, \quad . \quad . \quad . \quad . \quad . \quad . \quad . \quad (11)$$

so that

$$\frac{E^\circ}{H^\circ} = \frac{\mu\omega}{|k|} \quad . \quad . \quad . \quad . \quad . \quad . \quad . \quad . \quad (12)$$

According to (12) the ratio E°/H° is always positive. Since the chosen system of coordinates x, y and z is a right-handed system (*cf.* fig. 2) this means that the directions $\mathbf{E}^\circ$, $\mathbf{H}^\circ$ and the positive z-direction also form a right-handed system.

Thus we have found a solution of (5)-(6) which, apart from the sign of k and an arbitrary factor by which it can be multiplied, is determined unambiguously by (7) and (10)-(12).

Strictly speaking we should also verify that this solution complies with the differential conditions following from (3)-(4) just as (5)-(6) follow from (1)-(2). Such is not difficult to prove if need be. Suffice it to state that it is thereby found that the charge density ϱ must everywhere be zero.

From (10) we see that in general the constant k is a complex number, namely in all cases where $\sigma \neq 0$, that is to say when the medium is conducting. We shall see presently what this means. First we shall consider the case where $\sigma = 0$, i.e. where the medium is a perfect insulator. Then, according to the eq. (10)-(12):

$$k = \omega\sqrt{\mu\varepsilon}, \quad . \quad . \quad . \quad . \quad . \quad . \quad . \quad (13)$$

$$E^\circ/H^\circ = \sqrt{\mu/\varepsilon}, \quad . \quad . \quad . \quad . \quad . \quad . \quad (14)$$

$$\eta = 0,$$

the last equation signifying that $\mathbf{E}$ and $\mathbf{H}$ vibrate in phase. The physical significance of k is clear when bearing in mind that the wavelength λ of the wave (7) in the case in question (k real) is given by

$$\lambda = 2\pi/k\,. \quad . \quad . \quad . \quad . \quad . \quad . \quad . \quad . \quad (15)$$

From the well-known relation between the phase velocity v of a wave and its frequency and wavelength $v = \lambda\nu$ it therefore follows that

$$v = \frac{1}{\sqrt{\mu\varepsilon}}.$$

If the medium concerned is a vacuum then this phase velocity is equal to $c \approx 3 \cdot 10^8$ m/sec, the velocity of light in vacum, that is to say:

$$c = \frac{1}{\sqrt{\mu_0\varepsilon_0}}\ \text{m/sec} \quad . \quad . \quad . \quad . \quad . \quad (16)$$

Now (see eq. (IX))

$$\mu_0 = 4\pi/10^7\ \text{volt·sec/amp·metre.}$$

For the relation of amplitudes E°/H° we thus get in this case

$$\frac{E^\circ}{H^\circ} = \sqrt{\frac{\mu_0}{\varepsilon_0}} = \frac{4\pi c}{10^7} \approx 377\ \text{ohms} \quad . \quad (17)$$

Moreover we find:

$$k = \frac{\omega}{c}.$$

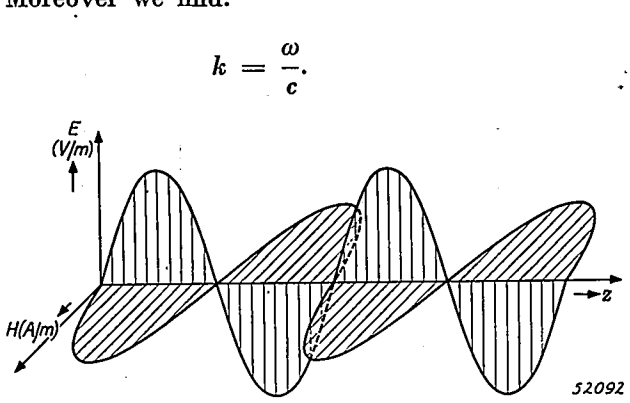


Fig. 3. Diagrammatic representation of the form of a linearly polarized, sinusoidal plane wave in vacuum ("instantaneous view").

The form of the wave in vacuum is represented diagrammatically in *fig. 3*.

If the medium is conducting ($\sigma > 0$), then k is complex and may be written as

$$k = k_1 - jk_2, \quad . \quad . \quad . \quad . \quad . \quad . \quad . \quad (18)$$

where k_1 and k_2 are real numbers. On account of (11) we therefore have

$$\tan \eta = k_2/k_1 \quad \ldots \ldots \quad (19)$$

Substituting (18) in (7) we obtain

$$\left.\begin{aligned} \mathbf{E} &= \mathbf{E}^\circ\, e^{-k_2 z}\, e^{j(\omega t - k_1 z + \eta)}, \\ \mathbf{H} &= \mathbf{H}^\circ\, e^{-k_2 z}\, e^{j(\omega t - k_1 z)}. \end{aligned}\right\} \quad \ldots \quad (20)$$

These formulae represent a wave damped in the direction of propagation, provided k_1 and k_2 are positive. Now k_1 and k_2 are determined by (10), except only for the sign. Let us therefore assume that k_2 for instance is always positive. It appears that then also k_1 is always positive. Thus we see that a plane electromagnetic wave in a conducting medium must necessarily be damped, or, in other words, there is then always an absorption of the wave. This is not surprising, for, if $\sigma > 0$, then the wave induces a (conduction) alternating current (density $\sigma\mathbf{E}$) in the medium; the Joule heat of this current is generated at the cost of the energy of the wave, this being manifested in the decrease of the wave amplitudes. Now the Joule heat amounts to σE^2 joule/m^3. If the medium is a very good conductor (large σ) then consequently the damping is strong, so that a wave penetrating such a medium travels only a very short distance before it becomes no longer perceptible. The greater the value of ω, the shorter is this distance. In a perfect conductor ($\sigma = \infty$) wave propagation is absolutely impossible. As a matter of fact, from the fundamental equations (1)-(2) it is immediately seen that in a perfect conductor the **E**, **H** alternating field must always be zero. We would further point out that in a conducting medium **E** and **H** no longer oscillate in phase ($\eta \neq 0$) and that both the wavelength and the ratio E°/H° are smaller than in the case of vacuum. In the limiting case of a very good conductor the form of the plane wave undergoes such an alteration in consequence of the strong damping that the sinusoidal character of the wave can hardly be recognized, as may be seen from *fig. 4*.

Considering the form of eq. (10) there are obviously two limiting cases to be discussed separately, namely $\sigma/\varepsilon\omega \ll 1$ and $\varepsilon\omega/\sigma \ll 1$. Since the total current density is given by

$$\sigma\,\mathbf{E} + \varepsilon \frac{\partial \mathbf{E}}{\partial t} = (\sigma + j\omega\varepsilon)\,\mathbf{E},$$

it corresponds in the first case to a practically pure displacement current: the medium behaves as an insulator. In the second case the total current is practically a conduction current, the medium acting as a good conductor.

First limiting case: $\sigma/\varepsilon\omega \ll 1$.

In this case the absorption of the electromagnetic wave is often called the dielectric absorption and one speaks also of dielectric losses. One then sometimes introduces a complex dielectric constant, $\underline{\varepsilon}$, that is to say one writes (10) in the form:

$$k^2 = \omega^2 \mu \underline{\varepsilon}$$

where

$$\underline{\varepsilon} = \varepsilon - j\sigma/\omega.$$

The well-known "loss angle" δ, which may be defined as the angle whose tangent is equal to the absolute value of the ratio of the imaginary to the real part of $\underline{\varepsilon}$, stands in a very simple relation to the phase difference η between **E** and **H**, for from the last two equations and eq. (11) it follows that

$$\delta = 2\eta, \qquad \tan\delta = \tan 2\eta = \sigma/\varepsilon\omega.$$

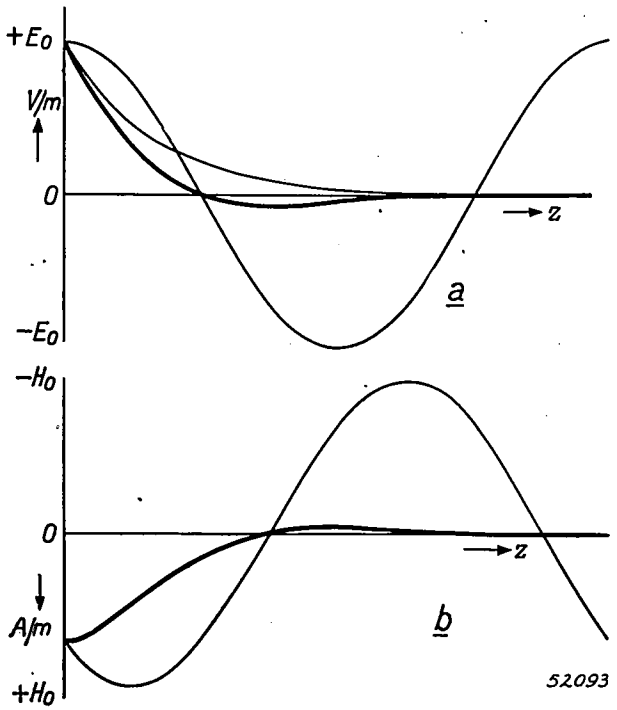


Fig. 4. Diagrammatic representation ("instantaneous view") of the structure of a linearly polarized, sinusoidal, damped plane wave in a well-conducting medium at high frequency ($\varepsilon\omega/\sigma \ll 1$). In (*a*) the value of the electric field strength and in (*b*) the value of the magnetic field strength are plotted vertically as functions of the distance z along the direction of propagation. The lightly-drawn sine curves represent the wave when there is no damping. By multiplying the values of these sine functions by the corresponding values of the damping factor (see (*a*), lightly drawn) one obtains the heavy curves, which thus represent the damped wave. There is a difference in the shape of these curves in (*a*) and (*b*) due to the phase difference between **E** and **H**, which amounts here to $\pi/4$. Since **E**, **H** and the direction of propagation are at right angles to each other and, moreover, form a right-handed system, in order to obtain a three-dimensional picture one would have to turn the plane of the drawing in (*b*) 90° about the z-axis, such that the positive direction of the H-axis points towards the reader. Both the ratio E°/H° and the wavelength are a factor of the order of $\sqrt{\varepsilon\omega/\sigma}$ smaller for a conducting medium than for vacuum.

The loss angle is therefore equal to twice the phase difference between **E** and **H**. From eq. (20) we see that the wavelength of the wave in a dielectric is $2\pi/k_1$. The damping of the wave amplitudes per wavelength is therefore, from (19):

$$e^{-k_2\lambda} = e^{-2\pi k_2/k_1} = e^{-2\pi\tan\eta} = e^{-2\pi\tan(\delta/2)}.$$

All these formulae are still exact. Introducing the assumption that $\sigma/\varepsilon\omega \ll 1$, we find with the aid of (10) and (18)

$$k_1 \approx \omega\sqrt{\mu\varepsilon}, \quad k_2 \approx \frac{\sigma}{2}\sqrt{\frac{\mu}{2}}, \quad \tan\eta \approx \eta = \frac{\delta}{2} = \frac{\sigma}{2\omega\varepsilon}.$$

A comparison of these formulae with (13)-(15) shows that to a first approximation the wavelength and the ratio E°/H° have here the same values as those for a wave in a non-conducting medium. Little is noticed of the damping of the wave amplitudes so long as $\sigma/\varepsilon\omega$ is very small, the damping factor per wavelength being $e^{-k_2\lambda} \approx e^{-\pi(\sigma/\varepsilon\omega)}$.

Second limiting case: $\varepsilon\omega/\sigma \ll 1$.

One may then to a first approximation entirely ignore the displacement current, that is to say the first term in the right-hand member of (10) can be omitted. We then obtain:

$$k^2 \approx -j\mu\sigma\omega$$

and since

$$\sqrt{-j} = (1-j)/\sqrt{2},$$

$$k \approx \sqrt{\frac{\mu\omega\sigma}{2}}(1-j),$$

that is to say

$$k_1 \approx k_2 \approx \sqrt{\frac{\mu\omega\sigma}{2}}, \quad \eta \approx \frac{\pi}{4}, \quad \delta \approx \frac{\pi}{2}.$$

A comparison of these formulae with (13)-(15) shows that in a good conductor an electromagnetic wave assumes an entirely different form from that in a non-conducting medium (see fig. 4). Here the ratio E°/H° and the wavelength are smaller than in a non-conducting medium by factors $\sqrt{\varepsilon\omega/\sigma}$ and $\sqrt{2\varepsilon\omega/\sigma}$ respectively (with $\varepsilon\omega/\sigma \ll 1$!). Moreover the damping is so strong that over a distance of one wavelength the field amplitudes become smaller by a factor 0.002, for in this case the damping factor of a wavelength amounts to

$$e^{-k_2\lambda} = e^{-2\pi k_2/k_1} \approx e^{-2\pi} \approx 0.002.$$

This strong absorption of the electromagnetic wave is closely related to the skin effect. From the theory of skin effect it is known that the so-called penetration depth d is given by

$$d = \sqrt{\frac{2}{\mu\omega\sigma}}$$

and this is found to be equal to $1/k_2$.

The significance of the penetration depth d follows from the fact that the amplitude of density of a high-frequency current in a conductor decreases proportionately with $e^{-z/d}$, where z represents the depth below the surface of the conductor. Now, in consequence of (20), the amplitudes of the **E** and **H** waves diminish according to exactly the same law with the same value of $d = 1/k_2$. This correspondence is easy to understand when the high-frequency current is construed as being caused by the electromagnetic field tending to penetrate into the conductor from the outside.

If for instance $\lambda = 10$ cm (in vacuum), then from the formula given above for the penetration depth d we find that for copper ($\sigma = 5{\cdot}8 \times 10^7$ ohm^{-1} × m^{-1}) this amounts to only $1{\cdot}2 \times 10^{-6}$ m.

Propagation of the waves in a homogeneous medium bounded by conductors

Boundary conditions

Contrary to what has been assumed in the preceding section, in reality a homogeneous medium is always bounded. The homogeneous medium air, for instance, in a cavity resonator or in a wave guide is bounded by metal walls. Such walls can of course be regarded as another homogeneous medium. The values of ε, μ and σ therefore make a jump on the boundary surface between air and metal. A similar situation occurs on the boundary between any two homogeneous media.

From what has been stated so far about the mathematical principles of the Maxwell theory it is by no means clear how such a situation has to be dealt with mathematically. We do know that plane (damped) waves can be propagated in each of the two media, but we do not yet know how the amplitudes and phases of a plane wave in one medium are to be "matched" with those of a plane wave in the other medium on the boundary surface. The fact that this matching cannot be arbitrary, so that some "matching rule" is essential, follows at once from the existence of the empirically established laws for the passage of a plane wave from one medium to another (laws of refraction and reflection).

It appears that such a general (*i.e.* not limited to plane waves) "matching rule", which finds expression in the existence of certain boundary conditions that have to be satisfied by **H**, **B**, **E** and **D** on the boundary surface, is indeed to be deduced from Maxwell's fundamental equations. Here we shall not formulate this matching rule in a general way but only for the particular case in which one of the two media is a perfect conductor ($\sigma = \infty$). Throughout this article metals will be replaced by perfect conductors in which, therefore, the electromagnetic field is exactly zero. This is certainly permissible (and in fact usual) as a first approximation, since, as we have seen in the example of plane waves, when the frequency is high the electromagnetic field scarcely penetrates into a good conductor. If the energy losses are of any interest — and in practice that is of course the case — then in a further approximation corrections have to be made for this slight penetration of the field into the metal.

The reason why the conductors are mostly assumed to have an infinite conductivity is that the boundary conditions become very simple if the electromagnetic field inside one of the two media is exactly zero. In the case that both media have finite conductivities the boundary conditions lead, on the other hand, in most problems to great mathematical difficulties.

The boundary conditions for a perfect conductor may now be formulated as follows. One resolves

E on the boundary surface between the conductor and the other medium (not necessarily vacuum) into a tangential component E_t and a normal component E_n; as positive direction of the normal we take the direction from the conductor to the other medium. The same is done with **H**. We then have on the boundary surface:

$$E_t = 0, \quad H_n = 0, \quad \ldots\ldots \quad (21)$$

$$\varepsilon E_n = s, \quad H_t = i, \quad \ldots\ldots \quad (22)$$

where s and i stand respectively for the density of a surface charge (in coulomb/m^2) and the density of a surface current (in ampere/m); this current is at right-angles to the direction of **H**, such that the (positive) direction of the normal of the surface, the direction of **H** and the direction in which i flows form a right-handed system.

In order to understand better the significance of the "surface current", think for instance of a wire through which a high frequency alternating current is flowing. Owing to the skin effect the density of this current will have measurable values only in a thin surface layer of the wire. Roughly speaking one may therefore say that the current flows "along the surface" of the wire. The density of this "surface current" will then be equal to the current intensity (in amperes) divided by the circumference (in metres) of the cross section of the wire. The density calculated in this manner is quite analogous to the quantity i occurring in equation (22) in the limiting case where the conductivity of the material of the wire becomes infinite.

Methods for solving the fundamental equations

In order to ascertain how the electromagnetic fields can propagate in vacuum when (perfect) conductors are present, two different courses can be followed.

One course is similar to that which we followed in the previous section: from equations (1) and (2), which have an integral form, by a suitable choice of integration contours we derive the Maxwell equations in the differential form, the equations (5) and (6) thus being a special case. The only point of difference, compared with what we did before, is that the electromagnetic field does not now depend upon one coordinate but upon all three. Once we have the Maxwell differential equations for the general case, then for any given configuration of conductors the problem is reduced to finding the solutions of a system of simultaneous differential equations with due observance of the boundary conditions (21) and (22). This method is perfectly general and in many cases in fact the only suitable one. It will be further explained, in connection with wave guides of a circular cross section, in Part II of this article (to be published in a subsequent number of this journal).

We shall first, however, follow another method which in principle is no less general though usually cumbersome. On the other hand, at least in simple cases, it expresses better what is physically essential in the solutions obtained. This method is based on the fact that the fundamental equations (1) and (2) are linear, *i.e.* they do not contain products of field components and consequently any linear combination of their solutions must also be a solution. For the unbounded, empty space this means that a situation where an arbitrary number of plane waves, with arbitrary direction and magnitude of the electric vector [7]), are propagated in arbitrary directions, corresponds to a solution of the fundamental equations. If there are (perfect) conductors present then this arbitrariness is considerably limited; only those superpositions of plane waves are permissible which satisfy the boundary conditions. For simple configurations of the conductors such permissible superpositions of plane waves can easily be found [8]). This will be illustrated in what follows with some examples.

Propagation of the waves between parallel conducting planes and in rectangular wave guides

Starting from the "superposition principle" outlined above we shall now consider how electromagnetic waves can be propagated with the three following configurations of conductors in vacuum;

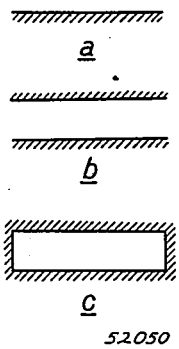


Fig. 5. Diagrammatic representation of the configuration of conductors dealt with in the text. *a*) one infinitely long and wide plane, *b*) two such planes parallel to each other, *c*) a rectangular wave guide, *i.e.* two pairs of planes as in (*b*), each pair being perpendicular to the other. In all three cases the plane of the drawing is perpendicular to the conducting planes.

[7]) By a "plane wave" is to be understood here and in the following pages a harmonic, linearly polarized, plane wave. For such a wave **H** is unambiguously determined by **E** and the direction of propagation.

[8]) The first to deal with the propagation of waves in wave guides as a problem of the superposition of plane waves was L. Brillouin (Rev. Gén. d'Electr. **40**, 227, 1936).

1) the space is bounded on one side, for instance underneath, by an infinitely long and wide, conducting plane (*fig. 5a*); 2) the space is bounded both underneath and on top, by two parallel planes (fig. 5*b*); 3) the space is bounded on four sides by two pairs of parallel planes, with the two pairs at right-angles to each other (fig. 5*c*). The last case represents a technically important example of a wave guide, namely that of a wave guide with a rectangular cross section.

One single plane wave

We begin by remarking that one single plane wave may be a permissible solution for the configurations of figs 5*a* and *b* but not for the wave guide of fig. 5*c*. In the cases of figs 5*a* and *b* it is indeed sufficient if the plane wave is chosen in such a way that its direction of propagation is parallel to the conducting planes and its electric vector is perpendicular to those planes. The boundary conditions (21) are then automatically satisfied, for then the normal component of **H** on the conducting planes and the component of **E** parallel to those planes are everywhere zero. From eq. (22) we then obtain immediately the values of the surface charge and surface current. Any other choice of the propagation direction of the plane wave or of the directions of **E** and **H** would not comply with the boundary conditions. Now it is readily seen that with the permitted choice of the plane wave one cannot add two other conducting planes (the case of fig. 5*c*) without coming into conflict with the boundary conditions (21) on these new planes. A single plane wave cannot, therefore, be propagated in a rectangular wave guide.

From this, however, one can draw farther-reaching conclusions. In the first place it is clear that a superposition of plane waves all having a direction of propagation parallel to the axis of the rectangular wave guide cannot produce an allowed wave either. In the second place the propagation of a purely transverse but possibly not plane wave in a rectangular wave guide — that is to say, a wave where both **E** and **H** have no component in the direction of the axis of the wave guide — is also impossible (because, as may be proved, this can be imagined as a superposition of plane waves all propagated parallel to the axis of the wave guide). The validity of this result is not confined to rectangular wave guides. So long as a wave guide consists of one conductor, that is to say so long as the boundary of its cross section consists of one continuous closed line (circle, ellipse, etc.), the fact remains that purely transverse waves cannot propagate in such wave guides. In the case of waves which can indeed be propagated in such wave guides the **E** and **H** fields always have a longitudinal component. On the other hand such does not hold hold for a wave guide consisting of two conductors, *i.e.* having a cross section bounded by two contours; in a coaxial cable for instance a purely transverse wave can indeed be propagated.

The situation described above, where a purely transverse plane wave is propagated between two infinite perfectly conducting planes, forms the basis for a rigorous treatment of a Lecher system consisting of two wide parallel metal strips at a short distance from each other.

It can easily be proved that with such a Lecher system the equations for the current and voltage are approximately equivalent to the differential equations for a plane wave in the previous section. It is only necessary to define the voltage in an unambiguous manner, since the current in the Lecher system is nothing else than the total surface current calculated from the boundary condition. We shall not go into that any further here, because a similar problem will be dealt with in Part II, *viz.* the rigorous deduction of the equations applying for a Lecher system consisting of two coaxial cylinders (the coaxial cable). We would only mention that the ratio $E^\circ/H^\circ = \sqrt{\mu/\varepsilon}$, for vacuum approximately equal to 377 ohms (see eq. (17)), then assumes the significance of the characteristic impedance of the Lecher system. For this reason one sometimes calls the quantity $\sqrt{\mu/\varepsilon}$ the characteristic impedance of the medium for plane waves.

Superposition of two plane waves

We shall now superpose one upon the other two plane waves having different directions of propagation and different **E** vectors but equal lengths E of these vectors and equal frequency $\nu = \omega/2\pi$. We shall show that by doing this in a suitable manner we find electromagnetic waves (of course not plane and not transversal) capable of propagation in the rectangular wave guide.

Obviously any combination of plane waves that is not allowed for the case of fig. 5*a* (or 5*b*) will certainly not be allowed for the case of fig. 5*b* (or 5*c*). We shall therefore first consider the simple case of fig. 5*a*.

Let us consider a plane wave that strikes the conducting plane at an angle in such a way that **E** is parallel to the plane. We shall call this wave the "incident wave". Let ϑ (see *fig. 6a*) represent the angle between the direction of propagation of this wave and the conducting plane. From what has been said above it follows that this wave is not an allowed solution of the problem even for $\vartheta = 0$. But by superposing on the incident wave a second plane wave, the "reflected wave", we can easily

construct an allowed solution. It is evident that in order to comply with the boundary condition $E_t = 0$ on a conducting plane we must choose $\mathbf{E}^{\text{refl}} = -\mathbf{E}^{\text{inc}}$ ("refl" and "inc" refer here and in the following to the reflected and incident waves respectively); both waves being plane, $\mathbf{E}^{\text{refl}}$ and $\mathbf{E}^{\text{inc}}$ will then everywhere be parallel. Having done this, we only have to choose $\vartheta^{\text{refl}} = \vartheta^{\text{inc}}$ in order to comply with the boundary condition $H_n = 0$. In this manner we arrive at the situation diagrammatically represented in fig. 6*b*. From simple considerations of symmetry it is not difficult to understand that the wave resulting from the superposition of the incident and reflected waves is propagated in a direction parallel to the conducting plane and perpendicular to $\mathbf{E}^{\text{inc}}$ (or $\mathbf{E}^{\text{refl}}$); in fig. 6*b* this direction is indicated by an arrow. Now what is the form of this wave? In order to answer this question fully the simplest way is to perform analytically the superposition of the incident and reflected waves, i.e. to write the expressions

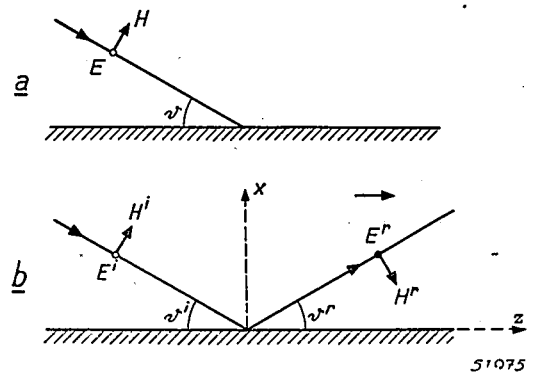


Fig. 6. Direction of propagation and position of the **E** and **H** vectors of the plane waves considered in the text, striking a conducting plane and reflected from it: *a*) the incident wave, *b*) the incident and the reflected wave (the arrow to the right of the illustration indicates the direction of the resulting wave). The **H** vectors lie in the plane of the drawing; the **E** vectors are at right-angles to it. ● signifies that an **E** vector is directed towards the reader, ○ that it has the opposite direction. The indices *i* and *r* refer to the incident and reflected waves respectively.

$$\mathbf{E} = \mathbf{E}^{\text{inc}} + \mathbf{E}^{\text{refl}}, \qquad \mathbf{H} = \mathbf{H}^{\text{inc}} + \mathbf{H}^{\text{refl}}.$$

If the system of coordinates x, y, z is chosen as indicated in fig. 6*b* (the equation of the conducting plane is then $x = 0$), then a simple calculation gives the following expressions

$$\left.\begin{aligned} E_y &= A \sin(xk \sin\vartheta)\, e^{j(\omega t - zk\cos\vartheta)}, \\ H_x &= A \sqrt{\frac{\varepsilon_0}{\mu_0}} \cos\vartheta \sin(xk\sin\vartheta)\, e^{j(\omega t - zk\cos\vartheta)}, \\ H_z &= A \sqrt{\frac{\varepsilon_0}{\mu_0}} \sin\vartheta \cos(xk\sin\vartheta)\, e^{j(\omega t - zk\cos\vartheta - \pi/2)}, \\ E_x &= E_z = H_y = 0 \end{aligned}\right\} \quad (23)$$

(A = an arbitrary constant, $k = \omega\sqrt{\mu_0\varepsilon_0} = \omega/c = 2\pi/\lambda$, where λ is the wavelength of each of the plane waves.)

This shows that the resultant wave is indeed propagated parallel to the conducting plane and perpendicular to its **E** vector. Its phase velocity v is

$$v = \omega/k \cos\vartheta = c/\cos\vartheta,$$

thus greater than c, whilst its wavelength λ_z is

$$\lambda_z = v/\nu = c/\nu\cos\vartheta = \lambda/\cos\vartheta\,. \qquad (24)$$

The form of the wave (23) is rather complicated. **E** and **H** are at right-angles to each other, as is the case with a plane wave, but whereas the **E** field is transverse the **H** field is not so: contrary to the case of a plane wave, here the magnetic field has a component in the direction of propagation. Such a wave is called a "transverse electric wave" (abbreviated "TE" wave) or "H-wave". Furthermore we see that the wave is no longer linearly polarized: the direction of **H** at each point of the space changes with the time, owing to H_x and H_z differing 90° in phase. Finally, we find that the wave is no longer plane either. The values of the **E**, **H** fields in a plane perpendicular to the direction of propagation (z-direction) depend upon x: for z = constant H_x, H_z, E_y vary sinusoidally with x, that is to say, along the x-direction the wave (23) behaves as a standing wave. In particular $H_x = 0$ and $E_y = 0$ (regardless of the value of t) in each plane which is parallel to the conducting plane and for which

$$x = \frac{m\pi}{k\sin\vartheta} = \frac{m\lambda}{2\sin\vartheta} \quad (m = 0, 1, 2\ldots) \quad (25)$$

applies. If we introduce the wavelength

$$\lambda_x = \lambda/\sin\vartheta \quad \ldots\ldots\ldots \quad (26)$$

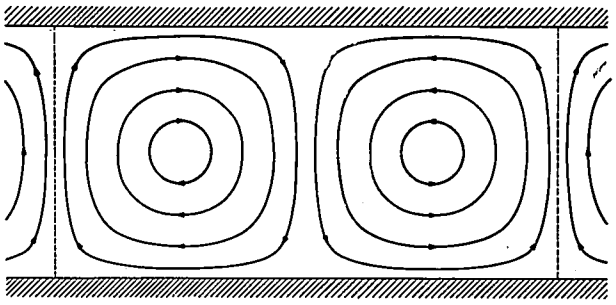
of the said standing wave, we can write instead of (25):

$$2x = m\lambda_x \quad (m = 0, 1, 2\ldots), \quad \ldots \quad (27)$$

which is self-explanatory.

The consequence of this is highly important. When a second conducting plane is applied above and parallel to the conducting plane $x = 0$ at a distance x given by (27) then the boundary conditions $E_t = H_n = 0$ are automatically satisfied also for this second plane; this means that the wave (23) is also an allowed solution of the problem of fig. 5*b* provided the distance between the conducting planes complies with (27). We can, however, verify the correctness of a still farther-reaching statement that the wave (23) — still under the condition (27) — is also an allowed solution of the problem of the rectangular

wave guide. The fact is that if we apply two other conducting planes at an arbitrary distance from each other parallel to the direction of propagation of the wave (23) and perpendicular to its



52094

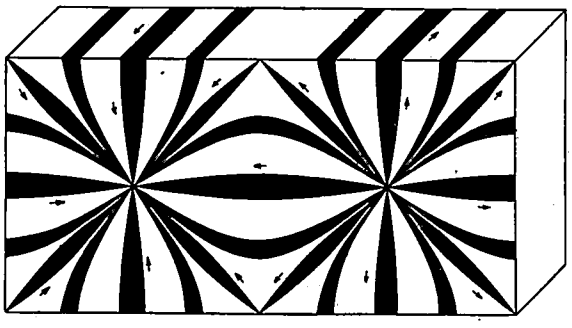
Fig. 7. The H-lines in the case of an H_{10}-wave in a rectangular wave guide ("instantaneous view"); a cross section parallel to one pair of walls (thus also parallel to the direction of propagation). The E-lines are perpendicular to the plane of the drawing. The H-lines are given by the equation

$$\sin 2\pi\xi \cdot \sin 2\pi\zeta = \text{constant},$$

where $\xi = x/\lambda_x$ and $\zeta = z/\lambda_z$. The distance between the two dotted vertical lines is equal to λ_z; the distance between the two horizontal lines representing the walls is equal to $\lambda_x/2$. The H-lines in the case of an H_{m0} wave are obtained by drawing the picture for the H_{10}-wave m times one above the other.

E vector (having the direction of the y-axis), then the boundary conditions (21) are likewise automatically satisfied at these two new conducting planes. Different values of m thus correspond to different forms of the wave ($m + 1$ is equal to the number of "nodal planes" of the standing wave along the x-direction). The H-waves of the type (23) are therefore denoted by H_{m0}; the second index 0 reminds us that the wave is not dependent on the y-coordinate.

The magnetic lines of force (for t = constant) of the H_{10}-wave are represented in *fig. 7*; E-lines are perpendicular to the plane of the drawing. In *fig. 8* we have a diagram representing the surface



52095

Fig. 8. Representation of the density distribution of the surface current on the walls of a rectangular wave guide through which an H_{10}-wave is propagated ("instantaneous view"). The width of the "lines of flow" perpendicular to the magnetic lines of force in fig. 6 is proportional to the current density and also — owing to the boundary condition (22) — proportional to the value of the magnetic field strength at the wall.

current density which follows from the boundary conditions (22).

For the above-described "construction" of the H_{m0}-waves we have taken a plane wave of which the electric vector **E** is parallel to the conducting plane and which strikes the conducting plane at an angle. If such a construction had been built up from an oblique incident plane wave whose magnetic vector **H** was parallel to the conducting plane, then we should have obtained in precisely the same way a wave — the "transverse magnetic" (TM-wave) or "E-wave", *viz.* an "E_{m0}-wave" — which could be propagated between two parallel planes (fig. 5*b*) but not in a rectangular wave guide (fig. 5*c*). From the analogy between an E_{m0}-wave and an H_{m0}-wave it immediately follows that, just as for an H_{m0}-wave **E** has the direction of the y-axis and does not depend upon y (see eq. (23)), for an E_{m0}-wave **H** must also have the direction of the y-axis and cannot be dependent upon y. Therefore, the two walls of the wave guide which are perpendicular to the y-axis could not possibly be applied in such a way as to satisfy the boundary condition $H_n = 0$ everywhere along those walls. Consequently it is not possible to obtain permissible E-waves in rectangular wave guides by the superposition of two plane waves. This would require the superposition of at least four plane waves. The E-waves are then found to be of a more complicated form: they behave as standing sinusoidal waves not only along the x-direction but also along the y-direction, and that is why they are called "E_{mn}-waves". By a suitable superposition of four plane waves it is possible to construct also the H-waves analogous to "E_{mn}-waves", called the "H_{mn}-waves".

The cut-off frequency

In the foregoing we have adapted, as it were, the position of the conducting planes to the form of the waves (23). From this one might be inclined to conclude that an H_{m0}-wave can only be propagated in a rectangular wave guide when there is a discontinuous series of values for the distance between two parallel walls. However, such a conclusion is incorrect. If the said distance is a then in eq. (25) we must put $x = a$ and determine from that the angle ϑ, which, just like m, plays the part of a parameter:

$$\sin\vartheta = \frac{m\lambda}{2a} \quad (m = 0, 1, 2 \ldots .). \quad . \quad . \quad (28)$$

With the aid of eq. (28) we can eliminate ϑ from eq. (23) and then obtain the following expressions for the H_{m0}-wave:

$$\left.\begin{aligned} E_y &= A \sin\frac{m\pi x}{a}\, e^{2\pi j\varphi}, \\ H_x &= A \sqrt{\frac{\varepsilon_0}{\mu_0}} \sqrt{1-\left(\frac{m\lambda}{2a}\right)^2} \sin\frac{m\pi x}{a}\, e^{2\pi j\varphi}, \\ H_z &= A \sqrt{\frac{\varepsilon_0}{\mu_0}} \left(\frac{m\lambda}{2a}\right)^2 \cos\frac{m\pi x}{a}\, e^{2\pi j(\varphi - 1/4)}, \\ E_x &= E_z = H_y = 0, \end{aligned}\right\} \quad (29)$$

where

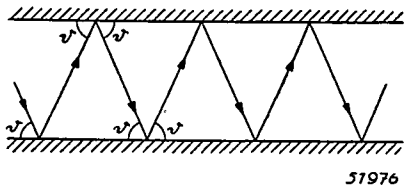
$$\varphi = \nu\left\{t - \frac{z}{c}\sqrt{1-\left(\frac{m\lambda}{2a}\right)^2}\right\}. \quad . \quad . \quad (30)$$

However, it is not always possible to determine a real angle ϑ from eq. (28), because a real angle ϑ can only be found from this equation when its right-hand side is $\leqq 1$, that is to say only if λ is not greater than a certain wavelength which is called the cut-off wavelength λ_c and which is given by

$$\lambda_c = \frac{2a}{m} \quad (m = 1, 2 \ldots.); \quad . \quad . \quad . \quad (31)$$

The frequency ν must therefore be greater than the cut-off frequency $\nu_c = mc/2a$.

If λ satisfies the condition $\lambda > \lambda_c$, that is to say if $\vartheta < 90°$, then the H_{m0}-wave may also be regarded as one plane wave (wavelength λ) reflected to and fro between a pair of parallel conducting planes and propagated in this zig-zag fashion in the z-direction



51976

Fig. 9. The zig-zag course of a plane wave between two planes the situation where the angle ϑ is almost 90° corresponds to a wave whose length is only a little smaller than the cut-off wavelength.

(see *fig. 9*). This interpretation leads to the conclusion that when $\lambda = \lambda_c$, *i.e.* $\vartheta = 90°$, the wave can no longer be propagated in the z-direction. We shall now verify this with the aid of the formulae given above, when it will at the same time be made clear what happens when $\lambda > \lambda_c$. Since, owing to (28) and (31),

$$\cos\vartheta = \sqrt{1-(m\lambda/2a)^2} = \sqrt{1-(\lambda/\lambda_c)^2}, \quad . \quad (32)$$

the z-dependence of the wave (29)-(30) is given by

$$e^{-2\pi j z\sqrt{(1/\lambda)^2-(1/\lambda_c)^2}}. \quad . \quad . \quad . \quad . \quad . \quad (33)$$

For $\lambda = \lambda_c$ the exponent becomes zero, that is to say the wave (29) is in fact no longer dependent upon z; it is only a standing wave along the x-direction. But the expression (33) shows us something more, *viz.* that for $\lambda > \lambda_c$ the wave (29) is damped because then the expression underneath the radical is negative, that is to say the exponent is a real number. For $\lambda > \lambda_c$ (29) thus represents a standing wave along the x-direction whose amplitude depends exponentially upon z.

The practical consequences of the existence of the cut-off frequency are now clear. An H_{m0}-wave cannot be propagated in a rectangular wave guide if its frequency ν is less than ν_c: if such a wave is admitted at the entrance of the wave guide it changes into a standing wave (perpendicular to the axis of the wave guide) whose amplitude decreases exponentially along the axis of the wave guide, so that at some distance from the entrance it can hardly be perceived.

This result can also be interpreted in the following manner. From (27) and (31) it is directly deduced that

$$\lambda_c = \lambda_x. \quad . \quad . \quad . \quad . \quad . \quad . \quad . \quad . \quad . \quad (34)$$

One may therefore say that a wave with $\lambda > \lambda_c$ cannot be propagated in the wave guide "because" its wavelength is too great to be able to form a standing wave in the x-direction which matches the given values of a and m.

From the foregoing it is evident that the damping of the standing wave (for $\lambda > \lambda_c$) is not an absorption phenomenon, for if the walls of the wave guide are perfectly conducting no heat is developed.

When we have to do with H_{mn} or E_{mn} waves, which therefore represent standing waves both in the x-direction and in the y-direction, the cut-off wavelength is given by:

$$\frac{1}{\lambda_c} = \sqrt{\left(\frac{1}{\lambda_x}\right)^2 + \left(\frac{1}{\lambda_y}\right)^2},$$

where

$$\lambda_x = \frac{2a}{m}, \qquad \lambda_y = \frac{2b}{n};$$

a and b being the lengths of the sides of the rectangular cross section of the wave guide. From this we see that the H_{10}-wave ($m = 1$, $n = 0$) has the smallest cut-off frequency, *viz.* (assuming $a > b$):

$$\frac{c}{\nu_c} = \lambda_c = 2a. \quad . \quad . \quad . \quad . \quad . \quad . \quad . \quad (35)$$

Consequently the H_{10}-wave is very important from the practical point of view.

It can generally be proved that with any wave guide there is a cut-off frequency $\nu_c > 0$ for every wave that is not purely transverse. Now we have already seen that a purely transverse wave cannot be propagated in wave guides having a cross section bounded by one single continuous line (*e.g.* rectangular, circular or elliptical wave guides). Such wave guides act as filters, "cutting off" the low-frequency components of any electromagnetic wave entering them.

In this connection it may not be superfluous to stress the fact that in this article we are concerned only with the problem as to what modes of propagation of electromagnetic waves are possible in wave guides. Here we leave out of consideration the no less important but more difficult problem as to which of the possible waves will actually be propagated in a wave guide when, for instance, a radiating aerial is placed at the entrance of the wave guide.

Damping of the waves owing to losses

In the foregoing we have assumed throughout that the conductors were perfect and that the medium through which the waves are propagated was vacuum. In actual wave guides the medium is mostly air and the walls are not perfectly conducting. Consequently waves are always attenuated in wave guides, for the air can lead to "dielectric losses" and the finite conductivity of the metal walls to the development of Joule heat. Under normal conditions the former effect is of course negligibly small compared with the latter.

Dielectric losses can be exactly calculated by superposing plane damped waves one upon the other in the manner described. As explained in a previous chapter, k then becomes a complex number: $k = k_1 - jk_2$. The amplitudes of the field vectors of the resultant wave are each multiplied by a factor $e^{-k_2 z}$; k_1 plays the part which $k = \omega/c$ plays in vacuum. If the conductivity of the dielectric is very small then $k_1 \approx k$, so that the values of the cut-off frequency are hardly affected.

The damping of the waves caused by losses in the walls is calculated only approximately. It is assumed that this damping finds expression in the form of a factor $e^{-\alpha z}$ by which all field amplitudes are multiplied. We shall not go into the question how α is calculated but would only state that it is essential to know how the surface current is distributed over the walls. The losses are calculated by imagining this current to be "spread out" in a layer the thickness of which is equal to the "penetration depth" d.

THE PART PLAYED BY OXYGEN AND NITROGEN IN ARC-WELDING

M.F. 9120.

by J. D. FAST.

621.791.753:669.1.014.6:541.123.28

The action of oxygen and nitrogen on iron and steel is dealt with here at some length as an introduction to an article that will follow in which the function of the coating of welding electrodes will be analysed. This article is devoted to an estimation of the solubility of oxygen and nitrogen in liquid as well as in solid iron and to a discussion of the harmful and the useful effects of these elements in electric welding. As harmful effects are discussed the causation of porosity and the adverse influence upon mechanical strength, whilst the useful effects discussed are the promotion of transfer of heat and transport of the metal across the arc. This leads to a discussion also of the part played by the reaction between oxygen and carbon.

When welding by the commonly applied method of Slavianoff an arc is struck between the workpiece to be welded and a metal rod called the electrode. The latter gradually melts during the welding and thus functions not only as electrode but also as filler rod.

At first no steps were taken to protect the molten metal against the attack of the oxygen and the nitrogen in the air, with the result that very poor quality welds were obtained. When unprotected rods of mild steel containing for instance 0.1% C, 0.1% Si and 0.4% Mn are used it is found that in the transfer of the metal to the workpiece the content of these elements is greatly reduced by oxidation. On the other hand the originally very small content of oxygen and nitrogen is increased to something like 0.15% N and 0.25% O, as a chemical analysis of the bead shows. Accordingly a microscopic examination of the deposited metal may show the presence of a considerable quantity of oxide and nitride. Furthermore, there appear to be a number of cavities in the metal due to the formation of carbon monoxide through oxidation of the carbon contained in the steel and, as will be demonstrated, also to the release of nitrogen during the cooling and solidifying of the metal.

In order to obtain welds with satisfactory mechanical properties it is therefore essential to protect the metal against the attack of oxygen and nitrogen while being transferred from the electrode to the workpiece.

In principle the simplest way to provide such a protection is to carry out the welding in a gas that is absolutely free of components which react with iron. Welding in hydrogen for instance has become well-known; use is thereby made of the large quantity of heat released by the recombination of the atomic hydrogen formed in the arc. This method, however, is a rather expensive one and is consequently used only in special cases. The same applies to welding in helium and argon, as recently developed.

A more economical protection is obtained by coating the electrodes with substances which during the welding process keep the oxygen and nitrogen away from the metal, either by the development of large quantities of other gases (organic substances) or by the formation of a sealing slag on the metal (mineral substances). Frequently a combination of both these processes is applied.

In our next article we shall go fully into the protection afforded by a slag, but first of all it is necessary to study more closely the effect of oxygen and nitrogen on iron and steel, as will be done in this article. The obsolete method of welding with bare electrodes will only be referred to in so far as it will help to give a better understanding of the part played by the coating.

We shall concentrate our attention particularly upon the questions that are of importance in the technique of welding, viz:

a) The solubility of oxygen and nitrogen in liquid iron between its melting point and boiling point; this gives us an idea of the maximum quantities that may be absorbed while welding.

b) The solubility of oxygen and nitrogen in solid iron, particularly alpha iron (the form of iron which is stable below 910 °C and is body-centred cubic); this helps to gain an insight into the effect of these elements upon the mechanical properties of welds.

c) The chemical reaction between oxygen and carbon dissolved in liquid iron; this reaction is apt to cause porosity in the welds and, what is still more important, provides the propelling force for the transfer of the metal from the electrode to the workpiece.

The injurious as well as the useful effects of oxygen and nitrogen in the welding process will be discussed in the latter part of this article.

The iron-oxygen system

Solubility of oxygen in liquid and in solid iron

If liquid iron is attacked by oxygen and the pressure of the oxygen exceeds a certain value then all the metal will be gradually transformed into liquid oxide. This can be read from the partial constitutional diagram of the iron-oxygen system (*fig. 1*), when it is borne in mind that to each percentage of oxygen and each temperature there corresponds a certain partial pressure of the oxygen.

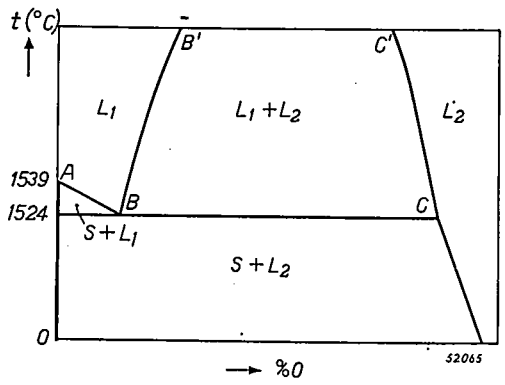


Fig. 1. Part of the constitutional diagram of the iron-oxygen system represented diagrammatically. S signifies solid iron, L_1 liquid iron with oxygen in solution, L_2 liquid iron oxide of variable composition. The line BB' is the solubility curve of oxygen in liquid iron. The solubility of oxygen in solid iron is so small that the solubility curve practically coincides with the t-axis. The position of the points C and C' does not differ much from the stoichiometric composition FeO.

Let us suppose that while maintaining a constant temperature (say 1600 °C) we cause the oxygen pressure above the liquid iron to rise gradually from zero. The state of saturation, indicated in the diagram by the solubility curve BB', will then be reached already at a very low oxygen pressure. At 1600 °C this pressure is about 10^{-8} atm. As soon as the state of saturation has been reached, then, in addition to the liquid metallic phase, a liquid oxide phase begins to form, the composition of which is given by the position of the line CC'. According to Gibbs' phase rule the pressure should remain constant (about 10^{-8} atm.) until all the metal has been transformed into this oxide phase.

If the number of independent components in a system is C and the number of phases P then according to Gibbs' phase rule the number of variables (degrees of freedom) F required to determine fully the state of the system is given by $F=C-P+2$. In the case in question for the area bounded on the left and right by the lines BB' and CC' we therefore have $F = 2-3+2 = 1$. Consequently in this area the state of the system is a function of only one variable, *e.g.* the pressure or the temperature. If we take the temperature for this variable then the pressure is a function only of the temperature. Consequently, when the value of the temperature is fixed, as we have done in this case by supposing the temperature to be constant at 1600° C, then also the pressure is fixed.

If at the constant temperature of 1600 °C the pressure of the oxygen is caused to rise further, then the liquid oxide, the composition of which on the line CC' was not far removed from the stoichiometric composition FeO[1]), gradually absorbs more oxygen. Finally at a pressure of one atmosphere an oxygen content is reached which is already greater than that corresponding to the formula Fe_3O_4.

In electric arc welding with bare electrodes the reaction time is so short that actually not all the metal is transformed into oxide, as is required by the thermodynamic equilibrium, but only a partial oxidation takes place. Immediately underneath the electrode a molten mass is formed, called the pool, consisting of a metallic phase containing oxygen and covered by a thin layer of liquid oxide. At the interface the compositions of these two phases will be as represented by the lines BB' and CC' in fig. 1. The average composition of the metallic phase, however, will be given by points a little to the left of BB' and that of the oxide phase by points a little to the right of CC'.

What is of particular importance in welding technique is the position of the line BB', i.e. the solubility of oxygen (or FeO) in liquid iron as a function of the temperature [2]). For the temperature range between 1800 °K and 2083 °K this solubility has been accurately determined by Chipman and Fetters [3]).

It is highly important to know the solubility also at higher temperatures, for there are indications that while passing from the electrode to the workpiece the metal is in many cases heated to the boiling point of iron. According to most experimental data the boiling point of iron lies somewhere between 2700 and 2800 °K.

By means of a few simple hypotheses regarding the thermal effect and the change in entropy taking place when liquid Fe is homogeneonsly mixed with liquid FeO, the following relation between solubility and temperature can be deduced [4]):

$$T = \frac{C}{R} \frac{1-2x}{\ln \frac{1-x}{x}} \quad \ldots\ldots \quad (1)$$

[1]) According to some investigators the line CC' lies to the left of the composition FeO whilst others place it to the right.
[2]) Of course the solubility can be expressed in % FeO as well as in % O.
[3]) J. Chipman and K. L. Fetters, Trans. Am. Soc. Metals 29, 953-967, 1941.
[4]) Cf. J. D. Fast, Philips Res. Rep. 2, 205-227, 1947.

T being the absolute temperature and x the solubility of FeO expressed as a molecular fraction, i.e. the number of molecules of FeO in the saturated solution divided by the total number of molecules. R is the gas constant and C a constant that has to be determined experimentally.

Formula (1) indicates that when plotting $(1-2x)/\log[(1-x)/x]$ as a function of T we should obtain a straight line through the origin. As shown in *fig. 2*, Chipman's and Fetters' measurements

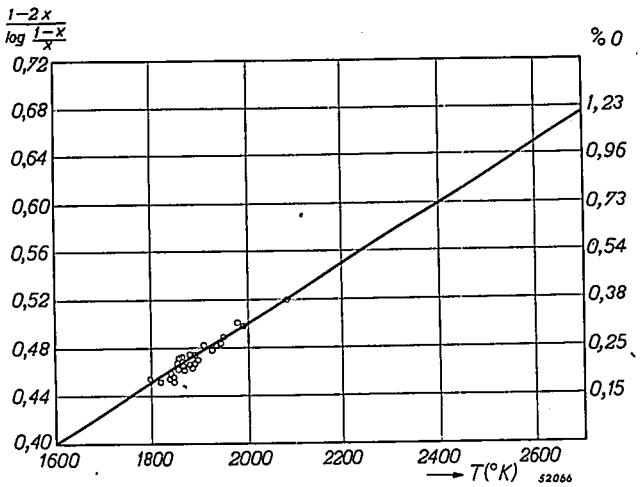


Fig. 2. The expression $(1-2x)/\log[(1-x)/x]$, where x indicates the solubility (expressed as molecular fraction) of FeO in liquid iron, as a function of the absolute temperature. To the right of the figure the values of solubility are given in wt%. The theoretical straight line (equation (1)) points to the invisible origin at 0°K. The experimental points (small circles) have been taken from the measurements of Chipman and Fetters (see footnote [3]).

satisfy this requirement quite well. The straight line in the diagram has been drawn in such a way as to point precisely towards the invisible origin at O°K. From its slope we find for the constant C in (1) the value

$$C = 18300 \text{ cal.}$$

The satisfactory agreement between theory and experiment encourages us to use equation (1) also for calculating the solubility at higher temperatures. These (calculated) solubilities can be read directly from fig. 2.

The solubility of oxygen in solid iron is so small that it could not be determined experimentally. In fig. 1 the solubility curve coincides with the t-axis.

Absorption of oxygen when welding with bare electrodes

Since the boiling point of iron lies at about 2750 °K, from fig. 2 it may be expected that when welding with bare electrodes the molten metal will always contain less than 1.2% of oxygen.

Of interest in this connection are the experiments carried out by Losana [5]). He used bare electrodes of different diameters and made of different kinds of steel. It was found that both the oxygen and the nitrogen content of the deposited metal increased as the thickness of the electrode decreased. In not a single experiment was a content found lower than 0.140% O, or higher than 0.953% O. The results of these experiments, therefore, are not in contradiction with fig. 2.

As an example taken from a series of experiments by Losana we give in *table I* the C, Mn, Si, P, S, O and N contents of the metal deposited from electrodes containing 0.10% C, 0.89% Mn, 0.17% Si, 0.015% P and 0.021% S (the balance being Fe).

Table I. Composition of the metal deposited in some of Losana's experiments [5]) when welding with bare electrodes containing 0.10% C, 0.89% Mn, 0.17% Si, 0.015% P and 0.021% S.

Wire dia. mm	C %	Mn %	Si %	P %	S %	O %	N %
1	?	?	?	?	?	0.720	0.218
2	0.026	0.054	0.039	0.010	0.019	0.550	0.180
4	0.048	0.070	0.053	0.014	0.021	0.302	0.130
6	0.068	0.124	0.058	0.014	0.022	0.140	0.105

For a more exact comparison with the theory the experiments should have been carried out with wire of pure iron. In the experiments referred to C, Mn and Si were, it is true, oxidized to a condiderable extent but by no means completely.

The drop in the oxygen content with increasing diameter of the electrode wire is probably related to the fact that the thicker the wire the larger are the droplets of metal transferred from the electrode to the workpiece. It may be that consequently the temperature of the metal crossing the arc is lower when thicker rods are used. Moreover, we have to take into account the fact that there is no time for the equilibrium of dissolution and the chemical equilibria to adjust themselves fully. In the following section we shall see from the example of the reaction between oxygen and carbon that these equilibria are in fact unable to adjust themselves in the process of welding.

The reaction between oxygen and carbon in electric arc welding

To a liquid iron phase containing small quantities of C and FeO (or O) in solution, in the state of

[5]) L. Losana, Metallurgia Italiana **26**, 391-403, 1934.

equilibrium there belongs a gas phase consisting of a mixture of CO and CO_2. The reactions that can take place between the components in the two phases are the following:

$$[FeO] + [C] \rightleftarrows [Fe] + CO \quad . . . . . \quad (2)$$

$$2\,[FeO] + [C] \rightleftarrows 2[Fe] + CO_2 \quad . . . . . \quad (3)$$

$$[FeO] + CO \rightleftarrows [Fe] + CO_2 \quad . . . . . \quad (4)$$

$$[C] + CO_2 \rightleftarrows 2\,CO \quad . . . . . \quad (5)$$

where the brackets indicate the components of the homogeneous liquid phase. Two of these equations, however, are sufficient to describe the equilibrium between the liquid and the gaseous phases, since (4) is the difference between (3) and (2), and (5) is equal to twice (2) less (3).

With the aid of thermodynamics and experimental data taken from literature it is possible to calculate the positions of the said equilibria as functions of the temperature of the steel (see the article quoted in footnote [4]). Without going into these calculations we give here in *table II* the equilibrium pressures of CO and CO_2 which should correspond to the C and O contents of the deposited metal given in table I. The calculations have been carried out for two temperatures, *viz:* 2300 °K and 2700 °K.

Table II. Calculated equilibrium pressures of CO and CO_2 (in atmospheres) corresponding to the C and O contents in table I.

% C	% O	2300 °K		2700 °K	
		P_{CO}	P_{CO_2}	P_{CO}	P_{CO_2}
0.026	0.550	10.4	1.23	14.3	0.75
0.048	0.302	11.3	0.79	15.3	0.47
0.068	0.140	7.7	0.26	10.3	0.15

The choice of 2300°K as lowest temperature is due to the fact that the highest oxygen content of deposited metal in table I of which also the C content is known is 0.55%, which according to fig. 2 would correspond already to a temperature of about 2250°K of the metal being transferred if the equilibrium between liquid iron and liquid ferro-oxide had indeed been established during the deposition process. The actual temperature was probably higher.

In the calculations which led to the pressures given in table II extrapolations were employed which may have caused errors of 10% in the results. This, however, does not detract from the conclusion obviously to be drawn from table II that when welding with bare electrodes conditions are far removed from the state of chemical equilibrium. The $(CO + CO_2)$-pressure cannot in actual fact have amounted to more than a fraction of one atmosphere.

This failure to reach states of equilibrium will prove to be of essential importance also when dealing with coated electrodes.

The iron-nitrogen system

Dissociation pressure of iron nitride

When iron was attacked by oxygen at high temperatures saturated solutions were obtained, as shown above, at O_2-pressures far below the partial pressure of this gas in the air. In the case of nitrogen the reverse is found: at high temperatures the state of saturation both for liquid and for solid iron is reached only at N_2-pressures far above the partial pressure of nitrogen in air. Consequently it has not yet been possible to reach the saturation concentrations for liquid iron. As we shall see farther on, it has however been possible to determine the concentrations corresponding to a nitrogen pressure of 1 atm.

For alpha iron [6]) it was possible to reach the condition of saturation by an artifice. Instead of N_2, mixtures of NH_3 and H_2 were caused to react with iron. As soon as the limit of solubility is exceeded a new phase is formed (the nitride Fe_4N), the dissociation pressures of which at various temperatures naturally correspond to the equilibrium pressures of the saturated solutions of nitrogen in iron. As we shall see below, these dissociation pressures can be calculated and will enable us to compute an upper limit for the solubility of nitrogen in alpha iron. We shall also see (table III) that more direct determinations of the position of the solubility line AC diagrammatically represented in *fig. 3* give greatly divergent values.

The explanation why NH_3 is so much more active than N_2 lies in the fact that the equilibrium

$$8\,Fe + 2\,NH_3 \rightleftarrows 2\,Fe_4N + 3\,H_2 \quad . . . \quad (6)$$

is reached comparatively quickly, whereas the reactions

$$N_2 + 3\,H_2 \rightleftarrows 2\,NH_3 \quad . . . . . \quad (7)$$

and

$$2\,Fe_4N \rightleftarrows 8\,Fe + N_2 \quad . . . . . \quad (8)$$

take place but very slowly. If, for instance, NH_3 is heated for a long time to 500 °C it dissociates almost entirely into hydrogen and nitrogen, since the

[6]) Alpha iron is the body-centred cubic form of iron which is stable below 910 °C. The modification of iron which is stable between 910 and 1400 °C and is face-centred cubic is called gamma iron. The body-centred cubic form is again stable between 1400 °C and the melting temperature (1540 °C) and this is now called delta iron.

stoichiometric gas mixture in the state of equilibrium at 500 °C and 1 atm contains only 0.12 vol % NH_3. When, however, iron is heated to 500 °C in a stream of $NH_3 + H_2$ the velocity of the gas can

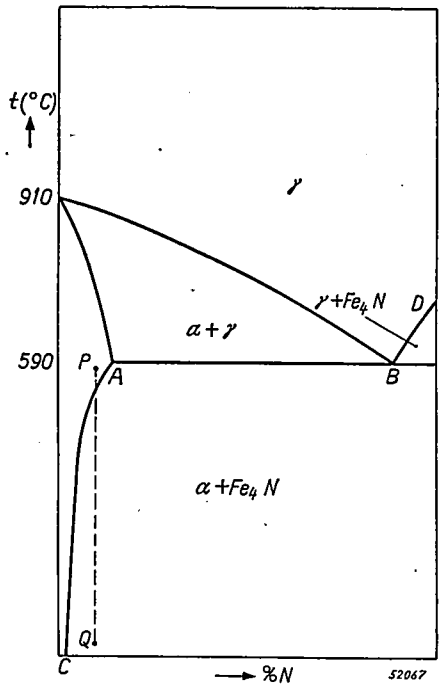


Fig. 3. Part of the constitutional diagram of the iron-nitrogen system represented diagrammatically. Here α and γ indicate respectively alpha iron and gamma iron. The solubility curve of nitrogen in solid iron is given by the lines *CA* and *BD*.

easily be chosen such that the percentage of NH_3 drops only very little. The iron then reacts with a mixture of NH_3 and H_2, which corresponds to very high nitrogen pressures in the state of equilibrium. By way of illustration, the constant of the reaction (7)

$$K_{NH_3} = \frac{p^2_{NH_3}}{p_{N_2} \cdot p^3_{H_2}} \quad \ldots\ldots \quad (9)$$

at 500 °C amounts to $1.5 \cdot 10^{-5}$. A gas mixture comprising 70 vol % NH_3 + 30 vol % H_2 of 1 atm thus corresponds at 500 °C to a nitrogen pressure

$$p_{N_2} = \frac{10^5}{1.5} \cdot \frac{(0.7)^2}{(0.3)^3} = 1.2 \cdot 10^6 \text{ atm},$$

whilst a mixture of 98 % NH_3 + 2 % H_2 corresponds even to a nitrogen pressure of about $8 \cdot 10^9$ atm [7]).

When mixtures of NH_3 and H_2 of varying composition are passed over iron at 500 °C then the formation of Fe_4N begins as soon as the NH_3 content rises above 20 vol %. The reaction takes place in the opposite direction as soon as the NH_3 content falls below 20 %. If we now substitute $p_{H_2} = 0.8$ and $p_{NH_3} = 0.2$ in (9) then we find that $p_{N_2} \approx 5200$ atm. Considering (7) and (8) this means that also the dissociation pressure of Fe_4N in equilibrium with Fe amounts to about 5200 atm N_2 at 500 °C.

In the same way we can determine the dissociation pressure for other temperatures, and from the experimental data available we deduce the following relation between the dissociation pressure of Fe_4N (in equilibrium with Fe) and the absolute temperature:

$$\log p = -\frac{1760}{T} + 5.99 \quad \ldots\ldots \quad (10)$$

According to this formula the dissociation pressure at 20 °C is already about 1 atm. The Fe_4N needles in steel, so well known in metallography, should, therefore, dissociate spontaneously; the fact that they continue to exist is due only to the inertia of this dissociation. It is the same as with iron carbide (cementite) Fe_3C, which in iron-carbon alloys should really dissociate spontaneously into iron and graphite but only does so at an imperceptibly low rate.

Solubility of nitrogen in solid iron

Some research workers understand by the solubility of nitrogen in iron something different from what we have understood it to be in the foregoing, in conformity with the conventional definition [8]). They understand it to be the amount of nitrogen contained in the metal in equilibrium with nitrogen of 1 atm. We have seen, however, that the true solubility say at 500 °C corresponds to a pressure of about 5200 atm. Now in order to be able to speak about the solubility at a certain nitrogen pressure without causing confusion we shall from now onwards call the (true) solubility as indicated in the constitutional diagram of fig. 3 by the lines *CA* and *BD* the maximum solubility.

Reliable data in respect to the solubility of nitrogen in solid iron are only available for a pressure of 1 atm. They are given by Sieverts and his collaborators [9]) and are represented by *fig. 4*.

According to Sieverts the solubility in alpha iron is 0.002 wt % at 890 °C and 0.0004 wt % at 750 °C. At these relatively low temperatures equilibrium is established so slowly that the values given

[7]) Of course these figures are not exact, because equation (9) only strictly applies as long as the gases behave as ideal gases. It would be better to substitute "nitrogen activity" for "nitrogen pressure".

[8]) This reads: solubility is the maximum quantity that can be absorbed without a new phase beginning to form.

[9]) A. Sieverts G. Zapf and H. Moritz, Z. physik. Chem. A **183**, 19-37, 1938.

are less reliable than those for gamma and delta iron (see note 6). Now the iron atoms in alpha as well as in delta iron form a body-centred cubic lattice and it is therefore to be expected that one continuous curve

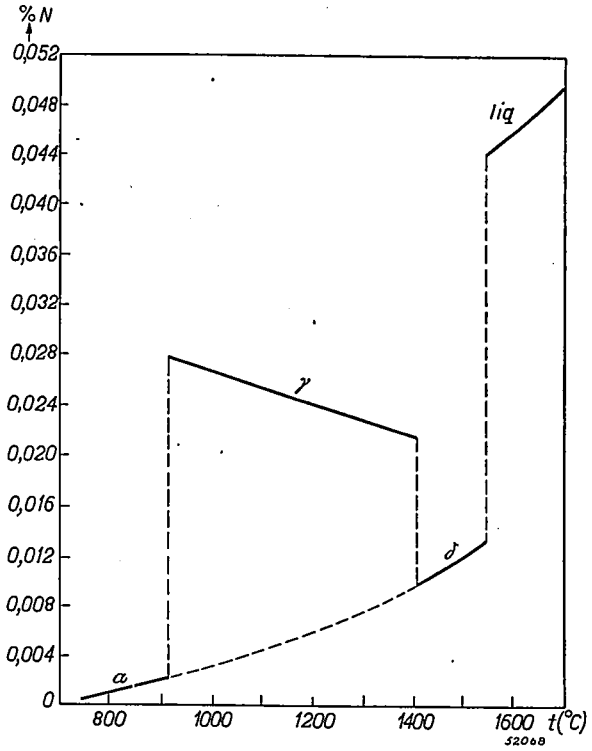


Fig. 4. Solubility of nitrogen in iron at 1 atm nitrogen pressure as function of the temperature. The curves drawn for solid iron correspond to the measurements of Sieverts and his collaborators (see footnote [9])) and for liquid iron to the measurements of Kootz (see note [14])). It is to be noted that for liquid iron various investigators find different values. For instance according to Chipman and Mutphy (Trans. A.I.M.E. **116**, 179-196, 1935) the solubility immediately above the melting point is about 10% lower and according to Sieverts about 30% lower.

can be drawn through the points of alpha and delta iron. This does indeed prove to be the case (see dotted line in fig. 4) and it makes the points for alpha iron more reliable. According to fig. 4 the solubility in the gamma phase, stable between 910 °C and 1400 °C, and the solubility in liquid iron are much greater than that in alpha (delta) iron.

Now in order to be able to say something about the *maximum* solubilities on the grounds of these experimetal data, we shall avail ourselves of the fact that the concentration of a bi-atomic gas in a metal is in general approximately proportional to the square root of the pressure.

From the example of nitrogen this can be realized as follows. The reaction constant K of the dissociation $N_2 \rightleftarrows 2N$ in the gas phase is given by

$$K = p_N^2/p_{N_2}.$$

The pressure of the atomic nitrogen p_N is thus proportional to the square root of that of the molecular nitrogen p_{N_2}. The nitrogen is dissolved in the metal in the atomic state and, since its concentration in iron is small, it will be proportional to p_N and thus also to $\sqrt{p_{N_2}}$. Here, at not very high temperatures p_{N_2} is virtually equal to the total pressure.

Now the temperature coefficient of the solubility in alpha iron is positive, so that the given solubility of 0.0004 % N at 750 °C is certainly an upper limit for the solubility (still at 1 atm) at temperatures lower than 750 °C. For the solubility C (in weight % N) at some other pressure we have

$$C < 0.0004 \sqrt{p_{N_2}} \quad \ldots\ldots \quad (11)$$

An upper limit of maximum solubility is then immediately found by substituting for p_{N_2} the dissociation pressure of Fe_4N as calculated from (10). If it is desired to avoid this pressure, which only arises as a secondary quantity, then one may combine directly the formulae (9) and (11) and write

$$C_{max} < \frac{0.0004\, p_{NH_3}}{\sqrt{K_{NH_3} \cdot p_{H_2}^3}}, \quad \ldots\ldots \quad (12)$$

where p_{NH_3} and p_{H_2} are the partial pressures of NH_3 and H_2 in the gas mixture of 1 atm at which the maximum solubility is reached and the formation of Fe_4H begins.

Thus we find the values given in column 2 of *table III* for the upper limit of maximum solubility.

The values of maximum solubility found experimentally by the various research workers do not by

Table III. Values of the upper limit of maximum solubility of nitrogen in alpha iron calculated for various temperatures, and the experimental values of maximum solubility found by various investigations.

Temp. (in °C)	Maximum solubility (in weight %)			
	calculated (upper limit)	measured		
590	0.040	0.5 [10])	0.42 [11])	0.13 [12])
550	0.035			0.05 [12])
500	0.030			
450	0.025		0.32 [11])	
400	0.020			0.02 [13])
300	0.010			0.01 [13])
200	0.005			0.005 [13])
100	0.002			0.001 [13])
20	0.0004			

[10]) A. Fry, Stahl und Eisen **43**, 1271-1279, 1923.
[11]) O. Eisenhout and E. Kaupp, Z. Elektrochem. **36**, 392-404, 1930.
[12]) D. Séférian, Etude de la formation des nitrures de fer par fusion et du systéme fer-azote. Paris 1935.
[13]) W. Köster, Arch. Eisenhüttenwes. **3**, 637-658, 1930.

any means agree one with the other, as may be seen from column 3 of this table. Remarkably enough, our calculated values correspond almost completely with Köster's experimental values [13]). Even the lowest values taken from literature are therefore probably to be regarded as an upper limit.

Solubility of nitrogen in liquid iron and absorption of this element when welding with bare electrodes

In the foregoing we have considered the solubility of nitrogen only in solid iron. In order to judge the maximum amount of nitrogen that might be absorbed during the process of welding we should have to know the solubility of nitrogen in liquid iron. Considering that welding is usually done in air, at a pressure of 1 atm, the partial pressure of nitrogen then being about 0.8 atm, the solubility at 0.8 atm nitrogen pressure is of particular importance to us.

Various investigators have determined the solubility of nitrogen in liquid iron at 1 atm nitrogen pressure. The highest and possibly the most reliable values were found by Kootz [14]). The solubility $C_{1\,\mathrm{atm}}$ at 1 atm as a function of the absolute temperature T can be represented, according to his measurements, by the formula

$$\log C_{1\,\mathrm{atm}}\ (\text{in wt. \% N}) = -\frac{1170}{T} - 0.715 \quad . \quad (13)$$

Substituting for T the boiling temperature of iron, about 2750 °K, we find a nitrogen content of 0.072 %. Considering that the nitrogen pressure is only 0.8 atm, this value has to be reduced to $0.072\sqrt{0.8} = 0.065$ %. For $T < 2750$ °K equation (13) would yield still smaller values of solubility.

Now Losana's measurements (see table I) and also those of other investigators show that when welding with bare electrodes nitrogen may be absorbed in quantities three to four times as much as the maximum quantity (0.065 %) conformable to equation (13).

In our calculations, however, it has been tacitly assumed that the liquid iron is in contact with nitrogen of the same temperature. In point of fact this is certainly not the case, for all available experimental data indicate that temperatures of at least 6000 °K are reached in the welding arc. At this temperature the concentration of atomic nitrogen in the gas phase is already about 10^5 times as great as that at the boiling point of iron [15]). Taking this into account it is surprising that not a still greater nitrogen content is found when welding with bare electrodes. As we shall see from what follows, in the deposition of the metal more nitrogen is indeed absorbed but this is partly released again in the cooling down and solidifying of the metal.

Injurious effects of oxygen and nitrogen

Porosity

As already stated, highly porous beads are obtained when welding with bare electrodes. Everywhere in literature we find that this is caused by the formation of CO as a result of the reaction between the oxygen absorbed while welding and the carbon always present in technical iron and steel.

Our foregoing considerations led us to presume that this is only half the truth and that also nitrogen is to be regarded as a cause of porosity. In order to investigate this we prepared an iron entirely free of carbon and made plates of it 10 mm thick and rods 4 mm in diameter. With these carbon-free rods beads were welded on the carbon-free plates and, as was expected, these were found to be almost as porous as the beads obtained when using normal technical wire and plates both containing about 0.1 % C.

Apart from the formation of CO there is obviously another cause of porosity, and this may be assumed to be the release of part of the dissolved nitrogen.

Mechanical strength

The mechanical strength of welds is very often judged by measuring the impact value, i.e. the energy required to break in half in one blow a bar of iron of certain dimensions in which a certain notch has been made.

Owing to the great porosity and the high oxygen and nitrogen content (see table I) welds made with bare electrodes have such a low mechanical strength that there is hardly any sense in measuring their impact value. In a subsequent article we shall see that welds made with modern coated electrodes have much lower but still relatively high oxygen and nitrogen contents, the nitrogen content varying from about 0.005 % to about 0.033 % according to the type of electrode and the oxygen content from about 0.03 to about 0.12 %. It appears that a lower nitrogen content is always accompanied by a lower oxygen content and a higher impact value. Since the oxygen and nitrogen contents vary in the same direction it is not possible to determine from tests on welds the effect that each of these elements separately has on the impact value.

We have therefore carried out a number of experiments with iron of the composition of the bare

[14]) T. Kootz, Arch. Eisenhüttenwes. **15**, 77-82, 1941.
[15]) J. D. Fast, Philips Res. Rep. 2, 382-399, 1947.

electrodes, first removing oxygen and nitrogen by repeated high-frequency melting in pure argon and then adding known quantities of one impurity at a time (nitrogen or oxygen) [16]). These experiments have shown that up to a content of 0.033 % nitrogen does not affect the impact value, whereas the addition of oxygen up to the aforementioned content of 0.12 % is accompanied by a gradual lowering of the impact value.

Furthermore, the experiments indicate that the great influence of oxygen on the impact value is due to the fact that this element is present in the form of an oxide which is partly contained along the crystal boundaries. Consequently the metal readily breaks between the crystals.

Ageing

Both after rapid cooling and after mechanical working steel is apt to be unstable, gradually increasing in hardness and decreasing in ductilily. One then speaks of "ageing", in the former case "quench ageing" and in the latter case "strain ageing". These processes may be accelerated by heating to 100 or 200 °C.

Ageing after mechanical working is particularly of great technical importance an a great deal has been published on this subject. Many investigators attribute this strain ageing to the presence of oxygen, whilst many others ascribe it to the presence of nitrogen. The cause of the controversy lies in the fact that the experiments have been carried out with technical steels containing both oxygen and nitrogen.

By studying this phenomenon with iron and steel, specially made in this laboratory, not containing both these impurities together, it has been possible to arrive at the definite conclusion that nitrogen causes strain ageing whereas oxygen does not.

Apparently this is related to the fact that nitrogen has a certain solubility in alpha iron (a solubility decreasing with temperature), whereas oxygen is practically insoluble in alpha iron (cf. figs. 1 and 3). Consequently supersaturated solutions of nitrogen in alpha iron may easily be obtained, for instance by rapid cooling from P to Q in fig. 3. If there is a great supersaturation there may be a spontaneous precipitation of finely divided Fe_4N (quench ageing). If there is only slight supersaturation (for instance after comparatively slow cooling) then one can imagine that mechanical working is necessary to start precipitation (strain ageing). It is also possible that in the latter case it is not so much a question of precipitation of a new phase as the occurrence of changes in concentration in the homogeneous solution, which have an adverse effect upon ductility.

As table III shows, the solubility of nitrogen in alpha iron at room temperature is at most a few ten-thousandths per cent and therefore even very small quantities of nitrogen may be expected to cause phenomena of ageing. This is borne out by our experiments.

Useful effects of oxygen and nitrogen

Transmission of heat

Wyer [17]) has pointed out that heat transfer to the metal is governed to a high degree by dissociation of the gas in the arc, not only when welding in hydrogen but also when welding in air.

Dissociation of the oxygen and nitrogen requires a great deal of energy and consequently the arc voltage is greater than that in a monatomic gas. The atoms recombine for the greater part on the surfaces of the electrodes. thereby releasing again their dissociation energy.

Transfer of the metal

Of fundamental importance is the influence that oxygen in combination with carbon exercises upon the transfer of the metal from the electrode to the workpiece.

At first sight it always appears strange that it should be possible to weld "overhead", the droplets being "shot" upwards against the force of gravity. Various investigators have already pointed out that one of the factors playing a part here is the production of gases during the melting of the metal.

To throw more light upon this question we have carried out some experiments with 4 mm wire made of the carbon-free iron mentioned in the section on "Porosity". Overhead welding was found to be impossible with bare electrodes of this kind. Droplets were formed at the end of the electrode but they ran downward along the rod. The experiments were repeated with the same kind of iron but with 0.1 % C added, when it was indeed found possible to obtain an upward transfer of the metal.

We have already seen (table I) that when welding with bare electrodes the C content drops to very low values as a consequence of the reaction with oxygen. The experiments described above give the impression that this reaction leads to small explosions in the melting metal which act as propelling forces upon the drops.

[16]) J. D. Fast, Philips Res. Rep., to appear shortly.

[17]) R. F. Wyer, Gen. Electr. Rev. 42, 170-172, 1939.

The experiments described seem to show that any other propelling forces which may act besides the development of CO and which have been summed up by Sack [18]) in this journal do not play any important part. These other forces must exercise their influence also when welding with carbon-free rods but they prove to be incapable of overcoming the force of gravity in the transfer of the metal.

Apart from the already mentioned objections attached to welding with bare electrodes, overhead welding with these electrodes, even if they contain carbon, is hardly practicable on account of the fact that owing to the absence of a "cup" much of the metal is thrown off laterally.

If the formation of CO in the metal is indeed the propelling force when welding with bare electrodes, then not only the absence of carbon (even when oxygen is present) but also the absence of oxygen (even when carbon is present) must neutralize the welding action proper. This conclusion is borne out by experiments of Doan and Smith [19]). They welded with bare electrodes in different gas atmospheres. In helium, argon and nitrogen the droplets just fall apparently under the action of gravity. There is no arc blow and no crater is formed (an elliptical depression in the molten or solidified pool underneath the tip of the electrode). Consequently there is little penetration. The addition of only a few per cent of oxygen to the inert gas was sufficient to make the welding normal; the droplets are then driven out with force, a crater is formed and the penetration is normal.

In welding with coated electrodes too the development of gases is fundamental for the transfer of the metal. With the best coated electrodes, however, these gases are not formed by the reaction between oxygen and the carbon in the metal because the coating affords protection against this oxidation. The production of gases then takes place in the coating and, as we shall see in a later article, constitutes one of the most important functions of the coating.

[18]) J. Sack, Philips Techn. Rev. 4, 9-15, 1939.
[19]) G. E. Doan and M. C. Smith, Welding J. 19, 110s-116s, 1940.

ABSTRACTS OF RECENT SCIENTIFIC PUBLICATIONS OF THE N.V. PHILIPS' GLOEILAMPENFABRIEKEN

Reprints of the majority of these papers can be obtained on application to the Administration of the Research Laboratory, Kastanjelaan, Eindhoven, Netherlands. Those papers of which no reprints are available in sufficient number are marked with an asterisk.

R 42: W. Elenbaas: influence of cooling conditions on high-pressure discharges (Philips Res. Rep. 2, 161-170, 1947, No. 3)

The influence of cooling on high-pressure discharges in tubes and in free air is theoretically discussed and for the case of discharges in tubes verified experimentally. The agreement between experiment and theory is satisfactory.

R 43: H. C. Hamaker, H. Bruining and A. H. W. Aten Jr.: On the activation of oxide-coated cathodes (Philips Res. Rep. 2, 171-175, 1947 No. 3)

To obtain a satisfactory emission from an oxide-coated cathode, the degassing of the tube and the various parts inside it must be carried out in a special order and the correct pumping procedure has to be found for each type of tube. One of the factors influencing the cathode-emission has been made the subject of a special investigation which led to the following conclusions: a) glass heated to 400 °C evolves a small amount of hydrochloric acid; b) in a vacuum tube this HCl reacts with the carbonate or the oxide to give $BaCl_2$ or $SrCl_2$; c) when the cathode is subsequently heated these chlorides evaporate and condense on the grid and the anode; d) under electron bombardment the chlorides decompose, thereby producing Cl-atoms or Cl-ions which poison the cathode.

R 44: F. A. Kröger: Photoluminescence in the quaternary system $MgWO_4$ - $ZnWO_4$ - $MgMoO_4$ - $ZnMoO_4$ (Philips Res. Rep. 2, 177-182, 1947, No. 3)

In the quaternary system (Mg, Zn) (W, Mo)O_4 four different crystal structures appear. The fuorescence and absorption of products of these structures are studied.

R 45: F. A. Kröger: Luminescence of solid solutions of the system $CaMoO_4$ - $PbMoO_4$ and of some other systems. (Philips Res. Rep. 2, 183-189, 1947, No. 3)

As shown in a previous paper, the fluorescence of solid solutions of (Zn, Mg)WO_4 can be interpreted simply as the superposition of the fluorescence of its two components; but in the systems (Ca, Pb) WO_4, (Sr, Pb)WO_4 and (Ba, Pb)WO_4 new emission bands were observed which were attributed to tungstate groups with mixed surroundings of lead and calcium, strontium or barium ions. In this paper the systems (Ca,Sr)WO_4, (Ca,Sr)MoO_4, and $(Ca,Mg)_3$ WO_6 are shown to behave as (Zn,Mg)WO_4, whereas (Ca,Pb)MOo_4 behaves as (Ca,Pb)WO_4.

R 46: R. Loosjes and H. J. Vink: The i,V-characteristic of the coating of oxide cathodes during short-time thermionic emission. (Philips Res. Rep. 2, 190-204, 1947, No. 3)

The potential differences existing across an oxide coating during short-time emission (condenser discharge with an "RC-time" of 10^{-4} sec) have been measured.

For this purpose a new measuring method was worked out. Using this method it was found that at current densities of about 5-10 A/cm² remarkable high potential differences exist across the oxide coating (50-200 V) at the normal working temperature (900-1100 °K) at which the experiments were carried out.

R 47: J. D. Fast: The reaction between carbon and oxygen in liquid iron. (Philips Res. Rep. 2, 205-227, 1947, No. 3)

The main subject of this article is the reaction between FeO and C. Assuming a mixture of liquid Fe and liquid FeO to possess a Gibbs entropy of mixing and a van Laar heat of mixing, the activity of FeO in liquid Fe is computed and compared with observed solubilities. Next the activity of C in Fe is derived by comparing the composition of CO-CO_2 gas phases in equilibrium with liquid iron and with graphite, using spectrocopic and thermal data. The quotient $(p_{CO} \cdot a_{Fe})/(a_{FeO} \cdot a_C)$ computed from the activities is a constant only if the C-concentration < 0.1 percent by weight. This is confirmed by independent arguments.

R 48: C. J. Bouwkamp: Calculation of the input impedance of a special antenna. (Philips Res. Rep. 2, 228-240, 1947, No. 3)

A calculation is given of the input impedance of antenna consisting of a vertical wire fed against a

system of two or four equal horizontal wires. The latter are placed end to end and symmetrically around the base of the antenna proper. The investigation is based on the assumption of sinusoidal current distribution. For a quarter-wave antenna the radiation resistance is found to be approximately 20 ohms, both for two-wire and for four-wire systems.

R 49: F. L. H. M. Stumpers: On a non-linear noise problem (Philips Res. Rep. 2, 241-259, 1947, No. 4)

A rectangular noise spectrum is applied to a valve with a non-linear current-voltage characteristic. The energy frequency spectrum is computed. It is shown that the partial spectra resulting around multiples of the original central frequency have different forms. They are distinguished by their order. If the characteristic is given in the form of a polynomial or of a power series, a formula is obtained fom which all partial spectra can be computed directly. Finally, the presence of one or more carriers is taken into account.

R 50: J. L. Meyering and M. J. Druyvesteyn: Hardening of metals by internal oxidation, II. (Philips Res. Rep. 2, 260-280, 1947, No. 4)

As was described in Part I, certain alloys of Ag, Cu and Ni with a few atomic % of a homogeneously dissolved metal having a suffiicent affinity for oxygen can be dispersion-hardened by diffusing O into them. Two conditions must be satisfied. Firstly the oxide must be formed not as a surface layer but dispersed in the interior of the alloy. In this connection the penetration of the reaction front and the oxide concentration was calculated. Secondly the dispersion must be very fine. The greater the affinity for O of the basic metal, the greater must be the affinity of the solute to produce oxide that conglomerates slowly enough. This was worked out in a tentative thermodynamical scheme.

In Part II diffusion coefficients of O in internally oxidized alloys of Ag and Cu are given. X-ray and and electrical resistivity measurements support the view that the MgO and Al_2O_3 particles that harden silver are very small. The mechanical properties are not much affected by long annealings at high temperature. Creep and recrystallization are slowed down considerably. A drawback is the intercrystalline brittleness of these materials, which is less serious when somewhat smaller hardness is aimed at. Single crystals are completely ductile. Some peculiar metallographic effects are explained.

R 51: T. H. Oddie and J. L. Salpeter: Minimum-cost chokes (Philips Res. Rep. 2, 281-312, 1947, No. 4)

A design method is developed for chokes carrying A.C. only, to enable the most economical dimensions to be found for any given electrical characteristics. Formulae and tables are given for rectangular types of chokes with and without limitations on the stacking height. It is also shown briefly how the method may be applied to chokes carrying D.C. with superimposed A.C.

R 52: A. J. Dekker and W. Ch. van Geel: On the amorphous and crystalline oxide layer of aluminium (Philips Res. Rep. 2, 313-319, 1947, No. 4)

Aluminium can be covered electrolytically with a porous layer of aluminium oxide, and oxidation afterwards in boric acid gives rise to the formation of a crystalline layer. The experiments described below show undoubtedly that this layer only fills up the holes of the amorphous Al_2O_3. Moreover, there is a correlation between the current density in oxalic acid and the porosity of the amorphous layer thus formed.

VOL. 10 No. 2, pp. 37-68 AUGUST 1948

Philips Technical Review

DEALING WITH TECHNICAL PROBLEMS RELATING TO THE PRODUCTS, PROCESSES AND INVESTIGATIONS OF THE PHILIPS INDUSTRIES

EDITED BY THE RESEARCH LABORATORY OF N.V. PHILIPS' GLOEILAMPENFABRIEKEN, EINDHOVEN, NETHERLANDS.

A DIAGNOSTIC X-RAY APPARATUS WITH EXPOSURE TECHNIQUE INDICATION AND OVERLOAD PROTECTION

By A. NEMET *), W. A. BAYFIELD *), and M. BERENDEI *).

621.386.1: 616-073.75

In order to obtain radiographs of the highest possible quality with a given diagnostic X-ray apparatus, in general it is desirable to choose the voltage at the X-ray tube, the tube current and the exposure time in such a way that the tube is loaded to the permissible focus temperature. With a universal diagnostic apparatus described earlier in this Review, this was achieved by allowing the operator to select the voltage and the exposure time only, the current then being adjusted automatically to its maximum permissible value. In many cases, however, a certain freedom of choice, together with a clear insight of other possible settings will be preferred. Owing to these considerations, Philips Electrical Ltd, London, has developed an apparatus featuring a clear survey of all permissible and non-permissible settings by means of a special signalling system, and an overload protection which on selecting a non-permissible setting (i.e. which would cause the X-ray tube to be overloaded) automatically renders impossible the switching on of the high tension generator. For complete reliability of the protection and the signalling system, severe demands were to be imposed on the reproducibility of the voltage, current and time setting. Among the measures taken with a view to meeting these requirements and described in this article, one of the most interesting is that regarding the voltage drop in the tube circuit: this voltage drop for every mA setting is brought to a constant value by means of a bank of resistances, from which the appropriate one is selected by the mA control handle and connected in series with the primary coil of the high tension transformer.

With fixed tube voltage, the radiation output of an X-ray tube increases proportionally as the tube current is increased. A limit to this is imposed by the development of heat in the focal spot: the temperature of the anode at this spot must not exceed a certain value. The current rating with which the permissible temperature will be obtained depends on the time during which the tube current flows.

Thus, when making a radiograph with a given X-ray tube, for every choice of tube voltage and exposure time a maximum permissible value of the tube current will exist. The relation between these three variables may be represented by a diagram with a series of curves, the so-called rating chart. As an example, *fig. 1* shows the rating chart of the "Rotalix" X-ray tube with 2 mm focus when working on full wave rectification.

With a given tube, where there is involuntary movement, sharper images will (other things being equal) be obtained on increasing the tube current, as this diminishes the exposure time necessary for producing the desired film density. Therefore, in general, it is desirable that the operator, when choosing tube voltage, current and exposure time for a radiograph, goes right to the limit of what he is allowed by the rating chart.

The designer of X-ray apparatus can proceed in different ways to aid the operator in using the tube always in the described optimal manner. The most radical solution of the problem consists in abolishing entirely the free choice of the tube current by the operator and in ensuring instead, by means of a suitable control mechanism, that on

*) X-Ray Development Laboratory, Philips Electrical Ltd, London.

choosing the voltage and the exposure time the current is rated automatically to its maximum permissible value. A diagnostic apparatus with this principle incorporated was described several years ago in this Review [1]).

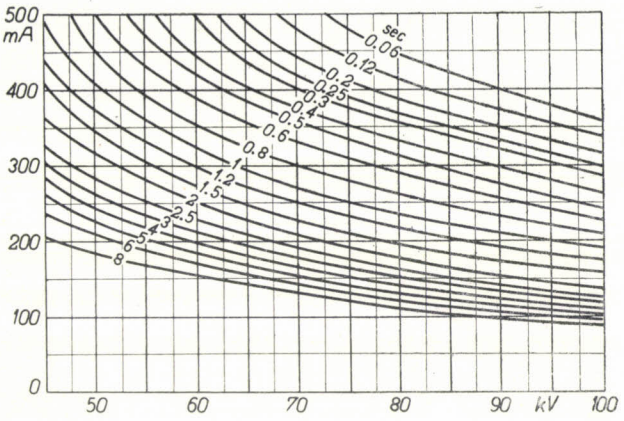


Fig. 1. Rating chart of a "Rotalix" X-ray tube with 2 mm focus when loaded with full wave rectified A.C. For a number of values of the exposure time, taken as a parameter, the maximum permissible tube current is plotted against the adjusted voltage (in kV_{peak}). Thus, for every combination of tube voltage, tube current and exposure time obtained from the chart, the focus is heated exactly to the permissible temperature.

There is no doubt that this method has important advantages and gives the most satisfactory results. There remains, however, the possibility that some operators may find that complete automatism is a disadvantage under certain circumstances. For instance, where it is desired to follow a known exposure technique or to develop and reproduce new exposure factors, greater flexibility is a desirable feature. Furthermore, with the completely automatic method referred to above it is not practicable for the manufacturer to make an apparatus delivering for every one of the hundreds of combinations of possible voltage and time adjustments the exact value of the corresponding permissible current. In a practical approximation, the tube current may be underrated by say 30 % for the most unfavourable combination [2]). Although in normal cases this does not mean an appreciable loss of quality of the radiograph, it is quite likely that for difficult objects the operator will miss this difference.

So it may be stated that, in addition to the radical method described, which is based on a complete automatisation, there is room for a less radical method, asking more deliberation from the operator and on the other hand offering him more latitude and more possibilities. A diagnostic apparatus (DX 4) making use of such a method and developed by Philips Electrical Ltd, London, will be discussed in this paper.

General description of the apparatus

As the apparatus, apart from the control method and some other features which will be described in detail, is designed on the same general lines as the diagnostic apparatus previously reported in this Review [1]), we shall only give a brief general description.

The apparatus consists of two units: the high tension generator cabinet — housing the high tension generator with its auxiliary gear and a remote controlled high tension switch — and the control table; these are linked by a flexible connecting cable. A maximum of three different X-ray tubes, one of which may be of the double focus type [3]), may be connected to the generator unit, so that

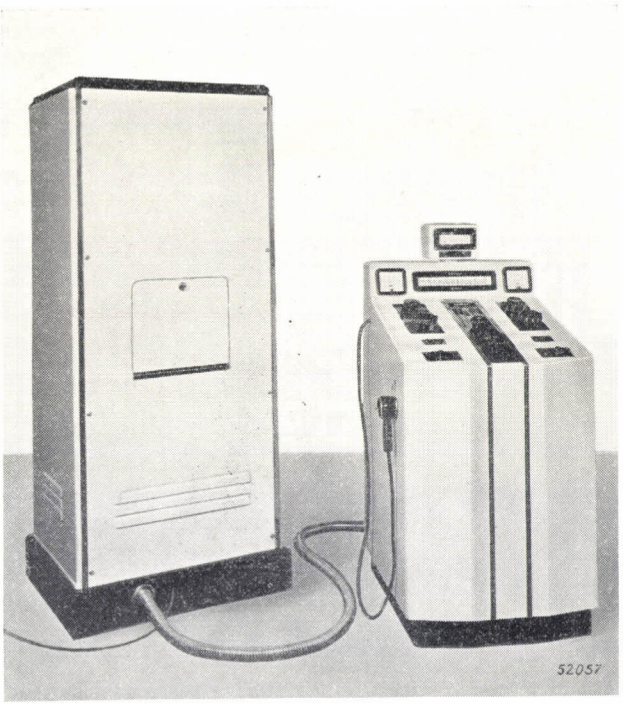


Fig. 2. The universal diagnostic X-ray apparatus described in this paper (D X 4) consists of two units: on the left hand the high tension generator cabinet, containing the high tension transformer, rectifying valves and a high tension switch, for supplying various X-ray tubes; on the right hand the control table containing the switch gear for energizing the X-ray tube for taking radiographs and for screening, control apparatus for making the desired settings for a radiograph, various meters and auxiliaries. A hand switch for taking exposures is attached to the control table by a flexible lead.

[1]) H. A. G. Hazeu & J. M. Ledeboer, A universal diagnostic X-ray apparatus, Philips Techn. Review **6**, 12-21, 1941.

[2]) Cf. the article mentioned under [1]).

[3]) A tube of this type is dealt with e.g. in Philips Techn. Review **8**, p. 327 (fig. 7), 1946 (No. 11).

four focal spots are available. By means of a focus selector switch in the control desk and the high tension switch mentioned above, any one of these may be selected.

The generator contains a high tension transformer and four rectifying valves of the high vacuum type in a bridge circuit. Thus, the output of the generator is pulsating D.C. By means of an autotransformer, the primary voltage of the high tension transformer is controlled so that the tube voltage may be varied between 45 and 100 kV_{peak} in 23 steps of $2^1/_2$ kV.

The generator also contains two filament transformers, for feeding the filaments of double focus X-ray tubes. A variable resistance in the primary circuit of these transformers permits the adjustment of the output current in 10 steps from 25 to 500 mA, mean value.

The switching of the high tension for producing a radiograph is effected by a time switch operating a high speed contactor, allowing 26 different time settings, from 0.02 to 9 seconds. During screening the time switch is inoperative, the tube current in this case being adjustable from 1 to 5 mA by means of a stepless control. The tube voltage control for screening is also stepless.

All these adjustments are read on calibrated scales on the control table.

In addition to the switches mentioned, the control table also contains a number of auxiliary switches such as room light switches, fan switches for X-ray tubes with fan cooling and a selector switch for the selection of external accessories such as a Potter-Bucky diaphragm, a serial changer for stomach radiography, a planigraph movement of tube and film, and so on. The limited scope of this article does not permit the description of all these more or less conventional details. As a substitute we give a few photographs of the complete apparatus and of the control table (*figs. 2* to *4*), the legends conveying some further information. Several important features will be discussed in connection with the control method, which we shall describe in the following section.

Control method and automatic overload protection of the tube

The idea of the control method incorporated in the present apparatus [4]) is to give the operator, when selecting voltage, current and exposure time, at any moment a clear survey of the relation between the combination actually selected and the series of other possible combinations, so that he may see how far he has approached the limit. At the same time the apparatus must contain a safeguard automatically rendering the exposure impossible when the operator has selected a combination which is not permissible, i.e. which would cause overloading of the tube.

Overload protection

We shall first consider the realization of the second object, the protection of the tube. For this purpose a relay contact is connected in series with the energizing circuit of the main contactor, the

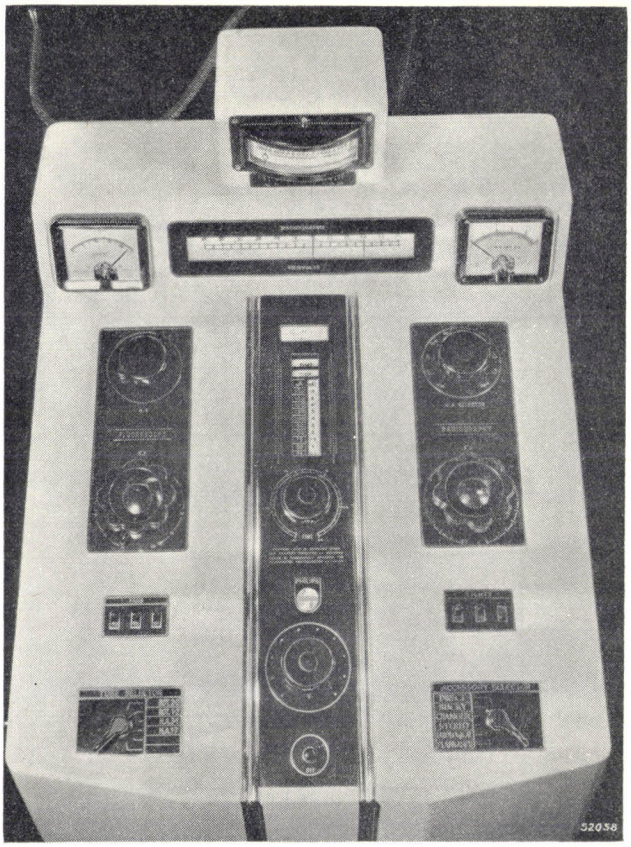


Fig. 3. Desk of the control table. On the left: the two control knobs for the tube current and tube voltage on screening; on the right: the corresponding handles for taking radiographs; in the centre; the exposure time selector with the signalling system described below. In the lower part: the tube and focus selector handle (left), a selector switch for various external accessories (right) and between these the "off" switch of the apparatus and the mains compensating switch. The mains compensation is checked on the meter on top left part, the meter on the opposite side indicating the tube current on long exposures (1—8 secs.). The same meter indicates on a separate scale the tube current on screening, and by a simple change-over it can be used for reading the filament current of the X-ray tube. This is an important help, as small deviations of the filament current, due to errors in the pre-setting or to small variations in the resistances of contacts, would impair the control technique described below. The top centre meter indicates the mAsec: it is switched on automatically with exposures of less than 1 sec; beneath this meter is the indicator of tube kilovoltage for radiography. The kilovoltage for screening is engraved on the corresponding control knob.

[4]) A. F. Jeans, Brit. Pat. 571243.

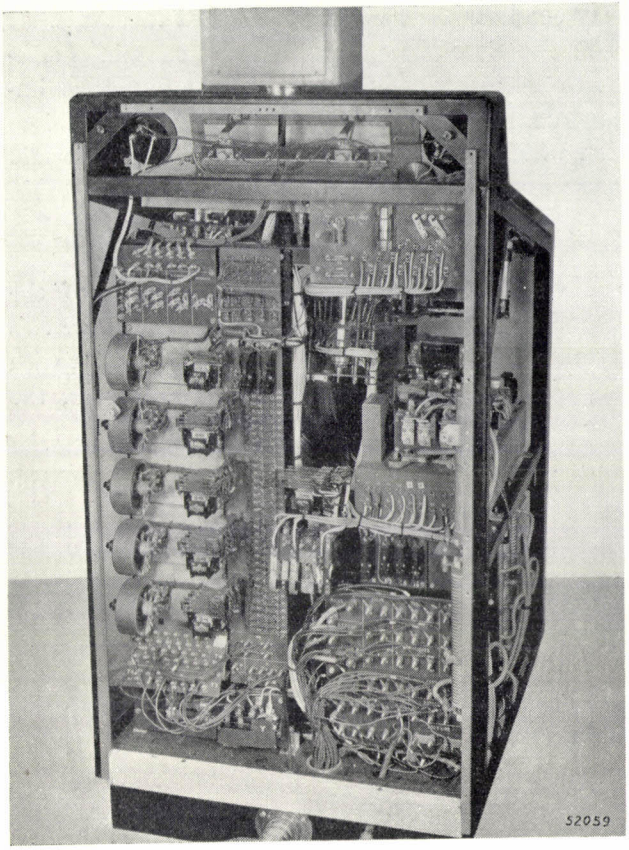


Fig. 4. Back view of the control table with panel removed. To the right from the centre the time switch is visible, to the left the control units for the setting of the tube current for the four different foci. The control mechanism proper is not visible on this photograph.

relay coil being supplied by the current in an auxiliary circuit. Whether the contactor can be operated by the time switch and the tube loaded will thus depend on the auxiliary circuit being closed. This circuit is interrupted in one place, and the connection between the two terminals, P_1 and P_2, is controlled by the selection of the tube voltage, tube current and exposure time in the following manner.

By means of selector arms (A_1, A_2) mounted on the shafts of the control knobs for the tube voltage and tube current, one of the terminals (P_1 in *fig. 5*) is connected, for every combination of selected voltage and current, to a corresponding contact stud S_i. The number of studs S provided is equal to the number of possible combinations of kV values and mA-values, i.e. in our case 23·10 = 230. Let us imagine that these contact studs are arranged on a rectangle, all studs corresponding to a common kV value lying on a vertical line and all studs with a common mA value on a horizontal line. Hence, the studs represent a picture of the coordinate system of the rating chart; cf. Fig. 5.

The second terminal (P_2) of the auxiliary circuit ends in a selector arm coupled to the exposure time control knob, which for every time setting connects this terminal to a corresponding contact stud of a series of 26 studs T.

Each contact stud S_i is linked permanently to the contact stud T_k belonging to the longest exposure time permissible with the combination "S_i" of voltage and current. Thus, when this "T_k" with the voltage-current combination "S_i" are selected, the auxiliary circuit is closed and the exposure can take place.

There exist, however, a number of other voltage-current combinations with the same maximum permissible exposure time "T_k". Such combinations are indicated by the curve of the rating chart belonging to that time (Fig. 1). All contact studs S corresponding to these combinations are also permanently connected to the contact T_k and hence linked mutually. These chains of connections, each chain belonging to one of the contacts T,

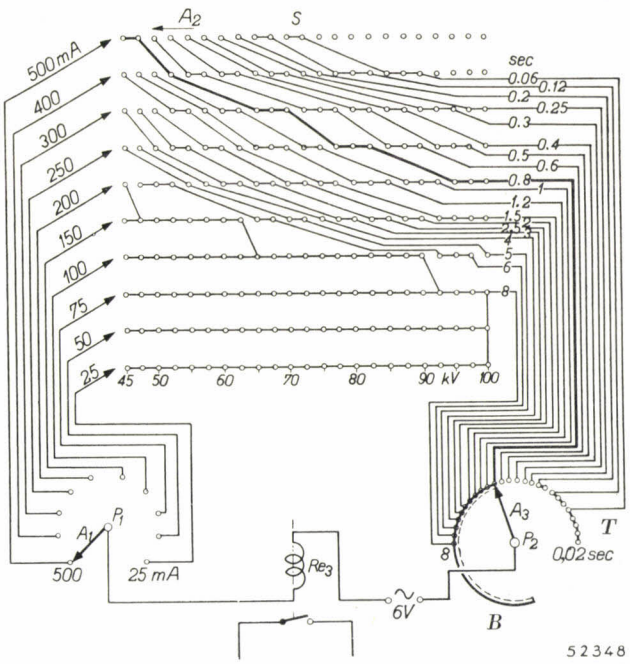


Fig. 5. Schematic representation of the auxiliary circuit used for the overload protection of the X-ray tube. If relay Re_3 is de-energized, the supply for the high tension transformer is interrupted and no exposure is possible. This depends,therefore, on a connection being established or not between the terminals P_1 and P_2. By means of selector arms A_1, A_2 coupled to the control handles for the current and the voltage settings (the form of A_2 will be explained in the following), the terminal P_1 is connected to one of the 230 contact studs S corresponding to the 230 possible voltage-curernt combinations. The selector arm A_3, coupled to the time control knob, connects terminal P_2 to one of the 26 contact studs T belonging to the 26 possible exposure time values. B is a wiper arm fastened to A_3. Due to the connections traced between chains of contact studs S on the one hand and contact studs T on the other hand, overload protection is achieved, as is explained in the article. (The connections traced apply to a "Rotalix" X-ray tube with chart shown in Fig. 1.)

appear as the series of chart curves in the coordinate system of the studs S in Fig. 5.

Finally, the selector arm of the contacts T is fitted with a wiper arm shown in the figure as a circular segment, which on selecting a contact stud T_k shortcircuits this stud with all those belonging to exposure times longer than T_k. Hence, when selecting T_k and then taking a voltage current combination for which a still longer exposure time than T_k would be permissible, the auxiliary circuit again will be closed and the overload protecting relay will be energized.

When, on the other hand, a time T_k is selected together with a voltage-current combination which would only allow a shorter exposure time than T_k, the auxiliary circuit remains open, as can be easily verified in Fig. 5; the relay is de-energized and the main contactor remains inoperative. In this way the overload protection of the tube is achieved.

As to the actual design of the system described, only the selection of the contact stud S_i needs some further consideration. The rectangle containing 23 columns of studs S and represented in fig. 5 is in fact bent round a circular drum coupled to the kV selector switch. A vertical row of ten brushes is in contact with this drum (at A_2). Depending on the position of the drum, the brushes are in contact with studs S of one of the 23 columns, this column corresponding to the kV value selected. The previously mentioned selector arm of the mA-control knob (A_1) connects the terminal P_1 of the auxiliary circuit to one of the ten brushes, each brush belonging to a fixed mA value. Thus, the terminal P_1 is connected with the contact stud S_i belonging to the selected voltage-current combination. The permanent links between the studs T on the one hand, and the chains of mutually connected studs S on the drum on the other hand, are maintained by means of series of slip rings at the end of the drum.

Fig. 6 shows a photograph of the drum with contact studs S. For every X-ray focus which may be fed through the apparatus a different system of mutual connections of studs S is required, corresponding to the rating chart of the focus under consideration. Therefore the drum contains four coordinate systems of studs as pictured in Fig. 5, mounted one above the other. The drum section belonging to the selected focus is brought into action by the focus selector switch on the control table. As generally only one of two foci allowing the maximum mA values of 400 or 500 mA will be used, two of the sections are fitted with seven rows of studs only instead of ten as described above. The wiring of the contact studs and slip rings is placed inside the drum.

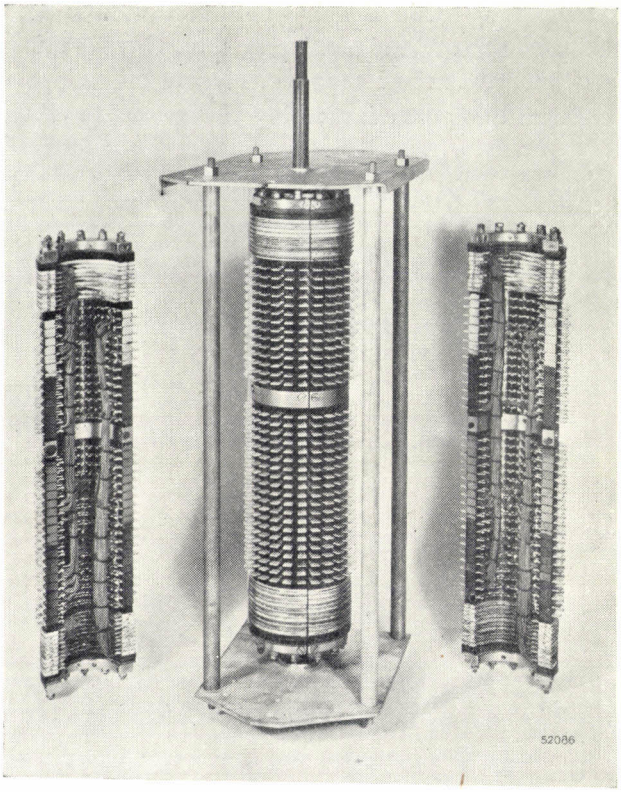


Fig. 6. Control drum with the 230 contact studs S from Fig. 5. The drum is mounted on the shaft of the kV control handle and contains in four sections four assemblies of similar contact studs S, corresponding to the four different foci to be energized by the apparatus. The wiring between studs S is placed within the drum, as is to be seen in the two half drums shown separately. The permanent connections with studs T (cf. Fig. 5) are maintained by means of slip rings visible on the ends of the drum (D in Fig. 7).

Signalling

The second object stated in the beginning of this chapter, viz. to give the operator for every setting a survey of the possible variations, is achieved by means of a signalling system making use of the auxiliary circuit already introduced. To each of the ten brushes mentioned above and corresponding to the ten possible mA values, a lamp is connected in the manner indicated in *Fig. 7*. The ten lamps are mounted on the control table under a window. With the aid of Fig. 7 it may be seeen that on selecting a kV value and a time setting all lamps will be alight that belong to mA values permissible for this combination (regardless of the actual mA setting as yet to be chosen). This enables the operator to see at a glance the range of mA settings from which he can choose.

For practical purposes generally not the mA value is regarded as of prime importance, but the number of mAsec, this number determining

the photographic density obtained with a fixed tube voltage. The signalling system, therefore, is so designed that the lamps when lighted illuminate a column of figures indicating the products of the

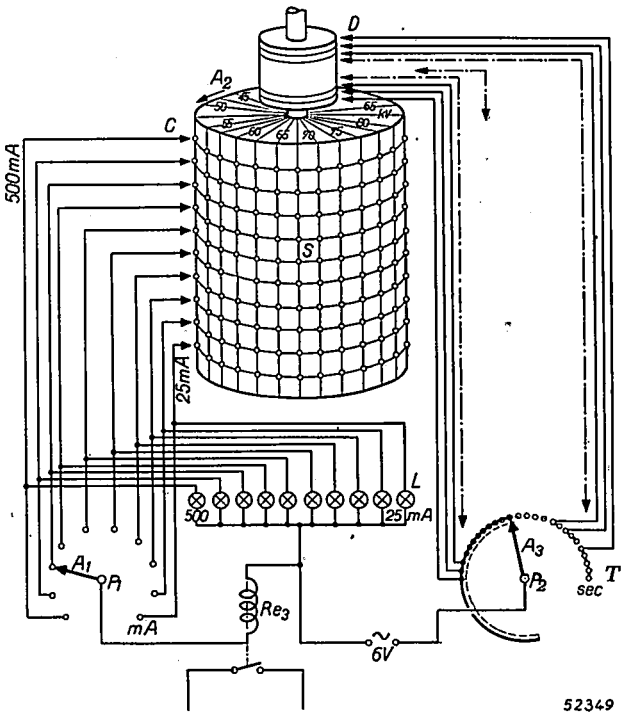


Fig. 7. Signalling system based on the auxiliary circuit shown in Fig. 5. Terminal P_1 is connected to a contact stud S by means of the ten brushes C corresponding to the ten possible mA values and selected by the arm A_1 coupled to the mA control. To each brush a lamp L is connected. When a kV value is selected by A_2 and an exposure time by A_3, all the lamps corresponding to permissible mA values will be alight, regardless of the mA value which may subsequently be chosen. The slip rings D maintain the necessary permanent connections between studs T and studs S.

mA values with the selected exposure time. This is obtained by arranging between the lamps and the window in the control desk a transparent rotating disc, coupled to the time selector handle and carrying 26 radial columns of ten mAsec figures each. Depending on the time setting, a different series of mAsec figures is visible through the window. Moreover, the window shows another column containing the ten (fixed) mA values, of which only the value adjusted at that moment is illuminated (by a simple signalling circuit not indicated in Fig. 7). This second column is placed opposite to the mAsec column, as is to be seen in *Fig. 8*.

Hence, the exposure can be switched on if the selected mA value is located opposite one of the illuminated mAsec figures. If, however, the selected mA value stands opposite a non-illuminated mAsec figure, the relay in the auxiliary circuit is de-energized and the X-ray tube cannot be loaded. At the same time, by the falling out of the relay a warning signal on the control table is lighted, informing the operator that the selected combination of voltage current and time is not permissible ("rating exceeded", cf. Fig. 8).

The usefulness of the above control technique is illustrated by considering the frequently occurring condition whereby the tube voltage and the number of mAsec necessary for optimal contrast and density of the radiograph are known. With the complete automatization formerly described (cf. the article mentioned in footnote [1]), only the kilovoltage and the exposure time, derived in advance from exposure tables, are to be selected. After the exposure the number of mAsec obtained is checked by means of a mAsec meter. If this number exceeds the prescribed value a shorter exposure would have been possible, with correspondingly less blurring of the image (it being presupposed that we are dealing with moving objects). With the present control technique, however, the operator, after having adjusted the tube voltage, is able to find immediately the shortest possible exposure time by turning the time control knob: he simply must

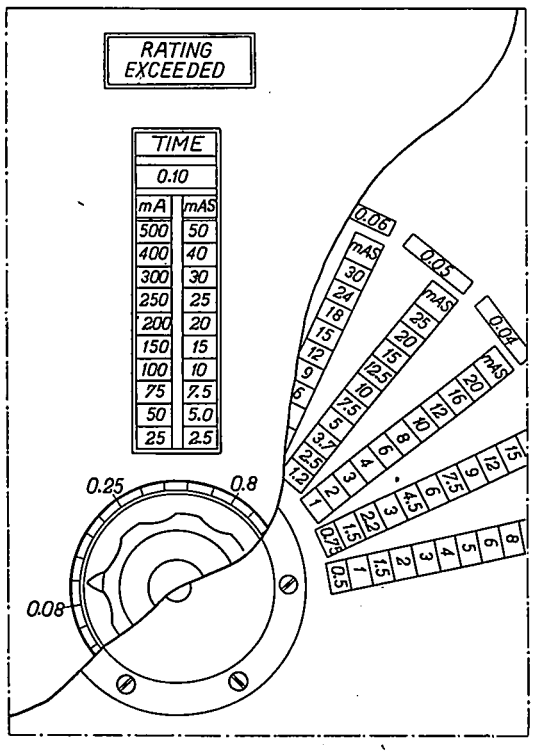


Fig. 8. Through an oblong window in the control desk the selected exposure time and mA value are read (the mA value in question being lighted in the mA column). Moreover, the operator sees at a glance which mAsec values the X-ray tube can withstand at the selected kilovoltage and exposure time: these are the numbers lighted in the mAsec column in the window. The mAsec indication is obtained by coupling to the time control handle a transparent disc carrying 26 different columns of mAsec numbers. When setting the time the correct column appears automatically in the window.

arrive at a setting where the prescribed mAsec value (or the one closest to it) will appear as the highest illuminated mAsec figure in the window. Then he has to adjust his mA control so that the illuminated mA figure appears opposite the mAsec figure in question.

Reproducibility of tube voltage and tube current

When considering the role the rating chart of the tube plays in the control technique described (Fig. 5), it will be evident that the voltage, current and exposure time obtained with the respective settings of the control handles must be accurately reproducible. This implies that their values must be largely independent of the mains supply voltage, and the high tension obtained must not be influenced by the current setting and vice versa. We shall now explain how these requirements have been met in the present apparatus.

As to the exposure time, we can chiefly refer to the description of the diagnostic apparatus repeatedly mentioned above [1]) (where similar requirements concerning the reproducibility were to be fulfilled). The contactor switching the high tension transformer abruptly on and off must handle loads up to about 40 kVA. Nervetheless, no heavy moving parts and contacts must be used, since the duration of the going in and falling out must be very short, lest its consistency be impaired by friction effects. A comparatively light design of the relay is made possible by fixing the phases of making and breaking the heavy current at the moments when the pulsating high tension passes through zero value. This "isochronic" switching is obtained with a circuit in which the contactor coil is energized by means of gas-filled, grid-controlled rectifying valves. The time switch developed for our apparatus and based on the above principles may be considered as a variant of the one formerly described (cf. the article mentioned under [1]).

The tube voltage

Three chief measures are taken to make the tube voltage correctly reproducible. The first one, which is well-known, consists in compensating mains fluctuations by applying the mains voltage to various tappings on the auto transformer (T_2 in *Fig. 9*) feeding the high tension transformer. The operator, who selects the tapping by a control handle, can check the adjustment on a voltmeter which must be made to read to the nominal input voltage of 230 volts.

Another cause of variation of the adjusted tube tension is the variable voltage drop, occurring in the transformer coils, in the high tension rectifying valves, etc. due to the load current of the X-ray tube. This voltage drop varies roughly proportionally to the current. Therefore, the second measure consists in "compensating" the voltage drop variations by means of a bank of resistances in the control table. For every mA setting a resistance is provided. The resistance corresponding to the selected mA value is connected in series with the primary of the high tension transformer ($R_{3,1}$, in fig. 9). (This, of course, is equivalent to inserting a certain resistance on the high tension side.) The resistances are so adjusted in the factory that the voltage drop produced in them always supplements the voltage drop in the tube circuit to give a constant total value, regardless of the mA setting.

At the maximum possible rating of the X-ray tube (500 mA at 85 kV_{peak}), during a short time a current of about 105 A flows through the primary circuit of the high tension transformer. As the switch for selecting the supplementary resistance has also to cope with these large currents, the transition resistance of its contacts must be extremely small (less than 0.001 ohm), lest a new and non-reproducible voltage drop be introduced. By means of a special design, making use of parallel silver contacts of the rubbing action (self cleaning) type, this has been attained with relatively small dimensions of the switch.

Apart from the voltage drop in the tube circuit another voltage drop occurs in the mains. With a current of about 100 amperes this voltage drop is far from negligible. If, for instance, the mains resistance amounts to 0.2 ohm, the voltage drop with that current is more than 20 volts, which may correspond to about 8 kV in the tube voltage. It is evident that the adjustment of the kV compensation, which is done in the factory before delivery, would be meaningless if afterwards the apparatus were to be used without taking into account the different local mains resistances that occur in different localities. Therefore, as a third correction, on installing the apparatus a padding resistance is added to the local mains resistance, giving a total of 0.4 ohm. The voltage drop caused by this constant total mains resistance is taken into account while adjusting the kV compensation in the factory and thus its effect on the adjusted tube tension is eliminated.

If the mains themselves have already a resistance larger than 0.4 ohm — which is undesirable and should be remedied if possible in order to obtain best results from the apparatus — the above described measure of "compensating" the mains resistance is impossible. Yet even in this case errors can be excluded, at least for smaller tube currents, if only the actual

mains resistance is known while adjusting the apparatus in the factory: to this end the excess mains resistance (over 0.4 ohm) is subtracted from each of the resistances which are adjusted for the kV compensation. However, for the largest tube currents, for which these supplementing resistances must be very small or even zero, subtracting the surplus is not possible and one must put up with substantial deviations in the kV settings.

entails a much larger voltage loss in the valve. It is not feasible to cope with this extra voltage drop in the voltage compensation described (i.a. because of its sensitivity to minor differences in valve properties). Moreover, a large voltage loss in the valves is detrimental to their life, the valves not being designed to dissipate the resulting high wattages on the anode. In view of these consequences, a small boosting transformer (T_5 in fig. 9) is incorporated, which

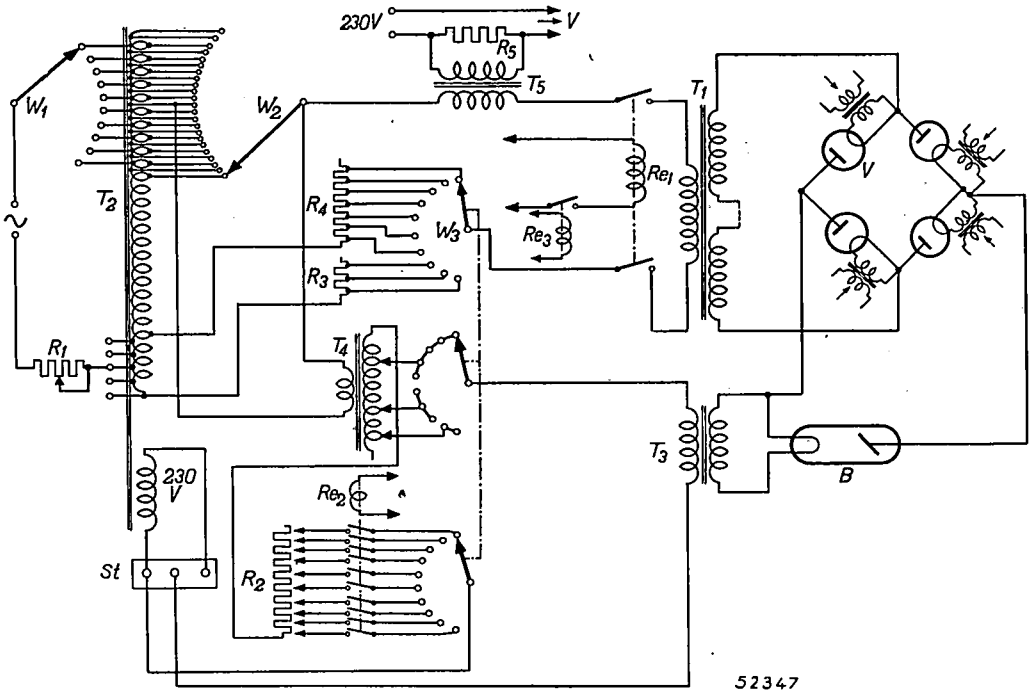


Fig. 9. Simplified circuit diagram of the DX 4 diagnostic X-ray apparatus. The high tension transformer T_1, the four rectifying valves V and X-ray tube B are connected in a conventional 4-valve rectifying system. T_1 is fed from an autotransformer T_2, connected to the A.C. mains through a mains adjusting resistance R_1. By means of the lower tappings of T_2 the apparatus is adjusted to the nominal mains voltage; the upper tappings, selected by the switch W_1, make it possible to keep the output voltage of the autotransformer constant, irrespective of mains fluctuations. W_2 is the kilovoltage selector. W_3, containing three selector arms on three decks, is the milliampere selector, which regulates in the first place the supply of transformer T_3 energizing the filament of the X-ray tube. The source of the filament current is a 230 V auxiliary winding on T_2, whose output voltage is stabilised by stabiliser St and then connected to T_3 via the filament-controlling resistance R_2 and compensating transformer T_4 (see text). The filament selector relay Re_2 is energized by the focus selector switch (not shown) connecting the correct filament resistance R_2 in the circuit. The top deck of W_3 selects the correct value of resistances R_3 and R_4, compensating for the variations of the overall voltage drop of the apparatus and the mains due to the load current. Re_1 is the high tension contactor switching the high tension circuit. Its coil is energized via a contact on the relay Re_3 whose coil is connected to the overload protection system (see text). Boosting transformer T_5 and resistance R_5 compensate for the drop in the valve filament supply due to load.

In the compensating method described it is presupposed that for a given kV setting of the transformer the voltage drop is entirely determined by the tube current. In reality it depends also on the selected voltage, due to the leakage impedance of the high tension transformer, but tests have shown that the errors caused by neglecting this effect are less than 2%.

A totally different phenomenon apt to give rise to voltage errors occurs within the rectifying valves. During heavy loads on the X-ray tube the valve filament supply voltage drops because of the voltage drop in the mains; this would cause the voltage-current characteristics of the valve to change in such a way that obtaining the desired current delivers an auxiliary voltage proportional to the current and in series with the filament voltage of the valves. The filament voltage is thus automatically maintained at the required level, in spite of variable tube loads.

The tube current

Controlling the tube current, as we have seen, is carried out by means of a variable resistance connected in series with the primary coil of the filament transformer feeding the filament of the selected focus. As the filament emission (and therefore the tube current) reacts very strongly to small

variations of the filament voltage, the setting of the tube current can only be reproducible if the mains supply voltage is kept constant. Therefore the tube filament, in accordance with conventional practice, is fed from a voltage stabiliser to eliminate mains fluctuations [5]).

Other measures would not be necessary if the X-ray tube were always functioning at complete saturation of the filament emission. In practice this is not so, because in every period of the tube voltage (pulsating D.C.) low voltage values will also occur. During these parts of the period the emission drawn from the cathode has not the saturation value, but the current is limited by space charge. The higher the peak of the tube voltage, the faster the low voltage values are run through and the larger will be the portion of the period where the current attains its saturation value. Hence, the mean value of the current set by the mA control knob, when not taking any precautions, must depend to some extent on the selected tube voltage.

To eliminate this effect, i.e. to make the calibration of the mA control handle independent of the kV setting, a compensating transformer is used (T_4 in fig. 9), the output of which is added as a correction to the output of the stabiliser mentioned above. The necessary correction voltage will depend on the tube voltage and also on the current setting. Accordingly the primary voltage of the compensation transformer is varied together with the kV control, while the output is taken from various tappings on its secondary coil, the appropriate tapping being chosen by a selector arm coupled to the mA control handle.

In contrast with the compensation of the voltage drop described before, the necessary correction for the current variations is different for each X-ray tube, or rather for each focus. This follows from the fact that the necessary correction depends on space charge conditions between filament and anode. Therefore, a different series of tappings on the compensation transformer must be used for each focus. The changing of the tappings when changing the focus is performed automatically by the focus selector switch in the control table. This switch simultaneously changes the variable series resistance (R_2 in fig. 9) provided for the mA control and which, of course, must be different for each focus too. On the photograph, Fig. 4, the necessary elements are visible, assembled in four units according to the four different foci. The fifth unit (the uppermost one) is common to all filaments and is used on screening.

The measures described in the last chapter in fact have made all settings on the control table quite reproducible. Thus, on the one hand complete reliability of the overload protection of the X-ray tube is achieved, while on the other hand the quality of the radiographs obtained will be for every setting in accordance with expectations.

---

[5]) In this case a simple boosting transformer as applied for the filament voltage of the valves (see above) is not sufficient, because the filament current of the X-ray tube must be kept constant much more rigidly.

ELECTROMAGNETIC WAVES IN WAVE GUIDES

by W. OPECHOWSKI.

538.566.5:621.392.26

PART II. COAXIAL CABLES AND CIRCULAR WAVE GUIDES.

Part I of this article dealt with the theoretical principles of the propagation of electromagnetic waves in wave guides, based upon the fundamental equations of the Maxwell theory. As an example of the application of the general theory, the case of rectangular wave guides was discussed at length; in order to find electromagnetic waves capable of propagation through such wave guides, a method was followed which is based upon the superposition of plane waves.

The subject of this Part II is the propagation of electromagnetic waves in cases where the conductors have the symmetry of a cylinder with circular cross-section (coaxial cable, circular wave guide, round wire). Examples of possible modes of propagation of the waves are deduced by a direct solution of Maxwell's differential equations.

In Part I of this article [1]) we dealt with the propagation of electromagnetic waves in rectangular wave guides. As an introduction we summarized the general mathematical formulation of the principles of the Maxwell theory, followed by a fairly exhaustive discussion of the harmonic, linearly polarized plane wave as an example of a simple solution of the fundamental equations of the Maxwell theory. Finally two methods were mentioned by which these equations can be solved for a given configuration of conductors. The manner in which we found the possible modes of propagation in rectangular wave guides was an example of one of these methods, namely of that where use is made of the fact that a superposition of a number of plane waves is always a solution of the Maxwell equations (principle of superposition).

In this second part we shall deal with electromagnetic waves in coaxial cables and circular wave guides. Both these configurations of conductors have the symmetry of a cylinder with a circular cross section: a circular wave guide is formed from a coaxial cable by removing the inner conductor. The propagation of electromagnetic waves along a round wire will come in for consideration as a matter of course: such a wire is in fact what remains of a coaxial cable after the outer cylinder has been removed.

The superposition principle being absolutely general, the waves which are theoretically possible with such configurations of the conductors could also be found by suitably superposing plane waves. This, however, would mostly be rather troublesome in this case, because one would have to carry out each time the superposition of an infinite number of plane waves.

We shall therefore use these configurations of conductors to demonstrate the application of the other general method for finding the possible modes of propagation of electromagnetic waves when conductors are present.

The first step in this method is, as we said in Part I, the deduction of Maxwell's differential equations from the fundamental equations of the theory, which we have written down in the integral form.

For easy reference we write down these fundamental equations again, but without the explanation of the notation used, for which we refer to Part I pp. 15-17:

$$\oint E_l \, \mathrm{d}l = -\mu \frac{\mathrm{d}}{\mathrm{d}t} \iint H_n \, \mathrm{d}S, \quad \ldots \quad (1)$$

$$\oint H_l \, \mathrm{d}l = \sigma \iint E_n \, \mathrm{d}S + \varepsilon \frac{\mathrm{d}}{\mathrm{d}t} \iint E_n \mathrm{d}S, \quad (2)$$

$$\oint\oint H_n \, \mathrm{d}S = 0, \quad \ldots \quad (3)$$

$$\varepsilon \oint\oint E_n \, \mathrm{d}S = \iiint \varrho \, \mathrm{d}\tau. \quad \ldots \quad (4)$$

To derive the Maxwell equations in differential form from the above equations one has to begin with the choice of the system of coordinates in which one desires to obtain these equations, for with the equations (1)-(4) no particular choice of the system of coordinates is assumed [2]). When a

[1]) Philips Techn. Rev. **10**, 1948 (No. 1).

[2]) Maxwell's differential equations can also be given a form in which no particular choice of the system of coordinates is assumed, this being done with the aid of symbols of the vector analysis ("curl", "div", etc.).

given configuration of the conductors shows a certain symmetry then one preferably chooses a system of coordinates adapted to that symmetry. The second step is to choose suitable integration contours and surfaces in (1)-(4).

The Maxwell equations in cylindrical coordinates

It is immediately obvious that for our problem cylindrical coordinates form the system indicated. With this system the coordinate surfaces are the planes g = const. and z = const. and the cylindrical surfaces r = const.; the three kinds of coordinate surfaces are perpendicular to each other. The three components A_z, A_φ, A_r of a vector A in a point of the space are defined as the orthogonal projections of this vector on the normals of the three coordinate surfaces intersecting each other in this point.

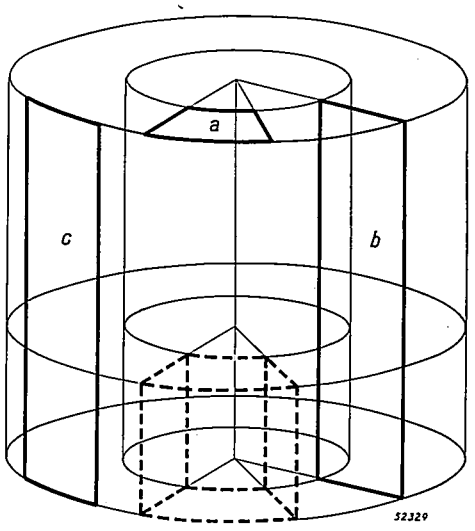


Fig. 1. Integration contours and surfaces for deduction of eqs (5)-(8) from eqs (1)-(4).

In order to derive the differential equations we choose the integration contours indicated in eq. (1)-(2) successively in the surfaces z = const., φ = const. and r = const., for instance in the manner shown in *fig. 1*. By applying eq. (1) successively to these three contours and the surfaces bounded by them and then differentiating each of the equations thus obtained with respect to the two remaining coordinates (in the case of the contour a in fig. 1, where the integration plane is z = const. with respect to φ and r; in the case of the contour b with respect to z and r; in the case of the contour c with respect to φ and z) one finds:

$$\frac{1}{r}\frac{\partial}{\partial r}(rE_\varphi) - \frac{1}{r}\frac{\partial E_r}{\partial \varphi} = -\mu\frac{\partial H_z}{\partial t}, \quad \ldots \quad (5a)$$

$$\frac{\partial E_r}{\partial z} - \frac{\partial E_z}{\partial r} = -\mu\frac{\partial H_\varphi}{\partial t}, \quad \ldots \quad (5b)$$

$$\frac{1}{r}\frac{\partial E_z}{\partial \varphi} - \frac{\partial E_\varphi}{\partial z} = -\mu\frac{\partial H_r}{\partial t} \quad \ldots \quad (5c)$$

By performing the same operations with eq. (2) one finds further:

$$\frac{1}{r}\frac{\partial}{\partial r}(rH_\varphi) - \frac{1}{r}\frac{\partial H_r}{\partial \varphi} = \sigma E_z + \varepsilon\frac{\partial E_z}{\partial t}, \quad (6a)$$

$$\frac{\partial H_r}{\partial z} - \frac{\partial H_z}{\partial r} = \sigma E_\varphi + \varepsilon\frac{\partial E_\varphi}{\partial t}, \quad \ldots \quad (6b)$$

$$\frac{1}{r}\frac{\partial H_z}{\partial \varphi} - \frac{\partial H_\varphi}{\partial z} = \sigma E_r + \varepsilon\frac{\partial E_r}{\partial t} \quad \ldots \quad (6c)$$

The differential form of eqs (3) and (4) can be derived in a similar manner when the closed surface indicated in these equations is chosen as represented by dotted lines in fig. 1. One finds:

$$\frac{1}{r}\frac{\partial}{\partial r}(rH_r) + \frac{1}{r}\frac{\partial H_\varphi}{\partial \varphi} + \frac{\partial H_z}{\partial z} = 0, \quad \ldots \quad (7)$$

$$\frac{1}{r}\frac{\partial}{\partial r}(rE_r) + \frac{1}{r}\frac{\partial E_\varphi}{\partial \varphi} + \frac{\partial E_z}{\partial z} = \frac{\varrho}{\varepsilon}. \quad \ldots \quad (8)$$

The equations (5)-(8) look rather complicated. We shall therefore at once specialize these equations to a few simple cases of practical importance.

The transverse cylindrical wave

We shall first consider the case of a purely transverse wave (radian frequency ω) being propagated in the direction of the z-axis, that is to say a wave for which E_z and H_z are zero. For the time being we shall not make any assumptions as regards the position of the conductors, expect of course that the z-axis is the axis of cylindrical symmetry. The simplest possibility now is a wave where $H_\varphi \neq 0$, $E_r \neq 0$ and all other components of the field are zero; **H** and **E** are thus at right angles to each other [3]). From (7) and (5a) it then immediately follows that H_φ and E_r do not depend upon φ; the electromagnetic field is therefore rotationally symmetrical. Further from (6a) it follows that the product rH_φ does not depend upon r. According to (8) the same holds for the product rE_r provided

[3]) It can be proved that the equally simple transverse wave with $E_\varphi \neq 0$, $H_r \neq 0$, all other components being zero, can in no case exist, which means to say that there the field amplitudes must be zero.

there are no charges in the space considered ($\varrho = 0$), which in the following we shall assume to be the case.

The wave must therefore have the form:

$$\left.\begin{aligned} E_r &= E_r^\circ(r) \cdot e^{j(\omega t - kz + \eta)}, \quad . \quad . \quad . \\ H_\varphi &= H_\varphi^\circ(r) \cdot e^{j(\omega t - kz)}, \quad . \quad . \quad . \quad . \end{aligned}\right\} \quad (9)$$

$$r \cdot H_\varphi^\circ(r) = C_1, \quad r \cdot E_r^\circ(r) = C_2, \quad (10)$$

where k, η, C_{10} and C_2 are constants still to be determined; $E_r^\circ(r)$ and $H_\varphi^\circ(r)$ are assumed to be real.

Now, by substituting (9) in (5b) and (6c) (these are all that remain of the eqs (5)-(8)), that is to say by writing:

$$\frac{\partial E_r}{\partial z} = -\mu \frac{\partial H_\varphi}{\partial t}, \quad . \quad . \quad . \quad . \quad . \quad . \quad (11)$$

$$-\frac{\partial H_\varphi}{\partial z} = \sigma E_r + \varepsilon \frac{\partial E_r}{\partial t}, \quad . \quad . \quad . \quad . \quad (12)$$

one easily finds

$$k^2 = \mu\omega(\varepsilon\omega - j\sigma), \quad . \quad . \quad . \quad . \quad (13)$$

$$k = |k| e^{-j\eta}, \quad . \quad . \quad . \quad . \quad . \quad . \quad . \quad (14)$$

$$\frac{C_2}{C_1} = \frac{E_r^\circ(r)}{H_\varphi^\circ(r)} = \frac{\mu\omega}{|k|}; \quad . \quad . \quad . \quad (15)$$

In writing (15) we have made use also of (10).

Eqs (13)-(14) are identical with eqs (10)-(11) in Part I, which hold for the constants k and η of a plane (damped) wave. (In this manner the use of the same symbols k and η in both cases becomes justified.) Also the expression (15) for the relation of the field amplitudes is identical with the corresponding expression for the plane wave (cf. (12) in Part I).

If one wishes to use the fact that the equations (14)-(15) apply for the plane wave (see eqs (7) and (9) in Part I)

$$\left.\begin{aligned} E_x &= E^\circ e^{j(\omega t - kz + \eta)}, \quad . \quad . \quad . \quad . \\ H_y &= H^\circ e^{j(\omega t - kz)}, \quad . \quad . \quad . \quad . \quad . \end{aligned}\right\} \quad (16)$$

then the validity of the same equations for the wave (9) can be proved without any calculation, for the eqs (11)-(12) are identical with the eqs (5b) and (6a) in Part I, which are satisfied by the plane wave (16).

The solution of the Maxwell equations (5)-(6) characterized by the eqs (9)-(10) and (13)-(15) is sometimes called the (damped) transverse cylindrical wave. In order to characterize this wave completely we must still determine the constants C_1 and C_2.

Now it is easily understood that in an unbounded homogeneous medium C_1 and C_2 are zero; in other words, a transverse cylindrical wave cannot be propagated in such a medium. The fact is that since $E_z = 0$ and ϱ and ε are finite the right-hand side of eq. (2) must be 0. This means that the line integral in the left-hand side is also zero. When one takes a circle r = const. as integration contour this line integral has the value $2\pi r H_\varphi^\circ$. Thus we obtain $2\pi r H_\varphi^\circ = 0$ and from that, owing to (10), $C_1 = 0$. From (15) it then follows that also $(C_2) = 0$. Therefore the amplitudes of the transverse cylindrical wave become in this case zero.

This manner of reasoning is no longer applicable, however, when we have along the z-axis a perfectly conducting wire (radius a). E_z still remains zero it is true, but since $\sigma = \infty$ we may have the product $\sigma E_z \neq 0$, implying a surface current along the surface of the wire.

In order to determine the constants C_1 and C_2 in this case, we shall employ the boundary conditions which have to be satisfied by the electromagnetic field at the boundary surface between two media. These boundary conditions were briefly discussed in Part I and formulated in eqs (21)-(22) for the case where one of the two media is a perfect conductor.

When the boundary surface is a cylindrical surface, as it is here, then on the basis of these equations we have at the boundary surface:

$$E_\varphi = 0, \qquad H_r = 0, \quad . \quad . \quad . \quad . \quad . \quad . \quad (17)$$

$$\varepsilon E_r = s, \qquad H_\varphi = i, \quad . \quad . \quad . \quad . \quad . \quad . \quad (18)$$

where s and i denote the density of the surface charge and of the surface current respectively (the amplitudes of these quantities will be denoted by s° and i°).

From (10) and (18) it now follows that:

$$C_1 = ai^\circ, \qquad \varepsilon C_2 = as^\circ. \quad . \quad . \quad . \quad . \quad (19)$$

The boundary condition (17) is already satisfied because for a transverse cylindrical wave E_φ and H_r are everywhere zero.

When the medium in which the wire is situated is a perfect insulator ($\sigma = 0$) then from eqs (13), (15) and (19) it is easy to convince oneself that the ratio i°/s° is equal to the phase velocity $v = \omega/k$ of the cylindrical wave.

In what follows we shall need also an equation to indicate the relation between $H\varphi$ and the total surface current $I = 2\pi a i$ along the wire. This equation follows immediately from (10) and (19):

$$H_\varphi(z, r, t) = \frac{I(z,t)}{2\pi r}. \quad . \quad . \quad . \quad . \quad . \quad (20)$$

In the region of very high frequencies a wire therefore plays only the role of a cylindrical boundary surface making it possible for a transverse cylindrical wave to be propagated in a certain direction. Actually, owing to the imperfect conductivity of the wire, the wave cannot be exactly transverse, that is to say E_z cannot be exactly zero. However, the higher the frequency, the smaller is the error resulting from putting $E_z = 0$.

In a coaxial cable it is of course possible for the transverse cylindrical wave to be propagated, since on the inside of the outer cylinder (radius b) the boundary conditions are automatically satisfied. There the total surface current is also $I(z,t)$ but the direction of the current is opposed to that of the surface current on the wire, i.e. on the inner conductor (radius a) of the cable.

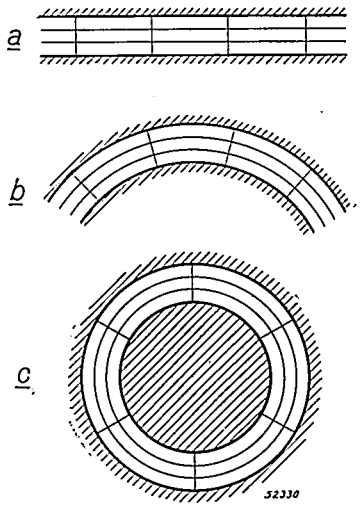


Fig. 2. The manner in which the magnetic lines of force (concentric circles) and of electric lines of force (straight lines) for a transverse cylinder wave in a coaxial cable (*c*) can be deduced from that for a transverse plane wave between two parallel flat planes (*a*) by gradually transforming the latter into curved surfaces (*b*). In all three cases the direction of propagation of the wave is perpendicular to the plane of the drawing.

The lines of force of the **E** and **H** fields are diagrammatically represented in *fig. 2c*. We take this opportunity to show also in figs 2*a* and *b* how the trend of the lines of force for the transverse cylindrical wave in a coaxial cable can be graphically "deduced" from that for the transverse wave between two flat planes (discussed in Part I) by gradually curving the planes. This is often a useful way of arriving at an idea of the trend of the lines of force also for a non-transverse wave without working out the solution of the Maxwell equations; this particularly applies in cases where an exact solution is practically impossible owing to mathematical difficulties. Of course the lines of force for a certain form of conductors must already be known.

If we now imagine the inner conductor to be removed from a coaxial cable then, in order to determine C_1 and C_2 of the transverse cylindrical wave within the space bounded by the outer cylinder, we can apply without any alteration the reasoning followed for the case of an unbounded homogeneous medium. In this manner we arrive again at the conclusion that $C_1 = C_2 = 0$. In other words, a transverse cylindrical wave cannot be propagated in a circular wave guide.. This result is a special case of the general theorem which we formulated in Part I, viz. that a purely transverse electromagnetic wave cannot be propagated in any wave guide the cross section of which is bounded by one single continuous closed curve. (The cross section of a coaxial cable is bounded by two closed curves; therefore the hypothesis does not hold in that case.)

Deduction of the "cable equations"

It can easily be proved that eqs (11)-(12) are equivalent to the well-known "cable equations" for the tension V and the current I in a coaxial cable. The proof is as follows. The current $I(z,t)$ is defined by (20) and the voltage $V(z,t)$ between the outer and inner conductors by

$$V(z,t) = \int_A^B E_l \, \mathrm{d}l \,, \quad \ldots\ldots \quad (21)$$

the path of integration lying entirely in the plane $z =$ const., whilst its end points A and B are situated on the outer and inner conductors; apart from this the path of integration is arbitrary.

It is easy to understand that in this manner the tension $V(z,t)$ is unambiguously defined.

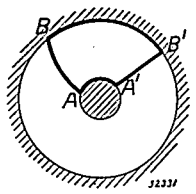


Fig. 3. Integration contour $ABB'A'A$ for proving that the tension V between the two conductors in the coaxial cable is unambiguously defined by eq. (21).

To make this clear it is noted that the integral $\int E_l dl$ along the closed path $ABB'A'A$ indicated in *fig. 3* must be equal to zero, regardless where the points A, A' and B, B' lie respectively on the inner conductor and on the outer conductor and

what the shape of the curves AB and $A'B'$ may be in the plane z = const., for since $H_z = 0$ the magnetic flux through the part of the plane z = const. bounded by $ABB'A'A$ is always zero. In accordance with the law of induction (eq. (1)) it follows from this that the said integral is indeed zero. Now:

$$\oint_{ABB'A'A} E_l \, dl = \int_A^B E_l \, dl + \int_B^{B'} E_l \, dl + \int_{B'}^{A'} E_l \, dl + \int_{A'}^{A} E_l \, dl$$

applies.

Since $E_\varphi = 0$, the second and fourth integrals in the right-hand side of this equation are zero, i.e.:

$$0 = \int_A^B E_l \, dl + \int_{B'}^{A'} E_l \, dl,$$

or

$$\int_A^B E_l \, dl = \int_{A'}^{B'} E_l \, dl,$$

from which the unambiguity of the definition (21) immediately follows.

When we substitute in eqs (11)-(12) the expression (20) for H_φ and then integrate these equations with respect to r in the manner indicated in the definition (21) of V, then after a little manipulation we find:

$$-\frac{\partial V}{\partial z} = L\frac{\partial I}{\partial t}, \quad \ldots\ldots \quad (22)$$

$$-\frac{\partial I}{\partial z} = GV + C\frac{\partial V}{\partial t}, \quad \ldots \quad (23)$$

in which

$$L = \frac{\mu}{2\pi} \cdot \ln(b/a), \quad C = \frac{2\pi\varepsilon}{\ln(b/a)}, \quad G = \frac{2\pi\sigma}{\ln(b/a)}, \quad (24)$$

where L, C and G denote respectively the series self-inductance, the shunt capacity and the shunt conductance per metre of the cable.

The conductors of the cable being assumed to be perfectly conducting, the term RI (R = resistance per metre) usually present in the right-hand side of equation (22) is of course absent, for this term describes approximately the losses in the conductors due to the development of Joule heat.

The cable equations (22)-(23), deduced here for a coaxial cable from the Maxwell equations [4]), also hold strictly for any configuration of two arbitrary conductors allowing the propagation of a purely transverse wave (naturally the expressions for L, C and G vary from case to case). We shall not give here the proof of this more general statement, the plausibility of which is so obvious.

[4]) We could, of course, have derived the cable equations (22)-(23) directly from the fundamental equations (1)-(2) without employing the differential equations (11) and (12) as intermediate stage.

In this connection we would make the following remark. In the general case the voltage V is defined also by (21). The unambiguity of this definition is based, as we have seen, only upon two facts: 1) that the component of **H** in the direction of propagation of the wave is zero, 2) that the tangential component of **E** at the surface of the conductors is also zero. The former follows from the transverse nature of the wave, the latter from the boundary condition. The current I has in the general case the same meaning as in the case of the coaxial cable, namely that of the total surface current along one of the conductors.

Rotationally symmetrical E and H waves [5])

In the foregoing it has been shown that a purely transverse cylindrical wave can only be propagated when there is a conductor along the axis of symmetry. Neither in free space nor in a circular wave guide can such a wave be propagated. The essential condition for the possibility of propagation of an electromagnetic wave in a circular wave guide is, therefore, that at least one of the field vectors **E** and **H** must have a component in the direction of propagation, i.e. in the direction of the axis of symmetry. The two simplest kinds of waves are then:

1) Waves where $H_\varphi \neq 0$, $E_r \neq 0$, $E_z \neq 0$, all other components of the **E** and **H** fields being zero. In accordance with what we have stated when dealing with rectangular wave guides, these waves and in general the waves for which $H_z = 0$ are called the "E-waves" (or "TM-waves").

2) Waves where $E_\varphi \neq 0$, $H_r \neq 0$, $H_z \neq 0$, all other components being zero. These waves are examples of "H-waves" (or "TE-waves").

In the case of each of these waves **E** and **H** are thus at right-angles to each other. From eqs (5)-(8) it now follows that with these two kinds of waves the **E** and **H** fields are not dependent upon φ; these waves are therefore rotationally symmetrical.

In Part I it has already been stated that in wave guides waves which are not purely transverse necessarily have a cut-off frequency; if the frequency of such a wave is lower than the cut-off frequency in a given wave guide then it is impossible for the wave to be propagated in that wave guide. In the following we shall briefly outline how one

[5]) The first publications on the theory of circular wave guides appeared in 1936: J. R. Carson, S. P. Mead and S. A. Schelkunoff, Bell Syst. Techn. J. **15**, 310-333, 1936; W. D. Barrow, Proc. Inst. Radio Engrs **24**, 1298-1328, 1936; L. Brillouin, Rev. Gén. d'Electr. **40**, 227-239, 1936. The practical importance of wave guides in general was first pointed out in the article by Barrow quoted above and in an article by G. C. Southworth, Bell Syst. Techn. J. **15**, 284-309, 1936, which latter article is complementary to the publication by Carson, Mead and Schelkunoff.

arrives at the cut-off frequency of the rotationally symmetrical E- and H-waves. We shall confine the discussion of these waves mainly to this point.

We assume that in both cases all components of the **E** and **H** fields have the same factor $e^{j(\omega t - hz)}$ expressing wave propagation in the z-direction, thus

$$H_\varphi = H_\varphi^\circ(r) \cdot e^{j(\omega t - hz)},$$

etc.

It will be found that as a rule the field amplitudes are complex numbers, which means to say that the various components of the **E** and **H** fields do not oscillate in phase [6]).

Rotationally symmetrical E-waves

By substituting in (5)-(6) H_φ, E_r, E_z, which have the form just mentioned, and taking the remaining components as zero, after an easy reduction one obtains the following equations for rotationally symmetrical E-waves:

$$\frac{d^2 H_\varphi^\circ}{d\varrho^2} + \frac{1}{\varrho}\frac{d\, H_\varphi^\circ}{d\varrho} + \left(1 - \frac{1}{\varrho^2}\right) H_\varphi^\circ = 0, \quad (25)$$

$$E_z^\circ = \frac{\sqrt{k^2 - h^2}}{\sigma + j\varepsilon\omega}\,\frac{1}{\varrho}\frac{d}{d\varrho}\,(\varrho\, H_\varphi^\circ)\,, \quad (26)$$

$$E_r^\circ = \frac{jh}{\sigma + j\varepsilon\omega}\, H_\varphi^\circ, \quad (27)$$

in which

$$\varrho = r\sqrt{\mu\omega\,(\varepsilon\omega - j\sigma) - h^2}\,;$$

if we denote the first term in the expression below the radical by k^2 (see (13)) then this expression can be abbreviated to read:

$$\varrho = r\sqrt{k^2 - h^2}\,. \quad (28)$$

The constant h will presently be determined by the boundary condition.

From these formulae it appears that E_r and E_z are unambiguously determined by H_φ.

Now the equation for H_φ is an equation very well known in mathematics, viz. the equation for the Bessel functions of the first order. Incidentally it may be stated that by replacing $1/\varrho^2$ by n^2/ϱ^2 ($n = 0, 1, 2 \ldots\ldots$) one obtains the equation for the Bessel functions of the nth order. Among the Bessel functions two kinds are distinguished. The Bessel function of ϱ of the nth order "of the first kind" [7]) is denoted by $J_n(\varrho)$. The Bessel functions $J_0(\varrho)$ and $J_1(\varrho)$, the only ones with which we shall be concerned here, are shown in *fig. 4;* these two functions are related by the following expressions:

$$\frac{dJ_0}{d\varrho} = -J_1 \quad \text{and} \quad \frac{1}{\varrho}\frac{d}{d\varrho}\,(\varrho\, J_1) = J_0\,. \quad (29)$$

Thus according to (25)-(27) and (29) the amplitudes of the rotationally symmetrical E-wave are given by

$$\left.\begin{aligned} H_\varphi^\circ &= A J_1(\varrho), \qquad E_z^\circ = A\frac{\sqrt{k^2 - h^2}}{\sigma + j\varepsilon\omega}\, J_0(\varrho), \\ E_r^\circ &= A\frac{jh}{\sigma + j\varepsilon\omega}\, J_1(\varrho)\,, \end{aligned}\right\} \quad (30)$$

in which A is an arbitrary constant.

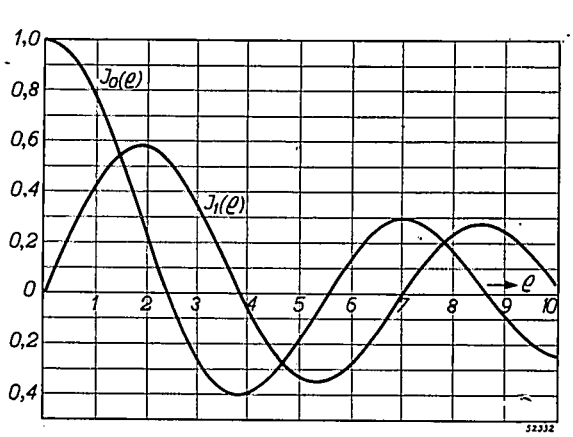


Fig. 4. Graphic representation of the Bessel functions $J_0(\varrho)$ and $J_1(\varrho)$.

We shall from now on assume that the wall of the wave guide is perfectly conducting. According to the boundary conditions (21) in Part I the tangential component E_t of **E** and the normal component H_n of **H** must therefore be zero at the wall.

Given that the wave guide has a radius b, the boundary condition $E_t = 0$ requires that $E_z(b) = 0$, that is to say

$$J_0(b\sqrt{k^2 - h^2}) = 0. \quad (31)$$

The boundary condition $H_n = 0$ is automatically satisfied, for the radial component of **H** here is everywhere zero.

From (31) one can determine h. The function $J_0(\varrho)$ has an infinite number of zero points ϱ_1, $\varrho_2, \ldots\ldots$, some of which are shown in fig. 4: ϱ_1 has the value 2.405, $\varrho_2 = 5.520$, $\varrho_0 = 8.654$, and so on. For the quantity h we therefore derive from (31) an infinite number of equations of the form

$$h_p = \sqrt{k^2 - (\varrho_p/b)^2} \qquad (p = 1, 2, \ldots), \quad (32)$$

[6]) In the case of the transverse cylindrical wave (9) we were able to assume that the field amplitudes are real because we explicitly introduced the phase difference η, which we have not done here.

[7]) We should come across the Bessel function of the "second kind" when discussing the E and H waves in a coaxial cable.

where the radius b of the wave guide is taken as given.

For air (or vacuum) we may put $\sigma = 0$. From (13) it follows that k^2 is then real, viz. $k^2 = \varepsilon\mu\omega^2 = \omega^2/c^2$.

Eq. (32) thus becomes:

$$h_p = \sqrt{(\omega/c)^2 - (\varrho_p/b)^2} \quad (p = 1, 2, \ldots). \quad (33)$$

Now only real values of h are of importance for our problem, because when h is imaginary this means that the wave is not propagated (this has been explained in Part I). From (33) we see that h can only be real when

$$(\omega/c)^2 - (\varrho_p/b)^2 \geqq 0,$$

that is to say when

$$\nu > \varrho_p c/2\pi b$$

or

$$\lambda < 2\pi b/\varrho_p.$$

Thus, just as in Part I in the case of rectangular wave guides, we meet here again the concepts "cut-off frequency" ν_c and "cut-off wavelength" λ_c:

$$\lambda_c = c/\nu_c = 2\pi b/\varrho_p. \quad \ldots\ldots \quad (34)$$

Only rotationally symmetrical E-waves with a wavelength $\lambda < \lambda_c$ can be propagated in a circular wave guide. A certain λ_c corresponds to every value of ϱ_p. The greatest cut-off wavelength for rotationally symmetrical E-waves is therefore

$$\lambda_c^{(1)} = 2\pi/2.405 = 2.61\, b, \quad \ldots \quad (35)$$

and this is found to be also the greatest wavelength that a wave can have in a circular wave guide.

Denoting the wavelength of the wave in the wave guide by λ_z (cf. the analogous notation in Part I), from (33) and (34) it follows that:

$$\lambda_z^{(p)} = 2\pi/h_p = 1/\sqrt{(1/\lambda)^2 - (1/\lambda_c)^2} \ldots\ldots \quad (36)$$

The z-dependence of the rotationally symmetrical E-wave is therefore given by

$$e^{-jh_p z} = e^{-2\pi j z\sqrt{(1/\lambda)^2 - (1/\lambda_c)^2}}. \quad \ldots\ldots \quad (37)$$

Precisely the same formula has been deduced in Part I for a rectangular wave guide (eq. (33) Part I).

For easy reference we again write down here the full expression (in the non-complex notation) for rotationally symmetrical E-waves in a wave guide with perfectly conducting wall:

$$\left.\begin{aligned} E_z &= (A/\varepsilon\omega)\sqrt{(\omega/c)^2 - h_p^2}\cdot J_0(\varrho)\cdot \sin(\omega t - h_p z),\\ E_r &= (Ah_p/\varepsilon\omega)\cdot J_1(\varrho)\cdot \cos(\omega t - h_p z),\\ H_\varphi &= A\cdot J_1(\varrho)\cdot \cos(\omega t - h_p z),\\ E_\varphi &= H_r = H_z = 0, \end{aligned}\right\} \quad (38)$$

in which

$$\varrho = r\sqrt{(\omega/c)^2 - h_p^2}; \quad \ldots\ldots \quad (39)$$

h_p is defined by (33).

Corresponding to a certain value of $p = 1, 2, \ldots$. there is an E-wave of a certain form, for p indicates the number of coaxial cylindrical surfaces in the wave guide for which $|E_z|$ is the maximum and E_r and H_φ are zero, when the axis of symmetry is also considered as a (degenerated) cylindrical surface; this statement can be verified with the aid of fig. 4. The electrical lines of force for a wave corresponding to ϱ_1 are shown in *fig.* 5, in the part lying between the two horizontal dotted lines representing the wall of the wave guide. The magnetic lines of force lie in planes $z =$ const. and are concentric circles. The density of the surface current and surface charge on the wall of the wave guide follows from the boundary conditions (18).

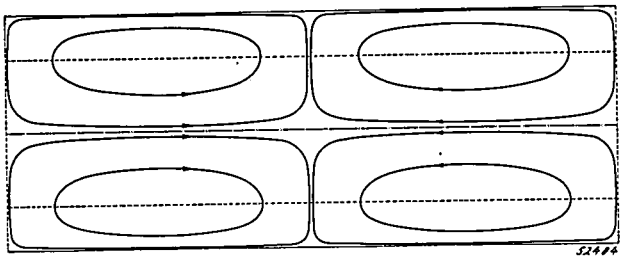


Fig. 5. Representation of the electrical lines of force for a rotationally symmetrical E-wave (corresponding to the smallest root of the eq. $J_0(\varrho) = 0$) and of the magnetic lines of force for a rotationally symmetrical H-wave (corresponding to the smallest root of the eq. $J_1(\varrho) = 0$ differing from zero) in a circular wave guide. In both cases the lines of force are determined by the equation

$$\varrho \cdot J_1(\varrho)\cdot \sin 2\pi\zeta = \text{constant}.$$

The variable ζ is given by $\zeta = z/\lambda_z$, in which λ_z is the wavelength of the wave in the wave guide (see eq. (36)) and the z-axis coincides with the axis of symmetry (dot-dash line) of the wave guide; the variable ϱ is proportional to the distance r from the axis of symmetry (see eq. 28)).

The plane of the drawing is thus an r-z-plane (or $\varphi =$ const.). In the case of H-waves the fully drawn horizontal straight lines represent the intersections of the wall of the wave guide with the plane of the drawing. The contours indicate the magnetic lines of force. The same contours also represent the electrical lines of force in the case of the E-wave, provided the wall of the wave guide is imagined as being removed to the dotted horizontal straight lines.

The solution (30) of eqs (5)-(6) forms also the basis of the theory of the skin effect in a circular wire, assuming σ to be finite inside the wire and zero outside it. Thus the

variable ϱ is complex. On the surface of the wire one then has to try to satisfy the boundary conditions, which in this case lead to rather complicated formulae, since neither of the two media is a perfect conductor.

Rotationally symmetrical H-waves

Rotationally symmetrical H-waves can be dealt with in exactly the same manner. A comparison of (5) with (6) shows at once that the expressions for the amplitudes of a rotationally symmetrical H-wave can be obtained by replacing $H_\varphi°$, $E_z°$, $E_r°$, $(\sigma + j\varepsilon\omega)$ and $(-j\mu\omega)$ in (30) respectively by $E_\varphi°$, $H_z°$, $H_r°$, $(-j\mu\omega)$ and $(\sigma + j\varepsilon\omega)$. The constant k^2 is not changed by this substitution since according to (13)

$$k^2 = (-j\mu\omega)\,(\sigma + j\varepsilon\omega).$$

This time, therefore, the boundary condition $E_t = 0$ does not lead to eq. (31) but to the following equation for the determination of h:

$$J_1(b\sqrt{k^2 - h^2}) = 0 \quad . \; . \; . \; . \quad (40)$$

Since $E_\varphi°$ and $H_r°$ (just as $H_\varphi°$ and $E_r°$ in the case of the E-waves) depend in like manner upon r, the boundary condition $H_n = 0$ is automatically satisfied. Eqs (34)-(37) hold, of course, also here, the only difference being that ϱ_p is no longer determined by the eq. $J_0(\varrho) = 0$ but by the eq. $J_1(\varrho) = 0$. The full expression for the rotationally symmetrical H-waves in the case when $\sigma = 0$ is obtained by replacing E_z, E_r, H_φ and ε in (38) respectively by H_z, H_r, E_φ and $(-\mu)$. The magnetic lines of force for a simple rotationally symmetrical H-wave are also given in fig. 5.

There is a peculiarity about the rotationally symmetrical H-waves to which we would draw attention. On the wall of the wave guide the magnetic field follows the direction of the z-axis ($H_r(b)$ being zero) and hence the surface current flows at right-angles to the z-direction: the lines of flux are circles perpendicular to the z-axis [8]). This is a striking example of the fact that at high frequencies there is no direct relation between the direction of the current and the direction of propagation of the electromagnetic wave along the conductor, thus also of the electromagnetic energy.

Apart from the rotationally symmetrical E- and H-waves considered above, in circular wave guides E- and H-waves may be propagated of which the **E** and **H** vectors depend also upon the angle coordinate φ. The form of these waves is deduced in a similar manner from equations (5)-(8), though the calculations in this case are somewhat more complicated; we shall not go into that further here.

Finally we would observe that in many technically important problems relating to the propagation of microwaves a rigorous solution of the Maxwell equations involves great mathematical difficulties; in the foregoing we have considered only exceptionally simple configurations of conductors. Nevertheless the methods that we have outlined are useful when seeking approximative solutions of more complicated problems. This will become evident when the technique of wave guides is dealt with in further articles to be published in this journal.

APPENDIX:

About the relation between wave guides and cavity resonators

If a circular wave guide is closed by applying a metal wall in any two planes perpendicular to the axis of symmetry then a (circular) cavity resonator is obtained. The characteristic modes of oscillation of such cavity resonators have already been dealt with in this journal [9]) [10]). In the method of treatment applied there, however, deductions were limited to that of the distribution of the current density in the walls of a circular, flat cavity resonator. We shall here outline briefly how one arrives at the expressions for the electromagnetic field in the space bounded by the walls of a circular cavity resonator (not necessarily flat).

Obviously in a stationary condition the electromagnetic field must bear the character of a standing wave. In the case of a standing electromagnetic wave the electrical and magnetic lines of force are not dependent upon the time; only the strength of the field changes with time (in the most simple case sinusoidally). In other words the expression for **E** or **H** for a standing wave must be a product of a function depending only upon time and a function depending only upon the place.

A standing wave (in a circular cavity resonator) can be imagined as originating from a superposition of two running waves in a circular wave guide having opposite directions of propagation but otherwise absolutely identical. We shall explain this further with the example of the rotationally symmetrical E-waves. The superposition referred to means that to the expressions (38) for the field components one has to add the expressions obtained from (38) when replacing h_p by $(-h_p)$. In this way we obtain:

$$\left.\begin{aligned} E_z &= (2A/\varepsilon\omega)\sqrt{(\omega/c)^2 - h_p^2}\,.\,J_0(\varrho)\,.\cos h_p z\,.\sin\omega t,\\ E_r &= -(2Ah_p/\varepsilon\omega)\,.\,J_1(\varrho)\,.\sin h_p z\,.\sin\omega t,\\ H_\varphi &= 2A\,.\,J_1(\varrho)\,.\cos h_p z\,.\cos\omega t,\\ E_\varphi &= H_z = H_r = 0. \end{aligned}\right\} \quad (41)$$

[8]) Related to this property of the rotationally symmetrical H-waves is the fact that an unlimited increase of the frequency ν is accompanied by a decrease of the energy losses in the wall of the wave guide right down to zero; for all other H and E waves the energy losses for $\nu = \infty$ become infinitely large.

[9]) C. G. A. von Lindern and G. de Vries, Flat cavities as electrical resonators, Philips Techn. Rev. **8**, 149-160, 1946 (No. 5).

[10]) G. de Vries, Electromagnetic cavity resonators, Philips Techn. Rev. **9**, 73-84, 1947 (No. 3).

This is indeed a standing wave, for **E** and **H** are products of sin ωt and cos ωt, respectively, and a function depending only upon the place.

The expressions (41) will represent a possible mode of oscillation of the **E** and **H** fields in a circular cavity resonator when the boundary conditions are satisfied at the two new walls (transforming a circular wave guide into a circular cavity resonator). If the two walls are introduced at $z = 0$ and at $z = l$ then at $z = 0$ the boundary condition $E_t = 0$ is automatically satisfied, since $E_r = 0$ for $z = 0$. To obtain $E_r = 0$ also at $z = l$, we must have $h_p l = 0$, and from this it follows that:

$$h_p l = \pm \pi q \ (q = 0,\ 1,\ 2 \ldots). \quad . \ . \ . \ . \ . \ . \quad (42)$$

The boundary condition $H_n = 0$ is automatically satisfied because H_z is everywhere equal to zero.

Now the condition (42) agrees with eq. (33) only when $\omega = \omega_{pq}$, where

$$\left(\frac{\omega_{pq}}{c}\right)^2 = \left(\frac{\pi q}{l}\right)^2 + \left(\frac{\varrho_p}{b}\right)^2. \qquad \begin{pmatrix} p = 1, 2, 3 \ldots \\ q = 0, 1, 2 \ldots \end{pmatrix} \qquad (43)$$

From eq. (43) it follows that a circular cavity resonator cannot oscillate at every frequency. Among the rotationally symmetrical standing waves (41) only those corresponding to the characteristic frequencies $\nu_{pq} = \omega_{pq}/2\pi$ represent a possible mode of oscillation.

According to (43) and (34) the lowest characteristic frequency ($q = 0$, $p = 1$) is equal to the lowest cut-off frequency of running E-waves in a circular wave guide.

$$\nu_{10} = \varrho_1 c/2\pi b. \quad . \ . \ . \ . \ . \ . \ . \ . \quad (44)$$

Not only the "standing E-wave" corresponding to (44) — here we introduce a term which is in line with the terminology used in the case of wave guides — but also all other standing E-waves with $q = 0$ have the property that their characteristic frequencies are independent of the length l of the cavity resonator; this follows from (43). From (41) and (42) it follows moreover that with these standing waves the electrical lines of force always run parallel to the axis of symmetry. In the case of "standing H-waves", which we shall not deal with here, the characteristic frequency is in no case independent of the length of the cavity resonator.

The electrical lines of force in the case of a standing E-wave ($q = 1, p = 1$) in a circular cavity resonator can be seen from fig. 5, provided the two new walls closing the wave guide on the left and the right are applied at suitably chosen places. By "suitably" we mean here a choice which satisfies the boundary conditions. A vertical straight line, which in fig. 5 would represent each of the new walls, must therefore exactly halve the contours. (In a similar manner the magnetic lines of force can be read from fig. 5 for the case of a standing H-wave in a circular cavity resonator.) Whereas, however, in the case of the wave guide fig. 5 was "an instantaneous recording", here this figure represents lines of force not changing with the time.

The current density i in the walls of the cavity resonator can also be easily calculated from eqs (41)-(43) if reference is made to the boundary condition $H_t = i$. For the "bottom" ($z = 0$) or the "cover" ($z = l$) of the cavity resonator we obtain in this manner, for $q = 0$,

$$i = H_\varphi = 2A \,.\, \mathrm{J}_1 (r\varrho_p/b) \,.\, \cos \omega t \,. \quad . \ . \ . \quad (45)$$

Fig. 2 of the article quoted in footnote [10]) is a representation of the current density distribution as obtained from (45) for $p = 1$ and $p = 2$.

Of course the mathematical expressions for electromagnetic waves in cavity resonators can also be deduced directly from the Maxwell equations, thus without employing the expressions for running waves.

THE ORIGIN OF THE GIORGI SYSTEM OF ELECTRICAL UNITS

by W. de GROOT. 537.71

This article gives an outline of the origin of the system of fundamental formulae in electricity and magnetism, the subject being dealt with in such a way as to give an insight into the Giorgi system of electrical units. These units are explained and particular attention is paid to what is called rationalization. This is followed by a review dealing historically with the c.g.s. systems, the practical system, the absolute and the international practical units. Finally the realization of the absolute ampere, ohm and volt is briefly described.

Introduction

The following is an outline of the development of the fundamental formulae in electromagnetism, given in such a way as to throw some light upon the Giorgi or M-K-S system of electrical units.

The unit of charge

Systems of formulae used in electro-magnetism are usually based upon the Coulomb law:

$$K = a\frac{Q_1 Q_2}{r^2},$$

where K is the mutual force between the charges Q_1 and Q_2 at a distance r between each other, and a is a constant that has still to be determined [1]). Once it has been decided in what units K and r are to be measured, then by ascribing a certain value to a one arrives at a definition for a unit of charges.

One may also regard the above formula as a particular case of a general law according to which

$$\mathbf{K} = Q_2 \cdot \mathbf{E},$$

where $\mathbf{E}$ represents the field strength vector [2]). In an electrostatic field, for a charge Q_1 carried along a path s from point *1* to point *2* we have the formula:

$$\frac{1}{Q_1}\int_1^2 K_s \,\mathrm{d}s = \int_1^2 E_s \,\mathrm{d}s = V_1 - V_2,$$

where K_s and E_s represent the components of the force and of the field strength respectively in the direction of s. This holds regardless of the path followed by the charge from point *1* to point *2*. V_1 and V_2 are the electrostatic potentials in the points *1* and *2* (already determined except for a constant). This determines the unit of potential difference, since the unit in which the energy $\int K_s \,\mathrm{d}s$ will be measured is already fixed.

An important step in the theory is the law of the superposition of electric fields: $\mathbf{E}$ is the vector sum of the separate $\mathbf{E}$'s originating in each of the charges. As a consequence, when we integrate in vacuum the component E_n of $\mathbf{E}$ across a closed surface A according to the normal of that surface and thus construct $\oint\!\!\oint E_n \mathrm{d}A$, the result is proportional to the total charge Q enclosed by that surface:

$$Q = \iiint \varrho \,\mathrm{d}\tau \backsim \oint\!\!\oint E_n \,\mathrm{d}A,$$

where ϱ represents the spatial charge density (charge per unit volume) whilst $\mathrm{d}\tau$ is a volume element within the enclosed surface. The value of the constant of proportionality (which appears to be $4\pi a$) is directly related to the choice of the unit of charge.

Following the example of Maxwell, the same fact can also be expressed by introducing a new vector $\mathbf{D}$ proportional to $\mathbf{E}$ and then requiring that the corresponding surface integral $\oint\!\!\oint D_n \mathrm{d}A$ shall be not only proportional but also equal to Q:

$$\oint\!\!\oint D_n \,\mathrm{d}A = Q. \quad \ldots\ldots \quad (1)$$

The integral of D_n across a part of a surface bounded by a closed curve is called the electric flux Ψ through that surface

$$\Psi = \iint D_n \,\mathrm{d}A.$$

Equation (1) then expresses the fact that the total electric flux Ψ through a closed surface is equal to the enclosed charge Q.

The relation between $\mathbf{D}$ and $\mathbf{E}$ can be represented by writing:

---

[1]) The Coulomb law has not been very accurately verified by direct observation of the force K. Later, it has been confirmed very accurately by indirect experiments, for instance by Cavendish, where it was proved that a charged body placed inside a closed conductive envelope lost all its charge to the envelope when contacted with it. See, for instance, J. H. Jeans, The mathematical theory of electricity and magnetism, Cambridge 1923, 4th edition, pp. 37-38.

[2]) From now onwards vectors, such as $\mathbf{E}$, will be printed in heavy type and the magnitude of a vector, such as E, in italics.

$$\mathbf{D} = \varepsilon \mathbf{E}, \quad \ldots\ldots\ldots \quad (2)$$

where the magnitude of ε again depends upon the units chosen.

The advantage of proceeding in this way is that account is also taken of the phenomena occurring when the dielectric is not an empty space but is wholly or partly filled with an insulating medium.

If the medium occupies only part of the space or if there are several media then, in addition to (2), boundary conditions also arise, namely $D_{n1} = D_{n2}$ and $E_{t1} = E_{t2}$, where the indices n and t relate to the components normal and parallel to the interface between the two media and the indices 1 and 2 indicate the media on either side of this surface.

The quantity **D** is termed the dielectric displacement. In any medium the value of ε differs from the value ε_0 applying in vacuum. The quotient

$$\frac{\varepsilon}{\varepsilon_0} = \varepsilon_r$$

is called the (relative) dielectric constant of the medium.

The electric current

A charge in motion represents an electric current. If v is the velocity of the charge Q then $\mathbf{I} = Q\mathbf{v}$ is the current and, in the case of an extensive charge, $\mathbf{S} = \varrho\mathbf{v}$ is the current density.

If S_n is the component of **S** perpendicular to an element $\mathrm{d}A$ of a closed area A then

$$\oint\oint S_n \, \mathrm{d}A = -\frac{\mathrm{d}}{\mathrm{d}t} \iiint \varrho \, \mathrm{d}\tau. \quad \ldots\ldots \quad (3)$$

The measuring of charges can also be reduced to the measuring of currents (think of the ballistic galvanometer). If we proceed in a manner similar to that described above for charges, the measuring of currents can in turn be reduced to the measuring of the forces that the conductors exercise one upon the other. We shall not attempt to explain this in detail but refer to textbooks on the subject. We would only remind the reader that a current conductor determines a magnetic field characterized by a vector **B**. A part of a second conductor (length $\mathrm{d}l$) through which a current **I** is flowing and which is perpendicular to the vector **B** is subjected to a force of the magnitude

$$K = B \cdot I \cdot \mathrm{d}l. \quad \ldots\ldots \quad (4)$$

In the absence of a coefficient this equation determines the unit for B; the direction of the force is given by Fleming's left-hand rule.

As regards the current giving rise to the field, we have it that in the vacuum the line integral $\oint B_s \mathrm{d}s$ taken along a closed curve surrounding the conductor is proportional to the current I flowing through the conductor:

$$I = \iint S_n \, \mathrm{d}A \backsim \oint B_s \, \mathrm{d}s.$$

In the same manner as for the electrotastic field, we can introduce beside the vector **B** a vector **H** which is proportional to **B** and for which the equation holds:

$$\oint H_s \, \mathrm{d}s = I, \quad \ldots\ldots \quad (5)$$

whilst **H** and **B** bear the relation:

$$\mathbf{H} = \frac{1}{\mu} \mathbf{B}. \quad \ldots\ldots \quad (6)$$

The advantage of this method of reasoning is again that we include at the same time the phenomena obtained when the vacuum is wholly or partly replaced by a paramagnetic or diamagnetic medium. In such a medium μ has a constant value, which differs however from the value μ_0 applying in the vacuum. The quotient

$$\frac{\mu}{\mu_0} = \mu_r.$$

is termed the relative permeability. For paramagnetic substances it is greater than unity and for diamagnetic substances less than unity.

Where there is more than one medium, separated by an interface, or where the vacuum is partly filled, there occur on the interface certain boundary conditions analogous to those for **D** and **E**. Besides the paramagnetic and diamagnetic media, ferro-magnetic media also occur. The phenomena occurring in these ferro-magnetic substances can again be described by the equations given above but then the relation between **B** and **H** is more complicated. In the simplest case (absence of hysteresis) $B = \mathrm{f}(H)$, where $\mathrm{f}(H)$ represents a function characteristic for the medium.

Variable fields [3])

So far we have been considering the case of charges in a state of rest and stationary currents. In the case of currents changing with the time t the law of induction applies, which says that: if $\iint B_n \mathrm{d}A = \Phi$ represents the surface integral of **B** across a surface bounded by a closed curve (Φ is called the magnetic flux) then there acts along the curve an electric force E_s according to the equation:

$$\oint E_s \mathrm{d}s = -\frac{\mathrm{d}}{\mathrm{d}t} \Phi. \quad \ldots\ldots \quad (7)$$

[3]) See also the article by W. Opechowski, Philips Techn. Rev. **10**, 14-26, 1948 (No. 1).

E and Φ are related by the "corkscrew rule".

In equation (7) there is no new coefficient and the equation sign applies as in (4). This is closely related to the law of the conservation of energy, which connects (4) and (7).

As Maxwell first demonstrated, in the case of a surface partly bounded by a closed curve there are values of $\oint H_s ds$ differing from zero not only when a charge is flowing through the surface but also when the electric flux $\Psi = \iint D_n dA$ bounded by the said curve changes with time, in which latter case

$$\oint H_s ds = \frac{d}{dt}\Psi. \quad \ldots\ldots \quad (8)$$

As a rule, when moreover a charge passes through this area then

$$\oint H_s \, ds = I + \frac{d}{dt}\Psi. \quad \ldots\ldots \quad (8a)$$

From eq. (7) we can deduce that for a closed area

$$\oint\oint B_n \, dA = 0, \quad \ldots\ldots \quad (9)$$

whilst from eq. (8a) it follows that

$$\oint\oint (S_n + \dot{D}_n) \, dA = 0, \quad \ldots \quad (3a)$$

which is agreement with (3).

Maxwell's equations

The equations (1), (9), (7) and (8*a*) are the well-known Maxwell equations, which together with (2) and (6) determine the properties of the electromagnetic field. Side by side with these we have the physically less fundamental but in practice important Ohm's law, according to which, in a large number of cases, there is a proportionality between the current density S and the electric field vector **E**:

$$\mathbf{S} = \gamma \mathbf{E}, \quad \ldots\ldots\ldots \quad (10)$$

where γ represents a material constant, the specific conduction.

The Maxwell equations are generally given in a differential form instead of in the integral form; they then read:

$$\begin{aligned} \text{div } \mathbf{D} &= \varrho, \\ \text{div } \mathbf{B} &= 0, \\ \text{curl } \mathbf{E} &= -\dot{\mathbf{B}}, \\ \text{curl } \mathbf{H} &= \dot{\mathbf{D}} + \mathbf{S}, \end{aligned}$$

$$\mathbf{D} = \varepsilon \mathbf{E}, \quad \mathbf{B} = \mu \mathbf{H}, \quad \mathbf{S} = \gamma \mathbf{E}.$$

One of the most important consequences of these equations is that an electromagnetic plane wave is propagated with the phase velocity

$$v = \frac{1}{\sqrt{\varepsilon \mu}}.$$

In vacuum this is the velocity of light c, so that

$$\varepsilon_0 \mu_0 c^2 = 1. \quad \ldots\ldots\ldots \quad (11)$$

The Giorgi units

As we have seen above, the units of all quantities occurring in electro-magnetism are fixed as soon as a choice has been made for the mechanical units of length, mass and time and, further, a unit has been fixed for the charge or the current intensity.

In 1901 G. Giorgi [4]) put forward a number of proposals in connection with these units:

1) In the the place of the centimeter, gram-mass and second (the basic units of the c.g.s. system, to which belong the dyne as unit of force and the erg as the unit of energy) Giorgi takes the meter (m), the kilogram-mass (kg) and the second (sec.). The unit of force in this system is the force which induces in 1 kg mass an acceleration of 1 meter/sec./sec. This unit of force is called the newton (N):

$$1 \text{ newton} = 10^5 \text{ dyne}.$$

The mechanical unit of work is the work performed by the force of one newton when the point of application moves 1 meter in the direction of the force. This unit is called the newton-meter = 1 joule (J);

$$1 \text{ joule} = 1 \text{ newton-meter (N·m)} = 10^7 \text{ erg}.$$

Thus the mechanical unit of work becomes equal to the electrical unit:

$$1 \text{ joule} = 1 \text{ watt·second} = 1 \text{ VAsec}, \quad . \quad (12)$$

provided one starts from the so-called absolute volt and ampere.

2) As unit of current intensity the ampere (A) is chosen. As we have just seen, it is best to understand by this the absolute ampere.

This may be defined, for instance, as the current required to flow through two infinitely long straight conductors (with negligible circular cross section) so that, given a mutual distance of one meter, the force per meter length equals $2 \cdot 10^{-7}$ newtons (resolution of the "Comité International des Poids et Mesures", to take effect as from January 1st 1948).

All other units follow from this choice. For the greater part they coincide with those of the already commonly used "practical" system of electric units, namely with the so-called absolute practical units.

What is new in this system, however, is the fact that Giorgi consistently uses the volt and ampere also in the units for the electromagnetic field quantities.

[4]) G. Giorgi, Unità razionali di electtromagnetismo, Atti dell' Assoc. electtr. Ital. **5**, 402-418, 1901.

The quantity E is measured in volts/meter, the quantity D in coulombs/m² ($\Psi = \iint D_n \mathrm{d}A$ in coulombs) and B in newtons/ampere·m, or, in other words, in volts·seconds/m².

The last manner of writing the quantity B reminds us of another way of determining B, *viz.* by applying the law of induction. The surface intregal Φ is measured in units of volt·second, also called the weber (Wb). For H the unit is ampere/m. The units for ε and μ are A·sec/V·m = farad/m and V·sec/A·m = henry/m respectively.

Rationalization

When using c.g.s. units one is accustomed to find factors of 4π in the formulae analogous to (1) and (5). In the "mixed system of Gauss" the formulae (1) and (5) generally read:

$$\oint\oint D_n' \, \mathrm{d}A = 4\pi Q,$$

$$\int H_s' \, \mathrm{d}s = 4\pi I,$$

where Q and D' are expressed in electrostatic units and I and H' in electromagnetic units. Here the field quantities have been accented to distinguish them from the quantities D and H meant in this article, which are determined by (1) and (5). The omission of the factor 4π, which in the case of the quantities D and H leads to a natural interpretation such as we have already applied above, results in certain differences between the old and the new form of known formulae. For instance Coulomb's electrostatic law now reads:

$$K = \frac{1}{\varepsilon} \frac{Q_1 Q_2}{4\pi r^2}, \quad \ldots . \quad (13)$$

and the formula for the force which two infinitely long conductors exercise upon each other over a distance l reads:

$$K = \mu \frac{I_1 I_2 l}{2\pi r}. \quad \ldots . \quad (14)$$

On the other hand the formula for the capacitance C of a plane capacitor with area A and distance between the plates s becomes:

$$C = \varepsilon \frac{A}{s},$$

and that of the self-inductance L of a long coil of n windings with area A for a coil length s becomes

$$L = n^2 \mu \frac{A}{s}.$$

It is therefore seen that the number π does not occur in formulae representing "homogeneous" cases but does appear in formulae relating to cases with spherical or cylindrical symmetry. This so-called rationalization (it is rational in that π occurs in the latter cases and not in the former ones) is an advantage of the manner of writing formulae (1) and (5) proposed by Giorgi and of the definitions for D and H embodied therein.

From formula (14) it follows, further, that since in vacuum $K = 2 \cdot 10^{-7}$ N, when $r = 1$ m, $l = 1$ m, $I_1 = I_2 = 1$ A,

$$\mu_0 = 4\pi/10^7 \text{ V·sec/A·m} \quad \ldots . \quad (15)$$

Taken together, (15) and (12) can also be construed as a way of defining the "absolute" electrical units.

Since $\varepsilon_0 \mu_0 c^2 = 1$, with $c = 2.99776 \cdot 10^8$ m/sec it follows that

$$\varepsilon_0 = \frac{10^7}{4\pi c^2} \approx 8.855 \cdot 10^{-12} \text{ A·sec/V·m} \quad . . \quad (16)$$

A remark is to be made in respect to the Coulomb magnetic law. As is known, a long coil acts as a rod magnet with "poles" at the extremities. From the north pole there is a flux $\Phi = \iint B_n \mathrm{d}A$ (taking the integral across the cross section of the coil). This flux can be taken as a measure of the pole strength, but with a given current this varies with the medium. Independent of the medium, however, is the quantity $\iint H_n \mathrm{d}A = P$. If Φ is chosen as pole strength then the force between two poles at a distance r is:

$$K = \frac{1}{\mu} \frac{\Phi_1 \Phi_2}{4\pi r^2} \ldots . \quad (17)$$

If P is taken as the pole strength then

$$K = \mu \frac{P_1 P_2}{4\pi r^2} \ldots . \quad (18)$$

Both these formulae give expression to Coulomb's law of magnetism. Formula (17) is, formally, analogous to (13) whilst (18) is analogous to (14). The case is more or less academic, since actually free magnetism does not exist [5]).

Historical notes

The c.g.s. systems so far usually employed go back to the two laws of Coulomb:

$$K_{\mathrm{el}} = \alpha \frac{Q_1 Q_2}{r^2} \quad \ldots . \quad (19)$$

and

$$K_{\mathrm{magn}} = \beta \frac{P_1 P_2}{r^2}, \quad \ldots . \quad (20)$$

where P_1 and P_2 represent the magnet pole strength, which laws have been formulated in analogy with Newton's law of attraction (about 1680).

After Oersted (1819) had determined how electrical currents act upon the poles of a magnet [6])

[5]) See also A. Sommerfeld, Über die elektromagnetischen Einheiten, Z. techn. Phys. **16**, 420-424, 1935, and "Verhandelingen aangeboden aan Prof. Dr. P. Zeeman", M. Nijhoff, The Hague, 1935, pp. 157-165.

[6]) Oersted spoke of the "electrical conflict". The title of his paper of 1820 read: "Experimenta circa effectum conflictus electrici in acum magneticum". He imagined that when a Volta battery is circuited with a wire the "two electricities" (+ and —) combine and that this turbulent process causes the magnetic action.

it was particularly Ampère [7]) (Sept.-Dec. 1820) who undertook a thorough investigation of these forces, as also the forces between conductors. With the aid of what is understood as the "current element" one can formulate Ampère's results in the same way as the Coulomb laws. The most familiar formula is that of Laplace[8]), which reads:

$$K = \delta \frac{I\,ds \cdot P}{r^2} \sin \varphi, \quad \ldots\ldots \quad (21)$$

indicating the force exercised by a current element Ids upon a magnet pole P at a distance r (φ is the angle between the directions of r and ds, K being perpendicular to those directions, whilst δ is a constant).

It was Ampère, too, who first introduced the concepts of current and tension as we know them to-day. The concept of resistance and the laws indicating the relation between current and voltage when applied to conductors are due to Ohm (1829).

From the formulae (20) and (21) Gauss developed (about 1830) the so-called electromagnetic system of units, following upon which Weber (about 1850) derived from (19) the electrostatic system. These systems were not officially adopted as c.g.s. systems until 1873. (Gauss worked at first with the millimeter as length unit and the milligram as mass unit).

In 1831 Faraday discovered the law of induction (7) and in 1864 Maxwell revealed its analogue (8). The introduction of the field concept began with Faraday and Maxwell. As is known, Maxwell was the first to prove that the relation between the electromagnetic and the electrostatic charge units is equal to the velocity of light (in centimeters per second).

Helmholtz (1882) and Hertz (about 1890) employed a mixed system of units where electrical units were measured in terms of e.s.u. and magnetic units in e.m.u. (generally called the "Gauss mixed system"). The three c.g.s. systems are characterized by the place occupied by the factors c ($\approx 3 \cdot 10^{10}$) and c^2 in the formulae.

The "practical" units

None of the above-mentioned systems of units was suitable for practical use in the developments taking place in electrotechnics. Through the activities of the British Association for the Advancement of Science (1867) there came to be adopted the now commonly used practical units of the ohm, volt and farad, to which were added by the "Congrès International des Electriciens" (1881) [9]) the coulomb, ampere and henry (originally sec·ohm = ohm·sec).

These units are equal to the electromagnetic units but for factors of powers of 10: 1 ohm = 10^9 e.m.u., 1 volt = 10^8 e.m.u., 1 farad = 10^{-9} e.m.u., 1 coulomb and 1 ampere = 1/10 e.m.u., 1 henry = 10^9 e.m.u. In 1935 the I.E.C. ("International Electrotechnical Committee") decided to apply Giorgi's M-K-S system in electrotechnics.

International units

Together with the adoption of the practical units there arose a need to define them by standards or standardized specifications. It would lead us too far to go into this at any length here and we shall only briefly relate how the so-called international ampere and ohm have so far come to be established:

1 int. amp. = the current which when passed through a specified silver voltameter will deposit silver at a rate of 1.11800 mg/sec.;

1 int. ohm = the resistance of a column of mercury of uniform cross-sectional area, 1.06300 m in length and 14.4521 g in mass at 0 °C.

From these two data there follows the international volt, which, moreover, has also been fixed by taking the e.m.f. of the Weston cell at 10°C as equal to 1.01830 V.

As was to be expected, upon further investigation these units were found to be practically but not precisely in agreement with the "absolute" or "theoretical" units. Various government laboratories have since then determined the relation of the international to the absolute practical units. The average equations of six laboratories (Germany, England, France, Japan, U.S.A., U.S.S.R.) are as follows [10]):

1 int. ohm = 1.00049 absolute ohm,
1 int. amp = 0.99985 absolute ampere,
1 int. volt = 1.00034 absolute volt,
1 int. watt = 1.00019 absolute watt (10^7 erg/sec).

Although the deviations are so small as to be of no importance for many practical measurements, where measurements have to be precise it is indeed of importance to know exactly what units have been used. In particular, the double definition of

[7]) See e.g. G. A. Boutry, Ampère ou la Pureté, Rev. trim. Canad. **33** 257-274, 1947 (No. 131).

[8]) Commonly known as the Biot-Savart law (1829), although these authors were only considering the special case of an infinitely long straight conductor.

[9]) See e.g. G. Giorgi, La métrologie classique et les systèmes d'unités qui en dérivent, Examen critique. Rev. Gén. Electricité **40**, 457-467, 1936.

[10]) See e.g. Mesures **11**, 379-380, 1946.

the international volt is apt to lead to mistakes [11]).

Mixed use of practical and c.g.s. units

Whilst the practical units came into general use for research as well as for engineering — largely as a result of the availability of standard instruments calibrated in these units, such as resistance boxes and meters — c.g.s. units continued to be used for describing electrical and magnetic fields. For this purpose powers of 10 are introduced in the formulae as coefficients, as for instance in the formula

$$V = -10^{-8}\frac{d\Phi}{dt},$$

indicating the relation between the electromotive force V induced in a winding of a transformer and the magnetic flux Φ, where V is expressed in volts and Φ in gauss·cm^2 (= maxwell). We have already seen how the proposals made by Giorgi have led to these factors also disappearing from the formulae.

Realization of the absolute ampere, ohm and volt

In 1910 at a conference held in Washington agreement was reached between the laboratories of the U.S.A., England, France, Germany, Japan and Russia in regard to the standards of resistance and e.m.f. In 1930 however the standards of the various countries were found to show intolerable discrepancies. The "Comité International des Poids et Mesures" has now decided to return as from January 1st 1948 to the absolute units, on the ground that modern measuring technique has been sufficiently developed to be able to realize these units at any desired moment. Several different methods of doing this are in use [12]).

One method for determining the ohm as an absolute measure, for instance, is to compare in a bridge circuit the self-inductance of a coil of known dimensions with the capacitance of an auxiliary capacitor, which capacitance is then compared with a resistance in a second measuring bridge. The absolute ampere is determined by the force acting between two conductors in accordance with the definition given above. Of course one does not use infinitely long straight conductors, but circular coils of exactly known dimensions and with a precisely known mutual position. The force is measured with a current balance. Since the force depends not only on the masses of the weights but also on the acceleration due to gravity at the place where the measurement is taken, it is necessary to measure the latter very accurately. When the absolute ampere and ohm are known, then the absolute volt is the voltage induced by a current of one ampere at the extremities of a resistance of 1 ohm.

The international units now play at most the part of secondary standards. That is why we have given above the relation between absolute and international units, as fixed for 1948. In a subsequent article in this journal some practical consequences of the use of the rationalized Giorgi system (with absolute volt and ampere) will be explained further.

[11]) See e.g. U. Stille, Die Umrechnungsfaktoren von internationale auf absolute elektrische Einheiten, Z. Phys. **121**, 24-53, 1943.

[12]) See e.g. L. M. Briggs, Rev. mod. Phys. **11**, 111-120, 1939.

CONICAL DISC SPRINGS

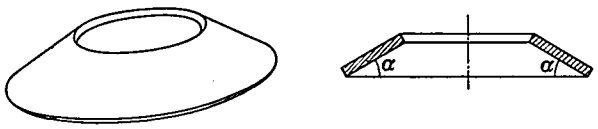
by J. A. HARINGX.

621-272.4

Relatively little use is made of the disc spring as resilient element in constructions. In respect to the amount of energy that can be absorbed a disc spring can certainly lay no claim to any fundamental superiority over the helical spring, but in certain cases it does make the construction simpler and more efficient. What these cases are will be discussed in this article, following upon a brief explanation of the properties of disc springs, some of which are rather remarkable. The designing of disc springs most suitable for a certain purpose is explained in more detail for two particular cases. It appears that the most favourable shape of the disc spring (for a given load and maximum permissible stress) can be very easily determined with the aid of appropriate graphs.

Among the various kinds of springs applied in the technique the conical disc springs (often called Belleville washers) are relatively little known. In recent times, however, they have been receiving more attention because they often help to simplify constructions.

A conical disc spring — in the following pages the adjective "conical" will mostly be omitted — consists of what we might call the "collar" of a truncated cone the vertex angle of which is approximately 180° (see *fig. 1*). In the limit case where this



52341

Fig. 1. Diagrammatic representation of a conical disc spring in the non-loaded state. On the left a view in perspective, on the right the meridian cross section. The angle α is actually much smaller than that indicated here, seldom exceeding 6°.

vertex angle is exactly 180° we have a round flat plate with a circular aperture at the centre. Although the disc spring therefore bears a certain resemblance to such a flat plate, the results of the theory of bent plates may not be used directly for disc springs, not even as an approximative solution. This is due to the entirely different nature of the stresses occurring. For instance, if a disc spring supported underneath is loaded with an axial force uniformly distributed along the upper rim it undergoes an axial compression and takes the shape as indicated by the full line in *fig. 2*. The outer edge is forced slightly outwards and stretched, whilst the inner edge is shortened. As a consequence, in addition to bending stresses there also arise radial and tangential stresses uniformly distributed over the thickness, which stresses do not occur in bent plates, at least not at small deflections.

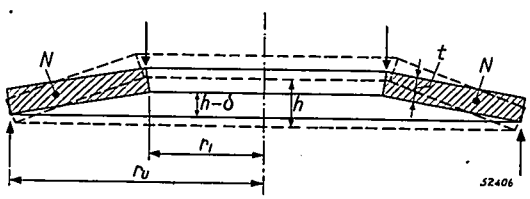
In this connection disc springs show some typical properties which will be discussed in this article. Then we shall consider how the disc spring should be shaped for a given load and maximum permissible stress in two particular cases, and finally we shall give some examples of the application of disc springs.

Properties of the disc spring

General properties

Looking at fig. 2 we see that the top and bottom edges of the disc spring lie in two parallel planes, not only in the original state but also in the loaded state, on account of the axial symmetry. If the spring is placed between two parallel "compression plates" the compressive force will therefore always be transmitted in an axial direction. Moreover, the shallow height allows of an element with great resilience being used in a small space. These two properties are highly important and in many cases make the application of the disc spring exceptionally attractive.

Furthermore, it is possible to combine several of these disc springs (say n in number) in the manner illustrated in *fig. 3a*. With this arrangement, given the same load, the compression is n times as great as that for one single disc. If, on the other hand, n



52406

Fig. 2. The meridian cross section of a loaded disc spring resulting from the meridian cross section of the non-loaded spring (in broken lines) after rotation around the points N. Both in the loaded and in the non-loaded state the top and bottom edges lie in two parallel planes. The inner and outer radii of the spring are indicated by r_i and r_u; h and t are respectively the height and thickness of the spring; δ is the compression.

springs are stacked in the manner indicated in fig. 3*b* a load n times as great is required to bring about the same compression. Of course both these methods could be used in combination one with the other, but it has to be pointed out that the system of stacking into what might be called a packet (fig. 3*b*) always gives rise to friction and wear, which is often troublesome.

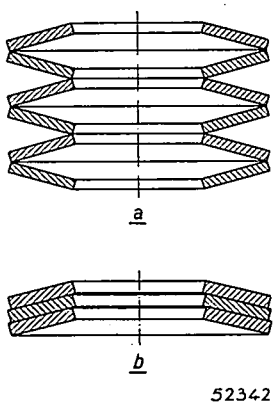


Fig. 3. *a*) A resilient column built up with disc springs. *b*) A resilient packet built up with disc springs.

The amount of energy that can be absorbed per unit of volume of the material is about a factor 3 less in the case of the disc spring than in the case of the helical spring. Thus, to reach the same effect, about three times as much material is required when using a disc spring. For the same amount of material the disc spring does, it is true, take up less space than the helical spring, but not so much less as to compensate this factor 3. When it is a matter of accommodating the largest possible amount of energy in a given space the disc spring is at a disadvantage by a factor of about 2, so that from this point of view there is no purpose in using a column of disc springs in the place of a helical spring. However, there are other reasons why a disc spring may after all be preferable as compared with the helical spring. In certain cases it is useful, for instance, to be able to adjust easily the rigidity of the resilient element (i.e. the load per unit of compression); whereas the rigidity of a helical spring already made cannot be altered, this is indeed possible with a column built up out of several separate disc springs. A further important point is that disc springs can be made in any engineering works, whereas the coiling of heavy helical springs requires some experience.

Relation between load and compression

Apart from the general characteristics of disc springs mentioned above, which are generally decisive for their application, in certain cases it may be advantageous to make use of the peculiar shape of the curves representing the relation between load and compression. We shall prove this with the aid of the theoretical formula expressing the said relation, viz:

$$\frac{P}{P_h} = 1 + \left[1 - \tfrac{1}{2}\left(\frac{h}{t}\right)^2\right]\left(\frac{\delta}{h} - 1\right) + \tfrac{1}{2}\left(\frac{h}{t}\right)^2\left(\frac{\delta}{h} - 1\right)^3. \quad (1)$$

The meaning of the symbols h, t, δ occurring in this formula can be found in the subscript to fig. 2: h and t are respectively the height and thickness of the disc spring; δ is the compression. Further, P is the axial load uniformly distributed over the edges of the disc spring, whilst P_h represents the force required to flatten the disc spring ($\delta = h$). A calculation shows that

$$P_h = \frac{Eht^3}{Mr_u^2}, \quad \ldots\ldots \quad (2)$$

where E is the modulus of elasticity, M a certain function of r_u/r_i, and r_u and r_i are respectively the external and the internal radius of the disc spring (see fig. 2).

From equation (1) it is seen that the relation between load and compression depends only upon the thickness of the spring, taking P_h as load unit and h as length unit.

Fig. 4 shows the relation between P/P_h and δ/h according to eq. (1) for various values of h/t. The curves appear to fall into two groups according as $h/t > \sqrt{2}$ or $h/t < \sqrt{2}$.

Where $h/t > \sqrt{2}$, that is to say for disc springs that are relatively thin, the curves show a maximum and a minimum. When a disc spring is compressed continuously, for instance by placing it between two parallel plates drawn closer together by turning a screw, the compressive force exercised by the disc spring upon the compression plates does not by any means change at a uniform rate, but in a certain range (between the maximum and the minimum) it decreases with increasing compression. When the ratio h/t is greater than $2\sqrt{2}$, the (P, δ)-curve intersects the abscissa, so that corresponding to a compression $\delta > \delta_1$ (see in fig. 4 the curve for $h/t = 3$) we find a negative compressive force. Since in this case a disc spring is incapable of exercising a negative compressive force (thus a tensile force) the spring loses contact with the compression plates and, being now unloaded, changes in shape until the stable state of equilibrium $\delta = \delta_2$ is

reached; in other words the disc spring suddenly gives [1]).

We now consider δ as a function of P instead of P as a function of δ, that is to say, instead of bringing the two compression plates closer together by means of a screw, we bring a continuously increasing force to bear upon the spring, for instance with the aid of weights. It will be clear that the disc spring will now give as soon as the force reaches the maximum in the (P, δ)-curve and the compression $\delta = \delta_1'$ will jump to the value $\delta = \delta_2'$ (see in fig. 4 the curve for $h/t = 2$).

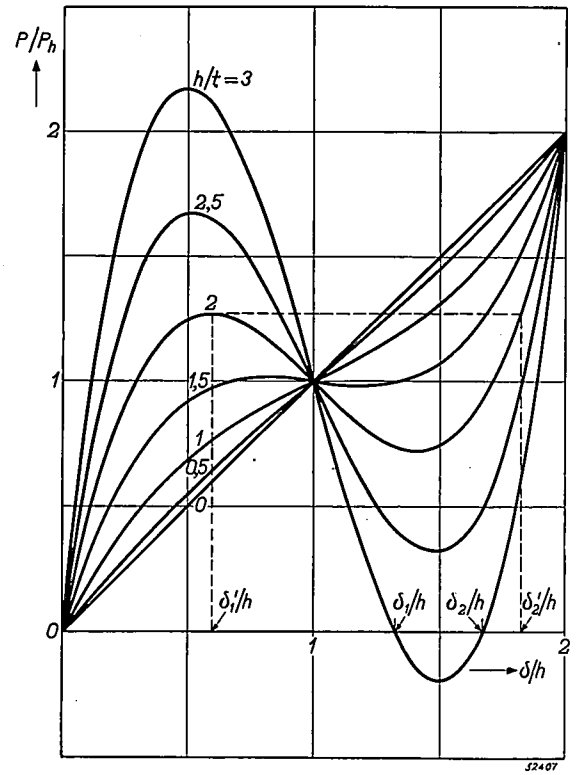


Fig. 4. The relation between the load P and the compression δ of a disc spring for different values of the ratio of the height h to the thickness t. The length unit is the height h of the disc spring and the load unit is the value P_h of the load at the flattened state of the spring.

Usually it is desired to avoid these phenomena of "giving". A construction must therefore be designed in such a way that the compressions actually occurring are always less than the compression corresponding to the maximum of the (P, δ)-curve.

Where h/t is less than $\sqrt{2}$ on the other hand the compressive force always increases at a uniform rate with the compression. The greater the thickness of the disc spring, the more the (P, δ)-curve approaches a straight line.

For $h/t = \sqrt{2}$, the curve representing the compressions round about $\delta = h$ runs practically horizontal. It is this peculiar property of the disc spring that is of great practical importance in certain constructions, in particular in those cases where the load is required to be independent of the compression. An example of such an application of the disc spring will be given presently.

Relation between the maximum stresses and the compression

An important property of any spring in practice is the relation between the maximum stresses occurring in it and the load or corresponding compression. The maximum stress may never exceed a permissible limit, which is to be regarded as a given material constant. In the case of a disc spring the maximum (compressive) stresses σ occur along the top rim on the inside. For σ the following formula holds

$$\sigma = \frac{E\delta h}{Mr_u^2}\left[C_1\left(1-\frac{\delta}{2h}\right)+C_2\frac{t}{h}\right], \quad \left(\frac{\delta}{h}<2\right), \ldots \quad (3)$$

where C_1 and C_2 are certain functions of r_u/r_i given by the theory; the other terms have already been defined.

Theoretical fundamentals of equations (1) to (3)

We shall now say a few words about the manner in which the behaviour of the disc spring represented by the equations (1) to (3) can be deduced. Since the problem of the disc spring has never yet been dealt with in an exact theoretical manner, we can only work upon the approximative calculation of Almen and Laszlo [2]). These authors introduce the supposition — which is after all only obvious — that the rectangular cross section of the spring lying in the meridian plane does not change in shape when loaded, but only turns about a "neutral" point, indicated in fig. 2 by the point N. This greatly simplifies the determination of the tangential elongations ε_t. Applying this conception consistently, they put the radial elongations ε_r as zero and calculate the tangential stresses σ_t with the aid of the equation $\sigma_t = m^2E\varepsilon_t/(m^2\text{-}1)$, where m represents Poisson's ratio = 10/3. The radial stresses then amount to $\sigma_r = \sigma_t/m = 0.3\,\sigma_t$. The approximation theory given by Almen and Laszlo can be partly checked with the flat "conical" disc spring ($h = 0$), the behaviour of which can be calculated with the conventional theory of the bending of flat plates. The shape of the flat disc spring (for instance in the case where $r_u = 2r_i$) in the loaded state does indeed deviate only very little from a cone, so that one can safely calculate the tangential elongations ε_t as those obtaining for the conical shape. The small deviation from the conical shape is due to the fact that there are practically no radial bending stresses: the outer or inner edges of the disc spring are free of load in a radial direction, and here the radial

[1]) We have a familiar example of this phenomenon in the case of certain containers closed by a metal lid that is slightly convex. When more than a certain limit pressure is applied to the centre of the lid this gives inward and the serrated rim is forced out.

[2]) J. O. Almen and A. Laszlo, The Uniform Section Disk Spring, Trans. Amer. Soc. Mech. Engrs. 58, 305-314, 1936.

stresses are in fact exactly zero. Towards the centre between the inner and outer edges they do, it is true, increase, but in the case that $r_u = 2r_i$ they reach at most a value of 0.065 σ_t and are therefore much smaller than the stresses 0.3 σ_t which would be present according to the calculation of Almen and Laszlo.. We may therefore expect a better approximation of the problem of the disc spring when we put instead of the radial elongations the radial stresses at zero, thus calculating the tangential stresses with the aid of the equation $\sigma_t = E r_t$. As a result of this correction the factor $1-\sigma^2 = (m^2-1)/m^2$ is eliminated from the denominators in the formulae of Almen and Laszlo. At the same time the differences between their calculation and the experimental result are likewise partly eliminated.

Except for the factor just referred to, eqs (2) and (3) given above are identical with those of Almen and Laszlo.

Design of disc springs

It is not the intention to deal here with the technical problem of the designing of a disc spring, or of columns of disc springs, in general terms. All we intend to do is to show briefly, with reference to two special cases, how the shape of a disc spring can best be chosen with the aid of suitable graphs.

First case

In the construction of a press in one of the Philips factories it was found useful to employ columns of disc springs built up in the manner indicated in fig. 3*a*. In order to minimize the number of springs in a column like this one has to use disc springs with a certain optimum value of the ratio of the external diameter to the internal diameter. For the greatest possible compression under a given load and given maximum stress this ratio should preferably be chosen equal to 2, as may be determined by a calculation applying for the case of a flat disc spring. Thus we put once for all $r_u/r_i = 2$, when the functions M, C_1 and C_2 occurring in equations (2) and (3) have respectively the values 0.69, 1.225 and 1.58.

Furthermore for constructional reasons disc springs which under the maximum load pass through the flat state cannot be used. If, therefore, we fix the minimum slope of the generatrix of the disc spring at say 0.04 we get the condition:

$$h - \delta = 0.04\,(r_u - r_i),$$

that is to say, since $r_u = 2r_i$,

$$\frac{h}{\delta} = 1 + 0.02\,\frac{r_u}{\delta} \quad . \quad . \quad . \quad . \quad . \quad (4)$$

Moreover, we have to take care that the maximum stresses σ in the spring, calculated according to eq. (3), never exceed a certain permissible limit.

To give a disc spring the greatest possible elasticity its material must allow of very great stresses. What the maximum permissible stresses are is a matter of experience. For plain carbon steel, for instance, σ may amount to 120-140 kg/mm², whilst in the case of quenched and tempered chromium-nickel steel stresses may occur as high as 180-200 kg/mm² (with thin disc springs even up to 220 kg/mm²). These are very high values and it is therefore inevitable that under these conditions local plastic distortions will arise, so that already under the first load the disc spring "settles" a little, thus reducing the height h. This must therefore always be taken into account when designing a disc spring. Should the load not be static, as tacitly understood so far, but dynamic then a repetition of such plastic deformations will in the long run prove fatal. Therefore in this case we must base our calculations on the fatigue strength of the material, which means that with a good kind of spring steel a stress variation of at most 100 kg/mm² is permissible.

Taking these requirements into consideration, not much freedom is left in the choice of the most suitable shape for a disc spring, for we have to work upon four equations (1)-(4) between seven quantities, P, P_h, δ, σ, r_u, h, t, which means that we can only freely dispose of three quantities. Now in the practical problem the load P and the maximum stress σ are given, so that really we are only free to vary one quantity, and for this it is well to choose r_u. By a simple conversion of the equations (1)-(4) we obtain two relations of the following form:

$$\frac{\delta}{r_u} = \Psi\left(\frac{P}{r_u^2}, \sigma\right) \quad . \quad . \quad . \quad . \quad . \quad (5)$$

and

$$\frac{t}{r_u} = \Phi\left(\frac{P}{r_u^2}, \sigma\right) \quad . \quad . \quad . \quad . \quad . \quad (6)$$

We shall not write down the rather complicated, though elementary, functions Φ and Ψ but give them in the form of graphs in *fig. 5*.

With P, σ and r_u given, we now find from equation (5) or from the right-hand graph of fig. 5 the value of δ/r_u, and from eq. (6) or the left-hand graph of fig. 5 the value of t/r_u. Only h is still unknown, and this we find from eq. (4).

The curves in the right-hand graph of fig. 5 are limited upward by a broken line defined by the condition $t/r_u < 0.25$. This condition has to be fixed because otherwise the thickness of the disc spring would exceed the practical limit. The bottom limit in the graph has been introduced in order to avoid too strong a deviation from the straight (P, δ) line and also as a safeguard against the troublesome "give" phenomena (cf. fig. 4). The upper and the

lower broken lines for the bottom limit correspond respectively to the condition $h/t < 1.0$ and $h/t < 1.2$.

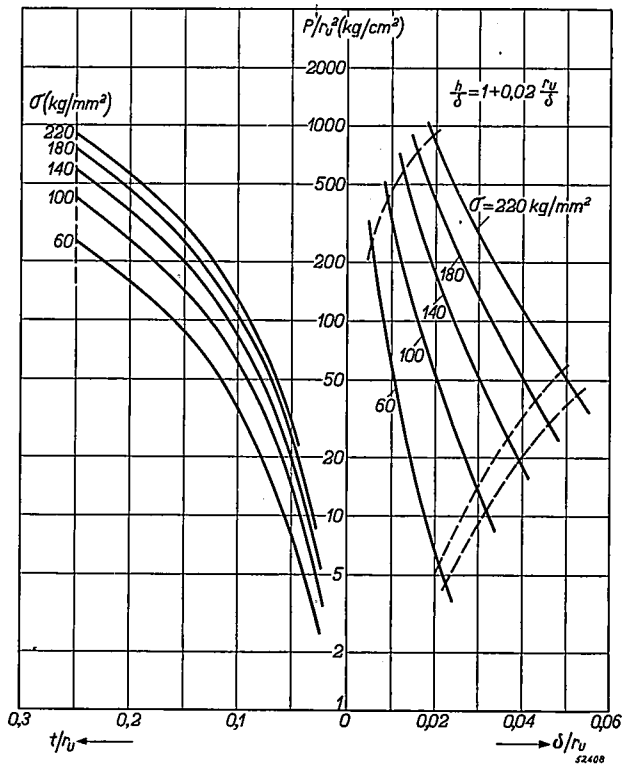


Fig. 5. Graph showing the compression δ and the thickness t of the spring for a given load P, maximum permissible stress σ and outer radius r_u (= $2r_i$) of the disc spring. The height h of the spring is calculated with the aid of the formula given (eq. (4)). This graph holds for the case where a disc spring has to be designed which allows of the greatest possible compression under a given load.

Tests made with disc springs calculated in the manner described above showed that the actual compression was smaller than calculated. Upon further consideration a very acceptable explanation of this was found. Disc springs stacked in a column are apt to slide one over the other on account of the sharp edges, and in order to avoid this the top edge and the bottom outer edge were slightly ground to provide a flat seating (see *fig. 6*). The compression being rather great, the slope of the cone becomes noticeably smaller and the flat-ground edges do not remain flat but become slightly

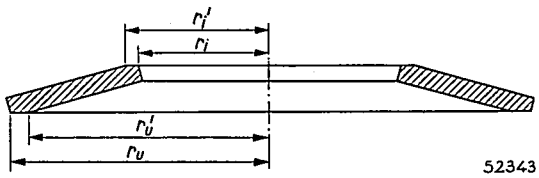


Fig. 6. When stacked up in a column the disc springs may easily slide over each other. To avoid this the top and bottom edges are slightly ground off to a flat plane as sketched here.

conical, so that the original contact planes of two adjacent disc springs begin to show some clearance. As a consequence the load is transmitted at circles with radii r_i' and r_u' respectively instead of at those of radii r_i and r_u respectively. Obviously $r_i' > r_i$ and $r_u' < r_u$.

Taking this fact into consideration we can still use eqs (5) and (6) as well as the corresponding graphs in fig. 5, with hardly any alteration. As a further consideration will show, we only have to introduce in place of the actual load P a fictitious load $P' = kP$ where

$$k = \frac{r_u' - r_i'}{r_u - r_i}.$$

However, the value then obtained for δ', from the modified eq. (5),

$$\frac{\delta'}{r_u} = f\left(\frac{P'}{r_u^2}, \sigma\right),$$

is not the actual compression δ. In order to arrive at δ, the value δ' has to be multiplied by the factor k:

$$\delta = k\delta' \quad \ldots\ldots\ldots \quad (8)$$

The compression values calculated in this manner agree well with the measured results.

Second case

As already stated, a typical property of the disc spring is the fact that when it is suitably dimensioned its compression can be varied between wide

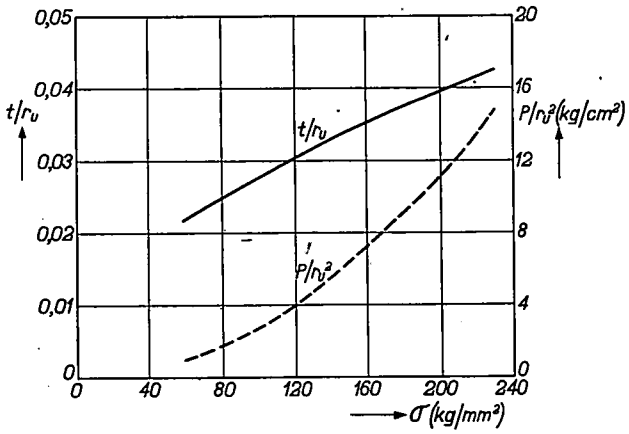


Fig. 7. Graph for designing a disc spring where the compression is required to be variable within wide limits under a constant load. In this case the ratio of the height h to the thickness t is 1.5. For a given load P and maximum permissible stress δ this graph gives the values of the outer radius r_u (= $2r_i$), the thickness t and the height h.

limits without hardly any change in load. If this property is to be utilised there must be a certain relation between the height and the thickness of the spring, namely $h/t \approx \sqrt{2} = 1.41$. For instance for

$h/t = 1.5$, P is found to be constant within the region $0.6\,h < \delta' < 1.4\,h$. This constant value of P depends only upon σ and r_u. In *fig. 7*, P/r_u^2 is plotted as a function of σ for $h/t = 1.5$ and $r_u = 2r_i$. When the load is given one can therefore find immediately from this graph what value has to be chosen for r_u (and r_i). Fig. 7 also gives the curve representing t/r_u as a function of σ, from which can be derived the required thickness and height of the spring for a given r_u.

Possibilities of application

The example already mentioned where a column of disc springs was required for a press lies in a domain where also a helical spring can be used. As stated when dealing with the properties of disc springs, in this case the disc spring does not offer any fundamental advantages over the helical spring and only secondary circumstances are decisive.

The specific field of application for the disc spring is rather to be sought in cases where the helical spring cannot be considered. For instance, advantage can be taken of the shallowness and excellent centering of the compressive force in the case of friction couplings, for fixing securely the parts of a motor commutator and wherever an elastic construction is desired to take up large impulses [3]).

An example of the application of a disc spring for a compressive force independent of the compression is given by Almen and Laszlo in the article quoted in footnote [2]). There it concerns the fixing of the tail-stock centre of a lathe. Owing to the generation of heat in the turning process the workpiece expands and if the centre does not "give" the workpiece gets jammed. By applying the disc spring construction this is avoided, for here the centre has axial freedom of movement without the axial force increasing to any appreciable extent.

---

[3]) Examples given by G. Ashworth, The Disk Spring or Belleville Washer. Proc. Inst. Mech. Engrs **155**, 93-100, 1946.

ABSTRACTS OF RECENT SCIENTIFIC PUBLICATIONS OF THE N.V. PHILIPS' GLOEILAMPENFABRIEKEN

Reprints of these papers not marked with an asterisk can be obtained free of charge upon application to the Administration of the Research Laboratory, Kastanjelaan, Eindhoven, Netherlands.

R 53: A. van der Ziel: Method of measurement of noise ratios and noise factors (Philips Res. Rep. **2**, 321-330, 1947, No. 5).

In this paper methods are described, as applied in this laboratory, for the measurement of noise ratios of impedances and of the noise factor of receivers. Instead of standard signal generators, saturated diodes are used as "standard noise generators". The noise voltages are amplified in a linear amplifier having a relatively small bandwidth (50-100 kc/sec), and detected by a thermocouple.

R 54: J. L. H. Jonker: Reflections in electron tubes (Philips Res. Rep. **2**, 331-339, 1947, No. 5).

The characteristics of some electron tubes show irregularities as a result of reflected electrons. By studying the peculiarities of these reflections at low potentials, it is possible to deduce their influence on the electric field between the electrodes, and in this way to explain the irregularities.

R 55: F. A. Kröger: The temperature dependence of the fluorescence of tungstates and molybdates in relation to the perfection of the lattice (Philips Res. Rep. **2**, 340-348, 1947, No. 5).

The quenching temperature of the photoluminescence of tungstates and molybdates is dependent on the perfection of the crystals, imperfect crystals having a low quenching point. This property may be explained in terms of the quenching theories of Mott and Seitz, as well as in terms of the theories of Peierls, Möglich - Rompe and Frenkel.

R 56: F. de Boer: Some characteristics of trigonal selenium crystals obtained from the vapour phase (Philips Res. Rep. **2**, 349-351, 1947, No. 5).

Trigonal selenium crystals of a size sufficient for conduction measurements have been prepared from the vapour phase. The majority of these crystals had the form of hollow needles showing slight deviations from the ideal monocrystal structure. A small fraction, however, consisted of thick and massive twin crystals, amongst which one rather well-developed monocrystal was found. All well-developed planes were prism planes.

R 57: F. de Boer: On the electrical conductivity of selenium crystals (Philips Res. Rep. **2**, 352-356,1947, No. 5).

For the specific resistance of selenium monocrystals parallel to the c-axis values ranging from 2.10^4 to 5.10^4 Ω cm were observed; it is made plausible that the specific resistance of a pure monocrystal is lying near the lower end of this range. The specific resistance at right angles to the c-axis was found to be 2.10^6 Ω cm. In addition some experiments on the influence of temperature and pressure on the conductivity were carried out.

R 58: L. J. Dijkstra: Elastic relaxation and some other properties of the solid solutions of carbon and nitrogen in iron (Philips Res. Rep. **2**, 357-381, 1947, No. 5)

The theory of elastic relaxation in α-iron caused by carbon and nitrogen in solid solution, as given for the first time by Snoek and later elaborated by Polder, predicts a strong anisotropy for the various crystal directions. This theoretical conclusion has been confirmed in a series of experiments carried out on prepared single crystals of iron in the (100)- and (111)-directions. For carbon it was possible to check the theoretical absolute magnitude of the effect. The question of the most probable place of the dissolved particles in the iron lattice is also discussed.

Finally at 20 °C the rate of segregation taking place in the form of a carbide or nitride has been determined by measuring the decrease in magnitude of the elastic relaxation in the course of time.

R 59 J. D. Fast: The dissociation of nitrogen in the welding arc (Philips Res. Rep. **2**, 382-398, 1947, No. 5)

For temperatures in the range from 5000-10000 °K the dissociation of nitrogen is computed on the basis of spectroscopic data and for three different values of the dissociation energy, viz. 7·383, 8·573 and 9·764 electron-volts; in view of a recent investigation by Gaydon and Penncy the highest value is probably the correct one.

At 10000°K and a pressure of one atmosphere the degree of dissociation is 99% at least; at 5000 °K 25.1% of the nitrogen will be dissociated if the dissociation energy amounts to 7.383 eV, but only 1.63% will be dissociated if the dissociation energy is 9.764 eV. Two cruder methods of computation give results that differ only slightly from these "exact" values.

R 60: J. Haantjes and B. D. H. Tellegen: The diode as converter and as detector (Philips Res. Rep. **2**, 401-419, 1947, No. 6)

The current through a diode, to which is applied, in addition to an A.C. voltage and a D.C. voltage, a small extra voltage v, can be developed into a power series of v whose coefficients are Fourier series. The magnitude of these coefficients is calculated for a diode that has a linear characteristic in the pass direction. By confining ourselves to the term linear in v, four-pole equations and equivalent circuits can be set up for the diode as converter and as detector. From these equivalent circuits various properties and quantities can be deduced. The fluctuations of the diode as converter can also be represented with the help of the equivalent circuit. Upon conversion as well as upon detection it is found favourable to give the diode a small internal resistance.

R 61: H. C. Hamaker: Radiation and heat conduction in light-scattering material (Philips Res. Rep. **2**, 420-425, 1947, No. 6)

In previous papers (see **R 35**, **R 38** and **R 39**) only simplified problems have been considered. For a fuller discussion of many practical questions of a similar kind some extensions of the theory are required. These are indicated, though no attempts are made to work them out in full detail.

R 62: N. Warmoltz: The time-lag in starting a low-pressure arc on a mercury or gallium cathode in connection with field emission and surface deformation (Philips Res. Rep. **2**, 426-441, 1947, No. 6)

For the contents of this article see Philips techn. Rev. **9**, 105-113,1947 No. 4

R 63: W. Elenbaas: The continuous spectrum of the high-pressure mercury discharge (Philips Res. Rep. **2**, 442-453, 1947, No. 6)

The intensity of the continuous spectrum of the high-pressure mercury discharge has been measured between $^1/_4$ and 25 atm for inputs from 20 to 60 watts/cm and for diameters between 6 and 60 mm. The ratio of the intensity of the continuum to the intensity of the yellow lines 5770/91 is almost independent of the input and increases linearly with the mean vapour density m/d^2. The ratio at $m/d^2 = 0$ is interpreted as being due to recombination of electrons with ions, whereas the contribution proportional to m/d^2 originates from molecular radiation.

A rough energy balance is given in which the line energies and the energies radiated in the two types of continuum occur. Using the equation, the absolute value of the intensity of the continuum of the U.V.-standard is found to be more than twice as high as the value measured by Rössler.

The discrepancy between the measured and calculated gradient between 1 and 5 atm disappears on using this energy-balance equation instead of that formerly used, in which the lines and the recombination spectrum were the only radiations taken into account. The remaining discrepancy at higher pressures is probably due to the diminution of the ionization potential at these high densities. The magnitudes of these diminutions necessary to account for the measured gradients are tabulated as a function of the mean vapour density.

R 64: J. W. L. Köhler and C. G. Koops: Absolute measurement of the time constant of resistors (Philips Res. Rep. **2**, 454-467, 1947, No. 6)

A new method is described for the accurate determination of the time constant of resistors in absolute measure, using as standards of reference a set of standard condensers with negligible losses as described in a previous paper (see Philips techn. Rev. **5**, 311-319, 1940)

R 65: F. L. H. M. Stumpers: On the calculation of impulse-noise transients in frequency-modulation receivers (Philips Res. Rep. **2**, 468-474, 1947, No. 6)

The effect of impulse-noise transients is calculated by means of a series expansion of the phase, the general term of which contains $[A(t)]^n$ when the amplitude $A(t)$ of the disturbance is smaller than the amplitude of the signal, and $[A(t)]^{-n}$ in the inverse case. The Laplace transform is used to calculate the effect in the filters. The large effect of phase-opposition during the capture time is accounted for.

VOL. 10 No. 3, pp. 69-96 SEPTEMBER 1948

Philips Technical Review

DEALING WITH TECHNICAL PROBLEMS
RELATING TO THE PRODUCTS, PROCESSES AND INVESTIGATIONS OF
THE PHILIPS INDUSTRIES

EDITED BY THE RESEARCH LABORATORY OF N.V. PHILIPS' GLOEILAMPENFABRIEKEN, EINDHOVEN, NETHERLANDS.

PROJECTION-TELEVISION RECEIVER

I. THE OPTICAL SYSTEM FOR THE PROJECTION

by P. M. van ALPHEN and H. RINIA

621.397.62:535.881

A series of articles will be published dealing with various parts of a projection-television receiver for home use. The first of these articles opens with a brief introduction on television in general and then proceeds to deal with the optical system for the projection. For this purpose Philips employ a somewhat modified mirror system with a Schmidt correction plate. The modification consists mainly in the addition of a plane mirror placed obliquely in the path of the light between the spherical mirror and the correction plate. The very fast optical system (numerical aperture 0.62 with a magnifying factor 8.7) is free of third order aberrations with the exception of the curvature of field. The latter has been corrected by giving the screen of the cathode-ray tube a certain curvature. In this manner a perfectly clear picture is obtained on a flat projection screen. This picture is just as bright as a cinema picture and is of such a size (32 cm × 40 cm) and brightness that the audience can easily observe it in a room with normal or slightly lowered lighting. Due to the compact construction of the optical part and of other parts to be described later, the whole apparatus can be housed in a cabinet of very reasonable dimensions.

In 1939 the technique of television had reached a stage of development where several transmitters were already regularly broadcasting a television programme and receiving sets were on the market. After the war this branch of broadcasting was revived and the number of transmitting stations now regularly working is gradually increasing; at the moment there are several scores of these, most of which are in the U.S.A. (in Europe there is one in London and another in Paris). In addition there are several transmitters of a more or less experimental character (among others there is one at Eindhoven in Holland). With this increasing number of transmitters the demand for television receivers is bound to increase, and it is in this connection that a series of articles are being published in this journal dealing with some important points in the development of these receivers. Before starting on the first of these articles it may well be worth while to sketch briefly the principle of present-day television [1]).

The "eye" of the transmitter is the iconoscope [2]) or its special form known as the "orthicon", upon the "retina" of which a picture is cast of the scene to be transmitted. This "retina" is periodically scanned by a beam of electrons, thereby producing electrical impulses the amplitude of which corresponds to the brightness of the successively scanned points in the image. These impulses are called video signals and modulate the transmitter.

In the receiver a cathode-ray tube is employed as the light source. Just as in the case of an oscillograph, a beam of electrons produces a spot of light on the luminescent screen of the cathode-ray tube. The beam periodically scans the image plane in synchronism with the beam in the transmitter, the strength of the current in the beam varying according to the modulation of the video signal received.

---

[1]) See for instance J. van der Mark, An experimental television transmitter and receiver, Philips Techn. Rev. 1, 16-21, 1936.

[2]) See the article quoted in footnote [1]), particularly page 18.

As a result the points scanned in succession on the screen show variation in brightness corresponding to those of the image transmitted.

To maintain the synchronization between the electron beam in the transmitter and that in the receiver special synchronizing signals are transmitted in addition to the actual video signal.

The television receivers placed on the market from 1936 to 1940 were mostly built for "direct view", the image observed being that produced on the luminescent screen of the tube [3]). In particular the large types of tubes for direct view, with a screen diameter larger than 30 cm, are expensive and difficult to handle. To give these large tubes the necessary strength (on a tube face 39 cm in diameter the atmosphere exercises a force much greater than 1000 kg) they have either to be made very thick or given a fairly large curvature. This curvature distorts the image observed, so that the effective area of the face is not proportional to the dimensions of the tube. The danger of implosion makes it necessary to provide special safety measures. Owing to the length of the tube — it increases roughly in proportion to the screen diameter — the cabinet has to be made of such large dimensions as to be incompatible with an aesthetic appearance.

All these objections, which arise when a good-sized image is required, were recognized at an early date and are now avoided, or at least considerably reduced, by the projection method. By this method a small image produced on the face of a likewise small cathode-ray tube is projected onto a viewing screen by optical means. Obviously this is the only way if a televised picture is to be viewed by a large audience, for instance in a theatre. But also for the home — and it is exclusively home receivers that we shall be speaking about in this series of articles — it is very convenient to have a picture of such a size that a fair number of spectators can easily see it without being strictly confined to one particular place. Philips marketed a tube for projection reception as far back as 1937 [4]). Since then, however, this projection system has undergone considerable development.

Below we shall describe the optical system with which the image of about 3.6 cm × 4.6 cm that is formed on the tube face is projected onto a viewing screen as a bright, sharp and flat picture of 32 cm × 40 cm. Due to the small dimensions of the tube and the special construction of the optical system it has been possible to house the whole apparatus in a cabinet of moderate dimensions (see *fig. 1*, in the subscript to which various particulars are given).



Fig. 1. Apparatus type SG 860 A for projection-television and for ordinary broadcast reception. The three control knobs in front of the television screen, taken from left to right, are for controlling the sharpness and the brigtness of the picture and adjusting the contrast between the light and dark parts. The five controls underneath the station dial serve for adjusting the selectivity and the volume, changing over from ordinary broadcasting to gramophone music or television, for tuning and for selecting the wave range. Behind the cloth screen below these controls is the loudspeaker. Small extension loudspeakers on either side of the projection screen serve only for television reception. The screen can be left folded down when not tuning in to television broadcasts.

Mirrors or lenses?

In order to project the image produced on the cathode-ray tube face onto a viewing screen one may use either concave spherical mirrors, or lenses, or a combination of both these elements. The question is which is to be preferred.

Let us first deal with some advantages of mirrors in general. In the first place they do not show any chromatic aberration. Further, the spherical aberration of a mirror is less than that of a lens with the same diameter and focal length, so that for a given

[3]) See e.g. G. Heller, Television receivers, Philips Techn. Rev. **4**, 342-350, 1939, in particular fig. 13. By "direct view" is to be understood here also the observation of the picture via a plane slanting mirror, with the cathode-ray tube having its axis in a vertical position an arrangement employed in some cabinet models.

[4]) M. Wolf, The enlarged projection of television pictures, Philips Techn. Rev. **2**, 249-253, 1937.

permissible aberration mirrors can be used with a larger aperture number (i.e. greater speed) than lenses. Moreover, mirrors of high aperture number are comparatively easy to make. Whereas the diameter of a lens is limited to about 50 cm, mirrors of 1.5 metre diameter are quite common, as for instance for searchlights. The cost of a mirror compares favourably with that of a lens of equal performance; a mirror has only one ground and polished face and need not be made of so-called optical glass. This is why astronomers usually prefer mirrors; the Mount Palomar Observatory has a mirror of 5 meters diameter, which surpasses any lens ever made.

But, compared with lenses, mirrors are not entirely free of drawbacks. Owing to the fact that they reflect the light, the image of the object is formed in the path of the incoming light rays, which are thus more or less intercepted. This is the reason why mirrors have found little favour in photography and in the projection of films, where preference is given to fast lenses. This was a disadvantage that weighed rather heavily at first also in the designing of an optical system for the projection of televized images, but by a special arrangement of the components, to which we shall refer presently, this drawback has in so far been overcome as to be more than outweighed by the advantages of a mirror.

The mirror system with Schmidt correction plate

We must first recall the fact that a spherical mirror, just like a lens, is subject to a number of image defects, or aberrations [5]). Confining our remarks to third-order aberrations, these are to be distinguished as spherical aberration, coma, astigmatism, distortion and curvature of field. In the article quoted in footnote [5]) it is shown how a diaphragm placed in the centre of curvature of the mirror neutralizes a number of these defects, leaving only spherical aberration and curvature of field. Further, it is stated that of these two remaining defects the spherical aberration can be eliminated with the aid of a Schmidt correction plate, which has been further discussed in a separate article [6]), where a detailed description is given of an extremely simple and inexpensive method developed by Philips for manufacturing these correction plates. The plates made by this method consist of a layer of gelatin applied to a flat glass plate and given the desired profile.

The only image defect (apart from aberrations of a higher order which are of less importance) is the curvature of field: a plane object is sharply focused on a curved surface that is approximately a spherical one. Conversely an object curved in a certain way will be sharply focused on a plane surface. If, therefore, the face of the cathode-ray tube is given a certain curvature then the projection will be flat, so that a sharp image can be obtained on a flat viewing screen. For more details the reader is referred to a later article specially devoted to the cathode-ray tube.

Modifications made in the Schmidt system

Schmidt developed his system for photographing the stars. Here the photographic film or plate — and not the object that is to be imaged — forms an unavoidable obstruction for some of the light rays that would otherwise be utilized by the optical system. In television projection it is just the other way round. Here we are faced with the question how to apply the cathode-ray tube in such a way that its face, which is here the luminescent object, comes to lie in the right position between the mirror and the correction plate, while the minimum of light is interrupted or lost in any other way. The positioning of the tube is rendered still more difficult owing to the fact that its anode carries a high tension with respect to earth (25 kV) and the tube itself is surrounded by coils for focusing and deflecting the electron beam.

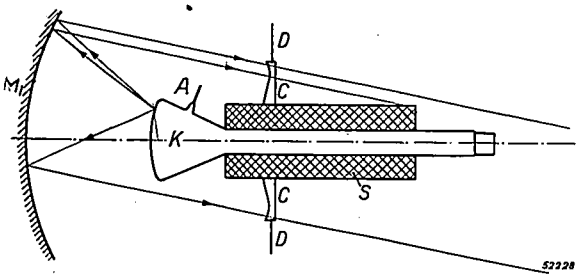


Fig. 2. Simple optical system for television projection but with considerable loss of light through interception. K = cathode-ray tube with anode connection A and focusing and deflection coils S. M_1 = spherical mirror, C = Schmidt correction plate, D = diaphragm. (In figs 2-5 the outgoing rays are drawn parallel for the sake of simplicity, but actually they converge upon a point on the projection screen, which is a relatively large distance away.)

An obvious construction is illustrated in *fig. 2*, where the neck of the tube, together with the coils, is passes through an aperture in the correction plate. Even if the tube were short enough to allow of its being accommodated entirely between the mirror and

[5]) See e.g. W. de Groot, Optical aberrations in lens and mirror systems, Philips Techn. Rev. **9**, 301-308, 1947 (No. 10).

[6]) H. Rinia and P. M. van Alphen, The manufacture of correction plates for Schmidt lenses, Philips Techn. Rev. **9**, 349-356. 1947 (No. 12).

the correction plate, the middle part of the correction plate would still lie in the shadow of the tube, so that the fact that in fig. 2 this part has had to be removed for the neck of the tube to pass through it does not constitute any additional drawback. There is, however, the drawback that the tube intercepts some rays coming from the edge of the image and striking the tube or the coils laterally (see fig. 2), though this effect can be reduced by providing for a smaller angle between these rays and the axis, thus by selecting a larger focal distance. This, however, would lead, with a given aperture number (a conception to be dealt with presently), to a larger diameter of the mirror, and this in turn would necessitate a larger cabinet. This solution could only be applied where the space is not limited, as for instance for television projection in a theatre.

A constructional objection against the central aperture in the correction plate is the fact that this aperture makes it extremely difficult to centre the plate. A simple solution for the centering of a plate not having a aperture in the middle will be referred to later on.

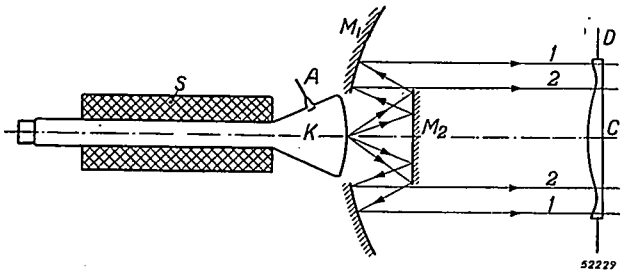


Fig. 3. Modified arrangement of the optical system where the light rays reach the spherical mirror via the plane mirror M_2. In this model the diameter of the plane mirror is such that the rays *1* emerging from the centre of the tube face and reflected from the edge of M_2 just pass through the edge of the correction plate *C*.

A method absolutely avoiding lateral shadow effect of the tube is represented in *fig. 3*. Here the tube screen is situated in an opening in the centre of the spherical mirror. The rays coming from the tube face strike a plane mirror (M_2) which reflects them onto the spherical mirror. Thus the dimensions of the tube and the coils are no longer restricted, since the tube and coils do not lie in the path of the light. But now we are faced with another difficulty, viz. the question as to how large the plane mirror has to be. Let us first consider only the rays emitted from the centre of the tube face. In fig. 3 the plane mirror is of such a size that the rays *1* striking its edge just pass through te edge of the correction plate. When we follow the rays coming from the edge of the tube screen and reflected by the plane mirror (beam between *3* and *5* in *fig. 4*) we see that these fall partly outside the correction plate and are thus held back by the diaphragm (e.g. *4* and *5* in fig. 4). Thus the useful beam emitted by a point on the edge is narrower than the beam

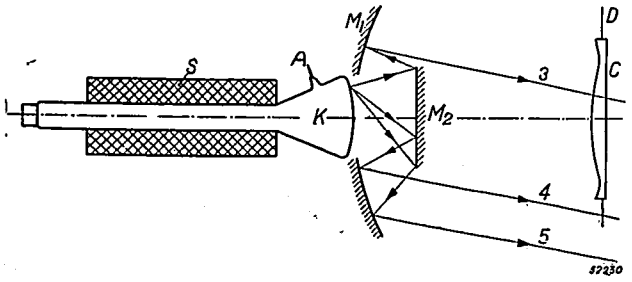


Fig. 4. The same arrangement as in fig. 3 but showing some rays emerging from the edge of the image on the face of the cathode-ray tube. Rays like *4* and *5* fall outside the correction plate.

coming from the centre. This manifests itself in the image on the projection screen as a sort of vignetting, that is to say the intensity of light in the corners is less than in the middle. This phenomenon can be counteracted by making the plane mirror larger, but then still more light rays are intercepted (*i.e.* the rays *2* in fig. 3). Thus a really satisfactory compromise is not to be found.

Finally it is to be remarked that a system such as that of fig. 3 has the disadvantage of being greater in length than that of fig. 2.

In the Philips optical system for televisoin projection (*fig. 5*) a plane mirror is also employed but placed at an angle of 45° to the axis of the spherical mirror. This plane mirror is not, optically speaking, situated between the tube screen and the spherical mirror, as is the case in fig. 3, but between the spherical mirror and the correction plate. The screen of the cathode-ray tube protrudes through an opening in the flat mirror, in such a way that the loss of rays coming from the centre of the tube screen is of practically the same magnitude as the loss of rays

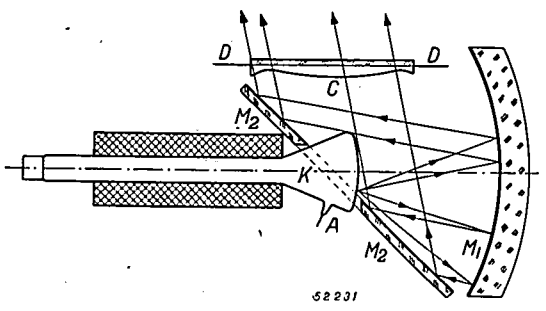


Fig. 5. The arrangement adopted for the Philips optical system. The plane mirror M_2 lies in the light path between the spherical mirror and the correction plate and makes an angle of 45° with the axis of the cathode-ray tube.

coming from the edges of the face. Vignetting thus arises to a much less extent than in the case of fig. 3; the tube does not hold back any light laterally (cf. fig. 2) on account of its being behind the mirror, where there is space enough for the coils, fixtures, connecting leads, etc.

The path of the light is folded, as it were, so that the construction of the apparatus can be very compact (*fig. 6*). The cathode-ray tube and the whole of the optical system can be housed in a dust-proof box, so that the tube face, the two mirrors and the gelatin side of the correction plate are kept clean. Only the flat, glass outer face of the correction plate can accumulate dust, but it is very easy to clean and there is no risk of the system being disturbed. The place occupied by the optical unit in the receiving set is shown in *fig. 7*.

A second plane mirror is affixed on the inside of the slanting cabinet lid (fig. 1 and 7) to throw the light beam passing through the correction plate onto the projection screen.

Characteristic quantities of a Schmidt system

We shall now consider for a moment what quantities are typical of a Schmidt optical system, for we have to refer to these in the next section dealing with the dimensioning of the optical system.

In the first place there is the focal distance, from which follow the distances for the object and image required for a certain magnification. The magnification, too, is a characteristic quantity.

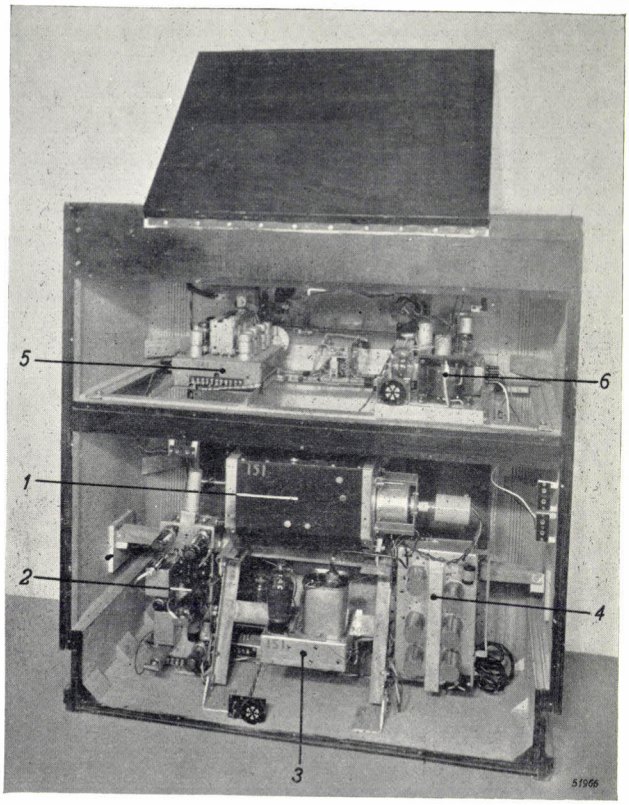


Fig. 7. Inside view of the receiving set SG 860 A (cf. fig. 1) seen from the back.
1 is the optical unit (cf. fig. 6),
2 apparatus for deflection of the electron beam,
3 high-tension unit (25 kV),
4 television receiver (picture and sound),
5 receiver for ordinary broadcasting
6 rectifier.

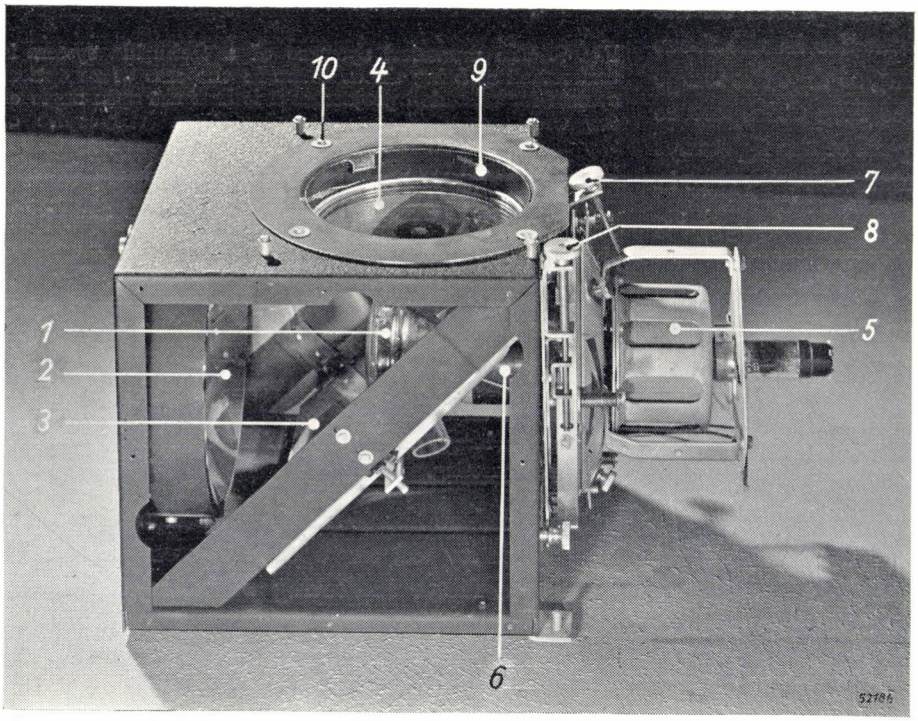


Fig. 6. The Philips optical system for projecting television pictures (one side of the mounting box removed). *1* is the face of the cathode-ray tube, *2* the spherical mirror, *3* the plane mirror, *4* the correction plate, *5* the focusing coil, *6* the deflection coils, *7* one of the adjusting screws for aligning the axis of the cathode-ray tube, *8* the screw for adjusting the distance between the tube screen and the spherical mirror, *9* screws fixing the correction plate holder after the plate has been set to the correct height, *10* fixing screws around which some play is left in the rim of the correction plate holder for the purpose of centering.

Just as a parabolic mirror gives a good image only with one object distance or image distance, viz. infinite, so a particular Schmidt system is suitable for only one such distance, thus for one particular magnification [7]). If the system were to be used

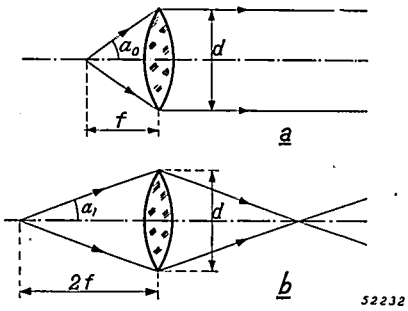


Fig. 8. *a*) Simple lens with light source in the focus and infinite projection of the image. The relative is understood to be $d/f = 2 \tan \alpha_0$.
b) The same lens with true-to-size projection. Here the relative aperture is $d/2f = 2 \tan \alpha_1$.

with some other magnification then the spherical aberration would not be completely eliminated. For every correction plate it is therefore necessary to specify not only the radius of curvature of the corresponding mirror but also the magnification for which it is calculated, the more so since this magnification cannot easily be derived from the form of a particular specimen.

Further, the "speed" is an important quantity in an optical system. In the case of lenses this is usually expressed by the relative aperture. For a simple lens this represents the ratio of the diameter d of the lens (or of the diaphragm) to the focal distance f. If the apex angle of the cone of rays striking the lens from a light point placed on the axis is 2α and if the light point lies in the focus (where α has the value α_0; *fig. 8a*), so that the image is formed at an infinite distance then the aperture number $d/f = 2 \tan \alpha_0$, If the path of the light rays is reversed then we get the situation which arises in photography when the object distance can be regarded as infinite, as is often the case. When, however, an object is photographed from close by, e.g. so that the picture is the actual size of the object (fig. 8*b*), then the speed of the lens is determined by an angle $\alpha_1 < \alpha_0$ (in this case $\tan \alpha_1 = {}^1/_2 \tan \alpha_0$). Accordingly, when taking a close-up photograph a longer exposure time is required than when the focusing is infinite (under otherwise the same conditions).

From this it appears that when specifying the value of d/f one should really mention the object or image distance used (or, what comes to the same thing, the magnification). Moreover, it is in fact not $\tan \alpha$, that might be derived from these data, but rather $\sin\alpha$ that gives a direct measure for the speed of an optical system. In relatively low-speed optical systems, such as those of the usual cameras, the value of α is so small that the difference between $\tan\alpha$ and $\sin\alpha$ is of no significance, but with the very high speeds that can be reached with the Schmidt system this difference is indeed of importance. The quantity $\sin\alpha$, also called numerical aperture, has long been commonly used for microscope objectives. It seems to us desirable to introduce this quantity also for Schmidt optical system, the more so since $\sin^2\alpha$ is the light-gathering power of the optical system for an object emitting rays according to Lambert's cosine law. (By "light-gathering power" is understood the ratio that the quantity of light entering bears to the total light emitted by the object.) The angle α is then to be understood as being half the apex angle of the cone formed by the rays which come from the centre of the image screen and farther on just pass through the edge of the correction plate (see *fig. 9*, where for the sake of simplicity the Schmidt system is represented in the simple form of fig. 2).

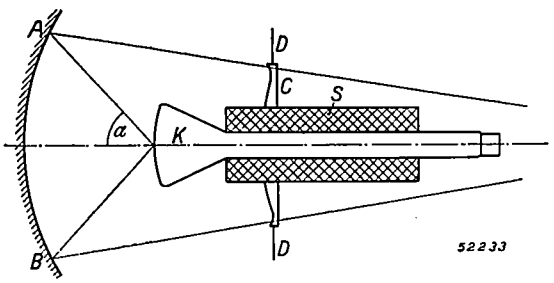


Fig. 9. The numerical aperture of a Schmidt system is understood as being sin α, where in the case of an optical system for television projection α is half the apex angle of the widest cone of rays emerging from the centre of the tube face and after reflection from the spherical mirror passing through the edge of the correction plate.

Of course it is thereby assumed that the spherical mirror is large enough to reflect these rays, its diameter from edge to edge being at least AB (fig. 9). *However, a still larger mirror does not at all imply a larger numerical aperture.* It is therefore incorrect to take the diameter of this mirror as a measure for the speed, as is sometimes done. This does not alter the fact that it does serve a purpose to take a mirror larger than AB, for this improves the situation for rays coming from the edge of the image on the face of the cathode-ray tube and reduces vignetting.

Finally there has to be mentioned as a characteristic quantity of an optical system the loss factor, a factor indicating what fraction of the amount of light entering the optical system is lost through interception, imperfect reflection and absorption.

[7]) Apart from the reciprocal value corresponding to the inverse direction of the light rays.

Dimensioning of the optical system

All dimensions of the optical system bear, roughly speaking, a direct relation to the focal distance. When aiming at keeping the size of the cabinet within reasonable limits one would therefore be inclined to choose a small focal distance. However, the cathode-ray tube sets a limit to this. This tube cannot be reduced to any size at will, because account has to be taken, *inter alia*, of the question whether a sufficiently fine light spot can be obtained. One might, it is true, try to work with a small magnification, but this would be disadvantageous because then the tube, being comperatively large, would intercept too much light; it may be taken as a general rule that the diameter of the tube face should be at most no more than half that of the correction plate, so that no more than one quarter of the light is intercepted.

The following rough calculation is intended to show the relation between the desired size and brightness of the projected image on the one hand and the diameter and the luminous flux of the cathode-ray tube together with some data of the optical system on the other hand.

We shall start from the size of the projected image 32 cm × 40 cm, area 0.128 m^2) and its brightness, assuming, to start with, that the latter is required to be equal to that of a good screen picture in a cinema (about 32 candles/m^2) [8]). If the light emitted from the projection screen were absolutely diffuse then in order to reach this required brightness a luminous flux of $0.128 \times 32 \times \pi = 13$ lumens would have to fall on the screen. Much less is required, however, if the screen is made of a translucent material, such as frosted glass. The fact is that when glass is frosted in a certain way the light falling perpendicularly on the back of the screen mainly emerges at the front also perpendicularly and is scattered only to a very small extent (we shall revert to this presently). Such a selectively scattering screen gives a gain, for instance, of a factor well over 4, so that a luminous flux of only 3 lumens is then required to fall on the screen. There is, however, some loss of light in the optical system through which the luminous flux has to pass, firstly on account of the interception previously referred to (about 25%) and further in the reflection from the mirrors and the passage of the light through the correction plate (together likewise about 25%), so that the loss factor amounts to about 0.5. Therefore, in order to get a yield of 3 lumens from the optical system about 6 lumens has to enter it.

But the luminous flux coming from the cathode-ray tube has to be even larger. The luminous flux taken up by the optical system expressed as a fraction of the luminous flux emitted by the cathode-ray tube is equal to the square of the numerical aperture, as already stated. If this aperture is say 0.62 then $6/0.62^2 \approx 15$ lumens has to be emitted from the tube face. It has been assumed again that the emission from the tube face follows approximately Lambert's cosine law; therefore the luminous intensity in the axial direction must be $15/\pi \approx 5$ candles. The light yield of luminescent substances lies between 1.6 and 3 candles/watt (averaging 2 candles/watt) so that for 5 candles luminous intensity about 2.5 W is required in the electron beam. The question as to what voltage and current are required to reach this wattage will be answered in a later article, but we may already say that the cathode-ray tube has sufficient reserve capacity to allow of a short peak current intensity 5 times as great as that mentioned. Thus a brightness can be reached 3.5 to 4 times as great as that from which we started (32 candles/m^2). (The fact that the brightness increases less than proportionately with the current intensity is due mainly to saturation phenomena in the luminescent substances.)

Regarding the cathode-ray tube we may also state that it has been found possible to reduce the face diameter to 6.3 cm (the size of the image on the face is about 3.6 cm × 4.6 cm). According to the rule given above the correction plate should have a diameter about twice that of the tube face, thus in this case about 12 cm. Taking this diameter and the figure of 0.62 given in the foregoing for the numerical aperture, it follows that a focal distance of about 10 cm is required. With these data given, all other dimensions of the optical system are determined.

The quality that can be reached with the Philips optical system is such that more than twice the present number of lines per image could easily be dealt with. (However, difficulties of quite a different nature, into which we cannot enter here, prevent such a raising of the number of lines.)

Fig. 10 is a photograph of an image televized by the experimental transmitter at Eindhoven and received with an apparatus of the type shown in fig. 1.

Focusing the optical system

To get a proper projection with a fast optical

[8]) In American literature brightness is usually expressed in foot-lamberts. The relation between this unit and the candle/m^2 unit is: 1 ft-lambert = 3.43 candles/m^2.

system it is necessary to focus very carefully. In the first place the centre of the correction plate must exactly coincide with the centre of curvature of the spherical mirror — or, in the case of the Philips optical system, with the projection of this centre on the plane mirror .This can be brought about in two stages : 1) by moving the correction plate in the axial direction until the centre of curvature (or its projection) just lies on the face of the plate; 2) by shifting the correction plate perpendicularly to its axis until its centre coincides with the point just referred to.

The importance of this latter centering will be clear when it is borne in mind that the thickness of the correction plate at the edge varies rapidly with the distance from the centre (see the article referred to in footnote [6]), so that only a very small deviation form the correct centering is sufficient to spoil the whole correction.

To facilitate these adjustments the centre of the correction plate is indicated by the point of a V-shaped mark. The two mirrors form a true image of this mark which just falls on the correction plate when this is at the correct height. By screwing the correction plate slightly upward or downward the position can be found where no parallax is to be observed between the mark on the correction plate and its projection on the mirrors. The correction plate holder is then secured in this position by means of the screws of which one is indicated by the number *9* in fig. 6. The second adjustment, shifting the correction plate in its own plane, has been made possible by leaving some play in the holes in the rim of the correction plate holder through which the fixing screws are passed (*10* in fig. 6). The correction plate is moved about until the point of the V mark coincides with the point of its projection on the mirrors, so that two V's together form a cross, after which the plate is secured by tightening the screws marked *10*.



Fig. 10. Photograph of a television picture transmitted from the experimental station at Eindhoven and received with an apparatus of the type illustrated in fig. 1. Number of lines 567 (interlaced scanning [9]), 50 frames per second.

In the second place the spherical face of the cathode-ray tube has to be correctly positioned with respect to the optical system. In the manufacture of the tube care has already been taken to give the face the radius of curvature corresponding to the optical system. The tube holder has been fitted into the receiver in such a way that its distance from the spherical mirror can be adjusted (see fig. 6). Furthermore, this tube holder allows of some play in the angle between the axis of the tube and that of the mirror, so that it is possible to align the centre

[9]) For interlaced scanning see e.g. Philips Techn. Rev. **3**, 285-291, 1938.

of curvature of the tube face in the axis of the mirror.

The projection screen

As already remarked in the introduction, one of the main advantages of a large picture is that several persons in one room can follow the television broadcast at their ease. To obtain a picture of such dimensions the projection method must be applied. We have also seen that by using a selectively scattering screen we have a welcome gain in the brightness of the picture, but it is to be noted that this can only be obtained at the cost of a reduction in the number of the audience or reduced freedom in the choice of position from which the picture can be viewed. Consequently we have to find a compromise.

We have already mentioned that frosted glass is a suitable material for a screen with selective scattering. Such a material can be characterized by its scattering curve $N = f(\Theta)$ (*fig. 11b*; for the meaning of N and Θ see fig. 11*a* and its subscript). In principle only two quantities of such a scattering curve are of importance: the maximum scattering factor N_0 and the angle at which N is a certain fraction of N_0. For this fraction we chose $^1/_2$; and we therefore speak of the half-value angle $\Theta_{1/2}$. This may be regarded as half the apex angle of a scattering cone forming approximately the boundary of the space within which a good view is possible. The scattering curves of different kinds of frosted glass answer approximately the equation $N_0 \sin^2 \Theta_{1/2} =$ constant, in which expression is again given to the compromise that has to be made between N_0 and $\Theta_{1/2}$.

An objection attaching to a material like frosted glass is that in vertical planes there is just as much scattering as in the horizontal direction. Now in vertical planes a much smaller half-value angle suffices, because the eye levels of tall and short, standing and sitting viewers differ much less than the width of the space in which several people have to be placed. A gain in brightness could therefore be reached by using a projection screen ribbed in such a manner that the half-value angle is smaller in the vertical plane than in the horizontal plane. The ribs, however, would have to be very fine, in fact smaller than the projection of the light spot on the projection screen. With the 8.7 × enlargement applied, the diameter of the image of the light spot is about 0.6 mm. Such a screen is rather difficult to make. Moreover, owing to the regular structure so-called moiré effects might easily arise.

So far Philips have been using a frosted glass projection screen with N_0 = about 4 and $\Theta_{1/2}$ = about 17° (fig. 11*b*). This angle is large enough for the picture to be easily observed by a fair number of spectators. Just as in a cinema, the distance between the audience and the screen must be at least 5 times the picture height; thus 1.6 m for a picture of 32 cm × 40 cm. This is necessary to be able to perceive the whole picture at one glance. At this distance the edges of the picture are observed at an angle of about 5° from the perpendicular to the centre of the picture, that is to say the image of the edges is cast upon the retina at a place where the visual acuity is reduced to $^1/_3$ of that in the middle of the fovea (the central part of the yellow spot). which experience shows to be just admissible. With $\Theta_{1/2} = 17°$ at the minimum distance of 1.6 m there is room for two people. There are, moreover, other reasons why the minimum distance has to be about 1.6 meters: at a shorter distance one can see the lines from which the picture is built op.

Finally, we have something to say about the lighting of the room in which the receiver is placed

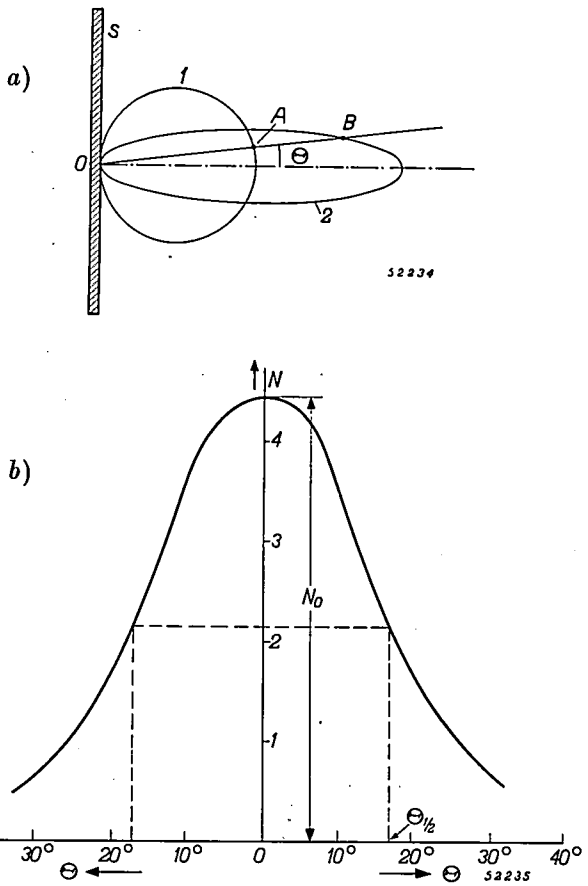


Fig. 11. *a*) When *S* represents a white, diffuse-reflecting plate (e.g. MgO) then the light incident at right-angles from the right is scattered in such a way that the part *OA* cut by the circle *1* on a radius vector (making an angle Θ with the perperdicular to *S*) is a measure for the intensity which *S* possesses in the direction given by the angle Θ. If, on the other hand, Θ is a frosted glass plate illuminated with equal intensity but this time from the left, then instead of the circle we find e.g. the ellipse *2*. The ratio *OB*/*OA* is called *N*.

b) Scattering curve $N = f(\Theta)$ of a particular kind of frosted glass.

and about the framing of the projection screen. In a blacked-out room the television picture is certainly very bright, but is gives an unnaturel impression and it is difficult to get that feeling of "living" with the scene. In the other extreme case of a very brilliantly lighted room attention is easily distracted from the picture, because it is less bright than its surroundings. The most favourable conditions for viewing are obtained when soft daylight is allowed to enter the room or normal or slightly toned down artificial lighting is used.

Another important point is the framing of the picture. It is best to use light colours, the effect being comparable to that of the frame round a painting or the white mounting round an etching; it appears to be an invaluable help for the imagination of the observers, bringing much more life into the picture. This effect is considerably enhanced by the small auxiliary loudspeakers set up on either side of the screen and reproducing mainly that part of the sound spectrum that is of most importance for speech.

THE RATIONALIZED GIORGI SYSTEM WITH ABSOLUTE VOLT AND AMPERE AS APPLIED IN ELECTRICAL ENGINEERING

by P. CORNELIUS. 537.713

Various systems of electrical units are in use today, these having been introduced in the course of the development of the theory or practical application of electricity in various fields. By an efficient combination of the conventional units the rationalized Giorgi system with absolute volt and ampere has been developed and made suitable to cover the whole range of electromagnetism. In this system several electrical quantities are given not only a different value but also a difinition different from that previously employed. As a result the current in conductors as well as the electrical and the magnetic field can all be dealt with in an analogous manner. In this article, after a brief review of the older systems, the rationalized Giorgi units are summarised and explained. The most important formulae for electromagnetism are tabulated in the form which they assume when expressed in these units. This table and several of the quantities occuring therein are discussed.

Introduction

The electrostatic c.g.s. system with its concepts of charge and potential follows naturally when one starts from the Coulomb's law and adopts the mechanical units cm, g, sec with the accompanying concepts of force and work as given.

The electromagnetic c.g.s. system with the concepts of magnet pole, magnetic field strength and electric current is obtained just as naturally when one starts from Coulomb's magnetic law, and the relation between current and magnetism is described for instance with the aid of the Biot and Savart law.

From electrostatics and electromagnetism one can arrive at a combined theory, based on Maxwell's laws with the inherent concepts of field. If, then, the two c.g.s. systems are taken as being equivalent, the so-called Gauss system is an obvious solution.

The theory of electromagnetism as represented by the Gauss system and the requirements of electrical engineering, in which "practical units" are employed, are reconciled in an extremely simple manner by means of the rationalized Giorgi system with absolute volt and ampere. This system is built up from the conceps of current and voltage. The concept "current", represented as a charge in motion or as the cause of magnetic phenomena, plays an important part also in the line of thought covering the three c.g.s. systems. The concept "voltage" on the other hand occupies a less prominent place in these systems and is represented therein as a difference in potential or as the line integral of the electric field strength. In electrical engineering, however, this concept of voltage is so fundamental as to be of predominant importance, for here it is commonly said that "the voltage drives the current through an impedance" and "that the voltage between two conductors causes an electric field". Regarded from this point of view the concepts of electromagnetism are of course often given a different aspect.

Bearing this in mind, the rationalized Giorgi system [1]) may be summarized as follows.

The rationalized Giorgi system

The rationalized [2]) Giorgi system is based, for all electrical and magnetic quantities and thus also for field quantities, upon the volt and ampere, the units with which everyone is familiar. Further, the usual electrical units of the ohm (Ω), the coulomb (C), the farad (F) and the henry (H) are maintained. The electrical field strength E is measured in volts per meter (V/m), and the magnetic field strength H in amperes per meter (A/m).

The electric flux Ψ passing from positive to negative charges is measured, like the charge Q itself, in ampere-seconds or coulombs. The displacement D (a better name is electric induction) may be regarded as electric flux density and is therefore measured in A · sec/m^2 or C/m^2.

The magnetic flux Φ, which encircles a conductor through which a current is flowing, or which is induced by the molecular circuit currents of permanent magnets or magnetized iron, is given in

---

[1]) Cf. W. de Groot [4]. (Figures between brackets refer to the bibliography at the end of this article). There the historical development of electromagnetism is outlined and the position occupied therein by the Giorgi system is shown. It also deals with the difference between the "absolute" and the "international" volt and ampere. The present article will show mainly how the rationalized Giorgi system with absolute volt and ampere can be applied in electromagnetism.

[2]) We are discussing here exclusively the rationalized Giorgi system. No attention is paid to the question whether the formulae given here may also hold for the non-rationalized system.

volt-seconds, also called webers (V · sec = Wb). The magnetic induction B can be regarded as magnetic flux density and is therefore measured in V · sec/m² or Wb/m².

Giorgi chose as the unit of length the metre instead of the centimetre, so as to give a simple relation between electrical and mechanical quantities (see below). The Wb takes the place of the maxwell, the Wb/m² the place of the gauss and the A/m the place of the oersted. In engineering the A/cm, under the name of ampere-turns per cm, has long been adopted in the place of the oersted. It is then a very short step to the A/m. The V/cm and also the Giorgi unit V/m have likewise already become of common use.

In the Gauss system the displacement D has the same dimensions as the electric field strength E at the same point, whilst moreover in vacuum D and E are identical. Giorgi on the other hand ascribes to D a value and a dimension different from E, not only in matter but also in vacuum. The same applies for the magnetic field strength H and the magnetic induction B. The advantages that are to be set against this complication will be seen farther on.

It is to be pointed out that this complication in the Giorgi system is partly met with also in the electrostatic and the electromagnetic c.g.s. system. It is true that in the electrostatic system $D = E$ in vacuum but $B = H/c^2$; in the electromagnetic system on the other hand $B = H$ in vacuum but $D = E/c^2$. As opposed to the advantage of the Gauss system that in vacuum $D = E$ and $B = H$, is the drawback that we find the factor c occuring in many important formulae.

From this it is to be seen that the difference between the electrical systems is not merely a question of numerical factors. Whereas calculating with say feet instead of metres does not in principle present any difficulties, the trouble when changing over from one electrical system to another is that quantities change not only in value but also in definition and dimension. This fact is not always sufficiently realized when the three c.g.s. systems are employed, because in these systems the electrical quantities are expressed in the same mechanical units.

It is, therefore, a great advantage of the rationalized Giorgi system that the definition, or at least the meaning, of the electrical quantities can easily be recognized from the unit.

From the internationally recognized decimal system of mass and length units Giorgi took the kilogram as mass unit and, as mentioned above, the metre as length unit. The unit of force in the Giorgi system is the newton (N), the force inducing in a mass of 1 kg an acceleration of 1 m/sec² (in some publications the rather misleading expression m/sec/sec is used instead). Provided one uses the "absolute" (instead of the "international") volt and ampere, the unit of mechanical work, the newton-metre, and the unit of electrical energy, the watt-second (= volt-ampere-second = joule (J)) are exactly identical:

$$1\,\mathrm{N \cdot m} = 1\,\mathrm{V \cdot A \cdot sec.}$$

The relation between the voltage, charge and current expressed respectively in the units of the volt, coulomb and ampere and the forces occuring in the corresponding fields thus assumes a simple form.

As an application of the Giorgi system a summary is given of the more important relations and laws of electromagnetism expressed in rationalized Giorgi units (*table I*). This table is discussed below.

At the end of this article two other tables are given in which the formulae and units of the older systems are compared with those of the rationalized Giorgi system.

We shall now discuss some of the quantities given in table I and explain the line of thought underlying the compilation of this table.

Field quantities

Owing to the historical development of electromagnetism, to which expression is given in the c.g.s. systems, when speaking of field quantities one is accustomed to thinking in the first place of forces. The electric field strength E is there defined as the force acting on the unit of charge and the magnetic induction B as the force acting on the unit of current element. According to this point of view D and H are auxiliary quantities for describing fields in matter and are superfluous when describing vacuum fields.

Since in the Giorgi system the field units are derived from the voltage and current units volt and ampere, it is advisable to replace the usual definitions of field quantities by others based upon measurements of voltage and current. When represented in this manner all four field quantities are of equivalent importance. E and B describe the electromagnetic field with the aid of voltage measurements, D and H with the aid of current measurements, regardless whether the field occurs in matter or in vacuum.

It is then found that by employing rationalized Giorgi units the current in conductors, the "current field", as well as the electric and the magnetic field can be dealt with in a manner which in many respects is similar.

The current field

In homogeneous as well as inhomogeneous cases[3])

[3]) There may be inhomogeneity in the current distribution, material, etc.

Table I. Some formulae expressed in rationalized Giorgi units

Current field	Electric field	Magnetic field
Ohm's law	Law of capacity ($\Psi = Q$)	Law of self-induction (1 turn)
$I = G\ V$	$\Psi = C\ V$	$\Phi = L\ I$
(A) (S) (V)	(C) (F) (V)	(Wb) (H) (A)
S (siemens) = A/V	C (coulomb) = A·sec F = A·sec/V	Wb (weber) = V·sec H = V·sec/A
Vector equations		
$S = \gamma\ E$	$D = \varepsilon\ E$	$B = \mu\ H$
(A/m²) (S/m) (V/m)	(C/m²) (F/m) (V/m)	(Wb/m²) (H/m) (A/m)
Relations between the field quantities		
a) in homogeneous fields		
$I = S\ A$	$\Psi = D\ A$	$\Phi = B\ A$
(A) (A/m²) (m²)	(C) (C/m²) (m²)	(Wb) (Wb/m²) (m²)
$V = E\ s$	$V = E\ s$	$I = H\ s$ *)
(V) (V/m) (m)	(V) (V/m) (m)	(A) (A/m) (m)
b) general		
$I = \iint S_n\ \mathrm{d}A$	$\Psi = \iint D_n\ \mathrm{d}A$	$\Phi = \iint B_n\ \mathrm{d}A$
(A) (A/m²) (m²)	(C) (C/m²) (m)	(Wb) (Wb/m²) (m²)
$V = \int E_s\ \mathrm{d}s$	$V = \int E_s\ \mathrm{d}s$	$I = \oint H_s\ \mathrm{d}s$
(V) (V/m) (m)	(V) (V/m) (m)	(A) (A/m) (m)
Homogeneous cases		
Conductance	Capacity	Self-induction (1 turn)
$G = \gamma\ A/s$	$C = \varepsilon\ A/s$	$L = \mu\ A/s$
(S) (S/m) (m²/m)	(F) (F/m) (m²/m)	(H) (H/m) (m²/m)
Power	Energy	
Conductor	Capacitor ($\Psi = Q$)	Coil (1 turn)
$P = I\ V$	$W = \frac{1}{2}\ \Psi\ V$	$W = \frac{1}{2}\ \Phi\ I$
(W) (A) (V)	(W·sec) (C) (V)	(W·sec) (Wb) (A)
Space density of the power	Space density of energy	
(in W/m³) = $S\ E$	(in W·sec/m³) = $\frac{1}{2}\ D\ E$	(in W·sec/m³) = $\frac{1}{2}\ B\ H$
(A/m²) (V/m)	(C/m²) (V/m)	(Wb/m²) (A/m)

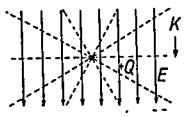
Maxwell equations

$$\oint E_s\ \mathrm{d}s = -\dot{\Phi} \ \ldots \ (\mathrm{V})$$
$$\oint H_s\ \mathrm{d}s = I + \dot{\Psi} \ \ldots \ (\mathrm{A})$$

For the surface A enclosing a part of the space:

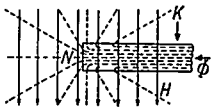
$$I \equiv \oint\oint S_n\ \mathrm{d}A = -\dot{Q} \ \ldots \ (\mathrm{A})$$
$$\Psi \equiv \oint\oint D_n\ \mathrm{d}A = Q \ \ldots \ (\mathrm{C})$$
$$\Phi \equiv \oint\oint B_n\ \mathrm{d}A = 0 \ \ldots \ (\mathrm{Wb})$$

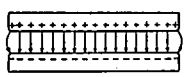
Laws of force



$K = Q\,E$

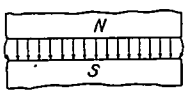
$K = \Phi\,H$

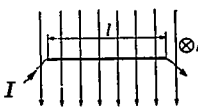




$K = \frac{1}{2}\,\Psi\,E$

$K = \frac{1}{2}\,\Phi\,H$





$K = I\,l\,B$

Energy equivalent: 1 V·A·sec = 1 N·m

Relation to velocity of light: $\varepsilon_0\,\mu_0\,c^2 = 1$

Value of μ_0: $\mu_0 = 4\pi/10^7$ ... (H/m)

*) In this table I represents the entire current surrounded by the flux, in technical language the ampere-turns; s in the case of a long coil is the length of the coil, and in the case of a toroid the length of the circular centre line.

the current in conductors is expressed, as stated by Ohm, by:

$$I = GV$$

(I ... (A); V ... (V); G is the conductance, unit A/V = Ω^{-1} = mho = siemens (S)).

In a homogeneous case we can divide the current by the cross section perpendicular to its direction and the voltage by the length in the direction of current. We may therefore write Ohm's law for specific quantities and take these quantities in the direction in which they have the greatest value. Thus we arrive at the vector equation of the current field [4]):

$$\mathbf{S} = \gamma \mathbf{E}$$

(S denotes the current density in A/m^2: E is the electric field strength in V/m and γ the conductivity in A/V·m = S/m). This relation, although it has been deduced for a homogeneous case, can likewise serve for describing inhomogeneous cases. In most cases the quantity γ is a scalar material constant. *The numerical value of γ is equal to the conductance of the "unit conductor"* (with dimensions: length = 1 m; cross section = 1 m^2) of the material in question in the case of homogeneous distribution of current.

The electric field

When the voltage on a capacitor is increased by 1 V then the same current impulse $\int I\,dt$ ... (A · sec) or quantity of charge Q ... (coulomb (C) = A · sec) is always taken up, regardless of the rate at which the voltage is increased. The value C of a capacitor denotes the magnitude of this current impulse or quantity of charge; the unit is the farad (F) = A · sec/V = C/V. The concept of capacitance and the phenomena related thereto may be described, following Faraday and Maxwell, as follows. Between the plates of a charged capacitor is an electric field. This field accumulates the energy .. (V · A · sec) used for the charge, and the voltage V.. (V) between the plates sets up an electric flux Ψ ... (A · sec), passing from the positive charge Q .... (A · sec) on one plate to the negative charge Q on the other plate, where the general relation is:

$$\Psi = Q = CV.$$

In a homogeneous case (plane capacitor in which the distance between the plates is small compared with the plate surface) the electric flux can be divided by the cross section perpendicular to its direction and the voltage by the length in that direction. Thus we write the ordinary law of capacitance for specific quantities and take these specific quantities in the direction in which they have the greatest value [5]).

Thus we arrive at the vector equation of the electric field:

$$\mathbf{D} = \varepsilon \mathbf{E}$$

(D denotes the displacement, i.e. electric flux density in C/m^2; E ... (V/m); ε is the "(absolute) dielectric constant" in A · sec/V · m = F/m).

This relation, though deduced for a homogeneous case, can likewise serve for describing inhomogeneous cases. In the simplest case the quantity ε is a scalar constant of the dielectric medium (matter or vacuum). *The numerical value of ε is equal to the capacity of the "unit capacitor"* (with dimensions: plate separation = 1 m; plate surface = 1 m^2) in the case of homogeneous field distribution [6]). ε ... (F/m) *performs the same function for the electric flux, as the conductivity γ* ... (S/m) *for the electric current.*

When using the absolute volt and ampere and substituting the velocity of light $c = 2.99776 \times 10^8$ m/sec, the value of the dielectric constant of the vacuum, called the "electric induction constant", is:

$$\varepsilon_0 = 10^7/4\pi c^2 \approx 8.855 \times 10^{-12} \ldots \text{(F/m)}.$$

[4]) Vector quantities, which in contrast with scalar quantities are characterized not only by a dimension and a numerical value but also by direction, are denoted by letters printed in heavy type (except in the tables). The equation given here expresses the fact that S and E bear a certain relation in value and also have the same direction.

[5]) The electric flux through a surface can be measured with the aid of electric induction. See e.g. R. W. Pohl [3], p. 29.

[6]) Homogeneous field distribution can be obtained by means of a guard ring, see fig. 1.

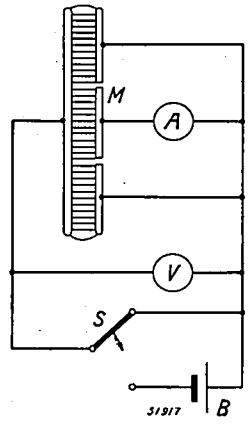


Fig. 1. Plane capacitor with guard ring. Inhomogeneity of the field occurs only at the outer edge of the ring. Only the charge of the middle part M is measured, where the field is homogeneous. A ballistic ammeter; B battery; S switch for charging and discharging the capacitor; V voltmeter.

From the Maxwell theory we have the fundamental relation

$$\varepsilon_0 \mu_0 c^2 = 1.$$

To derive the value of ε_0 one therefore has to remember, in addition to the velocity of light, only the value of the „magnetic induction constant" $\mu_0 = 4\pi/10^7 \ldots$ (H/m). The meaning of μ_0 is explained farther on.

The dielectric constant of a material dielectric is usually denoted by the product of its "relative dielectric constant" ε_r and ε_0:

$$\varepsilon = \varepsilon_r \varepsilon_0 \ldots \text{(F/m)}.$$

ε_r is a non-dimensional number, the material constant known of old.

The force exercised upon a charge $Q \ldots$ (C) in an electric field having the field strength $\mathbf{E} \ldots$ (V/m) is:

$$\mathbf{K} = Q\mathbf{E} \ldots \text{(N)}.$$

Whenever it is desired to regard the electric field strength E as a force vector this can also be measured not in V/m but in the identical unit N/C.

With the aid of the equation given above Coulomb's law can be deduced by calculating the field strength at the point where there is a charge Q_2 from the flux proceeding in spherical symmetry from a charge Q_1.

The magnetic field

When the current flowing through a loss-free coil is increased by 1 A, then the same voltage impulse $\int V \, dt \ldots$ (V · sec) always arises between the ends of the coil, regardless of the rate at which the current increases. The self-inductance L of a coil indicates the magnitude of this voltage impulse; the unit is the henry (H) = V · sec/A.

According to the method of representation followed by Faraday and Maxwell a current is surrounded by a magnetic field. This field accummulates the energy ... (V · A · sec) that is used for starting a current. The current $I \ldots$ (A) flowing in a coil of a single turn thereby gives rise to a magnetic flux $\Phi \ldots$ (V · sec = weber (Wb)) enveloping the wire, the general relation applying for a single turn being:

$$\Phi = L\,I.$$

Let us now consider a long coil of a single turn consisting, for instance, of a wide strip of metal. The width of the strip is the length of the coil (see *fig. 2*) [7]. In this coil the field is practically homogeneous, and negligible in the space outside the coil. Practically the entire "magnetomotive force" (A) of the enclosed current is used to drive the magnetic flux through the length of the coil.

In this homogeneous case the magnetic flux can be divided by the cross section perpendicular to its direction and the current by the length in that

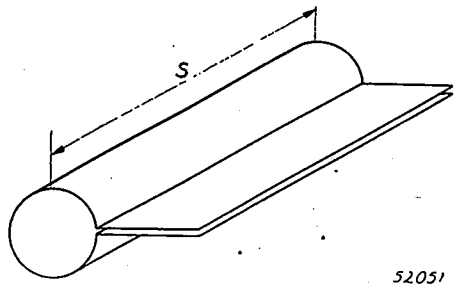


Fig. 2. Single-turn coil made from a wide strip of metal, the width of the strip being the length s of the coil.

direction. We therefore write the normal self-induction law for specific quantities and take these quantities in the direction in which they have the greatest value [8]. Thus we arrive at the vector equation of the magnetic field:

$$\mathbf{B} = \mu \mathbf{H}$$

(**B** denotes the magnetic induction, i.e. magnetic flux density, in Wb/m²; **H** is the magnetic field strength in A/m and μ the "(absolute) permeability" in V · sec/A · m = H/m).

Although deduced for a homogeneous case, this relation can also serve for describing inhomogeneous cases. In the simplest case the quantity μ is a scalar constant of the magnetic medium (matter or vacuum). *The numerical value of* μ *is equal to the self-inductance of the "unit coil"* (1 turn) having a length of 1 m and an enclosed area of 1 m²) in the case of homogeneous field distribution [9]). $\mu \ldots$ (H/m) *performs the same function for the magnetic flux,* as $\varepsilon \ldots$ (F/m) *does for the electric flux* (S/m) *for the current.*

In the case of ferromagnetic media μ is often still a scalar quantity but depending on H and the previous history of the material (hysteresis).

The permeability of the vacuum, called the "magnetic induction constant", when using the

[7]) This is the ideal solenoid, without any leakage of the magnetic field between the windings, which occurs in the case of a solenoid whose windings are mutually insulated.

[8]) The magnetic flux through a surface can be measured by means of an induction test. See e.g. R. W. Pohl [3], p. 74. The "magnetic tension" between two points ... (A) can be measured by the Rogowski method. See e.g. R. W. Pohl [3], pp. 76-80. For practical reasons this measurement is carried out as measurement of the impulse of an open voltage ($\int V dt$). When we imagine a Rogowski coil as having a negligible resistance and short-circuited with a resistance-free ammeter, then in this manner the "magnetic tension" can also be measured directly as a number of short-circuit ampere-turns.

[9]) Homogeneous field distribution can be obtained by using extension coils (see *fig. 3.*)

Table II. Comparative table of formulea

	Rationalized Giorgi	Gauss ($c \approx 3 \cdot 10^{10}$ cm/sec)	Electrostatic c.g.s. ($c \approx 3 \cdot 10^{10}$ cm/sec)	Electromagnetic c.g.s. ($c \approx 3 \cdot 10^{10}$ cm/sec)
Maxwell's laws	$\text{rot } E = -\dot{B}$ ... (V/m²) $\text{rot } H = \dot{D} + S$ ... (A/m²) $\text{div } S = -\dot{\varrho}$ ... (A/m³) $\text{div } D = \varrho$ ... (C/m³) $\text{div } B = 0$ ... (Wb/m³) $S = \gamma E$ ... (A/m²) $D = \varepsilon E$ ... (C/m²) $B = \mu H$ ... (Wb/m²)	$\text{rot } E = -\dot{B}/c$ $\text{rot } H = \dot{D}/c + 4\pi S/c$ $\text{div } S = -\dot{\varrho}$ $\text{div } D = 4\pi \varrho$ $\text{div } B = 0$ $S = \gamma E$ $D = \varepsilon_r E$ $B = \mu_r H$	$\text{rot } E = -\dot{B}$ $\text{rot } H = \dot{D} + 4\pi S$ $\text{div } S = -\dot{\varrho}$ $\text{div } D = 4\pi \varrho$ $\text{div } B = 0$ $S = \gamma E$ $D = \varepsilon_r E$ $B = \mu_r H/c^2$	$\text{rot } E = -\dot{B}$ $\text{rot } H = \dot{D} + 4\pi S$ $\text{div } S = -\dot{\varrho}$ $\text{div } D = 4\pi \varrho$ $\text{div } B = 0$ $S = \gamma E$ $D = \varepsilon_r E/c^2$ $B = \mu_r H$
Law of induction	$V = -\dot{\Phi}$ ... (V)	$V = -\dot{\Phi}/c$		$V = -\dot{\Phi}$
Plane capacitor	$C = \varepsilon A/s$ ... (F)	$C = \varepsilon_r A/4\pi s$ ... (cm)	$C = \varepsilon_r A/4\pi s$ ... (cm)	
Sphere	$C = \varepsilon \cdot 4\pi r$ ... (F)	$C = r$ ... (cm)	$C = r$ ... (cm)	
Long coil (n turns)	$L = n^2 \mu A/s$ ... (H)	$L = 4\pi n^2 \mu_r A/s$ ... (cm)		$L = 4\pi n^2 \mu_r A/s$ ... (cm)
Field strength in long coil (n turns)	$H = n I/s$ ... (A/m)	$H = 4\pi n I/c s$ ... (oersted)		$H = 4\pi n I/s$ ... (oersted)
Space density of energy	$\frac{1}{2} E D + \frac{1}{2} H B$ ... (W·sec/m³)	$\frac{1}{2} E D/4\pi + \frac{1}{2} H B/4\pi$ ... (erg/cm³)		
Force on a charge	$K = Q E$ ... (N)	$K = Q E$ ... (dyne)	$K = Q E$ ... (dyne)	
Coulomb's law	$K = Q_1 Q_2/\varepsilon \cdot 4\pi r^2$ ... (N)	$K = Q_1 Q_2/\varepsilon_r r^2$ ... (dyne)	$K = Q_1 Q_2/\varepsilon_r r^2$ ... (dyne)	
Force on charge in motion	$K = Q v B$ ... (N)	$K = Q v B/c$ ... (dyne)		$K = Q v B$ ... (dyne)
Force on straight wire	$K = I l B$ ... (N)	$K = I l B/c$ ... (dyne)		$K = I l B$ ... (dyne)
Force between two parallel wires	$K = \mu I_1 I_2 l/2\pi r$ ... (N)	$K = 2\mu_r I_1 I_2 l/c^2 r$ ... (dyne)		$K = 2\mu_r I_1 I_2 l/r$ ... (dyne)
Force between to charged plates	$K = \frac{1}{2} Q E = \frac{1}{2} \Psi E$ ... (N)	$K = \frac{1}{2} Q E = \frac{1}{2} A D E/4\pi$ ... (dyne)	$K = \frac{1}{2} Q E = \frac{1}{2} A D E/4\pi$ ... (dyne)	
Force between to plane magnet poles	$K = \frac{1}{2} \Phi H$ ... (N)	$K = \frac{1}{2} \Phi H/4\pi$ ... (dyne)		$K = \frac{1}{2} \Phi H/4\pi$ ... (dyne)

Table III. Comparison of the units of different systems

Notes: 1) It is to be borne in mind that the formulae denoting the relation between the various quantities may differ for the different systems (cf. table II).

2) *In this table c is the numerical value of the velocity of light in m/sec: 2.99776 · 10^8 ≈ 3 · 10^8.*

	Giorgi	Electrostatic c.g.s.	Electromagnetic c.g.s.	Gauss
Current I	A	1 e.s.u. = $1/10c$ ≈ $3.33\cdot10^{-10}$ ... (A)	1 e.m.u. = 10 ... (A)	1 e.s.u. = $1/10c$ ≈ $3.33\cdot10^{-10}$ ... (A)
Voltage V	V	1 e.s.u. = $c/10^6$ ≈ 300 ... (V)	1 e.m.u. = 10^{-8} ... (V)	1 e.s.u. = $c/10^6$ ≈ 300 ... (V)
Charge Q	1 C (coulomb) = 1 A·sec	1 e.s.u. = $1/10c$ ≈ $3.33\cdot10^{-10}$ ... (C)	1 e.m.u. = 10 ... (C)	1 e.s.u. = $1/10c$ ≈ $3.33\cdot10^{-10}$ ... (C)
Resistance R	1 Ω = 1 V/A	1 e.s.u. = $c^2/10^5$ ≈ $9\cdot10^{11}$ ... (Ω)	1 e.m.u. = 10^{-9} ... (Ω)	1 e.s.u. = $c^2/10^5$ ≈ $9\cdot10^{11}$ ... (Ω)
Capacitance C	1 F = 1 A·sec/V	1 cm = $10^5/c^2$ ≈ $1.11\cdot10^{-12}$ ... (F)	1 e.m.u. = 10^9 ... (F)	1 cm = $10^5/c^2$ ≈ $1.11\cdot10^{-12}$ ... (F)
Self-induction L	1 H = 1 V·sec/A	1 e.s.u. = $c^2/10^5$ ≈ $9\cdot10^{11}$ ... (H)	1 cm = 10^{-9} ... (H)	1 cm = 10^{-9} ... (H)
Electric flux Ψ ($\equiv \iint D_n \, dA$)	C ($\Psi = Q$)	1 e.s.u. = $10^{-1}/4\pi c$ ≈ $2.65\cdot10^{-11}$ ... (C)	1 e.m.u. = $10/4\pi$ ≈ $7.96\cdot10^{-1}$ ... (C)	1 e.s.u. = $10^{-1}/4\pi c$ ≈ $2.65\cdot10^{-11}$ ... (C)
Displacement, electric induction D	C/m²	1 e.s.u. = $10^3/4\pi c$ ≈ $2.65\cdot10^{-7}$ ... (C/m²)	1 e.m.u. = $10^5/4\pi$ ≈ $7.96\cdot10^3$ ... (C/m²)	1 e.s.u. = $10^3/4\pi c$ ≈ $2.65\cdot10^{-7}$ ... (C/m²)
Electric field strength E	V/m	1 e.s.u. = $c/10^4$ ≈ $3\cdot10^4$ ... (V/m)	1 e.m.u. = 10^{-6} ... (V/m)	1 e.s.u. = $c/10^4$ ≈ $3\cdot10^4$ ... (V/m)
Magnetic flux Φ ($\equiv \iint B_n \, dA$)	1 Wb (weber) = 1 V·sec	1 e.s.u. = $c/10^6$ ≈ 300 ... (Wb)	1 maxwell = 10^{-8} ... (Wb)	1 maxwell = 10^{-8} ... (Wb)
Magnetic induction B	Wb/m²	1 e.s.u. = $c/10^2$ ≈ $3\cdot10^6$ ... (Wb/m²)	1 gauss = 10^{-4} ... (Wb/m²)	1 gauss = 10^{-4} ... (Wb/m²)
Magnetic field strength H	A/m	1 e.s.u. = $10/4\pi c$ ≈ $2.65\cdot10^{-9}$ ... (A/m)	1 oersted = $10^3/4\pi$ ≈ 79.6 ... (A/m)	1 oersted = $10^3/4\pi$ ≈ 79.6 ... (A/m)
Force K	1 N (newton) = 1 kg·m/sec²	1 dyne = 1 g·cm/sec² = 10^{-5} N	1 dyne = 1 g·cm/sec² = 10^{-5} N	1 dyne = 1 g·cm/sec² = 10^{-5} N
Energy W	1 N·m = 1 W·sec = 1 V·A·sec = 1 J (joule)	1 erg = 1 dyne·cm = 10^{-7} N·m	1 erg = 1 dyne·cm = 10^{-7} N·m	1 erg = 1 dyne·cm = 10^{-7} N·m

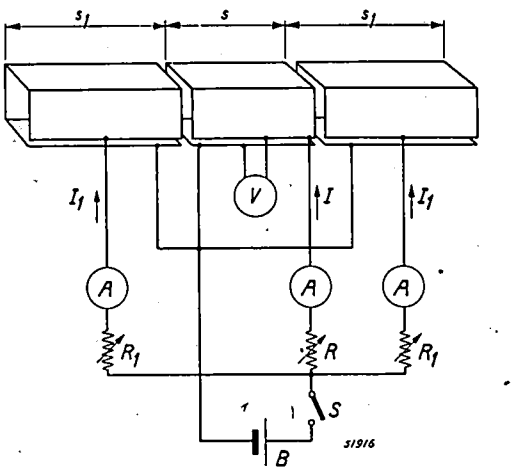


Fig. 3. Coil consisting of a centre piece with extension coils. Inhomogeneity of the field occurs at the ends. Only the voltage impulse of the centre piece is measured, where the field is homogeneous and equals I/s. A denotes ammeter; B battery, R and R_1 variable resistors for making $I_1/s_1 = I/s$; S switch for switching the currents I and I_1 on and off; V ballistic voltmeter not consuming any current.

absolute volt and ampere has the value:

$$\boxed{\mu_0 = 4\pi/10^7 \ldots (\mathrm{H/m}).}$$

Now that we have learnt the meaning of μ_0 we can remember the definition of the absolute volt and ampere from the following: the product of V and A is given by the energy equation $1\ \mathrm{N \cdot m} = 1\ \mathrm{V \cdot A \cdot sec}$: the quotient of V and A is given by $\mu_0 = 4\pi/10^7 \ldots (\mathrm{V \cdot sec/A \cdot m})$. The reader will now understand why in this article these two formulae — upon which the whole Giorgi system can be built up — have been given special prominence by framing them.

It is common practice to indicate the permeability of a material magnetic medium as the product of its "relative permeability" μ_r and μ_0:

$$\mu = \mu_r \mu_0 \ldots (\mathrm{H/m}).$$

μ_r is a non-dimensional number, the material constant known of old.

The force exercised upon a straight conductor of the length $l \ldots$ (m), when a current $I \ldots$ (A) is flowing through it and it is directed perpendicular to the direction of a homogeneous magnetic field, is at right-angles to these two directions and has the value:

$$K = IlB \ldots (\mathrm{N}).$$

Whenever it is required to regard the magnetic induction **B** as a force vector this can also be measured not in $\mathrm{Wb/m^2}$ but in the identical unit $\mathrm{N/A \cdot m}$.

By means of this equation one can find the force between two parallel conductors by calculating the induction caused at I_2 by the field strength due to I_1. It is with the aid of this force that the "Comité international des Poids et Mesures" has defined the absolute ampere [10]).

The foregoing should have made it clear how, by using the rationalized Giorgi system, one can deal in like manner with the important concepts of electromagnetism, viz. current field, electric field, magnetic field, and the phenomena related thereto.

For those who are accustomed to working with the older systems and now wish to change over to the rationalized Giorgi system it may well be useful to be able to compare the formulae and units of the old systems with those of the new one. For this purpose we have compiled *tables II* and *III*. For practical application particular attention is drawn to the note 1) to table III.

BIBLIOGRAPHY

[1] G. Giorgi, La métrologie électrique classique et les systèmes d'unités qui en dérivent. Examen critique, Revue Gén. d'Electr. **40**, 459-468, 1936.

[2] G. Giorgi, La métrologie électrique nouvelle et la construction de système électrotechnique absolu M.K.S., Revue Gén. d'Electr. **42**, 99-107, 1937.

[3] R. W. Pohl, Elektrizitätslehre, publ. Springer, Berlin, 1943 (8th and 9th editions).

[4] W. de Groot, The origin of the Giorgi system of electrical units, Philips Techn. Rev. **10**, 55-60, 1948 (No. 2).

[10]) W. de Groot [4], p. 58.

THE EFFECT OF THE MELTING POINT AND THE VOLUME MAGNETO-STRICTION ON THE THERMAL EXPANSION OF ALLOYS

by J. J. WENT.

666.1.037.5:669.018.47:536.413.2

When metal has to be sealed to glass it is first of all necessary that the expansion coefficient of the metal in a certain temperature range does not differ too much from that of the glass. It is investigated how the expansion coefficient of alloys is related to the drop in their melting point and what effect the volume magneto-striction has upon that coefficient in the case of alloys of ferromagnetic materials. An empirical rule is given for the composition of alloys with a small expansion coefficient. As a practical example the composition of an alloy consisting of iron, nickel, cobalt and copper which is suitable for sealing to hard glass is discussed.

Glass and metal can only be sealed together when both materials satisfy certain requirements. At temperatures lying between that for normal use and the minimum temperature at which one of these two materials is able to neutralize by plastic changes any stresses arising during the sealing of the glass to the metal, the expansion of the glass must within sufficiently narrow limits be equal to that of the metal [1]). In the second place the adhesion between the metal and the glass, either direct or via a skin of oxide, is of the greatest importance. Moreover, the materials have to answer a number of technological requirements, e.g. malleability, soldability, non-corroding, etc.

In this article we shall confine our discussions to those aspects of importance in the development of alloys which must satisfy certain requirements regarding thermal expansion. It will be shown that the thermal expansion coefficient of an alloy is related to its melting point and its magnetic properties. These relations make it possible to find from the data regarding the melting points on the one hand and the magnetic properties on the other hand an indication of the composition of alloys having expansion coefficients answering the requirements.

Expansion and melting point of elements

An empirical rule has long been known which gives the relation between the melting point and the linear thermal expansion for elements. According to this simple rule the total expansion from the absolute zero point to the melting point is the same for all elements. This is important, because usually the melting point is one of the best known data for any solid substance. The rule is in agreement with the fact that the higher the melting point the greater are the binding forces of the lattice (and thus the greater the hardness) at a certain temperature, which means that the expansion is less. By way of illustration, in *table I* some data are given for three metals with greatly different melting points.

Table I. The melting point, the total linear expansion from the absolute zero point to the melting point, the expansion coefficient between 0 and 100 °C and the hardness of three metals.

Metal	Melting point	Total linear expansion	Expansion between 0° and 100 °C per °C	Vickers hardness
W	3400 °C	$24 \cdot 10^{-3}$	$43 \cdot 10^{-7}$	250 kg/mm²
Cu	1083 °C	$23 \cdot 10^{-3}$	$165 \cdot 10^{-7}$	35 kg/mm²
Al	660 °C	$22 \cdot 10^{-3}$	$240 \cdot 10^{-7}$	15 kg/mm²

From a list of 38 elements (metals and non-metals) for which sufficient data on the expansion up to the melting point are known, we find for the total linear expansion

$$22.0 \times 10^{-3} \pm 3.5 \times 10^{-3}.$$

This relates to pure elements. It is exceptional, however, for an element to answer exactly the requirements in regard to thermal expansion. Yet there are cases where this is so. For instance tungsten and molybdenum can be used for sealing to hard glass, and platinum for sealing to soft glass. If, however, there are objections against using these elements, for instance becuase they are difficult to process (W and Mo) or because the material is too expensive (Pt), we have to investigate what alloys can be used for the purpose in view. Our thoughts then turn in the first place to real (homogeneous) alloys and not to a composition of different materials such as the so-called copper-clad wire, consisting of a nickel-iron core with a low expansion coefficient clad in copper with a high one

[1]) A. A. Padmos and J. de Vries, Stresses in glass and their measurement, Philips Techn. Rev. 9, 277-285, 1947 (No. 9).

In this last case a material can be obtained which has a well-matched average expansion in the radial direction but its use is restricted, by the inevitable anisotropy of the expansion, to special applications such as lead-in wires for lamps.

The alloys must be of such a composition that no phase changes take place within the temperature range in which they are to be used. Changes are almost always taking place in volume at the phase change and, moreover, there are usually great differences in the expansion coefficients between two phases of the same material .A familiar example of this latter phenomenon is the difference in the expansion coefficients β [2]) of the α -phase and the γ-phase [3]) of iron, the former being $\beta = 120 \cdot 10^{-7}$ and the latter $\beta = 170 \cdot 10^{-7}$. By adding suitable percentages of manganese or nickel the γ-phase of iron can be made stable at room-temperature. In that case the expansion coefficient of $170 \cdot 10^{-7}$ just mentioned still holds.

The above-mentioned rule, in so far as it is used to indicate the change of the expansion due to an admixture, no longer applies for alloys. Nevertheless, from the melting point a conclusion can be drawn as to the extent of the thermal expansion.

Melting point drop and thermal expansion of homogeneous alloys

The melting point of a metal is lowered when a second metal is added. It appears that in the case of homogeneous alloys a relation exists between the extent of this drop in melting point (when adding an alloy element) and the corresponding change in the expansion coefficient.

To explain this we shall start with iron. This metal is used preferably as the main component of an alloy for sealing not only because it is inexpensive but also because its expansion coefficient ($\beta = 120 \cdot 10^{-7}$) does not differ so very much from that of normal soft [4]) glass ($\beta = 95 \cdot 10^{-7}$), so that the addition of a second metal need only cause a relatively small reduction of the expansion coefficient.

In *table II* the change of the linear expansion coefficient (between 0 and 400 °C) is compared with the change in melting point resulting from the addition of another metal to iron. It is to be noted that in both cases extrapolation has been carried out to very small percentages of the material added.

It appears that the less the added metal reduces the melting point of the iron, the lower is the expansion coefficient, whilst the greatest reduction of the melting point is even accompanied by a slight increases of the expansion coefficient.

Table II. The changes taking place in the melting point of iron ΔT_s and in the linear expansion coefficient $\Delta\beta$, both per atomic percent, when a second element is added. In the last column the solubility of the added element is given.

Added element percent	ΔT_s per atomatic percent	$\Delta\beta$ between 0 and 400 °C per	Solubility in iron
Sn	— 10 °C	+ 0.31×10^{-7}	5 atom. %
Si	— 7	+ 0.04	25
Ni	— 3.3	— 2.0	18
Co	— 1.3	— 0.9	75
V	— 1.2	— 5.7	30
Al	— 0.5	— 0.9	20
Mo	— 0.5	— 6.7	4
Cr	0	— 5.9	40
W	0	— 8.3	3

The regularity of this phenomenon does not apply to quite the same extent in the case of cobalt and aluminium, for there the expansion coefficient is reduced less than would be expected from the general rule.

In *fig. 1* the change in the expansion coefficient $\Delta\beta$ of iron is plotted as a function of the quantity of material added. The initial slopes of the curves correspond to the values of $\Delta\beta$ given in table II The diagram in fig. 1 also indicates the extent to which the expansion coefficient of soft glass differs from that of iron.

It appears that only three elements are suitable for combining with iron to form a metal which can be sealed. Only in the case of the binary alloys Fe-Cr, Fe-V and Fe-Co (with a high Co-content) is the expansion coefficient, as compared with that of pure iron, sufficiently reduced before the limit of solubility is reached; this is due not only to the

---

[2]) In this article β is used to denote the linear expansion coefficient, which as is known, is defined for a specific substance by the relation $\beta = 1/l \cdot \mathrm{d}l/\mathrm{d}T$, where l is the length at the temperature T. Within small ranges of temperature this coefficient is so constant that we may write $l_{T'} = l_T\,[1 + \beta\,(T'-T)]$, where $l_{T'}$ and l_T are the lengths of a bar at T' and T °C respectively.

[3]) As is known, the iron atoms form a cubic lattice in both modifications (α and γ), but with this difference that in the case of alpha iron in addition to the corners the spaces in the middle of the cubic cells are also occupied (body-centred cubic structure), whereas in the case of γ-iron in addition to the corners the spaces in the middle of the cube planes are occupied (face-centred cubic structure). The reason why the modification that is stable from 900 up to about 1400 °C is denoted by γ and not by β is becauses at about 700 °C (the Curie point of iron) the magnetic α-iron stable at room temperature becomes nonmagnetic, and the non-magnetic phase having the same crystal structure as the magnetic phase is denoted by β-iron. The conversion at 900 °C might actually be called the $\beta \rightarrow \gamma$ transition.

[4]) Soft glass has a high expansion coefficient (β = 90 to $100 \cdot 10^{-7}$); hard glass has a low expansion coefficient (β = 40 to $50 \cdot 16^{-7}$).

relatively high $\Delta\beta$/atomic percentage ratio but also to the satisfactory solubility of the added element in iron. Of the alloys mentioned here the chromium iron alloys are well known and employed as sealing metals.

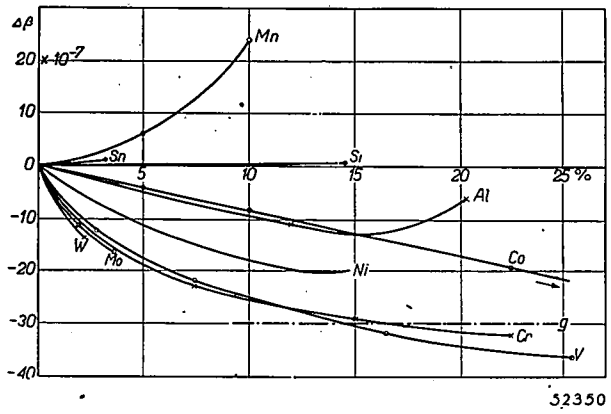


Fig. 1. Variation of the expansion coefficient of iron (between 0 and 400 °C) when a certain percentage of another metal is added in solution. The quantity of the second element is set out on a horizontal axis as an atomic percentage. The graph for Fe-Co, which runs almost straight, has to be extended further owing to the great solubility of this combination. The Fe-Al alloys show an irregularity due to a rearrangement in the lattice. The Fe-Mn alloys show differences in behaviour due to stabilisation of the gamma phase of iron at room temperature resulting from the addition of manganese. The horizontal dot-dash line denoted by g represents the expansion coefficient of soft glass compared with that of iron. It appears that only Fe-Cr, Fe-V and Fe-Co can be considered for sealing to soft glass.

With reference to fig. 1 it is also to be noted that alloys with an Si content greater than about 15 atomic percent have not been included. This is because with these alloys, just as the graph shows to be the case for Fe-Al, irregularities occur which are related to the fact that a rearrangement takes place in the lattice. By this it is to be understood that the Al and Fe ions, or the Si and Fe ions, are no longer arbitrarily distributed among the available lattice points, but alternate one with the other in a certain order. This tends to effect the expansion, whilst moreover the change from order to disorder or vice versa may be accompanied by changes in volume.

We have included in fig. 1 also the Fe-Mn alloys previously mentioned to show by an example how the expansion coefficient of these alloys increases as a result of the stabilization of the γ-phase of iron at room temperature through the addition of manganese, in spite of the fact that the melting point of iron is scarcely affected by Mn. The behaviour of manganese therefore is not in agreement with the rule for the relation between ΔT_s and $\Delta\beta$ as represented in table II.

Ordered arrangement in the lattice and phase changes undoubtedly affect the expansion, but since both these effects occur in relatively small temperature ranges they are not of great importance, and sometimes even undesired, for the application of alloys as sealing metals. It is a different matter, however, with the magnetic influence upon the volume, to which we shall now give attention.

Ferromagnetic properties and thermal expansion

Under the influence of an external magnetic field a ferromagnetic material appears to undergo changes in its form. This phenomenon is called magneto-striction [5]). A change takes place in dimensions in the direction of the magnetisation, with an opposite change in the directions perpendicular thereto, so that to a first approximation the volume is not changed. The change in the dimensions in the direction of magnetisation may be a lengthening or a shortening, the magneto-striction in the first case being said to be positive and in the second case negative. This change in length, which together with the magnetisation, reaches a saturation value, may be fairly considerable, amounting for instance to $60 \cdot 10^{-6}$ of the length. Further, accurate measurements have shown that there is another effect, a change in volume of the ferro-magneticum, called volume magneto-striction, which, however, only reaches a perceptible value when the field strengths are very high. This volume magneto-striction may result in either an increase or a reduction of the volume.

In order to indicate the relations for these phenomena and the effect they may have upon thermal expansion, we have to consider more closely our ideas of a ferro-magnetic material. Ferromagnetism arises from the fact that, owing to certain exchange forces, adjacent lattice elements each possessing a magnetic moment tend to equalize these moments. Such a representation would lead one to expect that without an external field any ferromagneticum would always show the saturation magnetisation corresponding to the best possible parallel placing of all these primary minute magnets, under the influence on the one hand of the exchange forces and on the other hand of the forces disturbing this regularity, viz. the thermal motion. The fact that such a material nevertheless often shows outwardly only small magnetisation or even no ferromagnetism at all is explained by the circumstance that although the saturation magnetisation exists in small regions (Weiss's domains) the ferro-magneticum is built up from a large number of these small regions which have mutually different directions of the magnetic moment. By applying an

[5]) Striction = contraction.

external magnetic field, in the first place the magnetic moments af all individual regions may, as far as is possible, become orientated in parallel directions. In the second place, by applying very high external fields one can improve the parallelization of the separate moments within each region in so far as they are disturbed by thermal agitation. The effect first mentioned produces the normal saturation of the ferro-magneticum as determined by measurement in an external magnetic field of moderate strength, and with this parallel orientation of the magnetic moments of Weiss's domains linear magnetostriction occurs. The second effect, which increases somewhat the saturation of the ferro-magneticum, is accompanied by the volume magneto-striction mentioned above. From this we derive the important rule that the volume is a function of the saturation.

From the foregoing it will be clear that saturation may be influenced by very strong external magnetic fields as well as by temperature. Therefore, volume magneto-striction may arise both from external magnetic fields and from variations in temperature. This change in volume with temperature has to be superimposed upon the normal thermal expansion. Obviously this applies only for temperatures below the Curie point, because above that ferromagnetism disappears entirely.

In general volume magneto-striction and thus also its influence upon expansion is very small; only in exceptional cases is there any great effect. For pure iron $1/V \cdot \mathrm{d}V/\mathrm{d}H$ (where V = the volume and H = the magnetic field) is about $6 \cdot 10^{-10}$ per oersted [6]) and for pure nickel even 6 times as small. $\mathrm{d}V/\mathrm{d}I$ (I = the magnetisation) can be calculated by multiplying the measured value of $\mathrm{d}V/\mathrm{d}H$ by $\mathrm{d}H/\mathrm{d}I$. In the case of strong magnetic fields, where a linear relation exists between I and H, this is a constant factor for any particular material. Further, it is possible to deduce $\mathrm{d}I/\mathrm{d}T$ from the curve giving the relation between the saturation I and the temperature T. The quantity that is of importance to us, $\mathrm{d}V/\mathrm{d}T = \mathrm{d}V/\mathrm{d}I \cdot \mathrm{d}I/\mathrm{d}T$, is then also known.

In the developing of alloys suitable for sealing to hard glass it is usually a matter of finding a composition having a lower expansion coefficient than that of the basic materials. This is attained when $\mathrm{d}V/\mathrm{d}H$ and $\mathrm{d}I/\mathrm{d}T$ are both large (in absolute value). (It is assumed that $\mathrm{d}V/\mathrm{d}H$ is positive, because $\mathrm{d}I/\mathrm{d}T$ is always negative.) It is therefore necessary to find alloy which satisfies these two conditions.

[6]) In Giorgi units $1/V \cdot \mathrm{d}V/\mathrm{d}H = 48 \cdot 10^{-9}$ m/A.

This can be explained further with reference to the diagram in *fig. 2* relating to the iron-nickel system. It appears that an alloy can be formed in which the volume mangeto-striction reaches the exceptionally high value of $3 \cdot 10^{-8}$ per oersted. If, now, at the same time the value of $\mathrm{d}I/\mathrm{d}T$ for this alloy is large, the expansion coefficient will be of the desired small value. In order to ascertain at what temperature a high value can be expected for this differential quotient we have to consider the variation of I as a function of temperature. It appears that I has a maximum value at the absolute zero point, and decreases from that point onwards, the decrease being rapid for temperatures not far

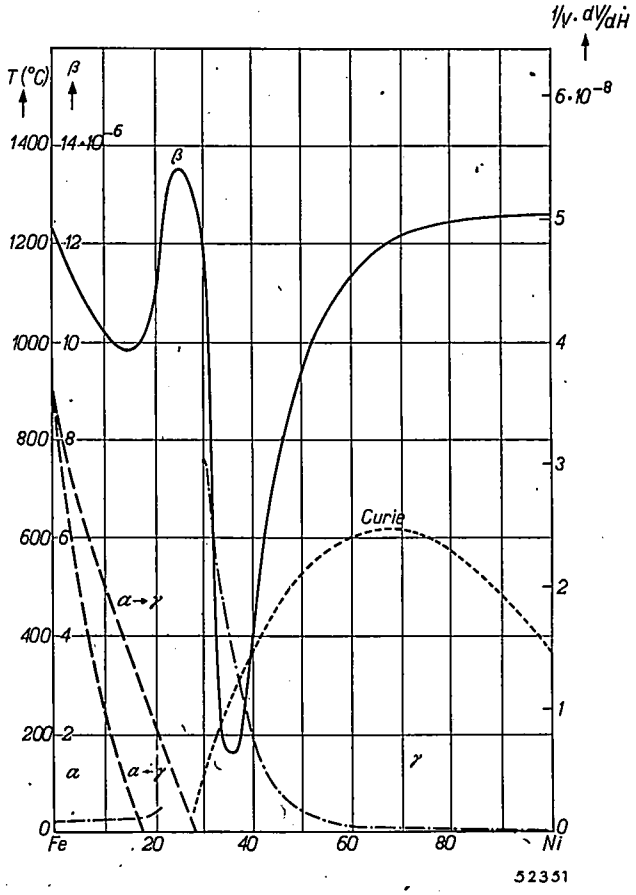


Fig. 2. Diagram of the Fe-Ni-system with the limits of the α and γ-phases, the value of the volume magnetostriction, the Curie points and the value of the linear expansions coefficient (between 0 and 100 °C). The alloy having a minimum expansion coefficient belongs to the gamma phase in a region which for the temperatures to be considered lies close to the $\alpha \rightarrow \gamma$ boundary. This alloy has a relatively low Curie point. On the left-hand axis we have the temperature and the value of the expansion coefficient (between 0 and 100 °C) and on the right the value of $1/V \cdot \mathrm{d}V/\mathrm{s}H$ per oersted as a measure for the volume magneto-striction. The line denoted by β relates to the expansion coefficient and the dot-dash line denotes the volume magneto-striction; the latter is interrupted in the region where this value cannot be determined. The curve marked Curie indicates how high the Curie temperature is for the alloys to be considered. For the phase transitions $\alpha \rightarrow \gamma$ and $\gamma \rightarrow \alpha$ different lines have been drawn because it makes a difference in the results whether these transitions are brought about by heating or by cooling.

below the Curie temperature T_1, where the zero value is reached. When an alloy is sought with a small expansion coefficient calculated for a range from 0 to T_2, the conditions in respect to dI/dT will only be met when T_2 is not much lower than T_1 [7]). In practice what this amounts to is that the Curie temperature of the alloy required must lie round about the transformation point of glass.

Fig. 2 also gives for the iron-nickel system the Curie temperature of the alloys as a function of their composition. It is seen that the alloy with a very large volume magnetostriction has a sufficiently low Curie temperature and is therefore suitable for the purpose. This is confirmed by the graph for the expansion coefficient (between 0 and 100 °C) as a function of the composition of the alloy, plotted in the same diagram.

An examination of fig. 2 shows that a composition of the alloy with a minimum expansion coefficient is not exactly the same as that of the alloy with a maximum volume magneto-striction. In this connection it has to be considered that the expansion coefficient is given for the range 0-100 °C and the volume magneto-striction has been measured at a temperature of 4 °C. The graph for the volume magneto-striction is interrupted at the point where the value of this quantity cannot be determined.

From fig. 2 we see that the alloy consisting of 63% Fe and 37% Ni has a very low expansion coefficient ($\beta = 1.5 \times 10^{-6}$). This alloy is of practically the same composition as the alloy "Invar", which has long been known and is used for making measuring rods, clock pendulums and suchlike.

Further it is to be seen from the diagram that in the iron-nickel system the alloy with a large volume magneto-striction belongs to the γ-phase in a region which, for the temperatures to be considered, lies close to the $\alpha \rightarrow \gamma$ limit. We have found confirmation of this emperical rule in the examination of other systems too. When we have to do with unknown systems this rule therefore offers an indication as to what alloys should be considered for examination. This also explains why we have indicated the phase limits in the graphs showing the variation of the volume magneto-striction and the expansion coefficient as functions of the composition. The transitions from the alpha to the gamma phase and from the gamma to the alpha phase are represented by separate lines, because different results are obtained with increasing and decreasing temperatures.

[7]) This is confirmed by the graph of σ (the saturation magnetisation per gram) for a Fe-Ni-Co alloy in fig. 7 in the continuation to this article.

It is obvious that, as found with the Fe-Ni system, with other systems a large volume magneto-striction alone is not sufficient either; in addition, dI/dT must be sufficiently large and dV/dH must have the desired sign.

Theoretically it is feasible that by a suitable choice of components an alloy can be made which has a negative expansion coefficient. *Fig. 3* shows that in the iron-platinum system this can indeed be done. Here again we find confirmation that the alloy with the minimum expansion coefficient belongs to the γ-phase and has a composition which, in the diagram of the system, lies close to the limit between the alpha and the gamma phases (at room temperature), whilst for this composition the Curie temperatuer is fairly low.

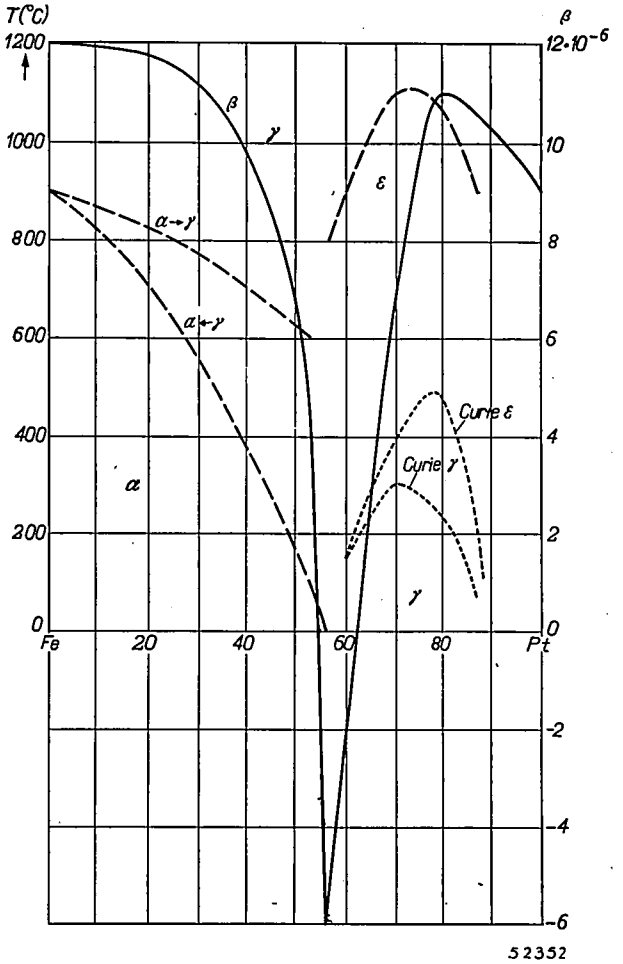


Fig. 3. The Fe-Pt system with the phase limits at room temperature, the Curie point value (both for the γ and for the ε -phase) and the value of the linear expansion coefficient (between 0 and 100 °C). ε=a body centred cubic phase in this system differing from the α-phase and partly bounded by the broken line. On the left-hand side we have the temperature and on the right the value of the expansion coefficient. It appears that the composition of the alloy can be chosen in such a way as to give a negative expansion coefficient. Here again we find confirmation that the alloy having a minimum expansion coefficient belongs to the γ-phase in a region which, for the temperatures to be considered, is close to the $\alpha \rightarrow \gamma$ boundary.

In the case of ternary systems also, we have found confirmation of the empirical rule mentioned above. Of course it also holds here that a large volume magneto-striction is not sufficient to give an alloy a low expansion coefficient, but that dI/dV must be sufficiently large as well.

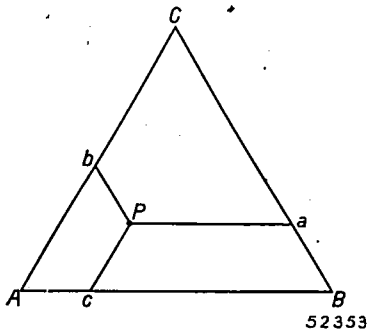


Fig. 4. In the equilateral triangle ABC, $Pa + Pb + Pc = AB$.

It is obvious, for these systems also, that the necessary curves for the volume magneto-striction, the Currie temperature and the expansion coefficient should be drawn in one diagram together with the phase limits. It is to be noted that when plotting such a diagram for a ternary system one usually starts from an equilateral triangle. The corners then correspond to the pure components A, B and C of the alloy, with the sides of the triangle representing the three binary systems AB, BC and CA, whilst a point inside the triangle characterizes a certain ternary alloy. Here we employ the theorems of planemetry which says that in an equilateral triangle the sum of the lines drawn from a point inside the triangle parallel to the three sides equals the side of the triangle. Thus in *fig. 4* $Pa + Pb + Pc = AB$. This enables us to find a point iside the triangle corresponding to an alloy composed for instance of 45% of the element A, 30% of the element B and 25% of the element C.

In such a phase diagram it is possible to set out the properties of the alloys as functions of their composition. For instance we can plot the phase limits at a certain temperature or draw lines showing what compositions have a certain Curie temperature. Lines can also be drawn between the points corresponding to compositions all having the same expansion coefficient.

Fig. 5 is an example of a phase diagram for a ternary system, viz. for the Fe-Ni-Co system. Here the phase limits are given at room temperature. It also shows with what compositions the Curie temperature is respectively 200 and 500 °C and gives a number of lines of equal expansion coefficient. It appears that by a suitable choice of components alloys can be produced with zero expansion coefficient. These alloys belong to the gamma phase in a region close to the transsition to the alpha phase (at the temperatures to be considered) with a relatively low Curie temperature. In fig. 5 the limit between the alpha and the gamma phases at —200 °C is also indicated because this will be referred to later on.

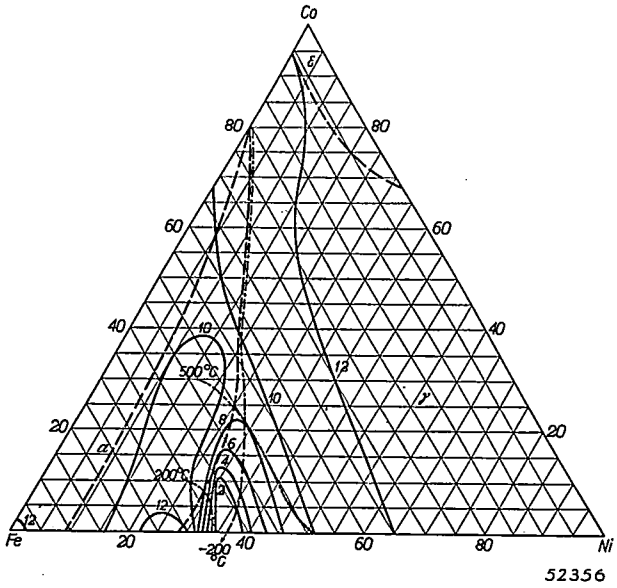


Fig. 5. The Fe-Co-Ni system with the phase limits at room temperature (——— lines) and, as far as the $\gamma - \sigma$ transition is concerned, at —200 °C (dot-dash lines). Further it is indicated what compositions have Curie point temperatures of 200 and 500 °C (----- lines), whilst a number of lines are given for equal expansion coefficients measured between 30 and 100 °C (full lines). The numbering of the latter curves indicates the value of this expansion coefficient × 10^6.

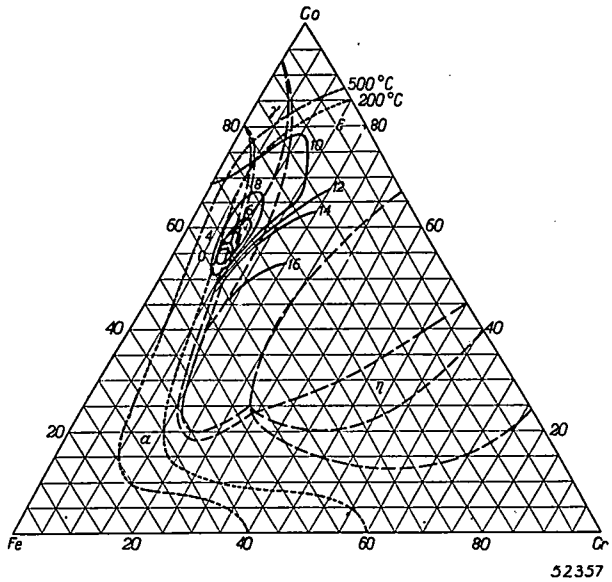


Fig. 6. The Fe-Co-Cr systems with phase limits at room temperature (——— lines), the composition of the alloys having a a Curie point temperature of 200 and 500 °C (----- lines) and a number of lines af equal expansion coefficient measured between 20 and 60 °C (full lines.) The numbering of the latter curves indicates the expansion coefffcient × 10^6.

As a second example *fig. 6* gives the phase diagram for the Fe-Cr-Co system. This shows the phase limits at room temperature, a number of lines of equal expansion coefficient (measured between 20 and 60 °C) and the compositions of the alloys having a Curie temperature of 200 and 500 °C respectively.

Here again we find confirmation of the rule that the alloys with small expansion coefficient lie in a region of the gamma phase close to the limit (for the working teperatures) of the alpha phase and at a point where the Curie temperature is sufficiently low.

Composing an alloy for sealing to hard glass

After this discussion of the two conditions which have to be met (high volume magneto-striction and relatively low Curie point) one may have obtained the impression that it is a simple matter to compose alloys for sealing glass to metal. In actual practice, however, difficulties are encountered. This is particularly the case when the metal has to be sealed to hard glass, i.e. glass with a high softening temperature and a small expansion coefficient. So far it has not even been found possible to find alloys suitable for sealing to glasses having an expansion coefficient less than about $40 \cdot 10^{-7}$.

In the first place it has to be borne in mind that the sealing is done close to the limit between the alpha and the gamma phases, with the risk that owing to the occurrence of the alpha phase, which has no considerable volume magneto-striction, the expansion coefficient again assumes the normal value of the α-phase and thus becomes much too high.

In the second place, while the Curie point has to be relatively low, it must be high enough so as not to remain too far below the softening temperature of hard glass. The magnetic effect upon the expansion is of course only possible below the Curie point; above that even the very high expansion coefficient of the γ-phase arises.

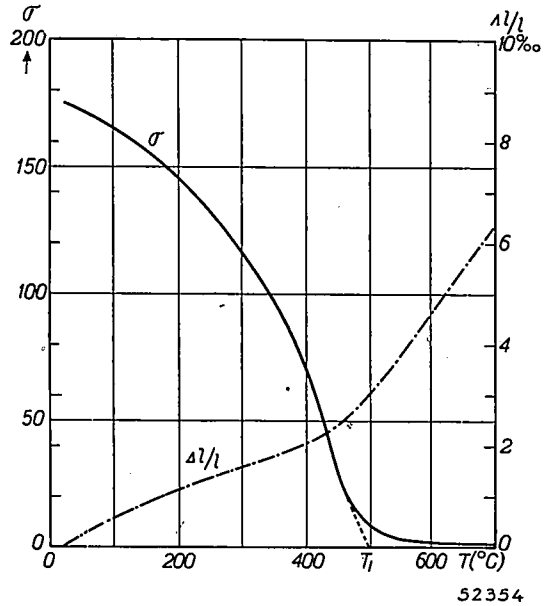


Fig. 7. Variation of magnetic saturation per gram ($\sigma = I_s/d$, where I_s is the normal saturation and d the density in grams) as a function of the temperature for a Fe-Ni-Co alloy having a small expansion coefficient below the Curie point temperature T_1. For the same alloy also the curve for the expansion $\Delta l/l$ is plotted as a function of the temperature.

We shall now deal with an example of the composition of a metal alloy for sealing to hard glass. In the past only molybdenum or tungsten could be used for this purpose on account of the expansion

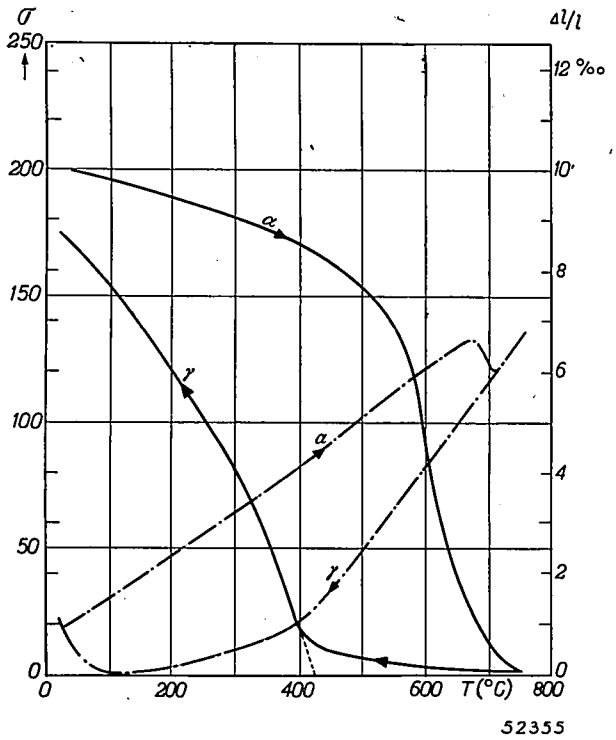


Fig. 8. Curves showing the expansion $\Delta l/l$ (dot-dash lines) and the magnetic saturation per gram σ as function of the temperature (full lines) for a Fe-Ni-Co alloy which may occur at the same temperature not only in the gamma phase but also in the alpha phase. (The alpha phase is obtained by first strongly cooling the material down.) The temperature is first raised to 750 °C and then lowered to room temperature, the curves thereby following the direction indicated by arrows.

coefficient having to be so low. We shall now take, however, the Fe-Ni-Co system, the phase diagram for which is given in fig. 5. It will be found that with this system it is just possible to make a suitable alloy for sealing to hard glass. For grades of glass intermediate between hard glass and quartz glass it has not been possible to find a suitable alloy for two reasons: the expansion coefficients of these kinds of glass are still lower than that of hard glass (less than $50 \cdot 10^{-7}$) and their softening points are too high, so that too high Curie temperatures are required for the sealing materials.

The conditions arising in our case may be seen from *figs. 7 and 8*, relating to two Fe-Ni-Co alloys, in the first of which the Ni content is somewhat higher and the Fe content somewhat lower than in the second alloy. In both diagrams the expansion and the saturation magnetisation are plotted as functions of the temperature. This

slope of the saturation-temperature curve shows that for temperatures not far below the Curie point the value of dI/dT is fairly high. From the slope of the expansion curve we can derive the value of the expansion coefficient β. Fig. 7 represents the position found with many such alloys. Above the Curie point the expansion coefficient of this material has the high value of $155 \cdot 10^{-7}$. At the Curie point the expansion coefficient begins to drop and from 400 °C onwards β drops to the rather small value of $60 \cdot 10^{-7}$, which however is still too high for hard glass. In the second alloy (to which fig. 8 relates) the Ni content is reduced so as to reach a lower expansion coefficient below the Curie point. It is found that β is no more than $25 \cdot 10^{-7}$ between 100 and 300 °C. But on the other hand there are the great disadvantages that owing to this reduction of the Ni content the Curie point is too low with respect to the softening point of the glass, and, as shown in fig. 5, at low temperatures the gamma phase is no longer stable. From this phase diagram it is to be deduced that at a tempeture of -200 °C the limit between the alpha and the gamma phases is partly shifted to the right. Consequently when this alloy is strongly cooled down, for instance in liquid hydrogen to -183 °C, the material is almost completely transformed into the alpha phase, with the result that the expansion coefficient ($\beta = 86 \cdot 10^{-7}$) and also the saturation temperature curve correspond to those of a normal alpha phase. When heating to 700 °C this alpha phase changes into the gamma phase. This transition is accompanied by a change in volume [8]), in this particular case a reduction, and at still higher temperatures the expansion coefficient has the normal value ($\beta = 160 \cdot 10^{-7}$) of the gamma phase. Upon the temperature being lowered again, the gamma phase continues to exist with its high expansion coefficient until (at about 425 °C) the Curie temperature of this phase is reached and the expansion coefficient has dropped to the very low value of $\beta = 25 \cdot 10^{-7}$. At 100 °C however this gamma phase again begins to change into the alpha phase, with all the attendant objections of changes in volume and increasing expansion coefficient.

Although it has been found possible to produce in this manner an Fe-Ni-Co alloy suitable for sealing to hard glass, the transition from the gamma to to the alpha phase at low temperature remains an undesirable feature of this material. Since it is established that with ternary systems no improvement can be made in this respect, the question arises whether the desired change can be brought about by adding a fourth component. One might think of elements which promote gamma formation in iron, such as Mn, Cu, C znd N, but most of these elements are unsuitable. Owing to their low degree of solubility C and N have to be cut out in practice, whilst Mn reduces the Curie point far too much. Copper, however, can be used because when a small percentage of Ni is replaced by Cu not only is the temperature lowered at which the $\gamma \rightarrow \alpha$ transition takes place but at the same time the Curie point is slightly raised, both of which changes are favourable for fusing the alloy to hard glass. This is proved by *table III*. By comparing line *4* with line *1*, *5* with *2* and *6* with *3* one finds that by adding this fourth element an alloy is obtained possessing properties which answer the requirements.

Table III. The expansion coefficient (for the range 0 to 350 °C) the Curie point and the temperature level of the $\gamma \rightarrow \alpha$ transition for some alloys of the Fe-Ni-Co-Cu system.

Ni	Co	Cu	Fe [9])	$\beta_{0\text{-}350\,°C}$	Curie-point	$\gamma \rightarrow \alpha$-transition
26.7%	17.2%	—	56.1%	$27 \cdot 10^{-7}$	390 °C	+ 100 °C
28.9	17.3	—	53.8	55	430	— 30
29.6	17.5	—	52.9	61	460	— 183
26.5	17.5	1.0%	55.0	35	420	+ 20
26.5	17.5	2.0	54.0	48	450	— 80
26.5	17.5	3.0	53.0	59	480	— 183

[9]) Possibly with impurities.

[8]) It is possible that the position of the Curie point may have some influence upon this change, because if it is so arranged that the $\alpha \rightarrow \gamma$ transition takes place not exactly at a temperature of the α Curie point then one finds separate irregularities for both effects.

ABSTRACTS OF RECENT SCIENTIFIC PUBLICATIONS OF THE N.V. PHILIPS' GLOEILAMPENFABRIEKEN

Reprints of these papers not marked with an asterisk can be obtained free of charge upon application to the Administration of the Research Laboratory, Kastanjelaan, Eindhoven, Netherlands.

1758: D. Polder: Nature of the hydrogen bond in patassium hydrogen fluoride (Nature **160**, 870, 1947, Dec. 20).

The doublet 1450, 1222 cm^{-1} in the infrared absorption spectrum of KHF_2 is ascribed by Ketelaar to a doubling of the fundamental asymmetric frequency ν_3, belonging to the vibration of a proton between two F-ions, due to a double minimum of the potential energy (analogeous to what happens in the NH_3 molecule). The validity of this conjecture is checked by measuring the temperature coefficient of the dielectric constant ($\varepsilon^{-1}\ d\varepsilon/dT$). A value 2.10^{-4} is found between $T = 80$ °K and $T = 300$ °K, whereas Ketelaar's data would yield a negative temperature coefficient between 0.01 and 0.001.

1759: C. J. Bouwkamp: A study of Bessel functions in connection with the problem of two mutually attracting circular discs (Proc. Kon. Ned. Akad. Wetenschappen, Amsterdam **50**, 485-497, 1947, No. 9)

Calculation of the potential energy of two coplanar, circular, homogeneous discs for an arbitrary law of force, in terms of integrals containing Bessel functions.

Sepcial attention is paid to the case where the potential energy between two point masses varies with the distance r as r^{-n}. The integrals so obtained are evaluated in terms of elementary functions, complete elliptic integrals of the first and second kinds, and hypergeometric functions.

R 66: K. F. Niessen: Indication of landing courses independent of weather conditions I. (Philips Res. Rep. **3**, 1-12, 1948, No. 1).

Discussion of the indication of straight landing courses with a small angle of elevation, independent of changes in the electric constants of the ground (as produced, for instance, by rain and snowfall). In this first part only infinitely small dipoles at unequal heights are considered.

R 67: A. van der Ziel and A. Versnel: Induced grid noise and total-emission noise (Philips Res. Rep. **3**, 13-23, 1948, No. 1).

In space-charge-limited triodes the fluctuations in the number of electrons that have sufficient energy to pass the potential minimum give rise, by electric induction, to a noise current flowing to the grid; the fluctuations in the number of the electrons returning in front of the potential minimum give rise, by electric induction, to a noise current flowing from cathode to grid. The first noise current is generally called "induced grid noise" and the latter "total-emission noise". Measurements are given of the noise resonance curve of the input circuit of pentodes at 7·25 m wavelength. It is shown that the asymmetry of the noise resonance curve of the input circuit of pentodes at u.h.f. is due to the phase relation between the induced grid noise and the normal shot-effect noise.

Further, it is shown that for diodes in the cut-off region at 7.25 m wavelength the total-emission noise may be described by assuming that the equivalent noise temperature of the "total emission conductance" is equal to the cathode temperature.

R 68: B. D. H. Tellegen: The determination of the integration constants when calculating transient phenomena (Philips Res. Rep. **3**, 24-36, 1948, No. 1).

A network is considered containing a voltage source v under the influence of which a current i flows in a certain branch. A method is given for calculating from the differential equation connecting i and v the discontinuities in i and its derivatives resulting from discontinuities in v and its derivatives. The method is applied to the calculation of periodic phenomena caused by periodic sources containing discontinuities.

R 69: H. J. Lindenhovius and J. C. van der Breggen: The measurement of permeability and magnetic losses of non-conducting ferromagnetic material at high frequencies (Philips Res. Rep. **3**, 37-45, 1948, No. 1).

A method is described for a rapid and accurate determination of the permeability and the magnetic losses of non-conducting ferromagnetic material.

For frequencies between 30 and 300 Mc/s this method makes use of a coaxial cavity resonator with end-capacitance, accurately tuned to the frequency of an oscillator to which it is coupled. One measures the changes in the resonance frequency

of this cavity resonator after successively inserting, concentrically with the inner conductor, a ring made of the ferromagnetic material to be tested and a ring of the same size made of a well-conducting metal. The susceptibility ($\chi = \mu - 1$) of the ferromagnetic material equals the ratio of these two frequency changes.

The magnetic losses can easily be computed from the band widths of the cavity resonator with and without the ferromagnetic ring. For frequencies above 300 Mc/s a coaxial Lecher system is used instead of the cavity resonator. A minor complication of a dielectric nature then arising is eliminated in a simple way. The equations are the same as for the cavity resonator.
Some data obtained with compressed iron powder and with "ferroxcube" are given.

R 70: F. A. Kröger, J. M. Stevels and Th. P. J. Botden: The influence of hexavalent uranium in glass (Philips Res. Rep. **3**, 46-48, 1948, No. 1.)

In glasses hexavalent uranium may be present as uranyl groups or as uranate groups. The uranyl groups give rise to fluorescence at room temperature, but both uranyl and uranate groups show fluorescence at low temperatures. It is shown that there is a direct relation between the emission bands and the absorption bands.

R 71: W. J. Oosterkamp: The heat dissipation in the anode of an X-ray tube, I (Philips Res. Rep. **3**, 49-59, 1948, No. 1).

The life of an X-ray tube is often determined by the rate of evaporation of the target, and hence by the maximum temperature occurring during an exposure. For a given inflow of heat through the focus, the temperature of the target may be computed from the equations of heat conduction. The requisite general equations are developed and are then applied to the problem of loads of short duration in tubes with stationary anodes.

R 72: J. F. Klinkhamer: Emperical determination of wave-filter transfer functions with specified properties, I (Philips Res. Rep. **3**, 60-80, 1948, nr. 1).

A method is decribed for determining wave-filter transfer functions $z\ (\lambda) = e_u/e_i$ with specified properties by means of measurements in an electrolytic tank, e_u being the output voltage, e_i the input voltage, and λ the complex frequency parameter. At the same time other functions are discussed which are equally useful in calculating the filter-network performance (the "characteristic functions" of Piloty). The position of the transmission bands, the permissible variation of the attenuation within these bands, and the position and the minimum attenuation of the attenuation bands are supposed to be given. As the method is applicable to filters with several transmission and attenuation bands, not necessarily equal in attenuation qualities, the new method is more general than that of Cauer, though it bears a close relation to the latter. In the case of one transmission band and one attenuation band, and in the case of several transmission and attenuation bands with equal attenuation qualities, the results of the two methods are identical.

VOL 10 No. 4, pp. 97-124 OCTOBER 1948

Philips Technical Review

DEALING WITH TECHNICAL PROBLEMS
RELATING TO THE PRODUCTS, PROCESSES AND INVESTIGATIONS OF
THE PHILIPS INDUSTRIES

EDITED BY THE RESEARCH LABORATORY OF N.V. PHILIPS' GLOEILAMPENFABRIEKEN, EINDHOVEN, NETHERLANDS.

PROJECTION-TELEVISION RECEIVER

II. THE CATHODE-RAY TUBE

by J. de GIER.

621.397.62:621.385.832

A description is given of cathode-ray tube type MW 6-2. This tube produces a television picture of about 3.6 cm × 4.6 cm which, by means of a suitable optical system, is enlarged and projected on a screen (32 cm × 40 cm). The electron beam is focused and deflected by means of magnetic fields. The tube is designed to operate with an anode voltage of 25 kV. The "gun" is a triode system with a spark-trap. In order to produce a white picture, a mixture of two luminescent substances is used, one of which gives a yellow light and the other a blue light. An important element in the construction is the reflector, consisting of a thin layer of aluminium applied on the inside of the luminescent screen. By means of this reflector the luminescent light radiated to the rear is thrown forward, so that little is lost. Other advantages obtained with this reflector include improved contrast between the light and dark parts of the picture and the avoidance of an ion spot. Discoloration of the glass, a phenomenon that has been found to be due both to X-rays and to electrons penetrating the glass, is also discussed; a glass has been developed which shows no discoloration.

In the previous paper [1]) of this series on television reception — which paper we shall refer to here as article I — a summary was given of a number of drawbacks of the so-called "direct viewing" method when a fair-sized picture is required. Briefly, the objections were as follows: when a large cathode-ray tube capable of withstanding atmospheric pressure is used, either the tube face (the carrier of the luminescent screen) has to be given a strong curvature or the glass has to be made very thick. The former causes the picture to be distorted whilst the latter involves considerable thickness (one centimeter or more for the largest tubes having a diameter of about 50 cm) of the glass through which the picture has to be observed; moreover, such a bulb is most awkward to handle. In either case the risk of implosion has to be considered, and precautions have to be taken against this danger. Obviously such a tube is expensive and the cabinet in which it is mounted has to be of comparatively large size.

From the point of view of the tube manufacturer there are still other objections to be raised: large machines are required for the sealing, pumping and other processes, a great deal of space is required in which to store the bulbs and the completed tubes, and the cost of packing and transport is considerable.

All these objections disappear when a small cathode-ray tube is used and the picture is enlarged by means of projection. In article I a description was given of the modified Schmidt optical system that has been designed in the Philips laboratory for this purpose. It has been calculated that the cathode-ray tube requires a power of 2.5 W to give the projected picture of 32 cm × 40 cm the brightness of a good cinema picture, which is about 32 candles per sq. metre. Although the tube is capable of producing a much higher degree of brightness, the calculations which are to follow will be based on these figures.

In article I the choice of the tube voltage and tube current, the product of which yields this power, was left open. Since this is a matter closely related to our aim of minimizing the size of the light spot describing the picture as it

[1]) P. M. van Alphen and H. Rinia, Projection-television receiver, I. The optical system, Philips Techn. Rev. **10**, 69-78, 1948 (No. 3).

passes to and fro across the window, this is the appropriate place to consider the choice of tube voltage and current, for the diameter of the light spot is directly related to several main dimensions of the cathode-ray tube and of the optical system, as will be evident from the following. In the ideal case the light spot is sharply defined and sp small that the lines of the television picture just become contiguous. The height of the picture on the tube window therefore equals approximately the number of lines [2]) multiplied by the diameter of the spot. From this picture height there follows the picture width — which bears a certain proportion to the height — and thus also the diagonal determining the diameter of the window (with the British television system for instance the width is 5/4 × the height and the diagonal 6.4/4 × the height; with the American system these ratios are 4/3 and 5/3 respectively). Consequently, the more the spot can be reduced in size, the smaller the cathode-ray tube and the optical system can be made.

Choice of current and voltage

In point of fact the light spot is not sharply defined, its brightness being maximum in the middle and decreasing towards the edge. Defining the spot diameter d as being the diameter of the circle where the brightness is half of that in the centre, we can write the formula for d [3]) as:

$$d = C\left(\frac{I_a}{V_a \cdot j_k}\right)^{\frac{1}{2}},$$

where I_a represents the current flowing through the tube, V_a the voltage across the tube and j_k the current density at the cathode, whilst C is a factor that can be disregarded in the present case. From this formula it follows that in order to obtain the smallest possible spot one must choose a low current, but on the other hand the highest possible voltage across the tube and current density at the cathode. By increasing the current density, however, there is a danger of shortening the lifetime of the tube, whilst increasing the voltage likewise leads to a limit above which the difficulties are disproportionately increased. It was found that with a voltage of 25 kV these difficulties can quite well be overcome and this voltage has therefore been chosen for the tube to be presently described [4]).

Naturally, steps have been taken to make it impossible for anyone to touch live parts. From the power of 2.5 W required for a satisfactory brightness of the picture on the projection screen it follows that a current of 0.1 mA is needed. With this current and a picture height of 3.6 cm good line definition is indeed obtained, even with the large number of lines (567) on which the experimental transmitter at Eindhoven is working, This gives a spot diameter of about 70 μ [5]). The cathode-ray tube, however, has so much reserve as to allow of higher current peaks (up to 0.5 mA), so that if it is desired the brightness can be appreciably increased (to about 120 candles/m², i.e. about 35 foot-lambert on the viewing screen, corresponding to a tube face brightness in the order of 10 000 c/m², or 3000 foot-lambert). The spot diameter is then increased, it is true, and the picture is thus less sharply defined, but as long as the lack of sharpness is confined to a few "high lights" this need not be troublesome.

The fact that the spot becomes larger when the current is increased can be seen from the formula given for d when it is borne in mind that then a larger surface of the cathode takes part in the emission, so that j_k does not increase so quickly as I_a. Moreover, when a high current is used account has to be taken of an effect which has been ignored in the deduction of the formula, namely the mutual repulsion of the electrons in the beam. This also means that the spot has a tendency to become larger.

The picture height of 36 mm leads to a diagonal of about 60 mm. The outer diameter of the tube face is about 65 mm.

Magnetic versus electric focusing and deflection

For the focusing as well as for the deflection of the electron beam either an electric field or a magnetic field can be used. In the case of a cathode-ray tube for a projection television receiver a maghetic field is to be preferred for both purposes, contrary to the case of a normal oscillograph tube for instance. This preference is due partly to the high voltage required for television tubes.

Let us first consider the deflection. If this were to be done electrostatically, a saw-tooth voltage of very large amplitude (of the order of 1000 V) would be required between the deflecting plates, owing to the high speed of the electrons. The generating of such a high saw-tooth voltage, which must satisfy stringent requirements of linearity, is no easy matter. Furthermore, the high D.C. voltage across the tube would involve the following difficulty. If the anode were to be earthed (as is usual with an oscillograph tube) the receiver supplying the video signal to the cathode

[2]) The numbers of lines at present employed are: 405 in the British, 455 in the French and 525 in the American television system.

[3]) See for instance G. A. Morton, Electron guns for television application, Rev. Mod. Phys. **18**, 362-378, 1946.

[4]) A specially suitable apparatus for this high D.C. voltage will form the subject of another article in this series.

[5]) During the flyback of the light spot from the bottom to the top about 10% of the number of lines is lost.

and control grid of the cathode-ray tube would have to have a high (negative) voltage with respect to earth. If, on the other hand, the cathode were earthed then the generators of the saw-tooth voltages would come under a high (positive) voltage with respect to earth. Either case leads to unpleasant complications. With magnetic deflection these difficulties do not arise. Electrically the coils exciting the magnetic deflection fields [6]) are separated from the tube and can therefore be kept at earth potential. Then the cathode can be earthed, so that the problem of insulation does not arise in the receiving set either.

deflected to the same extent. The diameter of the beam can be kept so small, however, that the inhomogeneity of the field within that diameter can be ignored in this case.

Now as regards the focusing a factor in favour of the magnetic method is the extreme simplicity that can then be given to the electrode system (the "gun"), for this system, to which we shall refer presently, then need only consist of a cathode, a grid and an anode, as diagrammatically represented in *fig. 1*. The focusing coil around the neck of the tube is then at earth potential, as are also the deflecting coils.

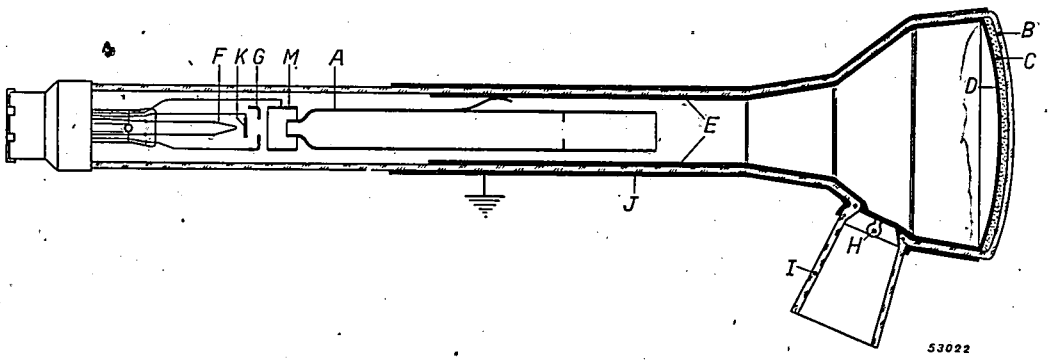


Fig. 1. Cross-section of the cathode-ray tube type MW 6-2 for projection television reception. F = filament, K = indirectly heated oxide cathode, G = grid, A = anode (the shape of these electrodes is only diagrammatically represented), B = spherically curved tube face, C = luminescent screen, D = reflector, E = conducting layer (continuation of D and at the same time forming connection to A), H = anode connecting lug, I = insulator for extending the leak path between the anode connection and the earthed conducting outer coating (J), M = spark-trap (referred to later).

A third argument in favour of magnetic deflection lies in the fact that a certain error occurs to a much less extent than it does in the case of electrostatic deflection[7]). The fact is that with electrostatic deflection the voltage between the deflecting plates causes the electrons to be accelerated on the side of the positive plate and retarded on the side of the negative plate. The accelerated electrons are deflected over a smaller angle than the retarded ones, so that the light spot, which is circular so long as it is in the middle of the tube face, when deflected is drawn out to a small line. In the case of magnetic deflection in principle such a deformation likewise occurs, though from a different cause: the deflecting magnetic field has not precisely the same strength at all points of the diameter of the electron beam, so that the electrons are not all

[6]) The apparatus supplying the saw-tooth currents for these coils will be described in a further article.

[7]) See for instance fig. 5 and the relative text of the article by J. de Gier and A. P. van Rooy, Improvements in the construction of cathode-ray tubes, Philips Techn. Rev. **9**, 180-194, 1947 (No. 6).

Constructional features of the new cathode-ray tube

In article I it was recalled that Philips brought onto the market a cathode-ray tube for television projection as far back as 1937 [8]). Since that time considerable improvements have been made in the construction, some of which will be discussed here. The appearance of the new tube (type MW 6-2) may be seen from the specimen *3* shown in *fig. 2*, the I_a characteristic of which is given in *fig. 3* as a function of the grid voltage V_g.

The electrode system

One demand that has to be met by an electrode system for a cathode-ray tube is that it must produce a sufficiently narrow electron beam. This is above all necessary to minimize the aforementioned aberration that occurs through deflection. Moreover, the largest diameter of the beam must still be small enough to ensure also that the maximum deflected electrons are kept a certain distance away

[8]) M. Wolf, The enlarged projection of television pictures, Philips Techn. Rev. **2**, 249-253, 1937.

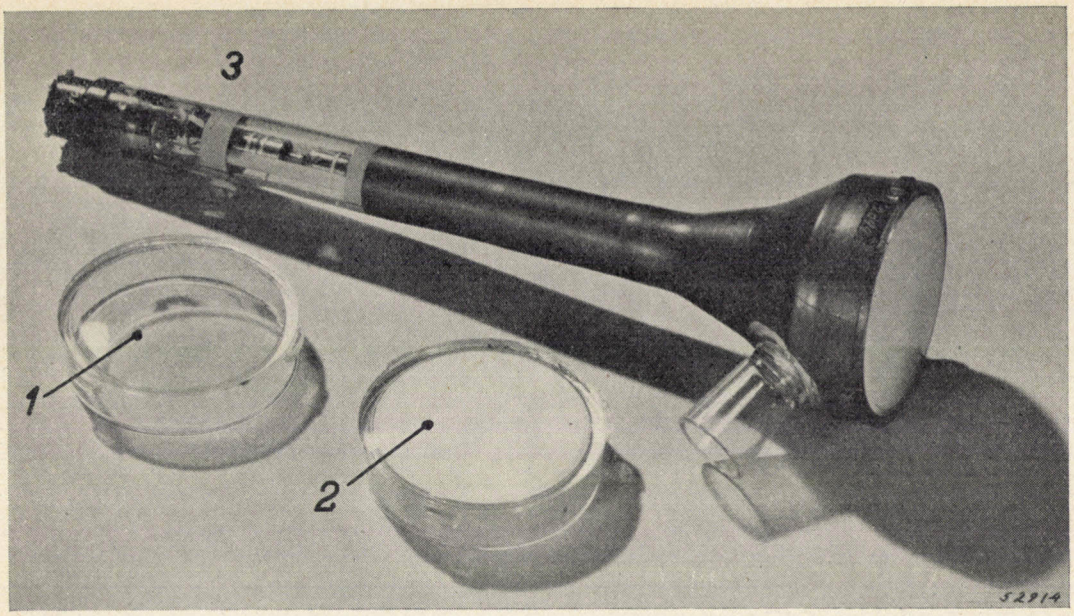


Fig. 2. *1* = tube face before the luminescent screen has been applied, *2* = tube face with luminescent screen, *3* = the complete tube MW 6-2.

from the edge of the anode and from the wall of the tube. On the other hand, however, the beam must not be so thin as to cause the mutual repulsion of the electrons to contribute perceptibly towards blurring of the light spot.

Further, the gun must be so arranged as to give a sufficiently steep $I_a = f(V_g)$ characteristic.

In the past it was thought that these demands could only be met by means of rather complicated constructions, for instance with a tetrode system comprising a "suction anode". It has been found, however, that also a triode system can produce

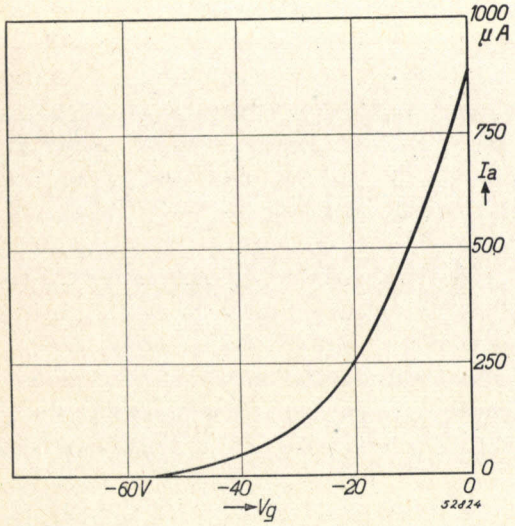


Fig. 3. Characteristic (anode current I_a as function of the grid voltage V_g) of the cathode-ray tube MW 6-2 for the normal values of the filament voltage and anode voltage (respectively 6.3 V and 25 000 V).

field conditions which meet the requirements, if special attention is given to the following: shaping of the anode and of the profile of the opening in the grid, distance between anode and grid, and insertion between anode and grid of a ring connected to earth (which ring, as will be seen later, has also another function).

A triode system such as represented in *fig. 4* is, for various reasons, by far preferable to the older and more complicated constructions. With those older constructions it was not easy to centre the narrow aperture in the grid and in the suction anode with the necessary precision and to keep it centered. With the triode system, on the other hand, the centering of the grid with respect to the anode, which has a large aperture, does not present any particular difficulties. Especially satisfactory in this respect is a system already described in this journal [9]) where the electrodes are supported by ceramic insulators in the form of a small rod having a groove filled with sintered glass in which the electrode supports are fused.

A particular feature of the triode system applied in the MW 6-2 tube is the so-called spark-trap. This is the ring-shaped electrode already mentioned (*M* in fig. 4) which is placed between the grid and the anode and connected to earth. The purpose of this spark-trap will be seen from the following. If some gas should be released in the tube, for instance owing to overloading, then with the high anode

[9]) See fig. 4 of the article quoted in footnote [7]).

voltage applied this might well give rise to a discharge between anode and cathode. This discharge might lead to a discharge between anode and cathode. The latter discharge might strike the grid and temporarily cause the grid voltage to be so highly positive as to damage the cathode [10]). The spark-trap is placed in such a position that any discharge can take place only between this trap and the anode and in such a way as not to strike the grid. Thus, in the event of a flashover, the spark-trap avoids damage to the tube.

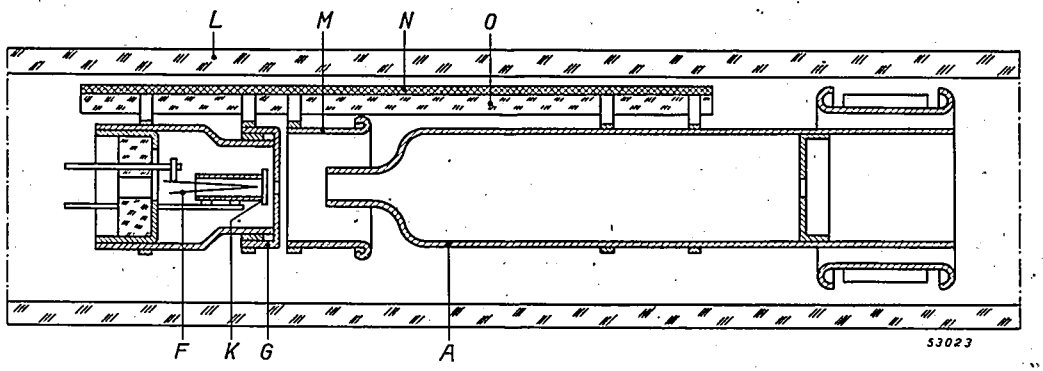


Fig. 4. Cross-section of the "gun" of the cathode-ray tube MW 6-2 enlarged about 2 ×. F = filament, K = cathode, G = grid, A = anode, L = tube wall, M = spark-trap, N = ceramic supporting insulator with glass filling G.

The tube face and luminophores

As already mentioned in article I, when a Schmidt optical system is used for the projection, the face of the cathode-ray tube has to be spherically curved in order to get a sharp projection on a flat screen [11]). The radius of curvature has to be about half that of the concave mirror. The tube face consists of a separately prepared piece of pressed glass (*1* in fig. 2). After the luminescent screen has been applied on the inside (*2* in fig. 2) the window is fused onto the conical part of the bulb.

In order to obtain the bluish-white tint that has been found best for black-and-white television pictures, a mixture of a yellow and a blue luminescent substance [12]) is used, in such proportions that the colour temperature amounts to about 6500 °K. Luminophores should be chosen which have only a short persistence, because otherwise there would be troublesome blurs following rapidly moving objects in the television picture. In the article referred to in footnote [12]) a number of silicates and sulphides are mentioned which give good results.

Reflector behind the luminescent screen

An important improvement is the reflecting layer of metal applied to the back of the luminescent screen, so that the light irradiated to the rear is reflected back again and thus contributes towards a greater brightness of the picture. Of course this layer must not obstruct the electrons in the beam, which have to penetrate through it, so that it must be extremely thin. Although the idea of such a reflector is nothing new, until 1940 it had not been applied to any extent worth mentioning, because no satisfactory method had as yet been found. The fact is that if the obvious method is employed — evaporating a suitable metal directly onto the luminescent screen — the result is usually just the opposite of what is required, the light yield being less than it would be without the metallic layer, instead of almost twice as great, as is to be expected theoretically. This adverse result is due mainly to the granular structure of the luminophores, the surface of which is like a mountain landscape, with the evapored metal precipitating for the most part on the peaks and in the valleys, and only little on the slopes; the layer on the slopes is thus more or less translucent and does not reflect so much light. Still more harmful is the effect of the metal precipitated in valleys which may be so deep as to reach down to the glass, for there a layer is formed which partly absorbs or reflects back the light emitted forwards.

During the war research was carried out in various countries in order to arrive at a process which

[10]) Cf. H. C. Hamaker, H. Bruining and A. H. W. Aten Jr. On the activation of oxide-coated cathodes, Philips Res. Rep. **2**, 171-176, 1947 (No. 3).

[11]) Looked at from the outside, the tube face must appear convex, in contrast to the tube of 1937 (see footnote [8])) which was used in combination with a lens and had a concave window.

[12]) F. A. Kröger, Applications of luminescent substances, Philips Techn. Rev. **9**, 215-221, 1947 (No. 7).

would give a good reflecting layer[13]). The solutions found are based on one of the two following principles: 1) first a filler is applied to the luminescent layer to fill up the valleys, the metal then being evaporated onto the plateau thus formed; 2) a film is stretched over the peaks so as to act as sub-layer for the metal. It is this latter principle that is applied in the Philips projection tube. With the process worked out at Eindhoven the film consists of an organic substance which, after the metallic layer has been applied, can be removed by burning or evaporation.

The metal commonly used for the reflector is aluminium, which combines a number of properties favourable for the object in view. Its reflectivity for light is high (85% can easily be reached), whilst owing to its fairly low atomic weight (27) electrons can readily penetrate through it. It is easily evaporated, for instance from an electrically heated tungsten or molybdenum wire. The thin layer of oxide, Al_2O_3, formed on the aluminium during the heating of the bulb and the pumping is transparent and does not affect the reflectivity; it has even a favourable effect, in that it protects the underlying aluminium layer against chemical attack in the manufacturing process and against atomisation by the impinging electrons.

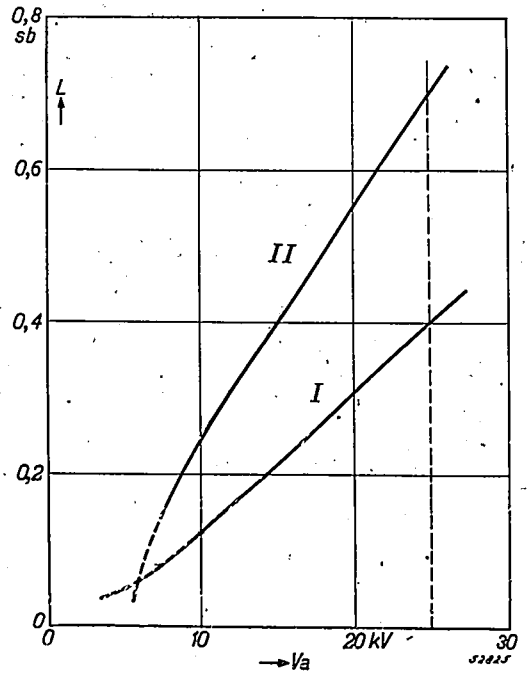


Fig. 5. Brightness L (in stilb = candle/m²) of a cathode-ray tube in the forward direction as function of the anode voltage V_a; *I*) without, *II*) with reflector behind the luminescent screen. In both cases the anode current was 200 μA.

[13]) See e.g.: D. W. Epstein and L. Pensak, Improved cathode-ray tubes with metal backed luminescent screens, R.C.A. Rev. 7, 5-10, 1946.

The layer of aluminium has to be of such a thickness as to be opaque but at the same time thin enough as to absorb only very little energy from the electrons. The first requirement is already met at a thickness of 0.5 μ, and since the penetration depth of electrons with a velocity of 25 kV is from 5 to 10 μ [14]) (according to the definition given to penetration depth) it is obvious that in such a thin layer rapid electrons will lose but little energy.

In *fig. 5* we have plotted as a function of the voltage the brightness of the tube face in the forward direction at a given intensity of current: *I*) without reflector and *II*) with reflector. It will be seen that at 25 kV the reflector yields a gain factor of about 1.8, and that at lower voltages this factor decreases. (This constitutes yet another argument for working with the highest possible voltage on the tube).

Other favourable effects of the reflector

The favourable action of the reflector is not confined to an increase in the useful quantity of light. Another desirable property is its high electric conductivity, which prevents potential differences arising between the anode and the luminescent screen and between different parts of the latter. As a consequence there is more freedom in the choice of the luminophores, since substances can be used which could not previously be considered on account of their weak secondary emission; in the absence of a metallic layer the use of substances deficient in secondary emission would lead to local negative charges on the screen, which would repel the electron beam (until the charges have sufficiently disappeared) and thus cause irregularly flickering spots in the picture.

Further, the aluminium layer enhances the contrast between the light and dark parts of the picture. Without this layer a bright part on the luminescent screen might radiate light to a dark part (both directly along a chord of the curved tube face and *via* reflection on the inner wall of the bulb cone); due to scattering, this light would also partly radiate towards the observer and thus reduce the original contrast.

Finally, the aluminium layer, provided its thickness has been properly chosen, is an effective remedy against the phenomenon called the ion spot. While the tube is working, negative ions are formed (negatively charged O-atoms, O_2-molecules,

[14]) See for instance P. Lenard, Quantitatives über Kathodenstrahlen, aller Geschwindigkeiten, Heidelberg 1925; E. Rutherford, J. Chadwick and C. D. Ellis, Radiations from radioactive substances, Cambridge 1930, chapter XIV; F. Rasetti. Elements of nuclear physics, London and Glasgow 1937, page 68.

OH-groups, etc.) which arise from gas residues or are released from the cathode. The mass of these ions being much greater than that of the electrons, they are not appreciably deflected in the magnetic field and thus tend to concentrate continuously on the middle of the screen. This concentration would result in a gradual decrease in the luminescence at that spot if there were no protective layer of metal. In course of time the picture would show a dark spot in the middle, the ion spot. The aluminium being a perfect safeguard against the ion bombardment, no trouble is experienced from this phenomenon.

Discoloration of the glass

In cathode-ray tubes at high anode voltages from about 15 kV upwards a phenomenon occurs which is not evident when lower anode voltages are used. This phenomenon is the discoloration of the glass of the tube face. After the tube has been used for some length of time, the rectangle of the television picture can be seen marked on the tube face in a certain colour (purple, brown or black according to the composition of the glass), when the tube is switched off. This may lead to as much as 20% absorption of light, but still more serious is the unpleasant tint given to the picture.

This phenomenon has been thoroughly investigated and it has been found that there are two causes for the discoloration: the soft X-rays arising from the electron bombardment on the luminescent grains, and the rapid electrons impinging directly upon the glass.

As already known from literature on the subject, the discoloration due to X-rays can be removed by heating the glass to 200-400 °C or exposing it for a long time to daylight.

The discoloration found in many kinds of glass as a result of the action of rapid electrons is of an entirely different type. In a cathode-ray tube this may occur when the luminescent layer is not of such a uniform thickness as to absorb all the electrons. For an optimum luminosity of the layer its average thickness must lie between narrow limits. It appears that with this average thickness it is possible for the electrons to pass through the layer, at least at the thinner parts, and still retain enough energy to penetrate into the glass. The discoloration due to this penetration of electrons cannot be so easily removed as that caused by X-rays. It is limited to a very thin layer only a few microns thick, whereas the discoloration due to X-rays may extend to a depth of a millimeter in the glass.

The extent to which these two effects occur in different kinds of glass varies considerably. Research undertaken by Philips has led to the composition of a special glass that shows neither of these two discolorations. A limiting factor in this research was the requirement that the new glass must be capable of being fused onto the glass of the other part of the bulb.

Conducting layers on the bulb

As in the case of all cathode-ray tubes, the inside of the bulb has to be covered with a conducting layer connected to the anode so as to prevent charging of the glass. Before the reflector described above was introduced reflection from the wall of the bulb had to be avoided, as otherwise there would be troublesome reflections of the picture. Consequently a dull black substance had to be used for the conducting layer, for instance graphite. This substance is often applied in the form of Aquadag, i.e. colloidal graphite suspended in a solution of organic components in water, the water being subsequently evaporated. From the tube manufacturer's point of view Aquadag has two drawbacks: 1) particles of graphite settling on the cathode greatly reduce the emission; 2) the organic components give off gases which can only be removed by very careful evacuation.

By using the reflector, which prevents any radiation of light to the rear, there is no longer any fear of reflections on the wall of the bulb, so that now there is no objection to the conducting layer on the wall being reflective. Obviously there-

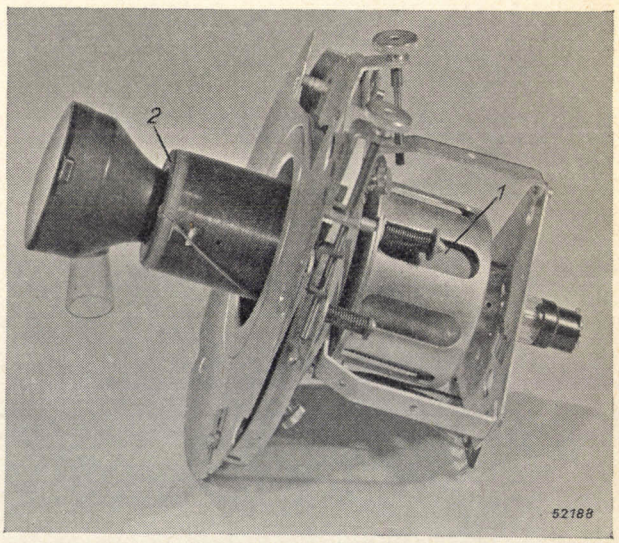


Fig. 6. The cathode-ray tube mounted in the holder for fixing it in position with respect to the projection optical system (cf. figs 6 and 7 of article I). *1* = focusing coil, *2* = cylinder containing the deflecting coils.

fore, instead of Aquadag, aluminium can now be used for the internal conducting layer, and this has in fact been applied in the MW 6-2 type of tube. This layer serves at the same time as a connection between the anode proper (A) and the anode connecting lug (H in fig. 1).

Aquadag is still used on the outside of the bulb to form a conducting layer connected to earth (J in fig. 1). Together with the layer of aluminium on the inside and the glass in between, this external layer forms a condenser helping to smooth the anode voltage. The capacitance is about 300 pF.

Data regarding focusing and deflection

Focusing of the electron beam is done by means of the coil *1* seen on the right in *fig. 6*, which has an iron magnetic circuit with an air gap of 1.2 cm. This circuit has about 800 ampere turns. The coil is fed from the high-tension supply unit of the receiver via a variable resistor with which the focusing can be adjusted.

The displacement x of the light spot on the screen of the tube MW 6-2, at 25 kV, is

$$x = 180\ lB,$$

in which l represents the axial lenght of the deflection coils (*2* in fig. 6) expressed in the same unit as x, and B the magnetic induction in the axis of the coils (in Wb/m²). The induction required with a 5 cm coil to carry the light spot across to the edge of the 4.6 cm wide picture is thus $2.3/(180 \times 5) = 2.6 \times 10^{-3}$ Wb/m² (in e.m.u.: 26 gauss).

With an anode voltage of 25 kV and an anode current of 0.1 mA the brightness on the tube face is approximately 3600 candles/m². In article I it was roughly calculated that in order to give the picture on the frosted glass viewing screen a brightness of 32 c/m² the face of the tube has to yield a luminosity of 5 candles in the axial direction, corresponding to a brightness of about 3000 c/m². The tube MW 6-2 thus amply answers the requirement. Moreover, as already stated, current peaks up to 0.5 mA are permissible, so that locally a much greater picture brightness can be achieved.

A TRANSPORTABLE X-RAY APPARATUS FOR MASS CHEST SURVEY

by H. J. DI GIOVANNI *), W. KES *) and K. LOWITZSCH *).

621.386.14:616-073.75

The transportable apparatus developed by North American Philips Co., Inc., for mass chest survey by fluorograms of groups of industrial workers, schoolchildren and others, is described. The pictures are recorded on 70 mm-film by a Fairchild camera with automatic film strip advance after every exposure, allowing 375 pictures to be made in uninterrupted succession. Constant average density of all pictures is achieved by the application of the photoelectric Morgan-Hodges timer, which automatically terminates the exposure when the film has received enough light from the fluorescent screen. In addition to these elements, the apparatus contains a series of other error-precluding devices, such as an interlocking mechanism actuated by the examinee's identification card, that serves to avoid a possible mix-up of the fluorograms. The weight of the total installation, based on a maximum X-ray tube rating of 100 kV, 200 mA, is only 1212 lbs; this is achieved through the extensive use of magnesium alloy castings. The apparatus may be disassembled in 12 pieces, thus allowing very rapid mounting and dismantling at the site of the day's assignment. A number of further details of the equipment are described, e.g. the vertical adjustment of the X-ray tube and screen, the control panel, the photoelectric timer, etc.

The modern fight against tuberculosis has been aided during the past ten years by a new diagnostic tool: the fluorogram. This is an X-ray picture of the thorax on a reduced scale, obtained by photographing the X-ray shadow picture appearing on a fluorescent screen; cf. *fig. 1*. Small size pictures, e.g. on 35, 45 or 70 mm roll film, have proved capable of giving information as to whether a lesion in the lung tissues is present or not. Owing to the small film size, the series examination of large groups of an entire population is possible at relatively low cost and at a remarkably fast time rate. Thus, the method has proved extremely valuable for finding cases of pulmonary tuberculosis in the so-called symptomless stage (which offers best prospects for a successful treatment); more detailed diagnoses in the cases thus located can be obtained subsequently by the conventional full size radiographs.

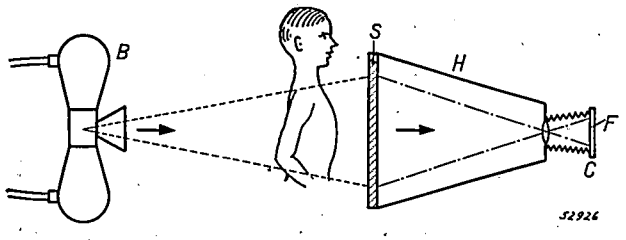


Fig. 1. General set-up for fluorography. The examinee is placed with his chest against a fluorescent screen S fixed to one end of a light-tight hood H. An X-ray tube B casts a shadow image of the chest on the screen. This image is photographed on a small size film F by means of a camera C fixed to the other end of the hood.

*) North American Philips Company, Inc., New York, N.Y.

The principle of the method of fluorography, which was first put into a practical form by de Abreu [1]) in 1936, was discussed in this Review in an article in 1940, in which a series of experiments showing the usefulness of the method [2]) was also described. In order to give an idea of the large scale on which the method has been applied in the interim, it may be mentioned that during the years 1941-1944, 20 million fluorograms were taken in the U.S.A. alone [3]).

It is obvious that the problems of organization for smoothly handling such enormous numbers of examinees become pre-eminent. They can be solved only with the aid of a highly specialized equipment, and the solution will be different for different groups of the population. A successful mass survey is most readily conducted with (though not restricted to) coherent groups such as soldiers, industrial workers, school children and hospital admissions. A few words will be said about the last of these groups at the end of this paper; as to the other groups, there are two possibilities of organization, viz., bringing the equipment to the examinees, or the reverse. If the number of examinees in a

[1]) M. de Abreu, Z. Tuberkulose **80**, 70-91, 1938; M. de Abreu and A. de Paula, Roentgenfotografia, Livr. Ateneu Rio de Janeiro 1940. There were a number of precursors, i.a. Köhler and Biesalski (1909), Caldwell (1911), Gardner (1932), who saw the importance of the method, but had no adequate technical means for its successful realization.

[2]) A. Bouwers and G. C. E. Burger, X-Ray Photography with the Camera, Philips techn. Rev. **5**, 258-263, 1940 (No. 9).

[3]) Cf. H. E. Hilleboe and R. H. Morgan, Mass Radiography of the Chest, The Year Book Publishers, Chicago 1945.

specific locality warrants the application of the first procedure — and if the locality affords a suitable power line supply or if a suitable gasoline generator is available —, this procedure should be adopted. It offers the advantages of causing the examinees to lose a minimum amount of time and of preventing them, as far as possible, from missing the examination. Therefore, in developing a radiographic equipment suited for general mass chest survey purposes, an essential requirement — in addition to the desired high quality of the pictures — was portability, to be achieved through low weight, small volume, and easy mounting and dismantling. Other important requirements which were to be met in order to make a large scale application feasible were: complete reliability, simple and quick operation by relatively unskilled operators, and safeguards against all kinds of possible errors.

Important contributions to the achievement of the latter aims were furnished by the development of automatic photographic cameras (Fairchild, Recordak), and of the automatic timing device of Morgan and Hodges [4]). Both devices, a few details of which will be discussed in the following pages, are incorporated in most of the commercially available types of apparatus which have been designed for mass chest survey purposes. They are included in the apparatus described in this paper,

[4]) R. H. Morgan and P. C. Hodges, U.S. Patent 2 401 289. Cf. R. H. Morgan, Am. J. Röntg. **48**, 220-228, 1942; Publ. Health Rep. **58**, 1533, 1943. — Previous attempts to develop such a device were made by H. Franke: Fortschr. Röntg. **42** (Kongressheft), pag. 153-154, 1930.

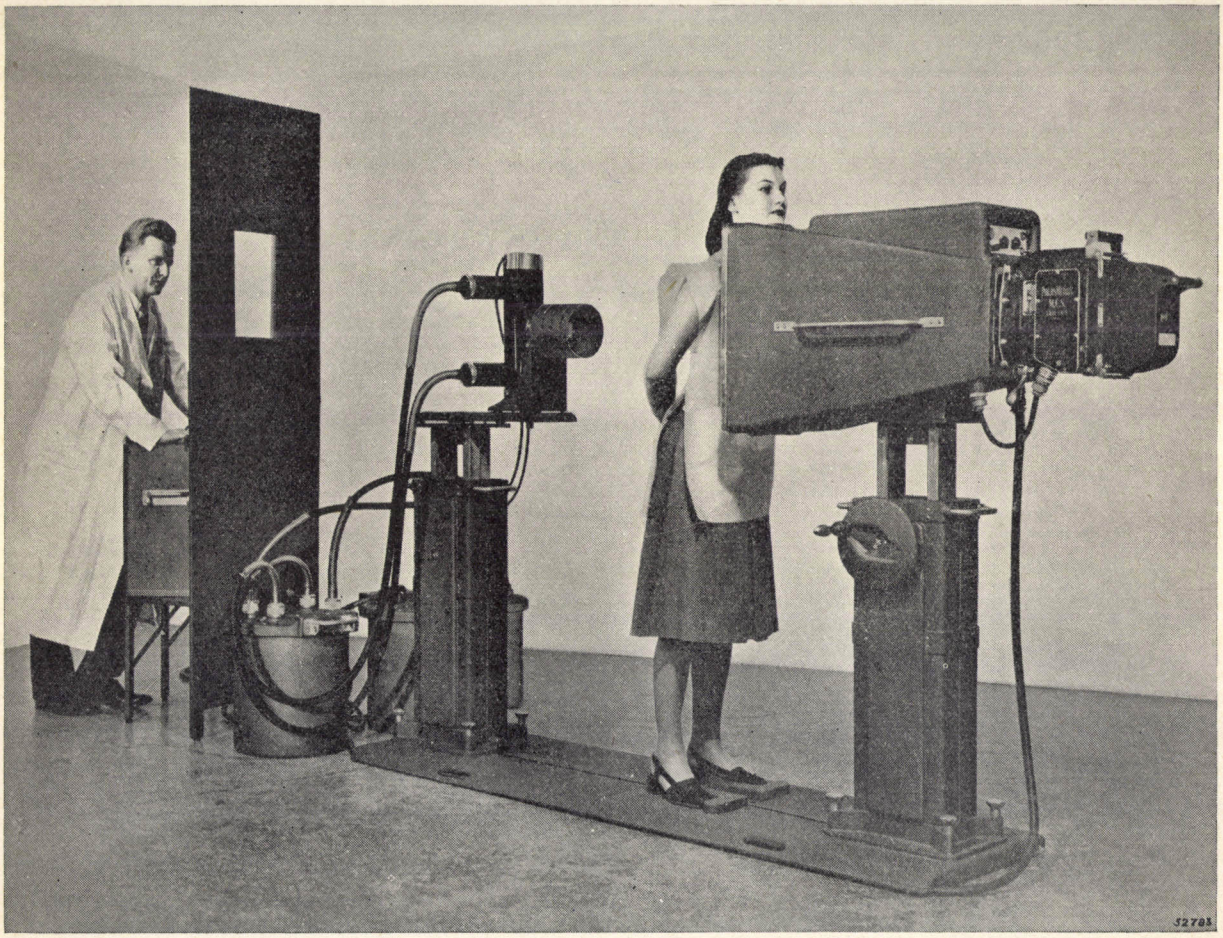


Fig. 2. Philips mass chest survey apparatus. X-ray tube and hood are mounted on two columns, clamped to a floor-plate. To the extreme right, the automatic Fairchild camera is fastened to the hood by two mounting hooks and two spring bands with a lock-type lever. The photoelectric timer is mounted in the top of the hood. The operator stands at the control panel behind a protective screen, where he can watch the examinee through a lead glass window. The three tank units located between the X-ray tube and the control panel, and linked to both of them by flexible cables, contain the two halves of the high tension transformer, each delivering up to 50 kV, and a bridge circuit with four high vacuum rectifying valves. In place of the two transformer units, which can supply 200 mA at 100 kV, a single unit can be optionally substituted delivering the total voltage of 100 kV with a maximum load of 100 mA. The leads connecting the camera and the photoelectric timer to the control panel are placed in a channel in the floor-plate.

along with a number of other features that warrant a more detailed description. This apparatus was developed by North American Philips Company, Inc., and has been in constant use at a number of Health Services throughout the U.S.A. and other countries during the past several years.

General description of the apparatus

A photograph of the complete equipment is reproduced in *fig. 2*. The X-ray tube and the hood with the camera, sketched in fig. 1, are mounted on two columns, whose relative position is fixed by a common floor-plate. The high tension generator consisting of three (or two) units, and a control stand for the operator are placed behind the X-ray tube. This arrangement requires a minimum of floor space and permits the working area around the unit to be kept free from obstructions such as cables, which is an important consideration when dealing with a more or less continuous stream of examinees.

The automatic Fairchild-camera, which is fastened to the small end of the hood, has been especially developed for miniature film radiography. It will accomodate a 100 foot strip of (unperforated) 70 mm roll film. After each exposure the film is transported automatically through one frame length by a small electric motor. Thus the task of the operator is facilitated and the risk of double exposures avoided. The picture size is 2.5″ × 3″, so that a 100 foot length of film permits 375 exposures to be taken without interruption for unloading and reloading the camera. Arguments concerning the most desirable picture size will not be appraised here. It may be stated, however, that — although smaller sizes are quite feasible and offer enhanced advantages of economy and easy handling — the 70 mm size has become rather popular because it permits the use of relatively coarse-grained and, therefore, very sensitive film material.

As a high speed optical system is of prime importance with fluorography, the Fairchild-camera contains a coated lens having an effective speed of f: 1.9 (with a subject-to-lens distance of 78 cm), designed especially for this purpose. The reconciliation of the contradictory requirements of a large aperture and of extremely sharp images was considerably simplified by the fact that a single invariable subject-to-lens distance is required and that the problem of chromatic aberration was rendered less serious because the types of fluorescent screen used for fluorography emit light with a fairly distinct maximum in its spectral distribution, either in the blue or in the green region.

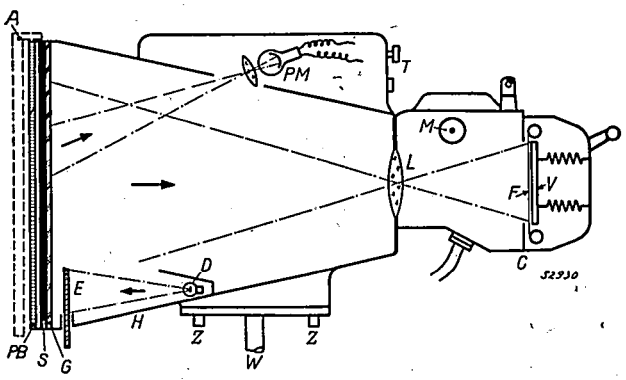


Fig. 3. Schematic cross section of the hood. In front of the screen *S*, which is backed by a clear glass plate *G*, a very fine meshed Potter-Bucky filter grid *PB* is placed, which reduces materially the scattered radiation and hence improves the contrast of the image. An adequately chosen rectangular portion of the chest image on the screen is projected by a lens onto the sensitive surface of the photo-multiplier tube *PM*, controlling the automatic timing of the exposure. The setting of the timer to the desired film density is done on the panel at *T*. Card *E* and lamp *D* are part of the identification and interlock system described in the following section. *W* and *Z* are pins for mounting the hood on its pedestal. *C* is the Fairchild "Fluoro-Record" camera, with lens *L* and motor *M* for automatic film transport. During the exposure the film *F* is pressed against the frame in the focal plane by a pressure-plate *V*; it is automatically released for transport after the exposure. X-rays transmitted by the fluorescent screen are almost completely absorbed by the camera lens and its steel fitting, so that no fogging of the film in the camera magazine will occur. If it is desired to make a full-size radiograph, an adaptor frame *A* for a cassette holder is hooked on the screen side of the hood.

The Morgan-Hodges-timer is placed in the top of the hood. This device controls the duration of the film exposure, de-energizing the X-ray tube automatically as soon as the given exposure that corresponds to the desired density of the fluorogram has been obtained. A cross-section of the hood showing the basic arrangement of the timer is given in *fig. 3*. An image of a portion of the fluorescent screen is focused by a lens on the light-sensitive cathode surface of a photo-multiplier tube. The electric current produced in the tube by the illumination charges a capacitor, and the voltage built up across it is applied to the grid of a relay-tube. When the voltage on the capacitor reaches a certain value, corresponding to a predetermined amount of light emitted by the fluorescent screen, the relay-tube is fired and interrupts the X-ray supply. A few more details of this mechanism will be described below.

The control-panel is shown in *fig. 4*. As it will be impracticable, in many cases, because of the limited time and supervisory personnel allotted, to determine and use the exact kilovoltage and current of the X-ray tube yielding best penetration and contrast with the specific chest dimensions of each individual examinee of a large group, medium values of e.g. 85 kV (peak) and 100 mA (mean value) are

ordinarily adopted. Other values need be used only with persons of very unusual proportions. For this purpose, the kilovoltage may be adjusted to 75, 85 or 100 kV, while the current is adjustable to 50, 100 and 200 mA. The highest mA-value should be used only in places where the local power line has sufficiently small resistance not to produce too large a voltage drop with this heavy load.

The tube current is made independent of line voltage fluctuations by means of a filament voltage stabilizer, and the kilo-voltage is made independent of the tube current by a set of compensating resistors, utilizing a method recently described in this Review [5]). These precautions are taken in this apparatus only to obtain consistent contrast and sharpness of the radiographs; in contradistinction to normal diagnostic radiography they are not necessary for obtaining consistent film densities, this being insured by the automatic timer.

The exposure time necessary for an average chest size of 22.3 cm and with 100 kV and 100 mA is about 0.185 sec. For extreme chest sizes, exposure times under the same conditions may vary from about 0.1 to 0.6 seconds. Of course, with a given kilovoltage and tube current, the exposure time must not be so long as to cause an excessive heating of the anode of the X-ray tube. In order to insure that the time limit which corresponds to the permissible tube rating will never be exceeded, and also to protect the X-ray tube in case the photoelectric timer should entirely fail to function, a safety timer is provided which interrupts the X-ray tube supply (regardless of the action of the photoelectric timer) after a given time, set in accordance with the permissible tube rating to any one of seven values between 0.25 and 2.5 sec. Incidentally, the permissible exposure times with mass chest surveys are influenced by the great number of exposures which must be taken with only short intervals between them (on many assignments, 200 or 300 per hour).

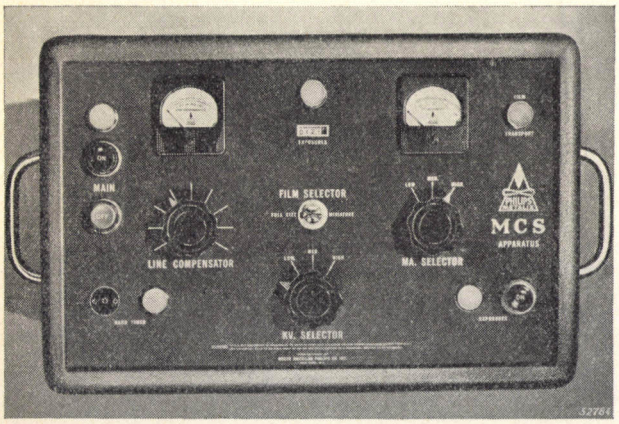


Fig. 4. View of the control panel of the apparatus. In the center is the switch for changing over from fluorography to full size radiography; below this switch is the control knob for kilovoltage selection, to the right, the mA-selector (with meter); to the left, the voltage adjusting knob (with meter) for compensating power line variations. Situated around these elements are pilot lights, the pushbutton for making the exposures and a register for counting the exposures. The circuits contained in the high tension generator, the photoelectric timer, the automatic camera and other devices are all connected to the control panel with plugs and jacks. All the plugs are coded and keyed in order to prevent the incorrect connection or accidental interchange of leads.

The height of the X-ray tube and the screen must be adapted to the height of the examinee. Therefore, a vertical adjustment of the hood by means of a crank-wheel is provided. The X-ray tube is linked to the hood by a chain running through a channel in the floor-plate, so that the tube follows the hood in its vertical movement. This mechanism is illustrated by *fig. 5*, in which a few more details of the design are also shown and explained. A foot form on the floor-plate and a chin-rest on the hood aid in rapid posturing of the examinee with respect to the screen.

The vertical adjustment may also be accomplished by means of a small motor provided with a special braking control developed for this specific purpose. The braking mechanism brings the fast running motor to a stop within two or three revolutions after the operating button has been released. This is very important when a quick adjustment is required, avoiding repeated overshooting.

Mechanical design of the equipment

As light weight is one of the most important requirements for transportable apparatus, magnesium was selected as the basic metal from which to fabricate the main assembly castings. Considerable experience has been gained before and during the last war by airplane manufacturers and aircraft parts foundries in handling this hitherto rather unfamiliar metal. For castings, the metal is generally used in the form of an alloy containing aluminum, small amounts of manganese, and sometimes zinc, e.g. 6% Al, 0.2% Mn, 3% Zn. The specific gravity of this alloy is about 1.8, i.e. it is about 1/4 that of iron and 2/3 that of aluminum, so that considerable saving in weight could be expected from the use of this material.

It is true that part of the gain achieved by the low specific weight is lost because of the less favorable mechanical properties of magnesium, viz., its low shock resistance and low elastic modulus, as compared with common aluminum alloys (the elastic modulus for the magnesium alloy mentioned above

[5]) A. Nemet, W. A. Bayfield and M. Berindei, A diagnostic X-ray apparatus with exposure technique indication and overload protection, Philips Techn. Rev. **10**, 37-45, 1948/49 (No. 2).

is 64×10^5 lb/in^2 (4.5×10^5 kg/cm^2), for aluminum alloys 100×10^5 lb/in^2). These properties require the adoption of thicker sections, added stiffening ribs, generous tapers from heavier to lighter sections and larger fillet radii (about twice those that would be used for iron castings). Nevertheless, the magnesium castings turn out to be lighter than if made of any other material. This is partly due to the fortunate fact that the provisions necessary for compensating for low elastic modulus and low shock resistance are similar.

Due to the extensive use of magnesium it was possible to reduce the total weight of the apparatus to 1212 lbs (with the 200 mA-generator; if the 100 mA-generator is used, the weight is only 1052 lbs).

Other important requirements for portable apparatus were mentioned above; small size, easy and quick mounting and dismantling. To reduce size,

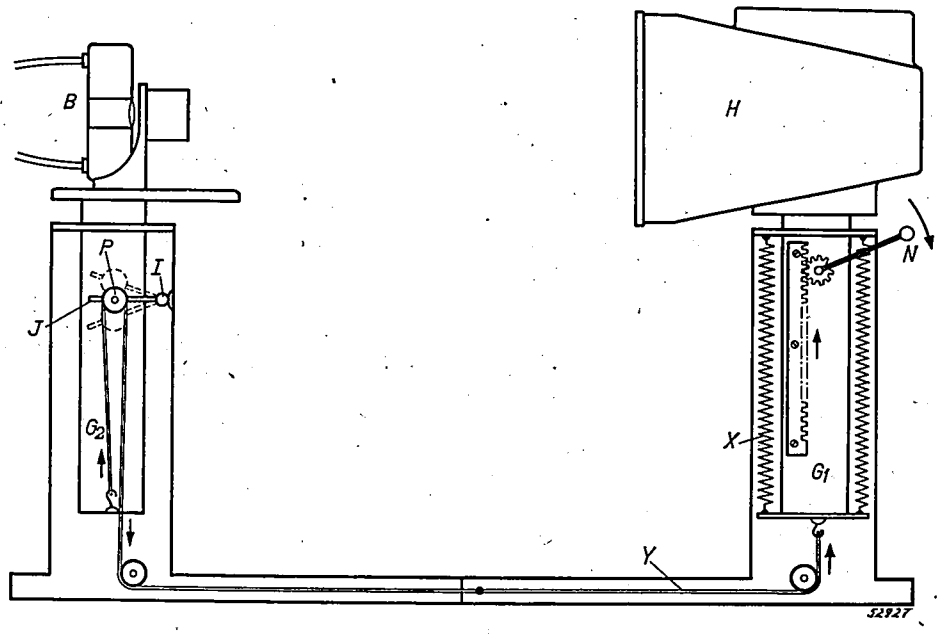


Fig. 5. The height of the hood H is adjusted by means of crank N and a rack and pinion drive. The X-ray tube B follows the hood in synchronous movement, due to the interconnection of the two supporting movable members G_1 and G_2 by chain Y. The total weight of hood and X-ray tube is, at a position of medium height, exactly counterbalanced by the tension of the springs X. Owing to the great length of these springs, their tension varies only slightly with the position of the hood; hence the counterbalanced condition is maintained to a good degree of approximation in all positions, and the adjustment of height requires negligible effort. (Counterbalancing by springs instead of by weight has the advantage of keeping the total weight of the apparatus and the inertia of the adjustable portions as low as possible.) The pulley P may be lowered or raised to two fixed positions other than the normal one by swinging the bearing arm J round its fulcrum I by means of a crank; in this way, stereoscopic pictures can be taken, as the X-ray source in one position of P is 5 cm below, and in the other one 5 cm above its normal height, thus producing two shadow images with the desired parallax. (In order to make separate sets of stereoscopic pictures, the roll film cassette of the camera can be substituted by a special adaptor for cut films; this is also most useful for making test fluorographs.)

In addition to their low density, magnesium alloys in general offer the advantage of very favorable machining characteristics, so that high tool speeds and deep cuts are possible. However, due to the unique mechanical properties, machining practice with respect to the cutter types and grinding and lubricating methods to be used is rather different from that in use for other metals. Ample data as to proper machining technique are available from the manufacturers of magnesium alloys [6]).

[6]) A curious detail of the machining of magnesium is the necessity of avoiding the hazard of fire: as is well-known, very fine magnesium chips are easily inflammable, as exemplified by the old-fashioned photographic flash powders. Therefore, special precautions are necessary in cutting and in disposing of the shavings.

the largest component parts (operator screen and floor-plate) are made collapsible. On the other hand, the number of pieces into which the unit is disassembled is kept to a minimum, in order to reduce the time necessary for mounting and disassembling. There are only 12 major pieces, and the whole unit can be set up or dismantled in 15 to 20 minutes. The objective of reducing the number of pieces was not, of course, allowed to interfere with the requirement that each single piece must be easily handled. Accordingly the transformer of the 200 mA-generator is designed as two units to divide the weight (each of the two sections weighs 196 lbs).

The speed of setting up results partly from the simple way in which the columns with the hood and

the X-ray tube are assembled. The columns are fastened to the floor-plate by four integral clamping screws. The hood is simply placed on its pedestal inserting a mounting stud in the corresponding hole, two small auxiliary pins ensuring proper alignment. The X-ray tube and the tube support bracket are mounted in a similar way, suitable indexing arrangements being provided. The hood, bracket and tube are heavy enough to remain securely seated in their proper places without requiring any sort of clamping. The chain connecting the hood and the X-ray tube is composed of two parts, each part, upon disassembling the unit, being retractable into its respective column where it can be fastened in place. This automatically locks the sliding section of the tube column, so as not to risk damage during transport.

Error-precluding devices

The apparatus contains several devices to prevent operators from making errors which would cause damage to the equipment or impair the usefulness of the survey. The automatic motor-driven camera and the automatic timer, as error-precluding devices, were mentioned above. A few others are described here.

During the survey the possibility of mix-ups resulting from improperly identified photographs is completely eliminated by an identification system visible in the lower part of fig. 3. For every examinee, an identification card *E* containing name, serial number or other data must be properly inserted in a card holder in the hood. The proper insertion of the card operates a relay system, which is connected in the circuit in such a way that until it is operated the X-ray tube cannot be loaded. During the exposure the identification card is illuminated by a lamp *D* and photographed on the lower part of the fluorogram. After the exposure the apparatus is automatically interlocked, and only the extraction of the card from the holder and the proper insertion of a new one (or of the same card again, if a second exposure of the examinee is desired) will re-establish the conditions necessary for energizing the X-ray tube.

The actual exposure is effected by simply pressing a pushbutton on the control panel (cf. fig. 4) and holding it down. The relay system actuated by this button switches on the illumination for the identification card in the hood, boosts the filaments of the rectifying valves and energizes the stator of the X-ray tube, rapidly accelerating the anode to full speed (this, of course, applies only to the case of a rotating anode tube; tubes with stationary anode may also be used). Approximately one second after the button is pressed the X-rays come on, this condition being indicated by a red pilot light on the control panel. When the proper exposure time has elapsed, the X-ray tube is automatically de-energized by the photoelectric timer and the red pilot light is extinguished. Now the pushbutton can be released, whereupon the automatic advance of the film strip to the next frame takes place.

Releasing the pushbutton at an earlier moment will terminate the exposure and de-energize the apparatus at once. Thus, the operation remains continuously under control and may be interrupted without delay if this should be necessary.

In addition to the proper insertion of a new identification card, there are other conditions necessary to prepare the apparatus for the next exposure. If the end of the film strip has been reached, or if the camera magazine was accidentally left unloaded, no exposures can be made. A similar condition will exist when the safety timer has terminated an exposure before actuation of the photoelectric timer. This is indicated by a white pilot light on the timer panel. When this light is on, a reset button on the panel must be depressed in order to restore the normal conditions. This serves to direct the attention of the operator to the fact that the density of the preceding fluorogram will be low, as the full exposure time was not received. He can try, in that case, to repeat the exposure with a higher kilovoltage, yielding better penetration of the chest under examination.

In addition to the red and white pilot lights already mentioned, a blue light on the control panel is provided which blinks during the moving of the film, and a light marked "Ready" verifying that all conditions for making the next exposure are fulfilled.

As the remarkable simplicity of operation is largely due to the use of the photoelectric timer, a description of a few details of this device seems worth while. A simplified circuit diagram is shown in *fig. 6*. The timer can be preset to produce a fixed average density of the fluorograms by adjusting the amplification factor of the 9-stage photomultiplier tube. For this purpose the accelerating voltage between successive electrodes in this tube may be varied between 25 and 100 V, causing the amplification factor to vary between 100 and 10^6 and hence allowing variation by a factor of 10^4 in the exposure of the film before the X-ray tube is switched off. As for the reproducibility of the density (or the product of screen brightness and

exposure time), it is clear from the above that the density obtained will be very sensitive to small voltage fluctuations on the phototube. Therefore, the voltage supply of the timer unit is stabilized. Another factor that had to be considered is the finite time required to open the contactor actuated by the ralay-tube of the timer. When no allowances for this are made, all exposure times t, "proposed" by the photo-multiplier tube, will be prolonged by this constant break-contact time T, which amounts to about 1/60 second. Thus, the desired inverse proportionality between the actual exposure time t' $(= t + T)$ and the brightness of the fluorescent screen (magnitude of photoelectric current) would not be strictly realized. To correct for this small but not insignificant error, a resistor R was inserted in the phototube circuit as shown in fig. 6.

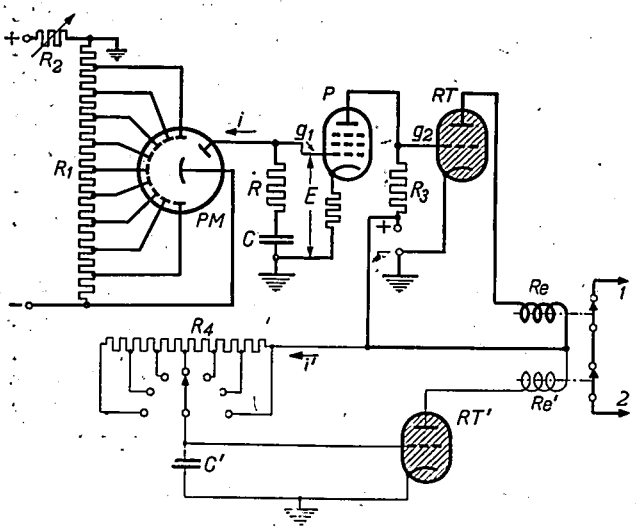


Fig. 6. Simplified circuit diagram of the photoelectric timer (heavy trace) and the safety timer (light trace). The current i of the photo-multiplier tube PM charges the capacitor C. This means that the potential of grid g_1 of pentode P will gradually grow more negative, the anode current of the pentode and hence the voltage drop on resistor R_3 will decrease, and the potential of grid g_2 of the relay-tube RT gradually will grow more positive. When the voltage on the capacitor C (plus resistor R whose role is explained in the text) reaches the value E, grid g_2 has become positive to such a degree that the relay-tube RT is fired, the relay Re is tripped and the power supply of the X-ray tube, conducted via *1-2*, is interrupted. (The relay-tube must be of a type firing at positive grid voltages.) The voltage between two successive electrodes of the photo-multiplier tube, tapped from potentiometer R_1, is controlled by the variable series resistance R_2. In this way the amplification factor, on which depends the density of the fluorogram attained, is adjustable between wide limits. — The relay Re' of the safety timer is tripped by the triggering of another relay-tube RT', whose grid potential (in contradistinction to the grid potential of RT), is rising at a rate independent of the screen illumination, owing to the capacitor C' being charged by a current i' derived from the power supply. By adjusting this current by means of the variable series resistance R_4, the safety timer can be preset to a desired exposure time limit. — After an exposure, both relay tubes are quenched by interruption of their anode circuit; similarly, both capacitors are discharged, and recharging begins when the X-ray tube again is loaded.

Without the resistor, the following equation would hold:

$$\frac{i \cdot t}{C} = E, \quad \ldots\ldots\ldots \quad (1)$$

where C is the capacitance of the capacitor, charged by the photoelectric current i, and E the voltage across it necessary for firing the relay-tube. Thus the total exposure time would be

$$t' = t + T = \frac{CE}{i} + T.$$

With the resistor, however, we have instead of (1):

$$\frac{i \cdot t}{C} + i \cdot R = E. \quad \ldots\ldots\ldots \quad (2)$$

Hence

$$t' = t + T = \frac{CE}{i} - RC + T.$$

Choosing R so that

$$RC = T,$$

we get

$$t' = \frac{CE}{i},$$

i.e. the desired constancy of the product $i \cdot t'$, which determines the density of the fluorogram, is achieved.

The automatic timer may also be used in making full size radiographs, if this is desired. In that case the timer is automatically set for proper full size radiograph density by throwing the corresponding switch on the control panel. The ease with which full size pictures may be taken in this way is very important for assignments in isolated places: as soon as the film has been processed and inspected, the suspicious cases thus discovered can be picked out for normal radiography with the same equipment.

In this section a few remarks are added concerning the reliability of the whole apparatus. Special care was devoted to this point, because on many assignments the apparatus is to be used at large distances from its home base so that possible troubles might cause considerable delay for want of proper servicing facilities. An important feature in this respect is that the X-ray tube, which is normally supplied with full-wave rectified a.c., can also be made to work on self-rectification (provided the type of tube adopted is suited for a.c. supply). In the normal case, the tank unit mentioned earlier, containing a complete bridge circuit of four high vacuum rectifying valves immersed in oil and a transformer for the filament current of the X-ray tube, is connected in series with the two high tension transformer units; cf. *fig. 7*. Obviously the rectifying valves and the X-ray tube are the most vulnerable parts of the equipment, possessing a limited (though very long)

life. As a rule, a spare X-ray tube is carried with the equipment, but it would hardly be feasible to carry along a spare specimen of the rather heavy rectifier unit as well, and replacement of a single rectifying valve at the site is not convenient because of the oil-filling. Therefore, the cathode unit (A') of the high tension transformer is provided with an additional filament transformer which is not in operation under normal conditions, but which renders it possible to connect the X-ray tube directly to the transformer, bypassing the entire rectifier unit. Thus, in an emergency, a survey already in progress can be continued with a.c. voltage on the X-ray tube. However, the rating of the tube will be lower in this case and one must be satisfied with a lower quality of the radiographs.

Similar provisions, insuring continuation of a survey in progress, have been made for the photoelectric timer and for the motordrive unit used for the vertical adjustment. Each of these can be readily detached and replaced in its entirety by another unit; or, if desired, a non-automatic hand- or clockwork-timer can be substituted for the photoelectric timer, and the manual adjustment substituted for the motor drive.

X-ray protection

In connection with an X-ray survey involving great numbers of exposures executed at all kinds of sites, in factories, class rooms, barracks etc., it is evident that special attention must be paid to X-ray protection. It need hardly be mentioned that the X-ray tube must be of the ray- (and shock-) proof type, allowing a cone of X-rays to emerge only in the direction of the examinee. A further conventional measure is the protection of the operator against the radiation scattered from the examinee, the fluorescent screen, etc.: he is placed behind a protective screen (cf. fig. 2) provided with lead glass windows. The protective screen consists of sheet steel and has a thickness of 1/16″, equivalent to 0.25 mm of lead. Weight reduction by selection of suitable material was not possible in this case, as the effectiveness of the screen in absorbing X-rays depends directly on its weight.

If the exposures are made with the help of other personnel standing near the examinee, these persons likewise must be protected by means of similar screens.

The danger that might arise for other persons through excessive exposure to radiation, even if the X-ray tube is pointed — as it should be — toward an outer wall or an empty room, is minimized with this apparatus by placing a diaphragm before the X-ray tube window, cutting off all the rays of the primary cone which would not strike the fluorescent screen. As provision is made for three different focal spot-to-screen distances, the distance desirable for full size radiography being different from that for fluorography, a different properly related position of the diaphragm is provided in the diaphragm holder for each of these distances (cf. *fig. 8 a, b, c*), in order to insure the exact limitation of the primary radiation to the screen in all three cases.

The radiation cone itself is not sharply limited, owing to the finite width of the focal spot (1.5 mm with rotating anode tubes, 4 tot 5 mm with stationary anodes); a "half-shadow" or penumbra, gradually widening at increasing distances from the tube, is present around the useful cone. This half-shadow region necessarily must fall outside the screen, lest a decrease of density toward the edges of the image be obtained. As is

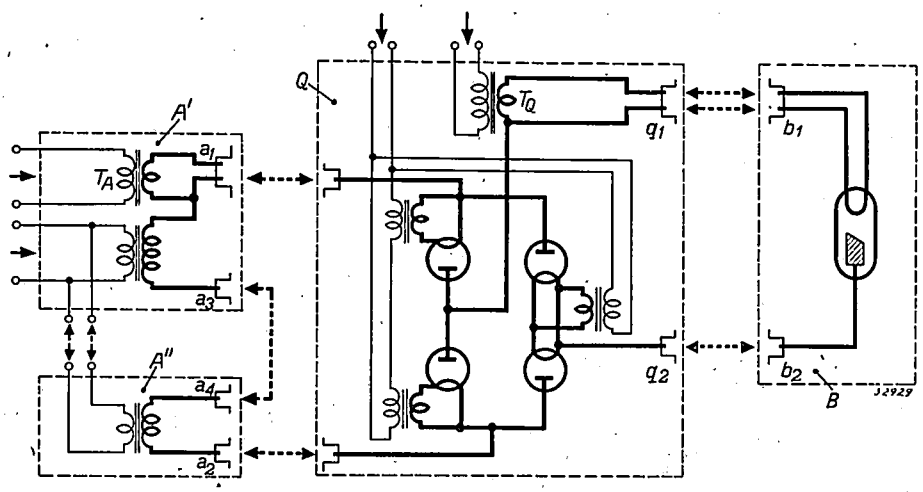


Fig. 7. Circuit diagram of the power supply of the X-ray tube (B). A' and A'': high tension transformer units, each delivering 50 kV, 200 mA. Q: rectifier unit, containing four rectifying valves and the filament transformer T_Q for the X-ray tube. The receptacles a_1 and q_1 are identical, and so are a_2 and q_2. Thus the entire rectifier unit Q can readily be eliminated in case of a breakdown of one of the valves, the cable from b_1 being plugged into a_1, that from b_2 into a_2; the spare filament transformer T_A automatically takes over the supply of the X-ray tube filament. The X-ray tube then is run with self-rectification.

seen from fig. 8*d*, the undesired half-shadow region will be reduced by placing the abovementioned diaphragm (D_1) at a greater distance from the tube. In order to be able to do so without unduly increasing the flange width of the diaphragm designed to absorb the useless outer parts of the primary cone, a second diaphragm (D_2) nearer to the X-ray tube is provided. This intercepts a large part (*IV*) of the useless outer rays, leaving the exact limitation of the remaining cone to be performed by the first diaphragm (D_1), whose size is in this way kept within reasonable limits.

Equipment for survey of hospital admissions

Among the groups of persons eligible for a systematic chest survey, hospital admissions have been named as one of the most important. Considering the fact that, in the United States, e.g. about 16 000 000 hospital admissions per year occur, it is seen that an appreciable part of an entire population could be surveyed in this way. With respect to organization, the examination of hospital admissions is a comparatively easy job, and with respect to possible consequences, the recognition of cases of tuberculosis with these persons (and with hospital personnel) is particularly important. Experience already obtained [7]) demonstrates that about 1.5 to 4.3% of the admissions (depending on age, living standard etc. of the groups examined) show significant tuberculous disease. Incidentally, 10 to 20% exhibit non-tuberculous abnormalities of the lungs, heart, spine or other parts visible on the radiographs.

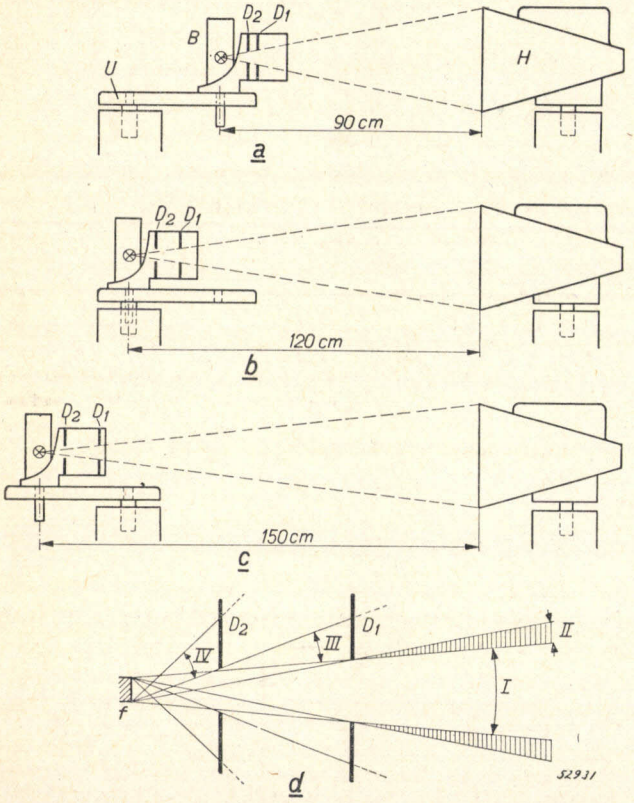
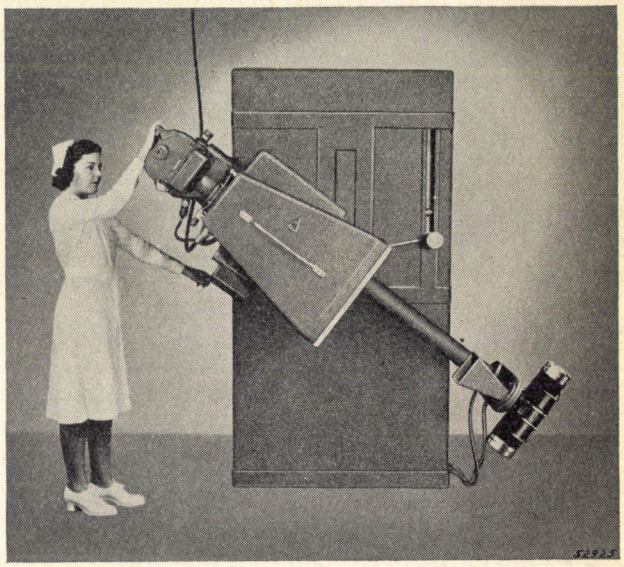


Fig. 8. Limitation of the cone of X-rays, emitted by the X-ray tube *B*, to the solid angle subtended by the hood *H* (screen surface) by means of diaphragm D_1. The tube can be fixed at three different distances from the hood, as the tube-supporting bracket *U* contains two holes for the alternative insertion of the tube dowel pin, and moreover, the bracket can be placed on its pedestal in a forward or backward direction (*a*, *b*, *c*). In accordance with these three different focal spot-to-screen distances, the diaphragm D_1 must be placed in the corresponding one of three different positions marked on the diaphragm holder. The auxiliary diaphragm D_2, which permits the size of diaphragm D_1 to be kept small, remains in a fixed position in all three cases. Owing to the finite width of the focal spot *f*, the cone of X-rays transmitted by the diagraphm is not sharply limited (*d*). Only part *I* of the cone may be used for the irradiation of the fluorescent screen; parts *III* and *IV* are absorbed by the flanges of diaphragms D_1 and D_2; part *II* is the half-shadow.



ig. 9. Mass chest survey equipment for hospital admissions. To enable fluorograms of incoming stretcher patients to be taken, the X-ray tube and hood can be swung to a vertical alignment.

X-ray equipment for this special survey work in hospital locations need not be transportable, but on the other hand, it must meet the requirement of being suited for both ambulant and non-ambulant patients. North American Philips Co., Inc., has designed a specially adapted equipment for this purpose, cf. *fig. 9*. The X-ray tube and the hood in this apparatus are mounted at opposite ends of a supporting arm which can be swung through an arc of approximately 100°, thus providing the possibility of horizontal radiography for patients lying on a stretcher. In other respects, this apparatus is essentially similar to the one described above.

[7]) The following statements are taken from a report issued in 1946 by the Council on Professional Practice of the American Hospital Organization. In this report is mentioned a 1943 questionnaire sent to 934 major hospitals, which revealed that 46 of them had already adopted the chest survey of all admissions as a routine practice. To-day it has undoubtedly been adopted by many more.

THE FUNCTION OF THE COATING OF WELDING RODS

by J. D. FAST.

621.791.753:66.046.58

In a previous article the physico-chemical factors playing a part in welding with bare rods have been discussed. In the present article the requirements that have to be met by the coating of welding rods are analysed. Firstly the nature of the forces bringing about the transfer of the metal is gone into and the circumstances are investigated under which iron oxide in the coating may cause porosity of the welds. The protection afforded by the slag against oxygen and nitrogen is discussed, starting from an ideal case where liquid iron is covered with a simple slag consisting solely of liquid SiO_2. Attention is then directed to more complicated slags and finally the coatings and slags applied in welding technique are discussed. It appears that satisfactory protection against oxygen can only be obtained if the use of oxides with a heat of formation less than about 100 kcal per gram atom oxygen is entirely avoided in the coating. Maximum protection against nitrogen requires the use of slags with low solubility for this gas. In additon to the requirements for protection against oxygen and nitrogen, for the transfer of the metal and the avoidance of porosity, the coating and the slag have to fulfil other functions, which are likewise discussed here. These requirements are so numerous and so divergent that it was necessary to develop various types of welding rods each possessing a certain number of favourable properties. The most important types manufactured by Philips are discussed.

Introduction

In a previous article [1]) we have seen that in order to make welds having satisfactory mechanical properties it is necessary to provide the welding rods with a coating. It is from the material of this coating that the slag is formed which has as its main purpose the protection of the molten metal against the attack of oxygen and nitrogen.

Coatings of greatly differing composition are used, which is not surprising considering the various functions of the coating in addition to affording protection against oxygen and nitrogen. In this article we shall go more closely into these various aspects.

When thought is given to the function of the coating and we ask ourselves what material is most suitable we must firstly bear in mind that in practice one is obliged to use oxides, among other substances. If these oxides have relatively little stability (this is manifest, inter alia, in a not very great heat of formation) the iron that has to be protected may already absorb a quantity of oxygen as a result of the reaction with such oxides. This applies particularly to rods which have a coating containing large quantities of iron oxide and with which we shall become acquainted in this article under the name of type Ph 46 electrodes. With this type of rod there can be hardly any question of protection against oxygen, though its coating does afford a certain amount of protection against nitrogen. Rods which in addition to iron oxide contain in their coating reducing metal powders (type Ph 50 electrodes) offer much better protection, but still there is no question of complete protection against oxidation. To reach this, one must absolutely avoid the use of iron oxides and other oxides having relatively little heat of formation. Such is the case with the electrodes type Ph 55 and Ph 56.

Now in the article quoted in footnote [1]) it was shown that the forces driving out the droplets of iron during the welding process are due, in the case of bare electrodes, to the chemical reaction between the carbon present in the metal of the welding rod and the oxygen absorbed from the atmosphere. Effective protection against oxidation, as offered by the coating of the electrodes type Ph 55 and Ph 56, eliminates this reaction almost entirely. Here the function of the development of CO is taken over by substances in the coating which generate large quantities of gas during the welding process. The coatings referred to contain alkaline-earth carbonates, substances which were already used before one was aware of this important aspect of their function.

The use of iron oxide has yet other drawbacks than those already mentioned. We shall see that owing to its presence welds made with the type Ph 46 electrodes always contain pores. Under normal circumstances such is not the case when the type Ph 50 electrode is used, but slight changes in the conditions may likewise lead to porous welds.

Remarkably enough, the coatings containing iron oxide appear to offer less protection also against

[1]) J. D. Fast, The part played by oxygen and nitrogen in arc-welding, Philips Techn. Rev. **10**, 26-34, 1948 (No. 1).

nitrogen than the coatings of the type Ph 55 and Ph 56 rods. At the end of this article (the closing paragraph in small type) we shall see that this is related to the fact that the slags formed out of the coatings containing iron oxide have greater solubility for nitrogen. In this connection it must be borne in mind that although it prevents direct contact between the metal and the atmosphere the slag is apt to absorb oxygen and nitrogen from the atmosphere and transmit this to the metal through diffusion and turbulences. In order to explain both this question and the reaction between coating (respectively slag) and metal we shall consider in this article an ideal case where liquid iron is covered with a very simple slag consisting of liquid SiO_2. After dealing with that case we shall discuss the more complex slags used in welding technique and investigate in how far the electrode coatings answer the requirements that have to be made. It will be found that these requirements are related not only to the protective action and the formation of gases but also, inter alia, to the melting range, the electron emission, the viscosity and the expansion coefficient of the material comprising the slag. The article closes with a more detailed discussion of the various types of welding electrodes. There a type will be referred to which has not hitherto been mentioned, the type Ph 48 electrode, which has relatively large quantities of organic materials in the coating.

The part played by gases coming from the coating in the transfer of the metal and in the penetration

When welding with the type Ph 46 and Ph 50 electrodes (which contain iron oxide in their coating) the carbon content of the metal is reduced by at least some hundredths per cent by oxidation, so that, just as is the case with bare rods, the reaction between oxygen and the carbon in the rod may contribute towards the transfer of the metal. That this is not the only determining factor when using coated electrodes, however, is evident from the fact that with the electrodes type Ph 55 and Ph 56 (coating: waterglass + CaF_2 + $CaCO_3$ + reducing metal powders) overhead welding can quite well be done, although with this type of electrode the slag affords such a good protection that there is virtually no reduction of the carbon content.

In order to ascertain the origin of the force which in this case drives out the droplets at such a high speed, we heated some of these rods for two hours in a stream of argon at 850 °C, thereby driving the chemically bound H_2O and CO_2 out of the coating. It was then found that after this heating it was no longer possible to make an overhead weld with these electrodes. At the tip of the electrode drops were formed which became larger and larger until ultimately they fell off. There was virtually no transfer to the workpiece at all. This is illustrated in *fig. 1.*

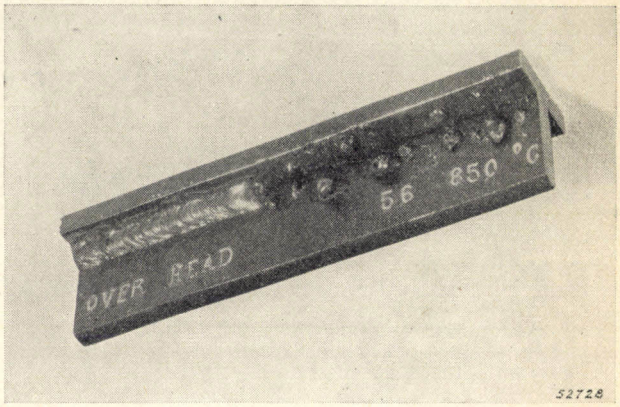


Fig. 1. The effect of heating a coated electrode (type Ph 56) for two hours in a stream of argon at a temperature of 850 °C. The left half of the workpiece shows an overhead weld made with a normal type Ph 56 rod. After a rod had been heated in the manner described it was found impossible to make an overhead weld, although an expert welder did his very best. As the right half of the workpiece shows, only a few drops of the welding material could be deposited on the workpiece, so that there was no question of any weld being made.

On the other hand the rods of this type when not previously heated to 850 °C are exceptionally suited for overhead welding. This is due to the fact that the smaller the oxygen content the greater is the surface tension and the viscosity of the molten metal. The oxygen content of the metal deposited from the type Ph 46 and Ph 50 electrodes is so high that when making overhead welds the liquid iron has a tendency to drip down out of the pool.

From the foregoing it appears that the gases driven out of the coating when welding with electrodes not previously heated to 850 °C tend to take over the previously described function of the formation of CO at the tip of the electrode. Under the influence of these released gases the drops are thrown off at a high velocity. Furthermore, a strong stream of hot gas blows against the workpiece and makes for good penetration (*fig. 2* illustrates what is meant by this). This jet action when welding with coated electrodes not heated to 850 °C is apparent also from the fact that after the welding is completed there is always a so-called crater [2]) in the solidified metal.

A good coating should therefore be capable of

[2]) In welding technique the crater is understood to be the oval depression in the solidified metal at the end of a bead.

producing a powerful stream of gas during the welding process. This requirement is usually met by adding carbonates or organic substances to the coating. The gases are evolved partly in the form of H_2O and CO_2 and partly (i.a. owing to

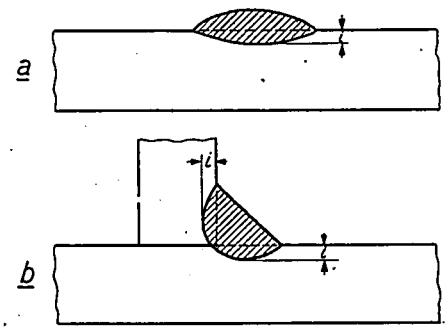


Fig. 2. The depth to which the metal of the workpiece is melted is called the penetration. This is indicated by the letter i: *a*) for a bead on a flat plate, *b*) for a horizontal fillet.

reaction with the reducing metal powders in the coating) as H_2 and CO. As shown experimentally by Mallett [3]), the water-gas equilibrium is established between these gases in the vicinity of the arc

$$H_2O + CO \leftrightharpoons H_2 + CO_2 \quad . \quad . \quad . \quad . \quad (1)$$

The arc gases from the type Ph 55 and Ph 56 electrodes have a very low content of H_2O and H_2. This is because these electrodes before leaving the factory are heated to such a temperature that the carbonates in the coating are not dissociated but the bound water is for the greater part expelled. Consequently when welding with this type of rod the molten metal can hardly absorb any hydrogen at all, with the great advantage that one need have no fear of encountering the difficulties likely to arise from the release of this gas. Without going into them more closely we may say that the main difficulties are the occurrence of porosity and, when welding steels having a relatively high carbon content, the occurrence of cracks in the transition zone ("underbead cracking").

The part played by iron oxide in the occurrence of porosity in beads

Apart from the so-called hydrogen porosity referred to above, under certain circumstances (particularly when using electrodes which have iron oxide in the coating) there may also be trouble from CO porosity. With the type Ph 50 electrodes, the coating of which contains, among others, iron oxide and reducing metal powders (ferromanganese and ferrosilicon), the proportions are so chosen that in normal working sound, non-porous welds are obtained.

If the reducing metal powders are removed from the coating, then owing to the increased development of CO in the molten metal the welds become highly porous. It is a remarkable fact that also reduced formation of CO seems to lead to porosity of the welds, as may appear from the following experiments.

Thick-walled tubes of mild steel (ext dia. 25 mm, int. dia. 4 mm) were closed at one end by welding and then filled with a rod of aluminium, titanium or zirconium of a high degree of purity and of such a length as to leave about 8 mm of the steel tube vacant. Then the open end of the tube was sealed by welding, but before doing so, this end was plugged with a conical steel pin in order to avoid oxidation of the Al, Ti ot Zr. The rods with a core made in this manner were then hammered and drawn out to wire of 4 mm gauge, cut to length (after removing the ends) and provided with coatings of the Ph 50 type. The beads obtained with these welding rods were highly porous, whereas 4 mm rods of ordinary mild steel with the same coating gave perfectly sound beads.

There is little room for doubt that the evolution of gas that always takes place in the molten pool is greatly reduced by the addition of Al, Ti or Zr to the core wire. In certain cases therefore reduced gas formation seems to have a tendency to increase porosity. This is probably to be attributed to the fact that when they are evolved very slowly the gases are more easily enclosed in the solidifying metal. This is in agreement with what has been experienced in the manufacture of steel [4]).

Further evidence of this is found in the fact that Doan and Smith, when carrying out welding experiments in helium and argon (see the article quoted in footnote [1])) obtained beads which were much more porous than when welding in the air. Here again there can be little doubt that when welding in helium or argon less gas is evolved in the molten pool than when welding in the air.

The equilibrium between liquid SiO_2 and liquid Fe.

Having considered the nature of the forces driving out the droplets at such a high speed when welding with coated electrodes, and having ascertained under what conditions the presence of iron oxide in the coating may lead to porosity of the

[3]) M. W. Mallett, Welding J. **25**, 396s-399s, 1946.

[4]) See for instance A. Hultgren and G. Phragmen, Trans. A.I.M.E. (Iron and steel division) **135**, 133-244, 1939.

welds, we shall now consider more closely the protection afforded by the slag against oxygen and nitrogen.

All slags employed in the technique of welding contain SiO_2 and we shall therefore first direct our attention to the equilibrium existing between SiO_2 and liquid Fe:

$$2Fe + SiO_2 \rightleftarrows 2FeO + Si. \quad . \quad . \quad . \quad (2)$$

The position of this equilibrium can be calculated by thermodynamic methods from heats of reaction, specific heats, heats of fusion and heats of solution [5]). In this reaction not inconsiderable quantities of FeO are formed, the greater part of which dissolves in the SiO_2 and the smaller part in the iron.

Table I gives the calculated Si and O equilibrium contents of the metal and the FeO content of the slag for different molar ratios of SiO_2/Fe and at a temperature of 2000 °K.

Table I. Calculated compositions of metal and slag for the equilibrium between liquid SiO_2 and liquid Fe at 2000 °K.

Molar ratio SiO_2/Fe	Metal		Slag
	wt % Si	wt % O	wt % FeO
1/16	0.12	0.083	3.45
1/8	0.15	0.074	3.09
1/4	0.20	0.064	2.67
1/2	0.28	0.054	2.23

The values given in table I are not claimed to be absolutely accurate, but anyhow they show that even in the absence of oxygen in the gaseous state not inconsiderable quantities of oxygen may be absorbed by the liquid iron by reaction with a chemically pure SiO_2 slag. At the still higher temperatures reached by the iron when arc-welding, the equilibrium relations are in this respect even still more favourable.

It is fortunate, however, that welding takes only so short a time that one always keeps fairly far away from the state of equilibrium. Moreover, table I shows that the iron also absorbs a quantity of Si much greater than is necessary for a complete binding of the dissolved oxygen to SiO_2 during the cooling process.

If air is present as a third phase we must also take into account (as already remarked) the fact that the slag does not offer complete protection against this, because it will always possess a certain degree of permeability for gases.

[5]) For these calculations reference is to be made to an article that will shortly be published in Philips Research Reports.

Permeability of the SiO_2 slag for oxygen and nitrogen

From measurements taken by various investigators it may be deduced that a wall of pure SiO_2 (quartz glass) 1 mm thick and with a surface area of 1 cm² under a pressure difference of 1 atm on either side of the wall allows quantities of oxygen to pass through which, for a temperature T between 950 and 1200 °K, are given by the equation

$$m = 1.2 \cdot 10^{-2}\, e^{-15600/T} \text{ gram } O_2/\text{hr}. \quad . \quad . \quad (3)$$

Under the same conditions and within the same temperature range the permeability for nitrogen is expressed as

$$m = 1.75 \cdot 10^{-3}\, e^{-12600/T} \text{ gram } N_2/\text{hr}. \quad . \quad (4)$$

This permeability is due to the fact that oxygen and nitrogen have a certain though small solubility in quartz glass. As a result there is apt to be a diffusion current from one side to the other. At first sight one might think that this must have serious consequences for arc-welding. However, even for a temperature of 2500 °K the order of magnitude of the permeability found with the aid of the formulae (3) and (4) is only 10^{-5} gr/hr. Of course we dare not by any means maintain that such a large extrapolation is permissible, but even if the permeability at 2500 °K were for instance a factor 100 greater than that found here it would be insignificant under the conditions of arc-welding.

In the composite slags actually used for arc-welding, which we shall consider more closely farther on, there may, however, be a much greater solubility and a much greater permeability. Moreover, at high temperatures the viscosity of the slags used in welding is so low that convection currents in the slag may also considerably accelerate the transmission of gas.

As soon as the slag contains a quantity of FeO in solution (and according to table I this is already the case in the state of equilibrium if we start with pure Fe and pure SiO_2 in the absence of a gas phase) the permeation of oxygen may also be brought about by an entirely different mechanism. On the outer surface of the slag oxygen can be continuously chemically bound, bivalent iron being converted into trivalent iron. This reaction can be expressed by the formula

$$4\,Fe^{++} + O_2 \rightarrow 4\,Fe^{+++} + 2\,O^{--}. \quad . \quad (5)$$

Inversely, at the boundary between slag and metal trivalent iron can again be reduced to bivalent iron:

$$2\,Fe^{+++} + Fe \rightarrow 3\,Fe^{++}, \quad . \quad . \quad . \quad (6)$$

iron being transferred from the metal to the slag. In the liquid slag there will then be a continuous transport (owing to convection and diffusion), ferro-ions (Fe^{++}) moving outwards and ferri-ions (Fe^{+++}) and oxygen ions moving inwards. Electrons too may contribute towards this transport, since at the high temperatures prevailing SiO_2 already possesses a certain degree of conductivity for electrons. Consequently the inward flow of the ferri-ions may be wholly or partly replaced by a movement of electrons in the opposite direction.

The various processes discussed lead to a continuous increase in the iron oxide content of the slag and if there were time enough ultimately all the iron would be taken up in the slag in the form of oxide.

Regarded from the point of view of the states of equilibrium, the slag therefore offers no protection at all, as could be predicted. The final stage is always the complete oxidation of the iron. In fact, however, slags do indeed afford protection against oxidation because in welding the reaction time is only very short, so that we keep at a safe distance from the state of equilibrium. Moreover, usually there are added to the slag-forming coatings of the welding rods reducing metal powders such as ferro-silicon (45% Si and 55% Fe), ferro-manganese (80% Mn and 20% Fe) and ferrotitanium (25% Ti and 75% Fe), which bind the oxygen penetrating into the slag and, if added in sufficient quantity, even deposit a metal with higher Si and Mn contents than those of the core wire. This brings us, however, into the domain of the slags as used in welding technique, which we shall consider further in the following.

Composite slags

When discussing in the two preceding sections the protection offered by a coating we confined our considerations to slags consisting entirely of SiO_2 or, after reaction with the liquid iron, of SiO_2 + a little FeO. We chose this course because it allowed a more or less quantitative treatment and because SiO_2 is an essential component of all slags used in practice.

Actually, however, welding is impossible with rods having a coating consisting almost entirely of SiO_2. Owing to its high melting point such a coating would not melt uniformly with the metal but would form a tube that becomes longer and longer until at last the distance between the core wire and the workpiece would become too great and the arc would be extinguished. It is therefore necessary to use coating containing other oxides in addition to SiO_2.

We shall mention here some experiments carried out with mixtures consisting of only three of these oxides, viz. SiO_2, CaO and Al_2O_3[6]). These experiments show that a state of equilibrium will no more be established between the components of the slag during welding than between the metal and the gaseous atmosphere (see the foregoing and the article quoted in footnote [1])).

In the aforementioned system two ternary compounds occur, anorthite $CaAl_2Si_2O_8$ ($CaO \cdot Al_2O_3 \cdot 2SiO_2$) with a melting point of 1550 °C and gehlenite $Ca_2Al_2SiO_7$ ($2CaO \cdot Al_2O_3 \cdot SiO_2$) with a melting point of 1590 °C. These compounds form a quasi-binary system with a eutectic point of 1385 °C. See the diagram in *fig. 3*.

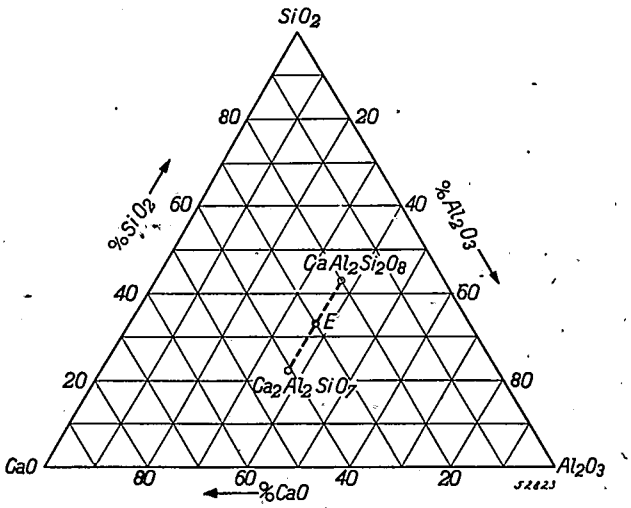


Fig. 3. In the ternary equilibrium diagram SiO_2 - CaO - Al_2O_3 two congruently melting ternary compounds occur, anorthite ($CaAl_2Si_2O_8$) and gehlenite ($Ca_2Al_2SiO_7$). These form a quasi-binary system with eutectic E of 1385 °C (see the dotted line).

For these experiments rods of mild steel (diameter 4 mm) were coated with mixtures containing 30% CaO, 37% Al_2O_3 and 33% SiO_2 (all % by wt), the composition of the aforementioned eutectic. This was done in three ways:

a) by coating with a mixture of $CaCO_3$, Al_2O_3 and SiO_2,
b) by coating with a mixture of anorthite and gehlenite, both obtained by mixing $CaCO_3$, Al_2O_3 and SiO_2 in the proportions corresponding to these compounds and sintering separately for a long time at 1340 °C [7]).
c) by coating with a eutectic obtained by melting $CaCO_3$, Al_2O_3 and SiO_2 in the right proportions in an oven.

---

[6]) Experiments by J. L. Meyering and W. P. van den Blink not published.

[7]) It is to be assumed that during the sintering the oxides are not fully converted into the compounds.

When welding with the rods coated in this manner that with the coating a) gave a slag with a much too low viscosity. The viscosity rose considerably, however, in the order a)-b)-c), so much so that as far as the viscosity is concerned the slag formed from the coating c) almost came up to the requirements made in practice. Still, even in the case c) the slag could not be said to be technically useful, because, inter alia, it did not sufficiently wet the metal. It showed a tendency to agglomerate into separate drops (see the next section). This was one of the causes of the great porosity of the beads obtained in these experiments.

The great difference in viscosity between these three slags of the same gross composition leads to the conclusion, already mentioned, that in the short welding time no state of equilibrium can be reached in the slags.

In agreement herewith, when measuring the viscosities of molten mixtures of CaO, SiO_2 and Al_2O_3 McCaffery [8]) found that after melting the viscosity needed a certain time (in some cases as much as one hour) to reach a constant value. One might imagine that in the welding experiments described when the coating a) is used a metastable eutectic liquid with a low viscosity is formed and that a much longer time would have been needed to cause the viscosity to rise through the formation of anorthite and gehlenite molecules.

In the following sections we shall consider the mixtures applied in actual practice. First of all we have to see what requirements these mixtures have to meet. At the same time it will be necessary to make a sharper distinction between coating and slag, because, as is evident from the foregoing, chemical reactions may take place during melting not only in the coating itself but also between the coating (or the slag) and the metal. As a consequence there may be great differences in chemical composition between the coating and the slag.

Requirements to be met by coatings and slags

As we have seen, the slags discussed in the preceding sections do not come up to the requirements met in practice. Moreover, only a few of these requirements have so far been mentioned.

Besides the conditions referred to in the foregoing, the coating and the slag have to satisfy the conditions that will be summed up below. Those discussed under a)-d) relate particularly to the coating and the others mainly to the slag.

a) *Cup formation*

As seen from the foregoing (in the beginning of the previous section), one of the first requirements to be met by the coating is that it must have such a low melting range as not to form too long a cup when welding. This is illustrated in *fig. 4*, a diagrammatic representation of the process of welding with coated rods. On the other hand, the melting range may not be so low as to prevent the formation of a cup, for the cup has the useful function of directing the arc and the stream of droplets passing from the electrode to the workpiece. A satisfactory cup is obtained when the melting range lies in the neighbourhood of 1200 to 1300 °C.

b) *Welding without interruptions*

Apart from their use with direct current, in many cases welding rods have to be used with alternating current, which is practically impossible with bare electrodes. The automatic reignition of the arc following every currentless moment when alternating current is used is closely connected with the electronic emission from certain components of the coating.

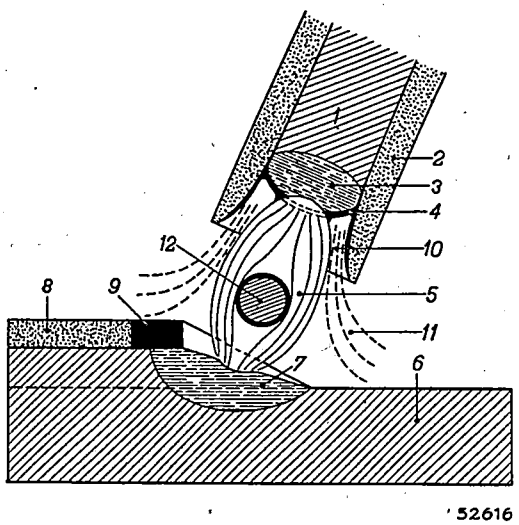


Fig. 4. Diagrammatic representation of the process of welding with a coated electrode (see J. Sack, Philips Techn. Rev. 2, 129-135, 1937). *1* core of the electrode, *2* coating, *3* liquid metal, *4* liquid slag, *5* electric arc, *6* workpiece, *7* pool, *8* solidified slag, *9* liquid slag, *10* cup, *11* protective gases, *12* droplet covered with slag.

c) *Cohesion between the metal and the metal of the workpiece*

In order to be sure of making a strong joint certain requirements are made as to the depth to which the metal of the workpiece is melted during the welding process, i.e. the penetration already mentioned. As we have seen, the depth of the penetration is directly related to the evolution of gases from certain components of the coating during the welding.

[8]) R. S. McCaffery, Trans. A.I.M.E. (Iron and steel division), **100**, 64-140, 1932.

d) *Mechanical properties of the weld.*

In some cases the requirement is made that the coating must have an alloying action, so that the deposited metal becomes richer in certain alloying elements (usually Mn and Si) than the original core wire. This requirement is made in order to obtain welds having special mechanical properties. Obviously this alloying action can only be fully brought about when the coating is of such a composition as to satisfy the primary requirement in respect to the protective action against oxygen and nitrogen, or, in other words, when it would already lead to very good mechanical properties even without an alloying action.

e) *Viscosity of the slag*

The viscosity of the slag formed from the coating may not be too high, as is, for instance, the case with slags having a very high SiO_2 content. It may not, however, be too low either, because then (particularly in the case of vertical and horizontal fillets) the slag would run off the weld too readily, with the risk of the still hot metal being exposed to the attack by oxygen and nitrogen.

f) *Spreading of the slag.*

The slag must not agglomerate. The condition that a drop of slag spreads itself out over liquid iron is expressed by

$$\sigma_{Fe} > \sigma_{slag} + \sigma_{Fe\text{-}slag} \quad . \quad . \quad . \quad . \quad . \quad (7)$$

where σ_{Fe} and σ_{slag} represent the surface tensions of iron and slag and $\sigma_{Fe\text{-}slag}$ denotes the iron-slag interfacial surface tension. If the condition (7) is satisfied then there is a reduction of the free energy in the spreading. The surface tension of the slag and the metal-slag interfacial surface tension must therefore be relatively low. This spreading also inproves the appearance of the weld.

g) *Breaking away of the slag*

The slag must have an expansion coefficient differing as much as possible from that of the metal, so that when it cools down it easily breaks away, preferably of itself. This is also promoted by porosity of the slag.

h) *Various other requirements*

Among various other requirements, it should be possible to use the rods in all positions and, further, the welding speed should be high.

The requirement a)-h) are so numerous and so divergent that it is impossible to satisfy them all at the same time, even with a coating consisting of a large number of components, so that the development of a coating for welding electrodes is always of the nature of a compromise. Different types of electrodes will be used according to whichever group of requirements weighs most. Below we shall discuss four of the most important types, which for the sake of simplicity we shall denote as *A*, *B*, *C* and *D*. First of all it is to be noted that with practically all types the coating materials are used in the form of fine powders, which are applied to the rods with the aid of potassium waterglass or sodium waterglass having a high SiO_2 content.

The different types of welding electrodes

Type A (e.g. Ph 46). For the simplest types of electrodes with inorganic coatings the powders consist for a large part of quartz and natural silicates (talc $Mg_3[Si_4O_{10}(OH)_2]$; kaolin $Al_4[Si_4O_{10}(OH)_8]$; asbestos $Mg_6[Si_4O_{11}(OH)_6] \cdot H_2O$, etc.). In order to reduce the melding range and viscosity, iron oxides (hematite Fe_2O_3; magnetite Fe_3O_4) and manganese oxides (pyrolusite MnO_2; hausmannite Mn_3O_4) and sometimes also titanium dioxide (rutile TiO_2) are added. Further, in order to promote electron emission and also to produce a stream of gas (see requirement c) alkaline-earth carbonates are added (calcareous spar $CaCO_3$, magnesite $MgCO_3$ and dolomite $CaMg(CO_3)_2$).

Owing to the high iron oxide content of the slags obtained with these rods, the oxidation of the weld metal is almost as serious as when using bare electrodes. The oxygen contents found in the welds are comparable to those for bare rods, given in table I of the article quoted under footnote [1]) whilst the C, Mn and Si contents are reduced to almost equally low values. The welds made with these rods have, therefore, poor mechanical properties compared with those obtained when using the types of electrodes *B*, *C* and *D*, though, owing to the much lower nitrogen content of the deposited metal, the mechanical properties are much better than those obtained with bare electrodes.

Rods of the type *A* are especially used in cases where mechanical strength is of minor importance and the main consideration is easy weldability and good appearance of the beads (for instance, for welding sheet metal and for very light constructions). The welds are internally porous owing to the reaction between oxygen and carbon in the molten metal.

Type B (e.g. Ph 50), In order to obtain electrodes which deposit a metal with better mechanical properties, appreciable quantities of ferromanganese and ferrosilicon are added to the coatings.

From the chemical point of view this solution of the problem is a remarkable compromise, because the coating then contains both oxidizing and deoxidizing substances. The exothermic chemical reaction between these substances, however, contributes towards a high welding speed. The mechanical properties of the deposited metal are more than sufficient for most applications. The oxygen content, however, is still rather high (about 0.12 wt % O), so that it is still possible to improve further the mechanical properties.

Type C (e.g. Ph 55). If rods are required with exceptionally good mechanical properties one should entirely avoid the use of iron oxides in the coating. The slag should only contain oxides of which the heat of formation ΔH per gram atom of oxygen (or rather the free enthalpy of formation ΔG) is very large. The oxides of *table II* for instance, can be used. By way of comparison we may state that the values of ΔH and ΔG for Fe_2O_3 and Fe_3O_4 lie between —67 and —60 kcal per gram atom of oxygen [9]).

Table II [9]). High-melting oxides with large heat of formation ΔH and a corresponding free enthalpy of formation ΔG.

Oxide	ΔH	ΔG
	kcal per gram atom of O	
Al_2O_3	—131	—124
BeO	—145	—
BaO	—133	—126
CaO	—152	—144
MgO	—146	—138
SiO_2 (quartz)	—104	— 97
TiO_2	—112	—106
ZrO_2	—129	—

With this type of rod fluorite (CaF_2) is added to the coating as a fluxing agent. The most commonly used rod of this type has a coating consisting mainly of CaF_2 + $CaCO_3$ in addition to waterglass, with additions of ferromanganese, ferrosilicon and ferrotitanium. The quantities used are as a rule such that the Mn and Si contents of the weld are higher than those in the core wire, thus giving greater mechanical strength and ductility (cf. requirement d). The O content of the deposited metal is only 0.03%.

A drawback attaching to these rods is the frequent extinction of the arc when working with alternating current, unless a welding machine is used with a dangerously high no-load voltage. This extinguishing of the arc is found to be particularly promoted by the calcium fluorite contained in the coating and can be eliminated by ensuring that this substance has less chance of getting into the immediate vicinity of the focus of the arc. This has been achieved by applying the coating in two or more layers around the rods, in such a way that the calcium fluoride is contained mainly in the outer layer. Such a "shell rod" is marketed by Philips under the type number Ph 56. This electrode can be used on alternating current at a no-load voltage of about 60 V without trouble being experienced from extinction of the arc.

Type D (e.g. Ph 48). The coating of this type of rod contains large quantities of organic substances which evolve a great deal of gas during the welding process and thus keep the oxygen and nitrogen away from the metal. At the same time the coatings contain slag-forming inorganic substances in respect to which the same remarks apply as have been made under the types *A*, *B* and *C*. The O content of the metal deposited from electrodes of the type *D* lies between that of the types B and C.

The core wire used in all these four types of electrodes is usually of mild steel. The differences between the various types and the metals deposited from them lie almost exclusively in the different coating. For special purposes there are also on the market electrodes having a core wire of entirely different composition, but these are left out of consideration here.

A disadvantage when welding with the types of rods described is that the welder must maintain a definite arc length (about 3 mm). If the arc becomes too long the weld has an irregular appearance and insufficient penetration, whilst further there is much loss from spattering. If the arc length is too short the electrode "freezes" to the workpiece. Particularly with havy gauge rods it is difficult to maintain the correct arc length.

In the latest types of welding rods this objection has been overcome by incorporating a large part of the iron in the coating in the form of a powder. This gives a coating of such thickness and strength as to allow of touch-welding with these rods. For a more detailed account of these so-called "contact" electrodes we refer to two articles that have been published in this journal [10]).

[9]) Following international usage that is gaining more and more ground, a quantity of heat (or work) added to a system is said to be positive. Consequently an exothermic chemical reaction has a negative heat of reaction.

[10]) P. C. van der Willigen, Philips Techn. Rev. **8**, 161-167 and 304-309, 1946. In these articles various other advantages are summed up which are connected with welding with contact electrodes. The "contact" electrodes corresponding to the types Ph 48, Ph 50 and Ph 55 are marked C 18, C 20 and C 15 (C = contact).

The absorption of nitrogen in arc-welding

Remarkably enough, the nitrogen content of the deposited metal varies with the type of rod in the same sense as the oxygen content. As a typical example, the metal obtained from the Ph 55 and Ph 56 (type *C*) has 0.03% O and 0.01% N, whilst the metal from the Ph 50 (type *B*) has 0.12% O and 0.03% N. This seems to indicate that the slag of the latter type absorbs nitrogen out of the air and passes it on to the metal more readily than the slag of the former type.

The apperance of the slags points in the same direction. Whereas the Ph 55 gives a dense crystalline slag, the Ph 50 produces a slag which is highly porous and vitreous. This leads one to suppose that at high temperatures the latter slag dissolves gases readily, part of the gas being subsequently released in the cooling process, thereby causing porosity. The fact that under certain circumstances oxidic masses of comparable composition can dissolve large quantities of gas is known from the volcanic phenomena [11]).

If nitrogen were one of the gases readily soluble in the Ph 50 slag we might find herein an explanation for the relatively high nitrogen content of the welds made with rods of this type. In order to check this, quantities of slag obtained from welding the Ph 50 and Ph 55 rods were pulverized (in order to avoid the complication of gases contained in the pores) and high-frequency heated in platinum crucibles in vacuo. The gases evolved in the melting of the slags were drawn off and analysed. From the slag of the Ph 50 about 2 cm^3 of gas (of 0 °C and 1 atm) per gram slag was released, accompanied by strong frothing. The slag of the Ph 55 did not froth and generated only a fraction of the amount of gas released from the other slag. *Table III* gives the composition of these gases in so far as they were not condensable at −80°C (the content of water vapour was not determined).

Table III. Composition (in volume per cent) of the gases released when melting slags from the electrodes Ph 50 and Ph 55.

Gas	Ph 50 vol. %	Ph 55 vol. %
CO_2	2	46
CO	23	51
CH_4	5	—
H_2	60	1
N_2	10	2

These figures may be taken as a confirmation of the supposition previously expressed that the higher nitrogen content of the metal deposited from the Ph 50 is related to the greater solubility of this gas in the slag.

[11]) See for instance P. Niggli, Das Magma und seine Produkte, Teil 1, Akademische Verlagsgesellschaft, Leipzig 1937.

ABSTRACTS OF RECENT SCIENTIFIC PUBLICATIONS OF THE N.V. PHILIPS' GLOEILAMPENFABRIEKEN

Reprints of these papers not marked with an asterisk can be obtained free of charge upon application to the Administration of the Research Laboratory, Kastanjelaan, Eindhoven, Netherlands.

1760: C. J. Bouwkamp: On the construction of simple perfect squares (Proc. Kon. Ned. Akad. Wetenschappen, Amsterdam, **50**, 1296-1299, 1947, No. 10)

Correction to a previous paper (these abstracts **1719-1721**). Construction of a simple, perfect, squared square of 55 elements.

1761: Balth. van der Pol: An electro-mechanical investigation of the Riemann Zeta function in the critical strip (Bull. Am. Math. Soc. **53**, 976-981, No. 10).

A known representation of Riemann's ζ-function ($\zeta(s)$), valid for $\mathrm{Re}\, s > 1$, is analytically continued in the strip $0 < \mathrm{Re}\, s < 1$. For $s = {}^1/_2 + it$ this representation may be written as the Fourier-integral of a certain saw-tooth function. The zero's and maxima of this integral are obtained by an electro-optical method, the Fourier-integral being approximated by a Fourier series. A disc carrying the saw-tooth function on its circumference rotates before a photoelectric cell. The amplitudes of the harmonics of the resulting periodical time function are plotted as a function of their number.

1762: A. Cramwinckel: The sensitivity of various phototubes as a function of the color temperature of the light source. (J. Soc. Mot. Pict. Eng. **49**, 523-529, 1947, No. 61).

A method is described for measuring the sensitivity of various types of phototubes (Cs_2O vacuum and gas-filled, Cs-Sb vacuum, Se) as a function of the temperature of the light source (tungsten ribbon lamp). The results are compared to the function giving the brightness of a complete radiator as a function of temperature. For light sources with high color temperature (3000 °K) the Cs-Sb cell is at least two times as sensitive as the Cs_2O vacuum cell.

1765: J. D. Fast: De rol van zuurstof bij het electrisch lassen (The influence of oxygen in electric arc welding, Meded. Vlaamse Chem. Ver. **10**, 1-21, 1948 Jan., in Dutch).

For the contents of this paper see Philips techn. Rev. **10**, 27-35, 1948 (No. 1), Philips Res. Rep. **2**, 205-227, 1947 (No. 3) and these abstracts No. **R 47**

1766: F. L. H. M. Stumpers: Distorsie van signalen met frequentiemodulatie bij doorgang door electrische netwerken. (Distorsion of frequency modulated signals, in electrical networks, T. Ned. Radiogen. **13**, 1-21, 1948 no. 1, in Dutch).

The distortion, introduced when a frequency-modulated signals passes through electrical networks, is calculated using Fourier analysis or the series of Carson and Fry. The methods used by these authors are studied and their series is shown to be not convergent but asymptotic. An alternative asymptotic series development is given, which is more adapted to F.M. The theory is applied to simple networks: single tuned circuit, coupled circuits. The production of harmonics as well as intermodulation is considered.

1767: A. Claassen and J. Corbey: On the electrometric determination of vanadium in steels (Rec. trav. chim. Pays Bas **67**, 5-10, 1948, No. 1).

Procedures are given for the electrometric determination of vanadium in alloy steels. In tungsten-free steels vanadium is determined by titration with ferrous sulphate under specified conditions of acidity. It is shown that this method gives low results for steels containing tungsten, due to the imcomplete reduction of the vanado-phosphato-tungstate complex; complete reduction however takes place by boiling with excess ferrous sulphate, enabling the determination to be finished by electrometric titration with standard permanganate. Small amounts of vanadium accompanied by large amounts of tungsten can only be determined by titration with ferrous sulphate when the amount of phosphoric acid is greatly increased.

1768 *: P. J. Bouma: Physical aspects of colour, an introduction to the scientific study of colour stimuli and and colour sensations, 312 pages, 113 figs, 15 tables and extensive list of references (Edited by Philips Gloeilampenfabrieken, Philips Technical Scientific Library Department, 1948).

For the contents of this book, being the English version of "Kleuren en Kleurindrukken" by the

same author (in Dutch), see the review given in Philips techn. Rev. **9**, 159, 1947. A few sections and minor contributions have been added, e.g. on colour equations, the systems of Ostwald and Munsell, heredity, etc.

1769*: E. J. W. Verwey and J. Th. G. Overbeek (with the collaboration of K. van Nes): Theory of the stability of lyophobic colloids, the interaction of sol particles having an electric double layer, 205 p., 54 fig. (Elsevier Publishing Company Inc. New York, Amsterdam, London, Brussels, 1948).

The purpose of this book is to explain the stability of hydrophobic colloids and suspensions and to develop as far a possible a quantative theory of this stability.

The basic concepts of this theory were the mutual repulsion consequent upon the interaction of two electrochemical double layers, and the attraction by the London-Van der Waals forces. The principal facts of stability could be explained by combining these two forces. Among other things, a quantative explanation of the rule of Schulze and Hardy has been given. For this purpose it was essential to use the unapproximated Gouy-Chapman equations for the double layer. The approximation of Debije and Hückel, however useful in the theory of electrolytes, appears to have only a very limited applicability in colloid chemistry.

The introduction of several refinements was necessary to explain various details. The quantitative agreement between theory and experiment made it necessary to reckon explicitly with the dimensions and the specific adsorbability of the ions. To this end, Stern's theory has been introduced.

Repeptization phenomena cannot be understood without the introduction of the Born repulsion, which, however, apart from this, is of very minor influence on the stability properties.

The results proved that the London theory also needed a certain rectification in the form of a relativistic correction, because the uncorrected theory led to conflicts with the experiments in the case of coarse suspensions. The book consists of three parts, dealing with the theory of a simple double layer, the interaction of two flat plates, and the interaction of spherical colloidal particles respectively. In an appendix a survey of theoretical work on the stability of lyophobic colloids by previous authors is given. See also Philips Res. Rep. **1**. 33-49, 1945/46.

1770: M. J. O. Strutt and A. van der Ziel: Application of velocity-modulation tubes for reception at U.H.F. and S.H.F. (Proc. Inst. Radio Engns **36**, 19-23, 1948 no. 1).

Upon introduction of the notions of gain and noise figure, it appears that preamplifier stages using velocity-modulation tubes are unsuitable at u.h.f. and s.h.f. under operational conditions considered hitherto. A special arrangement, connected with such a tube and consisting of three electrode pairs spaced along the electron stream, is considered in this paper. The first pair is connected to a resonance cavity or line, constituting a pre-circuit. The second pair is connected to the input, an the third pair to the output circuit. It can be shown that the transfer of initial spontaneous velocity fluctations to density fluctations along the electron stream may be neglected. The reserve effect is considered in an appendix, and it also is negligible under practical conditions. It is shown that, by the use of a properly detuned pre-circuit, the noise figure may be reduced from a few thousand to, say, 10 under optimal conditions retaining gain figures of, say, 100. The usefulness of the arrangement under consideration is discussed and estimated to be favorable under actual conditions of operation. With traveling-wave tubes noise figures below 10 are thought to be attainable by application of the present device.

VOL. 10 No. 5, pp. 125-156 NOVEMBER 1948

Philips Technical Review

DEALING WITH TECHNICAL PROBLEMS
RELATING TO THE PRODUCTS, PROCESSES AND INVESTIGATIONS OF
THE PHILIPS INDUSTRIES

EDITED BY THE RESEARCH LABORATORY OF N.V. PHILIPS' GLOEILAMPENFABRIEKEN, EINDHOVEN, NETHERLANDS.

PROJECTION-TELEVISION RECEIVER

PART III. THE 25 kV ANODE VOLTAGE SUPPLY UNIT

by G. J. SIEZEN and F. KERKHOF.

621.397.62:
621.396.615.17:
621.314.54

The power required for feeding the cathode-ray tube of a projection-television receiver amounts to only a few watts, at a direct voltage of the order of 20-30 kV. The method of supplying this power described here, in which a cascade rectifier is fed from a pulse generator, has several advantages over the more conventional method of stepping up and rectifying the A.C. mains voltage. The pulse generator consists of a coil taken up in the anode circuit of a pentode, the anode current of which is periodically and suddenly interrupted by a saw-tooth voltage on the control grid (frequency about 1000 c/s). The current interruption excites the oscillator circuit consisting of the inductance of the coil and its self-capacitance. The voltage peak across the coil can easily reach a value of the order of 10 kV. The desired direct voltage (in this cases 25 kV) is obtained with a rectifier, preferably consisting of a number of stages in cascade.

The cascade circuit is further analyzed. From the formulae derived it appears that with a non-controlled pulse generator a reasonable value of the internal resistance can only be obtained at a low efficiency. This difficulty has been overcome by applying to the pentode a control voltage derived from the peak voltage on the oscillatory circuit. The result is a low internal resistance in the range between no-load and full load, at a satisfactory efficiency, and a marked voltage drop when the load is excessive. The practical execution described here, employing a three-stage cascade rectifier, gives an output of 25 kV at 150 μA, and consumes about 11 W from a direct voltage source of 350 V. The internal resistance under no-load is about 5 megohms. The dimensions of the apparatus are only 18 cm × 10 cm × 15 cm (7″ × 4″ × 6″). In the oscillatory circuit good use has been made of "Ferroxcube".

Introduction

As explained in previous papers [1][2] (which will be referred to hereafter as I and II) on projection-television receivers, this method of reception provides a large-sized picture while at the same time the drawbacks attached to the use of large cathode-ray tubes for direct view are avoided. Thanks to the solution (described in the present series of articles) to the many problems arising with projection reception, the price of the receiving set has by no means increased in proportion to the size of the picture. The small cathode-ray tube, described in article II, allows a considerable saving compared with the tube which would be required for a direct vision picture of the same size as the projected picture. It is true that for the projection method an optical system is needed, but this need not contain any expensive components. As explained in article I, it has been found possible to keep the dimensions of the optical system very small, owing to a special positioning of the mirrors of which it is composed. This all helps to reduce the size of the cabinet and thus also the price.

Another component on which it is well worth economizing is the rectifier for feeding the cathode-ray tube with a voltage which in the present case amounts to 25 kV at a current of about 0.1 mA. Experience indicates that at such a high voltage a rectifier becomes cumbersome and heavy when the alternating voltage from the lighting mains

[1] P. M. van Alphen and H. Rinia, Projection-television receiver, I. The optical system for the projection, Philips Techn. Rev. 10, 69-78, 1948 (No. 3).
[2] J. de Gier, Projection-television receiver, II. The cathode-ray tube, Philips Techn. Rev. 10, 97-104, 1948 (No. 4).

is stepped up and rectified in the traditional manner. Moreover, in the event of a short-circuit the current would then become prohibitively high.

We shall now discuss a method whereby the rectifier is fed from a separate pulse generator working with a frequency of the order of 1000 c/s. This method has led to the construction of an inexpensive apparatus which is compact and has a good efficiency.

According to another method the saw-toothed time-base current for exciting the magnetic field for the horizontal deflection of the electron beam in the cathode-ray tube is used. This method is certainly economical but with such high voltages as 25 kV it has the drawback that the rectified voltage obtained is strongly dependent upon the amplitude of the horizontal deflection. Related to this is the fact that if the synchronisation should be lost the voltage would rise to impermissibly high values. Another drawback is that the load formed by the rectifier retards the fly-back of the electron beam. By employing the separate pulse generator described below these objections are avoided.

Still another method is known where the rectifier is fed from a separate high-frequency oscillator via a bandpass filter [3]). The most suitable frequency lies between 0.3 and 1.2 Mc/sec. This makes it necessary to provide good screening to prevent interference from these radio-frequencies. Furthermore, with this method the efficiency is low and the apparatus is rather bulky.

Principle and advantages of the pulse generator

The operation of the pulse generator is based upon the generation of voltage impulses when the current passing through a coil is interrupted. This interruption sets up an oscillation in the circuit formed by the inductance L of the coil with its self-capacitance C_p. If I_{max} is the strength of current at the moment of interruption then the peak value V_{max} reached by the oscillation voltage across the circuit is given approximately by

$$V_{max} = I_{max} \sqrt{\frac{L}{C_p}}, \quad \ldots\ldots \quad (1)$$

because the energy $^1/_2 L I_{max}^2$ accumulated in the magnetic field of the coil at the moment that the current is interrupted is found a little later as $^1/_2 C_p V_{max}^2$ in the electric field of the oscillator circuit (except for a small amount which owing to various losses has meanwhile been converted into heat).

Substituting in (1) for instance the following values: $I_{max} = 120$ mA, $L = 0.5$ H and $C_p = 50$ pF, we find $V_{max} = 12000$ V. This example shows that in this manner an alternating voltage with a peak value in the order of 10 kV can be obtained with values of L and C_p which can quite well be realized. Further, the current required can be supplied by an output pentode of moderate power with the coil in its anode circuit (*fig. 1*). The

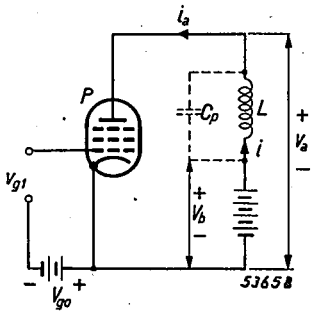


Fig. 1. Diagram of an pulse generator. L = self-inductance of a coil (with self-capacitance C_p) in the anode circuit of a pentode P.

current can then be interrupted very efficiently by suddenly making the control grid voltage of the pentode so negative as to block the anode current.

A rectifier with a cascade circuit [4]) can be connected to the terminals of the coil, and thus a direct voltage can be obtained amounting to a multiple of the input voltage peak V_{max}. We shall revert to this presently.

Although the shape of the curve of the anode current i_a prior to the interruption is of little consequence, a linear increase as seen in the curve for i_a in *fig. 2* has some advantages compared, for instance, with the case where I_a, being either zero or I_{max}, would have a rectangular shape. With the shape of curve shown in fig. 2 the efficiency is better and there is less risk of the valve being overloaded.

Such a shape can easily be given to the anode current by using for the control grid voltage of the pentode an alternating voltage (v_{g1}, fig. 1) of a saw-tooth shape (supplied by a separate generator) combined with a suitable chosen negative bias V_{g0}. After the current is interrupted the control grid voltage must be kept sufficiently negative for some time to block the anode current in spite of the high positive anode voltage then arising (see fig. 2, curve for v_a).

If T is the time between two successive interruptions and a is the fraction of T during which anode current is flowing (see fig. 2) then the constant voltage difference ΔV_a at the coil during the interval aT is:

$$\Delta V_a = L \frac{di_a}{dt} = \frac{L I_{max}}{aT},$$

[3]) O. H. Schade, Radio-frequency operated high-voltage supplies for cathode-ray tubes, Proc. I.R.E. 31, 158-163, 1943.

[4]) See for instance Philips Techn. Rev. 1, 6-10, 1936.

and hence the interruption frequency $f_i = 1/T$ is

$$f_i = \frac{a \Delta V_a}{L I_{max}}. \quad \ldots\ldots \quad (2)$$

For practical reasons the fraction a should preferably not be smaller than 0.25. The highest value of ΔV_a is equal to the difference between the direct voltage V_b supplying the anode circuit and the minimum anode voltage $V_{a\,min}$ required to prevent too high a screen grid current. If this minimum anode voltage is, say, 50 V and $V_b = 350$ V, thus $(\Delta V_a)_{max} = 300$ V, with $a = 0.25$ and with the values of L (= 0.5 H) and I_{max} (= 120 mA) previously quoted, from (2) we find:

$$f_i = \frac{0.25 \times 300}{0.5 \times 0.120} = 1250 \text{ c/s.}$$

This frequency is so much higher than the mains frequency that the smoothing of the rectified voltage can be done much more easily than would be possible with frequencies of the same order as the mains frequency.

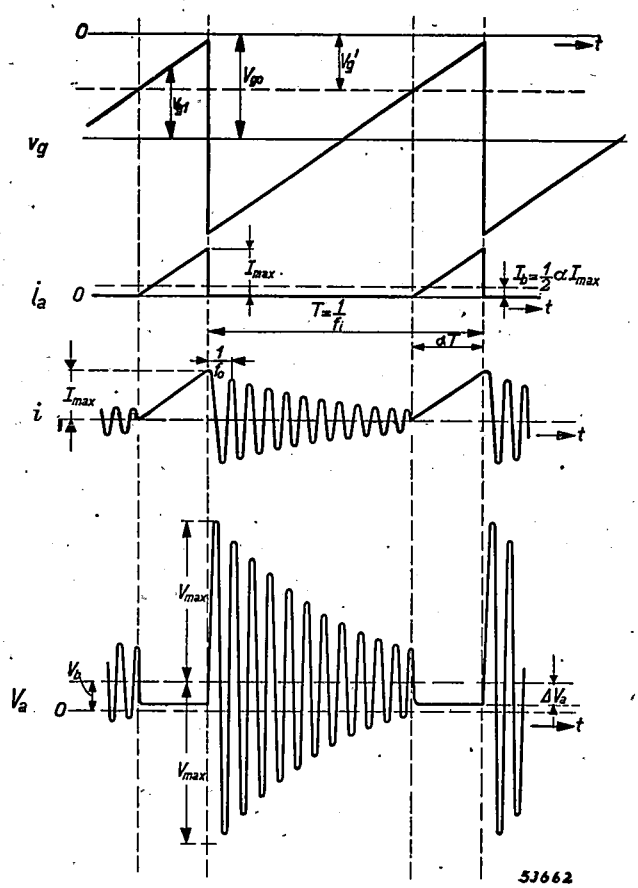


Fig. 2. Variation of voltages and currents with time t in the circuit of fig. 1. v_g = control grid voltage consisting of a bias V_{g0} and a saw-tooth voltage v_{g1} (period $T = 1/f_i$). During the time $a\,T$, the value of v_g exceeds that of V_g' and the anode current i_a is blocked. I_{max} = the value at which i_a is interrupted. I_b = mean value of i_a, i = current in the coil with the natural frequency f_0 of the circuit L-C_p, v_a = anode voltage of the pentode, V_b = D.C. supply voltage, ΔV_a = voltage drop in the coil while the anode current is flowing (interval aT), V_{max} = peak of the oscillatory voltage.

With $L = 0.5$ H and $C_p = 50$ pF the natural frequency f_0 of the oscillator circuit is 32000 c/s. This lies so far outside the range of radio-frequencies that there need be no fear of its giving rise to any interference.

Fig. 2 also gives the curves of the current i in the coil and of v_a as functions of the time t.

Before going into further details we would draw attention to the fact that the method described here allows of a very efficient control of the voltage, since in accordance with eq. (1) the voltage peak V_{max} (and thus also the direct voltage) is proportional to I_{max}, the value of which is very easily regulated with the control grid bias. It is then only a small step further to make this control automatic by governing the bias with the peak voltage V_{max}. In this way it is possible to obtain a highly constant direct voltage between certain load limits (in other words, the rectifier can be given a very low internal resistance), without the short-circuit current being much greater than the normal working current.

The rectifier

Theoretically V_{max} can be made any desired value; thus it could be chosen high enough to obtain the desired direct voltage (here 25 kV) with the aid of only one valve and one capacitor. There are, however, practical reasons why in our case preference is given to a lower value of V_{max}, combined with a voltage multiplication by means of a cascade circuit of valves and capacitors. The reasons for this are the following:

In the first place it has to be considered that with pentodes of medium size the maximum permissible peak value of the anode voltage (here $V_b + V_{max}$) is limited; with the type EL 38 for instance the limit is about 6 kV. One could try to keep the peak voltage below this limit by connecting the anode to a tap on the coil, which then acts as a step-up autotransformer. If one were to go so far as to render voltage multiplication unnecessary, either the coil would have to be very large or the anode current would have to be raised to a level exceeding the limit fixed for the EL 38.

The energy that the transformer has to supply with every pulse is fixed. It is $\frac{1}{2} L' I_{max}^2$, where L' is the self-inductance of the primary of the coil. If the step-up ratio is chosen so high as to be able to dispense with voltage multiplication in the rectifier, then the two extreme possibilities are the following. One, L' can be chosen equal to the value L yielding

according to eq. (1) the desired high voltage peak V_{max}. If this is done, because of the high step-up ratio, the whole coil is much larger than the primary part; or two, the inductance L'' of the whole coil can be chosen equal to L, but then L' is much smaller than L, so that according to eq. (1) the current I_{max} would have to be considerably increased.

In the execution chosen the voltage is stepped up only slightly (1:1.4), so that voltage multiplication is still necessary.

In the second place, as far as the valves are concerned we must remember that in a cascade circuit with n stages the voltage across each of the n valves is roughly only $2/n$ of the direct voltage V_h supplied. The employment of n valves each calculated for a voltage $2V_h/n$ may be preferable to using one valve that would have to carry the voltage $2V_h$.

different coils having the same value B, with the size of the air gap so chosen in each case as to give the maximum L, it is found that with all these coils the most favourable air gap forms approximately the same fraction λ of the length l, so that eq. (3a) becomes

$$V_{max} = B \sqrt{\frac{Ql\ (1 + \lambda\mu_r)}{\mu_0 \mu_r C_p}} \quad \ldots\ldots\ldots \quad (3b)$$

Thus the volume Ql of the ferromagnetic core is roughly proportional to V^2_{max}. (The self-capacitance C_p is assumed to be constant, but actually it increases with the size of the coil, so that the volume will increase with the voltage to a still greater extent than V^2_{max}.)

Thus, although there are a number of facts in favour of keeping the voltage V_{max} fairly low, it would not be rational to use a very large number of stages in cascade. Consequently a compromise has to be sought. In order to do so we shall consider the cascade circuit somewhat more closely.

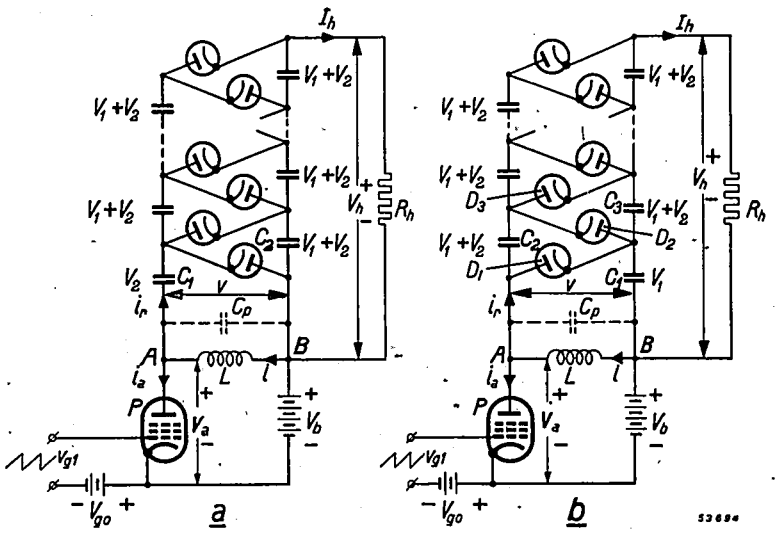


Fig. 3. Cascade rectifier, connected to a pulse generator, (*a*) with even number of stages, (*b*) with odd number of stages. V_h = direct voltage output, R_h = load resistor through which the direct current I_h flows; i_r = current taken up by the rectifier. For V_1 and V_2 see fig. 4.

A third point of consideration is the dimensions of the coil, which greatly increase with the value required of the peak voltage V_{max}.

The following will make this clear: From eq. (1) it is easily deduced that

$$V_{max} = B \sqrt{\frac{Q\ (l + \mu_r d)}{\mu_0 \mu_r C_p}}, \quad \ldots \quad (3a)$$

where B represents the magnetic induction, Q the cross section of the magnetic circuit, l the average length of the lines of force in the ferromagnetic core (of which μ_r is the relative permeability), d is the size of the air gap and μ_0 is the permeability of the vacuum ($= 4\pi \cdot 10^{-7}$ H/m) [5]. For

[5]) Here we are using Giorgi units (see for instance Philips Techn. Rev. **10**, 79-86, 1948 (No. 3). V_{max} is therefore expressed in V, B in Wb/m², Q in m², l and d in m, C_p in F, and μ_r is the permeability in relation to that of vacuum.

Cascade circuit

In a cascade circuit one of the input terminals coincides with one of the direct current terminals. Now in our case the negative terminal has to be earthed. From this it follows that that side of the circuit L-C_p (fig. 1) which is connected to $+ V_b$ has to be the negative pole. This leads to the arrangements indicated in *figs. 3a* and *b*, for an even and an odd number respectively of stages n in cascade. (It will be seen that small differences arise in the formulae applying in these two cases, both of which can in principle be used. Therefore one must differentiate between an even number of n and an odd number of n.)

To begin with we shall deal briefly with the variation of the voltages and currents with time; we shall confine our considerations to the steady state and introduce some simplifying assumptions which sufficiently approximate practical conditions. We shall ignore the internal resistance of the valves and assume that the capacitors in the cascade circuit have a capacitance that is not only large compared with C_p but also large enough to allow the ripple voltage on these capacitors to be ignored. Thus across each of the capacitors there is a pure direct voltage.

From fig. 3 it follows that immediately after every interruption of the anode current the voltage across the circuit L-C_p has a polarity where A is positive with respect to B.

We shall confine ourselves for the time being to the case where n is an *odd* number (fig. 3*b*). As soon as v has reached the value V_1 of the direct voltage across the capacitor C_1, the first diode (D_1) becomes conductive and thus the capacitance C_1 comes to lie in parallel to the much smaller capacitance C_p. The circuit voltage v cannot then rise to the peak value V_m which it would reach if there were no rectifier, but remains limited to the value V_1 (*fig. 4*, curve v). As soon as the current ceases to flow through the diode — that is to say at the end of the first rectifying interval t_{r1} —, v begins to drop, according to a cosine function with the initial value V_1.

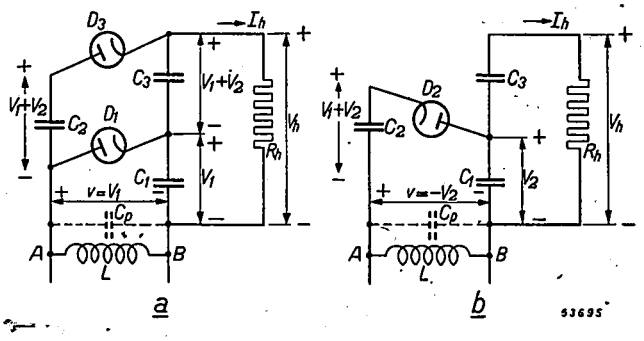


Fig. 5. These diagrams correspond to fig. 3*b* for $n = 3$. (*a*) is the situation during the first rectifying interval ($v = V_1$) when the diode D_2 (not shown) is non-conducting. (*b*) is for the second rectifying interval ($v = -V_2$); the diodes D_1 and D_3 which are then non-conducting have been omitted.

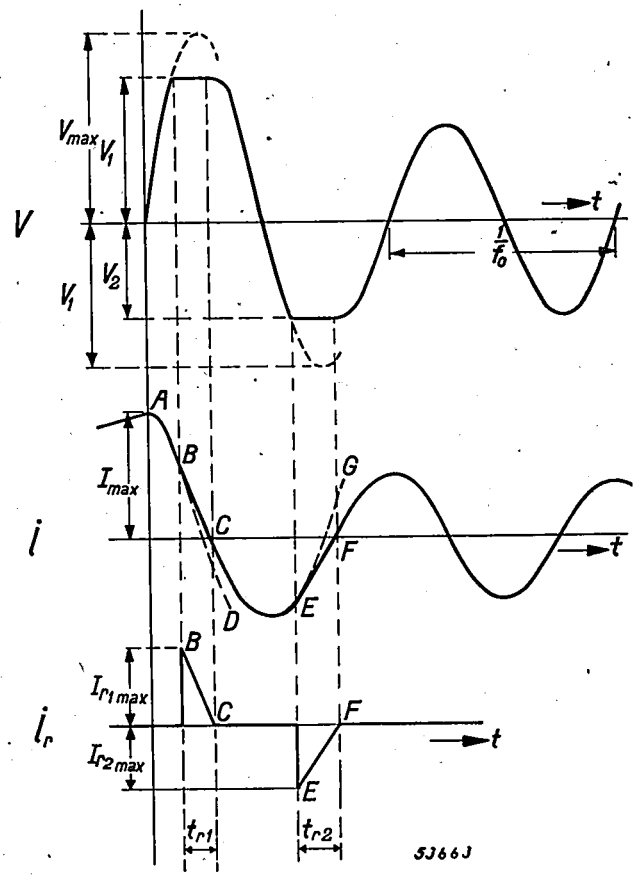


Fig. 4. Voltage and current curves as functions of t in the circuit according to fig. 3*b*. v = voltage at the coil, i = current through the coil, i_r = current taken up by the rectifying circuit. V_1, V_2 = amplitude of the first and second voltage peaks respectively; t_{r1}, t_{r2} = duration of the first and second rectifying intervals respectively.

As soon as v has become sufficiently negative, or in other words as soon as the circuit voltage, assisted by the voltage V_1 on the first capacitor, has reached the value existing on the second capacitor C_2, current is able to flow through the second diode (D_2 in fig. 3*b* and also in *fig. 5b*, which corresponds to fig. 3*b* for the case where $n = 3$ but in which the temporarily non-conducting diodes D_1 and D_3 have been omitted). From that moment onwards v is again kept constant (now at a value which we shall indicate by $-V_2$, see curve v in fig. 4), because the large capacitance formed by C_1 and C_2 in series is shunted across C_p. From fig. 5*b* we now read that the voltage at C_2 has the value $V_1 + V_2$. The second rectifying interval, t_{r2}, lasts until the current has fallen to zero.

Owing to the damping, the succeeding peaks of v are in absolute value smaller than V_2; consequently they cannot contribute towards the rectification. For every period T there are, therefore, only the two rectifying intervals mentioned.

During these intervals, as we have seen, the voltage on the circuit is constant, that is to say the current through C_p is then zero and the current i through the coil is a linear function of time. Owing to the continuity conditions, which oppose current surges through a coil and voltage surges on a capacitor, during the first interval the variation of i must follow the tangent BC to the damped cosine line ABD in the point B corresponding to the

beginning of the interval (fig. 4, curve i). Similarly, the variation in current during the second interval follows the tangent EF to the damped sine curve CEG. Since we are considering that part of the period T in which the anode current $i_a = 0$, during the rectifiying intervals the current i in the coil is equal to the current i_r (fig. 4, curve i_r) taken up by the cascade circuit.

In the foregoing we have only considered the first and second of the n diodes. Now what about the trend of the current in the other valves? In fig. 5a we again have the case of $n = 3$ for the situation during the first rectifying interval, omitting the diode D_2 which is then non-conducting. From fig. 5b we have already seen that C_2 was charged via D_2 up to the voltage $V_1 + V_2$. It is easily proved indirectly that the voltage at C_3 must likewise amount to $V_1 + V_2$. Now, during the first rectifying interval the cascade connection comprises not only the current path D_1-C_1 between the input terminals A and B but also a second path, C_2-D_3-C_3-C_1 shunted across the first one. Along this second path the voltages on C_2 and C_3 neutralize each other, so that the position is as if the diodes D_3 and D_1 were connected direct in parallel. Thus the current I_r is equally divided between the two branches.

This reasoning can of course be extended for odd numbers $n > 3$. It then leads to the deduction that the voltage $V_1 + V_2$ is present on all the cascade capacitors (except for the first, where the voltage is V_1), and that the n valves can be divided into two groups: one group of n_1 valves (in fig. 3b drawn more to the left) functioning simultaneously in the first rectifying interval, and a group of n_2 valves (more to the right in fig. 3b) which function during the second rectifying interval. It can easily be worked out that $n_1 = (n + 1)/2$, $n_2 = (n - 1)/2$.

Obviously a similar reasoning can be followed for an *even* number n (fig. 3a). Here it will suffice to state that the conclusion derived above holds also for $n =$ even, the only differences being that the voltage at the first capacitor is not V_1 but V_2 and that each of the simultaneously functioning groups of valves consists of $n/2$ valves.

Some important characteristics

After these qualitative considerations of the cascade circuit, we shall proceed to deal with some important characteristics. We shall first consider the external characteristic, namely the direct voltage output V_h as a function of $1/R_h/(R_h =$ load resistance). From this characteristic we shall later on deduce the internal resistance.

From figs 3a and b it is found that the direct voltage V_h across the output terminals is:

$$V_h = n_1 V_1 + n_2 V_2,$$

regardless whether n is an odd and even number.

At no-load apparently $V_1 = V_2 = V_{max}$, so that for the ratio y of V_h to the no-load voltage V_{h0} we can write:

$$y = \frac{V_h}{V_{h0}} = \frac{V_h}{nV_{max}} = \frac{n_1}{n}\frac{V_1}{V_{max}} + \frac{n_2}{n}\frac{V_2}{V_{max}}. \quad (4)$$

The unknown quantities V_1 and V_2 can be eliminated with the aid of the two energy equations

$$^1/_2\, C_p\, (V_{max}^2 - V_1^2) = n_1 V_1 V_h T/R_h, \quad (5)$$

$$^1/_2\, C_p\, (V_1^2 - V_2^2) = n_2 V_2 V_h T/R_h \quad (6)$$

Eq. (5) expresses that the energy given off by the oscillatory circuit during the first rectifying interval is used to replace that part of the charge that is drawn from n_1 cascade capacitors by the external load in one period T. At the moment of interruption of the anode current the energy in the electromagnetic field amounts to $^1/_2 LI_{max}^2$. Disregarding circuit losses, we may write for this $^1/_2 C_p V_{max}^2$. At the end of the first rectifying interval $i = 0$ and $v = V_1$, so that the circuit energy is then $^1/_2 C_p V_1^2$. Thus the left-hand member of (5) represents the energy that the circuit loses during the first rectifying interval. The load current I_h arises from the fact that the cascade capacitors give off a charge which flows through the resistor R_h. In one period T the charge flowing through R_h is $I_h T = V_h T/R_h$. During the first rectifying interval, n_1 of the n capacitors receive a supplementary charge. The source of this charge is the oscillatory circuit, the voltage of which is V_1. Thus the energy supplied is $n_1 V_1 V_h T/R_h$, as indicated by the right-hand member of (5).

Similarly it can be shown that (6) represents the energy transition during the second rectifying interval.

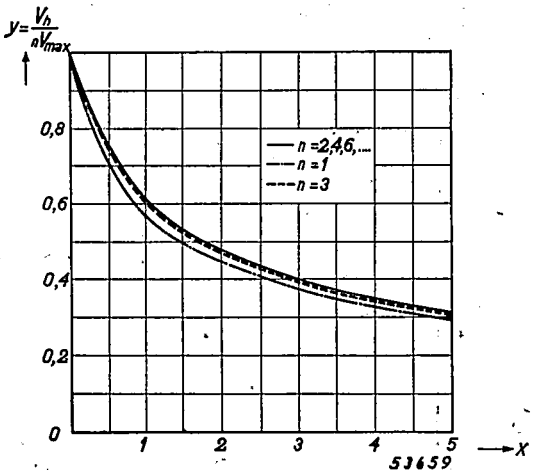


Fig. 6. The general external characteristic $y = f(x)$ where y is a measure for the direct voltage V_h and x is inversely proportional to the load resistance R_h. The upper curve applies for even values n, the lower one for $n = 1$, the middle one for $n = 3$.

We shall not go further into the elimination of V_1 and V_2 from (4), (5) and (6) here, because these calculations have already been published elsewhere [6]). The result is given in *fig. 6*, in which $y = V_h/V_{h0}$ is represented as a function of a quantity x proportional to $1/R_h$ which occurs in the calculation and is defined by

$$x = \frac{n^2}{C_p}\,\frac{T}{R_h} \quad \ldots\ldots\ldots \quad (7)$$

It is seen that one curve is found for all even values of n and a number of slightly deviating curves each for one odd value of n. The larger the odd number n with respect to unity, the closer the solution approaches that for an even value of n.

To give an idea of the order of size of x, we use the numerical values already applied: $T = 1/1250$ sec. and $C_p = 50$ pF, to which, when V_h and I_h amount respectively to 25 kV and 100 μA, can be added $R_h = 250$ megohms. Then $x = 0.064$ for $n = 1$; 0.26 for $n = 2$; 0.58 for $n = 3$.

As may be seen in fig. 6, in this range the curves fall steeply, which is already an indication that the internal resistance will be high. We shall find confirmation of this presently.

Besides $V_h = f(x)$, there are some other graphs of importance, namely those representing the trend of the voltages V_1 and V_2 each separately with x, and also the graphs for the peak values $I_{r1\max}$ and $I_{r2\max}$ of the pulses going to make up i_r (see fig. 4, curve i_r). With the aid of the foregoing considerations these characteristics can be derived from the eqs (4)-(7). The results are given in *figs. 7* and *8*, fig. 7 giving $V_1/V_{\max}$, and $V_2/V_{\max}$, and fig. 8 $I_{r1\max}/I_{\max}$ and $I_{r2\max}/I_{\max}$, as functions of x, respectively for n = even, $n = 1$ and $n = 3$.

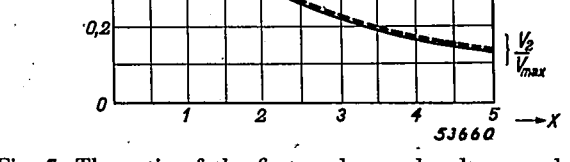


Fig. 7. The ratio of the first and second voltage peaks V_1 and V_2 to $V_{\max}$ as a function of x. Fully drawn curves apply to an even number n and the dotted curves to $n = 3$.

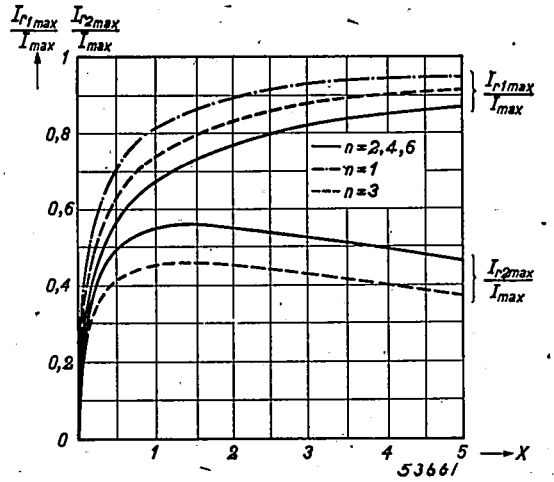


Fig. 8. The first and second current peaks $I_{r1\max}$ and $I_{r2\max}$ of the current I_r in the rectifying circuit, both in relation to $I_{\max}$, plotted as a function of x for n = even, $n = 1$ and $n = 3$.

From fig. 7 it is to be seen that as the load increases V_2 drops much more quickly than V_1, a phenomenon which will be referred to later.

Fig. 8 is of importance in choosing the number of stages n. It has been deduced above that the peak currents $I_{r1\max}$ and $I_{r2\max}$ are distributed respectively among n_1 and n_2 valves connected in parallel. Thus the peak current in each of the n_1 valves is found by dividing $I_{r1\max}$ by n_1, whilst $I_{r2\max}/n_2$ is the peak current in each of the other n_2 valves. If an even number of n is chosen, that is to say $n_1 = n_2 = n/2$ then according to fig. 8 the peak current in the n_1 valves is greater than that in the second group. If, on the other hand, $n = 3$, thus $n_1 = 2$ and $n_2 = 1$, the peak currents of the three valves are approximately equal, which obviously is the most economical. (Moreover, the choice of $n = 3$ is favourable also in other respects, such as the dimensioning of the coil in the anode circuit of the pentode).

Internal resistance and automatic control

With the aid of eq. (7) the internal resistance $R_i = -\mathrm{d}V_h/\mathrm{d}I_h$ can be expressed in the form

$$R_i = \frac{-n^2 y'}{y + x\,y'}\cdot\frac{T}{C_p},$$

where $y' = \mathrm{d}y/\mathrm{d}x$.

Here we shall pay particular attention to the value R_{i0} of the internal resistance when the load is very small, thus the slope of the characteristic $V_h = f(i_h)$ in its initial point on the V_h-axis. This initial value (which from now on for the sake of

[6]) G. J. Siezen and F. Kerkhof, Home projection-television, Part II. Pulse-type high-voltage supply, Proc. I.R.E. 36, 401-407, 1948 (No. 3), in particular pages 404 and 405.

simplicity we shall call "the" internal resistance) is found by putting $x = 0$ in the last formula and substituting for y and y' the corresponding values that can be calculated from the eqs (4)-(7). We than find an expression that can be converted into the following form:

$$R_{i0} = \frac{n_1^2 + n_1 n_2 + n_2^2}{2 n^2} \cdot \frac{V_b}{\Delta V_a} \cdot \frac{V_{h0}^2}{W_b}. \quad (8)$$

Here W_b represents the energy supplied by the direct voltage source (voltage V_b) in the anode circuit (fig. 1).

W_b is equal to the product of V_b and the mean value I_b of the anode current. From fig. 2, curve i_a, it can be read that $I_b = {}^1/_2\ \alpha\ I_{max}$.

The factor $(n_1^2 + n_1 n_2 + n_2^2)/2n^2$ has a value of ${}^3/_8$ for an even number n whilst for an odd number n it varies from ${}^1/_2$ for $n = 1$ to ${}^3/_8$ for $n = \infty$.

From (8) we see that with a given value of the voltages V_{h0}, V_b and ΔV_a, and with a given number of stages n, the internal resistance is inversely proportional to the power supplied W_b. A numerical example wil show that a considerable power W_b is needed to arrive at a reasonable value of R_{i0} (at least if no particular steps are taken, to which we shall refer presently).

Let us say that $n = 3$, $V_{h0} = 25$ kV, $V_b = 350$ V, $\Delta V_a = 280$ V, $R_h = 250$ megohms. To reach a value of R_{i0} amounting for instance to 2% of R_h (thus 5 megohms), according to (8) W_h must be well over 60 W. This means not only that the efficiency would be very low (the output being only a few watts) but that the anode current would have to have the high mean value of 175 mA.

This difficulty has been solved by using an automatic control voltage on the control grid of the pentode (fig. 1). This control voltage, which is dependent upon the amplitude of the voltage peaks on the circuit L-C_p, is obtained by rectifying the alternating voltage induced in a winding coupled to the coil L. This automatic control permits only a small drop in the direct voltage when the load current increases from zero to a certain limit, without any great amount of power having to be supplied; consequently eq. (8) then no longer holds. At loads exceeding the limit referred to, however, the voltage drops quickly. This is a valuable property of the system, since a short-circuit of the D.C. terminals is rendered relatively harmless thereby.

In order to increase the sensitivity of the control to the utmost extent two measures have been adopted:

1) The winding is connected in such a way that it is the voltage proportional to the peak V_2 that is rectified; as already observed (fig. 7), the variation with the load is greater in V_2 than in V_1.

2) A constant direct voltage bias is connected in series with the alternating voltage to be rectified; consequently, with fluctuating load the percentage of the variation in the resulting control voltage will be greater than that in the induced alternating voltage. Details of this device will be found below where a practical example is considered.

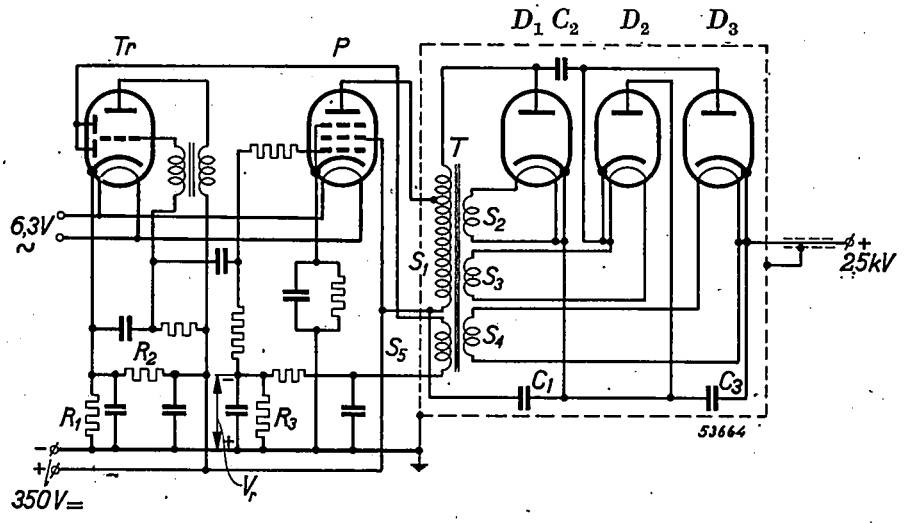


Fig. 9. Complete circuit diagram of pulse generator and rectifier. Tr = triode EBC 33 for producing the saw-tooth voltage, P = pentode EL 38 with the coil S_1 of the transformer T in the anode circuit. S_2, S_3, S_4 = cathode current winding of the diodes D_1, D_2, D_3 (type EY 51). S_5 = winding for control voltage V_r. The circuit is fed with 350 V direct voltage.

Practical execution

We shall now show the ideas set forth above have been realized in an apparatus supplying the cathode-ray tube of a projection-television receiver.

Fig. 9 is a circuit diagram of this supply unit, designed for a direct voltage of 25 kV and a maximum direct current of 150 μA (thus more than sufficient for the cathode-ray tube MW 6-2 [7]), described in article II), whilst at a small load the internal resistance does not exceed 5 megohms.

On the left-hand side of the diagram a blocking oscillator is shown with the triode EBC 33. This oscillator supplies a saw-tooth voltage (frequency about 1000 c/s) to the control grid of a pentode EL 38, in the anode circuit of which a part of the voltage across the cathode resistor R_1. This voltage is produced partly by the load current of the valve EBC 33 and partly also by an auxiliary current led through R_1 via a resistor R_2. The control voltage V_r ultimately appears across a resistor R_3 in the control grid circuit of the valve EL 38.

The five coils mentioned are wound on a ferromagnetic core of "Ferroxcube" [8]). Owing to the high relative permeability (about 800) and the low losses of this material, it is possible to keep the core small, and still maintain a high circuit quality. Figs. 10 and *11* show a form of the core ensuring a good magnetic screening.

Of course with the high voltages occurring here a transformer of such small dimensions cannot be operated in air. Consequently it is housed, together with the three diodes and the three cascade capacitors C_1, C_2, C_3, in a metal box filled with oil under vacuum and hermetically sealed.

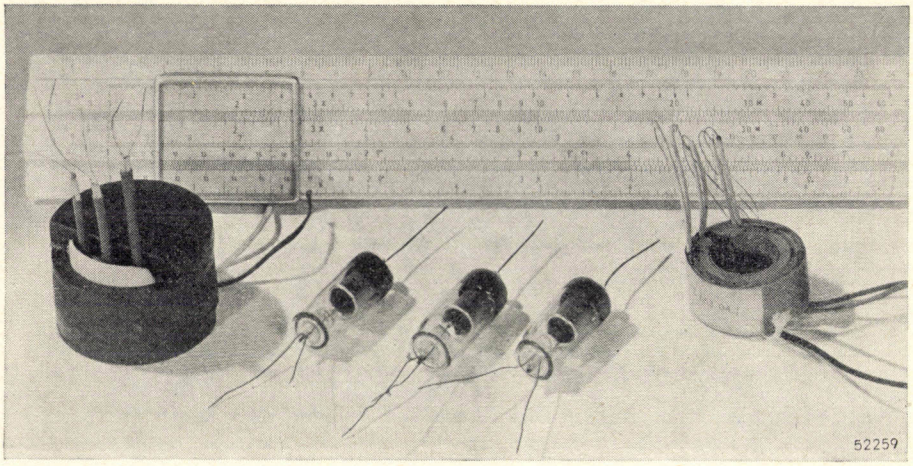


Fig. 10. In the middle the three diodes EY 51 (inverse peak voltage 20 kV, saturation current approx. 200 mA, length of the bulb 40 mm, diameter 14 mm). On the left the complete transformer T of fig. 9. On the rigth the coil of the transformer.

coil S_1 is connected to serve as autotransformer (T).

By employing voltage-trebling ($n = 3$) the peak voltage occurring at the coil S_1 is limited to about 8.5 kV. The rectifying valves (type EY 51, *fig. 10*) have been designed for a peak inverse voltage of 20 kV. The saturation current is about 200 mA. The power for heating the filaments (0.5 W) is drawn from a coil (S_2, S_3, S_4, fig. 9) consisting of a few windings coupled to S_1.

The alternating voltage required to furnish the control voltage V_r is induced in another winding (S_5) of the transformer T (fig. 9). This alternating voltage is rectified by means of the diodes contained in the valve EBC 33. For the bias — the object of which is to make the control voltage more dependent upon the load than the voltage across S_5 — use is made of

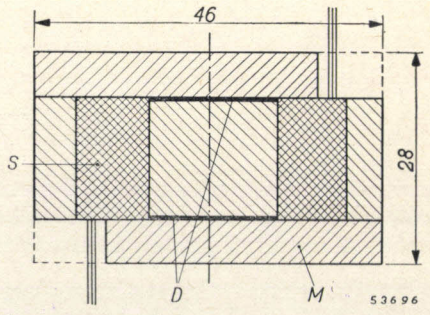


Fig. 11. Cross-section of the transformer T (confer figs 9 and 10) at approximately true size. S = coil, M = magnetic circuit consisting of four pieces of "Ferroxcube" and two air gaps D. Dimensions in millimeters.

[7]) Thanks to the presence of the smoothing capacitor to be mentioned presently, during a short time current impulses can be supplied which are much greater than 150 μA, without causing the direct voltage to drop too much.

[8]) J. L. Snoek, Non-metallic magnetic material for higb frequencies, Philips Techn. Rev. 8, 353-360, 1946.

The positive terminal is connected to the cathode-ray tube by means of a flexible cable insulated with polyvinyl chloride, a material which is not only a very good insulator but is also resistant to oil. The

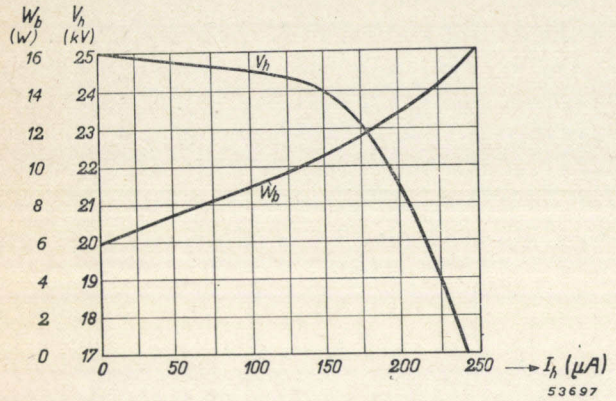


Fig. 12. Direct voltage output V_h and direct current power consumption W_b as function of the direct current output I_h.

outside of the cable has a conducting layer that is earthed. The end of the cable is provided with a plug which fits onto the anode connection of the cathode-ray tube and which contains a series resistor of 1 megohm. This serves a double purpose. In the first place, together with the capacitance between the inner and the outer envelope of the cathode-ray tube (about 300 pF), it forms a smoothing filter for the ripple voltage. In the second place it limits the current impulse which in the event of a short-circuit would discharge the cascade capacitors; without the resistor this would lead to undesired voltage surges.

In *fig. 12* the direct voltage output V_h and the dissipated power W_b are plotted as functions of the current output I_h. It is seen that V_h at first drops only a little when the current increases, but at $I_b >$ approx. 175 μA it drops sharply, and that W_h (9 W at 100 μA, 11 W at 500 μA) compares very favourably with the value which, as calculated above, would be needed without automatic control (60 W).

Fig. 13 gives an idea of the appearance of the apparatus that has been designed in this manner, the dimensions of which are approximately 10 cm × 15 cm × 18 cm (4″ × 6″ × 7″). As regards the place it occupies among the other component parts of the television receiver, reference is made to fig. 7 of article I.

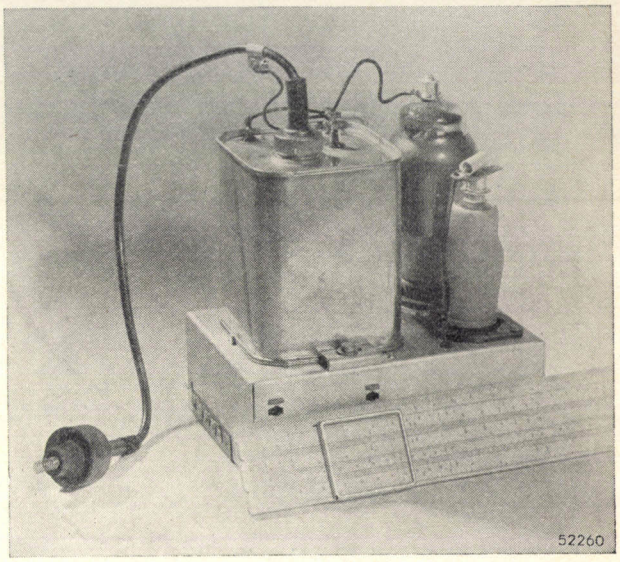


Fig. 13. The complete apparatus for converting 350 V direct voltage into 25 kV direct voltage. On the right the valves EBC 33 and EL 38 and to the left of these the oil-filled can containing the rectifying part. On the extreme left the cable for connecting the cathode-ray tube. The height of the apparatus is 18 cm (7″) and the base occupies 10 cm × 15 cm (4″ × 6″).

STABILIZATION OF THE ACCELERATING VOLTAGE IN AN ELECTRON MICROSCOPE

by A. C. van DORSTEN. 621.385.833:621.316.722.1

The accelerating voltage in an electron microscope must be kept constant to a high degree. The high-voltage generator constructed for the experimental electron microscope of the Institute for Electron-Microscopy at Delft (Laboratorium voor Technische Physica der Technische Hogeschool) had to answer special requirements because the tension had to be continuously adjustable within an extensive range (50-150 kV) and at any level within these limits it was also necessary to keep the voltage constant within 0.2‰ for at least 30 seconds. This article describes a method for stabilizing the voltage by employing a circuit with a high degree of feed-back. At the same time a solution is given for the problem related to the occurrence of relatively large capacitive currents, a problem typical of a system which supplies a small current at a relatively high voltage. With the method chosen the required voltage stability is mainly brought about by means of two regulating valves.

In order to derive full benefit from the high resolving power attainable with electron microscopes having magnetic lenses, the accelerating voltage of the electrons must be highly stable. After the appearance of the first magnetic electron microscopes about 1934, it was a number of years before one realized what requirements had to be met in this respect by the electrical apparatus. In a certain sence the progress made has gone hand in hand with the improvement of the voltage stability of the apparatus.

Permissible variations in voltage

In a previous article published in this journal [1]) it has already been shown how variations in the accelerating voltage affect the quality of the picture. When a magnetic lens is excited with a perfectly constant current its focal distance is proportional to the potential difference through which the electrons have passed. Consequently electrons having different velocities caused by different accelerating voltages do not converge into the same focal point. Optically this means that the lenses are subject to chromatic aberration. Whereas in optics this aberration can be neutralized by a combination of two kinds of glass, in the case of electron lenses such a neutralization is as a rule impossible.

Only such variations of the accelerating voltage are allowed therefore which lead to a blurring not worse than the minimum useful resolving power and certainly no greater than the image fault resulting from diffraction effects and spherical aberration.

The axial chromatic aberration, i.e. the variation of the position of the image measured along the axis, is independent of the lens aperture used, but the corresponding size of the circles of confusion is directly proportional therefore. Lest for a given minimum definition unnecessarily high demands should be made in respect of voltage stability, the aperture — which is given by the size of the condenser diaphragm and the degree of excitation of the condenser lens — must not be chosen too large. As a rule it will have to be smaller than the image of the source of the electron emission, the cathode, projected upon the object. This is, it is true, opposed to the desire to obtain an image as bright as possible, for which purpose the electron density in the beam where it strikes the object has to be raised as high as the object can withstand. However, the loss suffered in this respect owing to the defocusing of the condenser can easily be compensated by increasing the electron emission of the cathode, by heating it to a higher temperature. The resultant shortening of the lifetime of the cathode is not a serious loss, since the cathode is easily replaced.

In this article it will be explained how the accelerating voltage has been stabilized in the high-voltage generator for the electron microscope of the Institute for Electron-Microscope at Delft (Laboratorium voor Technische Physica der Technische Hogeschool). The arrangement and the properties of this instrument have already been described in the article referred to in footnote [1]). A quantitative consideration on the lines indicated above which we shall not go into further here, shows that for this electron microscope the voltage variations are not allowed to exceed about 0.2‰. Since this particular microscope is of an experimental character the high-voltage generator has been so constructed that the voltage can be continuously varied between 50 and 150 kV. Care had to be taken to ensure that within this extensive range the required degree of stability for any voltage setting would be maintained for a period of at least 30 seconds, the time which under normal conditions may be considered sufficient both for focusing the image and for recording the micrograph on a photographic film.

[1]) J. B. Le Poole, A new electron microscope with continuously variable magnification, Philips Techn. Rev. 9, 33-45, 1947, (No. 2).

Principle of the circuit

With the aforementioned requirements in mind we chose a circuit which includes two amplifying valves regulated in such a way as to keep the current intensity highly independent of the voltage supplied to the system. The constant current thereby obtained is passed through a high-stability resistor and the very constant potential difference thus obtained across the resistor forms the voltage source with the properties desired.

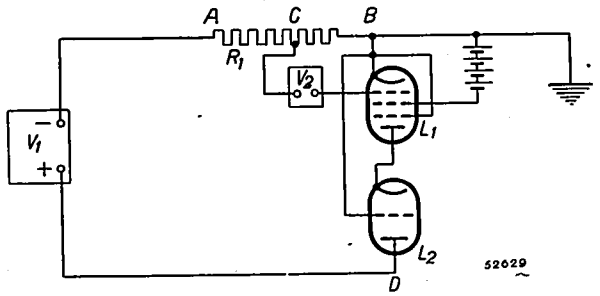


Fig. 1. Circuit diagram applied for the stabilization of the constant potential for an electron microscope. V_1 = the voltage supplied by the rectifier, V_2 = a highly constant reference voltage; R_1 is a high-stability resistor, L_1 a pentode and L_2 a triode. The electron microscope is shunted across the resistor between A and B.

The lay-out of this circuit is diagrammatically represented in *fig. 1*, where V_1 represents the voltage supplied by a rectifier, L_1 and L_2 are the two amplifying valves and R_1 is the high-stability resistor tapped at C in such a way that the part between C and D can be for instance one-thousandth part of the resistance between A and B. The point B and thus the positive side of the voltage on the electron microscope is earthed. The control grid of L_1 is connected to the point C via a highly constant reference voltage V_2. Owing to the voltage difference between B and C, the grid of L_1 becomes rather highly negative with respect to the cathode, but the compensating voltage V_2 holds it at a potential only slightly negative with respect to the cathode, so that the valve L_1 works at its normal bias.

Now, small changes in the grid voltage of L_1 cause large variations on the anode voltage. The voltage amplification obtained by this arrangement is practically equal to the amplification factor of the pentode, which can easily have a value of about 3000. By applying the voltage between cathode and anode of the pentode as grid voltage to a second valve L_2 — if necessary also compensated by a second reference voltage source — the voltage variation is once more amplified. If, for instance, a triode with a voltage amplification of 100 is chosen for L_2, the total voltage amplification becomes 300 000 ×, that is to say that a small variation in the grid voltage of L_1 is 300 000 times greater between cathode and anode of L_2.

It is easy to see that there is a persistent trend to a constant current through the resistor R_1. If with a rising voltage V_1 the current through R_1 increases, the point C would acquire a more negative potential with respect to B, as a result of which the voltage across L_1 would increase and, consequently, that across L_2 likewise. The higher voltage across the valves L_1 and L_2 reduces the voltage V_1, so that the assumed variation in the voltage between A and B is neutralized. The voltage variations of V_1 thus show themselves only as practically equal variations of the voltage of point D (in fig. 1) with respect to B. As long as the grid potentials of L_1 and L_2 remain within the normal range, in this manner a highly stable circuit is obtained.

The general control features of the circuit described here need not be discussed further since they are entirely analogous to those of other control circuits previously dealt with in this journal [2]). We shall confine our considerations to the details relating to the fact that here the voltages are much higher and the currents much lower than those found with stabilizing circuits for measuring and radio purposes.

The difficulties arising from the high voltage are not connected to problems of insulation and the like but rather in the occurence of displacement currents, the consequences of which may have a very disturbing effect upon the controlling properties.

Fig. 2 is another schematic diagram of the circuit including the high-tension transformer T

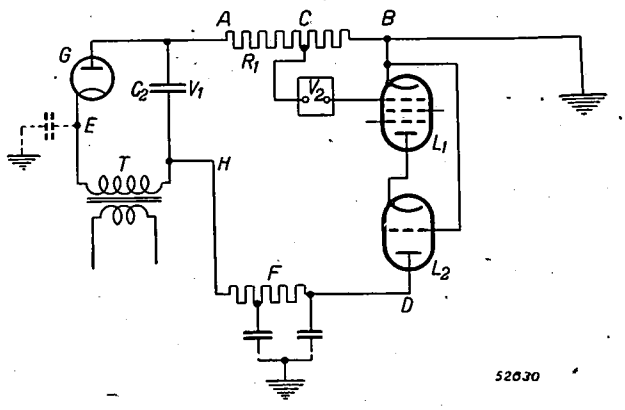


Fig. 2. Diagram of the system of fig. 1 further extended to include the high-tension transformer T and the rectifying valve G, a smoothing condenser C_2 as well as a filter F to eliminate the alternating voltage arising from the capacitive current flowing from the high-tension terminal of the transformer to earth.

[2]) H. J. Lindenhovius and H. Rinia, A direct current supply apparatus with stabilized voltage, Philips Techn. Rev. 6, 54-61, 1941.

and the rectifying valve G and showing (in dotted lines) the capacitance at the high-tension terminal E of the transformer T with respect to earth. Due to the alternating voltage at this point a current flows via this capacitance also through the valves L_1 and L_2. This capacitive current may reach a considerable amplitude which may even be many times greater than the useful direct current supplied by the apparatus.

This capacitive current from the supply transformer to earth occurs in principle also in highly stabilized direct voltage sources as developed for radio and measuring purposes (see the article quoted in footnote [2]), but owing to the low voltage and the relatively large direct current the ratio of the undesired alternating current i_c to the direct current i_g to be supplied is of an entirely different order of magnitude. In the high-tension apparatus for an electron microscope the ratio i_c/i_g may easily be a factor 10^5 greater than that of an apparatus for low voltages and large currents.

As a consequence of this capacitive current to earth, a considerable alternating voltage would come across the regulating valves L_1 and L_2 in fig. 2 and interfere with the whole control. In order to remedy this, a filter F can be introduced as shown in the diagram. It is in fact possible to eleminate this undesired voltage by this means, but there is a resultant undesired time lag.

Another and more effective method of eliminating this undesired capacitive current is to provide an electrostatic screening which prevents this current flowing to earth and directs it straight to the low-potential terminal H of the supply transformer T. This screening should envelop the windings of T as completely as is possible. An obvious solution is to choose the transformer box for this.

The presence of the filament transformer for the rectifying valve G, is likewise a cause of a capacitive leak current to earth. This can be rendered harmless by using an intermediate transformer and connecting the intermediate windings to the screen. In a rectifier for voltages of the size required here, 160 kV, for practical reasons two rectifying valves in a voltage-doubling circuit are to be preferred to one single rectifying valve, because this halves the inverse voltage. *Fig. 3* shows the circuit diagram incorporating these improvements.

Special attention has also been paid to the speed of regulating. A rapid variation, periodically or not, of the high negative potential at the point A in fig. 1 must be followed without troublesome inertia by a corresponding though much smaller potential change at the point C in the same figure, to which the grid of the control valve L_1 is connected. Since between A and C there is a resistance of 10^8 ohms, a small capacitance at the point C with respect to earth would already cause a delay in the corrective action of the control, which would defeat the object in view.

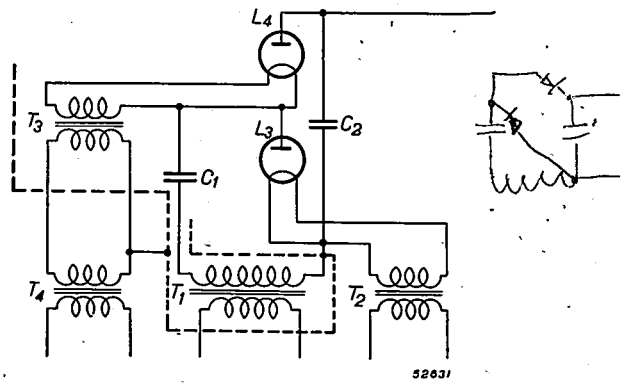


Fig. 3. Part of the circuit showing how voltage doubling is obtained for the high-tension rectifier. T_1 is the high-tension transformer, whilst the dotted line represents the transformer box acting as an electrical screen. The common circuit of the transformers T_3 and T_4 is connected to the screening box of T_1 in order to carry off the capacitive current.

This can be avoided by bridging the resistor between A and C with a condenser. This would then be in parallel with the electron microscope, which is undesired because in the event of a disturbance this condenser would discharge a high, undamped, current in the space between cathode and anode. By introducing a resistor in series with the capacitor the current can be sufficiently damped to ensure that in the event of such an interference the electron microscope suffers no harm.

Further, it is to be pointed out that in the practical application of this system it was found desirable to connect the apparatus supplying the compensating voltage V_2 between B and the cathode of L_1 instead of between C and the control grid of L_1. This was to avoid increasing the input grid capacity of the pentode by the capacitance unavoidable in this apparatus.

It has already been mentioned that the required degree of voltage stability has to be maintained for at least 30 seconds, the period considered sufficient for focusing and taking a micrograph. To meet this requirement not only must the mains voltage variations be compensated but care has also to be taken that no inadmissible changes take place in the circuit elements during that period. What is most to be avoided is a variation in the resistor R_1 and this requirement has been met by applying oil-cooling and selecting a resistance wire with a small temperature coefficient.

Before proceeding to give a further description of the high-voltage generator at Delft we must draw attention to the fact that the demands made

for that experimental electron microscope differed considerably from what is usually required of such an apparatus. In the first place it was quite unusual to require continuous adjustability in a range of 100 kV, whilst on the other hand the nature and purpose of the instrument left the designer more freedom as regards the dimensions of the installation, since it did not have to be set up in a particular small space. This made it possible, for instance, to use metal wire for the high-ohmic resistor R_1, shunted across the microscope proper, so that this resistor could be given exceptional properties but was much larger than carbon resistors; the wire is wound on a cylinder no less than 1.80 metres long.

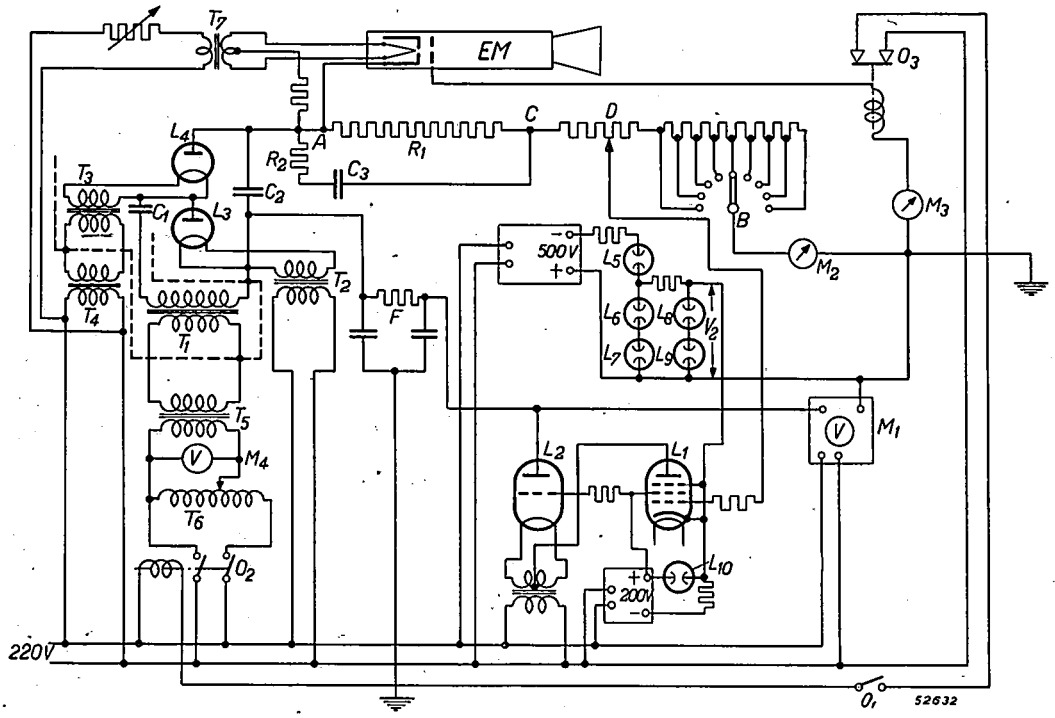


Fig. 4. Circuit diagram of the high-tension installation of the experimental electron microscope for 150 kV installed in the Institute for Electron-microscopy at Delft. *EM* is the electron microscope, L_1 and L_2 are a pentode and a triode repectively, L_3 and L_4 two rectifying valves, L_5-L_{10} neon stabilizing valves, M_1-M_4 measuring instruments, O_1-O_3 switches, T_1-T_7 transformers, F a filter. The box of the high-tension transformer is again represented by a dotted line. In so far as this circuit relates to the high-tension rectifier, the following is to be noted: The transformer T_1, connected on the primary side to the regulating transformer T_6 via the intermediate transformer T_5, supplies on the secondary side a voltage with a maximum peak value of 80 kV. C_1 is a condencer having a value of 0.05 μF. Since the load current is small (1-2 mA), at maximum voltage this condenser is charged almost up to 80 kV, the peak value of the transformer voltage, via the high-tension valve L_3 (type 28122). The pulsating voltage, amplitude about 2 × 80 kV, across this valve causes the condenser C_2, with a value of 0.025 μF, to be charged via the valve L_4 to a voltage of about 160 kV. The circuit of the regulating apparatus is explained in the text.

Description of the installation

The high-tension installation described in this article was made in the Philips Laboratory at Eindhoven. Its circuit diagram is given in *fig. 4*.

For the sake of clarity the description of the apparatus is divided into three parts: 1) the rectifier for the high tension, 2) the stabilized resistor, 3) the regulating apparatus with compensating device.

The rectifier for the high tension

For the reason already given, voltage-doubling with two valves was used for generating the high constant potential.

It is not necessary to go into the details of the circuit of this rectifier because it has already been fully described in this journal [3]). Numerical data are given in the legend of fig. 4.

The filaments of the valves L_3 and L_4 are fed via transformers. The secondary winding of the transformer supplying L_3 is insulated for 20 kV. The filament of L_4 is fed via a transformer insulated for 180 kV, connected to the mains on the primary side via an intermediate transformer insulated for 20 kV and with its secondary winding connected, like that of the valve L_3, to the box of the high-

[3]) Philips Techn. Rev. 1, 6-10, 1936; 2, 161-164, 1937.

tension transformer T_1, to carry off the capacitive current which otherwise, as explained above, would flow to earth. A metal screen can also be affixed to the box of this high-tension transformer to render the capacitive current from other parts of the installation harmless.

High-stability resistor

The high-stability resistor R_1 consists of a coil of resistance wire with a low temperature coefficient helically wound on a cotton core. This in turn is wound on a glass cylinder 12 cm in diameter which is mounted inside a vertical column consisting of sections of high-voltage grade "Philite" screwed one into the other. Rings of the same kind and similar ones of larger size have also been used for the jackets of the high-tension condensers C_1 and C_2, the filament transformers of the rectifying valve L_4 and the transformer T_7 for the electron microscope.

High-tension resistors made in this manner are apt to show sometimes irregular deviations in the resistance, this being due to the fact that in the process of winding breaks are apt to occur in the 15 μ thick wire; when the electric power is switched on, the cotton core becomes carbonized locally where those breaks occur and since these carbonized points are conductive, the interruptions are shunted thereby. The resulting very small increases of the resistance often pass unnoticed in the beginning. In order to eliminate such defects, while the column was being wound tests were made to make sure that the resistance increased strictly linearly with the length of the wound wire. The abnormal spots were detected by graphical means and the breaks bridged over. In this manner a resistor was produced which satisfied the most stringent requirements.

The regulating apparatus with compensating device

An important part of the regulating apparatus is the compensating device, which has to supply the highly stabilized voltage V_2. A small rectifier supplies 500 V direct voltage, from which, by means of a two-fold stabilization with successively three and two neon stabilizing valves L_5 to L_9 (type 150 A1) connected in series, the highly constant reference voltage V_2 is obtained, which together with the potential difference between the points B and D determines the voltage difference between grid and cathode of the pentode L_1 (type EF 6). The grid is connected directly to the point D, the sliding contact of the potentiometer. The point B is the contact arm of a tapped resistor with constant properties. In this manner it is possible to modify the resistance between the points B and D both step by step and continuously; for each setting there is a definite current passing through the total resistance between A and B. The difference between the constant voltage V_2 and the voltage between the points B and D thus brings the regulating valve into the working point. The adjustment is such that the anode voltage of the valve L_1 then amounts to about 200 V.

The voltage between the anode of L_1 and earth is now identical with the voltage between grid and cathode of the valve L_2 (type TA 8/300), but since the latter would then have too high a negative grid bias its grid is not connected directly to earth, as in fig. 1, but via a suitable voltage source. For this purpose the same voltage source can be used as is required to keep the screen grid of L_1 at a constant potential with respect to the cathode. In this case a small rectifier is used together with the

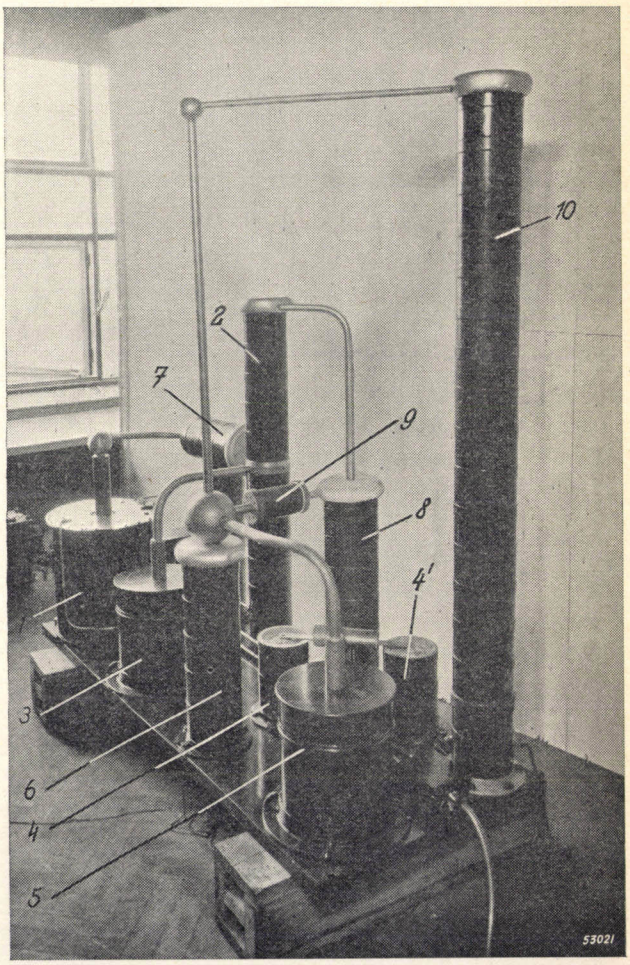


Fig. 5. The high-tension installation of the 140 kV electron microscope installed at Delft. *1* is the high-tension transformer, *2* the column with the two high-tension valves, *3* their filament transformers, *4* and *4'* the parts of the filter, *5* the filament transformer for the electron microscope, *6*, *7* and *8* condensers, *9* a smoothing resistor, *10* the high-stability resistor mounted on a cylinder 1.80 metres in length. (The smoothing condenser *6* and the smoothing resistor *9* are not shown in the diagram of fig. *4*; they would have to be shunted across C_2.)

neon stabilizing valve L_{10} (type 150 A1). This rectifier supplies a voltage of 150 V. In this manner a good adjustment of the valve L_2 is obtained, which can take up an anode voltage varying for instance between 1000 and 15000 V according to the grid voltage and thus ultimately dependent of the potential of the control grid of L_1.

The working voltage of the electron microscope is therefore selected by means of the adjustment of the resistor between B and D, the voltage applied by the rectifier being so adjusted, by means of the hand adjustment of the regulating transformer T_6, that the regulating valve L_2 comes to lie in the middle of the regulating range and thus takes up a voltage of about 7000 V. In order to check this adjustment, between the anode of L_2 and earth a valve voltmeter M_1 is connected which has an extremely high input resistance and acts practically speaking as an electrostatic voltmeter. This meter indicates the voltage fluctations that are "smoothed out". This renders it possible to check the working of the circuit at any time. Mains voltage fluctuations up to 5%, positive as well as negative, can be controlled in this manner. Larger deviations, which hardly ever occur in the form of fluctations, have to be adjusted with the aid of the regulating transformer T_6.

The circuit of fig. 4 further shows some of the devices already described above, such as the condenser C_3, which transmits the rapid variations to grid of L_1, and the filter F which suppresses what is left of the capacitive current, particularly the higher harmonics of the 50 c/s current.

Further, the diagram shows that some control meters have been introduced: M_4 is a voltmeter for the primary transformer voltage, M_3 a milliammeter for the emission current of the electron microscope, M_2 a milliammeter for the current passing through the potentiometer. O_1 is the switch controlling the excitation of the magnetic switch O_2 and thus the high-tension rectifier. O_3 is a overload relay which interrupts the energizing current of O_2 as soon as the current in the electron microscope reaches an abnormally high value, as may be possible for instance when gas is released or in case of a break in the vacuum system. This automatic cut-out comes into operation as soon as the current exceeds 2 mA. This device precludes discharges that may be harmful to the instrument.

Fig. 5 is a photograph of the high-tension equipment as installed.

Note

The circuit described here represents only one of the many methods that can be applied to obtain a stabilized high tension. The attractiveness of this method lies in its simplicity, the work being done in fact by only two regulating valves.

Finally it is to be noted that with the method described it would also be possible to introduce the regulating valves on the high-tension side of the resistor R_1. The problems connected with the capacitive current would not then arise, but on the other hand there would be difficulties of a constructional nature, particularly so when the voltage is high, as it is the case here.

A RAPID-ACTION STARTER SWITCH FOR FLUORESCENT LAMPS

by Th. HEHENKAMP.

621.327.43.032.433

With the usual types of starter switches for fluorescent lamps, namely the resistance and glow-discharge bimetallic starters, several seconds elapse between the switching on and the ignition of the lamp. Though in many cases of public utility lighting this is no objection, it is of more serious consequence in the illumination of the home, in which field the fluorescent lamp is gaining more and more ground. To overcome this difficulty a new solution has therefore been sought based on the consideration that the cathodes should first be sufficiently heated so as not to suffer any damage when the lamp is ignited. For this heating to take place in a reasonably short time (0.3 to 0.4 sec) a current has to be sent through the filaments which is greater than the stationary short-circuit current of the series choke. This heating current is obtained by utilizing a transient, the circuit being periodically closed and opened by a contact forced to vibrate by means of a coil shunted across it. The time normally elapsing between the switching on and the ignition of the lamp is 0.3 to 0.4 sec, and in unfavourable circumstances 0.5 to 1 sec. The new starter switch is interchangeable with the conventional glow-discharge bimetallic starter.

Tubular fluorescent lamps for general illumination purposes are as a rule of such a construction that the arc voltage amounts to about half the R.M.S. value of the mains voltage for which they are rated. A simple ballast (generally a choke) then sufficies to stabilize the discharge in the lamp [1]).

In order to ignite the lamp it has to be given a voltage impulse higher than the peak value of the mains voltage. Preferably the lamp should not be ignited before the cathodes have practically reached the working temperature, not only because the voltage impulse can then be smaller than when the cathodes are cold, but particularly because ignition with cold cathodes shortens the life of the lamps. For this reason automatic starters have been devised which pass a heating current through the filaments before igniting the lamp. Two types of starters hitherto used will be briefly described before proceeding to deal with a new type.

Starter switches hitherto used

The resistance-bimetallic starter

The so-called resistance-bimetallic starter (S_r, *fig. 1*) consists of a contact having one of its poles fixed to a bimetallic strip and a heating element r in the shape of a coil. Since the contact is originally closed, upon the mains voltage being switched on a current flows through the choke L, the two filaments and the heating element. We call this current the short-circuit current (I_k), because it flows when the lamp is short-circuited. After the filaments have been given time to reach the desired temperature, under the influence of the heat generated in the heating element the bimetal is curved far enough to open a contact and break the short-circuit current. When this opening of the contact takes place at a not too small momentary value of the current, owing to the self-inductance L it is accompanied by a voltage impulse that ignites the lamp. There then flows through the heating element the normal working current, which though less than the short-circuit current is still sufficient to keep the contact open. The cathodes are then maintained at the desired temperature by the discharge itself.

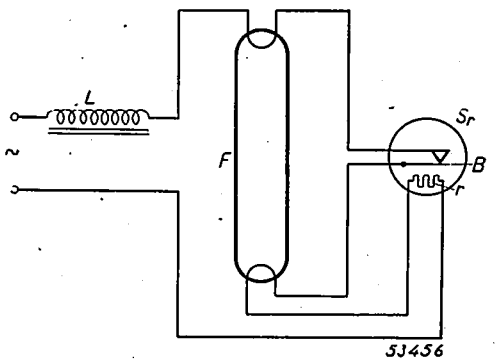


Fig. 1. Circuit diagram of the resistance-bimetallic starter (S_r). F = fluorescent lamp. L = ballast choke. B = bimetal. r = heating coil.

If, however, the opening of the contact takes place at about the zero point of the short-circuit current, then there is no voltage impulse sufficient to ignite the lamp. In such a case the circuit through the heating element remains broken until the bimetal is sufficiently cooled down for the contacts to meet again. This cycle is repeated until ignition of the lamp occurs.

The great objection against the resistance-bimetallic starter is that the initial state (heating element cold, contact closed) differs from the working state (heating element hot, contact opened). The fact is that when a lamp is switched on again a few seconds after it has been switched off, the contact

[1]) A. A. Kruithof, Tubular luminescence lamps for general illumination, Philips Techn. Rev. 6, 65-73, 1941.

is still open and one has to wait for the bimetal to cool down sufficiently to close the contact. The heating element, however, is then still at a considerable temperature and the contact will open again in a much shorter time than is normally the case. The cathodes of the lamp, which had on the other hand cooled down, are not sufficiently heated again in that short space of time and the voltage peak arising from the breaking of the circuit is not high enough, so that in such a case the lamp does not ignite until the starter action has been repeated several times. The re-ignition times with the resistance-bimetallic starter therefore amount to 10 to 15 seconds.

The glow-discharge bimetallic starter

The glow-discharge bimetallic starter (S_g, *fig. 2*) likewise consists of a contact having one pole fixed to a bimetallic strip. The heating of the latter however is not brought about by means of a heating coil but by a glow-discharge between the electrodes. The bulb containing these electrodes is filled with a gas of such a nature and pressure as to cause the ignition voltage of the glow-discharge to be lower than the peak of the lowest mains voltage (nominal 220-230 V [2])) but higher than the arc voltage of the fluorescent lamp.

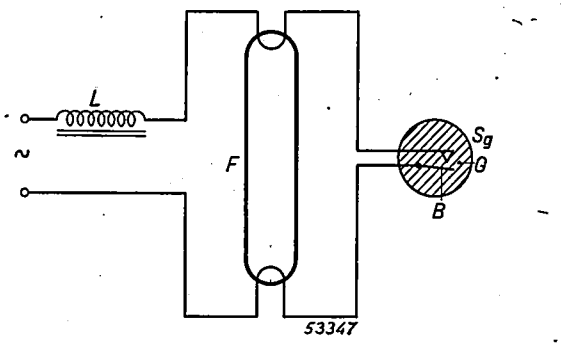


Fig. 2. Circuit diagram of the glow-discharge bimetallic starter (S_g). G = gas filling in which a glow discharge may take place and heat the bimetal. The other letters have the same meaning as in fig. 1.

Another fundamental difference compared with the resistance-bimetallic starter lies in the fact that in the initial state the contact of the glow-discharge bimetallic starter is open.

The latter type of starter works in the following way. As soon as the mains voltage is switched on a glow-discharge takes place in the starter and heats the bimetal, so that after a time the contact is closed. Not until then does the short-circuit current begin to flow and heat the lamp cathodes (the glow current already flowing did not play any appreciable part in this). Simultaneously with the closing of the contact the glow-discharge is extinguished. The bimetal thus cools down, the contact opens after a certain time and the short-circuit current is broken. The voltage impulse thereby arising may be sufficient to ignite the lamp, the cathodes having meanwhile been heated up. The arc voltage of the lamp then comes to lie across the starter, and no glow-discharge can take place; thus the contact remains open. As a rule, however, the first voltage impulse will not be sufficient to ignite the lamp; the cycle is then repeated, possibly several times.

On an average this cycle is repeated many more times with the glow-discharge bimetallic starter than is the case with the resistance bimetallic starter, for in the former case the glow-discharge is first started upon the contact being opened, the voltage peak remaining lower than would be the case without a glow discharge; consequently there is less chance for the lamp to ignite.

Apart from the drawback of this more frequent repetition of the cycle, the glow-discharge bimetallic starter has the objection that the short-circuit current does not begin to flow until the bimetal has been heated. In fact it takes as much as from 2 to 5 seconds before the lamp starts. With the resistance-bimetallic starter this delay is no more than 1 to 2 seconds.

Against this, however, there is the important advantage that with a glow-discharge bimetallic starter the initial state is the same as the working state, viz. no glow-discharge, contact open. Upon the lamp being switched off and then immediately switched on again there is therefore not the objection that arises in the case of the resistance-bimetallic starter.

Another advantage of the glow-discharge bimetallic starter, which though incidental is of practical importance, is the fact that it has only two connecting points (fig. 2), thus greatly simplifying the wiring. The resistance-bimetallic starter on the other hand has four connecting points (fig. 1).

In the course of the last few years various improvements have been made to both these types of starters with a view to minimizing the drawbacks referred to. In most applications the glow-discharge bimetallic starter has gained more favour and is now commonly employed both in Europe and in America.

[2]) At other nominal values of the mains voltage, say 110 V, 125 V, etc., an autotransformer is used with a secondary voltage of 220 V. This transformer may have such a leakage as to make a separate choke unnecessary. What is said in this article about starters applies also to the case where such a transformer is used.

The properties desired in an improved starter switch

The delay between the switching-on and the ignition of fluorescent lamps is no great objection when these are used in factories, offices, shops and suchlike, but they are beginning to be used on a steadily increasing scale for the illumination of the home [3]), where it more frequently happens that a dark room needs to be illuminated immediately upon switching on. In such cases a delay of a few seconds is most annoying. There is therefore undoubtedly a need for a starting device which, if not eliminating this delay entirely, will at least reduce it considerably.

The solution is not to be sought in the raising of the voltage impulse to such a level as to ignite the lamp immediately upon switching on, because this would be detrimental to the life of the lamp, since its durability depends in part upon the number of times it is switched on. In houses the number of times a lamp is switched on is greater than elsewhere, and if the lamp were to be ignited every time while the cathodes are still cold its length of service would be considerably shortened.

We must therefore maintain the requirement that upon the lamp being ignited its cathodes must already have been brought up to a sufficiently high temperature, the latter taking place so quickly as to avoid any inconvenience being experienced from the delay.

Furthermore, a very short re-ignition time is desired when a lamp is switched on again immediately after having been switched off.

Finally, the new starter must be interchangeable with the hitherto conventional glow-discharge bimetallic starter, likewise having only two terminals and the same small dimensions.

Ignition voltage and cathode temperature

The requirement made above, that prior to the ignition of the lamp its cathodes must have reached a sufficiently high temperature in the shortest possible time, leads to the following problems:

1) How high must the minimum temperature of the cathodes be upon ignition in order to avoid excessive sputtering?
2) With what heating current do they reach this temperature in a reasonably short time (e.g. $^1/_3$ sec.)?
3) How can this heating current be obtained?

As to the first question, the following is to be remarked. When the R.M.S. value V_0 of the sinusoidal alternating voltage that just causes the lamp to ignite is measured as a function of the cathode temperature ϑ it is found to follow a curve as indicated in *fig. 3*; raising ϑ above about 400 °C gives practically no further reduction of the ignition voltage.

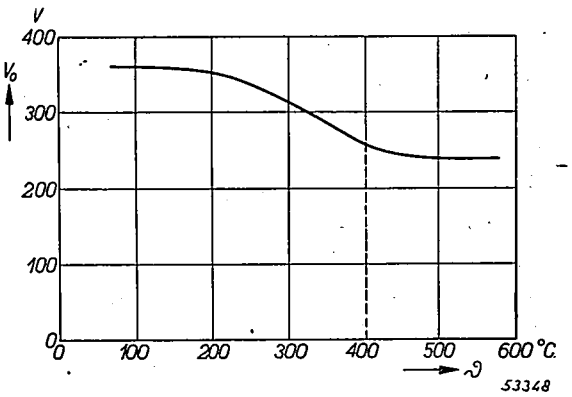


Fig. 3. Ignition voltage V_0 (R.M.S. value of a sinusoidal alternating voltage) of the TL 40 W fluorescent lamp, as function of the cathode temperature ϑ. This graph represents the average of the measured results taken with several lamps.

Now it is known from experience that when the ignition voltage is low there is also little sputtering due to the ignition. It is therefore to be taken as a fact — confirmed in practice — that ϑ need not be raised higher than 400 °C to give the lamp a long life.

The second question has been answered by measuring ϑ as a function of the time t at various constant values of the heating current. This measurement amounts to the recording of an oscillogram of the voltage across the filament while the constant heating current is passing through it. This voltage and current give the resistance of the filament, which resistance increases as the filament gets hot. (This increase of resistance has practically no effect upon the value of the heating current, since the resistance of the hot filament is still small in comparison with the impedance of the series choke.) From the curve representing this resistance one can deduce the temperature with the aid of the temperature coefficient. The wiring diagram used is represented in *fig. 4*, some details of which are explained in the legend.

An oscillogram of the heating voltage is given in *fig. 5*. The curves $\vartheta = f(t)$ derived from such oscillograms for a number of values of the heating current are reproduced in *fig. 6*.

The short-circuit current I_k of the ballast belonging to the TL 40 W lamp is 0.7 A at a mains voltage of 220 V. Extrapolation of the bottom curve in fig. 6 shows that with this current applied as heating current it takes more than 1 sec to reach the temperature of 400 °C. To cut this time down

[3]) L. C. Kalff and J. Voogd, Living-room lighting with tubular fluorescent lamps, Philips Techn. Rev. 8, 267-271, 1946.

to 0.3 sec a heating current of 1 A is required, i.e. a current generating per time unit twice as much heat as the normal short-circuit current I_k.

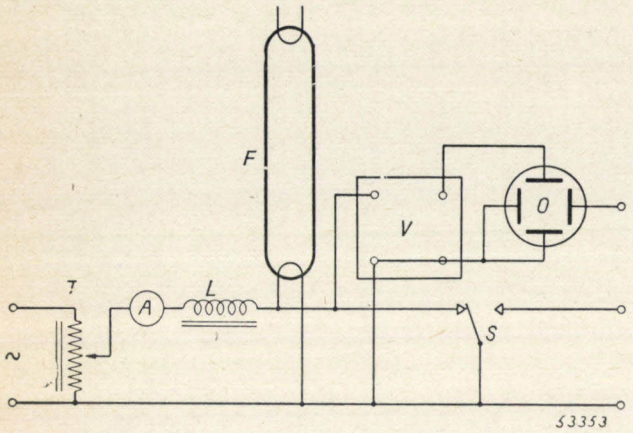


Fig. 4. Circuit diagram for recording the oscillogram of the heating voltage during the heating of the cathode, at constant heating current. F = fluorescent lamp, where the current passing through one of the filaments is preadjusted to the desired value (regulating transformer T, ammeter A). The secondary voltage of T being much higher than the heating voltage, and the excess being taken up in a choke (L), a preadjusted heating current undergoes practically no change while the cathode is heating up. When, with cold filament, the switch S is turned to the right, the filament is no longer short-circuited and the heating voltage, via the amplifier V, causes a vertical deflection on the oscillograph screen O. At the same time the right-hand contact of S activates a device which supplies a voltage rising proportionately with the time. This voltage causes the light spot to traverse the screen horizontally in about 0.5 sec.

The value of I_k could be raised to 1 A (while retaining the normal working current) by constructing the choke in such a way that the induction in the core is higher up in the saturation zone, but then this would involve a noticeable distortion of the working current and relatively large current variations following fluctuations in the mains voltage.

A better method has been found by utilizing the fact that the current arising when an alternating current circuit is switched on is apt to assume extra large values temporarily.

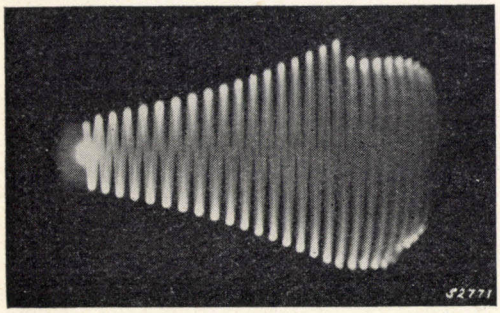


Fig. 5. Oscillogram showing the heater voltage of a TL 40 W lamp taken up in the circuit of fig. 4. The heating current is 1 A, 50 c/s. At first the heater voltage rises owing to the positive temperature coefficient. After 17 cycles ($^1/_3$ sec.) the heater voltage had risen to such a high level (12 V) as to cause a gas discharge to take place parallel to the filament, this accounting for the resulting drop in the heater voltage.

Transient occurring when switching on a circuit with self-inductance and resistance

When a circuit consisting of a self-inductance L with a resistance R in series is connected to an alternating voltage source $v = V_{max} \sin \omega t$, we have for the current i the differential equation

$$L \frac{di}{dt} + Ri = V_{max} \sin \omega t.$$

The solution of this equation for constant values of L and R is:

$$i = \frac{V_{max}}{Z} \sin (\omega t - \varphi) + Ce^{-\frac{R}{L}t} \quad . \quad . \quad . \quad . \quad (1)$$

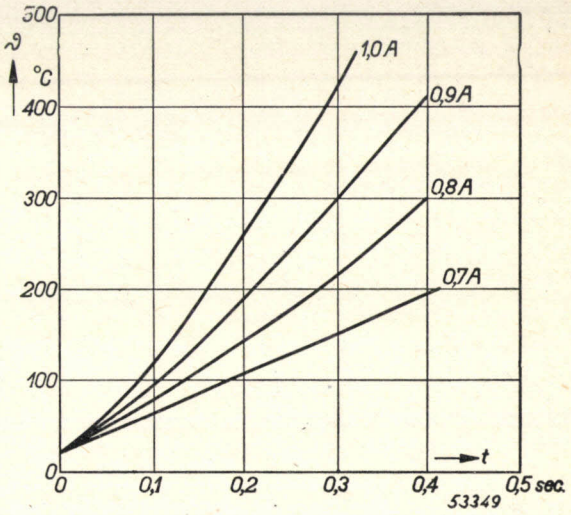


Fig. 6. Cathode temperature ϑ as function of the time t at constant values of the heating current.

The first term in the second member represents the stationary solution, where Z is the impedance, $\sqrt{\omega^2 L^2 + R^2}$, and φ is the phase difference between this stationary current and the mains voltage: arc tan $\omega L/R$.

The second term on the right-hand side of (1) represents the transient. The constant C is governed by the moment t_0 at which the circuit is switched on (the solution has to satisfy the condition $i = 0$ for $t = t_0$). Hence we have the following form of the solution applicable for all values of $t \geqq t_0$:

$$i = \frac{V_{max}}{Z} [\sin (\omega t - \varphi) - e^{-\omega (t - t_0) \operatorname{cotan} \varphi} \cdot \sin (\omega t_0 - \varphi)] =$$

$$= \frac{V_{max}}{Z} \cdot y. \quad . \quad . \quad . \quad . \quad . \quad . \quad . \quad . \quad . \quad . \quad . \quad . \quad . \quad (2)$$

In *fig.* 7 the quantity $y = iZ/V_{max}$, which is a measure for the current i, is plotted in a heavy

line as a function of ωt for one value of φ ($\varphi = 78°$, cotan $\varphi = 0.21$). The figs 7*a-d* relate to four values of the switching-on moment t_0 given in the legend. The dotted sine line represents the mains

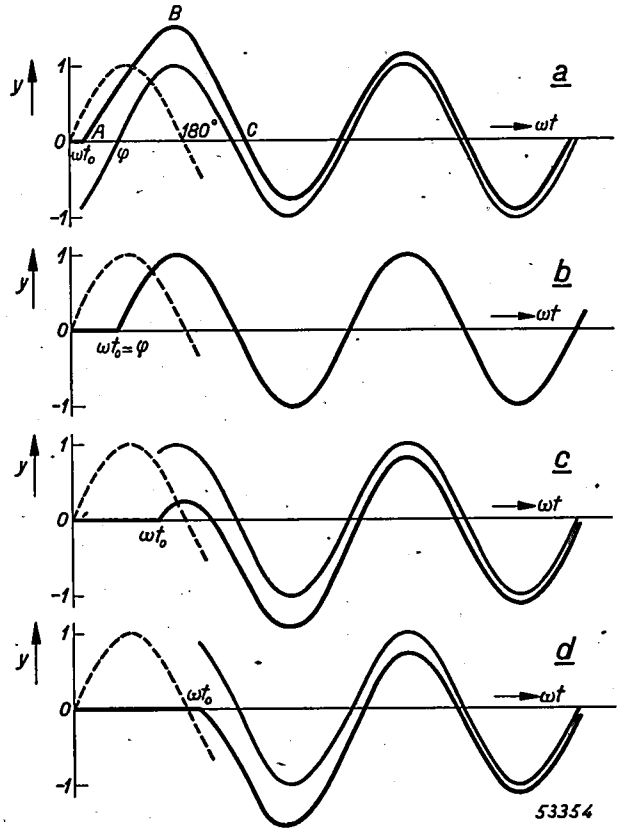


Fig. 7. Curves of the current arising when a circuit consisting of a constant resistance R and a constant self-inductance L connected in series is connected to an alternating voltage source $\vartheta = V_{max} \sin \omega t$. Plotted in heavy lines is $y = iZ/V_{max} = f(\omega t)$ according to equation (2) for $\varphi = 78°$ and *a*) $\omega t_0 = 18°$, *b*) $\omega t_0 = 78° = \varphi$, *c*) $\omega t_0 = 138°$, *d*) $\omega t_0 = 198°$. The dotted line represents the mains voltage: $v/V_{max} = \sin \omega t$; the light sine line represents the stationary current: $\sin(\omega t - \varphi)$.

voltage curve, the lightly drawn sine line representing the stationary current. From formula (2) and fig. 7*b* we see that the current follows the stationary curve immediately after switching on when $\omega t_0 = \varphi$, thus when the circuit is closed at the moment at which the stationary current, if present, would pass through zero. With other values of ωt_0 however a transient is superposed upon the stationary current (figs 7*a*, *c*, *d*). As a consequence the current peaks (in absolute value) are alternately higher and lower than those in the stationary state.

The new starter

Principle

In the new starter described here use is made of the high current peaks referred to above in order to get the desired rapid heating of the cathodes. The circuit L-R upon which we worked in the preceding paragraph is now composed of the self-inductance L_1 of the choke and the sum R_1 of the loss resistance of that choke and the resistance of the two filaments (*fig. 8*).

The desired heating cannot be obtained with only one current impulse (for instance ABC in fig. 7*a*), it being necessary to repeat the impulse during say from 15 to 20 successive periods, thus during an interval of time of about $^1/_3$ sec. This implies that the current must be repeatedly interrupted. The switching contact, which is shunted across the lamp just as in the case of the glow-discharge bimetallic starter (fig. 2), is therefore kept in vibration by a magnetic coil while the cathodes are heating up. This coil is connected across the contact (fig. 8), so that upon the armature being attracted the coil is short-circuited, the contact then opening, and so on. Once the lamp has been ignited the contact remains open, because then the arc voltage of the lamp across the magnetic coil is not sufficient to close the contact.

From the foregoing it will be evident that for proper functioning one is not entirely free in the choice of the moments at which the contact closes and breaks the circuit: as we have seen from fig. 7, it depends upon the switching-on moment what proportions the transient assumes, and the switching-off moment must be so chosen that the filaments are without current during the shortest possible time.

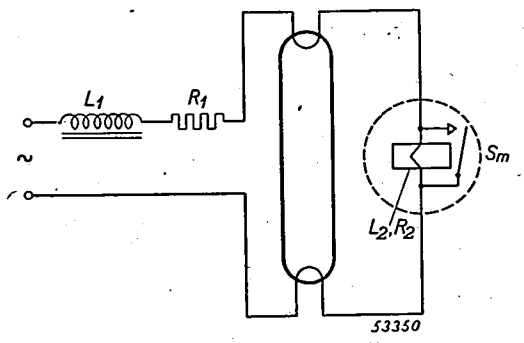


Fig. 8. Circuit diagram of the electromagnetic starter switch (S_m). L_1, R_1 and L_2, R_2 represent the self-inductance and resistance of the ballast choke (including the filaments) and of the magnetic coil respectively.

Another important point is that these moments must be so chosen that the heating effect is only slightly dependent upon small inevitable variations in the switching moments. A further quantitative analysis is therefore required, even though various effects arise which cannot very well be taken into account. Then there comes the question how to bring about the switching operations at the desired moments.

The chosen frequency f_c at which the contact vibrates is equal to the mains frequency f. This is not absolutely necessary, some other simple relation between f_c and f being possible, for instance $f_c = 2f$, or $2f/3$; the calculation in such cases is analogous to that given below for $f_c = f$. It appears that when $f_c > f$ the result is so strongly dependent upon the switching moments that for practical purposes this case is unsuitable. When $f_c < f$ another difficulty arises, to which we shall refer later. $f_c = f$ proves to be a satisfactory compromise.

Choice of the switching-on moments

First of all it is to be noted that with a given ballast the quantities R_1, L_1 and ω are fixed, thus also the impedance Z_1 and the phase angle φ_1. Thus for the 40 W lamp in question cotan φ_1 = approx. 0.21, φ_1 = approx. 78°; it is upon this value, for which the curves have been drawn in fig. 7, that the following calculations are based.

The amount of heat w generated by the passage of the current through each of the filaments (resistance R_f [4])) amounts to:

$$w = \frac{R_f}{\omega} \int_{\omega t_0}^{\omega t_0+\delta} i_1^2 \, \mathrm{d}(\omega t) = \frac{R_f}{\omega} \cdot \frac{V_{\max}^2}{Z_1^2} \int_{\omega t_0}^{\omega t_0+\delta} y_1^2 \, \mathrm{d}(\omega t). \quad (3)$$

where δ is the angle corresponding to the time elapsing between switching-on and a switching-off and y_1 is the expression between brackets in formula (2) for a given angle φ_1.

We shall now compare the quantity w given by (3) with the amount of heat w_s which could be generated in the same resistor R_f in the full cycle (2π) by the stationary current $i_s = (V_{\max}/Z_1) \sin(\omega t - \varphi)$, the R.M.S. value of which we have previously called I_k:

$$w_s = \frac{R_f}{\omega} \cdot \frac{V_{\max}^2}{Z_1^2} \int_{\varphi}^{\varphi+2\pi} \sin^2(\omega t - \varphi) \, \mathrm{d}(\omega t) = \frac{R_f}{\omega} \cdot \frac{V_{\max}^2}{Z_1^2} \cdot \pi.$$

The equation $k = w/w_s$ of these two quantities of heat is thus

$$k = \frac{1}{\pi} \int_{\omega t_0}^{\omega t_0+\delta} y_1^2 \, \mathrm{d}(\omega t) \quad \ldots \quad (4)$$

By integration we find k as a function of the two quantities t_0 and δ, which we still have available. *Fig. 9* shows $k = \mathrm{f}(\delta)$ for some values of ωt_0 (thin lines); the heavy line is the envelope of the series of curves and shows the greatest value of k that can be reached with a given δ. At first sight it appears that k, though being greater than 1 (maximum about 1.67), does not reach the required minimum value 2, so that apparently the method is inadequate. There is, however, an incidental circumstance

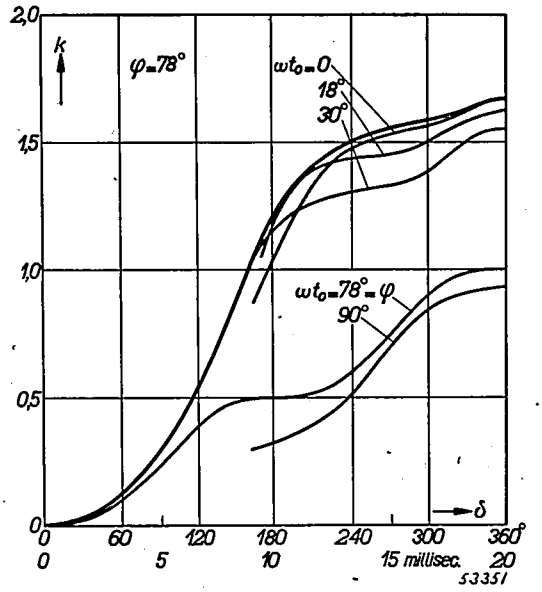


Fig. 9. Light lines: the quantity k of eq. (6) as function of the angle δ, which is proportional to the time during which the contact is closed, for cotan $\varphi = 0.21$ and some values of ωt_0. The heavily drawn envelope indicates the greatest value k which with given δ is obtained with the corresponding optimum value of ωt_0.

that has so far been left out of consideration, namely the fact that the core of the choke is rather highly saturated, not so highly as to cause inconvenience from the drawbacks already mentioned (current strongly distorted and greatly dependent upon the mains voltage), but to such an extent that the starting current impulse reaches much higher values than would follow from the above calculation. We shall not try to include this non-linear effect in the calculation but merely state that, provided t_0 and δ are favourably chosen, it is capable of raising k to the required value of 2.

The foregoing calculation for a linear self-inductance has by no means become valueless, since in spite of its imperfection it shows how t_0 and δ can best be chosen; it only has to be borne in mind that the actual values of k may be greater than calculated.

From fig. 9 it is seen that, as was to be expected, the curves with increasing δ rise continuously. Therefore δ should preferably approach a full period as closely as possible. It has to be taken into account, however, that it is not practicable to construct a synchronous switch that is closed for practically a whole cycle and opened only for a

[4]) In fact R_f depends upon temperature, and thus upon time; in a short time such as we are dealing with here (less than 1 cycle) R_f may however be taken as being constant. Even with a hot filament R_f is such a small part of the total resistance R_1 that we can ignore the change taking place in Z_1 and φ_1 while the filament is heating up.

small fraction of that time. Fig. 9 shows that very little of the greatest possible value of k need be sacrificed to get a much smaller angle δ, say $\delta = 200°$ (corresponding to 11 milliseconds), $k \approx 1.3$. With a further reduction of δ, however, k diminishes rapidly. Fig. 9 further shows that ωt_0 must lie round about 0, but that it is not very critical.

The switching mechanism

The switch as a whole is characterized by the current i_a in the magnet coil at which the armature is just attracted and the contact closed, and by the smaller current i_b at which the armature is just released. By i_a and i_b we mean the momentary values; we shall disregard for a moment the mechanical inertia of the armature itself.

We start from an interval of time during which the contact is still open and the current i_2 in the coil is increasing. As soon as i_2 has reached the value i_a the contact is closed and the coil short-circuited. The current i_2 does not then immediately fall to zero but continues to flow across the contact, decreasing exponentially according to

$$i_2 = i_a \cdot e^{-\frac{R_2}{L_2} t'}, \quad \ldots\ldots \quad (5)$$

where R_2 and L_2 are respectively the resistance and the self-inductance of the coil and t' is the time reckoned from the moment at which the contact closes.

As soon as i_2 has dropped to the value i_b the coil releases the armature, and at that moment $\omega t' = \delta$. From (5) it then follows that

$$\delta = \frac{\omega L_2}{R_2} \cdot \ln \frac{i_a}{i_b} \text{ radians} \quad \ldots\ldots \quad (6)$$

Here δ is known (see previous paragraph) and ω likewise, so that (6) is an equation which has to be satisfied by L_2, R_2, i_a and i_b.

It has already been said that the frequency f_c of the contact may also be lower than the mains frequency f, say $f_c = 2f/3$. The lower the frequency f_c, the larger the angle δ must be, that is to say the larger (according to (6)) L_2/R_2 must be (it would not help to increase the ratio i_a/i_b because δ is only proportional to the logarithm of this ratio). Any increase of L_2/R_2 however involves larger dimensions of the coil and cannot therefore be considered if one wishes to keep to the desired small dimensions of the switch.

A second equation between some of these quantities follows from the fact that the current i_a which just attracts the armature must be so small that in the stationary state the current reaches this value even at the lowest mains voltage occurring. Assuming that the mains voltage may drop to 20% below the nominal value, and ignoring L_1 with respect to L_2 and R_1 with respect to R_2, then we must have

$$i_a < \frac{0{,}8\, V_{\max}}{\sqrt{\omega^2 L_2^2 + R_2^2}} \quad \ldots\ldots \quad (7)$$

Another equation arises from the limit that has to be set for the power P taken up by the coil in the working state (thus when the lamp is ignited). Owing to the desired small dimensions of the starter switch, this power dissipation must be very small (< 1 watt). When the arc voltage of the lamp is indicated by V_b (= about 110 V) then

$$P = \frac{V_b^2}{\omega^2 L_2^2 + R_2^2} \cdot R_2, \leqq 1 \text{ watt.} \quad \ldots \quad (8)$$

The equations (6)-(8) furnish a guide for the designing of the switch. In its ultimate construction the characteristic quantities have the following values:

$L_2 = 28$ H, $\quad i_a = 10$ mA,
$R_2 = 12\,000\ \Omega$, $\quad i_b = 1$ mA.

The equations (7) and (8) are amply satisfied, since according to (7) i_a could amount to as much as 16.7 mA and according to (8) $P \approx 0.7$ watt. According to (6) however $\delta = 1.7$ radians $= 97°$. This calculated value is therefore much smaller than our target, but owing to some circumstances not so far taken into consideration the actual value is rather higher than the calculated value. In addition to the mechanical inertia, which delays both the moment of closing and that of opening, one must take into account the spark arising upon the contact being opened, so that the current is apt to flow longer than has been calculated above. Moreover, to ensure sufficient contact pressure, the armature is resiliently connected to the contact. Consequently when the armature is closed and the current in the coil is diminishing the contact will not open until the armature is released. As a result of all these effects, the actual value of δ becomes more than half a cycle, as is shown by oscillograms. As to the switching-on moment, a closer investigation would become rather lengthy, but oscillograms show it to lie in the neighbourhood of the desired value 0. The value of k corresponding to $t_0 \approx 0$ and $\delta \approx 200°$ is approximately 1.3 according to fig. 9. As already stated, owing to the saturation of the choke, k reaches a much higher value (about 2).

Constructional details

It will already have been noticed that i_a is much

greater than i_b, the ratio i_a/i_b being 10. This was necessary to keep the contact closed long enough (see equation (6)). This large ratio of the two currents has been obtained by designing the construction on the lines indicated in *fig. 10*. Here the armature is a small iron pin affixed to a leaf spring, one end of which is clamped while the other end carries the moving pole of the contact. A stop ensures a fairly high tension in the spring in the state of rest. The armature protrudes into an opening in the magnetic circuit. The dimensions are such that the magnetic flux passing through the armature in the closed state is far in excess of that in the state of rest. Consequently i_a is much greater than i_b.

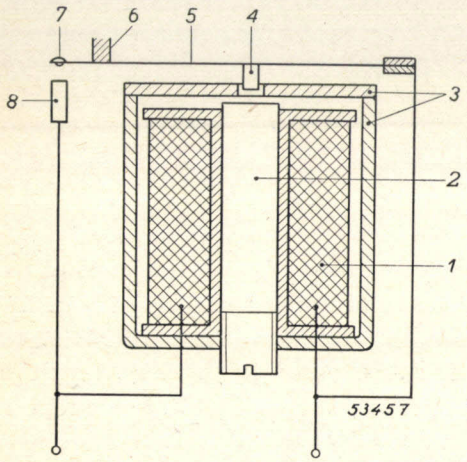


Fig. 10. Enlarged diagrammatic cross-section of the electromagnetic starter switch. *1* = coil, *2* = core, *3* = magnetic circuit, *4* = armature, *5* = leaf spring, *6* = stop, *7* = movable pole of the contact, *8* = fixed pole.

The explanation of this is as follows. Let us suppose that of the flux Φ in the core a part $p_a \cdot \Phi$ passes through the armature in the state of rest and a part $p_b \cdot \Phi$ in the closed state, whereby $p_a \ll p_b$ (say $p_a = 2\%$, $p_b = 20\%$). We assume that the bias in the spring is so great that the spring tension may be regarded as being practically constant, regardless of the position of the armature. Taking Φ_a as the value of Φ corresponding to the current i_a and Φ_b as the value corresponding to i_b, since in both cases the force exercised upon the armature just corresponds to the spring tension, we have by approximation $p_a\Phi_a = p_b\Phi_b$.

Since the flux is approximately proportional to the current passing through the coil, $p_a i_a \approx p_b i_b$, or $i_a/i_b \approx p_b/p_a$, which according to the supposition is large with respect to unity.

The core is partly threaded (fig. 10) so that it can be adjusted to the best position with a screwdriver.

In addition to the switching mechanism proper the starter must contain some other components. First of all there is a capacitor (6000 pF) connected in parallel with the lamp, with the object of suppressing radio interference while the lamp is ignited and to minimize sparking at the contact upon ignition. For the latter purpose it is necessary to have a resistor in series with the capacitor, so as to reduce the discharge current impulse upon the contact being closed. Room has to be found in the starter also for this resistor (R_3 in fig. *11a*), unless the arrangement of fig. 11*b* is adopted, where the filaments take over the current-limiting function of R_3. In that case, however, either the capacitor has to be placed outside the starter or the starter

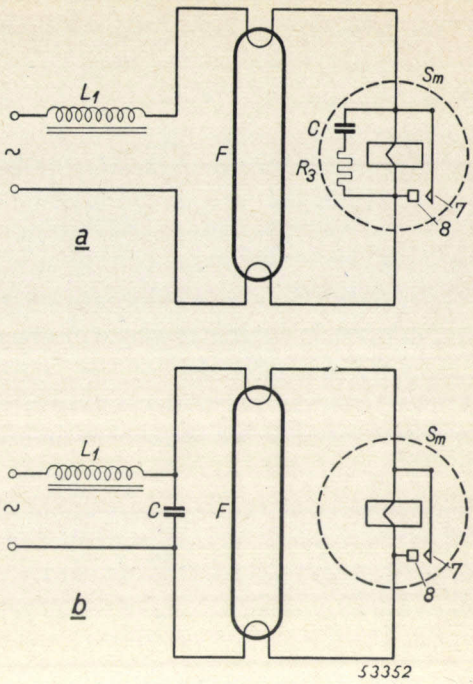


Fig. 11. Two ways of installing an anti-interference capacitor C, *a*) on the starter side of the filaments but in series with a current-limiting resistor R_3, *b*) on the mains side of the filaments, the resistance of the filaments performing the function of R_3. F = fluorescent lamp, L_1 = ballast choke, S_m = starter, *7* and *8* = respectively movable and fixed poles of the contact.

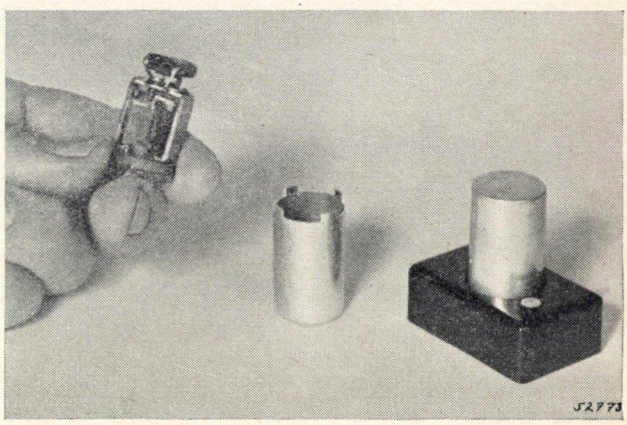


Fig. 12. The new starter switch. On the left opened, on the right placed in a holder.

itself has to be provided with two extra contacts, but then this type of starter would no longer be interchangeable with the glow-discharge bimetallic starter. The solution according to fig. 11*a* has therefore been given preference.

Fig. 12 shows the interior of this starter switch. The external dimensions are: diameter 20 mm, height 34 mm.

Fig. 13 shows how the starters can be mounted in a fixture.

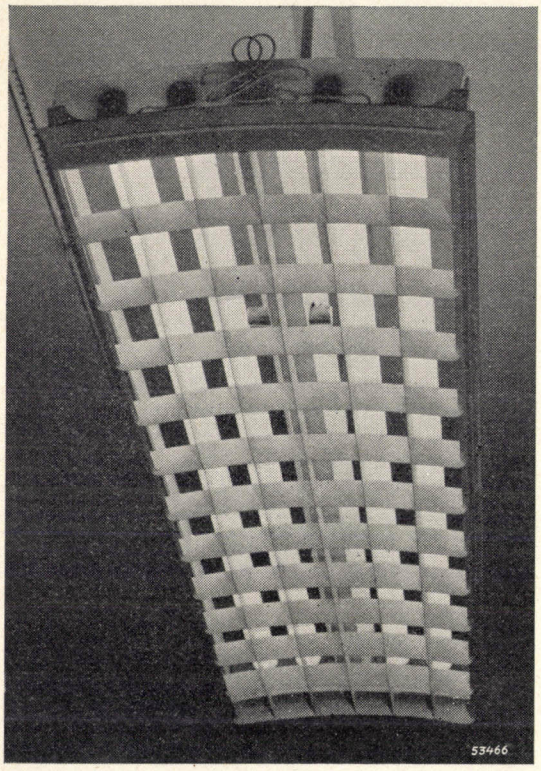


Fig. 13. Fixture (viewed obliquely from underneath) with four TL lamps. In the photo two of the four starters can be seen.

Results

Measurements have shown that under normal conditions the new starter ignites the lamp within 0.3-0.4 sec. An example of this is given in *fig. 14*, which is the oscillogram of the voltage across one of the filaments during the heating and ignition process. In fig. *15a* is the oscillogram of the current in the magnet coil (the exponentially diminishing part is clearly discerned); b is the oscillogram of the voltage peak across the lamp at each interruption.

These voltage peaks, which have an amplitude of about 2000 V, are much greater than the peak voltage at which according to fig. 3 the lamp ignites with cold cathodes (about $360/\sqrt{2} \approx 500$ V). From this it is not to be concluded, however, that the starter will ignite the lamp immediately after switching on, which would be entirely in disaccordance with the object. The ignition of the lamp, that is to say the starting of a glow discharge and the changing of that discharge into an arc, requires a much higher voltage when only a weak source of energy is available than is required when that source is a strong one. Fig. 3 only holds when a strong source of energy is used, such as the lighting mains. In the case of the starter, however, there is only the low energy available that is accumulated in the choke, and even the much higher voltage peaks which fig. 15*b* shows as occurring are not sufficient to ignite the lamp with cold cathodes.

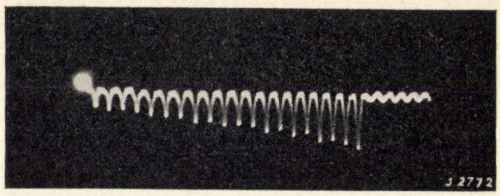
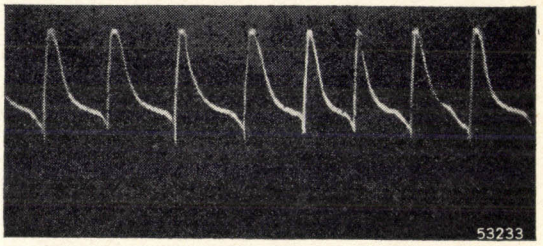


Fig. 14. Oscillogram of the voltage across one of the filaments of a TL 40 W lamp while heating up with the aid of the electromagnetic starter. After 20 cycles (0.4 sec) the lamp is ignited.

From the increase in amplitude of the heating voltage (fig. 14) it is to be deduced that the cathodes have in fact reached the right temperature before the lamp is ignited.



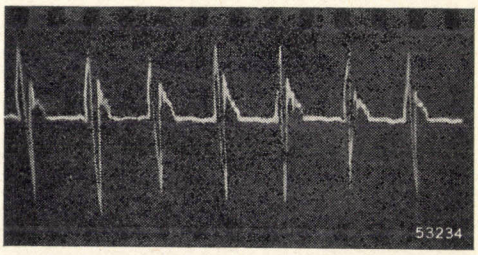


Fig. 15. Oscillogram of *a*) the current i_2 in the magnet coil (the differences in the intervals between the current peaks are due to irregularities in the film transport), *b*) the voltage peaks across the lamp while the cathodes are heating up. The amplitude of the peaks is about 2000 V.

If conditions are highly unfavourable (for instance low ambient temperature) it may take from 0.5 to 1 sec before the lamp ignites, but this is still shorter than the time taken with the older types of starters.

This new starter can be used not only for the 40 W TL lamp but also for the smaller 25 W type of lamp.

THE NEW CANDLE

by W. de GROOT.

535.241.42:535.233

This article is concerned with a circular letter sent out by the "Comité International des Poids et Mesures" bringing the "new candle" into use on the 1st January 1948. The brightness of a black body is calculated in terms of the new candle as a function of the temperature with the aid of Planck's radiation formula (with $c_2 = 14385\ \mu\ °K$). For the mechanical equivalent of light the value $M = 683$ new lumen/watt (nlm/W) is found.

Introduction

The "new candle", a unit for measuring luminous intensity, is the subject of an article [1]) which appeared in this journal in 1940, and it was to have been introduced on the 1st January of that year. Owing to the difficulties of international communication at that time its introduction was postponed; on the 1st January 1940 the "Comité International des Poids et Mesures" sent out a circular letter to the various countries asking them to await further advice ("nouvel avis") before changing the units.

It was not until 1947 that a second circular was despatched in which the 1st January 1948 was fixed as the date on which the new unit was to come into force. An unofficial translation of this circular reads as follows:

Concerning changes in photometric units

By virtue of the powers which were conferred on it by the Conférence Générale des Poids et Mesures in 1933, the Comité International, considering the resolution of the 1937 session (Procès-Verbaux du Comité International, 1937, pp. 236 and 64) and taking note of the desire expressed by the Comité Consultatif de Photométrie in 1939 (Procès-Verbaux, 1939, p. P28), with a modification concerning the date of application, decided that the "new candle" would come into force on the 1st January, 1948.

The present resolution constitutes the "further advice" of execution for which the circular of 1st January, 1940, signed by the President and Secretary of the Comité International des Poids et Mesures asked the various countries to wait, before proceeding with any change of unit. The Comité International adopts "résolution 3" unaltered concerning photometric units, submitted to them in 1939 by the Comité Consultatif de Photométrie (Procès-Verbaux, 1939, pp. P32-P35), the text of which is reproduced below:

1. *The present situation*

At the present time, the units of luminous intensity in use in different countries are based on flame standards or on the values assigned to certain electric incandescent lamps maintained in the National Laboratories. France, Great Britain and the U.S.A. agreed in 1939 to adopt a common unit, which was subsequently adopted in certain other countries. Various proposals had been made with a view to establishing a unit which should be based on a primary standard source, that is to say, one reproducible by means of a specification. Nevertheless, it is only in recent years that such a source has been shown to be practicably realised.

2. *The primary standard*

This standard, adopted in principle by the Comité International des Poids et Mesures in 1930 and 1933, is a total radiator (black body), at the freezing point of platinum, and the value of the unit of luminous intensity (adopted in 1937) is such that the brightness of 1 cm² of the standard is 60 units. The form in which the standard is actually realised is, in its essentials, that which was conceived by the National Bureau of Standards at Washington and which is described in the Procès Verbaux du Comité International des Poids et Mesures, 1931 (p. 249). The colour of the light furnished by this standard does not differ sensibly from that emitted by the flame standards and the incandescent lamp standards referred to in paragraph 1.

3. *Measurement of light sources having colour temperatures different from that of the primary standard*

Modern light sources (even if one excepts those which are markedly coloured) have colour temperatures considerably higher than that of the primary standard, and it is consequently necessary to define the following procedure by which these sources are to be evaluated. The method approved by the Comité International des Poids et Mesures in 1937 consists in using a procedure which is based on the relative luminosity curve adopted by this Committee; e.g. a coloured filter is used which, placed between the primary standard and the photometer, gives a colour comparable with that of the light to be measured. The transmission factor of this filter is determined from its spectral transmission curve by means of the relative luminosity curve adopted in 1933 by the Comité International des Poids et Mesures (Procès-Verbaux, 1933, p. 62).

4. *Definition of the units*

The photometric units may be defined as follows:

I. The new candle (unit of luminous intensity). — The magnitude of the new candle is such that the brightness of a total radiator at the freezing point of platinum is 60 new candles per cm.²

II. The new lumen (unit of luminous flux). — The new lumen is the luminous flux emitted in unit solid angle (1 steradian) by an uniform point source having a luminous intensity of one new candle.

[1]) G. Heller, The new luminous standard, Philips Techn. Rev. 5. 1-5, 1940.

5. *The Practical realisation of the units.*

While it should be possible to realise the primary standard at any time and in all laboratories possessing the necessary apparatus, in the majority of practical applications the reference standards will remain the secondary standard carbon or tungsten filament lamps, the luminous intensities of which will have been determined by reference to the primary standard. The precision of comparisons of these lamps between themselves is higher than the precision with which the primary standard can in practice be reproduced. Secondary standard lamps of this type will be maintained in the various National Laboratories and at the Bureau International des Poids et Mesures. Values attributed to these secondary standards with reference to the primary standard will be determined either by direct comparisons in one or more of the principal National Laboratories or indirectly by inter-comparison with other similar lamps whose values have been determined by direct comparison. Thus, the values assigned to the secondary standards maintained at the Bureau International and in each of the National Laboratories will be expressed in terms of the mean unit, which will itself be determined as the average of the results of all the laboratories, in which the primary standard will have been realised.

An analogous procedure will be used in case of lamps having colour temperatures higher that than of the primary standard, just as in the derivation of the lumen from the candle.

The brightness ("luminance") of a black body as a function of temperature

Since the new light unit is defined in terms of the brightness ("luminance") of the radiation from a black body at a prescribed temperature, it is obvious that we should know how this brightness ("luminance") varies as a function of the temperature.

We shall start from the conventional standpoint that the luminous intensity of a light source is determined with the aid of the international relative luminosity curve $V(\lambda)$, which reaches its maximum value (= 1) at the wavelength $\lambda = 0.555$ μ. Let $E(\lambda, T)\,d\lambda$ (measured in watts per cm^2) be the energy irradiated in the hemisphere, in the wavelength range λ, $\lambda + d\lambda$, per cm^2 of a black body of the absolute temperature T. This amounts to $M \cdot E(\lambda, T)\, V(\lambda)\, d\lambda$ lumen, where the constant factor M — thus defined — represents the so-called mechanical equivalent of the light.

By integration over all wavelengths of the visible spectrum one finds the total luminous flux emitted by 1 cm^2 in lumen:

$$\Phi = M \int_{0{,}38\,\mu}^{0{,}78\,\mu} E(\lambda, T)\, V(\lambda)\, d\lambda \quad . \quad . \quad . \quad (1)$$

According to Lambert's law the luminous intensity in the direction perpendicular to the respective plane of 1 cm^2, which is nothing else than the brightness ("luminance") B, is equal to $(1/\pi) \times$ the luminous flux, so that

$$B = \frac{\Phi}{\pi} = \frac{M}{\pi} \int E(\lambda, T)\, V(\lambda)\, d\lambda. \quad . \quad (2)$$

The determination of the new candle implies that for $T = T_{Pt}$, the freezing temperature of platinum, B must equal 60, so that

$$60 = \frac{M}{\pi} \int E(\lambda, T_{Pt})\, V(\lambda)\, d\lambda \quad . \quad . \quad (2a)$$

Eliminating M from (2) and (2a) by division, one arrives at

$$B = 60\, \frac{\int E(\lambda, T)\, V(\lambda)\, d\lambda}{\int E(\lambda, T_{Pt})\, V(\lambda)\, d\lambda}. \quad . \quad . \quad . \quad (3)$$

From this one can determine B by calculating $E(\lambda T)$ with the aid of Planck's formula

$$E(\lambda, T) = c_1 \frac{\lambda^{-5}}{e^{c_2/\lambda T} - 1}, \quad . \quad . \quad . \quad (4)$$

and substituting the value of T_{Pt}.

If $c_2/\lambda T > 7$ for all wavelengths of the visible spectrum, the denominator is equal to exp $(c_2/\lambda T)$ to a sufficient degree of accuracy (0.1%), so that formula (4) may be replaced by what is known as Wien's formula:

$$E(\lambda, T) = c_1\, \lambda^{-5}\, e^{-c_2/\lambda T} \quad . \quad . \quad . \quad . \quad . \quad . \quad (4a)$$

This is the case for $T < 3000$ °K ($\lambda \leqq 0.7\mu$), whilst if one is satisfied with an error of 1% in the middle of the spectrum ($\lambda = 0.6$ μ) formula (4a) can even be used up to $T \approx 5000$ °K.

Now the values of c_1 and c_2 are more or less uncertain[2]). As regards c_1, this does not give rise to any difficulty because this factor does not occur in equation (3), but the expression does depend on the value of c_2. In this article we shall put

$$c_2 = 14385\ \mu\ °K,$$

in agreement with the theoretical value $c_2 = c\,h/k$, (c = velocity of light, h = Planck's constant, k = Boltzmann's constant), which has been given by Dumont and Cohen[3]), viz. 14384.7 $\pm$ 1.9.

---

[2]) See for instance H. T. Wensel, The international temperature scale and some related physical constants, J. Res. Nat. Bur. Stand. **22**, 375-395, 1939 and [3]).

[3]) J. W. M. Dumont and C. R. Cohen, Our knowledge of the atomic constants F, N, m and h in 1947 and of other constants derivable therefrom. Rev. mod. Phys. **20**, 82-108, 1948 (No. 1); see also R. T. Birge, New table of values of the general physical constants (as of August 1941), Rev. Mod. Phys. **13**, 233-239, 1941 and Rep. Progress Phys. London **7**, 126-134, 1941.

Equation (3) depends upon the value of c_2 not only explicitly but also implicitly, since the value that has to be ascribed to T_{Pt} is likewise dependent on c_2 (2041.7 °K for $c_2 = 14385$).

In connection with the freezing point of platinum, it must be noted that temperatures above 1336 °K are usually determined by comparing the radiation of a black body monochromatically with that of a black body at the temperature of melting gold. The latter temperature is exactly known ($T_{Au} = 1336$ °K) because it can be measured with a gas thermometer. The temperature required then has to be derived from the measured ratio of radiations with the aid of Planck's (or Wien's) formula, taking a certain value of c_2 (the international temperature scale of 1931 prescribes $c_2 = 14320$ μ °K).

Using Wien's formula it then follows that

$$\frac{1}{T_{Au}} - \frac{1}{T} = \frac{\lambda}{c_2} \ln R, \quad \ldots\ldots\ldots \quad (5)$$

where R represents the monochromatic ratio of radiations referred to. If the unknown temperature T could be measured in some other way, for instance also with the gas thermometer, then we should have a means of determining c_2. Van Dusen and Dahl [4]) have recently done this for the melting points of Ni and Co, employing the gasthermometrical determinations of Day and Sosman obtained with the same samples of metal. They found $c_2 = 14382 \pm 6$ μ °K, which agrees with the "theoretical" value 14385, whilst at the same time it proves that the value of 14320 adopted in the international temperature scale is too low.

For the freezing point of platinum, which cannot be measured with a gas thermometer, one finds

$$R = R_0 = 299{,}0 \quad \text{for} \quad \lambda = \lambda_0 = 6528 \text{ Å} = 0{,}6528\ \mu.$$

From formula (5) it therefore follows that for T_{Pt}

$$\frac{1}{T_{Au}} - \frac{1}{T_{Pt}} = \frac{\lambda_0 \ln R_0}{c_2} = \frac{3{,}72125}{c_2}.$$

Introducing these values of T_{Pt} and c_2 in equation (3) we find for B as a function of T the figures given in *table I*. The dependence of B on T as graphically represented in *fig. 1* can be expressed, approximately, by the formula

$$\log B = 7{,}224^5 - 11{,}437\left(\frac{1000}{T}\right) + 0{,}648\left(\frac{1000}{T}\right)^2, \quad (6)$$

which holds for $T = 1000$ °K up to $T \approx 5000$ °K[5]).

Table I. The brightness ("luminance") B of a total radiator (black body) (in new c/cm²) as function of the absolute temperature T for $c_2 = 14385$ μ °K and $T_{Pt} = 2041.7$ °K.

T (°K)	B (T) (nc/cm²)
1000	0.000273
1200	0.0139
1400	0.243
1600	2.14
1800	11.76
2000	46.5
2041.7	**60**
2200	145
2400	373
2600	835
2800	1670
3000	3050
3500	10220
4000	25500
4500	51900
5000	91800

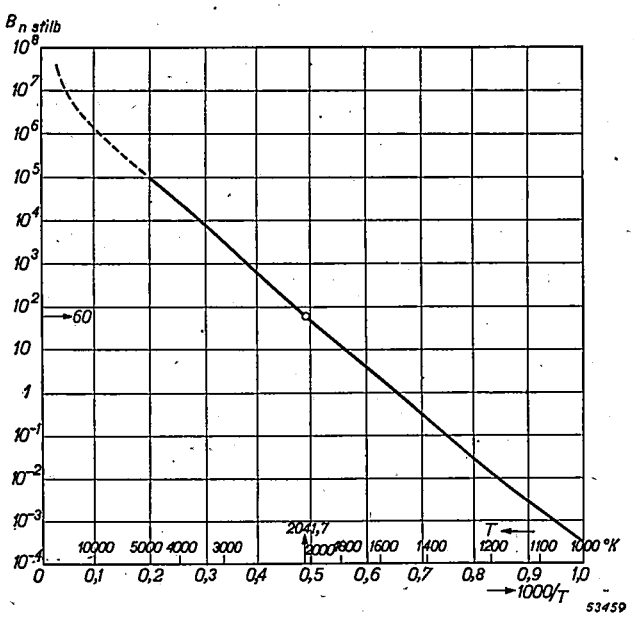


Fig. 1. Graphical representation of the brightness (luminance) B of a total radiator (black body) as function of the absolute temperature T, plotted from the values given in table I.

For $T > 5000$ °K, B increases with T more rapidly than is indicated by (6). It can be shown that for $T \to \infty$ log B approaches (const. + log T), whilst for $T = \infty$ log formula (6) would give $B = 7.2245$.

The mechanical equivalent of light

To calculate the mechanical equivalent of light M one can use equation (2a) in combination with (4) or (4a). It is seen that M is likewise dependent on the value of c_2, but it also depends on the value of c_1. The following equation can be deduced for the effect of these two quantities upon M

[4]) M. S. van Dusen and A. I. Dahl, J. Res. Nat. Bur. Stand 39, 291-295, 1947 (No. 3).

[5]) The fact that an equation of this shape must apply, at least as regards the first two terms, can be deduced from the fact that monochromatically, according to Wien's formula, the radiation and thus also the brightness ("luminance") are proportional to exp. $(-c_2/\lambda T)$. Since the wavelenght range of visible light can be regarded as a rather narrow band round about the wavelength $\lambda = 0.555$ μ, it follows that

$$\ln B = A - B/T,$$

where A is a constant and $B \approx c_2/0.555$. This formula has already been given by Nernst; see also W. Geiss, Das Licht, 13, 19-36, 1943 and E. F. Caldin, Proc. Phys. Soc. London 57, 440-443, 1945.

$$\frac{dM}{M} = -\frac{dc_1}{c_1} + \frac{dc_2}{775},$$ [6])

where c_2 is expressed in μ °K.

In the calculation of M, substituting for c_1 the value recommended by Birge (1941)

$$c_1 = 3{,}7403 \cdot 10^4\ W\mu^4/cm^2$$

and taking for c_2 the value

$$c_2 = 14385\ \mu\ °K,$$

we find $M = 683$ new lumen/watt [7]).

It would be highly desirable to compare this value with a direct experimental determination of the quantity M, but the literature on the subject gives only scanty data. In most cases calculated values are given (with different values for c_1 and c_2 and a different light unit). M may for instance be determined directly by measuring on the one hand the luminous intensity of the light source and on the other hand the spectral energy distribution in absolute units. This has been done by Krefft and Pirani [8]), among others, using a sodium lamp; the value found by them is $M = 694 \pm 15$ Hefner-lumen/watt $= 640 \pm 15$ new lumen/watt. The difference compared with the calculated value, 683 nlm/W, is thus rather considerable. It is desirable that similar measurements should be repeated, bearing in mind, however, that in practice the relative luminosity curve of any observer never corresponds precisely to the international relative luminosity curve V (λ). The observers will therefore have to be very carefully selected and preferably a large number of observers should participate.

[6]) The number 775 is the value of the product $\lambda_c \cdot T_{Au}$, where T_{Au} is the melting point of gold = 1336 °K and λ_c the so-called Crova wavelength at the freezing temperature of platinum, viz. $\lambda_c = \int \lambda E(\lambda, T_{Pt})\, d\lambda / \int E(\lambda, T_{Pt}) d\lambda = 0{,}58\ \mu$.

[7]) When calculating M with the value of c_2 which has been taken in the international temperature scale, namely $c_2 = 14320\ \mu$ °K, and with $c_1 = 3.7403 \cdot 10^{-16}$ W · m^2, we find $M = 627$ nlm/W. See also E. F. Caldin, Proc. Phys. Soc. London 58, 207-210, 1946.

[8]) H. Krefft and M. Pirani, Z. techn. Phys. 13, 367-369, 1932.

ABSTRACTS OF RECENT SCIENTIFIC PUBLICATIONS OF THE N.V. PHILIPS' GLOEILAMPENFABRIEKEN

Reprints of these papers not marked with an asterisk can be obtained free of charge upon application to the Administration of the Research Laboratory, Kastanjelaan, Eindhoven, Netherlands.

1719a: M. Gevers en F. K. du Pré: Power factor and temperature coefficient of solid (amorphous) dielectrics (Trans. Faraday Soc. 42A, 47-53, 1946).

For the contents of this paper, see Philips Techn. Rev. **9**, 91-96, 1947, No. 3 and these abstracts, No. **1726.**

The subject contained in this paper has been dealt with extensively in Philips Res. Rep. **1**, 197-224, 279-313, 361-379, 447-463, 1946.

1763: P. Bayens: The effect of operating conditions on the throwing power of cyanide cadmium plating solutions (Third Int. Conf. on Electrodeposition, No. 13).

Bright cadmium electrodeposits may be formed under widely different conditions, but for economic working, i.e. for high throwing power, with a given composition of the solutions there are narrow limits of temperature and current density. These limits are studied experimentally.

1771: C. J. Bouwkamp:Concerning a new transcendent, its tabulation and application in antenna theory (Quart, appl. Math. 4, 394-402, 1948).

The author discusses a new function $E_1(z)$ which is related to the integral sine and cosine functions in the same way as the latter are to the ordinary sine and cosine functions. Numerical evaluation is accomplished by power-series expansion (z small) and asymptotic expansion (z large). The gap is bridged by a Taylor-series method (z moderate). A six-decimal table covering the range $z = 0(0.2)20$ is included. Application of the new function to Hallén's antenna problem is indicated. Additional tables of antenna functions are given.

1772*: F. A. Kröger: Some aspects of the luminescence of solids (310 p. 72 figs., 27 tables Elsevier Publ. Cy, Inc., Amsterdam, New York, London, Brussels, 1948.

This book is a monograph, based on experimental work on luminophors, carried out in the Philips Research Laboratory at Eindhoven 1940-1945. It does not pretend to give a complete representation of the present knowledge regarding the phenomenon of luminescence in solids, nor does it give a general survey. It contains some hitherto unpublished experimental results together with theoretical considerations regarding certain aspects of this field of science. In chapter I a brief consideration is given to the energy levels of pure and disturbed crystals. Starting from the energy diagram it is shown that different types of luminescent effects must exist. Emissions of activated luminophors reported in literature have been tabulated and classified according to the diagram. Further attention has been paid to the different mechanisms of the excitation process and its most important attendant phenomenon.

Four further chapters are devoted to new experimental results concerning some particular systems, viz.: tungstates, molybdates and luminophors activated by manganese, uranium and titanium. For manganese the activating properties of the tetravalent ion have been discovered, beside those of the divalent ion already known.

In the sixth and final chapter the influence of temperature on the efficiency of luminescence has been considered both from the experimental and from the theoretical angle.

1773*: W. Elenbaas: Dissipation of heat by free convection (De Ingenieur **60**, 021-034, 1948, No. 7).

A body differing in temperature from the surroundings loses energy not only by radiation but also by conduction and convection. The general laws governing this latter dissipation of heat are investigated. The many quantities governing this transfer may be combined into a few dimensionless numbers by means of similarity considerations. This leads to an important simplification and facilitates the survey of experimental and theoretical results. The above mentioned considerations are first applied to bodies which may be characterized by one linear dimension only (the vertical plate, the horizontal cylinder, the sphere), and next to bodies characterized by two such quantities (the vertical cylinder of finite height, cooling ribs, the inner surface of vertical tubes).

This paper appears in full in Philips Res. Rep.

1774*: J. M. Stevels: Progress in the theory of the physical properties of glass (104 p., 26 figs., 22 + 5 tables, Elsevier Publishing Cy., Inc., Amsterdam, New York, London, Brussels, 1948.

Starting from the fruitful ideas of Zachariasen and their experimental affirmation by Warren and his coworkers, it was possible to get a much better and detailed knowledge of the structure of glass, and such properties as density, electric conductivity, dielectric losses and refraction.

In chapter I a survey is given of the knowledge of the structure of glass as far as it may be considered generally accepted.

Chapter II deals with the density of glass. With the aid of a new density relation, the physical background of which is amply discussed, various interesting conclusions are drawn about the structure of a number of glasses (especially of the borate glasses).

In Chapters III and IV the electric conductivity and the dielectric losses of glass are discussed. The general picture of the behaviour of the metallic ions, which jump from interstice to interstice in the network, is worked out extensively. This theory leads to a number of quantitative relations which are adequately checked experimentally.

In Chapter V a theory of the molecular refraction is given, based on the new conceptions.

Finally, in a number of appendices all the glasses mentioned in the book are listed comprehensively.

1775: K. ter Haar and W. Westerveld: The colorimetric determination of nickel as $Ni_{(4)}$ dimethylglyoxime (Rec. trav. Chim. Pays Bas, **67**, 71-81, 1948).

A description is given of a colorimetric determination of nickel as $Ni_{(4)}$ dimethylglyoxime, but in contrast to the customary methods, use is made of persulphate as oxidizing agent. The influence of other metallic ions has been investigated too.

It appears that, of the elements investigated Ag must be removed, while the alkaline earth metals give a sulphate precipitate which can be removed by centrifuging. The determination of Ni in the presence of Mn, Fe, Cu and Co presents the greatest difficulties. In many cases the writhers have succeeded finally in determining nickel in the presence of these elements without removing them. Thus it is possible to determine accurately 5% Ni and over in manganese, 0.25% and over in iron, 0.05% and over in copper and 0.05% and over in cobalt.

In general it has been established that the highest accuracy is obtained when full attention is paid to the following points:

1) the avoidance of ammonia
2) the regulation of the amount of dimethylglyoxime.
3) the acidity of solution.

If one of these points is not in order, the degree of accuracy becomes less. This is the case in the determination of Ni in the presence of cobalt and copper, where the presence of ammonia is a necessary condition for the formation of the colour.

It can be remarked that this method is extensively applied in the Philips Laboratory in the determination of Ni in chrome-iron, Mo and W compounds.

1776: C. Zwikker: Systematic relations existing between the properties of solid materials (Physica **14**, 35-47, 1948, No. 1).

When describing the properties of solids it is necessary to distinguish between "generalized forces" or intensity parameters (i) and "generalized displacements" or extensive parameters (e). The numerical factors occuring in the linear equations expressing the de as functions of the di are called by the author coefficients and those determining the di as function of the de, moduli.

Between the different moduli there exist systematic relations and likewise between the different coefficients. The relations are expanded to the quadratic effects. Care should be taken to distinguish between a modulus and the corresponding reciprocal coefficient.

The theory is extended to include systematic relations between "resistances" and "conductivities", of which relations examples are given too.

1777: F. A. Kröger, W. Hoogenstraten, M. Bottema and Th. P. J. Botden: The influence of temperature quenching on the decay of fluorescence (Physica **14**, 81-86, 1948, No. 43).

Temperature quenching causes a marked increase of the rate of decay of fluorescence. It is shown that both the efficiency of fluorescence and the decay are determined by the probabilities of the fluorescence transition and of a radiationsless transition. By combining data from measurements of the efficiency and the decay, it is possible to obtain the two transition probabilities separately, and both as a function of the temperature. The results with $(NH_4)_3UO_2F_5$ and Mg_2TiO_4. Mn^{4+} have been used to verify whether the raditionless process follows the theories of Mott and Seitz, or that of Möglich and Rompe; they are found to favour the former. A few examples are dealt with.

1778: B. D. H. Tellegen: Zijn er naast capaciteiten, weerstanden, zelfinducties nog andere soortgelijke grootheden denkbaar? (T. Ned. Radiogen. **13**, 73-98, Nr 3) in Dutch

The contents of this article are covered by those of Philips Res. Rep. 3, 81-101, 1948, No. 2 (see these abstracts **R** 73).

1779: C. Zwikker: Vectorial theory of gear wheel tooth profiles (Appl. Sci. Res. **A 1**, 139-150, 1948, Nr. 2).

The mechanical problem of the admissible gear tooth profiles is dealt with by a method using the geometry of the complex plane. This method is better known in the electrical branch of technical science, but may — as is shown in this paper — easily be generalized to a complete version of plane geometry and applied to mechanical problems.

1780: H. C. Hamaker: Current distribution in triodes neglecting space charge and initial velocities (Appl. Sci. Res. **B 1**, 77-104, 1948, Nr. 2).

A theory of the current distribution in triodes with positive grid is developed on the assumption that space charge and the initial velocities of both primary and secondary electrons may be neglected. This theory, which is originally due to De Lussanet de la Sablonière, has been put in a more lucid form, and a graphical method has been developed to check the applicability of this theory to any set of observations. From the graphs used for this purpose the different distribution functions which enter the equations can be read off in a very simple manner. In some cases theory and experiment are in excellent agreement; discrepancies occuring in other cases are discussed. In connection with these observations the basic assumptions underlying the theory are subjected to a closer scrutiny.

1781: A. van der Ziel: The virtual cathode problem for cylindrical electrodes (Appl. sci. Res. **B 1**, 105-118, 1948, Nr. 2).

After a general discussion on the influence of space charge upon the potential distribution between parallel electrodes, the case of coaxial cylindrical electrodes is investigated. The resultant current-voltage characteristics are calculated and it is shown that the curves obtained are similar to those of the wellknown case of plane electrodes. The theory may be useful for the development of cylindrical tetrodes and pentodes, especially for transmitting valves.

1782: N. Warmoltz: A powerful light source for the illumination of Wilson cloud chambers (Appl. sci. Res. **B 1**, 139-142, 1948, No. 2).

A capillary flash tube for the photography of the tracks in a Wilson cloud chamber is described. At an energy input of 500 watt. sec per flash with a choke of 10 mH in series with the flashtube the light output amounts to 15 000 lumen·sec per flash. At a rate of 8 flashes per minute the lifetime of the tube exceeds 1,000,000 flashes at the energy stated above. At about 320 watt·sec the light output is ample sufficient for photographing cloud chamber tracks.

VOL. 10 No. 6, pp. 157-188 DECEMBER 1948

Philips Technical Review

DEALING WITH TECHNICAL PROBLEMS
RELATING TO THE PRODUCTS, PROCESSES AND INVESTIGATIONS OF
THE PHILIPS INDUSTRIES

EDITED BY THE RESEARCH LABORATORY OF N.V. PHILIPS' GLOEILAMPENFABRIEKEN, EINDHOVEN, NETHERLANDS.

AN IMPROVED X-RAY DIFFRACTION CAMERA

by W. PARRISH*) and E. CISNEY*).

548.73:621.386.1:778.332

For obtaining high quality X-ray diffraction patterns with minimum exposure times, an improved Debye-Scherrer camera has been designed and is produced by North American Philips Co., Inc. Various factors entering the design of the camera and interrelated in their influence on the properties of the patterns are considered in this article. The necessary compromises between such properties as line intensity, line sharpness (resolution), contrast and line shape are favorably affected by several resources. Line intensity is improved without loss of resolution by using a rectangular collimating aperture for the X-ray beam. Contrast is enhanced by surrounding the primary beam on its path to and from the specimen by a collimator and exit tube, thus diminishing the film blackening resulting from radiation scattered in the air. It is shown that these "anti-air-scatter tubes" must have definite dimensions in order to insure the limitation of air scatter to a minimum without causing undesirable blind areas in the diffraction patterns and avoiding any scattering from the tubes themselves. The optimum forms of the tubes for different purposes have been computed, and the cameras can be provided with one of several systems designed in accordance with the results of these computations. The tubes are made easily interchangeable. Handling of the cameras in general is simplified to a considerable extent by the application of certain mechanical design principles outlined by Buerger.

In this article a description is given of an improved camera for the photographic recording of X-ray diffraction patterns of polycrystalline (e.g. powder) specimens according to the Debye-Scherrer method. There is no need to enumerate here the many purposes which these patterns may serve. It is sufficient to state that they are used extensively in research and industrial laboratories for the identification or chemical analysis of materials, for the examination of crystalline structure and grain size, and for the analysis of stresses, texture etc. [1]).

Fig. 1 illustrates the well-known principle of the Debye-Scherrer camera. This camera is a cylindrical enclosure along the axis of which the cylindrical specimen is mounted; the film strip is placed against the inner wall of the camera. The X-ray beam (made as monochromatic as practicable) enters the camera through an aperture in the cylindrical wall. Parts of this beam are diffracted at definite angles by the tiny crystals in the specimen and produce characteristic diffraction lines on the film, while the diffracted part of the (primary) beam passes on to a stop or receiver, or may leave the camera through an aperture in the opposite cylindrical wall.

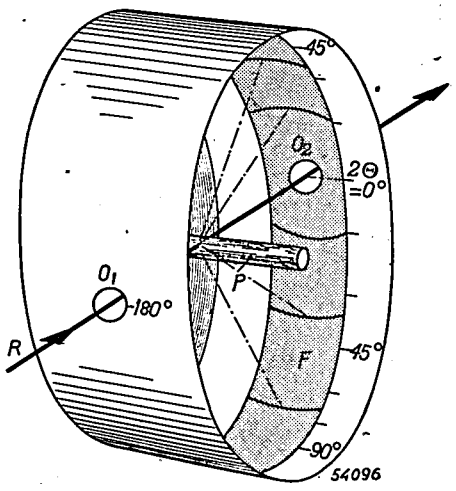


Fig. 1. Principle of the Debye-Scherrer camera. A monochromatic X-ray beam R enters the cylindrical camera through an aperture O_1 and is partly diffracted in the specimen P. The undiffracted part of the beam leaves the camera through the aperture O_2. The diffracted rays cause the lines (ring segments) of the diffraction pattern on the film F.

*) Philips Laboratories, Inc., Irvington-on-Hudson, N.Y., U.S.A.

[1]) A survey of the applications of the Debye-Scherrer method can be found, for instance, in Philips Techn. Rev. 5, 157-166, 1940. A few months ago an article in this Review was devoted to the "Geiger counter X-ray spectrometer", an apparatus also produced by North American Philips Co., Inc., and enabling the direct measurement of the intensity distribution of X-ray diffraction patterns (Philips Techn Rev. 10, 1-12, 1948 (No.1)). The Geiger counter method and the photographic method are well suited to supplement each other due to their different performance characteristics.

A well designed Debye-Scherrer camera should meet the requirements that, on the one hand, the recording of a pattern be made as easy and quick as possible, while, on the other hand, the highest possible quality of the resulting patterns be secured.

As far as ease of handling is concerned, the cameras produced by North American Philips Co., Inc., have been designed in the main in accordance with the cameras described a few years ago by M. J. Buerger [2]). The principles outlined by Buerger were aimed, among other things, at facilitating the alignment of the camera with the X-ray tube, the recovering of the alignment after temporary removal of the camera from its position, the centering of the specimen in the camera, the rapid mounting of the film, etc. The successful realization of such principles depends mainly on precise mechanical construction. Those are not the subjects which are extensively treated in this article, although some details relating to the aforementioned principles are given in *figs 2* and *3* and explained in the accompanying legends. On the contrary, this article deals much more thoroughly with the speed of recording and the quality of the patterns obtained.

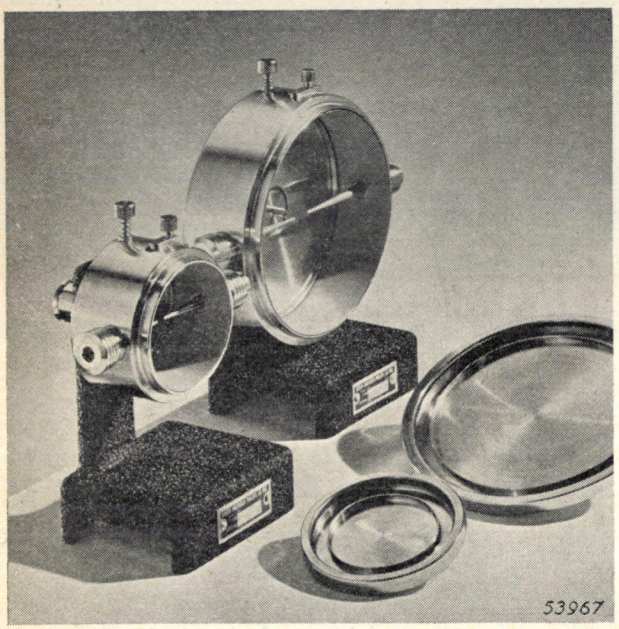


Fig. 2. The Debye-Scherrer cameras with diameters of 57.3 and 114.6 mm, as manufactured by North American Philips Co., Inc. Next to the cameras are the covers, fitting light-tight on the cameras, so that it is not necessary to make exposures in a dark room nor to cover the film with black paper. In each of these cameras the primary X-ray beam passes through two conical tubes between which the very thin rod-shaped specimen is mounted. After placing the specimen roughly on the axis of the camera it is accurately centered by means of a threaded "pusher" perpendicular to the axis. This is facilitated by slipping a small magnifying glass on the end of the exit tube. During the exposure the glass is replaced by a cap containing a small fluorescent screen, on which the primary beam and the shadow of the specimen may be observed. Thus the alignment of the camera and the centering of the specimen are checked. The fluorescent screen is covered at the inside with black paper, making the camera light-tight, and at the outside with lead glass, absorbing the remainder of the primary beam without obstructing the view of the fluorescent screen. The film is placed in the camera according to the Straumanis method: the film takes up nearly 360°, and two holes of normalized width of 9 mm are punched in it where the tubes are to be inserted. Careful design and machining of the tubes make it possible to remove them easily for mounting the film and to replace them in exactly the correct alignment. The film is expanded tightly against the inner wall of the camera by means of a movable finger which pushes one end of the film, the other end being fixed by a stop.

[2]) M. J. Buerger, The design of X-ray powder cameras, J. Appl. Phys. **16**, 501-510, 1945. Cf. also: M. J. Buerger, An X-ray powder camera, Amer. Mineralogist **21**, 11-17, 1936.

Properties involved in quality of pattern

Information about the nature of the X-rayed specimen can be deduced from the positions (i.e., the diffraction angles) of the diffraction lines, from their relative intensities and from the line shape. High quality patterns, therefore, will exhibit the following properties:

1) Recording of all lines that are of importance. This especially refers to very weak lines, which may often be important in quantitative chemical analysis by X-ray diffraction, and to lines at very small or very large diffraction angles (2Θ near zero or 180°, Θ = Bragg angle).
2) Great sharpness of lines. This will enable the diffraction angles to be determined very accurately and at the same time it will provide a good resolution of adjacent lines.
3) Good contrast of recorded picture, i.e., minimum and relatively uniform background density on the film in comparison to the density of the lines. A strong background would not only affect the observable recording of very weak lines mentioned in (1), but also impair the measurement of the correct relative intensities, for strong as well as for weak lines.
4) Good line shape, i.e., correct contour, uniform density, and constant intensity along the usable length of each line (insofar as the desired data do not actually depend on broadening, spottiness or specific intensity distribution of each line). This property is important for good definition of the position of the lines and for correct intensity measurements.

In order to meet the requirement of quick recording of patterns, especially in view of point (1), we must add to this list of desiderata:

5) High intensity of diffracted rays.

Camera design considerations relating to quality of pattern and speed of recording

When considering the design factors which influence the abovementioned properties it becomes apparent that in several instances the requirements are conflicting. For the sake of convenience let us start from the sharpness of lines.

Sharp definition of the lines mainly depends on the diameter of the camera, the width and divergence of the primary X-ray beam, and the thickness of the specimen.

Simple geometrical considerations show that the lines become sharper (i.e. narrower in relation to their mutual separation distances) with an increase

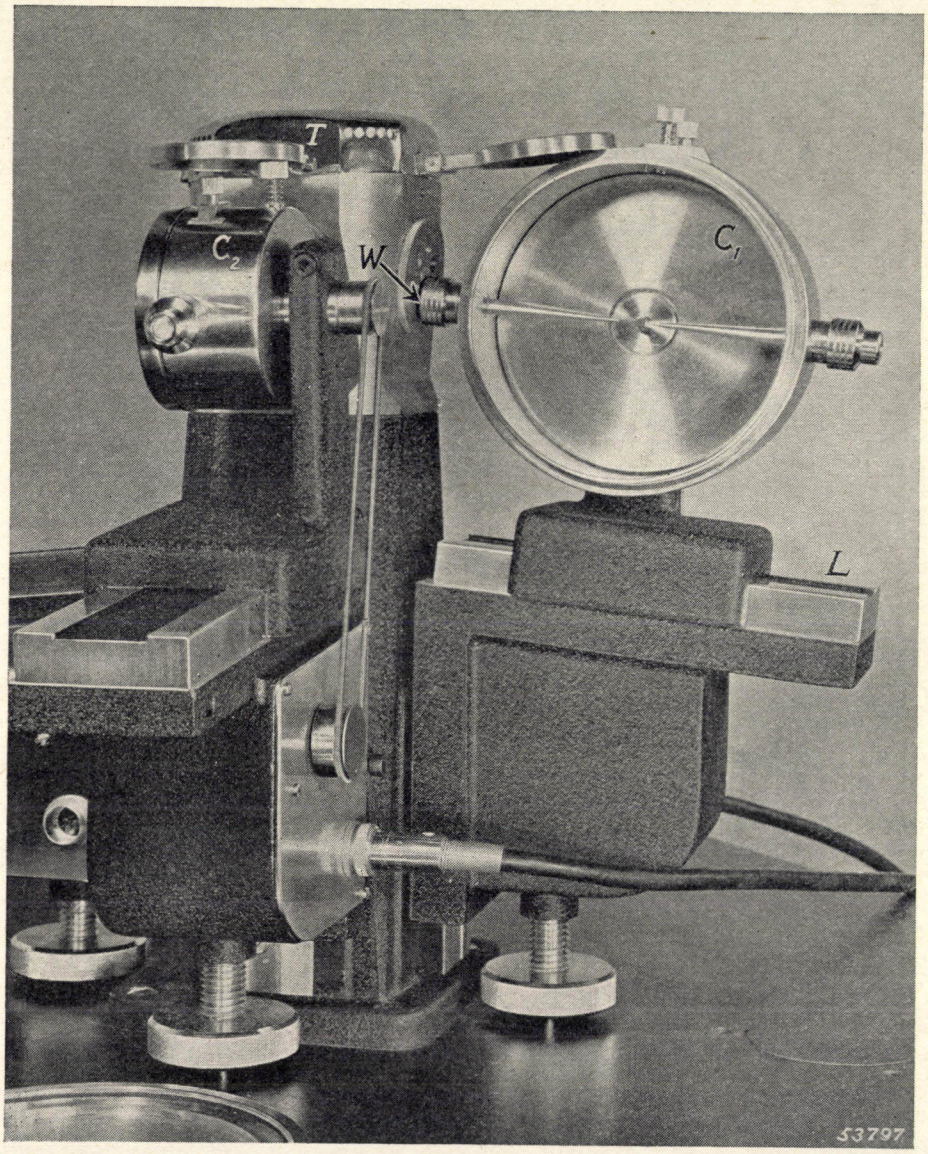


Fig. 3. The two cameras, C_1 and C_2, set up with an X-ray tube T on the desk of a Philips diffraction apparatus (the same tube can, as a rule, be used for from one to four cameras at the same time). Each camera is supported by a bracket and rests on a flat track L. The bracket being fixed, the camera may be rocked around and translated along the specimen axis; the track may be translated along and rocked about a vertical axis (parallel to the X-ray tube housing). This permits an easy aligment of the diffraction camera with the corresponding exit window (W) of the X-ray tube. Once aligned, the camera may be removed for film processing and reloading, and repositioned on the track without need for further alignment. Small and large cameras may be interchanged without altering the position of the track. The X-ray tube, too, is designed to allow changing tubes (e.g., for varying the target material) without affecting camera aligment. The tracks make an angle of 6° with the horizontal plane. Hence, if the camera is rocked around its axis so that the two tubes are parallel to the track, the X-ray beam used makes an angle of 6° with the horizontal face of the X-ray tube target. By slightly rocking the camera and raising the track this angle can be made smaller (e.g., 3°). While the exposure is being made the specimen is rotated continuously around its axis by a pulley attached to a small electric motor covered under the track.

in the diameter of the camera. Enlarging the camera, however, is soon limited by the rapid decrease in line intensity. In order to keep the exposure times within reasonable limits, one does not go any further, as a rule, with the camera type under consideration, than the frequently used 114.59 mm diameter. The Philips cameras possess diameters of 114.59 and 57.3 mm [3]).

Next, consider the divergence of the irradiating X-ray beam. Lines will be sharper for a smaller beam divergence, as may be seen from *fig. 4*. On the other hand, a larger area of the X-ray tube focus contributing to the irradiating energy corresponds with a greater divergence of the beam (the distance between focus and specimen, and the angle at which the anode surface is viewed being given). Hence, a compromise between line sharpness and line intensity again will be necessary.

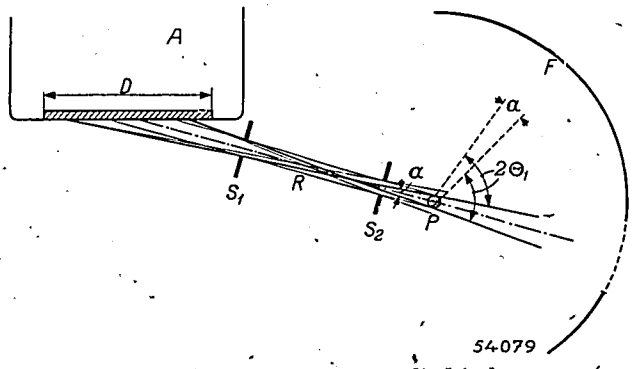


Fig. 4. Vertical cross-section of the cylindrical camera (not drawn to scale), showing film F, specimen P, anode A, focal spot D and beam collimating apertures S_1 and S_2. The divergence of the primary X-ray beam R (in this case limited by aperture S_1 and specimen diameter) is α. The same angular divergence appears between rays diffracted at the outermost points of the specimen cross-section and contributing to one diffraction line ($2\Theta_1$ = diffraction angle).

Finally the thickness of the specimen (which also determines the necessary width of the primary beam) should be considered. To obtain sufficiently sharp lines, the specimen must be extremely thin, in some instances 0.3 mm or even less. Evidently the X-ray energy diffracted by the specimen will, then, be very small. So we have once again the conflict between line sharpness and line intensity. In this case, however, other requirements mentioned above are involved in the conflict too. Diminishing the specimen diameter is apt to create a very unfavorable condition with respect to the contrast of the pattern and the line shape. This may be seen in the following way:

[3]) These seemingly odd diameter values have the advantage that the diffraction angles 2Θ are in a simple way numerically related to the line distances measured in mm on the film: 1° of 2Θ corresponds to 1 mm with the 114.59 mm camera, to $^1/_2$ mm with the 57.3 mm camera.

The main cause of the occurrence of a uniform background on the film, detrimental to contrast, is the scattering of the primary beam in the air through which it passes on its way through the camera [4]). Given a certain path length of the beam in air and assuming the beam width in all cases to be equal to the thickness of the specimen, the air volume contributing to the undesired scattering will decrease proportionately to this thickness. The volume of the specimen contributing to the desired diffraction, however, decreases according to the square of the specimen thickness, so that the air scatter will be relatively more pronounced the thinner the specimen.

Similarly, the unfavorable effect on the line shape may be understood. Given the average size of the crystals oriented at random in the specimen, the number of crystals irradiated decreases with the square of the specimen thickness, and so does the average number of spots from which each diffraction line is built up, while the line width on which the spots are distributed diminishes only proportionately to this thickness. Thus, the lines in the diffraction pattern will be less uniformly blackened and, in the extreme case, tend to get a spotty appearance on decreasing the specimen diameter. (This is quite noticeable in the examination of compounds of low crystal symmetry, for which a given type of lattice planes will attain an orientation suitable for reflecting only in a single or very few positions of the crystal.)

The various conflicts pointed out to exist between desired features and necessitating as many compromises in camera design, may have caused a somewhat gloomy impression as to camera performances which can be expected. Fortunately, there are several resources which favorably affect the necessary compromises and which have been applied in the Philips cameras with considerable success. One such resource, well-known for a long time, is the rotating of the specimen during the exposure (combined with a translation along its axis if desired); cf. fig. 3. This results in more crystals

[4]) We will not consider in this article causes such as possible fluorescence (X-rays or light) which is brought about by the primary beam in the specimen and which is non-directional, or the "white" (non-monochromatic) components of the X-ray beam which produce a diffraction spectrum for every wavelength that is present, all these spectra being superimposed to form a continuous background. These contributions to background (and hence indirectly also the contribution from air scatter) may be diminished by special measures for making the primary beam more monochromatic, e.g. by means of a "crystal monochromator". Such a device may also be used with the Philips cameras. The scattering of the beam at various apertures through which it passes will be discussed below.

coming temporarily in an appropriate position for contributing to a specific diffraction line and, hence, in diminishing the spottiness of lines. Other resources, also well-known but, in our case, applied in a novel manner, are concerned with the X-ray beam geometry and the reduction of air scatter. These will be treated to somewhat greater detail in the following parts of this article.

Geometry of beam collimating system

The desired beam shape is obtained by means of a collimator system, commonly consisting of two pinhole apertures (cf. fig. 4). When diminishing the specimen thickness to values of, say, 0.5 or 0.3 mm, the width of the X-ray beam had to be adapted to the specimen thickness by making the collimator apertures narrower. This was necessary, because all parts of the primary beam failing to strike the specimen do not add to the line intensity but only to the undesired air scatter. This necessity, however, applies only to the width of the beam in the "equatorial" cross-section of the camera and the specimen, represented in fig. 4. The width of the beam in a direction parallel to the specimen axis, need not be limited to the same content. This means that the beam need not be made rotation-symmetrical but that it can be given an oblong cross-section, by taking a rectangular slit rather than a circular pinhole as a first collimator aperture; cf. *fig. 5*. The obvious advantage of this is that a relatively long part of the rod-shaped specimen is irradiated, resulting in a higher intensity of the diffraction lines and, at the same time, in a more uniform blackening of the lines and truer relative intensities because a larger number of crystallites are irradiated [5]).

A limit to the slit length is set by the fact that with too great a divergence of the X-ray beam in a direction parallel to the specimen axis, the line sharpness and line shape will again begin to suffer. This is explained with reference to *fig. 6*. An ideal diffraction line is the intersection of the film with a cone of rays the apex of which lies in the specimen and the axis of which is the direction of

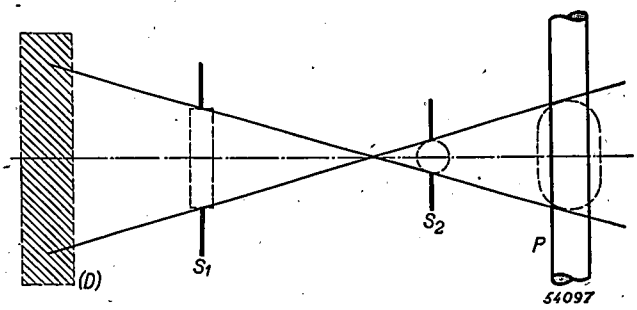


Fig. 5. Horizontal section of the primary X-ray beam. The first collimator aperture S_1 is made rectangular; S_2 is the circular second aperture; P, the specimen; D, projected focal spot. At P the X-ray beam has an oblong cross-section. (The cross-sections of D and of the beam at S_1, S_2 and P are turned in the plane of the drawing and indicated by dotted lines.)

the primary ray. With a diverging primary beam each ray will produce its separate diffraction cone. Each diffraction "line", then, is formed by the superposition of a continuous series of cones with different axes. This results in a broom-shaped broadening of each line on either side of the "equator" of the film, and in the case of a strongly diverging primary beam it also results in a line broadening at the equator itself. The effect is very noticeable at very small and large diffraction angles where the arcs form complete circles.

This well-known "slit effect" is not troublesome with the aperture dimensions chosen for our cameras. The first aperture is 0.5 mm wide and 2 mm long, the second one is circular, with a diameter of, say, 0.5 mm. The resolving power for adjacent lines proves to be hardly less than that of the usual systems with two circular pinhole apertures of 0.5 mm diameter, and it is certainly better than

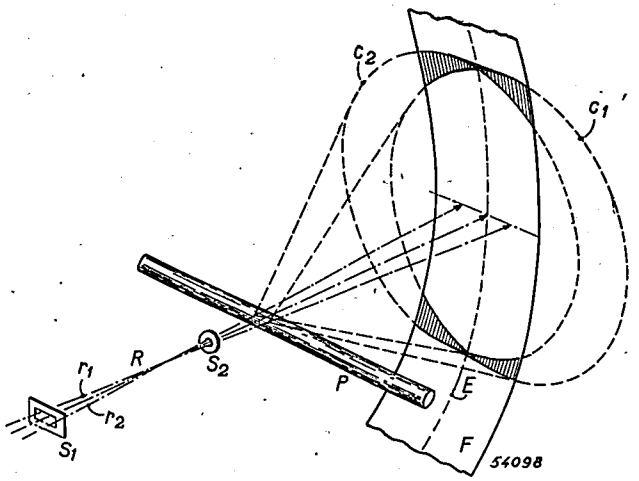


Fig. 6. Slit effect on shape of diffraction lines. Diverging rays of the primary X-ray beam R produce different cones of diffracted rays, each having its original ray as an axis. Diffraction lines on the film are obtained by the superposition of eccentric rings arising from the intersection of such cones with the film. c_1 and c_2 are the rings produced on the (virtually extended) film surface by the rays r_1 and r_2 respectively; E is the "equator" of the film F.

[5]) On the use of a rectangular first collimating aperture see e.g. F. Halla and H. Mark, Röntgenographische Untersuchung von Kristallen, Leipzig 1937, p. 156. The successful application of this device depends on extreme precision in the mechanical construction and particularly in the alignment of the slit with the focus and the specimen. Special precision techniques and tools have been developed for this purpose in the case of our cameras. The slit is punched out of a piece of lead by means of a special hob, which, when pressed further (without withdrawing), cuts a circle out of the lead. Thus the slit is automatically centered in a circular lead disc which may then be fixed at its proper place in the collimator tube.

that of a similar system with 0.75 mm apertures. Compared with the first system, an intensity factor of 3 is gained, when this collimator system is completely filled with radiation.

The value of 0.5 mm was chosen for the aperture widths because it was assumed that in general the specimen would be no thicker than 0.5 mm, and also because this value is well adapted to the focal spot dimensions of the Philips X-ray tubes supplied for use in the Philips diffraction apparatus. A few remarks should be made concerning this latter point.

The collimator system must, on the one hand, insure the beam width and divergence not to exceed the limits set by the desired resolution. On the other hand, it is desired that the radiation of the X-ray tube be used to good efficiency. This evidently will not be the case if the outermost points of the specimen circumference cannot "see" the full projected size of the focal spot because rays coming from the ends of the focal spot are cut off by apertures (cf. fig. 4). Therefore, we might say that the focal spot and the collimator system are well adapted one to the other if the first collimator aperture in fact could be omitted without affecting the beam shape [6]).

With the Philips X-ray tube mentioned above the focal spot is 9 mm long. At an angle of 3° from the face of the anode the projected width of the focal spot is 0.5 mm; in that case, rays from the entire focal spot pass through the apertures of size mentioned above to each point of the specimen cross-section, and the full radiation intensity is utilized. At an angle of 6°, however, which is more commonly used in diffraction apparatus, the projected width of the focal spot will be 0.9 mm, resulting in the ends of the spot not being used.

If the 3° angle is always used the only function of the first collimator aperture is to collimate the beam in case an X-ray tube having a larger focal spot than that of the Philips tubes is to be used.

A similar consideration applies to the 2 mm length of the first aperture: the dimensions of the focal spot of Philips X-ray tubes in this direction being on an average only 1.2 mm, the collimating action of the first aperture in this direction likewise becomes apparent only if other tubes, having wider focal spots, are used. With the focus width of 1.2 mm mentioned above, the first aperture is not completely filled by the beam and the intensity gain as compared with two circular 0.5 mm pinholes, therefore, is somewhat smaller than indicated above (gain factor about 2-2$^1/_2$).

Anti-air-scatter tubes

The deleterious effect of air scatter on the contrast of diffraction patterns can be eliminated by evacuating the camera. This technique, though applied in some cases, is not convenient in instruments for routine investigations. An alternative and much simpler resource consists in confining the primary beam on its path to and from the specimen within two metal tubes (see fig. 2). The entrance tube also contains the collimator system. Film background is reduced because the air path is now limited to the distance between the ends of the two tubes.

As is well known, incorporating the beam collimating system in a tube inside the camera has, moreover, the important advantage that the focus-to-specimen distance can be made smaller, entailing a considerable increase in intensity.

To reduce air scatter to a minimum one would prefer to bring the tubes as close as possible to the specimen. It is obvious, however, that sufficient space must be allowed around the specimen for the emission of the rays diffracted by the specimen. The diffraction lines at angles near 0° and 180° evidently are most liable to be intercepted by the rims of the tubes, and it was quite a common deficiency in cameras previously designed that "blind areas" were caused on the film at these diffraction angles, i.e., around the holes punched in the film at the entrance and exit region for the primary beam. Such a blind area is clearly visible in the pattern of a commercial soap reproduced in *fig. 7b*. On the other hand, fig. 7*a* exhibits the dense background which is produced, particularly near the exit film hole, if no exit tube or one of insufficient length is used.

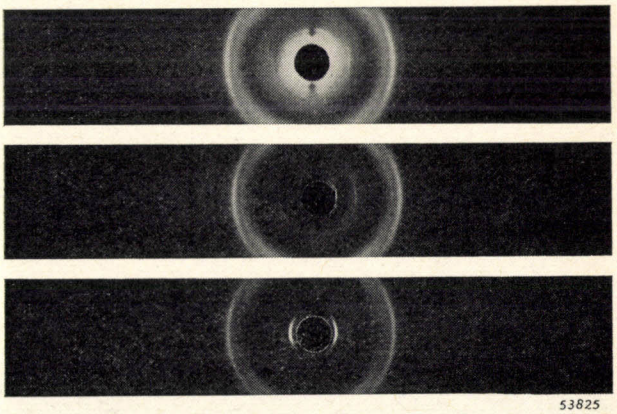


Fig. 7. Part of diffraction pattern of soap, containing the range of diffraction angles 2Φ from 0° to about 90°, taken with copper $K\alpha$ radiation and nickel filter.
a) No exit tube used. Considerable background occurs in the range of low diffraction angles, near 0°.
b) Badly designed exit tube. The tube, due to its contour, intercepts the diffraction lines which would otherwise be registered near the film hole (blind area effect).
c) Recorded with new 114.6 mm Philips camera. Background has been reduced to a minimum, without any blind area effect around the film hole, due to proper design of the collimator and exit tubes. Lines at small angles that could not be seen before are now reproduced very clearly.

Closer investigation shows that it is possible to compute specific dimensions of the anti-air-scatter tubes which give best results for different purposes. These computations have been made for our cameras and the tubes now employed have been designed in accordance with the results. For comparison, a pattern of the same specimen as in fig. 7*a* and *b* recorded with one of our improved cameras is

[6]) For a set-up without "first" collimator aperture, cf. A. Guinier, Radiocristallographie, Dunod Paris 1945, p. 80. The same principle is applied also in the Geiger counter spectrometer (cf. footnote[1])).

reproduced in fig. 7*c*. The occurrence of a "blind area" outside the film hole is completely avoided; some lines close to the hole, which could not be seen with previous systems on account of either background or blind area, can now be seen very clearly.

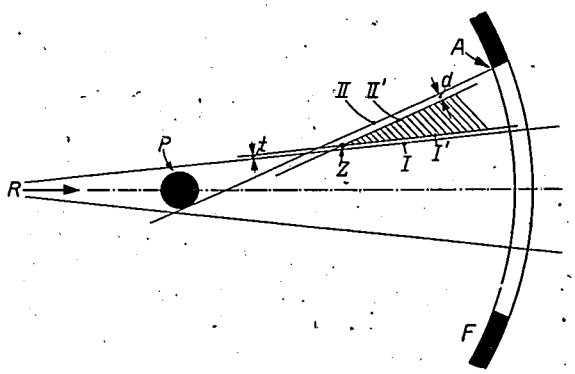
The line of thought for the computation of the tubes will be outlined below.

Computation of optimum form of anti-air-scatter tubes

Exit tube

Let us take the exit tube first; see *fig. 8*. The diameter of the camera, the diameter of the specimen and the diameter of the film hole are considered as being fixed. The primary X-ray beam — provisionally assumed to have rotational symmetry — is also considered to be given. The simplest form for the exit tube to take will be that of a truncated cone, with the base falling within the film hole while the width and the position of the tip still have to be chosen.

The exit port will, of course, have to receive the whole of the primary beam, whose edge is indicated by line *I* in fig. 8. The inner rim of the exit



54080

Fig. 8. Dimensioning of the exit tube. *R*, diverging X-ray beam; *P*, specimen; *F*, film; *A*, rim of the exit film hole. For the most favorable design the inner rim of the tip of the exit tube must lie at the point *Z*.

port will therefore have to be outside line *I*, measured from the axis, or rather outside line *I'*, drawn parallel to *I* in order to provide a certain clearance *t*, so that the tip of the exit port will not be touched by the beam (otherwise there would be considerable scattering from this tip and the scattered rays would reach the film without hindrance).

On the other hand, we want to introduce the requirement that the abovementioned blind area effect should be completely eliminated, i.e., that the exit port should not obstruct any rays diffracted from the specimen, not even for the lowest usable diffraction angles. That means that the whole of the specimen must be visible from the rim *A* of the film hole. The outer rim of the exit port will therefore have to be within line *II*, and the inner rim within line *II'* which has been drawn parallel to line *II* at a distance *d* equal to the thickness of the wall of the tube.

The two conditions stated above limit the allowable position of the inner rim of the exit port to the hatched region between lines *I'* and *II'*. To envelop the primary beam over the greatest possible distance it is necessary to place the inner rim of the exit port in the extreme corner of the hatched area, i.e., at the point *Z* where the lines *I'* and *II'* intersect.

Collimator tube

Similar considerations lead to the required shape of the collimator tube, though here the problem is more intricate, as the collimating of the primary X-ray beam also is involved. We shall provisionally adhere to the supposition that the beam is made rotation-symmetrical, thus that both collimating apertures are circular, their widths, $2s_1$ and $2s_2$ (which need not be equal), being determined in advance on grounds in part explained above. Also it is assumed that the position of the first aperture can be considered fixed on the strength of certain geometrical and physical considerations; we have placed it at a distance $a = 20$ mm in front of the entrance hole in the film. We are still free to choose the position of the second collimating aperture, of course within certain limits.

We can start once again from the fact that the part of the collimator lying inside the camera may be shaped as a truncated cone, with the base falling within the hole punched in the film at the spot where the beam enters the camera. We shall now have to choose the most suitable width and position of the opening at the strip of the tube.

First of all we have to observe that this opening cannot itself be successfully utilized as a second collimating aperture. The primary X-rays are strongly scattered at the edges of the beam-limiting apertures. If the second beam-limiting aperture were to be located at the end of the collimator tube this scattered radiation would reach the film unhindered and that result would be worse than the air scatter it is desired to eliminate. The second collimating aperture must, therefore, be placed inside the collimator tube, and the tube tip (scatter cup), in addition to its function of diminishing air scatter, must keep the rays scattered

by the aperture away from the film [7]). Thus we arrive at the configuration sketched qualitatively in *fig. 9*.

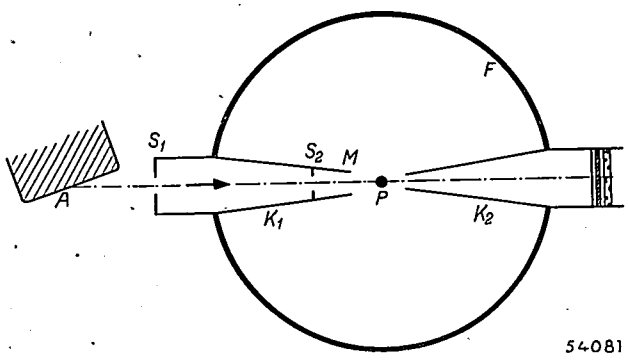


Fig. 9. Configuration of collimator and exit tubes K_1 and K_2 (qualitatively). The second beam-limiting aperture S_2 is inside the collimator tube, so that the rays scattered at this aperture are kept away from the film F by the tube port M (scatter cup). P, specimen, A, anode. (At the end of the exit tube, the three closures mentioned in the description of fig. 2 are indicated schematically.)

From *fig. 10* we can now deduce the conditions which have to be fulfilled by the collimator tube.

The tube tip must not cut off any part of the divergent beam formed by the apertures S_1 and S_2 (for if it did it would itself act as a second aperture). Hence the condition: 1) The inner rim of the scatter cup must be outside line I, measured from the axis, or rather outside line I' drawn parallel to I, again to allow for the necessary clearance t.

Furthermore, the scatter cup must intercept all scattered rays which, coming from the circumference of S_2, would fall outside the film hole on the opposite side of the camera (point A). Consequently: 2) The inner rim of the scatter cup must lie inside line III. The two conditions taken together indicate that the inner rim of the scatter cup must lie in the hatched region shown in fig. 10.

Finally, any blind area in the 180° region outside the entrance film hole must be avoided, which means that it must be possible to see the whole of the specimen unhindered from the rim C of the film hole. Hence it follows that the outer rim of the scatter cup must lie on the inside of line IV, or, if we draw a line IV' parallel to IV at a distance equal to the wall thickness of the tube: 3) The inner rim of the scatter cup must be on the inside of line IV'.

We see that all three conditions together still leave us free to place the rim of the scatter cup somewhere in the triangular part of the hatched field delineated by heavy lines. To envelop the primary beam over the greatest possible length, the rim of the scatter cup will have to be placed in the farthermost right-hand corner (W') of the triangle.

The position and the width of the collimator tube tip are thus fixed as soon as the position of the second collimating aperture S_2, as yet unspecified, has been established. When we vary this position we see that the more nearly horizontal line I (and I') becomes, and thus the smaller the divergence of the X-ray beam, the closer the point W' is brought to the specimen. It is therefore desirable to place the aperture S_2 as close to the specimen as possible. A limit to this is set because, as a closer examination will show, as S_2 is brought nearer to the specimen the apex (W) of the hatched area is shifted in the same direction. S_2 can only be shifted, therefore, until point W has reached the line IV', the delineated triangle in this case being reduced to that single point. The position of the second collimating aperture is then unambiguously established and the largest possible length of the collimator tube corresponds to this situation.

At the same time this position of the second aperture is also the most suitable for the design of the exit tube. In our discussion on this point with reference to fig. 8, which led to the tip of this tube being placed at point Z, we had assumed the primary beam to be limited by line I as given. It is apparent that point Z, too, now comes closer to the specimen the more nearly horizontal line I is made. The permissible lengths of both the collimator tube and the exit tube thus become a maximum when the position of S_2 is determined by the foregoing considerations [8]).

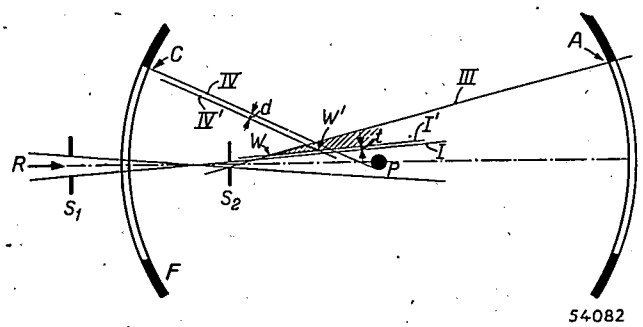


Fig. 10. Dimensioning of the collimator tube. R, X-ray beam; P, specimen; S_1 and S_2, apertures; F, film; C and A, rims of the entrance and exit film holes. With the position of S_2 being chosen arbitrarily as yet, for best results the inner rim of the collimator tube port must lie at the corner W' of the delineated triangle.

[7]) It is a common fault in many camera designs that this requirement is not met. The importance of the requirement was pointed out by M. J. Buerger, l.c. (1945), p. 505.

[8]) Incidentally, it should be pointed out that care must be taken to prevent rays scattered back from the wall inside the exit tube from returning through the tube tip and reaching the film. This requirement can easily be met by making this tube conical or by step-drilling it.

The optimum dimensions of the anti-air-scatter tubes can now be computed in an elementary, though not very simple manner, from the criteria established above. We introduce a system of coordinates ξ, η, having its origin O at the center of the entrance film hole as indicated in *fig. 11*. There are five unknowns: u, the ξ-coordinate defining the position of the second collimating aperture S_2; v and w, coordinates of point W, indicating the position and half the width of the collimator tube tip; x and y, coordinates of point Z, indicating the position and half the width of the exit tube tip.

According to elementary principles of analytic geometry we can write the equation for each of the straight lines I'-IV' in the form

$$\frac{\eta-\eta_1}{\xi-\xi_1}=\frac{\eta-\eta_2}{\xi-\xi_2},$$

where ξ_1, η_1 and ξ_2, η_2 are the coordinates of two fixed points through which the line is drawn. Since, according to the above, point W must be situated simultaneously on the lines I', III and IV', we get for the three unknowns u, v, w, the three equations:

$$I': \quad \frac{w+(s_1-t)}{v+a}=\frac{w-(s_2+t)}{v-u},$$

$$III: \quad \frac{w+s_2}{v-u}=\frac{w-f}{v-2R},$$

$$IV': \quad \frac{w+(r+d)}{v-R}=\frac{w-(f-d)}{v}.$$

Here R is the radius of the camera, r the radius of the specimen, d the wall thickness of the tube, t the desired clearance between the primary beam and the inner rim of the tube tip, f the radius of the entrance and exit hole punched in the film, s_2 half the width of the second collimating aperture; a and s_1 indicate the position and half the width of the first collimating aperture [9]). All these symbols stand for known numerical values.

Since point Z lies on the lines I' and II' we derive for the unknowns x and y the equations:

$$I': \quad \frac{y+(s_1-t)}{x+a}=\frac{y-(s_2+t)}{x-u},$$

$$II': \quad \frac{y+(r+d)}{x-R}=\frac{y-(f-d)}{x-2R}.$$

Elimination of u and v from the first three of these equations yields a rather cumbersome quadratic equation for w. After w is known, v and u may readily be computed, and likewise x and y with the help of u. We need not give here the detailed solutions and the computation of the numerical values.

Different types of anti-air-scatter tubes

In the above the rigorous requirement was set that nothing must be lost from the diffraction pattern, that is to say, the whole of the specimen must be visible from the rims of the film holes. In practice, however, this will never be required for the 0° section and the 180° section of the pattern at the same time. Organic compounds which often possess large interplanar spacings and, thereby, will produce very low angle diffraction lines, in general will not yield any "back-reflection" lines (near 180°). Conversely, inorganic compounds ordinarily give distinct back-reflection lines but rarely show lines corresponding to large spacings.

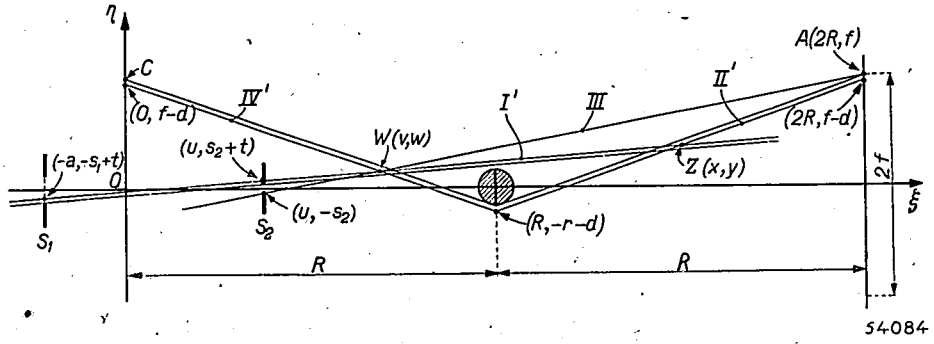


Fig. 11. The position of the second aperture S_2, and that of the points W and Z, indicating the best location and width of the tips of the two tubes, are given in the ξ, η-coordinate system by the coordinates u; v, w; x, y, respectively. The coordinates of all points used for the equations of lines I', II', III and IV' are indicated in the diagram.

Thus three different cases may be distinguished as regards the desired angle region of the diffraction pattern: the examination of forward diffraction only, of back-reflection only, and general work where neither very large nor very small angles are of interest but an optimal record of the entire "normal" angle region is desired. We have developed a number of different anti-air-scatter tube systems for these various purposes. Some of these are described below, the indicated figures corresponding to the 114.6 mm camera.

The first tube system (No. 77) is calculated for forward diffraction work. The rigorous blind area condition has been applied to the exit tube. Full line intensity is obtained at angles $> 4.5°$ (the minimum angle permitted by the film hole). Lines at angles larger than 90° need not be recorded in

[9]) These and the following equations contain two very obvious simplifications (cf. fig. 11): the circular cross-section of the specimen to which lines II and IV should be tangent was replaced by its vertical diameter; and the rim of the two holes in the curved film was assumed to have ξ-coordinates zero and $2R$, respectively. Actual computations showed that the latter simplification is permissible even in the case of the small camera ($2R$ = 57.3 mm) in which the film curvature is greatest.

this case. The collimator tube, therefore, has been extended so as nearly to touch the specimen. This has reduced the non-enveloped length of the primary X-ray beam to 19.9 mm.

An analogous tube system (No. 85) is made for back-reflection work. In this case only the collimator tube is subjected to the rigorous blind area condition, providing full line intensity up to angles of 175.5°. This tube system is used, e.g., for the precision determination of lattice constants. The non-enveloped beam length is 28.8 mm.

For the third case, i.e., all general work as in normal identification of compounds etc., the rigorous blind area condition has been replaced by a less rigorous one for both the collimator and the exit tube. This less rigorous condition consists in setting the requirement that, though not the entire specimen cross-section, at least part of it should be visible from the rim of the film holes. This means that a gradual intensity drop (a kind of "half-shadow") of the outermost lines towards the holes is allowed. *Fig. 12* illustrates the gain in tube length

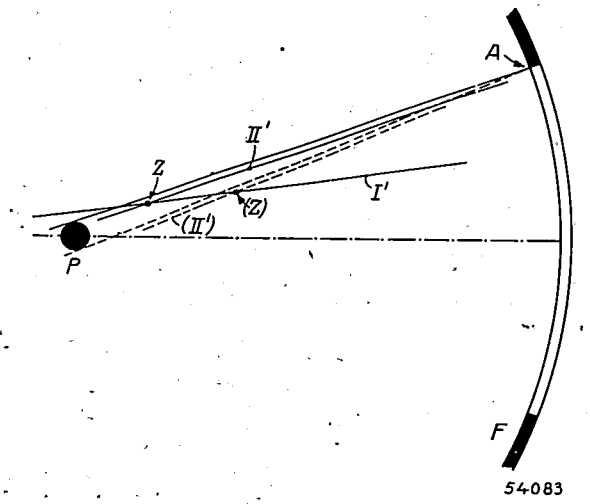


Fig. 12. For the strict requirement made above, viz., that the exit tube tip must not cause any obscuration of the specimen for points outside the film hole (rim *A*), in most practical cases the less strict requirement can be substituted that there should be no complete obscuration while a partial one could be tolerated. The former border line (*II'*) dotted in this diagram may then be replaced by the full line *II'*. The intersection point (*Z*) will come closer to the specimen, at *Z*. The exit tube may, therefore, be longer. Similar considerations apply to the collimator tube.

obtainable by substituting this less rigorous condition for the rigorous one. Accordingly, the non-enveloped primary beam path with the third system of tubes (No. 55) has been reduced to 10.9 mm! The air scatter is extraordinarily weak with this tube system. The intensity drop of the diffraction lines as they approach the film holes is noticeable at angles smaller than 6° and greater than 172.5°.

For cases where high intensity is of prime importance, and a smaller resolution and stronger background are permissible, a similar tube system having a wider second collimating aperture has been designed (0.9 mm; No. 73). The non-enveloped beam length is 30.2 mm for these tubes.

The same five equations as used above hold for the computation of the tubes with the less rigorous blind area condition, the only difference being that $+r$ has to be replaced by $-r$, as may easily be seen from fig. 12.

In the computation of collimator and exit tubes outlined above it was assumed that the X-ray beam has a circular cross-section. Its real shape, however, is oblong (fig. 5). In order to take in this oblong cross-section, a slit-shaped exit port evidently would be best suited. Nevertheless, for practical reasons the exit port, as well as the scatter cup, are made circular in all cases. This means that the exit port in the equatorial plane of the camera is about 3 times wider than is required for taking in the whole width of the primary beam. As a result, in order to prevent the occurrence of a blind region in the equatorial plane, the exit tube tip must be relatively a little farther away from the specimen, and the tube, therefore, has not the full theoretically feasible length. The difference is approximately compensated by the gain in length obtained by changing from the rigorous to the less rigorous blind area condition.

In *fig. 13* a number of patterns are reproduced which were recorded by the 114.6 mm camera, making use of the general purpose type No. 55 (films *a-e*) or of the forward-reflection type (film *f*) of anti-air-scatter tubes. The latter pattern has no blind area around the 0° film hole, the heavy broad diffraction ring in this region corresponding to a lattice plane spacing of ca. 15 Å, but has a large blind area around 180°. (The film of soap, fig. 7*c*, was also obtained with this type of collimator.) In the case of the former patterns (*a-e*), the very small partial blind area around both holes can be seen[10]). All the patterns are remarkable for their low background and their sharp and uniformly blackened lines. The exposure times for these patterns, taken with copper radiation at 45 kV_{peak}, 25 mA, were no longer than 1 to 2 hours, while a good pattern of quartz powder (*b*) could be obtained even with much shorter exposures (10 to 15 minutes).

Finally, it should be mentioned that for studies depending on differences in line shape, e.g., for the measurement of particle size by line broadening, or the examination of preferred orientations of crystallites by non-uniform line blackening, it is desirable to irradiate the specimen only along an axial length about equal to the diameter of the specimen. For this purpose collimators of a more conventional type having two circular pinholes are provided: with a first aperture of, e.g., 0.2 mm and a second one of 0.4 mm diameter, the beam

[10]) The blind area becomes visible by virtue of the faint residual background of the film which is caused mainly by white radiation diffracted by the specimen.

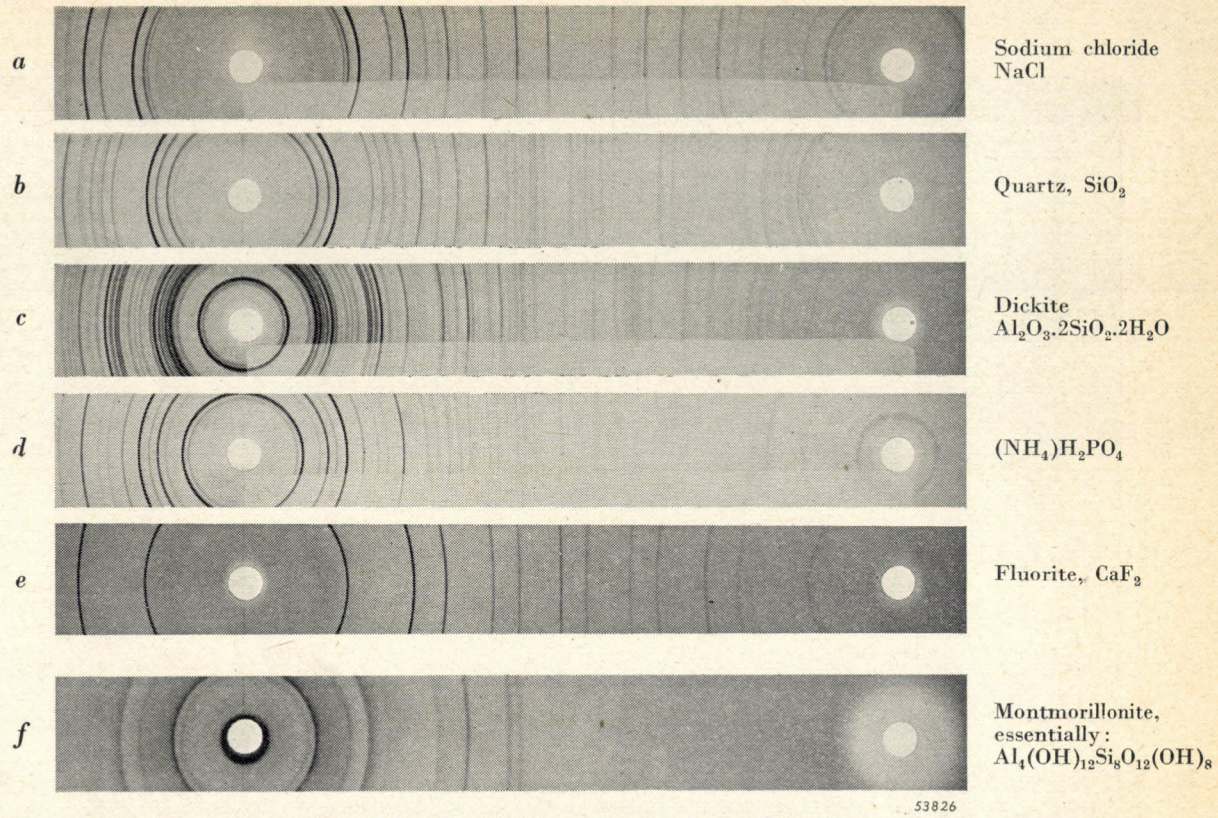
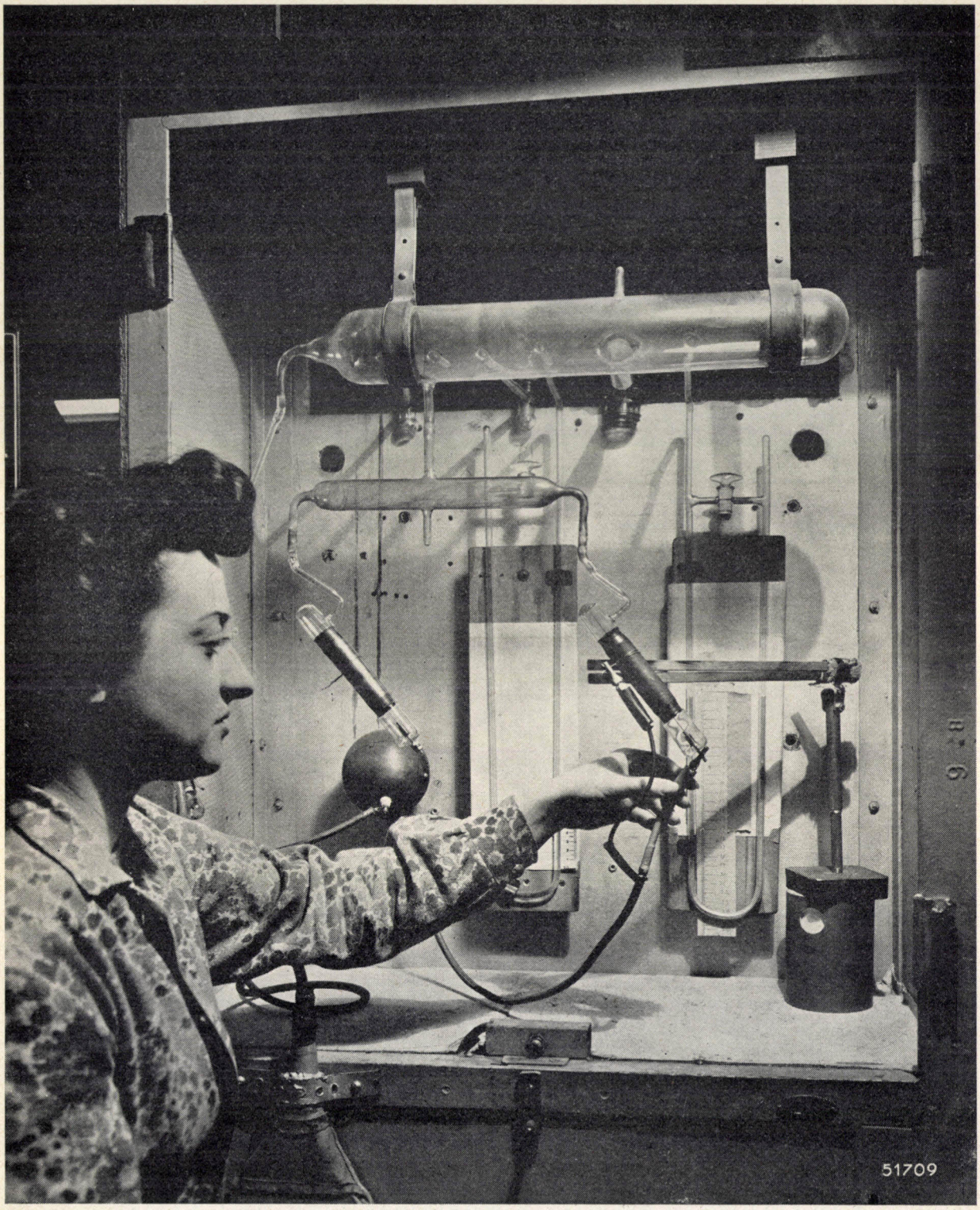


Fig. 13. Six diffraction patterns showing performance of new Philips 114.6 mm camera. All taken with copper radiation at 45 kV_{peak}, 25 mA, with exposure times of 1 to 2 hours; *a-e* with general purpose type tube system No. 55 causing small blind areas around film holes, *f* with forward-reflection (only) type causing a large blind area around 180° film hole but no blind area near 0° hole. For films *e* and *f*, a 0.015 mm nickel filter was placed before the window of the X-ray tube, eliminating the undesired copper $K\beta$-radiation so that only the $K\alpha$-diffraction pattern is recorded. For *a*, *c* and *d*, a similar filter sheet covering the lower part of the film was used, so that the major portion of the film represents unfiltered radiation; this technique has the advantage of more rapid exposures combined with easy identification of the undesired $K\beta$-lines. Film *b* was taken with no filter at all. The pattern of fluorite shown in *e* was recorded with black paper being placed over the whole film to prevent the film from being blackened by visible fluorescence caused by the X-rays striking this compound (cf. footnote [4]). In some of the original patterns faint broad diffraction lines are discernible around the 0° film hole; these are caused by a slight devitrification of the Lindemann glass capillary used for mounting the specimen.

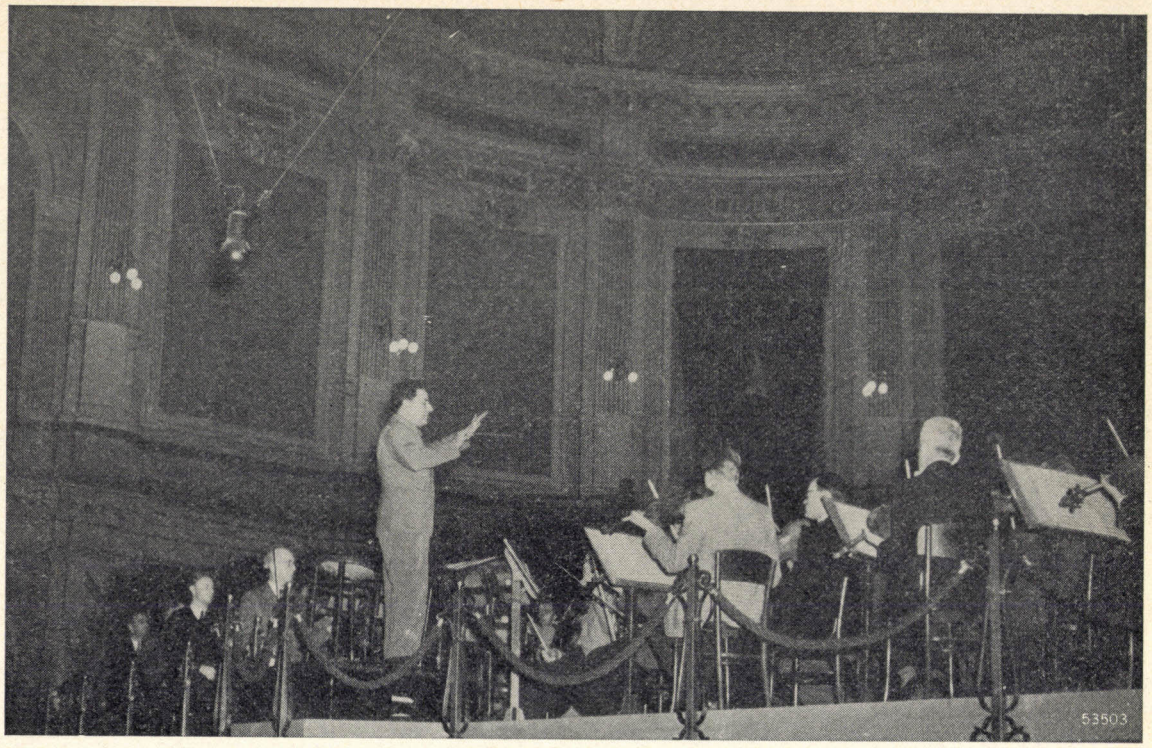
(of the 114.6 mm camera) has a width of 0.48 mm at the specimen. Of course intensity is low in this case; it is sacrificed to obtain optimum line shape.

High requirements are set for the precision of the machining in the manufacturing process of the collimator and exit tubes. It may be mentioned, for instance, that the inner diameter of the collimator tube tip must not deviate from the calculated dimensions by more than minus 0 and plus 5 microns. A similar precision is required for the tube fittings in order to insure the necessary exact alignment with the center of the camera. This requirement was made all the more difficult because it had to be combined with an easy interchangeability of the tubes of different types. A practicable solution was found in providing each tube with a precisely machined external surface fitting snugly into a receptacle in the camera wall, while the ultimate positioning on insertion results from matching of very accurately ground faces on the tube collar and the receptacle, these faces being normal to the beam axis.

EXHAUSTING GEIGER COUNTER TUBES



The photograph shows a phase in the manufacturing of Geiger counter tubes in one of Philips' American plants. These tubes, which are used for measuring X-ray or other radiation intensities, are filled with argon or other gases after the air has been exhausted. The gas filling process is checked by connecting the tube to a high voltage source and measuring the number of counts produced with a standard radio-active specimen. Gas ballast reservoirs and manometers for adjusting the pressure of the filling gas to the value desired are seen in the background.



DUPLICATION OF CONCERTS

by R. VERMEULEN.

534.76:534.86:785.1

By means of electro-acoustic sound equipment, experiments have been carried out in the Concertgebouw at Amsterdam and elsewhere in duplicating the presentation of ordinary concerts in a second auditorium. The equipment incorporates all the latest refinements in the technique of transmission and, in particular, the reproduction is stereophonic, with or without intermediate sound-recording; a new system of noise elimination, not discussed in this paper, enables an exact reproduction of the original dynamics of the music. Experience gained as a result of these experiments and an enquiry made at the time showed that such duplication of concerts provides musical enjoyment much more closely approaching that of the actual concert than what can possibly be had from gramophone or radio reproduction at home. This may ultimately prove a solution to the problem of the overflowing concert halls with which the larger cities are faced and with which they will doubtless have to cope to a still greater extent in the future. A number of features of the results of the experiment are discussed in this paper. In certain respects one might even venture to say that such duplicated concerts are superior to the actual performance. The main apparent point of difference between the actual concert and the reproduction, namely the absence of the visual contact between the audience and the performers, is reviewed from various angles.

Historical development of the concert

For many centuries in the history of the western hemisphere the arts were the exclusive privilege of kings, prelates and aristocrats, who alone were able to afford the luxury of retaining the services of performers in order that they might add to the enjoyment of their palaces the creations of these often very gifted servants. Music, therefore — with the exception of the church — was almost entirely the monopoly of the nobility. In those days an orchestra, whose function was to enchant small and select audiences, consisted of only a few musicians, often grouped around the harpsichord which was played by the conductor himself.

After the time of the French revolution and the American War of Independence, when social leader-

ship was transferred to the people, it was only natural that the latter should also assume the patronage of the arts and so themselves become the audience of the musician. The orchestra thus moved from the exclusive palace chambers to the public concert hall, and this change immediately paved the way to a marked growth, not only in the number of performers, but also in the diversity of their instruments. The wider variety in the timbre of the latter and the increased volume of sound in the larger halls — until then reserved only for renderings of the more specialized sacred music — were eagerly seized upon by composers for the creation of new styles.

It is not necessary to elaborate on the subject of present-day orchestras; one or more concert halls are to be found in all large cities of almost every country, with accommodation for audiences of hundreds, or even thousands: the "Concertgebouw" at Amsterdam seats 2000, the Royal Albert Hall, London, 10,000 and the instrumentalists in such cases will usually number anything from 80 to 120, playing some twenty different instruments.

The question of the moment is the direction in which the development will be likely to progress. Despite the confusion all around us there is a definite tendency to be observed: science continues in the creation of the means to enable ever increasingly larger groups of society as a whole to enjoy a certain prosperity. If such development is not to end in ultimate barbarism, it is however essential that this prosperity shall not be limited to material considerations; people must also be given access to intellectual spheres. To a certain extent literature has already furnished an opportunity of this kind. In the field of music it applies with equal force that this art should be enabled to reach larger and larger audiences, and the situation in which we shall find ourselves in the future and, for that matter, one which here and there exists today, is this, that the large concert halls of the present time will be far too small for the multitudes wishing to attend the concerts.

The problem presented by the masses

Two solutions immediately suggest themselves: the building of more concert halls, or an increase in the size of those to be built. Both solutions involve serious difficulties, however; the first, that is, more concert halls, would mean more orchestras and, even now, the contributions of audiences are usually insufficient to guarantee the performers a reasonable standard of living, rendering subsidies necessary. To draw still larger groups of music-lovers to the concert halls would at first mean that there would have to be a decline in the financial means of the average listener and, at the same time — although of less importance to the point at issue — in his artistic level. With the greater number of orchestras required subsidies would thus have to increase more than proportionally. Another, more fundamental objection is this, that it may be possible, in principle, to duplicate a well-balanced and accomplished orchestra, but not so the personality of the talented exponent. A symptom of this form of check-mate has been met with on many occasions, when a soloist, for example in the Concertgebouw, Amsterdam, has been obliged to give the same performance on two successive evenings. Needless to say, it is only by sheer necessity that a virtuoso is thus called upon to perform on mass-production lines and that this would never be done if there were any possibility of arranging for an audience twice the size to hear the single performance.

This difficulty can of course be met by the second of the above suggestions, i.e. larger concert halls, but here we encounter a financial obstacle; a larger hall will usually demand a larger orchestra, and the number of listeners per musician thus increases only slowly. Again, larger halls increase the element of risk for the producer and, in any case, this solution would come into consideration only in the larger cities; the rural population would not be benefited at all [1]). Finally, it is a very doubtful point whether it would be feasible to give satisfactory musical performances in such very large halls, since certain kinds of music would not lend themselves to such a magnification.

The failure of the most obvious "non-technical" remedies seems to indicate that in this sphere, too, science and in particular that of electro-acoustics must be called in to furnish the means of reaching a larger section of the public.

Gramophone and broadcasting

The conclusion just drawn actually seems to lag somewhat behind the facts, for what else are the gramophone and the radio if not a means for bringing music to the majority? Certainly, both go a long way towards meeting the demand, but in a manner which lacks those essential elements to be found only in the concert hall itself.

Take the case of a gramophone. It offers to

---

[1]) As an example of an effort to solve this problem, we may mention the open-air concerts given regularly since 1928 by the Philharmonic Symphony in the Lewisohn Stadium, New York (15,000 seats).

the individual the opportunity to hear a particular piece of music most suited to his mood at any given time. It is also obvious that the interpretation of a composition which the individual hears in recorded form is the most perfect it is humanly possible te achieve. On the face of it this would appear to be such an attractive proposition as to render the concerts superfluous, but the facts have disproved this; the development of the gramophone has not reduced concert audiences, but has on the contrary steadily increased them, as witness the very real problem which forms the subject of our discussion. Recorded music, even if representing the limit of perfection in reproduction (ignoring the fact that most of the equipment in present-day use is by no means perfect), has one inherent drawback in the rigidity or monotony which is an unavoidable outcome of the continued repetition of one and the same rendering. In the arts there is no measure of perfection that will satisfy everyone all the time; it is just that progressive recreation, each time with fresh nuances, that keeps art alive.

Radio broadcasting fulfils this need for live, albeit sometimes less perfect, interpretations. It also possesses other important characteristics, amongst others the facility for placing within reach of everyone a great diversity of music at low cost, in which respect it is a unique medium from the point of view of musical education. Even so, there appear to be reasons why broadcast music also lacks the power to rob the concert of its audiences, as borne out not only by the continuance of concerts, but, more especially, by the interest shown in the concerts played before audiences by broadcasting orchestras.

The reason, we think, is not to be sought in the technical imperfections still present in radio reception. Although both gramophone and radio have earned a place for themselves in the field of music, neither the one nor the other in its present popular form is capable of furnishing a solution for the problem that, in principle, reproduction of music in the home just does not satisfy all needs. Even with "technically perfect" reproduction it is undesirable, if not impracticable, to reproduce a concert at the same acoustical level within the confined space of the living room as in the concert hall. The dynamic contrasts which are so essential in the concert hall have to be levelled down in smaller spaces. What is even more important perhaps is the fact that it is often difficult in the home to isolate oneself from all kinds of disturbing influences, whilst, on the other hand, those positive psychological elements to be found in the concert hall itself are entirely absent. The fact that one forms part of an equally-minded community, drawn out of the daily slur of life into surroundings where the sustaining influence of architecture, lighting and acoustics is felt, is just as important in a concert as the effect of the artists personality.

Electro-acoustics in the hall

The conclusion, then, is that the final solution must be sought in the concert hall itself, and the most obvious step is to investigate further the potentialities of the courses of action already outlined above, i.e. more concert halls or larger ones, and to see whether electro-acoustics may possibly assist in removing some of the difficulties described.

By means of electro-acoustics, music can be made to fill larger halls without any augmentation of the orchestra. It is possible not only to employ ordinary amplification methods for the orchestra as a whole, using microphones and loudspeakers, but also to enhance the response of individual instruments in a manner as described in a previous issue of this Review, as applied to the violin [2]), or as universally employed in the electric guitar. It is not felt, however, that the best solution is to be found in this direction, firstly because of the objection raised in an earlier paragraph to the effect that much of our concert music, especially the older compositions, will not lend itself to diffusion in mammoth halls. Secondly, in this form of amplification there is always the danger of acoustic coupling between microphones and loudspeakers which can often only be avoided by adopting less favourable dispositions and characteristics of the microphones. Another factor to be contended with is the difference in time for the contributions from the primary source (the orchestra) and secondary source (the loudspeakers) to reach the audience; in extreme cases this will even produce echos.

The other alternative is more concert halls and here electro-acoustic equipment enables a single orchestra to suffice. The fundamental difficulty that a celebrated soloist cannot be duplicated is disposed of. In the light of present-day technique, *the simultaneous duplication of a concert* in another hall or, if desired, *in a number of halls can be effected to a high degree of musical perfection.* The effects of time lag, mentioned in connection with ordinary local amplification, are then absent, since there is no actual orchestra in the subsidiary hall(s).

[2]) R. Vermeulen, Perspectives for the development of the violin, Philips Techn. Rev. 5, 40-45, 1940.

The only weak link is the absence of the visual contact between audience and performers, which for some people is an indispensable feature: in the subsidiary hall this contact is of course lacking, although for that matter the position would not be very much better in a concert hall of very large proportions in view of the great distance between the platform and the major part of the accommodation in the auditorium. This point will be referred to later.

Equipment for the duplication of concerts

In order to realize the duplication of concerts, equipment has been built at the Philips Laboratories at Eindhoven, upon every component of which exceptional care has been bestowed, in an endeavour to approach as closely as possible to technical perfection. The aim was to ensure an aural impression in the subsidiary hall which would be as nearly as possible identical to that produced in the primary hall. By reducing to a minimum all imperfections in the reproduction it was ultimately found possible to carry out experiments calculated to put the original idea to the most stringent tests. A brief review of the equipment used, as well as of the results obtained from it, will now be given.

A general impression of the equipment may be obtained from *figs 1* to *3*, the legends of which also give a number of details. The installation is designed for the simultaneous duplication of a concert in one or more concert halls over telephone lines, as well as for subsequent reproduction at any desired time by means of a Philips-Miller sound record. In either case the reproduction is stereophonic [3]). The high and the low notes are reproduced by separate loudspeakers; the channels from the two microphones in the dummy head are separated only for the higher notes. For the low notes the contributions of the two microphones are mixed, since these do not contribute to the stereophonic effect to any great extent. Three output amplifiers are therefore needed and the output from these is on the generous side (60 W each), so that non-linear distortion may be avoided as much as possible. Careful design of all the components of the equipment ensure a flat frequency response characteristic up to 8000 c/s. The microphones used have already been described in a previous issue [4]). The Philips-Miller sound recording unit was made capable of meeting the special requirements by increasing the resonant frequency, this being possible by reason of the fact that the maximum recording amplitude of the double track required for stereophony is only half the normal track width [5]). Finally it may be mentioned that a special and very effective system was employed for the reduction of background noise and other interference to a sufficiently low level to ensure that the full dynamic range of the original performance would be reproduced without the audience being disturbed by the consciousness of the technicalities employed in the system. It is hoped that it will be possible to publish shortly an article in this Review on this important feature of the equipment.

This brief description will have made it clear to the reader that in the system in question many desiderata have been catered for which, for as far as the ordinary reproduction of music by means of radio and gramophone is concerned, still belong to the category of wishful thinking, even in the case of frequency modulation. The introduction of such elaborate devices for the reproduction of music in a hall need by no means be restricted to a model installation such as we had in view here. In considerations affecting reproduction in an auditorium the cost is relatively less important and there is therefore no reason why the equipment as described should not be regarded as a prototype.

The choice of the above mentioned frequency limit of 8000 c/s may need some explanation. In recent years there has been much controversy as to whether frequencies above 4000 or 5000 c/s are really appreciated, or whether the listening public prefer to do without them, even in the original music. From our own experiments we have gained the impression that the ear is particularly sensitive to discrepancies in this frequency range, whether these are to be attributed to non-linear distortion or to deviations from a flat frequency response characteristic. Omission of the sound spectrum above 4000-5000 c/s may be preferable to faulty reproduction, but it cannot be denied that it is just the higher notes that lend

[3]) A general description of the method employed by Philips in stereophonic reproduction will be found in an article by K. de Boer, Philips Techn. Rev. 5, 112-119, 1940. In the U.S.A. experiments were carried out some time ago, but with stereophony of a somewhat different form: these culminated in the telephonic duplication in a hall in Washington D.C. of a concert conducted by Stokowski in Philadelphia, a description of which appears in Bell System Techn. Journal, 13. 239-308, 1934 (Symposium on wire transmission of symphonic music and its reproduction in auditory perspective).

[4]) A. Rademakers, A condenser microphone suitable for stereophony, Philips Techn. Rev. 9, 330-338, 1947 (No. 11). In this connection see also J. J. Zaalberg van Elst, A low noise level circuit for use with condenser microphones, Philips Techn. Rev. 9, 357-363, 1947 (No. 12).

[5]) Regarding the Philips-Miller sound recorder see A. Th. van Urk. Philips Techn. Rev. 1, 135, 1936. This article also explains why the resonant frequency of the recorder is limited by the maximum amplitude to be recorded (formula 3). The adaption of the Philips-Miller system for stereophonic recording is described in Philips Techn. Rev. 6, 88, 1941 by K. de Boer.

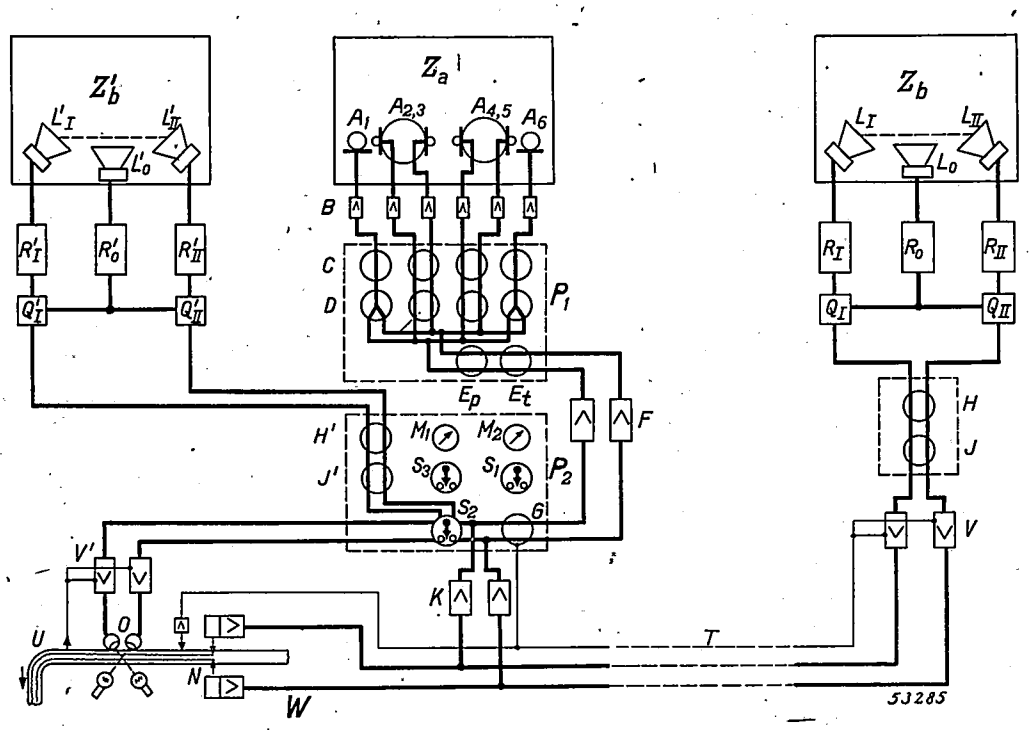


Fig. 1. Block circuit diagram of the equipment built in the Philips Laboratories, Eindhoven for the duplication of concerts. The orchestral music in the concert hall (Z_a) is picked up by a dummy head ($A_{2,3}$) containing two microphones. (In the photograph at the head of this article, showing a rehearsal in progress in the Concertgebouw Amsterdam, this dummy head will be seen suspended above, and just in front of, the platform.) Provision is made also for two microphones (single) (A_1 and A_6) and a second dummy head ($A_{4,5}$), to pick up the performance of soloists, groups of instrumentalists, or a choir. The signals from the 6 microphones are taken by way of 6 pre-amplifiers (B), and cables, to the mixing panel P_1, where the volume and the ratio between the two channels of each stereophonic unit are controlled (controls $D_{2,3}$ and $D_{4,5}$), together with the relative contributions of each of the 4 sources (A) with respect to the two resultant stereophonic channels (controls C, D_1 and D_6). The lower notes can be emphasized in both channels simultaneously (control E_p), whilst the over-all volume is controlled by means of knob E_t. The signals are then passed through intermediate amplifiers (F) to the control panel P_2 and thence by way of line amplifiers (K) either to a telephone line (T) connected to the secondary hall Z_b, or to the Philips-Miller unit W. In the case of direct reproduction in the subsidiary hall the signals are fed to filters Q_I and Q_{II} after re-amplification (V) and adjustment of the volume (control H) and the ratios of the stereophonic channels (control J). These filters separate the high and low registers; the former are taken to the loudspeakers L_I and L_{II} through the output amplifiers R_I and R_{II} and the auditory perspective is produced by disposing these two speakers a suitable distance apart. The low tones in each of the channels are combined, amplified by R_0 and passed to a loudspeaker L_0 which is placed between L_I and L_{II}.

Alternatively, if a phonogram is required, the output signals from the line amplifiers (K) are taken to two Philips-Miller recording units (N) where a stereophonic track is traced on the tape (U). For monitoring purposes, the sound record is reproduced almost immediately in the hall Z_b', the tape passing between the double optical pick-up unit O after leaving the recording heads. The signal thus obtained is amplified by V', readjusted at the control panel (H', J') and then passes through filters and output amplifiers Q' and R' to the loudspeakers L'. The operator, with his two panels P_1 and P_2 in the monitoring hall Z_b' thus hears the immediate result of his mixing and other adjustments.

Potentiometer G on the control panel enables the operator, who has a copy of the musical score before him, to reduce the loud passages and bring up the softer ones, in order to avoid overlooding the amplifiers, either when recording or when transmitting by telephone line, and on the other hand to reduce background noise etc. Although the dynamics of the music are thus compressed, they are subsequently fully restored, since the setting of the potentiometer control is transmitted separately to the subsidiary hall, or is recorded on the sound tape, as the case may be; these signals automatically vary the gain at V (or V' when reproducing from the tape) in the opposite sense as affected by G. The relevant connections are shown as lightly-drawn lines in the diagram.

The control panel also mounts two modulation meters M_1 and M_2 which can be plugged in to different points in the circuit (switch S_1). Switch S_2 enables the monitoring hall Z_b' (Q', R', L') to be connected directly to the signal from the control panel for monitoring in the case of direct line transmission or for comparing the recorded sound with the input signal. Different filters may be connected to switch S_3 for experimental purposes.

life and colour to the music. This, then, was the deciding factor in placing the limit at 8000 c/s; to reproduce higher frequencies does not seem to be worth while as the gain does not compare with the increase in the difficulties to be surmounted, such as background noise and so on.

Experiments and results

After a number of tests at Eindhoven, the equipment was installed in the Concertgebouw, Amsterdam, where a series of concerts given by the orchestra of that name were "duplicated": the main experiments consisted in recording the music and playing this back in an upper hall of the building.

The first of the concerts to be duplicated was conducted by Leopold Stokowski and we had

the privilege of submitting for his criticism test sound records made during rehearsals, good use being made of his comments in improving the recording. On another occasion a concert given in the Great Hall of the Concertgebouw under Paul Hindemith was duplicated simultaneously in the Small Hall, to which a number of persons had been invited (14 professional musicians and 27 others), this "audience" being requested to give their opinions on this method of musical reproduction by completing a questionnaire.

The more important results and experiences arising from these experiments may be summarised as follows.

Almost all who were given the opportunity to listen to these duplicated concerts were agreed that they provide a form of musical entertainment of very much higher value than the reception of ordinary broadcast music and quite comparable in many respects with the original performance; in the questionnaire mentioned above, an enquiry as to the listeners' opinion of the reproduction of the



Fig. 2. Mixing and control panel in operation during the recording of a concert. The mixing and „volume compression" is effected with the musical score and the experience gained during rehearsals as a guide. The control knobs referred to in fig. 1 can be easily identified from the photograph: a number of plug sockets will also be seen, these being employed for the connection of different meters, a telephone and a communication microphone (e.g. for speaking to the conductor).

Other concerts were similarly duplicated in the studio of Philips Acoustics Dept (E.L.A.) at Eindhoven, the music being transmitted from Amsterdam over a special telephone line, suitable for the transmission of music [6]).

orchestral timbre as such received a "good" from 85%, "moderately good" from 15% only. Stress is laid on the term "as such", since the general question whether it was considered possible to obtain genuine enjoyment from music produced in this manner — not taking as criterion the endeavour faithfully to reproduce the concert — was answered in the affirmative by 95% of the judges.

The effect of perspective produced by the stereophonic reproduction was unanimously considered to be a very great advance. In our own opinion the improvememt is not so much due to the possibility of discrimination between the different directions from which the sounds

[6]) We should like to express here our indebtedness to Mr. Stokowski for the interest he showed in the experiments and for the very fruitful discussions we were able to have with him. Our acknowledgements are also due to the Management of the Concertgebouw, the orchestra and, in particular their conductor Eduard van Beinum, for their very willing co-operation. We also tender our thanks to the Post, Telegraph and Telephone Service for the particular care bestowed on the overland connection in the transmission of the Amsterdam concerts to Eindhoven.

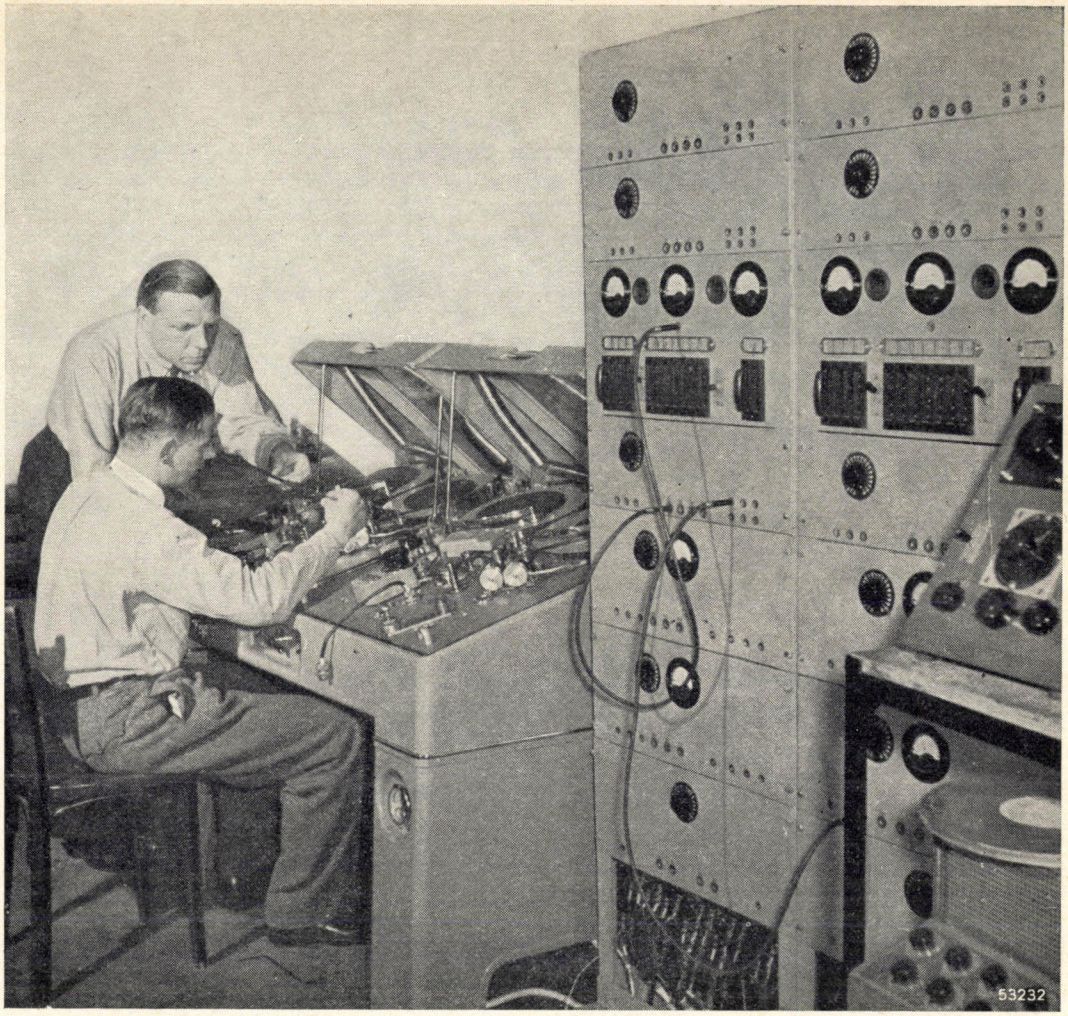


Fig. 3. The Philips-Miller unit, showing some of the amplifier racks etc. installed in the Concertgebouw, Amsterdam.

emanate (or even to follow the sources in the event of their movement), but should be sought more in the facility for picking out the characteristic sounds of the different instruments and the ability to hear the reverberations and possible extraneous sounds as being distinct from the rest.

This was, in fact, borne out by the answers in the questionnaires distributed in the Small Hall of the Concertgebouw, for although, owing to the peculiar unsymmetrical design of the hall, distortion in the stereophonic sound-"picture" at certain points in the hall was unavoidable[7]), nevertheless 95% of the replies attested to the positive value of this auditory perspective.

The impression was gained that the sound level of the reproduction in a given hall is likely to be fairly critical; variations of only 3db from the "most satisfactory" volume appear to have an adverse effect on the general appreciation, though this is of course a question of statistics. In the questionnaire relating to the experiment in the small hall 11% returned the opinion "too loud", 78% gave "good" and 11% "too soft", and from this the conclusion was drawn that the level, by and large, was satisfactory.

Another noteworthy fact is that during the duplication process the engineer at the control panel always has a tendency to bring out the bass notes stronger than they are heard in the actual performance; this was noticed by listening to the concert and the reproduction in turn, and this effect is considered worthy of attention because an exaggeration of the low tones is, in effect, a departure from the primary object, in this case the representation, with the utmost fidelity, of the tone picture as provided by the concert itself. At the same time, this is a peculiarity which is perhaps not unjustifiable from

[7]) The hall is oval in shape, with the platform at one end and a small balcony at the other. One of the sides has high windows covered with heavy curtains; the other is recessed, but is acoustically "hard".

the musical aspect: Stokowski once said "It is one of the greatest shortcomings of the orchestra that the deepest tones are relatively weak and so do not balance the middle and higher tones" [8]). Physically, the explanation of this deficiency is quite simple for, on the one hand, the sensitivity of the human ear is very much lower in the low-note zone than in the range of frequencies from about 1000 to 2000 c/s; on the other hand the radiation resistance for the low tones in the more usual sources of music (apart from organ pipes) is relatively low, owing to their limited dimensions [9]). That the most obvious step, the addition of more bass instruments, does very little to overcome the difficulty will be realised when it is remembered that even doubling of the number of bass players, say from 8 to 16, yields an increase of only 3db in the volume of sound contributed by that section. "Improvements" in orchestral music introduced by electro-acoustics in this respect (and possibly in other directions as well) would seem to suggest future possibitities which, however, the technician will approach only with the greatest diffidence.

The first item in the questionnaire already referred to was the point whether the absence of the orchestra was noticeable as a specific want. Opinions were fairly evenly divided, viz. 39% "Yes" and 41% "No", whilst 10% even considered the absence of the visual element to be an advantage. Of the professional musicians, remarkably enough, only 21 % replied in the affirmative and this seems to indicate that a musical education makes it easier for the individual to concentrate on the auditory impression, whereas it appears desirable for listeners who have received no special musical schooling to have something on which to focus their gaze. For the experiment in the Small Hall of the Concertgebouw the platform was screened by a thin white curtain, behind which the loudspeakers were placed, and a natural resting place for the eyes was therefore lacking; probably one of the most important problems in the duplication of concerts will be just this question of furnishing a suitable visual element that will not, however, distract the attention of the listener from the music. One will obviously expect the solution to come from television, since this is able to transmit a picture of the orchestra to the subsidiary hall, but we ask ourselves whether this would really serve the purpose, for it may be doubted whether the spectacle of a number of toiling musicians is actually the best possible background for the full enjoyment of music. Would it perhaps not be better, now that the opportunity presents itself, to turn this shortcoming to advantage and seek a "better" subject for the eyes to rest upon?

One simple solution which rather circumvents the problem and which would doubtless be considered unacceptable in most circles, is to darken the subsidiary hall. This was tried during the transmission of the concert to Eindhoven and it was generally agreed that in this way the music could be enjoyed to better advantage. Apart from the restfulness to the eyes in their vain roamings, the darkness without a doubt removes the cause of the sub-conscious conflict between the visual and aural impressions. The force of this aural impression is demonstrated by the well-known fact that sightless persons are able fairly accurately to judge the size and nature of a room upon entering it, by the sounds alone. A subsidiary hall will frequently be smaller than the primary one, especially in cases where a notable concert is given in one of the larger cities and duplicated simultaneously in the provinces. If the hall is darkened all visual impressions are removed and a sense of a much larger space prevails, more approaching that of the primary hall, of which the music bears the imprint.

It may be noted here that the acoustical requirements of the subsidiary hall need not conform to such stringent demands as those of the primary hall; in the latter the distribution of sound intensity is governed by numerous reflections from the walls and ceiling and, even in cases where the general acoustics can be considered good, there are inevitably some less satisfactory seats in the auditorium. In the subsidiary hall, however, the loudspeakers can be so disposed as to include the whole audience without any assistance from the walls (provided means of avoiding the visual conflict can be found, the walls are best covered with a good sound-damping material). Every member of the audience will hear the orchestra almost just as clearly as the microphones "hear" it and, as the latter are given the best possible places in the main concert hall, everyone in the subsidiary hall hears the music just as well as, or even better than if he were occupying the best seat. Whether it be for this reason, or possibly on account of the emphasized bass notes, we would not venture to say, but during the experiments remarks were heard stating that certain passages and instruments were more effective in the duplicated concert than in the original.

---

[8]) L. Stokowski, "Music for all of us", Simon & Schuster, New York, 1943, p. 189.

[9]) A. Th. van Urk and R. Vermeulen, "The radiation of sound", Philips Techn. Rev. 4, 225-234, 1939.

In conclusion

There is a deep-rooted conviction among many that the arts are so esoteric in character that the technical devices used for bringing them to the masses threaten to bring about a change in art itself. Even supposing this to be true, who can predict whether art would be poisoned and shrivel under the change, or whether on the contrary it will blossom forth anew? The troubadour, who brought the mythology of old as well as of fresh deeds to the knights in their castles certainly lost much of his attraction on the introduction of the printing press, but, even considering the quantity of lower-grade literature disseminated as a result of this invention, one can hardly assert that the letterpress has had a harmful influence on western culture. In the world of music, too, we feel that there is some justification for the hope that fresh technical discoveries will not be obstacles to the attainment of new and unexpected heights: they may even be the means of assisting this upward trend.

The developments described in the foregoing were primarily directed towards the most faithful possible reproduction of the so well known strains of the orchestral concert, and anything beyond this the technician cannot be asked to undertake; it is conceivable, none the less, that these limitations will ultimately be eased, when the artist comes to realise that he can employ these technical devices, which have released the orchestra from its traditional limitations, to create entirely fresh musical impressions.

A FLASH LAMP FOR ILLUMINATING VAPOUR TRACKS IN THE WILSON CLOUD CHAMBER

by N. WARMOLTZ and A. M. C. HELMER *).

539.16.08 : 771.447.4

A short description of the Wilson cloud chamber, which figures as an important adjunct in nuclear physical research as well as in investigations into cosmic radiation, is followed by a discussion of the conditions to be met by a flash lamp suitable for the illumination of cloud chamber tracks. A description is then given of a flash lamp specially designed by Philips for this purpose. The latter is an elongated, xenon-filled tube, across which a condenser, charged to several kilovolts, is discharged via a choke. The resultant flash has a duration of a few milliseconds. The lamp is simple in use, with a high efficiency, and the accompanying photographs give some idea of the results to be obtained. Finally, some of the characteristics of the lamp in question are discussed.

Introduction

One of the most important aids to nuclear physical research and the study of cosmic radiation is undoubtedly the cloud chamber, originally constructed in 1910 by C. T. R. Wilson, which has made it possible to render visible and make photographic records of the tracks described by ionised particles such as electrons, mesons and atomic nuclei, through the medium of a gas.

At an even earlier date it had been discovered in the course of laboratory experiments on the formation of clouds in a moist atmosphere, that the condensation of water vapour from super-saturated air takes place mainly on the particles of matter present in the air. Wilson subsequently found that when supersaturation takes place in air which is quite free from solid matter, water droplets are nevertheless formed, in this case on the available free ions. This fact was demonstrated by introducing radio-active materials — which emit high-velocity ionising particles in the form of α or β-rays — into or in the vicinity of the chamber, or by exposing the latter to X-rays or γ-rays.

Proceeding from these discoveries, Wilson developed an apparatus, the cloud chamber, for the demonstration of free ions in a gas by means of the condensation of water vapour which is brought into a state of super-saturation by expanding the gas, thus reducing its temperature.

When a high-velocity, charged, particle describes a path through the cloud chamber it produces in that path a train of ions, upon which condensation of the water vapour takes place during the subsequent expansion.

By brightly illuminating this trail of water droplets for a very short space of time, immediately after its production, that is, before the droplets can be displaced by gravity and diffusion, the path of the particles can be photographed and these observations can provide valuable information regarding the nature of the particles in question, as will be explained in the following.

The Wilson cloud chamber has, in fact, yielded very important results; by means of photographs of vapour tracks, Anderson in 1933 discovered the positron, whilst in the same year E. Curie and Joliot were able to observe the so-called materialisation of the photon, in the form of an electron-pair.

In the present article we are concerned mainly with the equipment required for the illumination of the tracks in question and, with this end in view, we shall first look more closely at the construction of the cloud chamber itself.

Details of the cloud chamber

In its modern form, the cloud chamber is an enclosed space having the shape of a flat box, of which the front wall is of glass, the rear wall consisting of a perforated metal plate, usually blackened to avoid the possibility of light reflections (see *fig. 1*). Behind this perforated plate a rubber diaphragm is stretched so as to separate the expansion space from the pressure chamber at the rear. The side wall of the expansion chamber is formed by a ground glass cylinder, or by a metal cylinder provided with a glass window, for lateral illumination.

The whole is rigidly assembled by means of clamps, bolts and gaskets. The pressure side is connected via a reducing valve to a cylinder of compressed air, so adjusted as to place that compartment under a pressure of 2 atm. At that side there is also an outlet valve, normally kept

*) Physical Laboratory of the Municipal University in Amsterdam.

closed by an electromagnet against the pressure within; when the electric current is interrupted the pressure opens the valve, which is very wide, allowing the pressure on this side of the chamber to drop rapidly to 1 atm: when this happens the rubber diaphragm is flexed towards that side and a uniform expansion of the gas in the front chamber takes place.

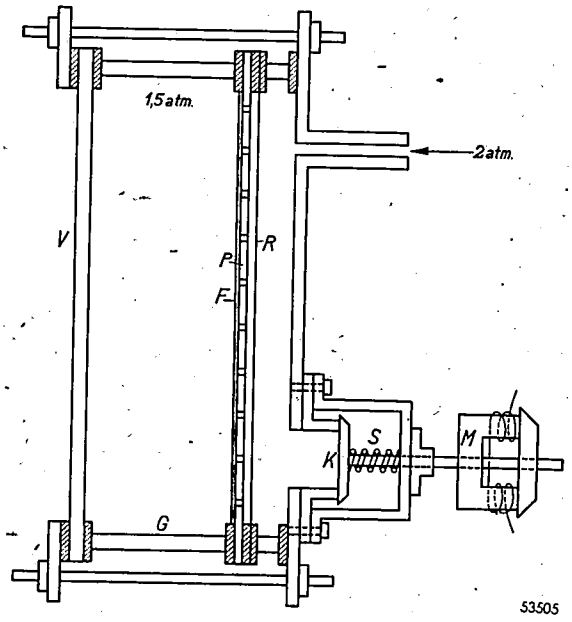


Fig. 1. Sketch of the Wilson cloud chamber in its present-day form. *V* glass front-plate; *G* glass cylinder forming the side wall; *P* perforated metal plate covered in front by a black velvet cloth *F* to prevent reflections of light; *R* rubber diaphragm. The valve *K*, which is held just closed at normal pressure by spring *S* and against higher pressures by the electro-magnet *M*, opens when the electric current is interrupted, thus allowing the gas in the chamber to expand.

The gas in the expansion chamber may for example consist of a mixture of argon and oxygen, at a pressure of about 1.5 atm and saturated with moisture, preferably partly alcohol and partly water vapour. Owing to the presence of the perforated plate, which is, moreover, covered with velvet, expansion within the chamber does not take place too abruptly and turbulences are thus avoided; this is essential since eddies would distort the vapour tracks to a high degree. When the tracks are to be photographed, a lamp producing an intense flash is operated either entirely by electrical means or by contacts on the outlet valve rod shortly after expansion has occurred.

As a result of the adiabatic expansion, a reduction in temperature and consequent super-saturation of the vapour takes place: it has been found that a vapour mixture of alcohol and water (corresponding to a liquid containing 50% alcohol), at an expansion ratio of less than 1.10 produces cloud effects only when the expanding gas is contaminated with particles of solid matter, but that with an expansion ratio of 1.10 to 1.11 droplets are also formed locally on the ions in the gas if it contains no particles of solid matter. Above this ratio of 1.11 arbitrary cloud formation occurs the intensity of which increases as the expansion ratio is increased, and for this reason it is usual to fill the cloud chamber with a gas mixture that is free from all extraneous matter and to employ an expansion ratio of between 1.10 and 1.11.

As already stated, an ionised particle travelling across the chamber leaves in its path a trail of ions: now, if expansion of the gas be made to take place in the ratio specified, shortly after the passage of the particle condensation occurs only on those ions formed along the track of the particle. Using a powerful lateral illumination, it is possible to observe the water droplets and therefore also the particle itself, through the glass front of the chamber. The concentration of the ionisation along the track, as evidenced by the number of droplets per centimetre of track length and the distance travelled by the particle (if the track ends within the chamber) often suffice to draw a conclusion regarding the nature of the particle.

The fact that droplets are formed on the ions at lower saturation values than those required for the appearance of droplets in the absence of ions can be elucidated theoretically.

A droplet of liquid is capable of existence in equilibrium with the surrounding vapour when the vapour pressure in the immediate vicinity is equal to the vapour pressure corresponding to a surface, the radius of curvature of which is *R*; the vapour pressure above a curved surface increases as the radius of curvature is decreased, and so also does the degree of saturation necessary for condensation.

Above a curved and at the same time electrically charged surface, however, the vapour pressure decreases as the radius is diminished below a certain value. For the same value of *R* below that value, the vapour pressure is reduced by the electrical charge and condensation on the ions sets in much more readily than the general condensation arising from the statistic vapour concentration.

When the cloud chamber is placed in a magnetic field of known strength, perpendicular to the front window of the chamber, the momentum of the particle can be determined from the curvature of its trajectory, as produced by the field. The strength of the field used will depend on the anticipated momentum of the particles to be registered, and varies from about 0.02 to 2 Wb/sq.m, which corresponds to 200 to 20,000 gauss.

The Wilson cloud chamber is an extremely useful instrument in the investigation of cosmic radiation and nuclear processes; not only that

the curvature of the tracks can be used to determine what particles are liberated on collision of the elementary particles with atomic nuclei of the gas molecules, or with the nuclei of the atoms of absorbent material specially introduced into the cloud chamber, but the resultant transfer of energy or momentum can in many cases also be calculated.

Fig. 2 is an illustration of a well-known example of impact between elementary particles and atomic nuclei: alpha-particles emanating from a radioactive substance shoot through the gas (in this case nitrogen) in the cloud chamber, and one of the tracks visible in the photograph will be seen to terminate in a fork which is produced by the collision of the alpha-particle with a nitrogen nucleus. The long limb of the fork, as may be concluded from the ionisation density and the range, is caused by ejection of a proton, and the short branch by

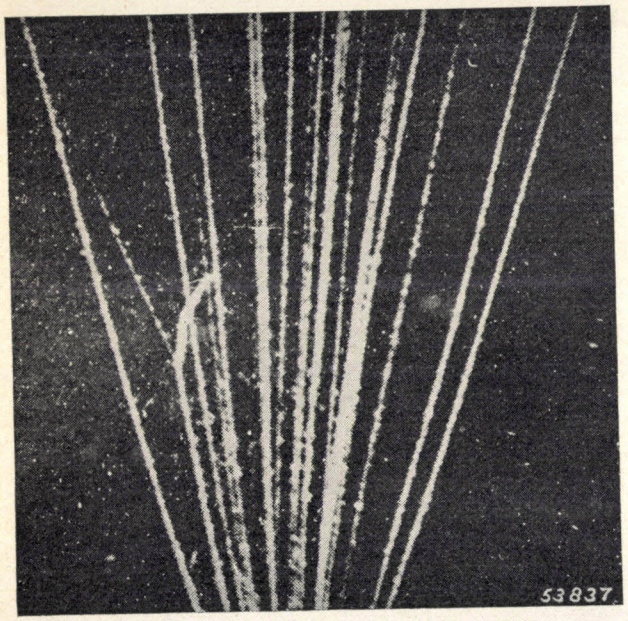


Fig. 2. Cloud chamber photograph showing collision between an alpha-particle and a nitrogen nucleus, causing ejection of a proton and the formation of an oxygen isotope (vide Blackett).

the nucleus which receives momentum at the impact. As no third track is visible, it must be concluded that the α-particle is trapped by the nucleus.

The resultant reaction [1]) may be represented by the formula:

$$_7N^{14} + _2He^4 \rightarrow _8O^{17} + _1H^1.$$

This was the first nuclear reaction to be ascertained: it was observed experimentally by Rutherford in 1919 as the result of the bombardment of nitrogen with α-particles and the result was fully confirmed by Blackett in 1923, using the cloud chamber.

In order that expansion may take place exactly at the correct moment when the cloud chamber is to be used for research on cosmic rays, one Geiger-counter is placed beside the chamber, facing in the direction from which the particles are expected to arrive, and a further counter on the opposite side. These counters produce a small current impulse when an ionising particle passes, which can be amplified as required by means of radio valves. The two counters are so connected that a relay is operated only when both counters are actuated: this means that the particle must pass through both counters as well as through the cloud chamber located between them. The relay operates the magnet of the outlet valve, which then connects the pressure chamber with the outer atmosphere and allows expansion to take place. Naturally, all this must be accomplished in so short a space of time that the ions cannot move too far from the point at which they are originally produced by the particle. Combinations of one or more cloud chambers and a larger number of counters in different positions in relation to each other may be employed for segregating the process to be observed from the many phenomena occurring in cosmic radiation.

This is only one method of employing the cloud chamber. Many other devices are also used to effect the expansion of the gas; in some cases arrangements are made to obtain alternate expansion and compression, preferably at high speeds and without any form of control [2]).

The illumination of the cloud-tracks

The trains of droplets which delineate the track of a particle can be observed only under a powerful form of illumination. Usually the light-source is placed at the side of the chamber to illuminate the droplets through a window or through the glass side wall of the chamber, so that they may be visible from the front by reason of the light which they scatter [3]).

---

[1]) W. de Groot, Nuclear Physics, Philips Techn. Rev. **2**; 97-102, 1937.

[2]) For a complete review of the applications of cloud chambers, the various processes thereby taking place and methods of measurement, reference should be made to the article by N. N. Das Gupta and S. K. Ghosh in the Review of Modern Physics, **18**; 225-290, 1946.

[3]) A method of illumination from a different angle with respect to the direction of observation is discussed in the article by Das Gupta and Ghosh mentioned in note [2]).

Many different illuminating methods will be found described in the literature on the subject under review: Blackett (1934) employed two systems, one of which consisted in discharging a condenser across a narrow mercury vapour discharge tube, whilst in the other these tubes were connected directly to the secondary side of a high tension transformer. The resultant current impulse, of some hundreds of amperes, produces a powerful flash of 0.1 to 0.01 seconds duration.

Overloaded incandescent lamps are also sometimes used, 110 V lamps being connected to 220 V mains: yet another method involves the use of continuously burning, super high pressure mercury vapour lamps (e.g. Philips SP 500 or SP 1000), the illumination period being controlled by means of a mechanical shutter.

The main requirements to be met by the illumination are as follows:

1) It should furnish uniform luminous intensity from the side in a drum-shaped chamber. A linear source of light of roughly the same length as the diameter of the drum is very suitable and can be used in conjunction with a cylindrical lens. A screen between the lens and the chamber will prevent light from reaching the front and rear walls and thus producing troublesome reflection.
2) It should produce a high intensity, for a very short period of time. The duration of the flash must be very short, since the diffusion of the water droplets as well as their displacement by the force of gravity tend to widen and distort the vapour track to a considerable extent.

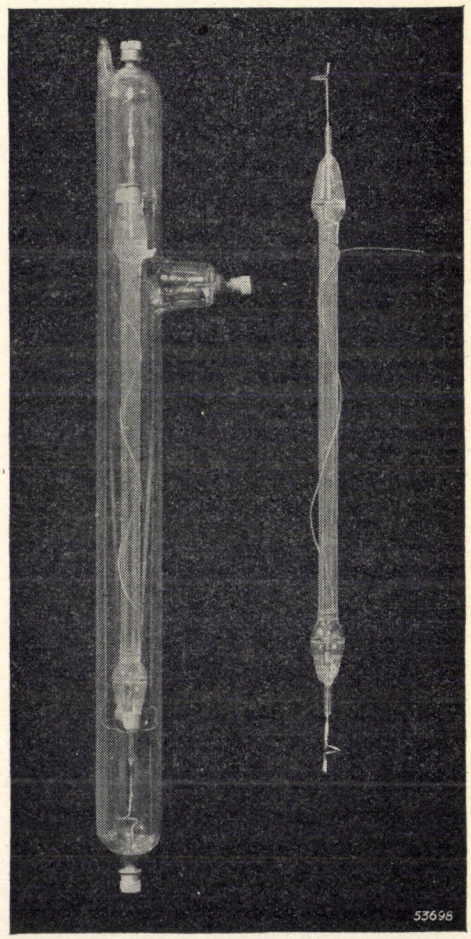
   This latter requirement is particularly important when a large cloud chamber is mounted vertically for the observation of cosmic rays. Since the trajectory of the high-velocity particles, moving in a magnetic field is only very slightly curved, the sagging of the track in a vertical plane might introduce large errors in the determination of the curvature. For this reason the duration of the flash must be less than 10 milliseconds.

   When the chamber is mounted horizontally, as is frequently done for nuclear research, the falling of the droplets does not result in immediate distortion, and longer illumination periods may be employed.

   Nevertheless, the short duration of the flash necessitates very high luminous intensities to ensure sufficient exposure of the photographic plate.
3) The moment at which the flash takes place must be controlled to within an accuracy of about 1 millisecond if the droplets are to be photographed at the most suitable moment after expansion has taken place. A little time may be allowed to permit the droplets to develop, but not too much, in view of the consequent blurring and distortion of the tracks, explained previously.
4) The lighting equipment must not increase the temperature of the cloud chamber, as this also causes distortion due to convection currents in the gas.

A flash lamp for the illumination

The above requirements are all fully covered by a gas-discharge lamp specially designed by us for the purpose; when operated by the discharge of a condenser it gives a flash of short duration.



a *b*

Fig. 3. Photograph of the flash lamp. *a*) the complete lamp, *b*) the flash tube proper.

Fig. 3 is an illustration of the lamp in question: *a*) the complete lamp and *b*) the discharge or flash tube proper, which is mounted in the outer tube to provide a robust, easily-handled unit: the use of this tube or jacket further ensures rigid mounting of the screw-type terminals for the connecting leads.

The discharge tube is made of quartz or glass and has an internal diameter of about 4 mm; the electrode seals and the electrodes themselves, which are both oxide-coated [4]), are accommodated in the widened ends.

If desired the length of the lamp, which is normally about 20 cm, can be adapted to the dimensions of the cloud chamber. The tube is filled with rare gas at a fairly high pressure, the gas used being xenon or krypton to ensure a high luminous output; this point will be dealt with later.

As the window of the cloud chamber is usually made of glass that will not pass ultra-violet rays, the jacket of the lamp is also made of ordinary glass, but for special purposes both discharge tube and jacket can be produced in glass which transmits ultra-violet rays.

The wire coiled round the inner tube serves as ignition electrode. The lamp is operated by the discharge of a condenser, charged to several kilovolts, which is connected to the lamp via a choke in the manner shown in the circuit diagram, *fig. 4*. The choke serves to increase the duration of the discharge, which, without the choke, would be only about 40 microseconds (dependent on the capacitance of the condenser), to several milliseconds, this having the advantage of prolonging the life of the lamp. The inductance of the choke may be 10 mH and the D.C. resistance should preferably be less than 1 Ω.

It has been found that the reduction in the total luminous output of the lamp due to the resistance of the choke in series with it will, in certain instances, have little or no effect on the ultimate blackening of the photographic plate, owing to the decrease in the sensitivity of the latter when the exposure period is reduced. The blackening of the photographic plate is determined by $I.t^p$, in which p is dependent on I and t (I = intensity and t = duration of exposure); in the range under consideration p is usually greater than unity. Consequently, for the same total amount of power input, an increase in the duration of the flash due to the choke may even blacken the plate to a greater extent, notwithstanding the reduced total emission of light.

The lamp just described is not only used as an adjunct to the cloud chamber, but it has a very wide range of application for photographing phenomena of very short duration in other fields as well. In such cases the choke can be omitted without detriment to the flash tube, provided the amount of power applied per impulse is reduced.

[4]) As both electrodes are oxide-coated, the direction of the current may be reversed when that electrode which is first used as cathode deteriorates in use; in this way the life of the lamp may be prolonged.

Ignition is established by a voltage impulse of about 10 kV, furnished by a low-power impulse generator: a condenser charged to 300 V and discharged through the primary winding of a transformer will serve the purpose. The high tension side is then connected directly to the ignition electrode.

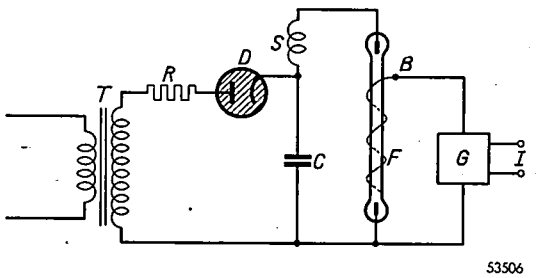


Fig. 4. Diagram of the flash lamp circuit. The condenser C, the value of which may be between 10 and 100 μF, is charged to the extent of several kilovolts by the transformer T and diode D, across a resistor R. An impulse delivered by the generator G and applied to the external electrode B provides a weak discharge in the flash lamp F, in consequence of which the condenser C discharges through the choke S. The resultant brilliant flash has a duration of a few milliseconds. The generator G is operated by applying a low voltage impulse to the terminals I; this impulse is produced either wholly electrically or partly mechanically when expansion takes place in the cloud chamber.

A very serviceable impulse generator may be provided by a radio valve with a choke in the anode circuit. The valve is so arranged as to pass a steady anode current at rest, the required voltage impulse across the choke being produced by suddenly rendering the grid negative.

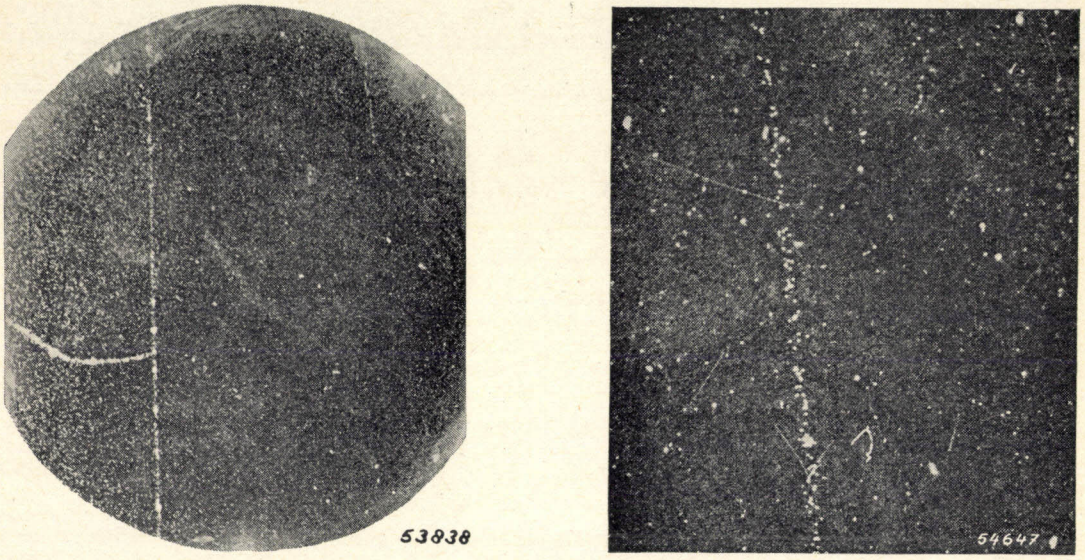
Results

Using a cloud chamber such as the one described in an earlier paragraph, in combination with the flash lamp under review, photographs have been taken of the tracks produced by cosmic rays, and these are reproduced in *figs 5* and *6*. The chamber was mounted vertically and the light from the lamp was concentrated by means of a cylindrical lens (glass tube filled with water).

Fig 5*a* depicts the track of a high-velocity electron or meson which has liberated a low-velocity electron by collision with a nucleus in the gas; owing to its lower velocity, this describes a more or less arbitrarily curved path. In fig. 5*b* a portion of a track is shown greatly magnified. Fig 6 shows what is probably a particle of the cosmic radiation (possibly a photon) liberating an electron and a meson, in the upper part of the cloud chamber; the meson has in turn produced a secondary particle, possibly an electron, but more probably another meson.

As will be seen from these reproductions, the tracks of the high-velocity particles can be faithfully recorded by means of the equipment with which we are concerned.

The exposures, which were about 2 milliseconds, were made 0.25 seconds after expansion of the gas in the chamber. The condenser was discharged through a choke of 0.7 mH having a D.C. resistance of 0.02 Ω and the camera used was a Contax, stopped down to f/5.6, the film used being Ilford HP 3.



a *b*

Fig. 5. Photographs of cloud chamber tracks taken with the aid of the flash lamp described above. *a*) High-velocity electron or meson colliding with a nucleus and liberating a low-velocity electron, the track of which is curved; *b*) Portion of a track greatly enlarged. These photographs and the next one have in no way been retouched. In the background a number of droplets will be seen which have condensed on particles of dust; it is essential that the definition of the tracks is such that the droplets can always be distinguished and counted under an ordinary magnifying glass.

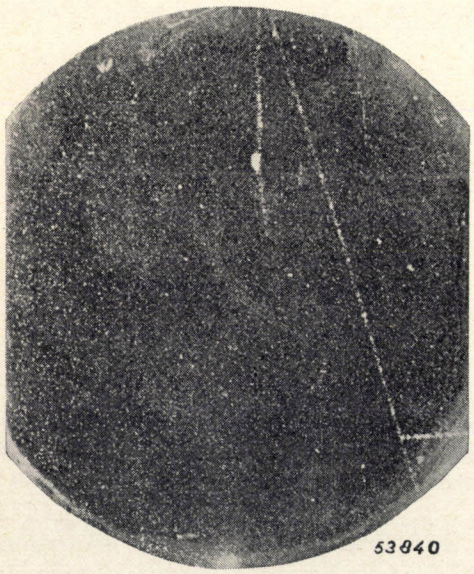


Fig. 6. Another example of a vapour track as photographed with the Philips flash lamp. This shows, in the upper portion of the chamber, a cosmic ray particle (possibly a photon) liberating an electron and a meson, producing in turn a secondary particle, possibly an electron, but more probably another meson.

The load on the flash lamp represented 320 wattsec as produced by the discharge from a 40 μF condenser, previously charged to 4 kV [5]).

The flash lamp itself, 20 cm in length, is found to have an effective life of more than 100,000 flashes, of an input of 500 wattsec, and at a rate of 8 flashes per minute; even at loads of 1000 wattsec the life is quite good, so that, if higher intensities are required for photographing less clearly defined tracks, or to permit of smaller lens apertures, higher loads may be safely applied to the flash lamp. It is of course also possible to employ two lamps, one each side of the cloud chamber, whilst if the latter is made with a glass cylinder as side wall the use

[5]) The light was radiated freely all round, only a part of it being effectively used. It is also possible, however, to apply a specular coating to the rear wall of the lamp and thus also to utilise the flux emitted at ths side.

of an annular lamp placed round the chamber offers considerable advantage.

Since the flash lamp functions without warming up (unlike some other types of light source) and as a single flash develops very little heat, there is no risk of convection currents being produced in the gas (requirement 4).

It has been shown, then, that the flash lamp fully meets the four conditions specified above, but it also possesses other favourable characteristics, namely:

a) since the lamp does not burn continuously, no screens or mechanical shutters are required;
b) the simple method of ignition dispenses with the necessity for relays and permits of the design of light, non-arcing apparatus, this being of particular advantage in cosmic ray research by means of aircraft;
c) the running costs are extremely low, since the power consumed is only that taken by the flash; no pre-heating is required, as in the case of mercury lamps.

Some characteristics of the flash lamp

Finally, let us look more closely at some of the properties of this flash lamp [6]).

It has already been stated that a rare gas is used for the filling the lamp, usually xenon or krypton, or a mixture of two or more such gases. The question which kind of gas gives the best results can be answered by means of *fig. 7*, in which the horizontal co-ordinate shows the voltage in kV to which a 100 μF condenser was charged to operate the flash-lamp. The vertical axis gives the total quantity of light from a single flash in arbitrary units.

These tests were carried out with the aid of a potassium photocell of the vacuum type, provided with filters to ensure an approximation of the sensitivity to the relative luminosity curve, in conjunction with a ballistic galvanometer.

The distance between the photocell and the light-source was varied to ensure that no saturation of the electron current occurred at the very high luminous intensities concerned. No saturation was found to take place at sufficiently high anode voltages (about 400 V), and the deflection of the galvanometer was therefore directly proportional to the total quantity of light emitted during the flash.

It will be observed from this figure that the heavier rare gases give a much greater quantity of light than the lighter ones, for which reason xenon is obviously the best medium for the filling of flash lamps; the measurements discussed in the following are therefore all based on the xenon-filled lamp.

A large portion of the light produced by the xenon-filled flash lamp comprises a continuous spectrum, similar to that of a black body at about 6000 °K, which means that the light is practically white. The sprectrum extends into the ultra-violet zone and a marked group of xenon lines also appears at the infra-red end; in the visible part of the spectrum some xenon lines are superimposed on the continuous spectrum. Specific absorption in the tube is found to be only very slight or entirely absent.

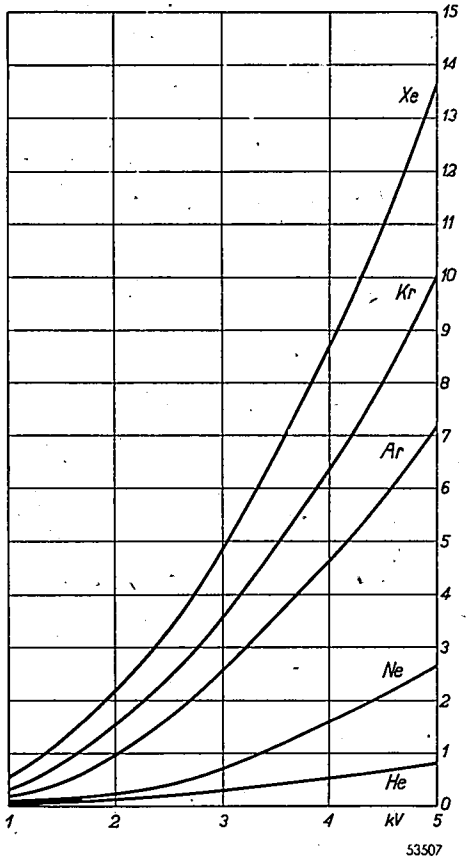


Fig. 7. Total visible quantity of light of a single flash (in arbitrary units), as a function of the voltage across a condenser of 100 μF, for helium, neon, argon, krypton and xenon (at the same pressure), as measured with a ballistic galvanometer and a photocell matched to the relative luminosity curve.

Tests were further carried out to ascertain what effect the gas pressure has on the quantity of light produced, and it was found that the latter increases steeply with the pressure (see *fig. 8*).

Fig. 9 illustrates the total quantity of visible light as a function of the applied power using a con-

[6]) For a description of a rather different type of flash lamp, developed for another purpose, see S. L. de Bruin: Apparatus for stroboscopic observations. Philips Techn. Rev. 8, 25-32, 1946.

denser of 100 μF; it will be seen that the efficiency at 400 wattsec without a choke is 42.5 lumen/watt, and 29.5 lumen/watt with an inductance of 7 mH and 1.1 Ω resistance in series with the lamp. The

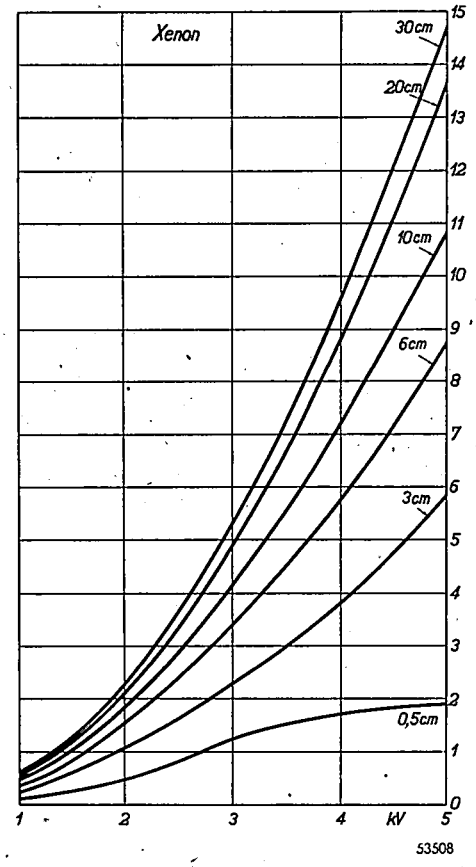


Fig. 8. Total visible quantity of light of the flash lamp (in arbitrary units), as a function of the condenser voltage, for xenon at different pressures.

measurements were carried out with a standard type of condenser, not specially designed for low inductance and resistance values.

In order to investigate the development of the discharge as a function of the time, measurements have also been made of the current, the voltage and the total quantity of light by means of a cathode ray oscillograph [7]). Figs *10a, b* and *c* are the reproductions of the oscillograms as taken without a choke in the circuit. Fig. 10*a* shows the current through the flash lamps, using a 20 μF condenser at a potential of 2 kV. With the object of determining the duration of the discharge, a sinusoidal voltage of a known frequency was photographed on the same plate. It was found that the current drops to one half of its peak value in 4×10^{-5} seconds; fig. 10*b* depicts the corresponding voltage on the lamp. The oscillogram in fig. 10*c* shows the variation in the total quantity of light emitted; in this case the difference in potential was taken across a resistor of 470 Ω connected in series with the above-mentioned photocell and passed to the oscillograph after having been amplified. The luminous intensity will also be seen to decrease to one half of its maximum after 4×10^{-5} seconds.

Let us now look at some of the results obtained with a choke in series with the flash lamp which are represented by *fig. 11*. Fig. 11*a* refers to the current; an initial positive flow of current lasting 1.2×10^{-3} sec is followed by a further wave in the opposite direction [8]). Fig 11*b* shows the fluctation in the light emission, of which the initial wave also covers 1.2×10^{-3} sec; the second wave is produced by the current flowing in opposite direction.

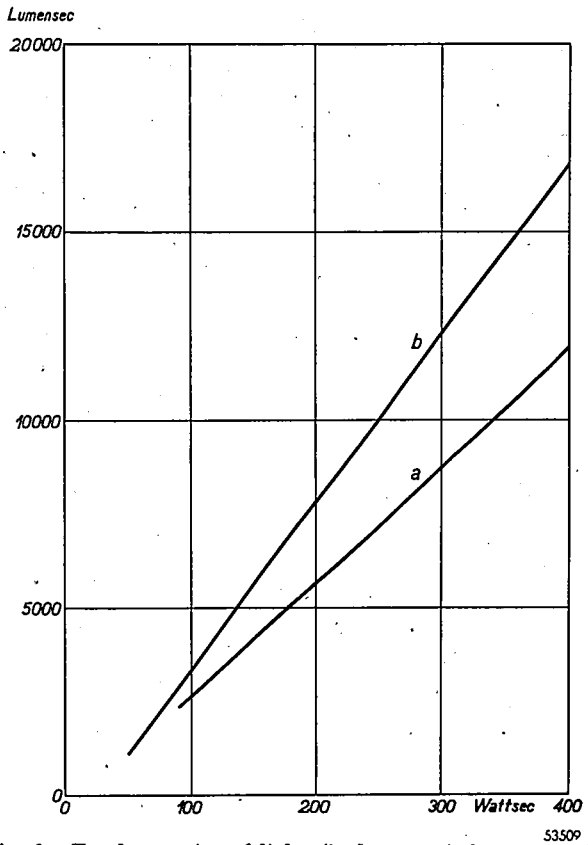


Fig. 9. Total quantity of light (in lumensec) from a single flash of a xenon-filled flash lamp as a function of the applied power, using a 100 μF condenser: *a*) with choke, *b*) without choke.

[7]) A description of the circuit used in this case is given in an article by N. Warmoltz, The ignition mechanism of relay tubes with dielectric igniter, Philips Techn. Rev. **9**, 105-113, 1947 (No. 4), see fig. 6. As is customary, the electron beam was suppressed during the inoperative period, the photograph being taken from the screen of the cathode-ray tube which has an acceleration of 5 kV, with a single sweep time base.

[8]) It is therefore advantageous when the choke is included in the circuit to employ a flash lamp in which both the electrodes are oxide-coated.

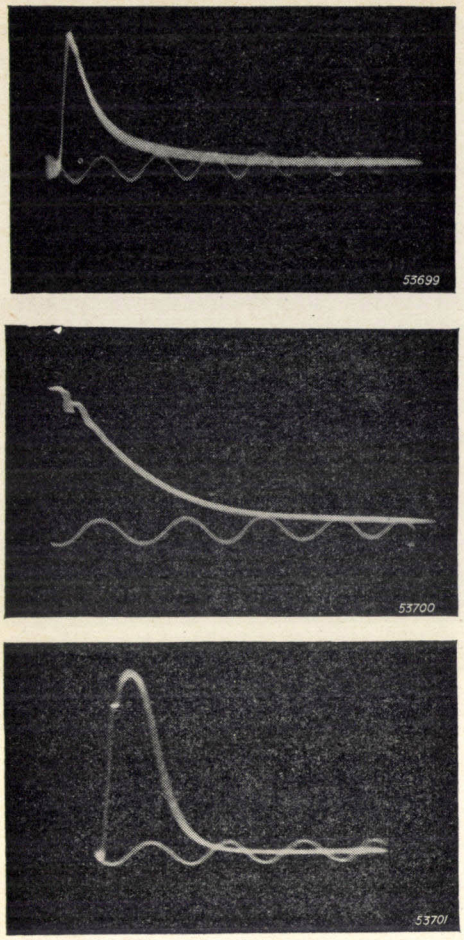


Fig. 10. Oscillogram showing current, voltage and total quantity of light during one flash (without choke): *a*) current curve with a condenser of 20 μF at a potential of 2 kV. The calibrating frequency is 15,000 c/s. At 4×10^{-5} sec the current is seen to have dropped to one half of the peak value. *b*) Corresponding variation in voltage: calibrating frequency 5000 c/s. *c*) Quantity of light (at the same voltage and capacitance). Calibrating frequency 15,000 c/s. As the emission also drops at one half of the maximum in 4×10^{-5} sec, the duration of the flash is almost the same as that of the current pulse.

When the choke is used, either for the purpose of prolonging the flash or to preserve the life of the lamp, it is advisable to keep the resistance of the coil as low as possible, since the inclusion of the choke has an adverse effect on the efficiency of the lamp, as will be seen from fig. 9 which demonstrates the lamp efficiency, with and without choke.

To obtain some idea of the value to be attributed to the choke which will not reduce the efficiency too much, let us turn for a moment to the question of the "resistance" of the flash lamp itself.

Fig. 12 shows the behaviour of the voltage on the lamp as a function of the current passing during one flash. The slope of the curve with respect to the horizontal is a measure of the lamp resistance.

The oscillogram commences at a point on the vertical co-ordinate (just visible in the photograph as a small spot). In the first moments the current increases rapidly, whilst the voltage decreases only slowly; owing to the high speed at which the whole process takes place the first branch of the curve (except the initial point to which we have just referred) is not visible in the oscillogram. From the second part of the curve it appears that the resistance increases with the time.

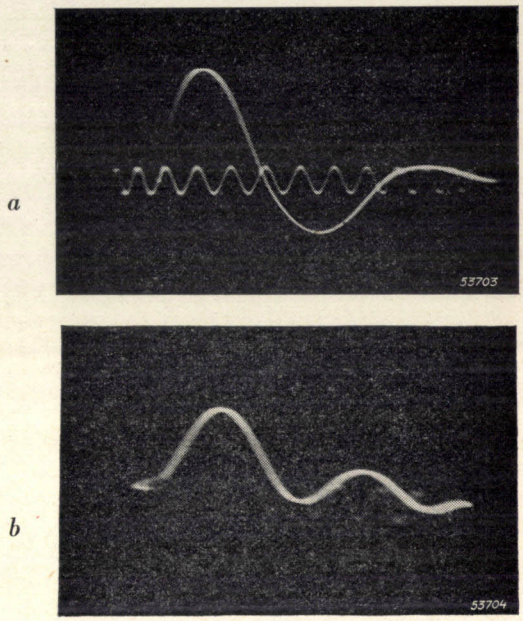


Fig. 11. Current and quantity of light as a function of time, a choke being connected in series with the flash lamp. For this measurement a choke having a self-inductance of 7 millihenry and a resistance of 1.1 ohm was used. *a*) Current as a function of time. The voltage was, once again, 2 kV and the condenser had a value of 20 μF. The calibration frequency was 2500 c/s. The duration of the first positive current wave is 1.2×10^{-3} sec. *b*) The quantity of light as a function of time.

The resistance is actually quite low, being 2 to 3 Ω at the moment when the current reaches its maximum value and increasing to about 6 Ω as the

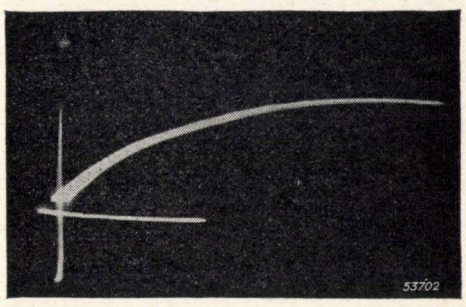


Fig. 12. Oscillogram illustrating the effective resistance of the flash lamp versus the time. The deflection along the horizontal axis is proportional to the current, and that along the vertical co-ordinate is proportional to the voltage; the slope of the curve with respect to the horizontal is thus a measure of the resistance of the lamp. For this test a potential of 4 kV was used, the condenser in question being 100 μF. If actual values are required, the different horizontal and vertical sensitivities must be taken into account.

current drops. The resistance of the choke, then, must be low in comparison with these values.

The measurements just described were effected with a xenon-filled lamp 20 cm in length, but experiments with other fillings and different lengths of tube have proved that both these factors will considerably affect the results of the measurements. If so desired, even shorter flash periods can be attained by a suitable selection of the physical dimensions and gas fillings of a lamp of this type.

If a flash lamp is to be employed on higher voltages than those which can be withstood by the lamp without breaking down (without ignition impulse), a relay tube that can withstand the higher potential may be placed in series with the lamp and this may be fitted with a mercury cathode capable of emitting the high peak currents [9]). The loss in energy due to inclusion of this tube does not exceed a few per cent.

[9]) A relay tube of this kind with a dielectric igniter is described in the article referred to in note [7]), and the tube in combination with a flash lamp in the article indicated in note [6]).

ABSTRACTS OF RECENT SCIENTIFIC PUBLICATION OF THE N.V. PHILIPS' GLOEILAMPENFABRIEKEN

Reprints of these papers not marked with an asterisk can be obtained free of charge upon application to the Administration of the Research Laboratory, Kastanjelaan, Eindhoven, Nederlands.

R73: B. D. H. Tellegen: The gyrator, a new electric network element (Philips Res. Rep. **3**, 81-101, 1948, No. 2).

Besides the capacitor, the resistor, the inductor and the ideal transformer a fifth, linear, constant, passive network element is conceivable which violates the reciprocity relation. This element is a four-pole in which the secondary current and voltage are proportional to the primary voltage and current respectively; it is denoted by the name of "ideal gyrator". By its introduction the system of network elements is completed and network synthesis is much simplified. The gyrator can be realized by means of a medium consisting of particles carrying both permanent electric and permanent magnetic dipoles or by means of a gyromagnetic effect of a ferromagnetic medium.

R74: H. Bremmer: On the theory of spherically symmetric inhomogeneous wave guides, in connection with tropospheric radio propagation and under-water acoustic propagation (Philips Res. Rep. **3**, 102-120, 1948, No. 2).

The conception of the atmposphere as a curved wave guide consisting of an inhomogeneous medium, through which radio waves and acoustic waves can be propagated, is worked out. The guiding effect is compared with that occuring in the propagation of acoustic waves through oceans. The properties of these two types of spherical wave guides are in many respects interrelated, but there are some essential differences which are brought to the fore. These differences are due to the fact that the product $r\mu$ (r = distance to the centre of the earth, μ = index of refraction) shows at least one minimum in the case of atmospheric propagation and one maximum in the case of oceanic propagation. As a consequence there is a difference, for instance, in the distribution of the times of arrival of consecutive rays orginating from a point source: in the first case the intervals between these times are smallest for the rays coming latest, in the second case they are smallest for the rays arriving earliest.

Some general remarks are made with respect to arbitrary spherically symmetric wave guides. For example, the concept of cut-off frequency is discussed from the point of view of the modes as well as from that of geometric optics.

R75: A. van der Ziel and A. Versnel: Measurements of noise-factors of pentodes at 7.25 m wavelength (Philips Res. Rep. **3**, 121-129, 1948, No. 2).

Measurements are given of noise factors of pentodes at 7.25 m wavelength as a function of the transformed antenna resistance, and the results are compared with the theory. Theoretically, induced grid noise might be partly suppressed by inserting a small resistor of e.g. 30 Ω in the cathode lead. This should reduce the noise factor, but in practice other effects cancel this reduction. It is shown that in many cases the selfinductance of the cathode lead increases the noise factor, but this may be counteracted by inserting a capacitor in the cathode lead, so that series resonance is obtained. Finally, the influence of internal feedback is investigated, and it is shown that it may give rise to an increase of the noise factor.

R76: K. F. Niessen: Indication of landing courses independent of weather conditions, II and III. (Philips Res. Rep. **3**, 130-139, 1948, No. 2).

This is a continuation of the theory given in **R66** (see these abstracts). In II and III the case is considered where the infinitesimal dipoles are replaced by antennae of final length, the landing course being indicated by antennae placed at different heights (II) or at equal heights (III).

R77: J. M. van Hofweegen and K. S. Knol A universal adjustable transformer for u.h.f. work (Philips Res. Rep. **3**, 140-155, 1948, no. 2.

A matching device for u.h.f. work is described with which any impedance can be matched to any other impedance by properly adjusting two shorting bridges. It consists of a screened two-wire Lecher system assymetrically loaded with respect to the screen. The device can also be used for coarse impedance measurements. Based on the same principle, a universal adjustable transformer using wave guides can also be made.

VOL. 10 No. 7, pp. 189-220 JANUARY 1949

Philips Technical Review

DEALING WITH TECHNICAL PROBLEMS
RELATING TO THE PRODUCTS, PROCESSES AND INVESTIGATIONS OF
THE PHILIPS INDUSTRIES

EDITED BY THE RESEARCH LABORATORY OF N.V. PHILIPS' GLOEILAMPENFABRIEKEN, EINDHOVEN, NETHERLANDS

EXPERIMENTAL TRANSMITTING AND RECEIVING EQUIPMENT FOR HIGH-SPEED FACSIMILE TRANSMISSION

I. GENERAL

621.397.3

by H. RINIA, D. KLEIS and M. van TOL.

In recent years a new system has been developed at Eindhoven for facsimile transmission and reception of drawings, photographs or printed matter capable of transmitting a document of quarto size (21 cm × 29.7 cm) in 8 seconds by means of a cable or by radio. The system is continuous: the documents, the size of which — apart from a limit on the width of 22 cm — is immaterial, are placed on an endless belt upon which they are electrically "stuck" for scanning by a rapidly rotating optical system. At the receiving end positive or negative reproductions, reduced 6 × in size, are "written" on a continuously moving film which then passes through the developing and fixing processes and can if necessary be printed immediately on sensitized paper, enlarged to the original size. The resolving power of the system is 5 lines per mm, which corresponds to the best reproduction obtainable from the older and slower types of equipment. A number of characteristic features and possibilities of application of the new system are reviewed in this article; a description of the mechanism, with details of the optical and electrical devices, will be presented in subsequent articles in this review.

In 1843, when Morse telegraphy was still in its infancy, a British physicist, Bain, demonstrated an apparatus by means of which it was possible to reproduce hand-written characters at a distance, over an electric circuit. In 1865 Caselli carried out in France a number of experiments with this so-called facsimile telegraph, which was then capable of handling 600 written words per hour. Around the year 1890 numerous other experiments in this direction were carried out in the United States and by 1907 a whole network was employed for a short time in Europa for the telegraphic transmission of illustrations for the daily press. After the first world war, mainly between 1922 and 1928, a number of facsimile systems were developed, incorporating considerable technical improvements [1]) and the resultant installations appeared to have come to stay. Since then, facsimile networks in Europa and America were extended more and more and permanent inter-continental connections were subsequently established: in 1931 there were more than 25 European stations in use, whilst by 1937 London was maintaining permanent picture-telegraph communication with many European capitals, as well as with New York, Buenos Aires and Melbourne.

This short and by no means comprehensive historical sketch is intended merely to show that facsimile transmission has for a long time occupied a definite place in the field of telecommunications, to supplement the well-established Morse telegraphy, telephony, teleprinting and — the latest acquisition to this family — television.

There can, in fact, be no doubt that in many spheres of application the possibility of transmitting documents and pictures in facsimile, by cable or radio, furnishes an essential adjunct to the conventional transmission of words, whether spoken or recorded in the form of standardised characters. The contents of a letter can thus be transmitted telegraphically without depriving it of its most individual character, the handwriting of the sender; a cheque, complete with signature, can

[1]) Among the more important systems at this time were those of Korn, 1922; Bartlane, 1922; Belin, 1924; Jenkins, 1924; American Tel. and Tel. (Bell system), 1924/5; RCA (Ranger), 1924/5; Siemens Karolus Telefunken, 1927; Westinghouse (Zworykin), 1928.

be reproduced for examination at places far removed from the point of origin within a matter of minutes only; technical drawings, details of which cannot be clearly expressed in words; weather charts showing the changes in meteorological conditions hour by hour; press-photographs; texts in languages not employing the letters of the alphabet, such as Chinese — these are but a few examples of the objects for which of picture transmission is the indicated method.

Efforts have recently been made in various quarters to create a still wider scope for facsimile transmission in our daily life, and developments are actually in progress in two different directions, viz.

1) In the United States a wider field is being sought for facsimile transmission in the form of a supplementary feature in broadcast transmissions, using relatively simple facsimile receivers, based on the systems of Finch, Hogan or Alden, which can be connected to any ordinary radio receiver in place of the loudspeaker. Listeners are thus to be provided in their own homes with a radio news-sheet containing actual photographs as well as many other items of visual interest. Endeavours are also being made to arouse interest in facsimile transmission for mobile services such as the police, fire brigade, taxis and aircraft, for the transmission of situation diagrams and written orders (also finger-prints etc. for the police) to and from headquarters; the pictures are recorded automatically and it is claimed that facsimiles are less liable to be misunderstood than verbal messages.

2) The other line of development is directed towards a speeding-up of the transmission itself and, with it, an intensification of the facsimile traffic between any two fixed stations. As far back as 20 years ago attempts in this direction were made by Alexanderson [2]) and Zworykin [3]), but these did not meet with any permanent success. It seems to us, however, that this failure should be looked upon as being analogous to the initial fate of the ordinary "slow" facsimile technique; the network installed in 1907 and referred to above very quickly disappeared from the scene. The years from 1924 onwards saw a more permanent establishment of "slow" facsimile telegraphy networks, partly owing to the improved picture quality and more reliable working, but partly also to the greater demand for this means of communication. It is obvious that the intensification of facsimile traffic by high-speed equipment will likewise become a fact only when the various favourable conditions mentioned above have been realized.

With this in mind, and after preparatory work which has taken some years to complete, Philips have developed in their laboratories at Eindhoven a new system of high-speed facsimile transmission in which the use of recent technical advances guarantees not only high quality of reproduction but also great reliability in performance. It may be expected that, in view of the present pattern of our social structure, the possibilities offered by the new system will open up fresh and very important applications.

In presenting a series of articles in this journal, giving a description of the new facsimile system, we begin with a review of its fundamental principles and major characteristics, followed by a brief resumé of some of its possible fields of application. Later articles will then deal with the construction of the transmitter and the receiver, the optical system, the electrical transmission circuits and, finally, the synchronisation of receiver and transmitter.

Salient features of the new system

In accordance with the system employed in all present-day facsimile transmission equipment, the picture to be transmitted is scanned by a spot of light which traverses narrow, parallel and contiguous lines; the amount of light reflected (or transfused), which varies according to the local blackness of the picture, is transformed by means of a photo-electric cell into a varying electrical voltage, the image-signal, which is transmitted to the receiver via a cable or by radio. In the receiver this signal may be used to control the intensity of a beam of light which moves synchronously with the scanning spot at the transmitting end, and "writes" the successive lines on a sheet of sensitized material, the varying intensity of the light reproducing faithfully the pattern of light and shade in the original.

The smaller the spot of light used for the scanning (and reproduction), the better the quality of the reproduced image; in the Philips equipment the diameter of the scanning spot in the transmitter is *1/5th of a millimetre*, so that, in principle, it is possible to reproduce details of that order of size. This corresponds to the best reproduction so far achieved by any of the slower picture-telegraph systems. For purposes of comparison, details of the "resolving power" of various other methods of

---

[2]) See, inter alia, F. Schröter, Handbuch der Bildtelegraphie und des Fernsehens, Springer, Berlin, 1932, p. 414.

[3]) V. K. Zworykin, Facsimile picture transmission, Proc. Inst. Rad. Eng. 17, 563-550, 1929.

reproduction are given in *table I* [4]). *Fig. 1* illustrates part of a document transmitted by the new Philips system.

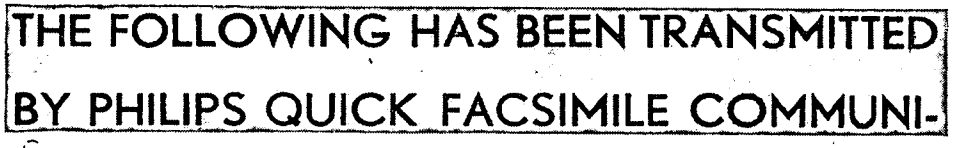
Table I. Resolving power, in lines per mm, of various reproduction methods.

Newspaper picture	2-4
Half-tone blocks Philips Technical Review . .	6
Ordinary slow facsimile transmission (105 lines per inch)	4
Philips high-speed facsimile system	5
Photographic reproduction on positive film	55

The new system is capable of handling documents up to a width of about 22 cm, i.e. the maximum width of conventional letter paper, and of any length. A sheet of quarto size (roughly the size of this page) 29.7 cm in length is *transmitted in 8 seconds*, whereas the more common facsimile systems require something like 8 minutes to reproduce a sheet of the same size (in some cases less, e.g. 2 to 3 minutes, but in many other cases still longer, viz. 20 minutes).

The number of image elements (that is, surface elements of the same size as the scanning spot) that can be transmitted per second over a given channel of communication is directly related to the maximum permissible modulation frequency in that channel. In our case, where the diameter of the spot is 0.2 mm, a sheet of the size on which this article is printed will contain 297:0.2 $\approx$ 1500 lines for scanning, and on each line there will be 210:0.2 $\approx$ 1000 image elements. Thus, 1.5×10^6 elements have to be transmitted in eight seconds, which, in the extreme case of the successive elements being alternately black and white, corresponds to 200,000 luminous fluctuations per second, or a *maximum modulation frequency of 100 kc/s*. A frequency band of such a width is available with ultra-short-wave transmitters, which are frequently used for permanent beam-communication between two stations. Similar bandwidths are usually also available in present-day cable networks for carrier telephony; the network in the Netherlands, for instance, even permits of modulation frequencies up to around 200 kc/s. For the rest, the limit of 100 kc/s is not so very critical in actual practice, since tests have shown that signals from our equipment, transmitted over a line allowing a maximum modulation frequency of 80 kc/s, still give reproductions of quite reasonable quality. In the event that the modulation frequency has to be still further limited, the transmission rate can be reduced accordingly, to maintain the same resolving power. For this purpose the speed of both the transmitter and the receiver must be reduced, which can quite easily be achieved with the synchronisation method employed.

a)



b)

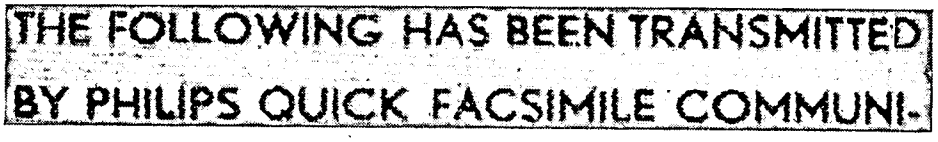


Fig. 1. Part of a document transmitted by the new high-speed facsimile system: *a*) the original; *b*) the facsimile. Both *a*) and *b*) have been enlarged to twice the size of the actual original: owing to the enlargement the effect of the blurring of the printing block (see table I) on the image quality is eliminated. For a fair comparison, the text should be observed from a distance of about 50 cm (twice the normal reading distance). The time required for transmitting the area shown in this example is about 0.06 sec.

It is a well-known fact that in ordinary telegraphy the total quantity of information (number of characters coded according to a given system) capable of transmission per unit of time is, theoretically, roughly proportional to the width of the available frequency band, irrespective of the type of equipment employed [5]). Similar considerations apply to facsimile telegraphy, the total quantity of "information" being represented here by the number of picture elements. In connection with this fact, three remarks have to be made. Firstly, for the performance of a facsimile system, the frequency band (that

[4]) The obvious course would be to include in our comparison the reproduction obtained in television, but in judging television pictures other criteria are involved, since we are then dealing with moving images. Moreover, these images are viewed at much greater distances than ordinary correspondence or newspaper photographs, in just the same way as, in the cinema, the distance is such that the whole of the picture can be observed without moving the eye.

[5]) See e.g. J. te Winkel, Carrier Telegraphy, Philips Techn. Rev. **8**, 206-213, 1946.

is, the number of picture elements that the equipment is capable of transmitting per second) is a better criterion than the actual area of picture transmitted per second, seeing that a given area could easily be transmitted more rapidly in a certain frequency band if one were contented with fewer lines per mm (e.g. if a larger scanning spot were used).

Secondly, with an ordinary facsimile system working 60 times more slowly than ours it is possible, for the same image quality and using a frequency band of 100 kc/s, to transmit roughly the same picture area per minute, provided the available band is divided into 60 channels, 60 transmitters and receivers being used. Needless to say, this would be far too cumbersome and uneconomical for a permanent link between any two given stations.

In the third place it is quite possible, in principle, to transmit documents by television, by photographing the image appearing on the screen, but, as the primary object of television is to transmit moving images, necessitating the transmission and reception of single images (of, say, 567 lines) in about 1/25 second, it requires an even much wider frequency band, namely 2000 to 3000 kc/s. The use of a frequency band of this width for facsimile work would be quite uneconomical at anything less than 20 to 30 times the speed of our new facsimile system. Whereas we consider that the speed of the Philips system will in many cases meet a practical demand, it seems doubtful whether a system working at a speed still 20 times higher would find regular employment. Furthermore, in order to be able to feed the documents into the machines fast enough, a film would first have to be made at the transmitting end, thus considerably complicating the process. Moreover the problem of the sensitivity of the recording material, which, as we shall see, played a very important part in the designing of our facsimile system, would be almost incapable of solution at very much higher speeds.

Any increase in the width of the frequency band employed is accompanied by a corresponding increase in the noise produced by fluctuations in the emission of electrons from the photocell and by the movement of the electrons in the resistor used for coupling the photocell to the amplifier. In our high-speed facsimile transmission, therefore, the noise level, taken absolutely, will be higher than in the slower systems; in spite of this, interference-free reproduction is assured by using a photocell with secondary emission amplification (electron-multiplier). The internal amplification of these valves may be of the order of 100,000, and the noise originating from the resistor in question is thus rendered quite negligible, whilst the apparatus itself is considerably simplified. In our case a *signal-noise ratio of 43 db* has thus been obtained, which is even better than with the majority of slow facsimile systems.

In the conventional, slower systems, scanning of the document is effected by wrapping it around a drum which rotates while an optical system slowly travels along the drum in the axial direction. The few seconds required to place a fresh document on the drum (or to replace the latter by another which has been previously loaded), do not make much difference to a transmitting time of several minutes per document, but in a system such as the one under review, in which the transmission time is a few seconds only, such repeated interruption of the transmission would be very prejudicious to the efficiency of the whole system; we have therefore made a departure from the now almost traditional drum system. As will be seen from the photograph of the equipment in *fig. 2*, the documents are simply placed on an endless belt moving at a speed of 30 cm per 8 seconds. They are stuck on to the belt by an electric charge. The documents, consisting of light or dark paper, with drawings, photographs, or hand-written, typed or printed text, are scanned by a rapidly revolving optical system at a certain point in their passage, an additional advantage of this *continuous scanning system* being that the documents need not necessarily be of the standard quarto size, 29.7 cm in length: *any length may be used* provided the width does not exceed approx. *22 cm* [6]).

As already mentioned, the equipment under discussion will transmit an image of 1.5×10^6 picture elements in 8 seconds. This means that the receiver is allowed only 1/200,000 sec. for the exposure of each element. The light-source, the luminous intensity of which must be capable of keeping in step with modulations up to 100 kc/s, is a special gas-discharge lamp which we have developed for the purpose. This lamp, together with a high-speed optical system, makes it possible to obtain the required density (max. 1.5) on *standard positive film* within the short space of time in question. The resolving power of this film is much higher than that of the scanning spot (see table I); the image in the receiver can therefore be recorded greatly reduced in size in comparison with the original, without any loss of definition, and the receiver has therefore been designed to give a reproduction *reduced 6 times in size*. The amount of film required is thus reduced by a factor of 36.

The 45 mm film passes continuously through the receiver, at a certain point in which a rapidly rotating optical system "writes" the lines on the

---

[6]) This principle of continuous scanning was first employed in 1928 by Alexanderson, but the essential increase in the transmission rate, which in our case was the main reason for adopting this method, could not be satisfactorily achieved with the means available in those days, At that time the avoidance of the necessity for loading the documents onto a drum and the advantage of freedom in regard to document size were regarded as primary factors.

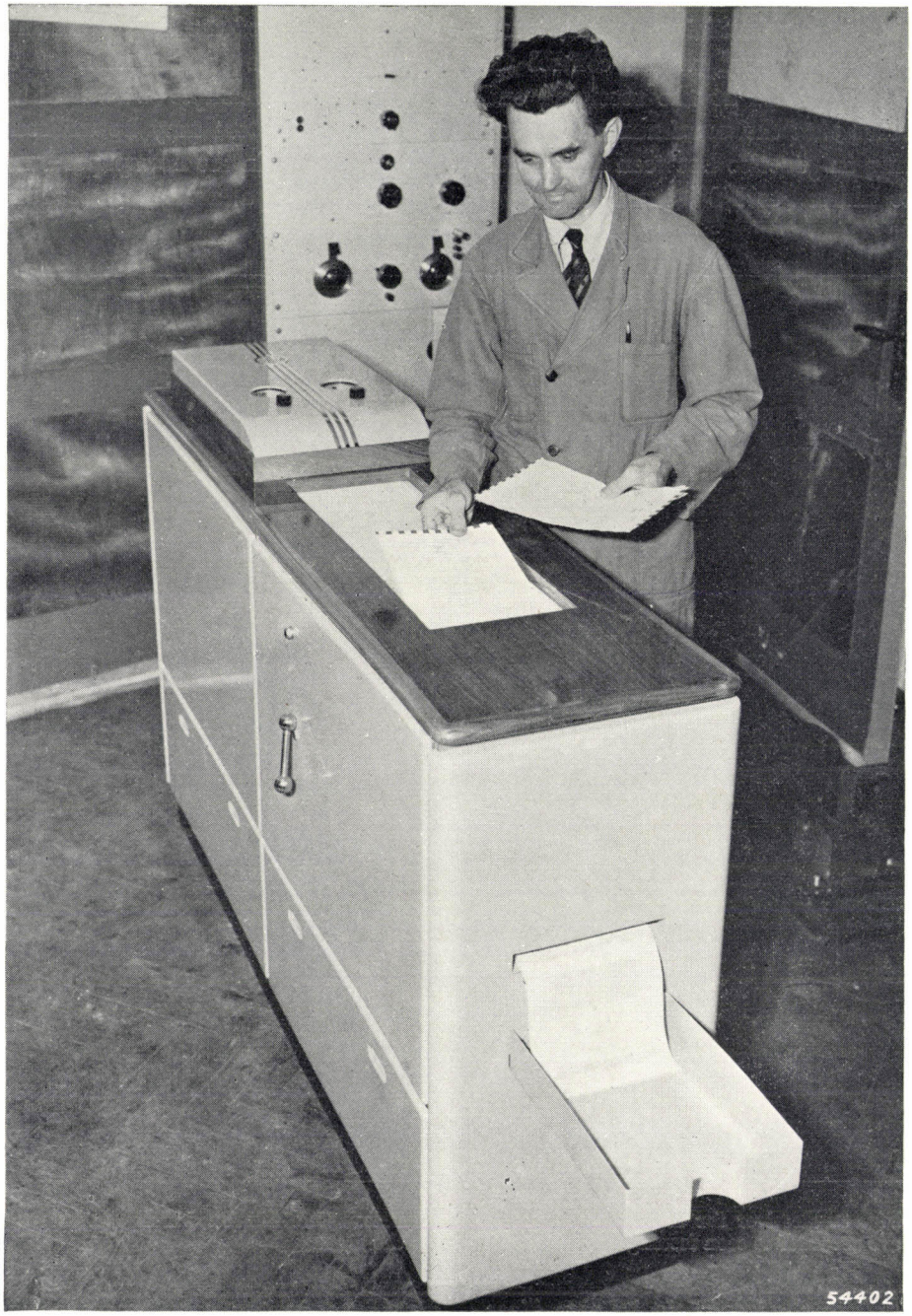


Fig. 2. Transmitter of the Philips high-speed facsimile equipment in operation. Documents of any size up to 22 cm in width are placed on an endless belt running just below the aperture in the table top. When finished with, they fall into the collecting tray seen at the front end of the unit.

film with the requisite intensity of every element. After development and fixing, the documents can be projected full-size while the film is still wet or, if required, one or more copies of each can be made in this way on an inexpensive photostat paper. *Fig. 3* depicts the receiving equipment in use.

In order to complete our review of this equipment it may be said that the receiver is very simply switched over to produce either a positive or a negative image of the original; further, the electrical circuit is such that the average brightness of the original document (the "direct current component" of the image signal) is correctly reproduced at the receiving end. The equipment is capable of transmitting black-and-white pictures or half tones (photographs) as required [7]).

Synchronisation of the revolving optical systems of the transmitter and the receiver is

[7]) The designation "picture telegraphy" is sometimes applied specifically to half-tone transmission and "facsimile transmission" exclusively to black-and-white, but we have not adopted this distinction.

effected by means of synchronising signals, transmitted with the image signal, which control the speed of the driving motor at the receiving end: this feature ensures that the maximum differences in phase occurring in practice between transmitter and receiver are limited to 1/2°, corresponding to a line displacement in the image, in its own direction, of only 0.5 mm. In the event of an interference (as may be caused by fading), the relative phasing corrects itself aperiodically in one second, this being the equivalent writing time of about 200 lines; the resultant displacement among the lines, even in the worst case, is therefore imperceptible.

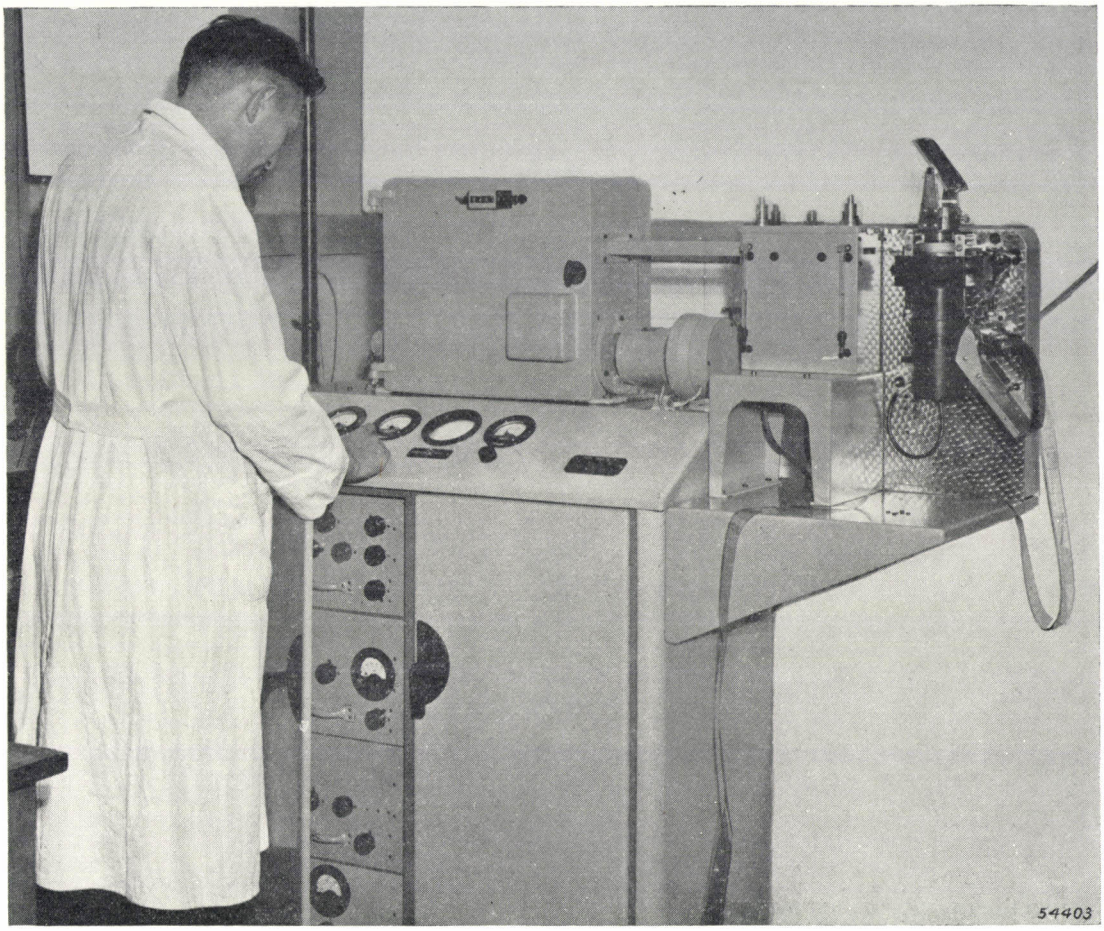


Fig. 3. Receiver for high-speed facsimile transmission. The film on which the images are recorded is seen issuing from the machine on the right.

Possible applications of the new system

Although picture telegraphy as such is, of course, primarily concerned with the transmission of pictures, it is obvious that there are not likely to be many places in the world with such a concentration of pictures to be transmitted that this high-speed facsimile apparatus could be loaded continuously. In connection with its applications, therefore, one of the first possibilities that came to mind is the transmission of illustrated text material. An example where all the advantages of the new system may be utilised to the fullest is to be found in the newspaper business.

It is quite a normal procedure to print and distribute in the provinces identical copies of a large city newspaper, possibly with the inclusion of a local-news page. The text of the more important news is usually transmitted to the appropriate point in the provinces by telephone or teleprinter, so that it will not lose too much of its news value. The ordinary teleprinter service will handle 1000 characters in $2^1/_2$ minutes, which means a period of some three hours for two pages each of 40,000 letters. Then the type has to be set, corrected and laid out before printing can be commenced. Using the new facsimile system, the same two sheets, divided into 8 quarto sheets, can be transmitted in about 1 minute. Re-setting of the type and the subsequent operations are then eliminated, since the reduced reproductions on the film can be

immediately used for making full-size blocks, from which the paper is then printed. The job of making these blocks involves very much less time and labour than the setting of type, whilst line drawings or photographs in the original paper can be reproduced along with the text without any difficulty.

Another use of the system, in which all its essential features can be employed, might be found in the transmission of ordinary letter post between the principal centres of a country. During the night, when carrier-telephony cables are more or less idle, a facsimile unit of the type under review would be able in five hours to transmit a good 2000 quarto-size letters, or proportionately more of a smaller size. In certain cases where identical letters are to be sent to numerous addresses it would mean a great advantage that the contents would have to be transmitted only once, since the receiver supplies a film of the letter (as a negative, if desired) and copies can be made on the spot. Again, the addressees can be furnished with two or more copies of any given letter, as is often required in business correspondence. If a filing system of all incoming items is to be maintained, the fact that a small film of each document received is immediately available may be very useful; microfilm archives of this kind are very widely employed today.

The particular advantages of this system might lead one to infer that it will oust the teleprinter, but this is not very likely, seeing that the latter, being intended for a more limited performance than the facsimile system, is able to perform its allotted task more economically. Let us for a moment look more closely at this question. From the figures given it follows that the teleprinter will transmit a message of roughly 4000 letters, this being the maximum contents of a typed sheet of letter paper, in about 10 minutes — our facsimile equipment does it in 8 seconds. At the speed in question the teleprinter, however, uses a frequency band of only 120 c/s, as compared with 100 kc/s for the facsimile system. Since the use of a cable calculated on the basis of the period of usage as well as on the required frequency band represents by far the greater portion of the operating cost, the teleprinter, despite its slow transmission powers, is more economical than the facsimile by a factor of 10 to 12. The explanation is quite simple. The teleprinter requires 7 impulses for each character transmitted, whilst the facsimile system transmits, per quarto sheet, 1.5×10^6 image elements, or 0.75×10^6 impulses, that is an average of 200 impulses per character. The teleprinter is able to function on such a small number of impulses because it employs both standardisation and code; textual matter is expressed in the form of a small number of standardised letter, figure and other symbols (about 50 in all), each of which is represented by only a small number of impulses (actually 7), spaced out in accordance with a certain code. This code has been given once for all to the receiving stations by means other than the transmission channel and is incorporated in the mechanism of the recording machines.

The facsimile system, on the other hand, transmits every individual peculiarity of the characters and faithfully measures out and reproduces all spaces and blank parts of the sheet. Its use is therefore economically justified only in cases where it is just those peculiarities of form that are important, as in hand-written correspondence, which simultaneously transmits something of the writer's own personality; or, again, where the blank parts are essential features, as in pictorial representations or specially "made up" textual subjects; or finally, in other cases as outlined above, where characteristic advantages of the system, swing the balance in its favour.

A DEMONSTRATION STUDIO FOR SOUND RECORDING AND REPRODUCTION AND FOR SOUND FILM PROJECTION

by the ELECTRO-ACOUSTICS DEPARTMENT. 725.81

At the commencement of 1948 a new demonstration studio was placed at the disposal of the Electro-Acoustics Department of the Philips Factories at Eindhoven. Known as the ELA Studio, it is equipped for demonstrations of various types of programme sources, amplifiers, loudspeakers and film projection equipment, as well as for sound recording by different systems. The acoustic properties of the studio are such that the reverberation time at the higher frequencies (0.9 sec at 2000 c/s) is only slightly less than at the lower frequencies (1.3 sec at 100 c/s), this having a very beneficial effect on the high note response. An elaborate relay system permits of any combination of a sound source (microphone, "Philimil" tape, magnetic tape, or radio receiver), an amplifier, and one or more loudspeakers. From the control desk one or several programmes can be passed to different recording equipment, viz. the Philips-Miller, the magnetic or the photographic equipment, or the gramophone recording unit. Arranged round the studio itself are a microphone room, "speech studio", projection, control and recording rooms.

For the effective demonstration of electro-acoustic equipment such as microphones, pick-ups, amplifiers, loudspeakers and so on, a hall possessing certain acoustic properties — amongst others those relating to reverberation time and sound insulation — is indispensable. This being so, the necessary devices to make rapidly any desired combination of these different apparatus is also essential, the final requirement being a certain degree of comfort in which to judge the results.

Prior to the war, the Electro-Acoustics Department had at their disposal a hall in one of the Philips factories which more or less met the conditions outlined, but this was completely destroyed in 1942.

It was then decided that as soon as the opportunity presented itself, a new hall was to be built and equipped, but with every modern facility and much wider scope; by this is meant that it would have to be suitable for soundfilm projection and for use as a studio for sound recording, for post-synchronisation of films and also for radio transmission.

A studio on these lines, called the ELA Studio (*EL*ectro-*A*coustics) was completed early in 1948. It includes a microphone room, "speech studio" and projection, control and recording rooms. *Fig. 1* gives a good impression of the finished studio arranged for film projection. The main measurements are: length 17.6 m, width 11.6 m, height 7 m (58′ × 38′ × 23′); a plan view of the whole project is given in *fig. 2*.

Before embarking on a technical description, let us say a few words about the architecture and acoustics.

Architecture

In the design of the studio the scope of the architect was in many respects limited. He was obliged to take into account the special conditions to be met in the matter of acoustics (see later paragraph), air-conditioning and heating; moreover, the electrical wiring was to be concealed from view and yet easily accessible at various points, but, notwithstanding all these restrictions a harmonious effect was created.

The lower part of the walls is panelled in dark walnut, and the same material is used for the panels covering the ventilation shafts and for the border of the ceiling. Above the dado the walls are covered with a thin fawncoloured fabric to conceal the sound-absorbing material with which they are lined, the severity of these surfaces being relieved by silk cords stretched over the fabric to form a diamond pattern.

The lighting is partly direct from lamps on the ceiling and partly indirect from cornices running along the top of the wall panelling; the latter lighting therefore mainly illuminates the upper part of the walls.

Acoustic properties

We must here distinguish between the acoustics and the sound insulation of the studio.

Acoustics of the studio

First of all, what are the requirements governing the acoustics, and in particular the reverberation time, of a hall intended to serve both for sound recording and the reproduction of sound by means of loudspeakers?



Fig. 1. The ELA Studio, arranged for film projection.

Clearly, the reverberation time must not be too long in either case, as this would mean too much merging of the individual sounds.

On the other hand, a recording studio must not be too "dead" acoustically, for in the extreme case, with no reverberation at all, musicians would find themselves in difficulty as their music would sound unnatural. Again, recordings made in an acoustically dead studio need to be played back in a room of outstanding acoustic properties (a rare occurence) if the music is not to sound too clipped.

A room in which is reproduced should not be too dead either, since the listener then does not really "experience" the reverberation already present in the recording; consequently for the proper reproduction of a recording containing only part of the requisite reverberation the room in which the recording is played requires a definite reverberation time.

In both cases, that is, for the recording of music as well as for its reproduction by means of loudspeakers, the reverberation times are therefore subject to certain limitations and the most suitable of these were found to be:

100 c/s	1.3 sec,
800 c/s	1.0 sec,
2000 c/s and higher	0.9 sec.

To ensure good intelligibility the reverberation time for speech should usually be shorter than for music; generally speaking, large halls are therefore less suitable for recording speech. For this reason a small speech studio and also a microphone room, have been included in the layout of the studio complex, both of these rooms being almost completely dead acoustically.

The reverberation time of a hall of the dimensions in question (1500 cub. m) would be far too long for both high and low frequencies if the walls were of bare brick. Moreover, the absorption of brickwork increases with the frequency; the reverberation time would therefore be longer for the low frequencies than for the high, which would cause the hall to sound "hollow".

It is a characteristic of almost all sound-absorbent material that the absorption increases with the frequency, in other words, when the absorption of the lower frequencies is satisfactory, that of the high frequencies is too great; this cannot be tolerated,

however, since sound depends for its brilliance upon these higher frequencies. In order to attain the reverberation times specified above, steps had to be taken in the construction of the studio to ensure extra absorption of the lower frequencies.

In the calculation of the reverberation time, the following fixed elements had to be taken into account:

1) the ceiling of plaster in the form of partitions (fig. 1) which diffuse the sound; also the wooden border round the ceiling;
2) the wood parquet flooring, partly covered with carpets;
3) those parts of the walls taken up by doors and windows.

Only the remaining parts of the walls were available for applying acoustic materials.

Measurements were duly taken from a large number of building and furnishing materials to determine their respective sound absorption coefficients as a function of the frequency, calculations in respect of various designs being based on these values.

The reverberation times of the ultimate project, as measured at different frequencies [1]) proved to be in complete agreement with the required values.

The wainscoting and the covering of the ventilatings hafts are in the form of wood panelling mounted on sound absorbent material, whilst above the panelling the walls are covered with various kinds

[1]) For the method employed in taking these measurements see W. Tak, The measurement of reverberation, Philips Techn. Rev., **8**, 82-88, 1946; also Measuring reverberation time by the method of exponentially increasing amplification, Philips Techn. Rev., **9**, 371-378, 1947 (No. 12).

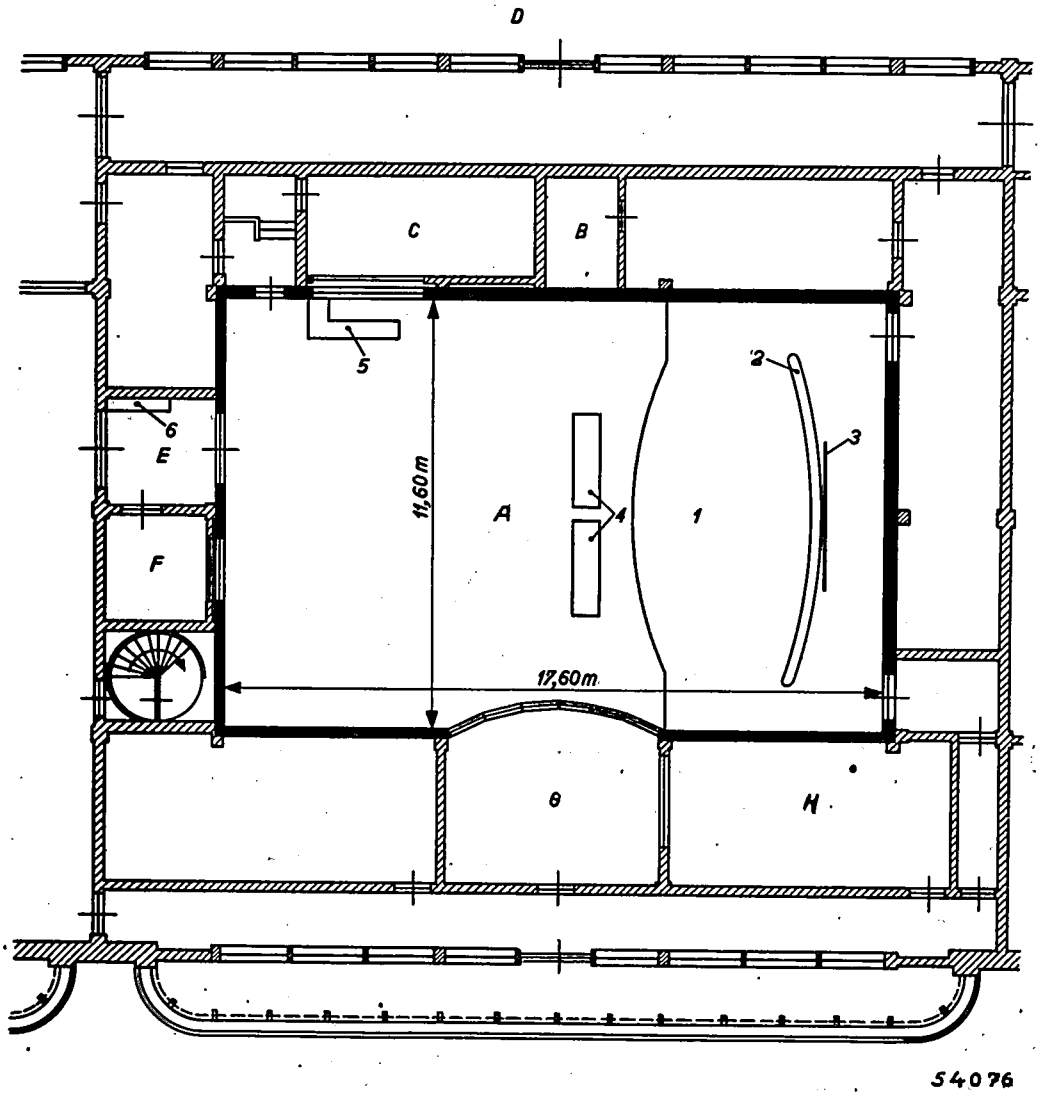


Fig. 2. Plan view of the studio and associated rooms, equipment etc. *A* = studio with *1* platform, *2* baffle, *3* projection screen, *4* demonstration tables with amplifiers, *5* desk with gramophones, master control panel etc, *B* = battery room; *C* = microphone room; *D* = roof terrace; *E* = vestibule with equipment for directional radio reception (*6*); *F* = speech studio; *G* = control room; *H* = sound recording room.

of wood fibre-board; both panelling and fibre-board are so constructed and mounted as to effectively solve the problem of ensuring sufficient absorption of the lower frequencies and not too much absorption of the higher ones. For the sake of appearance the fibre-boarding is covered with the thin material alluded to above which has little or no effect on the acoustics.

Sound-insulation

In order to prevent the entry of disturbing noises, the studio — weighing some 400 tons and being situated on the top floor of a building about 40 m (130′) in height — is insulated from the main building by several layers of bituminous material between the floor of the studio and its footings (*fig. 3*).

The ante-rooms are separated from the main studio by cavity walls, and any windows occurring in these walls are of double glass; the construction of the doors and frames is also such as to prevent the entry of any sounds from outside.

Let us now turn to the equipment: in the main this falls into three categories, viz.:

1) Electro-acoustic reproduction equipment;
2) Cinematographic equipment;
3) Sound recording equipment.

Electro-acoustic reproduction equipment

Programme sources

The ELA Studio is provided with the following "programme sources":

1) microphones,
2) gramophones,
3) playback equipment for Philips-Miller recordings,
4) playback equipment for magnetic recordings,
5) various radio receivers,
6) music lines (telephone lines for music transmission).

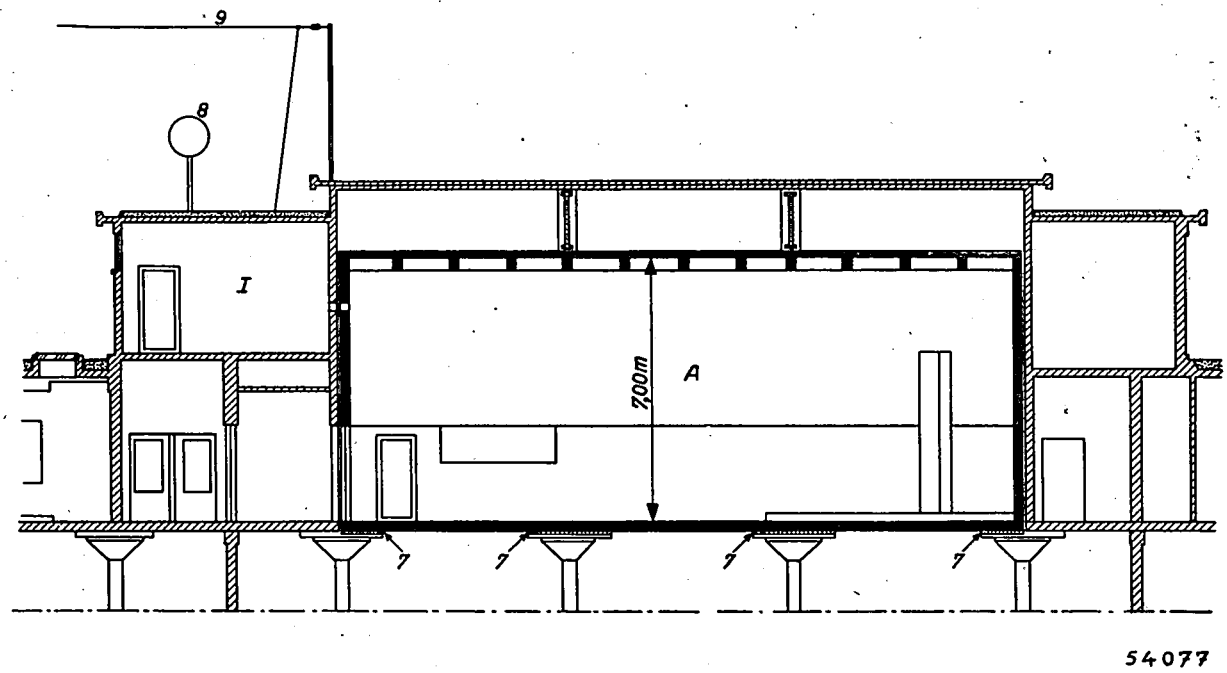


Fig. 3. Cross-section of side elevation. *A* = studio; *I* = projection room; *7* = sound-insulation; *8* = loop aerial; *9* = normal aerial.

Microphones of different types are provided in the microphone room (*fig. 4*).

For gramophone music there are three turntables (*fig. 5*), each fitted with three different pick-ups which can be switched into circuit as desired.

Mounted close to these is the Philips-Miller playback equipment and an ordinary radio receiver. A special receiver is also provided (*fig. 6*) for directional reception in cases where it is required to eliminate interference from other stations; this set is served by a loop aerial (fig. 3) which can be employed in conjunction with an ordinary aerial if desired [2]). The bandwidth of this

[2]) P. Cornelius and J.van Slooten, Installations for improved broadcast reception, Philips Techn. Rev. **9**, 55-63, 1947 (No. 2).

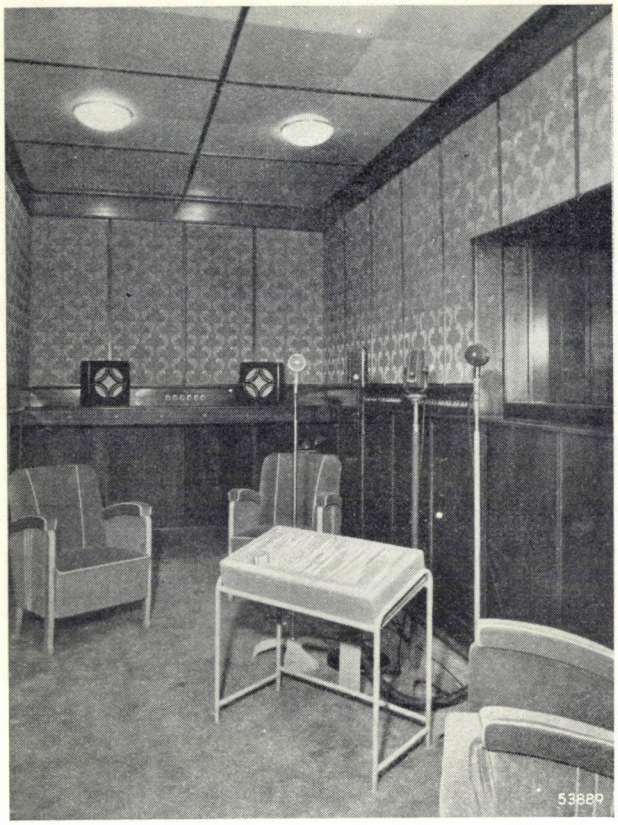


Fig. 4. Microphone room (*C* in fig. 2), with four different types of microphones. In the foreground a movable switch panel with push-buttons and pilot lamps. The two loudspeakers (in background) have been designed for radio relay.

receiver is variable to a greater extent than is the case with ordinary receivers; in fact the directional properties of the aerial system make it possible to receive broadcast transmission without interference at much greater bandwidths than whith conventional types of receivers.

Playback and recording equipment of the magnetic type is installed in the recording room.

Land-lines may for instance provide connection with the Concertgebouw, Amsterdam [3]), the Netherlands broadcasting studios etc.

Amplifiers

For demonstration the amplifiers are located on tables and along the wall in the main studio (*fig. 7*) and can be connected as required between any particular programme source and the loudspeakers by means of a system of relays, to which further reference is made in a following paragraph.

Loudspeakers

A large baffle stands on the platform of the studio (*fig. 8*), offering space for 12 loudspeaker units

[3]) A recent article in this Review contains a description of the experimental „duplication" in the ELA Studio of a performance given in the Concertgebouw; see R. Vermeulen Duplication of Concerts, Philips Techn. Rev. **10**, 169-177, 1948 (No. 6).

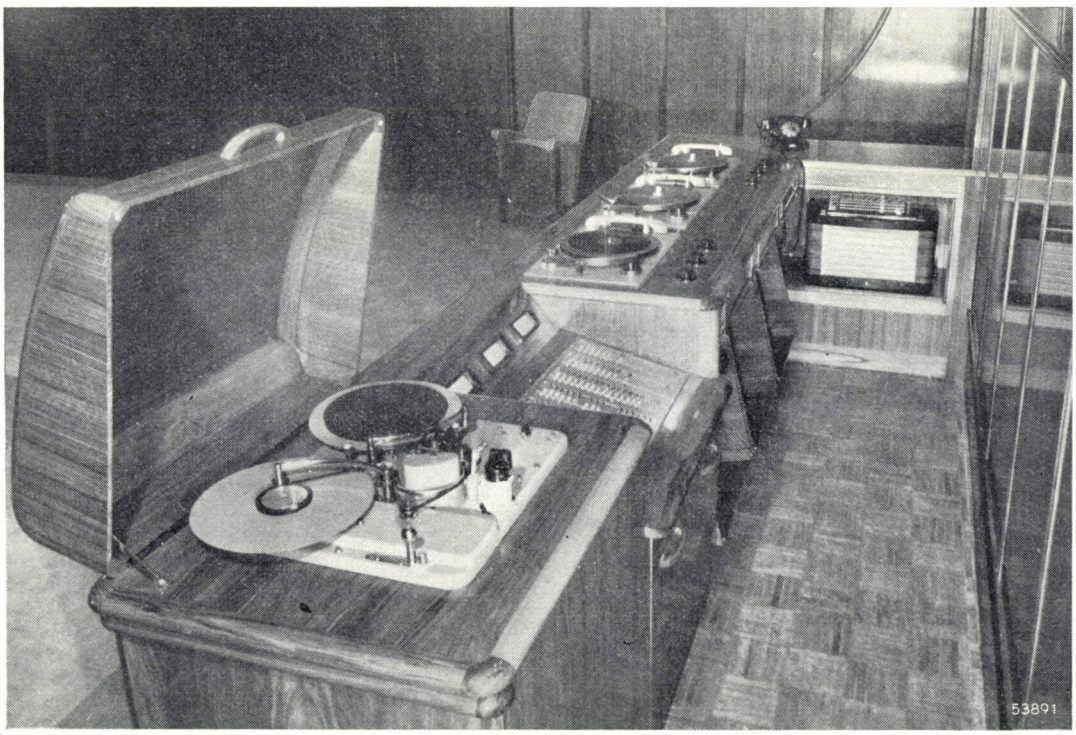


Fig. 5. Desk (5 in fig. 2) accomodating (from front to rear): Philips-Miller playback equipment, master control panel with push-buttons and pilot lamps, programme level-meters, three gramophones (each with three different pick-ups), radio receiver.

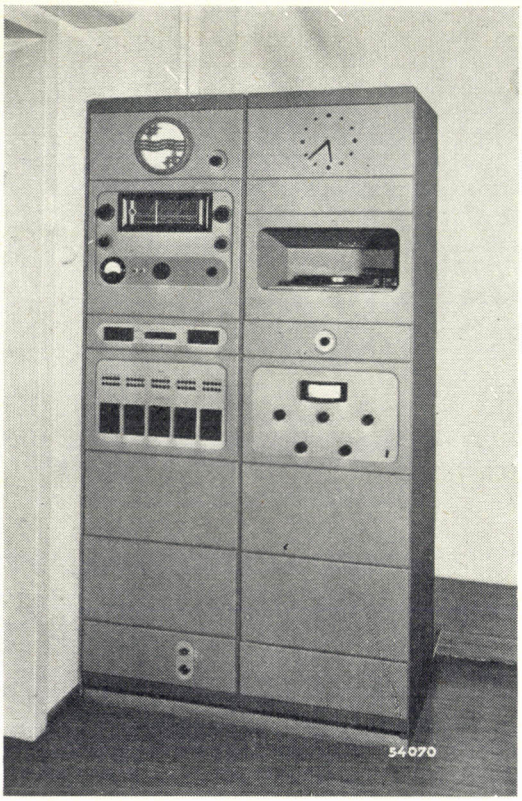


Fig. 6. Rack containing receiver for directional radio reception, monitor speaker, gramophone, programme level-meter and switch panel with correcting filters.

any one or more of which can be connected to each of the different amplifiers. Other speakers, for open-air reproduction, are located on the roof terrace; they can also be linked up with the amplifiers and programme sources mentioned.

The microphone room further provides facilities for listening to loudspeakers intended for use in small rooms or in the home, as for example, with radio-relay.

Stereophony

Needless to say, the studio is also equipped for stereophonic reproduction [4]) of stereophonically recorded sound either by the Philips-Miller or by the magnetic tape system, or as picked up in a remote concert hall by means of a stereophonic microphone unit. In the latter instance the ELA Studio is linked up with the concert hall by land-line (see footnote [3])), or by special radio transmission, employing two transmitters and two receivers.

Switching system

The system of switching is designed to establish rapidly any desired combination of programme source, amplifier and loudspeaker. Each of the sources of music can be connected to the amplifier input cables via relays, and the output of each of the amplifiers is passed through one of a second set of relays to an output line, to which a third group of relays connects one or more of the loudspeakers.

The various relays are operated by means of push-buttons on four parallel-connected control panels, two of which are fixed, namely the master panel in the studio and that on the terrace, whilst the other two are movable, one being in the studio and the other in the microphone room.

Each of these four panels enables a selection to be made from the available programme sources, amplifiers and loudspeakers, and, when the buttons on any one of these panels are depressed, pilot lamps light, not only at the buttons concerned, but also at the corresponding buttons on the other panels and at the particular apparatus put into circuit.

The cabling, which in the case of such a complex system is necessarily extensive, has partly a fairly high and partly a very low power level. In order to avoid the possibility of consequent cross-talk, the ducts containing the cables are divided into four compartments, each one screened from the other and containing groups of lines of roughly the same power level.

Cinematografic equipment

The centre part of the speaker baffle on the platform is folded back sideways when the projection screen (3.65 m × 2.75 m, or 12′ × 9′) is to be used. Behind the screen the cinema speakers are mounted, those for the low frequencies on a large wooden horn and those for the high frequencies on a multicellular metal horn.

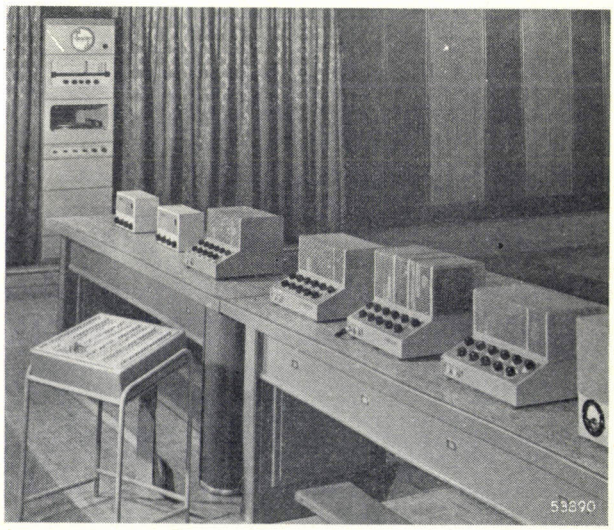


Fig. 7. Tables with demonstration amplifiers (*4* in fig. 2). On the left in the foreground is a movable control panel similar to that shown in fig. 4.

[4]) K. de Boer, Stereophonic sound reproduction, Philips Techn. Rev. **5**, 107-114, 1940.

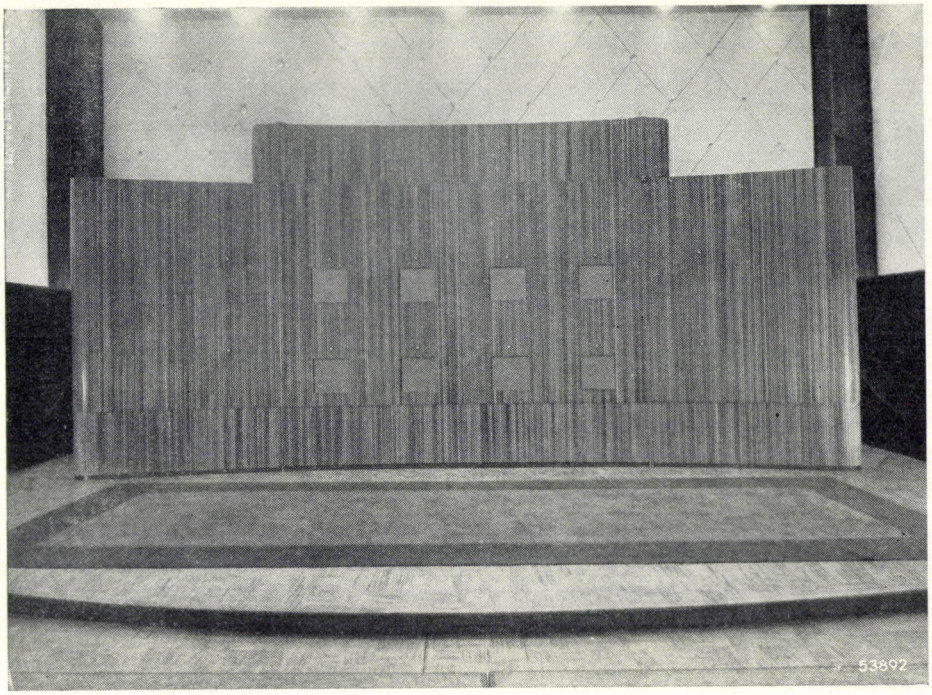


Fig. 8. Baffle on the platform of the studio (*2* in fig. 2) with 8 loudspeaker units (this number can be increased to 12). The centre part folds back sideways to reveal the projection screen (see fig. 1).

In the projection room there are two projectors (*fig. 9*) with the amplifier cabinet in between. Each of the high-intensity arcs is fed from a separate rectifier, housed in an adjoining room.

There is also accommodation for a third projector for demonstration or experimental purposes.

Panels with push-buttons and switches are mounted on the wall beside each of the projectors for controlling the rectifiers and the studio lighting. As regards the latter, this is provided by incandescent lamps (total consumption 20 kW). The dimmer for the studio lighting and the switch for the motor operating the curtain in front of the screen can be controlled from the projection room as well as from the studio itself; the sound volume, too, is controllable from both points.

All possible measures have of course been taken to minimize the risk of fire originating in the projection room; the windows between the latter and the studio are fitted with steel shutters (fig. 9), held open by electro-magnets when a film is being shown; in the event of the film catching fire the energizing current of these magnets is automatically cut off and the shutters drop.

Sound recording equipment

Various installations are available for the recording of sound, which may be derived from any of the following sources:

1) microphones in the main studio,
2) microphones in the speech studio,
3) music lines,
4) other sound sources.

The signals arrive at a four-channel mixing desk in the control room (*fig. 10*), from which a large window gives the operator a wide view of the studio.

Installations for the recording are located in an adjoining room. The four systems employed, which can record a same programme simultaneously, are:

1) Philips-Miller recording equipment,
2) magnetic recorder,
3) photographic sound recording installation,
4) gramophone recording unit.

A short description of each system may not be out of place. In the Philips-Miller system [5]), the sound track is cut electromagnetically in a "Philimil" tape, this being of celluloid with a transparent coating of gelatine, on top of which there is a very thin and opaque layer. The recorded sound can be reproduced during the recording process.

Copies of the "Philimil" recordings may be made either photographically [7]) or mechanically, accor-

[5]) R. Vermeulen, The Philips-Miller system of sound recording, Philips Techn. Rev. **1**, 107-114, 1936.

[6]) See R. J. H. Alink, C. J. Dippel and K. J. Keuning, The metal-diazonium system for photographic reproduction, Philips Techn. Rev. **9**, 289-300, 1947, (No. 10).

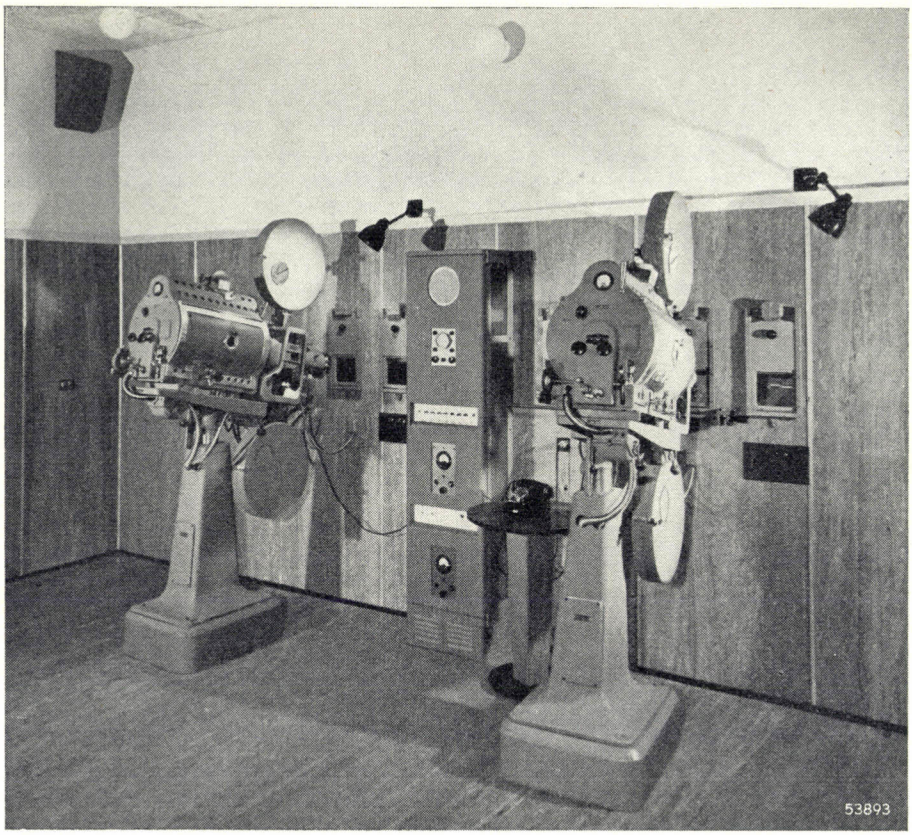


Fig. 9. Projection room, with two Philips Type FP 7 projectors and Type 2834 amplifier cabinet. On the wall, near each projector, the small panels which carry the pilot lamps, push-buttons and switches for changing-over the rectifiers and for controlling the studio lighting. The windows are fitted with automatic steel shutters. A communication speaker is seen in the left hand top corner.

ding to the particular purpose for which they are intended.

For film studio work perforated „Philimil" tape 35 mm in width is used; for broadcasting purposes the tape is only 7 mm wide and unperforated. Both varieties are handled in the recording room; *fig. 11* shows the 7 mm equipment.

With the magnetic system[7]) a sound track of varying remanence is produced in a tape of magnetic material; this also permits of immediate playback.

The latter feature is absent in the photographic system (also mentioned in the article

[7]) This system is employed for professional purposes only.

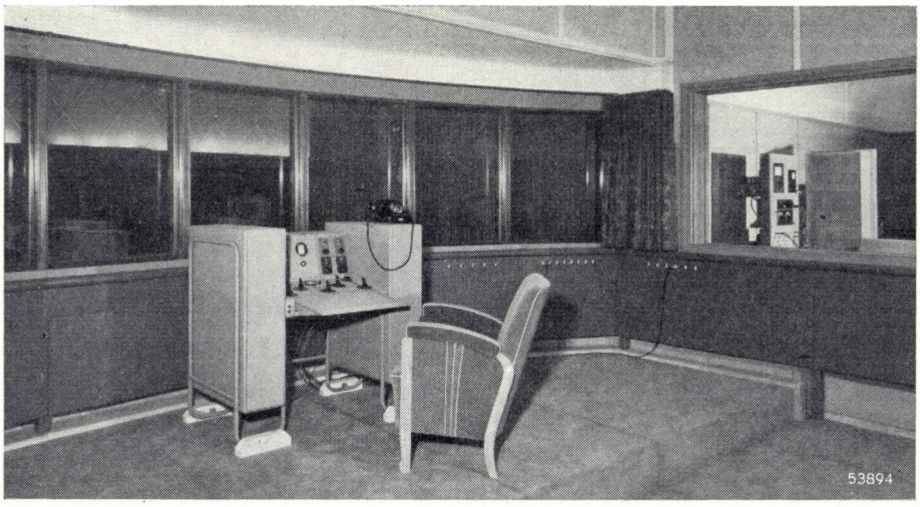


Fig. 10. Mixing desk in the control room (*G* in fig. 2). The bay-window provides a wide view of the interior of the studio. The window on the right gives on to the recording room.

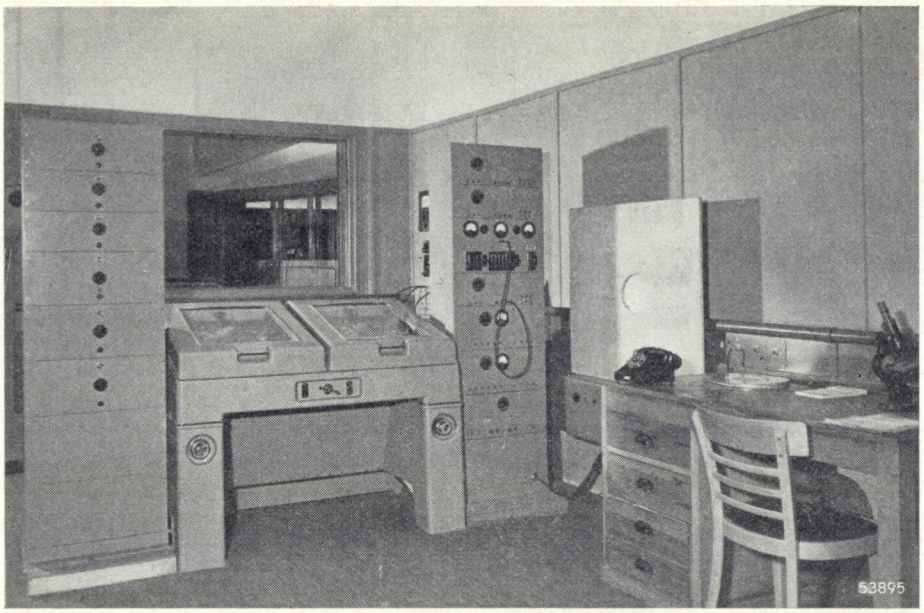


Fig. 11. Recording room (*H* in fig. 2). Centre: twin Philips-Miller recording equipment for 7 mm tape. Right: amplifier rack. Left: rack with power supply units.

referred to in footnote [5])), as in this case the sound track requires development and printing before playback is possible.

Gramophone records are normally cut on equipment adapted for the recording of sound on shellac discs; special apparatus is provided in the studio for the making of records on wax discs.

Another application of sound recording is the post-synchronisation of film-sound, facilities for which are also included in the studio equipment. The silent film is projected on the screen, the appropriate sound being produced either in the main studio or in the speech studio, and recorded on "Philimil" tape, or by the photographic process.

Intercommunication system

To establish communication between the studio and the ante-rooms, three different systems are in use, each of which has its own merits. These are:

1) house telephone,
2) a system of light signals,
3) microphones and loudspeakers.

With this we close our description, although many details have not been touched upon; it is intended only to give a general impression of the extensive electro-acoustic and cinematographic facilities with which this up-to-date studio has been equipped.

CERAMICS AND THEIR MANUFACTURE

by R. A. IJDENS.

666.3:621.315.612

The art of producing utensils and art wares from ceramic materials has been practised for centuries, but it is only since the end of the last century that these materials have been adapted for use in the electrical industry in the form of insulators and dielectrics for capacitors. The requirements imposed in the field of high-frequency equipment as regards the dielectric constant, dielectric losses, the coefficient of expansion and mechanical properties have greatly accelerated the development of this branch of the ceramic art and in this development Philips Laboratories at Eindhoven have played an important part. The aim of this article is to present a brief survey of the different methods employed in a factory in the preparation of ceramic materials; of the different ceramic compositions manufactured at Eindhoven at the present time and of the different purposes for which they are used. Reference is also made to the phase diagram of the system MgO-Al_2O_3-SiO_2, in order to illustrate the manner in which the characteristics of the final product are related to the composition of the ceramic mixtures.

Development of the ceramic art

The ceramic art as based on the manufacture of objects from inorganic materials dates back to antiquity: many centuries before the christian era it formed part of the culture of those days. The word "ceramic" is of Greek origin; in Hellas the potter was known as "kerameus" and the word "keramos" designated the plastic raw material employed by him.

A characteristic feature of the process is that the raw materials are mixed with a liquid (usually water) to a plastic dough before they are moulded into objects of the desired form, being subsequently fired at a high temperature to produce the necessary strength.

In principle, the manufacture of ceramic articles has changed very little in the course of time; it has merely undergone refinements and improvement and, with the growth of industry in general, has been adapted to mass production methods.

The selection and use of the most suitable raw materials for ceramics has always been a most important question; in fact it is not always easy tor ecognise exactly the right material, since chemical analysis and X-ray examination reveal but very little about the practical results that may be anticipated. These raw materials have always been of mineral origin, the most important being clay, which gives the ceramic mixture the required plastic consistency.

When electricity began to play such an important part towards the end of the last century, it was only a matter of time that a large demand for ceramic articles was developed by the electrical industry; insulators were needed for many different purposes and porcelain was quickly recognised as an excellent insulating material. Very soon all kinds of electrical components were being produced in porcelain or in some cases in steatite; these materials were, at any rate in the beginning, based on more or less classical compositions.

The development of the high-frequency technique, however, brought many changes in its train, for the well-known varieties of steatite and porcelain proved to be unsuitable for this purpose and new grades had to be developed; often it was to introduce new types of raw materials, to meet the demands of the electrical experts for more and more ceramics of widely divergent properties.

Ceramic materials for high frequencies

The fact that the earlier grades of porcelain and steatite were not suitable for high-frequency work must be attributed to their high dielectric losses under these conditions. It is a well-known property of an insulator that, when placed in an electric alternating field, it consumes part of the electrical energy and converts it into heat. Provided the heat thus developed corresponds only to a small proportion of the total amount of energy in the field, it can be represented approximately by the expression:

$$W = V^2 . 2\pi f . C . \tan\delta, \quad . \quad . \quad . \quad . \quad (1)$$

where V = the high-frequency voltage (r.m.s. value),
f = frequency,
C = capacitance,
δ = loss angle of the material.

The value of the capacitance depends upon two factors, namely the dielectric constant ε and a form-constant K, determined by the shape of the

insulator. Expression (1) can therefore also be written:

$$W = (V^2 . 2\pi f . K) . \varepsilon \tan\delta \quad . \quad . \quad . \quad (2)$$

In a given device or technical application, V, f, and usually also K are known in advance: ε and $\tan\delta$ are thus the only factors available for modification to ensure that the ceramic product will meet the particular demands with respect to the dielectric losses.

In principle, both ε and $\tan\delta$ are moreover dependent on the frequency. In the range of radio frequencies, however, ε may be regarded for all practical purposes as being independent of the frequency and, for most materials, $\tan\delta$ does not vary with the frequency to any great extent either, in this range. This means that, in view of expression (2), the dielectric losses of most materials, broadly speaking, increase in proportion to the frequency; thus, if it is required to limit the dielectric losses in electrical equipment or circuits working at high frequencies, the product $\varepsilon \tan\delta$ (the loss factor) must be kept as low as possible. In all cases where ceramics are employed in the construction of insulators (e.g. supports for high-frequency lines) every effort is therefore made to ensure low values of ε and $\tan\delta$.

In capacitors, however, it is usually desirable to aim at high values of ε with a view to restricting the physical dimensions of the capacitor itself, and here it is all the more important that $\tan\delta$ should be as low as possible: the first material to come into consideration for this purpose is titanium dioxide, the dielectric constant ε of which, in case of the pure material, is 115. At the same time, it is a drawback of this material in many of its applications that ε has a high negative temperature coefficient, viz. -8×10^{-4} per °C, which tends to produce variations in the tuning of an oscillatory circuit some time after the current has been switched on. If this is regarded as an obstacle, some other kind of dielectric must be employed, the dielectric constant of which has a very low temperature coefficient, and a lower value of ε may then have to be accepted. Mg_2TiO_4 and other oxide mixtures come into consideration for this purpose.

When capacitors of very small physical proportions are required, having much higher capacitance values than those under review, use may be made of certain titanates ($BaTiO_3$, $SrTiO_3$): in the Philips Laboratories, for example, two such titanates have been developed, of which $\varepsilon = 1200$ and 2500. The temperature coefficients of the dielectric constant of these materials vary considerably according to the range of temperatures concerned and, wherever their use is favoured, the higher loss factor must be accepted as inevitable.

The choice of ceramics for use as constructional material is quite frequently governed by the high stability of thier physical form and chemical composition. In the first place consideration must be given to the coefficient of expansion of the material to be used, for it is quite possible that the tuning of an oscillatory circuit may be upset as a result of the slightest expansion or contraction of certain components in the circuit, due to variations in temperature; if this is to be avoided, the use of materials having a low coefficient of expansion is indicated and, in some cases, this may be so important that the question of a low loss factor takes second place. In the following paragraphs it will be shown that such ceramics, having a low coefficient of expansion, can be produced from the three constituents MgO, Al_2O_3 and SiO_2. For the coefficients of expansion of some of the ceramics in common use see *table I*.

Table I. Coefficient of expansion of some of the more common ceramic materials.

Cordierite mixtures	1- 2 $\times 10^{-6}$ per °C.
Porcelain	3- 4
Steatite-porcelain	6- 7
Steatite	8- 9
MgO compounds	10-12

There is a very large outlet for ceramics in the manufacture of electronic valves, in the form of both supporting and insulating elements, and *fig. 1* shows a typical example. When intended for capacitors, or as insulating material to be used in the air, ceramics are needed which have been sintered to the point of impermeability, but for use under vacuum finely porous types are also quite suitable; the degree of importance attached to the insulating qualities of the material within the electronic valve depends upon how low the dielectric losses have to be, and it is a point in its favour that the porous structure seems to have the effect of reducing the dielectric constant in comparison with that of the denser materials of the same chemical composition.

Originally, ceramics for electro-technical purposes were supplied by makers of domestic and art wares, but today the development has in many instances been taken over and progressed by the electrical industries to meet the demand for the many different varieties of ceramics needed to keep pace with the increased scope of high-frequency techniques. This has taken place in the Netherlands amongst

other countries and, in recent years, numerous ceramic materials have been developed in the Philips Laboratories; manufacture was commenced on a regular scale just prior to the last world war [1]).

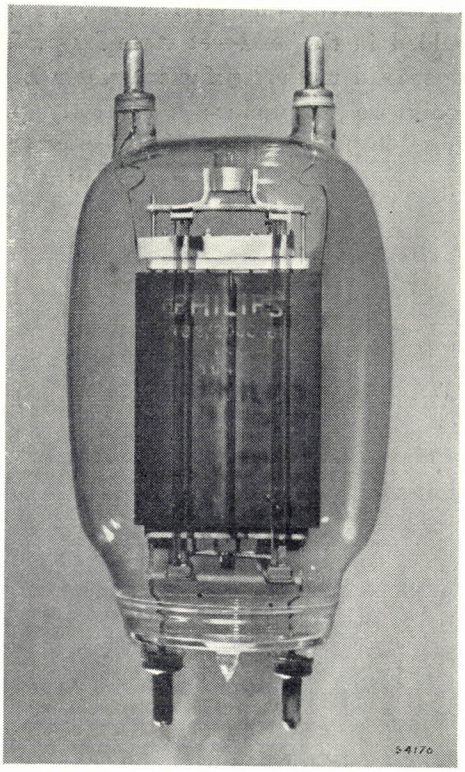


Fig. 1. A transmitting valve (type TB 3/2000) in which ceramic material is used for supports; the electrode system is fixed between ceramic rings.

We shall commence with a brief survey of the methods employed in the manufacture of ceramics and proceed to a discussion of various specific products used for insulation purposes, particularly in the sphere of high frequencies. It will be clear from the remarks that follow that the properties of the final product depend to a large extent on the raw materials used.

A review of titanium dioxide and allied substances for use as dielectric in capacitors, as well as the general uses of titanates, is reserved for publication in two following articles.

[1]) This article is devoted mainly to a discussion on ceramic insulating materials and dielectrics. Apart form these, two other groups of material have been developed by the Physical Laboratories, Eindhoven, namely ceramic resistance materials (semi-conductors) and ferro-magnetic substances for the cores of coils ("Ferroxcube"). These materials, which have found an extensive field of application, have already been desribed in an earlier issue of this Review by E. J. W. Verwey, P. W. Haayman and F. C. Romeyn, Semi-conductors with large negative temperature coefficient of resistance, Philips Techn. Rev. **9**, 239-248, 1947 (No. 8); J. L. Snoek, Non-metallic magnetic material for high frequencies, Philips Techn. Rev. **8**, 353-360, 1946.

Method of manufacture of ceramic products

The finished ceramic product may be regarded as having passed through five distinct phases of manufacture, viz.:

1) preparation of the ceramic mixture,
2) moulding,
3) drying,
4) firing,
5) finishing.

Preparation of the ceramic mixture

The raw materials may be divided into two categories:

The first group comprises the non-plastic constituents, usually present in large proportions in every ceramic mixture and having a major influence on the characteristics of the final product; typical examples of these materials are quartz, feldspar, steatite, magnesite, aluminium oxide and titanium oxide.

The second group comprises the plasticisers and these can be further classified as organic and inorganic; among the latter are kaolin, clay and bentonite, which form a plastic mass when mixed with water. After the firing these materials are still present in the ceramic mass, although chemically changed, and their influence is thus reflected in the final product, this being in certain cases a very desirable characteristic.

The organic plasticisers, which are usually referred to as binding agents or binders, may be electrocol (a farinaceous product), nitro-cellulose, tragacanth, etc. and these are added only in small quantities; once their function has been fulfilled during the moulding process, they are almost wholly burnt away in the subsequent firing operation. The properties of the resultant ceramics are thus governed entirely by the non-plastic ingredients. Organic binders are frequently necessary because inorganic plasticisers such as clay may impart to the final product qualities which tend to conflict with those required.

The raw materials of mineral origin are usually first broken up in mills of the crushing or edge-runner type, after which they are pulverised in a ball-mill. Sometimes — and this refers particularly to kaolin and clay — they are subjected to a precipitation process, being first brought into suspension and then allowed to settle. The raw materials are usually weighed dry to obtain a certain composition, after which they are milled wet in a base-mill. The slip is pumped to a filter press, passing through an electro-manget to remove any particles of iron present in it; the surplus water is removed in

the filter press through filter cloths at a pressure of some 6 to 8 atm. The paste is thus deposited on the cloths in the form of semi-solid slabs 2 to 3 cm in thickness and when these are sufficiently dry they are ground to a powder or to small granules according to the ultimate use to be made of the material.

If no clay or kaolin has already been added to the mixture as plasticiser, one of the inorganic binders previously mentioned is then mixed with the powder to form a plastic mass.

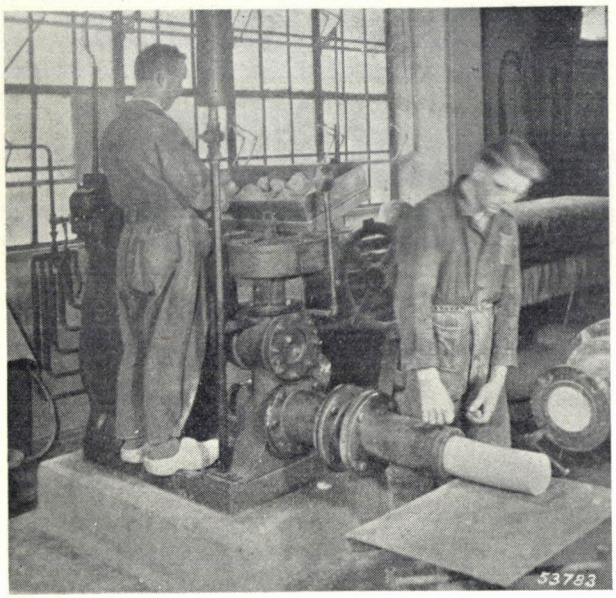


Fig. 2. De-airing pug-mill in operation.

The latter is next loaded into a de-airing pug-mill (*fig. 2*) for removal of all the air occluded during the preceding operations; if this were not done the final product would contain pores, cavities or even channels.

This preparatory processing is rather involved and occupies a considerable amount of time, but it is necessary to ensure complete homogeneity of the material before moulding is commenced.

Moulding

Any one of three different moulding processes may be employed.

In the first of these the powdered material, as it stands, or mixed either with a certain percentage of paraffin wax or a small amount of liquid (water, oil or kerosene), is moulded in dies. Most of the smaller ceramic articles employed for H.F. purposes are moulded in this way, in automatic or semi-automatic presses. We speak of dry moulding when the powder is used without the addition of a liquid, or when only paraffin wax has been added, but when the porcelain powder is admixed with water, kerosene and fat oil a pressing powder is obtained the plasticity of which is higher than that of the perfectly dry powder. By this "semi-wet" moulding method objects of rather more complex form may be shaped; objects with holes in horizontal directions, or those having thin vertical ridges, are therefore moulded in the semi-wet state for preference.

In the second method sufficient water is added to the mixture to produce a perfectly plastic mass suitable for moulding by the extrusion method or by rotary shaping (jollying).

To extrude a tube, a roll of the de-aired material is loaded into a cylinder on the underside of which a nozzle or die, with pin, are fitted, after the manner depicted in *fig. 3;* the respective sizes of the die and pin determine the outside and inside diameters of the ceramic tube thus produced.

For the rotary method a revolving disc, driven electrically or mechanically, is used, the plastic material being shaped by hand, just as on the potter's wheel of old, or special plaster moulds may be used for the purpose; this method is still used in the manufacture of many electrical components such as insulators for high or low tension.

The third moulding method involves the use of the ceramic powder suspended in so much liquid that the mixture is quite fluid, the products being moulded by casting in plaster moulds; owing to its high porosity the plaster absorbs the water, leaving a rigid layer of the material on the walls of the mould, and as soon as the required thickness has been obtained the surplus mixture is decanted. Upon drying, the ceramic moulding shrinks to such an extent that it comes away from the mould and can be easily removed; the plaster mould is then dried for further use.

Finally, it may be mentioned that dry-moulded or "biscuit" fired porcelain, which is ceramic material that has been fired half-hard, can quite well be turned on a lathe.

Firing

When ceramic articles have been moulded into the required shape they are first dried and then fired in a kiln at a temperature that will produce a sintering of the material. By sintering is meant the transition of the mixture from a powder to a coherent solid (which may or may not be porous), the temperature being raised to a level which is not far below the melting point. (If T_s be the melting point in degrees Kelvin, the material is heated to a point between at least $^2/_3\ T_s$ and T_s.) At this temperaure diffusion between the individual particles is accelerated and chemical reactions take

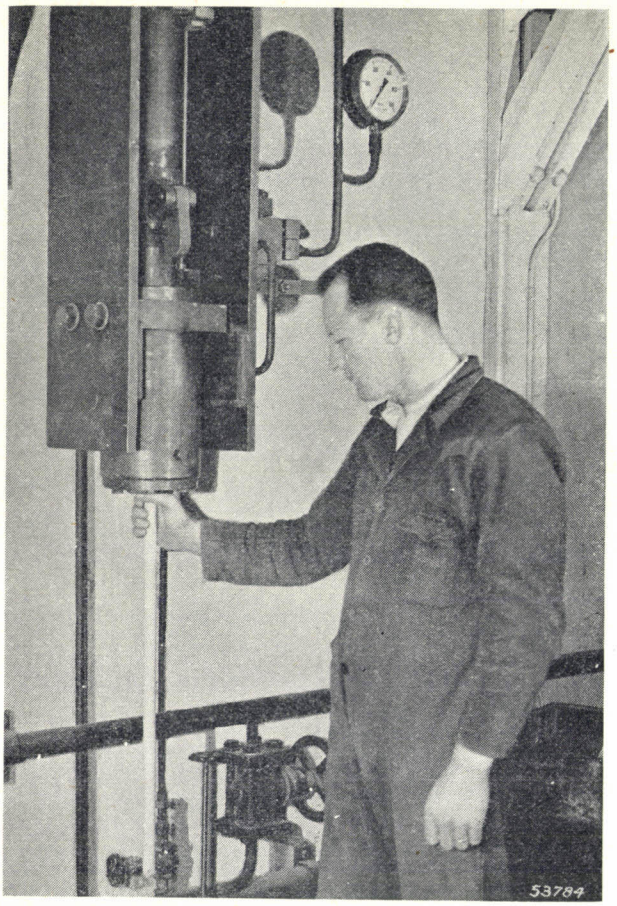


Fig. 3. Extrusion of ceramic tubes. A roll of de-aired raw material is placed in a cylinder, to the lower end of which a die and pin are attached. The inside and outside diameters of the tube are determined by the sizes of pin and die used.

place more quickly; sometimes this involves a change in the crystals to other modifications, whilst in other cases crystal growth may be promoted or entirely new compounds formed.

In the manufacture of some types of ceramics with which we are concerned in the following paragraphs it is essential that firing be carried out to the point where the material actually commences to melt; in this way we ensure that after the firing the crystals are embedded in a glassy matrix.

The ceramic objects are loaded into the kiln in "saggers" (*fig. 4*), to prevent foreign matter from the combustion gases settling on them, and the fully charged kiln is sealed up with brick before firing is commenced. *Fig. 5* depicts a charged kiln after firing has been completed. It takes some days to bring the temperature of the kiln to the required level, depending on the size of the charge.

Two kinds of kiln are in use, namely annular and tunnel furnaces, the first of these being charged and fired periodically. The tunnel kiln has the advantage that it works continuously, with less loss of heat. The articles to be fired are loaded onto trucks and these are drawn through the "tunnel" in regular succession, each truck therefore passing through exactly the same temperature cycle. Such kilns are usually fired by coal gas or producer gas.

The temperature is controlled by means of Seger cones, the material of the latter being such that they soften and curl over, or melt when the temperature of the kiln reaches a certain point. It is also possible to measure the temperature by different kinds of pyrometers (of the thermo-electric or optical type). In comparison with thermo-elements, Seger cones have the advantage that the measurement actually refers to $\int T dt$ (where T is the temperature as a function of the time); they therefore give a better indication of the effect of the heat upon the material in the kiln.

During firing, the material shrinks appreciably, sometimes as much as 30%; the actual amount of shrinkage depends on the composition of the mixture and the method employed in the moulding. As far as dimensions are concerned ceramic articles must therefore be designed with very definite tolerances.

Finishing

After firing and subsequent slow cooling, it may be necessary for the articles to undergo certain

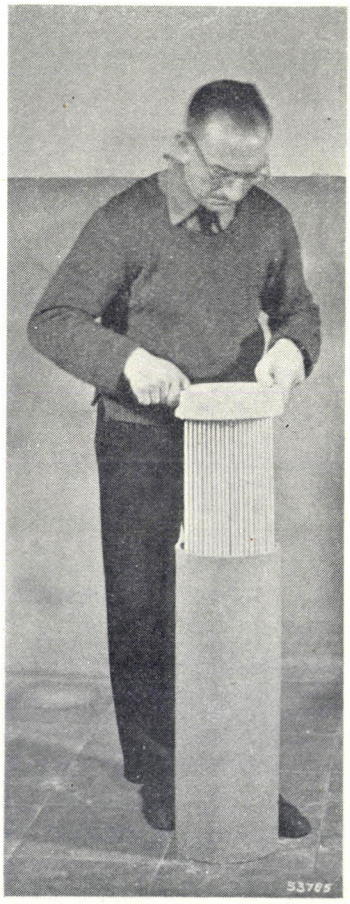


Fig. 4. One type of sagger used for loading ceramic articles into the kiln; it prevents soiling of the articles by the combustion gases.

finishing operations. In some cases they have to be ground, and this can be done by the centreless, circular or horizontal methods. *Fig. 6* illustrates a centreless grinder on which rods and tubes are being trued up, whilst *fig. 7* shows a method of grinding ceramic discs flat and parallel. The finishing or "drilling out" of holes can be carried out only with diamond-tipped tools. Frequently it is necessary to metallise ceramic articles, i.e. to apply a thin film of metal to them, as in the case of capacitor parts, whilst for other purposes it may be found desirable to glaze the surfaces of the material, which, owing to their natural dull finish,

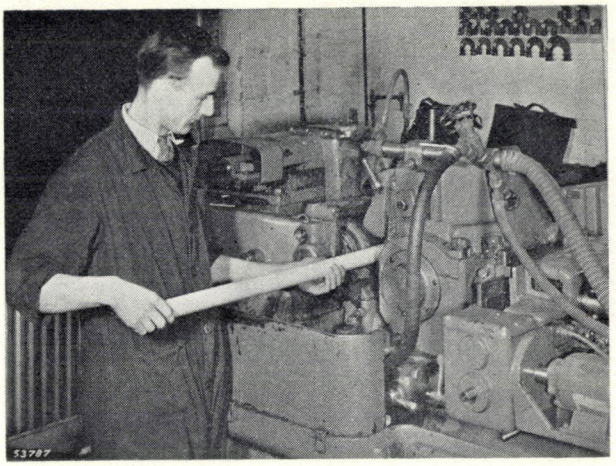


Fig. 6. Grinding ceramic rods and bars on a centreless grinder.

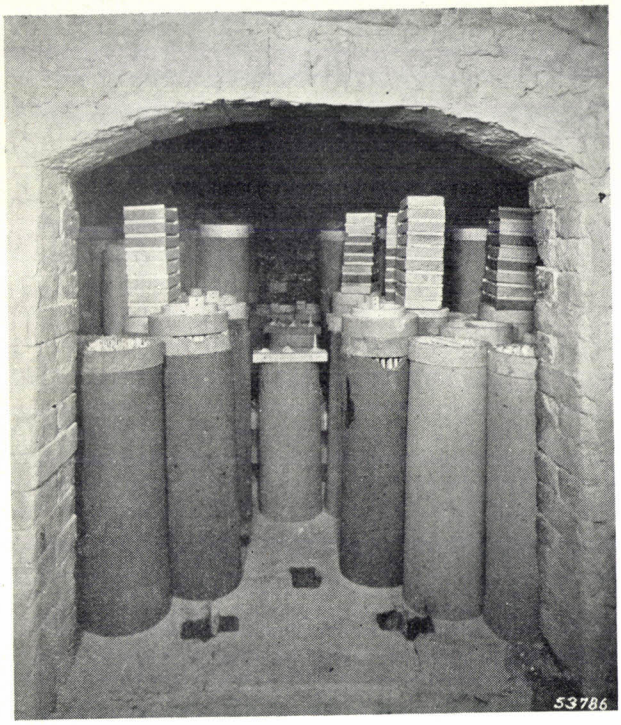


Fig. 5. Kiln charged with fired ceramics. Before firing is commenced the kiln is sealed with brick. The fact that this photograph was taken after firing is borne out by the fact that the Seger cones have melted.

would otherwise very quickly; become soiled. A thin layer of glaze is then applied, after which the article is heated for a little while in a furnace.

Some ceramic mixtures and products

The more important ceramic mixtures used in the manufacture of electrical components, a brief survey of which will now be given, all belong to the ternary system $MgO\text{-}Al_2O_3\text{-}SiO_2$, as represented in the phase diagram in *fig. 8* [2]). The names shown in the different phases indicate the crystalline structures produced in those zones upon cooling mixtures of the different compositions given, and, since sintering entails a commencement of the molten stage, it may be expected that the crystals concerned will be met with in the ceramic material.

Those mixtures which correspond to zone *A* in fig. 8 [3]) are of great importance. They are porcelains built up on a basis of steatite, that is to say the latter substance ($3MgO.4SiO_2$. 1 to 2 H_2O) is employed as primary ingredient; to this is added a sintering agent, mostly clay (aluminium hydrosilicate), sometimes with additions of barium carbonate and potash feldspar ($K_2O.Al_2O_3.6SiO_2$, in which the K_2O may be partly replaced by Na_2O).

The fired material is mechanically strong and dense and consists of enstatite crystals ($MgO.SiO_2$) surrounded by a glassy matrix [4]).

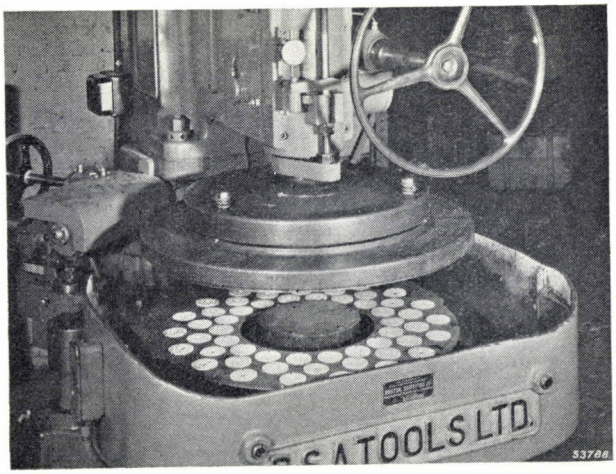


Fig. 7. Grinding machine as used for finishing ceramic discs. These are ground between two flat plates until they are themselves quite flat and parallel.

[2]) Constructed by G. A, Rankin and H. E. Mervin; Amer. J. Sci. **45**, 301-325, 1918, and improved by J. W. Greig, ibid, **13**, 1-44, 1927.

[3]) This Philips product is made under the trade name of "Kersima".

[4]) The conditions governing this phase have been discussed in detail in an article by J. M. Stevels, The vitreous state, Ph. Techn. Rev. **8**, 231-237, 1946.

One of the conditions essential for high mechanical strength of the porcelain is that the crysstalline phase shall be as extensive as possible, and the structure fine-grained. On the other hand, the vitreous phase must not be overlooked, since the composition in the latter state has a very decided effect on the resistance of the final product to temperature variations.

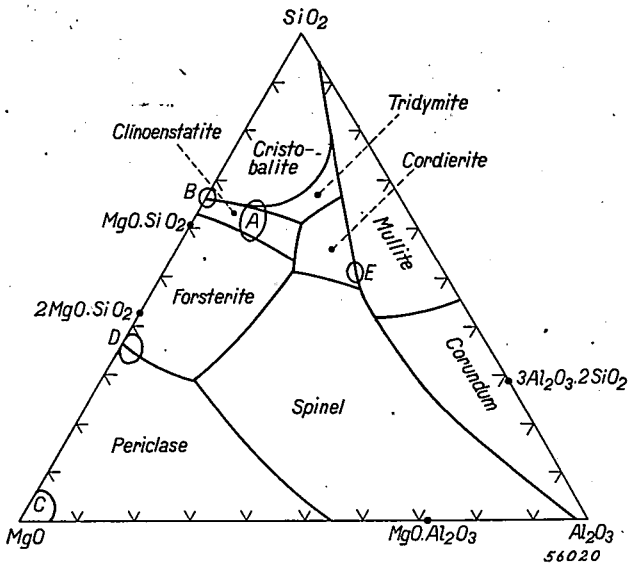


Fig. 8. Phase diagram of the ternary system MgO-Al_2O_3-SiO_2. The names in the various zones indicate the crystalline form produced in these zones upon cooling a molten mixture of the given compositions. The letters *A*, *B*, *C* and *D* indicate the points where the more important compositions occur in the preparation of ceramic mixture as discussed in this article.

The quality of the surface of the porcelain, which may be either smooth and "soft", or rough and stone-like, is governed mainly by the crystal size in the fired product, whilst on the other hand the chemical composition of the material is a criterion for the dielectric properties, and in this connection MgO (and also BaO, which is sometimes added) has a beneficial effect, as it assists in reducing dielectric losses; Al_2O_3 is neutral, whereas SiO_2 and alkalies have the opposite effect. Ultimately, the mechanical strength of the final product will depend very largely on the origin of the steatite used, for there are grades of this material with which, although chemically pure, there is little to be achieved, despite the admixture of sintering agents and other media that may appear necessary. Again, apart from the origin of the raw material, the firing curve is of great inportance: if the material is fired too high, products are obtained in which the crystals have grown too much, resulting in a material of poor mechanical properties; at too low a temperature the fired product will be porous.

Incidentally, those mechanical and dielectric properties which are desired in the final product are not the only factors that decide the composition of the batch. In practice an important question is whether a given mixture will lend itself to easy firing or not; for example it is a great advantage from the aspect of manufacture if the true sintering range — representing the difference in temperature between the beginning of "fusing" and actual "melting" — at a temperature of, say 1370 °C, is 20 degrees instead of only 10.

According to their composition, the substances occurring in zone *A* in the diagram show dielectric losses varying between $\tan\delta = 4\times10^{-4}$ and 25×10^{-4} (at 1500 kc/s). In judging the suitability of the material for constructional purposes, the modulus of rupture will also be found an important property, and this should be 1200-2000 kg/cm³. The ceramics in question are employed for capacitors and components working continuously at high frequencies.

A second group of ceramics corresponds to the composition represented by *B* in the diagram, fig. 8 [5]), these being also on a steatite basis. They differ from those mentioned above in that they are dense, but porous, and they are widely used for insulation and constructional purposes in electronic valves (spacers).

The most commonly used composition in this *B*-zone is modified by the addition of barytes and sand to yield a coefficient of expansion such that the material can be employed for sealing to normal soft glass; the mechanical properties are fair, and the modulus of rupture is about 700 kg/cm³. Measured in vacuo, at room temperature, $\tan\delta$ is in the neighbourhood of 10×10^{-4} (at 1500 kc/s) and even at higher temperatures (provided less than 1000 °C) the loss factor, owing to the addition of the above-mentioned substances, is less than that of most of the better known insulating materials.

Of these ceramics in the *B* region, other outstanding features are that the fired product can be machined and that the skrinkage during the firing operation is only small; owing to this latter characteristic many mouldings can be made to very much finer tolerances than in the case of materials in zone *A*. *Fig. 9* illustrates a number of the articles made as part of the normal mass production of the Ceramics Factory at Eindhoven, using the materials with which this paragraph is concerned.

[5]) These materials are known under the trade name "Kerpora".

In the zones marked *C* and *D* in fig. 8 two other interesting materials occur, that is, interesting from the point of view of the coefficient of expansion, which is fairly high for the different mixtures in these groups, namely 10 to 12×10^{-6}. These mixtures are built up from a basis of MgO [6]) and this explains why they are so difficult to process, seeing that magnesium oxide reacts with water in very much the same way as unslaked lime. The addition to these substances of organic solvents or binders further involves a number of technical difficulties.

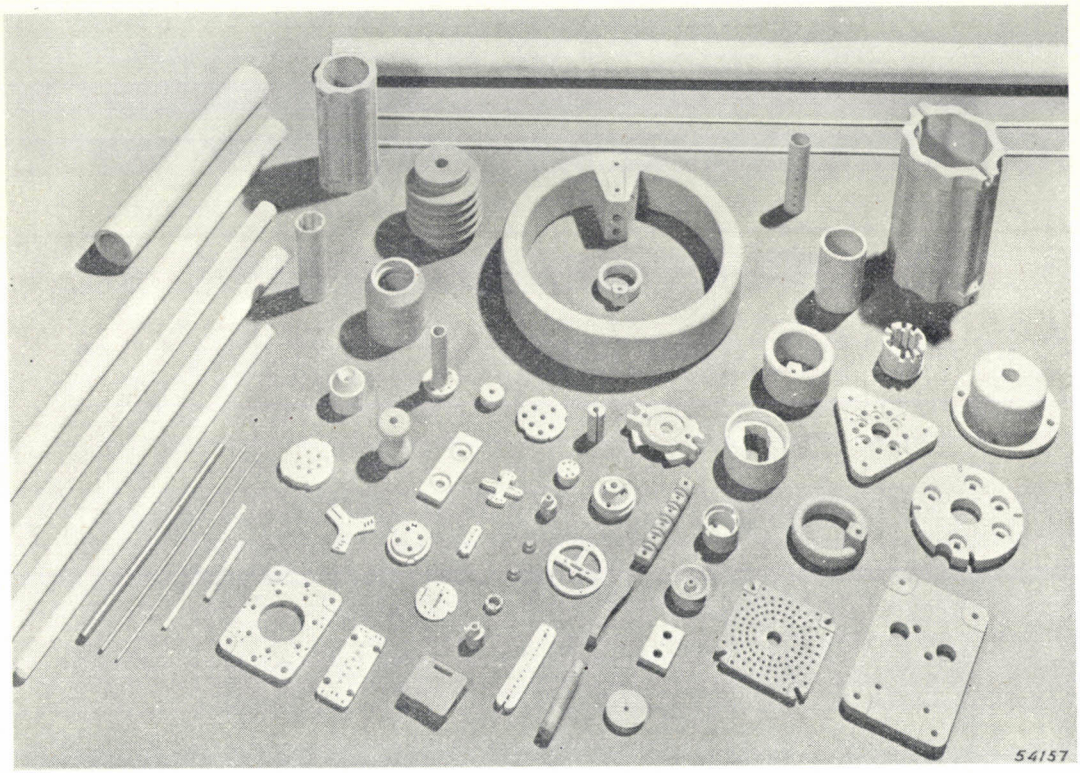


Fig. 9. Examples of ceramic components for electrical purposes, as produced by normal mass production methods in the Ceramics factory at Eindhoven. These articles are manufactured from materials known under the trade names "Kersima" and "Kerpora".

The first mixtures to be made in this range (*C*) consisted almost entirely of magnesium oxide. Now the melting point of MgO is extremely high, viz. 2800 °C, so that when it was required to manufacture, for special purposes, a closely sintered material at the conventional firing temperature (< 1400 °C) it was found necessary to add a sintering agent; the latter had to be chosen with care, however, in order not to change the coefficient of expansion out of all proportion.

Another group (zone *D*), which was developed at a later date, more nearly resembles forsterite ($2MgO.SiO_2$). Here the objections mentioned above are not so pronounced (difficulty in preparation and selection of suitable sintering agents). By prefiring the MgO with the requisite quantity of steatite it is not possible entirely to suppress the reaction of MgO with water, but it can certainly be greatly reduced, whilst the sintering process is thereby also facilitated, since the melting point of forsterite is not higher than 1880 °C.

Compositions occurring in zones *C* and *D* are eminently suitable for the manufacture of bodies for wire-wound resistors. Special development in this direction has ensured that the coefficients of expansion of both the wire and the body in which it is wound do not differ to any great extent. When the resistors are fired in the enamelling process, therefore, the turns do not get loose and there is no risk of short-circuiting.

In zone *E* in the diagram we have mixtures of a composition similar to that of the mineral cordierite ($2MgO.2Al_2O_3.5SiO_2$), known for its low coefficient of expansion, which, according to various investigators, is $1.2\text{-}2.0 \times 10^{-6}$. If it were actually possible to produce ceramics of this composition very low coefficients of expansion might be

[6]) The trade name of these materials is "Kermanox".

expected, but in practice this is very difficult, since there is no sintering range; the material either remains porous or melts completely. However, by carefully selecting the raw materials (sillimanite, steatite, feldspar, clay and kaolin) and accepting a slightly higher coefficient of expansion, it is possible to obtain a sufficiently dense material (porosity $\leqslant 2\%$), although the mechanical properties are only fair (modulus of rupture 750 cm^3). Owing to its very slight expansion with increases in temperature (coeff. exp. $\leqslant 2 \times 10^{-6}$), this material is very well adapted for coil formers and the construction of oscillatory circuits where variations in capacitance are to be kept as small as possible.

BASIC PRINCIPLES FOR THE FORMULATION OF ILLUMINATION STANDARDS

by A. A. KRUITHOF and A. M. KRUITHOF. 535.241.46:535.736

Utilising the experiments of H. C. Weston, the authors have compiled a table relating to visual tasks as characterised by contrast and visual angle of the details to be observed, from which table it is possible to ascertain the illumination level necessary to guarantee a certain degree of visual performance. The table is based (in so far as visual efficiency is concerned) upon the "relative performance" as defined by Weston. The values of the relative performance given may be employed in place of the more usual qualifications such as "adequate", "good" and so on. Having regard to economic, technical and possibly other points of view, this table is useful in cases where it is required to lay down standards with respect to practical illumination levels.

Physiological aspect and economics of the problem

In the designing of a lighting system it is necessary on the one hand to know something of the manner in which the visual function is influenced by the character of the lighting, i.e., the light distribution, colour, degree of glare, if any, and so on. On the other hand, the most satisfactory illumination level for the task in hand has also to be found. This latter problem, which amounts to the establishing of standards relating to the most suitable illumination level, is the subject of our article.

The considerations upon which such standards must be based are partly physiological in character and partly questions of an economical (and technical) nature: the former factor involves the establishment of a scale of qualification for the illumination levels. In the simplest possible language it is a question of levels of illumination to be attributed to such qualifications as "very good", "good", "sufficient" and so forth, solely from the aspect of the ability to see. In this article this physiological element only will be considered. The economics of the problem do not come into consideration till the question is raised whether in a given instance e.g. for a particular country the standard should be "very good", "good" or "sufficient" when paying attention, among other factors, to local electricity tariffs. (Of course "Inadequate" levels need not be taken into account.) As far as this economical side of the question is concerned, different authorities on the subject appear to hold views are are diametrically opposed to each other, but the simplest answer is surely that wealthy nations (or individuals) are able to afford very good, and therefore expensive, lighting whilst the poorer nations have to be content with something less. On the other hand it is often pointed out that poorer countries cannot afford to bear losses in the processes of production and are therefore obliged to apply the best possible illumination, whereas the affluent may be less careful. These points are mentioned not so much with a view to entering into a discussion of them as to demonstrate the fact that the applications of the physiological principles (the scale of qualifications) constitute a subject in themselves.

The visual task and its performance

It is proposed to term an illumination level "good" when the visual task to be carried out at that level is easily performed.

Although we are still very far from our ultimate objective in making this general statement, it does immediately indicate the course to be followed. The qualification of a given illumination level will depend on the visual task to be performed. In order, then, that the scale of values shall be applicable to every conceivable task and also to make comparison possible with the scales which have already been prepared by numerous other workers in this field, it is necessary to decide upon a measure of the difficulty of a task. Furthermore, the yardstick for the rating will be the ease of its performance and here, too, a quantitative measure is required. Experiments will therefore have to determine the effect of a given level of illumination on this "ease of performance", in relation to different tasks. Finally the scale of qualifications is to be established.

Examples of varying visual rasks are: reading a book, drawing, reading measuring instruments, operating a calculating machine, sewing, or crude or fine assembly work in factories, If we are to express the element of difficulty in such tasks in the form of figures, it must be characterised by means of certain factors which have to be capable of measurement. Such factors might be the following:

1) The size of the detail to be distinghuished,

which is evaluated by measuring the visual angle: a subtended angle of 1′ (one minute of arc) corresponds to 0.1 mm as seen at a range of 30 cm, and it is useful to grade certain common detail sizes in stages, as in *table I.*

Table I. Size of detail to be perceived in different grades of work.

Type of work	Size of detail d	
	Limits	Average
Coarse	$> 4.5'$	approx. 6′
Normal	2.2′ - 4.5′	approx. 3′
Fine	1.2′ - 2.2′	approx. 1,5′
Critical	0.5′ - 1.2′	approx. 1′

2) The contrast between the brightness of the task and that of its background. This is defined by $c = (B_1\text{-}B_2)/B_1$, where B_1 is the brightness of the background and B_2 that of the task, which is assumed to be darker than the background). For convenience, common contrasts are also tabulated in *table II.*

Table II. Classification of contrast c between task and background.

Classification	Value of contrast c	
	Limits	Average
Good	0.6 - 1.0	0.8
Fair	0.3 - 0.6	0.4
Poor	0.15 - 0.3	0.2
Very poor	< 0.15	0.1

As far as the effect of the lighting is concerned, it is not the illumination (in lux) that determines the facility of perception, but the brightness level, which, apart from the illumination, is also governed by the reflection factor of the background, and in a review of this kind it is usual to assume one particular reflection factor: in this case let us take 0.9. *All illumination levels mentioned in the following will thus relate to this reflection factor.* For tasks in which the reflection factor of the background is less, higher illumination levels are to be taken in proportion.

As regards the ease of performance of visual tasks, different investigators have made use of different criteria: Luckiesh and Moss [1]) and Waller [2]) assume certain factors to indicate how "far" the task lies above the threshold of visibility (as delineated in diverse ways). Efforts can also be made to employ as a measure of the ease of performance the degree of fatigue after a certain period of observation, in the manner discussed in a previous article in this review [3]).

Weston, in his investigations, adopts as a measure of performance the time taken for the observation in conjunction with the percentage of errors made [4]) and this conception appears to us very attractive, since it entails data which are not only capable of easy measurement but which have a very obvious practical value for expressing the ease of performance of a task; the arguments put forward in the following paragraphs are therefore based on Weston's experiments.

For a clear understanding of the problem it should be pointed out that the salient features of detail-size and contrast are in themselves not enough fully to characterize a given task. In general, it is moreover necessary to take into account the period of time during which the observations are made, whether these periods are broken by resting or waiting time and, again, whether the task involves any element of responsibility and so on. A table of recommended illumination levels compiled from observations relating to tasks entailing different sizes of detail and contrast values should therefore also indicate the circumstances, in accordance with the above. Then, when the appropriate illumination level for a given task is selected from the table, any differences in the factors referred to can be taken into account as far as possible by means of positive or negative allowances on the recommended level.

There is also another point of view, namely that the characteristics of the task and the ease with which it is performed, when examined closely, cannot easily be discriminated from each other, for the features of the task may be regarded as a measure of the difficulty or ease of performing it and there can be little sense in making a distinction between the degree of difficulty and the ease of performance of a task. The only significance of such a distinction is that the first must be looked upon as an independent variable and the latter as a dependent variable (with the illumination as parameter). This is clearly seen from the duration of the observation (rate of observation) introduced in the article referred to in footnote [3]) as characterising the task itself: Weston, however, employs it to characterise the performance of the task.

Weston's measurements: the concepts "performance" and "relative performance"

In Weston's experiments his subject was asked to examine charts showing a large number of open rings (Landolt's rings) with the slit directions distributed at random (*fig. 1*). The task consisted

[1]) M. Luckiesh and F. K. Moss, Visibility, its measurement and importance in seeing. J. Frankl. Inst. **220**, 431-466, 1935.

[2]) A. Waller, "Zichtbaarheid", diss, Utrecht 1945.

[3]) A. A. Kruithof and H. Zijl, Illumination levels in offices and dwellings. Phil. Techn. Rev. **8**, 242-248, 1946. The considerations regarding fatigue mentioned in this article were based mainly on measurements by M. Luckiesh and F. K. Moss. Trans. Ill. Eng. Soc. **34**, 571, 1939.

[4]) H. C. Weston, Industrial Health Research Report No. 87, H. M. Stationery Office, London, 1945.

in identifying and crossing off on each chart rings of a given orientation.

The detail to be observed — the slit in the ring — is of a given size and a given contrast on each

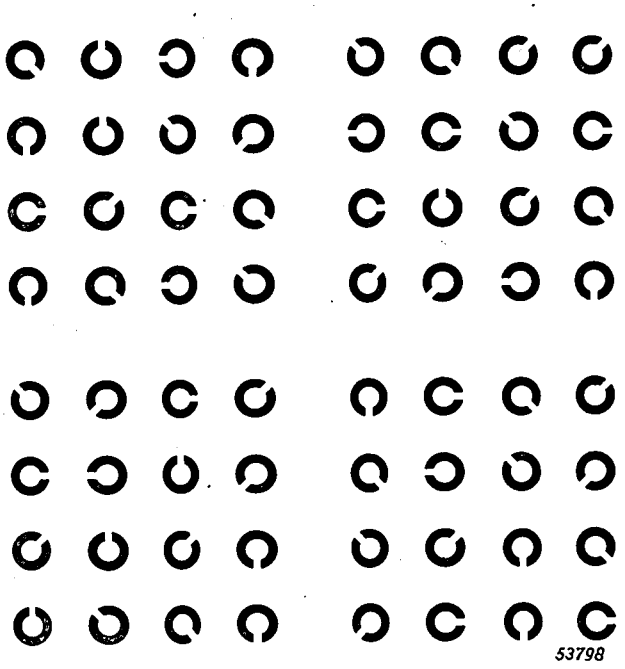


Fig. 1. Part of one of Lansolt's ring-charts, as used by Weston in his experiments. The diameter of the rings and therefore also the size of the slit (i.e. the detail to be observed) varies from one chart to another. The contrast, determined by the difference in reflection factor of the rings and the paper on which they are printed, also varies among the different charts. The rings are printed in eight different positions and the subject is required to mark off all rings having a certain orientation, being allowed as much time as he may deem necessary. This period of time, in conjunction with the number of rings overlooked, serves as a measure of the performance. The tests as carried out were in series of 1 minute duration with intermediate rest breaks of about $^1/_2$ minute, covering a total working period of $1^3/_4$ hours.

individual chart and Weston expressed the per*formance of the eye for a given task as the quotient of the accuracy of the result* (i.e. the ratio of rings marked correctly, to the total number of rings of the given orientation) *and the time required by the operator to determine the orientation of one ring.*

This quotient was taken by Weston to be the performance; he measured the average performance of a number of subjects, as a function of the illumination level for different sizes of detail and contrast. Some of his results are reproduced in *fig. 2.*

In this way, in principle the effect of the illumination on the performance of a task is known and it only remains to establish a standard of qualifications. In this connection Weston introduced the concept "relative performance": the curves in fig. 2, each of which refers to a particular task, do not rise indefinitely, but begin to drop at very high illumination levels ($>$ 20,000 lux, approx.) due to the fact that the disability glare begins to take effect. There is therefore a maximum performance for every task, and the relative performance is the ratio of the actual to the maximum possible performance. Our appraisal of an illumination level will thus have to be higher as the maximum performance for the task in question is more closely approached, i.e., as the relative performance more nearly reaches unity. The standard, then, will have to establish a relationship between the qualifications "sufficient", "good" etc. and certain relative performance values. This point will be referred to later.

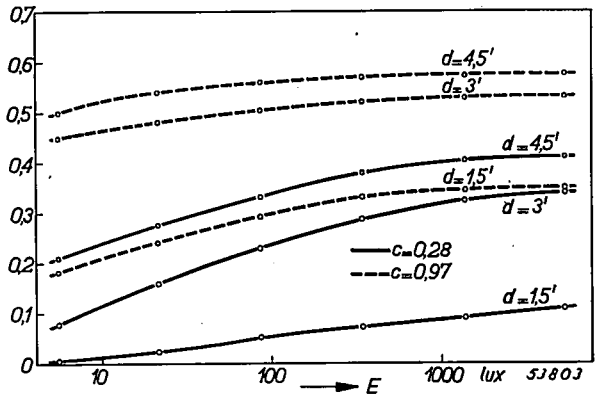


Fig. Performance as a function of the illumination E in lux, according to Weston. Each case refers to a particular task, i.e. size of detail d and contrast c. (In Weston's tests each contrast value was based on a different reflection factor of the background, i.e. the paper on which the rings were printed; in view of our remarks in the previous paragraph, we have converted Weston's illuminatoin values to agree with a constant reflection factor of 0.9.)

Reshaping Weston's data into a lighting table

In measurements such as those carried out by Weston there is bound to be a certain amount of deviation among the results, even though these be the averages taken from groups of different observers. Obviously, the differences thus arising

[5]) The performance of a task usually involves both an observation and a subsequent action (in the above case the marking of the ring identified). Both phases occupy a certain amount of time and they both present an opportinuty for making a mistake. Now, in order to obtain a true measure of the visual efficiency — this being our ultimate object — the errors in the action and the time taken to complete it should not be included. Weston therefore made a separate record of the time taken in marking a ring, and deduced this from the total time measured. The task in question is so simple (this being the reason why it was selected) that a correction for errors in the action are not necessary. In any case, an error in the performance of the task can consist only in the omission of a ring (the marking of a ring pointing in the wrong direction, in which case it would not be known whether the fault lies in the observation or in the action, was such a rare occurrence that it could be neglected).

between the various quantities cannot be allowed to pass into the final recommendations to be issued to lighting engineers, and fig. 2 gives a graphical representation of performance versus illumination level as smoothed by Weston.

Since in practical applications of the data the particular task is in each case the starting point, it is desirable from the point of view of easy interpolation also to smooth out the ratios in regard to the effects represented by the parameters, viz. size of detail and contrast, which means the removal of irregularities in the spacing of the curves shown in fig. 2. This has been done by plotting, as a function of the contrast, the illumination required to ensure a certain relative performance, thus producing a family of curves with the relative performance as parameter; for every size of detail concerned a different set of such curves is used, see *fig. 3*.

In this manner the irregularities in the functions are smoothed out (thus guaranteeing more reliable interpolation for any required contrast value), whilst ensuring that the curves also tally with known data concerning the threshold of vision.

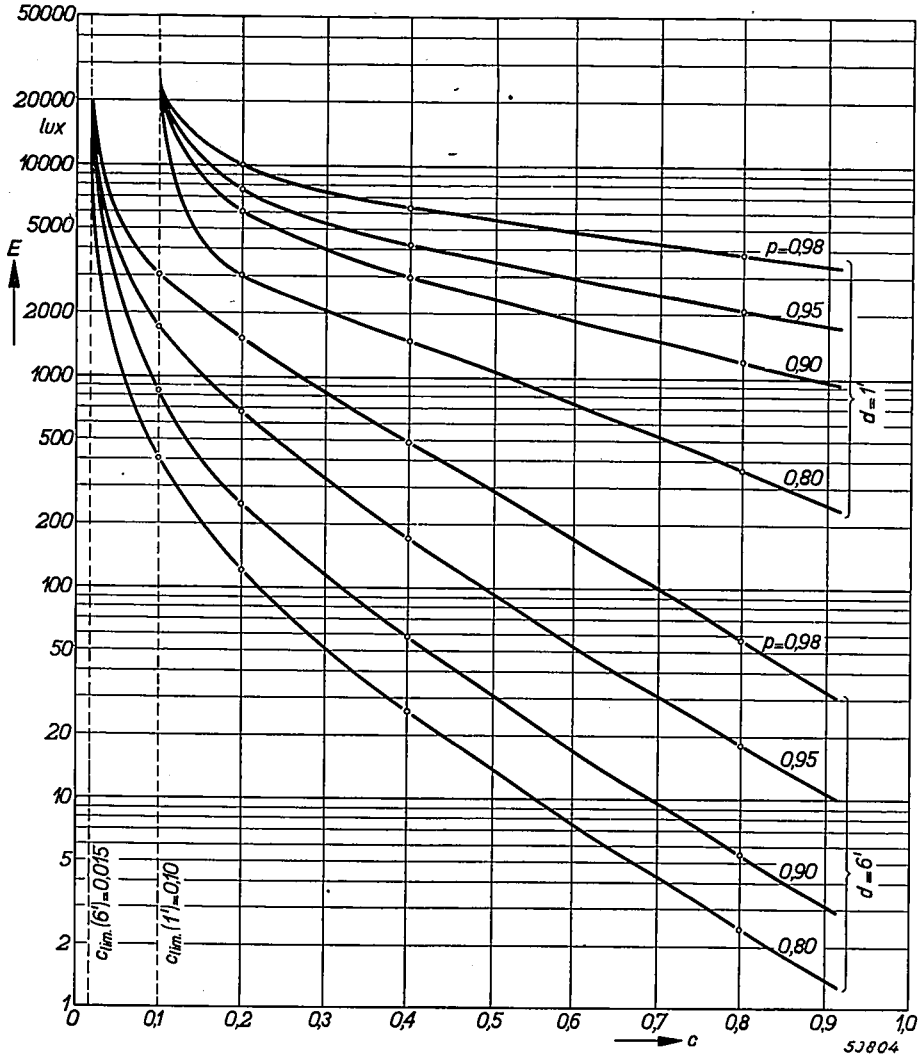


Fig. 3. Illumination E in lux required to ensure a given relative performance p on the basis of a given detail size d plotted against the contrast c. In this manner it is possible to "smooth out" and interpolate Weston's data in regard to the effect of the contrast. The curves are also subject to the condition that each group relating to the same detail size must approach the vertical line corresponding to the least perceptible contrast c_{lim}, for that detail size.

Even though the illumination level be raised to the point of disability glare, it is not possible to see an object of a given size if the contrast between that object and its background lies below a certain minimum value, and in *fig. 4* [6]) this minimum is shown plotted against the size of the object. At such very high illumination levels

[6]) H. Siedenhof, Das Licht **11**, 35, 1941. A. Kühl, Z. Instrumentenkunde **60**, 292, 1940.

the effect is that each of the groups of curves in fig. 3, relating to a certain size of detail, must approach the vertical line on which the contrast is at its corresponding minimum value, for, if tasks are to be undertaken at such low contrast values, a very high illumination will be needed to yield even the smallest performance.

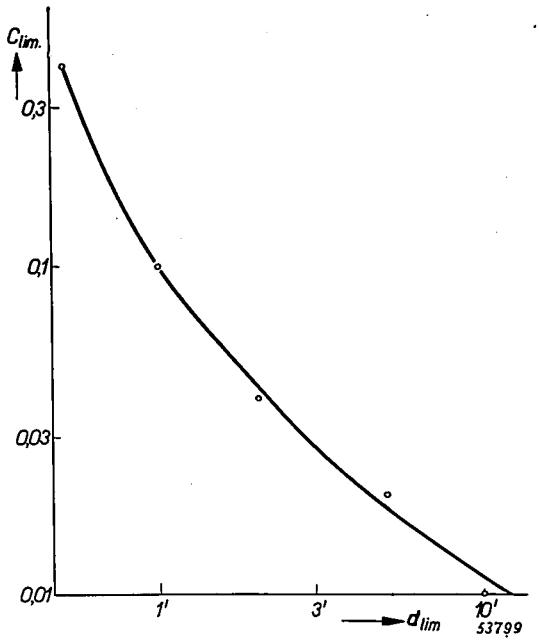


Fig. 4. Relation between the least perceptible contrast c_{lim} and smallest perceptible detail d_{lim} (derived from data by both Siedentopf and Kühl).

The data have also been smoothed out as far as the detail size is concerned (with the contrast as parameter for the groups of curves) and here, too, it has been found possible to correct the curves by enforcing the condition that each group for a particular contrast value will approach the vertical line at the appropriate threshold of perception of detail.

In this way the illumination levels shown in *table III* were obtained.

Stages of difficulty of task and performance

To ensure reliable interpolation once more, the successive columns (and lines) of the table should refer to tasks the difficulty of which increases in roughly constant steps. From table III it will be seen that, as far as this requirement is concerned, the gradations of detail size and contrast adopted in tables I and II answer the purpose very well. For example, if we proceed from the illumination levels specified for a task: detail size $d = 1.5'$, contrast $c = 0.2$, the illumination value required to ensure a specified relative performance will be seen to

Table III. Illumination in lux required to ensure given values of the relative performance of tasks involving different values of contrast c and detail size d (reflection factor of background 0.9). In comparison with Weston's original experimental results, the illlumination levels have been smoothed out, partly with the aid of fig. 3.

Size of detail d \ Contrast c / Relative performance p	0.1	0.2	0.4	0.8
1′	0.98		9900	6300	3800
	0.95		7500	4300	2050
	0.90		5400	2900	1200
	0.80		3100	1500	360
1.5′	0.98	9900	6600	3900	1600
	0.95	8100	4500	2400	750
	0.90	5700	3300	1500	370
	0.80	3300	1650	610	97
3′	0.98	5800	3600	1600	260
	0.95	4100	2250	780	110
	0.90	2500	1300	320	34
	0.80	1300	550	130	12
6′	0.98	2900	1600	480	57
	0.95	1700	700	170	19.5
	0.90	880	260	59	5.4
	0.80	420	120	26	2.6

increase just as much [7]) when changing the task to $d = 1.5'$, $c = 0.1$ (one step to the left) as when changing to $d = 1'$, $c = 0.2$ (one step upwards). Expressing this in another way, it may be said that the reduction in contrast from $c = 0.2$ to $c = 0.1$ renders the task more difficult to the same extent as the decrease in detail size from $d = 1.5'$ to $d = 1'$. If we now apply the same argument to a task $d = 3'$, $c = 0.2$ and $d = 6'$, $c = 0.2$, it will further be seen that the steps in the difficulty factor from $d = 3'$ to $d = 1.5'$ and $d = 6'$ to $d = 3'$ are for all practical purposes the same as from $c = 0.2$ to $c = 0.1$: in other words the three steps of the element of difficulty lying between the four grades of detail size d are practically the same.

[7]) In all these arguments it should be borne in mind that there is no object in striving towards too high a degree of accuracy when making comparisons between illumination levels. Owing to the fact that individual differences in visual performance are found to be considerable even for such quantities as contrast sensitivity and visual acuity, which are easily measured, variations up to 30% between anticipated and actual illumination need not be regarded as serious. In the ultimate levels recommended it is probable that greater discrepancies will occur as a result of subjective appraisal of the allowances, which latter, as mentioned above, are required to counterbalance numerous differences between the actual circumstances governing both a particular task and the type of task as selected from the table.

This may be verified by a comparison of the illumination levels in the columns for contrast $c = 0.4$ and $c = 0.2$, $c = 0.8$ and $c = 0.4$. Further, the three difficulty steps between the four gradations of contrast are not only aproximately equal, but also approximately the same as the steps corresponding to the detail size. There remains only the question whether the four stages in the relative performance p have been suitably chosen; in this case it is required that the transition from a specified value of p to the next higher stage shall in each instance represent a step of a given size in the relative difficulty factor [8]).

To check this point the obvious procedure is to calculate the factor (g) by which the illumination should be increased in order to raise the relative performance to the next higher stage. Admittedly, this factor is by no means a direct measure of the difference between the difficulty in the one stage of performance and the next, as is borne out at once by the fact that for a given performance step, say from 0.80 to 0.90, entirely different increment factors for the illumination level are found in different parts of the table. The same holds good when calculating from the table the factor (f) by which the illumination has to be increased to compensate for one step in the difficulty of the task (i.e. reduction of contrast or size of detail), at a constant value of p. Curiously enough it is found that both factors depend only on the illumination level taken as the starting point for the steps in difficulty and performance respectively and, owing to this fact, we are entitled to draw a comparison, in respect of any initial level, between the factor g, corresponding to one step in performance, and factor f which relates to one step in contrast.

Accordingly, we find that the performance steps 0.98/0.95, 0.95/0.90, 0.90/0.80 are, on an average, equivalent to 0.63, 0.59 and 0.65 times the value of one contrast step; the four performance stages 0.98, 0.95, 0.90 and 0.80 selected are thus quite equally spaced.

If the average factor f as calculated from the table be plotted as a function of the illumination level, there will naturally be a considerable scattering of the points, but a smooth curve drawn through these will give the average factor f as shown in *fig. 5*. These average factors enable us to apply a final correction to table III: what we have actually done is to equate the illumination levels relating to the four equally difficult tasks in the diagonal $d = 6'$, $c = 0.1$ to $d = 1'$, $c = 0.8$, with the average values

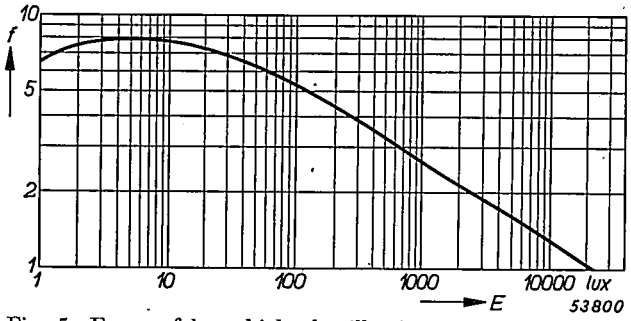


Fig. 5. Factor f, by which the illumination level must be increased in accordance with table III to maintain the same relative performance when the difficulty of the task is increased one step. It appears that this factor, within quite reasonable limits, depends only on the starting level. The curve has been drawn as a smooth line through the somewhat scattered points relating to the values of f calculated from the table. It meets the line $f = 1$ at about 20 000 lux, and this agrees with the established fact that vision does improve any further at levels beyond 20 000 lux (apart from tasks the difficulty of which is less than one stage removed from the threshold of perception).

found for these tasks in table III (correcting the four levels so that their ratios agree with the average factors g as derived above); we have then calculated the levels for all other tasks by means of the factor f, as read from fig. 5. At the same time, each calculated value has been rounded off in a manner frequently employed in illuminating engineering, viz. to the nearest of a series of values (excepting factors of 10) [9]): 1 - 1.25 - 1.6 - 2.0 - 2.5 - 3.2 - 4.0 - 5.0 - 6.3 - 8.0 - 10. The standarised table thus obtained is given below (*table IV*).

In the same way that this table is derived on the basis of Weston's definitions end experiments, it would also be possible to prepare a table according to the methods of Luckiesh and Moss, or Waller, alluded to in the opening paragraphs [10]). It might be interesting to see whether the different tables could be brought into line with each other, but here we cannot go into this matter any further.

Practical uses of the lighting table

It may now be asked to what interpretations as "sufficient", "good", etc. the above stages for the relative performance 0.80, 0.90, 0.95, 0.98 refer. By assuming a particular task and making a comparison between the relative data (inter alia

[8]) This again illustrates the fact that if attempts are to be made to discriminate between „difficulty" and "performance" ,it is merely a question of the choice of dependent and independent variables: it would be quite feasible to include the requirement of a certain relative performance in the delineation of the task and say that the latter becomes more difficult as the demands in respect of the level of performance are made more stringent.

[9]) As an approximation, these values form a geometrical series in the ratio of $\sqrt[10]{10}$ and thus divide the factor 10 into 10 equal intervals.

[10]) *Note at time of going to press.* More recent research in this field, introducing slightly different definitions, may be found in E. Simonson and J. Brozek: Effects of illumination level on visual performance and fatigue, J. Opt. Soc. Americ. *83*, 383-397, 1948 (No. 4).

Table IV. Illumination in lux required for four values of the relative performance of tasks involving different contrast c and detail d (reflection factor of the background = 0.9). The illumination values given differ from those in table III in that they are calculated with the aid of the smoothed-out factor f in accordance with fig. 5 and subsequently rounded off as explained in the text.

Detail size d	Relative performance p	Contrast c 0.1	0.2	0.4	0.8
1′	0.98		10000	6300	4000
	0.95		8000	4000	2000
	0.90		5000	2500	1000
	0.80		4000	1600	500
1.5′	0.98	10000	6300	4000	1600
	0.95	8000	4000	2000	800
	0.90	5000	2500	1000	320
	0.80	4000	1600	500	100
3′	0.98	6300	4000	1600	500
	0.95	4000	2000	800	160
	0,90	2500	1000	320	50
	0.80	1600	500	100	12.5
6′	0.98	4000	1600	500	100
	0.95	2000	800	160	25
	0.90	1000	320	50	6.3
	0.80	500	100	12,5	1.6

from the article mentioned in note [3])), it would be possible to give a general answer to the effect that a relative performance of, say 0.90 to 0.95, may be considered "good": this is in fact the standard suggested by Weston. In actual practice, however, the question and its answer are hardly relevant, for, with a little experience, the value of the relative performance can be employed directly as an indication of the quality of the lighting system, thus avoiding the detour by way of the descriptions "good", etc. employed in the introduction merely to clarify the point at issue.

In continuation of the remarks contained in the opening paragraphs, we now have the means of recommending a certain relative performance p to be the ultimate object under any given set of economic conditions. Conversely it will be useful to ascertain what average performances can be realised on the basis of the lighting tables now in use in various countries. It will be found, for example, that the German (pre-war) tables correspond to $p = 0.80$ to 0.85 for a task of average difficulty, and the latest American tables to $p = 0.95$ to 0.98. For very easy tasks the illumination levels recommended in the tables of every country concerned correspond to performances of roughly $p = 1$. This is not difficult to understand, since the highest relative performance values can be achieved for easy tasks at relatively low illumination levels. Performance can then no longer be a criterion of the required illumination and other considerations, such as a bright atmosphere in the place of work, will be brought forward as the reason for the recommendation of much higher illumination levels than those specified in table IV for such tasks.

If the lighting table is to be employed in connection with industrial tasks it will be advisable to remember that the differences in "relative performance" with respect to various illumination levels do not correspond in general to equally large differences in production figures. The concept "performance" employed in this article is solely a measure of the ease of performance of the visual element of a task: in a practical task involving more or less complex actions in step with visual observation (in accordance with note [5])) the influence of the illumination on the final result, i.e., the "production", may be appreciably less than its effect on the "visual peformance", since the time needed for the manual part of the task and the corresponding risk of error are independent of the illumination level.

VOL. 10 No. 8, pp. 221-256 FEBRUARY 1949

Philips Technical Review

DEALING WITH TECHNICAL PROBLEMS
RELATING TO THE PRODUCTS, PROCESSES AND INVESTIGATIONS OF
THE PHILIPS INDUSTRIES

EDITED BY THE RESEARCH LABORATORY OF N.V. PHILIPS' GLOEILAMPENFABRIEKEN, EINDHOVEN, NETHERLANDS

A MINIATURE X-RAY APPARATUS FOR DENTISTS

by J. FRANSEN.

616.314-073.75

For taking intra-oral radiographs of the teeth and mandible only a small X-ray intensity is needed. An apparatus for this purpose, therefore, need only be of small power (e.g. 160 W) with a relatively low tube voltage (45 kV_{peak}). Moreover the voltage and current do not have to be variable. These simplifications have made it possible to construct for dental use an X-ray apparatus of extremely small dimensions and light weight (4.5 kg). The X-ray tube, built on the lines of a modern radio valve, is only 6 cm ($2^3/_8$″) long. The X-ray tube and the high tension transformer are contained in a shield filled with oil. The filament current is drawn from a winding on the high tension transformer. The tube current is nevertheless sufficiently insensitive to mains voltage fluctuations, the cathode being made to work in the space-charge range instead of the saturation range. The circuit used for this purpose also has an additional stabilizing action. This article deals with all these points and describes the construction of the transformer as well as the apparatus as a whole.

The making of X-ray photos of the human denture and the designing of an apparatus for that purpose are in every respect much simpler problems than those usually encountered in medical X-ray practice, the most important differences being the following:

1) The object to be photographed does not make any involuntary movements like those of the lungs, heart and stomach, so that from the point of view of sharpness of definition a longer exposure time can be allowed.
2) The part of the body to be X-rayed (the mandible) is at most 2-2.5 cm thick, so that the focus of the X-ray tube can be brought close to the object (and thus to the film) without any troublesome distortion in the shadow picture. Since all parts of the object are close to the film, there is also little geometrical blurring of any parts.
3) Thanks to the nature and thinness of the object, relatively little radiation is absorbed. Due to the closeness of the focus to the film and the possibility of long exposure with a reasonably sensitive film, there is no need for an intensive radiation for radiography [1]). The advantages thus offered are:
   a) A relatively small-power X-ray tube suffices.
   b) Particularly, a low tube voltage can be chosen. This is not only an advantage from the constructional point of view but with such thin objects it is even an essential condition in order to get proper contrasts in the picture.
   c) The small power required can be dissipated on a relatively small focus, thus enhancing the definition of the radiograph.
4) In intra-oral radiography there are very little differences in the thickness and composition of the layers of tissue that have to be penetrated, so that there is no need for the tube voltage and the current to be made variable; small differences in absorption can easily be compensated by varying the exposure time if the same average film blackening is required.
5) Corresponding to the smallness of the objects, is a small size film. There is therefore no need, from the point of view of expense, for screening instead of radiographing. As a matter of fact there is an objection against screening, because

[1]) There is, it is true, also a factor having the opposite effect. Owing to the relatively high demands made in respect to the sharpnesss of dental photographs, no intensifying screens are applied to the film, because these would cause considerable blurring due to their granular structure. This means that the intensity has to be about 10 times as great as that needed when intensifying screens are used. Still the gain in intensity obtained by the aforementioned factors is by far the greater.

of the considerable screen-blurring and the large X-ray dose that would have to be given to the patient. The X-ray apparatus need not, therefore, bear any considerable loads.

The fact that the requirements to be met in the design of a dental X-ray apparatus can easily be satisfied does not by any means imply that the product is technically less interesting. As a matter of fact these simple conditions made it possible to improve considerably upon other diagnostic apparatus of a higher capacity, as far as small dimensions, simple construction and handiness are concerned. In *table I* some data of a new apparatus ("Oralix") specially designed by Philips for dentists are compared with those of a universal diagnostic apparatus ("Medio D" [2]). *Fig. 1* is a photograph showing the apparatus mounted on a dental chair.

The description that will now be given of this

[2]) H. A. G. Hazeu and J. M. Ledeboer. A universal apparatus for X-ray diagnosis, Philips Techn. Rev. **6**, 12-20, 1941. A dental apparatus built on principles similar to those described here and weighing even less was demonstrated by Bouwers already in 1937 at the fifth international roentgenological congress at Chicago (see A. Bouwers and W. J. Oosterkamp, Amer. J. Radium Therapy, **41**, 444-447, 1938), but owing to manufacturing problems this apparatus was not produced in any large numbers.



Fig. 1. The "Oralix" miniature X-ray unit developed by Philips. The aparatus (see directions of the arrows) is shown on an arm attached to a dental chair.

Table I. Comparison between some data of a universal diagnostic apparatus ("Medio D") and those of the new dental X-ray apparatus ("Oralix").

	"Medio D"	"Oralix"
Tube voltage	45-100 kV_{peak}	45 kV_{peak}
Tube current for radiography	100-250 mA	5 mA
Tube current for screening	3 mA	—
Time range	0.02-8.0 sec	0.1-6.0 sec
Focus width	1.2 or 2.0 or 3.5 mm	0.8 mm
Load-capacity, intermittent	13 kW	160 W
Load-capacity, continuous	150 W	(16 W)
Weight of X-ray tube	20 kg	4.5 kg
Weight of generator	300 kg	
Length of X-ray tube	30 cm	6 cm

miniature apparatus will show how the utmost advantage has been taken of the aforementioned possibilities for a small and simple construction.

The X-ray tube

The X-ray tube is made of hard glass and insulated in oil. As already described on more than one occasion [3]), this allows of a considerable reduction in the length of the insulation required for the tube voltage, and thus in the length of the tube. In our case, where a voltage of only 45 kV_{peak} was required, the minimum length of tube was in fact so small that the problem arose how to fit in the cathode and anode with their leads in such a way as to profit from this possibility of reducing dimensions.

The solution found is shown in *fig. 2*. Instead of the cathode being fused into the tube with the conventional pinch, as is done for larger X-ray tubes, the base of the tube is made flat and of hard glass, following the example of modern radio valves. Fused into the base are four molybdenum pins, which can act at the same time as connecting pins, leads, and as supports for the cathode system mounted in the tube. The solid tungsten anode is attached to a molybdenum pin carried through the top of the tube by the usual fusing technique. The resultant small dimensions are illustrated in fig. 2.

The filament is placed in a cathode cap which ensures focusing of the emitted electrons upon the small area of 0.8 mm × 3 mm on the anode (line focus, which in oblique projection has the apparent dimensions of 0.8 mm × 0.8 mm).

The thin anode pin cannot contribute much to carrying off the heat generated on the focus from the anode outwards. The anode therefore has to dissipate this heat for the greater part by radiation.

The following calculation shows that the anode is indeed able to do this. The heat developed during an exposure time of 6 seconds (the maximum exposure time this apparatus permits) is equivalent to 950 Wsec for an A.C. voltage of 45 kV_{peak} and 5 mA average tube current. The mass of the anode being 66 grams, the heat capacity is 9.4 Wsec/°C. The rise in temperature while making one radiograph is thus roughly 100 °C. Since at the most one has to reckon with intermittent working with one exposure of such a length per minute, the anode cannot cool off to room temperature after each photograph is taken, so that a certain higher starting temperature has to be reckoned with. While a photograph is being taken the anode temperature must not be allowed to rise above 850 °C, so that the starting temperature may be 750 °C at the utmost. Thus the anode has to cool off each time from 850 to 750 °C within one minute and by radiation. Now the formula for the total radiation of a black body of temperature T_1 °K is:

$$P = \delta \cdot (T_1^4 - T_0^4) \text{ W/cm}^2,$$

where $\delta = 5.8 \times 10^{-12}$ W/cm² degree and T_0 is the ambient temperature. The radiation of polished tungsten is much less, at 1100 °K for instance being equal to that of a black body at a temperature of 659 °K. In the case of our anode we can take it that radiation takes place at an average temperature between 1023 and 1123 °K, thus equal to that of a black body of about 640 °K. From the formula above we find that the radiation is $P = 0.92$ W/cm². The surface area of the anode being 13 cm², it radiates about 700 W sec/min, whilst 950 Wsec is added.

The excess of about 250 Wsec is carried off via the anode pin by conduction.

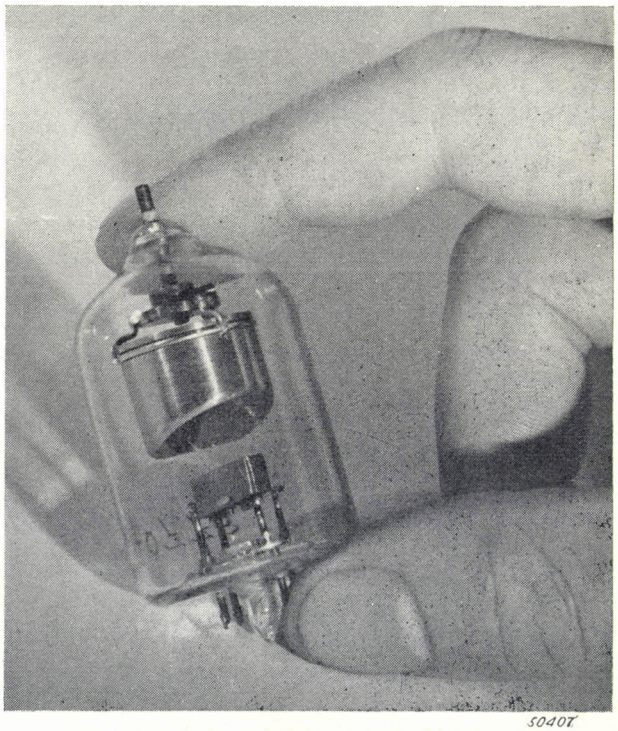


Fig. 2. X-ray tube for the "Oralix" miniature X-ray apparatus. The tube is designed to work on A.C. with 45 kV peak and 5 mA (mean) for max. 6 seconds per minute.

[3]) See, for instance, J. H. van der Tuuk, Hard glass X-ray tubes in oil, Philips Techn. Rev. **6**, 309-315, 1941.

The heat irradiated is first absorbed by the oil surrounding the tube and then imparted to the shield. In addition to its insulating effect the oil therefore has a cooling function.

The supply and stabilization of the tube current

A diagram of the circuit for feeding the X-ray tube is given in *fig. 3*. The secondary voltage from the high-tension transformer is conducted direct to the X-ray tube. The voltage for the filament is

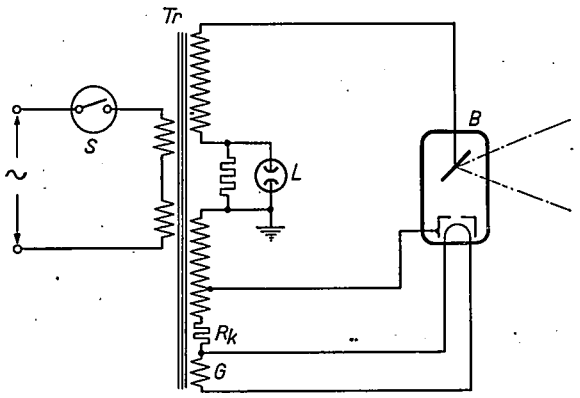


Fig. 3. Circuit diagram of the "Oralix" X-ray unit. *Tr* high tension transformer with symmetrical voltage with respect to earth; *B* X-ray tube; *G* heating-current winding; R_k resistor for applying a negative "grid bias" to the tube so that the filament works in the space-charge range of the characteristic curve; *L* pilot lamp; *S* time switch.

taken from a separate winding mounted on the secondary winding. Tube voltage and filament voltage are therefore in a fixed ratio. This simple method is possible in our case because neither the tube voltage nor the tube current need be varied, these being adjusted to the fixed values of 45 kV_{peak} and 5 mA (average value) respectively.

In normal X-ray apparatus where the tube current has to be variable the filament voltage is supplied by a separate small transformer; it can then be adjusted independently of the tube voltage, by adjusting the primary voltage on that transformer which is at a low potential. For a sensitive adjustment of the tube current the tube is caused to work in the saturation range of cathode emission; in fact, the saturation value of the cathode emission depends very strongly upon the cathode temperature. In this way a 50 % variation in the tube current is possible with a variation of only 10% in the filament voltage.

In our case, where only one fixed value of the tube current is required, working in the saturation range of the cathode is not only unnecessary but even undesirable, because otherwise the tube current would be highly sensitive to small fluctuations in the mains voltage. Since such a fluctuation generally passes unnoticed — in non-adjustable apparatus the voltage is not usually checked — and hence the current variation cannot be compensated by changing the exposure time, the film blackening would not be reproducible to the desired extent.

For this reason in our case the X-ray tube must not be allowed to work in the saturation range but rather in the space-charge range of the cathode emission.

In order to bring this about, one could try to reduce the action of the anode on the cathode through the opening of the cathode cap. This action, which can be defined as the reciprocal value of the amplification factor, will be denominated as the "transudation" (in foreign literature the common term is "Durchgriff"). A reduction of this "transudation" involves changing the configuration of the electrodes, for instance making the cathode cap narrower or placing the filament farther down in the cap. Such a method, however, would defeat its own object because, although the tube current is then much less sensitive to fluctuations in the filament voltage, the possibility is lost of obtaining the nominal value of tube current by adjusting the filament voltage in the manufacture. As a result one would be limited to extremely narrow tolerances in the electrode arrangement to obtain the nominal tube current without further adjustment.

Another course has therefore been chosen. The cathode cap, which in normal X-ray tubes is always at the potential of the filament, has been given a separate lead through the tube base. A voltage is now applied to the cap which is negative with respect to the filament. This "grid voltage" (v_g) is taken from a resistor (R_k) in the circuit through which the tube current flows; see fig. 3.

A diagram, as given in *fig. 4*, of the i_a-v_g characteristics of the X-ray tube — which can here be dealt with in a manner similar to that applied to a triode in the radio technique — shows that by this means the tube is indeed made to operate in the space-charge range. Each characteristic refers to a certain value of the anode voltage, the three fully-drawn curves relating especially to the peak values of the anode voltage in respect of the nominal, the maximum and the minimum mains voltages occurring ($V_{n\,nom}$, $V_{n\,max}$ and $V_{n\,min}$ respectively). At any moment the grid voltage is

$$v_g = -R_k \cdot i_a \quad \ldots\ldots\ldots \quad (1)$$

In each mains cycle the working point of the tube, which has the co-ordinates v_g and i_a, travels to and fro along the straight line given by eq. (1) and drawn through the origin — the working line —

thereby intersecting the family of characteristics according to the momentary values of the anode voltage passing through. The point where the working line intersects the curve $V_{n\,\mathrm{nom}}$ gives the peak

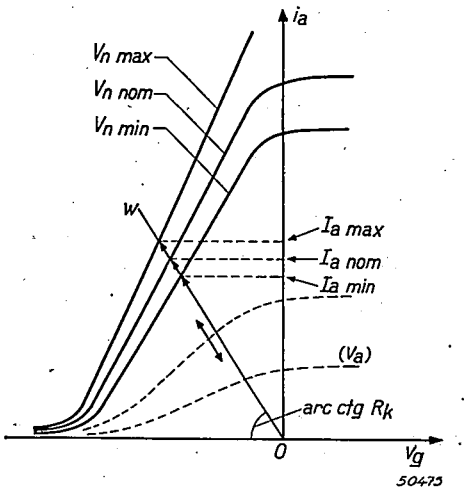


Fig. 4. Diagram of the i_a-v_g characteristics for the X-ray tube. Owing to the condition $v_g = -R_k i_a$, the working point has to move along the line w drawn through the origin. Each curve corresponds to a certain anode voltage. During a cycle of the alternating voltage supply the family of curves is intersected along the working line. The characteristic for the anode peak voltage occurring at the nominal value $V_{n\,\mathrm{nom}}$ of the mains voltage produces the peak value $I_{a\,\mathrm{nom}}$ of the tube current. With fluctuating mains voltage (between $V_{n\,\mathrm{max}}$ and $V_{n\,\mathrm{min}}$) there is relatively little variation in the tube current, owing to the characteristics deviating but little in the sloping part (space-charge range). Since with fluctuating mains voltage V_n the heating temperature of the cathode will fluctuate as well, the dotted curves for the instantaneous values v_a of the anode voltage will also vary slightly each time; for the sake of simplicity this is not shown here.

value $I_{a\,\mathrm{nom}}$ of the tube current (in our case about 15 mA, corresponding to the previously mentioned mean value of 5 mA). It is seen that the working point is always within the sloping part of the curves (the space-charge zone), where they deviate much less than in the saturation zone.

This method avoids the difficulty of too small tolerances in the electrode configuration. Fig. 4 shows that owing to the oblique traject of the working line the tube current I_a is less affected by small deviations in the characteristic, regardless whether these deviations are caused by variation of the mains voltage (thus of the filament voltage) or of the electrode configuration. Consequently, when a tube is being inserted in the apparatus there is no need to pay attention to the unavoidable small differences that exist between various tubes; the desired nominal tube current is obtained with sufficient accuracy without any adjustments.

To complete the picture *fig. 5* gives the corresponding diagram for the case where the X-ray tube is worked in the normal manner, thus with $R_k = 0$, in the saturation zone. Here the working line is the ordinate axis ($v_g = 0$) and it is seen that for the peak values of the anode voltage the working point enters the saturation range of the curves, resulting in the great differences between $I_{a\,\mathrm{max}}$ and $I_{a\,\mathrm{min}}$.

A comparison of the families of curves given in figs 4 and 5 shows that in fig. 4 the saturation values are much higher. This is necessary to bring the point of intersection of the working line on the characteristic for $V_{n\,\mathrm{nom}}$ on the same level as in fig. 5, thus to obtain the desired nominal tube current $I_{a\,\mathrm{nom}}$. The higher saturation is obtained by increasing the emission of the filament, for instance by heating it to a higher temperature.

In the foregoing we have dealt with the i_a-v_g diagram of our X-ray tube in a manner similar to that applied for a radio valve. Actually, however, there is an important difference, also in the qualitative sense. In the case of a radio valve the filament voltage is usually kept constant, so that in the i_a-v_g diagram of such a valve the characteristics corresponding to different anode voltages (V_a) all have the same slope. Where we have a working line like that in fig. 4 the relative variation of the tube current I_a corresponding to a variation in the anode voltage is always equal to the relative variation of V_a. In the case of our X-ray tube, however, the filament voltage also varies together with the anode voltage. Consequently the curves become steeper as V_a increases and the beam diverges, resulting in a relatively stronger variation of I_a.

It now appears that circuiting with the resistor R_k has another particular advantage compared with the other method of bringing the working point within the space-charge range (reducing the

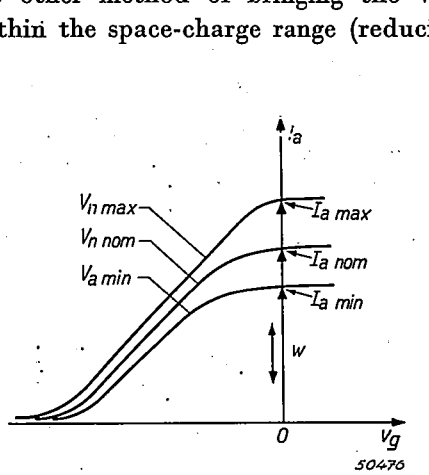


Fig. 5. Diagram corresponding to that in Fig. 4, for the case where the X-ray tube operates in the normal manner, with the filament working in the saturation range. Here the working line w is the ordinate axis ($v_g = 0$). The variations of I_a accompanying fluctuations in the mains voltage V_n are very considerable.

"transudation"). With the latter method, where $R_k = 0$, the working line of the diagram is the ordinate axis ($v_g = 0$), so that the diverging family of characteristics is intersected in the

vertical direction [4]). As a result any variation in V_a causes about twice as large a variation in I_a. In Fig. 4 on the other hand, where $R_k > 0$, the characteristics are intersected obliquely, so that their divergence is much less felt and I_a varies for instance by a factor of only $1^1/_2$ with respect to V_a.

Obviously this additional stabilizing action — just like the effect of rendering the tube current insensitive to the tolerances in the electrode configuration — will be all the more successful the larger the resistor R_k is chosen, for the working line in fig. 4 will then be flatter. But then, unless other steps are raken, the point of intersection of the working line on the characteristic $V_{n\,\mathrm{nom}}$ will be lower. Now, to be able to choose a large value of R_k and still reach the prescribed value of $I_{a\mathrm{nom}}$ for the tube current with the given characteristic, a positive grid bias has, in addition, been applied. This is obtained by connecting the cathode cap to a tapping of the high tension transformer as indicated in fig. 3 instead of connecting it direct to R_k. The resultant grid voltage is then at any moment

$$v_g = fv_a - i_aR_k, \quad \ldots\ldots \quad (2)$$

where f denotes the fraction of the high-tension coil to which the tapping is made. The working point for any moment can be found from the dotted line construction in *fig. 6*. Inversely, by starting from given values for $I_{a\,\mathrm{nom}}$ and R_k, with this construction it is possible to determine the required value of $f\,V_{a\,\mathrm{nom}}$ and thus of f.

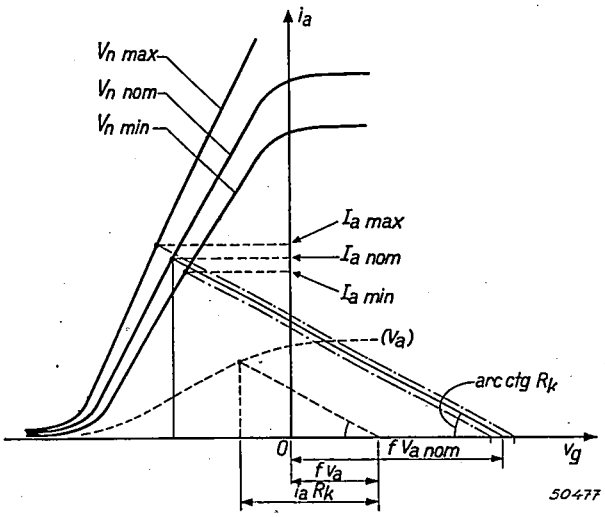


Fig. 6. In order to stabilize the tube current still more than in fig. 4 the resistor R_k has been made larger, and in order to obtain the same value for $I_{a\,\mathrm{nom}}$ a positive grid voltage component fv_a has been added. The resultant grid voltage v_g is at any moment the difference between fv_a and i_aR_k. The dotted lines indicate how the position of the working point is found at any moment (v_a, thus fv_a, and R_k given). The $I_{a\,\mathrm{nom}}$ and (dot-dash lines) $I_{a\,\mathrm{max}}$ and $I_{a\,\mathrm{min}}$ values can be constructed in the same way.

[4]) In order to obtain the same nominal tube current as indicated in fig. 4 the whole family of curves has to be imagined as being displaced to the right; this corresponds to a reduced transudation.

Since for the case of fig. 6 the working line cannot be indicated offhand, one cannot immediately visualize the "additional stabilization" given by the R_k method as compared with the method of reducing the "transudation". This can be found, however, by a simple calculation. For the X-ray tube, considered as a triode, in the space-charge range (the part where the characteristics show a straight slope) the equation holds:

$$i_a = S\,(v_g + \frac{v_a}{\mu}), \quad \ldots\ldots\ldots \quad (3)$$

where S is the slope and $1/\mu$ the "transudation". By substituting v_g from (2) we obtain

$$i_a = \frac{S}{1+SR_k} \cdot (f + \frac{1}{\mu})\,v_a \quad \ldots\ldots \quad (4)$$

This equation holds for any moment, thus for instance also for the peak values I_a, V_a and the value of S corresponding to V_a. By taking the logarithms on both sides of the equation and differentiating we find

$$\frac{\mathrm{d}I_a}{I_a} = \frac{\mathrm{d}V_a}{V_a} + \frac{\mathrm{d}S}{S\,(1+S\overline{R_k})} \quad \ldots\ldots \quad (5)$$

This equation confirms in the first place the statement that in the most favourable case, i.e. when the slope S of the characteristics is independent of V_a, the relative tube current variation is not greater — but never less either — than the relative mains voltage variation. Actually we may take it that S is approximately proportional to the filament voltage, thus also proportional to V_a. For $R_k = 0$ it then immediately follows from (5) that $\mathrm{d}I_a/I_a = 2\mathrm{d}V_a/V_a$ (see above). We may furthermore write for our X-ray tube $S \approx 10^{-4}$ A/V. Hence

$$\begin{aligned} \text{for } R_k = \quad & 0 \text{ ohm}: & \frac{\mathrm{d}I_a}{I_a} &= 2\,\frac{\mathrm{d}V_a}{V_a}, \\ R_k = \quad & 5000 \text{ ohms}: & &= 1{,}7\,\frac{\mathrm{d}V_a}{V_a}, \\ R_k = \quad & 10\,000 \text{ ohms}: & &= 1{,}5\,\frac{\mathrm{d}V_a}{V_a}, \\ R_k = \quad & 40\,000 \text{ ohms}: & &= 1{,}2\,\frac{\mathrm{d}V_a}{V_a}. \end{aligned}$$

By applying the indicated values of the resistance, the tube current variation for 10% mains voltage fluctuation is thus reduced to 20, 17, 15 and 12% respectively.

In practice a limit is set to the increasing of R_k by the fact that also the positive grid voltage contribution fv_a has to be chosen higher. In the half cycle when no tube current is flowing (v_a negative) the whole of the voltage fv_a (in this interval negative) comes to lie between the grid and the filament, and if this is too great it causes insulation troubles. Moreover, the effect of increasing R_k diminishes the higher the R_k values are chosen (see eq. (5)).

In the designing of the "Oralix" apparatus we have chosen $R_k = 40\,000$ Ohms, at which value

the tube current variation is only 1.2 times the mains voltage fluctuation causing that variation. The total gain obtained compared with the traditional circuiting of X-ray tubes where they work in the saturation range is shown graphically in *fig. 7*, where the tube current is plotted as function of the relative mains voltage.

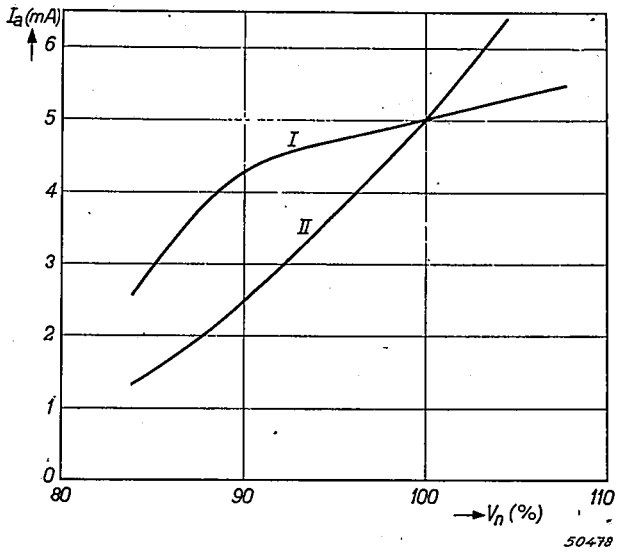


Fig. 7. With the apparatus described $R_k = 40\,000$ ohms has been chosen. Here the average tube current I_a is plotted as a function of the relative mains voltage V_n (% of the nominal value) and follows the curve *I*. If the X-ray tube were worked in the usual manner in the saturation range of the filament then the relation would be as represented by curve *II*.

As regards the film blackening, which is the criterion, it must not be forgotten that this is, of course, also affected by the tube voltage variation itself. Practice has shown that with $R_k = 40\,000$ ohms mains voltage fluctuations up to $\pm 5\%$ can be allowed without any appreciable difference in the film blackening.

It is also to be pointed out that the negative grid bias on the cathode cap affects the shape of the potential field between filament and anode and therefore also the focusing effect of this field upon the electrons. Consequently this must be taken into account when deciding what shape is to be given to the electrodes. Since the total grid voltage does not vary proportionately with the tube voltage, variations in the mains voltage cause such a slight change in the size of the focus as to make this effect imperceptible in practice.

Construction of the high-tension transformer

The high-tension transformer and the X-ray tube are both mounted in a common shield. In order to derive full advantage from the small dimensions of the tube every attempt has been made to minimize also the transformer dimensions. The shell type of transformer has therefore been chosen, with the shell extended so as to envelop about five-sixths of the circumference of the coils. This construction, which had already been applied to a small X-ray apparatus previously described [5]), has a very much smaller volume than the usual type. *Fig. 8* gives a clear picture of the construction. The iron circuit is made in two halves and after the coils, likewise made in two parts, have been fitted in, these two halves are placed face to face and tightly drawn together with bolts.

For easy shaping the shell is made by casting; the central part of the core is laminated and cast in the shell. To keep the eddy current losses in the non-laminated shell as low as possible the effect of the lamination is imitated by giving the shell the ribbed profile seen in fig. 8, whilst the material chosen is an iron alloy having a low electric conductivity. Nevertheless, with such a construction relatively large losses are unavoidable, but considering the small power of the apparatus such losses can be accepted from the economic point of view. We have therefore not hesitated to take advantage of this by allowing for a relatively heavy loading of the copper and the iron, thereby making it possible to reduce the dimensions and weight to the utmost. The losses only become objectionable when the heat thereby dissipated to the surroundings via the shield begins to obstruct the free dissipation of the "useful" heat generated on the anode (useful because this heat bears a fixed though very large ratio to the useful X-ray energy generated). This only occurs when the losses become about as great as the anode dissipation (160 W), a limit that is not reached with this apparatus. Incidentally, it was only possible to reach such small dimensions due to the oil dielectric in which the transformer and X-ray tube are placed and which greatly simplified the insulation problem (for a voltage of 25 kV_{peak} with respect earth.)

The copper losses of the high-tension transformer are in fact somewhat more limited than would be expected from the foregoing. They cause a voltage loss in the half cycle when the current is passing through the tube, with the result that in order to obtain a tube voltage of 45 kV_{peak} in this half cycle a higher no-load voltage is required, that is to say a higher voltage in the half cycle when there

[5]) A. Bouwers, Some new principles in design of X-ray apparatus, Radiology 22, 163-173, 1934. See also H. A. G. Hazeu, Small apparatus for medical X-ray examination, Philips Techn. Rev. 6, 225-234, 1941. The apparatus described there ("Centralix") worked with a higher voltage than the "Oralix", being designed for applications different from those occurring in dental practice.

is no load. Above a certain limit, therefore, the allowing of copper losses does more harm owing to the larger dimensions required to ensure sufficient insulation than the good derived from limiting the volume of copper. In our case the voltage drop is about 6 kV_{peak} for 5 mA (mean) tube current.

As already stated, the shield is filled with oil. The heat developed while the apparatus is working causes the oil to expand, whilst at lower temperatures, such as may prevail during transport, the volume of the oil is reduced. In order to ensure that these volume changes at temperatures between

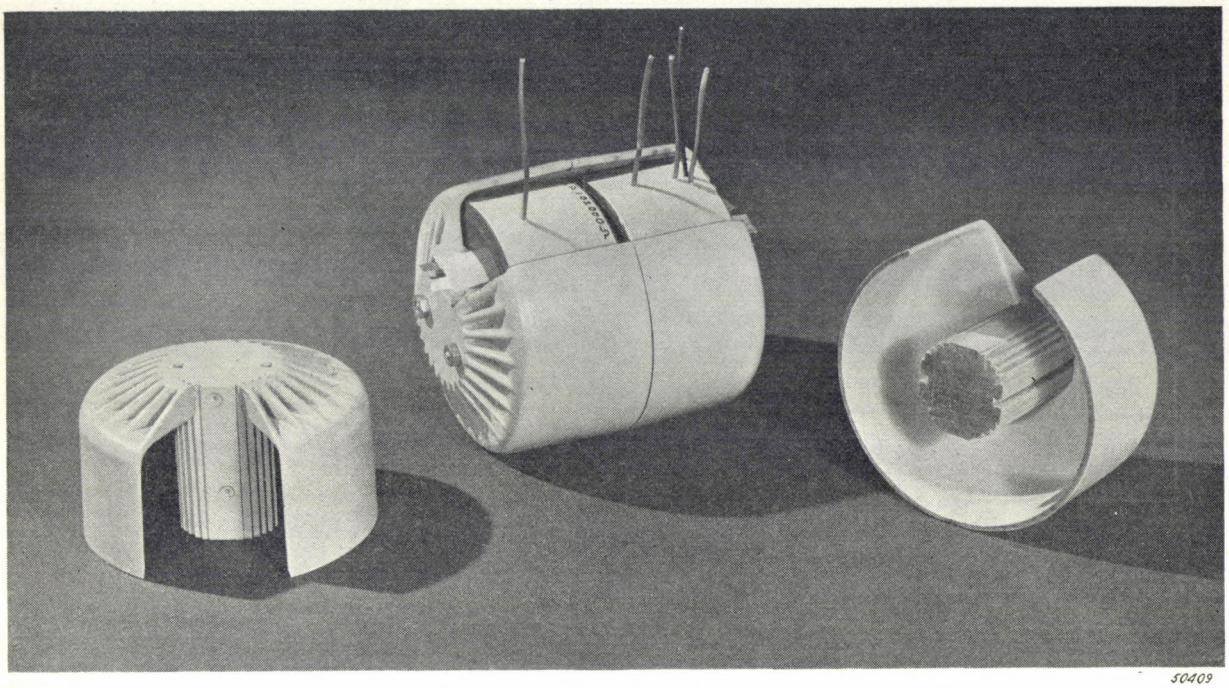


Fig. 8. In the middle, the high-tension transformer, completely assembled. On either side are the two halves of the iron circuit of a second specimen. Note the laminated central part and the cast shell extending over 5/6ths of the circumference.

Assembly of the apparatus

The manner in which the X-ray tube and the high-tension transformer are mounted in a common shield, likewise made in two halves, is shown clearly in *fig. 9*.

−10 and +60 °C do not cause any appreciable differences in pressure, an expansion vessel has been fitted into the shield in the form of a side tube shaped like an accordion.

The shield is made of brass. The X-rays emerge

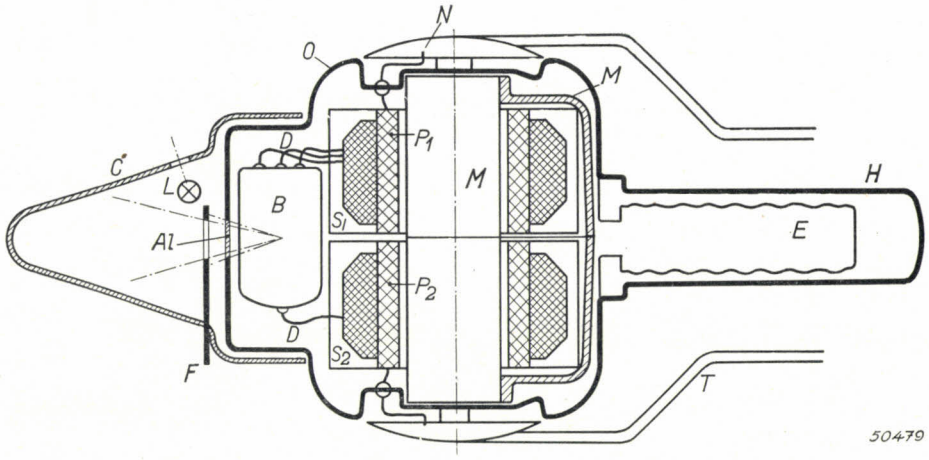


Fig. 9. Cross-sectional plan of the X-ray apparatus. *M* iron circuit of the high-tension transformer. P_1, P_2 halves of the primary coil, S_1, S_2 halves of the secondary winding, *D* connections to the X-ray tube *B*, *O* brass shield with aluminium window *Al*, *H* handle, *E* expansion vessel for the oil filling, *C* "Philite" directing cone, *T* bracket, *L* signal lamp, *F* exchangeable diaphragm, *N* mains lead.

through an aluminium window soldered in the brass wall. At this window the insulating layer of oil between the X-ray tube and the casing is only 3 mm thick. Owing to these measures the X-rays emitted are only slightly absorbed: the inherent filtration of the apparatus is equivalent to only 1 mm aluminium. This is of importance in connection with the fact that also the objects to be photographed absorb relatively little of the rays, about as much as 2 to 8 mm aluminium. On the other hand, the natural filter may not be much less than 1 mm aluminium because otherwise too many soft X-rays would be emitted, which, while not taking part in the image formation to any appreciable extent, might lead to an unnecessary amount of radiation being absorbed at the surface of the skin.

An exchangeable diaphragm can be placed in front of the window through which the X-rays emerge, thereby adapting the beam aperture to the size of the film, 2 × 3 or 3 × 4 or 4 × 5 cm. This adaptation is required because, if the beam is unnecessarily wide, the rays scattered in the object cause a loss in contrast in the X-ray picture [6]). If the same size of film is always used then as a rule there is no need to change the diaphragm, since the distance from focus to film is practically constant (about 12 cm). This distance is fixed on account of the fact that a directing cone of "Philite", the axis of which coincides with the axis of the X-ray beam, is mounted on the shield and pressed against the patient's face at the required spot (see fig. 11).

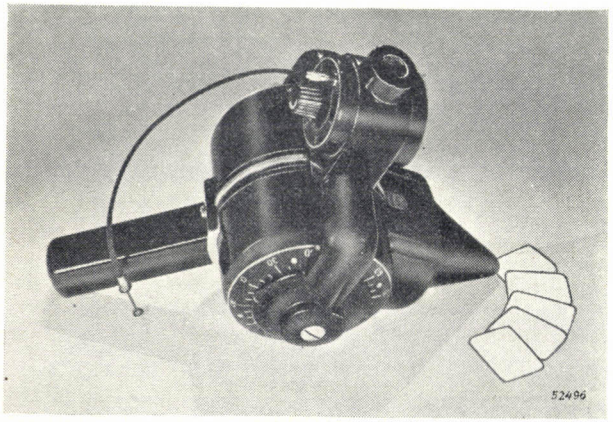


Fig. 10. Close-up of the miniature dental X-ray apparatus designed for suspension from a pulley (see fig. 11). Note the time switch on the trunnion. (In the design for mounting on a standard arm — see fig. 1 — the time switch is mounted in a separate hand switch.) The graduated scale is provided for adjusting the apparatus to the angle with respect to the "occlusal plane" required for radiographing each part of the denture. — Beside the apparatus are to be seen some dental films in their packing. Each packet contains two small films coated with emulsion on both sides; thus a duplicate is automatically made of each photograph. Behind the film in each packet is a tin foil protecting the films against fogging caused by the soft X-rays thrown back by the thumb of the patient when holding the film while the photograph is being taken.

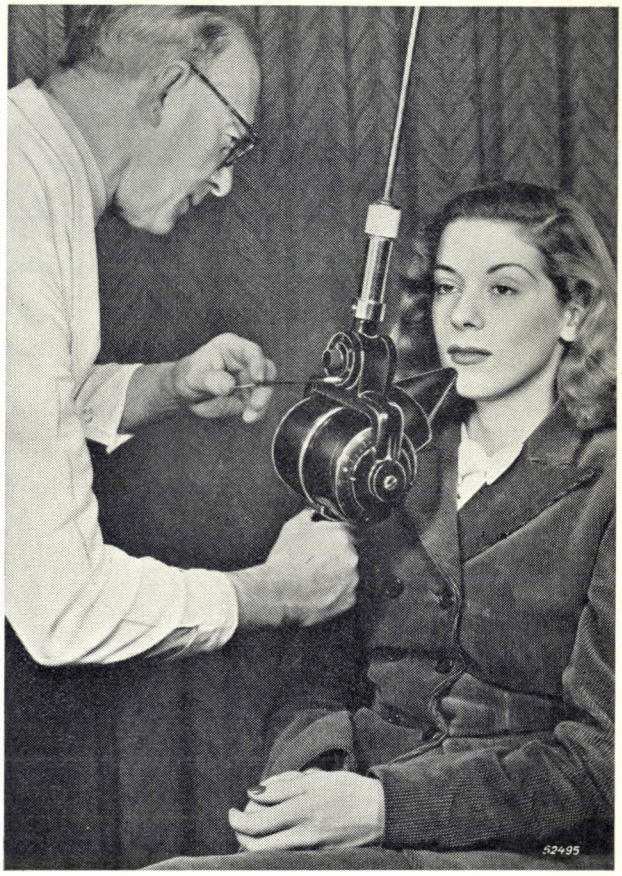


Fig. 11. The "Oralix" apparatus in use. The X-ray film is placed in the patient's mouth. (As a rule the patient has to press the film with the thumb against the part of the denture to be photographed.)

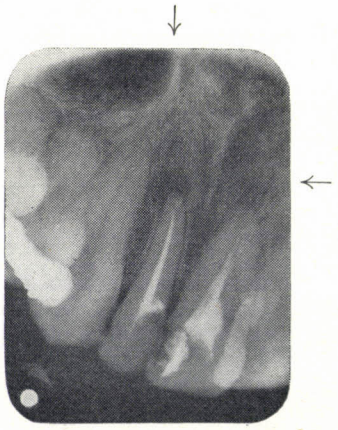


Fig. 12. Radiograph of part of an upper mandible taken with the "Oralix" apparatus, magnified 1.2 times. An inflammation is to be seen at the root of the second right-hand incisor (follow the arrows). The root channel is made clearly visible by a contrasting filling.

[6]) See, for instance, W. J. Oosterkamp, Eliminating scattered radiation in medical X-ray photographs, Philips Techn. Rev. 8, 183-192, 1946, No. 6.

A small neon pilot lamp is fitted in the director cone and connected in the tube current circuit. When tube current is flowing this lamp lights up and can be seen through a slit during the course of the exposure.

Fig. 10 is a close-up photograph of the whole apparatus. The shield, which is rotatable around the horizontal axis, is held in a trunnion by means of which the apparatus can either be attached to an adjustable stand (see fig. 1) or suspended from the ceiling by means of a pulley wire (*fig. 11*). The bracket itself is rotatable round the vertical axis, so that the beam can be guided in any direction desired, for which purpose a handle has been provided on the shield. (The expansion tube referred to farther back is contained in this handle.) The mains lead is connected to the bracket, which (in the case of the pulley construction) also has a time switch for adjusting the exposure time (e.g. between $^1/_2$ and 3 seconds). This and the starting of the time switch by means of a wire relaxer are the only manipulations required for operating the apparatus, apart, of course, from aligning the film and the apparatus with the object to be photographed, and possibly a selection of diaphragm.

Finally in *fig. 12* a typical dental radiograph taken with the "Oralix" apparatus described is reproduced.

CERAMIC MATERIALS WITH A HIGH DIELECTRIC CONSTANT

by E. J. W. VERWEY and R. D. BÜGEL. 621.315.612.4:537.226.2

In electrical engineering, ceramic materials are very widely used for insulation purposes and as dielectric for capacitors. In the latter instance preference is given to a material having a high dielectric constant and low dielectric losses and here the choice is limited almost exclusively to pure titanium dioxide (rutile), or a mixture in which the latter figures as chief ingredient. Admixtures, sometimes necessary for the purpose of reducing the dielectric losses to a value below the permissible maximum, tend also to reduce considerably the dielectric constant of the TiO_2, and the purpose of this article is to investigate in how far the value of this constant is related to other properties of the material. A disadvantage of pure titanium dioxide is that the temperature coefficient of its dielectric constant is highly negative, The Philips Laboratories at Eindhoven have worked out various methods for reducing this temperature coefficient to zero by using suitable admixtures. By way of example, a description is given of a series of capacitors of small dimensions with a ceramic dielectric as used in radio receivers and other equipment incorporating high-frequency circuits.

Ceramic materials are widely employed for insulating purposes in electrical engineering: high values of the capacitance of the insulated conductors to earth, or in respect of other conductors, will, in general, involve a certain amount of hazard and such capacitances are therefore kept low by exercising care in the design and by employing a suitable ceramic material, i.e. one having a low dielectric constant.

The requirements imposed on insulating materials used as dielectric in capacitors are very different, however: here a high dielectric constant is usually an advantage, and certain ceramic materials can be produced which possess this property. Further, a suitable choice of the raw materials and methods of preparation will ensure that the resultant material meets certain other requirements to which capacitors usually have to conform, e.g. that the dielectric losses will not be too high and that the dielectric constant will not vary too much with the temperature.

Dielectric constant of titanium dioxide and the effects of admixtures

Those materials which have a high dielectric constant and which have so far been adopted for electrical purposes usually contain a major proportion of titanium dioxide, owing to the fact that this material (as also a number of titanates) belongs to the very small group of substances the dielectric constant of which is exceptionally high. In nature titanium dioxide (TiO_2) occurs in the form of three different modifications, namely anatase, brookite and rutile. Wherever titanium dioxide is mentioned in the following we mean rutile, this being the stable modification, having at the same time the greatest density as well as the highest index of refraction and dielectric constant.

The two last mentioned qualities are dependent, moreover, on the orientation of the (tetragonal) crystal. In the direction of the major axis they are higher than in either of the two transverse axes: the indexes of refraction are 2.903 and 2.661 (for light of the wavelength of the D-line) and the respective values of the dielctric constant are 172 and 86 (as measured on a large crystal of the mineral rutile). In a close-sintered specimen [1]), which will contain a large number of arbitrarily oriented small crystals, an average value of approximately $(172 + 86 + 86) : 3 = 115$ may be obtained for the dielectric constant, but in actual practice it is very difficult to reach this figure. In the first place a titanium dioxide compound sintered to such an extent as to seal effectively all the pores on the surface will still contain air-occlusions at the crystal faces, and this has the effect of reducing considerably the apparent dielectric constant. Moreover, such a compound inevitably contains certain impurities, the dielectric constant of which is generally on the low side, so that in actual fact the dielectric constant ε of technical mixtures is generally lower than that of the pure titanium dioxide. If an impurity becomes dissolved in the titanium dioxide lattice, producing mixed crystals, it is not immediately clear why this should produce such a marked effect in the way of a decrease in the value of ε, but if the impurity occurs as a secondary distinct phase, having in itself a much lower ε-value, then as a rule the dielectric constant of the

[1]) Vide R. A. IJdens, Ceramics and thier manufacture, Philips Techn. Rev. **10**, 205-213, 1948/49 (No. 7).

mixture will obviously be considerably reduced by the presence of this secondary substance.

Let us suppose, for the sake of convenience, that the secondary phase occurs in the form of layers perpendicular to the direction of the electric field, so that the lines of force traverse a dielectric whose constant is alternately high and low. The example may be further simplified by taking the case of a capacitor consisting of only two layers, i.e. a flat capacitor of which the two electrodes are a distance d apart, with a dielectric comprising a layer of titanium dioxide the ε-value of which is ε_1), and another layer, in contact with it, of a substance having a low dielectric constant (ε_2) and a thickness of xd. According to the theory of dielectrics, the field in a capacitor of this kind will conform to the requirement that the product of field strength and ε must be constant throughout. The potential difference V betweeen the two electrodes is then divided (see *fig. 1*) into two parts V_1 and V_2, so that:

$$\frac{V_1 \varepsilon_1}{(1-x)d} = \frac{V_2 \varepsilon_2}{xd} = \frac{V\varepsilon}{d}, \quad \ldots\ldots \quad (1)$$

where q is the apparent dielectric constant of the whole. Since $V = V_1 + V_2$, expression (1) gives us:

$$\frac{1}{\varepsilon} = \frac{1-x}{\varepsilon_1} + \frac{x}{\varepsilon_2}. \quad \ldots\ldots\ldots \quad (2)$$

Let $\varepsilon_1 = 100$ and $\varepsilon_2 = 5$. The following values of ε will then be found in relation to x:

x	ε
0.000	110
0.005	99
0.01	91
0.05	54
0.10	36

Although this is only a very simplified example, it nevertheless demonstrates the marked reduction in the value of ε produced by the smallest admixtures in the dielectric: impurities to the extent of only about 0.5% immediately reduce the value of ε to a point below 100. Generally, such impurities are already present in the raw materials, or may be introduced in the course of the further processing. Small air-gaps between the crystals of the sintered mixture, or cavities within the mass, have an even more pronounced effect (since in that case $\varepsilon_2 = 1$). It therefore follows that the value of ε can be raised to 100 or slightly more only by taking the most stringent precautions.

It is hardly to be expected that expression (2) will provide an accurate quantitative criterion of the effect of admixtures or air-occlussions in titanium dioxide upon the value of ε, since we have based our example on an extremely simplified case which will certainly not be met with in general practice. It is possible, none the less, in the same way to construct expressions in respect of other, rather more complex examples, for instance where the one medium, in the form of ellipsoidal particles arbitrarily oriented, is enclosed within the other [2]). The appropriate expression may then be readily simplified to suit spheroidal particles, more or less flat particles (in which case one dimension of the ellipsoid is small in relation to the others), or needle-like particles (with one dimension large in contrast with the others). It may be anticipated that such hypotheses would more closely approximate actual conditions.

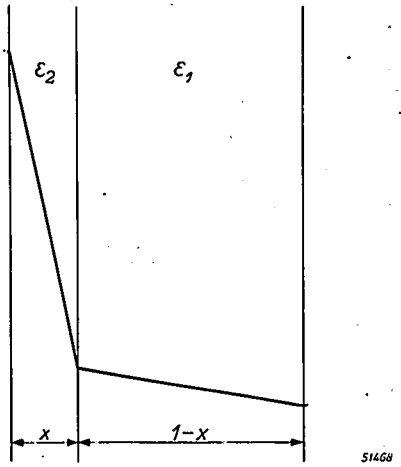


Fig. 1. Diagram showing the drop in potential in a double-layer capacitor. The thickness of the layers is indicated by xd and $(1-x)d$: the dielectric constants are respectively ε_2 and ε_1.

We are more particularly interested in the case where the secondary substance occurs in the form of flat, plate-like particles. If titanium dioxide be contaminated with a small quantity of a secondary substance it may be expected, in general, that the latter will accumulate at the crystal boundaries and thus reveal some analogy to flat particles having a low dielectric constant. When the calculation is carried out in respect of this particular case, to determine the effect of admixtures on the value of ε, it will again be found that the addition of relatively small quantities of substances having a low dielectric constant produces an exceptionally

[2]) D. Polder and J. H. van Santen, Physica, 12, 257-271, 1946.

sharp decrease in the apparent dielectric constant of the titanium dioxide mixture.

Reasons for the high dielectric constant of TiO_2

Let us for a moment investigate the causes of the extremely high dielectric of titanium dioxide.

The dielectric constant of a substance is defined as follows: when the space between the electrodes of a capacitor is filled with an insulating substance of dielectric constant ε, the charge on the electrodes, at a given potential, is ε times as great as when that space is empty; this constant is always greater than unity. The effect of such a medium, of which $\varepsilon > 1$, upon the charge in a capacitor is an outcome of the fact that it is built up of positive and negative charge-carriers which are able to migrate among themselves but which are nevertheless limited to their positions of equilibrium.

In a substance such as TiO_2 two possibilities have to be taken into account: firstly the chemical structure is strongly polar, so that TiO_2 may be imagined, as an approximation, as being built up from Ti^{4+}-ions and O^{2-}-ions which are able to undergo a limited amount of displacement in an electric field. Each ion, moreover, consists of a positively charged nucleus within a cloud of negatively charged electrons which in turn will also move with respect to each other in an electric field.

Consequently, in a homogeneous substance every volumetric element dv will have a dipole moment Pdv equal to the product of the displaced charge and the distance over which the negative charge has been displaced, with respect to the positive charge. The dipole moment per cubic centimetre (the polarisation P) is nil when $\varepsilon = 1$ and is proportional to $\varepsilon - 1$. Further, provided the field is not too strong, the displacement of the charge is proportional to the applied electric field E. This is expressed by:

$$P = \frac{\varepsilon - 1}{4\pi} E \quad \ldots\ldots\ldots \quad (3)$$

The magnitude of the polarisation, and therefore also that of the dielectric constant of the material, is very closely related to the degree to which the above-mentioned charge displacement takes place in the electric field.

The atomic characteristic determining such charge displacements in the atom is what may be termed the polarisability of the atom. Let us first assume that this is the only active characteristic. In the case of a substance consisting of only one type of atom the same electric field influences each of the atoms. Suppose that the value of this field at the atom be F, then the dipole moment μ generated in the atom is proportional to F and also to the polarisability α, so that:

$$\mu = \alpha F.$$

If the number of atoms per cubic cm be N, then the polarisation is:

$$P = N\mu = N\alpha F \quad \ldots\ldots \quad (4)$$

The effective field strength in the immediate vicinity of the atom however is not identical with the external field strength as applied, since the dipoles generated in the other atoms produce an additional field. The relation between F and E within a space of cubic symmetry is rendered by:

$$F = E + \frac{4\pi}{3} \cdot P,$$

(as given by Lorentz), so that formula (3) immediately gives us:

$$F = E + \frac{\varepsilon - 1}{3} \cdot E = \frac{\varepsilon + 2}{3} \cdot E \quad \ldots\ldots \quad (5)$$

Elimination of P and F from (3), (4) and (5) then finally yields:

$$\frac{\varepsilon - 1}{\varepsilon + 2} = \frac{4\pi}{3} N\alpha \quad \ldots\ldots\ldots \quad (6)$$

Expressions (3) to (6) are given in electrostatic units, but according to the rationalised Giorgi system [3]) they would take the following form:
From the formula:

$$D = \varepsilon_r \varepsilon_0 E = \varepsilon_0 E + P,$$

in which ε_0 is the (absolute) dielectric constant of a vacuum, whilst ε_r represents the (relative) dielectric constant of the material, it follows that:

$$P = (\varepsilon_r - 1)\varepsilon_0 E \quad \ldots\ldots\ldots \quad (3')$$

In the local field F the dipole moment is:

$$\mu = \alpha F,$$

where α is again the polarisability, but which, as will be seen presently, now has another physical dimension. If N be the number of atoms per cubic metre then:

$$P = N\mu = N\alpha F \quad \ldots\ldots\ldots \quad (4')$$

The relation between E, F and P is now:

$$\varepsilon_0 F = \varepsilon_0 E + \frac{1}{3} P,$$

from which, in view of (3'), it follows that:

$$F = E + \frac{\varepsilon_r - 1}{3} E = \frac{\varepsilon_r + 2}{3} E \quad \ldots\ldots \quad (5')$$

Elimination of P and F from (3'), (4') and (5') then gives us [4]):

[3]) See e.g. W. de Groot. Philips Techn. Rev. **10**, 55-60, 1948/49 (No. 2) and P. Cornelius, Philips Techn. Rev. **10**, 79-86, 1948/49 (No. 3).

[4]) See e.g. R. W. Pohl, Elektrizitätslehre, Springer, Berlin, 1943 (p. 58).

$$\frac{\varepsilon_r - 1}{\varepsilon_r + 2} = \frac{1}{3\varepsilon_0} N\alpha \ldots\ldots\ldots \quad (6')$$

If we ascribe to the term α/ε_0 the form α', then (6') can be written as:

$$\frac{\varepsilon_r - 1}{\varepsilon_r + 2} = \frac{1}{3} N\alpha' \ldots\ldots\ldots \quad (6'a)$$

The quantity α', as also α in (4) and (6), has the dimension of a volume; on the other hand, α in (4') and (6') bears the dimension

$$\text{A·sec·m} : \text{V/m} = \text{A·sec·m}^2/\text{V}$$

Indicating the term α in (4) and (6) by α_{esu}, we have:

$$\alpha' \ldots (\text{m}^3) = 4\pi \cdot 10^{-6}\, \alpha_{esu} = 1.26 \cdot 10^{-5}\, \alpha_{esu} \ldots (\text{cm}^3)$$

and

$$\alpha \ldots (\text{A·sec·m}^2/\text{V}) = \frac{10}{c^2}\, \alpha_{esu} = 1.11 \cdot 10^{-16}\, \alpha_{esu} \ldots (\text{cm}^3)$$

(c = speed of light in m/sec = $2.99776 \cdot 10^8$).

The second term of expression (6) is designated as p_e, in which the index e indicates that the electrons are displaced in the atom. From the derivative it thus follows that the dielectric constant is determined by a term p_e which is proportional to both the number of atoms N per cubic cm and their polarisability α. In a substance such as TiO_2, which is composed of two kinds of atoms, p_e is governed by the polarisability of the Ti^{4+}-ion and the O^{2-}-ion together. Thus, N is the number of TiO_2 "molecules" per cubic cm and α is the sum of the polarisability values of the individual atoms.

The dielectric constant in question, being determined exclusively by the displacement of the electrons in the atoms with respect to the nucleus, may be measured in an alternating field of so high a frequency that displacement of the ions in respect to each other does not take place: for this purpose electromagnetic waves at a frequency higher than about 10^{13}, i.e. of visible light, can be employed, so that it is permissible to use Maxwell's law:

$$\varepsilon_{opt} = n^2,$$

where n is the index of refraction of the substance having ε_{opt} as the optical dielectric constant.

Conversely, it is possible to proceed from the index of refraction to obtain some idea of the magnitude of p_e and α. For TiO_2 the average value of n is about 2.74. As far as the electronic contribution to the polarisability is concerned, TiO_2 should therefore have a value of $\varepsilon_{opt} = 7.5$. Applying formula (6) in this case [5]), p_e would then be $6.5/9.5 = 0.68$.

[5]) Admittedly this is not strictly correct, since the crystal lattice of TiO_2 does not conform to the condition that the encompassment of each ion shall be cubic-symmetrical. Nevertheless, it is quite feasible to apply this formula as an approximation, especially considering that we are employing the average value of n^2 (average of the three crystal planes). The difference is not so great as to affect the final conclusion in any way.

It is necessary, further, to take into account the polarisation arising from the displacement of the ions with respect to each other, and in this case we can similarly define a term p_i; hence:

$$\frac{\varepsilon - 1}{\varepsilon + 2} = p = p_e + p_i.$$

It will now be clear that in a substance such as TiO_2, of which the index of refraction is already relatively high, the part played by p_i in the total value of p — in comparison with p_e — need be only small in order to yield a high value of ε, since, if $p = 1$, the value of ε would already be infinitely high. From the experimental value of $\varepsilon = 110$ it follows that in the case of titanium dioxide $p = 0.97$, which is a close approximation of $p = 1$. For the contribution in respect of the ion displacement we now have $p_i = 0.29$, which, compared with the polarisability of other ion crystals, may be considered normal.

Our conclusion is that the high dielectric constant is due to the combination of a high index of refraction n and the fact that the value of p_i is not too low.

The dielectric losses of titanium dioxide and the effects of admixtures

It now having been ascertained that ε is high in the case of TiO_2 in the pure state and that admixtures result in a sharp decline in this value, the obvious aim will be to maintain the greatest possible purity in the preparation of this substance, before processing it in the form of ceramic material. This, however, is easier said than done, for the preparation and processing of TiO_2 involves a number of difficulties, added to which is the fact that a high value of ε is not the only requirement to which insulating materials have to conform. In many cases it will be found that admixtures to the TiO_2 are unavoidable.

When TiO_2 is to be used as basic material for capacitors there is no doubt that a high value of ε is very important, but it is also essential that the dielectric losses shall be low, especially in cases where the capacitor is to be employed in circuits working on high frequencies. The amount of these dielectric losses is customarily expressed as the value of $\tan\delta$, in which δ represents the angle of loss. Material which is to be employed for high-frequency capacitors usually has to conform to a value of $\tan\delta$ not exceeding 10^{-4} to 10^{-3} [6]).

[6]) For comparative purposes the average value of $\tan\delta$ with respect to certain non-ceramic insulating materials may be noted, viz: mica 1×10^{-4}, ebonite 81×10^{-4}, paper 140×10^{-4}, celluloid 450×10^{-4}.

Material prepared from reasonably pure titanium dioxide has a high value of ε, but its dielectric losses are intolerably high, partly owing to the high sintering temperature and its pronounced tendency at this temperature to evolve oxygen and revert to lower oxides, such as Ti_2O_3, which are semi-conductors [7]) and therefore useless for dielectric purposes. Even the smallest proportion of such oxides, too small to be determined by chemical analysis, will be sufficient to increase the loss factor $\tan\delta$ far beyond the permissible limit. This reducing effect becomes all the more marked according as the surrounding gases during the firing contain less oxygen and greater proportions of reducing agents.

It is, however, difficult to avoid these unwanted constituents. Owing to the dissociation just mentioned, it is impossible to indicate the melting point of titanium dioxide with any accuracy, but it is certainly above 1700 °C. A temperature of about 1500 °C — which is relatively close to the melting point — is therefore necessary to sinter the material closely, and such high temperatures are best obtained by gas firing, in the large kilns generally employed in the ceramic industry. It will be readily understood, then, that the exclusion of reducing gases from the firing space is an extremely difficult matter; in fact, when titanium dioxide material is fired in a gas kiln considerable reduction does actually take place.

One way of counteracting this effect it to add other substances to the TiO_2. Several substances, for instance clay, reduce the sintering temperature of the mixture, so that these lower oxides are not so easily formed. Various substances will, moreover, decrease the tendency towards the actual reduction itself, and in this way a raw material can be produced the loss factor of which is within the prescribed limit. In the meantime, however, ε will be found to have dropped as low as 60 or 80. Efforts have therefore to be made to evolve a composition, as well as a method of preparation, which will ensure satisfactory values both of ε and $\tan\delta$. It has been found possible in some cases to effect this by cooling the fired product in such a way as to introduce re-oxidation and thus nullify the reducing effect of the sintering process; this may be done by re-heating to a slightly lower temperature (about 1200 °C) in air or, even more simply, by retarding the cooling of the titanium dioxiode products after the normal sintering. In this way a temperature zone is passed through in which the oxygen dissociation-pressure of the material is sufficiently low to permit of the re-formation of stoichiometrically pure titanium dioxiode, the reaction rate remaining high enough to allow this re-formation to take place within the space of a few minutes. None the less, from the fact that the two measures referred to do not always yield the desired result, or at any rate not to a sufficiently high degree, it follows that the above mentioned partial reduction of the material is not the only source of a high loss factor.

There is no certainty regarding the origin of the dielectric losses occurring in the purest possible TiO_2 after full re-oxidation has been assured, but means have been found to limit these losses to a considerable extent by observing certain special precautions in the processing of the product. The first of these essential, is a rapid cooling after sintering and subsequent re-oxidation to stoichiometric TiO_2, which means that the sintered product is first cooled slowly to about 1100 °C, after which the cooling rate is accelerated.

The fact that we can obtain in this way a material with a low loss factor has led to the assumption that the previously mentioned dielectric losses (which appear to be present after complete re-oxidation) must be ascribed to the presence of impurities in the material. Closer investigation has shown, in fact, that traces of alkali metals (Na, K), and especially alkaline earth metals (Ca, Ba), have a very adverse effect on the dielectric losses.

Once this was known, a second method of reducing the loss factor to within the proper limits was made available to us. We therefore start with the purest possible titanium dioxide, in which the content of the deleterious oxides mentioned has been reduced to the technical minimum and in which the effects of any remaining unwanted oxides have been neutralised by the addition of small quantities of other oxides. It might be argued in spite of this, as mentioned above, that even one or two tenths of one per cent of impurities would be enough to reduce the dielectric constant from 110 to less than 100, but in actual practice the method in question has yielded satisfactory results. By basing the product on TiO_2 which is extremely pure by technical standards, so that any necessary additions may be limited to a minimum, it has been found possible to produce a titanium dioxiode having an ε-value of 100 to 105, with $\tan\delta$ at most a few times 10^{-4} (at a frequency of 1500 kc/s).

It is a noteworthy fact, too, that the method in question enables us to obtain a ceramic material the loss factor of which is low not only at 1500 kc/s but also at 10 kc/s. If use is made of TiO_2

[7]) See article by E. J. W. Verwey, Electronic conductivity of non-metallic materials, Philips Techn. Rev. **9**, 46-53, 1947 (No. 2).

containing a large percentage of clay the most favourable case will yield dielectric losses which are low at 1500 kc/s but high at 10 kc/s, as demonstrated in *fig. 2*, in which tanδ is shown plotted as a function of the frequency, with the two different mixtures as parameters.

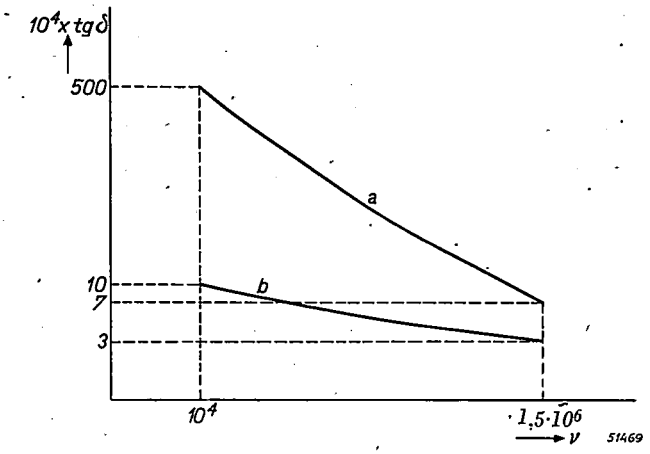


Fig. 2. The value of tanδ as a function of the frequency of the alternating current applied. The frequency ν of the current in c/s and the value of tanδ are shown plotted on logarithmic co-ordinates. Curve *a* refers to titanium dioxiode to which a high percentage of clay has been added, and curve *b* to technically pure TiO_2 in which the inevitable impurities, of oxides of alkaline-earth metals, have been neutralised by small quantities of other oxides.

Temperature coefficient of the dielectric constant

Once it has been assured, by a careful choice of the composition and the method of preparation of the ceramic material, that the final product will have a high value of ε and a low tanδ, attention must be paid to a final factor, the temperature coefficient of the dielectric constant, for, in the case of titanium dioxide, the value of ε is very highly dependent on the temperature. Curiously enough, this temperature coefficient, in contrast with that of nearly every other material, is negative, i.e. $1/\varepsilon \cdot d\varepsilon/dT = -8.10^{-4}$. This means that an increase of, say, 12.5 °C in the temperature of a capacitor having TiO_2 as dielectric causes the capacitance to decrease by 1%.

In certain applications such a high coefficient is a decided disadvantage. Take as an example the case of a capacitor in the tuning circuit of a radio receiver tuned at room temperature to a given station: as soon as the capacitance changes, which it will do after a little while owing to the increase in the working temperature of the set, the tuning will be upset. On the other hand there are cases where the high negative temperature coefficient may prove an advantage in compensating the coefficient in other components in the circuit, which is usually of the opposite sign.

It may well be asked what the relation is between the temperature coefficient of the dielectric constant and the other characteristics of titanium dioxiode. According to expression (6), the temperature coefficient of ε is determined by that of Na. Clearly, as a result of the thermal expansion the number of atoms per cubic cm decreases as the temperature is raised; in other words, the dielectric constant decreases with rising temperature. This effect may be counteracted by the variation in a with T, but in the case of a substance such as TiO_2 it appears that the value of a as calculated from the rather approximate formula (6) depends very little upon the temperature, so that the temperature coefficient of ε is determined almost wholly by the thermal expansion. At high values of ε, small variations in N result in relatively marked changes in ε, as will be seen from the relationship between these quantities in accordance with expression (6). The high temperature coefficient of TiO_2 is thus directly related to the high value of ε.

In the case where $d\varepsilon/dT \approx 0$, as roughly approximated in TiO_2, the following may be derived from formula (6):

$$\frac{1}{\varepsilon} \cdot \frac{d\varepsilon}{dT} = \frac{(\varepsilon-1)(\varepsilon+2)}{3\varepsilon} \cdot \frac{1}{N} \cdot \frac{dN}{dT} \quad \ldots\ldots (7)$$

If we introduce an average linear coefficient of expansion:

$$\beta = -\frac{1}{3N} \cdot \frac{dN}{dT}$$

expression (7) may be written in the form:

$$\frac{1}{\varepsilon} \cdot \frac{d\varepsilon}{dT} = -\frac{(\varepsilon-1)(\varepsilon+2)}{\varepsilon} \beta \quad \ldots\ldots (8)$$

which, at high values of ε, becomes:

$$\frac{1}{\varepsilon} \cdot \frac{d\varepsilon}{dT} = -\beta\varepsilon \quad \ldots\ldots\ldots (9)$$

The temperature coefficient is thus negative in such substances and is also proportional to the average linear coefficient of expansion.

It is necessary here to stress the fact that there are also many substances, especially those whose dielectric constant is low, in regard to which variations of a with the temperature also play a part.

It has already been mentioned that the high negative temperature coefficient is a disadvantage in many applications of the material in question. By adding other substances having a positive temperature coefficient it is possible to produce a mixture the temperature coefficient of which is very low, or even zero, but this can be done only at the cost of a high value of ε, as may be expected in the light of the remarks made in the opening paragraphs of this article. Let us now look at one or two examples of ceramic mixtures of this kind.

For many years MgO has been known as a suitable constituent; the sintered product in this case yields a material consisting in part of magnesium titanate, and provided the proportions are suitably

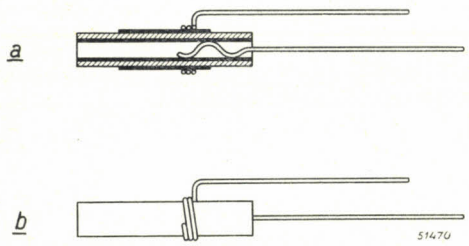


Fig. 3. Type "A" ceramic capacitor: *a* cross section, *b* side view. The length varies between 15 and 40 mm, whereas the capacitance may be from 33 to 1200 pF. The electrodes comprise two silver layers, the inner connecting lead being mounted by pressing the spiralized extremity into the ceramic tube.

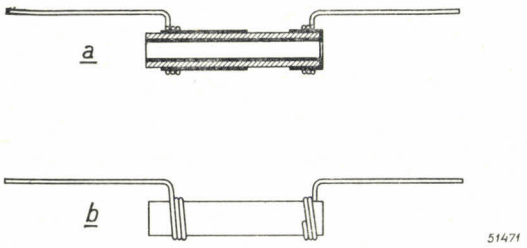


Fig. 4. Type "B" ceramic capacitor. *a* section, *b* side view. Dimensions are the same as for type A. In this case the lead connected to the inner electrode is mounted on the outside.

chosen $1/\varepsilon \cdot d\varepsilon/dT$ is for all practical purposes zero. The dielectric losses of this material are very low ($\tan\delta = 1 \times 10^{-4}$ at 1000 kc/s) but the dielectric constant is not much more than 12 to 18.

Another method consists in the addition of steatite, which will also give an ultimate temperature coefficient of 0, with very low losses, but ε is then only about 10.

Philips have developed a special mixture, using CeO_2 as a constituent. It was found that the dielectric constant of this substance is still fairly high, viz. about 35, whilst the temperature coefficient, dependent to some extent on the purity of the oxide, is generally weakly positive [8]). Therefore, mixtures prepared from CeO_2 and TiO_2, the temperature coefficient of which is to be roughly zero, must contain a very large proportion of CeO_2, a typical example being 85 mol% CeO_2 and 15 mol% TiO_2. This mixture is thouroughly sintered at 1220 °C, a temperature very much lower than that required for pure TiO_2. The dielectric constant is approximately 40, with $\tan\delta$ approx. 8×10^{-4} at 1000 kc/s.

Another possibility which we have investigated concerns admixtures of SnO_2. 50 mol% SnO_2 and 50 mol% TiO_2 yields a temperature coefficient of roughly zero. The firing temperature is certainly very high, being 1550 °C, but the losses are extremely low ($\tan\delta \approx 1 \times 10^{-4}$ at 1000 kc/s), whilst for the mixing ratio in question ε is 25.

Finally, mention should be made of ZrO_2 as a possible constituent: this may be introduced in a number of ways. In the first place, if not more than 1 or 2 % zirconium oxide is added, $\varepsilon \approx 60$ and $\tan\delta \approx 5 \times 10^{-4}$ at 1000 kc/s, but $1/\varepsilon \cdot d\varepsilon/dT$ is then still markedly negative (-6×10^{-4}). Alternatively, the admixture of ZrO_2 can be increased until $1/\varepsilon \cdot d\varepsilon/dT$

[8]) The spreading of the values is related partly to the losses. According to the rule of Gevers and du Pré (Philips Techn. Rev. **9**, 91-96, 1947, (No. 3), for this material that contribution towards the temperature coefficient which is related to the dielectric losses is roughly equal to 0.06 $\tan\delta$: at $\tan\delta = 10^{-3}$ this is therefore $+ 0.6 \times 10^{-4}$.

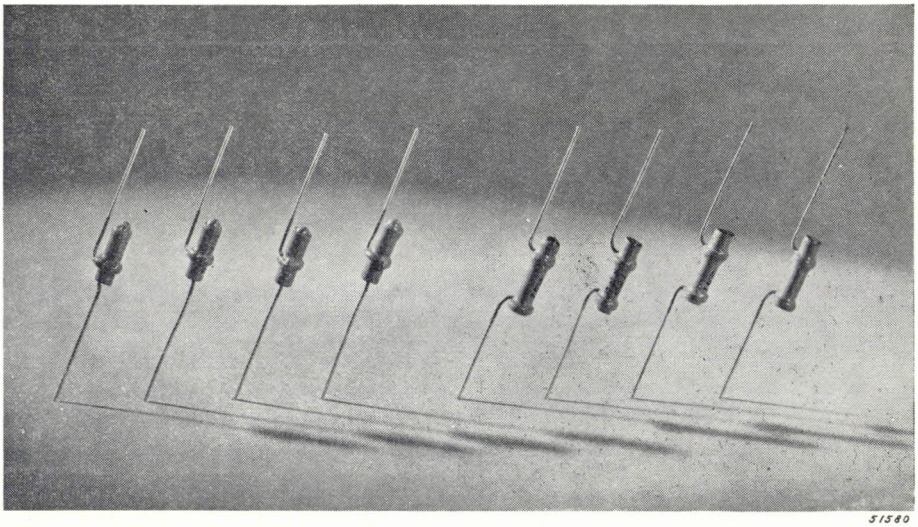


Fig. 5. Two groups of ceramic capacitors as supplied ready for use. On the *left* 4 capacitors of the "A" type; on the *right* the "B" type.

≈ 0, but, although this shows the same dielectric losses, ε will be found to have dropped to the order of 30. In this case, moreover, a high sintering temperature is needed.

From these examples it will be seen that variations in the ceramic mixtures will produce widely divergent dielectric properties, and it is on the basis of these experimental results that the composition of ceramic materials is determined, to meet the particular requirements to which any given product may have to conform.

Capacitors made of ceramic material

We close the present article with a brief reference to one particular application of ceramic materials for capacitors: these comprise a range of miniature capacitors for which a high dielectric constant is required to suit the capacitance values concerned. *Figs 3* and *4* show the method of construction.

These components, the length of which varies from 15 to 40 mm [9]), are manufactured in capacitances varying from 33 to 1200 pF. The tolerance ranges are 20, 10, 5 and 1%, although the maximum guaranteed accuracy is ± 1 pF. The maximum working voltage is 600 V, but each capacitor is factory-tested on 1500 V, A.C. 50 c/s, for 1 hour. As far as the dielectric losses are concerned, $\tan\delta$ is less than 20×10^{-4} in the "A" type (at 1500 kc/s) and less than 10×10^{-4} in the "B" type. The insulation resistance is higher than 5000 megohms. On the score of mechanical strength it may be said that the ends of these small capacitors can be loaded to the extent of 2 kg without rupture.

Fig. 5 illustrates a group of these components. These may be employed in radio receivers and other high-frequency circuits.

[9]) In the very low capacitance values (3.3 to 27 pF, similar capacitors are made with glass as dielectric. The dimensions then lie between 15 and 30 mm.

A TRANSMITTING VALVE COOLER WITH INCREASED TURBULENCE OF THE COOLING WATER

by M. J. SNIJDERS.

621.396.694.032.42

Although air-cooling has certain advantages for transmitting valves, water-cooling has the preference where the most intensive cooling effect is required, for example in transmitters working on very short waves. It appears that considerable improvement on the usual methods of cooling can be obtained by increasing the turbulence of the water in the cooler. One very effective method of achieving this is to inject the water into the cooler by means of concentric rings with jets arranged round the anode; the jets of water set up considerable turbulence in the water within the cooler. This method has been adopted for valve types PAW 12/15 and TAW 12/35, as it has been found in practice that, above a certain anode temperature (about 90 °C), a layer of copper oxide forms on the surface of the anode, which is such a poor thermal conductor that the latter tends to become overheated. In comparison with the old type of cooler, for the same flow of water per minute and the same dissipation, the spray method results in the peak anode temperature remaining about 40 °C lower and therefore well below the critical value of 90 °C. The dimensions of both types of cooler are the same and the new system can therefore be easily incorporated in existing equipment. The increased cooling effect provided by the system under review offers the possibility of obtaining a given transmission power from smaller valves than heretofore and/or at lower wavelengths.

Transmitting valves whose dissipation lies above a certain value are usually artificially cooled, this having the effect of considerably reducing the minimum practical dimensions of a given valve; this dissipation value lies at about 3 kW.

In most cases this cooling is effected by arranging for a flow of water along the anode, which constitutes part of the wall of the valve itself (*fig. 1*). According to another method, which is being applied more and more of late, air is blown along the anode, in this case provided with suitable cooling fins. In an earlier issue of this journal [1]) a description was given of a new form of cooling fins and a special method of air distribution which will permit of air-cooling even with the largest transmitting valves. As pointed out in that article, air-cooling has certain distinct advantages over water-cooling and there can be no doubt that it will supersede the latter in many instances. Nevertheless, water-cooling will often be given preference, especially when the valve is to operate on the higher frequencies, in which case the ratio of output power to dissipated power is much less favourable than on the lower frequencies. Furthermore, at very high frequencies, capacitances have to be kept as low as possible, not only between the electrodes in any one valve, but also between the anodes of two valves in a push-pull circuit, mounted close together for compactness. All this means that every effort is made to keep the dimensions of both valve and cooler as small as possible; as far as the valve itself is concerned, this in turn leads to high specific loads (i.e. dissipation per sq. cm anode area) and therefore also highly efficient cooling. As regards the latter, the water-cooler has the advantage of its smaller dimensions in comparison with the air-cooler, so that, if the maximum dissipation of the anode is demanded, water-cooling will be preferred. In the following we propose to discuss the new method of cooling more fully.

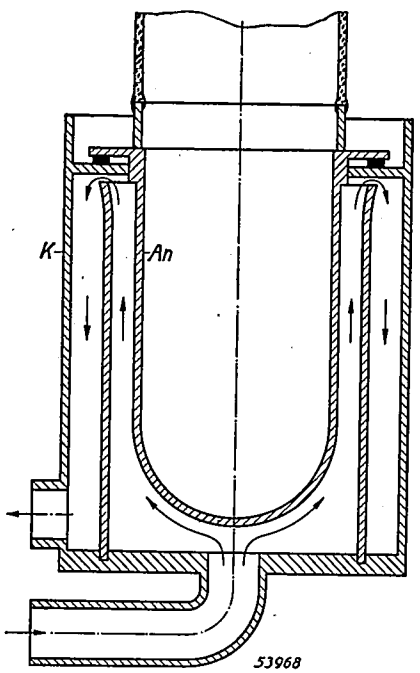


Fig. 1. *An* = anode of transmitting valve mounted in cooler *K* through which water flows.

[1]) H. de Brey and H. Rinia, An improved method for the air-cooling of transmitting valves, Philips Techn. Rev. 9, 171-178, 1947 (No. 6).

Open and closed cooling systems

In an "open" system the used cooling water is allowed to run to waste.

In the closed system the used water, the temperature of which has been raised, is cooled down in a special cooling device and used again; in other words a fixed quantity of water is kept in circulation.

For medium-sized transmitters, in which the water consumption is not very high, the simplest form of cooling system, i.e. the open type, is usually adopted, provided the quality of the available water supply is good enough, that is to say sufficiently free from elements that tend to fur the anodes, (this point will be referred to in detail later). Boiler scale is a very bad conductor of heat and therefore reduces the cooling effect, with the result that the valve ultimately runs the risk of being overheated. If only "hard" water is available then the closed system, where all the injurious constituents forming the scale speedily disappear, will have to be used. Moreover, even the initial deposit can be avoided by filling the cooling system with distilled water; it is only necessary to top up the water occasionally, to make good the small losses due to evaporation and leakage.

In large transmitters, requiring for instance a flow of water of about 500 litres (100 gallons) per minute, the closed system will always be preferable in view of the saving to be made on the cost of the pure water required for the open system.

Various methods are available for use in connection with the "return cooling" of the used water: small installations mostly employ an equipment very similar to the cooling system of a motor-car; in the larger transmitting stations use may be made of cooling towers, reservoirs or surface coolers in which the circulating (primary) water imparts its heat to running (secondary) water. The latter solution is shown in *fig. 2* (the closed type of system employed in the main Netherlands broadcasting stations).

The purity of the secondary cooling water need not be particularly high, as experience has shown that deleterious substances are not deposited in the return cooler, this being due to the fact that the temperature of the primary water is fairly low (at most 30 °C). The secondary supply may therefore consist of unpurified well-water, which is comparatively cheap.

Another advantage of the closed system, provided distilled water is used, is evident from what follows. The anode of the transmitting valve to be cooled carries a very high D.C. potential with respect to earth (possibly 20 kV) and also a high superimposed h.f. alternating voltage. Now, for the purposes of electrical insulation, the cooling water for the anode is fed and carried away through long insulating tubes. In order to save space these tubes

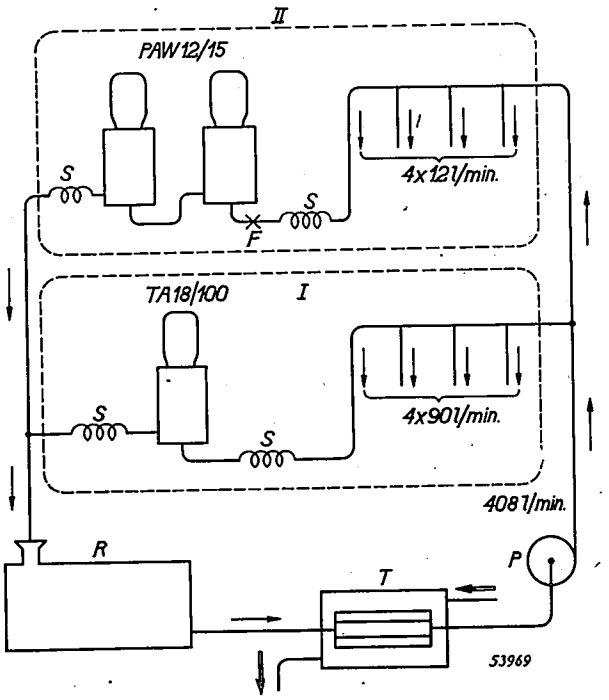


Fig. 2. Diagram of the closed cooling system as employed in the Netherlands broadcasting stations. The flow of the primary water is indicated by single arrows; that of the secondary water by double ones. P = pump, I = output stage, II = driver stage, S = coiled ceramic tube (for electrical insulation), R = reservoir, T = return cooler.

The output stage (I) comprises four valves type TA 18/100, plus two reserve valves not shown in the diagram. When the latter are put into service the cooling water is switched over simultaneously with the electrical connections. The driver stage (II), incorporating four PAW 12/15 valves, is arranged differently: in this case the cooler of each of the functional valves is connected in series with that of the associated reserve valve. In the figure only one of the four pairs is shown. At the point F a filter may be fitted (to be discussed later).

(preferably made of ceramic material) are usually arranged in the form of a coil (S fig. 2). Although the tubes themselves are non-conductive, there is nevertheless a certain leakage of current through the stream of water. This loss can be limited to a minimum by filling the closed system with distilled water, which has a low conductivity. The efficiency of the transmitter is thus considerably improved.

Possible causes of deposit on the anode

We have already mentioned the possibility of furring in the case of the open cooling system. It might be inferred, in view of the foregoing, that there would be no questoin of any kind of deposit in a closed cooling system containing distilled

water, but in practice furring does actually take place, owing to the circulating water picking up substances from the walls of the system, thus forming compounds which are deposited on the anode. For example, if the water is in direct contact with concrete, as may be the case if a reservoir as represented in fig. 2 is used, boiler scale will form on the anode; such reservoirs should therefore always be lined with chlorinated rubber paint to prevent the water from coming into direct contact with the concrete.

It has been found at a number of transmitting stations that, even though such precautions are taken and distilled water is used, a heat-insulating deposit — albeit not boiler scale — tends to form on the anode.

In fact a hard, black deposit has been found on the anodes of the PAW 12/15 and TAW 12/35 (*fig. 3*) as employed in different broadcasting stations where closed cooling systems were in use; this layer proved to be copper-oxide (CuO), which, although not such a poor conductor of heat as scale, may nevertheless lead to overheating of the valve.

Measures to prevent the deposit of copper-oxide

These copper-oxide deposits can of course be removed from time to time by sanding or pickling, but such operations, involving as they do the dismantling of the valve and subsequent re-inserting in the cooler, incur considerable risk of breakage (not only of the glass, but also of the tungsten filament, which in time becomes brittle).

One way of preventing the occurrence of copper-oxide would be to arrange matters so that at least one of the elements of which it consists cannot appear at the anode. Since the water is exposed to the air at a number of points (as in the reservoir, see fig. 2), the solution of oxygen can hardly be prevented. The presence of copper itself is even more difficult to avoid, as in the first place the anode is made of this material and, moreover, the whole cooling circuit, pumps, cocks and other equipment must necessarily consist of non-corroding material. Tinning of such components, as well as of the anode itself, would effectively prevent all direct contact between copper and water, but we found a much simpler method of preventing the formation of copper-oxide, consisting in a reduction in the temperature of the anode by intensifying the cooling. An improved type of cooler, which forms the subject of the present article, has been specially developed for this purpose.

In fact there are a number of indications that a reduction in the anode temperature reduces the formation of copper-oxide and that below a certain temperature limit it is almost entirely absent. The indications in question, as observed in a number of broadcasting stations, are the following:

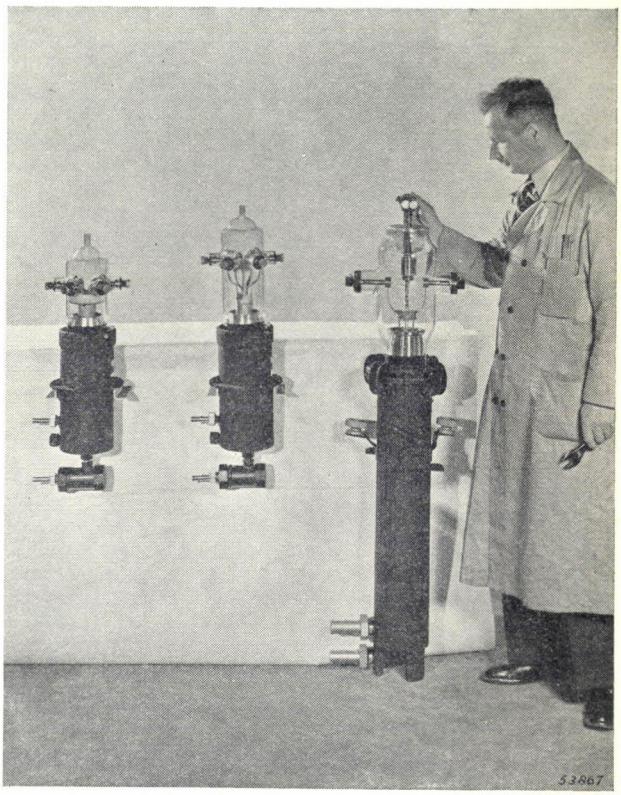


Fig. 3. The three transmitting valves mentioned in this article. From left to right: the pentode PAW 12/15, the triode TAW 12/35 and the triode TA 18/100.

1. Copper-oxide appeared more abundantly at the hottest parts of the anode.
2. More copper-oxide per unit of time was produced in heavily loaded valves of the type PAW 12/15 than in the more lightly loaded valves.
3. Type TA 18/100 valves (fig. 3) as used in the same transmitter and employing the same cooling water as the two previously mentioned PAW 12/15 valves (see fig. 2) showed no copper-oxide deposit, even under the heaviest loads. In fact, the anode temperature of the valves TA 18/100 appeared to be lower in this case than that of the valves PAW 12/15, as was proved by provisional measurements by means of thermo-couples soldered to the anodes. For the results of the measurements see *table I*. (For practical reasons these measurements were carried out under static load [2]), calcu-

[2]) The temperature under static load is less uniformly distributed over the anode than in the case of dynamic loading. This point is dealt with more fully in connection with the more accurate measurements described in the following paragraphs; the values given in table I are the outcome of less provisional, precise measurement.

lated to give the same dissipation as in the most heavily loaded valves in the transmitter.

The formation of copper-oxide appeared to cease at temperatures between 55 and 94 °C; according to later measurements the actual limit is in fact about 90 °C.

Table I. Measured temperatures of transmitting valves. t', t'' = temperature of cooling water at inlet and outlet of the cooler respectively, A = flow of water, P_{tot} = total dissipation calculated from $t''-t'$ and A, t_a = anode temperature measured with thermo-couple (roughly at the hottest place).

Type	PAW 12/15	TA 18/100
t' (°C)	20	20
t'' (°C)	30	26
A (l/min)	12	90
P_{tot} (kW)	8.4	37.7
t_a (°C)	94	55

The cooling of the valve PAW 12/15 in comparison with that of the valve TA 18/100

The problem, therefore, was how to keep the anode of the PAW 12/15 at a sufficiently low temperature.

The differences in the anode temperature as shown in the above table are not to be accounted for by the specific anode load of the PAW 12/15 in that particular transmitter being higher than that of the TA 18/100, for as a matter of fact the specific load on the PAW 12/15 was 23 W/cm² and that on the TA 18/100 26 W/cm².

The reason for the difference in temperature is apparent, however, when the speeds of flow of the water are compared: this speed, v, is obtained from the quotient of the flow A and the cross-sectional area O of the annular water-jacket surrounding the anode. In both cases O was 10.6 cm², and the values of A, as shown in the table, were 12 and 90 l/min, or 0.2×10^{-3} and 1.5×10^{-3} m³/sec respectively, so that, for the PAW 12/15:

$v = 0.2 \times 10^{-3}/10.6 \times 10^{-4} = 0.19$ m/sec.

and for the TA 18/100:

$v = 1.5 \times 10^{-3}/10.6 \times 10^{-4} = 1.4$ m/sec.

In the case of a laminary flow of cooling liquid over a heated surface the transfer of heat from the latter to the liquid takes place exclusively by conduction (radiation may be ignored here); now, the coefficient of thermal conductivity — i.e. the amount of heat transferred to the cooling agent per unit of the surface area, per unit of time and per degree difference in temperature — is independent of the rate of flow of the medium.

However, even at the lower of the two above-mentioned speeds the flow of water is turbulent and the volume elements of the water therefore acquire a component of speed in a radial direction as well as axial speed v as calculated above; the hotter volume-elements are thus transported to the colder places and vice versa. Due to this radial component convection occurs, as a result of which the coefficient of thermal conductivity is much greater than when attributed to conduction only. Furthermore, turbulence in the water involves another factor, in that, owing to the eddies, each aqueous element may come into repeated contact with the surface to be cooled, taking up an amount of heat each time. Thus the stronger the turbulence, the smaller the differences in temperature occurring in a radial direction within the water-jacket.

The radial component of the speed of flow required for an efficient transfer of heat increases with the axial speed v of the water [3]). It might be possible to increase the speed in the case of the PAW 12/15, for instance by increasing the flow of water A per minute, but such a solution would be uneconomical in many respects. Another way out would be to reduce the cross-section O, but in practice there are limits in this direction considering that the anode and water-jacket are only 3 mm ($^1/_8$") apart, whilst allowance must also be made for the fact that the anode is not always perfectly cylindrical.

Other means have therefore to be sought to increase the turbulence of the water in the cooler.

The spray cooler

A very high degree of turbulence can be obtained by injecting the water into the cooler in a suitable manner, and *fig. 4* gives details of a very practical method. The water is sprayed from a number of jets placed in a ring round the anode and sets up inside the filled cooler a violent circulation the main direction of which — accompanied by subsidiary eddies in other directions — is indicated by the dotted lines in the diagram.

Fig. 5 shows the ultimate arrangement as applied to the valve PAW 12/15; a similar form of cooler has also been developed for the valve TAW 12/35. The water enters a channel at *1* which is drilled in the bronze bottom of the cooler and subsequently branches into four ducts, each of which leads to a vertical tube through which the water reaches three jet-rings. Finally, the water leaves the cooler at *5*.

[3]) It is actually less than proportional, e.g. in some cases proportional to $v^{3/4}$; see A. Schack, Der industrielle Wärmeübergang, Düsseldorf 1940, 2nd edition, p. 60.

The external dimensions of the cooler are exactly the same as those of the old type.

Calculations

The design of the new cooler is based on the same flow of water as the old type (12 l/min = 2.64 gallons/min = 200 cm³/sec for the valve PAW 12/15), so that it may be substituted for existing

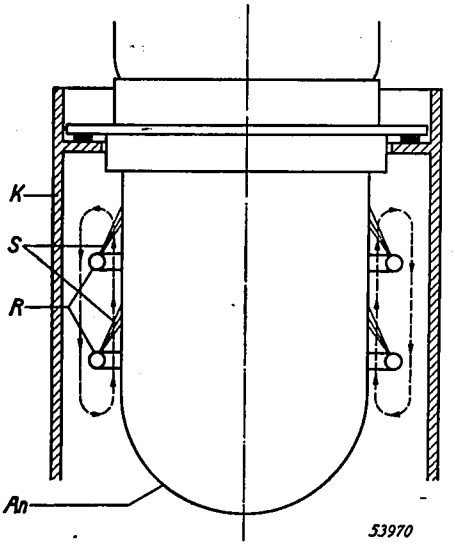


Fig. 4. Principle of the spray cooler. R = injector rings producing jets of water S, which keep the cooling water in violent motion. An = anode, K = cooling jacket.

equipment without necessitating the installation of pumps for larger quantities/minute or higher pressures.

The speed of flow of the water, v_0 (in m/sec), passing from the jets is rendered by the expression

$$v_0 = \sqrt{2gh},$$

where g is the gravitational acceleration (in m/sec²) and h the difference between the pressures (in m water column) in front of and behind the jets. If h be the total drop in pressure in the cooler — for which we maintain of the old cooling device (h = 1 m in the case of the value PAW 12/15) — the exit speed will be

$$v_0 = \sqrt{2 \times 9.81 \times 1} = 4.4 \text{ m/sec.}$$

Since there is also a certain drop in pressure in the other parts of the cooler and h is thus slightly less than 1 m, we shall assume that $v_0 \approx 4$ m/sec.

From this assumed flow of water it follows that the jets must have a total orifice area of 200/400 = 0.5 cm². The question as to the most suitable number of holes into which this area can be divided is governed by the fact that, on the one hand, a large number of holes promotes more uniform cooling, whereas on the other hand — and this is a more practical consideration — small holes are more liable to become clogged.

In view of this latter factor, a diameter of 1 mm has been taken for the jets, necessitating 60 holes to give a total area of 0.5 cm².

To eliminate any possible risk of stoppages the simple filter shown in *fig. 6* has been designed. This is fitted at the inlet of the cooler (at F in fig. 2).

Other points to be taken into consideration were the most suitable number of rings among which to divide the 60 jets, the most satisfactory height in respect of the anode at which to place them, the most effective angle for the jets of water, etc. These problems were solved experimentally, mainly with the aid of temperature measurements (discussed in

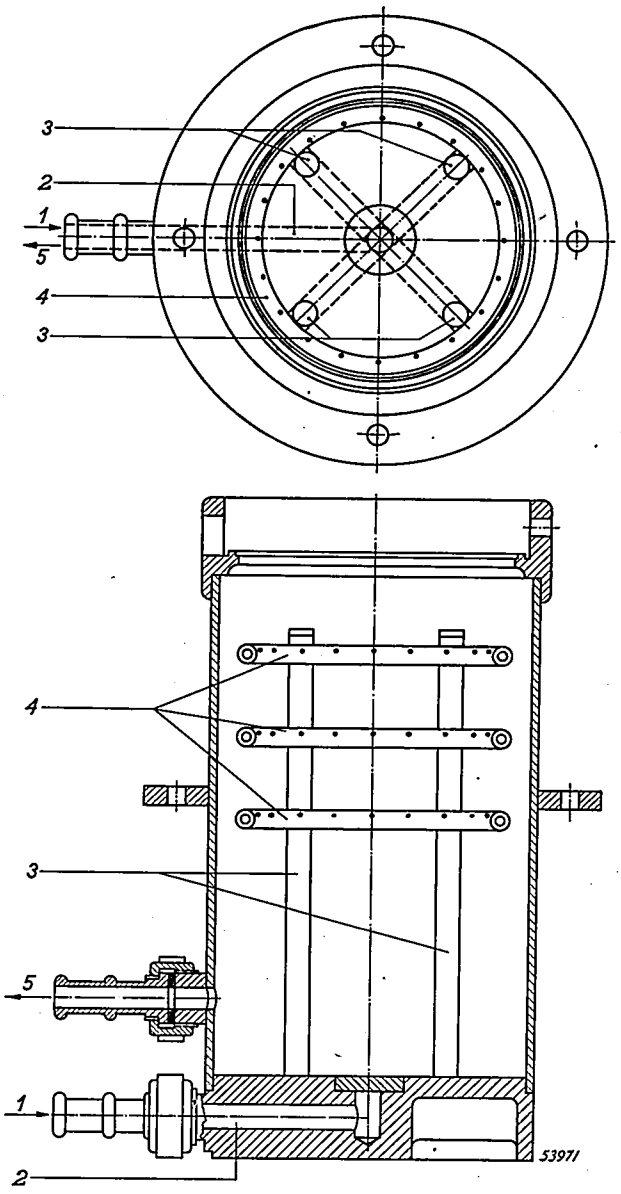


Fig. 5. Top view and vertical cross-section of the spray cooler. The cooling water enters at *1*, flows through duct *2* and branches into four tubes *3*, thus reaching the three jet-rings *4* and ultimately leaving the cooler at *5*.

the next paragraph) taken with a cooler so constructed that the factors in question were variable. As will be seen from fig. 5, the number of rings has been fixed at three. The most satisfactory angle for the jets of water was found to be obliquely upwards towards the anode, at an angle of 30° from the vertical.

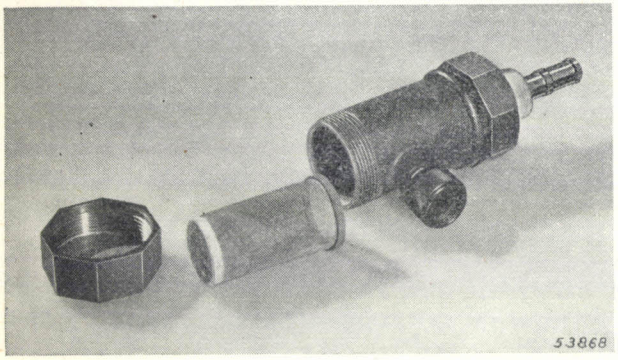


Fig. 6. Simple filter made of metal gauze. It is included in the water system at the inlet of the spray cooler (at *F* in fig. 2) and can be easily mounted on the latter (see left-hand and centre valves in fig. 3).

Measurements

To ensure accuracy of measurement of the anode temperature, five thermo-couples were provided along each of four longitudinal lines on the anode (*fig. 7a* and *b*).

A few remarks may be added in regard to the place and the construction of these thermo-couples.

1) The lines on which the latter were placed were chosen exactly in the centre of the open spaces between the grid supports, for the following reason. It is very difficult to carry out temperature measurements on an oscillating valve, so that for practical reasons a static load had to be applied. The control grid is then at a steady negative potential which produces a marked shadowing or screening of the grid supports; the current density at those parts of the anode immediately behind these supports is therefore much lower than in the intervening spaces and those sections of the anode will therefore become less hot. Points of measurement were therefore decided upon lying in the centre of the open space between the supports in order to avoid taking the measurements under too favourable conditions (fig. 7*a*).

It is not sufficient to limit the measurements to only one such row of points, in view of small but inevitable asymmetries in the locations of the electrodes with respect to the anode.

When the valve oscillates — under normal working conditions — the grid potential periodically assumes values in the region of zero, so that over an average period of time the effects of both the asymmetry and the screening of the grid by the supports are much less pronounced than under static load. For this reason the values indicated in the following figures are averages of the four measurements. These averages will show a fairly close agreement with the temperatures of the anode under dynamic load.

2) The thermo-couples were actually arranged in the following way in order that they might interfere as little as possible with the flow of water. At each of the points *0-5* on the longitudinal line (fig. 7*b*) a dimple was drilled in the copper anode. In each of the dimples *1-5* a thin constantan wire was soldered and at *0* a thin copper wire, the solder just filling the dimple. The six wires were insulated and carried outside through a water-tight seal in the cooler, the five constantan wires in conjunction with the copper acting as thermo-couples.

Fig. 8 shows the anode temperature of the valve PAW 12/15 plotted against the vertical distance *y* from the rim of the anode. The valve in question was operating at the maximum total rated dissipation of 14.25 kW [4]), with a cooler feed of 12 litres (2.6 gallons) of water per minute at 9 °C. As will be seen, the old cooler gives local temperatures in excess of 100 °C (curve *I*), whereas in the case of the new cooler (curve *II*) the highest temperature reached is barely above 60 °C.

The variation in the average temperature at the hottest part of the anode with the total dissipation is demonstrated in *fig. 9* (curve *I* for the old cooler

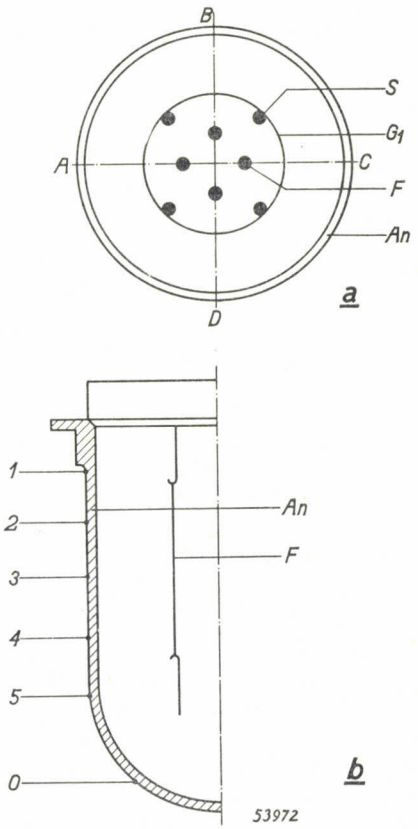


Fig. 7. (*a*) Horizontal and (*b*) vertical cross-section of the transmitting valve PAW 12/15 fitted with thermo-couples. *F* = filament, G_1 = control grid (not shown in *b*), *S* = grid supports, *An* = anode. Five constantan wires (*1-5*) are soldered at points along each of four longitudinal lines *A*, *B*, *C* and *D* and these, together with the copper wire *O*, form the poles of five thermo-couples.
Screen- and suppressor-grids are not shown.

[4]) Of which 1.83 kW is filament power, and 0.42 kW screen grid dissipation.

and curve *II* for the new type); curve *II* lies on a level which is some 40 °C lower than curve *I* and is at every point well below the critical value (90 °C) at which copper-oxide commences to form.

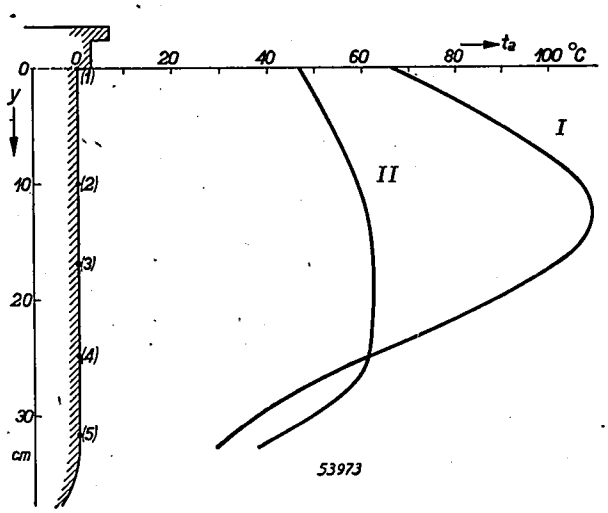


Fig. 8. Anode temperature t_a as a function of the distance y from the upper rim of the anode of a valve PAW 12/15. Curve *I* refers to the old cooler (fig. 1) and curve *II* to the spray type of cooler (fig. 5), 12 litres (2.6 gallons) of water per minute being used in each case. Total disssipation 14.25 kW. Temperature of cooling water at inlet of the cooler 9 °C, at the outlet 26 °C. The numbers (*1*)-(*5*) on the left indicate the positions of the thermo-couples.

Lines t' and t'' in fig. 9 indicate respectively the temperature of the cooling water at the inlet and outlet of the cooler.

For comparative purposes the quantity of water per minute required by the old cooler to maintain the anode at the temperature ensured by the new cooler was also measured with respect to a given dissipation: this was found to be 85 litres/min as compared with 12 litres/min in the new type of cooler.

Practical results

Comparative tests have been carried out in one of the Netherlands broadcasting stations with the PAW 12/15 valves mounted in the old and in the new type of cooler, under identical conditions of load and cooling water supply. After 170 hours operation the anode in the old type of cooler showed considerable deposits of copper-oxide, whereas the valves in the new cooler were entirely free from deposit after 4000 working hours, thus avoiding the necessity of periodical dismantling and reassembly, which is the most frequent cause of early failure of the valves.

Equally satisfactory results have been reported from another transmitting station employing TAW 12/35 valves, where heavy deposits of copper-oxide used to occur in the old type of cooler. During transmissions valves in the old type of cooler tended to "sing" loudly, indicating that the anode temperature was locally in excess of 100 °C; the normal amount of water used was 20 litres (4.4 gallons) per minute. With the new coolers the equipment was entirely free from mechanical noises and there was an entire absence of copper-oxide, although the flow of water was reduced to 16 litres (3.5 gallons) per minute, the pressure drop in the new cooler being somewhat higher than that in the old one.

After the filter shown in fig. 6 had been mounted no trouble was experienced from clogging of the jets.

Further possibilities

The introduction of the new cooler is important not only from the point of view of the increased life of the valves to which it has been adapted, but especially because this method of cooling paves the way to the design of smaller valves for a given power rating, seeing that the increased cooling effect permits of higher specific loads. This will be of advantage more especially in the case of valves working on very high frequencies, since the inter-electrode capacitances of these valves must be kept low and anode diameters small with a view to keeping the electron transit times between cathode and anode short (the transit time is one of the

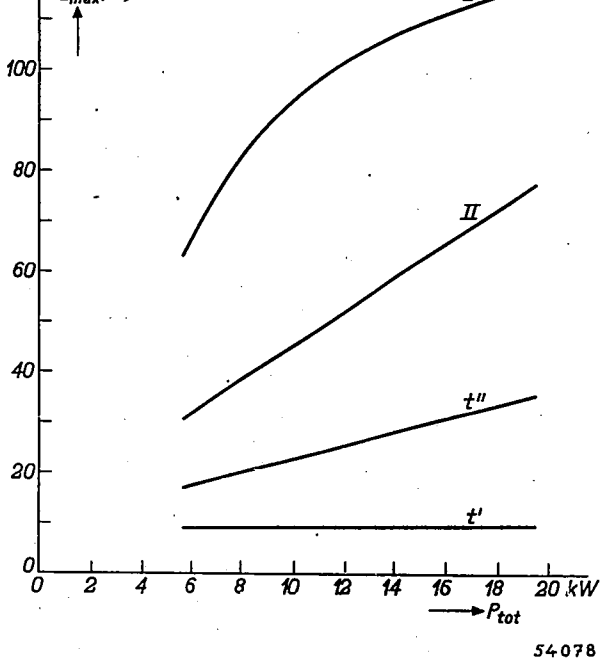


Fig. 9. Anode temperature $t_{a\,max}$ at the hottest points of measurement (*I* for the old cooler, *II* for the new one) as a function of the total dissipation P_{tot}, also temperatures t' and t'' of the water respectively at the inlet and outlet of the cooler. Flow of water 12 l/min.

factors limiting the frequencies which the valve can handle). In these cases, as far as the cooling is concerned, even better results can be anticipated than those obtained from valves PAW 12/15 and TAW 12/35 as described above, for in later types there will be more freedom in choosing the pressure drop permissible in the cooler; when a greater pressure drop is allowed than that assumed in the foregoing, more intensive turbulence and still greater cooling effects are obtainable. Since the pressure drop in the cooler always represents but a small fraction of the pressure difference required to force the water through the insulating coils, increases in this pressure drop are of little significance in comparison with the total pressure to be supplied by the pumps.

SOFT IRON FOR THE ELECTROMAGNET OF A CYCLOTRON

by J. J. WENT.

669.127.5:621.318.322

Investigation is made into the properties to be ascribed to a soft iron suitable for the construction of electromagnets as used in cyclotrons. The more important characteristics of ferromagnetic materials are first discussed, such materials being classified in four groups. A number of possible applications are then indicated for each group, after which it is shown that the iron from which electromagnets are made must possess high saturation values and relatively high remanence. Taking into consideration the general picture which ferromagnetic materials should present, it is then seen that the last-mentioned requirement can be met only when care is taken to minimise internal strains and any non-magnetic constituents that may be present. Since these desiderata are also conducive of a low coercive force, the same grades of iron can also be employed for the iron cores of relays. Finally, details are given of the conclusions drawn from this review as applied to a practical test in the manufacture of the iron used for a cyclotron built by Philips for the Institute for Nuclear-Physical Research at Amsterdam.

Introduction

In the field of nuclear-physical research the cyclotron is an extremely useful apparatus, which has accordingly been adopted in various countries; a unit built by Philips is in use at the Institute for Nuclear-Physical Research at Amsterdam.

The cyclotron is an apparatus by means of which it is possible to impart to charged particles enormous speeds (corresponding to direct voltages of 10 million volts or more). One of the major components of the equipment is an electromagnet of very large proportions; 200 tons of iron were used in the construction of the magnet for the cyclotron under review, so that it was well worth while ascertaining beforehand the particular magnetic properties to which the metal should conform to give the best results. The outcome of these investigations is reviewed in this paper.

For a clearer understanding of the various questions involved, let us first call to mind some of the more general characteristics of ferromagnetic material, as this will enable us to classify the different materials according to their desired properties. Proceeding from considerations regarding the magnetic structure of ferromagnetic substances, we shall then be able to look into possible methods of influencing the properties of such materials. This will in turn explain the reasons for the choice of the particular kind of iron used in the construction of the cyclotron in question. A brief description will then be given of the method employed in the manufacture of this iron.

In the closing paragraph of this article it will be shown that the type of iron developed for the electromagnet of the cyclotron is also very suitable for the iron cores of relays as used in large numbers in automatic telephone exchanges.

The hysteresis curve with and without demagnetisation

The properties of ferromagnetic materials are known to be characterised by the relation between the magnetic induction, or flux density B — or the magnetisation J — and the magnetising field strength of force H. Let us consider J as a function or H, the relation between which is represented by a hysteresis curve. As the Giorgi system of units is employed in this article it is better, in plotting the curve, not to make use

of H, but of $\mu_0 H$ (μ_0 is the permeability of a vacuum) for the abscissa. In the Giorgi system both $\mu_0 H$ and the magnetisation J are expressed in terms of Wb/m², and the abscissae and ordinates are then of the same denomination.

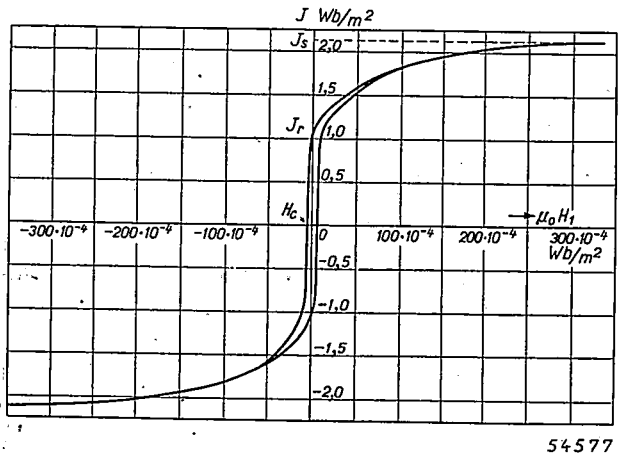


Fig. 1. Hysteresis curve of a ferromagnetic material. The curve relates to a closed magnetic circuit (e.g. an iron ring) and furnishes the relation between the magnetisation J and the field strength H_1 obtaining in the iron. At a high value of the field strength the magnetisation reaches a saturation point J_s. When it is subsequently reduced gradually to zero, J_s decreases to the remanence value J_r. Should an entire absence of magnetisation be desired, it is necessary to introduce a coercive force H_c the direction of which is opposed to that of the original magnetisation. The magnitude of the field strength H_1 is found by plotting $\mu_0 H_1$ (μ_0 being the permeability of a vacuum) in Wb/m² as abscissa; from this the field strength in oersted can be obtained by multiplying the resultant values by 10^4. The magnetisation J is similarly expressed in Wb/m². To obtain the corresponding values under the c.g.s. system the quantities must be multiplied by $10^4/4\pi \approx 800$.

When an ordinary hysteresis curve such as the one shown in *fig. 1* is examined, three important features are immediately apparent. At a high value of the magnetising force H the magnetisation attains a saturation value J_s; when the magnetising force is gradually reduced from this point to zero the magnetisation itself does not return to zero but goes no further than J_r, the remanence value, which is usually roughly equal to 0.5 J_s. Should an entire absence of magnetisation be desired, an external magnetic field H_c, the coercive force, must be applied in the opposite direction to that of the original field [1]).

Hysteresis curves, which are thus representative of one of the properties of a material, may be plotted from a closed magnetic circuit, e.g. a closed iron ring of uniform thickness, to which a magnetic field is applied. The field may be produced by a current flowing in a coil wound on the ring.

[1]) The coercive force is sometimes referred to as the strength of the field that must be applied to ensure a flux density of $B = 0$. In relation to the types of material discussed in this article (the coercive force of which is relatively low) this makes but little difference in practice.

In an electromagnet we are not concerned with a closed circuit; in this case the circuit is interrupted by an opening known as the air-gap. It is important to know the relation between the magnetisation and the field strength H as determined by the coil in a circuit of this kind.

Even when the air-gap in the ring alluded to above is no wider than 0.25% of the total length of the iron, the form of the curve in fig. 1 undergoes a considerable change, as shown in *fig. 2* (curve *b*), representing the "shifted" curve.

A simple calculation will serve to reveal the nature of this change; it is actually brought about by the fact that in this case the field strength H_1 acting on the iron is no longer equal to the magnetic field strength H produced by the coil. The presence of the free end faces in the air-gap — which may be regarded as magnetic poles — sets up a demagnetising field in the iron.

To demonstrate this let us take the case of an iron ring (*fig. 3*), having in it a gap l_2 in width, the length of the iron as measured along the centre line being l_1 ($l_1 + l_2 = l$).

Suppose the air-gap to be so small that the spreading of the magnetic lines of force at the gap may be ignored; the magnetic flux density in the iron, B_1, will then be equal to that in the air, B_2. If we represent the (absolute) permeability by μ (μ_1 in iron; μ_2 in air), then $B_1 = B_2 = \mu_2 H_2$, where $\mu_2 = \mu_0 = 4\pi \cdot 10^{-7}$ H/m.

Now, assume that a current flowing in a coil wound round the ring produces an "external" magnetising force H; the

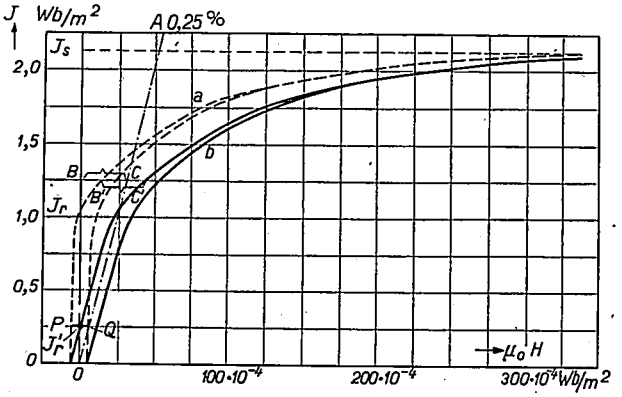


Fig. 2. The shifted hysteresis curve of an iron ring having in it an air gap the width of which is 0.25% of the total circumference. This curve illustrates the relation between the magnetisation and the "external" field strength H as determined by the current in the coil. The figure also shows how this shifted curve (*b*) may be derived from curve (*a*) (the "material" curve, fig. 1), by graphical transformation. Since, in order to obtain a certain magnetisation value J_1, the abscissa $\mu_0 H$ of a point on curve *a* must be augmented by NJ_1 (N being the demagnetisation factor), a line *OA* is drawn subtending an angle with the positive J-ordinate, the tangent of which is N. It is thus possible to read the value of NJ for every value of J (e.g. $B'C' = BC$). The quantity J_r in the case of curve *b* must be replaced by the apparent remanence J_r', which is considerably less. If, as the result of a low coercive force H_c, in conjunction with a high value of J_r, curve *a* is nearly enough perpendicular to the H-ordinate, then $J_r = \mu_0 H_c/N$. This will be apparent from the figure, provided $\overline{PJ_r'} = \overline{J_r'Q}$.

latter is understood to be the force that would be set up by the coil without the iron. Taking the magnetising force within the iron to be H_1 and in the air-gap H_2, then:

$$Hl = H_1 l_1 + H_2 l_2 \quad \ldots\ldots\ldots \quad (1)$$

Making use of the fact that the flux density is equal to the magnetisation augmented by the flux density in vacuum, we then find (J_1 being the magnetisation of the iron) that:

$$B_1 = J_1 + \mu_0 H_1 \quad \ldots\ldots\ldots \quad (2)$$

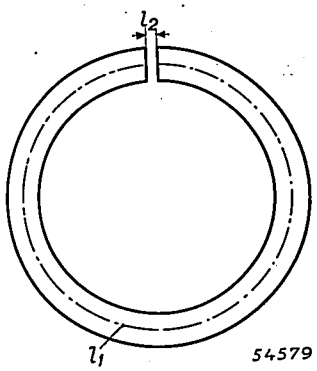


Fig. 3. Iron ring with air-gap l_2 in width; the length of the iron measured along the centre line is l_1.

In view of this, eq. (1) becomes:

$$Hl = H_1 l_1 + B_1 l_2/\mu_0 = H_1 l + J_1 l_2/\mu_0$$

or

$$\mu_0 H_1 = \mu_0 H - N J_1, \quad \ldots\ldots\ldots \quad (3)$$

assuming that $l_2/l = N$.

It follows, then, that the magnetising force H_1 obtaining in the iron, owing to the presence of the air-gap, is smaller than the magnetizing force H as produced by the electric current. This fact may be so expressed that the iron is partially demagnetised by the opposing or demagnetising force NJ_1/μ_0.

The magnitude of the demagnetising force is determined by N, which in our example is the ratio between the width of the air-gap and the total length as measured along the centre line of the ring; in other words it is a magnitude depending wholly on the geometrical data of the magnetic circuit. N is actually known as the factor of demagnetisation.

Of the three quantities J_s, J_r, and H_c, J_s and H_c are not affected by this demagnetisation, but the remanence J_r changes to the apparent remanence J_r'. The order of size of the latter, as applied to fig. 1, depicting a hysteresis curve in which H_c is not too high, depends almost entirely on the values of H_c and N, but hardly at all on J_r, as will be readily appreciated.

Suppose the magnetisation curve of a closed ring has been plotted, for which purpose J is ascertained as a function of H, and it is desired to derive from it the shifted hysteresis curve relating to the case where an air-gap produces a demagnetisation effect as characterised by a factor N. Let us now see how this can be done by graphical transformation.

The measured hysteresis ("material") curve yields the magnetising force $H_1 = f(J)$ within the iron. In a closed magnetic circuit the "external" magnetising force $H = H_1$, but according to eq. (3) $H_1 = H - NJ_1/\mu_0$ for a ring with air-gap. Thus, if we wish to know the relation between H and J we must make this distinction that without air-gap $H = f(J)$ and with air-gap $H = f(J) + NJ_1/\mu_0$, as illustrated by the shifted hysteresis curve. The latter can therefore be obtained from the original hysteresis curve by augmenting the abscissa $\mu_0 H_1$, for a given value J_1 of the magnetisation, by NJ_1. This is illustrated in fig. 2 for part of the curve in fig. 1. In order to determine graphically the quantity NJ_1, a line OA is drawn through the origin to subtend with the positive J-ordinate an angle the tangent of which is N.

If we are concerned with a material having only a low coercive force ($\mu_0 H_c = 0.1 \times 10^{-4}$ to 10×10^{-4}, i.e. 0.1 to 10 oersted), with normal $J_r = 0.5\ J_s$, the hysteresis loop at the point $\mu_0 H = -\mu_0 H_c$ is almost perpendicular to the H-ordinate and in this case the apparent remanence $J_r' = \mu_0 H_c/N$. This is immediately apparent when a line is drawn parallel to the H-ordinate through the point of intersection of the left-hand branch of the shifted hysteresis curve in fig. 2 and the J-ordinate (J_r'). Let the intersecting points of this line with the left-hand branch of the curve a and line OA be respectively P and Q; if the left-hand side of the curve a is practically perpendicular to the H-ordinate then $\overline{PJ_r'}$ and consequently also $\overline{QJ_r'} \approx \mu^\circ H_c$, from which it will at once be seen that $J_r' = \mu_0 H_c/N$.

In the situation shown in fig. 1, which concerns a fairly high coercive force ($\mu_0 H_c = 5 \times 10^{-4}$ Wb/m^2), the remanence is thus reduced to 0.20 of its original value at an air-gap width of 0.25%; were $\mu_0 H_c$ to be 0.5×10^{-4} Wb/m^2, J_r would even drop to 0.02 of that value.

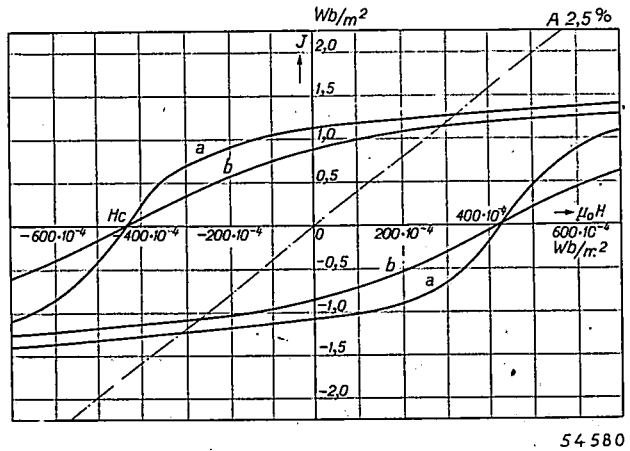


Fig. 4. Hysteresis curve for a material the coercive force of which is high. Curve a refers to the case where the demagnetisation (as in a closed iron ring) is zero, and curve b (the "displaced" hysteresis curve) to a ring with 2.5 % air-gap. It is seen that the apparent remanence in this case is governed mainly by the actual remanence and the factor of demagnetisation.

On the other hand, if the coercive force is quite high ($\mu_0 H_c = 100 \times 10^{-4}$ to 1000×10^{-4} Wb/m^2) as in *fig. 4*, then J_r' is only slightly less than J_r. For the above-mentioned air-gap of 0.25%, $J_r' = 0.985\ J_r$, whilst, for the demagnetisation illustrated in fig. 4 produced by a value of N which is 10 times higher, J_r' is still 0.80 J_r. In this

case J_r' is thus determined mainly by the remanence and the factor of demagnetisation.

When it is considered, finally, that low values of H_c have narrow hysteresis loops, i.e. enclosing only a small area and consequently corresponding to low hysteresis losses, whereas high values of H_c give wide loops and high hysteresis losses, the following classification of ferro-magnetic materials according to their characteristics will be obvious as far as 1) and 2) are concerned; in 3) and 4) other properties are involved which often have to be taken into account as well.

Classification of ferro-magnetic materials and their applications

Distinction is made between materials with:

1) high H_c values ($\mu_0 H_c > 100 \times 10^{-4}$ Wb/m^2), i.e. magnetically "hard" materials,
2) low H_c value ($\mu_0 H_c < 10 \times 10^{-4}$ Wb/m^2) i.e. magnetically "soft" materials,
3) high magnetic saturation,
4) high electrical resistance, owing to which eddy current losses may be small.

When reviewing the applications of ferro-magnetic materials it will be found in every case that one or more of these characteristics are concerned, though possibly not just those which are desired.

In electro-magnets the aim is to produce the greatest possible magnetic flux in the iron with the least possible magnetising force. This means that the material should conform to category 3) above, but efforts will also be made to ensure that high saturation values at the lowest possible value of the magnetising force, in other words, a relatively very high remanence and not too wide a hysteresis loop, are obtained, as otherwise the return branch of the curve will yield high magnetisation at low field strength values, but not the ascending branch. The last mentioned requirement means that H_c must not be too high.

Permanent magnets, intended to produce intense magnetic fields within air-gaps, must be made from materials answering to requirement 1), for, notwithstanding the considerable demagnetisation by the air-gap, the apparent remanence must be high. Requirement 3) must, however, be satisfied as well, since high saturation is needed in order to ensure a high remanence J_r.

Materials employed for high-frequency work will, in the first place, be required to conform to requirement 4). "Ferroxcube", a type of material developed in recent years in the Philips Laboratories at Eindhoven, being non-metallic and having a high electrical resistance, is exceptionally suitable for the purpose, the more so since it also satisfies requirement 2), in that its hysteresis losses are very low.

In low-frequency technique requirements 2) and 4) are also important (e.g. in transformers), but 4) does not then carry so much weight, since a laminated construction easily reduces the eddy current losses to reasonable proportions, especially if iron alloys be used having a resistance several times higher than that of pure iron. It is an advantage, then, if the material satisfies requirement 3) as well, and this can be achieved by making use of the high saturation value of metallic iron, thus reducing to a great extent the physical dimensions of transformers.

In the case of relays, such as are used in large numbers in automatic telephone work, yet other requirements have to be specified: a relay is required to "close" on a certain relay current, that is, under a given "external" field. This might indicate requirements similar to those of other electro-magnets. What is more important, however, is that the relay should open when the relay current ceases to flow; in other words the remanence should be low. Generally speaking, this can be achieved by arranging for a small air-gap also in the "closed" position (e.g. by inserting a non-magnetic "anti-freezing" plate), so that the apparent and not the true remanence is involved. On the other hand, it is at least equally important for the coercive force to be as light as possible, and also that this value shall not increase in course of time; if the coercive force is not free of all tendencies to vary, even the best relay will stick in the end. This point is referred to again in the closing paragraph of this article.

Before going into the question of the manner in which the above requirements were fulfilled in practice in the manufacture of the iron for the electro-magnet of the cyclotron, let us try to form a clear mental picture of a ferro-magnetic material. Without entering too deeply into theoretical considerations regarding ferro-magnetism, it will be useful to mention one or two corollaries of the theory, limiting our review, however, mainly to those results which may explain the origin of a high remanence and low coercive force.

General conclusions to be drawn regarding a ferro-magnetic material

According to the usual conceptions, ferro-magnetic material in the unmagnetised state may be divided into a number of small elementary domains, called Weiss domains, the area of which is nor-

mally between 10 and 100 μ, the substance within these domains being fully saturated. When the condition of the material is such that it is wholly demagnetised or, at any rate, differs considerably from the condition of saturation J_s at the temperature considered, the magnetisation vectors of these zones are all differently oriented. The fact that the magnetisation in each elementary domain has a very definite direction means that from a magnetic aspect the different directions are not equivalent; in other words there apparently exist anisotropic magnetising forces which may be attributable to the following causes.

In the first place the magnetisation appears to follow certain preferential crystallographic directions, which may vary still further between different metals and alloys. In the case of pure iron the three mutually perpendicular, cubic, directions of the (body-centred) iron crystal may be said to provide preferential energy directions for the magnetisation, which means that the potential energy is lowest when the magnetisation is oriented in one of these preferential directions. The difference in the magnetic energy between the directions of easiest and most difficult magnetisation is sometimes referred to as the crystal energy E_k.

In the second place, preferential directions may occur as a result of internal strains, which are in turn connected with the phenomenon of magneto-striction. When a ferro-magnetic material is magnetised by an external field of increasing strength, those elementary domains which are favourably oriented with respect to this external field gradually grow at the expense of the less favourably oriented, so that the magnetisation vector comes to lie roughly in the direction of the field. At intense flux densities all these vectors ultimately assume that direction. The material thereby undergoes a change in form, dependent upon the variations in the direction of magnetisation, and reverts to normal when the field is removed. Conversely, elastic modifications of form must have an effect on the direction of magnetisation among the elementary domains. The magnitude of the preferential energy thus produced is determined by the product of the magneto-strictive constant λ (which is equal to the relative longitudinal variation between the fully demagnetised and saturated conditions of the material) and the amplitude of the fluctation in the internal strain σ_i.

Which of the above-mentioned anisotropic influences will tend to predominate depends on whether E_k is greater or less than $\lambda\sigma_i$. Even when E_k is very high as compared with $\lambda\sigma_i$, however, — and this is usually so in the case of iron — the anisotropic influence of the strains may still play an important part, since it is quite possible that, as a result of the magneto-striction, the preferential direction will almost coincide with one of the three crystallographic, preferential directions, thus involving a preference along this single axis instead of along three.

Thirdly, the form of the ferro-magnetic material has a direct bearing on the direction of magnetisation: this is related to the fact that the demagnetisation factor of such materials differs between one direction and another, and so also, therefore, does the strength of the demagnetising field. Even if we ignore the external shape of the material the "internal" form remains an important factor. This latter is governed by small non-magnetic inclusions [2]) such as are present in all ferro-magnetic metals which are not absolutely pure. It would appear that, from the point of view of energy, it is much better for the magnetisation to run as far as possible parallel to such non-magnetic surfaces. This may be explaned by the fact that in the adverse case, independent magnetic poles will occur at the free surfaces, producing an opposed magnetic field.

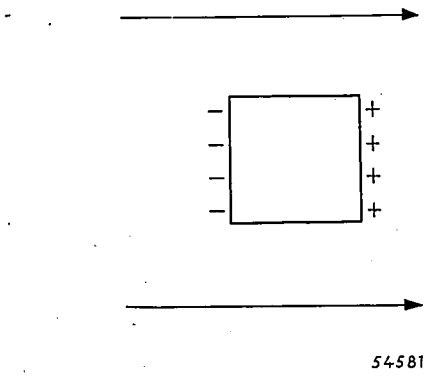


Fig. 5. How free magnetic poles occur in a cubic air-cavity. The arrows indicate the direction of magnetisation in the iron.

Let us suppose that a cubic air-cavity were to exist within an elementary domain (see *fig. 5*) and that this is required to produce no disturbance in the magnetisation around the cavity; in that case the magnetic flux density B_1 in the iron and that in the air, B_2, would have to be equal. This will occur provided no demagnetising poles are formed, i.e. when the magnetisation runs parallel to the air surface. If the non-magnetic inclusion be at all

[2]) When we speak here of non-magnetic inclusions we also mean those which, although magnetic, are less ferro-magnetic than the basic metal.

elongated in shape, magnetisation in the direction of the arrow (*fig. 6*) will be more favourable, from the aspect of the energy, than in the transverse direction.

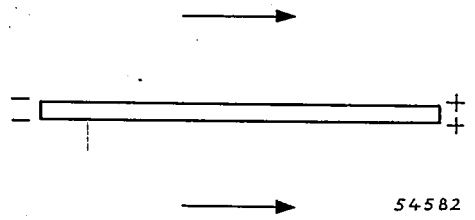


Fig. 6. How free magnetic poles occur if a non-magnetic inclusion has an elongated shape.

Moreover, non-magnetic inclusions tend to produce internal strains and thus also manifest themselves by their magneto-strictive effect.

Let us now see how the remanence and coercive force fit into the ferro-magnetic picture as sketched in the foregoing.

Remanence

The following simple considerations will serve to illustrate the relation between remanence and saturation.

Take the hypothetical case of a polycrystalline material in which so many anisotropic influences are at work that the preferential directions in the material as a whole are completely arbitrary. It might be expected of such a material in the fully demagnetised state ($J = 0$ and $H = 0$), such as might be produced by cooling the metal as from the Curie point in an external field of $H = 0$, that each elementary domain would have a certain optimum preferential direction, being the best from the point of view of energy, and that all the magnetisation vectors would thus be distributed at random over a sphere, in the manner illustrated in *fig. 7a*. If the metal be then saturated by means of a high magnetising force H in the direction indicated by the arrow in fig. 7, all the magnetisation vectors will assume this orientation (fig. 7*b*). When the field is removed the old preferential directions will be restored, but, since any two opposed directions are then equal as regards energy, the vectors will occupy only half the sphere (fig. 7*c*). This will gives us $J_r = J_s \overline{\cos \alpha}$, in which the vinculum over the "cos α" indicates that an average must be taken in respect of all angles occurring in this case over a hemisphere; this, then, yields $J_s = 0.5\ J_s$.

Now, it is possible to produce metals in which $J_r > 0.5\ J_s$, and we shall indicate the relevant requirements to be satisfied, together with the reasons for them. We shall suppose that fluctuations in the internal strain σ_i are so small that $\lambda\sigma_i \ll E_k$ and, further, that non-magnetic inclusions are either entirely absent or so large in proportion as to be magnetically innocuous (their dimensions being of the same order as the elementary domains). We then have to reckon only with the anisotropic crystallographic structure; the magnetisation vectors in all the elementary domains will then be oriented in one of the crystallographic preferential directions. After saturation in accordance with fig. 7*b*, the remanence of iron will not be as shown in fig. 7*c*, but as in fig. 7*d*, since the cubic axis most closely approximating the direction of the field will be the preferential direction taken. The half-angle of the sector of a sphere, thus occupied, is about 58°, this being the angle between a body diagonal and one edge of a cube. It is clear that this half-angle cannot be greater than 58°, for this will in any case include at least one of the axes of the cube functioning as preferential direction. In this case the remanence is found from the mean of $J_s \cos \alpha$, not with respect to the hemisphere (90°), but over a sector of the sphere the half angle of which is 58°, so that:

$$J_r = 0.78\ J_s.$$

The above argument thus provides the requirements to be satisfied by the iron to ensure a high remanence value, viz. the internal strains must not be great and non-magnetic inclusions

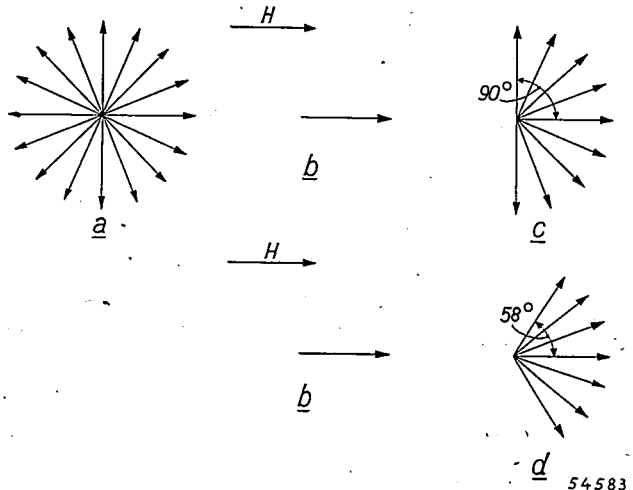


Fig. 7. Diagrammatic representation of the direction of the magnetisation vectors of the elementary domains of a polycristalline, ferromagnetic material.

a) in the fully demagnetised state the directions of the vectors are arbitrarily distributed;

b) when the material is saturated by means of an external magnetising force H, all the vectors assume the direction of H;

c) after the external magnetising force is removed, the vectors will be distributed over half a sphere;

d) when $\lambda\sigma_i \ll E_k$ (where E_k relates to a cubic structure) and the non-magnetic inclusions are absent or have very little influence, the vectors are contained within a sector of a sphere having a half-angle of 58°.

must be as few as possible. The same conditions, albeit for a different reason, also ensure a low coercive force.

The coercive force

In order to demonstrate the relation between strains and inclusions on the one hand and the coercive force on the other, it would be necessary to penetrate rather more deeply into the theory of the coercive force than can be done in this paper. A few words will, however, be said on the subject.

As already pointed out, the "magnets" in the elementary domains are parallel to each other, so that each domain is always saturated, at any rate as far as the temperature movement permits. At the boundary between two such domains a transition occurs between the preferential direction of one domain and the other, and in this transitional area, which may be referred to as the "wall" of the elementary domain,

1) the magnets are no longer parallel to each other, which means a loss of energy, and
2) they assume a direction of magnetisation which need not necessarily be the same as the local preferential direction, this likewise involving loss of energy.

The "wall" thus possesses a certain amount of energy per cm^2 of its area.

Now, it appears that the macroscopic magnetisation of magnetically soft metals takes place at relatively low values of the coercive force, by reason of a displacement of these walls, in consequence of which the domains which are more easily magnetised with respect to the external field increase in size, whilst the less favourably oriented domains are "absorbed". The magnitude of the coercive force of the material is determined by the facility (at low H_c) or the difficulty (at higher H_c) with which the walls can be displaced.

What, then, are the obstacles to these displacements of the walls? In the first place it may be imagined that the energy of the wall itself is a function of the locality where the wall occurs, either by reason of the fact that the energy per cm^2 varies owing to fluctations in the strain (σ_i), or because there may be non-magnetic inclusions in the wall which reduce the total wall area to be taken into account. In these wall displacements small amounts of energy have to be constantly added, disappearing again in the form of heat. Both the fluctuations in strain and the non-magnetic inclusions thus tend to increase the coercive force.

Finally, it should be noted that within the elementary domains themselves internal strains set up minor variations in the direction of the magnetisation, whilst inclusions produce small fluctuations in the intensity of the magnetisation, both these effects resulting in a loss of magnetising energy.

It has been stated above that non-magnetic inclusions represent demagnetising energy. Without going into quantitative calculations, from the diagrams *a* and *b* in *fig. 8* it will be readily seen that

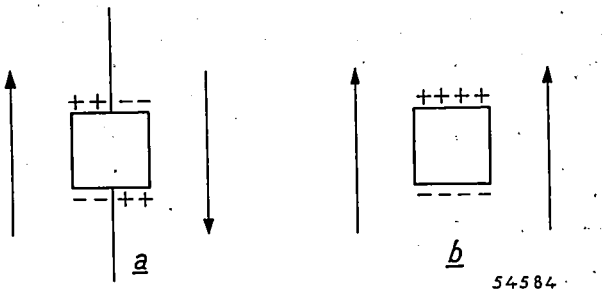


Fig. 8. Effects of the "wall" of an elementary domain on the magnitude of the demagnetising energy arising from non-magnetic inclusions.
a) A cubic inclusion at the boundary between two elementary domains.
b) The inclusion within a single elementary domain. In the second instance the demagnetising energy is much greater than in the first.

the demagnetising energy in case *b* is much greater than in case *a*. When the wall shown in fig. 8*a* is moved so that the inclusion lies well within a single elementary domain, there is not only the increase in energy due to the increase in the wall area but also an increase due to this augmented demagnetisation energy. The shape and dimensions of the inclusion determine which of the two effects predominates. The fluctuations in the direction of magnetisation in the body of an elementary zone, alluded to above, also give rise to hypothetical magnetic charges and thus also to variations in energy when the location of the wall is changed. In this way, depending on the location of the wall, fluctuations in energy may have the effect of increasing the coercive force.

The conclusion to be drawn is that the conditions to be met by the iron to ensure a low coercive force are: low internal strains and as few non-magnetic inclusions as possible, i.e. the same as for a high remanence.

Iron for the electromagnet of a cyclotron

In the light of the foregoing considerations it is clear that the ferromagnetic material employed in the construction of electromagnets should satisfy the requirements mentioned above as regards internal strains and non-magnetic or only weakly magnetic inclusions. Furthermore, we must ensure

high saturation J_s in order to obtain a high remanence in an absolute sense.

Starting out from the latter requirement, it is important to note that the magnetic saturation value of pure iron is already quite high, namely 21 000 $\times$ 10^{-4} Wb/m² (approx. 1700 c.g.s. units). Still higher values can be obtained only by the addition of large proportions (15 to 35%) of cobalt, which is very costly; the J_s value then rises slightly, viz. to 2.25-2.50 Wb/m². Any other element that is soluble in iron will reduce the saturation point. It might be asked: Why not then use an iron that is pure and free from strain? But it is not possible to produce such iron on a technical scale, so that we have to ascertain how, and in how far, the detrimental elements in the iron can be eliminated.

In the list of ever-present constituents of iron which are highly detrimental from the aspect of magnetisation of the soft metal, carbon is the outstanding element. Carbon, which is practically insoluble in iron at ambient temperatures, usually occurs in the form of cementite (Fe_3C), which is meta-stable at these temperatures, the more stable form at such temperatures, namely graphite, being much more difficult to produce. Despite the fact that cementite is in itself still slightly magnetic, it has a much more adverse effect, appearing as it does as inclusions, than non-magnetic graphite, if only for the reason that a given percentage of carbon produces a much greater volume of cementite than graphite, viz. 4.5 times as much. A content of 6.7% carbon by weight is sufficient to convert the whole of the iron into cementite.

The simplest means of removing the carbon from the iron consists in burning it out with oxygen, to form CO, and this can be done during the smelting process, either by forcing air through the metal or by adding sufficient quantities of iron oxide, for instance in the form of ore. The latter method is employed by the firm of De Muinck Keyzer of Utrecht, the suppliers of the iron used for the electromagnet of the cyclotron at Amsterdam. This oxidation process was carried out in a Siemens-Martin furnace, in which the iron was melted under a layer of molten slag, just so long until the carbon content dropped below 0.06%. The metal ultimately contained an excess of oxygen, which was then removed immediately before casting by adding so much aluminium that about 0.5% Al is left in the melt; this had the effect of fixing the oxygen in the form of Al_2O_3, an important part of which finished up in the slag. In addition to the 0.5% Al, 0.5% Si was added, in view of the fact that any carbon still present in the iron should preferably take the form of graphite. Although, in contrast with cementite, graphite is the stable modification at low temperatures, it is so difficult to produce that, unless special precautions be taken to ensure its formation, very little of it appears at all. Now, both silicon and aluminium possess the property of being able to promote the formation of graphite. These two elements were added to the melt as a mixture, because it was felt that the graphite-forming properties would be more pronounced in the combined than in the separate elements.

The addition of Al and Si naturally has the drawback that they both tend to reduce the saturation induction of the iron; the J_s value of the iron produced in the above manner is about 2.0 Wb/m² and the chemical composition is roughly as follows:

Fe	98.9 %
C	0.05%
Si	0.45%
Al	0.35%
Mn	0.25%.

This reveals the fact that part of the aluminium used for the de-oxidation disappeared in the slag; manganese is a comparatively innocuous element occurring in all technical grades of iron.

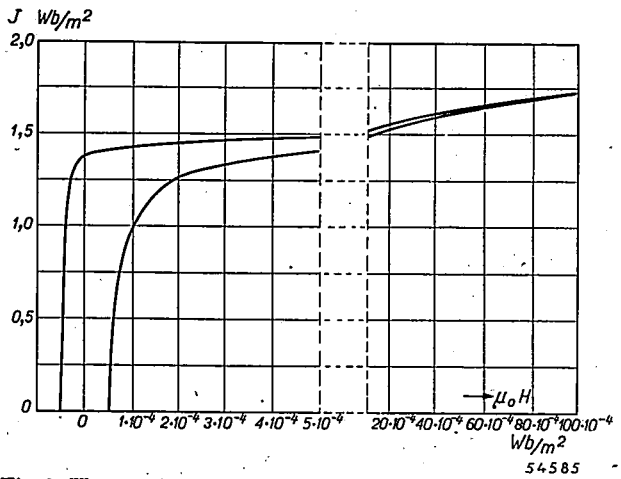


Fig. 9. Hysteresis curve of the iron used for the electromagnet of a cyclotron. The saturation induction J_s is 2.0 Wb/m², but this is attained at so high a field strength that it cannot be read from the graph. The remanence is approximately 70% of J_s, and the coercive force is very low ($\mu_0 H_c = 0.5 \times 10^{-4}$ Wb/m²). For $\mu_0 H_c > 5 \times 10^{-4}$ a different scale is used from that in respect of $\mu_0 H_c < 5 \times 10^{-4}$.

Fig. 9 illustrates the hysteresis curve of a casting made from the iron in question: the remanence is about 70% of the saturation of 2.0 Wb/m² and the latter is reached at so high a field strength that it can no longer be read from the graph. This, then, is an example of a metal in respect of which $J_r > 0.5\ J_s$. For a technical grade of iron the coercive

force is very low, viz. $\mu_0 H_c = 0.5 \cdot 10^{-4}$ Wb/m², this being an average. Needless to say, different casts yield varying values, but the coercive force is in every case so low that it lies between 0.3×10^{-4} and 0.7×10^{-4} Wb/m².

Table I. Comparative magnetic properties of different kinds of soft iron.

Grade of iron	Magnetising force (in $\mu_0 H$) to give $J = 1.5$ [3] [4] Wb/m².	Coercive force ($\mu_0 H_c$ in Wb/m²).
Mild steel	20×10^{-4}	$(1.5\text{-}3) \times 10^{-4}$ *)
Hyperm 0 (free-cutting quality)	23×10^{-4}	$(0.8\text{-}1{,}5) \times 10^{-4}$
Dynamo iron	16×10^{-4}	1×10^{-4}
Hyperm 0 (standard)	12.5×10^{-4}	$(0.5\text{-}1) \times 10^{-4}$
Armco iron	10×10^{-4}	1×10^{-4} *)
Cyclotron iron	8×10^{-4}	$(0.3\text{-}0.7) \times 10^{-4}$
Wemco iron (99.95 Fe)	1×10^{-4}	0.05×10^{-4}

*) The metals are subject to variation on ageing (H_c increases).
[3]) Corresponding to 1200 c.g.s. units or 15 000 gauss.
[4]) To obtain the flux density in oersted, multiply these values by 10^4.

To what extent the characteristics of the iron developed for the cyclotron excel over other grades of soft iron will be seen from *table I* showing the magnetising force to be applied to yield a magnetisation of 1.5 Wb/m², together with the coercive force. Hyperm 0 is a special kind of iron used by Krupp for relays. Wemco iron, mentioned last in the table, is included to show what can be attained under the most carefully controlled conditions in the laboratory, although not of course on a technical scale; no practical use can therefore be made of it.

The magnetic properties desired in soft iron for a cyclotron are related to the field strength required in the air gap. The desiderata and values given above apply to the cyclotron built for the Institute for Nuclear-Physical Research at Amsterdam. If, for a cyclotron of the same capacity, the dimensions of the pole shoes should have to be reduced, higher field strengths would be needed and the saturation value J_s of the soft iron would have to be raised, necessitating a different choice of the composition of the material.

Iron as used for relays

It has already been pointed out that iron used for the cores of relays must show the lowest possible values of the coercive force. Further we have shown that the properties of iron intended for the electromagnet of a cyclotron (low internal strain and absence of non-magnetic inclusions) ensure a low coercive force. The obvious inference is that the same iron which is suitable for the cyclotron will also be a very satisfactory material for the manufacture of relays.

In passing, we stated above that the coercive force of the iron used for relays must not increase as a result of ageing. The coercive force must be low in order to ensure a low apparent remanence. This is important, as it makes it possible for the relays to be so adjusted as to prevent sticking. If the coercive force does increase with the age of the relay the apparent remanence may even become so high that the relay will fail to open altogether. Many ordinary technical grades of iron do possess this disadvantage. The causes of this phenomenon may be sought in a precipitation process in which especially nitrogen and, to a certain extent, also carbon are the harmful elements, since they tend to separate in the form of nitrodes and carbides. Nitrogen is almost wholly insoluble in iron at ambient temperatures and only slightly soluble at elevated temperatures, but the γ-phase of iron, which is stable between 900 and 1400 °C, has a great solubility for nitrogen. However, when iron containing nitrogen is cooled down this element does not immediately pass out of solution as a nitride; in other words, the solution is super-saturated and if nitrides are formed in the course of time they occur in the iron in a very finely divided form, disturbing the crystal lattice and producing internal strains and non-magnetic inclusions, both of which increase the coercive force. To counteract this effect, silicon and aluminium should also be added to the iron, not only because they fix and remove the nitrogen as well as the oxygen, but also because they reduce the temperature range within which the iron is in the face-centred and not in the body-centred phase. Such percentages of these elements as are mentioned in a preceding section will reduce the range in question from 900-1400 °C to 1000-1300 °C; the smaller this range can be made and the higher the transition temperature between the body-centred and face-centred phases, the smaller the content of nitrogen that will remain in the super-saturated solution. The type of iron under review, to which small quantities of Si and Al are added, is perfectly free from any tendency towards ageing; heating of the metal for 500 hours at 100 °C has not the slightest effect on the coercive force.

ABSTRACTS OF RECENT SCIENTIFIC PUBLICATIONS OF THE N.V. PHILIPS' GLOEILAMPENFABRIEKEN

Reprints of these papers not marked with an asterisk can be obtained free of charge upon application to the Administration of the Research Laboratory, Kastanjelaan, Eindhoven, Netherlands.

1719b: E. J. W. Verwey and J. Th. G. Overbeek: Long distance forces acting between colloidal particles (Trans. Faraday Soc. **42B**, 117-123, 1946).

The writers have made an extensive investigation on the theory of the long distance forces acting between the particles in a colloidal solution, more especially in the case where the particles are surrounded by an electrical double layer. The paper gives a brief summary of these investigations preceded by a critical discussion of the work of previous authors.

For more extensive information, see these abstracts, Nr. **1769.***

1764: E. J. W. Verwey: De vrije energie van phasengrenzen (Kon. Vl. Acad. Wet. Lett. Sch. Kunsten; symposium Grenslaagverschijnselen, gehouden te Brussel, 5 en 6 Juli 1946, blz. 20-37, 1947). (The free energy of phase boundaries, in Dutch).

The free energy of a phase boundary has been considered for a number of simple cases. It is shown that in the cube face of most alkalihalides the negative ions are shifted outward, the positive ions inward. The deformations have the effect of lowering the free surface energy. The surface energy of water can roughly be understood by considering its ice-like structure and the forces acting between the molecules. The effects of dissolved substances on the surface tension of liquids is discussed qualitatively and the considerations are extended to the case of an interface of two liquids where an electric double layer may be present.

1764a: J. Th. G. Overbeek: Wisselwerking van electrochemische dubbellagen. Stabiliteit van hydrophobe colloiden (Kon. Vl. Acad. Wet. Lett. Sch. Kunsten; symposium Grenslaagverschijnselen, gehouden te Brussel, 5 en 6 Juli 1946, blz. 130-156, 1947). (Interaction of electrochemical double layers. Stability of hydrophobic colloids; in Dutch).

Considerations on the structure of the electrochemical double layer lead to a relation between the charge and the potential of a surface in contact with a solution of an electrolyte. It is shown that the surface charge will be diminished by the interaction of two double layers, causing a repulsion. Apart from this repulsion the London-van der Waals attraction has to be taken into account. Attraction and repulsion are given in the form of potential curves. If the combined potential curve shows a maximum of sufficient height, the corresponding sol is stable. Important conclusions are: a proof of the validity of Schulze and Hardy's rule for the concentration of electrolyte necessary to flocculate a hydrophobic sol, an estimate of the London-van der Waals constant, a proof of the instability of a solution with very small colloidal particles ($< 10^{-7}$ cm). Slow flocculation of a hydrophybic sol is a selfretarding process. The stability of coarse suspensions demonstrate that the London-van der Waals forces must decay more rapidly than according to customary theory, owing to a retardation effect. The reader is further referred to these abstracts, No. **1769***.

1764b*: W. Ch. van Geel: Doorgang van electronen door grenslagen (sperlaaggelijkrichters en sperlaagfotocellen) (Kon. Vl. Acad. Wet. Lett. Sch. Kunsten; symposium Grenslaagverschijnselen, gehouden te Brussel, 5 en 6 Juli 1946, blz. 172-192, 1947). (Passage of electrons through barrier layers; barrier-layer-rectifiers and -photocells; in Dutch).

In this paper the passage of electrons through insulating layers is considered. This phenomenon chiefly depends on the nature of the adjacent electrodes. Barrier layers, *a*) between two metals, *b*) between a metal and a semi-conductor, *c*) between a metal and an electrolyte and *d*) between a metal and a semi-conductive photosensitive substance are dealt with in succession. Various theories, based on tunnel-effect, cold emission and double layers are shortly described and compared with experimental results.

1783/85: H. Rinia, J. de Gier and P. M. van Alphen: Home projection television, I. Cathode ray tube and optical system; G. J. Siezen and F. Kerkhof: Id. II. Pulse-type high-voltage supply;

J. Haantjes and F. Kerkhof: Id. III. Deflection circuits (Proc. Inst. Radio Engr. **36**, 395-411, 1948, No. 3).

The contents of these papers are more extensively dealt with in Philips techn. Rev. **10**, 1948/49, Nos 3, 4, 5, 10 and 12, under the title: "Projection television receiver".

1786: H. C. Hamaker: Een systematische vergelijking van de statistische eigenschappen van hedendaagse steekproef-schema's (Statistica **2**, 19-39, 1948, No. 1/2). (A systematic comparison of the statistical properties of present-day sampling-schemes; in Dutch).

A survey of various sampling schemes, carried out with the aid of the "random walk diagram", leads to the conception that it must be possible to effect the same degree of inspection by the application of different schemes. The degree of inspection of a scheme is contained in its "operating characteristic", which is specified by two constants viz: its centre q_0, for which $P = {}^1/_2$, and its slope s in this point, defined by $s = -(\mathrm{d}P/\mathrm{d}q)_{q=q_0}$, q being the quality of the batch and P the chance of it not being rejected. It is shown that, if the operating characteristics of two different sampling schemes possess the same values of q_0 and s, the two characteristics are almost completely coincident. Thus two sampling schemes having the same q_0 and s will give identical inspection performances, and are consequently defined as "equivalent". A comparison of the sample sizes of equivalent schemes leads to a general definition of the "efficiency" of a scheme. On this basis single, double and sequential schemes are intercompared.

1787: J. L. Snoek: Dispersion and absorption in magnetic ferrites at frequencies above one Mc/s (Physica **14**, 207-217, 1948, No. 4).

The phenomena of absorption and dispersion observed in magnetic ferrites at frequencies above one Mc/s are discussed making the assumption that at these frequencies no contribution to the magnetisation is made by the Bloch boundaries.

For pure and unstrained polycrystalline aggregates of cubic crystals the following relation between the critical frequency and the initial susceptibility is found to be equal to ${}^2/_3\ |g|\ M$ where $g = e/mc = 1{,}76 \cdot 10^7$ emu and M the magnetic moment per cm³. In deriving this equation the damping is assumed to be small. It is further shown that internal stresses tend to increase the losses at lower frequencies and make the rise in tan δ with frequency less steep. This is actually borne out by experiment.

1788: W. Opechowski: On the anisotropic exchange interaction and the behaviour of copper potassium sulphate at very low temperatures (Physica **14**, 237-248, 1948, No. 4).

Formulae are given for the specific heat and the magnetic susceptibility of a crystal, calculated on the assumption that the interaction between magnetic atoms is a sum of the anisotropic (direct or indirect) exchange interaction and the magnetic interaction. These formulae are applied to the case of copper potassium sulphate which has been investigated experimentally by De Klerk at temperatures below 1° K. Unfortunately, no unambiguous theoretical conclusions seem to be possible.

1789: H. Brinkman: Réflexion résultante par plusieurs couches parallèles (Revue d'optique **27**, 31-33, 1948, No. 1). (Resulting reflection by a number of parallel layers; in French).

A simple deduction is given of T. Smith's formula for the reflection of a system of $(m-1)$ parallel non absorbing layers. This formula expresses that the ratio between the resulting reflectivity and the resulting transmission equals the sum of the corresponding ratios for the separate layers, taking into account repeated reflexions and considering the different rays as incoherent (thick specimen or white light). The resulting reflexion is minimal if the refractive index of each layer is equal to the geometric mean of the indices of adjacent layers. In good approximation it may be said that for given initial and final mediums the reflexion then is $1/m$ of the reflexion existing in the case of one optical surface.

VOL. 10 No. 9, pp. 257-288 MARCH 1949

Philips Technical Review

DEALING WITH TECHNICAL PROBLEMS
RELATING TO THE PRODUCTS, PROCESSES AND INVESTIGATIONS OF
THE PHILIPS INDUSTRIES

EDITED BY THE RESEARCH LABORATORY OF N.V. PHILIPS' GLOEILAMPENFABRIEKEN, EINDHOVEN, NETHERLANDS

EXPERIMENTAL TRANSMITTING AND RECEIVING EQUIPMENT FOR HIGH-SPEED FACSIMILE TRANSMISSION

II. DETAILS OF THE TRANSMITTER

621.397.61

D. KLEIS, F. C. W. SLOOFF *) and J. M. Unk *).

In the transmitter of the high-speed facsimile transmission system developed by Philips the documents to be transmitted are held electrostatically on a conveyor belt by a D.C. voltage of several kV. A rotating optical system, around which the conveyor belt is curved perpendicular to its direction of movement, scans the paper in parallel lines at the rate of 180 lines per second. The rotor comprises three identical scanning units set at angles of 120° to each other, so that it is only necessary for the conveyor to curve through 120°. The three scanning systems in turnproject a scanning spot $^1/_5$ mm in diameter on the document to be scanned and at the same time concentrate the diffusely reflected light on a stationary secondary-emission photo-electric cell. A carefully designed optical system, using a film projection lamp as light-source, produces at the photo-electric cell a luminous flux of 0.20 for black and 0.70 millilumen for white parts of the document. As the signal supplied by the photo-electric cell when scanning white is 43 db above the noise level, the latter produces no visible fluctuations in the tone of the received image.

The performance of the facsimile transmission system evolved in the Philips Laboratories at Eindhoven may be outlined very briefly as follows. A continuous flow of drawings, photographs or other documents can be transmitted over a cable or radio link at the rate of 80 cm² per second (a sheet of quarto size in 8 seconds), details in the original as small as 0.2 mm being clearly reproduced. The receiver furnishes a reproduction which is reduced 6 × in size, on a 45 mm film.

The function which this new facsimile system will fulfil as a complementary to the 60-times slower systems and other means of communication has already been reviewed in a previous issue [1]). A more detailed description of the apparatus, comprising the mechanical and optical features of the transmitter, follows. The receiver will be dealt with in a similar way in another article, whilst the electrical circuits will be discussed in a later article to appear in this journal.

*) N.V. Philips' Telecommunicatie Industrie (formerly N.S.F.), Hilversum.

[1]) H. Rinia, D. Kleis and M. van Tol, Part I of this article: General Data, Philips Technical Review, **10**, 225-231, 1948 (No. 8).

General arrangement of the transmitter

In accordance with the principle employed in every modern facsimile transmitter, the documents or images to be transmitted are scanned by a light-spot travelling across the page in successive parallel lines; the varying amount of reflected light is then converted by means of a photo-electric cell into a fluctuating electric voltage which is transmitted to the receiver.

In the usual slow facsimile systems scanning is effected by means of a rotating drum, around which the document is wrapped. An optical system is made to traverse slowly in a direction parallel to the axis of the drum in such a way that the scanning spot describes a helix of very fine pitch around the drum. Although this method is quite satisfactory in the slower facsimile systems, it is not suitable in a rapid system. In fact, placing a new document on the drum and restoring synchronism between receiver and transmitter for each transmission involves a loss of time of several seconds. When dealing with transmission times of only a few seconds this loss of time would affect efficiency to an intolerable extent.

It is true that in some systems the necessity of

stopping the drum has been avoided, the "copy" being fed to it automatically. However satisfactorily this device may work at rotation speeds of about 3 revolutions per second, it would be impossible at 60 times that rate, which would be required by the short transmission time mentioned previously.

A new scanning method has therefore been devised in which the respective movements of the paper and the scanning device have been interchanged. The documents are thus fed continuously. *Fig. 1* illustrates the manner in which this is achieved.

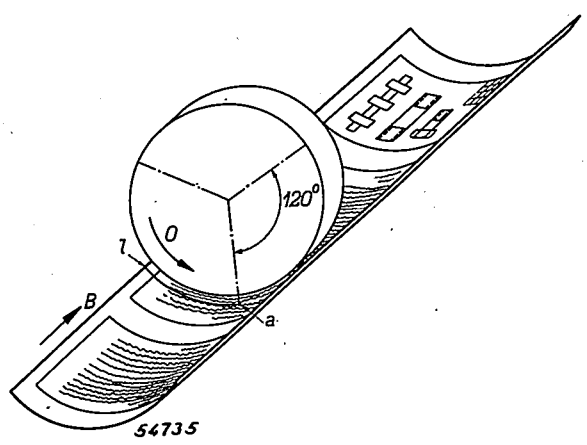


Fig. 1. A conveyor belt *B* with the documents upon it passes in front of a rapidly rotating scanning system *0*, the axis of rotation of which is parallel to the direction of travel of the belt, so that scanning takes place in the form of parallel lines. *l* represents one of these lines, with the scanning spot at the point *a*. The rotor embodies three optical systems set at 120° to each other, so that it is only necessary to curve the belt through 120°.

The copy to be transmitted is placed one sheet after another on an endless belt 22 cm in width. Subsequently the belt passes a rapidly rotating optical system which causes a scanning spot, 0.2 mm in diameter, to trace a line across the belt. Sharp definition of the spot is maintained by curving the belt at the point where scanning takes place, across its own direction of travel and around the same axis as that of the optical system. Since it is obviously not practicable to deform the belt to the extent of an entirely closed cylinder, it is curved only through 120° about its axis. The rotor comprises three identical optical systems set at 120° apart. The scanning spot of one of these scanning units traces its path across the belt in one-third of a revolution and is followed by the second spot, tracing the same path, during which time the belt moves on slightly, and so on. The belt and the rotor are coupled together by means of a reduction gearbox in such a way that the successive scanning lines on the paper — 0.2 mm in width — are exactly contiguous.

The desired curvature of the conveyor belt is produced by a cylinder, coaxial with the rotor (omitted for convenience in fig. 1), against which the advancing belt is thrust by a number of rollers. A slit in the wall of this cylinder permits the scanning light beam to pass through.

The manner in which the three scanning spots are obtained and the subsequent path of the light are illustrated in *fig. 2*. A stationary lamp is mounted in the geometrical axis of the rotor and three small condensers, arranged as an equilateral triangle around the axis of the unit, serve to concentrate the light rays onto three diaphragms. The three light beams admitted by the latter are then reflected in a radial direction from three flat mirrors into three objective lenses mounted in the periphery of the rotor. The foci are so calculated that the image of the light-source is reproduced by the condenser, in the aperture of each objective, whilst the latter — a microscope objective — focuses a reduced image of its associated diaphragm onto the paper.

The objective lens also serves to concentrate the light reflected from the illuminated spot on the paper (the reflected light of which is constantly varying in intensity during the scanning process), onto a stationary photo-electric cell mounted in the geometrical axis of the rotor. For this purpose an oblique mirror with central hole (S_1 in fig. 2) is located just in front of the objective; the light from the lamp passes through the hole in this mirror and floods the centre part of the objective. On the paper diffuse reflection of the light takes place and the reflected light floods the whole objective, a large portion of it falling on the mirror around the central hole. The mirror reflects this part of the beam, in a direction parallel to the rotor axis, onto a second mirror fixed to another rotor disc mounted on the rotor shaft. The latter mirror deflects the beam towards the centre of rotation, where a third mirror passes it to the photo-electric cell. The two last mentioned mirrors are also arranged in threes, each pair being set at 120° with respect to the others.

During the time that scanning spot *I* is passing over the conveyor belt, that is during 1/3 of a revolution, the photo-electric cell receives light from optical system *I*; as soon as scanning spot *II* commences its path across the belt the cell receives light from system *II*, but this change-over will not be noticed by the photo-electric cell, provided the various systems are properly adjusted and the luminous intensities carefully balanced. The same applies to the change-over from system *II* to system

III, which follows one-third of a revolution later.

The shaft with the two rotor discs makes 60 revolutions per second, so that 180 lines are scanned in this time. This represents 1440 lines in 8 seconds, corresponding to a length of copy of 28.8 cm or roughly the length of a quarto sheet (21 × 29.7 cm).

The photo-electric cell is a multiplier type and, as will be shown later, the current produced in it under normal operating conditions, varying with the reflecting properties of the paper scanned, is about 70 μA for white. This current passes through a resistor, and the alternating voltage across it is amplified to about 25 V (peak), the resultant signal being suitable, inter alia, for the modulation of the carrier wave of a radio transmitter. The electrical equipment must be capable of handling signals at frequencies of 0 to 100,000 c/s without attenuation, since on the one hand the constant average brightness of the copy (frequency 0) has to be reproduced in the receiver at the correct level, whilst on the other hand fluctations in the luminosity up to 100,000 c/s must be transmitted in order to reproduce accurately details corresponding to the size of the scanning spot (0.2 mm).

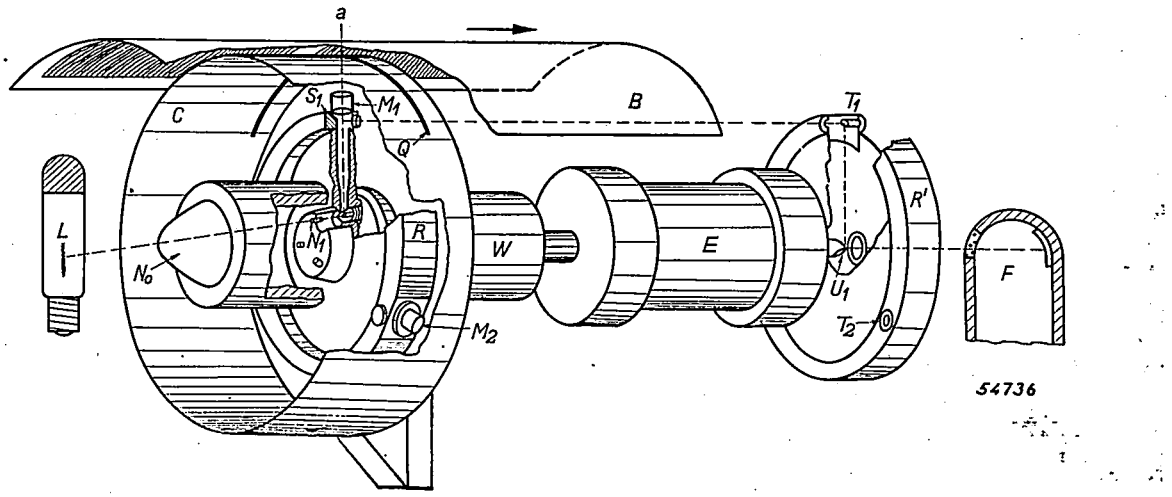


Fig. 2. The rotary scanning system, cut away to show some of the interior detail. The conveyor belt B, onto which the scanning spot (a) is projected, runs above the scanning system (not below it as shown for the sake of convenience in fig. 1). The documents are thus scanned from below, this arrangement presenting no difficulty in view of the method of adhesion empoyed, as described later.
C is a stationary cylinder, against which the belt is thrust; Q slot; E motor driving the rotor discs R and R'; W reduction gearing by means of which the slow travel of the belt is derived from the rotor drive.
The optical system, comprising a stationary lamp L, a stationary photo-electric cell F, an auxiliary condenser N_0 — which is not indispensible, but ensures a reduced (more concentrated) image of the lamp filament — and three sets of mirrors and lenses: the index 1 refers to the first of these; 2 refers to the second, whilst the third set is not visible in the sketch. N_1 condenser and behind it a diaphragm and mirror (not designated by letters); S_1 mirror with central hole; M_1 objective; T_1, U_1 mirrors.

The conveyor belt

After this brief review of the general design of the transmitter, details of some of the special features will now be given.

As long ago as 1928 Alexanderson endeavoured to realise the scanning principle which we have now adopted [2]), but he employed a rotor with two scanning heads, necessitating a curvature of the copy through 180° at the scanning point. This deformation made it very difficult to keep the documents smooth while in motion and the mechanical methods adopted for this purpose were not very reliable.

The difficulty arising from the transportation of the paper has now been overcome primarily by using three instead of two scanning units, which results in much less deformation of the paper, and secondly by applying a new electrical method of holding the paper firmly against the belt.

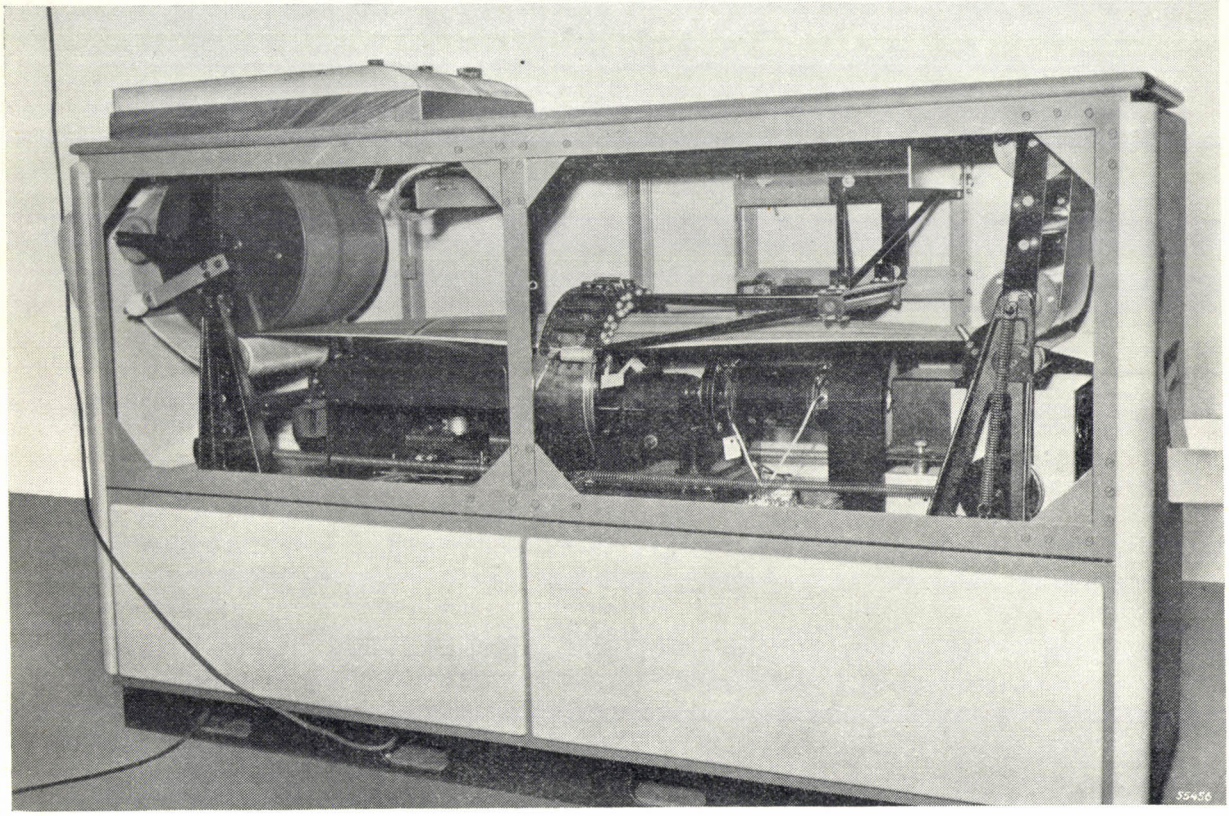
This method is based on the electrostatic attraction that occurs between the two electrodes of a capacitor. The belt itself is made from "Astralon", a

[2]) See e.g. F. Schröter, Handbuch der Bildtelegraphie und des Fernsehens, Springer, Berlin 1932, p. 414.

member of the polyvinychloride family of plastics [3]) that has a high breakdown voltage and an unusually good surface resistance. The belt, 0.5 mm in thickness, functions as a dielectric between a permanently earthed metallic layer on its inner side and the paper, which, although a very poor conductor, may nevertheless be regarded as a conductor for these purposes. The conveyor, with the documents on it, passes underneath and in close contact with an endless belt of brass gauze (see *fig. 3*) which is maintained at a high positive potential (7 to 10 kV) with respect to earth, by a simple high tension unit.

[3]) "Astralon", known also as Igelit MP-A, is a mixed polymerisation product of 80% vinyl chloride, 10% dimethyl maleate and 10% diethyl maleate. It is employed as a substitute for celluloid, to which it bears a very close resemblance, although chemically entirely different.

a)



b)

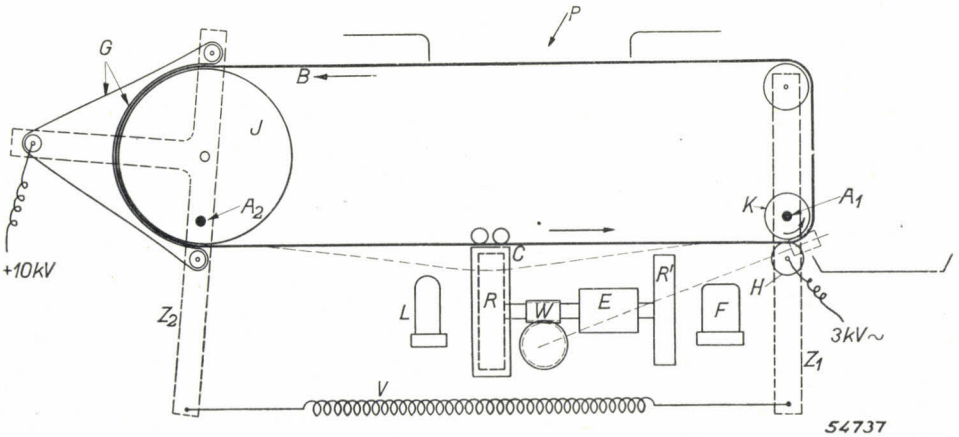


Fig. 3*a*) Photograph of the transmitter, *b*) schematic cross-section. The conveyor belt *B* is driven in the direction of the arrow by roller *K*. The documents are fed onto the belt at *P*. Passing over the drum *J*, the papers run between the belt (which is metallised and earthed on the inside) and a brass gauze belt *G*, maintained at a high potential with respect to earth. Due to the charge thus induced, the papers are held electrostatically to the belt. At *C* the belt curves round the scanning cylinder; the lateral curvature is clearly seen in the photograph (*a*). The documents are discharged by roller *H*, which carries a high alternating voltage; at this point they are therefore released from the belt and drop into a collecting tray. The drum *J* and all the rollers over which the belt runs are carried on two rockers Z_1 and Z_2 which are pivoted at A_1 and A_2; a spring *V* holds the belt taut, thus ensuring uniform movement of the latter at the scanning point. *E* motor driving *R* and *R'* and, through reduction gears *W*, the roller *K*. *L* lamp. *F* photo-electric cell.

During the period (approx. 15 seconds) that the paper is in contact with the brass belt an electrical charge is gradually built up in the paper and on the "Astralon" belt and is retained during the necessary travel of the latter. The paper thus adheres firmly to the belt, so much so, in fact, that a force of 0.5 kg/dm^2 would be required to detach it tangentially. The insulation properties of the paper (in not too humid an atmosphere) are sufficient to prevent the charge from leaking away prematurely towards the earthed scanning cylinder; even the short contact with the latter produces no appreciable discharge.

After passing the scanning cylinder the belt runs between a metal roller H and a driver roller K which carries the belt along by friction, without slip. Roller H carries an alternating voltage of about 3 kV, derived from the high tension unit already referred to and which discharges the capacitor formed by the "Astralon" with its metallisation and the paper document. Once the capacitor has been discharged, the paper drops off the belt at a point beyond H into a collecting tray [4]).

Another great advantage of this fixing method is that the documents are not limited to any particular size; they may be of any length and up to any width not exceeding the width of the conveyor belt itself.

In the process of feeding the documents onto the belt it is possible that the hands may touch it and tend to slow it down. In order to prevent this from producing irregularities in the movement of the belt along the scanning head, all the rollers over which the belt passes are carried by a pair of rockers, pivoted on shafts A_1 and A_2 (fig. 3*b*), the belt being kept taut by a spring between the lower ends of these rockers. If the belt should be retarded at a point P, the roller K can nevertheless continue to pull the belt over a short distance; the extra belt length is ensured by the fact that the left-hand rocker makes a slight clockwise movement. The spring also pulls over the right-hand rocker in the same direction, the part of the belt which is moving towards that side thus remaining taut in spite of the braking effect at P. Since the pivot A_1 is also the shaft of the driving roller K, the latter, however, will retain its position. Consequently the length of belt between the driving roller and the fixed point C where scanning takes place remains constant and, provided that the retardation is not of long duration, the movement of the belt at C remains practically unaffected by the movements of the rockers.

It will be seen that this simple form of compensation is made possible only by the fact that the documents are fed in and scanned at opposite sides of the belt; in other words the documents are scanned whilst they are "suspended". This again illustrates the importance of the very efficient adhesion of the documents on the belt.

The scanning system

The path of the light through one of the scanning units is illustrated diagrammatically in *fig. 4*. In order to ensure a reasonable luminous flux at the photo-electric cell, notwithstanding the small size of the scanning spot of which the reflected light is picked up and in spite of the considerable losses incurred in the complicated path of the light beam, it is essential to employ a luminous source of great brightness and an objective of very high f. number (numerical aperture). The light-source is a projector lamp of 400 W, 110 V, with highly concentrated filament, giving a brightness of 2270 candles/cm^2 (average of the whole area of the filament). A microscope objective of numerical aperture 0.3 is used for projecting the image. The focal distance of the objective is such that, with the sum of object- and image-distance amounting roughly to the radius of curvature of the paper (as governed by the width of the belt), an image of the diaphragm, reduced 4.5 times, is produced on the paper. In view of the required width of 0.2 mm for the scanning spot, the diameter of the diaphragm is thus 0.9 mm, this being a convenient size for manufacture and adjustment.

The objective M serves to concentrate both the incident and the emergent rays. The size of the hole in the mirror (S, fig. 4) determines what part of the objective aperture will be available for each of these two functions; there will obviously be an optimum size for the hole. Let the diameter of the objective be D and that of the hole d; the total aperture is then $A \sim D$, the effective part for the incident light is $A_1 = A \cdot d/D$ and the part for the returning beam $A_2 = \sqrt{A^2 - A_1^2} = A\sqrt{D^2 - d^2}/D$. The luminous flux received by the photo-electric cell is proportional to $A_1^2 \cdot A_2^2$, that is $\sim d^2\,(D^2 - d^2)$, which assumes a maximum at $d^2 = D^2 - d^2$, i.e. $d = {}^1/_2\, D\sqrt{2}$. The hole in the mirror must there-

[4]) This method of discharging, whereby every point of the conveyor belt is successively exposed to an alternating voltage the amplitude of which upon approaching and leaving the roller H subsequently increases from 0 to 4 kV and then decreases back to zero, is somewhat analogous to the well-known manner of demagnetisation of a magnet by means of a decaying alternating current. In this case it is the charged condition of the "Astralon" which is annihilated by the alternating field. It may be noted that the process of "charging" the paper and belt is actually rather more complicated than would appear from this very brief description. Very thin layers of air between the paper and the belt play a very important part, in that they induce a "charge pattern" on the "Astralon" which appears to a great extent responsible for the very considerable adhesion.

fore roughly be 0.7 times the aperture of the objective; the effective numerical aperture of the latter for each of the two functions is thus $A_1 = A_2 = 0.7\,A = 0.21$. (If the reflection from the paper is more or less specular instead of purely diffused, better results are obtained if A_2 is slightly greater than A_1.)

In principle it would be possible to employ a microscope objective having a higher numerical aperture than 0.3, but this has not been done for two reasons: in the first place, with a larger aperture the "image distance", that is the distance from the paper to the face of the objective, between which fact that both the light-source and the photo-electric cell had to be located stationary in the geometrical axis of the rotor, so that they had to be mounted on either side of the motor and reduction gear-box. The aforementioned lenses also seal the cavities in the discs and tend to keep the mirrors etc. free from dust. These discs, rotating at 3600 r.p.m., act in much the same way as a vacuum-cleaner, so that, without obturation, the light received at the photoelectric cell would soon be reduced too much by contamination of the mirrors and lenses.

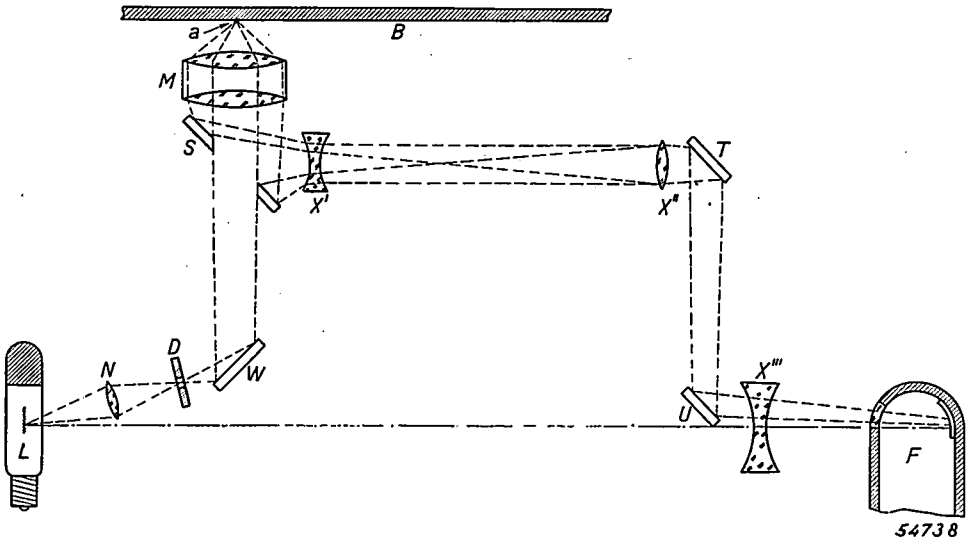


Fig. 4. Path of the light beam in one of the three optical systems in the rotor. L lamp; N condenser (the auxiliary condenser N_0 in fig. 2 is now not shown). D diaphragm; W mirror; S mirror with central hole; M microscope objective; a scanning spot on the conveyor belt B; T and U mirrors; F photo-electric cell. X', X'', X''' lenses to focus the rays and ensure that these are fully received by the mirrors and the photo-electric cell.

the fixed cylinder with its scanning slot has to be mounted, would be rather too small. Secondly, the depth of focus would be reduced. A certain amont of depth of focus is essential in view of the necessary tolerances in the focusing, possible slight eccentricity of the rotor with respect to the cylinder supporting the moving belt, possible vibrations of both these components, or small irregularities in the paper adhering to the belt. Should the distance vary for any of these reasons to the extent of + or − 0.1 mm, the diameter of the scanning spot would increase from 0.2 mm to $0.2 + (2 \times 0.1 \times 0.21) \approx 0.24$ mm at a numerical aperture $A_1 = 0.21$, which may be regarded as permissible.

From fig. 4 it will be seen that the light deflected by mirror S passes through three more lenses; these prevent any spreading of the beam, thus ensuring that it will be entirely intercepted by the mirrors in the rotor and by the photoelectric cell. The relatively great distance between the two rotor discs, necessitating this precaution, is due to the

Let us now approximately calculate the luminous flux Φ received by the photo-electric cell. Let B be the average brightness of the filament of the lamp and F the area of the scanning spot: the luminous flux falling upon that area — ignoring losses in the optical system — is then:

$$\Phi_1 = \pi B F A_1^2.$$

We will assume that the reflection from the paper is wholly diffuse, the reflection factor being r_w at the whitest parts and r_z at the darkest (e.g. those covered by printing ink). Of the luminous flux $r_w\,\Phi_1$ emitted by the white paper within a solid angle of 2π, the objective area available for the return beam receives the fraction $r_w \Phi_1 A_2^2$. If q be the factor by which the light is attenuated due to reflection losses in the optical system, the ultimate luminous flux at the photo-electric cell when white paper is being scanned is given by:

$$\Phi_w = \pi q r_w B F A_1^2 A_2^2.$$

As the light from the lamp has to pass through a total of 20 glass-to-air interfaces in its path to the photoelectric cell, each time with a loss of 4% due to reflection, and is further reflected 4 times at a (metallic) specular surface at an angle of 45°, each time with a loss of 20% due to absorption, q may be calculated to have a value of $0.96^{20} \times 0.80^4 \approx 0.18$. The reflection factor r_w of white paper may be put at 0.85 and that of the blackened parts at about 0.25. Putting: $A_2 = A_1 = 0.21$, $B = 2270$ candles/cm^2 and $F = \pi \cdot (0.01)^2$ sq.cm, the luminous flux will be $\Phi_w \approx 0.70$ millilumens. Scanning of the black portions similarly gives $\Phi_z = \Phi_w \cdot r_z / r_w \approx 0.20$ millilumens.

The photo-electric cell; the signal

By means of a secondary-emission photo-electric cell the very small available luminous flux can be made to deliver a signal of adequate strength relative to the unavoidable "noise" interference; an ordinary photo-electric cell would not be capable of this, as will be explained below.

A standard photo-electric cell of the vacuum type delivers roughly 20 μA per lumen. At the values of luminous flux mentioned above, currents of between 4×10^{-9} and 14×10^{-9} A would have to be handled. In practice, a reduction in the sensitivity of a photo-electric cell in course of time has to be allowed for, whilst the luminous flux itself will also tend to decrease owing to gradual blackning of the projector lamp bulb and accumulations of small quantities of dust etc. on the numerous surfaces of the optical system. Allowing for a suitable safety factor, the operating current should therefore have a value which is a factor of 10 lower, that is between 4×10^{-10} and 14×10^{-10} A for black and white respectively.

By including a resistor $R = 10{,}000\ \Omega$ in series with the photo-electric cell a signal voltage varying between 4 and 14 μV is available for feeding to the input of an amplifier. A noise voltage occurs in the resistor in question the magnitude of which, according to a well-known formula, is expressed as $\sqrt{4kTR \cdot \Delta f}$, where k is the Boltzmann constant, T the absolute temperature and Δf the effective frequency band employed. Since we have to take a value as high as 100 kc/s for Δf (see above), the noise voltage in the resistor will be 4 μV. In the case of the black parts of the document we therefore have a noise signal of the same order as the signal strength desired and this (assuming that the reproduction of half-tones is required) would be intolerable. The position might be improved by using a resistor of a higher value, as the signal increases in direct proportion to R and the noise only in proportion to $\sqrt{R}$. If R is much higher than the above-mentioned value of 10,000 Ω, frequencies in the region of 100 kc/s in the photo-current would, however, be severely attenuated on account of the unavoidable capacitances in parallel with R (e.g. the input capacitance of the first amplifier valve).

The use of a secondary-emission cell greatly improves the situation. Owing to the internal gain in the successive secondary-emission stages very much higher photo-currents are produced; a tube developed by Philips, containing 8 stages and employed in the facsimile transmitter under review, yields a current of 1 A/lumen [5]). For the same resistor in series with the photo-electric cell, and again allowing a factor of safety of 10 for ageing of the tube, reduction of luminous flux etc. (see below), the available signal is 0.2 V for black, so that the noise in the resistor is no longer of any importance. The remaining difficulty is the Schottky effect, that is the fluctation in the emission by the photo-cathode and secondary-emission electrodes, also present in the ordinary type of photo-electric cell, but which could be ignored in that case when compared to the noise originating in the load resistor.

The fluctuation in the electron stream is represented by $1.4p\sqrt{2e I_a \cdot \Delta f}$, where e is the charge of the electron, I_a the current supplied by the photo-cathode and p the internal gain factor of the tube (the factor 1.4 in this expression is applicable to modern types of secondary-emission tubes in which each electron releases an average of 5 secondary electrons). With $p = 50.000$ and I_a (on white) $= 14 \times 10^{-4}$A, the signal current is 70 μA and the ratio of noise to signal approximately 0.007, which is quite reasonable (43 db). There is also the advantage that when the luminous flux decreases the noise-to-signal ratio increases only in proportion to $\sqrt{I_a}$ (in the case of noise due to the resistor the proportion is $1/I_a$!). On black, too, the amount of "noise" is very small, being only 1% of the signal. This means that variations in the density of the reproduction due to this noise are hardly perceptible even in the black parts where they are proportionally greatest.

The above-mentioned sensitivity of the secondary-emission cell (1A/lumen) requires a potential of about 150 V per stage and this, in the case of a

[5]) A description of a secondary-emission photo-cell is given in Philips Techn. Rev., 3, 138, 1938. At the time a magnetic field was employed for focusing the electrons onto the successive secondary-emission electrodes, but nowadays electrostatic focusing is preferred, as being the simpler method.

new light-source and freshly cleaned optical system, with new valves in the amplifier and so on, will give a signal of from 2 to 7 V. In actual practice the tube is so adjusted that, with the equipment in the new condition, the signal is reduced to the previously mentioned level, i.e. 10 times lower, by reducing the sensitivity of the secondary-emission cell. This is effected merely by reducing the voltage applied per stage. As soon as the equipment shows signs of ageing the signal can be restored to the original level by raising the voltage on the photo-electric cell. A control knob, with meter for measurement of the signal, is fitted to the exterior of the equipment for this purpose.

An oscillogram of the signal as produced by the transmitter when scanning typescript on white paper is reproduced in *fig. 5*.

The commencement of each line is indicated by an extra high voltage peak (whiter than white) and the end of the line by an extra low value. The first of these impulses is used for synchronisation of the receiver, whilst the combined impulses — as will be explained in the fourth article in this series — ensure that the various tones are all faithfully reproduced at the receiver. This is rendered possible by ensuring that the amplitude of these impulses is constant; in fact this amplitude corresponds to 110% and 0% reflection respectively. These impulses are generated optically by the scanning spot, which, just before striking the conveyor belt and immediately after leaving it, passes two areas the reflection from which effectively gives these two values. The area that gives "110% reflection" is a frosted aluminium plate. Obviously this plate cannot reflect 110%, but the more or less specular reflection (which does not conform to Lambert's law) results in a luminous flux through the part of the objective available for the return beam, which is just as great as that which would be supplied to it by a perfectly diffuse surface capable of reflecting 110% of the light falling upon it.

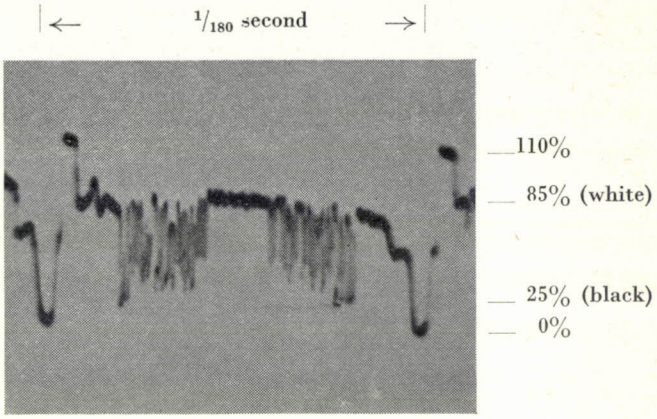


Fig. 5. Oscillogram of signal generated by the transmitter when scanning a typewritten letter: the levels corresponding to black and white are shown at the right. The periodic impulses of extra high and extra low amplitude (equivalent to 110 % and 0 % reflection respectively) provide a density reference scale and permit synchronisation of the receiver with the transmitter.

EXPERIMENTAL TRANSMITTING AND RECEIVING EQUIPMENT FOR HIGH-SPEED FACSIMILE TRANSMISSION

III. DETAILS OF THE RECEIVER

621.397.62

by F. C. W. SLOOFF *), M. VAN TOL and J. M. UNK *).

In the Philips high-speed facsimile transmission system the signal received, the strength of which varies according to the light and shade of the image being scanned, is employed at the receiver to control the current flowing in a gas-discharge lamp. The varying amount of light from this lamp is projected in the form of a spot onto a film by an optical system rotating in synchronism with the rotor of the transmitter. The film is curved to the cylindrical shape of the rotor and passes the latter continuously, so that the light spot traces on it parallel lines exactly corresponding to the scanning lines at the transmitter. Owing to the very high resolving power of the positive film used, the image can be reproduced in the receiver at 1/6th of the original size, with consequent economy in film. To this end, the diameter of the rotor is only 1/6th the diameter of the rotor at the transmitter, and the recording spot is similarly one-sixth the size of the scanning spot (i.e. 33 μ). In this case, too, the rotor carries three identical optical systems and the film is curved only through 120°. Tolerances governing the relative position, size and intensity of the spot in the three optical systems are essentially very small and extreme precision in manufacture of the rotor and in assembly is necessary. Whereas in the case of the scanning spot at the transmitter a circular form is the most suitable, a substantially rectangular shape is better for the recording spot. This is produced by focusing onto the film the image (reduced 4×) of a rectangular diaphragm having all four sides adjustable. The lamp, which is capable of following modulating frequencies up to 100 kc/s and the luminous intensity of which is sufficient to produce a density of 1.5 on the film in 5 μsec, is a gas-discharge lamp filled with mercury vapour and argon at low pressure. The discharge is concentrated within a tube 1 mm in width. A steady current flows through the lamp to assist it in following the necessary high modulation and to give the light-versus-current characteristic the desired form for linear reproduction.

The mechanical features of the Philips high-speed facsimile transmitter have been described in a previous article [1]), and here the mechanical and optical details of the receiver will be reviewed.

General arrangement of the receiver

The type of signal supplied by the transmitter is depicted in fig. 5 of the previous article. In the receiver this signal, suitably amplified, is applied to a lamp specially developed for the purpose and with a luminous intensity capable of keeping in step with every variation of the signal strength. The light from this lamp is used in conjunction with an optical system to provide a recording spot which is synchronised with the scanning spot at the transmitter (i.e. at the same speed and in phase) and traces a succession of straight contiguous lines on a strip of light-sensitive material, thus exposing the latter to a degree determined by the instantaneous values of the signal strength.

The transmitter scans 180 lines per second and each line, 22 cm in length, comprises 1100 image-elements of the size of the scanning spot (0.2 mm dia.). The receiver, therefore, must be capable of reproducing 180 × 1100 image-elements per second, each with its own individual density, which means that only 1/200,000 sec. is available for the exposure of the sensitized film for each elemental area corresponding to a similar image-element in the original.

Although the luminous intensity of the recording lamp cannot be increased to a very high level, since this would interfere with its ability to be modulated up to 100 kc/s, and although the focal aperture of the optical system in the receiver, like that of the transmitter, is limited by requirements relating to depth of focus and image distance, it has nevertheless been found possible to ensure sufficient density within the very short time available by using ordinary positive film as recording material.

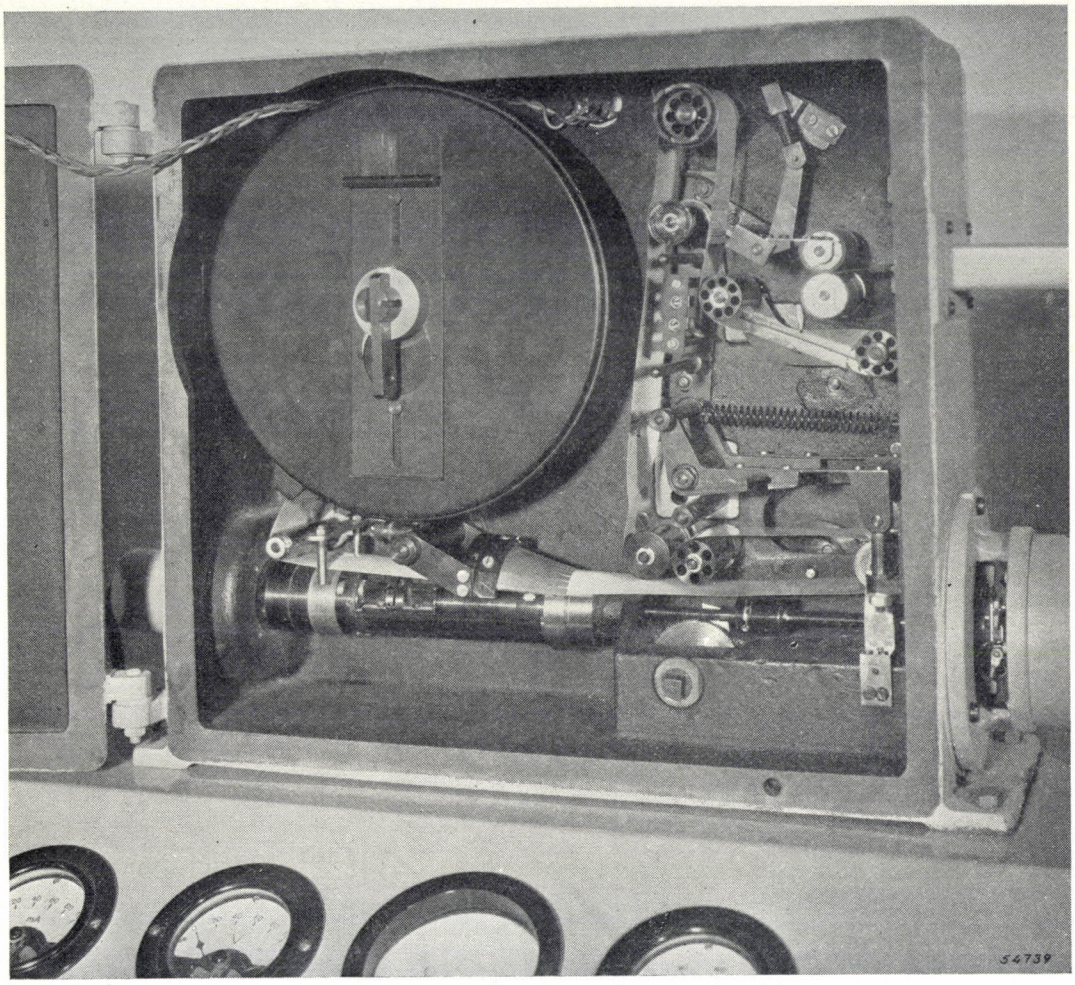
This material is certainly more costly than the recording paper used in the slower types of facsimile equipment. The resolving power of the film (55 lines per mm) is, however, very much higher than is necessary for a scanning and recording spot of 0.2 mm. The receiver is therefore designed to work with a light-spot 1/6th of the size and to give a reproduction 1/6th (linear) of the size of the

*) N.V. Philips' Telecommunicatie Industrie (formerly N.S.F.), Hilversum.

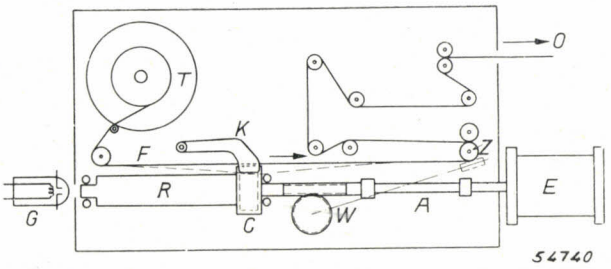
[1]) D. Kleis, F. C. W. Slooff and J. M. Unk, Details of the transmitter, Philips Techn. Rev. **10**, 257-264, 1949 (No. 9).

original document. The consumption of film is thus reduced to 1/36th of what it would otherwise be and the cost is therefore of very little importance.

The actual construction of the receiver is similar to that of the transmitter; see *fig. 1*. A 45-mm film continuously passes through the machine and at a given point is curved around a cylinder the radius of which is only 1/6th of that of the scanning cylinder at the transmitter. A rotor mounted coaxially in this cylinder and revolving in synchronism with the transmitter rotor at 3600 r.p.m. carries three identical optical systems, spaced at 120°. Each of the latter contains a diaphragm illuminated by the lamp, which is stationary in the axis of the rotor. An image of this diaphragm, 33 microns in size, is projected onto the film as the recording



a)



b)

Fig. 1. *a*) The receiver with cover open. *b*) Schematic cross-section. The rotor *R* and the stationary recording cylinder *C* are 1/6th the diameter of the corresponding parts of the transmitter. The 45 mm film *F* from the spool *T* is curved over the cylinder *C* by a specially shaped spring: at this point a light-spot 33 μ in width produced by the optical system in the rotor and originating in a gas-discharge lamp *G*, which is modulated by the incoming signal, traces parallel lines on the film. The rotor driven by motor *F* by means of a flexible shaft *A* is synchronised with the rotor of the transmitter. Roller *Z* pulls the film through the machine and is coupled to the motor by a reduction gear *W*. At *O* the film passes into a tank where it is automatically developed and fixed.

spot. The movement of the rotor causes each of the light-spots from the three optical systems to trace a line 33 μ in width across the surface of the film. The rotor and the film-feed mechanism are coupled together by suitable gearing to give a rate of feed of film equal to 1/6th of the speed of the conveyor belt in the transmitter, that is 33 μ per line or 6 mm per second. The film spool contains about 120 metres of film, sufficient for recording 2400 documents of quarto size, without interrupting the operation, covering a total working period of $5^1/_2$ hours.

The exposed film is developed and fixed continuously and automatically in a developing tank mounted on the receiver. Subsequently each document recorded on the film can be immediately enlarged to the original size. As each document can be exposed as a whole, exposure times of a few seconds can be applied. Moreover the lamp employed for the purpose may be of high intensity, so that the film can be enlarged on ordinary photostat paper.

In principle, any one of three different methods could be used for the enlarging process, viz:

1) to run the film through the enlarger continuously together with a strip of printing paper;

2) to project the documents one by one on separate sheets of paper, compensating the continuous movement of the film in the usual manner by means of a moving optical system;

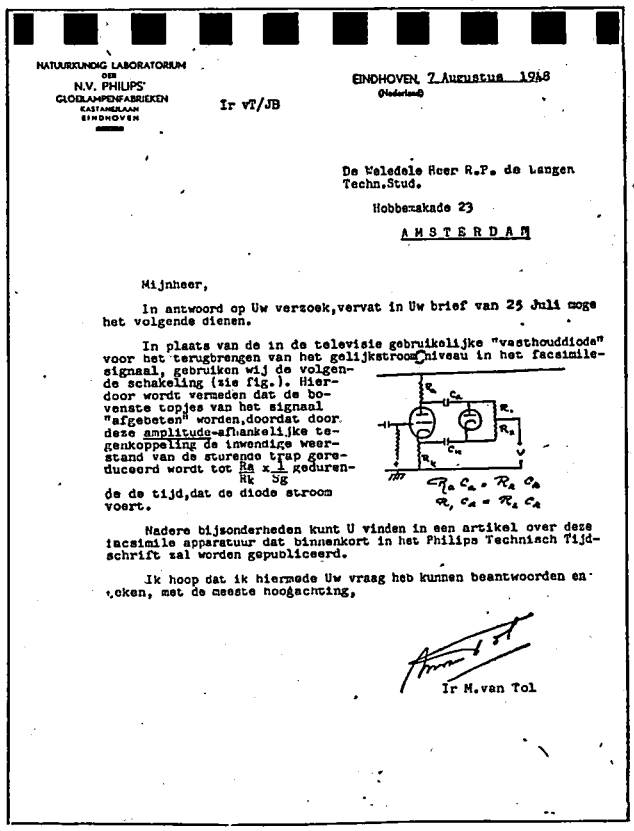
3) as 2), but in this case the compensating optical system can be dispensed with by feeding the film through the enlarger intermittently instead of continuously.

If the latter method is to be fully automatic, some form of mechanism is required to ensure that the film moves forward each time at the commencement of each document, even though the original documents may not be fed into the transmitter at regular intervals; this could be effected by various means suited to the particular purpose for which the high-speed facsimile system is to be used. For the transmission of letter post the following system has been evolved. A row of equally spaced black squares is printed at the top of each letter in the manner shown in *fig. 2*. Scanning of these produces a periodic signal at a frequency of 4 kc/s of about $^1/_3$ second duration, and this signal energizes a tuned circuit in the receiver, arranged so as to operate with a suitable delay and this in turn operating a punching mechanism via a relay. In this way a hole is punched in the film to register the commencement of each separate communication. (The method of perforation does not affect the movement of the film at the recording point.) When the film is approaching the printing machine the punched holes in it serve to control the click-mechanism on the film drive by means of a "feeler".

A brief survey of some of the other features of the equipment may be of interest.

The recording lamp

The problem of modulating a beam of light at high frequency is encountered not only in facsimile transmission but in many other spheres as well, e.g.


NATUURKUNDIG LABORATORIUM
DER
N.V. PHILIPS'
GLOEILAMPENFABRIEKEN
EINDHOVEN

Ir vT/JB

EINDHOVEN 7 Augustus 1948
(Nederland)

De Weledele Heer R.P. de Langen
Techn.Stud.
Hobbemakade 23
AMSTERDAM

Mijnheer,

In antwoord op Uw verzoek, vervat in Uw brief van 25 Juli moge het volgende dienen.

In plaats van de in de televisie gebruikelijke "vasthouddiode" voor het terugbrengen van het gelijkstroomniveau in het facsimile-signaal, gebruiken wij de volgende schakeling (zie fig.). Hierdoor wordt vermeden dat de bovenste topjes van het signaal "afgebeten" worden doordat door deze amplitude-afhankelijke tegenkoppeling de inwendige weerstand van de sturende trap gereduceerd wordt tot $\frac{Ra}{Rk} \times \frac{1}{Sg}$ gedurende de tijd, dat de diode stroom voert.

$R_a C_a = R_s C_s$
$R_1 C_2 = R_2 C_2$

Nadere bijzonderheden kunt U vinden in een artikel over deze facsimile apparatuur dat binnenkort in het Philips Technisch Tijdschrift zal worden gepubliceerd.

Ik hoop dat ik hiermede Uw vraag heb kunnen beantwoorden en teken, met de meeste hoogachting,

Ir M.van Tol

Fig. 2. When the facsimile equipment is to be used for letter post a row of black squares is printed at the top of each letter head. The signal generated by scanning these squares operates a punching mechanism in the receiver which pierces a hole in the film at the proper point. By this means the subsequent movement of the film is made to control a click-mechanism and to register the film correctly for each enlargement separately.

in television, light-beam telephony, etc. This problem has been solved in different ways to suit the various well-known requirements, either by using a constant light-source in conjunction with an optical device of which the transmission factor is varied mechanically or electrically (as in the Kerr cell), or, again, by direct modulation of the power supply of different types of light-source such as in an incandescent lamp, a gas-discharge lamp or a cathode-ray tube. A modulated incandescent lamp or a gas-discharge lamp provide simple solutions, but owing to the thermal inertia of the filament an incandescent lamp is not suitable for modulation frequencies of 100 kc/s. A specially designed gas-discharge lamp, however, has been found capable of fully meeting these modulation requirements.

Before going into details it will be useful to mention one or two other requirements entailed in the design of this part of the equipment. The brightness of the discharge must be high enough to produce on positive film a density [2]) equal to 1.5 or

[2]) This is $\log I_0/I$ when the portion I of the luminous flux I_0 falling upon an exposed film is transmitted.

rather more if possible in the exposure time of 5 μsec. Further the light beam has to be constant over a sufficiently wide angle in order to fill the rotating optical system with light, without necessitating large distances between lamp and rotor (or a very long rotor; see below). For practical reasons the required currents and voltages must not be too high and, finally, the characteristic (relation between luminous intensity and current or voltage) of the recording lamp must conform to certain other requirements.

Effective modulation of the beam can be expected only from a discharge lamp having a comparatively low gas temperature. In the case of an elevated gas temperature such as usually accompanies high gas-pressures and which, it is true, is very advantageous from the point of view of a high luminosity (high-pressure and super-high-pressure mercury vapour lamps), the thermal inertia is usually so great that the emission of light is unable to follow closely any rapid variation in the applied power. One way of obtaining a gas discharge at a low temperature, but nevertheless with a very high brightness is to concentrate the so-called positive luminous column in a very narrow tube (nozzle) and use the light emitted in the longitudinal direction, this being the principle of Ewest's "Lichtspritze" [3]). In this type of lamp the anode, in the form of a ring, is placed in front of the nozzle mentioned above; the use of an incandescent cathode ensures relatively low ignition and working potentials, with long life. Existing types have proved capable of modulation up to 15 kc/s and of producing the desired density on film in about 100 μsec.

The lamp developed by Philips is based on similar lines. Modulation is effected by varying the current. A few details of the methods employed to obtain the required higher brightness and better modulation response may be of interest.

Concentration of the luminous column within a nozzle of very small dimensions not only increases the brightness but also the modulation response. This will be appreciated when it is considered that there will be little inertia in the discharge if a surplus of ions can disappear quickly and a shortage of ions can quickly be made good by new ones. For the disappearance of ions a short transit time between the electrodes, that is a short discharge path, is necessary. The recombination of ions, which also assist in eliminating any surplus, can be promoted by reducing the diameter of the nozzle, due to the fact that recombination takes place mainly at the walls, whilst the ratio of wall-area to volume is inversely proportional to the diameter.

For the highest possible modulation response, therefore, a reduction of the cross-sectional area of the nozzle and of the length of the discharge is the solution. At a certain point, however, these conditions will conflict with the requirement that the brightness must also be high. Light being emitted longitudinally, it is evident that any reduction in the length of the discharge must have an adverse effect on the brightness (selective absorption is of minor importance at the low gas-pressures in question). For a given diameter d the nozzle therefore has to be of such a length as to furnish the required width of beam (relation of diameter to length of the nozzle). Similarly, regarding the effect of the diameter the modulation response and brightness are no longer proportional to each other when a certain point is reached, since the current density in the nozzle is limited by the admissible temperature of the wall. For a given wall temperature and angle of emission, a rough calculation will prove the brightness to be $\sim\sqrt{d}$ and the necessary current $\sim\sqrt{d^3}$. As soon as the permissible wall temperature is reached any increase in brightness therefore actually demands a larger diameter of the nozzle. In that case, however, the required power of the source of current, which following on the above increases directly as the third power of the brightness, must also be taken into consideration.

Another important factor in the design of the recording lamp by means of which the modulation response as well as the brightness can be effected is the choice of gas-filling. Both these properties appeared to be very suitable when the lamp was filled with a mixture of argon and nitrogen at a few millimetres mercury-pressure. Theoretical considerations may well explain that a good modulation response is thus obtained: both argon and nitrogen particles are relatively light and thus involve only short transit times. Moreover, it appears to be important that by colliding with nitrogen molecules, metastable, excited argon atoms, which owing to their long life would delay and therefore unfavourably influence the modulation response, can lose energy. From the aspect of spectral distribution of the light emission, too, an argon-nitrogen mixture is favourable, as the emission is preponderantly blue and violet, these being the colours to which positive film is most sensitive. However, a well-known disadvantage of this gas mixture of a gas discharge in which the current density is high is that in the course of time the nitrogen disappears

[3]) H. Ewest, Z. Techn. Phys. 12, 645, 1931.

from the mixture, presumably through its combining with the cathode metal to form a nitride.

Excellent results, without disadvantages, are obtained with a mercury-vapour discharge at very low pressure, containing argon to keep the ignition voltage down to a low value. Theoretically the modulation response will not be so good as in the case of the gas-filling previously mentioned, since the heavy mercury atoms require much longer transit times. This has been confirmed in practice, but it has nevertheless been found possible to obtain the desired modulation up to 100 kc/s with adequate brightness [4]) (argon-nitrogen mixtures actually made it possible to record modulation frequencies up to 300 kc/s). This result is partly due to the dimensioning of the nozzle, which approximates the optimum compromise, viz. 1 mm wide and 5 mm long with anode and cathode as close as possible to the ends of the nozzle. Good modulation response is partly due to the fact that a certain steady current is allowed to flow through the lamp even in the absence of signals, thus ensuring a reserve of ions which enables the formation of the required fresh ions to take place much more rapidly when the signal increases from zero than if the discharge were completely extinguished.

The relation between the luminous intensity and the lamp current is by no means linear, as might be considered desirable at first sight. In practice, however, this is not a disadvantage, but even an advantage, since it partly assists in compensating for the very pronounced non-linearity in the density curve of the positive film in question. In connection with this, the actual value of the steady current of the lamp is of special importance. The density of the enlarged print made from the film negative can in this way be made to approximate very closely the density of the original document, which is the essential requirement for a true reproduction of half-tones. If the facsimile apparatus were to be used only for the transmission of black-and-white images the characteristics of the lamp used would not be very important; the only requirement would be a sufficiently high intensity to expose the film to the necessary degree for the black part of the image.

A further advantage of the mercury-vapour filling is that the maximum luminous flux required is attained for a current of only 70 mA (at a working voltage of 30 V), so that it is possible to feed the lamp from a single output valve of the EL 6 type (argon-nitrogen necessitates three of these valves in parallel).

The design of the lamp used is shown in *fig. 3a*, whilst a photograph of the lamp is given in fig.3*b*.

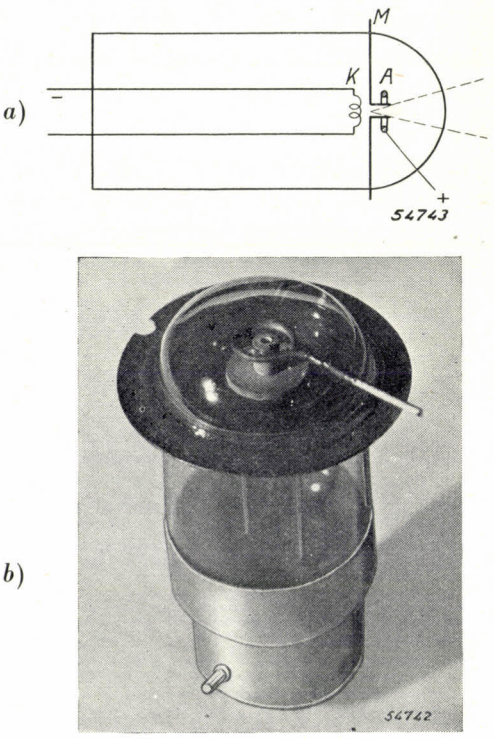


Fig. 3. *a*) Schematical cross-section, *b*) photograph of the lamp. A concentrated discharge of relatively high brightness occurs in the narrow tube nozzle between the cathode and the annular anode *A*. Due to the carefully proportioned system of electrodes, the luminous flux is capable of responding accurately to current modulations up to 100 kc/s. The tube is mounted on a molybdenum disc *M*, which also serves for alignment purposes.

To prevent the discharge from taking any path other than through the nozzle the latter is fixed to a molybdenum disc sealed into the glass bulb and dividing the lamp into two separate compartments for the anode and cathode, the connection between these compartments being formed by the nozzle. At the same time this molybdenum disc, which projects outside the wall of the bulb and which can be manufactured with a high degree of precision, facilitates centring of the light-spot exactly in the axis of the rotor in the receiver.

The optical system of the receiver

Fig. 4 is a cross-sectional diagram of the rotor, showing details of the optical system. A set of three mirrors (S_1) arranged around the axis of the rotor transmit radially three beams of light from the stationary lamp at angles of 120°. Each beam is then deflected in a direction parallel to the axis by

[4]) The spectral distribution of the light of the mercury discharge is in fact even more favourable than that of argon-nitrogen.

another mirror (S_2) and is concentrated by a condenser onto a diaphragm. A microscope objective of numerical aperture 0.3 then throws a 4 times reduced image of the diaphragm via a final mirror (S_3) onto the film.

The numerical aperture of the objective, which together with the brightness of the lamp determines the luminous flux of the light-spot, was not made larger for the reason already given in connection with the transmitter, i.e. the distances must not be too small as otherwise the depth of focus will be insufficient. To manage with the same depth of focus as in the transmitter, the absolute tolerances in eccentricity of the rotor or cylinder, vibration etc. are only 1/6th of those which are admissible in the transmitter, in view of the corresponding reduction in size. In fact these tolerances have to be even closer, since fluctuations in the size of the spot in the receiver are more troublesome than in the transmitter; variations of as little as 20% will give the image a badly striped appearance. The relative dimensions of the three light-spots therefore must not differ more than about 6 microns, and similarly tangential or axial discrepancies in the location of the spot must not exceed 6 μ. Irregularities in the motion of the film and axial movement of the rotor are subject to the same tolerance. The luminous flux of the three light-spots individually must not differ more than 10%.

To satisfy such requirements it was necessary to maintain a degree of precision in the manufacture of the rotor approaching the limits of practical achievement [5]). All the lenses and mirrors as well as the diaphragms are adjustable, so that the proper location, size and brightness of each of the light-spots can be adjusted individually. Axial movement in the rotor is restricted to the necessary degree by carefully machined thrust bearings at each extremity, whilst, moreover, the rotor is protected from vibration as much as possible by coupling it to the motor by means of a flexible shaft. Uniformity in the movement of the film is maintained by keeping it taut between the recording cylinder and the driving roller. An advantage in using film is that it can be easily curved to make close contact with the cylinder; this is effected by means of a curved spring.

At this point the reason for a reduction factor of only 4 being chosen for the projection of the diaphragm onto the film will become clear. A larger factor would have been more convenient from the point of view of handling the diaphragm (now only 0.13 mm in width), but this would have necessitated a longer light path and therefore a longer rotor, which in turn would have increased the problem of the bearings and the suppression of vibrations.

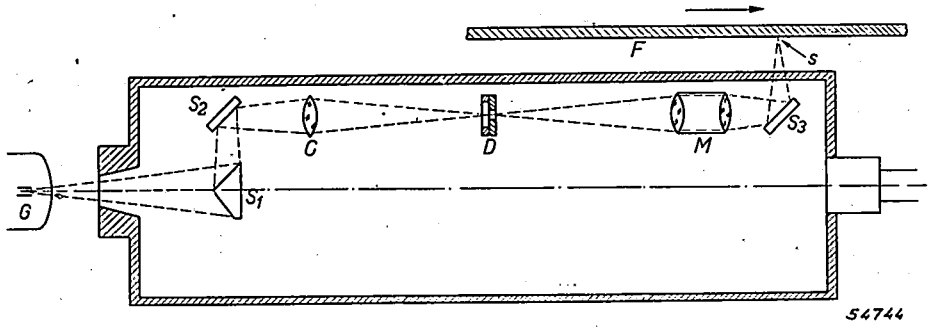


Fig. 4. Diagram of one of the three optical systems in the rotor. G stationary recording lamp; S_1, S_2 mirrors; C condenser; D diaphragm; M microscope objective; S_3 mirror, s recording light-spot on the film F.

From the known reduction in the size of the image in the diaphragm it is a simple matter to determine the aperture of the beam of light from the lamp, to which reference has frequently been made in the text. In order to fill the objective with light, the angle β in *fig. 5* must be made at least equal to angle α as determined by the reduction factor and the numerical aperture of the objective. It is advisable to have an image

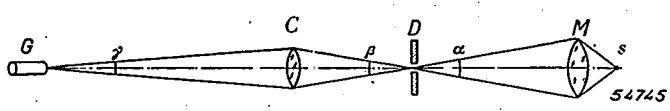


Fig. 5. The light-path in one of the three optical systems, from the light source G to the recording light-spot s, determining the conditions governing the aperture γ of the light beam. C condenser; D diaphragm; M objective.

of the light-source as formed in the diaphragm by the condenser, with a diameter of approximately 0.5 mm in order to allow sufficient latitude in the location of the diaphragm. The diameter of the nozzle of the recording lamp is 1 mm, so the image of it produced by the condenser must be reduced 2 times, from which it follows that $\gamma \approx {}^1/_2\,\beta$, that is $\gamma > {}^1/_2\,\alpha$. A larger aperture is advantageous, other things being equal,

[5]) Acknowledgements are due to Mr. H. Grandjean Perrenod-Comtesse of N.V. Philips' Telecommunicatie Industrie, who played a very active part in the mechanical construction of the rotor and other parts of the receiver, notably the above-mentioned punching device.

and the distance between light-source and condenser and between the latter and the diaphragm (which also determines to some extent the length of the rotor) can then be made smaller.

The shape of the recording spot at the receiver and of the scanning spot at the transmitter

To avoid a striped appearance of the image the lines traced by the three light-spots must not only be actually contiguous but each line, measured across its width, must be of equal density. The

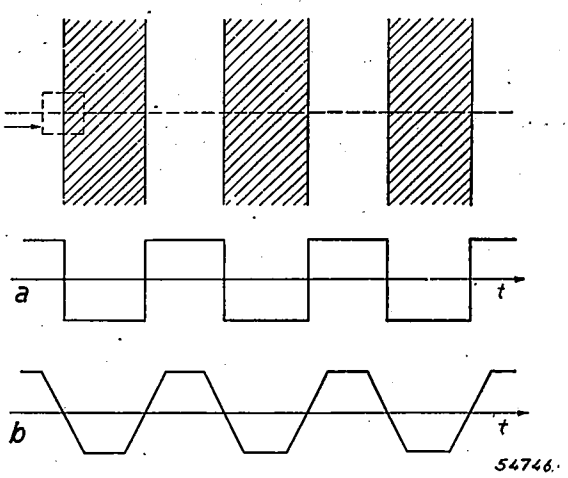


Fig. 6. *a*) Idealised signal supplied by the transmitter when scanning a black and white grid. *b*) Pattern produced on the film by modulation of the luminous intensity of the receiving lamp, in accordance with (*a*). Owing to the finite width of the recording spot the boundaries between the black and white lines of the grid as reproduced are not sharply defined.

light-spot, therefore, must not be round but rectangular. Of course the most obvious shape would hen be square, but this does not actually give the best results. Suppose that the transmitter is scanning a grid of black and white lines, which in the idealised case would give a signal consisting of pure square waves, see *fig. 6a*. The recording spot will vary in brightness in an exactly similar manner, but owing to the finite length of the spot in its travelling direction the transition between black and white will be blurred (fig. 6*b*). In order to limit this effect the longitudinal dimension in question is made slightly smaller than the width, viz. in the ratio of about 2 : 3. The spot cannot be made much shorter as this would reduce the exposure time at each point on the film below the required level.

If the exposed lines on the film, the centre distances of which are 33 μ, are to be really contiguous, the image of the diaphragm must be slightly less than 33 μ in width; scattering of the light in the film then ensures an effective width of spot of exactly 33 μ,

It must of course be possible to adjust the three diaphragms in the prescribed form and, further, to render each one displaceable as a whole. Each of the diaphragms therefore comprises the aperture between four blades, all lying in the same plane and each one capable of a small amount of adjustment in this plane.

In this connection it should be realised that the requirements imposed by the scanning spot in the transmitter are very different from those to which the recording spot in the receiver must conform. The function of the former is merely to make possible the measurement of the local "blackness" of the document or, in fact, its average value within an area equal to the smallest detail to be transmitted, i.e. a square of 0.2 mm × 0.2 mm. Since we are prepared to accept the fact that no detail will be distinguishable within an area of that size, it is also permissible in principle to assume that the density is uniform within that area. It therefore makes very little difference if the scanning spot covers slightly less than the whole area. In the transmitter it is thus quite permissible to employ a circular spot, which involves much less difficulty in manufacture than the rectangular form. Curiously enough it can be shown that, as far as the scanning spot is concerned, a circular form is actually better for the purpose than a square (or rectangular) form. Let us once more assume the transmission of a black and white grid, in which the width of the lines is equal to the resolving power of the scanning spot (i.e. its "longitudinal" dimension). The resultant signal will not be of rectangular wave-form as argued above, but in the case of a rectangular spot will be triangular or "saw-toothed", see *fig. 7a*, for when the light-spot

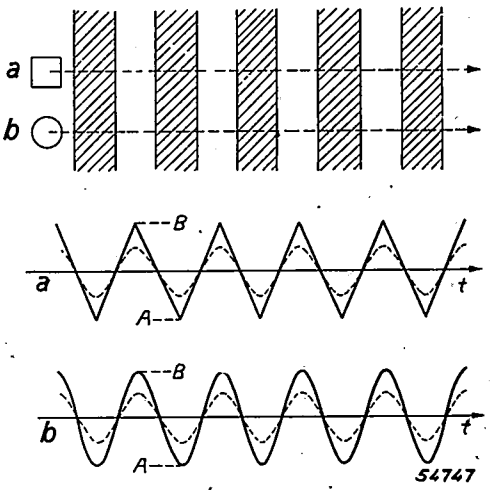


Fig. 7. *a*) Signal produced by the transmitter when scanning a grid as shown, using a rectangular scanning spot (length of spot equal to the width of the grid lines). *b*) The same as applied to a circular scanning spot (diameter equal to the width of the grid lines).

moves from a black line to a white one the increase in that part of it which is filled with "white" is linear with time, hence the increase in signal strength is linear from the lowest value (A in the black) to the highest (B in the white). The boundaries between the black and white lines will therefore be reproduced with a lack of definition even if there were no blurring effect caused by the recording spot at the receiver. In the case of a circular spot, however, the luminous flux intercepted in the scanning of the grid follows the sinusoidal (dotted line) curve shown in fig. 7. It is true that the slope at the steepest parts of the gradient, which determines the extent of the blurring, is then exactly the same as in the case of the saw-tooth characteristic, but as the levels of black and white (A and B respectively) must be the same in both cases, after amplification the curve takes the form shown in fig. 7*b*, from which it will be seen that the slope is now much steeper than that of the saw-tooth curve. The round scanning spot, therefore, ensures better definition.

These considerations apply only where the satisfactory reproduction of half-tones is concerned; for purely black and white images a different method of amplification is employed and the circular scanning spot no longer has any advantage over the rectangular. In this case the signal is actually cut off sharply at top and bottom after suitable amplification and the arbitrary cut-off levels are employed as "black" and "white" respectively. This, however, brings us into the province of the electrical circuits, which are to be reviewed in the following article.

GLASS TRANSMITTING VALVES OF HIGH EFFICIENCY IN THE 100 Mc/s RANGE

by E. G. DORGELO.

621.385.13:621.316.615

A new series of glass transmitting valves introduces a reversion from the flat type of electrode to the older arrangement of concentric cylindrical electrodes. A number of reasons are given for the change, based on electrical, mechanical and thermal considerations. Apart from the cylindrical arrangement of the electrodes, the more outstanding features of the new valves are a spiral cathode of thoriated tungsten, a non-emissive grid, a graphite anode with horizontal cooling fins in the form of a cotton-reel, and a shield to reduce the temperature of the bottom edge of the envelope and the base (thus keeping the electrical insulation high), the whole being assembled in an "all-glass" envelope, without the usual moulded base. In the triodes this shield is connected to the grid, enabling the valves to be employed in grounded-grid circuits without neutrodyne even at 200 Mc/s. In the tetrodes this shield is attached to the screen-grid, and neutrodyning is necessary only at frequencies above 100 Mc/s (approx). Various details are given of the triode TB 2.5/300 and the tetrode QB 2.5/250 (anode dissipations 135 and 125 W respectively). At 100 Mc/s the efficiency is still 70 to 65%. Similar valve types for higher power are in course of development.

Comparison between the cylindrical and flat types of electrode system

The very oldest types of transmitting and receiving valves were usually made with a straight filament as cathode, with coaxial, cylindrical [1]) grid and anode.

At a later stage the single filament was extended to a number of wires, all suspended in the same plane and surrounded by a flat grid and also a flat anode. The reason for this development was a desire to obtain a characteristic (anode current as a function of the grid voltage) with the highest possible slope. This arrangement necessitated a longer cathode, and by designing a filament in the form of a flat zig-zag with one face of the grid on each side of it a form of construction resulted which ensured mechanical rigidity as well as an enhanced effect of the grid potential on the anode current.

In recent years, however, there has been a growing tendency to revert to the original cylindrical construction, though in a modernised form. The fact that this does not adversely affect the slope of the characteristic is mainly due to the improved assembly methods, which have led to a considerable reduction in the space between grid and cathode.

We shall now briefly analyse the reasons for this change in policy, under the headings of electrical, mechanical and thermal considerations.

Electrical advantages of the cylindrical electrode system

a) Let us first compare the potential distribution, in the direction from grid to anode, in a valve having cylindrical, coaxial electrodes with that in one having flat electrodes, for the same potential difference and equal spacing of the electrodes. In the cylindrical system the potential increases more rapidly than in the flat system; it follows that the electron transit time in the former must be shorter than in the latter, for the electrons more rapidly acquire velocities approaching the final velocity (which is determined solely by the potential difference between anode and cathode). This immediately gives the cylindrical arrangement the advantage, since the transit time, when it becomes comparable with the oscillation time, reduces the efficiency.

b) In the cylindrical construction the current density is highest at points close to the cathode and decreases as the distance from the cathode becomes greater. Owing to this an undesired effect, namely a decrease in the space-potential, is not so pronounced, as will be seen from the following.

In high-frequency transmitting valves the lowest possible capacitance between grid and cathode is essential. Moreover, as already stated, the electron transit time in this part of the discharge space must be short. This implies that there must be small cathode and grid areas and also short distances between these electrodes, resulting as a matter of necessity in high values of the current density within the space in question. When flat electrodes are employed the electron paths are parallel and the current density in the grid-anode space is also high; in this region it tends to produce a local decrease in the space-potential (when the latter drops to zero we speak of a "virtual cathode") which causes part of the electrons to be thrown back. The grid current then rises at the cost of the anode current. The effect in question is less evident

[1]) In the following the term cylindrical is to be understood in the limited meaning of rotation-symmetrical.

in a valve having cylindrical electrodes, where the electron paths diverge and the current density in the grid-anode space is accordingly lower than between cathode and grid.

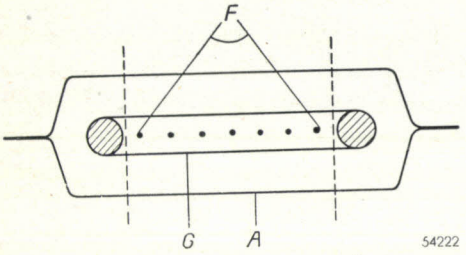


Fig. 1. Cross section of a triode with flat electrode system. F = filament, G = grid, A = anode. Only that part of the electrodes between the dotted lines is effective; parts outside that area add to the stray capacitances.

c) In the flat system of electrodes, a plan view of which is depicted in *fig. 1*, the effective part of the system lies within the area between the dotted lines; the parts outside those limits have an adverse effect, owing to their relatively large contribution towards the inter-electrode capacitances and also to the longer transit time of electrons which have penetrated to those outlying zones. With the cylindrical construction there are no such zones.

Mechanical advantages

A second group of advantages of the cylindrical arrangement is mainly to be found in the mechanical features.

d) In directly-heated transmitting valves the cathode often consists of a tungsten filament to which a small percentage of thorium oxide has been added [2]). To ensure a high specific emission the filament is heated during the manufacturing process in a gas containing carbon, thus producing a superficial layer of tungsten carbides [3]).

It is a well-known fact that such carburized filaments are not strong mechanically, owing to the brittleness of the carbide layer, in which cracks very easily occur and lead, in turn, to internal fracture. Risks of filament breakage can be considerably reduced by employing a spiralised filament, since a spiral can easily withstand small variations in length as well as lateral displacement.

Although in principle it would be quite possible to arrange a number of spirals in a row, i.e. in one plane, the more obvious solution is to employ a cylindrical configuration. In that case it is usual to assemble two (or more) spirals on the same cylindrical plane (see *fig. 2*), with the top ends of the spiral attached to a robust axial support, this arrangement being very resistant to shocks.

The springs usually employed to keep the straight filament taut are then not necessary, and this eliminates also the extra capacitance normally introduced by such springs, as well as the often complicated discs of insulating material required to hold the springs in position and insulate them from each other. The absence of these spacers in turn removes a source of dielectric losses.

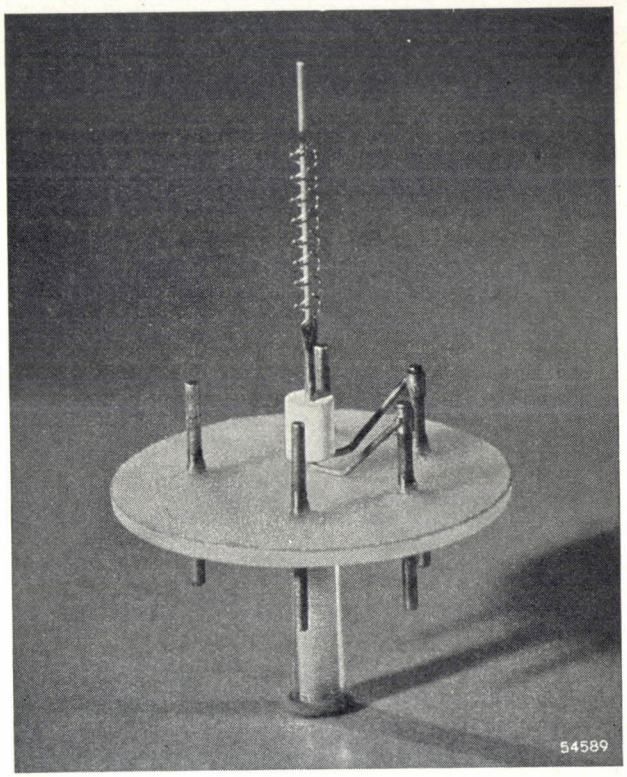


Fig. 2. Cathode consisting of two coaxial spirals of thoriated tungsten.

e) The manufacture of anodes of cylindrical form is very simple. If the material is to be graphite, as in the case of the valves under discussion, the whole anode, including any desired cooling fins, can be turned from a solid piece. When the anode becomes hot the circular form is maintained. Small discrepancies in the diameter or a slight eccentricity have little effect on the inter-electrode capacitances or electrical characteristics.

f) The fact that the electrodes all take the form of concentric cylinders simplifies assembly and facilitates accurate centring of the electrodes mutually. Rotary mounting and sealing machines permit

---

[2]) See S. Dushman, Electron Emission, Trans. Am. Inst. El. engrs. **53**, 1054-1062, 1934.

[3]) C. W. Horsting, Carbide structures in carburized thoriated-tungsten filaments, J. Appl. Phys. **18**, 95-102, 1947 (No. 1).

highly concentrated mechanisation in the manufacturing processes (*fig. 3*).

Thermal advantages

Finally, the cylindrical electrode system offers a number of advantages from a thermal aspect (though these might in part equally come under the heading of mechanical advantages).

Further, the cylindrical arrangement is well adapted to the "cage" type of grid (*fig. 4*), which consists of a rather large number of rods mounted like describing lines of the surface of a cylinder, with hardly any winding wire. These grids are very robust and self-supporting and they are highly conductive to heat as well as to high-frequency currents. This type of grid is employed in the

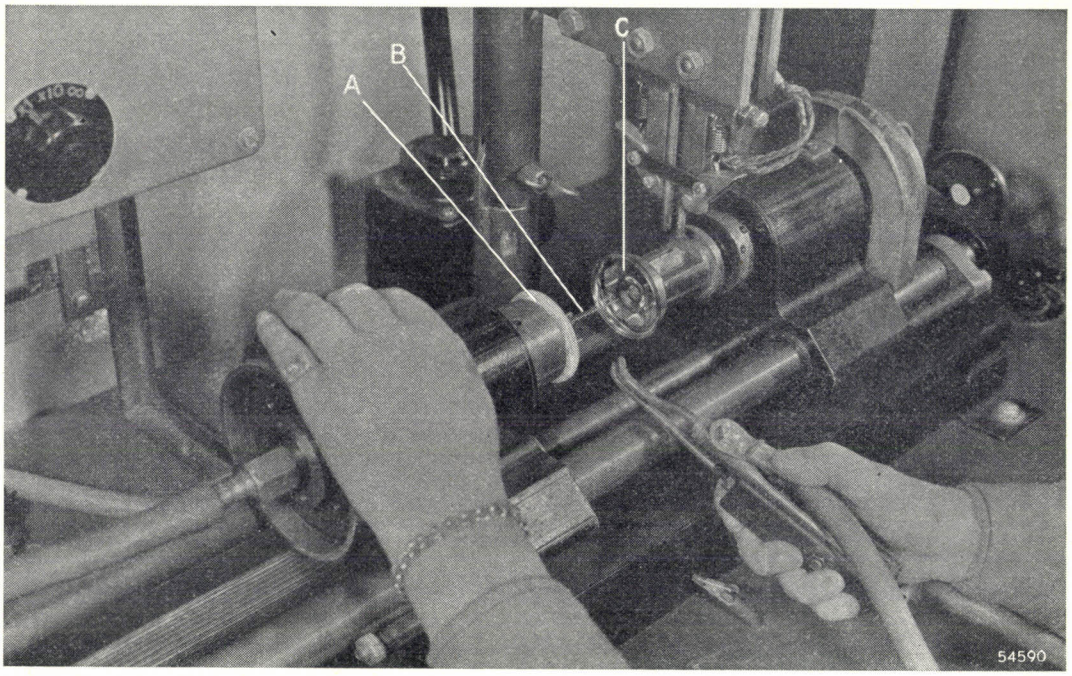


Fig. 3. Machine used for mounting cylindrical electrode systems. *A* = powder-glass base with leading-in pins and filament *B* (cf. fig. 2), *C* = shield to which the grid is connected. By rotating the machine head against which the glass base *A* is held by a vacuum, the operator accurately centres the filament in the grid, then welds the latter in position by means of the special welding pliers seen in the photograph. Extreme left: control knob for timing the weld.

g) The spirals of which the cathode consist are free to expand, even though the extremities are anchored; moreover, in a given valve type the expansion is uniform between one specimen and another.

The latter also applies to the grid and anode. At given temperatures of the electrodes, measurement of the internal capacitances yields almost the same results in every case.

h) With the flat grid one of the greatest sources of trouble is the irregular expansion of the turns of wire; the greatest expansion occurs at the centre, where it is hottest, and the turns at that point tend to go awry. If they buckle inwards they are likely to touch the filament. In the case of helical grids there is much less distortion and in any case this takes place outwards, so that there is no risk of shorting to the filament.

valves described in the following paragraphs (except in the smallest models).

i) The electron stream to an anode of cylindrical form is uniformly distributed over the whole periphery. The same applies to the temperature, not only at points along the length of the anode but also along the wall of the bulb, a fact that favours good operating conditions.

The radiation of heat from the anode can be facilitated by providing cooling fins, either vertical or horizontal, the latter being preferable, as the anode can then be manufactured by machining on a lathe (*fig. 5*). The size of the cooling fins depends to a large extent on the distribution of the temperature over the cross section through the axis of the bulb. This point is referred to more fully in a following section.

The shape of the anode with horizontal "fins" is

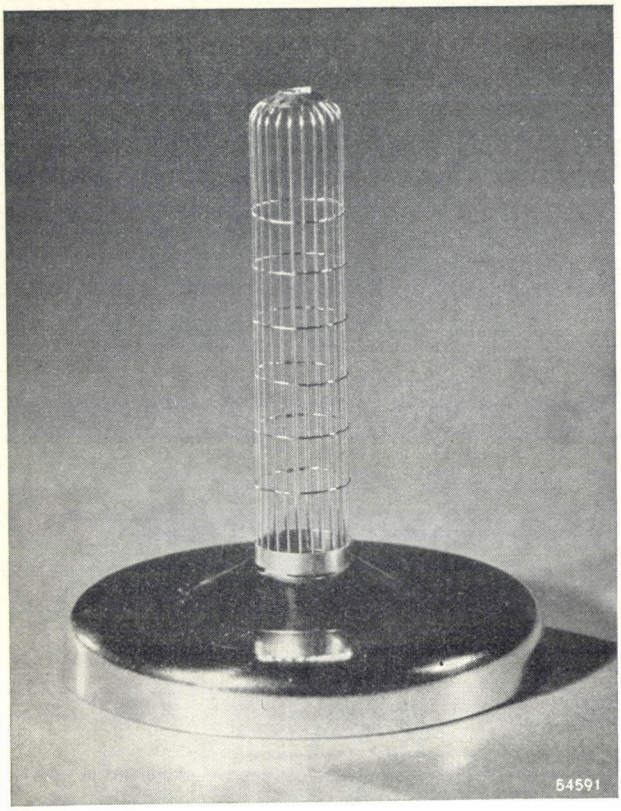


Fig. 4. Cage type of grid with shield at the base to screen the cathode electrically and part of the glass envelope thermally.

somewhat reminiscent of the domestic cotton reel; hence these valves are sometimes referred to as "cotton-reel valves".

A new range of transmitting valves of cylindrical construction

The various factors outlined above have led to the design of a new range of transmitting valves, two of which, the triode TB 2.5/300 and the tetrode QB 2.5/250, are already in production, others being still in course of development.

Before discussing the electrical characteristics of these valves, let us first look at some features of the electrodes and envelope.

The electrodes

The cathodes in the new valves are of spiralised thoriated tungsten, of the type mentioned above, these being carburized to increase the emissivity.

Until now, two difficulties have stood in the way of a universal application of this type of cathode. Firstly, thorium evaporated from the cathode and deposited on the grid very quickly produces electronic emission from the latter, whilst, secondly, the only known metal that will ensure a sufficiently low emission of gas (the emission of a thoriated cathode is destroyed by the merest traces of oxygen), and which is suitable for use for the grid and anode, is tantalum, which is costly.

The first of these obstacles has been overcome in the new range of valves by coating the grid with a substance that absorbs thorium, which, when once diffused within the basic material, is harmless. Moreover, owing to the effective thermal radiation of the anodes with their cooling fins, the temperature of the grids in these valves does not rise considerably and there is therefore little risk of grid emission.

As regards the second point, the discovery of the gas-absorbing properties of zirconium [4]) has made it possible to employ the thoriated tungsten cathode on a much larger scale, in conjunction with an anode of less costly material, such as molybdenum, nickel, or graphite.

The latter lends itself well to the manufacture of anodes with cooling fins from one solid piece (fig. 5), as already pointed out above. The amount of gas given off by the anode — and by the other electrodes as well — after the bulb has been exhausted is very small indeed when zirconium is applied to the anode in the form of a thin layer,

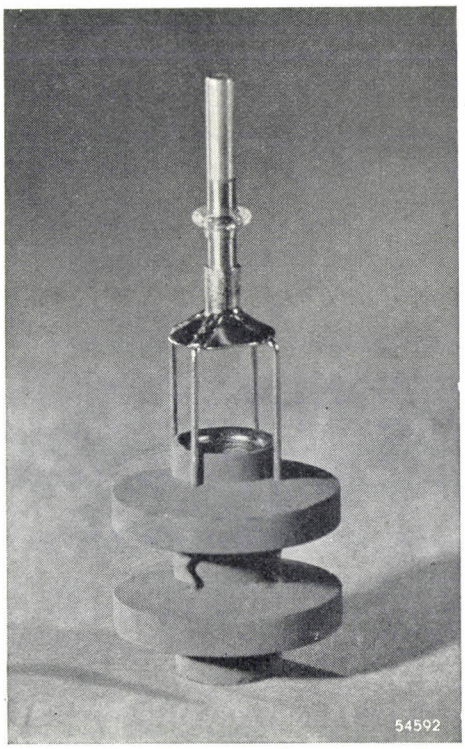


Fig. 5. Circular anode of graphite, with cooling fins, shaped more or less like a cotton-reel. The four molybdenum rods on which the anode is mounted are poor conductors of heat but provide good electrical conductivity.

[4]) J. H. de Boer and J. D. Fast, Rec. Trav. Chim. Pays-bas **55**, 459-467, 1936; J. D. Fast, Metals as getters, Philips Techn. Rev. **5**, 217-221, 1940.

this being the method employed in the production of the valves under discussion. The high thermal capacity of these anodes constitutes a safeguard against momentary heavy overloads. In fact the anodes are able to withstand overloads of some duration, as witness the fact that one of these valves, intended for a dissipation of 135 W, with a final temperature of 800 °C, was overloaded to the extent of 900 W for half an hour without detriment to the valve.

Four rather thin molybdenum rods are used to support the anode, this arrangement being better than a single thick rod, which, for the same resistance at high frequencies, would have to have a diameter equal to four times the thickness of the thinner rods, since, due to skin-effect, the electrical conductivity is proportional to the periphery and not to the cross section. At the same time the thermal conductivity of one such thick rod would be four times as high as that of four thinner ones together, and the anode lead-in might become too hot. Owing to the distribution (and adequate length) of the rods, the anode lead-in remains comparatively cool.

At a rising frequency and a constant input potential the losses within the valve will increase. Forced air-cooling (by means of a small fan which can simultaneously cool other parts of the transmitter) becomes necessary only at frequencies above 100 Mc/s, at maximum input voltage.

Envelope, leading-in pins and contact pins

The new valves are of the so-called "all-glass" construction. The envelope, at the top of which the anode connection is located, is closed at the bottom end by a flat, pressed powder-glass base [5]) containing five molybdenum leading-in pins, these being sealed into the base in one operation (*fig. 6*).

Of these five pins two are for the filament. In triodes the other three are attached to the grid, whilst in tetrodes only one serves this purpose, the remaining two being attached to the screen-grid. The intention is that when the valves are used on very high frequencies three grid pins or, similarly, the two screen-grid pins be connected in parallel in order to reduce the self-inductance and resistance (and therefore also the losses which result from the mainly capacitive grid current).

The conventional valve base has been dispensed with, and the leading-in pins, which are of molybdenum, serve at the same time as contact pins. This arrangement has been made possible only by the introduction of a sealing process which leaves the molybdenum in a ductile condition, thus avoiding breakage of the pins in use.

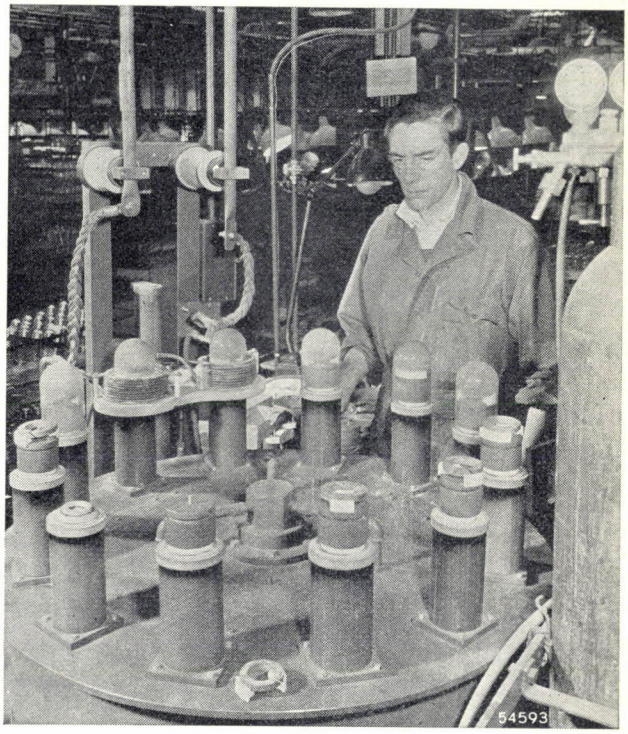


Fig. 6. Mechanical sealing of leading-in pins into the powder-glass base. Heating is brought about by h.f. induction in graphite jigs.

As these leading-in pins are thinner than the customary contacts in this class of valve, sleeves are soldered to them to give them the desired diameter. The arrangement of the pins (*fig. 7*), too, is such that the valves can be used in current types of valve-holders.

Considerable attention has been given to the distribution of temperature over the bulb surface, and the cooling fins on the anode have been carefully proportioned to ensure that a large portion of

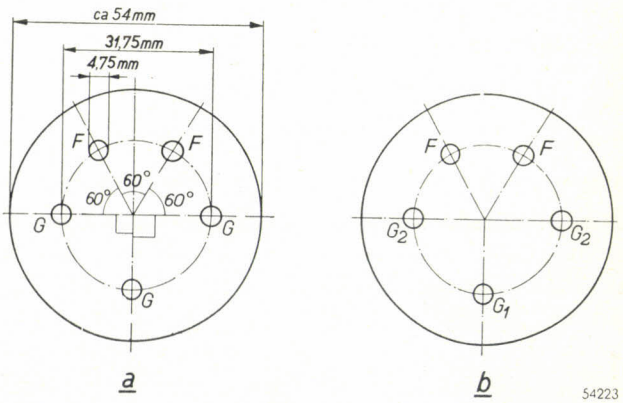


Fig. 7. Arrangement of contact pins in *a*) triode TB 2.5/300, *b*) tetrode QB 2.5/250. F = filament; G = grid (with shield), G_1 = control grid, G_2 = screen grid (with shield).

[5]) E. G. Dorgelo, Sintered glass, Philips Techn. Rev. **8**, 2-7, 1946.

the heat developed is radiated in an axial direction. This produces an extra supply of heat to the glass around the top seal containing the anode pin, so that there will be only a slight difference between the temperatures of the lead-in itself and the surrounding glass (see *fig. 8*, curve *a*). Thermal capacities are such that this applies not only under normal working conditions but also whilst the valve is warming up or cooling off.

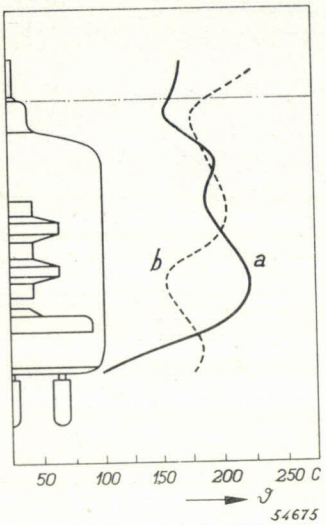


Fig. 8. Temperature ϑ of the anode lead-in (above the dot-dash line) and along the wall of the bulb (below the dot-dash line). The curve drawn as a full line (*a*) refers to the TB 2.5/300, a half-section of which is shown on the left. The dotted line (*b*) was plotted from a valve of similar rating without cooling fins and fitted with the conventional base. In both instances a static load of 125 W was applied. In the TB 2.5/300 there is very little difference between the temperatures of the anode lead-in and the surrounding glass; a cold zone occurs at the base of the valve, ensuring high insulation resistance.

Much wider differences in temperature occur in a similar valve not provided with cooling fins (fig. 8, curve *b*).

In a previous article in this journal [6]) we have mentioned the electrical conductivity of glass, which under certain conditions tends to reach critical levels at high temperatures; in view of this, special kinds of glass have been developed the conductivity of which is low. The valves now under discussion do not, however, call for the use of any special kinds of glass, since sufficient insulation is guaranteed by the long vitreous path between the anode pin and the connections to the other electrodes, which path moreover includes a "cold" zone (fig. 8, curve *a*). This cold zone is ensured by the presence of a metal shield in the valve (figs 4 and *9*) which protects the bottom of the envelope, as well as the base, from the effects of thermal radiation.

This shield also fulfils an electrical function, to which reference will be made presently.

The cold zone would not exist if the valve were fitted with the usual type of base, which tends to prevent the dissipation of heat through the bulb. This is illustrated in fig. 8, curve *b*, which shows the distribution of temperature along the envelope of a valve with base. The temperature in the region of the bottom contacts is in this case so high that it is essential to blow air through the base, necessitating a fairly complicated valve holder.

---

[6]) E. G. Dorgelo, Several technical problems in the development of a new series of transmitter valves, Philips Techn. Rev. **6**, 253-258, 1941.

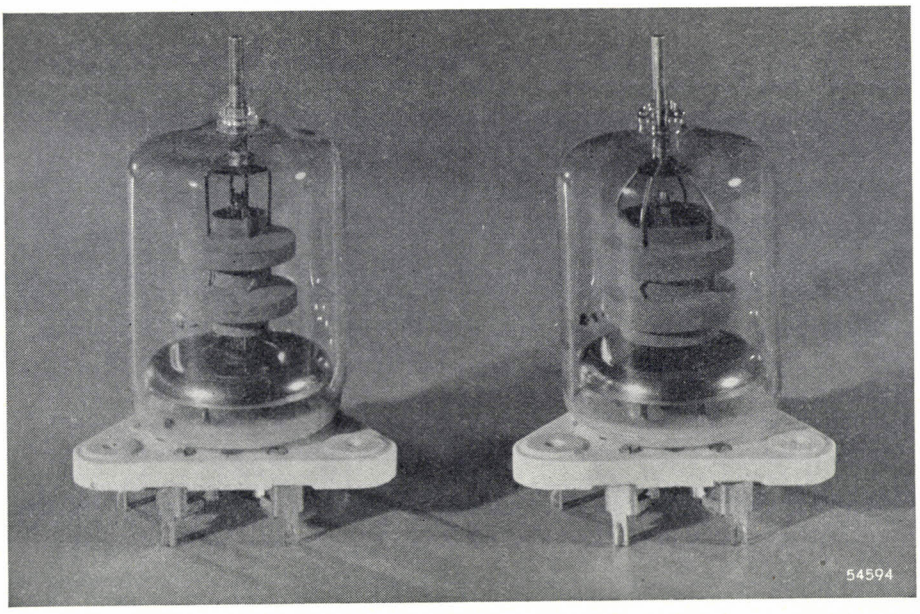


Fig. 9. On the left the triode TB 2.5/300 (anode dissipation 135W), on the right the tetrode QB 2.5/250 (anode dissipation 125W). Height of valves (including the pins) about 123 mm (5″).

Electrical data relating to the TB 2.5/300 and QB 2.5/250

The triode TB 2.5/300 is designed for an anode dissipation of 135 W and the QB 2.5/250 for 125 W. The construction of both types is based on the various factors outlined above and the characteristics are shown in *figs 10* and *11*; the filament in each case takes 5.4 A at 6.3 V.

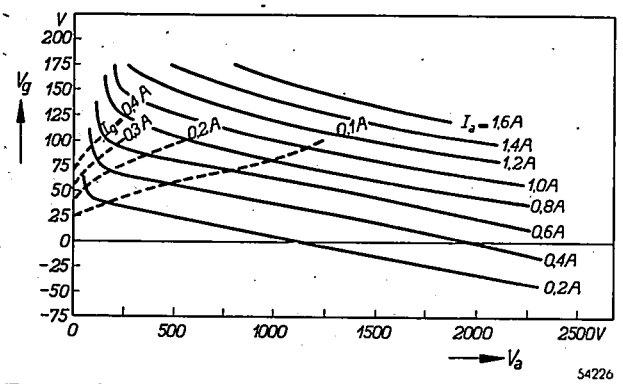


Fig. 10. Characteristics of the triode TB 2.5/300. In place of the characteristics anode current I_a as a function of the grid voltage V_g at constant V_a, or $I_a = f(V_a)$ at constant V_g, the increasingly popular characteristics $V_g = f(V_a)$ at constant I_a are shown (full lines). The broken lines refer to $V_g = f(V_a)$ for a constant grid current I_g.

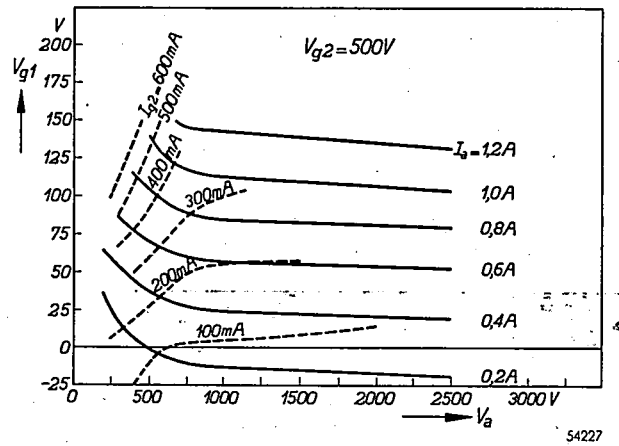


Fig. 11. Characteristics of the tetrode QB 2.5/250 for a screen grid voltage V_{g2} = 500 V. Full lines: control grid voltage $V_{g1} = f(V_a)$ at constant I_a; broken lines $V_{g1} = f(V_a)$ at constant I_{g2}.

In the triode the shield mentioned above is connected to the grid, thereby greatly reducing the capacitance C_{ak} between anode and cathode. The valve is thus rendered very suitable for use in grounded-grid circuits. Usually these circuits employ two valves in push-pull (*fig. 12*), in which case the input circuit is between the cathode and the output between the anodes. Neutrodyne capacitors are then unnecessary, even at the highest frequency at which the valve still works efficiently (200 Mc/s); the amount of coupling between input and output circuits due to the capacitance C_{ak} is in any case very small and is, moreover, almost wholly compensated in this frequency range by the self-inductance of the three connections to the grid and the shield, which are connected in parallel.

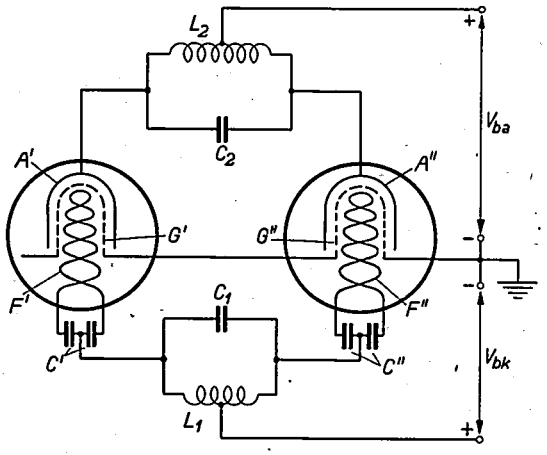


Fig. 12. Grounded-grid circuit employing two triodes in push-pull. G', G'' = earthed grids (and shields). L_1-C_1 = input circuit connected to the filaments F', F''. A', A'' = anodes to which the output circuit L_2-C_2 is connected. C', C'' = capacitors for h.f. decoupling of the filaments. V_{ba}, V_{bk} = D.C. voltages applied between anode and grid and between cathode and grid respectively.

In the tetrode the shield is attached to the screen grid, resulting in a low capacitance C_{ag_1} between anode and control grid. Neutrodynisation is unnecessary on frequencies below about 100 Mc/s. It is not the place to enter here into methods of avoiding coupling between circuits at higher frequencies; suffice it to say that this can be done very simply by interconnecting the screen grids of the two valves in push-pull via a variable capacitor.

Both valve types are intended to serve a large number of different purposes, such as for broadcasting and communication transmitters, oscillators for industrial or medical application (h.f. heating, diathermy, etc.). The efficiency is as high as 65-70% (*fig. 13*) at a frequency of 100 Mc/s, this rendering

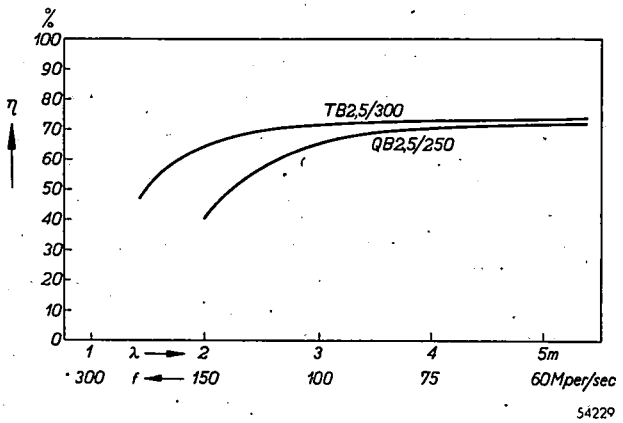


Fig. 13. Efficiency η (as defined in table III), as a function of the wavelength λ (or frequency f), of the TB 2.5/300 and QB 2.5/250. At 100 Mc/s the efficiency η is still as high as 72 % and 65 % respectively.

Table I. Several class C telegraphy ratings for the triode TB 2.5/300 used as amplifier and oscillator. Voltages are with respect to earth. Where two valves are used the values of current and power are per valve.

Application	Freq. (Mc/s)	V_{ba} (V)	V_{bg1} (V)	V_{bk} (V)	V_{g1max} (V)	I_a (mA)	I_{g1} (mA)	P_{g1} (W)	P_{ba} (W)	P_a (W)	P_o (W)	η (%)
As amplifier:												
Cathode grounded	60	2500	—200	0	350	200	40	14	500	135	365	73
Cathode grounded	60	1500	—120	0	270	200	40	11	300	100	200	67
Grounded grid (fig. 12) .	100	2000	0	150	—	200	40	50	400	130	280	70
As oscillator	150	1700	—130	0	—	200	40	—	340	135	205	60

Table II. As Table I for the tetrode QB 2.5/250, used as amplifier.

Circuit	Freq. (Mc/s)	V_{ba} (V)	V_{bg_1} (V)	V_{bg_2} (V)	V_{g1max} (V)	I_a (mA)	I_{g1} (mA)	I_{g2} (mA)	P_{g1} (W)	P_{ba} (W)	P_a (W)	P_o (W)	η (%)
Cathode grounded	20	3000	—170	400	300	150	15	50	4.5	450	125	325	72
Cathode grounded	60	2500	—170	400	300	170	15	50	4.5	425	125	300	70.5
Cathode grounded	100	2000	—150	400	280	170	15	50	6	340	120	220	65

the valves particularly suitable for transmitters working on wavelengths of a few metres, such as frequency-modulation and television transmitters. The good efficiency at these frequencies is directly due to the short transit time, low series-resistance of cathode, grid and anode connections, the low internal capacitances (ensuring a low current in the grid connection) and the very small quantity of materials employed in which dielectric losses occur.

At lower frequencies, too, these valves will give excellent service, e.g. in modulators and a.f. amplifiers.

Further details of frequency, voltages, current , powers and efficiencies for some of the more characteristic adjustments of the TB 2.5/300 and QB 2.5/250 are given in *tables I* and *II;* a list of the symbols employed is provided in *table III*.

Transmitting valves for higher powers

The principles outlined in the foregoing have also been followed in larger types of transmitting valves which are at the moment in an advanced stage of development.

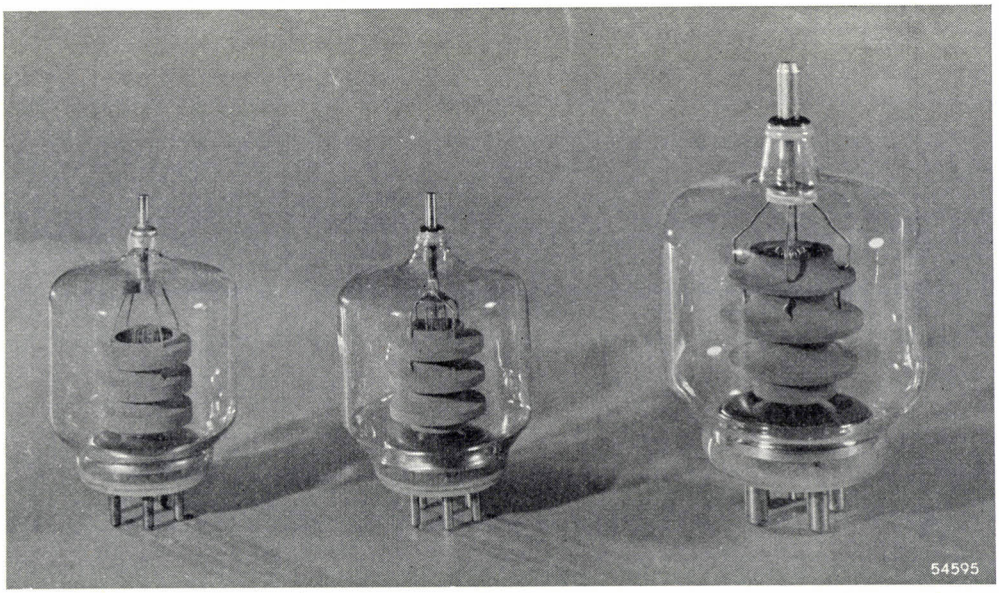


Fig. 14. Larger transmitting valves (still in development) based on the same lines as the TB 2.5/300 and QB 2.5/250. From left to right: tetrode with 250 W anode dissipation, triode with 270 W anode dissipation, triode with 540 W anode dissipation. Height of valves (incl. pins) about 147 and 205 mm (6″ and 8″) respectively.

Table III. Explanation of the symbols employed in tables I and II.

V_{ba}	= D.C. anode voltage
V_{bg1}	= D.C. control grid voltage
V_{bk}	= D.C. cathode voltage
V_{bg2}	= D.C. screen grid voltage
$V_{g1\,max}$	= peak alternating grid voltage
I_a	= D.C. anode current
I_{g1}	= D.C. control grid current
I_{g2}	= D.C. screen grid current
P_{g1}	= driving power
P_{ba}	= D.C. input
P_a	= anode dissipation
P_o	= h.f. output
η	= efficiency, defined as W_o/W_{ba} (the power to the filament, the control grid and the screen grid, if any, thus being disregarded).

Fig. 14 depicts two triodes designed for an anode dissipation of 270 W and 540 W, and a tetrode for 250 W.

The two smaller types are rated for 2 to 3 kV and the larger one for 3 to 4 kV anode voltage, supplying an output of 500 to 800 W and 1200 to 1600 W respectively (Class C). Owing to the efficient internal screening and the low inter-electrode capacitances amongst other things, these ratings are obtainable at frequencies of 100 Mc/s and even higher.

As will be seen from fig. 14, the larger types are also manufactured according to the "all-glass" technique, with cylindrical electrode systems. In order to secure complete similarity throughout the whole range of valves, the design has been based on laws of conformity; the specific loading of the electrodes and envelope is therefore practically the same in all types, ensuring the same high degree of reliability.

The two smaller valves in fig. 14 fit the same valve-holder as the TB 2.5/300 and QB 2.5/250; the larger one has pins of a different size but it nevertheless fits a current type of holder.

FORCING TULIPS WITH ARTIFICIAL LIGHT

by R. van der VEEN.

631.588.5

Tulips blooming in the early spring are usually forced in greenhouses, in daylight and at a temperature of about 20 °C. Experiments are now described showing that it is possible to obtain these early blooms by forcing the plants under artificial light in sheds insulated on all sides against any loss of warmth. The new method has several advantages, namely earlier blooms, better quality of both plant and flower, and reduced running expenses.

Forcing bulbs in greenhouses

Long before blossom time in the bulb-fields, tulips are on sale in flower shops, having been "forced" by a process in which warmth and light are the main factors.

Tulips which have appeared on the market in the early spring have so far always been forced in greenhouses: the grower sets his bulbs in the autumn, that is, towards the end of September or early October, placing them close together in "seed boxes", about 50 to a box. These boxes have to be kept in a fairly cool place, protected from frost; actually experience has shown that the best results, with slow growth, are obtained at a constant temperature of 9 °C. In practice it is usually considered sufficient to bury the boxes in the ground, as this has been found to provide the most satisfactory conditions for the development of the plant.

When the young plant is about 6 cm above the bulb (usually towards the end of December, or early January), the boxes are transferred to the greenhouse, where they are left in the daylight and at a temperature of some 21-22 °C. From that moment growth takes place very much more rapidly and, depending upon the particular sort of tulip, they will be in bloom within a period of 15 to 30 days. To obtain good results the two factors mentioned above must however be closely watched, viz. a temperature of slightly more than 20 °C, and sufficient daylight.

This, then, is a brief outline of the general method employed in growing early tulips. Needless to say, in times of fuel shortage it is rather a problem to maintain the greenhouses at the correct temperature, so much so that when there are periods of sharp frosts it is in many cases impossible, and as a result the early tulip crop fails.

The proper heating of greenhouses in very cold winters is rendered more difficult by the manner in which these greenhouses are usually built: generally they consist of a metal framework with glazed roof and sides and this is the main cause of dissipation of the heat within; most greenhouses are, in fact, a prolific source of fuel wastage. This great disadvantage of the design, from the point of view of economy, is discounted, however, since light is an absolute necessity for the proper development of the plants.

Experimental forcing of tulips by artificial light

It is quite an obvious question, therefore, whether it would not be possible to force the bulbs in houses which are effectively insulated to prevent thermal losses and to provide the requisite amount of light by artificial means.

In general it might be said that the amount of light needed for the satisfactory growth of plants would be far too large to justify the exclusive use of artificial light from the economic point of view. On biological grounds there are no objections to this, but an illumination of about 2000 to 4000 lux would be involved for the greater part of each day and this would be considered costly.

The forcing of bulbs, however, is quite another matter. Sustenance for the proper development of the leaves and flower are already in reserve within the bulb, and light is not needed as a source of energy in the assimilation processes: it is concerned mainly with the form and direction of the growth. An important function of light is the production of chlorophyll. Furthermore a considerable quantity of light will have a retarding effect on the growth, thus preventing the plant from growing too tall and straggly. Blue light promotes the formation of anthocyanin in many plants, this being the substance that imparts a vivid red colour to the bloom.

In 1930, J. W. M. Roodenburg, in collaboration with Philips Laboratories, Eindhoven, carried out several experiments in the forcing of tulips by artificial light, but the results obtained at the time did not appear to justify experiments on a larger scale. In the spring of 1946, however, Roodenburg, J. D. W. van Geel and C. Schoutsen [1]) once more took up the question of

[1]) Mededelingen van den Directeur van de Landbouw, 1948, p. 25.

forcing bulbs by artificial light and the results obtained, combined with the fuel shortage, induced van Geel to try this method on a larger scale. These trials, which yielded remarkable results, will now be reviewed in brief.



Fig. 1. Tulips forced under incandescent lamps in a thermally insulated shed.

A gladiolus drying shed at Bovenkarspel was covered in on all sides with wood-fibre sheet ("Kramfors" board) to a thickness of an inch to provide effective thermal insulation, thereby shutting out all light. A stove, together with a ventilator, kept the temperature constant at 22 °C. The whole shed was fitted up with electric light: a wooden ledge about 110 cm in width was built along the whole length of the walls, with electric lamps of 75 W each mounted in rows above them, about 75 cm apart and at the same distance from the bulb boxes placed on the ledge. This installation represented about 90 W per square metre of illuminated area. The lamps were kept burning 9 hours a day. To get the most benefit from the light available the ceiling and walls of the shed were whitewashed.

The first batch of bulbs to be forced, of the "Krelage's Triumph" variety, showed exceptional development right from the start: the boxes of bulbs were placed in the shed on 18th December and the blooms began to appear 17 days later. For comparison a number of bulbs from the same lot were set in a greenhouse for forcing in the conventional manner. Not only was the quality of the tulips in the lighted drying shed definitely better, but the proportion of stragglers was very much smaller, being only 4% as against a normal 10 to

15%. The fact that these tulips were of better quality than those in the greenhouse is undoubtedly due to the better facilities for the control of light and heat in the shed, where the plants were not exposed to the vagaries of the weather.

January. Again the growth and quality were good, the blooms being superior to those of the plants forced in the greenhouse.

Following on these practical experiments we have conducted a number of further, smaller trials in



Fig. 2. A view of the drying shed at Bovenkarspel where large-scale experiments have been carried out in forcing tulips under artificial light.

The tulips grown in this way attracted very much attention in trade circles and experts pronounced them to be excellent. A striking feature was the great length of stem, combined with sufficient rigidity, this being a quality of considerable importance from the point of view of market value.

In view of the success obtained with "Krelage's Triumph", another batch of bulbs was put down, this time the much slower-growing "Bartigon" tulip, these being placed in the shed on 16th

collaboration with van Geel to ascertain whether less light might do or whether a different type of light might yield still better results. Some details of these experiments are given below.

The lighting employed in the main experiment, consisting of 75 W lamps (90 W per m^2) for periods of 9 hours per day, proved to be just sufficient. A reduction in the power of the lamps to 40 W produced tulips of only fair quality; the colour of the leaf was too light and the blooms were on the

pale side, proving that the amount of light was inadequate to produce the essential chlorophyll in sufficiently large quantities. The shed was also lighted continuously, instead of only 9 hours a day, but in this case the growth was on the whole much too profuse, the leaf formation being so heavy as to produce difficulties in bunching. At the same time, the colour of both leaf and bloom was very good, as was also the length of stem. On an average, the flowers appeared some days before the others under 9 hours lighting per day.

Trials were also carried out with fluorescent lamps of different types, some of them giving mainly red or mainly blue light. With a power of 67 W per m^2 for 9 hours per day, the growth and quality of the tulips were excellent, but the general development was not quite so rapid as in the case of incandescent lamps, possibly because the fluorescent lamps give less infra-red radiation. The use of light sources of larger power, continuously alight, again resulted in a much more rapid growth, especially with red radiation.

It still remains to ascertain the optimum duration, intensity and colour of the lighting. It will then be possible to treat the various kinds of tulips differently in accordance with the particular characteristics most desired. Some types will be required to have a longer stem, while for other firmer stems, more leaf, or possibly a more vividly coloured flower may be desired. When the effect of artificial light upon the growth of the plant has been investigated more fully it should be possible to meet all these specific demands. The use of fluorescent lamps will be found preferable, since these offer a choice of either more red or more blue light. Experiments in that direction are now being conducted by the Agricultural Mechanisation Commission of North Holland, as well as in the Philips Laboratories at Eindhoven.

Saving in costs when artificial lighting is used

We have shown, then, that tulips forced under the light of incandescent electric lamps in thermally insulated sheds flower earlier and are of better quality than those forced in greenhouses.

The question whether this method will be universally adopted depends very largely on whether the running expenses are higher or lower than those of the old method. This point was investigated very carefully during the large-scale experiment at Bovenkarpsel. It was found that the cost worked out as follows, per day and per square metre of bulb-box:

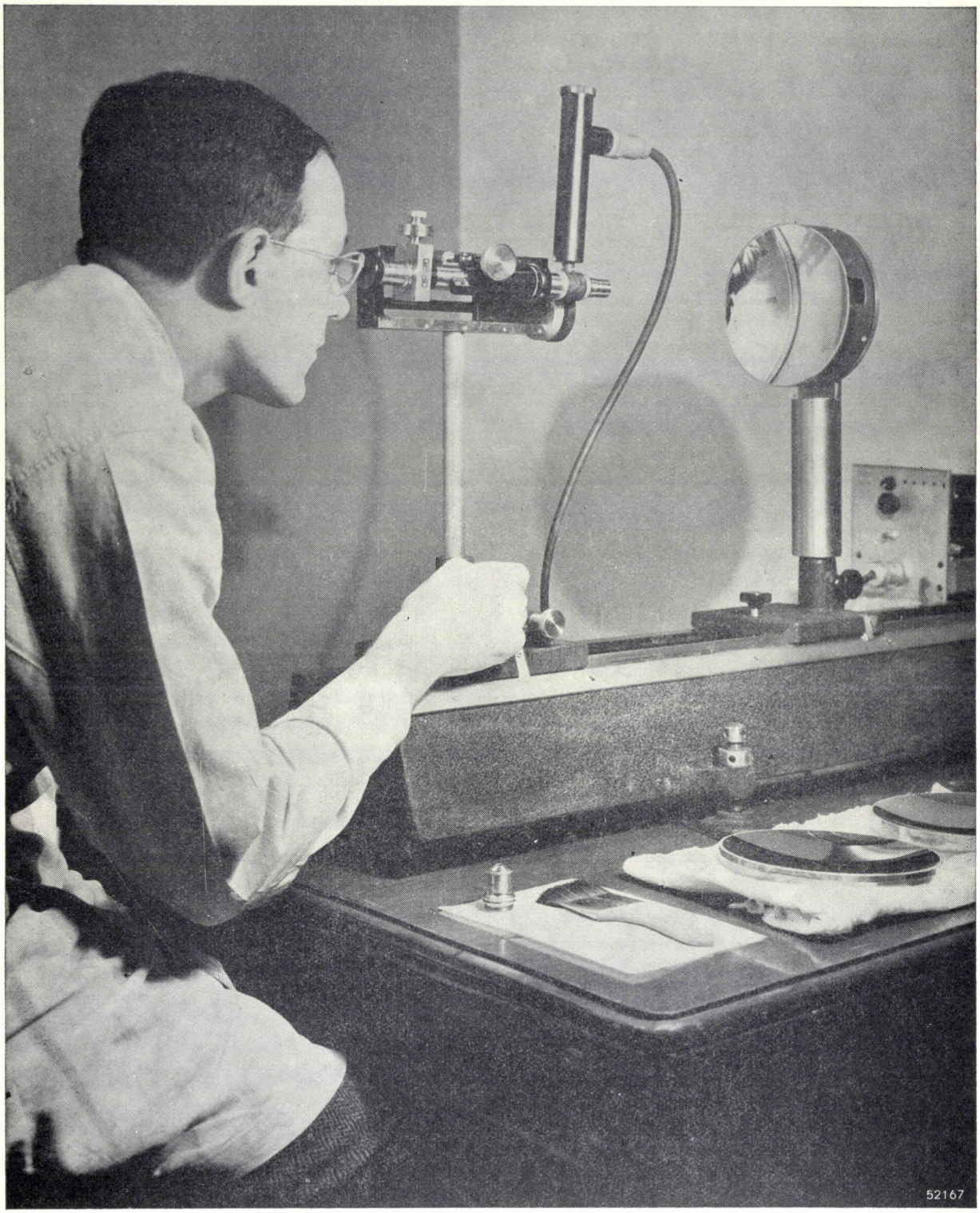
heating	*f* 0.011
electric current	*f* 0.024
lamps	*f* 0.009
total	*f* 0.044.

Against this, the cost of heating per m^2 of bulb-box in a greenhouse heated with oil fuel was found to be *f* 0.104 and in two other greenhouses heated with solid fuel *f* 0.051 and *f* 0.052. It must be remembered that these figures apply to the mild winter of 1947/48 and that in a very severe winter the cost of heating greenhouses is higher, whereas the costs for enclosed sheds remain almost the same, in which case the financial advantages of the new method are of even greater importance.

Apart form the saving on the fuel account, especially during a severe winter, a point in favour of incandescent lamps (or fluorescent lamps) is that the results will be more reliable and in many instances the construction and maintenance of special greenhouses will be unnecessary, seeing that existing sheds can be employed for the purpose.

Many growers in the Netherlands have already started converting their drying sheds for the forcing of tulips by artificial light, and this system is also receiving considerable interest in other countries.

EXAMINING MIRRORS FOR PROJECTION TELEVISION



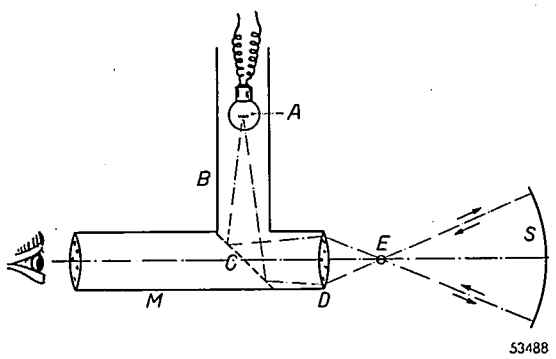
The quality of the concave spherical mirror of the Schmidt optical system used in projection televison receivers [1]) is examined with the aid of the apparatus shown in this picture (photo taken at Philips Laboratories, Inc., Irvington-on-Hudson, N.Y., U.S.A.). The principle of the apparatus is explained with reference to the schematic sectional plan given here.

Light from a small intense source (e.g. a "concentrated arc lamp") mounted in the side tube *B* passes from a partially reflecting plate in the horizontal microscope tube *M* through the micros-

[1]) Cf. P. M. van Alphen and H. Rinia, Philips Techn. Rev. **10**, 69-78, 1948/49 (no. 3).

cope objective. The distance of the source from the partially reflecting plate being suitably chosen, a reduced image of the concentrated source is formed by the objective at point E, in the plane to which the combination of microscope objective and eye piece is permanently focused. This image (which cannot be seen through the microscope owing to the direction of the rays), serves as a point source projecting a wide-angle light beam towards the spherical mirror. The image of this point source that is formed by the spherical mirror is viewed through the microscope in normal fashion, the only effect of the partially reflecting plate through which the rays must pass being a decrease in the brightness of the image. Any defects in the mirror are manifested through astigmatism, excessive spot size or non-uniform light distribution in the image observed.

In order to avoid superposition of the inherent aberrations which would otherwise be produced even with an ideal spherical mirror, it is necessary for the light source (E) to be located at the center of the curvature of the mirror. The feature of the set-up described here is that this is done automatically when adjustments are made for obtaining the best possible focus of the image observed. These adjustments consist in positioning the microscope to bring the image to the center of the field of vision, and varying its distance from the spherical mirror by means of a thumb screw. When the best focus is obtained the image must lie at point E, in the plane to which the microscope is permanently focused. The point source at E and the image of it that is formed by the spherical mirror and seen through the microscope therefore coincide, i.e., both lie at the center of curvature of the mirror



M microscope tube
B side tube of microscope
A partially reflecting plate
D microscope objective
E position of real image of *A* projected through *D*
S spherical mirror being examined.

ABSTRACTS OF RECENT SCIENTIFIC PUBLICATIONS OF THE N.V. PHILIPS' GLOEILAMPENFABRIEKEN

Reprints of these papers not marked with an asterisk can be obtained free of charge upon application to the Administration of the Research Laboratory, Kastanjelaan, Eindhoven, Netherlands.

1790: H. Bremmer: On the propagation of radio waves around the earth (Physica **14**, 301-318, 1948, No. 5).

Some questions about the propagation of radio waves around the earth are discussed. They concern successively:

1) an extension of Sommerfeld's ϱ-formula, applicable to the curved earth,
2) a reduction of Maxwell's vector equations to a scalar wave equation in the case of a spherically symmetric medium,
3) the reduction of the field corresponding to orthodox tropospheric refraction to the field existing without refraction.
4) a geometric-optical derivation of the attenuation factor in Austin-Cohen's formula for long-wave propagation,
5) the sky-wave field near the antipode of the transmitter,
6) a discussion of the day-light absorption for short waves,
7) the course of the rays and the field of cosmic radio waves.

1791: N. G. de Bruijn: Logarithmic solutions of linear differential equations (Phil. Mag. (7) **39**, 134-140, 1948, No. 2).

Starting from an expression given by Balth. van der Pol for $K_n\ (2\sqrt{x})$, where K_n is the Bessel function of the second kind, the author develops a method to derive similar expressions for "logarithmic" solutions of other 2nd order linear differential equations. Bessel's equation, Legendre's equation and the equation $xy'' + (1+x)\,y' - y = 0$ are given as examples. The last equation has as solution

$$\sum_{o}^{\infty} \frac{\mathrm{d}}{\mathrm{d}m}\left(\frac{x^m}{\Pi(m)}\right) = e^x \,\mathrm{li}\,(e^{-x}),$$

a result also derived by B. van der Pol with the aid of operational calculus.

1792: H. C. Hamaker: Toevalscijfers (Statistica **2**, 97-106, 1948, No. 3). (Random sampling numbers; in Dutch.)

This paper describes a simple dice-throwing technique, using a ten-faced regular prism, for producing random sampling numbers. The technique has been tested in various ways on series of up to 40,000 throws without showing evidence of bias.

1793: H. B. G. Casimir and D. Polder: The influence of retardation on the London-Van der Waals forces (Phys. Rev. **73**, 360-372, 1948, No. 4).

The influence of retardation on the energy of interaction between two neutral atoms is investigated by means of quantum electrodynamics. As a preliminary step, a discussion is given of the interaction between a neutral atom and a perfectly conducting plane, and it is found that the influence of retardation leads to a reduction of the interaction energy by a correction factor which decreases monotonically with increasing distance R. This factor is equal to unity for R small compared with the wavelengths corresponding to the atomic frequencies, and is proportional to R^{-1} for distances large compared with these wavelengths. In the latter case the total interaction energy is given by $-3\hbar c\alpha/16\pi R^4$. where α is the static polarizability of the atom. Although the problem of the interaction of two atoms is much more difficult to handle mathematically, the results are very similar. Again the influence of retardation can be described by a monotonically decreasing correction factor which is equal to unity for small distances and proportional to R^{-1} for large distances. In the latter case the energy of interaction is found to be equal to $-\ 23\ hc\ \alpha_1\alpha_2/8\pi R^7$.

VOL. 10 No. 10, pp. 289-324 APRIL 1949

Philips Technical Review

DEALING WITH TECHNICAL PROBLEMS
RELATING TO THE PRODUCTS, PROCESSES AND INVESTIGATIONS OF
THE PHILIPS INDUSTRIES

EDITED BY THE RESEARCH LABORATORY OF N.V. PHILIPS' GLOEILAMPENFABRIEKEN, EINDHOVEN, NETHERLANDS

EXPERIMENTAL TRANSMITTING AND RECEIVING EQUIPMENT FOR HIGH-SPEED FACSIMILE TRANSMISSION

IV. TRANSMISSION OF THE SIGNALS

by D. KLEIS and M. van TOL.

621.397.242

The transmitting apparatus of a facsimile equipment supplies a voltage which varies in accordance with the blackness of the successively scanned image elements. This "facsimile signal" has a Fourier spectrum beginning at the frequency zero and extending, in the case of the Philips system for high-speed facsimile transmission, to 100 kc/s. In the transmission of the signal to the receiving apparatus, where it has to control a gas-discharge lamp which records the image on a film, there are particularly four stages of importance: amplifying, modulating, reversal and slicing. Modulation on a carrier wave is necessary because the carrier-telephone cables suitable for the transmission do not pass the lowest frequencies of the signal. A carrier of 100 kc/s is used, thus equal to the highest signal frequency; the lower side band is transmitted. At the receiving end no demodulation in the ordinary sense of carrier-telephony is required, and a conventional full-wave rectifier will perform this function satisfactorily. The signal has to be amplified before it is modulated, and in the receiver amplification again takes place in order to modulate an output valve supplying the recording lamp. Alternating voltage amplifiers are used, which, it is true, do not transmit the direct-voltage component of the signal (average blackness of the image, frequency "zero"), but the exact position of all signal levels can be reconstructed by the periodical transmission of impulses with a given level and the use of *C-R* coupling elements with an auxiliary diode. For this principle, known in television, an improved circuit has been applied in our system. A reversal stage permits the recording on the film to be made either positive or negative. The slicer can advantageously be so set that for black-and-white documents, for instance, parts with a reflection coefficient of 60% and more are recorded as white and those with a reflection coefficient of 40% or less as black.

The fundamental principles of the telegraphic transmission of pictures (facsimile telegraphy) may be summarized as follows. A small spot of light is made to traverse narrow contiguous lines on the picture. With the aid of a photocell the varying intensity of the reflected (or transfused) light, which is a measure for the local shades of blackness of the picture, is converted into a fluctuating voltage, the facsimile signal. This signal is transmitted to the receiving station by cable or radio. There, the fluctuating voltage is used to bring about a varying blackness on a light-sensitive material which is recorded line for line in the same way as done with the original document in the transmitting station.

The Philips system for high-speed facsimile transmission [1]) is carried out with a scanning spot of 0.2 mm diameter traversing lines 22 cm long at a rate of 180 lines per second. Thus the scanning rate corresponds to the transmission of the blackness of 200,000 "picture elements" per second. In the receiving station the blackness is recorded on a light-sensitivite material (positive film) with the aid of a gas-discharge lamp the current of which is varied in accordance with the signal received.

The mechanical and optical apparatus used in the transmitter and the receiver respectively for scanning and recording the picture are described in parts II and III of this series of articles. In the present article some details of the electrical circuits employed for the transmission of the signals will be dealt with.

---

[1]) „Experimental transmitting and receiving equipment for high-speed facsimile transmission", I. General, by H. Rinia, D. Kleis and M. van Tol, Philips Techn. Rev. **10**, 189-195, 1948/49 (No. 7), II. Details of the transmitter, by D. Kleis, F. C. W. Slooff and J. M. Unk, Philips Techn Rev. **10**, 257-264, 1948/49 (No. 9), III. Details of the receiver by F. C. W. Slooff, M. van Tol and J. M. Unk, Philips Techn. Rev. **10**, 265-272, 1948/49 (No. 9), These articles will be referred to as I, II and III.

Transmission links

In *fig. 1* a block diagram is given representing the most important transmission elements that the signal passes through on its way from the photocell in the transmitter to the recording lamp in the

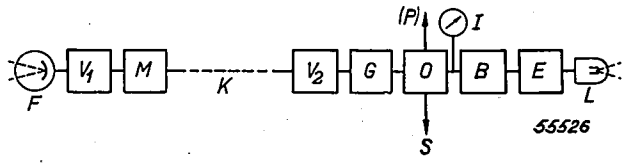


Fig. 1. Diagrammatic representation of the path followed by the facsimile signal from the photocell F at the transmitter to the recording lamp L at the receiver. V_1, V_2 amplifiers; M modulator; K cable; G rectifier; O reversal stage and synchronising separator (S) and, if required, arrangements referred to in article III for punching the films (P); I level meter; B slicer; E output stage.

receiver. This refers to transmission by a carrier-telephone cable. The transmission elements have mainly the following functions:

1) amplification of the signal (amplifier V_1 in the transmitter, V_2 in the receiver);
2) modulation of the signal on a carrier-wave for transmission via the cable (modulator M), and "demodulation" in the receiver (rectifier G);
3) reversal, if desired, of the "polarity" of the signal, for positive or negative reproduction of the original (stage O in the receiver);
4) slicing of the signal if only "black" and "white" have to be reproduced and no half-tones (stage B and the output stage E of the receiver).

In the output stage E the signal is brought to the required level to be able to feed the recording lamp.

We shall not give here any systematic description of all parts of the block diagram in fig. 1, but shall confine ourselves to a more or less fundamental consideration of the manner in which the four above-mentioned functions are performed, beginning with a discussion of the signal to be transmitted.

The facsimile signal

When one line of a normal letter is scanned a voltage, which varies in the manner represented schematically in *fig. 2a* (cf. also the oscillogram of fig. 5 in article II), will be obtained across the resistor through which the current from the photocell in the transmitter is conducted. This signal voltage reaches the level C when scanning white paper having a reflection coefficient of say 85%. It drops to the level B when the scanning spot crosses a black line, for instance of a written or typed letter; the reflection coefficient of the "black" of such a line amounts mostly to 20—25%. At the beginning of each line the scanning spot passes over an aluminium plate the specular reflection of which results in an impulse at the level D corresponding to a reflection coefficient of 110% (see article II). At the end of the line the spot passes over an opening with reflection coefficient zero, so that the voltage drops momentarily to zero (level A).

The signal voltage for black, level B, amounts to approx. 0.2 V and that for white, level C, to approx. 0.7 V (see article II). The overall "amplitude" of the signal, i.e. the distance between the levels A and D, is thus about 0.9 V.

When, instead of a normal document with black lettering on white paper, a document with white lettering on black paper is scanned (e.g. a negative photostat print) then a signal is obtained as represented in fig. 2*b*. There the voltage is mostly at the level B rather than at C. When instead of a letter a photograph with half-tones is scanned then the

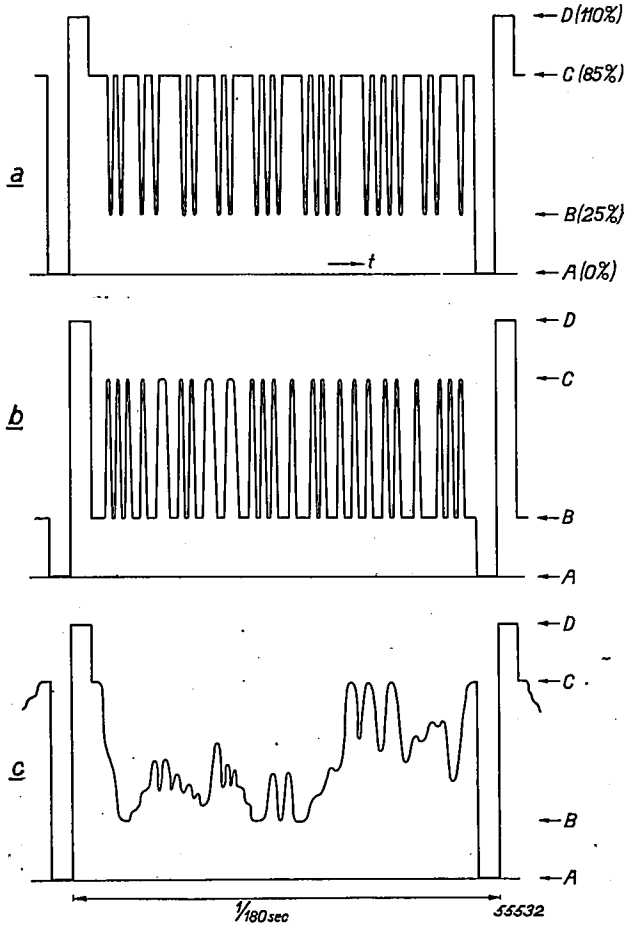


Fig. 2. Wave form of the facsimile signal obtained when scanning one line: *a*) white background with black lettering, *b*) black background with white lettering, *c*) half-tone illustration. On the white parts of the paper the coefficient of reflection may be for instance 85%: level C; on the darkest parts about 25%; level B. Pulses with the fixed levels D and A, corresponding to coefficients of reflection of 110% and 0% respectively, are transmitted with the signal at the beginning and end of each line.

signal will take a form as shown in fig. 2*c*, all levels between *B* and *C* being possible, corresponding to the various shades of grey.

If a Fourier spectrum of the facsimile signal is constructed it will be found to contain frequencies from zero up to 100,000 c/s. The highest frequency occurs when the document has alternating white and black lines 0.2 mm in width perpendicular to the scanning lines. The 200,000 "picture elements" transmitted per second then have alternating levels *C* and *B* answering to a (fundamental) frequency of 100 kc/s. (Actually the signal then also contains harmonics of this fundamental frequency, but these are not essential for the separate reproduction of the lines.) The lowest frequencies occur when the document has uniform grey parts which more or less gradually vary in blackness in a direction perpendicular to the scanning lines. The extreme case is the component with frequency zero (direct-voltage component) answering to the average brightness of the document being transmitted.

Owing to the occurrence of the low frequencies, from zero onwards, these signals differ from most other signals occurring in telecommunication technique.

Amplification of the facsimile signal

The amplifiers in the transmitter and in the receiver must transmit equally well all the frequencies occurring in the signal. This is essential because otherwise, owing to the distortion of the signals, any shade of grey in the documents being transmitted would not always be recorded with the same degree of density.

As regards the high frequencies this requirement does not give rise to any fundamental difficulties. For the very low frequencies, however, in particular for the component of the frequency zero, somewhat exceptional measures have to be taken, since with a normal alternating-voltage amplifier the very low frequencies are greatly attenuated owing to the *C*—*R* coupling between successive stages, whilst the direct-voltage component is entirely lost; the differences in the average brightness of successive documents and also of parts of one document would not be correctly reproduced in in that case.

In order to explain the remedy applied — which with some modifications has been taken from television technique where the same problem arises — it will be considered what happens to the signals for various documents when passing through a *C*-*R* coupling element.

We shall consider separately the case of a white document with black lettering and that of a black document with white lettering. Across the input *e*-*f* of the coupling element drawn in *fig. 3* we get a signal according to fig. 2*a* or fig. 2*b* (in both cases

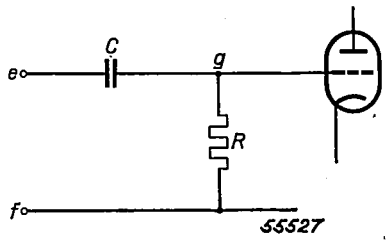


Fig. 3. *C*-*R* coupling between two stages of a conventional A.C. amplifier.

augmented with a D.C. component originating from the anode direct voltage of the preceding amplifying stage). The corresponding grid potential will also be as shown in figs. 2*a* and 2*b* respectively. Since, however, the blocking capacitor *C* removes the D.C. component between *e* and *f* of the current through the resistor *R*, the mean potential of *g*, taken over a sufficiently long time, will always be equal to the potential of *f*. With respect to this given zero level we therefore get a grid potential varying according to *fig. 4a* in the case of a white document with black lettering and according to fig. 4*b* in the reverse case. If the amplifying valve shown in fig. 3 is the output valve of the receiver then it is clear that in the two cases in question any signal level, for instance level *C*, produces entirely different currents in the recording lamp and is therefore reproduced on the film with different densities.

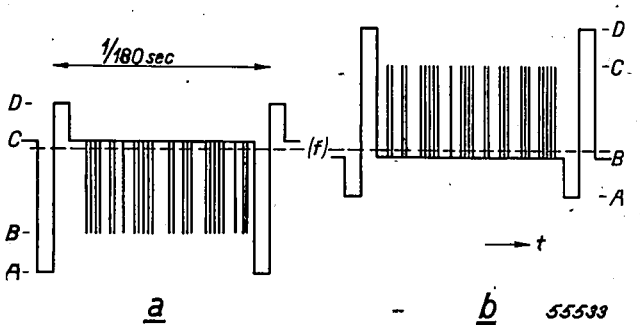


Fig. 4. Variation of the potential at point *g* of fig. 3 (*a*) when a signal according to fig. 2*a* is applied to the input *e*-*f* and (*b*) with signal shown in fig. 2*b*.

When in the transmitter a black document immediately follows a white one the form of the signal voltage at *g* will be as shown on the left-hand side of *fig. 5*. The time constant *R*·*C* of the inter-valve circuit determines the rate at which the mean potential of *g* again reaches the potential of *f* after the transition. This change in potential is observed on the film as a gradual decrease of density of the black document.

In our case, therefore, the normal A.C. amplifier mixes things up, because the reproduction of each signal level will be influenced by the average blackness of the preceding picture lines scanned. This way of expressing things is better suited for our purpose than the more usual consideration of the transmitted frequencies from which we started above.

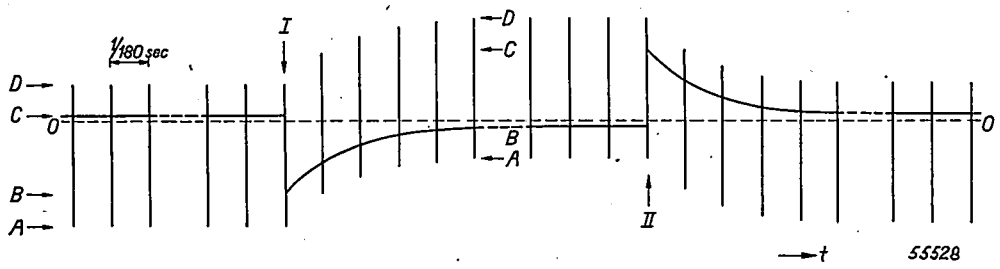


Fig. 5. Variations of the potential at point g in fig. 3 when scanning first a normal white original, then (step I) a black original, followed again by (step II) a white original. The units of time are much shorter than in fig. 4; only the impulses between the successive lines and the background level (first C, then B, and again C) are indicated.

The remedy applied by us to overcome this trouble consists in shunting a diode across the resistor R of the last inter-valve circuit; see *fig. 6*. Thus, no matter whether the signal between e and f follows the lines of fig. 2*a* or those of fig. 2*b* the peak potential of g of the signal (level D) will always be substantially equal to the fixed potential at point f; as soon as g becomes positive with respect to f, the diode conducts and in a very short time the capacitor C becomes sufficiently charged and the potential difference between g and f drops to zero. In this way, therefore, the grid of the output valve always has the same potential (namely practically that of the diode-cathode) for the signal peaks with level D, corresponding to the reflection coefficient of 110 %. Further, it is arranged that the amplitude of the signal at the input e-f, i.e. the difference between the levels A and D, has a suitably chosen and constant value for all documents, independently of any gradual changes in the scanning lamp, optical system or photocell of the transmitter or in the amplifying valves, etc. For this purpose a special measuring circuit has been designed to give a direct reading of the said difference on a meter (see I in fig. 1; for reasons stated later, this measuring device is connected prior to stage B and not to the input of stage E). The amplification of the signal received is adjusted by hand until the meter indicates the prescribed amplitude. Thus also level A, corresponding to the fixed reflection coefficient of 0%, is always at a certain grid potential of the output valve and accordingly B (black), C (white) and all intermediate tones are likewise recorded correctly. Consequently all shades of grey in each document are recorded with their proper density.

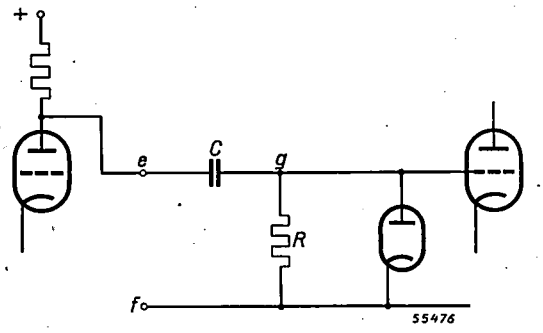


Fig. 6. C-R inter-valve coupling with diode (D.C. restoration circuit).

It is to be seen that this has been made possible by the periodical transmission of the fixed levels A and D, which furnish as it were a scale for the reflection coefficient. It is an important feature that the impulses A and D are obtained by optical means, by reflection from "calibrated" surfaces, and not for instance electronically. Thus the scale is always correct, even when the brightness of the lamp illuminating the scanning spot drops somewhat or when the losses in the optical scanning system increase (see article II).

The essence of the method described is that in the last stage of the receiver the correct mutual position of the signal levels is restored for all documents or parts of documents with the aid of two reference levels A and D and the method of coupling according to fig. 6. In principle, therefore, it is not necessary to maintain the exact position of the signal levels for the intermediate stages of the transmission. Nevertheless the coupling described has also been used in some intermediate stages with the object of improving the conditions under which the amplifying valves work. If a signal, as shown in fig. 5, is applied to the grid of a valve

the overall grid swing is equal to the level between A and D plus the difference between levels B and C (the latter being due to the change from white to black). If, on the other hand, all maxima are lined up by means of the diode circuit, the grid potential only varies between the levels A and D and the swing is thus reduced to about two-thirds of its previous value. Thus the signal can more easily be brought into the linear part of the valve characteristics and a greater amplification can be reached.

D.C. restoration circuit

During the scanning of each line between two impulses D, the diode is non-conducting. In this period of time the capacitor is discharged to a small extent by the resistor R. The potential of g thus shows a small and almost linear increase with time, which is, of course, superimposed upon the signal. The charge, however, is restored by the diode during the short interval of the impulse D (5% of the scanning period of a line). The increase of potential is thus not accumulative and only results in a slight drift of the signal level (cf. figs 2*a* and *b* and *figs* 7*a* and *b*); this drift is kept small by giving the coupling circuit a large time constant RC.

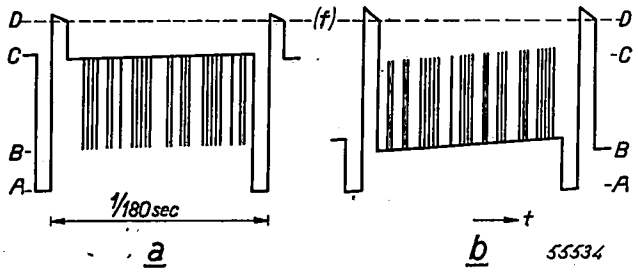


Fig. 7. The effect on the wave form of fig. 4 when the circuit of fig. 6 is used. The potential at g of fig. 6 assumes a fixed value for the maxima (level D) of the signal regardless whether the signal at e-f varies according to fig. 2*a* (*a*) or accroding to fig. 2*b* (*b*). The drift due to the discharge of the capacitor through R is superimposed on the potential variation while each line is being scanned. Here the drift is very much exaggerated for the purpose of illustration.

The drift referred to, however, also plays a useful part. Suppose that a signal which has already passed through one or several stages of A.C. amplification (without a diode in the coupling circuits) is applied to the input of the coupling circuit of fig. 6 and that this signal shows a discontinuity like that on the right-hand side of fig. 5 (at a change from a black to a white document). After the discontinuity the potential first drops with an initial slope corresponding to the resultant time constant $(RC)_t$ of the preceding stages. In principle, after the first peak is reached, owing to the tendency of the potential to drop, the diode loses control, with the result that level D departs (at least temporarily) from the fixed potential at which it is desired to be maintained. This falling tendency is counteracted by the aforementioned linear increase of potential occurring during the scanning of each line as a consequence of the discharge current. It can in fact be entirely compensated so that in each peak the diode can perform its conductive function. This compensation is obtained when the time constant RC of the coupling circuit with diode does not exceed [2]) a certain fraction of $(RC)_t$. Considering that RC is required to be as large as possible (see above) and $(RC)_t$ becomes smaller according to the number of coupling circuits without diode employed, all of which contribute to the decline in potential, it is also for this reason of importance to keep the number of amplifying stages without diode in the coupling to a minimum.

A drawback of the simple diode circuit according to fig. 6 is that during the maximum of the signal when the diode is conducting, the anode load is shunted by the much lower resistance of the diode and a portion of the top (D) of the signal is clipped off. This objection is particularly of importance when it is desired to use a rather high value of the anode load in order to obtain large signal voltages with relatively low anode currents.

In order to meet this requirement a modified D.C. restoration circuit has been designed, which is shown in *fig. 8*. It would carry us too far to analyze the working of this circuit; the effect previously mentioned occurs to a much smaller extent, this being attributed to the lower internal resistance

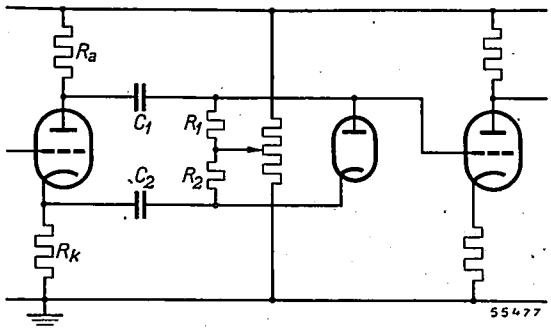


Fig. 8. Modified D.C. restoration circuit. The most important advantage of this circuit is that the flow of current through the diode no longer influences the anode alternating voltage of the preceding amplifier valve. The following conditions must be satisfied:

$$R_aC_1 = R_kC_2,$$
$$R_1C_1 = R_2C_2.$$

[2]) This applies for the case where the resistor R is connected directly to the cathode of the diode. The product RC can be considerably increased if a positive voltage is applied in series with R, but such details are beyond the scope of this article.

presented by the preceding stage when the diode is conducting [3]). This circuit has an additional advantage which will be dealt with below.

Modulation and demodulation

The facsimile signal transmitted by the apparatus occupies a frequency band of 100 kc/s. In many countries carrier-cable circuits are available which can transmit a frequency band of this order and over which this facsimile signal can therefore be transmitted. The circuits in the Netherlands, for instance, are designed for frequencies of 8 to 208 kc/s, thus for a total bandwidth of 200 kc/s [4]).

As the example just mentioned shows, such cable circuits are not suitable for the transmission of low frequencies. Bearing in mind what has been explained above about the amplification of the facsimile signal, one might readily suppose that this property of the cable could easily be compensated by the diode-coupling circuit in the receiver, which restores the correct level proportions when the mean level varies gradually (components with very low frequencies). D.C. restoration, however, is based upon the impulses D and A at the beginning and end of each line, and these impulses, the fundamental frequency of which is 180 c/s, are not transmitted by the cable either. Therefore, for cable transmission the signal is first modulated with a carrier, thus shifting the low Fourier components to a suitable frequency range within the transmitted frequency band of the cable.

For this modulation we apply the principle of the double push-pull connection of valves as employed in carrier-telephony, the best known example of which is the ring modulator [5]) as shown in *fig. 9*.

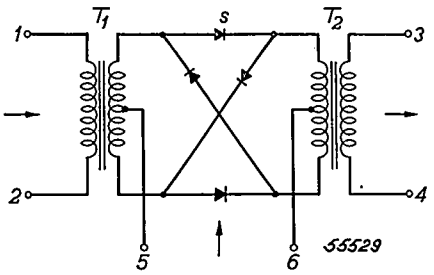


Fig. 9. Circuit diagram of the ring modulator. Between the transformers T_1 and T_2 four selenium rectifying cells are connected as it were in a ring.

[3]) This is the well-known feature of a cathode follower, some resemblance to which is found in the circuit described. In this case, however, the circuit can theoretically give a stage gain greater than unity.

[4]) See for instance G. H. Bast, D. Goedhart and J. F. Schouten, A 48-channel carrier telephony system, I. Choice of the method of modulation, Philips Techn. Rev. 9, 161-170, 1947 (No. 6).

[5]) See for instance F. A. de Groot and P. J. den Haan, Modulators for carrier-telephony, Philips Techn. Rev. 7, 83-91, 1942.

In carrier-telephony technique the carrier, which is of more or less a high frequency, is applied to the terminals *5-6* and the low frequency signal to be transmitted (microphone currents, frequencies q) to terminals *1-2*. The output obtained at terminals *3-4* consists of a voltage alternating with the carrier frequency (p) and varying in amplitude in accordance with the signal voltage. The Fourier spectrum shows that this output voltage contains the sideband frequencies $p+q$ and $p-q$ and some higher modulation products ($3p \pm q$, $p \pm 3q$, etc.); the carrier frequency p itself does not occur, due to the balancing of the circuit with respect to the terminals *5-6*. Neither are there any of the frequencies q at the output [6]). One of the side-bands, for instance the lower one $p-q$, is selected for the transmission after suppression of all other modulation products by means of appropriate filters.

In our case we have to proceed on different lines. With the double push-pull circuit of fig. 9 the amplitude of the modulated carrier is proportional to the difference between the instantaneous and the mean value of the signal voltage, being actually proportional to the absolute value of that difference. For facsimile signals, the D.C. component of which is not transmitted by the transformer at the input *1-2*, this leads to peculiar consequences. Suppose, for instance, that at *1-2* a signal is applied obtained from a document having an average brightness just half-way between B (black) and C (white). The carrier-amplitude for level B at the output of the modulator would then be the same as for signal level C; entirely black and entirely white could not then be distinguished!

For this reason the carrier is applied to the terminals *1-2* and the signal to *5-6*. In this case, too, a voltage fluctuating with the carrier frequency is obtained at the output *3-4*; its amplitude is at any moment proportional to the instantaneous absolute value of the voltage across *5-6*. The signal level D is fixed at a certain potential value, viz. zero, in the manner described above, in a preceding stage. (This comes to the same thing as if an opposed direct voltage equal to the signal voltage for level D were connected in series with the signal.) Since the voltage across *5-6* never changes in polarity but only varies between the value zero (for level D) and a maximum (for the level A), the phenomenon described above can never occur. If, for instance, the signal is as shown in *fig. 10a*, the output will be an alternating voltage according to fig. 10*b*.

The carrier frequency is chosen equal to the

[6]) For details see reference quoted in footnote [5]).

highest frequency in the signal band (q_{max} = 100 kc/s) or if necessary slightly higher or lower. For the transmission the lower side-band p-q is used. *Fig. 11* shows that this side-band lies within the same frequency range as the original Fourier spectrum (q), viz. between 0 and 100 kc/s, but reversed with respect to that spectrum; the

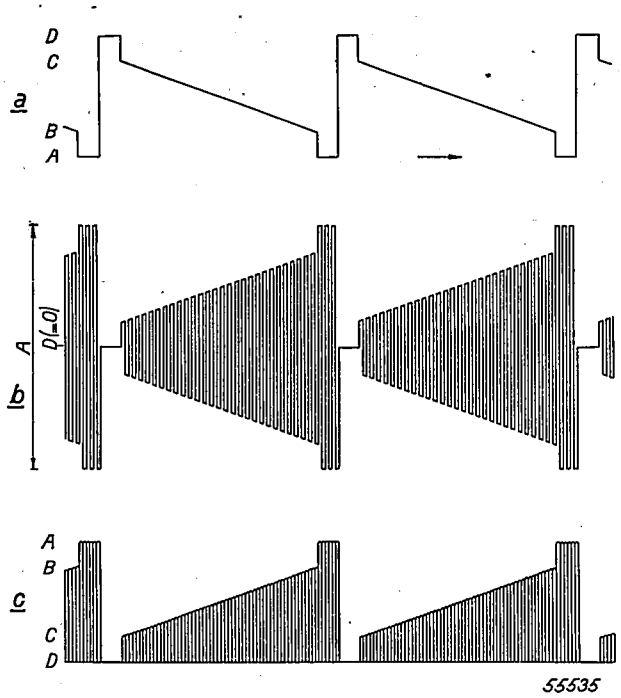


Fig. 10. *a*) Facsimile signal of a document black at one side and white at the other and in between (in the direction of the scanned lines) all intermediate tones. The average brightness lies half-way between the levels *B* and *C*. *b*) Modulated carrier obtained across the output *3-4* of the modulator when the signal (*a*) is applied at the input *5-6* in series with a direct voltage equal and opposed to the signal voltage for level *D*. *c*) Result of a full-wave rectification of (*b*).

low Fourier components of the signal now lie near 100 kc/s and the high ones near 0 kc/s. In the transmission by cable therefore only the highest Fourier components (e.g. from q = 92 to 100 kc/s) are affected, and this does not lead to any appreciable loss of definition in the received record.

This method of modulation is satisfactory for present requirements, namely that a transmission band can be used beginning at the lowest frequencies (thus not for instance for a band of 100-200 kc/s or higher), without having to employ multiple modulation. No trouble is experienced from the original signal, although its frequencies lie within the transmission band, because owing to the balanced circuit of the modulator the signal across *5-6* does not occur at the output. If desired it is also possible here to filter out the upper side-band $p+q$ of the modulated signal, so that the cable, if it can be used for frequencies higher than 100 kc/s, can be kept available for telephony channels located in this frequency range in the normal way.

In order to regain the "low-frequency" signal from the transmitted modulated carrier in the receiver (fig. 10*b* [7])) it could be demodulated according to normal carrier-telephony practice. This is normally carried out by applying it to a modulating circuit according to fig. 9, a voltage with a carrier frequency p being applied to the other input. However, in the case of facsimile transmission a simplification is possible. By merely rectifying the incoming signals with a full-wave rectifier one obtains a voltage as shown in fig. 10*c*. This corresponds practically to the original signal (with the previously mentioned D.C. component) but broken up at twice the carrier frequency $2q$. Remarkably enough this voltage (after the necessary amplification and slicing; see below) can be used directly to modulate the recording lamp: the flickering caused by the pulsating excitation has a frequency such that only small specks would appear having a breadth and distance apart equal to 16.5 μ. As the recording spot itself has a breadth of 33 μ these specks are just fully obliterated, so that no lattice is visible on the record.

If the carrier frequency is slightly higher or lower than 100 kc/s — which in itself is not of much consequence — then the flickering specks are not exactly half the width of the recording spot and they are not fully obliterated. The result is that unless steps are taken to suppress the double carrier frequency (which can actually be done with a very simple filter) some evidence of flickering will be found on the film.

This is the reason why in the method of modulation described the level *D* (the brightest white) is made to correspond to the carrier amplitude zero. In principle it would also be possible to make the carrier amplitude zero for the level *A*

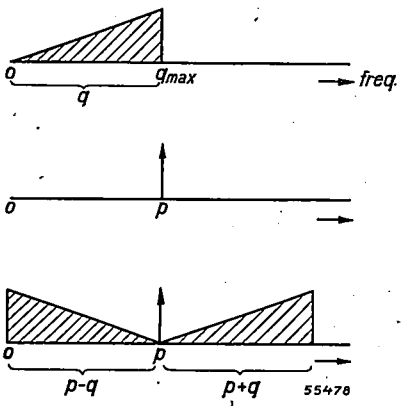


Fig. 11. Frequency allocation of the original facsimile signal (q = 0 up to $q = q_{max}$ = 100 kc/s), of the carrier (p = 100 kc/s), and of the side-bands p-q and $p+q$ obtained by modulation.

[7]) Owing to suppression of the frequencies above 100 kc/s ($p+q$) the voltage wave form transmitted differs slightly from fig. 10*b*, but this deviation (corner of the steep transmissions rounded off) can be ignored here.

(absolutely black) and the maximum for D. In the way chosen, however any stripes can only occur in the black and grey, and not on the white background where they would be more noticeable.

For those accustomed to carrier-telephony practice this direct use of the voltage according to fig. 10*c* may seem surprising, because it is not immediately clear how the original spectrum can be restored from the inverted Fourier spectrum of the voltage according to fig. 10*b*, for there has been no inversion of the frequency band as is the case when demodulating in the normal way. Without going deeper into the matter here we just mention it to illustrate once more that, however useful it may be to consider the frequencies

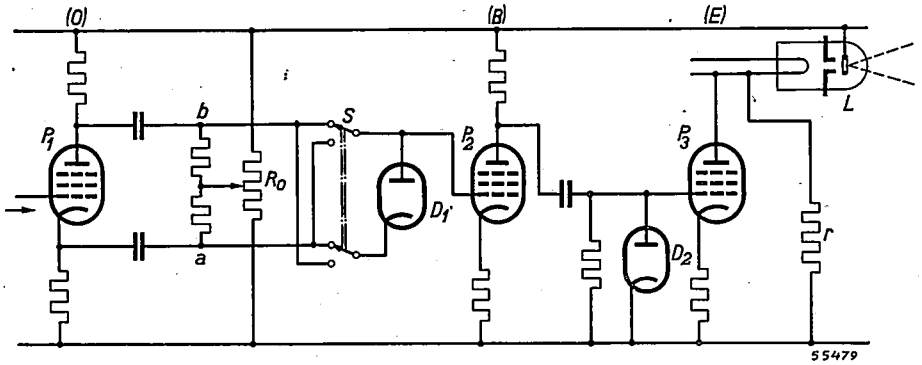


Fig. 12. The last three stages of the transmission, in the receiving apparatus (*O*, *B*, *E* of fig. 1). *L* is the recording lamp fed by the output valve P_3.

when judging properties of transmission, such considerations do not lead to the simplest insight when the form of the signal becomes a factor to be taken into account.

It may also be worth while to explain the following. If the signal from the photocell is strong enough to be modulated on a carrier directly, without amplification, and if it is then not demodulated until the output stage is reached in the receiver, the abovementioned problem as to how to transmit the "scale" of the facsimile signal can be solved in a much simpler way. Each signal level then corresponds to a certain carrier amplitude right from the beginning and it can easily be arranged for the scale of carrier amplitudes to be faithfully reproduced in a scale of grid voltages controlling the output valve. This is what is done in most systems for slow facsimile transmission; all kinds of methods, partly mechanical and partly electrical, are employed for the modulation. In our case, however, the signal is too weak for direct modulation so that pre-amplification is necessary. Further, in our system the "demodulation" takes place before the output stage is reached, as shown in fig. 1, in order to provide for the slicing without any great complications, a process which will be discussed below. It is for these reasons that the unconventional method of transmitting the limits for black and white had to be adopted; although this method may be somewhat difficult to understand, its practical realization is quite simple.

Reversal and slicing

Fig. 12 is a basic circuit diagram of the amplifying stages in the receiver designated in the block diagram of fig. 1 by items *O*, *B* and *E*.

P_3 is the output valve (EL6), the anode current of which traverses the recording lamp *L*. A given negative feed-back is provided by a non-bypassed cathode resistor in order to obtain the best possible linear relation between anode current and grid voltage (signal voltage). As maximum current it is desired to use the anode current supplied by the valve at a grid voltage zero with respect to earth [8]); the current is cut off at a grid voltage of —15 V. For the recording lamp to give negative reproduction of the original on the film the valve must in principle pass maximum current for the signal level *C* (original white) and zero current for the signal level *B* (original black). This is achieved in the following manner. The signal amplitude from *A* to *D* is adjusted to 26 V (using meter *I* in fig. 1; see above) and with the aid of the diode D_2 the signal peaks are maintained at such a potential that the signal lies within the "grid base" of the valve as shown in *fig. 13b*. The parts of the signal more negative than *B* fall beyond cut-off and therefore have no effect.

Since with increasing anode current of an amplifying valve the voltage drop across the anode resistor increases, the lower (less positive) the grid voltage of the valve P_2 the more positive is the anode potential of this valve. Therefore, in order to get on the grid of P_3 the signal as sketched in fig. 13*b*, the grid voltage of P_2 is made to vary according to fig. 13*a*: here the signal is reversed. Moreover a further diode D_1 fixes the potential of the "peaks" *A* and ensures that the signal falls in the grid base of valve P_2 in such a way that the signal levels "below" *C* (i.e. the pulses *D*) are cut off. (By the diode D_2 level *C* is then actually fixed and not level *D*.)

The combined stages P_2 and P_3 thus effectively confine the signal between the limits *B* and *C*.

[8]) The valve is capable of delivering still larger instantaneous currents, but these are not used because the maximum current may persist for long periods of time, as will be seen later.

Actually all that is attained is that the grid base of the output valve available for linear reproduction is utilized to the full. The slicing, however, is of more essential significance when, instead of photographs, originals have to be transmitted which are only black and white.

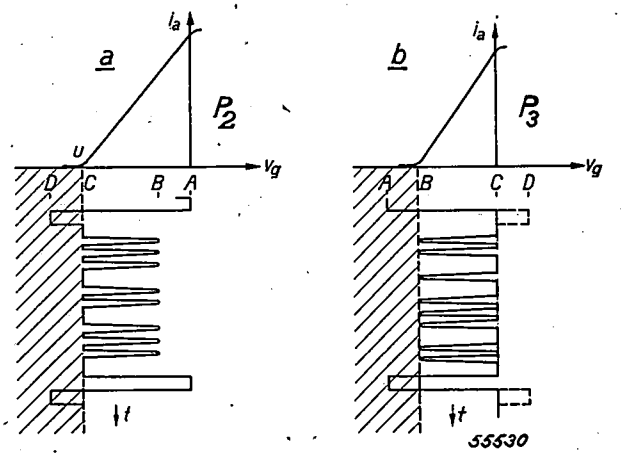


Fig. 13. i_a-v_g characteristics of the fed-back valves P_2 and P_3. *a*) The signal (at the bottom on the left) is applied to the grid base of the amplifier valve P_2 so that the levels "below" C (i.e. the maxima of the impulses D) come to lie below the cut-off point u of the characteristics. This is made possible by maintaining level A at a fixed potential and the amplitude A-D constant. *b*) The position of the signal in the grid base of the output valve P_3 is such that the maximum current flows at the level C (white) which is kept at a fixed potential, and the levels below B (black) lie below the cut-off point. Thus the signal is confined to the limits C and B.

In this case, where it is only a matter of getting the best possible contrast between black and white, the signal is amplified to give an amplitude of say 65 V measured between A and D. It is applied to the grid of the output valve in such a way that the slicing takes place at a signal level B' corresponding for instance to a 40% coefficient of reflection in the original. The maximum current is now already obtained at a signal level C' corresponding to a coefficient of reflection of 60%; see *fig. 14*. The parts of the signal with levels between C' and D are sliced by the preceding stage P_2 in the manner described above. The advantage of this method is, in the first place, that the transitions between black and white are more sharply defined than would be the case with the process according to fig. 13. The impulses corresponding to the lines on the paper traversed by the scanning spot get steeper flanks and thus the blurring caused by the finite diameter of the scanning spot in the transmitter (see article III) is partly compensated. In the second place one now gets a perfectly uniform white background and uniform black letters, whereas the "white" and "black" signal levels B and C used in fig. 13 contain all sorts of noise and random fluctuations such as caused by smudges or spots on the paper or by small irregularities in the focusing of the optical system in the transmitter [9]).

The cut-off levels can be varied by adjusting the gain of the preceding stages and setting the D.C. grid potential of P_2 with the potentiometer R_0 in fig. 12.

In this chapter we have pre-supposed that the output valve had to supply the maximum current at the signal level corresponding to white in the original. On the film we then get a negative reproduction. It is clearly possible that also a positive reproduction can be obtained on the film by "reversing" the signal before it reaches the grid base of the output valve, in the manner as shown in fig. 13*a* for the valve P_2: maximum current then has to flow through the recording lamp at the signal level B (or B' if slicing is applied for black and white documents) and zero current at the signal level C (respectively C'). With the circuit of fig. 12 this is very easily done. If the amplification of P_1 is made equal to 1, the coupling circuit with the modified diode connection applied between the valves P_1 and P_2 actually supplies a balanced signal at the output. Thus the potential of point a varies inversely to that of point b, which we have so far been using. The desired reversal of the signal — with the level D given a fixed potential value on the grid of P_2 — is therefore obtained by reversing the diode connections by means of the switch S. By adjusting the said fixed potential value with the aid of R_0 the reversed signal is again applied in the correct manner to the grid base of the valve P_2.

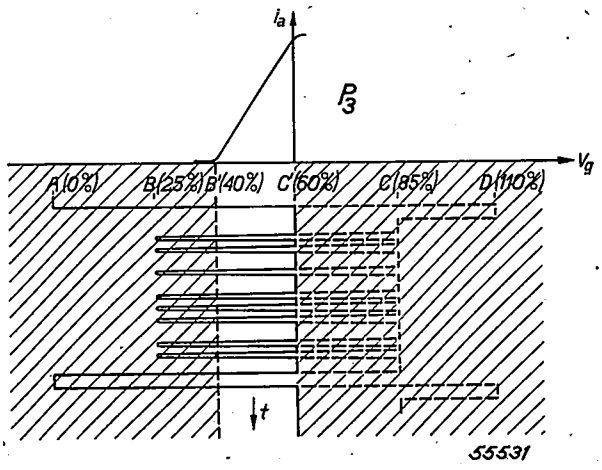


Fig. 14. By strongly amplifying the signal in advance it can be applied to the grid bases of P_2 or P_3 in such a way that these valves act as slicers operating at the levels B' and C' instead of B and C. In this manner black-and-white documents are reproduced with much more contrast and noise and smudges are eliminated.

[9]) Distortion due to the drift of grid potential in the diode circuit according to fig. 6 is also eliminated by slicing.

Linearity of the reproduction

Finally, the linearity of the complete system has to be considered. The transmitter amplifiers and other links in the chain are substantially linear, that is to say the current supplied by the ouput valve is in a linear relation to the reflection coefficient of the picture elements scanned. In the receiving apparatus, however, certain non-linear elements occur, notably the recording film, the printing paper on which an enlarged positive copy is made, and the recording lamp.

Assume for a moment that the recording lamp had a linear characteristic, that is to say that a linear relation existed between the luminous intensity of the lamp and the current of the output valve. As regards linearity the reproduction through the whole of our system would then be just as good or as bad as could be produced by ordinary photography. It is well known that the non-linearity of the film and that of the printing paper can be made to compensate each other to a considerable degree.

The characteristic of the discharge in mercury and argon, which is used for the recording lamp (see article III), however, is not quite linear. By introducing the resistor r in fig. 12 a small standing current is allowed to flow through the lamp and in this way the curvature of the characteristic can be utilized to improve upon the abovementioned compensation.

This procedure is, of course, only applicable to negative recording and if the inversion described above is used, thereby directly obtaining a positive reproduction, no compensation is obtained. This, however, is of little importance since the reproduction of a positive copy on the film need only be considered when it is intended to make subsequent prints on normal photostat paper (giving a positive print from a positive), but in view of the very steep characteristics of photostat papers this is only possible for documents having no half-tones anyhow, where the linearity of the reproduction is of no account and, owing to the process of slicing described, we even intentionally depart from linear circuit conditions.

ON THE ILLUMINATION OF TRAFFIC TUNNELS

by A. M. KRUITHOF.

628.971.8:535.241.46

A traffic tunnel, for instance one under a river, cannot be illuminated in a practicable manner to the same level of brightness as exists outside in full daylight. An example of such a tunnel will be dealt with to demonstrate the trouble experienced by the driver of a motor vehicle passing through the tunnel, due to the great change in the level of brightness. The nature of these troubles can be considered from the point of view of brightness adaptation and from that of glare. It appears that the data regarding adaptation to brightness are inadequate to provide a basis upon which anything definite can be concluded about the quality of vision. Various performances of the eye, i.a. contrast sensitivity, are reduced by the glare. Data available in the literature on the subject give no satisfactory explanation of the difficulties. Here the results are discussed of a laboratory experiment carried out to investigate the change in contrast sensitivity when approaching and entering a tunnel. The conditions assumed in the case of the tunnel chosen as an example resemble those existing in the tunnel under the river Meuse at Rotterdam. If in the light of these investigations the visual conditions of such a tunnel are to be further improved, this would be possible by raising the brightness in the entrance of the tunnel, which in practice can be done by tempering the daylight just outside the entrance.

Introduction

In modern town planning it has often been found necessary to build a tunnel under a river passing through the town. In the execution of such a project one is faced with a number of problems, one of which is the question how such a tunnel should be illuminated to meet the conditions of safety for fast-moving traffic.

To illuminate the traffic tunnel so intensely as to give inside it the same level of brightness as exists in the daytime on a thoroughfare outside is technically almost impossible and certainly not justified economically. It cannot therefore be avoided that inside such a tunnel the brightness is on a lower level than outside and it takes some time for one's eyes to get adapted to the lower level of brightness. Pedestrians do not as a rule experience any difficulty, for when they descend by escalators or enter the tunnel in any other way there is usually time enough for the eye to adapt itself sufficiently to the changed conditions to be able to distinguish the objects and pass through the tunnel without any trouble. For a motorist, however, travelling at a speed of say 35-40 miles per hour, the time in which the eye has to become adapted to the transition is so short that unless special measures are taken traffic is apt to be seriously endangered.

In this article we shall first try to picture the troubles arising for the motorist when passing through a tunnel under certain conditions taken here as an example.

We shall then investigate further the physiological phenomena which in this case may throw some light upon the quality of vision.

These considerations have led to some experiments being carried out in regard to the behaviour of contrast sensitivity under changing conditions, the results of which experiments will be dealt with at the end of the article.

Example of a traffic tunnel

Let us assume that we have to do with a tunnel for fast traffic about 1 kilometre in length and with separate tubes for each direction of traffic say 7 metres wide and 4 metres high; this width is sufficient to allow of one motorist overtaking another.

It is assumed that for the first 100 metres the illumination inside each tunnel is such that the horizontal brightness amounts to 65 c/m^2; after this 100 metres the lighting of the tunnel itself begins, the brightness of which is taken as 3 c/m^2, which is maintained right up to the exit of the tunnel. Further it is assumed that the lamps inside the tunnel are so arranged that there is no noticeable unevenness in the brightness and that there is no glare. Moreover it is taken for granted that the motorists maintain a speed of 35-40 miles per hour when passing through such a tunnel and that they do not use their headlamps.

The visual field of a motorist passing through the tunnel

When travelling at 35-40 miles per hour on a normal motor road most drivers direct their gaze on a point about 200 metres ahead. During a short interval this distance may be reduced to say 100 metres. If the eye is dropped to a still shorter

distance the road appears to slip past at such a great speed as to be troublesome and very fatiguing for the observer.

When approaching a tunnel along an open road the driver will usually have a field of vision with high level of brightness, varying of course considerably according to the weather and the state of the road surface. On a sunny day when snow is lying on the ground the level of brightness may be as much as 3×10^4 c/m^2, whereas on a dark rainy day it may be no more than 10^2 to 10^3 c/m^2.

For the greater part of the driver's field of vision this high level of brightness is maintained up to a few moments before he enters the tunnel, when he very soon finds himself inside where the brightness is at first 65 c/m^2 and a moment later only 3 c/m^2.

The question now is whether the human eye is capable of adapting itself to this low level of brightness within the time available. Upon leaving the tunnel, on the other hand, the eye is called upon to adapt itself rather suddenly from a low to a high level of brightness.

Various aspects from which vision in the tunnel is to be judged

The physiological processes taking place in the eye when entering and leaving the tunnel might be regarded as a form of adaptation to brightness.

Coming from very bright surroundings the motorist finds himself rather suddenly in a very much less bright environment. What he then experiences bears a certain resemblence to what takes place when one suddenly steps out of a brightly lighted room into complete darkness, or when the lights are suddenly extinguished in a room, with this difference, however, that in the case of the tunnel there is not absolute darkness because, as we have assumed, there is still anyhow a brigthness of 3 c/m^2.

When using the expression "adaptation of the eye" it implies more or less that it is here a matter of phenomena to which the eye is subject in its entirety. We must not overlook the fact, however, that already when approaching the tunnel the retina is in an exceptional state as regards the distribution of light, since some hundreds of metres before the tunnel entrance is reached the driver will be casting his eyes ahead to see whether there are any obstacles in the tunnel. He will keep his gaze fixed on the tunnel entrance and as a consequence the centre of his field of vision will be formed by an ever-expanding field of low brightness.

The driver's attempts to distinguish details in the field considered will be hampared by the high level of brightness of the rest of the visual field formed by the wall round the tunnel entrance, the part of the sky visible above it, and the road surface between the driver and the tunnel. This high level of brightness will result in glare and affect the vision in the central field. For this reason the physiological process taking place in the eye is in the second place to be regarded as a blinding process, at least when entering the tunnel.

Thus, while approaching the tunnel entrance, the motorist suffers from glare from the environs of the entrance, but when a moment later he enters the tunnel the high level of brightness has entirely disappeared, though he will still be troubled from its after-effects. So long as there is still the high level of brightness one speaks of a simultaneous glare, but when it has disappeared one speaks of successive glare [1]).

At the transition from the entrance lighting to the lighting inside the tunnel the same processes take place as when entering the tunnel, though at lower levels of brightness.

Both aspects of the problem, adaptation and blinding, will be investigated further in this article.

Before a motorist leaves the tunnel he already has a bright field of vision in dark surroundings at some distance from the exit. The dark surroundings tend to concentrate attention on the bright visual field and favourably affect the observation. Moreover, the fact that the bright visual field gradually becomes larger is also to be regarded as favourable. We shall revert to this later.

Illumination of the tunnel considered from the aspect of adaptation to brightness

The human eye has two kinds of light-sensitive elements, those which are used for high levels of brightness and for colours and those with which low levels of brightness are observed. When we have been for some time in a brightly illuminated space we see with the elements for high levels of brightness (the cones). When we leave the lighted room and suddenly enter a dark one then the faintest glimmer of light we are capable of observing with these elements corresponds to a brightness of something like 0.1 c/m^2. This is called the threshold value of brightness, with respect to the brightness to which the eye had become adapted in the brightly illuminated surroundings.

When we stay a long time in a dark room this

[1]) The various forms of glare have already been discussed at length in this journal, see P. J. Bouma, Philips Techn. Rev. 1, 225-229, 1936.

threshold value brightness drops in about 30 minutes to 6.4×10^{-6} c/m^2 (the graphical representation of this change is called a threshold value curve). The elements for low levels of brighness (the rods) also become gradually sensitive in the dark surroundings, their sensitiveness increasing in all by a factor of 15,000, at which level practically the uttermost limit of light sensitivity (the absolute threshold value) has been reached.

So much for the process of darkness adaptation. The opposite process, of adaptation to light, takes place much quicker. Upon leaving a dark room and entering a brightly illuminated one the eye is usually very soon adapted to the new situation after some blinking.

Both adaptations, to darkness and to light, take place relatively slowly, although the latter is much quicker than the former. The eye, however, has a special property which in the first moments of the change of brightness enables us to neutralize the change at least partly. This property is the power of the pupil of the eye to expand and contract, its diameter varying roughly from 2 to 8 mm according to the brightness observed.

The change in the threshold value as a function of time can be investigated, for a certain degree of brightness to which the eye is adapted, by determining the lowest perceptible brightness at different moments after the high brightness has been removed.

In the example of a tunnel with which we are concerned here the level of brightness assumed in the tunnel itself is still within the range of vision for the cones. Also the time it takes a motorcar to pass through the tunnel is so short that the use of the other elements can be left out of consideration. Consequently we shall only investigate the variation of the threshold value brightness in so far as it is observed with the cones.

Fig. 1 shows such a threshold value curve [2]). It starts from a situation where the eye was adapted to a brightness of 3×10^4 c/m^2 and indicates the change in the threshold value brightness for a natural pupil diameter. With this curve it is possible to ascertain whether we are able to perceive anything when we have to change suddenly from a certain initial brightness to a lower level of brightness, for if the latter lies above the threshold value perception is in principle possible.

In addition to the threshold value curve, in fig. 1 we have indicated by horizontal lines: the brightness to be expected outside the tunnel on a very bright day with snow: $B_1 = 3 \times 10^4$ c/m^2, on a bright day without snow: $B_2 = 2.5 \times 10^3$ c/m^2, on a dark day: $B_3 = 2.5 \times 10^2$ c/m^2; the brightness at the illuminated tunnel entrance: $B_4 = 65$ c/m^2 and that inside the tunnel itself: $B_5 = 3$ c/m^2.

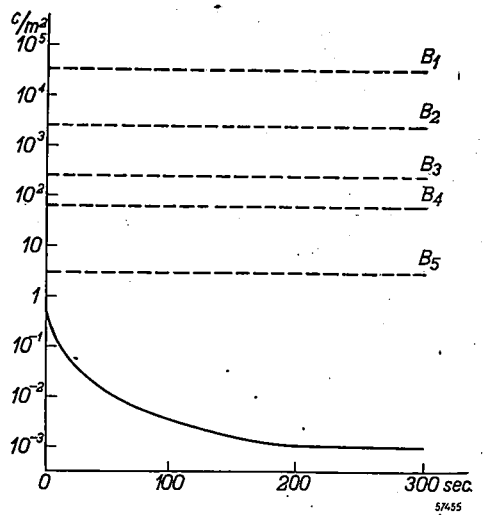


Fig. 1. Threshold value curve for the human eye at an initial brightness of 3×10^4 c/m^2. The curve indicates for this initial brightness the variation of the threshold value brightness as function of time in so far as the eye elements for high brightness are used. The horizontal lines give the degrees of brightness that may be expected in the case of the tunnel considered here as an example: B_1, B_2 and B_3 are the brightnesses outside the tunnel respectively on a sunny day with snow, in clear weather without snow and on a dark day; B_4 is the brightness under the entrance lighting and B_5 that under the normal tunnel lighting.

From this graph it appears that the brightness of the entrance lighting (B_4) lies above the threshold value curve appertaining to the initial brightness in the case of a bright day with snow (B_1). In the transition from B_1 to B_4 (and this is the most unfavourable case that can occur with the tunnel) the eye will therefore most certainly be able to perceive something. Even in the transition from B_1 to B_5 vision is still possible, since the line corresponding to the brightness B_5 likewise lies above the threshold value curve. If the brightness outside the tunnel is B_2 or B_3 it follows a fortiori that the eye is still capable of perception after transition to the brightnesses B_4 and B_5 respectively.

After 60 seconds — the time it takes a motorist to drive through the tunnel — the threshold value brightness has not yet reached its minimum.

It is of importance to note from fig. 1 that after entering the tunnel a motorist is still able to observe things, but it remains the question whether the conditions of vision are adequate for safe traffic.

One might try to obtain an impression of the quality of vision in the tunnel by comparing the

[2]) This curve was calculated according to the theory of Moon and Spencer (J. Opt. Soc. Amer. 35, 45-65, 1945), which represents the phenomena with sufficient accuracy for our purpose.

brightness prevailing there with the threshold value brightness of the motorist's eye.

Suppose that this threshold value brightness is n times lower than the brightness in the tunnel or becomes so many times lower after a certain time. If, either immediately or after some time, n is sufficiently high then one can easily observe any obstacles in the tunnel. The value that this factor n should have depends upon the requirements considered necessary for safe traffic and visual comfort.

For the case of the tunnel considered here as an example, immediately after entering it the ratio of the brightness in the entrance to the threshold value that the eye can perceive is on a very bright day 120, whilst on a dark day the ratio is higher. The question whether this ratio is high enough for adequate visual conditions can only be answered by experimental investigation.

The data available regarding adaptation to brightness are insufficient to allow any conclusion being drawn about the state of vision in the tunnel. We must not, however, confine our considerations to this adaptation as the cause of the change in the threshold value brightness, but must also take into account the behaviour of other physiological properties of the eye which likewise change during the process of adaptation. It is therefore necessary to look more closely into these properties of the eye under the conditions given.

The phenomena on leaving the tunnel thus stand in an entirely different light. Apparently it is the case that during the short stay in the tunnel only a slight adaptation takes place in the motorist's eye, and it is thus understandable that the motorist has no trouble when leaving the tunnel.

Further consideration of the tunnel lighting as a problem of glare

It has already been noted that the phenomena upon entering and passing through the tunnel can also be regarded from the aspect of glare and that we have to differentiate between simultaneous and successive glare.

To be able to study the glare of the various impressions of brightness upon the eye under different conditions it is desirable to express this effect numerically. This is usually done by measuring in how far a certain performance of the eye declines in a particular case of glare.

Thus we are able to measure the decline of contrast sensitivity, of visual acuity, of speed, of perception, etc.

We shall devote attention mainly to contrast sensitivity. This is one of the most important factors governing vision on the road; it is more readily affected by glare than any other factors and easy to measure, whilst much is already known about it. The other factors mostly show a corresponding behaviour.

Contrast sensitivity is defined as B: ΔB, where ΔB is the increase or reduction in brightness just perceptible which can be introduced into a part of the field of vision when the whole of the latter originally had a brightness level B. If somewhere in the field of vision there is an object with a considerably higher brightness than B, for instance a source of light, then that object (or source of light) will give rise to a certain glare manifest in a reduction of the contrast sensitivity.

Measurements of contrast sensitivity in an inner field surrounded by another of high brightness have been carried out by Schuhmacher [3]). These measurements, however, are only of partial use for our purpose, for we have assumed that the brightness of the illuminated tunnel entrance, forming the actual visual field of the motorist before entering the tunnel, amounts to 65 c/m^2, whilst it is further assumed that the surroundings of this field on a sunny day will reach the very high brightness of 3×10^4 c/m^2. Schuhmacher's data do not extend so far as regards the ambient brightness, but they nevertheless go to show that very high contrasts are required for anything to be seen in the given circumstances. From his results it may actually be concluded that with a centre field of 65 c/m^2 the ambient field may certainly not exceed 640 c/m^2 if a contrast sensitivity of 40 is to be reached, and that for the same contrast sensitivity with an ambient field of 6400 c/m^2 the centre field must have 3200 c/m. In this connection it is of importance that the angles of vision from which Schuhmacher took his measurements were of the same order as those which would occur in the case of the tunnel we are considering.

Looking at these figures one would conclude that the tunnel illumination which we have had in mind is quite worthless.

It appears, however, that the lighting of the Meuse tunnel in Rotterdam, which corresponds fairly well to the case we are considering, is indeed reasonably useful, though there is room for some improvement.

Apparently the physiological process with its greatly varying character, whereby the previous situation still has its influence upon the next, cannot be so easily divided into parts, with the result that

---

[3]) Das Licht **11**, 134-135, 1941.

the statically determined data given in literature cannot be applied to our case directly.

Both the considerations of brightness adaptation and those of glare led us, therefore, to take measurements of contrast sensitivity under conditions corresponding to those under which a motorist finds himself when approaching and entering a tunnel.

Contrast sensitivity measurements when approaching and entering the tunnel

A model was constructed and the bright surroundings of the tunnel entrance were imitated by fitting up a large screen of 3 m × 3 m made of tracing paper which could be strongly illuminated from the back. In the centre of this screen, S_1, first a rectangle of 12 cm × 20 cm was cut out and then another of 42 cm × 70 cm, and about 15 cm behind these openings another screen, S_2, with a low brightness was set up. Spots of light, V, 1 and 3 cm in diameter and of high brightness could be projected on this second screen.

We now place side by side in the left-hand column a description of the conditions at the tunnel being imitated and in the right-hand column a description of the manner in which this has been arranged and how the measurements were taken.

A motorist is travelling along an unobstructed road at 35-40 miles per hour on a very bright sunny day. In the distance is the tunnel he has to pass through.

The test person takes up a position 2 metres away from the screen. S_2 is 12 × 20 cm and V has a diameter of 1 cm. The brightness of S_1 averages 6400 c/m² and S_2 65 c/m².

A certain contrast is adjusted between S_2 and V. The test person is asked to adapt his eye for a few minutes to the high brightness of S_1.

At about 70 metres distance from the tunnel the motorist wants to see whether the entrance is free and so directs his gaze upon it and tries to see into the tunnel.

At a given moment the test person is asked to look at S_2 and to say whether he sees the contrast there. The contrast is changed several times in order to determine the threshold of the contrast sensitivity.

After two seconds the motorist has approached to within 35 metres of the tunnel and tries to see whether there are any obstacles inside it. He will have been directing his gaze continuously upon the tunnel entrance from a distance of 70 metres away.

The test person takes up a position one metre away from the same device. He is again asked to adapt his eye to the high brightness. At a given moment he has to look at S_2 and 2 seconds thereafter the threshold of the contrast sensitivity is again determined.

As the motorist drives on farther the tunnel entrance appears to become larger and any obstacle observed is perceived under an angle increasing in size. After almost two seconds the motorist has reached to within 10 metres of the tunnel entrance.

The screen S_2 is enlarged to 42 × 70 cm and the light spot V is given a diameter of 3 cm. The observer takes up a position 1 metre away from the screen. His field of vision now gives him the same impression as what the motorist gets at a distance of about 10 metres away from the tunnel. The test subject first adapts his eye again to the high brightness. At a certain moment he looks at S_2 and 4 seconds later the threshold of the contrast sensitivity is determined once more.

While travelling the last 10 metres before entering the tunnel the motorist finds his field of vision changes considerably in a very short time. Whereas at first the tunnel with its low brightness occupied a small part of the field of vision, it soon fills almost the whole of it. This is the case at the moment the car enters the tunnel.

The beginning of the test is the same as in the previous paragraph except that 4 seconds after the test person looks at S_2 the brightness of S_1 is brought down to the level of that of S_2. At this moment the test subject starts a stop-watch going. A certain contrast is focused on S_2 and the subject stops his watch as soon as he is able to perceive this contrast. By varying the strength of the contrast the change in contrast sensitivity can be determined as a function of time.

Results of these measurements are represented in the lower half of *fig. 2*. The observations were made with five test subjects, three of whom were less than 30 years of age and two a few years older. The fully-drawn line represents the average contrast sensitivity of these subjects. The spread of the measurements is indicated by the dotted lines. The results of the two older persons show no systematic deviation from those of the other three; neither was this to be expected, since the decline of contrast sensitivity of persons over 30 years of age is only very small during the first few years and the spread of the results is relatively large.

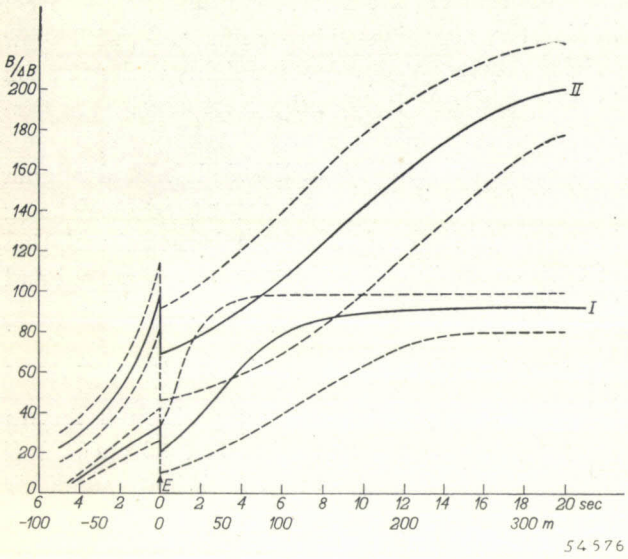


Fig. 2. The results of a laboratory test regarding the change of contrast sensitivity when the brightness and the ambient brightness of the field of vision are changed. The lowermost fully-drawn line indicates the variation of the contrast sensitivity of the eye as it will be according to the test when approaching and entering the tunnel if the brightness of the entrance illumination is 65 c/m² and the ambient brightness 6400 c/m². The uppermost fully-drawn line represents the same variation with an entrance illumination of 600 c/m². In both cases dotted curves are plotted to indicate the spread of the observations taken with 5 test subjects. On the vertical axis the contrast sensitivity $B/\Delta B$ is plotted and on the horizontal axis the distance from the entrance E of the tunnel and the time it takes a car to cover this distance when travelling at a rate of $37^1/_2$ miles per hour.

According to the results of these tests the contrast sensitivity at about 70 metres distance from the tunnel would be about 7, rising to 33 upon approaching the tunnel, then suddenly dropping to 20 and rising again fairly quickly in the tunnel to a maximum value of about 90.

It is to be observed that a contrast sensitivity of 7 (contrast 15%) is not, it is true, so very bad, but when judging the results of these tests it must be borne in mind that they have been carried out by observers possessing a very good contrast sensitivity. In fact it is not the average value that should be considered but rather the least satisfactory results. Further it should be taken into account that during these tests the test subject is much more at ease and thus better able to observe things than he is on the road, and that the obstacle was large and its position known to the test person. Bearing these considerations in mind we must therefore conclude that with the brightnesses assumed the results of our experiments will not always guarantee good vision at the entrance to and inside the tunnel under all circumstances. This led us to investigate in how far the results would be improved if the brightness of the entrance lighting were raised from 65 to 600 c/m². Results obtained from the measurements then taken are represented in the upper half of fig. 2, from which it is to be seen that there is a considerable improvement right at the outset.

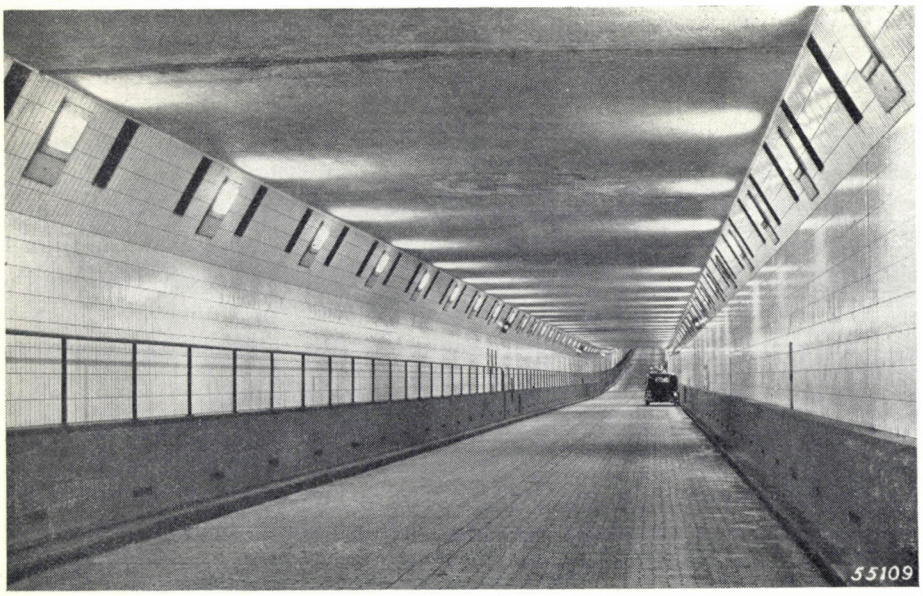


Fig. 3. A view inside the traffic tunnel under the Meuse at Rotterdam, which was opened in 1942. To meet the requirements of fast traffic two tubes were built side by side 1072 metres long, each 7.5 metres wide and 4.2 metres high, with a road width of 6 metres. For the illumination Philips sodium lamps with a flux of 2500 lumen were used, installed in shallow ornaments fitted in niches in the upper half of the tunnel walls slanting forward. The distance between the light points is 6 metres. This illumination gives a brightness inside the tunnel of 3 c/m².

The Meuse tunnel at Rotterdam

It has already been remarked that this, the only large traffic tunnel in the Netherlands, has an illumination closely resembling that of the tunnel upon which we have based our investigations.

A full description of the lighting installation of this tunnel has been given by Van Riemsdijk and Alpherts.

Two photographs of this tunnel (*figs 3* and *4*) are reproduced in this article to give an idea of the effect of the lighting. When we drove through the tunnel by way of a test we found that in sunny weather vision into the tunnel before entering it was not entirely satisfactory, neither when approaching from the southern end nor from the northern end. As soon as one got inside the tunnel it became better, though even then it cannot be said that there was great visual comfort.

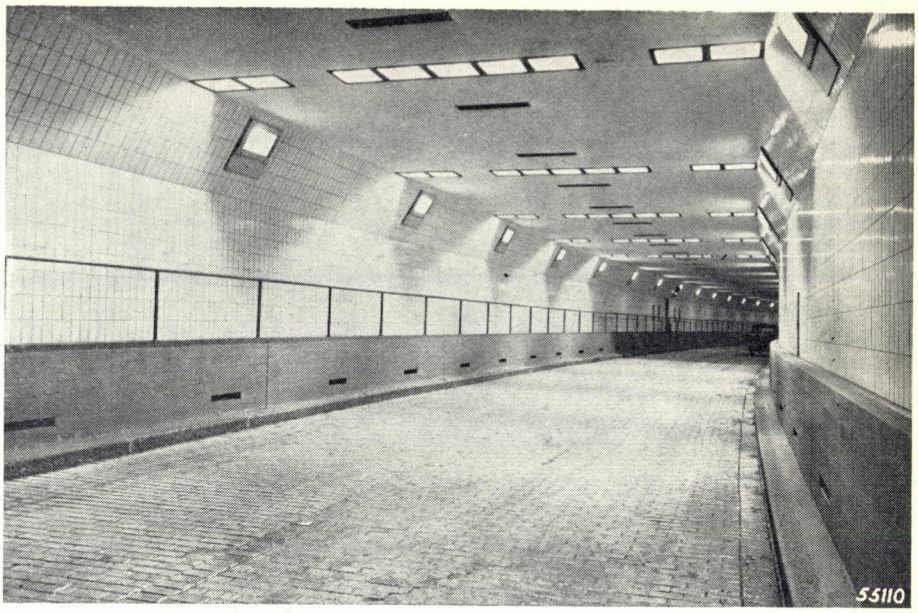


Fig. 4. The entrance lighting of the Meuse tunnel at Rotterdam. This entrance or threshold lighting consists of 5 strips of light at intervals of 6 metres in the ceiling. On the right-hand bank of the Meuse, where the tunnel entrance lies NNW, the first light strip is 15 metres from the entrance, whilst on the left-hand bank where the entrance is SE the first strip is 21 metres from the entrance. Each light strip contains 9 fittings, side by side, with mirror reflectors throwing the light opposite to the direction of the traffic. The sodium lamps used have a flux of 10000 lumen. The entrance lighting is divided into two groups so that if necessary on a dull day only half the lighting can be switched on (this was the case at the time this photograph was taken).

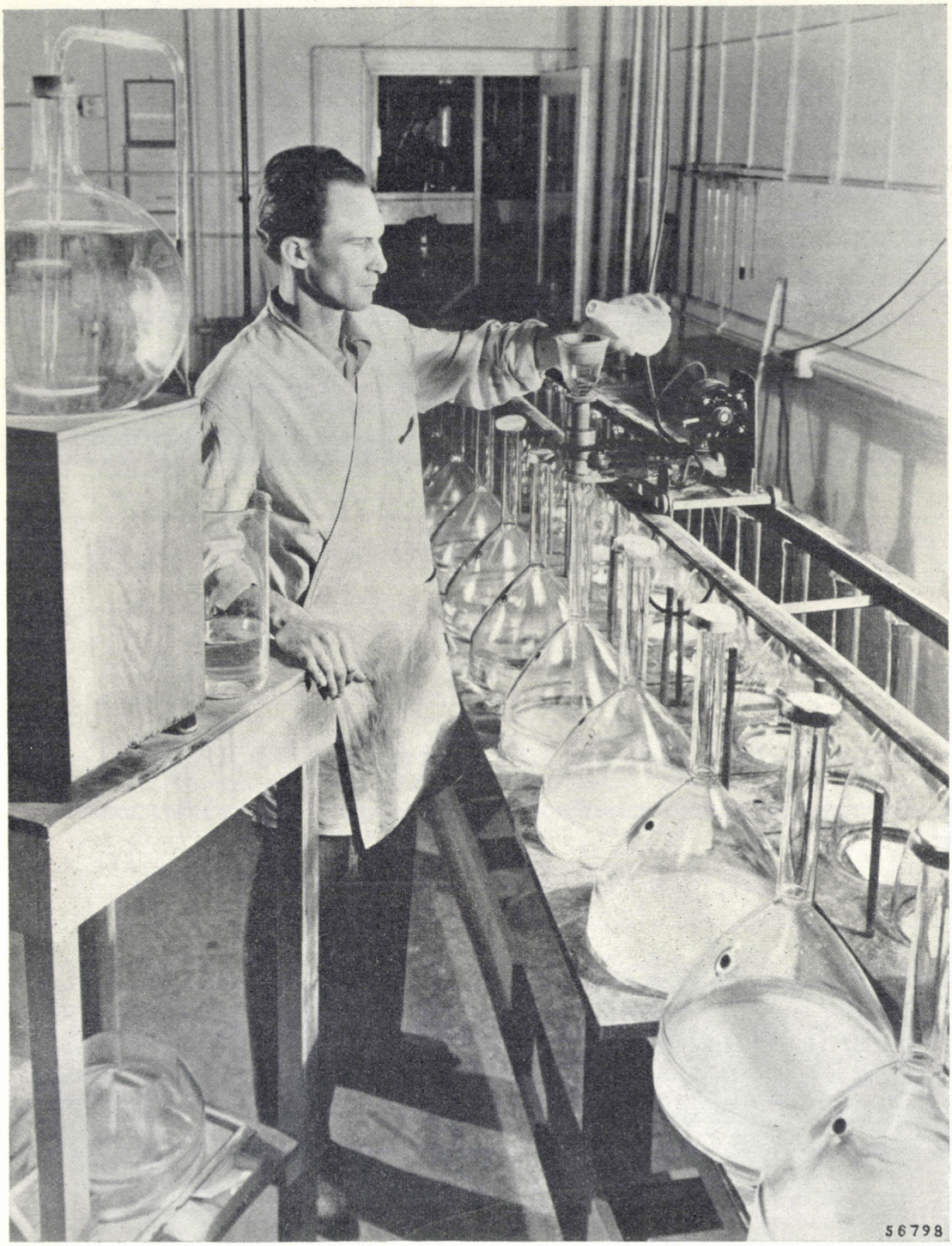
The experience that the vision before entering the tunnel was not quite satisfactory is in accordance with the results of the tests represented in fig. 2. Usually under the conditions prevailing here a contrast sensitivity of 40 is considered the minimum required for reasonable visual comfort, and this is not reached along the last 100 metres before entering the tunnel, neither is it attained just inside the entrance.

From fig. 2 it can also be seen what increase in contrast sensitivity may be expected if in the case of the Meuse tunnel the brightness of the entrance illumination were to be raised to 600 c/m^2. This does not mean to say, however, that we consider it essential to raise the brightness to such a high level, this being a matter that has to be decided according to the requirements made as regards visual comfort.

If the brightness of the entrance illumination has to be considerably raised it is not very well possible to do so by using more powerful lamps. The best solution in this case is to temper the daylight in front of the tunnel entrance, which can be done in various ways. The best known method is to extend the entrance end of the tunnel and to build that extension with a roof in which louvres are let in.

When the plans were being drawn up for the Meuse tunnel consideration was given to such a roof construction letting in the daylight over a length of about 100 metres in front of the actual tunnel, but for aesthetical reasons, among others, this was dispensed with.

DEPOSITION OF SCREENS IN TELEVISION TUBES



Cathode ray tubes for television must be provided with very homogeneous fluorescent screens. Such screens are obtained by deposition of phosphor particles from a dispersing liquid in the following way. After the tube has been filled with a pure liquid to a depth of 2″, a concentrated solution of phosphor mixture is introduced into the tube by pouring it into a rotating glass funnel closed at the end and provided with small holes arranged circumferentially around the stem. The solution flowing down the stem is ejected in a number of tiny streams through the holes and, thus, sprayed evenly over the liquid surface. In this way, the required homogeneous distribution of the phosphor particles in the liquid is obtained.

(Photograph taken at the Dobbs Ferry, N.Y., plant of North American Philips Company, Inc.)

PROJECTION-TELEVISION RECEIVER

IV. THE CIRCUITS FOR DEFLECTING THE ELECTRON BEAM

by J. HAANTJES and F. KERKHOF.

621.397.62:537.533.72

In the Philips projection-television receiver the elctron beam is deflected in a cathode-ray tube magnetically. For this purpose two saw-tooth current generators are needed, one for the horizontal and one for the vertical deflection. With interlaced scanning the frequency of the vertical deflection is equal to the mains frequency (50 or 60 c/s). The frequency of the horizontal deflection depends i.a. upon the number of lines making up a picture and is between about 10,000 and 16,000 c/s. The saw-tooth generators each comprise an oscillator stage and an output stage; the two output stages differ considerably owing to the great difference in frequency at which they operate. In this article first the output stage for the horizontal deflection is described, then that for the vertical deflection, after that the deflection coils and finally the oscillator stages. The output stage for the horizontal deflection contains an "efficiency diode" which ensures a linear saw-tooth shape and also returns to the supply source the energy which at maximum current is accumulated in the magnetic field of the deflection coils. Owing to the fact that this energy is regained, and also due to the use of magnetic material with low losses ("Ferroxcube"), it has been possible to limit the D.C. power consumption of this output stage to 8 W. The output stage for the vertical deflection is characterized by a compensating network connected in series which produces from the saw-tooth input voltage a grid voltage of such a form as to cause the deflection current to assume the right saw-tooth shape, without the output transformer having to have the very high self-inductance which would be required without this network. An additional advantage of the arrangement described is that it allows of a reduction of the direct current consumption, so that in this output stage only 3 W is needed. Apart from an outer layer of iron wire, the deflection coils contain no iron. The two oscillator stages are blocking oscillators supplying a saw-tooth voltage and controlled by the synchronization signals from the transmitter.

Introduction

In all television systems of the present day the scanning in the transmitter and in the receiver is done along horizontal lines which are traversed successively from top to bottom. It is also the common practice nowadays to apply interlacing, that is to say, first a picture is scanned consisting only of lines with odd numbers, then a picture of the intermediate lines of even numbers, then again a picture of odd lines, and so on. (Such a picture consisting of half the number of lines is called a frame; thus a complete picture consists of two frames.) Briefly, the advantage of interlaced scanning lies in the fact that with a given total number of picture lines the brightness of the picture can be increased to a higher level before flickering becomes troublesome [1]). The comparison between interlaced and non-interlaced scanning is explained in *fig. 1*.

In the article just quoted it has also been explained why it is necessary for the frequency of the vertical deflection to be chosen equal to the mains frequency. That is why the television systems in Europe work with 50 frames per second and those in America with 60.

The number of lines per complete picture differs rather considerably in the various countries: the British work with 405 lines, the French with 455,

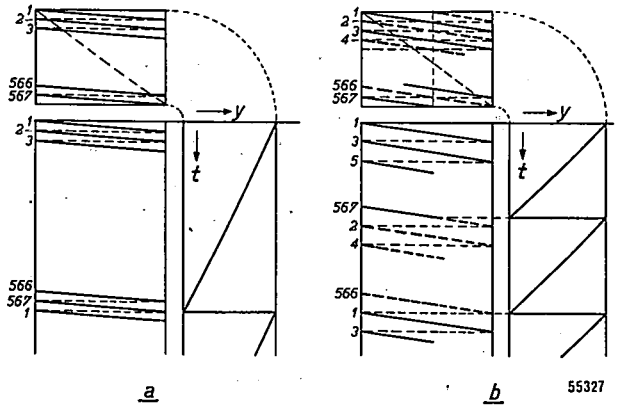


Fig. 1. *a*) Non-interlaced, *b*) interlaced scanning with for instance 567 picture lines. In the case of scanning without interlacing the order in which the lines are scanned is 1, 2, 3, 4 .... 566, 567, 1, 2, and so on. With interlaced scanning alternately the odd lines 1, 3, 5, ... 567 and the even lines 2, 4, ... 566 (indicated by broken lines) are scanned. To the right of each of the figures the vertical deflection y is plotted as function of the time t; in *b*) the frequency of the vertical scanning is twice as high as in *a*). The fly-back time of the light spot is assumed to be infinitely short.

[1]) J. van der Mark, Television, Philips Techn. Rev. **1**, 321-326, 1936.

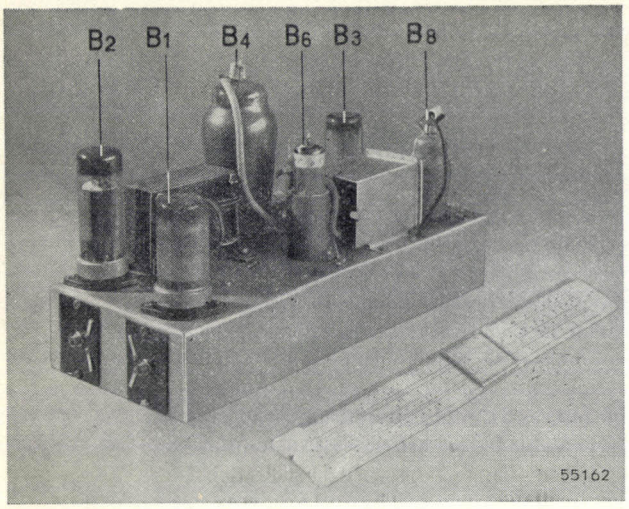
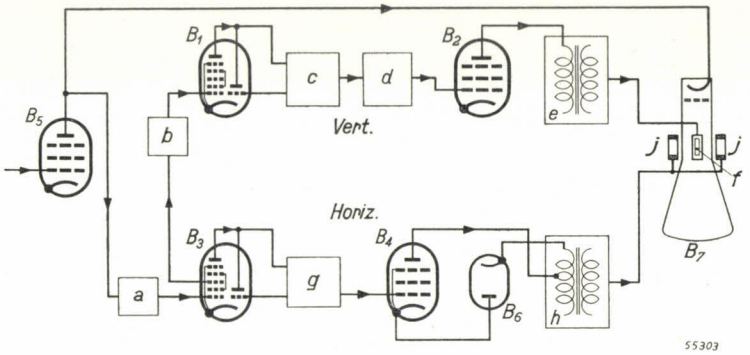


Fig. 2. *Left:* Chassis with synchronizing and deflecting system of the Philips projection-television receiver; *below:* block diagram of the same including the output valve B_5 of the video receiver and the cathode-ray tube B_7.
Horizontal deflection. Oscillator stage: triode part of B_3 with network *g*. Output stage: pentode B_4, diode B_6, transformer *h*, deflection coils *j*.
Vertical deflection. Oscillator stage: triode part of B_1 with network *c*. Output stage: compensating network *d*, pentode B_2, transformer *e*, deflection coils *f*.
Synchronization. From the synchronization signals the networks *a* and *b*, in combination with the heptode parts of B_3 and B_1, derive voltages which synchronize the oscillator stages.
Valves: B_1 and B_3 = heptode-triode ECH 21, B_2 = pentode EBL 21, B_4 = pentode EL 38, B_6 = diode EA 40, B_8 = triode EBC 33 (the function of B_8, which is not referred to further in this article and is omitted in the block diagram, is to suppress the beam current in the cathode-ray tube in the event of a breakdown in the deflecting apparatus, so as to avoid damage to the luminescent screen owing to the light spot remaining stationary or describing only one line).
Supply: 350 V direct voltage, about 15 W (including consumption of the oscillator stages and the synchronization).
Dimensions: Base area 11.5 cm × 29 cm, height 18 cm (roughly 5″ × 12″ × 7″).



the Americans with 525 and the experimental transmitter at Eindhoven with 567.

According to the British system, for instance, in each frame, lasting $^1/_{50}$ second, $202^1/_2$ lines have to be scanned, thus the frequency of the line-scanning in England is $202^1/_2 \times 50 = 10{,}125$ c/s. With the American television system this frequency is $(525/2) \times 60 = 15{,}750$ c/s.

The deflection of the electron beam in a cathode-ray tube, on the screen of which the television picture is scanned, can be brought about with the aid of an electrostatic or a magnetic field. In a previous article [2]) in this series the reasons were summed up which led to magnetic deflection being applied in the projection tube MW 6-2 both for the horizontal and for the vertical direction. Consequently the receiver has to be equipped with two saw-tooth current generators, one working on the mains frequency and the other on a frequency of the order of 10,000 c/s.

These two saw-tooth generators have to run absolutely synchronously and in phase with the corresponding generators in the transmitters scanning the picture, and for this purpose synchronizing signals are transmitted as already described in this journal [3]).

In *fig. 2* a photograph and block diagram are given of the synchronizing and deflecting apparatus used in the Philips projection-television receiver. The cathode-ray tube has two pairs of deflecting coils: *f* for the vertical, *j* for the horizontal deflection. Each pair of coils is fed with a saw-tooth current via a transformer. This current is generated with a saw-tooth voltage derived from a blocking oscillator. The latter consists of a network (*c* and *g* respectively) in combination with the triode part of the valves B_1 and B_3 respectively. The output valve B_5 of the receiver proper supplies on the one hand the output signal direct to the cathode-ray tube, in which this signal modulates the current intensity according to the brightness of the image points, and on the other hand it supplies the synchronizing signals to the heptode parts of B_3 and B_1, which parts are coupled to the triode parts and thus control the relaxation oscillations of the latter.

[2]) J. de Gier. Projection-television receiver, II. The cathode-ray tube, Philips Techn. Rev. **10**, 97-104, 1948 (No. 4).

[3]) Television receivers, Philips Techn. Rev. **4**, 358-366, 1939.

In the following we shall deal successively with the output stage for the horizontal deflection (from valve B_4 to the coils j, fig. 2,) the output stage for the vertical deflection (from the network d to the coils f), the deflection coils and the two oscillator stages (networks c and g with corresponding triodes). The synchronization will be dealt with in a subsequent article.

The output stage for horizontal deflection

There are various methods for generating a saw-tooth current in the deflection coils. One that immediately presents itself, and is in fact sometimes used, is that according to *fig. 3*, in which the

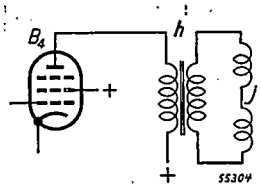


Fig. 3

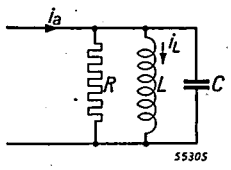


Fig. 4

Fig. 3. Pair of deflection coils coupled via a transformer to the anode circuit of a pentode. Signification of the letters as in fig. 2.

Fig. 4. Equivalent circuit for fig. 3. L = self-inductance formed by the primary self-inductance of the transformer and the self-inductance of the deflecting coils transformed to the primary side connected in parallel, C = sum of the anode and stray capacitance, R = loss resistance, i_a = anode current, i_L = current in the self-inductance.

coils are coupled via a transformer to the anode circuit of a pentode, to the control grid of which a saw-tooth voltage is applied.

For this system we have the equivalent circuit of *fig. 4*. Here the self-inductance L consists of the parallel connection of the self-inductance of the primary transformer coil and the self-inductance of the deflecting coils transformed to the primary side. The capacitance C is the sum of the capacitance of the transformer windings and that of the anode. The resistor R represents the internal resistance of the valve and the losses of the transformer.

The oscillator circuit thus formed with parallel damping is fed with a current i_a the wave form of which is identical with that of the saw-tooth voltage at the grid; i_a thus rises each time linearly from zero to a certain maximum, then flying back to zero (in a decay time which for the sake of simplicity we shall ignore here), and so on. The question now is what form the current i_L will take in the coil, for it is this current that excites the magnetic deflecting field.

Without going into the wave form of i_L in detail, it can be stated that every fly-back of the current i_a gives an impulse to the oscillator circuit (see *fig. 5* and its caption) and if this circuit is less than critically damped the oscillations set up by this will disturb the linearity of the current i_L (fig. 5*d*). It is therefore necessary that the damping should at least have the critical value. More than critical damping is not desired, because then i_L can only slowly follow the fly-back of i_a (fig. 5*f*) and as a consequence the fly-back time of the light spot becomes unnecessarily long. The most favourable condition is the critical damping, for which R must have the value R_{cr} given by

$$R_{cr} = \tfrac{1}{2}\sqrt{\frac{L}{C}}.$$

Since usually R is greater than R_{cr}, the condition of critical damping can be reached by shunting an additional damping resistor across the transformer.

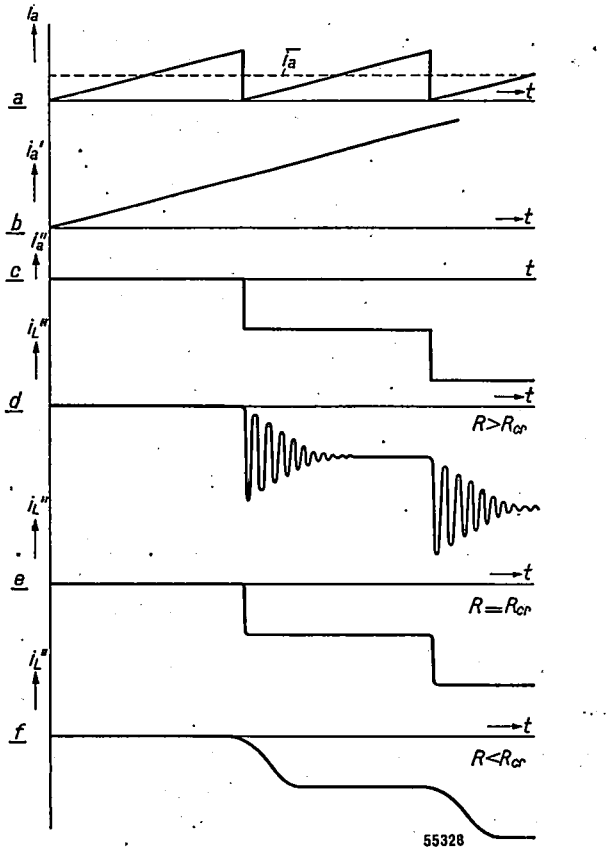


Fig. 5. Wave form of the currents in the diagram of fig. 4 as function of the time t. The saw-tooth anode current i_a (*a*) can be imagined as being composed of a current i_a' continuously rising in a straight line (*b*) and a current i_a'' dropping step for step (*c*). The current i_a' brings about in L a current i_L' (not drawn here) likewise continuously rising in a straight line. The steps in i_a'' excite the L-C circuit, thereby giving rise to a current i_L'' in L which, according to the degree of damping, has the shape shown at *d*, *e* or *f*. At *d* the damping is too small ($R >$ the critical value R_{cr}), at *f* it is too large ($R < R_{cr}$), whilst $R = R_{cr}$ at *e*, which is the most favourable condition. The total current i_L is obtained by adding the current i_L' to i_L''.

With critical damping the decay time of the current i_L lasts well over one oscillation period T_0 of the undamped circuit ($T_0 = 2\pi\sqrt{LC}$). Now in every television system there is a certain time available for the fly-back this varying from 15 to 11% of the time required for the scanning stroke. It is not always easy to choose L and C of such values as to make T_0 shorter than the fly-back time available, because L is more or less fixed by the desired frequency and amplitude of the saw-tooth current, whilst C is limited to a certain minimum by the unavoidable stray capacitances.

Another objection is that in every cycle the magnetic energy accumulated in the deflection coils at the end of the stroke is converted in a resistance into heat, and in the case of the horizontal deflection this happens to the order of 10,000 times per second. This means that a considerable direct-current power has to be supplied to the anode circuit, thus requiring an expensive power rectifier and a high-power pentode.

A slight improvement can be obtained by connecting a capacitor of suitable value in series with the damping resistor, but this is by no means adequate.

It is therefore much more satisfactory to employ a system whereby the energy of the deflection coils is for the greater part regained, and we shall now describe such a system.

Recovery of the energy accumulated in the deflection coils

The fact that with the circuit according to fig. 3 the energy in the deflection coils is lost in the form of heat upon each fly-back is actually due to the primary current of the transformer being conducted through a valve (the pentode B_4), in consequence of which this current has a D.C. component ($\overline{i_a}$ in fig. 5*a*), so that with a supply voltage V_b there is a power dissipation $\overline{i_a} V_b$. The primary D.C. component is of no consequence for the secondary saw-tooth current — with which we are concerned — and therefore $\overline{i_a}$ may be equal to zero. If this could be realized then i_a would be a purely alternating current and the energy supplied to the deflection coils during one half-cycle would be equal to the energy which these coils return to the supply source during the other half-cycle. On an average the power consumption would then be zero.

This condition is reached in the following imaginary experiment (with coils without resistance). Let us consider *fig. 6*, representing the manner in which a saw-tooth current can be generated in a deflection coil L (with capacitance C) by periodically connecting it to a battery via a switch.

So long as the switch is closed the current i_L in the coil (provisionally assumed to be free of losses)

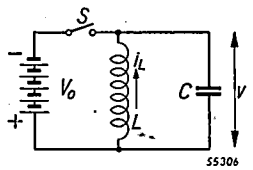


Fig. 6. By closing and opening the switch S periodically at the right moments a saw-tooth current can be generated in the coil with self-inductance L. V_0 = battery voltage. C = self-capacitance, v = voltage across the coil.

increases linearly with the time t in the ratio $di_L/dt = V_0/L$ (V_0 = battery voltage). When at the moment $t = t_1$ the current i_L has reached the value I_L required for the maximum deflection the switch is opened. In the circuit L-C an undamped oscillation is then set up the initial state of which is given by the current I_L in the coil and the voltage $-V_0$ across the capacitor. The current and voltage then change according to sine functions shifted 90° with respect to each other (*fig. 7*) until after slightly more than a half-cycle of this oscillation, at $t = t_2$, the voltage has again become $-V_0$, the

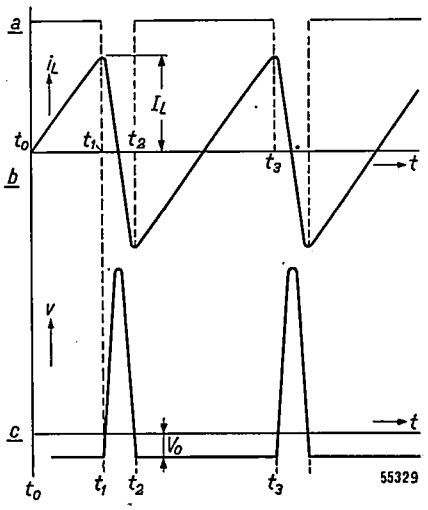


Fig 7. *a*) The straight line represents the closed position of the switch S (fig. 6) and the interruptions the open position. *b*) The wave form of the current i_L in L, *c*) that of the voltage v across L.

current then being $-I_L$. At this moment the switch is again closed. The rate of change of the current is then once more determined by $di_L/dt = V_0/L$ until it reaches the value $+ I_L$ and the switch is again opened, and so on.

In this manner a saw-tooth current is obtained rising linearly and dropping sinusoidally (fig. 7*b*).

In one half-cycle of i_L just as much energy is taken from the voltage source as is supplied to it in the other half-cycle. On an average therefore the battery does not deliver any energy during a cycle, as is only to be expected in a circuit with no energy dissipation. If, however, there are losses in the coil then of course the battery has to supply the corresponding power. The main thing is that with this arrangement the circuit energy is not lost in a damping resistor but returned to the battery (or to the source of energy used instead of it).

As already stated, the flyback covers about half a cycle of the natural oscillation, so that in this respect, as compared with the arrangement of fig. 3, there is a gain of a factor 2 in the duration of the flyback.

A third point in favour of the arrangement of fig. 6 is the fact that when the switch is closed no oscillations can arise during the scanning stroke, so that (at least in the case of a coil without resistance) a purely linear rise of the current is assured.

Efficiency diode

The question now, however, is how to produce a switch which is kept closed (for two directions of current) during the scanning stroke (t_2-t_3, fig. 7) and opened during the flyback (t_1-t_2).

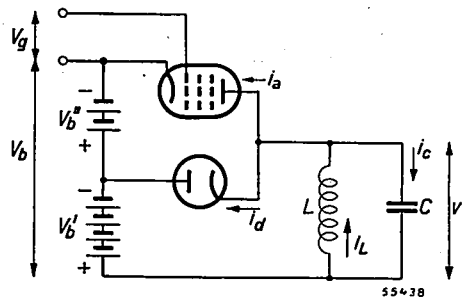


Fig. 8. The switch S (fig. 6) can be formed by means of a pentode and a diode connected in the manner indicated. The diode permits the energy accumulated in the magnetic field of the coil to return to the part V_b' of the battery; the part V_b'', the voltage of which is equal to the anode voltage V_a of the pentode, supplies the energy lost in the pentode.

In *fig. 8* a circuit is shown which approximates the ideal case of fig. 6. As switch we have here for one direction of current a pentode (controlled, as before, by a saw-tooth voltage) and for the other direction a diode, the anode of which is connected to a suitably chosen point of the anode battery. The working of this switch is as follows (see *fig. 9*).

Let us start at a moment when current is passing through the pentode. We assume for the time being that the pentode works in a range of the characteristics where the anode current is blocked during a part of the cycle and rises linearly during the remaining part (fig. 9*e*). For the present the coil resistance is ignored. The voltage v on the coil is then constant at V_b—V_a (V_a = anode voltage of the

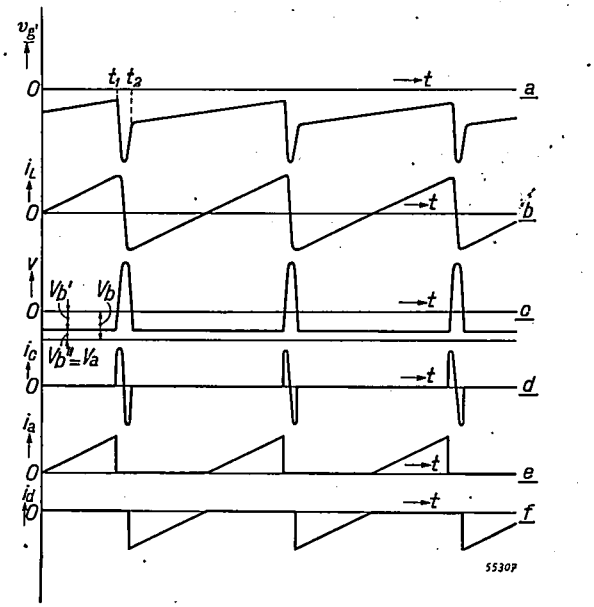


Fig. 9. Voltages and currents in the system according to fig. 8. *a*) voltage v_g on the control grid: negative bias plus saw-tooth voltage plus, during the flyback, negative peak. *b*) current i_L in L. *c*) voltage v across L. *d*) current i_C through C. *e*) anode current i_a of the pentode. *f*) current i_d through the diode.

pentode), the current i_C through the capacitors is zero, whilst the current i_L in the coil is equal to i_a and increases linearly with time. This is maintained until there is a pulse in the saw-tooth grid voltage ($t = t_1$); i_a is then blocked and the circuit formed by the coil and its self-capacitance starts to oscillate (fig. 9) in the same way as indicated in fig. 7.

Meanwhile the anode voltage rises to a high positive value. In order to keep the valve blocked in spite of this, a negative peak is superimposed upon the saw-tooth grid voltage (fig. 9*a*). The manner in which this peak is obtained will be made clear in the description of the oscillator stage.

At $t = t_2$, slightly more than half a cycle of the natural oscillation after t_1, the voltage v across the circuit reaches again the value V_b—V_a (fig. 9*c*). The diode then becomes conducting, since the tapping to which it is connected is so chosen as to have exactly the voltage $V_b'' = V_a$ with respect to the negative pole of the anode battery. The current i_L, which has meanwhile reversed, now flows through the diode, so that energy is returned to the part V_b' of the supply source lying between the tapping and the positive pole. If the internal resistance of the diode is negligible then as long as current is passing through

this diode the voltage $V_b' = V_b - V_a$ across the coil is just as great as was the case when the pentode provided for the passage of the current. In both cases the rate of change of the current will therefore be $di_L/dt = V_b'/L$.

The bias on the control grid of the pentode is adjusted in such a way that as soon as the diode current becomes zero the pentode conducts again, the process then repeating itself. The various currents and voltages in the circuit are represented in fig. 9*a-f*.

Thus we succeed in getting a pure alternating current flowing through the primary of the transformer, as well as through the part V_b' of the battery. In each cycle this part thus receives just as much energy as it supplies. The other part, with the voltage V_b'', supplies the energy lost in the pentode.

The diode has actually a dual function. In the first place it gives the circuit energy an opportunity to return to the supply source, much to the benefit of the efficiency of the circuit (hence the name efficiency diode). In the second place, as long as it is conductive, the diode guarantees a constant voltage across the coil, thus absence of oscillations. According to fig. 9*f* however the interval during which the diode is conducting covers only half of the scanning stroke, but this is easily remedied so as to ensure that the diode continues to be conducting during the whole of the scanning stroke. All that is needed is to adjust the pentode bias in such a way as to cause the pentode to become conducting a little earlier than indicated in fig. 9*e*.

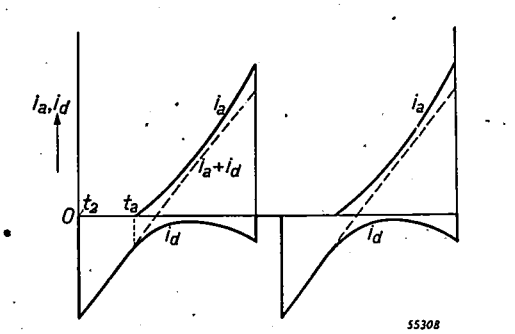


Fig. 10. By causing i_a to start earlier than indicated in fig. 9*e* its wave form will be as represented in this graph. As a consequence of the "excess" of i_a, during the whole of the scan i_d continues to flow and $i_a + i_d$ continues to rise in a straight line.

The situation then is as shown in *fig. 10:* from $t = t_2$ to $t = t_a$ only the diode is conducting, thus $i_L = i_d$ (both negative when taking the current directions indicated in fig. 8 as being positive). At $t = t_a$ current i_a (positive) also begins to flow through the pentode; this current i_a is in excess of what is required for the linear increase of $i_L = i_a$, but this is compensated by i_d, which does not now fall to zero. So long as i_d differs from zero there is a constant voltage V_b' across the coil and consequently linearity of i_L is ensured. Provided i_a is not too small, its exact wave form is immaterial; the pentode characteristics need not by any means be linear (as assumed above), neither is the wave form of v_g of any particular importance. In practice these are advantages that are not to be underestimated.

Nevertheless there is a drawback attaching to this arrangement which makes it unsuitable for practical use. The fact is that in practice one will not use a battery but a rectifier. To get the tapping one then needs a potentiometer formed of resistors the resistance of which must be relatively low if the potential of the tapping is to be sufficiently fixed.

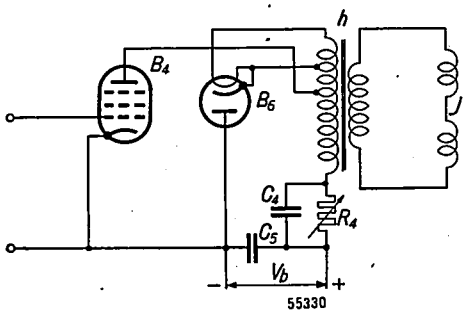


Fig. 11. Variation of the system according to fig. 8. Here there is no longer need to tap the supply voltage (V_b), which in this case is supplied by a rectifier. This system is applied in the Philips projection-television receiver. R_4 = variable resistor for adjusting the picture width. C_4, C_5 = smoothing capacitors. The meaning of the other letters is as indicated in fig. 2.

The power that is lost in these resistors would for the greater part neutralize the gain in efficiency. This could be avoided by connecting two rectifiers in series (the one with the voltage V_b' not then having to supply any power), but this is of course rather cumbersome.

Fig. 11 shows how we have solved this difficulty. The diode is connected between the negative pole of the anode voltage source and the end of the extended primary winding on the transformer. The extension has been so chosen that exactly the voltage V_a is induced in it when the voltage V_b' is lying across the original primary coil. This arrangement is therefore equivalent to that of fig. 8 without the necessity of a tapping on the supply source.

Deviation from linearity due to resistance of the coils

In the foregoing we have all along ignored the resistance of the deflection and transformer coils. Actually these coils do have a certain resistance and

as a consequence when a direct voltage is applied the current i_L will not vary according to a linear but to an exponential function, the rate of change di_L/dt decreasing during the scanning stroke. The relative decline p of di_L/dt during the forward stroke is a measure for the deviation from the straight line.

If we imagine transformer and deflection coils to be replaced by a self-inductance L and a resistance r connected in series, then a simple calculation shows that approximately

$$p = \frac{r}{f_h L},$$

in which f_h represents the frequency of the horizontal deflection.

If, for instance, we allow $p = 0.1$ (thus 10% drop in the velocity of the light spot when scanning one line, which is not yet disturbing) then with $f_h = 15{,}000$ c/s, $r/L < 1500$ sec^{-1}. This condition can be met without much trouble.

Practical execution

The pentode must be able to carry a high positive anode voltage, which during the fly-back may well rise to 4000 V[4]). For this reason the pentode type EL 38 is used, which has a top connection for the anode.

The efficiency diode gets much about the same high anode voltage, but negative, and moreover it must have a low internal resistance. Added to this there is the following difficulty as regards the filament current consumption. The filament cannot be fed from a transformer connected to the mains because this would involve a prohibitive capacitance parallel to the transformer (h, fig. 11) which would increase the fly-back time. That is why the solution has been chosen as already indicated in fig. 11, where an extra winding has been provided on the transformer h for feeding the heater; this means, however, that the power available for the heater is very limited.

Since none of the existing diodes answered all these requirements a new type (EA 40) was developed, the heater of which consumes only 1.4 W and which also satisfies the other requirements.

The transformer coupling the deflection coils to the anode circuit has a core of the non-metallic material "Ferroxcube"[5]), which has a high permeability and very small losses. This also helps to keep the power consumption low.

Connected in series with the primary of the transformer is a variable resistor shunted by a capacitor (fig. 11). In this resistor an adjustable part of the supply voltage V_b is lost, the remaining voltage determining the amplitude of the saw-tooth current and thus the width of the picture on the screen of the cathode-ray tube. (It is to be noted that with the arrangement described the amplitude of the saw-tooth current cannot be controlled by adjusting the amplitude of the saw-tooth voltage applied to the control grid!).

Thanks to the principle of economy described and the low losses, the power for which the output stage and the power pack have to be dimensioned is very low: for the full picture width (about 46 mm) and $f_h \approx 15{,}000$ c/s the current consumption (incl. screen-grid current) is 23 mA at a supply voltage of 350 V. This amounts to a consumption of 8 W, which compares very favourably with the power of about 30 W that would be required without the efficiency diode.

The output stage for vertical deflection

We have seen that the value of r/L of the coils for the horizontal deflection amounts to about 1500 sec^{-1}. With the frequency of the line-scanning (10,000 c/s and higher) these coils constitute a mainly inductive load in the anode circuit with which they are coupled. The pair of coils for the vertical deflection will as a rule have a value of r/L of the same order, but in this case the frequency is so low (50 or 60 c/s) that the coils will mainly act as a resistance; that is to say, at the energy accumulated in the magnetic field when current is at a maximum is small compared with the energy lost in the resistance of the coils during one cycle. There is therefore little sense in trying to recover the field energy in this case.

With this low value of the frequency of the vertical deflection a difficulty arises which does not occur with the line-scanning. This is explained with the aid of the equivalent diagram (*fig. 12*) of

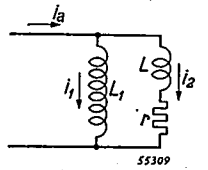


Fig. 12. Equivalent diagram (for low frequencies) for the anode circuit of a pentode feeding the coils for the vertical deflection via a transformer. i_a = anode current, L_1 = self-inductance of the primary transformer coil, L and r = self-inductance and resistance of the deflecting coils transformed to the primary side.

[4]) The manner in which such high voltages arise is explained in the previous article in this series: G. J. Siezen and F. Kerkhof, Projection-television receiver, III. The 25 kV anode voltage supply unit, Philips Techn. Rev. **10**, 125-134, (No. 5), in particular p. 126.

[5]) J. L. Snoek, Non-metallic magnetic material for high frequencies, Philips Techn. Rev. **8**, 353-360, 1946.

the anode circuit of the pentode feeding the coils for vertical deflection via a transformer. L and r represent the self-inductance and the resistance of the deflection coils transformed to the primary side; L_1 is the self-inductance of the primary transformer coil. In view of the low frequency the self-capacitance of the coils may be disregarded here. The parallel circuit is fed with a linear saw-tooth current i_a.

By the same definition as used before we employ a quantity p to indicate in how far the current i_2 in the L-r branch deviates from linearity. By this means we easily deduce the equation

$$\frac{r}{L_1 + L} = p f_v,$$

where f_v = the frequency of the vertical deflection. With f_v say 50 c/s and $p = 0.1$, this means that $r/(L_1 + L)$ must be less than 5 sec^{-1}. Now, for a good matching to the valve a value of r is required amounting at least to 5000 Ω. Hence $L_1 + L$ must be greater than 1000 H. The value of L being only a few H, the primary self-inductance must be very high and this could only be attained with an expensive transformer.

To overcome this difficulty the following method is sometimes applied. Instead of the transformer a choke is used, the deflection coils in series with a blocking capacitor being connected in parallel to this choke. The choke is given the same value of r/L as that of the deflection coils, so that the wave form of the current is the same in both branches (apart from the direct current, which flows only through the choke) and thus also equal to that of i_a. With this method, however, the deflection coils must have a high impedance for the sake of matching; consequently they must consist of a large number of turns of thin wire. This is not only rather costly but also objectionable from the manufacturing point of view on account of the risk of the wire breaking. Another drawback attaching to high-impedance deflection coils is the high voltage arising across them.

Compensating network

In the system which we employ a transformer is used which has a much lower self-inductance; the great deviation in the linearity of i_L which would result from this is compensated by a network which brings about a certain distortion of the input voltage. This network (d, fig. 2) may consist of two capacitors and a resistor (C_1, C_2, R_1) connected in the manner shown in *fig. 13*. The conditions which have to be met by C_1, C_2 and R_1 in order to give i_L the same wave form as that of the (saw-tooth) input voltage v_1 are deduced below.

To reach the similarity mentioned it is necessary that the Fourier series in which i_L can be developed and that in which v_1 can be developed should differ term for term by only a constant factor in amplitude and have the same phase angle term for term.

A simple calculation shows that for any arbitrary harmonic with the angular frequency ω we must have in the grid circuit

$$V_2' = \frac{1 + j\omega C_1 R_1}{1 + j\omega(C_1 + C_2)R_1} V_1' \quad \ldots \quad (1)$$

and in the anode circuit

$$I_L' = \frac{j\omega L_1}{r + j\omega(L_1 + L)} I_a', \quad \ldots \quad (2)$$

where V_2', V_1', I_L' and I_a' denote the amplitudes of the harmonics of v_2, v_1, i_L and i_a respectively. Further

$$I_a' = SV_2' \quad \ldots \quad (3)$$

where S = slope of the pentode B_2. Eliminating V_2' and I_a' from (1), (2) and (3) we arrive at

$$I_L' = \frac{j\omega L_1 - \omega^2 L_1 C_1 R_1}{j\omega\{L_1 + L + (C_1 + C_2)R_1 r\} - \omega^2(L_1 + L)(C_1 + C_2)R_1 + r} S V_1', \quad (4a)$$

which may be written as

$$I_L' = \frac{ja\omega - b\omega^2}{jc\omega - d\omega^2 + r} S V_1' \quad \ldots \quad (4b)$$

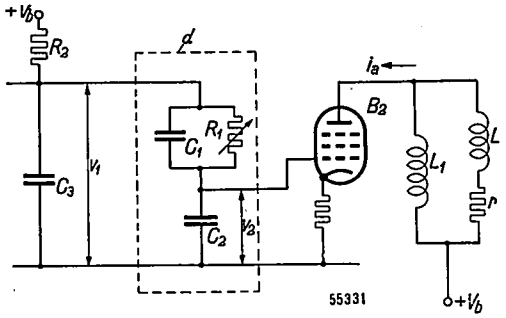


Fig. 13. d = compensating network consisting of the fixed capacitors C_1 and C_2 and the variable resistor R_1. It is connected between the oscillator stage and the output stage for vertical deflection. C_3 and R_2 belong to the oscillator stage; B_2, L_1, L and r (see fig. 12) belong to the output stage.

If the fraction in (4b) were a real quantity and (4b) independent of ω we should have the desired equality of phase and proportionality of amplitude for all harmonics, but this is prevented by the term r in the denominator. Therefore the first condition for attaining our object is that r must be negligible compared with the other terms in the denominator. We shall see presently to what this condition leads, but for the moment we shall assume that r may be omitted. The remaining fraction does then indeed become real and independent of ω when

$$a : c = b : d,$$

that is to say when

$$\frac{L_1}{L_1 + L + (C_1 + C_2)R_1 r} = \frac{L_1 C_1 R_1}{(L_1 + L)(C_1 + C_2)R_1}, \quad (5)$$

or

$$\frac{C_2}{C_1(C_1 + C_2)R_1} = \frac{r}{L_1 + L} \quad \ldots \quad (6)$$

C_1, C_2 and R_1 must therefore be chosen of such values as will comply with (6).

Putting $a/c = b/d = 1/q$ then (4b) may be written as

$$I_L' = \frac{ja\omega - b\omega^2}{q(ja\omega - b\omega^2) + r} SV_1'.$$

Thus r becomes all the more negligible as the value of q increases. Now, according to (5)

$$q = \frac{L_1 + L}{L_1}\left(1 + \frac{C_2}{C_1}\right).$$

By choosing

$$C_2 \gg C_1 \quad \ldots\ldots\ldots \quad (7)$$

we can always make q large enough to allow of r being ignored in the denominator of (4b). This condition $C_2 \gg C_1$ implies that the amplitude of v_1 must be much greater than the desired amplitude of v_2.

Finally we have to bear in mind that the network must not constitute more than a very small load on the oscillator stage, because otherwise the voltage v_1 would not retain its saw-tooth shape. This means that the current taken up by the network must be small compared with the charging current of the capacitor C_3 (fig. 13) in the oscillator stage. This results in another condition having to be met by C_1, C_2 and R_1, which we shall not go into here.

In practice C_1 and C_2 are fixed capacitors and R_1 is a variable resistor so adjusted that the wave form of i_L approaches the ideal as closely as possible; this is in fact managed in a very satisfactory way.

Saving of current

The fact that the distortion of the current in the compensating network is by no means small appears from *fig. 14a*, showing the wave form of

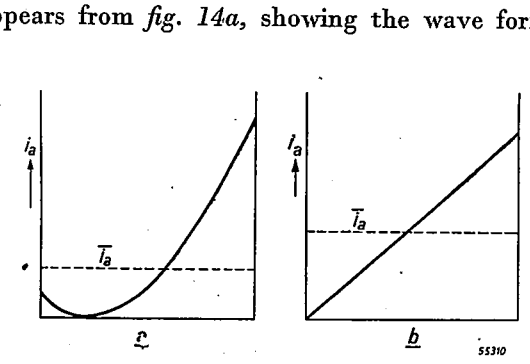


Fig. 14. Anode current i_a during the scanning stroke as function of t, *a*) when using the compensating network (fig. 13), *b*) without this network, with the same value of I_L. In the case *a*) the average value $\bar{i}_a$ may be more than 40% lower than in the case *b*).

the anode current during the scan; it deviates considerably from the straight line (fig. 14*b*). In both these graphs, drawn for the same difference between the initial and final values of i_a, thus for the same amplitudes of i_L, also the average value $\bar{i}_a$ of the anode current is indicated: in the case *a*), where the compensating network is applied, $\bar{i}_a$ is much lower than in the case *b*). In the case *a*) $\bar{i}_a$ depends upon the ratio r/L_1 and the calculation shows that it is smallest when

$$\frac{r}{L_1} = 3.45\, f_v \text{ sec}^{-1};$$

$\bar{i}_a$ is then more than 40% lower than in the case *b*).

In practice the average anode current consumed amounts to only 6 to 7 mA. With a screen-grid current of 2 mA and a supply voltage of 350 V this means that the power consumption of this output stage is only about 3W.

Practical execution

Fig. 15 gives a complete diagram of the output stage circuit for the vertical deflection.

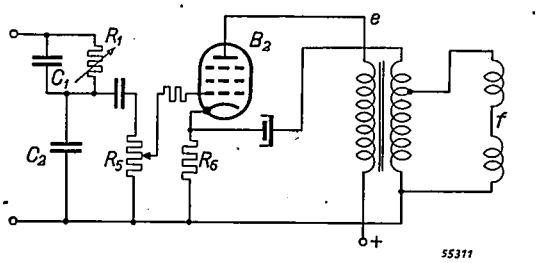


Fig. 15. Complete circuit of the output stage for vertical deflection. C_1-R_1-C_2 = compensating network (fig. 13), R_5 = potentiometer for adjusting the picture height, R_6 = cathode resistor to which feedback is applied. For the rest see the legend in fig. 2.

Across the output of the compensating network an additional potentiometer is shunted (of such a high resistance as to have no noticeable effect upon the network), with which the amplitude of the control grid voltage, thus also the amplitude of the deflection current, can be adjusted for controlling the picture height.

The pentode is of the EBL 21 type.

Just as in the output stage for the horizontal deflection, during the fly-back there is a high positive voltage peak on the anode and while this lasts the anode current has to be kept cut off. This is again brought about by superimposing a negative voltage peak on the grid voltage at the moment in question.

From fig. 15 it is to be seen that negative feedback has been applied; the secondary winding of the output transformer supplies current through a resistor in the cathode lead of the pentode. Negative feedback is a well-known means of reducing non-linear distortion [6]) which may arise from the curvature of the valve characteristic or from the self-inductance L_1 being more or less dependent upon the anode current.

---

[6]) B. D. H. Tellegen, Inverse feed-back, Philips Techn. Rev. 2, 289-294, 1937.

The deflection coils

Fig. 16 gives an idea of the shape of the deflection coils. One pair of coils is fitted closely around the neck of the cathode-ray tube whilst the other pair is fitted around the first pair.

It has been deduced above that for the pair of coils for the horizontal deflection r/L must be less than 1500 sec^{-1}. This would easily be complied with if ample use could be made of iron, but this may only be applied around the tube in a strictly rotationally-symmetrical fashion, because the focusing field — which is present also in the deflection coils — causes a disturbing astigmatism of the light spot as soon as there is the least deviation from rotational symmetry. What we have done is to wind a few layers of iron wire around the insulating cylinder enveloping the deflection coils (fig. 16). This appreciably improves the quality of the coils (reduction of r/L).

Fig. 17 shows the cathode-ray tube fitted in the holder with the deflection coils and the focusing coil.

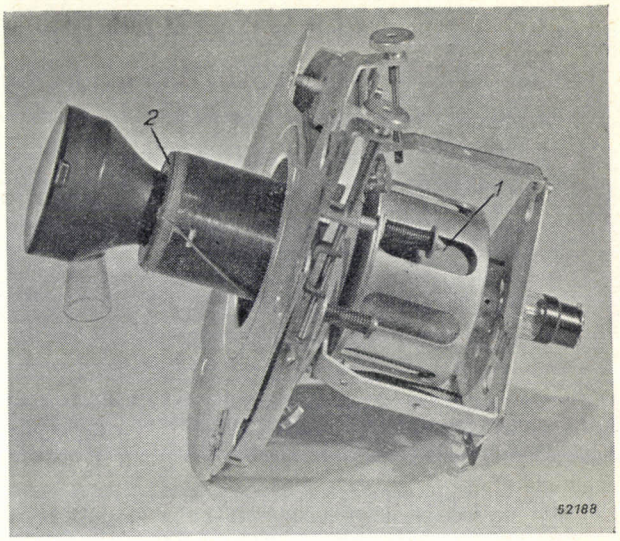


Fig. 17. Cathode-ray tube MW 6-2 placed in the holder with focusing coil (*1*) and deflection coils (*2*).

point P and the voltage across the capacitor changes according to an exponential function with the time.

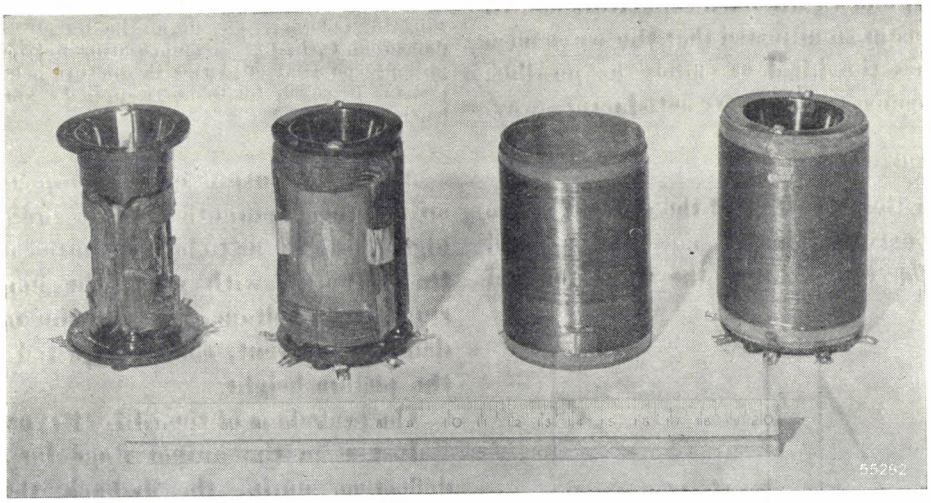


Fig. 16. From left to right: cylinder with one pair of deflection coils, the same with the second pair of deflection coils, envelope wound with iron wire, complete set of deflecting coils.

The oscillator stages

We have seen that a saw-tooth input voltage is required for each of the output stages. These voltages are supplied by relaxation oscillators, viz. blocking oscillators, the working diagram of which is represented in *fig. 18*. In essence such an oscillator consists of a triode with strong positive feedback, a grid capacitor and a grid leak. During oscillation the grid current causes the grid capacitor to be charged to such an extent as to interrupt the oscillation for a certain time, during which period an opposite charge flows across the grid leak to the Owing to the grid leak being connected to a point having a high voltage however, the rate of change of the voltage across the capacitor may to a good approximation be regarded as being linear.

This saw-tooth voltage serves as output voltage of the oscillator stage. Its frequency is adjusted by means of the variable grid leak R_2.

In *fig. 19* we again have a diagram of the blocking oscillator — the one for the vertical scanning — but with the addition of the correcting network (C_1-R_1-C_2). There is an additional resistor R_3 across which the grid current, during its short existence, a voltage pulse is developed which likewise forms part

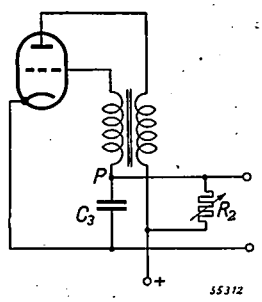


Fig. 18. Diagram of a blocking oscillator. Across the capacitor C_3 a saw-tooth voltage occurs the frequency of which can be adjusted by means of the resistor R_2.

of the output voltage. It has already been shown in the foregoing why these impulses are needed: they have to keep the output valve blocked at the high positive anode voltage arising during the fly-back.

Accurate synchronization with the scanning in the transmitter is assured by the triodes of the oscillator stages, to which at the right moments a pulse is applied which renders the valves conducting just before current would begin to flow naturally. For this purpose, as already stated in the introduction, the triode is coupled to a heptode (fig. 2) controlled by the synchronization signals. We shall revert to this in more detail in a subsequent article.

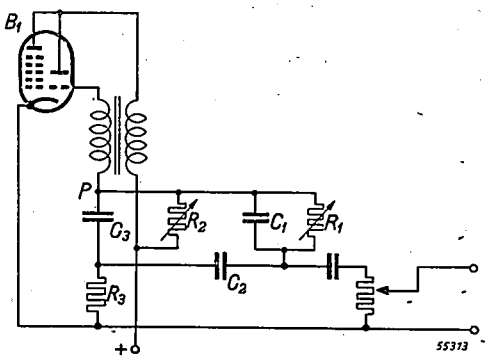


Fig. 19. Diagram of the oscillator stage for vertical deflection, including the compensation network C_1-R_1-C_2. B_1 = heptode-triode, C_3 and R_2 the same as in fig. 18, R_3 = a resistor across which the grid current develops a voltage peak which blocks the output valve during the fly-back.

STORING SEED POTATOES IN ARTIFICIALLY-LIGHTED CELLARS

by R. van der VEEN.

628.978:631.563.8:633.491

Seed potatoes are usually kept in what are known as clamps. They then lose much of their nutriment owing to the formation of long sprouts, which have to be removed. Since light checks sprouting, in may cases glass storage places have been resorted to, but as this method also has its drawbacks a more efficient manner of storing has been sought. This article describes an experiment for storing seed potatoes in an artifically-lighted cellar. It has been found that fluorescent lamps are much better than incandescent lamps for checking sprouting. One would think that this is to be ascribed to destruction of the auxin in the tubers, as it takes place mainly through blue light. A closer investigation into the nature of the active rays showed however that red light has a much stronger checking effect than blue light. These experiments lead one to suppose that, mainly or exclusively through red light, an inhibitor is developed in a potato.

The treatment of seed potatoes

Potatoes intended to be kept for planting out are cropped in the months June, July or August, and then have to be kept eight or nine months before the planting season starts. In order to check as far as possible the loss of nutritive substances through excessive breathing or drying up, soon after being cropped the potatoes are temporarily stored either in clamps or in barns until the autumn, when they are transferred to the winter storage places.

In January or February, and sometimes as early as December, one or more sprouts begin to grow out of each potato. How far these sprouts develop depends upon the kind of potato and the storage conditions, such as temperature, light and humidity. Usually these sprouts are broken off in January, after which the potato begins to sprout anew. If these new sprouts grow too long they, too, have to be removed, and this is disadvantageous for future growth in the field. The best results are obtained with potatoes which at the time of planting have short stubby sprouts and which have only to be "desprouted" once.

Seed potatoes are nowadays an important product of the Netherland's agriculture, which is also of importance for export. It is therefore not surprising that in recent years considerable attention has been paid to the problem of how seed potatoes can best be stored.

It is a known fact that the sprouting of potatoes is particularly checked by cold and by light. A temperature of 2-4 degrees centigrade will stop sprouting even without light, and undoubtedly good seed potatoes would be obtained if they could be kept at that low temperature, but this is not practicable. Neither the growers nor the dealers have storage places which can be kept at a constant temperature of 2-4 °C, independently of the outside temperature. Neither would it be economically justified to store seed potatoes in cold-storage depots, supposing that these were available in sufficient numbers.

At a temperature of 5-9 °C in the dark there is too much sprouting, but with a little light even at that temperature sprouting is sufficiently checked. The application of light, however, is difficult of realization with the present storage places. Until recently all seed potatoes were kept in clamps and even at the present day most of them are stored in this way. So as to profit from the favourable effect of light, in the Netherlands several storage places for seed potatoes have been made of glass in recent years. These are sheds with double walls of frosted glass, and in some of them there is also glass in the roof. In frosty weather the temperature inside these sheds is kept above freezing point by heating; in warm weather they are well ventilated so as to keep the temperature as low as possible. However, it has not been found practicable to keep such a storage place at a constant temperature. The greatest difficulty is in the spring when the weather is fine and sunny, the temperature inside the shed then often rising to 20 °C, which leads to considerable sprouting. Although such a storage place is to be preferred to a clamp, still it does not offer the ideal solution of the problem. The fluctations in temperature, moisture and light are too uncertain factors for the growers and dealers. In severe winters the results are satisfactory but in mild winters the potato develops too many and too long sprouts.

This had induced us to investigate whether better results cannot be reached by storing seed potatoes in cellars and providing artificial light to check sprouting.

The use of artificial light in the storing of seed potatoes

An underground cellar has the advantage that the temperature inside it is practically constant; on comparatively warm winter days the temperature is low and during cold periods it is above freezing point.

In cooperation with Mr. W. H. de Jong of the Central Institute for Agricultural Research (Centraal Instituut voor Landbouwkundig Onderzoek), extensive practical tests were carried out in a cellar of the "Lilbosch" Abbey at Pey-Echt (Limburg). The seed potatoes were stored in the usual way in shallow boxes made with high corners and stacked one on top of the other so as to leave an open space between. When artificial light is employed it is thus able to penetrate between the boxes, though of course where there are dense stacks of them, those farthest away receive only little light.

One part of the test cellar was illuminated with ordinary incandescent lamps and another part with fluorescent lamps of the "daylight" colour. This lighting was started on 3rd January 1948 and left burning continuously up to 31st March, when the potatoes had to be planted out.

In the part illuminated with incandescent lamps there were six 100-W lamps installed in a section 7 × 8 metres. At the end of the test the potatoes kept in this section were in a better condition than those which had been kept in clamps, but even so some difficulties arose.

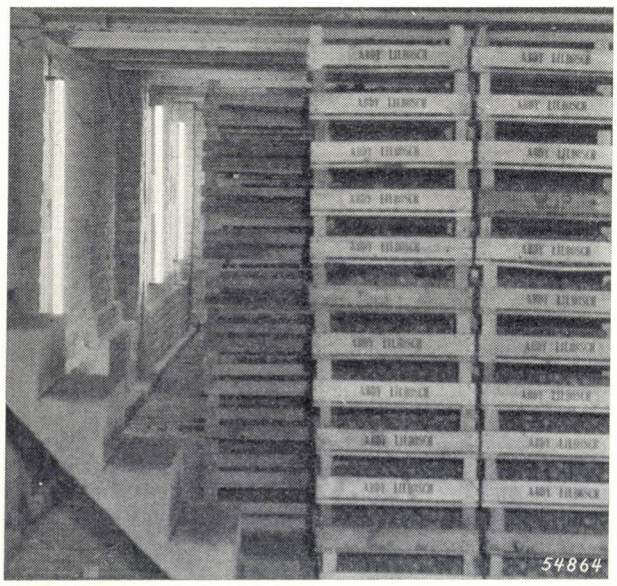


Fig. 1. A cellar in the "Lilbosch" Abbey at Pey-Echt (Limburg) where seed potatoes are being stored under the light from fluorescent lamps. In each section of 7 × 8 metres there are five TL lamps of 40 W. The boxes are stacked in such a way that the rays of light can penetrate into the farthest corners. It has been found that with this arrangement the sprouting of the potatoes is sufficiently checked.

In the first place it was found that the potatoes in the immediate vicinity of the lamps began to sprout rather strongly, notwithstanding the fact that they were receiving a fair amount of light. This is to be explained by the radiation of heat from the incandescent lamps, the temperature of these potatoes being raised so high that the light was incapable of checking the growth of sprouts.

A second objection is that in incandescent lamps light is radiated from a central point, in consequence of which there is little uniformity in the radiation. There were found to be a number of more or less large spaces where hardly any light could penetrate, as a result of which sprouting was not checked.

In the part of the cellar illuminated with fluorescent lamps five TL lamps of 40 W were installed in each section of 7 × 8 metres, placed at intervals of 3 metres. Since these lamps were mounted vertically against the wall (*fig. 1*) the light was able to penetrate between the boxes, so that as soon as a sprout began to grow it at once came into the light. With the lamps mounted in this way there are no shadow spots.

Fluorescent lamps produce scarcely any heat radiation, so that the potatoes in the immediate vicinity of the lamps do not sprout any earlier than the others and there is no need to rearrange the boxes after a certain time.

Thus the TL lamps yielded much better results than the incandescent lamps. The sprouts which had developed towards the end of March were stubby and tight, so that the potatoes (varieties: "Eersteling" and "Bintje") could quite well be planted mechanically. It was found that with the arrangement chosen, with the stacks extending up to 3-4 metres away from the lamps, even the boxes farthest away still received sufficient light. *Fig. 2* shows potatoes stored in a clamp in comparison with those which had been radiated with fluorescent light.

Unfortunately these experiments at Pye-Echt did not begin until January 3rd and it was necessary in the beginning to break off sprouts that had already formed. If we had been able to start with the irradiation of the potatoes back in November there would most probably have been no need to break off any sprouts. It is intended to repeat this experiment next winter and to see whether it is in fact necessary to keep the lamps alight continuously or whether it is sufficient to switch the lamps on for say 8 to 12 hours per day. The fact that irradiation with TL lamps yielded much better

results than that with incandescent lamps has to be ascribed, in the first place, to the shape of these TL lamps and their smaller heat radiation, though also the spectral composition of the radiated light will

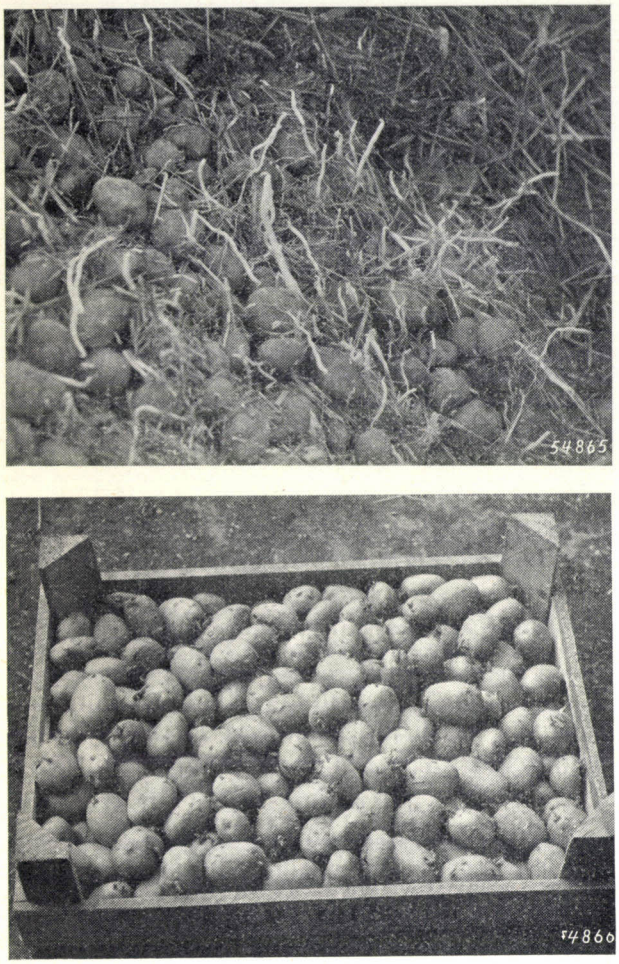


Fig. 2. Comparison between potatoes kept in the clamp (above) and others taken from a cellar illuminated with TL lamps (below). The former have developed long sprouts, in consequence of which the potatoes have lost much of their nutriment. The others have short stubby sprouts making these potatoes most suitable for planting out.

undoubtedly play an important part. It is therefore worth while investigating the kind of light which checks the sprouting of potatoes most. It is moreover of interest to ascertain what amount of light — using light of a certain wavelength — is just capable of sufficiently checking sprouting.

The optimum colour for irradiating potatoes

In order to investigate the effect of the colour of the light used, we irradiated one lot of potatoes with various intensities of blue and another lot with different intensities of red light. For the first lot a TL lamp was used with magnesium tungstate as luminophore and the addition of a blue filter. For the second lot a lamp with cadmium borate was used, with a red filter. The spectral distribution of the light from the two lamps is graphically represented in *fig. 3*. The irradiation took place at a temperature of 14 °C.

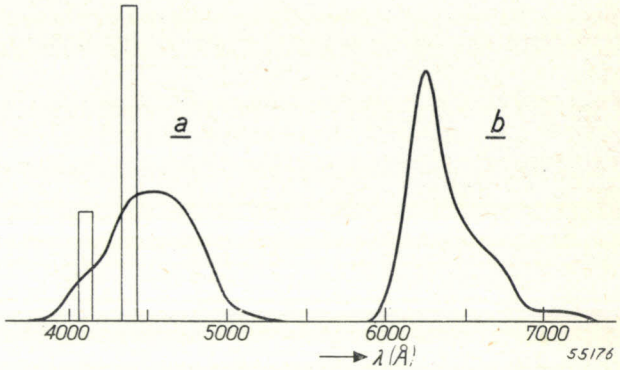


Fig. 3. The spectral distribution of the light from two fluorescent lamps used for the experiments regarding the influence of light rays on the sprouting of potatoes. The two rectangles relate to the light from two mercury lines. The area of these rectangles is a measure for the relative energy contribution of these spectral lines. The part *a* shows the spectral distribution for the TL lamp with blue light, the part *b* that for the TL lamp with red light.

There has been very little research into the mechanism of the sprouting of potatoes and the checking of same. It is known that the growth of the sprouts takes place under the influence of auxin, a hormone occurring in the growing parts of all higher species of plants. It is obvious to presume that the growth will be checked by the destruction of this auxin. It is known that blue-violet light has this effect but that red rays are of little influence.

Even in the smallest concentrations auxin is highly active, $5 \cdot 10^{-11}$ gram giving a measurable reaction in growth. Since such minute quantities cannot be measured chemically, the presence of this substance is determined by means of a quantitative biological analysis, a brief description of which follows.

In the seedlings of oats (Avena) this auxin is formed in the tip and when the tip is cut off the seedling ceases to grow, but if the tip is put back onto it then growth starts again at once. Auxin is mainly transported perpendicularly downwards. When the tip is put back over only part of the decapitated seedling the latter starts growing on one side and not on the other, so that it bends over. This curvature is used as a measure for the amount of auxin present. The unit (called the Avena unit) is the amount of this hormone which produces after 90 minutes in an oat seedling a curvature of 10°. To determine the auxin content of the tissue of a plant the auxin is diffused in a small block of agar which is then placed on a decapitated seedling in such a way as to cover only half of the wound. The curvature resulting after a certain time is used to indicate the number of Avena units of auxin present.

The auxin that is chemically distinguished as auxin-a is photo-stable, that is to say its activity cannot be influenced by irradiation. In weak acid solutions, however, this auxin-a readily changes, accompanied by separation of a molecule of H_2O, into auxin-a-lactone, a substance which is equally active

as a stimulus to growth but which is photo-labile. Under the influence of ultra-violet light this substance changes, not reversibly, into lumi-auxone, again accompanied by separation of a molecule of H_2O, and this substance has no longer a growth-stimulating action. In the absence of ultra-violet irradiation this transformation in the vegetable tissue would not take place if it were not for the fact that in the presence of carotene (invariably found in plant tissues) the reaction also takes place under the influence of rays from the blue-violet part of the visible spectrum. In vitro too it has been found possible to render auxin mixed with carotene inactive by means of small quantities of visible light. It appears that this result is mainly to be ascribed to the light of wavelengths occurring in the absorption spectrum of carotene. In agreement with this is the fact that growth reactions due to light are strongest — if we leave out ultra-violet light — under the influence of blue-violet light (wavelength 4300-4600 Å). The carotene present then causes the partial destruction of the growth stimulus.

expected, the sprout which had been under light of an intensity up to about 30 erg/cm²·sec being perceptibly checked in their growth. All the sprouts, including those which had not been checked at all or scarcely so, were turned more or less to the light owing to the auxin on the exposed side having suffered greater destruction than on the unexposed side. The sprout that had received about 2 erg/cm² · sec was still somewhat phototropically directed; this is also the minimum radiation intensity at which oat seedlings show a curvature under the influence of light.

There was an unexpected phenomenon with the potatoes that had been exposed to red light. In the first place the sprouting of these potatoes too was checked, so much so that it was even noticed

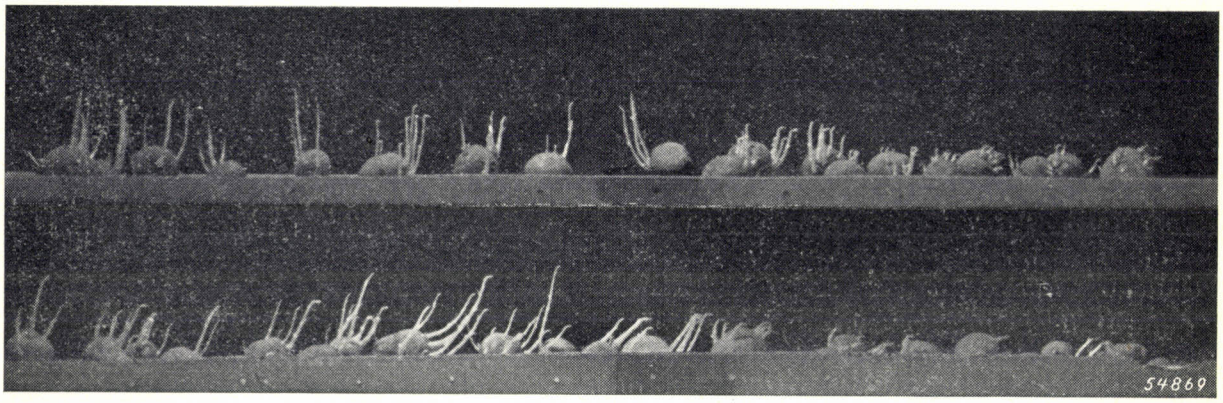


Fig. 4. Potatoes (variety "Eersteling") sprouting at a temperature of 14 °C under irradiation with the two kinds of fluorescent light of the composition represented in fig. 3. The light is incident from the right. The photos have been taken after 3 weeks irradiation. *Above:* irradiation with red light, the intensity diminishing from right to left from 3 to 0.1 erg/cm² · sec. *Below:* irradiation with blue light, the intensity diminishing from right to left from 80 to 2 erg/cm² · sec.

In the light of the results obtained form experiments concerning the destruction of auxin it was to be expected that the growth of the sprouts in seed potatoes would be most strongly checked by blue-violet light and that red rays would have but little effect.

Experiments carried out in cooperation with Prof. E. C. Wassink in the Laboratory for Physiological Research of Plants (Laboratorium voor Plantenphysiologisch Onderzoek) at Wageningen (Holland) were so arranged that the light fell continuously upon the potatoes from one side, as would be the case in the storage of potatoes. Thus, the farther they were away from the lamp the less light fell upon the potatoes. *Fig. 4* shows how the irradiation checks the development of the sprouts.

The results under blue light were in fact as under a very much lower luminous intensity than with blue light, intensities of 1 erg/cm² · sec producing noticeable results. But what was most surprising was the fact that the checked sprouts

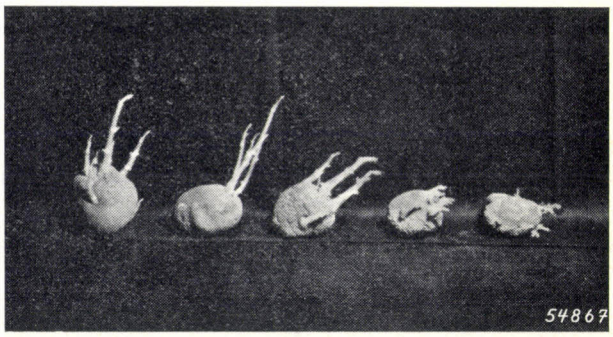


Fig. 5. Potatoes sprouting under blue light incident from the right. The intensities of illumination were, from right to left, respectively 80, 50, 15, 7 and 2 erg/cm² · sec.

under red light had not grown towards the light not even under much stronger radiation.

The phenomena observed under irradiation with the two kinds of light are clearly seen in *figs. 5* and *6*, showing some potatoes taken from the experiment to which fig. 4 relates. One can see what sprouts have grown under blue light and under red light respectively; the legends indicate the intensity with which the potatoes were irradiated.

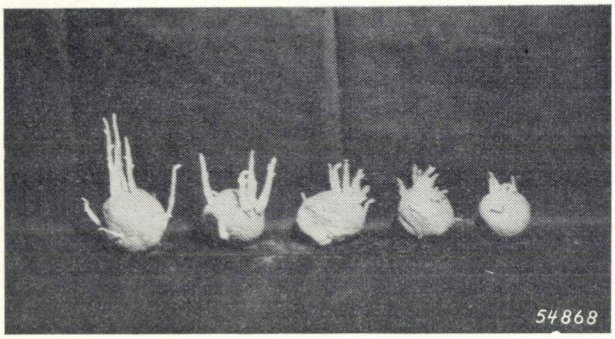


Fig. 6. Potatoes sprouting under red light incident from the right. The intensities of illumination were, from right to left, respectively 3, 1.5, 0.8, 0.3 and 0.1 erg/cm^2·sec.

From these experiments it appears that the checking of sprouting, — at least under the influence of red light — is not to be accounted for by reason of a growth-stimulating substance being rendered inactive by the light. Rather it is to be supposed that, under red light, a growth-checking substance in the potatoes is activated which then, contrary to auxin, would appear to diffuse through the sprouts in a horizontal direction. The result of this would be that instead of growing in the direction of the light they grow vertically upwards, at least in so far as they develop at all. The question whether this hypothesis of the activation of a growth-checking substance is correct is to be further investigated experimentally.

Very little is known in botany about growth-checking substances, although in recent years some substances have been extracted from plants which are found to check growth. For instance P. Larsen [1]) describes the growth-checking action of parasorbinic acid from tomato juice and of anemonin from Ranunculus. No investigations have yet been made into the formation of such substances under the influence of light.

Our experiments now having shown that red light has the strongest checking action upon the sprouting of potatoes, in the further experiments it will be advisable to use TL lamps of the "warm-white" colour instead of those of the "day-light" colour. This should be taken into account when fitting up storage cellars for seed potatoes with artificial light.

[1]) Amer. J. Bot. **34**, 349-356, 1947.

ABSTRACTS OF RECENT SCIENTIFIC PUBLICATIONS OF THE N.V. PHILIPS' GLOEILAMPENFABRIEKEN

Reprints of these papers not marked with an asterisk can be obtained free of charge upon application to the Administration of the Research Laboratory, Kastanjelaan, Eindhoven, Netherlands.

1794: F. A. Kröger and J. E. Hellingman: The blue luminescence of zinc sulfide (J. Electrochem. Soc. **93**, 156-171, 1948, No. 5).

It is shown that the ions Cl^-, Br^-, and I^- play an essential part in the formation of the blue centers of ZnS-Ag, ZnS-Zn, and ZnS-Cu phosphors. The centers are assumed to be Zn^+Cl^-, Ag^+Cl^- and Cu^+Cl^-, respectively (or the corresponding bromides and iodides), and to occupy normal zinc and sulfur sites in the zinc sulfide lattice. The spectral distribution of the fluorescence is the same for the centers containing chlorine or bromine ions; Ag, Zn, and Cu cause bands at slightly different wavelengths.

A difference in peak positions for wurtzite and sphalerite is explained by the difference in separation between the upper occupied and the lower empty band of the base lattice.

1795: A. H. W. Aten Jr., C. J. Dippel, K. J. Keuning and J. van Dreven: Denaturation and optical rotation of proteins (J. Colloid Sci. **3**, 65-66, 1948, No. 1).

It is fairly generally admitted that denaturation consists of a loosening of the native configuration of a protein, followed by refolding according to a less regular pattern. This denaturation is sometimes reversible. However, not all characteristics of the native substance are equally well reproduced in the regenerated product. The writers measured the optical rotation of solutions of regenerated seralbumin. No difference was observed, within the accuracy of the experiments (3°), between the rotation of native and regenerated seralbumin.

1796: J. L. Snoek and J. F. Fast: Metastable states of nickel characterized by a high initial permeability (Nature, London, **161**, 887, 1948, June 5).

In textbooks on the subject it is usually tacitly assumed that the initial permeability μ^0 of a ferromagnetic material not subject to ordering, ageing or allotropic transformations, is a unique function of the temperature. In contradiction to this the writers found for Ni that the temperature curve for μ^0, when taken at rising temperatures, differs markedly from the curve obtained at decreasing temperatures. Slightly tapping or demagnetizing the sample brings μ^0 down to values which — though mutually different — are independent of the previous heat treatment.

1797: L. J. Dijkstra and J. L. Snoek: Effect of lattice distortions on the mean rate of propagation of large Barkhausen discontinuities (Nature, London **161**, 886, 1948, June 5).

The experiments of Sixtus and Tonks on the propagation of large Barkhausen discontinuities have been repeated and extended, using slightly more refined methods. The relation $V = A\,(H - H_0)$ between the mean rate of propagation V and the external field H, where A and H_0 are certain constants, is found to be strictly valid in all cases investigated. Experiments on a 60 Ni 40 Fe alloy showed that A is very sensitive to defects in the lattice structure. Experiments at different temperatures (93 °K—368 °K) showed that A/R, where R is the resistance, is practically independent of the temperature.

1798: J. van der Vliet: Investigations on sterols II. Vitamin-D_2 and -D_3 in irradiated sterol from the mussel (Mytilus edulis) (Rec. Trav. chim. Pays-Bas **67**, 246-256, 1948, No. 4).

The following compounds have been detected in the sterol fraction from the mussel after irradiation with ultra-violet light: Vitamin-D_2 and -D_3 and a compound closely related to -D_2 and having a vitamin-D structure, but which is practically devoid of anti-rachitic action. A mixture of this compound with vitamin D_2 has been isolated in a crystalline state (-D_x).

1799: J. van der Vliet: Investigations on sterols III. The provitamins-D from the mussel (Mytilus edulis) (cf. these abstracts, No. **1741**) Rec. Trav. chim. Pays-Bas **67**, 265-281, 1948, No. 5).

In a further investigation on the sterol fraction from the mussel the following degradation products have been obtained by oxidation of the ultra-violet irradiation product: formaldehyde, the well known degradation ketone $C_{18}H_{22}O$ from vitamin-D_3, methyl-isopropyl-acetaldehyde and isopropyl-acetal-

dehyde. The latter aldehydes were detected by conversion into and isolation of the corresponding acid amides.

Qualitative and quantitative consideration of the results compared with similar degradations of calciferol and an irradiation product from 7-dehydrocholesterol, as well as biological data, lead to the conclusion that "mussel provitamin-D" is composed of: 7-dehydrocholesterol (about $^3/_6$ part), ergosterol (about $^1/_6$ part), $\triangle^{5,7,22}$-cholestatriene-3-ol. (between $^1/_6$ and $^2/_6$ part) and 2nd component of provitamin-D_x ($< {}^1/_6$ part).

The last two components probably cannot, or at least to a small extent only, be activated antirachitically.

1800: J. M. Stevels: Les propriétés optiques du verre en rapport avec sa structure (Verres et Refractaires **2**, 2-12, 1948, No. 1). (The optical properties of glass in relation to its structure; in French.)

The writer recapitulates the well-known rules of Zachariasen regarding the conditions anorganic compounds (chiefly oxydes) should comply with, in order to be able to occur in the form of a glass (see Philips techn. Rev. **8**, 231-236, 1946). Especially the relation between colour and structure of homogeneous glasses is studied. The absorption is shifted to decreasing wavelengths according as the Madelung potential on the place of an oxygen ion increases, e.g. going from borate glasses, via silicate glasses to phosphate glasses. However, certain ions may occur, which have a specific absorption and thus cause a colour of their own. A network-modifying ion as a rule has a narrow absorption band. If the same ion occurs as network former the absorption is much broadened and especially extended to the larger wavelengths. Between both functions of the ion an equilibrium exists, which may be influenced by outer circumstances, e.g. by heat treatment or by admixing special ions, such as Be^{2+}, Ti^{4+}, B^{3+}. In this way the influence of the structure on the specific absorption of Fe^{3+}, Cu^{2+}, Co^{2+}, Ni^{2+}, U^{6+} and Mn^{2+} may be understood. This is extensively discussed in the case of Fe and briefly in the other cases too.

1801: J. de Jonge and R. Dijkstra: Decomposition of o-hydroxydiazonium compounds by light. (Rec. Trav. chim. Pays Bas **67**, 328-342, 1948. No. 6).

Conditions could be found for decomposing a solution of an o-hydroxybenzene-diazonium compound into a colourless product. Such an irradiation product couples with diazonium salts in slightly acidic solution to red-shaded dyes according to a bimolecular reaction. However, it is not stable in solution at room temperature, but is converted slowly into a non-coupling dimeric form. The irradiation of the diazonium salt gives rise to a new, weak acid function that disappears again on heating with evolution of CO_2. Titration curves show that the o-hydroxy-benzene- and o-hydroxynaphthalene-diazonium compounds are decomposed in a similar way. Two irradiation products of o-hydroxynaphthalene diazonium compounds have been isolated. The results are completely understood by assuming the conversion of the benzene-nucleus into a five-membered ring, as recently concluded by Süs from other experiments.

1802*: J. D. Fast: Entropie (Amsterdam, Centen 1948; 270 p., 25 fig., 32 tables) (in Dutch).

The author aims at giving, in as simple terms as possible, a survey of the fundamentals of I) thermodynamics, II) quantum mechanics, and statistical mechanics as far as needed for the illustration of the concept of entropy. Part III deals rather extensively with the calculation of gas entropies from simple molecular models and from spectral data.

1803*: P. Cornelius: Korte samenvatting der electriciteitsleer (Meulenhoff, Amsterdam, 1948; 88 p., 7 fig., 3 tables). (A short survey of the theory of electromagnetism; in Dutch.)

In this booklet the author gives a short survey of the theory of electromagnetism indicating important simplifications. The reader is supposed to be more or less acqainted with the basic notions.

The author mainly aims at stopping discussions on electrical units by introducing the Giorgi system of electrical units in its rationalised form. In this connection, starting from the concept of current and voltage, the current field in a conductor (Ohm's law), the electric field of a capacitor and the magnetic field of a coil are dealt with in much the same way. The author emphasizes that the didactics of electromagnetism should be renewed according to his method of exposition, which is much related to that of R. W. Pohl (compare Philips Techn. Rev. **10**, 79-86, 1948, No. 3).

VOL. 10 No. 11, pp. 325-352 MAY 1949

Philips Technical Review

DEALING WITH TECHNICAL PROBLEMS
RELATING TO THE PRODUCTS, PROCESSES AND INVESTIGATIONS OF
THE PHILIPS INDUSTRIES

EDITED BY THE RESEARCH LABORATORY OF N.V. PHILIPS' GLOEILAMPENFABRIEKEN, EINDHOVEN, NETHERLANDS

EXPERIMENTAL TRANSMITTING AND RECEIVING EQUIPMENT FOR HIGH-SPEED FACSIMILE TRANSMISSION

V. SYNCHRONIZATION OF TRANSMITTER AND RECEIVER

by D. KLEIS and M. van TOL.

621.397.335

The motors which bring about the scanning of the picture areas in the transmitter and in the receiver of the Philips apparatus for high-speed facsimile transmission have to run synchronously with a tolerance of no more than 0.6 degree in their relative phase. This requirement cannot be met with synchronous motors, nor with the system of stabilization by means of tuning-fork generators much used for low-speed facsimile transmission. A new method of synchronization had, therefore, to be developed. A regulating device was employed which reacts to phase deviations between the motors in the transmitter and the receiver, combined with a similar device reacting to differences between the speeds of the two motors. These devices are controlled by synchronizing pulses produced by the optical rotor in the transmitter and transmitted to the receiver together with the facsimile signal, and with the aid of pulses produced by a small generator coupled to the shaft of the receiver motor. Moreover, in the transmitter a device is used which stabilizes the speed of the transmitter motor, so that the synchronization only needs to provide a correction for small variations in the transmitter. With this method it has been possible to reach the necessary phase constancy; in the event of a disturbance the equilibrium is aperiodically restored, with such an inertia that the edge of the recorded picture does not show any disturbing undulation.

Synchronization is a problem of prime importance in all systems of picture transmission, both in facsimile telegraphy and in television. On the transmitting side there is a picture surface traversed by a scanning spot, and at the receiving end a picture surface traversed by a recording spot. Both surfaces are identical and one can imagine them as being divided equally into minute surface elements. To reproduce the transmitted picture in the receiver without any geometrical distortion, the scanning spot and the recording spot must be "synchronized", which means that they must move continuously over corresponding areas of the two picture surfaces at exactly the same moment [1]).

The picture surface is always scanned along parallel, adjacent lines. We can therefore express the synchronization condition in a somewhat more concrete form by saying that the scanning spot and the recording spot have to start traversing each line simultaneously and must take the same length of time to cover a line. If the recording spot starts sometimes too early and sometimes too late then the lines in the picture obtained show individual displacements in their own direction; see *fig. 1*. It is not necessary (and not possible) to exclude such displacements entirely, but the tolerances in this respect are rather small; with a picture width of say 20 cm a maximum line displacement of 1 mm, i.e. 1/200 of the line length, is admissible. Of course such a displacement cannot be allowed between adjacent lines; there must be a gradual transition, so that the edge of the picture shows an undulation with a not too small wavelength. As a normal requirement it is taken that this "wave" must have a wavelength of at least 4 cm (fig. 1).

For the numerous systems of facsimile telegraphy

[1]) The transmitted signal has always a finite though very short transit time, T. On closer examination it is seen therefore that the recording spot, the intensity of which is governed by the signal obtained from the scanning spot, must traverse the picture elements with a delay T with respect to the scanning spot. It is not therefore absolutely correct to say that the scanning and recording spots pass over corresponding elements of the two picture areas at exactly the same moment, but this is of no consequence whatever for our further considerations.

already existing a number of methods of synchronization have been worked out, none of which however was suitable for our new facsimile system working at a transmission speed about 60 times higher than

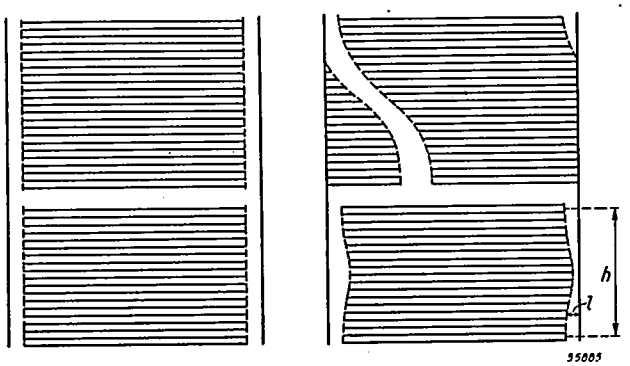


Fig. 1. Diagrammatic representation of the position of the parallel lines scanned on the picture area in the transmitter (left) and recorded on the picture area in the receiver (right). The fully-drawn and the broken lines at the edge indicate the picture area and the actual picture respectively. In the time required to traverse the short distance between these two lines the transmitter does not emit any picture signal.
Upper half: An example of inadequate synchronization. Here the receiver has a phase disturbance which for some length of time increases and then remains constant. *Bottom half:* The synchronization is considered adequate if the displacement of the picture edge (variation of the distance l) does not exceed 1/200 line length, i.e. about 1 mm, and the undulation of the edge has a wavelength (h) of at least 4 cm.

the existing systems. Some simple quantitative considerations will make this clear. The method of synchronization devised for this new system will then be described on broad lines.

For the details of the construction of the transmitter and the receiver in the Philips high-speed facsimile system we refer to the four previous articles published in this journal, which will be referred to as I-IV [2]).

Synchronous motor and tuning-fork oscillator

Since the synchronization can be reduced to the producing of an identical frequency at the transmitter and receiver, it seems obvious to take advantage of the standard frequency at our disposal in the a.c. mains. In that case the movements of the scanning spot and the recording spot are both brought about by synchronous motors fed from the mains. This method is of course confined to those cases where the mains available for the transmitter and for the receiver are interlinked and therefore always have the same frequency. In such cases this method is indeed successfully applied for low-speed facsimile systems.

Why is this not possible with our system?

In low-speed facsimile transmission the scanning rate is usually about 3 lines per second. The driving two-pole synchronous motors (the most favourable for our purpose) run at the rate of 50 r.p.s. (3000 r.p.m.) in Europe and 60 r.p.s. (3600 r.p.m.) in America, thus making about 20 revolutions in scanning one line. For a permissible displacement of 1/200 line length between transmitter and receiver a phase displacement of $20 \times 360°/200 = 36°$ can be allowed between the motors at the transmitting and receiving ends. The phase displacements between the terminal voltages of the two local mains likely to occur through fluctuations in the instantaneous load will as a rule be well below this limit of 36°. If, therefore, the mutual phase of the scanning elements in transmitter and receiver is properly adjusted at the beginning of the transmission, no prohibitive displacements need be feared.

With our high-speed facsimile system the rate of scanning is 180 lines per second (see article II). A driving synchronous motor would therefore make only $^1/_3$ revolution in scanning one line. The permissible phase displacement between the motors at the transmitting and receiving ends would thus not be more than $^1/_3 \times 360°/200 = 0.6°$. One could not possibly reckon on such a phase constancy of the mains.

Consequently synchronous motors cannot be considered for our purpose, not even if it could be expected that interlinked mains would be available at the transmitting and receiving ends.

In very many cases, especially in international communications, this latter condition will certainly not be complied with and for this reason other methods of synchronization have had to be developed already for low-speed facsimile systems. Practically all these methods result in the generation of an oscillation with a frequency of great constancy at the transmitter and receiver, this oscillation being used to control the speed of the motor for the scanning device. The two frequencies are rendered as accurately identical as possible by local adjustment of the frequency-governing element, for instance a tuning fork.

Whereas with the method of synchronous motors the mean speeds are identical and only disturbances due to phase shift fluctuations have to be considered, with these other methods the possible small

[2]) Experimental transmitting and receiving equipment for high-speed facsimile transmission.
I, General, by H. Rinia, D. Kleis and M. van Tol, Philips Techn. Rev. **10**, 189-220, 1948 (No. 7).
II. Details of the transmitter, by D. Kleis, F. C. W. Slooff and J. M. Unk, Philips Techn. Rev. **10**, 257-264, 1948 (No. 9).
III. Details of the receiver, by F. C. W. Slooff, M. van Tol and J. M. Unk, Philips Techn. Rev. **10**, 265-272, 1948 (No. 9).
IV. Transmission of the signals, by D. Kleis and M. van Tol, Philips Techn. Rev. **10**, 289-298, 1948 (No. 10).

frequency differences of the local tuning fork oscillator must be considered. The smallest difference in frequency will result in an additional small phase shift of the motors in each cycle. After a large number of cycles this displacement will have accumulated considerably. Suppose that the tuning forks vibrate at such a frequency that p cycles occur during the scanning of one line. A picture to be transmitted may be 30 cm long, so that given a line width of 0.2 mm the picture may contain in all 1500 lines. Each tuning fork then makes 1500 p vibrations per picture. If at the end of the picture the line displacement is not to exceed the value of 1/200 line length, the number of vibrations of the tuning fork must not be more than $p/200$ out in the 1500 p, that is to say the frequency deviation must not be more than 1 : 300,000.

This requirement can reasonably be met with tuning forks or other vibrating elements if they are very carefully made, but this will not bring us any farther than ensuring that one picture is properly recorded. In order to avoid the consecutive pictures being displaced farther and farther across the picture area, the phase of the scanning device in the receiver has to be corrected after every picture. With the usual low-speed facsimile transmission there is no difficulty in having this correction made for instance by the operators, but in our case, when it takes no more than 8 seconds to transmit a picture of the length mentioned, the operators would have to make this correction every 8 seconds, which of course is out of the question. Or, to put it the other way round, to allow of a correction being made say only once every 10 minutes, a frequency constancy of 1 in 2×10^7 would be required. Even with the best means available (quartz oscillators in thermostats) this cannot be attained.

There are two possible ways of overcoming these difficulties. According to the first method one is satisfied with a frequency constancy merely sufficient, as described above, for one picture or even less, and an additional mechanism is provided which after every picture or at the required shorter intervals automatically controls the phase of the scanning device in the receiver and where necessary makes a correction to annihilate the phase deviation. By the second method speed is not governed by local tuning devices — which would not possess sufficient frequency constancy anyhow — but the speed of the receiver motor is controlled by a frequency which is derived from the transmitter motor and transmitted together with the picture signal.

The synchronization in our facsimile system may be regarded as a combination of these two methods It will be seen why neither the first nor the second method alone will suffice.

Stabilizing the speed of the transmitter motor

If one has the means of getting the speed of the receiver motor to follow exactly any speed variations of the transmitter motor then, in principle, it is not essential that the transmitting speed should be kept to a high degree of constancy. However, the smaller the speed variations of the transmitter, the easier it will be, of course, to follow them at the receiver with the necessary accuracy. For this reason, in our facsimile equipment steps have been taken to stabilize the speed of the transmitter motor, and it is well to describe this stabilization first.

The transmitter motor is a direct current motor, the armature of which is fed from a simple (non-stabilized) mains rectifier, whilst the field current is supplied by an output valve of the type EL6. The speed of such a motor is approximately inversely proportional to the magnetic flux in the armature. The motor can therefore be accelerated by reducing the field current and slowed down by increasing the field current. For the normal speed of 60 r.p.s. the current to be supplied by the output valve has to be 55 mA, for which the grid voltage of the valve has to be about —8 V. To stabilize the speed it is arranged that the grid potential of the output valve becomes more positive as the motor begins to rotate at a higher speed. The resulting increase of the anode current flowing through the field winding then counteracts the increase in speed.

This regulating voltage at the grid of the output valve is derived in the following way. On the shaft of the motor a small generator is fitted which at a speed of 60 r.p.s. produces an alternating voltage with a frequency of (for instance) 180 c/s. This alternating voltage is applied to an L-C circuit tuned to a frequency slightly higher than 180 c/s, such that the resonance curve has its steepest slope at 180 c/s; see *fig. 2*. Consequently the amplitude of the voltage across the circuit will vary considerably when the frequency of the alternating voltage supplied, that is to say the speed of the motor, changes but slightly. The voltage across the circuit is now rectified, and the direct voltage obtained — from which is to be subtracted a constant bias determining the working point — serves as control grid voltage of the output valve. A block diagram of this stabilizing circuit is given in *fig. 3*.

Let us now consider the working of this stabilization more closely. In the event of an interference,

for instance a slight variation in the armature voltage or in the load of the motor, which has the tendency to change the speed, the field current changes to such an extent as to compensate the effect of the interference very rapidly. This means

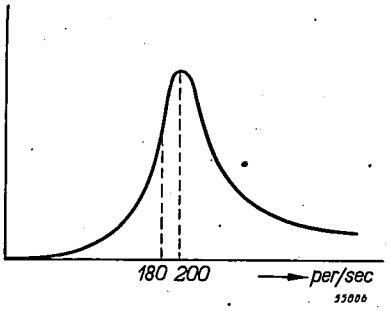


Fig. 2. Resonance curve of the tuned circuit employed for stabilizing the speed of the transmitter motor.

that the equilibrium corresponding, say, to a changed armature voltage, is already obtained with an extremely small change in speed. An actual and permanent small change in the speed, however, is indispensable. The effect of the stabilization therefore is only that the speed change required for the new equilibrium is considerably reduced as compared with the case where there is no stabilization.

In our installation the reduction factor has been made very large by keeping the damping of the *L-C* circuit low, namely by limiting the damping effect of the coupled rectifier with the aid of a special circuit (cf. fig. 6). In this way a resonance curve is obtained with steep sides, and the anode current of the output valve (i.e. the field current of the motor) will therefore greatly vary with the speed, due also in part to the high mutual conductance of this valve. In our case, for an interference due to variation of the armature voltage, the reduction factor is 270. For a variation of the load it is still higher.

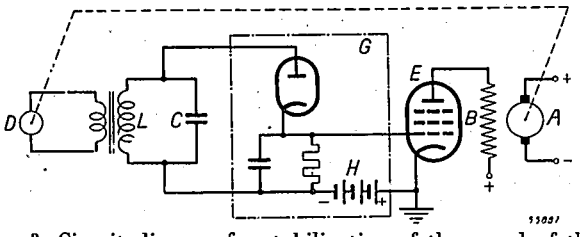


Fig. 3. Circuit diagram for stabilization of the speed of the transmitter motor. *A* armature fed from a mains rectifier; *B* field winding excited by the anode current from the output pentode *E*. On the motor shaft is a small generator *D* producing an alternating voltage which causes the tuned *L-C* circuit to oscillate. The voltage across the circuit is rectified by the rectifying circuit *G* and the direct voltage thus obtained, which varies considerably with the speed of the motor, is applied to the grid of the output valve. As the speed increases, the anode current of *E* rises and the stronger excitation slows down the armature. The right working point on the characteristic of the output valve is adjusted with the grid bias *H*.

The effect of a change in the natural frequency of the *L-C* circuit, on the other hand, cannot be reduced by this stabilization, as will be readily seen. It can therefore be said that the degree of constancy of the speed is practically determined by the constancy of the values of *L* and *C* in the circuit. For our purpose a variation in the speed over long periods to the extent of 1% or more could be allowed, so that no very stringent requirements had to be made as far as this circuit is concerned.

Other points of importance in the stabilization, such as automatic starting, inertia of adjustment, the possibility of instability arising, etc., cannot be dealt with here. It is to be noted, however, that the nominal speed can be altered by changing the capacitor in the *L-C* circuit. Another means by which small changes could be made in the nominal speed would be to change the abovementioned constant negative grid bias of the output valve, which is added to the regulating voltage. We shall presently see why this is of importance.

Regulating the speed of the receiver motor

In the first place the receiver is equipped with a speed-stabilizing device very much resembling that in the transmitter. The motor is of the same type; the field current is supplied by an output valve; the latter is controlled by the rectified voltage of a tuned circuit which in turn is excited by an alternating voltage of 180 c/s obtained from a small generator on the motor shaft. Here again negative grid bias is added to the regulating voltage for correctly adjusting the working point of the valve.

The result of this stabilization is that the effect of mains voltage fluctuations, etc., on the speed of the receiver motor is very greatly reduced, as is the case with the transmitter. At the same time, however, it affords a very simple means of satisfying the desire for the *speed of the receiver to be continuously controlled by that of the transmitter*. For this purpose an alternating voltage of a frequency proportional to the speed of the transmitter motor is transmitted by cable from the transmitter to the receiver [3]). There this voltage is applied to a tuned circuit corresponding to that in the transmitter, and the rectified voltage of this circuit is used for stabilizing the receiver motor, instead of the constant grid bias of the output valve. At the end of the previous section we have already pointed out that with the regulating method

[3]) One might use for this the already mentioned voltage of the generator on the shaft of the transmitting motor. Actually we use the "synchronization signals" referred to already in articles II and IV. This point is considered further in what follows.

described the nominal speed can be adjusted by choosing a suitable value for this grid bias. Now in this manner a variation in the speed of the transmitter will cause also a variation of the nominal speed at which the stabilization of the receiver is working. A block diagram of this method of synchronization is shown in *fig. 4*.

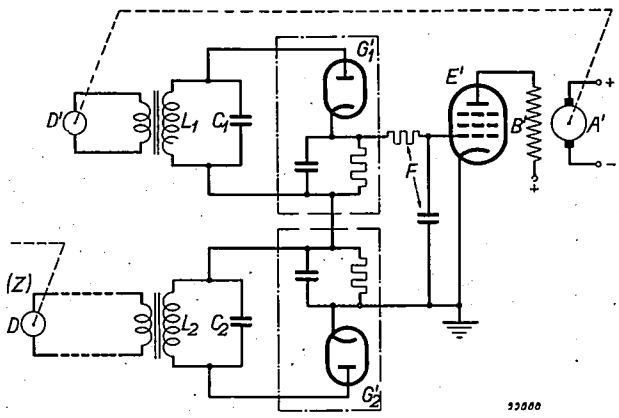


Fig. 4. Block diagram of the speed regulation of the receiver motor. The system is based upon a similar method of stabilization of the speed as applied in the transmitter (fig. 3): the small generator D' is mounted on the shaft of the armature A' of the receiver motor; the alternating voltage generated acts upon the circuit L_1—C_1; the circuit voltage rectified by G_1' controls the output valve E', the anode current from which flows through the field winding B'. Instead of a constant grid bias (H in fig. 3) for the output valve, here the voltage from the circuit L_2—C_2 rectified by G_2' is used, this circuit being caused to oscillate by means of an alternating voltage (Z) derived from the rotation of the transmitter motor and transmitted together with the picture signal. F is a smoothing filter.

However, our object in view is still not by any means reached, as the reader may already have observed. The receiver now reacts to a small change in speed of the transmitter, but in the event of an interference in the receiver itself, for instance a mains fluctuation, there will be an independent change in speed which is necessary for the new equilibrium and which, in spite of the large reduction factor of the stabilization, may be much greater than is permissible. Moreover, the influence of the local frequency-governing elements, which in the foregoing led to the rejection of the method of synchronization with tuning-fork generators, is not by any means eliminated. In fact there is no actual synchronization here; the control is not affected by the question whether the speeds in the transmitter and the receiver are actually equal; it only causes the speed of the receiver to vary in the corresponding degree to that of the transmitter. The nominal speeds of transmitter and receiver are governed by the local L-C circuits, which by no means possess the necessary frequency constancy of 1 in 2×10^7, so that after a short time, even in the absence of other disturbances, prohibitive phase displacements would arise.

The solution has been found in the principle of the other means already outlined: an automatic control, in our case functioning continuously, which has a direct phase-correcting action. This we shall now proceed to describe. We shall leave for the moment the question what function is then performed by the speed control already dealt with.

Regulating the phase of the receiver motor

As already stated, the receiver motor drives a small generator supplying the alternating voltage required for stabilizing the speed. This generator consists of a fixed magnet with an inductor and a rotating armature with three teeth. The teeth are so shaped that as one of them passes the magnet a voltage pulse is generated in the inductor. When the motor is running at the nominal speed of 60 r.p.s. there are thus 180 pulses per second. The fundamental frequency of 180 c/s filtered out of these pulses is used for the speed-stabilizing system (fig. 4). The impulses themselves are required for the phase control now to be described.

The synchronizing alternating voltage of the transmitter, mentioned above, also consists of pulses. These are obtained by optical means, i.e. by the three rotating, optical scanning systems in the transmitter (see article II): alongside the edge of the document to be scanned is a somewhat specular aluminium plate; an pulse of constant height and duration is thus introduced in the facsimile signal at the beginning of each scanning line. These pulses, which serve not only for the synchronization but also for reconstructing the scale of blackness of the picture (see article IV), are transmitted along the cable together with the signal; thus no separate channel is needed for the synchronization signals.

To achieve the speed regulation in the receiver already described (fig. 4) the fundamental frequency of 180 c/s is again filtered out of the transmitted pulses and used. For the phase regulation, however, the transmitter pulses are converted by means of a simple network into a saw-tooth voltage, and to this are added the pulses of the receiver generator. When the two motors are running at the same speed a purely periodical voltage is obtained in the form as represented in *fig. 5*.

The position of the pulse on the "back" of the saw-tooth is apparently directly related to the mutual phase of the transmitter and the receiver. By suitably positioning the inductor in relation to the armature on the shaft of the receiver motor it

can be arranged that for the desired phase relation (the recorded line in the receiver beginning at the edge of the picture plane) the pulse just comes to lie midway between the fly-back surges of the saw-teeth.

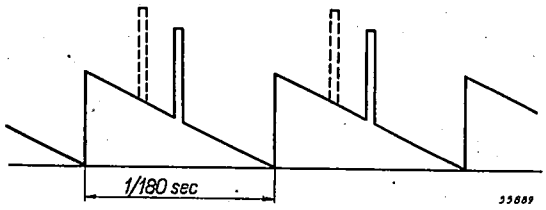


Fig. 5. Saw-tooth and periodical pulse added together. The saw-tooth voltage is derived from the rotation of the transmitter motor, the pulse voltage from the rotation of the receiver motor. When the motors are running at the same speed the pulse takes up a fixed position on the "back" of the saw-tooth; this position depends upon the phase relation of the motors. When the phase relation changes, the pulse is displaced along the saw-tooth, its top becoming higher or lower (for instance as shown by the dotted lines).

This voltage according to fig. 5 is conducted to a rectifying circuit which supplies a voltage equal to the difference between the peak of the pulse and the mean value. This direct voltage is applied, in series with an adjustable bias, to the grid of an output valve the anode current of which forms part of the field current for the receiver motor; see *fig. 6*.

In the event of the receiving motor lagging in phase behind the transmitting motor for some reason or other, the pulses come to lie farther to the right on the saw-tooth. Thus, its top lies lower, the output voltage of the rectifier is smaller, and when the polarity is suitably chosen the grid voltage of the output valve becomes more negative and as a consequence the field current of the motor is reduced. The result is that the motor is accelerated, so that it begins to make up for the phase lag in relation to the transmitter motor. In this way the original phase relation between transmitter and receiver is restored.

The equilibrium is also determined in part by the grid bias of the regulating valve. By varying this bias the phase relation between transmitter and receiver can be adjusted at the beginning of a transmission. For this purpose the potentiometer with which the grid bias is varied is provided with a control knob on the front panel. Also mounted on the front panel is a meter indicating the phase difference, whilst furthermore the form of the voltage illustrated in fig. 5 can be checked with the aid of a small cathode-ray oscilloscope. These devices are shown in the photograph reproduced in *fig. 7*.

If the cause of a phase displacement persists then it is not possible for the phase to be fully restored, just as we have seen with the methods of regulation first described. The effect of an interference is only reduced, that is to say the new equilibrium is already obtained at a very small displacement of phase. It is found possible to make the reduction factor sufficiently large to satisfy our demands as regards the phase constancy (maximum phase shift 0.6°). This is achieved, apart from other means, by making the saw-tooth steep, thus the amplitude of the saw-tooth voltage high (about 250 V), so that even small phase displacements result in a considerable change in the amplitude of the pulses.

For the control to act at any mutual phase position of transmitter and receiver, the amplitude of the pulse must, wherever it lies, exceed that of the saw-tooth; the amplitude of the pulse must therefore be made at least equal to that of the saw-tooth. The amplitude of the pulse and

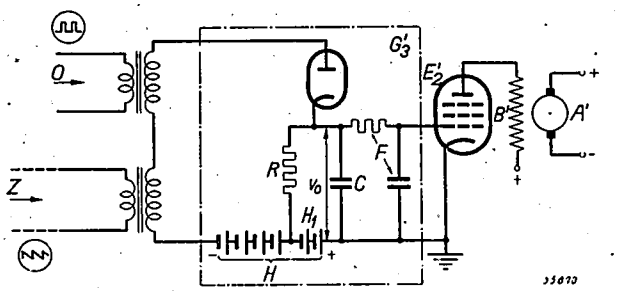


Fig. 6. Diagram of the phase regulation. Again an output valve is used (E_2') to supply a part of the current for the field winding B' of the receiver motor. This valve is controlled by the output voltage of the rectifier G_3', this being proportional to the difference between the peak value and the mean value of the A.C. input voltage. The input voltage for the rectifier is the voltage illustrated in fig. 5; part of this voltage is supplied by the receiver (O) and part of it by the transmitter (Z). The variable bias H ensures that the voltage v_0 in the right phase position assumes the value of −8 V corresponding to the desired working point of the output valve.

The rectifying circuit differs somewhat from the simple case illustrated in figs 3 and 4. It has the advantage that the voltage across the resistor R is reduced to the difference between the voltage v_0 and the part H_1 of the base, i.e. in the undisturbed state about 7 V, as against v_0—H, i.e. for instance 370 V, with the normal system. Hence, of the total variation range (250 V) of the peak height of the impulses — independently of their undisturbed position on the back of the saw-tooth — for the regulating effect only a part amounting to H_1 (= 15 V) is used, which just matches the grid base of the output valve. In this case too, the ripple of the grid voltage is only proportional to the voltage across R instead of the peak value of the inpulses. Consequently the RC-constant of the rectifying system (and also of the smoothing filter F) could be made sufficiently small to render the delay of the regulation described below innocuous.

Thanks to the reduction of the voltage across R much less energy is dissipated in this resistor than is the case with the normal system. It is for this reason that the principle of the system sketched is actually also applied for the rectifiers in figs 3 and 4. The smaller dissipation is of importance because it is accompanied by less damping and thus gives a sharper resonance curve for the preceding L-C circuit, as has already been pointed out above.

that of the saw-tooth voltage must be kept accurately constant, because any variation would just as well cause the voltage across the rectifier to change as would a phase displacement. Consequently the incoming pulses of the transmitter and the receiver are not applied directly but first limited to a constant level in the usual way.

speed difference is neutralized and its cause can only bring about a displacement of the equilibrium to a somewhat different phase relation, as we have already seen above [4]).

It may now be asked why, then, this phase control alone does not suffice.

Phase control can only be effective when the speeds

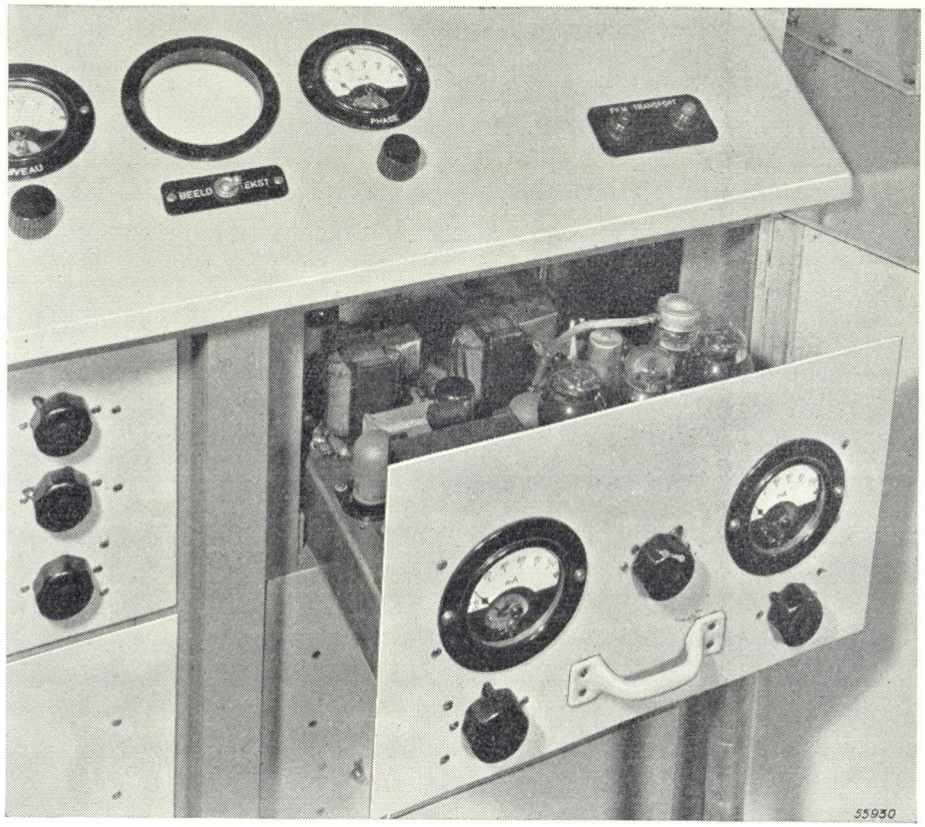


Fig. 7. The synchronization system for the receiver is for the greater part mounted on a single chassis which slides into the receiving cabinet. On the slanting top panel of the cabinet can be seen the meter and the control knob for reading and adjusting the phase relation between transmitter and receiver. To the left of these is the screen of the cathode-ray oscilloscope on which the oscillogram of the voltage for the phase regulation (fig. 5) can be produced by closing the switch. On the front panel of the synchronization chassis one sees the potentiometer knob and the two milliammeters with which the contributions from the two output valves of the speed and phase regulations towards the field current are adjusted (see caption of fig. 8). Immediately behind the front panel are the output valves, between which is one of the amplifiying valves for limiting the pulses supplied by the transmitter and the receiver.

Necessity of regulating speed in addition to phase

It is readily understood that phase regulation automatically implies that the speeds of the transmitting and receiving motors must be strictly equal. The smallest difference in speed manifests itself as a continuously increasing phase displacement. Owing to the pulse being shifted farther and farther on the saw-tooth this phase displacement in turn gives rise to an increasing deviation of the field current, and with a constant speed difference the correcting torque on the motor therefore becomes larger and larger. Thus the

of the transmitter and receiver are already practically equal. If there is any appreciable difference in the speeds then the pulse runs very rapidly over the back of the saw-tooth right to the end and then begins again at the other end. The rectified voltage would therefore have to rise and decay at the same rate. Owing to the necessary smoothing of the output voltage of the rectifier, however, the

[4]) In the terminology of control technique the phase control might be termed an "integral control" of the speed. Integral controls have the property of being able to make the mean value of the quantity to be adjusted exactly equal to a prescribed value.

grid voltage of the output valve corresponds to the average peak height, and consequently the total effect of the rapid phase variations upon the speed of the motor is nil. (As a matter of fact this would also be the case without smoothing, because the inertia of the armature would render rapid variations of the torque ineffective.)

The incapability of the phase control to correct large speed deviations is particularly manifest in the fact that when the receiver motor is started it will as a rule not be brought up to the desired speed. This is actually done by the speed control. After being switched on the receiver motor starts running and tries to reach the rated speed to which the speed stabilization is set. The speed regulation by means of the synchronization signals corrects this in so far that it brings the speed of the receiver anyhow very close to the speed of the transmitter. This means that the pulse in fig. 5 runs more and more slowly over the saw-tooth until the phase control comes into operation and keeps the pulse in a certain position. The phase relation can then be further adjusted by hand, as explained above.

Though easy starting is in itself sufficient justification to apply speed control in addition to phase control, there is a second reason for this which we regard as being still more important. In order to explain this reason we must first look at one side of the problem that has so far been neglected, namely the behaviour of this regulation as a function of time. In the description given above we have spoken only of the state of equilibrium, but how is a new equilibrium attained after an interference has taken place?

If the angle of rotation of the transmitting motor with respect to an arbitrary initial position is Φ, then in the event of an interference the angle of rotation of the receiver motor with respect to the corresponding initial position will not be exactly equal to Φ, but $\varphi = \Phi + \psi$. Thus ψ is the undesired phase deviation. Now there are a number of torques acting upon the shaft of the receiver motor. The normal field present when there is no disturbance in the running of the motor supplies a driving torque M_0. Friction sets up a braking torque, which for our purpose we can express to a sufficient approximation by $M_r = a + b\,\dot{\varphi}$, in which a and b are constants. The phase control yields a correcting torque M_c, which is opposed to the phase displacement ψ and which for small deviations we can take as being proportional to ψ: $M_c = c\psi$. Similarly the speed control yields a correcting torque M_d proportional to the speed difference $\dot{\varphi}-\dot{\Phi}$, thus $M_d = d\dot{\psi}$.

Using I to denote the moment of inertia of the armature and the rotor of the scanning device coupled to it, for the rotation of the receiver motor we have the differential equation:

$$I\,\ddot{\varphi} - M_0 + (a + b\,\dot{\varphi}) + M_c + M_d = 0.$$

Substituting $\varphi + \Phi + \psi$ and putting $\ddot{\Phi} = 0$, since we shall assume the transmitter motor to rotate at a constant speed, we then have

$$I\,\ddot{\psi} - M_0 + a + b\dot{\Phi} + b\dot{\psi} + M_c + M_d = 0.$$

This equation must also hold for the undisturbed state where ψ, $\dot{\psi}$, $\ddot{\psi}$ M_c, M_d are all nil. Hence $M_0 = a + b\dot{\Phi}$, so that our equation becomes

$$I\,\ddot{\psi} + b\dot{\psi} + M_c + M_d = 0. \quad \ldots\ldots \quad (1)$$

Let us now first consider the effect of the phase control alone. For the time being we therefore take the term M_d as being zero. Substituting $M_c = c\psi$, we then see that eq. (1) assumes the form of the well-known equation for a damped oscillatory vibration without an external force acting upon the vibrating system. From this we can at once conclude that when an arbitrary deviation ψ is introduced and the system is further left to itself the relative phase ultimately returns to its original value ($\psi = 0$). The relation of the damping term (coefficient b) to the other terms will determine whether this return of the relative phase to its original value takes place in an oscillatory manner or aperiodically.

This, however, is still incomplete. We have to take into account the fact that both in the phase control and in the speed control there is a delay time τ respectively τ_1. This is for a large part attributable to the RC-constant of the rectifying circuits supplying the grid voltage for the regulating valves and that of the smoothing filters, and also for a part to transients, for instance in the tuned circuits, and to the hysteresis of the iron circuit of the motor. The delay means that the correcting torques M_c and M_d at the instant t are determined by the phase and speed deviations respectively which were present at a time τ respectively τ_1 earlier. Thus:

$$M_c(t) = c\,\psi(t-\tau); \qquad M_d(t) = d\,\dot{\psi}(t-\tau_1).$$

If we now develop both these expressions in progressions according to Taylor we get:

$$M_c(t) = c\,[\psi(t) - \tau\,\dot{\psi}(t) + {}^1/_2\,\tau^2\,\ddot{\psi}(t) - \ldots],$$

$$M_d(t) = d\,[\dot{\psi}(t) - \tau_1\,\ddot{\psi}(t) + \ldots].$$

For these qualitative considerations we may ignore higher terms of the series. By substituting these expressions we derive from eq. (1):

$$(I + {}^1/_2\,c\tau^2 - d\tau_1)\,\ddot{\psi} + (b - c\tau + d)\,\dot{\psi} + c\psi = 0 \ldots (2)$$

As is to be seen, the coefficients of the equation for the vibration are altered owing to the retardation effects. In particular it is to be noted that now the damping term may also become negative (b, c and d according to their definition are positive), namely when c is too large. The phase deviation ψ will then fluctuate around the zero value; but the fluctuations will become larger and larger. This phenomenon may indeed occur in practice and would, of course, render the control useless. This is all the more unwelcome because a high value of the coefficient c, indicating the "amplification" of the phase regulation, is desired for a large reduction factor in this regulation.

This now, is where advantage is again taken of the speed regulation. The contribution of this regulation towards the damping term consists in the positive quantity d appearing in eq. (2). By making d large, we can therefore always make the damping positive, even when c has a very large value. In particular, regardless of the choice of c, we can now give the damping such a value as to render the system aperiodic, this being the most favourable condition for our purpose. In order to facilitate this we have kept the delay time τ as small as possible, inter alia by arranging the aforementioned rectifying circuits in such a way that they can have a short RC-time without causing any excessive ripple in the direct voltage supply (cf. fig. 6). As may be seen from eq. (2), the delay time τ_1 of the speed control has no effect upon the damping.

A high value of τ_1, as also of d, however has an adverse effect upon the inertia term. Its effect is adverse because the aperiodic response of the system should be such that the final value is reached at a sufficiently slow rate. At the beginning of this article it has been stated that the edge of the picture may take the shape of a wave with a minimum wavelength of 4 cm. This means that a phase displacement of the maximum value may be made to disappear (or brought to the new final value) only after 2 cm picture length, that is to say after about $^1/_2$ second. The inertia term in eq. (2) must be made sufficiently large to bring this about. It was found, however, that this requirement could be easily met, independently of the reduction factors and delay times of the two controls, by increasing the moment of inertia I with the aid of a flywheel on the motor shaft.

Finally we give in *fig. 8* a simplified diagram of the whole synchronization system, showing how the phase control and the speed control have been combined. Each of the controls works on a separate output valve yielding a contribution to the field current of the receiving motor [5]). A resistor (R_a) shunted across the output valves ensures that there is a certain field even when the valves are cut off, thus

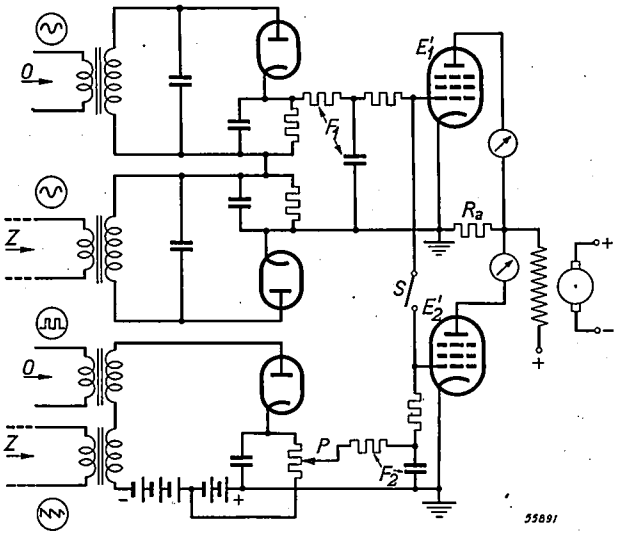


Fig. 8. Combination of phase control and speed regulation. The voltages O are derived from the receiver motor, Z from the transmitter motor. By means of the potentiometer T the "amplification" of the phase regulation — which provides sufficient reserve for the sensitivity required — can be purposely reduced so as to obtain the desired aperiodical damping effect of the speed regulation upon the phase variations. This adjustment applies only for a given ratio of the anode currents of the two output valves. This ratio is given the right value (in this case the value 1) by slightly varying the grid bias of E_1', which is supplied by the rectifier G_2' (see fig. 4). This is checked with the aid of the two milliammeters in the anode circuits. By closing the switch S the effects of the phase regulation voltage and the speed regulation voltage upon the two output valves are "mixed"; this, however, is not essential for the working of the synchronization system. F_1 and F_2 are smoothing filters.

allowing for automatic starting (without the armature current reaching an excessive value); this also ensures that in the event of failure of the control voltages the motor will not race. The adjustment of the desired aperiodic damping of the phase variations is brought about not by the choice of the coefficient d, that is the amplification of the speed regulation, but by the choice of c, the amplification of the phase control, with the aid of the potentiometer P. The motive for this lies in the fact that the reserve in the sensitivity of the phase control in the synchronization circuit proved to be much greater than that in the speed control.

[5]) Actually the two controls are "mixed", for although two regulating valves are used we apply to the grid of each valve a voltage composed of fractions of the two regulating voltages.

THE ILLUMINATION OF COAL-MINES AND THE ATTENDANT RISK OF EXPLOSIONS

by G. D. RIECK.

622.476.4:622.81

When fire-damp occurs in coal-mines and it is mixed with air it is apt to cause explosions as soon as it comes into contact with a hot object. This article first deals with the steps that can be taken against this danger when oil lamps and electric incandescent lamps are used. It is then discussed how the danger of explosion may arise when fluorescent lamps are employed. An adequate safeguard is to apply a type of circuit in which the fluorescent lamp is ignited while the cathodes are cold. In mines the lamps are not switched on and off frequently, so that there is no fear of the life of the lamps being very much shortened owing to this method of ignition.

In coal-mines, especially at the coal face, there is very frequently a certain amount of fire-damp. Mixed in certain proportions with air, this gas is apt to ignite when coming into contact with a body heated to a high temperature. That is why the lamps that miners have to use in their work are apt to be the cause of disastrous explosions. The steps that have to be taken to safeguard miners against this danger are related to the method of illumination applied.

The risk of explosions was particularly great when the miners used an unprotected oil lamp, and it was therefore of great importance when Davy invented his safety-lamp in 1815. In this lamp the oil flame is screened off by a fine-meshed metal gauze. When a combustible mixture of fire-damp and air penetrates to the flame it ignites, but the hot combustion gases cannot spread the combustion through the gauze to the surroundings, filled with the same combustible gas. The gauze must have a certain mesh width (a maximum of 0.05 cm is prescribed). Provided the rate of flow of the combustion gases is not too high no explosion can then take place, although the gauze may be heated even to glowing temperature. Another advantage of this safety lamp is that the colour of the flame betrays the presence of mine gas.

Incandescent lamps for the illumination of mines

At the turn of the last century electricity began to be used more and more for the lighting of mines. At first only incandescent lamps were employed. An incandescent lamp can only cause an explosion when its bulb bursts in an atmosphere dangerously charged with fire-damp and the filament happens to keep glowing. This risk is not a great one and is most likely to occur close to where the coal is being hewn out, for example owing to a flying piece of coal hitting the lamp.

The breaking of a bulb, whereby the filament or at least a part of it is left glowing in a space charged with combustible fire-damp, need not always cause an explosion [1]). The conditions under which an explosion occurs or can be prevented have been investigated with an apparatus designed by Fripiat and represented diagrammatically in *fig. 1*. By this means it has been found, for instance, that the risk of explosion can be avoided by using a thin filament in the lamp [2]). But lamps with a thin filament easily break and naturally do not yield much light. The risk of explosion can also be reduced by lowering the incandescent temperature of the wire, but then the efficiency of the lamp is much less. This is a great objection particularly for mine lamps of low power, which are fed from accumulator batteries. To get a reasonable efficiency a high incandescent temperature is required and the filament must be made of a metal having a very high melting point, such as tungsten. This material, however, oxidizes very quickly when exposed at a high temperature to air or mixtures of air and fire-damp, then flaming up and burning through; although the mixture of air and methane may not be immediately ignited by the hot wire (its incandescent temperature is at least 2000 °C) the flame arising when the wire burns through will most certainly set fire to the mixture.

When considering the risk of explosion one has to differentiate between the portable lamps (battery-fed), which the miners carry in their hand or have fixed to their caps, and the larger lamps used as fixed light points connected to the mains. The latter are usually located in well-ventilated galleries where there is so little danger that as a rule no special precautions need be taken. The portable

[1]) Extensive experiments have been carried out in this connection, inter alia, by J. Fripiat, See "Annalen der Mijnen België", 64, 105-144, 1943.

[2]) A platinum wire less than 0.1 mm in diameter caused to fuse by means of an electric current in a mixture of air and methane does not ignite the gas.

lamps are usually protected with an outer envelope (a wire-gauze screen would intercept too much light) and, moreover, in many cases mechanical safeguards are applied so that in the event of the outer bulb being broken a spring throws the lamp out of the fitting, thereby precluding any possibility of current continuing to flow through the filament. These measures, however, do not offer absolute safety, there still being a certain, though small risk, it being possible for a hole to be made right through the outer envelope and the inner bulb of the lamp without the safety mechanism being brought into operation, because this only reacts when the outer envelope is almost completely destroyed. The tungsten filament would then continue to glow at a high temperature and any mixture of air and fire-damp coming into contact with it would ignite; this is an exceptional risk of only sporadic occurrence. There is also even a possibility of the after-glow of the filament in the thrown-out lamp igniting the gas mixture, but in by far the majority of cases the safety mechanism will avert the risk of explosion.

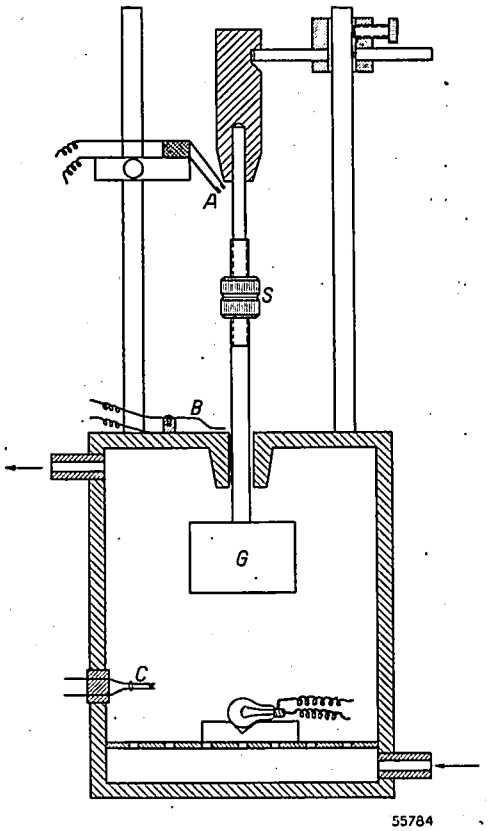


Fig. 1. Diagrammatic representation of an apparatus for testing mine lamps in respect to the danger of explosion. Such an apparatus was first designed by J. Fripiat. It consists of a metal explosion vessel with one wall of paper or cellophane. A mixture of air and methane flows into the vessel at the bottom and leaves it again through an opening at the top. The lamp to be tested is laid on a block resting on the bottom of the vessel. A metal weight G can be dropped onto the lamp to destroy the bulb. The nut S is first so adjusted that the filament of the lamp is not destroyed by the falling weight. Various electrical contacts are provided so as to be able to study the phenomenon of the combustion when that arises. The falling hammer closes a contact at A which starts the horizontal time-base of a cathode-ray oscillograph, and at B a contact is closed the moment that the lamp bulb is smashed, thereby bringing about a vertical deflection in the oscillogram. The moment of ignition of the gas mixture is recorded with a constant delay owing to the flame igniting a small piece of gun-cotton at C, thereby breaking the contact between two interconnected resilient plates. In many cases there is no need for these recording apparatuses when the object of the test is merely to ascertain whether ignition takes place or not.

Fluorescent lamps for the illumination of mines

In recent times there has been more and more a tendency to use fluorescent lamps (TL or MCF lamps)[3]) for the illumination of mine galleries. These can be used for permanent lighting points and small types can serve as portable light sources. These fluorescent lamps with their high efficiency and relatively low surface brightness have certain advantages for mine lighting because the black walls of the galleries reflect but little light and therefore call for rather powerful light sources. With the low level of brightness found in mine galleries a light source with a high brightness may easily cause troublesome glare. In this article we shall not go into the question whether the advantages of TL lamps outweigh the disadvantages, such as larger dimensions and higher initial cost. Here we are only concerned with the question in how far these lamps involve risk of explosions and what countermeasures have to be taken.

The fluorescent lamp requires stabilizing and an automatic starter. There are various types of starters in use: resistance-bimetal, glow-bimetal and electromagnetic starters [4]). For the problem that we are studying it does not matter much with what type of starter the fluorescent lamp is fitted. Let us assume that it is a glow-bimetal starter; the circuit normally used for this is represented in *fig. 2*. As soon as the mains are switched on a glow discharge takes place in the starter and heats the bimetal, with the result that after a time the contact is automatically closed. The choke is then short-circuited across the cathodes and the short-circuit current heats them. The glow discharge now being extinguished, the bimetal cools down, thereby opening the contact and cutting off the short-circuit current. The resultant voltage impulse ignites the lamp, the cathodes of which have mean-

[3]) A. A. Kruithof, Tubular luminescence lamps for general illumination, Philips Techn. Rev. **6**, 65-73, 1941.

[4]) These types have been described in an article by Th. Hehenkamp, A rapid-action starter switch for fluorescent lamps, Philips Techn. Rev. **10**, 141-149, 1948 (No. 5).

while reached a high temperature. Should the lamp fail to ignite, the process is automatically repeated, the cathodes being brought to glowing temperature each time. Once the lamp has been ignited no other current flows through the cathodes

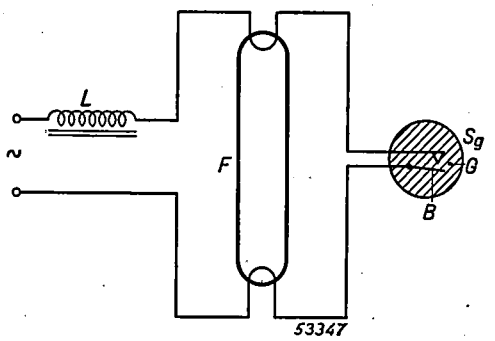


Fig. 2. The normal circuit of the glow-bimetal starter (*Sr*) of a fluorescent lamp (*F*). *G* = gas filling, in which a glow discharge may take place which heats the bimetal (*B*). *L* = ballast choke.

than that of the gas-discharge. This discharge ensures that the cathodes are kept at a temperature high enough for the lamp to burn.

An explosion can only take place in the event of the glass tube of the fluorescent lamp breaking. In order to investigate how great the risk of explosion may be in such an event, we purposely broke TL lamps having the starting mechanism of fig. 2 in a Fripiat apparatus charged with a combustible mixture of air and fire-damp [5]). An explosion took place every time about 1 second after the breaking of the lamp. This is understandable when it is borne in mind that after the destruction of the lamp the starter still tries to ignite it. The short-circuit current will cause the rather thick wires of the cathodes to glow at a much higher temperature than that brought about by the normal discharge, and the glowing cathodes then cause the gas mixture to explode.

When the glass tube of a fluorescent lamp is broken one must indeed reckon with the possibility of the electrodes remaining intact. This is much more likely to be the case than with the so much smaller incandescent lamp, the filament of which, moreover, is much more fragile. To counteract the risk of explosion a construction is applied whereby a broken lamp is automatically thrown out of its fittings, so that no current can flow through the cathodes. Just as is the case with incandescent lamps, however, here again such a construction has the drawback that the tube of the lamp may be cracked or a piece of glass may be knocked out of it and leave a leak, without the lamp being ejected. Although the lamp is then extinguished, the very first time the starter tries to ignite it again the gas mixture in the lamp will explode.

The firing of the gas mixture in the tube need not necessarily lead to an explosion of the gas mixture in the surroundings. Tests have shown that a crack in the lamp or a very small hole (e.g. 0.5 mm in diameter) is not sufficient to allow of an outward propagation of the explosion taking place inside the tube; this may be compared to the effect of a metal gauze (as used in the Davy safety-lamp) in checking the spread of an explosion. In the event, however, of larger holes being made (e.g. 1 cm in diameter) and also if in consequence of the explosion inside the lamp the cracked tube falls to pieces, then the explosion is indeed spread outwards.

A better and more adequate method of avoiding explosions is to arrange for the lamp to be ignited while the cathodes are cold. This is possible when the circuit arrangement as sketched in *fig. 3* is applied, whereby the electrodes are not previously heated by a short-circuit current. In other cases this method of ignition is usually avoided in view of its attendant drawbacks. Obviously, if the electrodes are not preheated and no other measures are taken then as a rule a much higher voltage impulse is required to bring about the ignition, and in some cases this necessitates a special starter having a rapid current-breaking action. When small power lamps are used (25 or 40 W), however, the normal starter usually suffices.

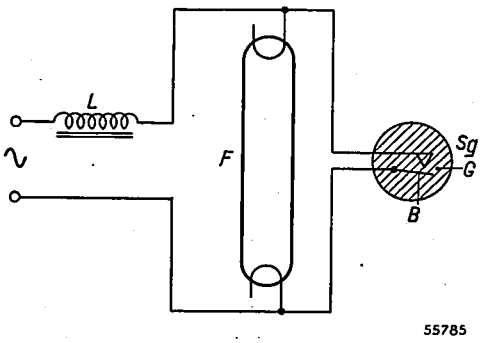


Fig. 3. A method of connecting the starter of a TL lamp which avoids the risk of explosion when the lamp is used in mines. With this arrangement the lamp is ignited with cold cathodes. For the meaning of the letters see fig. 2.

As a second objection it is mostly argued that with this method of ignition the electrodes suffer more and thus have a shorter life. For the lighting of mines, however, this is not of such great importance because the periods of operation are long and the lamp does not have to be switched on and off so frequently. Thus the advantages of this method of ignition most certainly outweigh the disadvantages.

[5]) The tests were carried out with fluorescent lamps of special dimensions, so constructed as to fit in the testing apparatus.

We have carried out a number of tests with fluorescent lamps in a circuit according to the scheme of fig. 3. Experiments with a broken or leaking TL lamp fitted with electrodes like those of the TL 40 W lamp, whereby under these conditions no ignition takes place, did not give rise to any explosion, as was only to be expected considering that the cathodes remained cold. Such a lamp when ignited and placed in a Fripiat apparatus in a mixture of air and fire-damp and then broken to pieces did not cause any explosion either, the working temperature of the electrodes not being high enough to ignite the gas mixture after the discharge had been extinguished. Consequently a TL lamp used in the manner described above may be considered safe under any circumstances.

Care must be taken that the starter mechanism itself does not involve the risk of explosion. A resistance-bimetal starter, for instance, will certainly cause an explosion if the heating wire should be switched on while in combustible surroundings. In our tests an electromagnetic starter working normally while in contact with a mixture of air and fire-damp did not result in any explosion spreading to the surroundings. When, however, the ignition failed (for instance owing to a defect in the lamp) and the starter therefore continued to operate for an abnormal length of time, there was indeed a risk of explosion. No serious troubles, however, are to be expected from starters, it always being possible to place these in metal containers, and it is most unlikely that such a container would break without throwing the starter mechanism out of order.

Finally we would point out that our experiments were carried out with mixtures of air and methane of different compositions. We started with natural fire-damp of the composition: about 39% CH_4, 4% CO_2, 4% O_2, 9% H_2, 44% N_2 and 0.2% higher hydrocarbons. To produce a highly explosive mixture of this gas with air a quantity of O_2 was first added to the fire-damp such as to give the same ratio of oxygen to nitrogen as that in air, after which this gas mixture was diluted with air to a mixture containing 7-8% CH_4. It appeared that mixtures of air with this percentage of methane are the most dangerous as regards ignition temperature [6]), rate of propagation of the flame and suchlike. Tests were also carried out with a technical methane containing unsaturated hydrocarbons, instead of the natural fire-damp. These admixtures increase the combustibility of the mixtures of air and methane, but in no single instance did an explosion take place when the lamp was ignited with cold cathodes.

[6]) The ignition temperature of these mixtures is about 650 °C.

A DIRECT-READING DYNAMIC ELECTROMETER

by J. van HENGEL and W. J. OOSTERKAMP. 621.317.723.082.742:621.386.82

A description is given of a direct reading d.c. electrometer. It is based on the dynamic principle, the direct voltage being converted into an alternating voltage with the aid of a parallel-plate capacitor, the capacitance of which changes periodically as one plate is kept stationary while the other is kept in vibration. The alternating voltage is applied to an amplifier with conventional valves; the output voltage is rectified and the conducted direct voltage measured with a moving-coil meter. In order to keep the amplification constant, a high degree of negative feedback is applied by connecting the output d.c. voltage wholly or partly in opposition to the voltage to be measured. This makes it necessary to use a special rectifying circuit which is sensitive to the polarity of the a.c. input voltage. Due in part to the direct-voltage feedback, the (apparent) input resistance reaches extremely high values (more than $10^{15}\ \Omega$). Two instruments are discussed: a millivoltmeter (full deflection at 100 mV) for laboratory measurements, and a dosimeter for X-rays (in combination with an ionization chamber and a measuring resistor). The dosimeter has a scale calibrated in r/min and covers a very wide measuring range, from $4 \cdot 10^{-7}$ r/sec (fraction of the tolerance dose) to 200 r/sec (contact therapy). For the calibration a standard-current generator has been designed which supplies a calibrated current of 10^{-9} A.

In many investigations in the field of physics and of electrical engineering the tension of direct-voltage sources which have a high internal resistance have to be measured. It is then essential that the voltmeter used should draw as little current as possible, so that the difference between the e.m.f. of the voltage source and the measured voltage under load is kept as small as possible.

Sometimes, when small direct currents are to be determined, the voltage produced across a high-ohmic resistor through which the currents flow is measured. Such cases occur not only in physical investigations but also, as will be shown farther on, in the daily routine of X-ray therapy. In these cases, too, one must have a voltmeter with very high resistance, since the meter bridges the measuring resistor and thus sets an upper limit to the resistance formed by the parallel connection of the two, thus limiting the sensitivity of the circuit.

In the cases mentioned one may often advantageously use an electrometer. This is an instrument in which the deflection is brought about by the electrostatic effect of charges and which therefore, in principle, consumes no current at all (apart from the charging current required to give the instrument a deflection, and the leakage current due to the finite insulation resistance).

A special form of electrometer is a triode — or, more generally, an electronic valve with a control grid — so arranged that no grid current flows through it. The word "no" is not to be taken too strictly, since owing to various causes the grid current is not generally absolutely zero; such causes may be imperfect insulation between the grid and other electrodes, ionic current flowing to the grid, or thermionic and photo emission from the grid. The methods applied in the special triode for use as an electrometer (type 4060) have already been described in this journal [1]). Within a wide range of conditions the grid current of this triode can be reduced to less than 10^{-14} A.

Here an electrometer will be described which, at full deflection, has a current consumption even 10^2 to 10^3 times smaller, so that the internal resistance of the source of the voltage to be measured, or the resistor through which the current to be measured flows, may be a corresponding factor larger. Moreover, this instrument has the advantage that, as opposed to some other electrometers, it gives a direct reading, whilst furthermore no special valves are required, only normal pentodes and rectifying valves being employed.

Principle of the dynamic electrometer

Our instrument is a further development of the dynamic electrometer described by Dorsman [2]), the principle of which is as follows. The direct voltage to be measured is applied via a high-ohmic resistor to a capacitor one of the plates of which is kept in vibration (for instance, with the aid of a loudspeaker system — see *fig. 1* — and a

[1]) H. van Suchtelen, The electrometer triode and its applications, Philips Techn. Rev. **5**, 54-59, 1940.

[2]) C. Dorsman, A p_H-meter with a very high input resistance, Philips Techn. Rev. **7**, 24-32, 1942; see also P. H. Clay, thesis, Amsterdam 1942; H. den Hartog and F. A. Muller, Physica **10**, 167-172, 1943 and **11**, 161-166, 1943; Hl. de Vries, Physica **13**, 449-452, 1947; H. Palensky, R. K. Swank and R. Grenchik, Rev. sci. Instr. **18**, 298-314, 1947.

valve oscillator), so that the capacitance varies periodically. Just as in the case of a condenser-microphone, an alternating voltage is produced across the capacitor which at a given amplitude of vibration is proportional to the direct voltage

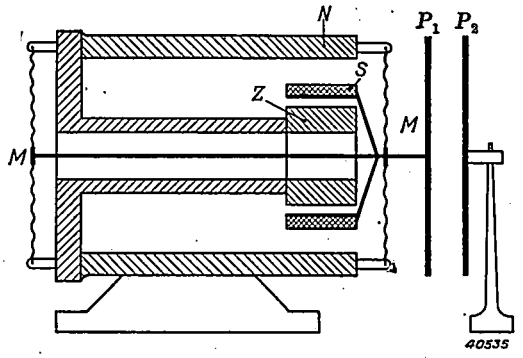


Fig. 1. Vibrating capacitor in cross section. N, Z = poles of a permanent magnet, S = coil of the electrodynamic driving system, M = diaphragm springs, P_1 = vibrating plate, P_2 = stationary plate of the capacitor.

applied. This alternating voltage is led via a coupling capacitor (C_2, *fig. 2*) to a normal a.c. pentode amplifier. The input resistance of the electrometer is mainly governed by the insulation of the coupling capacitor and that of the vibrating capacitor. With amber, polystyrene and similar substances as insulating material (and if desired as dielectric in the coupling capacitor) both capacitors can be given a much higher insulation resistance than is possible with an electrometer triode.

The electrometer described by Dorsman was designed for measuring the potential of a "glass electrode", from which potential the acidity (p_H) of a solution can be derived. The method of measuring is a zero method: the voltage to be measured is applied to the input of the electrometer in opposition to a reference voltage derived from a compensator, the latter voltage being so adjusted that the alternating voltage at the output of the amplifier is zero; this is observed on a cathode-ray indicator connected to the output. When the output voltage is zero the two d.c. input voltages are equal, so that the unknown potential may be read from the compensator calibrations.

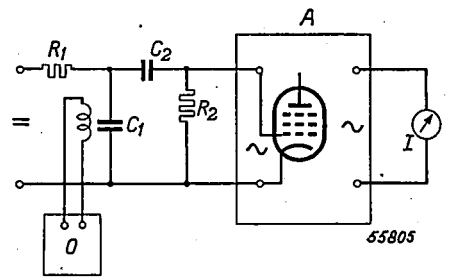


Fig. 2. Circuit diagram of the dynamic electrometer. C_1 = vibrating capacitor, the driving coil of which is connected to an oscillator O; R_1 = high-ohmic series resistor counteracting changes in the charge of C_1 when the system is vibrating, C_2 = coupling capacitor, R_2 = grid leak resistor, A = alternating voltage amplifier, I = indicator.

The zero method is suitable for the accurate measurement of very low voltages and has, moreover, the advantage that variations in the amplification or in the amplitude of the vibrating capacitor (due, for instance, to mains voltage fluctuations) only affect the precision of the adjustment and not the reading.

For many purposes, however, a direct-reading instrument is to be preferred, where no adjustments have to be made for every measurement, so that one's hands are left free and, moreover, the work can be done more quickly. It is then obvious that there should be connected to the output of the electrometer amplifier a measuring instrument provided with a scale calibrated in the units of the quantity to be measured, for instance mV.

Of course the favourable features of the zero method were to be retained as far as possible, and therefore the amplifier had to be of such a type that its amplification factor is reasonably constant, both in the event of mains voltage fluctuations and in the case of a variation of the characteristics of the valves. This requirement of constancy in the amplification has made it necessary to introduce drastic modifications of the electrometer amplifier used for p_H-measuring before it was possible to realize a direct-reading instrument.

Following these lines we have so far made two types of direct-reading dynamic electrometers for laboratory work, one as a mV-meter with very high impedance for general laboratory use, the other provided with a scale in röntgens per minute for measuring X-ray doses (with the aid of an ionization chamber). The circuit arrangements of both these types are mainly the same.

Direct-voltage feedback

The desired constancy of the amplifying factor is obtained by applying feedback [3]) to a high degree, by returning the output voltage E_2 (*fig. 3*) either wholly or in part to the input and there connecting it in opposition to the voltage to be measured, E_1. The output voltage must therefore be a direct voltage (which can thus be measured with a moving-coil meter); it is obtained with the aid of a rectifier connected to the output of the amplifier. Thus the feedback is a direct-voltage feedback.

[3]) B. D. H. Tellegen, Inverse feed-back, Philips Techn. Rev. 2, 289-294, 1937.

Across the vibrating capacitor is the direct voltage E_1—E_2. The vibration sets up a proportional alternating voltage v_1.:

$$v_1 = a_1 (E_1 - E_2),$$

which is amplified by a factor a_2 to the a.c. output voltage v_2:

$$v_2 = a_2 v_1 = a_1 a_2 (E_1 - E_2).$$

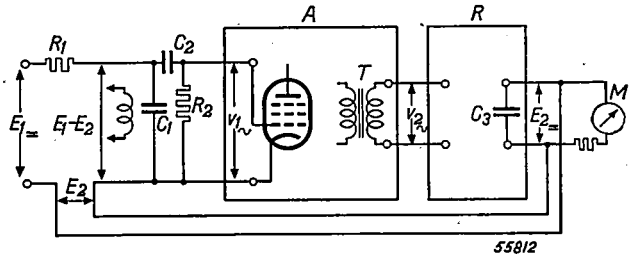


Fig. 3. Circuit diagram of the direct-voltage negative feedback system applied in our electrometer. E_1 = direct voltage to be measured; E_2 = d.c. output voltage; v_1, v_2 = a.c. input and output voltage, respectively of the amplifier A; T = transformer; R = rectifier with smoothing capacitor C_3; and M = moving-coil voltmeter. The other letters have the same meaning as in fig. 2.

From this the rectifier produces the direct voltage E_2 proportional to the amplitude of v_2 (proportionality factor a_3):

$$E_2 = a_1 a_2 a_3 (E_1 - E_2).$$

Thus we have for the ratio p between the d.c. output voltage E_2 and the direct voltage to be measured E_1:

$$\frac{E_2}{E_1} = p = \frac{a_1 a_2 a_3}{1 + a_1 a_2 a_3} = \frac{A}{1 + A}, \quad \ldots \quad (1)$$

when $A = a_1 a_2 a_3$.

The factors a_1, a_2 and a_3 depend more or less upon the properties of the oscillating, amplifying and rectifying valves respectively and upon the supply voltages (and thus the mains voltage). If however, it is arranged that $a_1 a_2 a_3$ is always large with respect to unity, then $p \approx 1$ and therefore practically constant, in spite of fluctuations in the values of a_1, a_2 and a_3. Now a_1 and a_3 are both smaller than unity, but a_2 can be made so large that in fact $A = a_1 a_2 a_3 \gg 1$. This requirement has been met in both forms of construction of our electrometer.

A limit is set to the raising of the value of A owing to the fact that at a higher amplification the system would become unstable, that is to say it would oscillate at a frequency depending upon the time constants of the circuits contained in the system. The larger the time constants, the more the amplification can be raised, but the adjustment time of the instrument becomes longer.

With the method of feedback applied the direct voltage across the vibrating capacitor is not E_1 but only E_1—E_2, which may well be 30 times smaller than E_1. This means that the leakage current flowing across the capacitors C_1 and C_2 at a given insulation resistance is reduced. It is partly due to this fact that the (apparent) resistance between the input terminals is exceptionally high.

As regards the a.c. losses in the resistors R_1 and R_2 (and the resistor R_5 to be discussed farther on), it must be noted that these are supplied by the oscillator driving the vibrating capacitor. These losses, therefore, do not form any load upon the voltage source to be measured.

Rectification

If the rectifier (R, fig. 3) were arranged according to one of the conventional methods, where the direct voltage obtained depends only upon the amplitude and not upon the phase of the a.c. input voltage, an unstable situation would arise, as may be seen from the following numerical example.

Let $A = 30$, thus, according to eq. (1), $p = 30/31$, and let E_1 be 100 mV, thus $E_2 = (30/31) \cdot 100 = 97$ mV. (The scale of the moving-coil meter to which E_2 is applied is such that the instrument indicates $E_2/p = E_1$, in this case 100 mV). E_1—$E_2 = 3$ mV.

Let us suppose, further, that E_1 suddenly drops to 94 mV. Since E_2 cannot change quickly, E_1—E_2 becomes at first —3 mV, in consequence of which v_1 and v_2 maintain the same amplitude but change polarity, which amounts to a phase shift of 180°. An ordinary rectifying system, however, is insensitive to this change and E_2 is kept at 97 mV. The situation is now unstable: any further drop of E_1 is accompanied by a rise in the absolute value of E_1—E_2, and also in the output voltage E_2. The negative feedback is turned into a positive feedback.

Besides this hypothetical experiment, any normal switching-on leads to instability, since E_2 builds up in an oscillatory way, so that there will be moments when E_1—E_2 is negative and the pointer of the instrument swings beyond the end of the scale.

To avoid this instability a rectifying system has been designed in which, when v_2 changes 180° in phase, E_2 tends to drop and to restore the proper polarity of E_1—E_2. When E_2 has reached p times the new value E_1 — in the example just given, therefore, $(30/31) \cdot 94 = 91$ mV — equilibrium is again obtained, E_1—E_2 again having practically its

original value (+ 3 mV). At this lower value of E_2 (91 mV) the meter indicates the exact value of E_1 (94 mV).

Fig. 4 represents the rectifying system in question. The polarity of v_2 is compared with that of the alternating voltage v_3 derived from the oscillator driving the vibrating capacitor. Special measures (to which we shall refer later) have been taken to ensure that the phase difference between v_2 and v_3 can only be either 0° or 180°.

This systems functions in the following way.

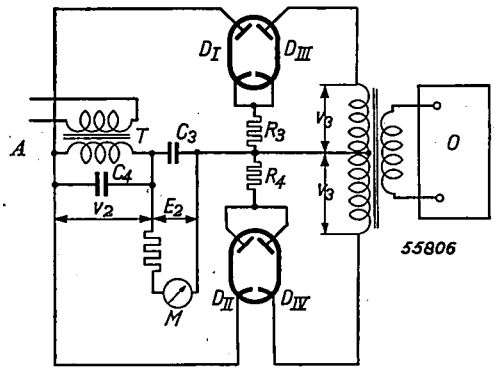


Fig. 4. Circuit of the phase-sensitive rectifier. T = output transformer of the amplifier; C_4 capacitor with which T is tuned; C_3 = smoothing capacitor; D_I-D_{III} and D_{II}-D_{IV} = double diodes (EB 4); O = oscillator also driving the vibrating capacitor.

For alternate half cycles [4]) the alternating voltage v_0 causes current to flow through the diodes D_{III} and D_{IV} and the resistors R_3 and R_4. During these half cycles voltages are developed across these resistors which, apart from voltage losses, are equal to v_3. The resistors also form part of the circuits via which the smoothing capacitor C_3, across which the output voltage E_2 is developed, either receives charge from the transformer T (via the diode D_I) or is discharged (via the diode D_{II}). When the phase shift between v_2 and v_3 becomes 180° then — as will be explained below — a change takes place in the ratio of the quantities of the charge fed to and drawn from C_3 per cycle, thus changing E_2 in the desired direction.

Let us first consider the situation where the direct voltage across the vibrating capacitor has the normal polarity (E_1—$E_2 > 0$). The system must be then so adjusted that v_2 has the polarity at which A is positive with respect to the terminal of T connected to C_3 (fig. 4) during the half cycles in which D_{III} and D_{IV} are non-conducting; within these half cycles the capacitor C_3, receives a charge via D_I (so long as $v_2 > E_2$) and gives off a charge via D_{II} (so long as $v_2 < E_2$) these valves not being blocked by the voltages v_3. During the other half cycles the diodes D_{III} and D_{IV} are conducting and, as we have seen, across each of the resistors R_3 and R_4 there lies the voltage v_3. This voltage is chosen high enough to block the diodes D_I and D_{II}; thus the voltage v_2 does not cause any current to flow. As a result the voltage E_2 adjusts itself in such a way that the capacitor C_3 receives (via D_I) per cycle just as much charge as it gives off (via D_{II} and via the meter connected to C_3).

We shall now consider the case where E_1—$E_2 < 0$. The polarity of v_2 at which A is positive with respect to the terminal of T connected to C_3 then occurs during the half cycles in which D_{III} and D_{IV} are conducting, and consequently — just as was the case before — D_I and D_{II} are blocked. During the other half cycles (D_{III} and D_{IV} non-conducting) no charge can flow to C_3 via D_I (v_2 has the wrong polarity for that) but charge can flow from C_3 through D_{II}. Thus the case in question (E_1—$E_2 < 0$) leads to a drop in E_2, as was desired.

With this system two valves suffice if double diodes (type EB4) are used as indicated in fig. 4.

Any voltage superimposed upon v_2 with a frequency different from that of v_2 and v_3 as a rule contributes little or nothing towards E_2. In other words, the rectification is selective, so that an interfering voltage with the mains frequency or resulting from "microphonic effect" will have little influence. The selectivity is still further increased by tuning the transformer T (fig. 4) with a parallel capacitor (C_4) to the frequency of vibration (125 c/s, midway between two harmonics of 50 c/s, so chosen as to avoid trouble from these harmonics). Although this circuit has so much damping that the voltage gain is of little significance, harmonics of v_2 are effectively suppressed.

Amplifier

From the explanation of the functioning of the rectifying system it will be clear that changes in the phase angle between v_2 and v_3 will affect the amplitude of E_2. When, in the amplifier, circuits are used with little damping and tuned to the frequency of the vibration — as is the case in the amplifier designed for p_H-measurements (see footnote [2])) — then the phase of v_2 changes considerably with small variations in the frequency of vibration or in the event of a slight detuning. In order to avoid this we have not used any tuned circuits in the amplifier for our electrometer (the circuit T-C_4 previously mentioned — fig. 4 — is so strongly damped as not to endanger phase stability). We employ a resistance-coupled amplifier (*fig. 5*) with two stages. The value of the coupling capacitors C_5 and C_6 has been so chosen that, in combination with the resistors R_5 and R_6 respectively, they bring about an appropriate phase shift such as to bring

[4]) For the sake of convenience we speak of "half cycles" although actually the intervals referred to differ slightly from half a cycle. We shall not go into this because it is of no consequence for our arguments.

v_2 exactly in phase with the reference voltage v_0 (fig. 4), as is desired for the rectification.

The dimensions of the circuit C_2-R_2-C_5-R_5 are such that voltages having the frequency of vibration are little attenuated in contrast with interference voltages derived from the first or second harmonics of the mains frequency. Thus the overall selectivity is improved. As an illustration of the strong filter action obtained in this manner it can be stated that an interfering voltage of 200 mV r.m.s., 50 c/s, superimposed upon an input direct voltage $E_1 = 10$ mV, does not affect the meter reading.

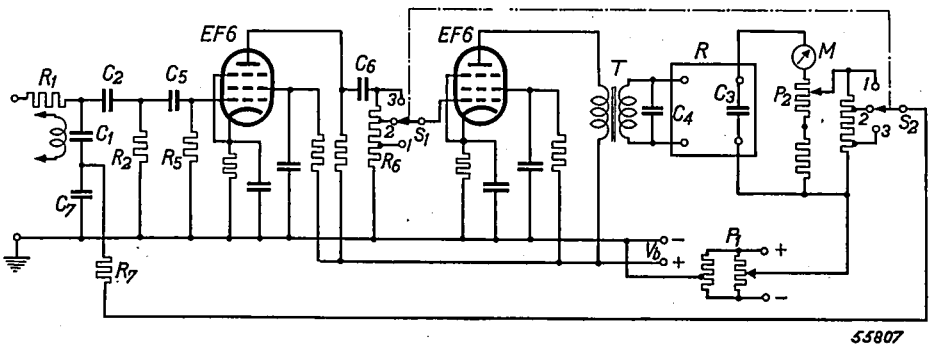


Fig. 5. More detailed diagram of the direct-reading electrometer (cf. fig. 3). R_5, C_5 and R_6, C_6 = circuits for bringing v_2 into phase with v_3; R_7, C_7 = smoothing circuit via which the d.c. output voltage (or a part of it) is returned to the input; S_1, S_2 = switches for varying the sensitivity: in position *1* the full deflection is at 1000 mV input voltage, in position *2* at 300 mV, in position *3* at 100 mV; P_1 = potentiometer for zero point correction; P_2 = potentiometer for scale correction; V_b = supply voltage. The other letters have the meaning given in figs 2 and 3.

Fig. 6 shows how little the reading is affected by mains voltage fluctations, due to the method of negative feedback applied; a variation in the mains voltage from the nominal value (100%) to 90% or 110% gives at most a difference of 1% on the meter.

Further details of the electrometer

The electrometer was designed for 100 mV at full deflection, corresponding to an accuracy within about 1 mV. This relatively low voltage-sensitivity enhances the reliability of the instrument and has, moreover, the advantage that as a rule no trouble is experienced from statistical current fluctuations. With this degree of sensitivity the direct voltage across the vibrating capacitor at the full deflection amounts to about 3 mV.

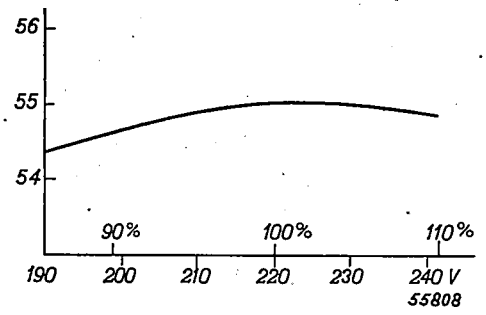


Fig. 6. Variation of the deflection (nominally, e.g., 55 scale divisions) as a function of the mains voltage fluctuations. If the mains voltage (rated value 220 V) fluctuates between 90% and 110% the variation in deflection is less than 0.5 division.

In cases where voltages higher than 100 mV have to be measured a switching device is used; this will be dealt with presently.

The reading is taken from a moving-coil meter giving full deflection when a current of 50 μA is flowing through the coil.

Zero adjustment is made in the first place, as far as the meter itself is concerned, with the normal zero adjustment of the pointer. In addition there is an electrical correction: by means of the potentiometer P_1 (fig. 5), connected to a small auxiliary direct voltage, any changes in the contact potential on the plates of the vibrating capacitor can be compensated.

The calibration of the meter can be corrected with the aid of the potentiometer P_2.

In the types already constructed the resistance between the input terminals of the electrometer is more than $10^{15}\,\Omega$ and the input capacitance about 40 pF.

Still more favourable values can be reached by applying the variation of the input circuit illustrated in *fig. 7* (so far this has not been normally applied). The insulation of the non-earthed input terminal is screened with a guard ring brought to the potential E_2. As we have already seen in the case of the capacitors C_1 and C_2, owing to this measure the insulation is only loaded with the voltage E_1—E_2 = about $E_1/30$. As a consequence the apparant input resistance is greatly increased and the apparent input capacitance many times reduced.

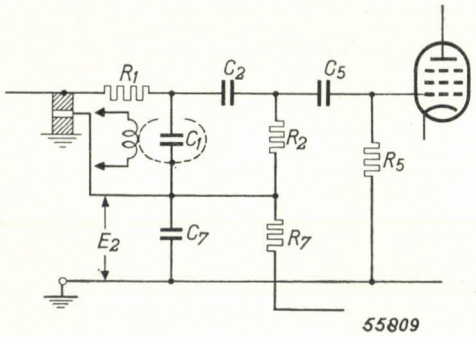


Fig. 7. Modification of the input part of the system according to fig. 5. In the insulator of the input terminal is a guard ring brought to the potential E_2, as is also the screening of C_1, so that the insulation at that spot is only loaded with the voltage E_1-E_2. This greatly increases the apparent input impedance and reduces the apparent input capacitance.

Practical application as laboratory voltmeter

Fig. 8 gives an illustration of the electrometer developed upon the principle described and intended for use as a laboratory instrument for taking measurements in cases where a very high input resistance is required. The circuit is that represented in fig. 5 (but without the switches S_1 and S_2) and in fig. 4. After what has already been said, this instrument needs no further explanation.

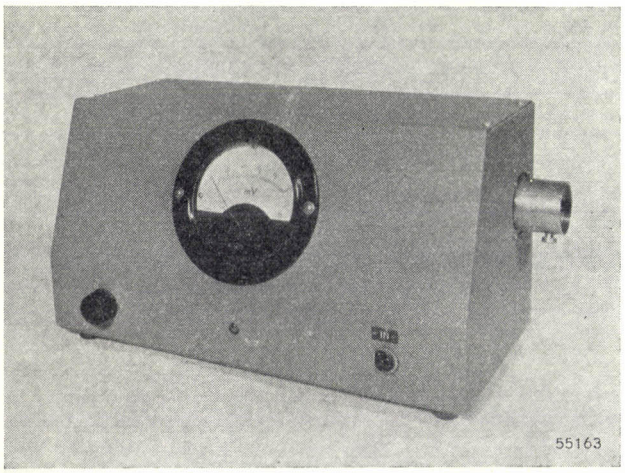


Fig. 8. Direct-reading dynamic electrometer for laboratory use. Full deflection at 100 mV input voltage. Input impedance $> 10^{15}\ \Omega$, input capacitance about 40 pF.

Practical application as dosimeter for X-ray therapy

The dosage of X-ray or gamma irradiation is expressed in terms of the röntgen unit (r), which is based upon the ionizing action of the rays and is defined as follows (Chicago 1937):

"The roentgen shall be that quantity of X or gamma radiation such that the associated corpuscular emission per 0.001293 gram of air produces, in air, ions carrying 1 e.s.u. of quantity of electricity of either sign".

A well-known method of measuring X-ray doses which is of course based on this definition is the following: an ionization chamber — a vessel containing a given quantity of air (or some other gas) and two electrodes between which a direct voltage is applied — is exposed to the rays, which ionize the gas and thus make it partially conducting. A current therefore flows between the electrodes. The potential difference should be large enough to cause the current of ions to reach its saturation value but must remain below the striking voltage. A current intensity of 3.33×10^{-10} A per cm^3 air (of one atm. and 0° C) in the ionisation chamber corresponds to 1 r/sec.

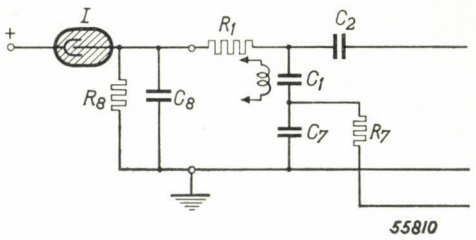


Fig. 9. Input circuit of the electrometer connected to an ionization chamber I with measuring resistor R_8 and smoothing capacitor C_8, for measuring the dose rate of X-ray irradiation. The other letters have the meaning given in fig. 5.

In order to measure the current it is passed through a high-ohmic resistor (R_8, *fig. 9*) and the voltage developed across it is measured. In view of the very weak current an electrometer is required for this purpose, and, given its exceptionally low current consumption, the electrometer described is particularly suitable.

Since the X-ray tube is fed with a more or less pulsating direct voltage (sometimes even with an alternating voltage) there is a certain "ripple" in the radiation, thus also in the ionization current thereby generated. A capacitor (C_8) shunted across the measuring resistor keeps the ripple voltage across the resistor sufficiently small.

Measuring range

The measuring range for which the dosimeter had to be designed is very wide: on the one hand it was desired to be able to measure the very large dose rates (doses per unit of time) which occur in contact therapy [5]) (up to 200 r/sec), while on the other hand it had to be possible to measure also fractions of the very much smaller dose rate corresponding to the amount of radiation that the tissues of the human body can bear without being

[5]) See, e.g. H. A. G. Hazeu, J. M. Ledeboer and J. H. van der Tuuk, An X-ray apparatus for contact therapy, Philips Techn. Rev. 8, 8-15, 1946.

damaged (e.g. 0.1 r/day, i.e. about 10^{-5} r/sec) [6]). These limits thus differ by a factor 10^9.

We shall now consider in what way the desired range in sensitivity of the instrument can be realized.

1) Volume of the ionization chamber. The current supplied by the ionization chamber is approximately proportional to its volume. A series of ionization chambers differing greatly in size therefore already permit an extensive measuring range to be covered. Of course the dimensions cannot be chosen arbitrarily, since one has to take into account the spatial distribution of the field of radiation in which the measurement is to be taken. For contact therapy we use a chamber of 25 mm^3, for deep therapy one of 6 cm^3 and for measuring tolerance doses one of 35 cm^3 or of 150 cm^3.

2) Gas filling. Usually the ionization chamber is in communication with the outside air and is thus filled with air under atmospheric pressure. Consequently for very accurate measurements corrections have to be applied for temperature and barometric pressure.

If it is decided to use a sealed ionization chamber then this can be filled with some other gas under a different pressure. If high sensitivity is required then a gas is chosen with a high atomic number and not too low pressure. The higher the atomic number of the gas, the greater is the absorption of the X-rays (at least if the rays are not very "hard") and thus also the greater the ionization brought about in the gas. In krypton (atomic number 36), for instance, the ionization current is about 400 times as large as that in air (atomic number of nitrogen 7 and of oxygen 8). An ionization chamber filled with krypton therefore renders good service for measuring very small dose rates. There is the disadvantage, however, that then the meter reading is dependent upon the hardness of the rays, so that a different calibrating constant has to be used for different qualities of radiation.

3) Measuring resistance. The higher the measuring resistance, the greater is the sensitivity. We use measuring resistors having a value between 50 MΩ and 2000 MΩ. Since the resistance between the input terminals of our electrometer is much higher, the measuring resistance can be further increased if required, but it is not easy to make resistors of such a high value which are sufficiently stable.

It is possible to do without the measuring resistor. Then the ionization current charges the input capacitance of the electrometer. The voltage reading follows the rising input voltage. The ionization current can be calculated from the values of the input capacitance and the time, measured by a stop watch, within which the needle covers a given distance on the scale. With this method it is advantageous to employ the system shown in fig. 7.

4) Switching-over of the electrometer itself. The measuring range can of course also be extended by giving the electrometer itself various degrees of sensitivity. In our instrument this has been done in the manner indicated in fig. 5: full deflection is obtained at an input voltage of 1000, 300 or 100 mV, according to whether the switches S_1 and S_2 are in the position *1*, *2* or *3*.

In the designing of this switching method we started from the consideration that the sensitivity of the moving-coil meter had to be kept unchanged, so that at the full deflection E_2 has the same value (about 970 mV) in all the three positions.

If, in order to get lower sensitivity, the moving-coil meter were shunted, then for the full deflection a higher alternating voltage would be required at the input of the rectifier and also a larger amplitude of the auxiliary alternating voltage v_3 supplied by the oscillator to the rectifier (fig. 5). The latter might result in a heavy loading of the oscillator; moreover the load would change when switching over to a different sensitivity, which might impair the constancy of the oscillator frequency and amplitude.

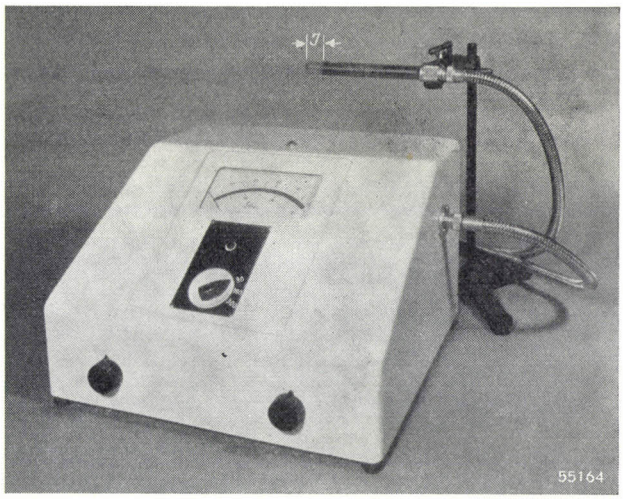


Fig. 10. Electrometer constructed as dosimeter, with scale in r/min. I = ionization chamber.

In the positions *2* and *3* (fig. 5) for max. 300 and 100 mV respectively only the part aE_2 of E_2 tapped off by S_2 is used as feedback voltage, the fraction being so chosen that it is always approximately equal to the same fraction p (≈ 0.97) of E_1. As may be seen from *table I*, in the positions *1* and *2* the direct voltage $E_1 - aE_2$ across the vibrating capacitor is then respectively 10 and 3 times as high as in the position *3*; thus the amplification can be reduced to $^1/_{10}$ or $^1/_3$. This is brought about

[6]) It is customary to express these tolerance doses per unit of time in r/day or in r/sec, whereas the dose rates for therapeutical purposes are expressed in r/min. For the sake of clarity we use here only r/sec.

with the switch S_1. The amplification cannot reach such values as to give rise to danger of oscillation. Table I shows the voltages produced at full deflection.

Table I. Direct voltages at full deflection in the three positions of the switches S_1 and S_2 (fig. 5). E_1 = voltage to be measured, E_2 = output voltage, aE_2 = negative feedback voltage, $E_1 - aE_2$ = direct voltage across the vibrating capacitor.

Position		1	2	3	
E_1	=	1000	300	100	mV
E_2	≈	970	970	970	mV
aE_2	≈	970	291	97	mV
$E_1 - aE_2$	≈	30	9	3	mV

For various fields of applications of X-rays a summary is given in *table II* of the possibilities mentioned sub (1), (2) and (3) which form a favourable combination, whereby E_{1max} may be made 1000 or 100 mV.

the anode current is practically independent, within wide limits, of the anode voltage. The anode current, however, is far too high for our purpose and therefore a capacitative current divider is used consisting of the capacitors C_9 (5 μF) and C_{10} (50 pF) bearing the relation of 10^5 : 1. The anode current is divided in the same ratio. The smaller of the partial currents passes through the measuring resistor R_8.

The current i passing through R_8 and C_{10} a period of time t after switching on is calculated as follows

$$i = \frac{C_{10}}{C_9 + C_{10}} I \left[1 - \exp\left(-\frac{C_9 + C_{10}}{C_9 C_{10} R_8} t\right)\right],$$

where I represents the anode current. When $C_9 \gg C_{10}$ one may write:

$$i \approx \frac{C_{10}}{C_9} I \left(1 - \exp \frac{-t}{C_{10} R_8}\right).$$

Even with $R_8 = 2000$ MΩ the time constant $C_{10} R_8$ is still only 0.1 sec, so that we very soon get

$$i \approx \frac{C_{10}}{C_9} I.$$

Table II. Table of the dose rates occuring in various fields of applied röntgenology, the ionization chambers used by us when measuring the doses, and the currents and voltage thereby obtaining.

Application	Dose rate to be measured	Ionization chamber		Ionization current	Measuring resistor R_8	E_1	E_1/sec
		volume	gas				
	r/sec	cm³		A	MΩ	mV	mV/sec
Contact therapy	0.5 - 250	0.025	air	$4 \cdot 10^{-12}$ - $2 \cdot 10^{-9}$	500-2000	8 - 1000	—
Deep therapy	0.1 - 5	6	air	$2 \cdot 10^{-10}$ - 10^{-8}	100	20 - 1000	—
Tolerance doses	$4 \cdot 10^{-7}$ - 10^{-5}	150	Kr *)	$2 \cdot 10^{-12}$ - $5 \cdot 10^{-11}$	2000	4 - 100	—
Tolerance doses	10^{-6} - 10^{-5}	25	air	10^{-14} - 10^{-13}	∞ **)	—	0.6-6 **)

*) The data given on this line apply for about 80 kV across the X-ray tube.

**) Measured without measuring resistor and with the system according to fig. 7. The ionization current can be calculated from the rate at which E_1 increases and the value of the input capacitance.

With a given ionization chamber and a given measuring resistance the moving-coil meter can be calibrated directly in r/sec or r/min (*fig. 10*). The electrometer itself, as already stated, is insensitive to mains voltage fluctuations and variations in the mutual conductance of the amplifying valves, but changes in the measuring resistor (R_8, fig. 9) may cause errors. In order be able to check the instrument, including this resistor, at any time, we have constructed a reference current generator, an apparatus supplying a very small, constant, known current which, when passed through the measuring resistor, gives a characteristic reading of the electrometer.

Reference current generator

The system applied for this accessory is diagrammatically represented in *fig. 11*. Use has been made of the familiar property of a pentode that

The process of calibration is as follows. When the switch S_3 is closed the anode current is adjusted to

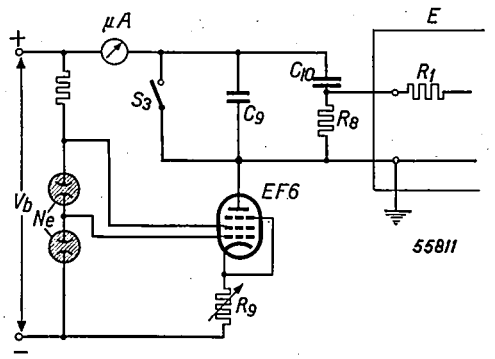


Fig. 11. Circuit diagram of a reference current generator supplying a current of 10^{-9} A for calibrating the dosimeter. V_b = supply voltage, Ne = neon tubes for stabilizing the voltage, R_9 = variable cathode resistor for adjusting the anode current of the pentode to 100 μA; C_9-C_{10} = capacitative current divider 10^5 : 1; R_8 = measuring resistor; E = electrometer.

100 μA with the aid of a variable cathode resistor. When S_3 is opened a current of $10^{-5} \times 100$ μA $= 10^{-9}$ A flows through R_8, which should give a characteristic reading on the electrometer. Any deviation from the correct deflection can be corrected with the potentiometer P_2 (fig. 5). After about 15 sec the capacitors C_9 and C_{10} are so far charged as to cause the anode voltage to drop below the limit at which the anode current is constant; the current then rapidly diminishes. The interval of 15 seconds is long enough for the correction to be carried out.

SECONDARY EMISSION IN OUTPUT VALVES

by J. L. H. JONKER.

621.396.645:621.385.5:537.538.8

Secondary electron emission is often an undesired phenomenon, which may, for instance, have a very adverse effect upon the functioning of tetrode amplifying valves. Known counter-measures are: 1) concentration of the space charge between screen grid and anode, 2) a third grid at low potential, 3) covering the anode with a layer of a substance from which secondary electrons cannot easily emerge. It is discussed why the means under 1 and 2, separately applied, frequently do not yield to the desired result, especially in the case of output valves As output valves, therefore, pentodes are usually employed in which advantage is also taken of the space charge. Output valves fed from an anode battery, however, operate with too small an anode current to be able to profit from the action of the space charge. Moreover, the supply voltage is low, and as a result the secondary emission consists of proportionately fewer slow, "real" secondary electrons and more rapid, reflected electrons. The latter are capable of passing the suppressor grid more easily. It appears that in such output pentodes the application of the third counter-measure leads to very much better characteristics and a higher output, with a given distortion. The new output pentode DL 41 for battery supply, with prepared anode, gives for instance with 10% distortion an output of approx. 260 mW, as against 200 mW for a similar valve with bare anode.

When electrons impinge upon the surface of a conductor or an insulator at a certain velocity some of them are reflected while the others penetrate into the material and transmit their energy to the electrons already in that material. In consequence some of the latter electrons, given a favourable direction of movement, emerge from the surface bombarded. This is the well-known phenomenon of secondary emission —by which one usually has in mind all the electrons coming from the bombarded surface, the emitted as well as the reflected ones. Several articles have already been written on this subject in this journal [1]).

Whereas in some cases good use can be made of this secondary emission, in others it is a most undesirable phenomenon and means have to be sought to suppress it as far as possible.

A familiar form of an electronic valve in which secondary emission may be highly injurious is the tetrode. The (primary) electrons which pass through the openings in the screen grid may strike the anode with considerable force and thereby liberate secondary electrons. When the tetrode is used as an amplifier, due to the anode load, the anode potential consists of an alternating voltage superimposed on the direct voltage. As a result the anode voltage may be temporarily lower than the constant screen-grid voltage. When this is the case the electrons are attracted towards the screen-grid, thereby considerably reinforcing the screen-grid current at the cost of the anode current i_a. In the characteristics representing i_a as a function of the anode voltage v_a irregularities then occur in the form saggings (*fig. 1*) which are apt to give rise to distortion. The anode current may not only drop to zero but may even be reversed in sign.

Means of suppressing secondary emission have already been discussed in this journal [2]) and consist mainly of the following measures:

1) concentration of the space charge between screen grid and anode,
2) the application of a third grid (at low potential),
3) covering the anode with a layer of a substance tending to prevent the emergence of electrons from the anode [3]).

[1]) See for instance H. Bruining, Secondary electron emission, Philips Techn. Rev. 3, 80-86, 1938.

[2]) J. L. H. Jonker, Phenomena in amplifier valves caused by secondary emission, Philips Techn. Rev. 3, 211-216, 1938.

[3]) A similar effect is obtained when fins or vanes are provided perpendicular to the anode surface as mentioned in the article quoted in footnote [2]). Such fins are not considered here.

Hitherto it has not been usual to apply more than one of these counter-measures simultaneously in one particular type of valve, though there are cases where a combination of (1) and (2) has been applied. In this article we shall show how in a certain case a particularly favourable effect can be produced by the combination of (2) and (3), that is, the application of a third grid and at the same time a prepared anode.

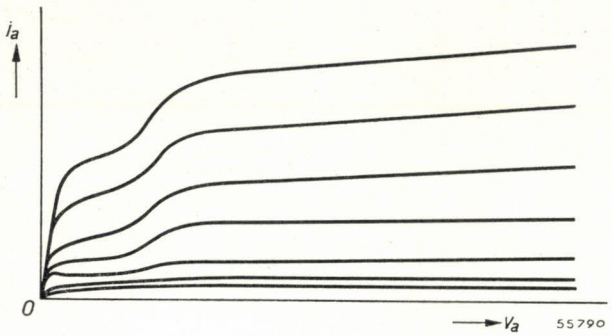


Fig. 1. Characteristics of a tetrode: anode current i_a as function of the anode voltage v_a at a constant value of the screen-grid voltage. Owing to secondary electron emission there is some sagging in the characteristics which gives rise to distortion.

First of all we shall consider briefly the measures referred to under (1) and (2), when we shall see the circumstances under which they fall short of their purpose.

Concentration of space charge

If a potential minimum is produced between screen grid and anode then, provided there is sufficient depth of the minimum, secondary emission is counteracted. A potential minimum can be obtained, for instance, by causing a concentration of the space charge between the said electrodes, this method often being used in tetrodes and, as we shall see, sometimes also in pentodes. Such a concentration may be brought about, for example, by giving the electrodes a certain shape and position, whereby the electrons are concentrated into one or more beams.

When one is dealing with output valves where it is of importance that the anode current and anode voltage should reach the largest possible amplitudes with the least possible distortion, the potential minimum should be present at widely divergent momentary values of that anode current and voltage. The meaning of this is illustrated in *fig. 2*, where the static characteristics of an output pentode ($i_a = f(v_a)$) are represented for one constant value of the screen-grid voltage V_{g2} and for a series of constant values of the control-grid voltage V_{g1} as well as a collection of working characteristics[4]). (Substantially the same applies for a tetrode.) In the case of the latter characteristics there was a loudspeaker connected to the anode

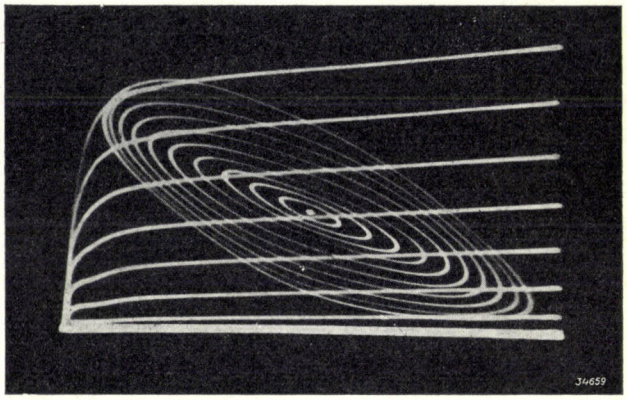


Fig. 2. Characteristics $i_a = f(v_a)$ of a pentode. The elliptical curves are the paths described by the working point when the load impedance in the anode circuit consists of a loudspeaker and a sinusoidal alternating voltage with stepwise increasing amplitude is applied to the control grid. It is seen that at a certain value v_a there may be widely different values of i_a.

circuit and a series of sinusoidal alternating voltages of increasing amplitude were applied to the control grid. In the absence of distortion the working characteristics would be pure ellipses.

It is seen that with varying amplitude of the a.c. grid voltage a large area of the plane of the characteristics is covered and that at a certain value of the anode voltage various values of the anode current are possible. In order to avoid distortion — in so far as this arises through secondary emission — secondary emission has to be suppressed in the whole of this area. It will appear that this cannot very well be realized without applying other means at the same time.

Let us first suppose that the valve is of such a construction that with a high anode current there is a sufficiently strong space charge to counteract secondary emission; the trend of the potential v in the space between screen grid and anode then follows a curve similar to curve (*1*) in *fig. 3*. With equal potentials of screen grid and anode, but with a small anode current, the minimum however disappears completely (curve *2*, fig. 3). If it had been arranged for a sufficient minimum to be present already with small anode currents then it might well fall too low, even to about zero ("virtual cathode"), when large

[4]) A method by which such characteristics can be recorded is described by A. J. Heins van der Ven, Testing amplifier output valves by means of the cathode-ray tube, Philips Techn. Rev. 5, 61-68, 1940.

anode currents are flowing. In that event some of the electrons are no longer able to reach the anode and then again considerable distortion takes place.

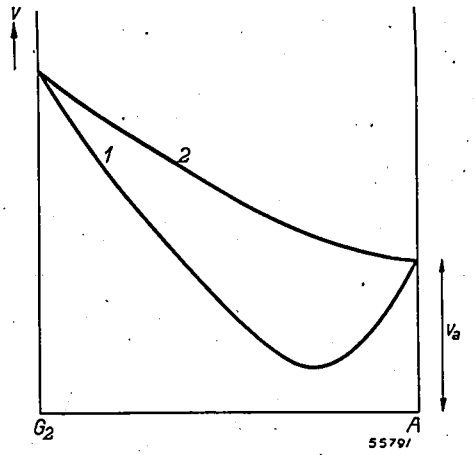


Fig. 3. The potential v between the screen grid (G_2) and the anode (A) of a tetrode with concentrated space charge. Curve *1* applies for a high anode current and curve *2* for a low anode current. In curve *2* the potential minimum has disappeared.

Such a state of affairs must be prevented at all costs. In the case of output tetrodes the usual practice is to mount screens between the screen grid and the anode which are connected to the cathode and to a certain extent counteract the transition of secondary electrons when the anode current is small. These screens are to be regarded as a simplified form of a suppressor grid, which we shall now consider.

Third grid

Secondary emission can also be suppressed by providing the tetrode with a third grid (making the valve a pentode) and connecting this so-called suppressor grid to a point where the potential is sufficiently lower than that of the anode [5]).

The suppressor grid should preferably have a large pitch. Therefore we have to differentiate between the (constant) voltage V_{g3} of the suppressor grid wires and the potential existing in the meshes of the suppressor grid. The instantaneous value of this potential depends upon V_{g3}, the anode voltage and the screen-grid voltage, and it may to a good approximation be identified with the effective potential $v_{3\text{eff}}$ that has to be given to the plane of the suppressor grid.

With an efficient construction it can be arranged that when $V_{g3} = 0$ the value of $v_{3\text{eff}}$ is kept lower than v_a for greatly differing values of v_a (*fig. 4*, curves *1* and *2*) independently of the anode current. It is this independency of the anode current that constitutes the great advantage of the pentode compared with a tetrode with concentrated space charge.

When v_a drops to very low values then, under the influence of the screen-grid voltage, $v_{3\text{eff}}$ may become higher than v_a (curve *3* in fig. 4) and thus draw the secondary electrons away from the anode instead of returning them to it.

When $V_{g3} = 0$ the potential $v_{3\text{eff}}$ is given by

$$v_{3\text{eff}} = \frac{D_1 v_{2\text{eff}} + D_2 v_a}{1 + D_1 + D_2} \quad \ldots\ldots\ldots \quad (1)$$

in which $v_{2\text{eff}}$ = effective potential in the plane of the screen grid (which in practice can be taken as being approximately equal to V_{g2}), D_1 = "Durchgriff" (reciprocal of amplification factor) of the anode in the suppressor grid. Fig. 4 has been plotted for $D_1 = D_2 = 0.5$.

For the limit case where $v_a = v_{3\text{eff}}$, when there is no longer any potential minimum, it follows from eq. (1) that

$$v_a \approx \frac{D_1}{1 + D_1} V_{g2} \quad \ldots\ldots\ldots \quad (2)$$

To keep this limit value of v_a as low as possible one must therefore make D_1 small. To this end one might make the suppressor grid out of closely wound wire turns, but then this would obstruct too much the passage of the electrons to the anode, and as the result the screen-grid current would be greatly increased at the cost of the anode current. Therefore one preferably applies a large pitch suppressor grid placed as far away from the screen grid as possible in order to keep D_1 small [6]).

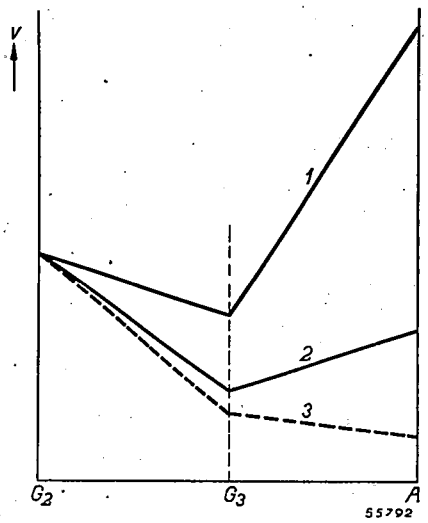


Fig. 4. The potential v between the screen-grid (G_2) and the anode (A) of a pentode in a plane passing midway between two wires of the suppressor grid. G_3 = suppressor grid at zero potential. Curve *1* applies for a high instantaneous value of v_a and curve *2* for a low ditto; in both cases there is a potential minimum in the meshes of G_3. This is no longer the case with curve *3*, applying for a still lower value of v_a.

[5]) See, e.g., British patent 287 958, priority 1926 (G. Holst and B. D. H. Tellegen.)

[6]) For a more extensive treatise on these matters see J. L. H. Jonker, Pentode and tetrode valves, Wir. Engr. **16**, 274-286 and 344-349, 1939.

In order to suppress secondary emission at very low instantaneous values of anode voltage, at least at a high anode current, modern output pentodes use also a concentration of space charge between suppressor grid and anode, this being brought about by suitable choice of the shape, size and spacing of the electrodes. The suppression is then only inadequate in the area where low values of i_a and v_a occur simultanously, but, as will be seen from fig. 2, this zone lies outside the working range of the valve.

Combination of suppressor grid and prepared anode

We now come to the third means by which secondary emission can be counteracted, the coating of the anode with a layer which the electrons cannot easily leave. Here it may be a question either of the nature of the substance forming the layer or of the form of that substance, or the solution may be found in both. As regards its nature it is obvious to choose a substance having a coefficient δ of secondary emission lower than that of the anode, which usually consists of nickel plate (by δ is understood the number of secondary electrons leaving the bombarded electrode as an average per primary electron). The form of the substance is of still more importance than its nature: a flocculated form is highly favourable because the secondary electrons cannot easily emerge from the numerous cavities in and between the flakes ("labyrinth effect"). A distinction has to be made between the coefficient δ (just mentioned) relating to a flat plane of material in a non-porous state and the coefficient δ_{eff} referring to materials in some other form. With a nickel plate covered, for instance, with floccular soot, values of δ_{eff} can be reached 3 to 5 times as low as the δ value of pure nickel plate.

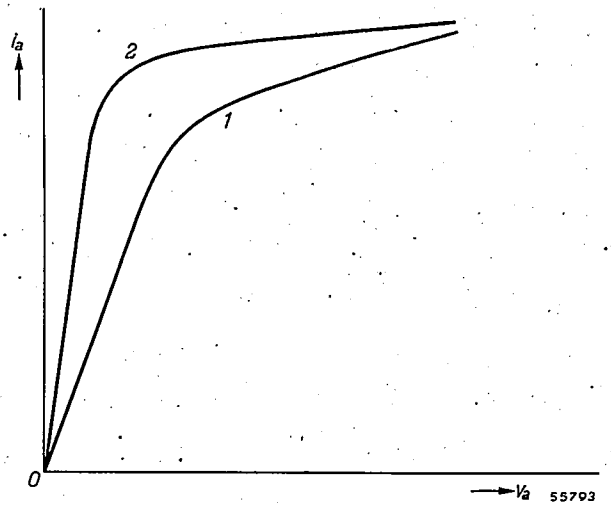


Fig. 5. Curve *1* is the characteristic $i_a = f(v_a)$ of a normal pentode and curve *2* that of a pentode in which the anode has a coating with a low secondary emission.

When this remedy is applied in a well-designed pentode, the suppressor grid of which is of such dimensions that the characteristics (curve *1* in *fig. 5*) no longer show any irregularities that are to be attributed to secondary emission, then a prepared anode as mentioned above does nevertheless give an improvement (curve *2* in fig. 5): the flat part of the characteristic is more horizontal and the bend in the curve is shifted to higher values of i_a and lower values of v_a. This means that for the working characteristic larger ellipses can be allowed — thus the valve can yield a greater output — before a certain amount of distortion arises.

To explain this rather unexpected effect we have to consider more closely the properties of secondary electrons.

Velocity distribution of secondary electrons

When a conductor is bombarded with electrons having a velocity V_1 electron volts then the emerging electrons have various velocities V between 0 and V_1. *Fig. 6*, relating to a nickel plate, shows the curve of the velocity distribution of these electrons in the case of primary electron velocities V_1 of 50, 150 and 250 eV. In every case a large proportion of emerging electrons are found to have a velocity of about 5 eV. These are the "real" secondary electrons. The curves show a peak at a velocity but little lower than V_1; this peak corresponds to the reflected electrons, i.e. the primary projectiles which have almost entirely retained their energy after the collision. (As already remarked in the introduction, the reflected electrons, too, are usually reckoned to belong to the secondary electrons.) The part of the curve lying between the two peaks represents those electrons which through the collision have lost a larger or smaller part of their energy.

From fig. 6 it appears that with lower velocities of the primary electrons the number of "real" secondary electrons relatively decreases whilst the number of reflected electrons increases.

In a tetrode or pentode it is particularly these reflected electrons which, owing to their high velocity, are easily capable of overcoming the repellent action of the potential drop between anode and screen grid and which are thus absorbed by this grid. This holds for any value of v_a, so that, as opposed to the "real" secondary electrons, the reflected electrons cannot give rise to any inflection points in the characteristics $i_a = f(v_a)$. What does happen, however, according to fig. 6, is that with falling anode voltage the number of reflected electrons becomes greater, which means that as v_a decreases the characteristic assumes a steeper slope,

as illustrated by curve *1* in fig. 5. When v_a drops to such low values to be about equal to or less than $v_{3\text{eff}}$ then the real secondary electrons also pass over to the screen grid and thus bring about a further reduction of i_a. In this way bends may arise in the characteristic which cause distortion when they lie within the working range.

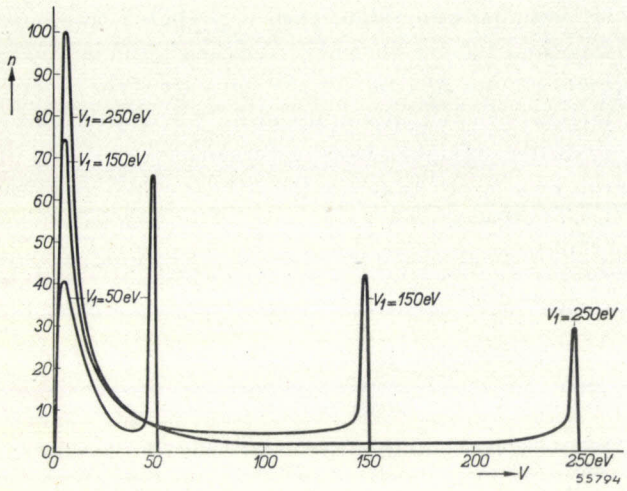


Fig. 6. Velocity distribution of secondary electrons obtained when a nickel plate is bombarded with primary electrons having a velocity V_1 of 250, 150 and 50 eV respectively. As function of the velocity V a quantity n is plotted which is proportional to the number of secondary electrons having the velocity V; $n = 100$ has been taken arbitrarily for the highest peak of the three curves. The peaks at $V \approx 5$ eV correspond to the "real" secondary electrons, the peaks at $V \approx V_1$ correspond to reflected electrons.

For the case of nickel coated with a porous layer of soot we have the curves of *fig.* 7. Here it is seen that the fast electrons have been relatively greatly reduced in number. The real secondary emission, too, is reduced: for the pure nickel plate $\delta = 1.2$ and for the plate covered with soot δ_{eff} is only 0.36 (in both cases at $V_1 = 250$ V). When such a coating is applied to the anode of a pentode the resultant reduction of the secondary emission manifests itself in the previously mentioned improved shape of the characteristic $i_a = f(v_a)$ (curve *2* instead of curve *1*, fig. 5).

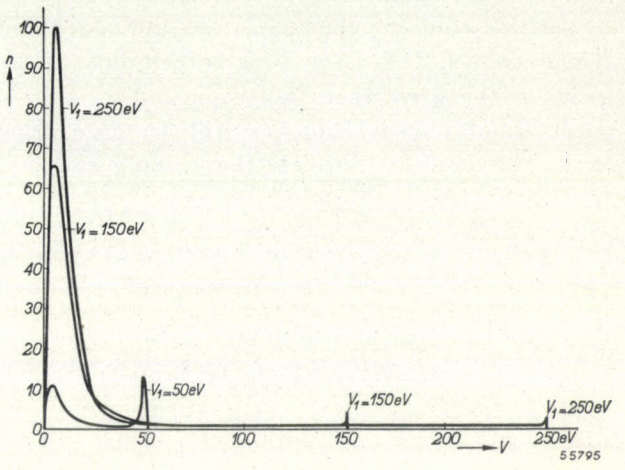
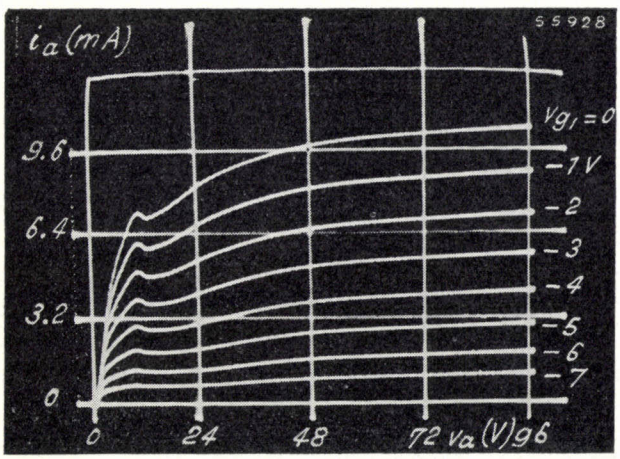


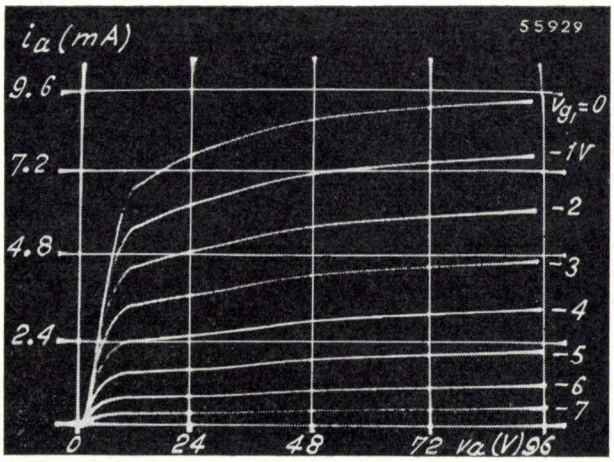
Fig. 7. As in fig. 6, but for the case where the nickel is coated with a porous layer of soot. The reflected electrons have lost much importance. To compare the ordinates with those of fig. 6 it is to be borne in mind that the area between a curve and the V-axis is a measure for the (effective) coefficient of secondary emission. For $V_1 = 250$ eV in fig. 6 $\delta = 1.2$ and in this figure $\delta_{\text{eff}} = 0.36$, from which it follows that the "real" secondary emission has likewise been reduced.

Output pentode for battery supply

The difficulties arising from secondary emission are felt most strongly in the case of valves which are supplied from an anode battery. The supply voltage is usually rather low (45 to 135 V) and, as we have seen from fig. 6, the fast reflected electrons are most



a



b

Fig. 8. Charcteristics $i_a = f(v_a)$ of two similar pentodes, (*a*) with bare anode, (*b*) with coated anode, at $V_{g2} = 90$ V and $V_{g3} = 0$. In (*a*) decided secondary emission occurs, whereas in (*b*) it does not. Attention is drawn to the very low value of v_a at which in the case (*b*) the bend occurs in the characteristics. The latter series of characteristics apply for the new output pentode (DL 41) designed for battery feed.

numerous when the voltage is low. Moreover, having regard to the useful life of the battery, a low mean anode current has to be used, so that the contributory help from the action of the space charge is for the greater part lost. It is therefore desirable, in particular for output valves fed from an anode battery, to reduce the number of secondary electrons and especially the reflected ones. This is best effected by coating the anode with porous soot or a similar material as referred to above.

The result is to be seen in *fig. 8*. In fig. 8*a* the characteristics $i_a = f(v_a)$ of a pentode with a normal nickel anode are shown [7]), and in fig. 8*b* we have the characteristics of a similar pentode provided with a prepared anode (type DL 41). Particularly at low anode voltages the latter characteristics have a very much more favourable shape. This is manifest in the maximum output that the DL 41 valve can yield with a given degree of distortion: with 10% distortion it is about 260 mW compared with 200 mW from a similar valve without anode coating [8]).

[7]) Recorded with a cathode-ray tube, cf. footnote [4]), but with an improved apparatus by means of which also a network of coordinates is plotted automatically.

[8]) Measured with a battery voltage of 120 V, $V_{g2} = 120$ V and a load resistance of 24000 Ω in the anode circuit.

ABSTRACTS OF RECENT SCIENTIFIC PUBLICATIONS OF THE N.V. PHILIPS' GLOEILAMPENFABRIEKEN

Reprints of these papers not marked with an asterisk can be obtained free of charge upon application to the Administration of the Research Laboratory, Kastanjelaan, Eindhoven, Netherlands.

R 78: W. J. Oosterkamp: The heat dissipation in the anode of an X-ray tube, II. Loads of short duration applied to rotating anodes (Philips Res. Rep. **3**, 161-173, 1948, No. 3).

The maximum temperatures occurring in the target of an X-ray tube, or in the copper backing behind it, are computed on the same principles as adopted in the first part of the paper (see these abstracts, No. **R 71**), but this time for a rotating anode. It is shown that for the short exposures the lateral dissipation of heat may be disregarded. Exposures lasting less than one revolution and those lasting several revolutions are dealt with separately. From the resulting formulae the rating capacity is computed as a function of the time of exposure and is found to agree closely with life-tests.

R 79: Balth. van der Pol: Mathematics and radio problems (Philips Res. Rep. **3**, 174-190, 1948, No. 3). The contents of this paper are the same as that of No. **1759.**

R 80: A. van Weel: Developments in radio-receiver circuits for the ultra-short-wave range (Philips Res. Rep. **3**, 191-212, 1948, No. 3).

Push-pull converter stages are described in which the antenna signal is used in push-pull whereas the local-oscillator voltage is supplied in parallel. The input circuit of the mixing valve is tuned to both frequencies at the same time. Special measures to prevent the local-oscillator voltage from penetrating into the antenna are described. Diode and triode mixing stages are dealt with in detail. It proves to be possible to design self-oscillating triode converter stages, as a consequence of which a separate local-oscillator valve is made superfluous and the noise that might be induced by this valve is eliminated. (Partly dealt with in Philips Techn. Rev. **8**, 193-198, 1946.)

R 81: C. J. Bouwkamp: On the theory of coupled antennae (Philips Res. Rep. **3**, 213-226, 1948, No. 3).

The purpose of this paper is to provide formulae for the self and mutual impedances of an antenna system consisting of two identical, centre-fed, parallel, cylindrical wires. Tables of auxiliary functions are given, facilitating numerical investigation in the range $1 < 2\pi l/\lambda < 2$, $0 < d/l < 2$, $\Omega = 2\ln(2l/a) > 10$, where $2d$ is the length of each antenna, d their mutual distance, $2a$ the wire diameter, and λ the wavelength.

R 82: W. W. Boelens: Valve characteristic giving linear modulation when a feedback resistor is inserted in the cathode lead (Philips Res. Rep. **3**, 227-234, 1948, No. 3).

It is well known that a high-frequency voltage can be modulated with a low-frequency signal by applying both voltages to the control-grid of a radio valve. If the I_a-V_g characteristic is quadratic there will be no distortion in the modulation. The

available valves, however, generally have a characteristic that is not quadratic. A feed-back resistance in the cathode lead was found to improve the linearity of the modulation; there was an optimum value for this resistance.

The theoretical question was put as to what valve characteristic would give linear modulation with a given feed-back resistance. This problem is solved in the present article and a simple answer is found. Two graphs are drawn for the characteristics with the feed-back resistance as a parameter.

R 83: J. M. Stevels: Some investigations in the system Na_2O-PbO-TiO_2-SiO_2 (Philips Res. Rep. 3, 235-238, 1948, No. 3).

A number of diagrams are given showing the vitreous and the crystalline regions in the systems Na_2O-SiO_2-Pb_2TiO_4, Na_2O-SiO_2-$PbTiO_3$ and Na_2O-SiO_2-$PbTi_2O_5$.

R 84: F. L. H. M. Stumpers: Noise in a pulse-frequency-modulation system (Philips Res. Rep. 3, 241-254, 1948, No. 4).

The optimum filter for pulse-frequency-modulation is derived for any given pulse form and large signal-to-noise ratio. For some special pulse forms she signal-to-noise ratio is calculated and it is shown that normal frequency modulation gives a better result. A method is given for the calculation of the noise spectrum, which is valid for all signal-to-noise ratios, though the intricacy of the formula restricts the possibilities for application. The noise threshold is estimated and the suppression of the modulation by noise is calculated.

R 85: A. van der Ziel and A. Versnel: The noise factor of grounded-grid valves (Philips Res. Rep. 3, 255-270, 1948, No. 4).

Measurements are given of the noise factor of grounded-grid valves at 7.25 m wavelength. In such valves part of the output noise currents also flows through the input circuit, thus giving rise to a partial noise suppression.

A general theoretical treatment of the problem is given, dealing with the influence of circuit losses, dielectric losses, transit-time effects, field inhomogeneities, and of an independent noise current in the output circuit which is not present in the input circuit. This theory is applied to grounded-grid triodes and to grounded-grid pentodes and secondary-emission valves. The experimental results for grounded-grid triodes agree qualitatively with theory. The experiments prove that a loose antenna coupling is favourable for a low noise factor, but that complete suppression of noise is impossible.

R 86: J. D. Fast: The equilibrium between liquid silica and liquid iron (Philips Res. Rep. 3, 271-280, 1948, No. 4).

The equilibrium between liquid SiO_2 and liquid Fe is computed with the aid of experimental data from the literature and thermodynamic considerations. The possible sources of error are discussed.

R 87: J. L. Meijering: Retrograde solubility curves, especially in alloy solid solutions (Philips Res. Rep. 3, 281-302, 1948, No. 4).

Using Gibbs's entropy of mixing and Richards's rule for the entropy of fusion of metals, a graph is derived thermodynamically, which serves to predict whether a solidus (curve representing the concentrations of mixed crystals in coexistence with liquid) is retrograde, i.e. shows a maximum with respect to the temperature axis. The result for the metals is checked with experimental data and is extended to other retrograde phenomena (solidus curves in systems of non-metals, retrograde allotropic transformations and retrograde solubility in liquids).

R 88: W. J. Oosterkamp: The heat dissipation in the anode of an X-ray tube, III. Continuous loads (Philips Res. Rep. 3, 303-317, 1948, No. 4).

In this paper (cf. **R 78** and **R 71**) the effect of continuous loads is considered in the case of both a stationary and a rotating anode.

VOL. 10 No. 12, pp. 353-388 JUNE 1949

Philips Technical Review

DEALING WITH TECHNICAL PROBLEMS
RELATING TO THE PRODUCTS, PROCESSES AND INVESTIGATIONS OF
THE PHILIPS INDUSTRIES

EDITED BY THE RESEARCH LABORATORY OF N.V. PHILIPS' GLOEILAMPENFABRIEKEN, EINDHOVEN, NETHERLANDS

A 48-CHANNEL CARRIER TELEPHONE SYSTEM

II. MECHANICAL CONSTRUCTION

621.395.44

by G. H. BAST *), D, GOEDHART and J. F. SCHOUTEN.

For the expansion of the Netherlands inter-district telephone network that is now in hand the 48-channel carrier system developed by Philips in cooperation with the Dutch P.T.T. is being applied on a large scale. This system works with triple modulation. The form in which the system is being employed differs considerably from the usual construction. All the equipment belonging to one individual channel which is identical for all channels, is contained in one drawer; the respective components comprise 80% of the equipment for the whole system, excluding carrier feed and repeaters. Thus the installation contains 48 identical channel drawers. The rest of the apparatus is contained in two sets of four (smaller) group-repeater, drawers one group-combining drawer and one system-repeater drawer. The panels slide into racks and are connected to the rack wiring with the aid of socket blocks and four-pin plugs. In the case of a breakdown in one channel the defective drawer is removed and replaced by a spare one. This method of working and mechanical construction offers great advantages and has been made possible by drastic reduction in the volume (by a factor of 4 to 5) of all components compared with former installations; this is due for a large part to the application of the new magnetic material "Ferroxcube" for the cores of the filter coils. The result of the saving in space allows of the whole of the equipment (including signalling) for the 48-channel system being mounted on the front and back of only two racks.

In many countries the long-distance telephone networks are being considerably expanded, partly in order to catch up with the arrears in the normal expansion and partly also with a view to shortening the delay on long-distance calls, thus making better use of the advantages of full-automatic working.

In the Netherlands, too, the number of connections in the inter-district network is being considerably increased, inter alia by employing on a large scale the 48-channel carrier-telephone system developed by Philips in cooperation with the P.T.T.

As its name implies, with this system 48 calls modulated on carriers can be transmitted over one pair of conductors simultaneously. Of each call the audio-frequencies between 200 and 3400 c/s are transmitted in a channel having a width of 4 kc/s. The 48 channels together cover the frequency band from 12 to 204 kc/s. Thus full use is made of the frequency range for which the Dutch carrier telephone cables are suitable, provided steps are taken according to the most recent ideas to prevent cross-talk between the pairs of conductors.

With this system a triple modulation system is used, the frequency allocations of which are indicated in *fig. 1*. For a detailed description of the method of modulation we refer to an article previously published in this journal [1]). We shall only recapitulate here the main points. Each conversation to be transmitted is brought into a basic channel of 60-64 kc/s by means of a pre-modulator. The undesired modulation products, in particular the lower side-band, are suppressed by a channel band filter, which is identical for all the 48 basic channels. In the next stage each twelve of these basic channels are modulated with

*) Of the Netherlands P.T.T.

1) G. H. Bast, D. Goedhart and J. F. Schouten, A 48-channel carrier telephone system, I, Choice of the method of modulation, Philips Techn. Rev. 9, 161-170, 1947 (No. 6).

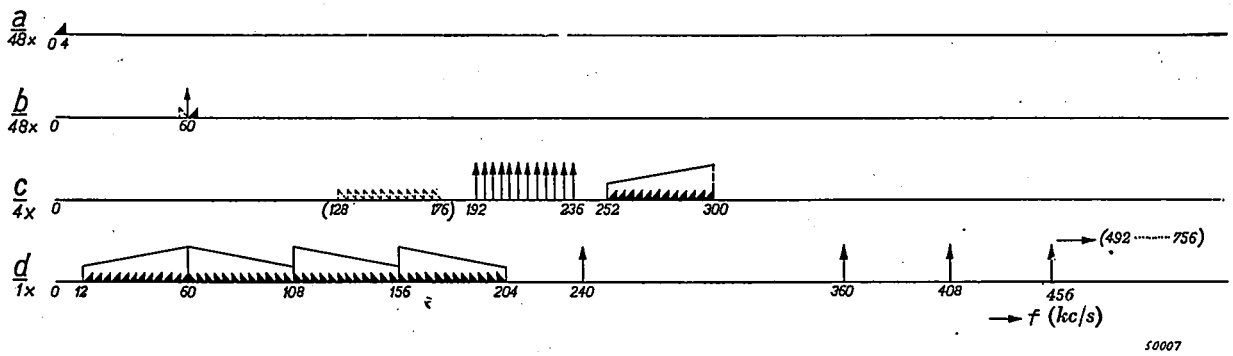


Fig. 1. Frequency allocation of the method of modulation of the 48-channel system. *a*) Low-frequency channel in the frequency range 0-4 kc/s. The ascending line indicates the rise of the audio-frequencies. *b*) Pre-modulation with 60 kc/s carrier. From each low-frequency channel a basic channel is formed lying in the frequency range 60-64 kc/s. The undesired lower side-band suppressed by the channel band filter is denoted by dotted lines. *c*) Second modulation with the 12 different carriers 192, 196, ... 236 kc/s for twelve basic channels. The result is a basic group in the frequency band 252-300 kc/s. *d*) Third modulation with the four carriers 240, 360, 408 and 456 kc/s for four basic groups. Thus the 48 channels are brought into their final position in the 12-204 kc/s band.

12 different carriers and combined into one basic group in the band 252-300 kc/s. Owing to the high frequency of the basic channel all undesired modulation products fall outside this band and can therefore be suppressed by a common group band filter. Finally, in the third modulation stage by means of four carriers the four basic groups are assembled to form a super-group lying in the band 12-204 kc/s. The undesired side-bands are here again suppressed by a common super-group filter, which owing to the wide separation of sidebands can be very simple.

The demodulation of the incoming calls takes place in three entirely analogous modulation stages.

The apparatus for the 48 channel-system is represented in *fig. 2* in a block diagram (for one direction only; an identical apparatus is required in the opposite direction of transmission).

In this article we shall go more fully into the construction of the apparatus for this 48-channel system. Both in its general set-up and in its detailed construction the form given to this system differs considerably from what has been usual so far in carrier-telephone installations.

The fact that the choice of the method of modulation and the mechanical construction of the apparatus have been dealt with in two separate articles does not mean that they are really two separate things. On the contrary, the choice of the method of modulation is governed in no small degree by the principles of the mechanical construction, as we hope will be made clear from what follows.

Principles underlying the mechanical construction

Without confining our ideas to any specific method of modulation we may say that for a multi-channel carrier system a number of modulators, filters, amplifiers, etc. will be needed for each channel. In large terminal stations there are frequently a number of cables in various directions which in all may comprise several hundreds or may be even some thousands of channels. In such stations there are consequently an enormous number of components. This fact largely governs the form to be given to any carrier system. The mounting of such a large number of elements in a not excessively large space, the localizing of a defective element in the case of a breakdown, the surveying of the whole when carrying out the necessary maintenance tests, the provision of the necessary spare components, all constitute problems of the first order which have to be taken into account. The matter is still further complicated by the consideration that the station can never be regarded as being a definitive installation: it must always be possible to extend the number of connections or to alter their distribution in different directions without too much difficulty.

In the designing of the 48-channel system the primary aim was to arrive at a more rational and more economical solution of the aforementioned fundamental problems. An essential condition was to reduce the dimensions of the components as compared with former constructions. A drastic reduction of the transducers, accompanied by an improvement of their frequency characteristics, was made possible by employing the new magnetic material "Ferroxcube" for the cores of the coils [2]). This material has therefore played an important part in the development of the new system.

[2]) G. L. Snoek, Non-metallic magnetic material for high frequencies, Philips Techn. Rev. 8, 353-360, 1946. See also the article quoted in footnote 1.

We shall now proceed to describe the general set-up of the apparatus for this system, with reference to an older type by way of comparison.

Distribution and mounting of the apparatus in racks

In many existing carrier systems the following method of construction is used. In the station there is a rack (possibly more than one) in which all the channel band filters and modulators are mounted, also racks with channel repeaters and racks with

For actual operation, however, such a construction has its disadvantages. It involves very extensive and complicated wiring, due to the fact that components of each channel are distributed among a number of racks. When carrying out the usual test measurements for the regular overhaul one has to check all these racks in succession for each channel. In the event of a breakdown in any one channel all the racks have to be checked to trace the defect, whilst to repair it all sorts of soldered

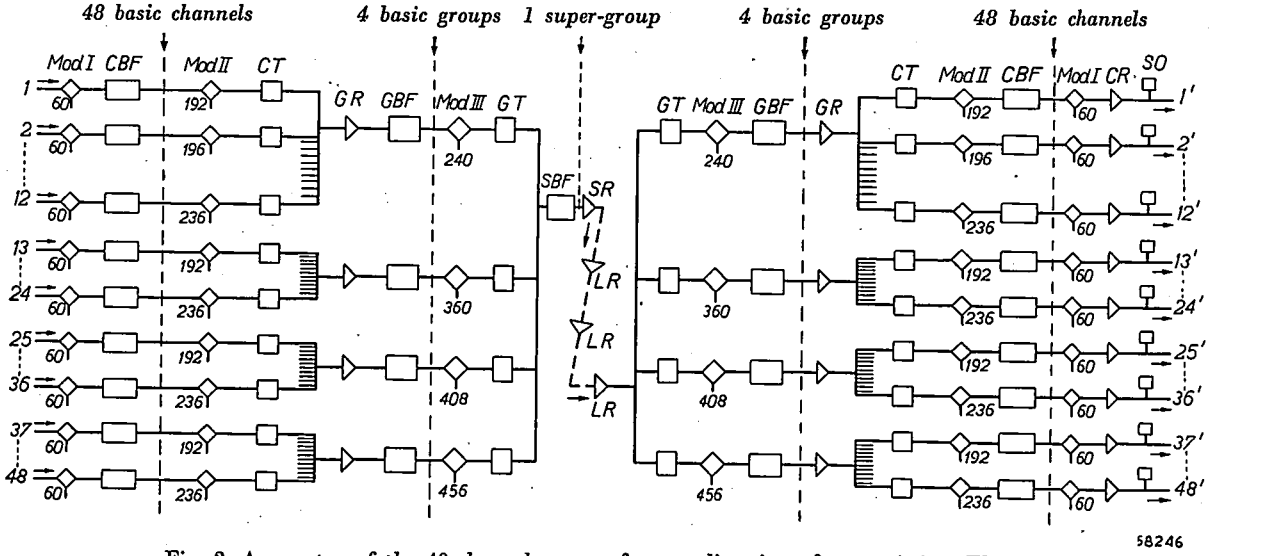


Fig. 2. Apparatus of the 48-channel system for one direction of transmission. The subscribers' lines at the transmitting end are numbered from *1* to *48* and those at the receiving end from *1'* to *48'*. *Mod I* is the pre-modulator, *CBF* a channel band filter, *Mod II* second modulator, *CT* channel transducer; *GR* group repeater, by means of which the audio signals of 12 bundled channels attenuated through modulation and filtering are again amplified sufficiently high above the noise level; *GBF* group band filter, *Mod III* third modulator, *GT* group transducer, *SBP* super-group band filter; *SR* system repeater raising all 48 channels to the level desired for transmission along the cable. *LR* line repeaters connected to the cable at distances of 25 km, the last repeater being in the terminal station itself.
At the receiving end in each channel there is a channel repeater *CR*, which compensates the attenuation by the last stages of the demodulation, and the signal receiver *SO*, which deals with the signals for dialling, etc.

signal receivers, etc. These elements are mounted on panels and a series of such panels are fixed onto a rack one above the other; see *fig. 3*. The leads of each apparatus are soldered to terminals grouped together on a block for each panel. On the other side of the terminal blocks are the soldered wire connections between the panels and between the racks.

This may in a certain sense be regarded as a surveyable or at least a systematic construction, and it was considered an advantage that the transducers and modulators, which as regards their properties are the most sensitive to temperature changes, are kept apart from the elements containing sources of heat (repeater valves, supply transformers).

connections have to be loosened and then resoldered. The complicated wiring, and in particular the numerous soldered connections, make it difficult to expand or alter the systems in a station. The large number of soldered connections was also awkward for the manufacturers: the desire to minimize the amount of soldering work to be done in the station itself meant that the factory had to deliver a rack complete with all its apparatus already mounted, and considering the heavy weight of the completely mounted racks this involved many difficulties.

Let us compare with this the fundamentals of the construction of the new 48-channel system. Two racks of this system are illustrated in *fig. 4*. Owing to the method of modulation by far the greater part of the apparatus is identical for all channels. All

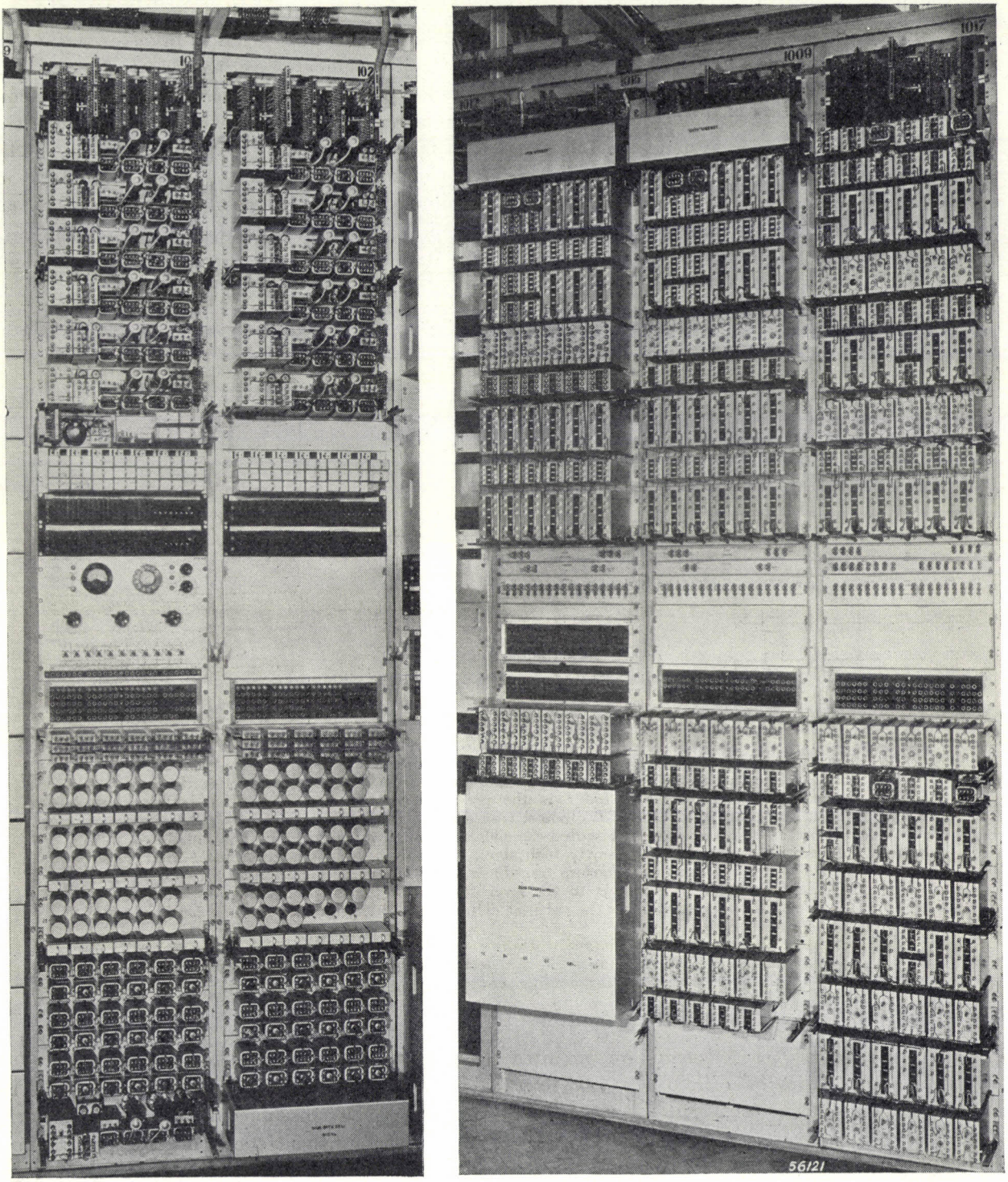


Fig. 3. Part of a carrier telephone equipment (Philips 17-channel system) built in a manner that has been customary in the past. On the right, racks with filters and modulators (the covers of most of the panels have been removed); on the left racks with signal receivers (at the top) and relays and transformers (at the bottom).

components that are identical are assembled for each channel and housed in a drawer, both those for transmission and those for reception. Thus in the 48-channel system we have 48 absolutely identical channel drawers containing the major part (about 80%) of the equipment: in each drawer there are mounted, among others, a pre-modulator, a channel band filter and a second modulator for the transmission path, together with the same elements for the reception path and, moreover, a channel repeater (including attenuation equalizer) and a signal receiver. The racks are built in the form of open

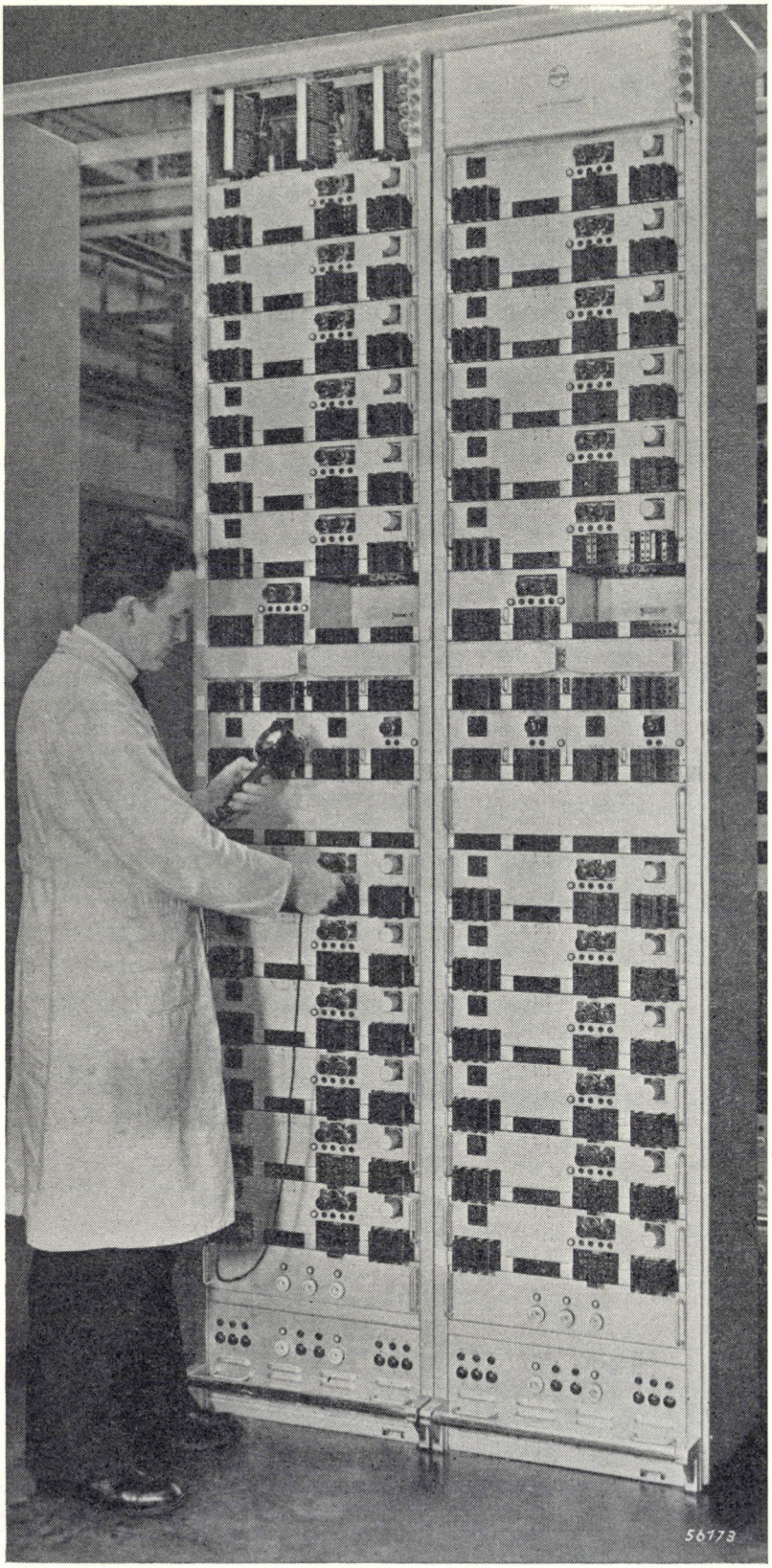


Fig. 4

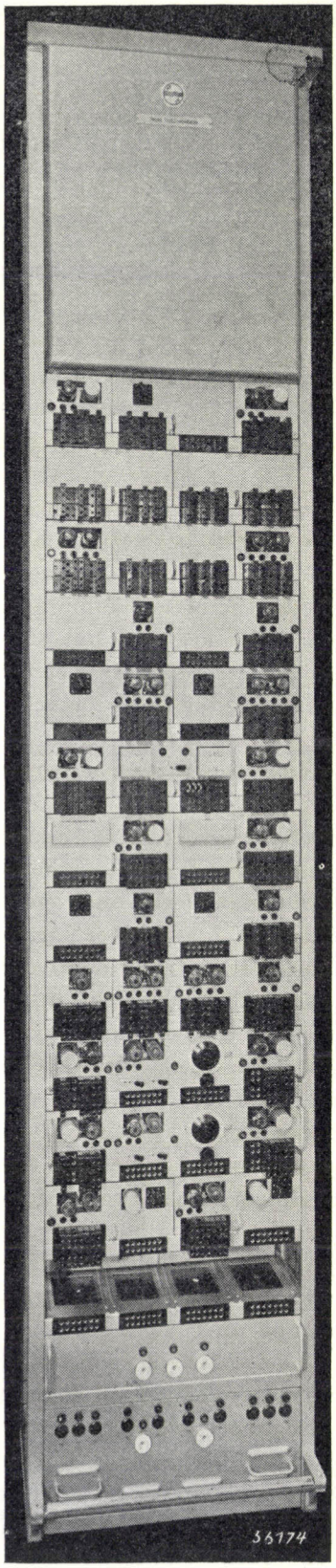


Fig. 5

Fig. 4. Racks of the 48-channel system. The apparatus is contained in sliding drawers. All components belonging to one channel which are identical for all channels, are mounted in one drawer. Thus the system has 48 identical channel drawers containing 80% of the whole equipment. Further there are eight group-amplifying drawers, a group-combining drawer, a system-repeater drawer, spare drawers and drawers with sundry accessories. The complete apparatus of a 48-channel system (excluding the carrier supply) is contained on the front and back of the two "system racks" shown here.

Fig. 5. Carrier supply rack of the 48-channel system. With the apparatus on the front and back of this rack 6 × 48 channels can be supplied.

cabinets with shelves between which the drawers can be pushed in from the front and back. Socket blocks form the terminals for the wiring of the drawer and come to lie in line with corresponding blocks on the rack shelves, to which blocks the rack wiring is connected. The drawer is connected up by a set of four-pin plugs. On one side of the rack there is room for 12 channel drawers. Further there is room for two drawers containing the apparatus, separated for transmission and reception, for filtering out and amplifying a basic group; for a drawer making up one super-group from four basic groups; and further for other various drawers.

The manner in which the apparatus is combined simplifies the wiring of the racks. For the overhauling of a channel all measuring points are found to lie close together. In the case of a breakdown of a channel there is no need first to trace the defect in the corresponding drawer (a signal lamp shows which drawer is out of order) but one simply removes the whole drawer, after taking out the connecting plugs, and replaces it by a spare. Since all the channel drawers are identical, in principle only one spare drawer has to be kept in reserve for the whole system of 48 channels and there is no risk of a mistake being made in the replacement. The defective drawer can then be taken to a workshop for examination and repair. A similar procedure is followed also for other parts of the apparatus, for instance the mutually identical group-repeater drawers, so that ideal conditions for the organisation of telephone services are very well approximated: in the stations themselves there is nothing else to be done than to replace components, repairs being carried out by specially trained workmen in a workshop which can serve several stations.

Such a method of construction as described here obviously has its advantages also for the manufacturer. All the channel drawers being identical, they can be built in large series. Racks and drawers are built up complete in the factory and can be transported to the repeater station in separate units. Of course the cables between the racks have to be connected in the station itself after the empty racks have been set up in position, and once this has been done there is no need for any further soldering. Then the drawers only need to be placed in the racks and connected up with plugs, the installation then being ready for the final check-over before being put into operation. One might compare it to the erection of pre-fabricated houses and ships [3]).

Presently we shall go into the construction of the drawers and their parts in more detail, but before doing so we have something to say about the importance of the reduction in size of all the components. It was only because all the equipment for an individual channel could be made sufficiently small, and of light weight to be handled easily by one man, that the principle of sliding channel drawers became a practicable proposition. Moreover, this was in itself of course highly important with a view to limiting the dimensions of the station as a whole: the complete apparatus of this 48-channel system is now contained in no more than two racks, as compared with 8 or 10 in former equivalent systems.

The principle of building racks of telephone installations in the form of sets of drawers and mounting the apparatus in sliding drawers with socket blocks was already applied by the Dutch P.T.T. about 1936 for the line repeaters of the low-frequency telephone networks. These repeaters formed natural units of not too large a volume. It was then applied mainly because of the advantages offered for easy expansion: starting for instance with 40 repeaters per rack, the installations could be expanded as required up to a maximum of 100 repeaters per rack simply by adding more repeater drawers.

In addition to the apparatus of the system proper, the installation of the station comprises a carrier supply apparatus and the line repeaters with attenuation equalizers for the incoming carrier cables. These parts are mounted on separate racks, the carrier supply for six 48-channel systems occupying only one rack. In *fig. 5* a photograph is reproduced of a carrier supply rack, details of which we shall not go into in this article.

We shall conclude this general review by drawing attention to the fact than on each side of the rack there is a complete basic group of 12 channels, which can be dealt with as an independent group. This means that it is possible to start with a 12-channel system, for instance when there is not much traffic along a cable, and to extend it as the traffic increases by adding further groups to build up a 24-, 36- or 48-channel system (provided of course that the cable itself and the line repeaters are calculated to take that number). It is also possible, for instance, to split up an existing 48-channel system into two equal halves of two groups each

[3]) The first installation according to the system described (with 24 instead of 48 channels) was supplied by Philips in October 1947 for the station at Chur in Switzerland, where the number of connections had to be extended at short notice for the 1948 Olympic Winter Games. This was a striking example of how delivery can be expedited owing to the easier transportation (in this particular case all the drawers were transported by plane) and the fact that the racks in the station can already be connected up before the drawers arrive.

(24 channels) and to conduct the calls from the two halves to two different cables. Thus, compared with former systems, this installation is much more flexible.

Details of equipment

In fig. 2 a block diagram has been given of the major components of the apparatus for the 48-channel system. In *fig. 6* it is now shown in more detail how the equipment is distributed in drawers. With the aid of this diagram we can explain some details of this distribution.

As already stated, in each channel drawer there is, among others, the pre-modulator, the channel band filter and the second modulator, for the transmission and receiving paths; see the part *I* framed in fig. 6. The second modulator is, it is true, fed with a different carrier frequency for each of the 12 channels of a group, but these frequencies come from the rack wiring, there being no difference in the modulators themselves. Thus the drawers are identical, only the position of the drawer in the rack determining which of the 12 bands between 252 and 300 kc/s will appear at the output of the drawer.

The channel transducers (*CT*) on the other hand do indeed differ for the 12 channels. Therefore, in order to keep the channel drawers identical, these filters are not mounted in the channel drawer, each of the twelve pairs of different filters being fitted in the corresponding shelf of the rack. This does not involve any great complication in the manufacture, since the coupling filters are extremely simple (see the article referred to in footnote [1])).

A repeater and group band filter constitute the main components of each group-repeater drawer. These drawers, for transmitting and receiving ends, are likewise framed in fig. 6 (parts *IIa* and *IIb* respectively).

Then there are the four group modulators with group transducers (*GT*) contained in a group-combining drawer (the framed part *III* in fig. 6) for the transmitting and receiving ends together. Each basic group can be connected to each of the four modulators, so that if desired, by adding a second group-combining drawer — in the normal 48-channel system there is only one —, the system can be split up for instance into two 24-channel systems in the same frequency range, e.g. in the

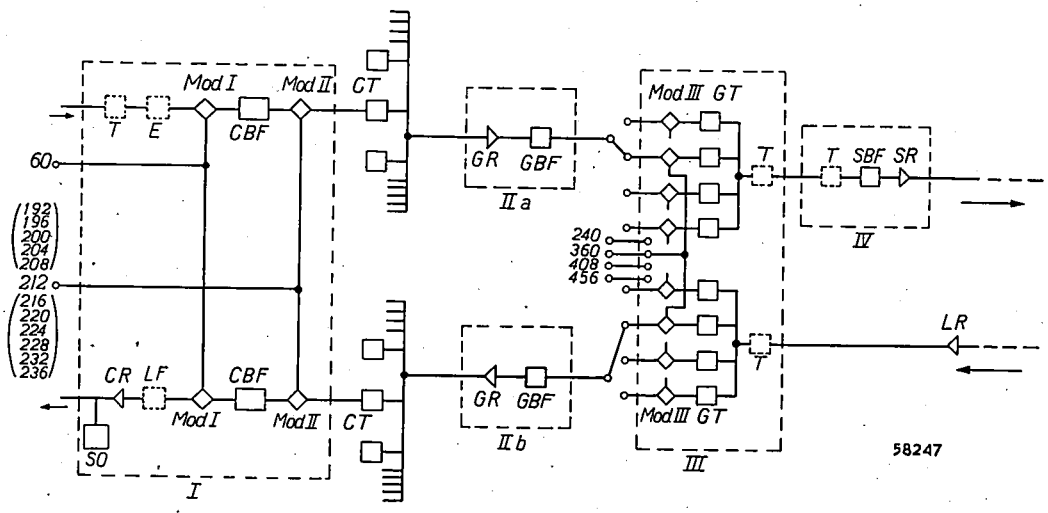


Fig. 6. The combining of the equipment of the 48-channel system in drawers. There are 48 identical drawers *I*, each containing practically the whole of the equipment of an individual channel both for transmitting and for receiving. This has been made possible owing to the apparatus being identical for all channels, due to the method of modulation chosen. Only the channel transducers *CT* differ for the 12 channels of the group and they are therefore not contained in the channel drawers *I* but in the rack shelves on which the drawers are placed. Further, there are four identical group-repeater drawers *IIa* for transmitting and four similar drawers *IIb* for receiving, one group-combining drawer *III* and one system-repeater drawer *IV*. The meaning of the letters is as given under fig. 2. Some less essential elements which were left out in fig. 2 are indicated here in dotted lines: *E* equalizer, *T* transformers for matching or separation, *LF* low-pass filter for suppressing what is left of any carrier leaking through from the adjacent channel (which would be audible as a whistling note of 4000 c/s).

In some installations it may not be desired to consider the signal receiver acting as the last element on the reception side as belonging to the carrier-apparatus. This applies to stations where signal receivers are already installed for all outgoing telephone lines. For such cases as this a somewhat different type of channel drawer is made without signal receiver; an example of this is the Swiss installation mentioned in footnote 3.

frequency band 12-108 kc/s. On the side of the rack where there is no group-combining drawer another drawer can be inserted containing measuring apparatus or suchlike. Finally, in the 48-channel system there is one drawer containing the super-group filter and the system repeater (the part *IV* framed in fig. 6). The super-group filter is not a band filter but can be a simple low-pass filter, as may be readily understood from an examination of the modulation system in fig. 1.

Right at the bottom of each rack is the alarm apparatus and the power supply, i.e. the filament transformers; the anode voltages are supplied by the storage batteries installed in every terminal station. At the top of the rack are the terminal blocks for connecting up the inter-rack cables. The wiring of the rack itself is contained in the side walls of the rack and in the shelves between the drawers. The wiring in the open sides of the outermost racks in a row is screened off by covering plates.

All the terminal connections on the socket blocks fitted on the shelves for the channel drawers are in duplicate, so that test measurements can be taken or an aged valve can be replaced without interrupting a conversation taking place along a channel in the corresponding drawer; this is done by connecting the spare channel drawer to the corresponding shelf by means of patching cords, so that this can take over temporarily the function of the operating channel drawer. In order to facilitate this connection with patching cords to all channels the spare drawer is placed in the middle of the rack. For normal service measurements on drawers the connecting plugs are used as measuring points.

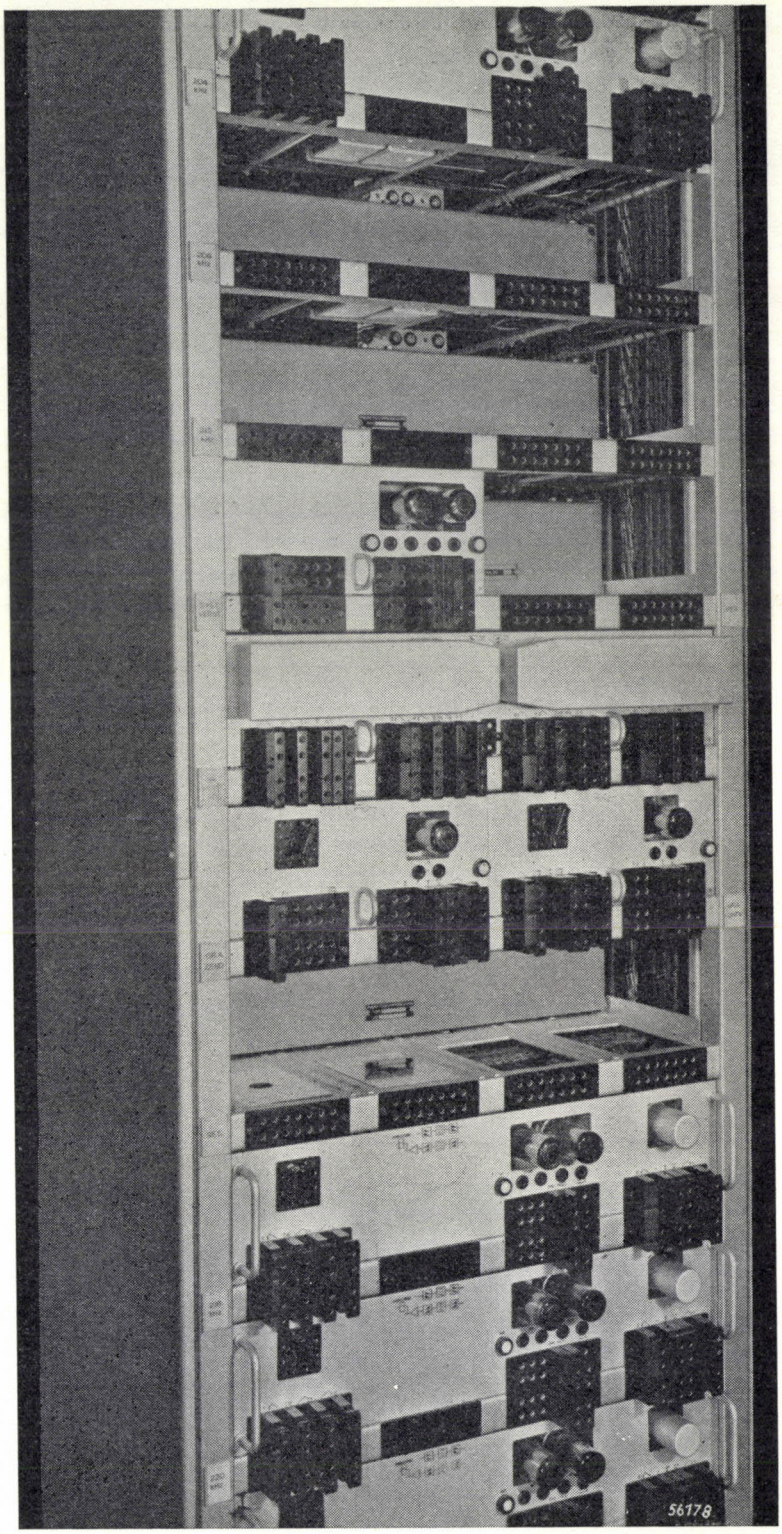


Fig. 7. Close-up of a system rack of the 48-channel system. The compartment for the spare channel drawer (in the middle) and a half compartment for a spare system-repeater drawer have been left open; higher up two channel drawers have been taken out to show the wiring in the shelves and in the side walls of this rack. In the shelves may also be seen the small cans containing the channel transducers. The connection between the rack wiring and the drawers is made by means of sets of four-pin plugs fitting into the socket blocks.

Fig. 7 shows how the channel drawer with a spare drawer, two group-repeater drawers, a group-combining drawer and the system-repeater drawer are arranged on one side of the rack. This photograph also shows some of the details mentioned above, such as the placing of the channel transducers, the wiring, etc.

Construction of drawers and components

This distribution of the components in drawers allows not only of a splitting up of the equipment into natural units but also of standardization of the dimensions of the drawers. In the racks there are only two types of drawers, whole and half ones; in the carrier-feeding rack, which we are not dealing with here, there are also quarter drawers. This standardization is of importance for the manufacture of the installation and obviously allows of the space available in the rack being fully utilized.

Of course also the space inside each drawer has to be utilized to the best advantage. To this end the dimensions of the cans in which most parts, such as filters, transformers, etc., are contained are likewise standardized. Except those contained in the band filters all cans are of the same height and width, though there are four different depths. Thanks to this uniformity of height the wiring inside the drawer can be kept entirely in one plane, making it easily surveyable and facilitating not only the wiring up in the factory but also repairs where necessary. The photograph of a channel drawer in *fig. 8* clearly shows this "two-dimensional" wiring and the compact arrangement of the components in the drawer.

The cans are not filled up with a compound, as they used to be, but are sealed by soldering. This results in a great saving in weight, so essential for sliding out the drawers, whilst there is still sufficient protection against the influence of moisture on the insulating material and dielectrics in the components. Each can has two pins underneath fitting into holes in the bottom of the drawer and secured with nuts. The drawers are put in the racks upside down so that no dust can settle in them. The repeater valves, of which there are for instance two in each channel drawer — one for the channel repeater and one for the signal receiver —, protrude at the front of the drawer; this facilitates replacement and, moreover, contributes towards an adequate heat transfer. This also avoided the previously mentioned point about inadvisability of the modulators being mounted on one rack together with the heat-spreading valves. Nevertheless the filters

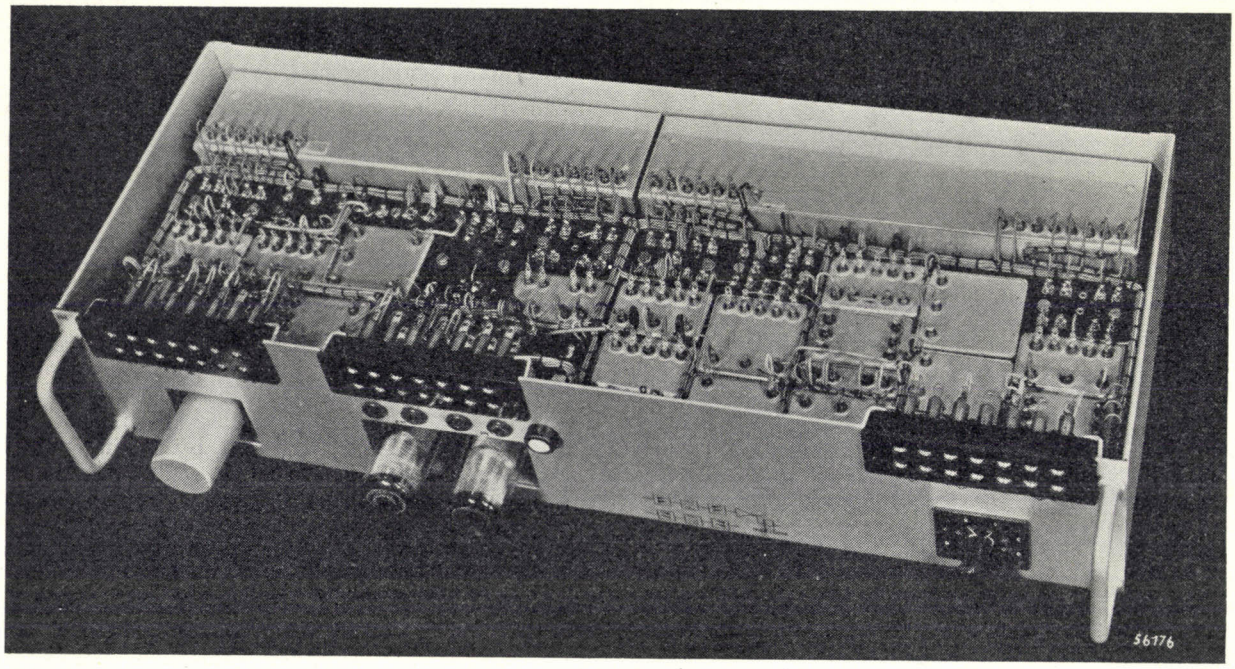


Fig. 8. Channel drawer ready to be put into the rack. The channel band filters for the transmitting and receiving ends are contained in two long cans, which are slightly higher than the others and occupy the rearmost part of the drawer. All other components (e.g. modulators, transformers, equalizers, condensers, etc). are contained in cans all of the same height and width and with standardized depths. In this way all the space available in the drawer is filled up compactly and the wiring is kept flat. The repeater valves (one for the channel repeater and one for the signal receiver) protrude, so that they can easily be replaced and do not cause undesired heating of the components in the drawer. In the middle of the front plate of the drawer is a signal lamp which lights up in the event of a defect arising in the drawer. By means of a control knob on the right-hand side of the front panel (on the left if the drawer is placed in the rack upside down) the gain of the channel repeater can be adjusted to the right value while the drawer is being tested.

and modulators are placed as far away as possible from the valves by mounting them right in the back of the channel drawer; this precaution has proved to be quite satisfactory, the influence of the conduction of heat to the filters being imperceptible.

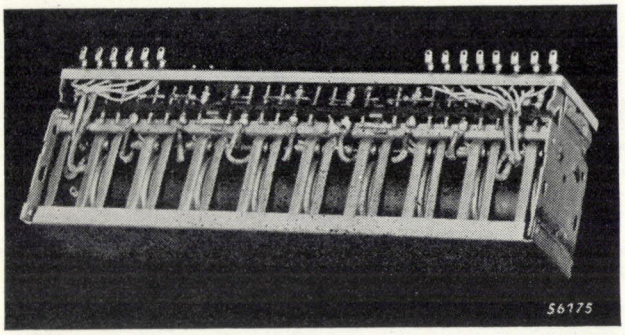


Fig. 9. Channel band filter, opened. The coils (at the bottom) and the condensers (at the top) are arranged in the same order as is usually followed when drawing the circuit diagram of such a filter (see fig. 9 of the article quoted in footnote [1]). Owing to the high permeability of the "Ferroxcube" cores, the coils can be placed side by side without screening.

The internal construction of the channel band filter is shown in *fig. 9*.

The very considerable reduction in the size of the parts, to which reference has been made several times already, is illustrated in *fig. 10*. There we see a channel band filter compared with the corresponding filter of an older system (the Philips 17-channel system [4])). This reduction in size, made possible by employing "Ferroxcube", will be realized when one considers that the channel filters in earlier systems often represented about half of the channel equipment. But also the other parts have been drastically reduced in volume. In the case of the modulators this has been achieved by an artifice. Each modulator contains four small selenium rectifiers, an input transformer and an output transformer. Since however, as shown in fig. 6, there is a filter adjoining one side of each modulator, the transformer on that side could be dispensed with by making an extra winding on the core of the first (or last) filter coil and letting the coil itself function as the other winding of the transformer.

The reduction reached in the size of the cans, compared with the former normal dimensions, would have been incomplete if it had not proved possible at the same time to reduce the seals of the cans considerably. Fig. 10 shows the comparatively long ceramic seals of the old cans, which have now been replaced by a construction with a glass bead tinned round the circumference and soldered into an opening in the top of the can. The sealing beads of all the cans in a drawer come to lie in one continuous rectangular pattern, thereby giving the flat wiring the aspect of compactness as seen in fig. 8.

Finally it is to be mentioned that only one type of repeater valve is used in the installation. This valve, a pentode (type 18040), has been specially designed for the desired universal application. Moreover, being built according to the C-technique (all-glass envelope with flat base), it is of much smaller dimensions than the valves formerly employed in telephone installations; see fig. 10. Thus here again the principles of reduction and standardization have been applied, such as characterize the construction of the whole of the 48-channel system.

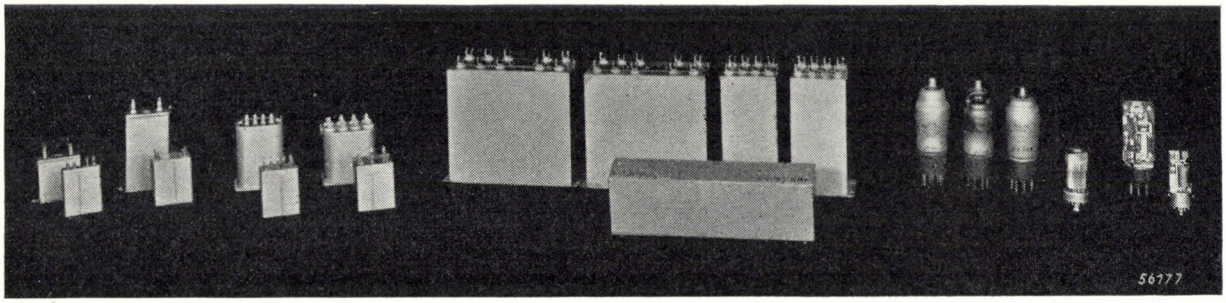
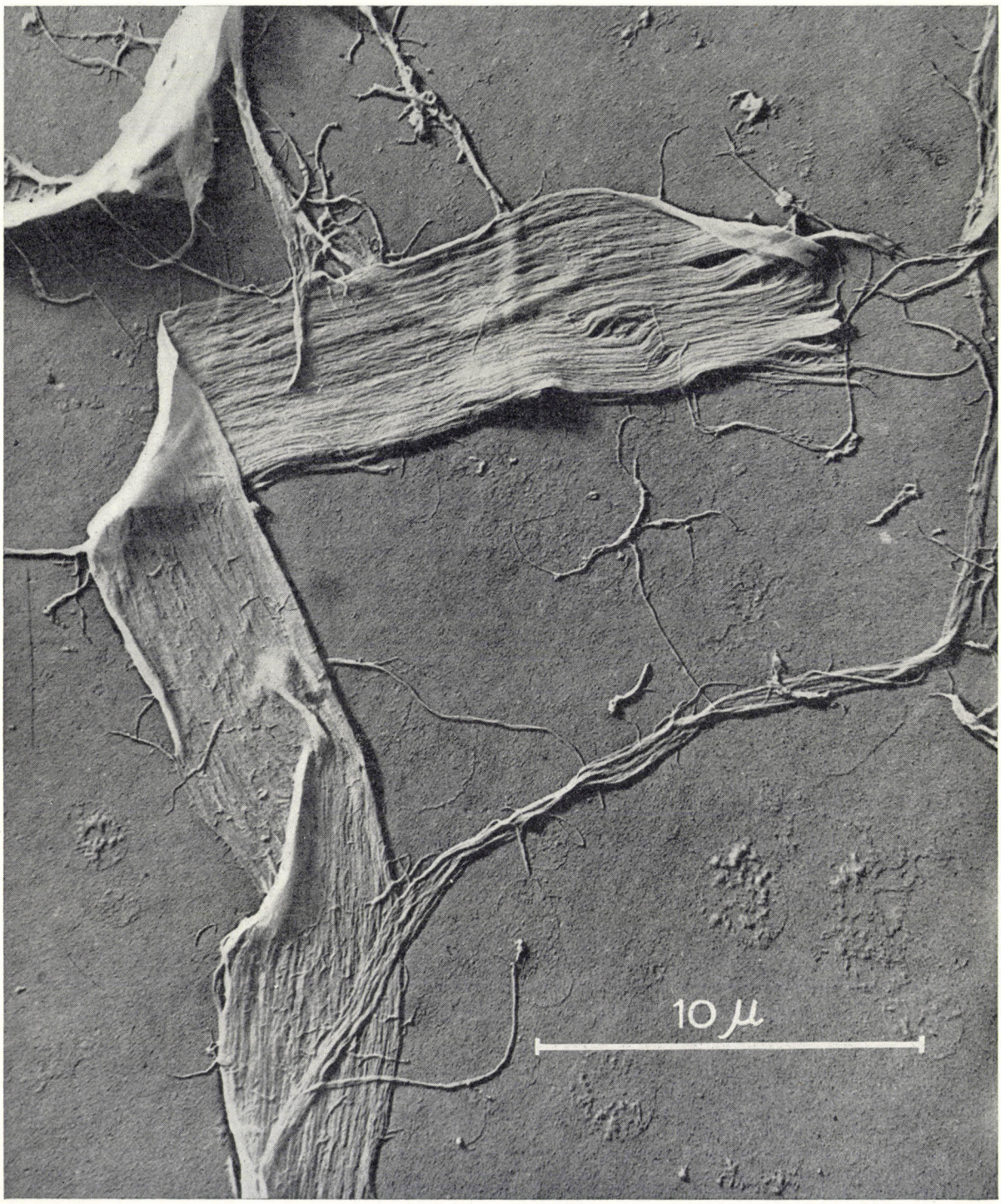


Fig. 10. Comparison of components of the 17-channel system (placed at the back) with those of the new 48-channel system (in the front). From left to right: two condensers, two transformers, a channel band filter (in the old system consisting of four boxes), the repeater valves and a relay. The reduction of the dimensions in the new system and the standardization of the parts are clearly seen: the two condensers and transformers are now in cans of the same width and height; only in the depth are there four different dimensions. Whereas formerly three types of valves were used, viz. types 18013, 18014 and 18015, now there is only one type, 18040.

[4]) See Th. J. Weijers, Filters for carrier-wave telephony installations, Philips Techn. Rev. 7. 104-112, 1942.

CELLULOSE FIBRE

PHOTOGRAPH TAKEN WITH THE PHILIPS ELECTRON MICROSCOPE EM 100



This is a fibre of a special kind of paper used, inter alia, as dielectric for high-tension capacitors. The photograph clearly shows that the fibre (which happens to be narrower than normal specimens) is in itself of a fibrous structure with fibrils about 80 mμ in width.

The magnification is comparatively small (6000 times) but the resolving power is remarkably high. The large field of vision at such small magnifications is a characteristic feature of the EM 100.

Before being placed in the microscope the specimen was "shadowed" in a well-known manner to bring it out clearly in relief: it was exposed in vacuum to a directed beam of vaporized gold. The electrons are strongly scattered by atoms of gold, so that the picture shows less blackening of the parts where gold has been precipitated, whereas the parts of the specimen lying in the "shadow" when the beam of gold was directed upon it, received no gold and thus show up in the picture as real deep black shadows.

PROJECTION-TELEVISION RECEIVER

V. THE SYNCHRONISATION

by J. HAANTJES and F. KERKHOF.

621.397.62:621.397.335

The video signal sent out by a television transmitter contains both picture and synchronisation signals, of which latter there are two kinds, one for the horizontal and one for the vertical scanning. In previous articles it has been shown how in a receiver the synchronisation signals are separated from the picture signal and how the two kinds of synchronising signals are separated one from the other by means of two *R-C* circuits. As regards the vertical synchronisation this method is not accurate because the moment at which the voltage on the corresponding capacitor passes a threshold value is not sharply defined, and this may lead to a troublesome "pairing" of the lines forming the television picture. Here a circuit is described which is free of this evil. In this system a resistor is again used in series with a capacitor, but it is from the resistor that the voltage is taken. At a certain point in the vertical synchronising signal this voltage shows a peak with a steep front. This peak synchronises the saw-tooth generator for the vertical deflection. — The number of valves can be minimized by using two heptode-triode valves (ECH 21), the triode system of which forms part of the saw-tooth generator for the horizontal and vertical deflections respectively. The method described is suitable for all present-day television standards.

The series of articles on the Philips projection television receiver is now concluded with a description of the manner in which the synchronisation of the horizontal and vertical deflections is achieved in this set.

In the previous article [1]) mention was made of the two blocking oscillators each supplying a saw-tooth voltage for controlling an output stage. The output stages produce saw-tooth currents which flow through the deflection coils and thus periodically deflect the electron beam in the cathode-ray tube in the horizontal and in the vertical direction. This deflection must of course be accurately in phase with the movement of the electron beam scanning the picture in the transmitter. To ensure synchronism, in addition to the picture signal synchronising signals are transmitted which, by means of certain circuits which will be described later, introduce a current pulse just at the right moment in the triode of each of the saw-tooth oscillators.

All the characteristic data of a television transmitter — the form of modulation (positive or negative, see below), the form of the synchronising signals, the manner of scanning (interlaced or not), the number of lines per picture, the number of pictures per second and other data of a similar nature — are collectively referred to as the television standard. So far there is very little international uniformity in regard to television standards; most closely approximating each other are the British and French standards, which differ only in the number of lines per picture and in a few details of the synchronising signals. We shall deal here briefly with two of the points mentioned, the form of the modulation and the synchronising signals.

Positive and negative modulation; the two kinds of synchronising signals

In Great Britain and France "positive (amplitude-) modulation" is used, that is to say the greatest brightness in the picture to be transmitted corresponds to the maximum carrier-wave amplitude (100%) whilst zero brightness corresponds to a given lower amplitude (black level) lying for instance at 30%. The synchronising signals consist of a variation of the carrier amplitude between this black level and zero according to rectangular pulses [2]).

In the U.S.A. on the other hand "negative (amplitude-) modulation" is usually employed, the maximum picture brightness corresponding to the zero carrier amplitude and the black level lying at, for instance, 75% of the maximum amplitude, whilst the synchronising signals are formed by block-shaped pulses between the black level and 100%. The experimental transmitter at Eindhoven

[1]) Projection-television receiver, IV. The circuits for deflecting the electron beam, by J. Haantjes and F. Kerkhof, Philips Techn. Rev. **10**, 307-317, 1949 (No. 10). This article will further be referred to here as article IV.

[2]) See, for instance, the article on television receivers, Philips Techn. Rev. **4**, 342-350, 1939.

(Netherlands) likewise works with negative modulation.

It is not the place here to weigh up the advantages and disadvantages of the two systems, but it is to be remarked that for the synchronisation system to be described here it makes no difference whether positive or negative modulation is employed.

There are two kinds of synchronising signals to be distinguished, those for the synchronisation of the lines (horizontal deflection of the electron beam in the cathode-ray tube) and those for the synchronisation of the frames (vertical deflection).

Line synchronisation takes place after the tracing of each line; the moment at which a line has to begin is determined by the carrier amplitude being made zero (in the case of positive modulation) or 100% (in the case of negative modulation) for a certain time interval once per line; see *fig. 1a*. Apart from certain details, this applies for all television standards.

The signals for the vertical synchronisation differ rather more, but there is international uniformity in so far that after each frame during an interval of at least 10 T no picture signals are transmitted (thus at least 10 lines per frame or at least 20 lines per complete picture are lost), during which interval the video signal alternates in a rectangular manner in an alternating rhythm, partly at twice the line frequency and partly at the line frequency itself. By way of example, figs 1*b* and *c* give the form of the signal for vertical synchronisation according to the British and French standards [4]).

Separation of the signals

In *fig. 2* the block diagram of the synchronisation and deflection apparatus (the deflection apparatus was discussed in article IV) is given once again.

[4]) Fig. 1 of the article quoted in footnote [2]) represents the form of the synchronising signals that were used at the time (1939) by the B.B.C.; they differ somewhat from the present form.

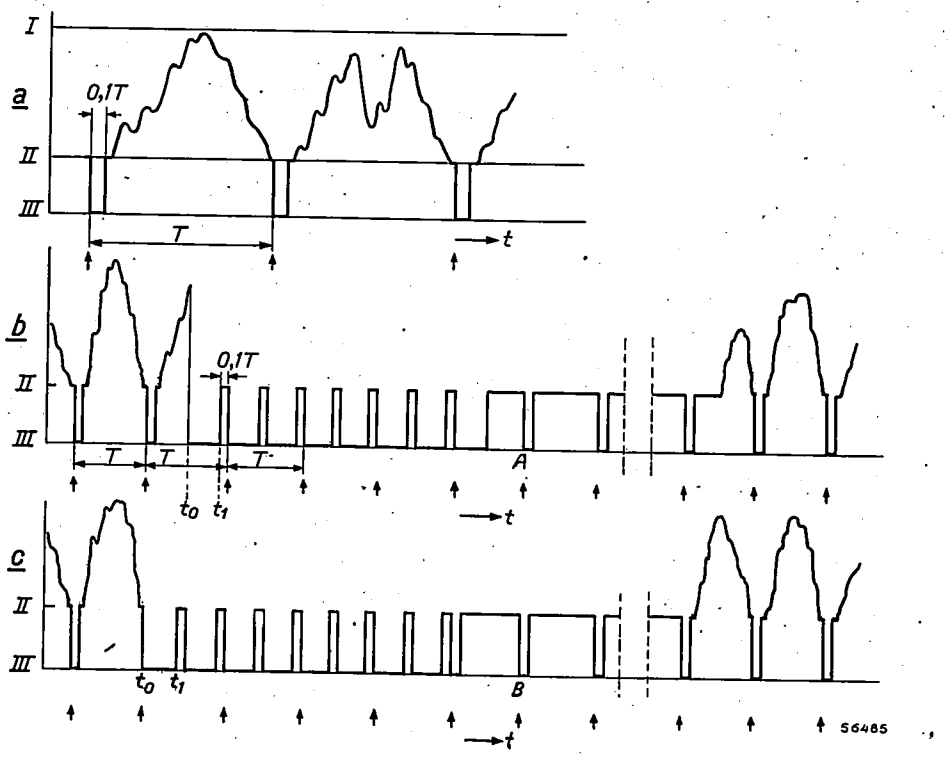


Fig. 1. Form of the video signal. *a*) The picture signal of a few lines with the line-synchronising pulses in between. *I* = level of greatest brightness, *II* = black level, *III* = level of the peaks of the synchronising signals. With positive modulation *I* corresponds to a modulation depth 100%, *II* corresponds to 30% and *III* to 0; with negative modulation *I* corresponds to 0, *II* to 75%, *III* to 100%. T = line period. — On another scale of the time t the signals for the vertical synchronisation to the British and French standards are represented under *b*) and *c*), this being what precedes an even and an odd frame respectively [3]), t_1 indicating the instant at which the vertical synchronisation takes place with the new system. The vertical arrows indicate the instants of horizontal synchronisation (line-synchronisation).

[3]) Here the words even and odd can be interchanged.

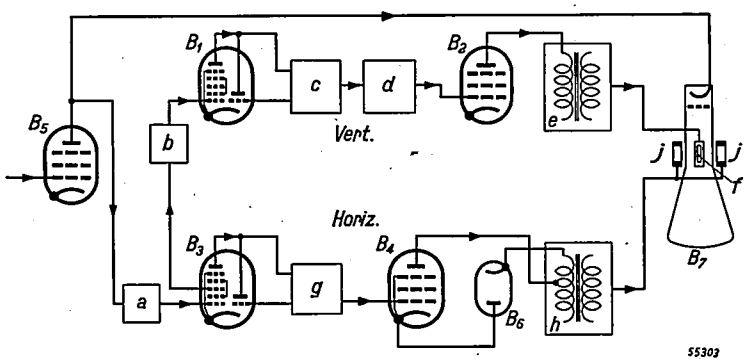


Fig. 2. Block diagram of the synchronisation and deflection apparatus. B_5 = output pentode of the video receiver, B_7 = cathode-ray tube with deflection coils f and j. For the horizontal deflection there is a driver stage (triode of B_3 and network g) and an output stage (pentode B_4, efficiency diode B_6 and transformer h), and for the vertical deflection likewise a driver stage (triode of B_1 and network c) and an output stage (compensating network d, pentode B_2 and transformer e). a is a source of negative grid bias, b is a network for separating the synchronising signals.

In this diagram the output valve (B_5) of the video receiver has been included. With our circuit the control grid of this valve receives a signal of the form represented in fig. 1. (To bring this about either for positive or for negative modulation the stages preceding B_5 have to be arranged differently for these two methods of modulation.)

The output signal from B_5, the polarity of which is opposed to that of the input signal (fig. 1), directly controls the cathode-ray tube and thus causes variation in brightness on the screen in accordance with the picture being transmitted.

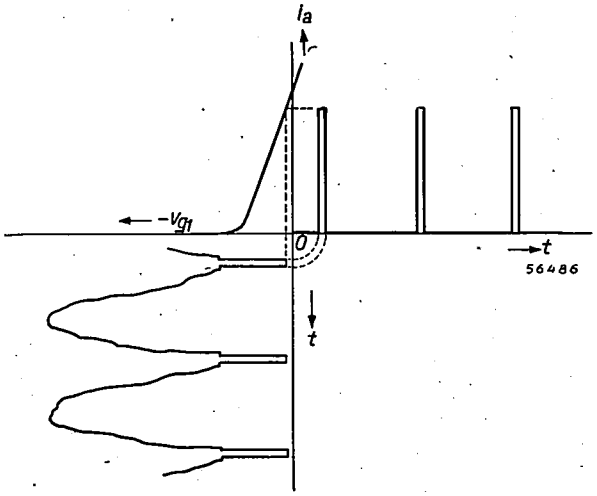


Fig. 3. The video signal is applied to the biased control grid of an amplifying valve in such a way that only part of the amplitude of the synchronising signals initiates anode current (i_a); the other part falls in the cut-off region. v_{g1} = control-grid voltage.

But at the same time this output signal from B_5 is applied to the control grid of an amplifying valve which has a bias so chosen that the black level is clipped off. With the given polarity of the video signal supplied by B_5 the picture signal makes the grid still more negative (*fig. 3*). In this manner the picture signal is suppressed. The synchronising signals on the other hand form pulses which cause anode current surges.

This is how the synchronising signals are separated from the video signal. However, they still consist of a mixture of synchronising signals for the two directions of deflection and they have to be separated so that each one of them can act upon the oscillator for which it is destined.

The last-mentioned separation has most commonly been brought about [5]) by feeding the combined synchronising signal (i.e. the output voltage of the valve in which the picture signal is clipped off) to two series-circuits consisting of a resistor and a capacitor R'-C' and R''-C'' (*fig. 4*). With a suitable choice of the time constants $R'C'$ and $R''C''$ ($R'C'$ smaller than the width of the line-synchronising pulses, thus $R'C'$ less than 0.1 T, and $R''C'' \approx T$) voltages of the form sketched in *figs 5b* and *c* appear across the resistor R' and the capacitor C''. This is what takes place with the synchronising signals according to the British and French standards (fig. 5*a*). The fact that the polarity is as indicated in fig. 5*a* follows from fig. 3.

The voltage across R' has peaks of periodicity T (and during a signal for vertical synchronisation peaks of periodicity $^1/_2\,T$) which are well suited for line synchronisation. We are still applying this method, as will be seen farther on.

Owing to the choice of $R''C''$ the voltage v_C'' across C'' (fig. 5*c*) shows only insignificant variations in the line-synchronisation pulses, but with the wider pulses of the vertical synchronisation this voltage can vary to a larger extent. When it passes a certain threshold value it is able to initiate in a valve an anode current which causes the light spot to travel up the screen from bottom to top.

However, the moment at which v_C'' passes the threshold value is not sharply defined, for two reasons. In the first place the value of v_C'' at which the vertical-synchronising signal begins to operate (fig. 5) is not always the same, this initial value being the remainder of the voltage which the preceding line-synchronising pulses have produced in C'', whilst the value of this remainder depends upon

[5]) Cf. the article quoted in footnote [2]), figs 9 and 10.

the time that has elapsed between the last line-synchronising pulse and t_0. This period of time, in the case of interlaced scanning, is alternately equal to $^1/_2\,T$ and to T (cf. figs 1*b* and *c*). In the first

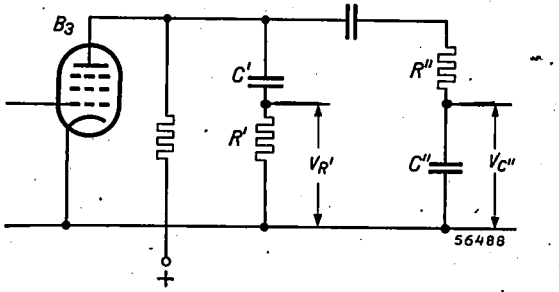


Fig. 4. B_3 = amplifying valve to which the video signal is applied (cf. fig. 3). The two kinds of synchronising signals present in the output voltage are separated by the networks C'-R' and C''-R'' with different time constants: $C'R' < 0.1\ T$, $C''R'' \approx T$. The horizontal synchronisation is brought about by the voltage $v_{R'}$ across R'; the vertical synchronisation, according to the old method, is brought about by the voltage $v_{C''}$ across C''.

case $v_{C''}$ has a certain start and thus the synchronisation is brought about slightly earlier than the synchronisation of the previous or the following frame. The result is that the lines of the even frames do not come to lie exactly half-way between those of the odd frames but have a tendency to "pair" (*fig. 6*). Obviously this detracts from the fineness of the raster.

This cause of pairing can be eliminated by having a series of so-called equalizing pulses preceding each vertical-synchronising signal, so that the varying duration of the interval mentioned above no longer has any effect. American transmitters employ such equalizing pulses. However, there are other causes of "pairing" which are not eliminated by this means, as we shall presently see.

The second cause of the vertical synchronisation not being sharply defined lies in the fact that the threshold value that $v_{C''}$ has to exceed shows fluctuations which cannot be entirely avoided. In particular, when the threshold voltage has a ripple

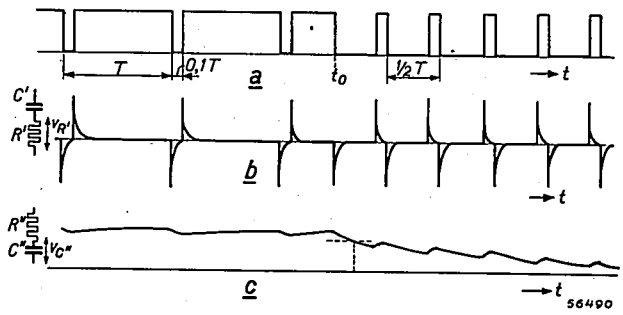


Fig. 5. Voltages in the circuit according to fig. 4. *a*) Output voltage of the valve B_3 (some line-synchronising pulses followed by a signal for vertical synchronisation); *b*) the voltage $v_{R'}$; *c*) the voltage $v_{C''}$.

of the line frequency — and such a ripple may easily arise, for instance via the common supply — this also leads to undesirable pairing of the lines.

Both causes are in fact to be traced to one origin: the gradual rise of the voltage $v_{C''}$. If it were possible to derive from the signal for the vertical synchronisation a pulse with a steep front, such as is shown for instance by the line synchronising pulses illustrated in fig. 5*b*, then there would

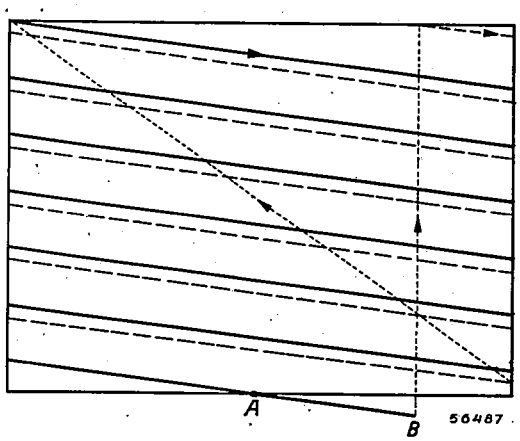


Fig. 6. Pairing of the lines of a television picture arises owing to the flyback not taking place at A but for instance somewhat later, at B. Odd lines are fully drawn, even lines are broken (see footnote [3])), flyback (from bottom to top) dotted lines; flyback times are assumed to be infinitely short.

be none of these troubles. The manner in which the vertical synchronisation can be brought about by means of a steep front will appear from what follows.

Vertical synchronisation with steep front

The method of vertical synchronisation that we are now applying is based upon the following.

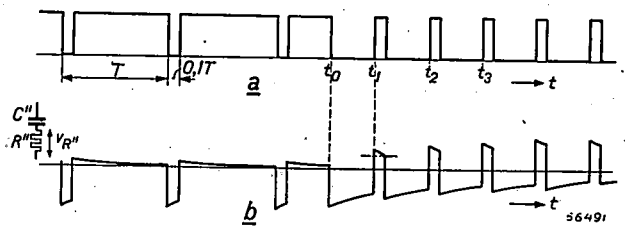


Fig. 7. *a*) The same synchronising signals as in fig. 5*a* applied to a circuit C''-R'' with $C''R'' \approx T$. Instead of the voltage across C'', for the vertical synchronisation use is made of the voltage $v_{R''}$ across R'' illustrated under *b*. The vertical synchronisation is brought about by a positive pulse with steep front at $t = t_1$.

The synchronising signals (*fig. 7a*) are again conducted to an R-C circuit with a time constant $\approx T$. Instead of taking the voltage across the capacitor we now take that across the resistor, as is done for the horizontal synchronisation. This voltage

has the form represented in fig. 7*b*. As will be seen, at $t = t_1$ there is a pulse with a steep front. The instant t_1 follows t_0 (at which the signal for the vertical synchronisation begins) after a fixed interval $0.4\,T$, which is governed by the transmitter. The pulse at t_1 is therefore excellently suited for vertical synchronisation. Further details are described below, where we shall at the same time have an opportunity to go into some details of the horizontal synchronisation.

Practical execution

The circuit is represented in *fig. 8*. For the suppression of the picture signal, in the manner depicted in fig. 3, use is made of the heptode part of the heptode-triode B_3 (fig. 2). The synchronising signals thereby occur on the two electrodes serving as output of the heptode, viz. the anode and third grid. The lines are synchronised via the anode and the frames via the third grid.

result, each line-synchronising pulse develops a voltage peak in the positive sense on the grid of the triode and thus initiates current through this valve just at the right instant. This keeps the line-frequency oscillator in the right phase. (Actually there is no resistor R_7, but there is an equivalent resistor R_7' across the other coil of the transformer, which resistor also performs the function of damping the oscillator circuit formed by the transformer with its self-capacitance.)

The signal for the vertical synchronisation brings about a series of peaks with an interval of only $\frac{1}{2}\,T$ on the triode grid. The "interposed" pulses however are ineffective, because the voltage across the capacitor C_3' (fig. 8) is then of such a high value as to keep the valve cut off in spite of the peak in the positive direction.

As already stated, the third grid of the heptode system of B_3 (fig. 8) acts as second output electrode. It is particularly suitable for this function because it is screened from the anode by the fourth grid,

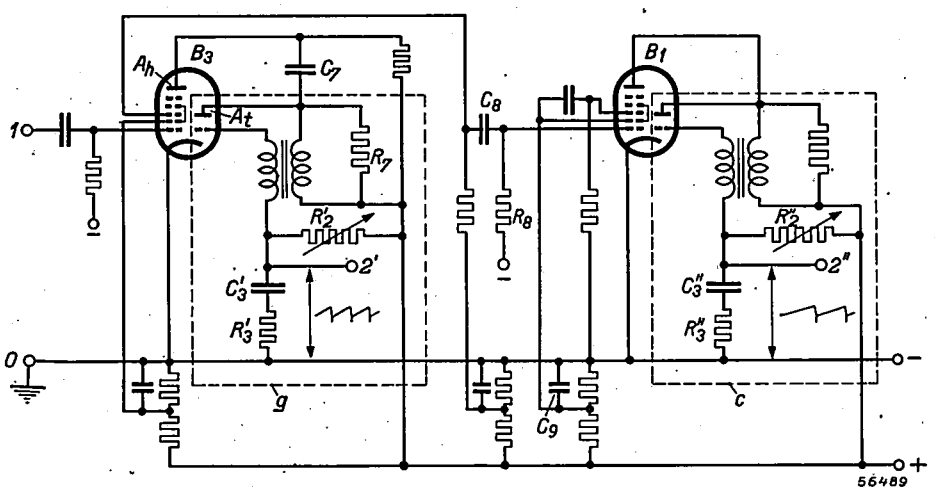


Fig. 8. Complete synchronisation circuit (including the driver stages). *0-1* = input for the video signal, B_3 and B_1 = heptode-triodes ECH 21, g = blocking oscillator for the horizontal deflection (output terminal *2'*), c = ditto for the vertical deflection (output terminal *2''*). R_7 = damping resistor. The circuit C_7-R_7 corresponds to C'-R' (fig. 5*b*), the circuit C_8-R_8 corresponding to C''-R'' (fig. 7*b*). C_9 = smoothing capacitor of small value.

Let us first consider the line-synchronisation, which needs little explanation. The anode A_h of the heptode is connected to a network C_7-R_7 which corresponds to C'-R' of fig. 4 and carries the voltage pulses from A_h to the anode A_t of the triode. Thus the voltages at A_h and at A_t follow the form indicated in figs. 5*a* and 5*b* respectively. The triode forms part of the saw-tooth oscillator for the line frequency.

The transformer bringing about the coupling between the grid circuit and the anode circuit of the triode is connected in such a way that a voltage drop at A_t causes a voltage rise at the grid. As a

which is made in the form of a screen grid, and thus is affected very little by the high voltage peaks (with the line frequency) occurring at the anode. It is, however, essential that the mean voltage on the third grid should be fairly low, such with a view to the proper distribution of the cathode current between the various grids and the anode; the third grid is therefore connected to a tapping on the supply source, as may be seen in fig. 8.

In series with the third grid is a resistor across which voltage pulses occur having the form of the synchronising signals. A coupling element C_8-R_8 transmits these pulses to the control grid of the

heptode system of the valve B_1. This coupling element is the aforementioned R-C circuit which transforms the synchronisation signals (fig. 7*a*) into the form represented in fig. 7*b*. The sign of the voltage across R_8 and the value of the bias on the control grid are such that only positive peaks of the pulses occur in the grid base. Only at these peaks — in fact, as will appear presently, only at the first of these peaks — can anode current flow through the heptode (B_1). The anode of this heptode is coupled to the anode of the triode system contained in the same valve and generating the saw-tooth voltage of the frame-frequency. The coupling

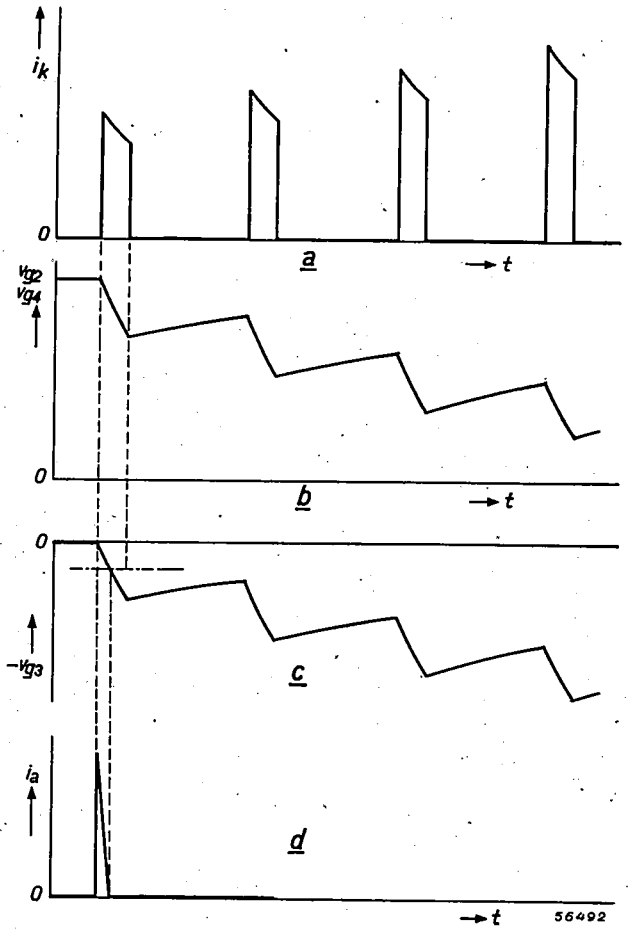


Fig. 9. The wave-form as function of t, during a vertical synchronising signal, of
a) the cathode current i_k in the heptode system of B_1 (fig. 8),
b) the voltage $v_{g2} = v_{g4}$ on the two screen grids,
c) the voltage v_{g3} on the third grid,
d) the anode current i_a.
After the first pulse in v_{g3} anode current surges no longer occur until the next signal for vertical synchronisation comes through.

may consist of a connection between the two anodes. The voltage on this coupling shows a polarity which is the reverse of that in fig. 7*b*., but the coupling transformer again ensures that the synchronising pulse reaching the grid of the triode has a positive sign.

Thanks to the steep front of the pulses on R_8 there is no fear of any of the difficulties arising which occur in the case of a gradually rising grid voltage (fig. 5*c*).

In one respect, however, a small precaution has to be taken in this system. The triode grid of B_1 receives not only a positive pulse at the instant t_1 (fig. 7) but also a number of successive pulses at t_2, t_3, and so on, and furthermore, after the signal for the vertical synchronisation has stopped, line-synchronising pulses following one upon the other at an interval of time T (fig. 1*b* or 1*c*). These latter pulses on the triode grid of B_1 are undesirable.

At the instants that these line-synchronising pulses occur the grid current discharging the capacitor C_3'' and starting to flow at t_1 has dropped almost to zero; the instant at which this current becomes zero is subject somewhat to the effect of the pulses previously referred to. Now in itself this would be no objection if the pulses always had the same time interval with respect to t_1, but this is not the case, as may be seen from figs 1*b* and *c*. The line-synchronising pulse A lies $^1/_2\,T$ closer to t_1 than the corresponding pulse B. In other words, with the even frames the capacitor C_3'' would begin to charge itself again at a moment slightly different from that in the case of the odd frame. This would mean again a certain tendency towards pairing.

This risk is avoided by so arranging the circuit that the first current surge through the heptode (B_1) itself causes the anode circuit to be blocked for a time, so that further pulses do not occur. By the time that the next signal for vertical synchronisation comes through, the charge bringing about the negative grid bias has leaked away sufficiently to allow of the valve functioning again normally.

This blocking of the anode circuit takes place in the following way (see fig. 8). The two screen grids of the heptode (B_1) are fed via a common series resistor and are connected to the cathode via a smoothing capacitor (C_9) of small value. As soon as current begins to flow through the heptode the voltage on the screen grids drops. This voltage drop is transmitted via a coupling capacitor to the third grid, which was previously at zero potential but then becomes negative. With each successive cathode current surge (*fig. 9a*) the voltage on the three grids again drops (figs 9*b* and *c*). Already at the first voltage drop the voltage on the third grid falls below the cut-off limit and the anode current is kept at zero (fig. 9*d*). Thus only one anode current surge takes place, and that is the one that brings about the vertical synchronisation.

Concluding remarks

The synchronisation system described can be used for all present-day television standards and is

entirely free of pairing of the picture lines. It is employed in the Philips projection-television receiver but is of course equally suitable for "direct-vision" receivers.

The form of execution with two heptode-triode valves (type ECH 21) described here has the advantage of requiring the smallest number of valves, but it is not the only possiblility. For instance, with a few small alterations, the heptode systems could each be replaced by a pentode, and the two triode systems could be combined into one double triode.

A photograph of the receiver built on these lines was given in article IV (fig. 2).

ABSTRACTS OF RECENT SCIENTIFIC PUBLICATIONS OF THE N.V. PHILIPS' GLOEILAMPENFABRIEKEN

Reprints of these papers not marked with an asterisk can be obtained free of charge upon application to the Administration of the Research Laboratory, Kastanjelaan, Eindhoven, Netherlands.

1804: J. van der Vliet: Investigations on sterols, IV. The configuration of the junction between rings C and D in cholesterol. (Res. Trav. chim. Pays Bas **67**, 343-348, 1948, No. 6.)

The ketone $C_{18}H_{32}O$, obtained by the oxidation of vitamin-D_3 and which still contains the rings C and D of the original sterol, appears to be readily converted into an isomer and the same holds for its semicarbazone. This isomerisation is to be explained by the conversion of the trans-hydrindane into the cis-hydrindane configuration. From this it is concluded that the junction between the rings C and D in vitamin-D_3, 7-dehydrocholesterol and cholesterol very probably has the trans-configuration.

1805: A. H. W. Aten Jr. and J. v. Dreven: A simple apparatus for the measurement of diffusion rates (Trans. Faraday Soc. **44**, 202-204, 1948, No. 4.)

The method proposed by the writers consists in filling the pores of a porous disc with the solvent, after which the disc is immersed e.g. for two hours in a beaker containing the solution for measurement which is kept at a constant temperature.

After this the contents of the disc are sucked into a beaker and the liquid in the beaker is analysed.

1806: P. C. van der Willigen. Warm-scheuren in lasrupsen en blauwbrosheid (Lastechniek **14**, 95-102, 1948, No. 8). (Hot-cracking in welds and blue-brittleness; in Dutch).

The author discusses some aspects of hot-cracking in welds, the most important of which are:

1) Differences in sensitivity for hot-cracking are often accompanied by differences in blue-brittleness (measured by notch impact tests).
2) The blue-brittleness of the material deposited is to be ascribed to the joint action of impurities. the differences between various types of electrodes and especially to the N- and O-content.
3) A characteristic difference in the various types of welding electrodes is the H-content immediately after welding. This is presumably also a cause of the difference in sensitivity for hot-cracking.

1807: H. C. Hamaker: Toevals-frequenties, een hulpmiddel bij de constructie van kunstmatige steekproeven van grote omvang (Statistica **2**, 129-137, 1948, No. 4). (Random sampling frequencies, a short-cut technique for the artificial constructions of large-size random samples; in Dutch.)

In this article a short-cut technique is described to arrive at artificial random samples of, say, 500 or 1000 scores, making use of previous records of the frequencies of two-digit random sampling numbers.

1808*: H. J. Vink: Het geleidingsmechanisme van de oxydekathode (Thesis, Leiden 1948, 170 pp., 63 fig. 5 tables). (The conduction mechanism of the oxide cathode; in Dutch.)

The resistance of a normal BaSr oxide coating is studied as a function of the temperature and at various degrees of formation. The $\log R$-T^{-1} characteristic is proved to consist of different parts, each part corresponding to one of the different results mentioned in the literature on the subject. It is impossible to explain the results on the basis of modern theory of electronic and ionic conduction of solids alone. Therefore a new theory is given, taking into account the conduction through the electron gas present between the emitting grains

of the porous oxide coating. Starting from reasonable assumptions as to the electron emission of separate grains, it is proved to be theoretically possible to calculate a resistance of the same order of magnitude as that experimentally observed; at the same time certain peculiarities of the characteristics may be explained in this manner.

1809: P. W. Haayman en G. W. Oosterhout: Eigenschappen en toepassing van halfgeleiders als weerstandsmateriaal met grote negatieve. temperatuur-coëfficient (Electrotechniek **26**, 342-347, 1948, No. 21). (Properties and application of semi-conductors having a high negative temperature coefficient of the electrical resistance; in Dutch).

In this paper a survey is given of the properties of semi-conductors and of their most obvious applications in electric circuits, such as protection against high currents, compensation of a high positive temperature coefficient, resistance thermometer, bolometer, wattmeter, artificial horizon, voltage stabilizer and adjustable resistance without moving contact.

R 89: B. D. H. Tellegen: The synthesis of passive, resistanceless four-poles that may violate the reciprocity relation (Philips Res. Rep. **3**, 321-337, 1948, No. 5).

The most general, passive, resistanceless four-poles of a certain order that may violate the reciprocity relation are investigated. They can be realized by means of inductances, capacitances, ideal transformers and ideal "gyrators" (cf. **R 73**). Of every order there are two types of four-pole, which can be transformed one into the other by connecting an ideal gyrator to any of their terminal pairs. The necessary and sufficient conditions of realizability are derived.

R 90: W. Elenbaas: Dissipation of heat by free convection, Part I (Philips Res. Rep. **3**, 338-360, 1948, No. 5).

This article is identical to that published in "De Ingenieur" (see these abstracts, No. **1773**).

R 91: A. van Weel: A new principle for transceivers (Philips Res. Rep. **3**, 361-370, 1948, No. 5).

It is shown that the self-oscillating triode mixing stages described in a former article (see these abstracts, No. **R 80**) offer distinct advantages for transceiver circuits, the most important of which is the possibility of switching from transmitting to receiving, and vice versa, fully electrically without any mechanical switching in the antenna circuit. As a consequence, switching in an ultrasonic frequency can be used, making it possible to establish a two-way communication. A system is described for stabilizing the frequency of both the transmitting oscillator and the local oscillator for reception with the aid of one cavity resonator.

R 92: J. H. van Santen and G. H. Jonker: The temperature dependency of the index of refraction of heteropolar solids (Philips Res. Rep. **3**, 371-377, 1948, No. 5).

While the electronic polarizability of molecules does not vary much with temperature it is found that the electronic polarizability of heteropolar lattices shows a pronounced dependency on temperature. A tentative explanation is suggested based upon the assumption that the electronic polarizability of heteropolar lattices is mainly of an electron-transfer type.

R 93: J. F. Klinkhamer: Empirical determination of wave-filter transfer functions with specified properties, Part II (Philips Res. Rep. **3**, 378-400, 1948, No. 5).

Continuation of a previous article (see these abstracts, No. **R 72**, where the contents of the present paper are indicated).

Erratum

The code number of the article AN IMPROVED X-RAY DIFFRACTION CAMERA published in Philips Techn. Rev. Vol. 10, No. 6, 1948, p. 157, should read **548.73:621.386.1:778.332** instead of **548.73:621.386.1:788.332**

SUBJECT INDEX, VOLUMES 1—10

Volume		Year	Volume		Year
1	—	1936	6	—	1941
2	—	1937	7	—	1942
3	—	1938	8	—	1946
4	—	1939	9	—	1947/1948
5	—	1940	10	—	1948/1949

The number in heavy print beside each subject indicates the volume, and the following number the page.

Aberrations, optical 9,301
Acoustics of auditorium, see **Auditorium acoustics**
Adhesive force of lacquers . . . 8,147
Adsorption phenomena at metal contacts 5,238

Aerial:
- communal — ("Antennaphil") 1,246
- loop —, aerial effect 7, 65
- loop —, combination with normal 9, 55
- receiving — ("Philastatic") . 4,320
- rotating directional — for PCJ-transmitter 3, 59
- sensitivity to local interference 6,302

Aerodromes:
- illumination and beaconing . 4, 93
- illumination by mercury lamps 6, 33
- radio beacons 2,370

Aeroplane radio:
- position and course finder 2,184
- transmitter-receiver V.R. 18 1,114
- transmitter-receiver with course finder (photograph) . 2,182

After-effect phenomena 8, 57

Air engines:
- theory 8,129
- development 9. 97
- construction 9,125

Amplifiers
- D.C. amplification with magnetron 8,361
- inverse feed-back, see under that title
- noise, see under that title
- stabilized amplifiers . . . 9, 25; 9,309
- transient characteristic . . . 6,193
- use in telephony 2,209

Amplifier installations, see **Sound amplification**
Amplifier valves, see **Radio valves**

Analysis:
- mixtures of argon and nitrogen 5, 88
- polarography 4,231
- X-ray diffraction for — . . 1,158; 5,157

Antenna, see **Aerial**
Architecture and illumination 2, 8
Arc-welding, see **Welding**
Armatures, testing dynamo — . 4, 88

Artificial resin:
- X-ray diffraction diagrams . 2,256
- see also under "**Philite**"

Artificial respiration, apparatus 4,325
Audiometer 6,234

Auditorium acoustics:
- E.L.A.-studio 10,196
- intelligibility 3,139
- optical models:
  - principle, distribution of intensity 1, 46
  - directional distribution . 5,321
- reverberation:
  - theory 3, 65
  - measurement, principle . 8, 82
  - measurement, apparatus 9,371
- sound absorption 3,363
- theatre Utrecht 7, 9

Austempering of steel 6,279

Band-spread, see **Radio receiving sets**
Barretters 3, 74
Batteries, emergency supply systems with — 9,231

Beacons for aerodromes:
- light beacons 4, 93
- radio beacons 2,370

"Bi-Arlita" lamp (coiled coil) . . 1, 97

Bicycle dynamo:
- construction 3, 87
- investigation 6,215

Bicycle rear lights and reflectors 5,335

Biological effect of ultraviolet radiation:
- cure of rickets (vitamin D) 3, 33
- erythema and conjunctivitis 2, 20

"Biosol"-lamp 2, 18
Black-out illumination, see **Illumination**

Blended light:
- different kinds 5,341
- developments ML lamps . . 7, 34

Blocking of oscillators:
- investigated with oscillograph 3,251
- theory 7,171

Blocking-layer photocells 8, 65
Blocking-layer rectifiers, see **Rectifiers**

Brightness:
- in connection with blackout problems 6,161
- definition and significance . 1,142
- of mercury lamp and sun . 1, 62
- of night sky 5,296

Broadcasting:
- motor van for — 4, 73
- short wave station PCJ . 3, 17
- — studio equipment, see under that title
- — studio, investigation with optical model 5,321
- — transmitters, Netherlands . 6, 1

Bulbs (flower-)
- influence of X-rays 2,321
- forcing of tulips 10,282

Bullet finder 5,309

Cable testing, see **Power cables**
Cancer Institute, Amsterdam, X-ray installation 4,153
Candle, new 5, 1; 10,150
Carrier telegraphy 8,206
Carrier telephony, see **Telephony**
Cathanode 1,367

Cathode-ray oscillograph:
- construction:
  - GM 3150 1,147
  - GM 3152 4,198
  - GM 3156 (tool-making) 5,277
  - GM 3159 (with two push-pull amplifiers) 9,202
- applications
  - armatures, testing in mass production . . . 4, 88
  - "blocking" of oscillators 3,251
  - chemical analysis (polarography) 4,231
  - cooling of hardening oils 9,147
  - electronic switch as auxiliary 3,148; 4,267; 9,340
  - frequency measurement 3,341
  - frequency modulation . 3,248
  - fuses 4,118
  - gas discharge lamps, current and voltage . . . 3,148
  - hysteresis loop 3,341
  - I_a-V_a diagrams 3,339
  - mechanical stresses . . . 5, 26
  - mechanical vibrations . 5,230
  - modulation depth . . . 3,248
  - pitch of orchestras . . . 4,205
  - power mains 3, 50
  - resonance curves of receiving sets 4, 85
  - stresses on Diesel engine parts 6, 94
  - watches, measuring of rate 9,317
- see also under **Cathode-ray tubes**

Cathode-ray tubes:
- beam intensity control . . . 1, 91
- construction, improvements . 9,180
- electrode system, potential field (photograph) 4,229
- focussing of electron beam . 1, 33
- post-acceleration tube . . . 5,245
- scanning speed:
  - apparatus for measuring 3,216
  - calculation, measurement, practical conclusions 2,148
  - increase by post-acceleration 5,245
- secondary emission of screen 3,211
- television tube with magnetic deflection 4,342
- television tube for projection with lens system 2,249
- television tube for projection with mirror system . . . 10, 97

applications:
characteristics of output valves 5, 61
characteristics of transmitting valves 4, 56
phase angles, measurement 5,208
pressure indication . . 5,348 / 6, 22
recording with high speed scanning 2,148
applications in which an ordinary oscillograph apparatus is used, see under Cathode-ray oscillograph
Cavity resonators . . . . . 8,149 / 9, 73

Ceramics:
survey 10,205
titanium dioxide 10,231
Change-over to emergency apparatus in communication systems 8,310
Chrome iron for metal-glass joints 2,306
Cinematography, light sources for — 7,161
Coal mines, illumination of — . . 10,334
Cold emission 4,100

Colours:
chromatic adaptation of the eye 9,257
— deviations, control 6,186
— diagram (I C I-triangle) . 2, 39
perception of colour 1,283
— stimulus and sensation . . 9, 2
Colour photography, additive method 5, 48

Colour rendering of light sources: improvement:
blended-light lamps . . 5,341
incandescent lamps ("Philiphane"-glass) . . 3, 47
mercury lamps (luminescence) 3,272
method of comparison of "white" light sources . . . 2, 1
photometer for investigation 4, 66

Condensers:
ceramic — 10,231
electrolytic — 2, 65
linear action tuning — . . . 4,277
low-loss — 5,300
power — 1,178
pressure — 4,254
10 000 kVA battery 7,182
Condenser microphone, see Microphones

Conduction in solids:
non-metallic materials . . . 9, 46
semi-conductors with large negative temp. coefficient . 9,239
Conical disk springs 10, 61

Contacts, electrical:
contact pressure, control . . 6, 61
convergence resistance . . . 4,332
transition resistance (influence of adsorption) 5,238
vibration of contact springs 7,155
Contact arc welding, see Welding
Contact therapy, X-ray apparatus for — 8, 8
Contrast and visibility, see Eye
Converting D.C. into A.C., see Vibrators

Cooling methods:
air cooling of transmitting valves 4,121
idem, improved method . . 9,171
spray cooler 10,239
Copper wire, non-ferrous 8,315
Course finder for aeroplanes . . 2,184
Crystal structure, see Structure analysis
Current regulation by barretters 3, 74
Cyclotron, iron for electromagnet 10,246

Damping mechanical vibrations, see Mechanical vibrations
Deaf-aid apparatus 4,316
Debye-Scherrer camera 10,157
Decibel, definition and use . . . 2, 47
Decimal classification 3, 27
Demonstration studio for electro-acoustic purposes 10,196
Density meter 5,331

Diamond:
crystal defects 2,254
dies 5, 14

Dielectric constant:
materials with high — . . . 10,231
temp. coeff. of — and losses 9, 91

Dies:
diamond 5, 14
hard-cemented carbide . . . 4,309
Directing instrument for femur-neck nailing 8,237
Directional hearing, see Stereophony
Disk test for machinability . . 1,183 / 1,200

Distortion:
in coil-loaded cables 4, 79
in the ear 4,172
of magnetic origin 2,193
measurement of — in loud-speakers 4,354
in output valves 5,189
in sound film with oblique slit 6,110
reduction by feed-back, see Inverse feed-back
Dosimeter for X-rays 10,338
Drying lamp 9,249
Dynamo for bicycle, see Bicycle dynamo
Dynamo pocket torch 8,225
Dynatron 3,133

Ear:
directional hearing 6,359
distortion 4,167
perception of pitch 5,286
sensitivity 2, 47
sharpness of hearing 6,234
Elastic constants of metals . . . 6,372
Electro-acoustic demonstration studio 10,196
Electrolytic condensers 2, 65

Electrometer with vibrating condenser:
for p_H-measurement 7, 24
direct reading — 10,338
Electrometer triode . . . . . 4, 68 / 5, 54
Electron, 50 years history . . . 9,225
Electronic conductivity of non-metallic materials 9, 46
Electron counter, see Geiger counter

Electron diffraction diagrams:
different applications 5,161
recording with electron microscope 9, 33
texture investigation 7,178
Electron emission, secondary, see Secondary emission

Electron microscope:
investigation of emitting metallic surfaces 1,312
investigation of α-γ transition in iron 1,317
with continuously variable magnification 9, 33
for 100 kV (photograph) . . 9,179
for 400 kV 9,193
stabilization of accelerating voltage for — 10,135

Electronic switch:
application in oscillography 3,150
GM 4196 4,267
GM 4580 9,340

Electron trajectories:
in magnetron 4,189
in multigrid valves 5,131
model for investigation of — 2,338
Electronic valves, see Radio valves
Emergency apparatus, change-over 8,310
Enamelled wire 3, 40
Epicyclic gearing 9,285
Equalization of telephone cables 7,184
Equivalent networks with highly saturated iron cores 2,276
Exhibition illumination, see Illumination
Expansion, thermal, of ferromagnetic alloys 10, 87

Eye:
characteristics at low brightness levels 1,102
colour perception, see Colours
contrast and visibility:
in road lighting 1,166
in tunnel lighting . . . 10,299
in X-ray fluoroscopy . . 4,114
glare 1,225
night blindness 9,211
sensitivity 5,296
speed of vision and visual acuity 1,215

Facsimile, equipment for high speed — transmission:
general data 10,189
transmitter 10,257
receiver 10,265
transmission 10,289
synchronisation 10,325

Fastness-to-light meter:
description 1,277
radiation intensity 2,282
Femur neck nailing 8,237

Ferrites:
"Ferroxcube", see under that title
crystalline structure 9,185
application in semi-conductors 9,239

"Ferroxcube":
development and properties 8,353

applications:
carrier telephony . . 9,161; 10,353
pulse generator television 10,125
saw-tooth generator . . 10,313
transformer frame aerial 9, 62

Field strength measurement:
accuracy 5,149
recording apparatus 2,216
Field strength in high-voltage installations 6,270

Film projection:
incandescent lamps for — . 8, 72
— with water-cooled mercury lamps 4, 2

Filters, electrical:
general theory 1,240
practical calculation 1,270
low pass — 1,298
high pass and band pass — . 1,327
table 1,332
transient phenomena 1,363
— for carrier telephony . . . 7,104
influence of losses 7,138
Filters for oil, see **Oil filters**
Fitting for road lighting 5,222

Flashlight lamps:
"Photoflux"
description 1,289
peak time of flash . . . 4,148
synchronizers for — . . 2,334
gas-discharge —
for stroboscope — . . . 8, 25
for Wilson chamber . . 10,178

Flickering:
improvement by luminescence 3,272
of electric light sources . . 6,295
Fluctuations, see **Noise**

Fluorescence:
phenomena, theory 3,125
— and phosphorescence, different forms 3,241
— of solids, theory 6,349
applications:
general survey 9,215
in low pressure mercury lamp, see **Fluorescent lamps**
in high pressure mercury lamp 5,341
for testing and research 3, 5
for X-ray screens . . . 9,321

Fluorescent lamps (tubular):
principles 3,272
application in coal mines . . 10,334
application in living rooms 8,267
construction:
for high voltage 4,337
for low voltage 6, 65
starter switch for — . . 10,141

Foundry:
high-frequency furnace . . . 1, 53
X-ray testing of castings . . 2,377
Frequency analysis, recording apparatus 7, 50
Frequency, measurement of —, with oscillograph 3,341

Frequency-changing valves:
diode as — 6,285
four-beam octode 3,266

Frequency characteristics, recording:
automatic recording apparatus 4,354
tone generator for — 5,263

Frequency modulation:
comparison with amplitude modulation 8, 89
control with oscillograph . . 3,248
principles 8, 42
ultra short wave link with — 8,121; 8,193
Fuses, testing with oscillograph 4,118

Galvanometer 7,113; 7,128
Gases, detection of poisonous . . 8,341

Gases, permeability of metals for:
theory 6,365
experiments 7, 74

Gas-discharges:
comparison of sodium and mercury lamp 1, 2; 1, 70
excitation and ionization in positive column 3,157
high frequency oscillations in sodium lamps 1, 87
light emission in positive column of mercury, sodium, neon 3,197
luminescent tube-wall with low pressure mercury column 3,272

Gas-discharge lamps:
A.C. circuits for — 2,103
flicker 3,272; 6,295
oscillographic investigation . 3,148
photometry 1,120; 5,166
recording — for facsimile . . 10,265
see also **Gas-discharges** and **Lamps**
Gas-filled photocells, time lag . . 4, 48

Gas-filled rectifier valves:
physical principles 2,122
see also **Rectifiers**
Gearing, epicyclic — 9,285

Geiger counter:
application in tracer method 8,330
electron counter, description 6, 75
X-ray spectrometer with — . 10, 1
Getters 5,217
Giorgi units 10, 55; 10, 79

Glare:
in road lighting 1,225
in tunnel lighting 10,299

Glass:
alloys for sealing to — . . . 10, 87
composition, properties, use . 2, 87
joints with metals (chrome iron) 2,306
metal leads through glass . 3,119
sintered glass 8, 2
stresses in glass 9,277
vitreous state 8,231
Glow discharge tube for voltage stabilization 8,272

Gramophone records:
simple apparatus for recording 4,106
speed of playing 2, 56
stereophony on — 5,182

Hardening oils, investigation of cooling process 9,147

Hard metal ("hard cemented carbides") 4,309
Hardness, definition and measurements 2,177
Hearing aid apparatus 4,316
Heliographic printing, mercury lamps for — 6,250
High frequency furnace with valve generator 1, 53

High voltage:
assembly of 10^6 V generator (photograph) 4,159
field strength in — constructions 6,270
impulse voltage generators, see under that title . . . .
generator for 10^6 V on the cascade principle 1, 6
generator with stabilized voltage 10,135
installation Cavendish Laboratory 2,161
rectifying valves, see **Rectifiers**
X-ray tube — construction . 4,153

Hysteresis:
distortion caused by — . . . 2,193
measuring apparatus for soft iron 2, 84
oscillographic recording . . . 3,341

Iconoscope 1, 18

Illumination:
aerodromes 4, 93; 6, 33
architecture and — 2, 8
black-out illumination:
brightness of night sky . 5,296
concept of brightness . 6,161
filter method 5, 93
principles 4, 15
blended light 7, 34
coal mines 10,334
efficiency of installations . . 7, 97
exhibitions:
Liège 1939 . . . . . 5, 42
Paris 1937 2,361
"Well-lighted House" . . 4,174
indirect —, light distribution on reflection 5,125
— intensity in offices and homes 8,242
League of Nations Palace, Geneva 3,175
linear light sources:
illumination intensity, shadows, reflections . . 4,181
reflecting surfaces . . . 5, 16
calculation of installations 6,147
living room —, see under that title
principles of public — . . . 2,110
railway yards 4, 61
road lighting, see under that title
ships ("Nieuw-Amsterdam"). 3,356
standards for illumination levels 10,214
streets:
principles 2,142
reflector 5,222
tennis-courts 1,252
theatre Utrecht 7, 1
traffic tunnels 10,299
work benches 3, 53

Impedance measurement:
with resonant Lecher system 8, 16
with non-tuned Lecher system 8,278
Impulse generator (carrier supply) 8,137

Impulse-voltage generators:
for 2×10^6 V 1,236
up to 4×10^6 V and 80 kW sec 3,306

Incandescent lamps:
assembly of 10 kW lamp (photograph) 4, 41
"Biarlita" lamp (coiled-coil) 1, 97
bicycle rear lights 5,335
— for cinematography . . . 7,161
colour rendering, see under that title
efficiency, improvements . . 6,334
— for film projection 8, 72
flickering 6,295
lighthouse lamps 4, 29
— for photography 6,259
"Protector" lamp 4, 15
series connection 6,105
— for testing fastness-to-light 1,277
tungsten ribbon lamps . . . 5, 82
see also **Illumination**
Indicator for internal combustion motors, see **Pressure indicator**

Infrared radiation:
drying with — 9,249
surveillance system 1,306
therapeutic use
large apparatus 6,202
"Infraphil" 8,177
Intelligibility of speech 3,139

Inverse feed-back:
principle and possibilities for application 2,289
applications:
in electrometer amplifier 10,339
for expansion in sound reproduction 3,204
in receiving sets 1,264
in repeaters 2,209
for stabilization of amplifiers 9, 25; 9,309
Ionosphere, radio investigation of 8,111
Iron content of copper wire . . 8,315
Iron for cyclotron magnet . . . 10,246
Iron filament in barretters . . . 3, 74
Iron lung 4,325
Iron, transition α to γ — 1,317
Isotopes, see **Tracers**

Krypton, in incandescent lamps 6,334

Lacquers, adhesive force 8,147
Lamps, see **Blended light**
Flashlight lamps
Fluorescent lamps
Gas-discharge lamps
Incandescent lamps
Mercury lamps
Sodium lamps
also **Illumination**
Laryngophone 5, 6

League of Nations Palace, Geneva:
electro-acoustic equipment . 3,322
illumination 3,175
Lecher systems 6,240
Liège, illumination of Water Exhibition 1939 . . . . . 5, 42
Light distribution of projectors . 9,114
Light sources, see **Lamps**
Lighthouse lamps 4, 29
Lightning, electrical data 2,225
Linear light sources, see **Fluorescent lamps and Illumination**

Living room lighting:
with fluorescent lamps . . . 8,267
illumination intensity . . . 8,242
"Well-lighted House" 4,174

Loading coils:
magnetic core material . . . 2, 77
X-ray examination of core material 2, 93
use, see **Telephony**

Losses:
— by after-effect phenomena 8, 57
connection with temp. coeff. of dielectric constant . . 9, 91
influence on networks . . . 7,138
magnetic — 8,353
measurement phase angles . 5,300

Loud speakers:
directional effect, sound diffusers 4,144
efficiency 4,301
electrical megaphone 4,271
testing 4,354
Luminescence, see **Fluorescence and Fluorescent lamps**
Luminous standard 5, 1; 10,150

Machinability, estimation by disk test 1,183; 1,200

Magnets:
calculation 5, 29
lifting power 5,195
use in dynamo 8,225

Magnetic material:
hysteresis measurements . . 2, 84
— for loading coils 2, 77
non-metallic — for high frequencies 8,353
soft iron for cyclotron . . . 10,246

Magnet steel:
high power steel 6, 8
theory, properties of different kinds 2,233
use for magnets 5, 29
Magnetostriction, effect on thermal expansion 10, 87

Magnetron:
as direct current amplifier . 8,361
theory 4,189
use in transmitter 2,299

Mains:
oscillographic investigation . 3, 50
protection against surge voltages 2,225
Manometers for high vacua . . . 2,201

Manufacture, methods of checking:
cathode-ray oscillograph for testing 4, 85
universal testing set for radio valves 2, 57
X-ray control of assembly . 3,186

Material testing:
automatic — with ionization chambers and X-rays . . . 3,228
electron microscope for — . . 1,312; 1,317
fastness-to-light 1,277; 2,282
hardness 2,177
machinability 1,183; 1,200
X-ray testing:
apparatus 5, 69
examples:
assembly 3,186
castings 2,377
riveted joints . . . 2,350
welds 3, 92
method 2,314
see also **Structure analysis and Texture investigation**
Measuring bridge, simple apparatus (Philoscop) 2,270

Mechanical stresses, investigation:
with cathode-ray oscillograph (varying —) 5, 26; 6, 94
— of glass 9,277
with X-ray diffraction . . . 1,373

Mechanical vibrations:
of contact springs 7,155
damping of — 1,370
pick-up for investigation of —, with oscillograph 5,230
vibration-free mountings . . 9, 16; 9, 85
Megaphone, electrical 4,271
Melting point, connection with thermal expansion 10, 87
Mercury-cathode valves, see **Rectifiers**
Mercury dropping electrode . . . 4,231

Mercury lamps:
"Biosol" lamp 2, 18
colour rendering, see under that title
comparison with sodium lamps 1, 2; 1, 70
for heliographic printing . . 6,250
high pressure —, air cooled:
HP 300 1,129
HPL (fluorescence) . . 5,341
HPL for photography . 4, 27
in enlarging apparatus . 3, 91
high pressure —, water cooled:
for aerodrome 6, 33
brightness 1, 62
for film projection . . . 4, 2
properties and applications 2,165
low pressure —, with fluorescence, see **Fluorescent lamps**
see also **Blended light and Illumination**
Metal leads through glass, see **Glass**
Metal-vapour lamps, see **Gas-discharge lamps**

Microphones:
calibrated — 1, 82
condenser microphone:
construction 9,330
circuit with low noise level 9,357
laryngophone 5, 6
survey of different types . . 5,140
Mirror for telescope 1,358

Mixing stage with triodes, self-oscillating 8,193
Modulation depth, measured with oscillograph 3,248
Modulators for carrier telephony 7, 83
Moisture content, determination 9, 13
Molybdenum, texture 7,120
Moving coil meters, non-ferrous copper wire for — 8,315

Multipliers:
construction with magnetic focussing 3,133
construction with electrostatic focussing 5,253
applications
television transmitter . . 2, 72
facsimile transmitter . . 10,257
X-ray camera-photography 10,107
Multireflection tube 8,257

Music:
duplication of concerts . . . 10,169
fortissimo and pianissimo . . 2,266
perception of pitch 5,286
pitch intervals 2, 47
pitch of orchestras, statistics 4,205
pitch, standard 5,243
playing speed of gramophone records 2, 56

Musical instruments:
church bells 5,293
compass of various — . . . 2, 47
violin, amplification of sound 5, 36

Neon lamps for irradiation of plants 1,193

Networks:
duality of —, and geometrical configurations 5,324
equivalent —, with highly saturated iron core 2,276
filters, see under that title
influence of losses 7,138
Neutrons, production and use . . 3,331
Nickel-iron strip, texture . . . 2, 93; 7, 45
"Nieuw Amsterdam", illumination 3,356
Night-blindness, testing for . . . 9,211

Nipkow disk:
construction 4, 42
interlaced scanning 3,285
use in television transmitter 2, 72

Noise:
causes of — 6,129
in amplifiers 2,136
in amplifier valves 2,329
in receiving sets 3,189
in sound film reproduction . 8, 97
in ultra short wave reception 5,172; 6,178
microphone circuit with low noise level 9,357
"Normandie", sound distribution 1, 22

Nuclear physics:
apparatus for transmutation (1250 kV) 6, 46
neutrons, production and use 3,331
survey 1937 . . . . . 2, 97

Octaves and decibels 2, 47
Offices, illumination intensity . . 8,242

Oil-filters, magnetic:
action of — 6,169
construction 2,295
Operational calculus in electrical filter theory 1,363
Optical aberrations 9,301
Optical models for investigation auditorium acoustics, see **Auditorium acoustics**
Optical telephony 1,152

Oscillations:
relaxation oscillations . . . 1, 39
see also **Mechanical vibrations**
Oscillator, for testing radio sets . 6,154
Oscillator, see **Triode-oscillator**

Oscillograms, distortion:
causes in the amplifier . . . 5,281
causes in the tube 4,199; 5,245
Oscillograph, see **Cathode-ray oscillograph**

Paris, illumination World Exhibition 1937 2,361
Peak voltage meter 7, 20
Pearls, X-ray testing for genuineness 1, 60; 2,156
Pentodes, see **Radio valves** and **Transmitting valves**
Perception of colour 1,283
Perception of pitch 5,286
Permeability of metals for gases, see **Gases, permeability of metals**
Phase angles, measurement with cathode ray tube 5,208
"Philiphane" glass, influence on colour rendering 3, 47

Philips-Miller system of sound recording:
principle 1,107
sound recorder 1,135
sound-track cutter 1,211
recording strip 1,231
machine for recording and reproduction 5, 74
stereophonic recording . . . 6, 80
use in motor van 4, 73
copying of sound track . . 9, 65; 9,289
"Philishave" dry shaving apparatus 4,350

"Philite":
properties and manufacture . 1,257
use, table of properties . . . 3, 9

"Philoscop" measuring bridge:
description 2,270
polarography with — 4,231
resistance measurement of liquids with — 3,183

p_H-measurement:
with electrometer triode . . 5, 54
with vibrating condenser . . 7, 24
Phosphorescence, see **Fluorescence**

Photocells:
principles and development . 2, 13
blocking-layer — 3, 65
application:
optical telephony . . . 1,152; 4, 68
photometry 4,260; 5,166
surveillance system . . 1,306
time lag of gas-filled — . . . 4, 48
— with amplification by secondary emission, see **Multipliers**
Photocurrent, measurement with electrometer triode 4, 66; 5, 54
"Photoflux" lamp, see **Flashlight lamps**

Photographic reproduction:
of sound film 9, 65
metal-diazonium system . . 9,289

Photography:
colour photography, additive method 5, 48
enlarging apparatus with mercury lamps 3, 91
flashlight lamps, see under that title
incandescent lamps for — . . 6,259
lamps for cinematography . 7,161
— with mercury light (HPL lamp) 4, 27
— with sodium light 2, 24

Photometry:
definition of brightness . . . 1,142
general problems 1,120
new candle 5, 1; 10,150
physical — 4,260
spectral — (block method) . 4, 66
subjective — 5,270
technical — of gas-discharge lamps 5,166
tungsten ribbon lamps for — 5, 82
Pick-up for mechanical vibrations 5,230
Pitch, see **Music**
Planigraphy 5,309

Plants, irradiation of:
experiments with neon light 1,193
forcing of tulips 10,282
seed potatoes 10,318
Poisonous gases, detection of . . 8,341
Polarography 4,231
Positive column, see **Gas discharges**
Potatoes, storing in artificially-lighted cellars 10,318

Potential fields, investigated with electrolytic tank:
method 4,223
applied to igniter of relay valve 8,346
Potter-Bucky diaphragm 8,183
Powder metallurgy 4,309

Power cables:
localization of flaws 7,113
testing apparatus 7, 59
Pressure condensers 4,254

Pressure indicator:
construction 5,348
recording of diagrams . . . 6, 22
Projection, see **Film projection**
Projectors, light distribution of — 9,114
Protection of overhead lines . . 2,225
"Protector" lamps 4, 15
Push-button tuning, see **Radio receiving sets**
Pyrometer, optical, in hardening department 6, 30

Quartz glass, metal leads 3,119

Radiation measurements:
comparison of fastness-to-light apparatus and sun . . 2,282
density meter 5,331
with ionization chamber and electrometer triode 5, 58
photographic (X-ray dosage) 1, 62
X-ray dosimeter 10,338

Radio interferences:
causes and transmission . . 3,235
combating — 4,237
— due to sodium lamps . . 1, 87
sensivity of aerials to — . . 6,302
Radio investigation of the ionosphere 8,111

Radio receiving sets:
aerial, see under that title
aeroplane radio, see under that title
band spread:
principles, different types 4,284
simple system 6,265
car radio 3,112
compression and expansion . 3,204
directional reception 9, 55
diversity reception 9, 55
frequency characteristics . . 5,115
h.f. oscillator for testing — . 6,154
magnetic tuning, negative feed-back 1,264
noise, see under that title
push-button tuning
with linear action condenser 4,277
with motor 3,253
resonance curves, control in mass production 4, 85
secret production in war time 8,337
superheterodyne principle, demonstration 1, 76
super-regenerative reception . 5,315
see also **Telephony, ultra short wave connections**

Radio valves:
characteristics, recording 3,339
with oscillograph 5, 61
construction, all-glass — . . 4,162
construction, glass or metal 6,317
diode for frequency changing 6,285
electron trajectories in — . . 5,131
influence of transit times and space charge; amplification with negative anode . . . 1,171
influence of transit times, self-induction, mutual induction of connections 3,103
noise of — 2,329
pumping plant (photograph) 3,147
series of small — ("Rimlock") 8,289
testing set for — 2, 57
secondary emission in —:
application 3,133
counteracted in output valves 10,346
harmful results 3,211
special valves:
diode as effects changer 6,285
diode for voltage measurement 7,124
diode, magnetically controlled 8,361
double cathode connection (EF 51) 5,357
electrometer triode . . . 5, 54
four-beam octode . . . 3,266
gasfilled triode 1,367
output valves for low voltage 10,346
output valves, power and distortion 5,189
ouput valves, testing with oscillograph 5, 61
push-pull amplifier valve (EFF 50) 5,172
see also **Transmitting valves**
Radiowaves, propagation 4,245
Railway yards, illumination . . . 4. 61

Rare gases:
analysis of argon-nitrogen mixtures 5 88
manufacture of 4,128
Rear lights for bicycles 5,335
Receiving sets, see **Radio receiving sets**
Receiving valves, see **Radio valves**
Recrystallization, X-ray investigation 2, 29

Rectifiers:
blocking-layer rectifiers:
construction, theory . . 4,100
use of selenium — . . . 5,199
small selenium — . . . 9,267
cascade generator:
for 1200 V 6, 75
for 25 kV (television) . 10,125
see also: **High Voltage**
controllable unit 20 kV, 18 A 1,161
high voltage valves:
for cascade generators . 1, 6
for X-ray diagnostics . 8,199
hot-cathode rectifier valves
principles of gas-filled — 2,122
relay valve (DCG 5/30) 1,163
mercury-cathode valves:
with dielectric igniter 8,346 / 9,105
with metal envelope . . 1, 65
preservation rectifier 9,233
with stabilized voltage, see **Stabilization of voltage**
for telephone exchanges . 1,295 / 6, 39
voltage impulses in 9,135

Reflection:
brightness coefficients of road surfaces 3,313
light distribution upon — by different materials 5,125
— with linear sources of light 5, 16
reflectors for bicycles 5,335
Relaxation oscillations 1, 39

Relay valves:
rectifier unit with — DCG 5/30 1,161
— as timing devices in welding 1, 11
see also under **Rectifiers**

Resistance measurement
apparatus for — 2,270
— of liquids 3,183
Resistors, automatic starting — . 1,205
Resonance circuits, u.h.f. 6,217
Resonance curves of receiving sets, measurement 4, 85
Reverberation, see **Auditorium acoustics**
Ribbon lamps 5, 82
Riveted joints, X-ray examination 2,350

Road lighting:
installed systems:
measurements 4,292
Purley Way, Croydon (photograph) 1,230
physiological principles
survey 9,149
general properties of eye 1,102
brightness and apparent brightness 1,142
contrast sensibility and richness of contrast . . 1,166
visual acuity and speed of vision 1,215
glare 1,225
principles of public lighting . 2,110
reflection of road surface:
desired brightness and contrast 2,239
distribution of brightness . . . . . 3,313 / 5,222
visibility meter for judging — 1,349
street lighting, see **Illumination (streets)**
"Rotalix" X-ray tube . . . . 3,292 / 8, 33

Scanning speed, see **Cathode-ray tubes**

Schmidt-optical system:
principle 9,301
correction plates, manufacture of — 9,349
for projection-television . . . 10, 69
testing of spherical mirror . 10,286

Secondary emission:
emission of different materials 3, 80
undesired effects in amplifier valves . . . . . 3,215 / 10,346
applications:
cathode-ray tube 3,214
dynatron, multiplier, amplifier valves 3,133
amplification of photo-electrical currents, see **Multipliers**
Selenium photocell 8, 65
Selenium rectifiers, see **Rectifiers (blocking layer —)**
Semi-conductors with large negative temperature coefficient . . 9,239
Shaving apparatus, "Philishave" 4,350
Short waves, see **Ultra short waves**
Short-wave therapy, generator . 7,147
Signalling in carrier telephony . . 8,168

Sintered glass:
description, properties . . . 8, 2
use in transmitting valves . 10,273
Soap film models of electrical networks 7,138
Soapstone, X-ray testing 1, 60

Sodium lamps
applications in photography 2, 24
comparison with mercury lamps . . . . . 1, 2 / 1, 70
h.f. oscillations in — 1, 87
principles and development 2,353
see also **Illumination**

Sound:
absorption 3,363
amplification:
apparatus for improving defective hearing . . . 4,316
League of Nations Palace 3,322
megaphone 4,271
"Normandie" 1, 22
principles, applications . 3,221
audiometer 6,234
auditorium acoustics, see under that title

electro-acoustic demonstration studio 10,196
intensity of different sources 2, 54
pitch, perception of 5,286
radiation:
pressure measurements . 1, 82
theory and models . . . 4,213
recording:
gramophone records, simple apparatus 4,106
machines for sound film 5, 74
Philips-Miller system, see under that title.
reproduction:
compression and expansion 3,204
duplication of concerts . 10,169
fortissimo and pianissimo 2,266
in radio apparatus . . . 5,115
spectra:
acoustic spectroscope . . 4,290
light diffraction by sound film 3,298
recording apparatus for frequency analysis . . 7, 50
stereophony, see under that title
synthetic sound 4,167
tone generator 5,263
units . . . . . 2, 47 / 5,243
Sound diffusers in loud speakers . 4,144

Sound film:
copying with metal-diazonium system 9,298
distortion with oblique slit . 6,110
light diffraction by — . . . 3,298
machines for recording and reproduction 5, 74
noise in reproduction, counteracting 8, 97
Philips-Miller system, see under that title
problems in reproduction of — 9, 65
Spinels . . . . . 9,185 / 9,239

Springs:
conical disk — 10, 61
helical — 9, 85
Spring balance 1,126
Stability of triode-oscillator . . . 7,171

Stabilization of voltage
D.C. generator, — by means of triodes 3, 97
"preserving" rectifier 9,231
rectifier for telephony exchanges 6, 39
— with highly saturated iron core 2,276
stabilizing tube 8,272
voltage supply, low tension . 6, 54
voltage supply for electron microscope 10,135
Starter switch for fluorescent lamps 10,141
Starting resistors, automatic . . 1,205

Steel:
austempering 6,279
examination with disk test 1,183 / 1,200
magnet steel, see under that title

Stereophony
apparent elevation 9, 8
condenser microphone for — 9,330
deaf-aid apparatus with — . 4,316
duplication of concerts . . . 10,169
formation of images 8, 51
localization "in front" and "behind", angle of elevation 6,359
principles 5,107
recording on gramophone disk 5,182
recording on Philips-Miller film 6, 80
Street lighting, see Illumination
Stroboscope 8, 25

Structure analysis, X-ray:
methods:
apparatus with Geiger counter 10, 1
Debye-Scherrer-camera . 10,157
general 1, 29
"sensitive" lines 1,253
X-ray tube for — . . . 3,259
applications
survey 5,157
analysis of mixtures . . 1,158
crystal defects 2,254
crystal size 2,255
identification . . . . 1, 31 / 1,158 / 1,188
mixed crystals . . . . 1,220 / 1,253
recrystallization 2, 29
strains 1,373
texture investigation, see under that title

Studio equipment:
broadcasting studios 4,136
electro-acoustical demonstration studio 10,196
new principles of construction 6,139
peak-voltage meter for — . . 7, 20
see also Auditorium acoustics
Superheterodyne reception, demonstration model 1, 76
Super-regenerative receiver . . . 5,315
Surge protection of overhead lines 2,225
Surveillance system with infrared rays 1,306
Switchboard wire for telephone installations 6, 85
Synchronization, see Facsimile and Television
Synchronizers for flash-light photography 2,334
Synthetic sound 4,167

Telephony:
carrier telegraphy 8,206
carrier telephony:
on coil-loaded cables . . 4, 20
distortion in loaded cables 4, 79
carrier supply (17 channels) 8,137
equalization of cables (17 channels 7,184
filters (17 channels) . . 7,104
maintenance measurements 8,249
modulators 7, 83
principles 6,325
selenium rectifiers for modulators 9,267
signalling with carrier waves 8,168
48-channel system
method of modulation . 9,161
construction 10,353
change-over to emergency apparatus 8,310
loading coils
core material 2, 77
use 1,353
optical telephony 1,152
rectifiers for small telephone exchanges . . . . . 1,295 / 6, 39
repeaters 2,209
switchboard wire 6, 85
ultra short wave — connections:
Eindhoven-Nijmegen . . 2,299
Eindhoven-Tilburg, first installation 2,171
Eindhoven-Tilburg, with frequency modulation 8,121 / 8,193
with moving automobiles 5,315
for the tropics 6,120
Telescope mirrors 1,358

Television:
amplifier, transient characteristic 6,193
experimental installation . . 1, 16
Nipkow disk, construction . 4, 42
projection of pictures . . . 2,249
receiving sets . . . . . 2, 33 / 4,342
projection-television receiver:
cathode-ray tube . . . 10, 97
deflecting circuit 10,307
high-voltage supply . . 10,125
optical system 10, 69
synchronisation 10,364
testing of mirror 10,286
transmitter with interlaced scanning 1,321
idem, transportable 3, 1
transmitter with Nipkow disk 2, 72
idem, with interlaced scanning 3,285
9 kW experimental transmitter 7,129

Temperature measurement:
with pyrometer 6, 30
with thermo-elements . . . 5,214

Texture investigation:
chrome-iron cups 2,158
cross-rolled molybdenum . . 7,120
electrolytic nickel coating . . 1, 95
electron diffraction, aluminium mirrors 7,178
methods, pole figure 7, 13
nickel-iron strip . . . . . 2, 93 / 7, 45
soapstone, pearls 1, 60

Theatre Utrecht:
acoustics 7, 9
illumination 7, 1

Therapy:
infrared — 6,202
infrared — with "Infraphil" . 8,177
short wave — 7,147
X-ray —, see under that title
Thermo-elements for temperature measurement 5,214
Thermo-junctions 3,165
Titanium dioxide as dielectric . 10,231

Tone generator:
for 440 c/s, with string . . 4,205
up to 16000 c/s 5,263
up to 100 000 c/s 8,251
Topology and electrical networks 5,324

Tracers:
isotopes used as tracers . . 8,296
technique of tracer method . 8,330
Transforming D.C. into A.C., see Vibrator
Transient characteristic of amplifier 6,193

Transmitters:
- broadcast — in the Netherlands . . . 6, 1
- rotating directional aerial for PCJ transmitter . . . 3, 59
- short wave station PCJ . . 3, 17
- television —, see **Television.**
- **transmitter-receiver installations:**
  - for aeroplanes . . . 1,114
  - for automobiles . . . 5,315
  - for the tropics . . . 6,120
  - Eindhoven-Nijmegen . . 2,299
  - Eindhoven-Tilburg . . 2,171
  - idem, with frequency modulation . . . 8,121, 8,193

Transmitting valves:
- air-cooled — . . . 4,121, 9,171
- characteristics, recording with cathode-ray tube . . . 4, 56
- development till 1937, manufacture . . . 2,115
- discharge phenomenon (Rocky Point effect) . . . 6,208
- gas-filled triodes . . . 1,367
- hum of — . . . 5,100
- pentodes . . . 2,257
- **for ultra short waves:**
  - technological problems . 6,253
  - for 100 M.c/s . . . 10,273
  - magnetrons, see under that title
  - velocity modulation valves, see under that title
- use in h.f. furnace . . . 1, 53
- use for short wave therapy . 7,147
- water cooled, with increased turbulence . . . 10,239

Transmutation, 1250 kV-apparatus for — . . . 6, 46

Triodes, see **Radio valves and Transmitting valves**

Triode-oscillator
- analysis of action . . . 7, 40
- stability . . . 7,171

Tuberculosis-detection by large scale X-ray examination:
- organization . . . 1,335
- principle of X-ray camera photography . . . 5,258
- apparatus for mass chest survey . . . 10,105

Tulips, forcing of . . . 10,282

Tungsten:
- preparation . . . 4,309
- recrystallization . . . 2, 29
- thorium in — . . . 1,188
- working (photograph) . . . 5,121
- α- and β-modification . . . 1,190

Tungsten ribbon lamps . . . 5, 82

Tunnels, illumination . . . 10,299

Ultra short waves
- cavity resonators . . . 8,149, 9, 73
- impedance measurements, see under that title
- Lecher systems . . . 6,240
- noise in — reception . . . 5,172, 6,178
- resonant circuits for — . . . 6,217
- **valves:**
  - behaviour of amplifier valves at v.h.f. . . . 1,171, 3,103
  - amplifier — with double cathode connection . . 5,357
  - push-pull amplifier — . . 5,172
  - diode as frequency changer . . . 6,285
  - diode for voltage measurement . . . 7,124
  - magnetron . . . 4,189
  - velocity modulation valves, see under that title
  - transmitting valves . . . 6,253, 10,273
  - wave guides . . . 10, 13, 10, 46
- telephone links, see **Telephony**

Ultraviolet radiation:
- **biological effects:**
  - general . . . 2, 18
  - vitamine D . . . 3, 33
- industrial application for luminescence research . . . 3, 5

Units:
- decibel . . . 2, 47
- **Giorgi — :**
  - origin . . . 10, 55
  - in electrical engineering 10, 79
  - new candle . . . 5, 1, 10,150
- phon . . . 5,243

Vacuum gauge . . . 2,201

Velocity-modulation valves:
- principles and theory . . . 8,214
- multireflection tube . . . 8,257

Vibrations, see **Mechanical vibrations**

Vibrators
- for connecting A.C. sets to D.C. mains . . . 2,346
- improved construction . . . 6,342
- transforming D.C. voltage in car radio . . . 3,112

Violin, perspectives in development . . . 5, 36

Visibility meter:
- principle and construction . 1,349
- use, results of measurements 4,292

Vitamine D . . . 3, 33

Voltage regulation, see **Stabilization of voltage**

Watches, measuring of rate with oscillograph . . . 9,317

Wave guides, electromagnetic waves in — . . . 10, 13, 10, 46

Welding:
- coating of welding rods . . 10,114
- **contact arc welding:**
  - principles, Contact electrodes . . . 8,161
  - penetration and speed . 8,304
- efficiency of welding rods . . 3,352
- fusing of electrodes, investigated by X-ray cinematography . . . 1, 26
- mechanical properties of joints 6, 97
- methods, and kinds of rods . 2,129
- oxygen and nitrogen, rôle in arc welding . . . 10, 26
- porosity of welds . . . 7, 91
- relay valves as timing devices 1, 11
- tensile strength of weld metal 3,279
- transfer of material (overhead welding) . . . 4, 9
- twin current welding unit . 1,338
- X-ray testing of welds . . . 3, 92

Wilson cloud chamber, flashlamp for — . . . 10,178

Work bench illumination . . . 3, 53

X-ray:
- **diagnostics:**
  - apparatus for mass chest survey . . . 10,105
  - camera photographs . . 5,258
  - fluoroscopy (protection against radiation, observation of objects) . . . 4,114
  - fluoroscopy with enlarged image . . . 8,321
  - high voltage rectifier valves for — . . . 8,199
  - localization of objects (projectiles) . . . 5,309
  - miniature apparatus for dentists (Oralix) . . . 10,221
  - organization of tuberculosis detection . . . 1,335
  - scattered radiation in X-ray photographs . . . 8,183
  - small apparatus (Centralix, Practix) . . . 6,225
  - universal apparatus with automatic current adjustment . . . 6, 12
  - universal apparatus with exposure technique indication . . . 10, 37
- **diffraction diagrams:**
  - Debye-Scherrer-camera . 10,157
  - spectrometer with Geiger counter . . . 10, 1
  - survey of interpretation and applications . . . 5,157
  - for special applications, see under **Structure analysis and Texture investigation**
- directing instrument for femur-neck nailing . . . 8,237
- dosimeter . . . 10,338
- irradiation of flower bulbs . . 2,321
- material testing, see under that title
- **photographs:**
  - camera photographs . . 5,258
  - density meter for X-ray films . . . 5,331
  - short exposure times (10^{-6} sec.) . . . 5, 22
  - stereoscopic — . . . 5,309
  - welding process (transfer of drop) . . . 1, 26, 4, 9
- protection against radiation 1, 62, 4,114
- scattered radiation in — photographs . . . 8,183
- **screens:**
  - blurring of image . . . 9,364
  - light-emission . . . 9,321
- structure analysis, see under that title
- **therapy**
  - contact — apparatus . . 8, 8
  - with 10^6 V tube . . . 4,153
  - 400 kV-installation . . . 8,105
- **tubes:**
  - for structure analysis . 3,259
  - for therapy up to 10^6 Volts . . . 4,153
  - hard glass — in oil . . . 6,309
  - with rotating anode (Rotalix-tube) . . . 3,292, 8, 33
  - small-focus tube . . . 8,321

Zirconium
- preparation and use . . . 3,345
- use as getter . . . 5,217

AUTHOR INDEX, VOLUMES 1–10

The figures in heavy type indicate the volume and those in normal type the page on which the articles are to be found.

Addink, C.C.J. and Balth. van der Pol
The pitch of musical instruments and orchestras . **4.** 205

Alexander, J.W.
A vibrator for the connection of alternating current receiving sets to the direct current mains **2.** 346
A car radio **3,** 112

Alink, R.J.H., C.J. Dippel and K.J. Keuning
The metal-diazonium system for photographic reproduction **9,** 289

Alma, G. and F. Prakke
A new series of small radio valves **8,** 289

Alphen, P.M. van
A photometer for the investigation of the colour rendering reproduction of various light sources **4,** 66
— and H. Rinia
The manufacture of correction plates for Schmidt optical systems **9,** 349
Projection-television receiver, I. The optical system for the projection **10,** 69

Amstel. J.J.A. Ploos van
Small selenium rectifiers **9,** 267
— and W.G. Burgers
The electron microscope as an aid in metallographic research **1,** 312
Electron-optical observations on the transition of alpha to gamma iron **1,** 317

Aninga, J.B. and G.C.E. Burger
An apparatus for artificial respiration ("Iron lung") **4,** 325

Assum, A.H. van and A.L. Timmer
A surveillance system using infra-red rays . . . **1,** 306

Aten Jr., A.H.W. and F.A. Heyn
The use of isotopes as tracers. **8,** 296
The technique of investigations with radioactive and stable isotopes **8,** 330

Bakker, C.J.
Some characteristics of receiving valves in short-wave reception **1,** 171
The causes of voltage and current fluctuations . **6,** 129
Radio-investigation of the ionosphere **8,** 111

Bast, G.H., D. Goedhart and J.F. Schouten
A 48-channel carrier telephone system
I. The method of modulation **9,** 161
II. Mechanical construction **10,** 353

Bayfield, W.A., M. Berindei and A. Nemet . .
A diagnostic X-ray apparatus with exposure technique indication and overload protection. . **10,** 37

Beek, M. van de
Air-cooled transmitting valves. **4,** 121
A nine kilowatt experimental television transmitter **7,** 129

Beljers, H.G.
A recording apparatus for the analysis of the frequency of rapidly varying sounds **7,** 50

Berg, J. ter
Quantitative considerations of electric welding . . **3,** 352
On the porosity of welds **7,** 91

Bergmans, J.
The brightness of road surfaces under artificial illumination **3,** 313
— and W.L. Vervest
A new fitting for roadlighting. **5,** 222
— and H.A.E. Keitz
Determining the light distribution and luminous flux of projectors **9,** 114

Berindei, M, W.A., Bayfield and A. Nemet
A diagnostic X-ray apparatus with exposure technique indication and overload protection . . . **10,** 37

Bleeksma, J., H.J. Di Giovanni and G. Kloos
X-ray spectrometer with Geiger counter for measuring powder diffraction patterns **10,** 1

Blok, L.
High-frequency oscillations in sodium lamps . . **1,** 87
An apparatus for the measurement of scanning speeds of cathode ray tubes **3,** 216
Radio-interference **3,** 235
Combating radio interferences **4,** 237
A tone generator **5,** 263
— and H.J. Köster,
An apparatus for the investigation of sharpness of hearing (audiometer) **6,** 234

Boeke, J.
Electrical detection of traces of poisonous gases in the atmosphere **8,** 341
A new electrical method for determining moisture content **9,** 13
— and H. van Suchtelen
Rapid chemical analysis with the mercury dropping electrode and an oscillograph or measuring bridge as indicator **4,** 231

Boekhorst, L.C.J. te
The universal decimal classification **3,** 27

Boer, J. de
Absolute sound-pressure measurements **1,** 82
The playing speed of gramophone records . . **2,** 56
Sound amplification and public address **3,** 221
Sound diffusers in loudspeakers **4,** 144
An electrical megaphone **4,** 271
The efficiency of loudspeakers. **4,** 301
Microphones **5,** 140
— and K. de Boer
The laryngophone **5,** 6
— and R. Vermeulen
Optical model experiments for studying the acoustics of theatres **1,** 46

Boer, K. de
Stereophonic sound reproduction **5,** 107
Experiments with stereophonic records. **5,** 182
Stereophonic recording on Philips-Miller film . . **6,** 80
The formation of stereophonic images **8,** 51
A remarkable phenomenon with stereophonic sound reproduction **9,** 8
— and J. de Boer
The laryngophone **5,** 6
— and A.Th. van Urk
A simple apparatus for sound-recording **4,** 106
Some particulars of directional hearing **6,** 359
— and R. Vermeulen
On improving defective hearing **4,** 316

Boldingh, W. Hondius
Impulse voltage installations **3,** 306
The testing of power cables with direct current voltage. **7,** 59
The localization of cable flaws **7,** 113
— and W.J. Oosterkamp
A 400 kilovolt installation for X-ray therapy . **8,** 105

Boosman, H.B.R.
The new broadcasting transmitters in the Netherlands **6,** 1

Bourdrez, J.P. and N.A.J. Voorhoeve
The electro-acoustic installation in the League of Nations Palace in Geneva **3,** 322

Bouma P.J.
Characteristics of the eye with special reference to road lighting **1,** 102
The definitions of brightness and apparent brightness and their importance in road lighting and photometry **1,** 142
The perception of brightness contrast in road lighting **1,** 166
Visual acuity and speed of vision in road lighting **1,** 215
The problem of glare in high-way lighting . . . **1,** 225
The perception of colour **1,** 283
Colour reproduction in the use of different sources of "white" light **2,** 1
The representation of colour sensation in a colour space-diagram or colour triangle. **2,** 39
The colour reproduction of incandescent lamps and "Philiphane glass" **3,** 47
Illumination and black-outs **4,** 15
Measurements carried out on road lighting systems already installed **4,** 292
Natural illumination and visibility at night . . . **5,** 296

The concept of brightness in connection with black-out problems 6, 161
The flickering of sources of electric light 6, 295
Perception on the road when visibility is low . . 9, 149
— and E.G. Dorgelo
The sodium lamp, from laboratory experiment to street lighting 2, 353
— and G. Holst . . . . . .
How can one judge the efficiency of road lighting? 1, 349
— and A.A. Kruithof . . . . . .
Colour stimulus and colour sensation 9, 2
Chromatic adaptation of the eye 9, 257
Bouman, H.J.J.
Demonstration model illustrating superheterodyne reception 1, 76
Rectifiers for telephone exchanges 1, 295
Boumeester, H.G.
Development and manufacture of modern transmitting valves 2, 115
— and M.J. Druyvestein
Gas-filled triodes 1, 367
Bouwers A.
The localization of objects in the human body . 5, 309
— and G.C.E. Burger
X-ray photography with the camera 5, 258
— and P.G. Cath
The maximum electric field strength for several simple electrode configurations 6, 270
— and F.A. Heijn . . . . . .
An apparatus for the transmutation of atomic nuclei 6, 46
A simple apparatus for counting electrons . . . 6, 75
Bremmer, H. and Balth. van der Pol
The propagation of wireles waves round the earth 4. 245
Brey, H. de and H. Rinia
An improved method for the air-cooling of transmitting valves 9, 171
— H. Rinia and F.L. van Weenen
Fundamentals for the development of the Philips air engine 9, 97
Bruin, S.L. de
The investigation of rapidly changing mechanical stresses with the cathode ray oscillograph . . . 5. 26
An apparatus for stroboscopic observation . . . 8. 25
— and C. Dorsman
An electron switch 4, 267
A cathode ray oscillograph for use in tool making 5. 277
Bruining, H.
Secondary electron emission 3. 80
Bügel R.D. and E.J.W. Verwey
Ceramic materials with a high dielectric constant 10, 231
Burger, G.C.E. and J.B. Aninga
An apparatus for artificial respiration ("Iron lung") 4, 325
— and A. Bouwers
X-ray photography with the camera 5, 258
— B. Combee and J.H. van der Tuuk
X-ray fluoroscopy with enlarged image 8, 321
Burgers, W.G.
Practical applications of X-rays for the examination of materials
I 1, 29
II 1, 60
III 1, 95
IV 1, 158
V 1, 188
VI 1, 220
VII 1, 253
VIII 1, 373
IX 2, 29
X 2, 93
XI 2, 156
XII 2, 254
The use of X-rays and cathode rays in chemical and metallographic investigations 5, 157
— and J.J.A. Ploos van Amstel
The electron microscope as an aid in metallographic research 1, 312
Electron-optical observations on the transition of alpha to gamma iron 1, 317
Carpentier, E.E.
A cathode-ray oscillograph with two push-pull amplifiers 9, 202
An electronic switch with variable commutating frequency 9, 340
Casimir, H.B.G.
A magnetron for D.C. voltage amplification . . . 8, 361
Cath, P.G.
A simple electrical measuring bridge 2, 270
A new principle of construction for radio valves . 4, 162
— and A. Bouwers
The maximum electric field strength for several simple electrode configurations 6, 270
Cisney, E. and W. Parrish
An improved X-ray diffraction camera 10, 157
Claassen, A.
A simple arrangement for the measurement of the specific resistance of liquids 3, 183
— and W.Ch. van Geel
Electrolytic condensers 2, 65
Clausing, P.
A speed-increment test as a short-time testing method for estimating the machinability of steels . 1, 183
The disk test as a rapid method for estimating the machinability of steel 1, 200
Coeterier, F.
The multireflection tube, a new oscillator for very short waves 8, 257
Cohen Henriquez, V.
Compression and expansion in sound transmission 3, 204
The reproduction of high and low tones in radio receiving sets 5, 115
Combee, B., G.C.E. Burger and J.H. van der Tuuk
X-ray fluoroscopy with enlarged image 8, 321
Cornelius, P.
The sensitivity of aerials to local interferences . 6, 302
The aerial effect in receiving sets with loop aerial . 7, 65
The rationalized Giorgi system with absolute volt and ampere as applied in electrical engineering . 10, 79
— and J. van Slooten
Installations for improved broadcast reception . . 9, 55
Cramwinckel A.
The sound-recording cutter in the Philips-Miller system 1, 211
— C.J. Dippel and G. Heller
The damping of mechanical vibrations 1, 370
Custers, J.F.H.
A new apparatus for testing the fastness-to-light of materials 1, 277
The recording of rapidly occurring electric phenomena with the aid of the cathode ray tube and the camera 2, 148
The radiation intensity of the Philips fastness-to-light meter 2, 282
Quantitative considerations in colour photography by the additive method 5, 48
Considerations on the texture of metals 7, 13
The texture of nickel-iron strip 7, 45
The texture of cross-rolled molybdenum 7, 120
The investigation of texture with electron rays . 7, 178
Dam, A. van, A. Horowitz and W.H. van der Mei
The dry-shaving apparatus "Philishave" 4, 350
Dippel, C.J.
A very sensitive spring balance 1, 126
The recording strip in the Philips-Miller system . 1, 231
— R.J.H. Alink and K.J. Keuning
The metal-diazonium system for photographic reproduction 9, 289
— A. Cramwinckel and G. Heller
The damping of mechanical vibrations 1, 370
— and K.J. Keuning
Problems in photographic reproduction, in particular of sound-films 9, 65
Dorgelo, E.G.
Alternating-current circuits for discharge lamps . 2, 103
Water-cooled mercury lamps 2, 165
Several technical problems in the development of a new series of transmitter valves 6, 253
Sintered glass 8, 2
Glass transmitting valves of high efficiency in the 100 Mc/s range 10, 273
— and P.J. Bouma
The sodium lamp, from laboratory experiment to street lighting 2, 353

Dorsman, C.
A pH-meter with a very high input resistance . 7, 24
— and S.L. de Bruin
An electronic switch 4, 267
A cathode ray oscillograph for use in tool making 5, 277
— and H. Rinia
Television system with Nipkow disc 2, 72
Dorsten, A.C. van
Stabilization of the accelerating voltage in an electron microscope 10, 135
— W.J. Oosterkamp and J.B. Le Poole
An experimental electron microscope for 400 kilovolts 9, 193
Douma, Tj.
Voltage impulses in rectifiers 9, 135
— and P. Zijlstra
Recording the characteristics of transmitting valves 4, 56
Druyvesteyn, M.J.
The determination of the elastic constants of metals 6, 372
— and H.G. Boumeester
Gas-filled triodes 1, 367
— and J.G.W. Mulder
Physical principles of gasfilled hot-cathode rectifiers 2, 122
du Pré, F.K. and M. Gevers
A remarkable property of technical solid dielectrics 9, 91
— and H. Rinia
Air engines 8, 129
— and J.L. Snoek
Several after-effect phenomena and related losses in alternating fields 8, 57
Duinker, D.M.
Relay valves as timing devices in seam-welding practice 1, 11
The use of selenium valves in rectifiers 5, 199
Dijk, B. van
Several problems of X-ray fluoroscopy 4, 114
Ehrnreich, H.
Heavy-current condensers 1, 178
Embden, H.J. Meerkamp van
Telescope mirrors 1, 358
Joints between metal and glas 2, 306
— and B. Jonas,
New kinds of steel of high magnetic power . . . 6, 8
Eringa, D.
A universal testing set for radio valves 2, 57
Fast, J.D.
Zirconium and its compounds with a high melting point 3, 345
The preparation of metals in a compact form by pressing and sintering 4, 309
Metals as getters 5, 217
The permeability of metal walls for gases 6, 365
Experiments on the permeation of gases through metal walls 7, 74
The part played by oxygen and nitrogen in arc-welding 10, 26
The function of the coating of welding rods . . . 10, 114
Feiner, H. and J. Hoekstra
Switchboard wire for telephone installations . . . 6, 85
Fransen, J.
A miniature X-ray apparatus for dentists 10, 221
— and J.M. Ledeboer
Generators for short-wave therapy 7, 147
Frederik, W.S.
Testing for nyctalopia (night-blindness) 9, 211
Fremery, F. de and G.J. Levenbach
Carrier-telephony on loaded cables 4, 20
— and J.W.G. Wenke
New principles of construction for the electro-acoustic installation of studios 6, 139
The measurement of peak voltages in a studio installation 7, 20
Funke, J. and P.J. Oranje
The development of blended-light lamps 7, 34
Geel, W.Ch. van
Blocking layer rectifiers 4, 100
Blocking layer photocells 8, 65
— and A. Claassen
Electrolytic condensers 2, 65
Geiss, W.
The development of the coiled-coil lamp 1, 97
Improvements in the efficiency of electric incandescent lamps 6, 334
Gevers, M. and F.K. du Pré
A remarkable property of technical solid dielectrics 9, 91
Gier, J. de
A cathode ray tube with post-acceleration . . . 5, 245
Projection-television receiver, II. The cathode-ray tube 10, 97
— and A.P. van Rooy
Improvements in the construction of cathode-ray tubes 9, 180
Giovanni, H.J. Di, J. Bleeksma and G. Kloos
X-ray spectrometer with Geiger counter for measuring powder diffraction patterns 10, 1
— W. Kes and K. Lowitzsch
A transportable X-ray apparatus for mass chest survey 10, 105
Gisolf, J.H. and W. de Groot
Fluorescence and phosphorescence 3, 241
Goedhart, D., G.H. Bast and J.F. Schouten
A 48-channel carrier telephone system,
I. The method of modulation 9, 161
II. Mechanical construction 10, 353
— and G. Hepp
Carrier supply in an installation for carrier telephony 8, 137
— and J. de Jong
Carrier-wave telephony 6, 325
Graaf, J.E. de
The examination of the macrostucture of raw materials and products with the help of X-rays
I 2, 314
II 2, 350
III 2, 377
IV 3, 92
V 3, 186
X-ray apparatus for the macroscopic examination of materials 5, 69
— and W.J. Oosterkamp
X-ray tube for the analysis of crystal structure . 3, 259
— and J.H. van der Tuuk
Automatic macroscopic examination of materials with X-rays 3, 228
Gradstein, S.
A modern high-voltage equipment 1, 6
Relaxation oscillations 1, 39
The equipment of broadcasting studios 4, 136
Radio receiving sets with linear action tuning condensers 4, 277
Groot, F.A. de
Signalling in carrier telephony 8, 168
— and P.J. den Haan
Modulators for carrier-telephony 7, 83
Groot, W. de
Nuclear physics 2, 97
Fluorescence 3, 125
Fifty years of electrons 9, 225
Optical aberations in lens and mirror systems . 9, 301
The origin of the Giorgi system of electrical units 10, 55
The new candle 10, 150
— and J.H. Gisolf
Fluorescenc and phosphorescence 3, 241
— and H.A. Klasens
The light-emission of X-ray screens 9, 321
Haan, P.J. den and F.A. de Groot
Modulators for carrier-telephony 7, 83
Haantjes, J.
Judging an amplifier by means of the transient characteristic 6, 193
— and F. Kerkhof
Projection-television receiver,
IV. The circuits for deflecting the electron beam 10, 307
V. The synchronisation 10, 364
Haayman, P.W., E.L. Heilman and E.J.W. Verwey
On the crystalline structure of ferrites and analogous metal oxides 9, 185
— F.C. Romeyn and E.J.W. Verwey
Semi-conductors with large negative temperature coefficient of resistance 9, 239
Hagendoorn, P.J. and M.F. Reynst
An electrical pressure indicator for internal combustion engines 5, 348

The recording of diagrams with the electrical pressure indicator 6, 22
Halbertsma, N.A.
The loudspeaker and sound-amplifying installation on the T.S.S. "Normandie" 1, 22
Work-bench illumination 3, 53
Reflecting surfaces in the neighbourhood of linear sources of light 5, 16
— and G.P. Ittmann
Illumination by means of linear sources of light . . 4, 181
— and J.A.M. van Liempt
Incandescent filament lamps for series-connection 6, 105
Lamps for use in photography 6, 259
Hardenberg, J.J.C.
The transport of sound film in apparatus for recording and reproduction 5, 74
Haringx, J.A.
Magnetic oil filters 6, 169
The vibration of contact springs 7, 155
Vibration-free mountings with auxiliary mass . . 9, 16
The practical construction of vibration-free mounting with auxiliary mass 9, 85
Conical disc springs 10, 61
Hazeu, H.A.G.
Small apparatus for medical X-ray examination 6, 225
— and M. Kiek
An alternating current dynamo with a flat characteristic for bicycle illumination 3, 87
— and J.M. Ledeboer
A universal apparatus for X-ray diagnosis . . . 6, 12
— J.M. Ledeboer and J.H. van der Tuuk
An X-ray apparatus for contact therapy 8, 8
Heel, G.L. van
The illumination and beaconing of aerodromes . 4, 93
Hehenkamp, Th.
A rapid-action starter switch for fluorescent lamps 10, 141
Heilman, E.L., P.W. Haayman and E.J.W. Verwey
On the crystalline structure of ferrites and analogous metal oxides 9, 185
Heins van der Ven, A.J., see **Ven, A.J. Heins van der**
Heller, G.
Comparison between discharge phenomena in sodium and mercury vapour lamps I 1, 2
A high-frequency furnace with valve generator . . 1, 53
Comparison between discharge phenomena in sodium and mercury vapour lamps II 1, 70
The photometry of metal vapour lamps 1, 120
The mercury vapour lamp HP 300 . . . . . 1, 129
A film projection installation with water-cooled mercury lamps 4, 2
The magnetron as a generator of ultra short waves 4, 189
Radio sets with station dials calibrated for short waves 4, 284
Television receivers 4, 342
The new luminous standard 5, 1
— C.J. Dippel and A. Cramwinckel
The damping of mechanical vibrations 1, 370
Helmer, A.M.C. and N. Warmoltz
A flash lamp for illuminating vapour tracks in the Wilson cloud chamber 10, 178
Hengel, J. van and W.J. Oosterkamp
A direct-reading dynamic electrometer 10, 338
Hepp, G.
Measurements of potential by means of the electrolytic tank 4, 223
Automatic change-over to an emergency apparatus in a communication system 8, 310
— and D. Goedhart
Carrier supply in an installation for carrier telephony 8, 137
Heyboer, J.P.
Five-electrode transmitting valves (pentodes) . . 2, 257
A discharge phenomenon in large transmitter valves 6, 208
Heyn, F.A.
The production and use of neutrons 3, 331
— and A.H.W. Aten Jr.
The use of isotopes as tracers 8, 296
The technique of investigations with radioactive and stable isotopes 8, 330
— and A. Bouwers
An apparatus for the transmutation of atomic nuclei 6, 46
A simple apparatus for counting electrons . . . 6, 75
Hoekstra, J.
Properties and applications of enamelled wire . . 3, 40
— and H. Feiner
Switchboard wire for telephone installations . . . 6, 85
Hofweegen, J.M. van
The measurement of impedances particularly on decimetre waves 8, 16
Impedance measurements with a non-tuned Lecher system 8, 278
Holleman H.C.A.
The manufacture of rare gases 4, 128
Measurements in the Philips rare gas plant . . . 5, 88
Holst, G. and P.J. Bouma
How can one judge the efficiency of road lighting? 1, 349
Hondius Bolding, W. see **Boldingh, W. Hondius**
Horowitz, A., A. van Dam and W.H. van der Mei
The dry-shaving apparatus "Philishave" 4, 350
— and J.A. van Lammeren
Radio receivers with push-button tuning 3, 253
Horst, H.L. van der and J.G.W. Mulder
A controllable rectifier unit for 20 000 Volts/18 amperes 1, 161
Houwink, R.
Properties and applications of artificial resin products 1, 257
Ittman, G.P.
The production of sharp fluorescent spots in cathode ray tubes 1, 33
Control of the beam intensity in cathode ray tubes 1, 91
An oscillograph apparatus 1, 147
Position finding and course plotting on board an aeroplane by means of radio 2, 184
— and N.A. Halbertsma
Illumination by means of linear sources of light 4, 181
Jansen, Joh.
The distribution of the light reflected by different ceiling and wall materials 5, 125
Jonas, B.
The sealing of metal leads through hard glass and silica 3, 119
— and H.J. Meerkamp van Embden
New kinds of steel of high magnetic power . . . 6, 8
Jong, F.H. de and N.A.J. Voorhoeve
Voltage regulation of direct current generators by means of triodes 3, 97
Jong, J. de
Maintenance measurements on carrier telephony equipment 8, 249
— and D. Goedhart
Carrier-wave telephony 6, 325
Jonker, J.L.H.
Phenomena in amplifier valves caused by secondary emission 3, 211
Electron trajectories in multi-grid valves 5, 131
Secondary emission in output valves 10, 346
— and A.J.W.M. van Overbeek
A new frequency-changing valve 3, 266
— and M.C. Teves
Technical applications of secondary emission . . 3, 133
Jurriaanse, T.
A voltage stabilizing tube for very constant voltage 8, 272
Kalff, L.C.
Illumination and architecture 2, 8
Illumination at the International Exhibition in Paris 1937 . . . . . 2, 361
The illumination of the League of Nations Palace in Geneva 3, 175
The illumination of passenger ships 3, 356
The well lighted house 4, 174
Interesting lighting effects of the Liege Water Exposition 5, 42
The illumination of the new municipal theatre in Utrecht 7, 1
— and J. Voogd
Living room lighting with tubular fluorescent lamps 8, 267
Keitz, H.A.E.
Rear lights and reflectors for bicycles 5, 335
A method of measuring in the investigation of bicycle dynamos 6, 215

— and J. Bergmans
Determining the light distribution and luminous flux of projectors 9, 114
Kerkhof, F. and J. Haantjes
Projection-television receiver,
IV. The circuits for deflecting the electron beam . 10, 307
V. The synchronisation 10, 364
— and G.J. Siezen
Projection-television receiver, III. The 25 kV anode voltage supply unit 10, 125
Kes, W., H.J. Di Giovanni and K. Lowitzsch
A transportable X-ray apparatus for mass chest survey 10, 105
Keuning, K.J., R.J.H. Alink and C.J. Dippel
The metal-diazonium system for photographic reproduction 9, 289
— and C.J. Dippel
Problems in photographic reproduction, in particular of sound-films 9, 65
Kiek, M. and H.A.G. Hazeu,
An alternating current dynamo with a flat characteristic for bicycle illumination 3, 87
Klasens, H.A.
The blurring of X-ray images 9, 364
— and W. de Groot
The light-emission of X-ray screens 9, 321
Kleis, D., H. Rinia and M. van Tol
Experimental transmitting and receiving equipment for high-speed facsimile transmission, I. General 10, 189
— F.C.W. Slooff and J.M. Unk
Experimental transmitting and receiving equipment for high-speed facsimile transmission, II. Details of the transmitter 10, 257
— and M. van Tol
Experimental transmitting and receiving equipment for high-speed facsimile transmission,
IV. Transmission of the signals 10, 289
V. Synchronization of transmitter and receiver . 10, 325
Kleynen, P.H.J.A.
The motion of an electron in two-dimensional electrostatic fields 2. 338
Klinkhamer, H.A.W.
The Philips twin current welding unit 1, 338
Equivalent networks with highly saturated iron cores with special reference to their use in the design of stabilisers 2, 276
A rectifier for small telephone exchanges 6, 39
Emergency supply systems with accumulator batteries 9, 231
Kloos, G., J. Bleeksma and H.J. Di Giovanni
X-Ray spectrometer with Geiger counter for measuring powder diffraction patterns 10, 1
Klute, J.W. and J.F. Schouten
The influence of losses on the properties of electrical networks 7, 138
Knol, K.S. and M.J.O. Strutt
A diode for the measurement of voltages on decimetre waves 7, 124
Köhler, J.W.L.
Optical telephony 1, 152
Non-linear distortion phenomena of magnetic origin 2, 193
Thermojunctions 3, 165
Koole, P.
Measurement of the adhesive force of lacquers . . . 8, 147
— and J.J. Went
A method for the control of colour deviations 6, 186
Koops, C.G.
The measurement of very small phase displacements 5, 300
Köster, H.J. and L. Blok
An apparatus for the investigation of sharpness of hearing (audiometer) 6, 234
Kröger, F.A.
Luminescent substances 6, 349
Applications of luminescent substances 9, 215
Kruithof, A.A.
Time lag phenomena in gas-filled photoelectric cells 4, 48
Tubular luminescence lamps for general illumination 6, 65
— and P.J. Bouma
Colour stimulus and colour sensation 9, 2
Chromatic adaptation of the eye 9, 257
— and H. Zijl
Illumination intensity in offices and homes . . . 8, 242
— and A.M. Kruithof
Basic principles for the formulation of illumination standards 10, 214
Kruithof, A.M.
On the illumination of traffic tunnels 10, 299
— and A.A. Kruithof
Basic principles for the formulation of illumination standards 10, 214
Kuntke, A.
An impulse-voltage generator for two million volts 1, 236
A generator for very high direct current voltage . 2, 161
Kuperus, J.
On the construction of vibrators for radio-sets . . . 6, 342
Lammeren, J.A. van and A. Horowitz
Radio receivers with push-button tuning 3, 253
Lange, C. de
Pressure condensers 4, 254
Langen, L.H. de
The application of magnetic oil filters to lubricating systems 2, 295
Leblans, L. and H. Rinia
The Nipkow disc 4, 42
Ledeboer, J.M.
An apparatus for the measurement of the photographic density of films 5, 331
— and J. Fransen
Generators for short-wave therapy 7, 147
— and H.A.G. Hazeu
A universal apparatus for X-ray diagnosis . . . 6, 12
— H.A.G. Hazeu and J.H. van der Tuuk
An X-ray apparatus for contact therapy 8, 8
Levenbach, G.J. and F. de Fremery
Carrier-telephony on loaded cables 4, 20
— and H. van de Weg
Non-linear distortion in loaded cables 4, 79
The equalisation of telephone cables 7, 184
Leydens, P. and J.A.M. van Liempt
The significance of a constant peak time in photoflash bulbs 4, 148
Liempt, J.A.M. van
The "Philora" sodium lamp and its importance to photography 2, 24
The use of the "Philora" HP mercury discharge lamp in an enlarging apparatus 3, 91
The role of mercury lamps with fluorescent bulbs in photography 4, 27
— and N.A. Halbertsma
Incandescent filament lamps for series connection 6, 105
Lamps for use in photography 6, 259
— and P. Leydens
The significance of a constant peak time in photoflash bulbs 4, 148
— and E.L.J. Matthews
Black-out by the filter method 5, 93
— and J.A. de Vriend
The "Photoflux", a light-source for flashlight photography 1, 289
The adjustment of synchronizers for the "Photoflux" photo-flash bulb 2, 334
The testing of electric fuses with the cathode ray oscillograph 4, 118
Lindenhovius, H.J. and H. Rinia
A direct current supply apparatus with stabilized voltage 6, 54
Lindern, C.G.A. von
Wireless telephony with moving motorcars . . . 5, 315
A telephone installation on ultra short waves for the tropics 6, 120
— and G. de Vries
An ultra short wave telephone link between Eindhoven and Tilburg 2, 171
A decimetre wave radio link between Eindhoven and Nimeguen 2, 299
Resonance circuits for very high frequencies . . 6, 217
Lecher systems 6, 240
Flat cavities as electrical resonators 8, 149
Lips, E.M.H.
The measurement of the hardness of metals and alloys 2, 177

Loon, C.J. van
Improvements in radio receivers 1, 264
A simple system of bandspread in short-wave reception 6, 265
Lowitzsch, K., H.J. Di Giovanni and W. Kes
A transportable X-ray apparatus for mass chest survey 10, 105
Manders, Th.J.J.A
Aerodrome illumination by means of water-cooled mercury lamps 6, 33
Light sources for cinematography 7, 161
Incandescent lamps for film projection 8, 72
The "Infraphil", an apparatus for infra-red therapy 8, 177
The drying lamp and its most important applications 9, 249
— and L.J. van der Moer
Lamps for lighthouses 4, 29
Mark, J. van der
An experimental television transmitter and receiver 1, 16
Television 1, 321
A transportable television installation 3, 1
Matthews, E.L.J.
The blended-light lamp and other mercury lamps with improved colour rendering 5, 341
— and J.A.M. van Liempt
Black-out by the filter method 5, 93
Meerkamp van Embden, H.J., see Embden,H.J. Meerkamp van
Mei, W.H. van der, A. Horowitz and A. van Dam
The dry-shaving apparatus "Philishave" 4, 350
Meulen, M.J.C. van der
A motor van for sound recording by the Philips-Miller system 4, 73
Moer, L.J. van der and Th.J.J.A. Manders
Lamps for lighthouses 4, 29
Moerel, P.G. and A. Rademakers
Non-ferrous copper wire for moving-coil meters . 8, 315
Mol, W.E. de
The influence of X-ray treatment on flower bulbs (hyacinths and tulips) 2, 321
Mulder, J.G.W.
A new metal rectifying valve with mercury cathode 1, 65
Surge protection of low-tension overhead lines . . 2, 225
Barretters 3, 74
— and M.J. Druyvestein
Physical principles of gasfilled hot-cathode rectifiers 2, 122
— and H.L. van der Horst
A controllable rectifier unit for 20 000 volts, 18 amperes 1, 161
Mulders, H. and W. Six
The use of amplifiers (repeaters) in telephony . . 2, 209
Nemet, A., W.A. Bayfield and M. Berindei
A diagnostic X-ray apparatus with exposure technique indication and overload protection . . . 10, 37
Nordlohne, P.J.H.A.
The experimental short wave broadcasting station P.C.J. 3, 17
A rotating directional aerial for short wave broadcasting 3, 59
Nijenhuis, W.
Measurement of phase angles with the help of the cathode ray tube 5, 208
"One out of Many"
Secret production of radio receivers in occupied territory 8, 337
Oosterkamp, W.J.
X-ray photographs with extremely short exposure times 5, 22
Eliminating scattered radiation in medical X-ray photographs 8, 183
— A.C. van Dorsten and J.B. Le Poole
An experimental electron microscope for 400 kilovolts 9, 193
— and J.E. de Graaf
X-ray tube for the analysis of crystal structure . . 3, 259
— and J. van Hengel
A direct-reading dynamic electrometer 10, 338
— and W. Hondius Boldingh
A 400 kilovolt installation for X-ray therapy . . . 8, 105
Opechowski, W.
Electromagnetic waves in wave guides,
I. General theoretical principles; rectangular wave guides 10, 13
II. Coaxial cables and circular wave guides . . 10, 46
Oranje, P.J.
Technical photometry of gas-discharge lamps . . 5, 166
— and J. Funke
The development of blended-light lamps 7, 34
Overbeek, A.J.W.M. van and J.L.H. Jonker
A new frequency-changing valve 3, 266
Padmos, A.A. and J. Voogd
Mercury lamps for use in making heliographic prints 6, 250
— and J. de Vries
Stresses in glass and their measurement 9, 277
Parrish, W. and E. Cisney
An improved X-ray diffraction camera 10, 157
Penning, F.M.
High-vacuum gauges 2, 201
Velocity-modulation valves 8, 214
Plaats, G.J. van der and A. Verhoeff
A directing instrument for the operative treatment of fractures of the neck of the femur 8, 237
Ploos van Amstel, J.J.A., see Amstel, J.J.A. Ploos van
Pol, Balth. van der and C.C.J. Addink
The pitch of musical instruments and orchestras . . 4, 205
— and H. Bremmer
The propagation of wireless waves round the earth 4, 245
— and Th. J. Weijers
Electrical filters
I 1, 240
II 1, 270
III 1, 298
IV 1, 327
V 1, 363
Polis, L.L.C.
"Philite" as a structural material 3, 9
Poole J.B. Le
A new electron microscope with continuously variable magnification 9, 33
— A.C. van Dorsten and W.J. Oosterkamp
An experimental electron microscope for 400 kilovolts 9, 193
Posthumus, K.
The hum due to the magnetic field of the filaments in transmitting valves 5, 100
Prakke, F. and G. Alma
A new series of small radio valves 8, 289
Pré, F.K. du, see du Pré, F.K.
Rademakers, A.
A condenser-microphone for stereophony 9, 330
— and P.G. Moerel
Non-ferrous copper wire for moving-coil meters . . 8, 315
Reynst, M.F. and P.J. Hagendoorn
An electrical pressure indicator for internal combustion engines 5, 348
The recording of diagrams with the electrical pressure indicator 6, 22
Richards, C.L.
A television receiver 2, 33
Rieck, G.D.
The illumination of coal-mines and the attendant risk of explosions 10, 334
Riemens, J.
Temperature measurements with the optical pyrometer in the hardening department 6, 30
Rinia, H.
Television with Nipkow disc and interlaced scanning 3, 285
— and P.M. van Alphen
The manufacture of correction plates for Schmidt optical systems 9, 349
Projection-television receiver, I. The optical system for the projection 10, 69
— and H. de Brey
An improved method for the air-cooling of transmitting valves 9, 171
— H. de Brey and F.L. van Weenen
Fundamentals for the development of the Philips air engine 9, 97
— and C. Dorsman
Television system with Nipkow disc 2, 72
— and F.K. du Pré
Air engines 8, 129

— D. Kleis and M. van Tol
Experimental transmitting and receiving equipment for high-speed facsimile transmission, I. General 10, 189
— and L. Leblans
The Nipkow disc 4, 42
— and H.J. Lindenhovius
A direct current supply apparatus with stabilized voltage 6, 54
Romeyn, C.
The V.R. 18 transmitting and receiving equipment 1, 114
Romeyn, F.C., P.W. Haayman and E.J.W. Verwey
Semi-conductors with large negative temperature coefficient of resistance 9, 239
Roodenburg, J.W.M. and G. Zecher
Irradiation of plants with neon light 1, 193
Rooy, A.P. van and J. de Gier
Improvements in the construction of cathode-ray tubes 9, 180
Sack, J.
How does a welding electrode fuse? 1, 26
Welding and welding rods 2, 129
The tensile strength of deposited weld metal . . . 3, 279
Overhead welding 4, 9
Schouten, J.F.
The diffraction of light by sound film 3, 298
Synthetic sound 4, 167
An acoustic spectroscope. 4, 290
The perception of pitch 5, 286
Non-linear distortion of sound film with oblique light slit 6, 110
— G.H. Bast and D. Goedhart
A 48-channel carrier telephone system,
I. The method of modulation 9, 161
II. Mechanical construction 10, 353
— and J.W. Klute
The influence of losses on the properties of electrical networks 7, 138
Schouwstra, P. and G. Zecher
Tubular luminescence lamps 4, 337
Severs, J.
An electrodynamic pick-up for the investigation of mechanical vibrations 5, 230
Siezen, G.J. and F. Kerkhof
Projection-television receiver, III. The 25 kV anode voltage supply unit 10, 125
Six, W.
The use of loading coils in telephony 1, 353
— and H. Mulders
The use of amplifiers (repeaters) in telephony . . 2, 209
Slooff, F.C.W., D Kleis and J.M. Unk
Experimental transmitting and receiving equipment for high-speed facsimile transmission, II. Details of the transmitter 10, 257
— M. van Tol and J.M. Unk
Experimental transmitting and receiving equipment for high-speed facsimile transmission, III. Details of the receiver. 10, 265
Slooten, J. van
The communal aerial 1, 246
Receiving aerials 4, 320
The functioning of triode oscillators with grid condenser and grid resistance 7, 40
Stability and instability in triode oscillators . . . 7, 171
— and P. Cornelius
Installations for improved broadcast reception . . . 9, 55
Smelt, J.
Glass for modern electric lamps and radio valves . . 2, 87
Snoek, J.L.
Magnetic cores for loading coils 2, 77
Magnet steels 2, 233
A permanent magnet which can lift 3500 times its own weight 5, 195
Non-metallic magnetic material for high frequencies 8, 353
— and F.K. du Pré
Several after-effect phenomena and related losses in alternating fields 8, 57
Snijders, M.J.
A transmitting valve cooler with increased turbulence of the cooling water 10, 239
Stegwee, J.G.C.
Experiments on the austempering of steel. 6, 279
Stevels, J.M.
The vitreous state 8, 231
Strutt, M.J.O. and K.S. Knol
A diode for the measurement of voltages on decimetre waves. 7, 124
— and A. van der Ziel
The behaviour of amplifier valves at very high frequencies 3, 103
A new push-pull amplifier valve for decimetre waves 5, 172
A variable amplifier valve with double cathode connection suitable for metre waves 5, 357
The noise in receiving sets at very high frequencies 6, 178
The diode as a frequency changing valve especially with decimetre waves 6, 285
Suchtelen, H. van
Applications of cathode ray tubes
I 3, 50
II 3, 148
III 3, 248
IV 3, 339
Application of cathode ray tubes in mass production 4, 85
The electrometer triode and its applications . . . 5, 54
Measuring the rate of watches with a cathode-ray oscillograph 9, 317
— and J. Boeke
Rapid chemical analysis with the mercury dropping electrode and an oscillograph or measuring bridge as indicator 4, 231
Tak, W.
The measurement of reverberation 8, 82
Measuring reverberation time by the method of exponentially increasing amplification 9, 371
Tellegen, B.D.H.
Inverse feed-back 2, 289
Geometrical configurations and duality of electrical networks 5, 324
Teves, M.C.
The photo-electric effect and its application in photo-electric cells 2, 13
A photocell with amplification by means of secondary emission 5, 253
— and J.L.H. Jonker
Technical applications of secondary emission . . 3, 133
Timmer, A.L. and A.H. van Assum
A surveillance system using infrared rays 1, 306
Tol, M. van and D. Kleis
Experimental transmitting and receiving equipment for high-speed facsimile transmission,
IV. Transmission of the signals 10, 289
V. Synchronization of transmitter and receiver . 10, 325
— D. Kleis and H. Rinia
Experimental transmitting and receiving equipment for high-speed facsimile transmission, I. General 10, 189
— F.C.W. Slooff and J.M. Unk
Experimental transmitting and receiving equipment for high-speed facsimile transmission, III. Details of the receiver 10, 265
Tromp, Th.P.
Technical problems in the construction of radio valves 6, 317
Tuuk, J.H. van der
The "Rotalix" tube for X-ray diagnosis 3, 292
A million volt X-ray tube 4, 153
Hard glass X-ray tubes in oil 6, 309
X-ray tubes with rotating anode ("Rotalix" tubes) 8, 33
High-voltage rectifier valves for X-ray diagnostics . 8, 199
— G.C.E. Burger and B. Combee
X-ray fluoroscopy with enlarged image 8, 321
— and J.E. de Graaf
Automatic macroscopic examination of materials with X-rays 3, 228
— H.A.G. Hazeu and J.M. Ledeboer
An X-ray apparatus for contact therapy 8, 8
Unk, J.M., D. Kleis and F.C.W. Slooff
Experimental transmitting and receiving equipment for high-speed facsimile transmission, II. Details of the transmitter 10, 257

— F.C.W. Slooff and M. van Tol
Experimental transmitting and receiving equipment for high-speed facsimile transmission, III. Details of the receiver 10, 265
Urk, A.Th. van
The sound recorder of the Philips-Miller system . . 1, 135
Auditorium acoustics and reverberation 3, 65
The use of modern steels for permanent magnets . . 5, 29
— and K. de Boer
A simple apparatus for sound recording 4, 106
Some particulars of directional hearing 6, 359
— and R. Vermeulen
The radiation of sound 4, 213
Uyterhoeven, W.
Electrical phenomena in the positive column at low pressure 3, 157
Emission of light in the positive column at low pressure 3, 197
— and G. Zecher
Low-pressure mercury discharge within a luminescent tube 3, 272
Veegens, J.D.
A cathode ray oscillograph 4, 198
— and M.K. de Vries
A simple high frequency oscillator for the testing of radio receiving sets 6, 154
— and J.J. Zaalberg van Zelst
The accuracy of measurements of field strength . 5, 149
Veen, R. van der
Forcing tulips with artificial light 10, 282
Storing seed potatoes in artificially-lighted cellars . 10, 318
Ven, A.J. Heins van der
Testing amplifier output valves by means of the cathode ray tube 5, 61
Output and distortion of output amplifier valves under different loads 5, 189
Verhoeff, A.
Epicyclic gearing for low powers 9, 285
— and G.J. van der Plaats
A directing instrument for the operative treatment of fractures of the neck of the femur 8, 237
Vermeulen, R.
The Philips-Miller system of sound recording . . 1, 107
Octaves and decibels 2, 47
The relationship between fortissimo and pianissimo 2, 266
Auditorium acoustics and intelligibility 3, 139
Auditorium acoustics and sound absorption . . . 3, 363
The testing of loudspeakers 4, 354
Perspectives in the development of the violin . . 5, 36
Standardization of acoustic quantities 5, 243
Optical experiments with models on the directional distribution of sound in halls 5, 321
The acoustics of the auditorium of the new municipal theatre in Utrecht 7, 9
Duplication of concerts 10, 169
— and J. de Boer
Optical model experiments for studying the acoustics of theatres 1, 46
— and K. de Boer
On improving defective hearing 4, 316
— and A.Th. van Urk
The radiation of sound 4, 213
Vervest, W.L. and J. Bergmans
A new fitting for road lighting, ... 5, 222
Verwey, E.J.W.
Electronic conductivity of non-metallic materials . 9, 46
— and R.D. Bügel
Ceramic materials with a high dielectric constant . 10, 231
— P.W. Haayman and E.L. Heilman
On the crystalline structure of ferrites and analogous metal oxides 9, 185
— P.W. Haayman and F.C. Romeyn
Semi-conductors with large negative temperature coefficient of resistance 9, 239
Voogd, J.
Physical photometry 4, 260
Tungsten ribbon lamps for optical measurements . 5, 82
Subjective photometry 5, 270
— and L.C. Kalff
Living room lighting with tubular fluorescent lamps 8, 267
— and A.A. Padmos
Mercury lamps for use in making heliographic prints 6, 250
Voorhoeve, N.A.J. and J.P. Bourdrez
The electric-acoustic installation in the League of Nations Palace at Geneva 3, 322
— and F.H. de Jong
Voltage regulation of direct current generators by means of triodes 3, 97
Vriend, J.A. de and J.A.M. van Liempt
The "Photoflux", a light-source for flashlight photography 1, 289
The adjustment of synchronizers for the "Photoflux" photo-flash bulb 2, 334
The testing of electric fuses with the cathode ray oscillograph 4, 118
Vries, G. de
Electromagnetic cavity resonators 9, 73
— and C.G.A. von Lindern
An ultra short wave telephone link between Eindhoven and Tilburg 2, 171
A decimetre wave radio link between Eindhoven and Nimeguen 2, 299
Resonance circuits for very high frequencies . . 6, 217
Lecher systems 6, 240
Flat cavities as electrical resonators. 8, 149
Vries, J. de and A.A. Padmos
Stresses in glass and their measurement 9, 277
Vries, M.K. de and J.D. Veegens
A simple high-frequency oscillator for the testing of radio receiving sets 6, 154
Warmoltz, N.
Potential distribution at the igniter of a relay valve with mercury cathode 8, 346
The ignition mechanism of relay valves with dielectric igniter 9, 105
— and A.M.C. Helmer
A flash lamp for illuminating vapour tracks in the Wilson cloud chamber 10, 178
Weel, A. van
An experimental transmitter for ultra-short-wave radio-telephony with frequency modulation . . . 8, 121
An experimental receiver for ultra-short-wave radio-telephony with frequency modulation . . . 8, 193
Weel, J.G.A. van
Systematic X-ray examination for the detection of pulmonary tuberculosis 1, 335
Weenen, F.L. van
The construction of the Philips air engine . . . 9, 125
— H. de Brey and H. Rinia
Fundamentals for the development of the Philips air engine 9, 97
Weg, H. van de
The equalization of telephone cables 7, 184
— and G.J. Levenbach
Non-linear distortion in loaded cables 4, 79
Wenke, J.W.G. and F. de Fremery
New principles of construction for the electro-acoustic installation of studios 6, 139
The measurement of peak voltages in a studio installation 7, 20
Went, J.J.
An apparatus for hysteresis measurements on soft magnetic materials 2, 84
The electrical resistance of metal contacts 4, 332
Adsorption phenomena at metal contacts 5, 238
The effect of the melting point and the volume magneto-striction on the thermal expansion of alloys 10, 87
Soft iron for the electromagnet of a cyclotron . . . 10, 246
— and P. Koole
A method for the control of colour deviations . . . 6, 186
Werfhorst, G.B. van de
Public lighting, principles of road lighting . . . 2, 110
Public lighting, principles of street illumination . 2, 142
Technical considerations in the lighting of country roads 2, 239
Werner, W.
The control of contact pressures 6, 61
Westmijze, W.K.
A new method of counteracting noise in sound film reproduction 8, 97

Weyers, Th.J.
Filters for carrier-wave telephony installations . . 7, 104
Frequency modulation 8, 42
Comparison of frequency modulation and amplitude modulation 8, 89
— and Balth. van der Pol
Electrical filters
I 1, 240
II 1, 270
III 1, 298
IV 1, 327
V 1, 363
Willigen, P.C. van der
Automatic starting resistances ("Starto" tubes) . 1, 205
The mechanical properties of welded joints . . . 6, 97
Contact arc-welding 8, 161
Penetration and welding speed in contact arc-welding 8, 304
Winkel, J. te
Carrier telegraphy 8, 206
Wolf, M.
The enlarged projection of television pictures . . 2, 249
Wijk, A. van
Spectral distribution of the radiation from the "Biosol" 2, 18
The use of ultraviolet radiation in industrial luminescence research 3, 5
Lamp manufacture and vitamine research 3, 33
An apparatus for treatment with infrared radiation 6, 202
IJdens, R.A.
Ceramics and their manufacture 10, 205
IJzeren, E.A. van
The dynamo pocket torch 8, 225
Zaalberg van Zelst, J.J., see **Zelst, J.J. Zaalberg van**
Zecher, G. and J.W.M. Roodenburg
Irradiation of plants with neon light 1, 193
— and P. Schouwstra
Tubular luminescence lamps 4, 337
— and W. Uyterhoeven
Low-pressure mercury discharge within a luminescent tube 3, 272
Zelst, J.J. Zaalberg van
Stabilised amplifiers 9, 25
Constant amplification in spite of changeability of the circuit elements 9, 309
Circuit for condenser microphones with low noise level 9, 357
— and J.D. Veegens
The accurary of measurements of field strength . . 5, 149
Ziegler, M.
The causes of noise in amplifiers 2, 136
A recording field-strength meter of high sensitivity 2, 216
Noise in amplifiers contributed by the valves . . 2, 329
Noise in receiving sets 3, 189
Ziel, A. van der and M.J.O. Strutt
The behaviour of amplifier valves at very high frequencies 3, 103
A new push-pull amplifier valve for decimetre waves 5, 172
A variable amplifier valve with double cathode connection suitable for metre waves 5, 357
The noise in receiving sets at very high frequencies . 6, 178
The diode as a frequency changing valve especially with decimetre waves 6, 285
Zijl, H.
The illumination of railway yards with sodium lamps 4, 61
The calculation of lighting installations with linear sources of light 6, 147
Efficiencies of lighting installations 7, 97
— and A.A. Kruithof
Illumination intensity in offices and homes . . . 8, 242
Zijlstra, P.
Radio landing beacons for aerodromes 2, 370
— and Tj. Douma
Recording the characteristics of transmitting valves 4, 56